





NASA Reference Publication 1224, Volume I

A High-Resolution Atlas of the
Infrared Spectrum of the Sun
and the Earth Atmosphere
from Space

A Compilation of ATMOS Spectra
of the Region from 650 to 4800 cm⁻¹
(2.3 to 16 μm)

/ Volume I. The Sun

Crofton B. Farmer
Robert H. Norton
Jet Propulsion Laboratory
California Institute of Technology



National Aeronautics and Space Administration
Office of Management
Scientific and Technical Information Division
Washington, DC 1989

Library of Congress Cataloging-in-Publication Data

Farmer, Crofton B.

A high-resolution atlas of the infrared spectrum of the Sun and Earth atmosphere from space : a compilation of ATMOS spectra of the region from 650 to 4800 cm⁻¹ (2.3 to 16 [symbol for Greek letter mu]m) / Crofton B. Farmer, Robert H. Norton.

p. cm. -- (NASA reference publication ; no. RP-1224)

Bibliography: v. 1, p.

Contents: v. 1. The Sun -- v. 2. Stratosphere and mesosphere, 650 to 3350 cm⁻¹.
1. Spectrum, Solar--Atlases. 2. Infrared spectrum--Atlases.

I. Norton, Robert H. II. Title III. Series: NASA reference publication ; 1224.

QB551.F37 1989

523.7'028'7--dc20

89-600203

CIP

Contents

I.	Introduction	1
II.	The ATMOS Instrument	1
III.	The Spacelab-3 Observations	3
IV.	Data Reduction	3
V.	Description of the Spectra	6
	A. Instrumental Lines	6
	1. Artifacts	6
	2. Residual Gas	7
	B. Detector Nonlinearity	7
	C. Frequency Reference	8
VI.	Availability of the Spectra in Digital Form	9
	References	11
	Spectra	13

Figures

1.	Layout of the key components of the interferometer optical system	3
2.	A view of the ATMOS interferometer with its dust cover removed	3
3.	Mounting arrangement of the interferometer and electronic subunits on the payload bridge structure in the shuttle cargo bay	4
4.	Low-dispersion plots of the 1100 to 1900 cm ⁻¹ region of the unapodized solar (a) and atmospheric (b) spectra	7
5.	Residual spectrum obtained by taking the ratio of the single-sided, high-Sun average spectra of the two cat's-eye symmetry cases	8

Tables

1.	Transmission frequency ranges of the ATMOS optical filters	2
2.	Summary of the observed solar occultations by filter and geographical location during the Spacelab-3 flight	4
3.	Listing of the ATMOS Spacelab-3 spectral database	5
4.	(a) Correlation coefficients for SS06 high-Sun spectra.....	6
	(b) Correlation coefficients for zonal average solar spectra	6
5.	List of principal "artifact" features	8

I. Introduction

During the period April 29 through May 2, 1985, the Atmospheric Trace Molecule Spectroscopy (ATMOS) experiment was operated as part of the Spacelab-3 (SL-3) payload of the shuttle Challenger. The instrument, a modified Michelson interferometer covering the frequency range from 600 to 5000 cm^{-1} (2 to $16\text{ }\mu\text{m}$) at a spectral resolution of 0.01 cm^{-1} , recorded infrared spectra of the Sun and of the Earth's atmosphere at times close to entry into and exit from occultation by the Earth's limb as seen from the shuttle orbit of 360 km. Spectra were obtained that are free from absorptions due to constituents of the atmosphere (i.e., they are "pure solar" spectra), as well as spectra of the atmosphere itself, covering line-of-sight tangent altitudes that span the range from the lower thermosphere to the bottom of the troposphere. This atlas, which is believed to be the first record of observations of the continuous high-resolution infrared spectrum of the Sun and the Earth's atmosphere from space, provides a compilation of these spectra arranged in a hardcopy format suitable for quick-look reference purposes; the data are also available in digital form.

A number of infrared solar atlases have been published over the past fifty years that, of necessity, have presented "solar-telluric" spectra containing lines originating in both the solar and Earth atmospheres, because the observations were made from ground-based sites or, in some cases, aircraft or balloon platforms. From the viewpoint of studies of the Sun itself, the use of the infrared solar spectrum has thus been restricted to those spectral intervals that are not masked by the strong absorption lines of constituents of the Earth's atmosphere (water vapor, carbon dioxide, methane, etc.) present in the atmospheric path above the observation site. Since the fundamental bands of diatomic molecular species, including NH, CH, OH, and CO and their isotopic variants, occur in this frequency region, the ability to analyze the many lines of these bands that would become accessible in a spectrum free of telluric absorptions would allow the determination of accurate solar abundances of C, N, and O, and their isotopic ratios. Similarly, detailed studies of the compositional structure of the Earth's atmosphere have suffered from contamination of the telluric features by absorptions of solar origin (for example, infrared measurements of the vertical distribution of carbon monoxide in the upper atmosphere have been hampered by the strong absorptions of carbon monoxide in the solar photosphere). Because the spectrum of transmitted solar infrared radiation has been the source of such a large part of our knowledge of the composition and structure of the Earth's

atmosphere, the potential value of such data, when coupled with the advantages of altitude and global coverage gained by making the observations from a platform above the atmosphere, provided a strong motivation for the development of the ATMOS experiment.

The advent of the Space Transportation System (STS)—the combination of the space shuttles and their supporting tracking and data relay satellites—has provided, within the past decade, the necessary payload-weight and high-data-rate capabilities to allow complex, high-spectral-resolution instruments to be operated in Earth orbit. Thus, the solar spectrum can be recorded without interference from Earth atmospheric absorptions, and this "pure solar" spectrum can then be used to ratio out the solar features from the solar-telluric spectrum recorded as the Sun passes behind the Earth's atmosphere during the occultation periods of the orbit. Such observations were made by the ATMOS instrument during its first flight. The present edition of the spectra is in two volumes: the first contains the solar spectra covering the entire frequency range of the instrument (650 to 4800 cm^{-1}), and the second covers the atmospheric spectra for tangent altitudes between 23 and 80 km , at approximately one-scale-height intervals (8 km), for the frequency range from 650 to 3380 cm^{-1} . Extensions of the atlas will be made in additional future volumes to include the extreme altitude and frequency limits of the acquired atmospheric spectra.

Detailed descriptions of the ATMOS experiment's scientific background, descriptions of the instrument's design and observation technique, and an account of the SL-3 mission and the results obtained therefrom can be found in References 1 and 2. A brief description of the instrument design's pertinent aspects is given below, followed by a discussion of the manner in which the interferograms and spectra have been processed.

II. The ATMOS Instrument

The ATMOS system's design was based on the requirements of the atmospheric measurements, since these were more stringent than the requirements for observations of the Sun itself. Consequently, the instrument's performance (in terms of the signal-to-noise ratio in the final spectra) favored the solar spectra, where a large number of high-speed scans could be averaged together. The scan time was determined by the need for a useful vertical resolution in the altitude profiles of concentration of the upper atmospheric constituents to be derived

Table 1. Transmission frequency ranges of the ATMOS optical filters.

Band 1 600–1200 cm ⁻¹	Band 2 1100–2000 cm ⁻¹	Band 3 1580–3400 cm ⁻¹	Band 4 3100–4700 cm ⁻¹
CO ₂	CO ₂	CO ₂	CO ₂
H ₂ O	CH ₄	CO	H ₂ O
O ₃	H ₂ O	CH ₄	
		H ₂ O	
		O ₃	
		N ₂ O	
NH ₃	H ₂ O ₂	NO	HF
HNO ₂	HO ₂	(NO ₂)	(HCN)
(HNO ₃)			
HNO ₄			
CCl ₃ F	(NO)	HDO	
CCl ₂ F ₂	NO ₂	(H ₂ O ₂)	
CHCClF ₂	N ₂ O ₅	H ₂ CO	
CH ₃ Cl	HNO ₃		
CCl ₄		HCl	
COF ₂	HOCl	(CH ₃ Cl)	
COClF	CF ₄	OCS	
CIO	SO ₂	HCN	
ClONO ₂			

from the spectra. From modeling considerations, it was decided that the vertical sampling interval should not be greater than half the atmospheric scale height, or about 4 km. Since occultation rates (i.e., the rate of change of altitude of the Sun-spacecraft tangent point) for the shuttle are typically 1.5 to 2 km/s, this translates to an instrument scan time of 2 s. In order to minimize the effect of smearing caused by the changing air mass as the interferogram was acquired, the instrument design was implemented so that a two-sided interferogram was produced every two seconds, with the zero path difference position at the center of the scan.

To further optimize the measurements in terms of the instrument performance and data rate under orbital conditions, the overall wavelength range to be covered was divided into several narrower bands by means of optical filters; these filters were chosen to be compatible with the alias limits of sampling at every second or every third fringe of the reference HeNe laser. The frequency ranges covered by the filters are shown in Table 1, which also lists the atmospheric molecules whose infrared transitions

occur within each band. Filters 1, 2, and 3 were used with a sampling interval of two laser fringes; for Filter 4, the interferogram was sampled every third fringe. (Data taken with Filters 5 and 6, which were used infrequently, are not included here.)

The conceptual design for an instrument capable of being put into Earth orbit and making the required observations was carried out at the Jet Propulsion Laboratory (JPL) between 1974 and 1977. At the end of this design study period, work on the final design and construction of the ATMOS instrument was begun at Honeywell Electro-Optics Center. Detailed descriptions of the instrument can be found in References 1 and 3.

The instrument consisted of four main parts: the suntracker, the foreoptics and frame camera, the interferometer and scan control system, and the electronic subunits, including the closed-cycle detector cooler. The instrument was mounted via vibration isolators to a temperature-controlled plate, which was itself mounted on a bridge structure across the aft end of the shuttle cargo bay. Figure 1

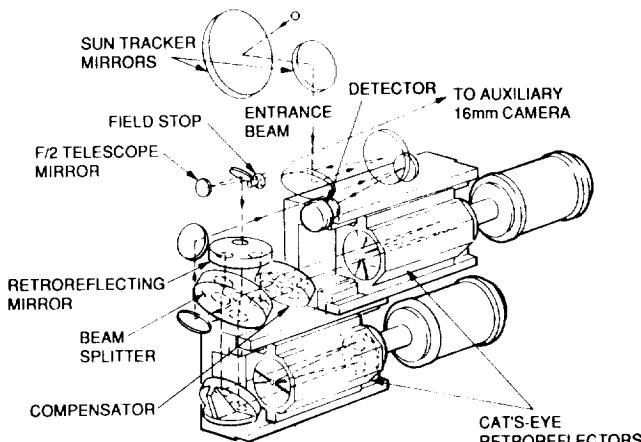


Figure 1. Layout of the key components of the interferometer optical system

is a schematic diagram of the optical system, and Figure 2 shows the interferometer and suntracker with the instrument cover removed. The overall assembly of the ATMOS optical and electronic subunits and their mounting arrangement on the bridge structure are illustrated in Figure 3.

An important aspect of the instrument design was the use of a thin aluminum cover that attached to the baseplate, enclosing all but the suntracker and camera. The pressure within the cover was maintained at ambient through a vent fitted with a desiccant filter designed to provide a clean, dry environment under all conditions (in particular, during the reentry phase). This filter prevented complete evacuation of the air inside the cover, even after several days in orbit, so that small residual lines of H_2O and CO_2 appeared in all of the spectra. These lines provided a valuable frequency reference for the rest frame against which the relative Doppler shifts of the solar and atmospheric lines could be verified.

The suntracker was able to acquire and track the Sun over the entire hemisphere above the shuttle wing plane; the tracking accuracy was 0.4 mrad, with a stability of 0.06 mrad. Solar radiation entered the foreoptics through a ZnSe window and was recollimated after passing through a selectable field stop of 1, 2, or 4 mrad. Energy that did not pass through the field stop was reflected to the frame camera, which recorded, at the beginning of each scan, the position of the interferometer's field-of-view superimposed on the solar disk. This feature was included to make sure that the relative position of the field-of-view on the disk did not drift during an occultation and also to be able to observe the shape of the solar image and the behavior of the tracker as the Sun approached the Earth's limb.

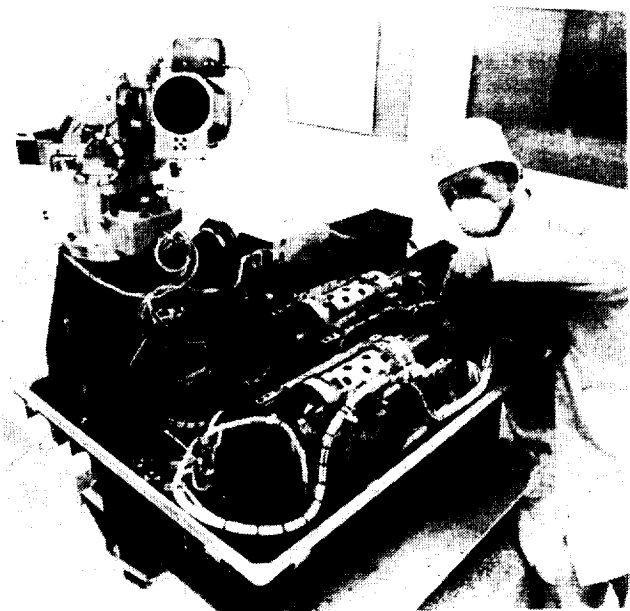


Figure 2. A view of the ATMOS interferometer with its dust cover removed.

III. The Spacelab-3 Observations

The SL-3 mission (STS flight 51B, on the shuttle Challenger) was launched at 21:00:30 GMT on April 29, 1985. The ATMOS observations included 19 complete occultation events, the geographic locations of which are listed in Table 2. The high-rate data stream (15.76 Mbps) was relayed via the NASA Tracking and Data Relay Satellite System (TDRSS) and recorded on the ground. The overall bit error rate in this process was 5×10^{-7} , averaged over the entire data set. However, errors occurred in bursts of several thousand bits, rendering an affected interferogram unusable, but having little impact on the experiment as a whole; the majority of interferograms were thus received error-free, with about 2% only of the spectra being lost because of uncorrectable bit errors.

The final data set contained a total of 1363 spectra, of which 510 were atmospheric and 853 were solar. Table 3 lists the inventory of ATMOS SL-3 spectra, with details of the time interval and number of scans corresponding to each occultation.

IV. Data Reduction

The initial reduction of the SL-3 data involved two principal tasks: (1) error-checking and reformatting the data from the recorded telemetry stream, followed by (2) Fourier transformation of the

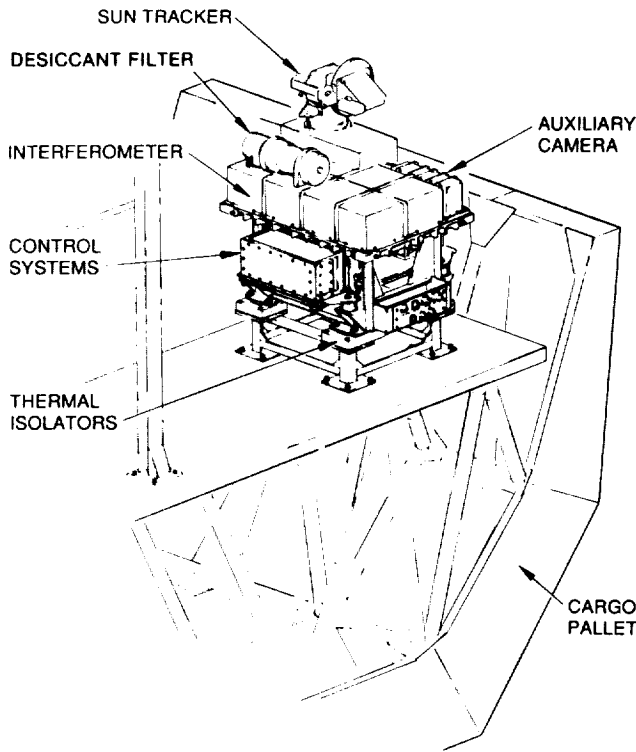


Figure 3. Mounting arrangement of the interferometer and electronic subunits on the payload bridge structure in the shuttle cargo bay.

interferograms to spectra. The Fourier transform program performed the nonlinear phase correction of the interferogram and a real-to-complex in-place Fourier transform. For phase correction, a short double-sided transform of the interferogram was carried out, and the phase spectrum and then its conjugate were calculated, with the inverse Fourier transform of the conjugate phase spectrum yielding the interferogram phase-correction function. After phase correction, all interferograms were zero-filled so that a 1-million-point real to 524,288-point complex transform could be performed. The spectra recorded with Filter 4, employing a sample interval of three HeNe laser fringes, resulted in an alias having a width of 2633.3 cm^{-1} (extending from 2633 to 5267 cm^{-1}), and a point spacing of 0.00502 cm^{-1} . All other spectra are contained within aliases extending from 0 to 3950 cm^{-1} , with point spacings of 0.00753 cm^{-1} .

The spectra have been apodized and interpolated by a factor of 5 (i.e., 4 additional points have been inserted between the original primary points), thus making the spectral point spacing used in this atlas 0.001506 cm^{-1} for frequencies below 3382 cm^{-1} , and 0.00100 cm^{-1} for frequencies above it. An intermediate apodizing function (number 2 in Reference 4) was used.

Table 2. Summary of the observed solar occultations by filter and geographical location during the Spacelab-3 flight.

Start Time (MET ^a)	Occ. Type	Opt. Fil.	Start Lat.	Start Lon. (E)
00/07:13	SR01	3	-50.10	118.25
00/08:08	SS01	1	36.87	277.60
00/18:52	SS02	1	36.18	117.31
00/19:27	SR02	3	-49.12	294.55
00/21:55	SS03	2	34.53	70.68
01/00:55	SS04	4	35.82	25.69
01/01:34	SR03	6	-49.10	203.09
01/02:28	SS05	1	34.80	2.26
01/07:01	SS06	3	32.90	292.66
01/08:33	SS07	2	33.65	270.20
01/10:05	SS08	1	33.73	247.39
01/15:18	SR04	4	-47.28	355.90
01/16:49	SR05	2	-47.80	333.43
01/18:21	SR06	1	-47.15	310.09
01/19:53	SR07	5	-46.97	287.07
02/01:22	SS09	3	29.95	16.84
02/02:53	SS10	4	30.28	354.13
02/04:25	SS11	3	29.00	330.65
02/05:51	SS12	2	28.65	307.61
02/07:27	SS13	3	29.65	285.23

^aMission Elapsed Time.

Although there were sufficient numbers of molecules of water vapor and carbon dioxide in the optical path to cause the instrumental lines discussed below, the internal instrument pressure was too small to require an air-to-vacuum frequency correction to the SL-3 data set. Evidence for the frequency stability of the HeNe reference laser has been given by Brown et al. (Reference 5), who reported an uncertainty of 0.0003 cm^{-1} in the frequency of a single-line, single-spectrum measurement.

During the SL-3 mission, the vast majority of the ATMOS observations were made at times close to the occultation entry and exit intervals; only a limited number of spectra were recorded at "high Sun," i.e., when the Sun was well away from the Earth's limb. This was done so that solar-only scans would be associated with each of the sets of occultation spectra of the atmosphere, and also so that the experiment observation timelines and the use of spacecraft resources would be simplified as much as possible. Thus, data that were free from telluric absorptions were obtained at the beginning of each sunset and at the end of each sunrise. From examination of the spectra, it was established that atmospheric lines of

Table 3. Listing of the ATMOS Spacelab-3 spectral database.^a

Filter	Ocnn.	GMT Range	m:ss	Spectra
1	SS01	850430000952-001232	2:40	72
	SS02	850430105146-105427	2:41	73
	SS05	850430183034-183237	2:03	58
	SS08	850501020836-021107	2:31	69
	SR06	850501102408-102650	2:42	78
2	SS03	850430135503-135757	2:54	77
	SS07	850501003711-003921	2:10	60
	SR05	850501085216-085515	2:59	81
	SS12	850501220001-220224	2:23	62
3	SR02	850430112950-113158	2:08	58
	SS06	850430230521-230742	2:21	52
	SS09	850501172500-172721	2:21	65
	SS11	850501202815-203044	2:29	68
	SS13	850501233132-233359	2:27	68
4	SS04	850430165817-170109	2:52	55
	SR04	850501072056-072336	2:40	71
	SS10	850501185637-185904	2:27	55
	SUN2	850501115547-115801	2:58	68
5	SR07	850501115547-115801	2:14	55
6	SR03	850430173651-173903	2:12	50
	SUN1	850501085838-090125	2:47	68

^aThe ATMOS Spacelab-3 observation record summarized here pertains to spectra from the Fourier transformation of two-sided interferograms. Scans that contained telemetry dropouts have been excluded.

NO at 1900 cm^{-1} could be detected at altitudes up to 140 km, while lines of CO_2 at 2350 cm^{-1} were detectable to altitudes slightly above 150 km. (It should be noted that the presence of atmospheric CO_2 lines at the highest altitudes could be detected only by means of a cross-correlation technique in which the entire band was included in the calculation. The lines were quite invisible to the naked eye.) It was decided, therefore, to adopt 165 km as the "boundary" between the atmosphere and space; all spectra taken at tangent altitudes greater than 165 km would be assumed to be solar-only, while the spectra at lower altitudes would be considered to contain atmospheric absorptions.

Because the variation in the radial velocity between the spacecraft and the Sun was so slight during the acquisition of the solar-only scans, it was possible to average all such spectra on a point-by-

point basis. This produced a solar reference spectrum for each occultation. To test the validity of this procedure, a cross-correlation at zero frequency lag was performed between the individual spectra and the occultation average. The results are shown in Table 4; the minimum correlation found (i.e., the worst case) is 0.999517, indicative of the very high degree of correlation that exists between the individual spectra. Average spectra were produced in this way for each of the SL-3 occultations and were used as the reference spectra in obtaining the (atmospheric) transmission spectra, which are referred to here as "ratio" spectra.

A similar point-by-point averaging procedure was employed to obtain zonal average solar spectra—the grand average of all solar spectra taken with a particular optical filter and at the same radial velocity. There was concern that the changing orbit

Table 4(a). Correlation coefficients for SS06 high-Sun spectra.

Spectrum	Coefficient
A50430230521	0.999906
A50430230523	0.999896
A50430230543	0.999884
A50430230545	0.999516
A50430230547	0.999883
A50430230554	0.999882
A50430230556	0.999885
A50430230607	0.999876
A50430230609	0.999884
A50430230611	0.999547
A50430230613	0.999859

Table 4(b). Correlation coefficients for zonal average solar spectra.

Filter	SS02	0.999998
	SS05	0.999997
	SS08	0.999996
Filter 2	SS03	0.999992
	SS07	0.999998
	SS12	0.999989
Filter 3	SS06	0.999944
	SS09	0.999976
	SS11	0.999988
	SS13	0.999994
Filter 4	SS04	0.999977
	SS10	0.999990

of the spacecraft might result in significant frequency shifts during the mission. This was found not to be the case; calculation of the cross-correlation coefficient at zero lag between any of the occultation average solar spectra and the grand average gives a worst-case value of 0.999944, again demonstrating a high degree of correlation between the individual, the occultation average, and the zonal grand average spectra. The latter set constitutes the ATMOS solar spectrum presented as Volume I of this atlas.

The raw spectra are characterized by a background intensity distribution that results from the combined shapes of the relative response functions of the instrument optical components and detector, and the spectral brightness temperature distribution of the Sun itself. This characteristic shape of the spectral background is illustrated in panels (a) and (b) of Figure 4, in which low-dispersion plots of the 1100 to 1900 cm⁻¹ region of the solar and atmospheric spectra are reproduced. In the atlas presentation of the solar spectrum, no attempt has been made to correct for, or remove, this background shape, since no independent radiometric calibration of the data was undertaken during the SL-3 observations. As discussed later, the solar spectrum contains instrument residual absorption lines and other artifacts, in addition to the lines of solar origin, superimposed on this continuum.

In the case of the atmospheric spectra, the instrument response function and the solar spectral intensity distribution, as well as the solar and instrument-related lines, have been removed by the process of taking the ratio of the atmospheric spectra and the corresponding occultation average solar

spectrum. The resulting spectra contain only lines that originate in the Earth's atmosphere, superimposed on a unit-transmittance background; a low-dispersion plot of the atmospheric ratio spectrum is shown in panel (c) of Figure 4.

V. Description of the Spectra

All dimensions in the atlas are metric: a linear frequency scale has been chosen, with a dispersion of 1 cm⁻¹ = 3.5 cm. In the case of the solar spectra (Volume I), the intensity scale (i.e., the height of the mean continuum level in each panel) is set at 8.0 cm, with a vertical offset between the sunrise and sunset tracings of 2.0 cm. For the atmospheric spectra (Volume II), the zero to unit-transmittance scale has a height of 5.0 cm, with a vertical offset between spectra of 2.5 cm.

A. Instrumental Lines

1. Artifacts. From the earliest operation of the ATMOS instrument, it was evident that the spectra recorded with this instrument contained several absorption-like features that were neither solar nor atmospheric in origin. It was clear that these "artifacts" were not atmospheric, as they were equally strong in the high-Sun spectra as they were in atmospheric spectra with significant line-blanketing. To test whether they were of solar origin or were inherent to the instrument itself, the processing software was modified to produce spectra from one-sided Fourier transforms of the data. These spectra were grouped according to whether the

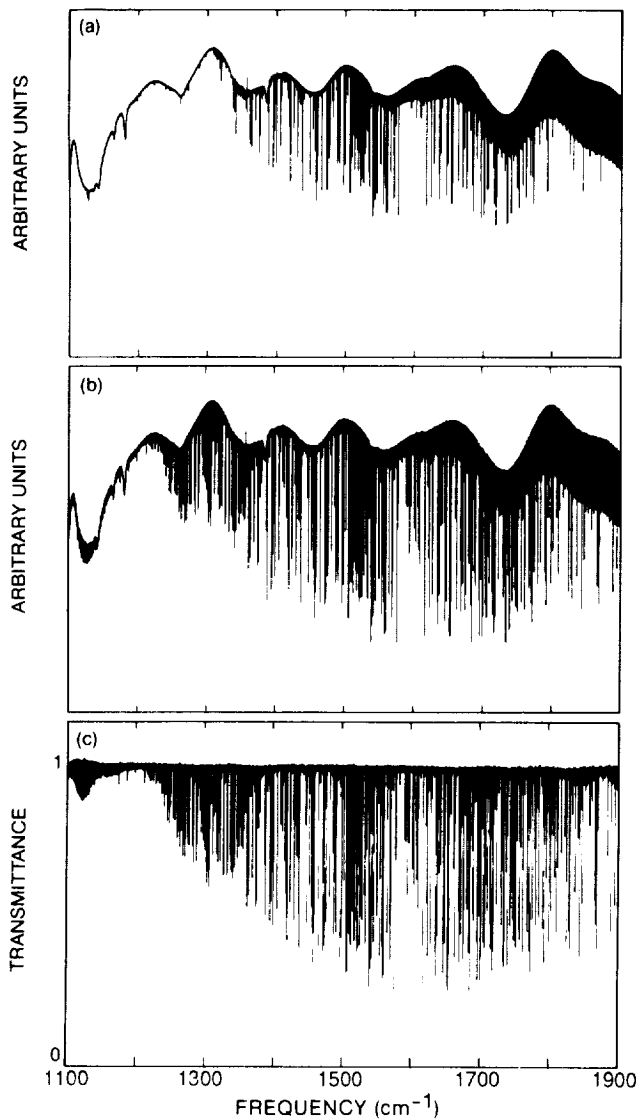


Figure 4. Low-dispersion plots of the 1100 to 1900 cm⁻¹ region of the unapodized solar (a) and atmospheric (b) spectra. The corresponding atmospheric ratio spectrum is shown in the lower panel (c).

inboard cat's-eye was close to the beamsplitter or away from it. It was then seen that the depths of the spurious features were much greater in the case of the spectra from those portions of the scan where the inboard cat's-eye was farthest from the beamsplitter. (The true solar lines revealed themselves to be independent of the cat's-eye position.) By averaging all available single-sided, high-Sun spectra, and then taking the ratio of the resultant averages of the two symmetry groups, an "artifact spectrum" was produced in which all trace of the filter and detector

response characteristics, solar lines, and absorptions due to the residual gas in the instrument (CO₂ and water vapor) were removed. This spectrum is shown in Figure 5; a list of frequencies of the artifacts is given in Table 5.

2. Residual Gas. The desiccant filter incorporated into the instrument cover acted as a barrier that prevented complete evacuation of the gas inside the interferometer; consequently, lines of the strongest bands of this residual gas are superimposed on all of the spectra. To date, no molecular species other than water vapor and CO₂ has been identified as contributing to these lines, which, like the artifacts, are Doppler-shifted with respect to the atmosphere at sunset and sunrise. It should be pointed out that the possibility exists that some or all of the observed residual gas may be outside the instrument, i.e., associated with the spacecraft as products of the propulsion or attitude control systems. Evidence to the contrary is provided by the fact that a rotational analysis of the gas temperature gives a value of 301 ± 2 K, consistent with the temperature of the instrument enclosure. However, the location of the gas has not been determined conclusively.

The equivalent column amount of residual water vapor appeared to remain constant at about 9.2×10^{-3} cm-atm during the time when the ATMOS observations were made; the CO₂, on the other hand, showed evidence of a slight decrease, with the average amount of the CO₂ being approximately 1×10^{-4} cm-atm. Since the sunset and sunrise zonal average spectra are compiled from the respective filter and occultation averages, which have different effective observation times during the mission, the intensities of the instrumental CO₂ lines appear to be greater in the sunrise spectra than in the sunset spectra in some spectral regions, and vice versa in others. (See, for example, 670 cm⁻¹ vs. 2350 cm⁻¹ in the solar spectra.)

B. Detector Nonlinearity

In the ATMOS instrument, interferometrically modulated solar radiation is focused onto a HgCdTe detector that receives mean photon flux levels of up to 10^{21} photons·cm⁻²·s⁻¹. It has been shown experimentally (Reference 6) that, for flux levels in excess of 10^{19} photons·cm⁻²·s⁻¹, the minority carrier lifetime in HgCdTe photoconductors is no longer constant, but is proportional to $(\text{flux})^{2/3}$, giving rise to an electrical conductivity proportional to the cube-root of the flux. Consequently, the ATMOS spectra exhibit symptoms of nonlinearity; viz., the spectra

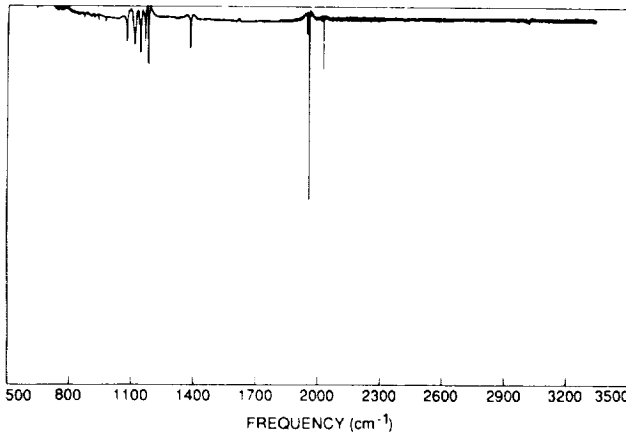


Figure 5. Residual spectrum obtained by taking the ratio of the single-sided, high-Sun average spectra of the two cat's-eye symmetry cases. The features revealed by this process are the instrument artifacts listed in Table 5.

are offset by their autocorrelation function, and phase errors are not fully eliminated by the symmetrization-convolution algorithm. Both of these effects are potential sources of systematic errors in the quantitative analysis of the spectra.

Work by Toon (Reference 7) has shown that interferograms deformed in this way can be corrected, provided the harmonic components introduced by the nonlinearity have not been lost in the data-sampling and -recording process. The procedure involves adding the DC electrical offset back onto the signal values, cubing, subtracting the offset, rescaling, doing the phase correction, and, finally, performing the fast Fourier transform (FFT). This correction was applied to all of the spectra recorded with Filters 1 and 2, which were sufficiently narrow that the information required for the correction was available. For data taken with Filters 3 and 4, the spectral bandpasses of which were almost as wide as the alias, the harmonic information was rejected in the signal processing circuitry, so that the nonlinearity correction could not be made *post facto*. Thus, the spectra at frequencies greater than about 2000 cm^{-1} show larger zero offsets than do those at lower frequencies.

C. Frequency Reference

The apparent frequencies of the spectral lines are affected by variations in the components of the

Table 5. List of principal "artifact" features.

Frequency (cm^{-1})	Approximate Depth (%)	Comments
870.1	1	
902.0	0.5	Diffuse
919.1	1	
937.8	2	
973.1	1.5	
1075.7	4	
1106.0	2	
1113.7	5	
1134.3	1	
1136.0	1	
1142.4	6	
1164.7	4	
1180.9	8	
1384.4	5	
1949.8	2.5	
1958.85	45	
2028.95	7	

instrument's relative velocity with respect to the Sun and the atmosphere as the spacecraft's orbital position changes. In order to provide the least chance of ambiguity in the identification of lines, the following convention has been adopted. For the solar spectra (Volume I), the sunset and sunrise zonal averages are displayed (sunset above, sunrise below), with the frequencies of the observed spectra having been corrected for the component of the relative velocity along the Sun-spacecraft line. Thus, lines whose positions appear shifted between the sunset and sunrise spectra are of instrumental origin (i.e., residual gas or instrument artifacts) and are easily distinguished.

The atmospheric zonal average spectra that constitute Volume II of the atlas have been taken from sunset occultations only; here again the spectra have been corrected to bring the atmospheric lines to the velocity rest frame. However, prior to application of the frequency correction, the spectra were ratioed against the zonal average solar spectrum, as described in Section IV; thus, the lines of solar origin, the instrument photometric background shape, and the instrument lines and artifacts have all been removed. The resulting atmospheric spectra are in transmittance form, and the ordinate of the plotted panels can be used as an approximate linear transmittance scale; the unit-transmittance level is marked adjacent to the respective tangent altitude

for each spectrum. The corresponding zero-transmittance levels are marked on the left-hand side of each panel.

VI. Availability of the Spectra in Digital Form

A digital version of the atlas is available in CD-ROM form; copies of this disk, or of any of the raw unprocessed spectra listed in Table 3, can be obtained by writing to:

National Space Science Data Center
NASA/Goddard Space Flight Center
Greenbelt, MA 20771

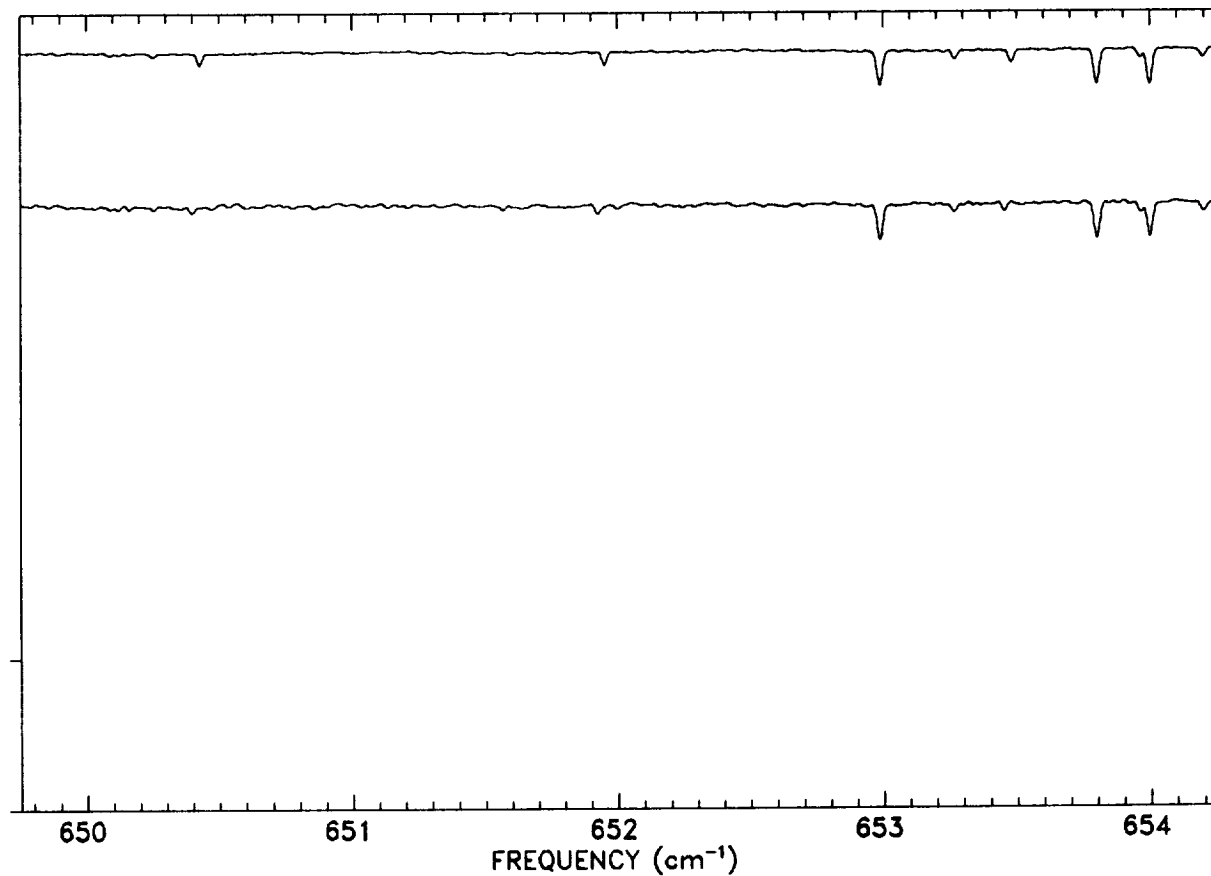
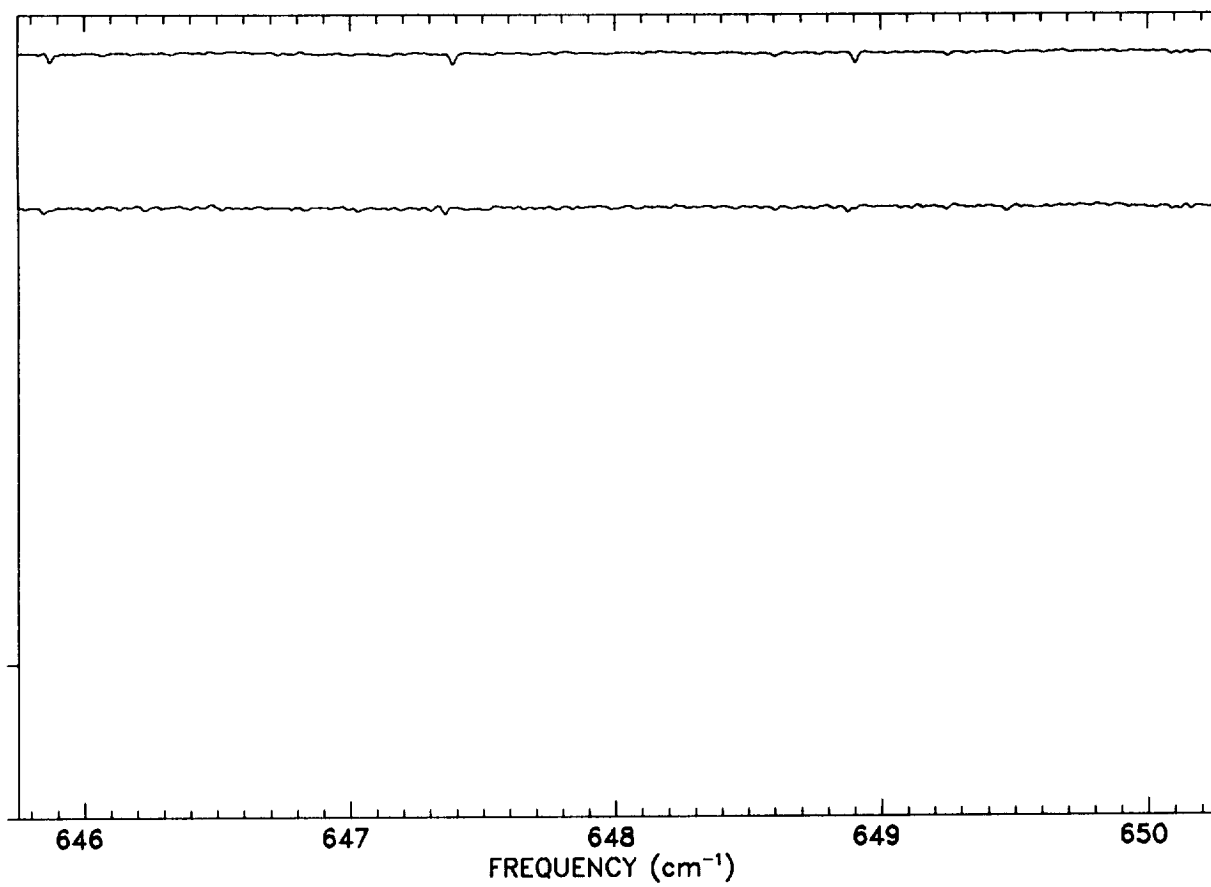
In addition, interested users can access the data using the extensive display and analysis software available at the ATMOS Data Analysis Facility by writing to the authors at:

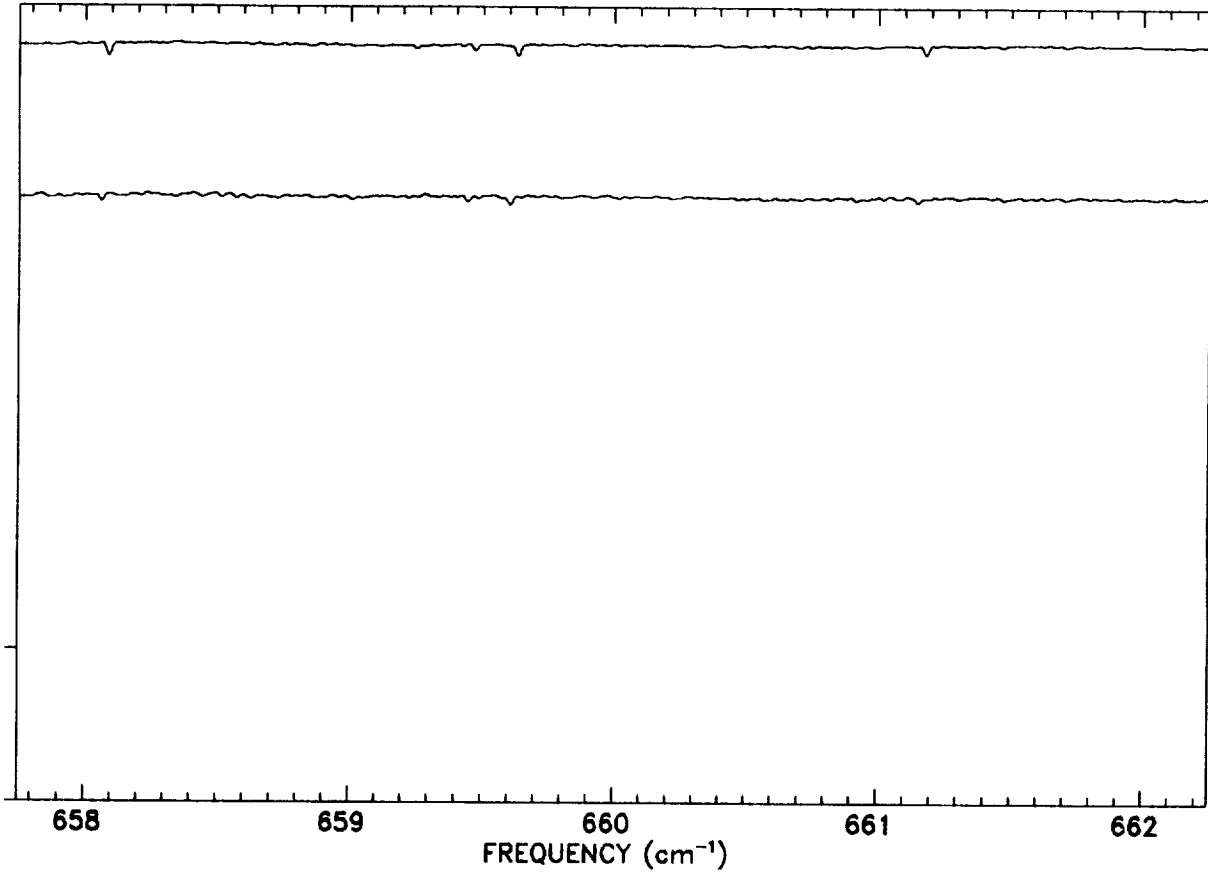
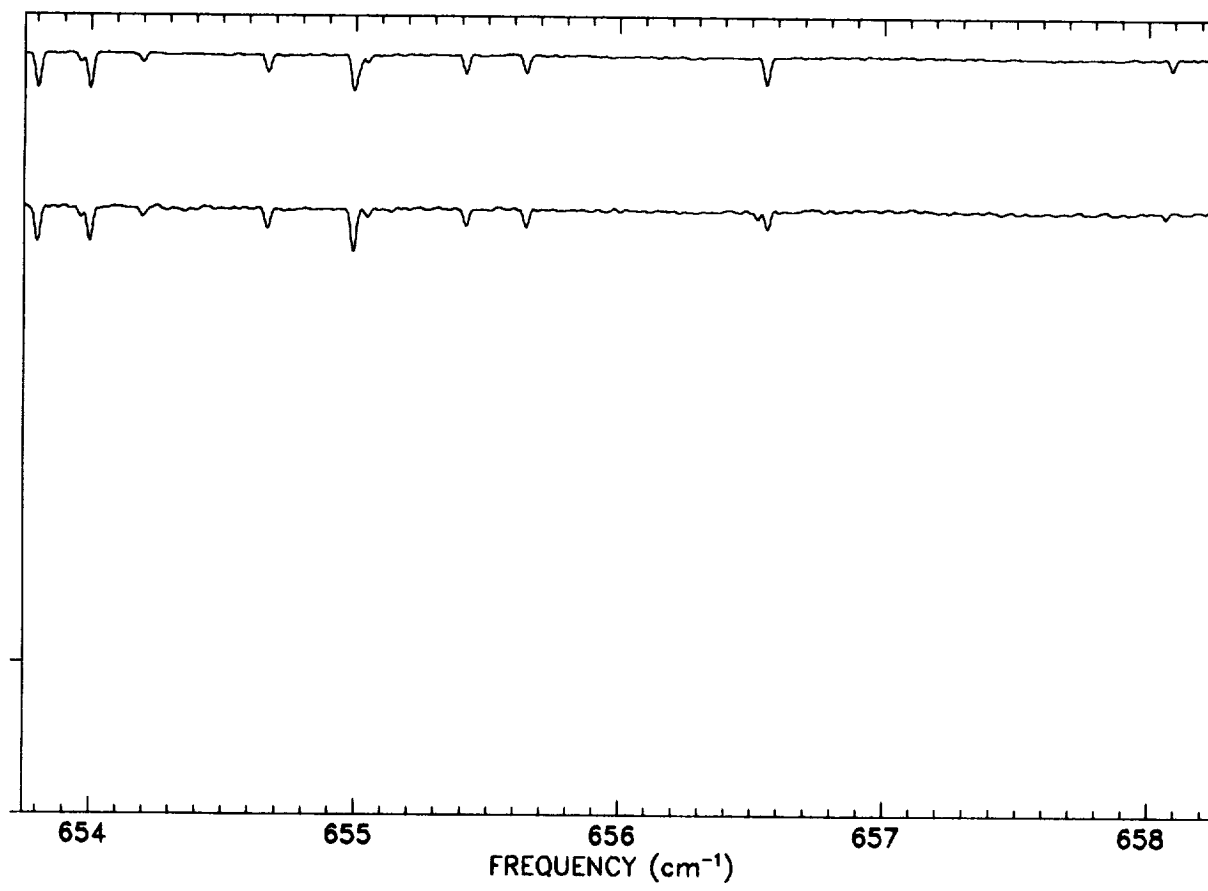
Jet Propulsion Laboratory
4800 Oak Grove Drive
Pasadena, CA 91109

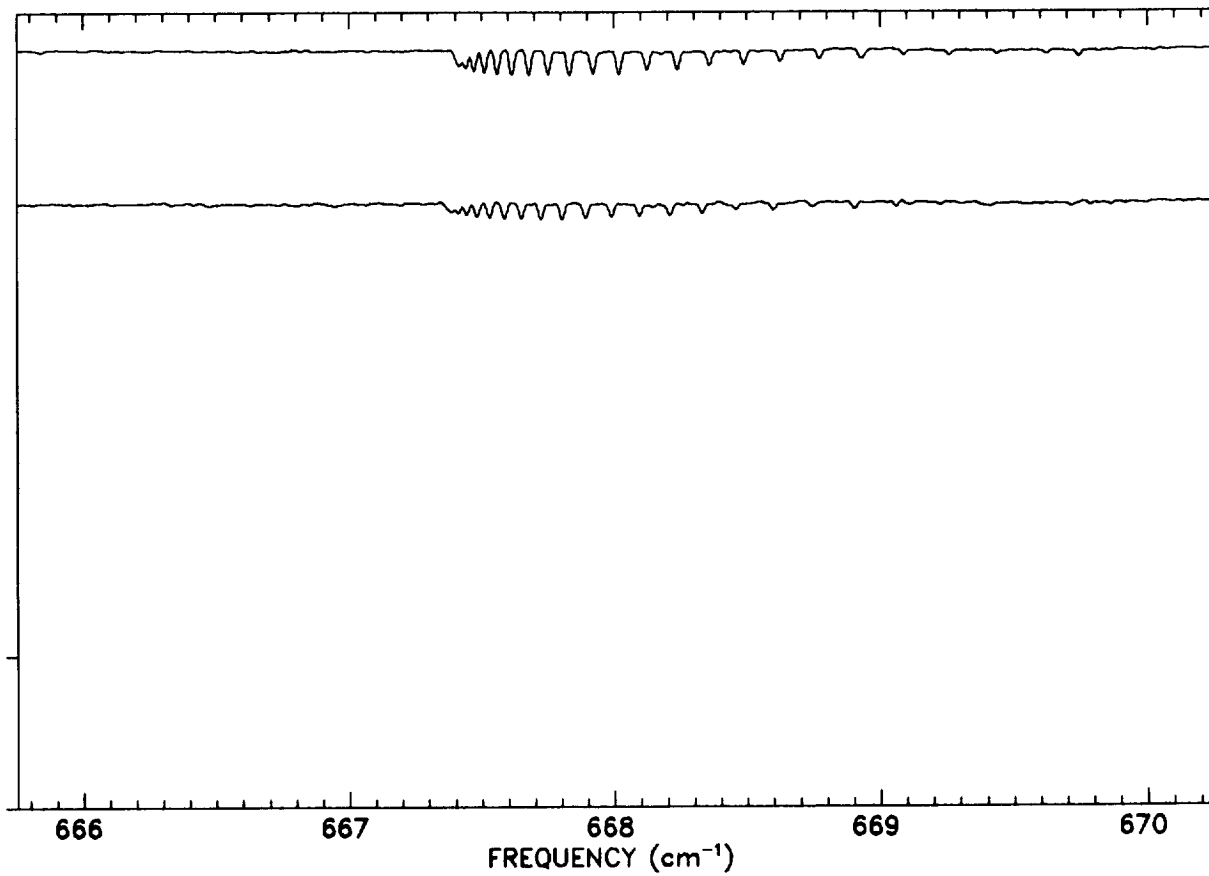
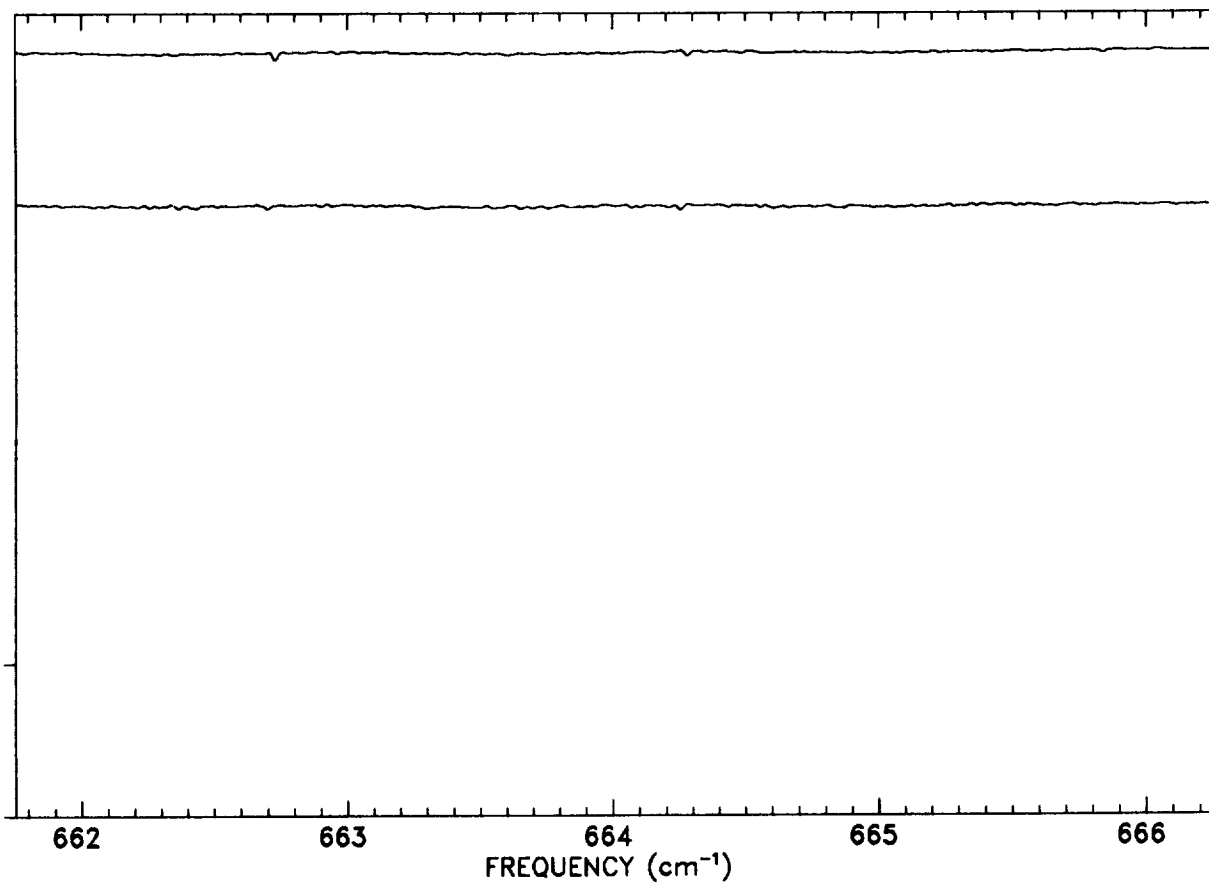
References

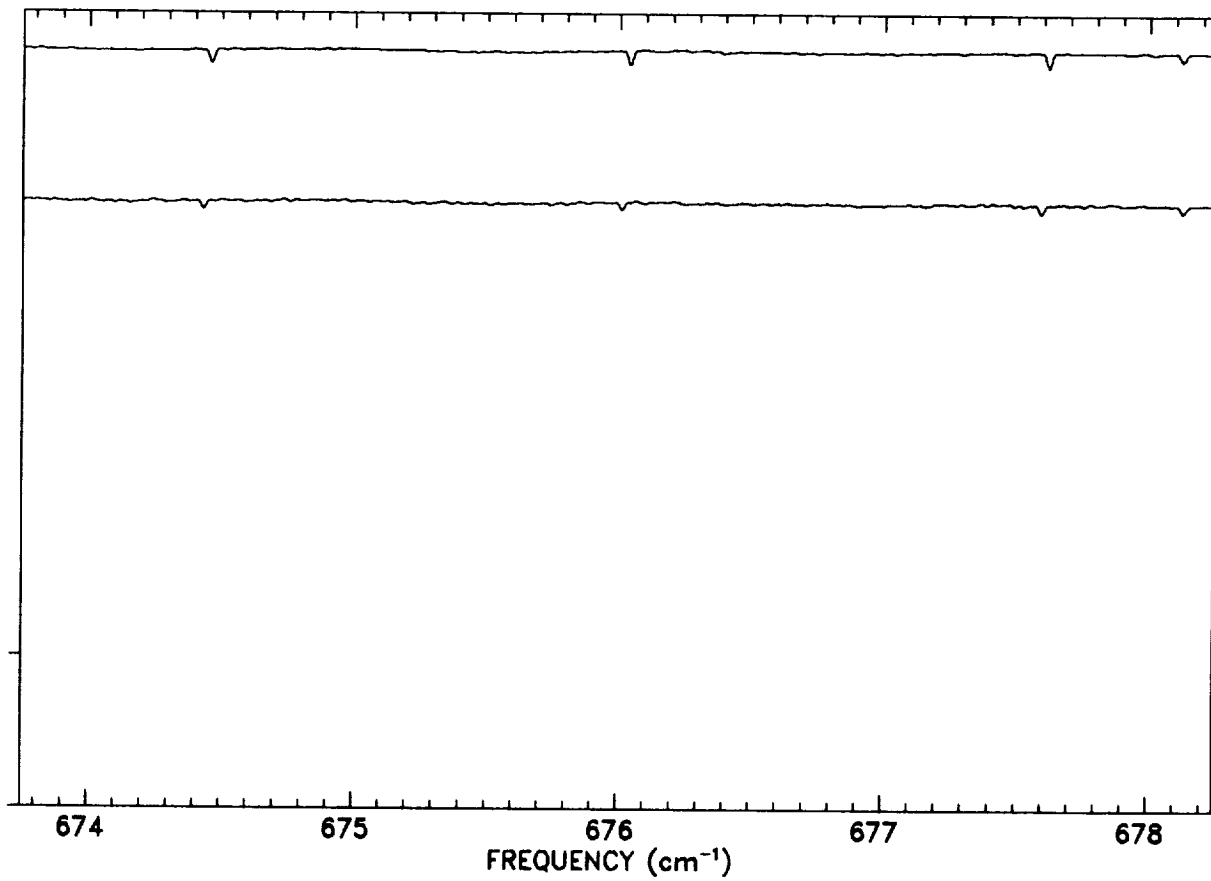
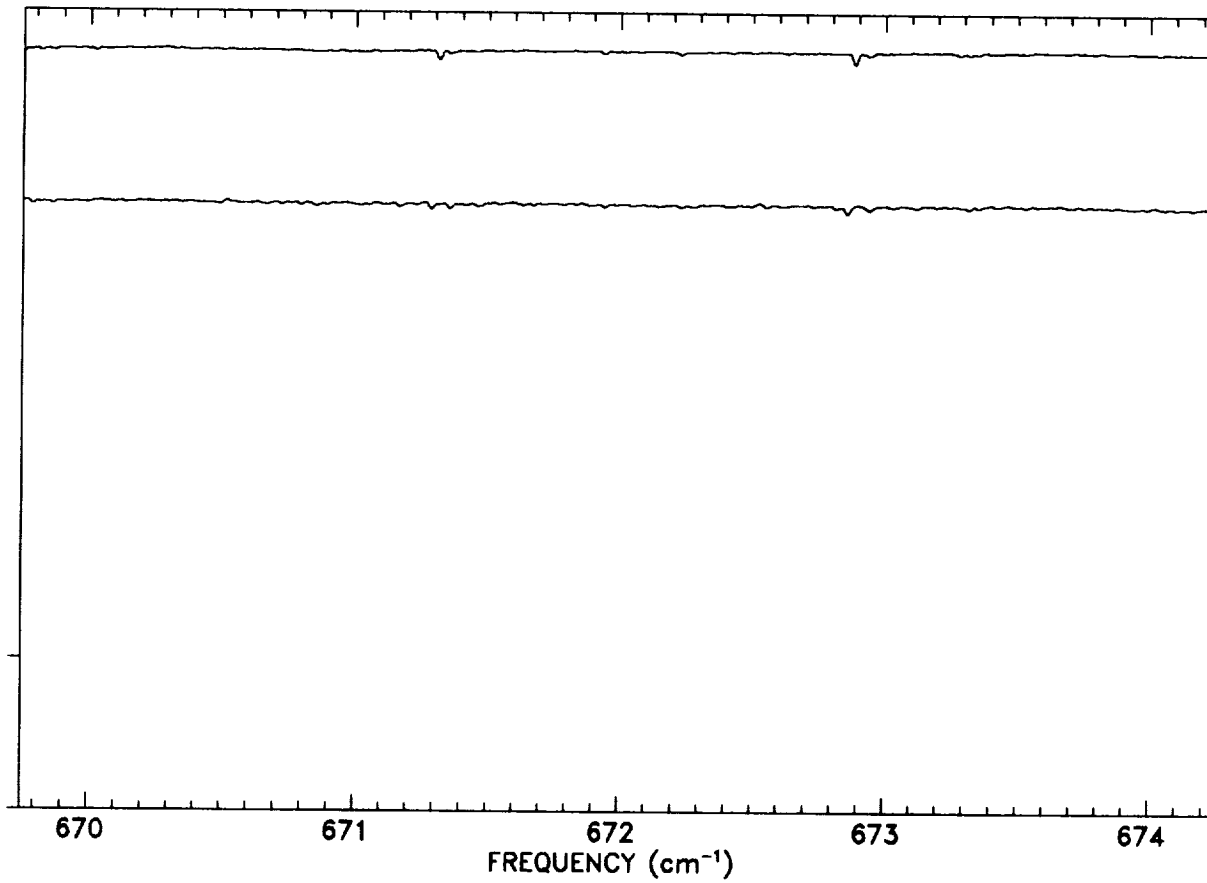
1. C.B. Farmer, O.F. Raper, and F.G. O'Callaghan, *Final Report on the First Flight of the ATMOS Instrument During the Spacelab-3 Mission, April 29 Through May 6, 1985*, JPL Publication 87-32, Jet Propulsion Laboratory, Pasadena, California, October 1, 1987.
2. C.B. Farmer, "High Resolution Infrared Spectroscopy of the Sun and the Earth's Atmosphere from Space," in *Proceedings of the 6th International Conference on Fourier Transform Spectroscopy* (G. Guelachvili, R. Kellner, and G. Zerbi, eds.), *Mikrochimica Acta (Wien)*, **1987, III**, 189–214, 1987.
3. P.G. Morse, "Progress Report on the ATMOS Sensor: Design Description and Development Status," *AIAA Sensor Systems Conference Proceedings*, Paper No. 80-1914-CP, 1980.
4. R. Beer and R.H. Norton, "New Apodizing Functions for Fourier Spectrometry," *J. Opt. Soc. Am.*, **66**, 3, 259–264, 1976.
5. L. Brown, C.B. Farmer, C.P. Rinsland, and R.A. Toth, "Molecular Line Parameters for the Atmospheric Trace Molecule Spectroscopy Experiment," *Appl. Optics*, **26**, 23, 5154–5182, 1987.
6. F. Bartoli, R. Allen, L. Esterowitz, and M. Kruer, "Auger-Limited Carrier Lifetimes in HgCdTe at High Excess Carrier Concentrations," *J. Appl. Phys.*, **45**, 2150–2154, 1974.
7. G.C. Toon, to be published.

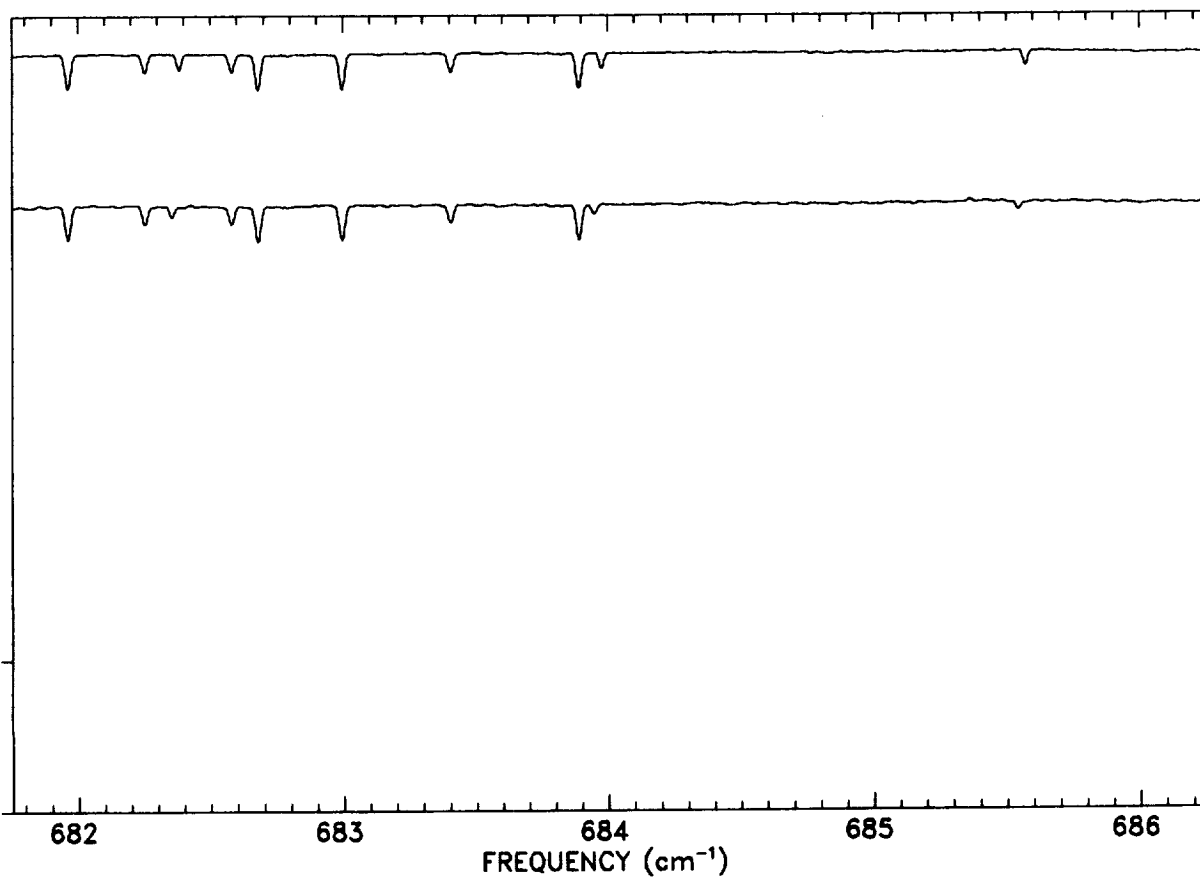
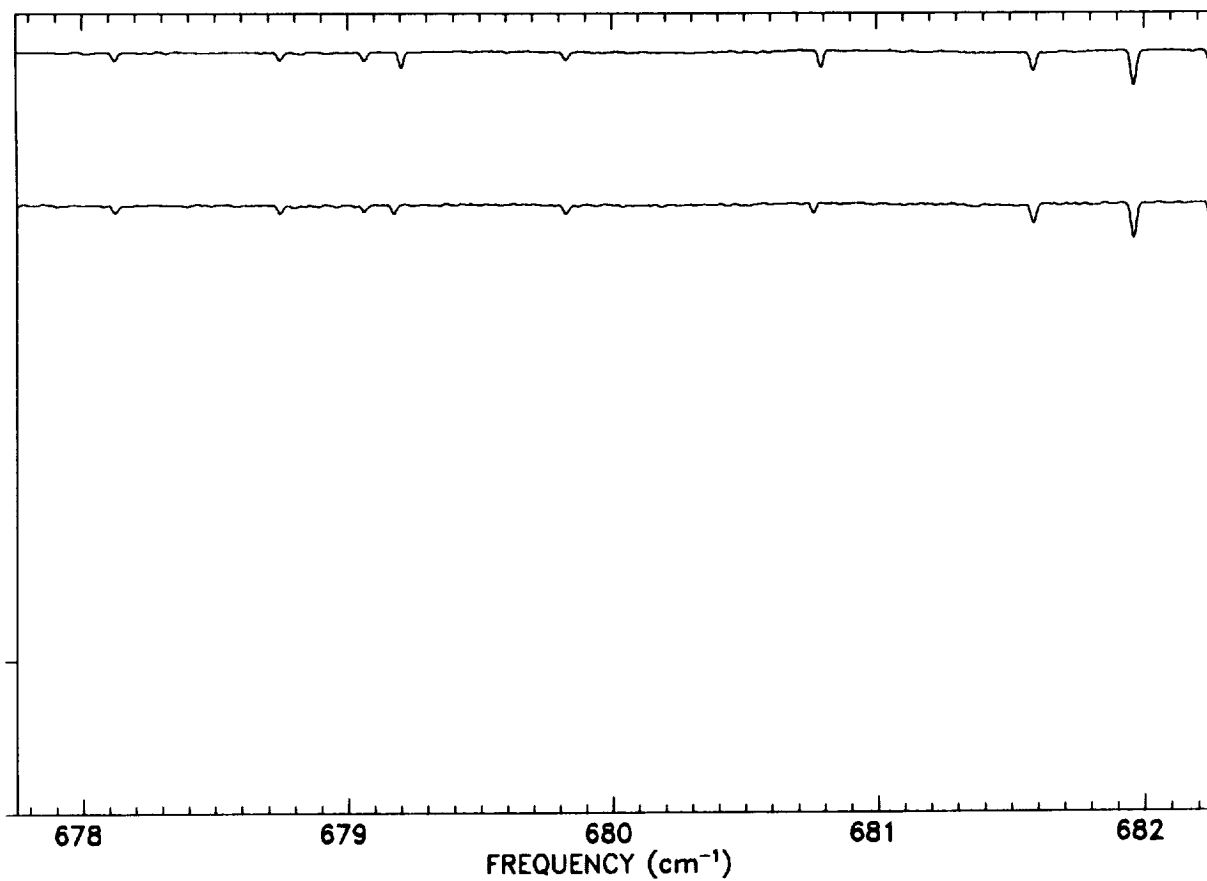
PRECEDING PAGE BLANK NOT FILMED

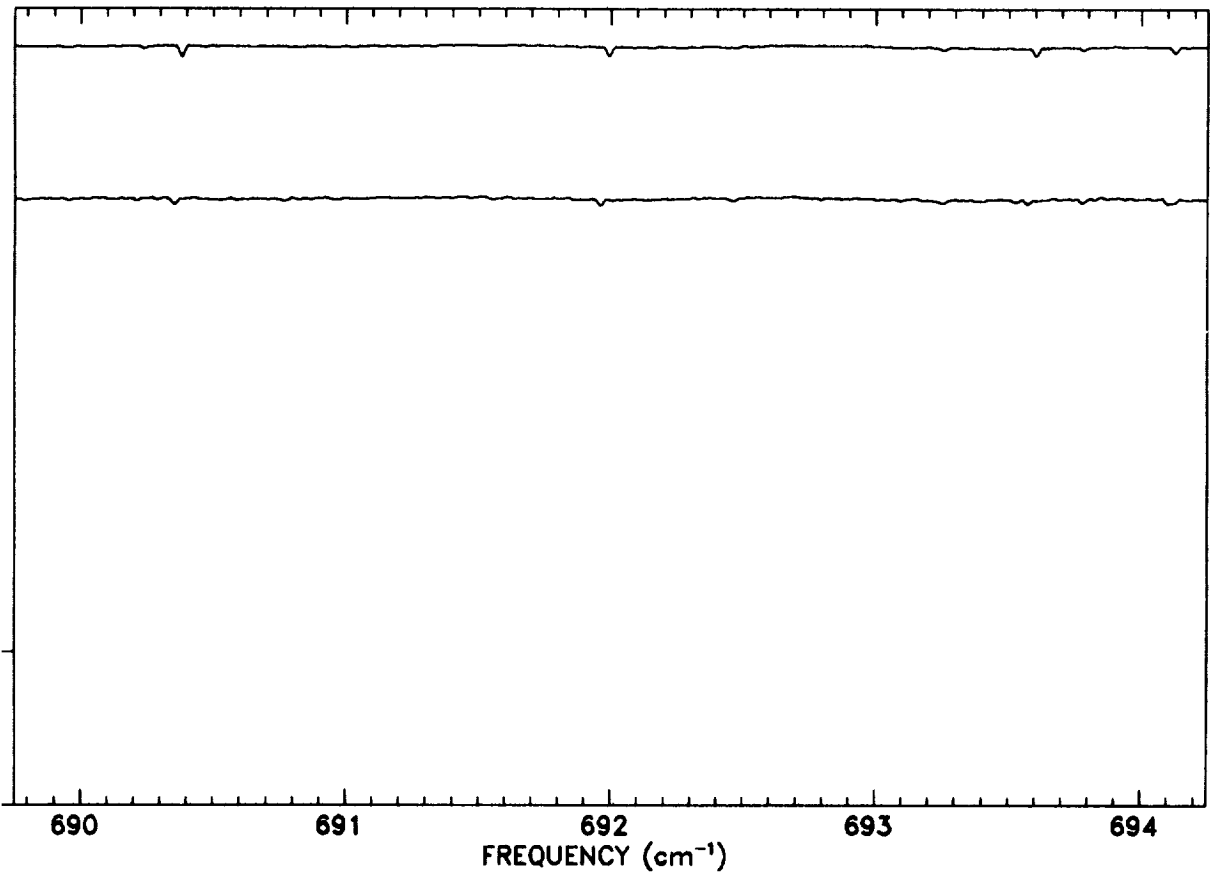
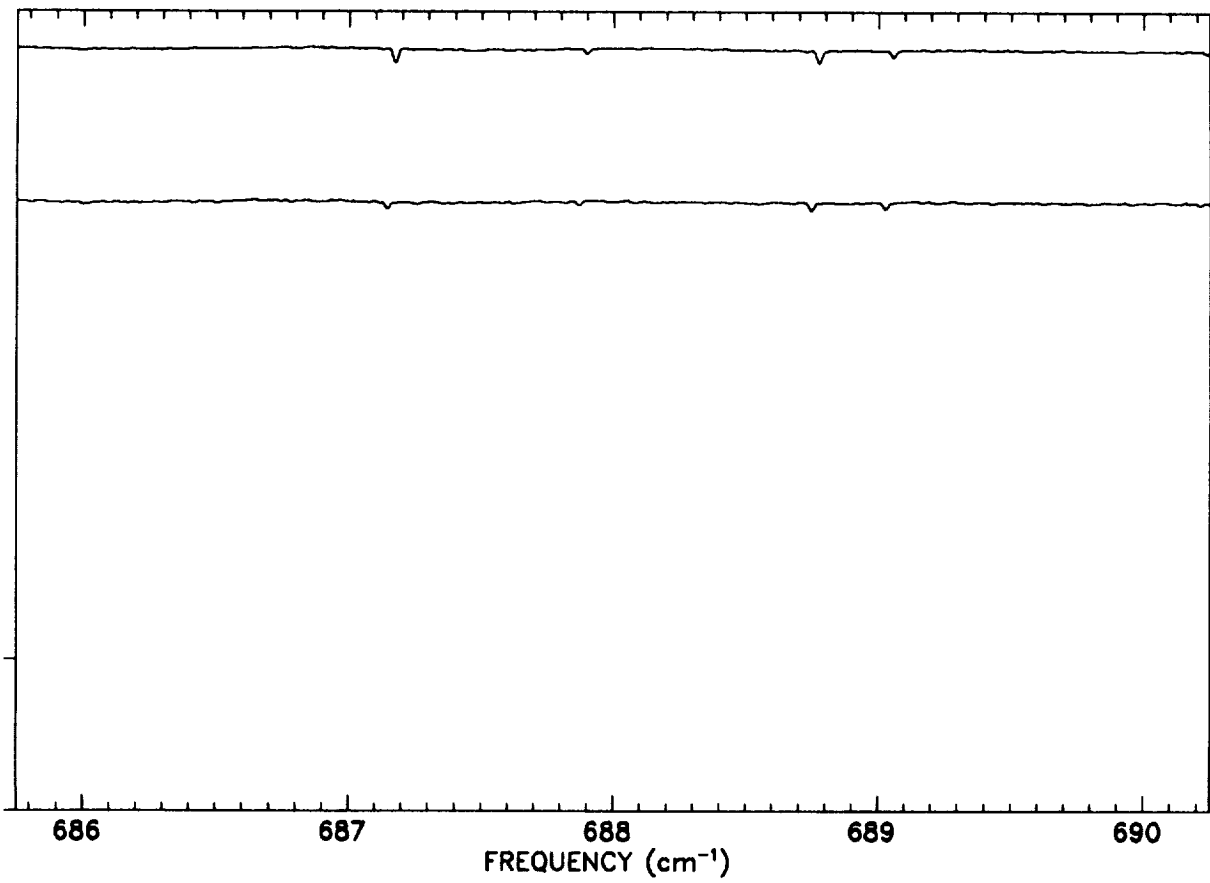


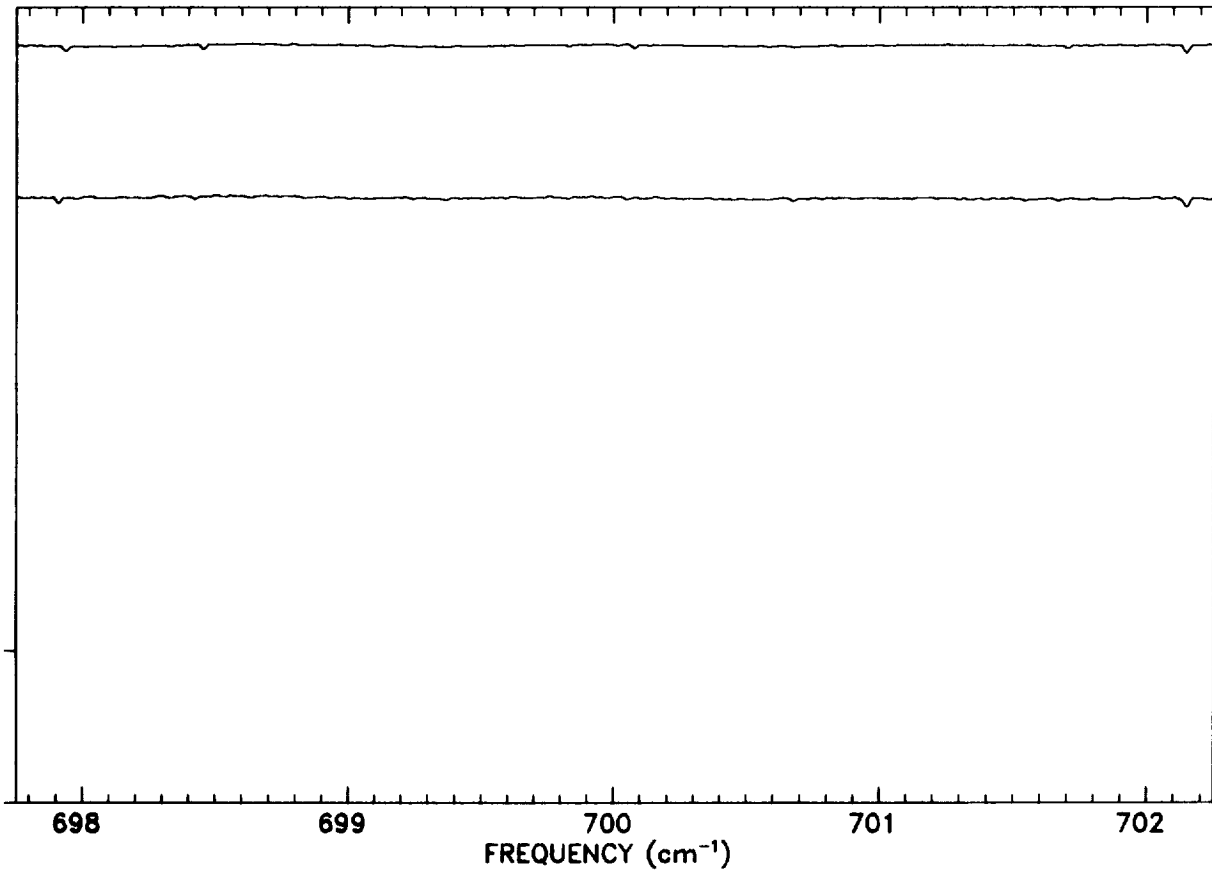
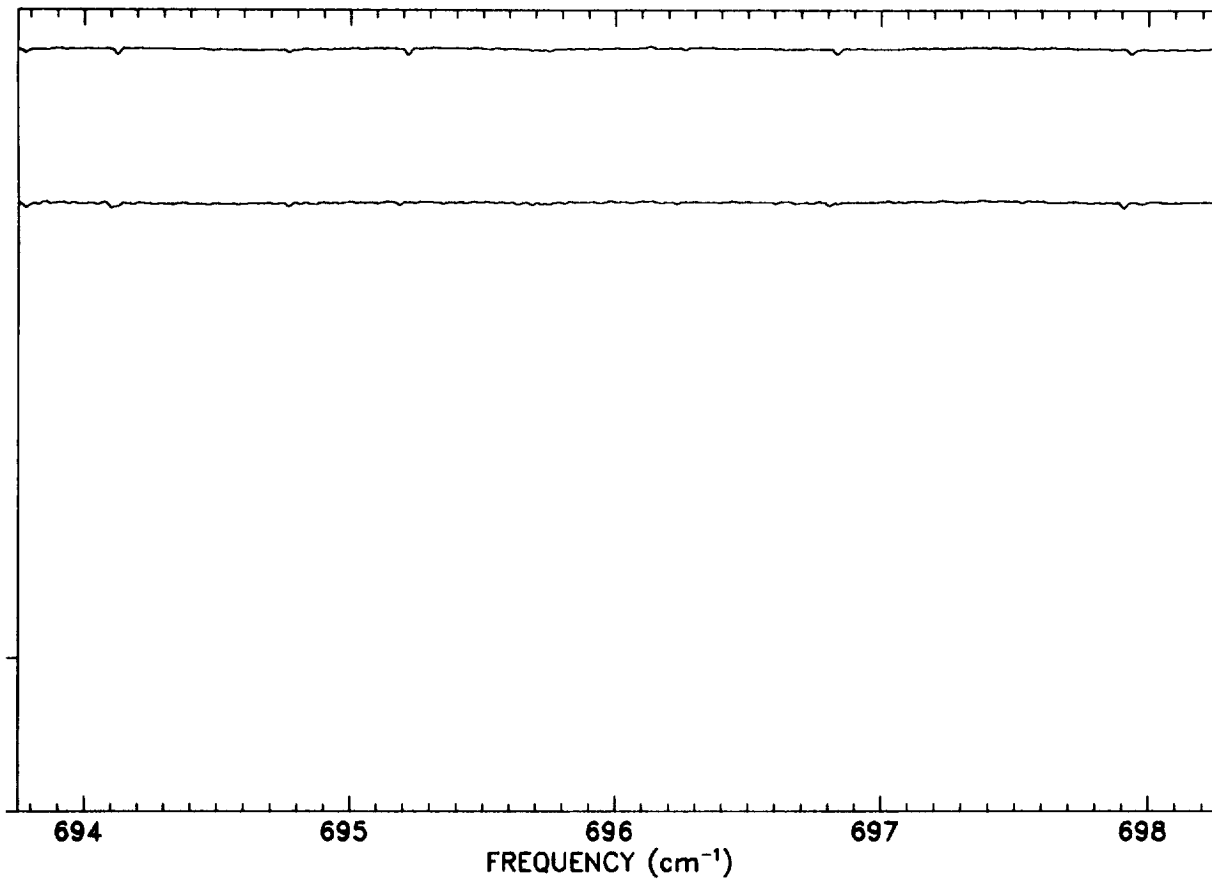


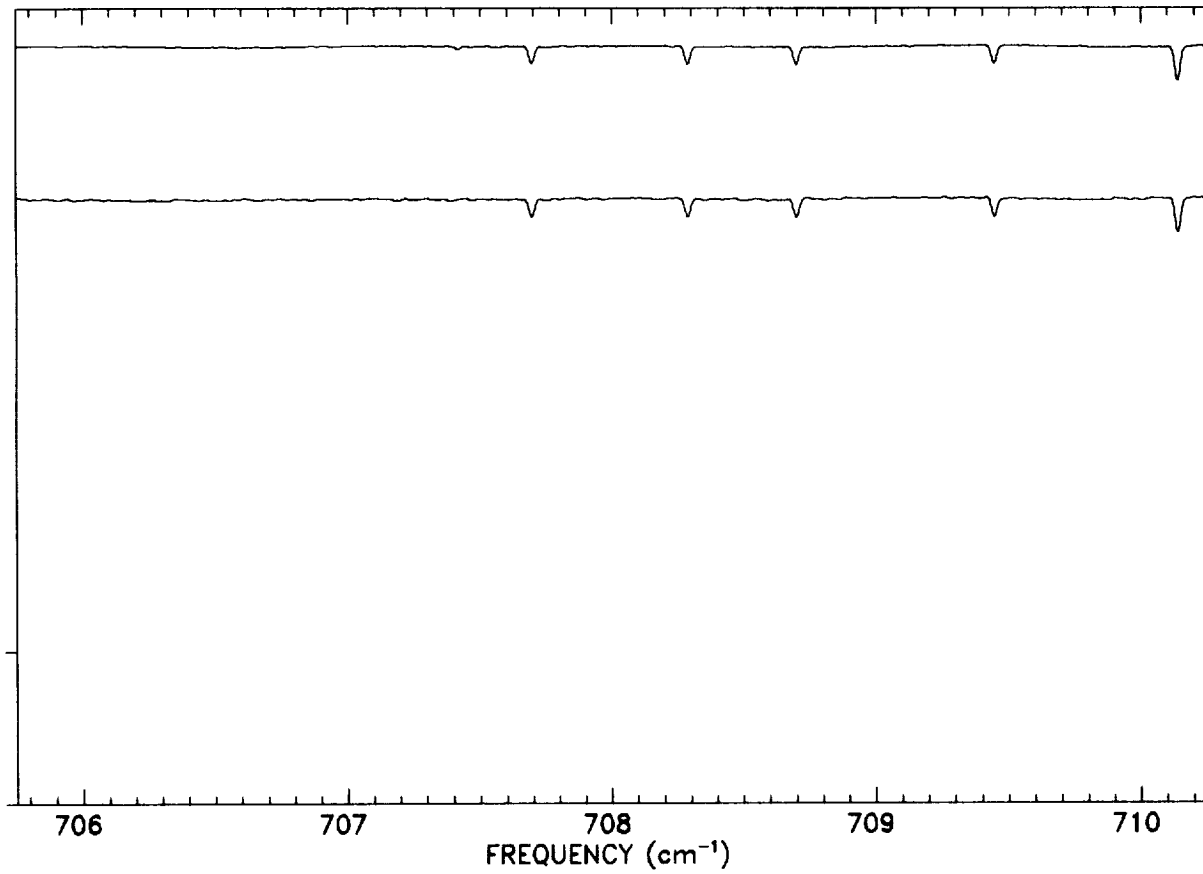
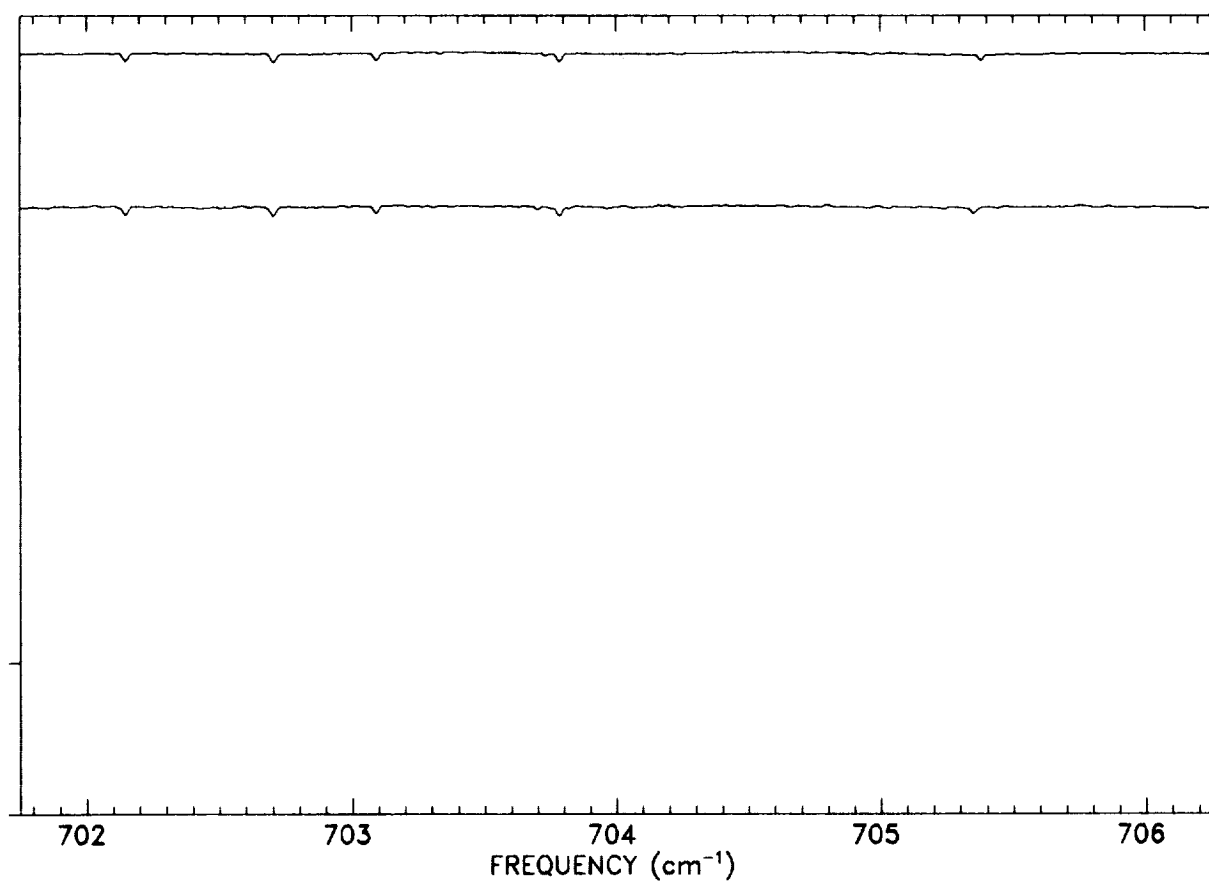


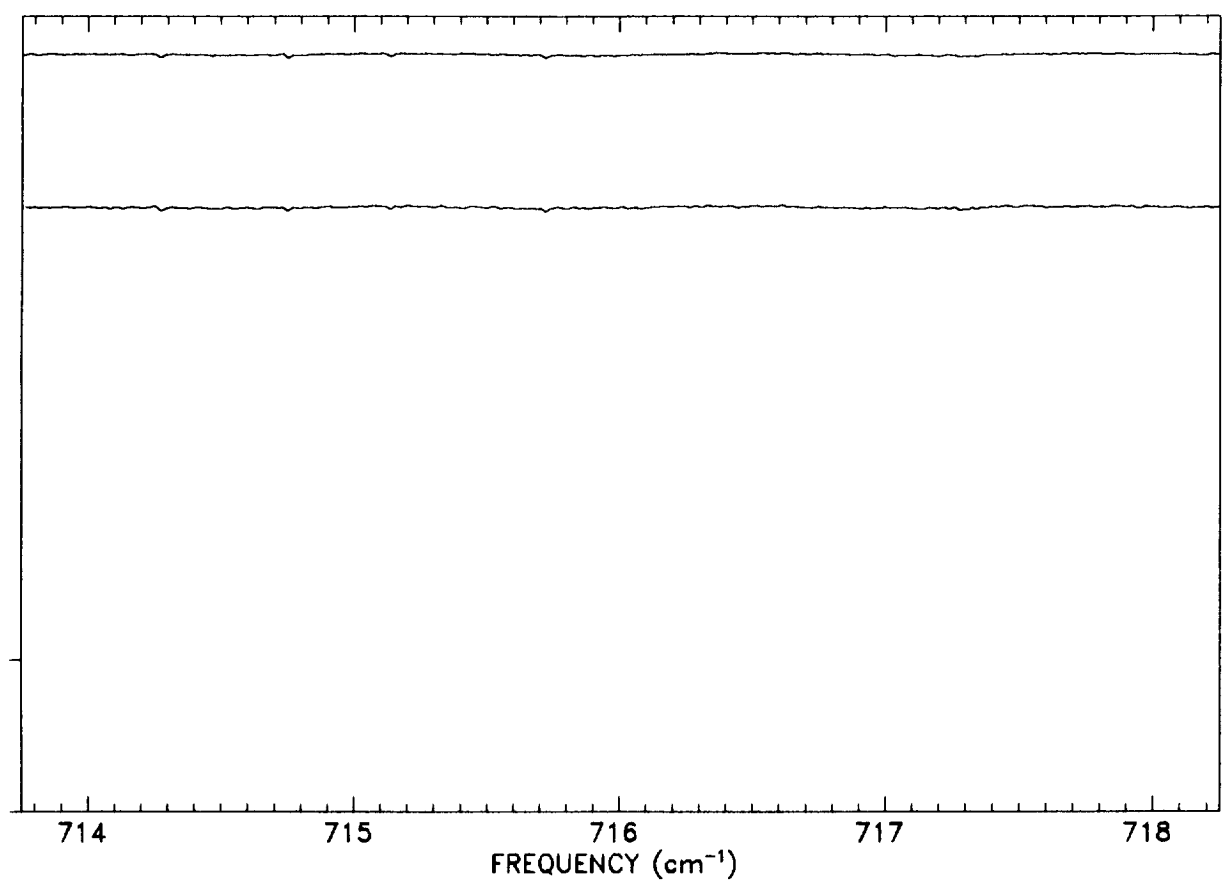
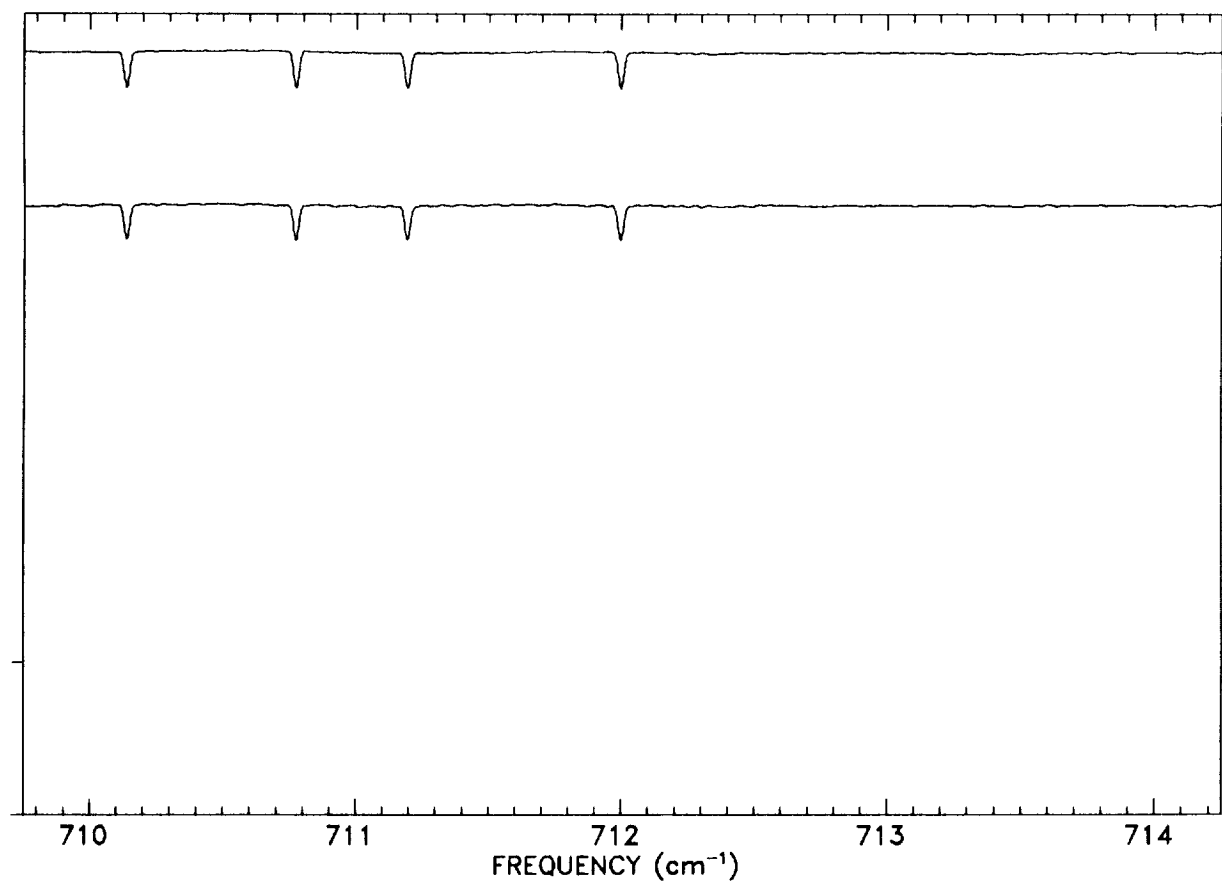


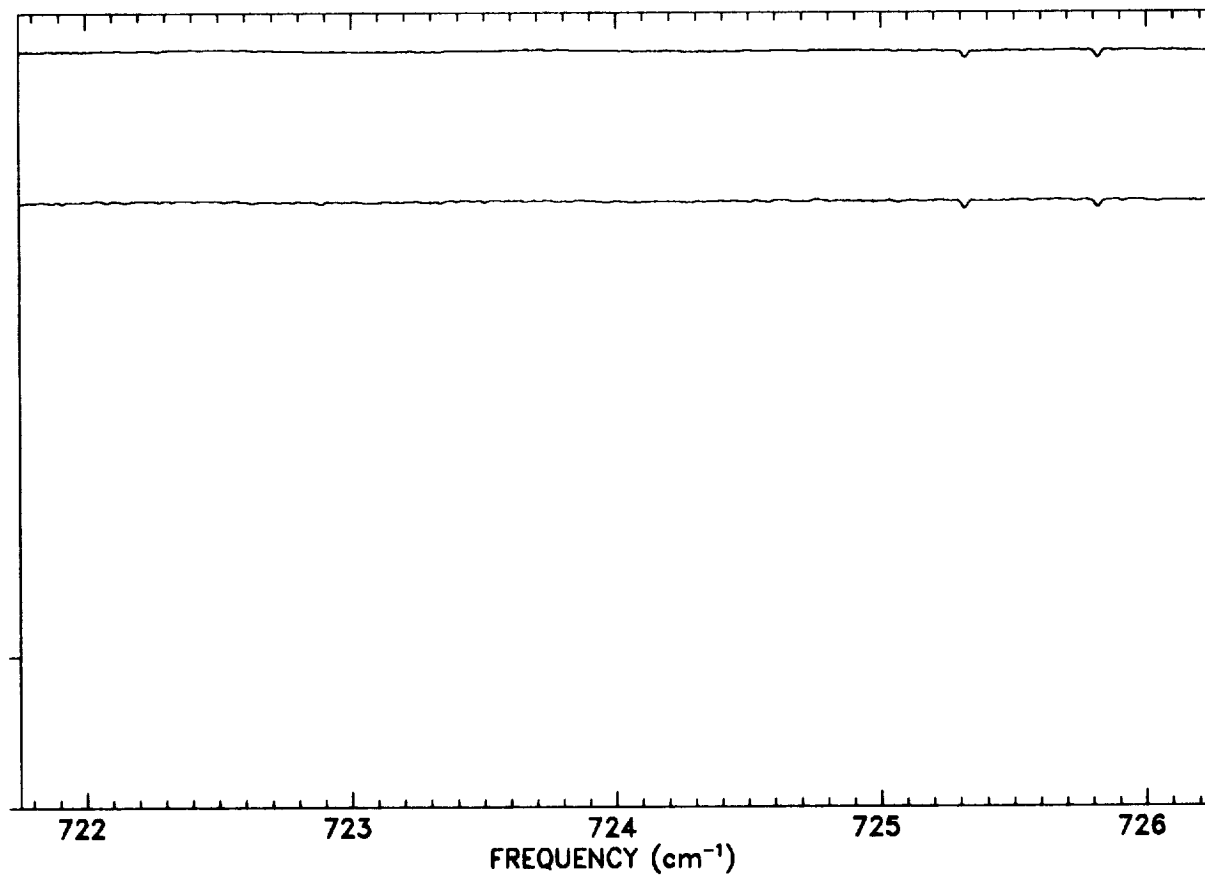
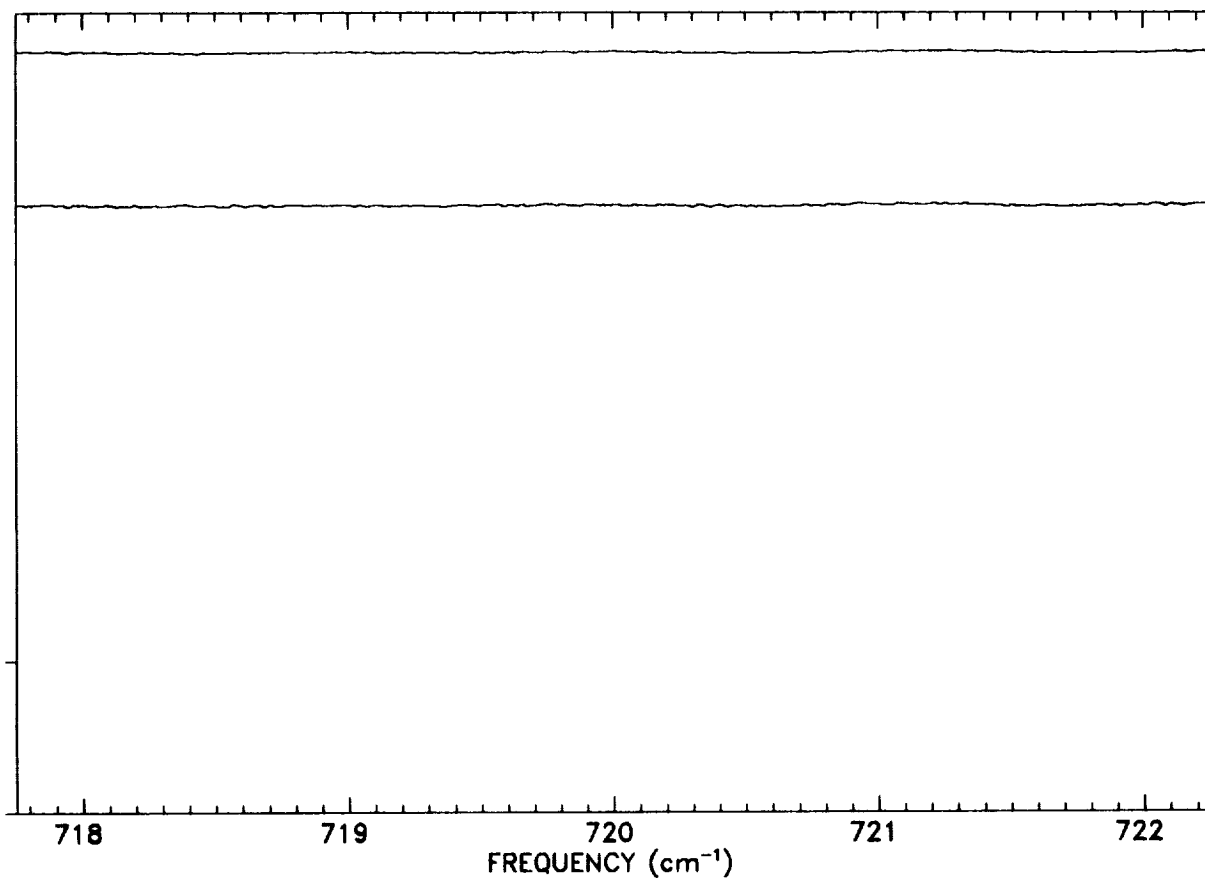


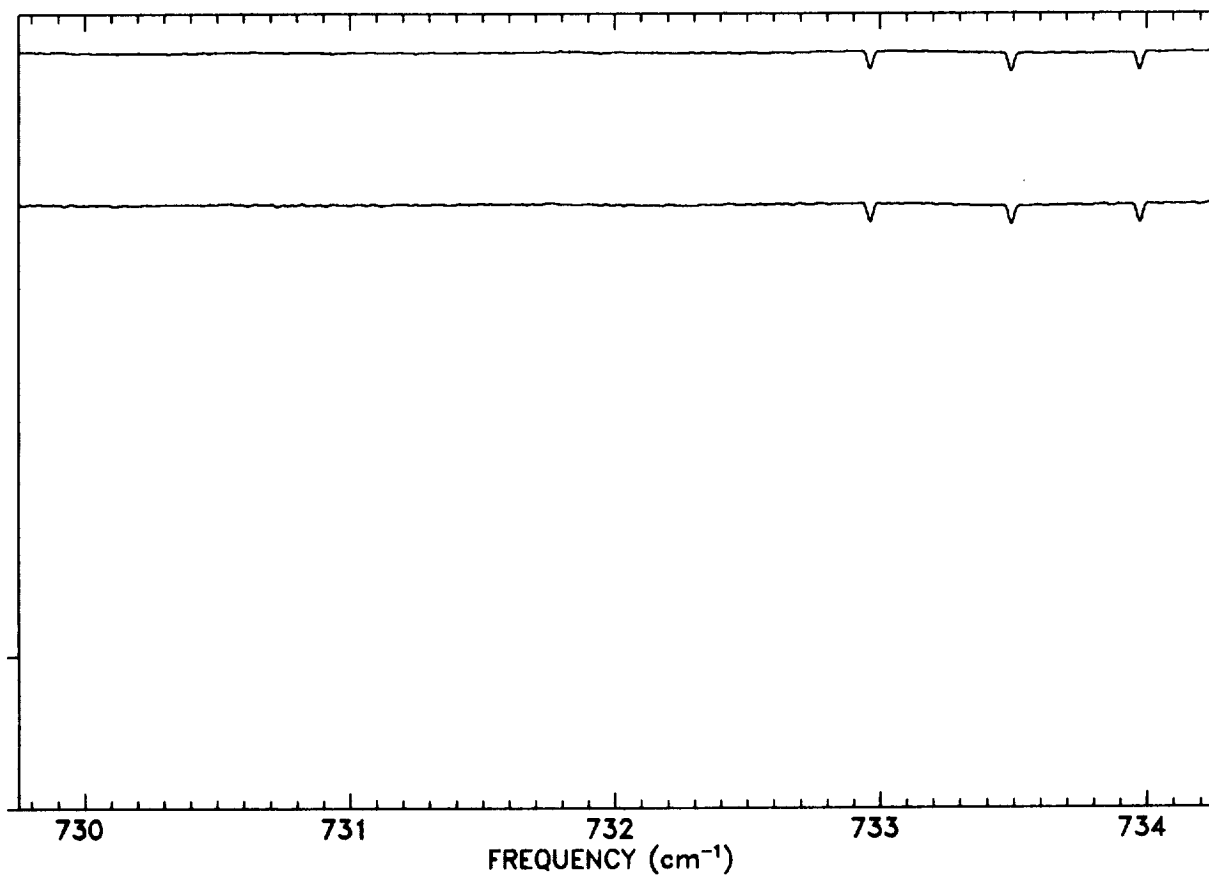
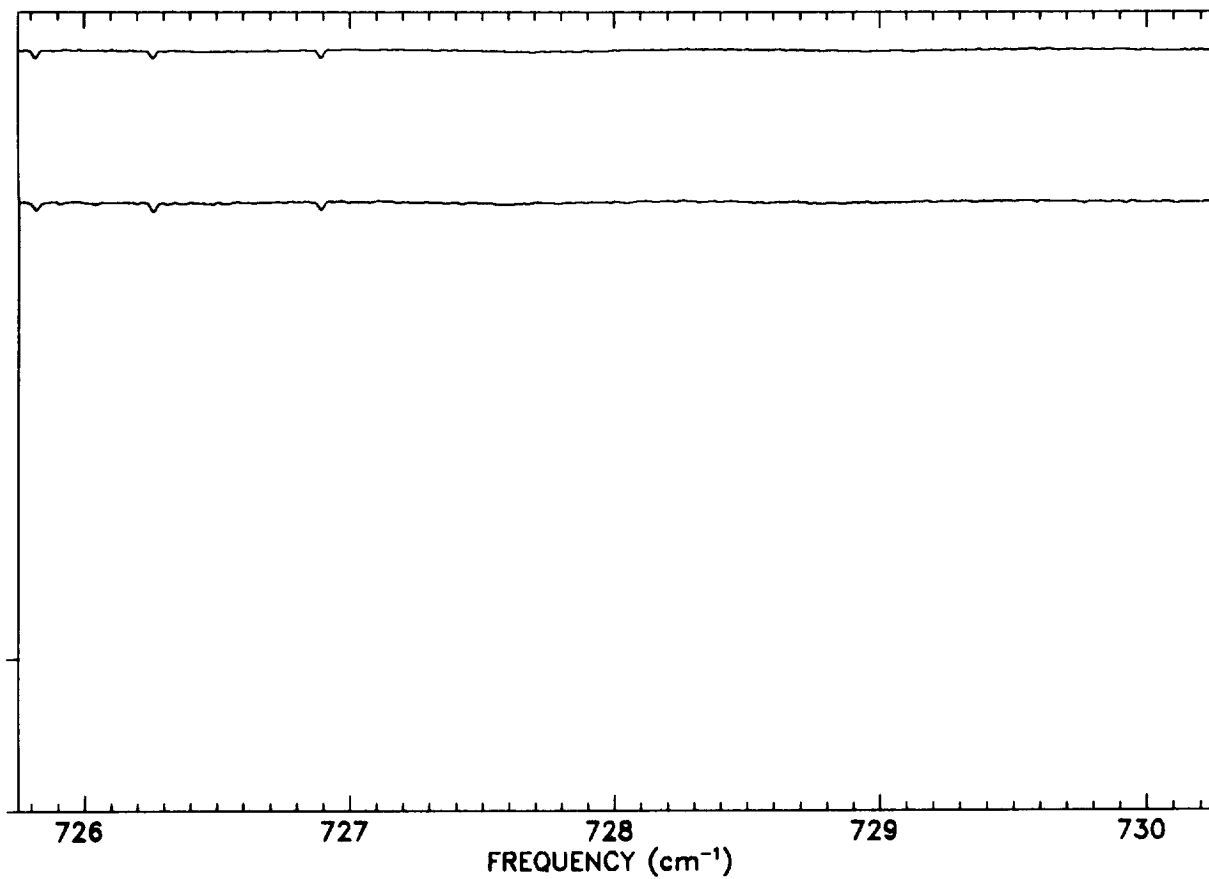


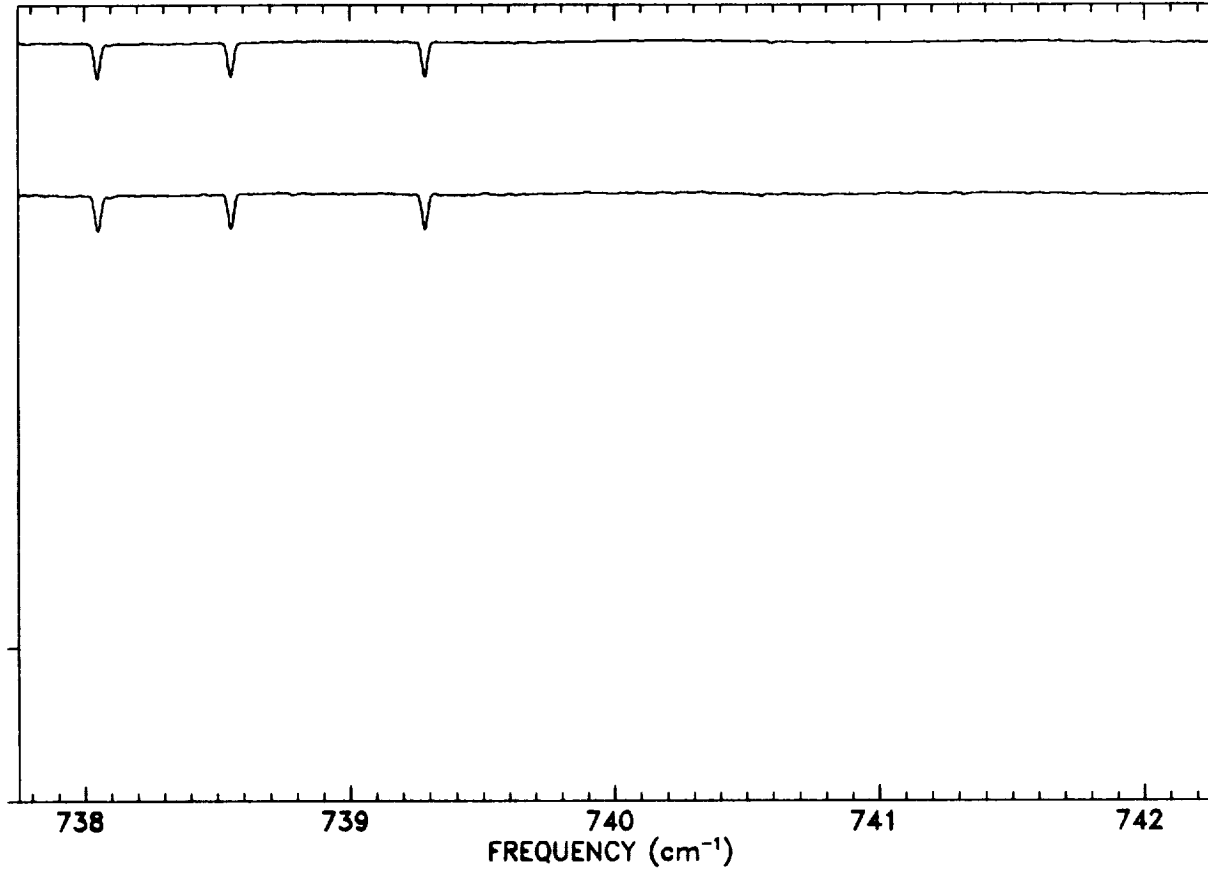
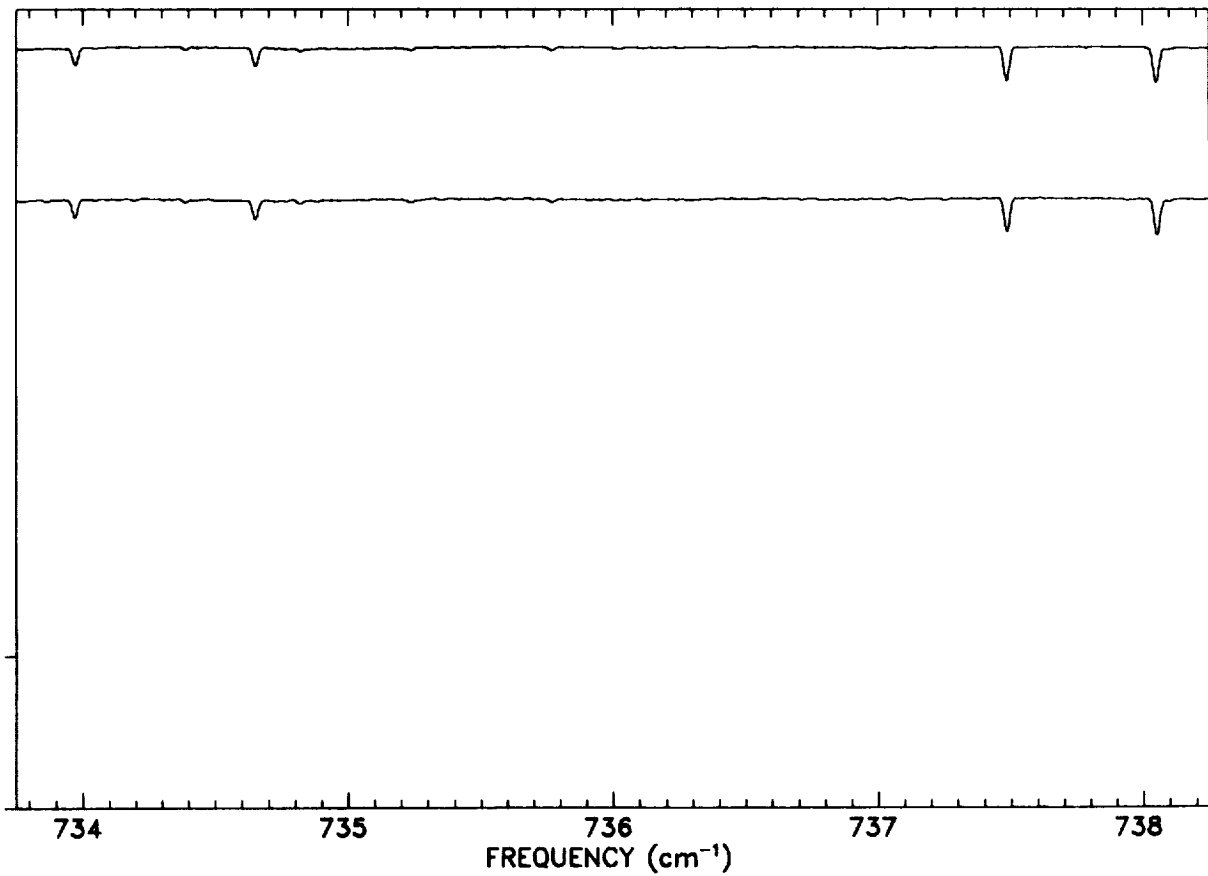


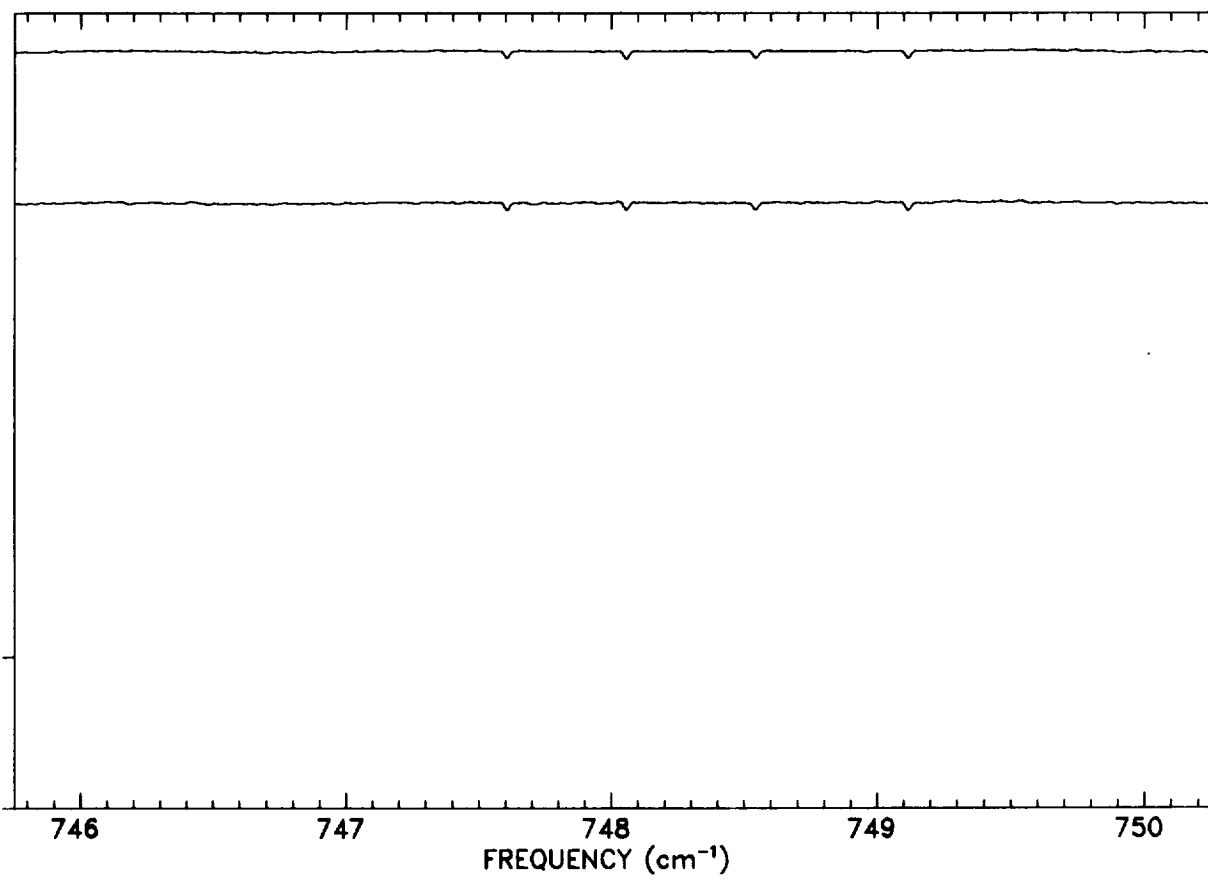
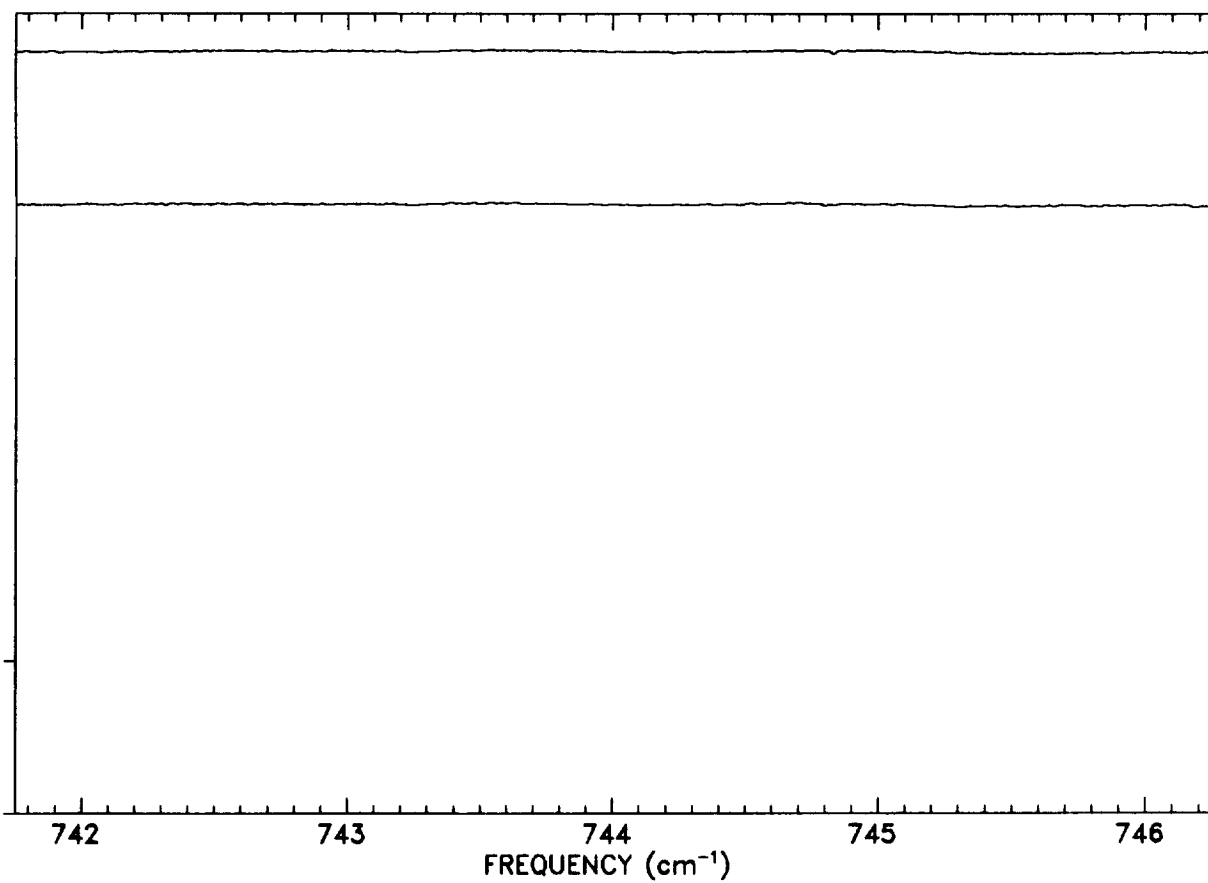


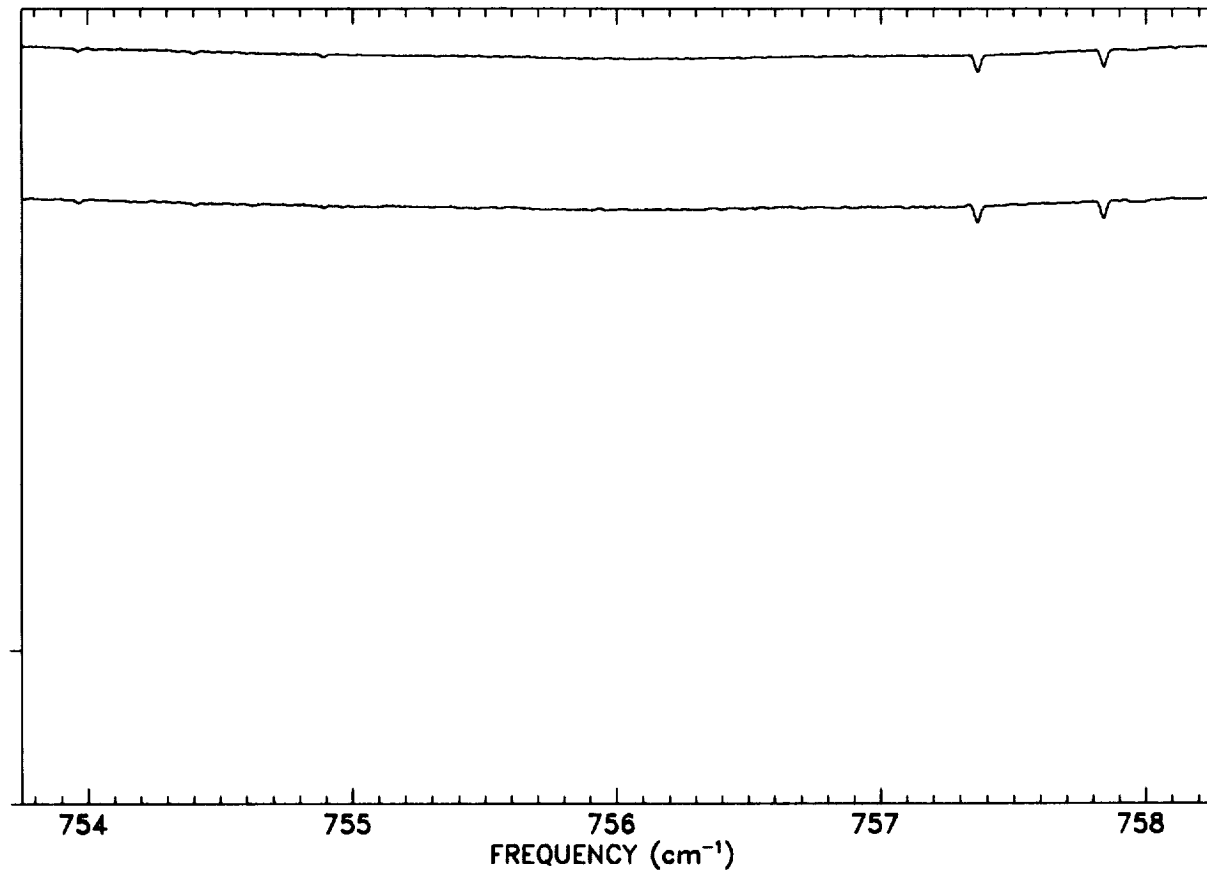
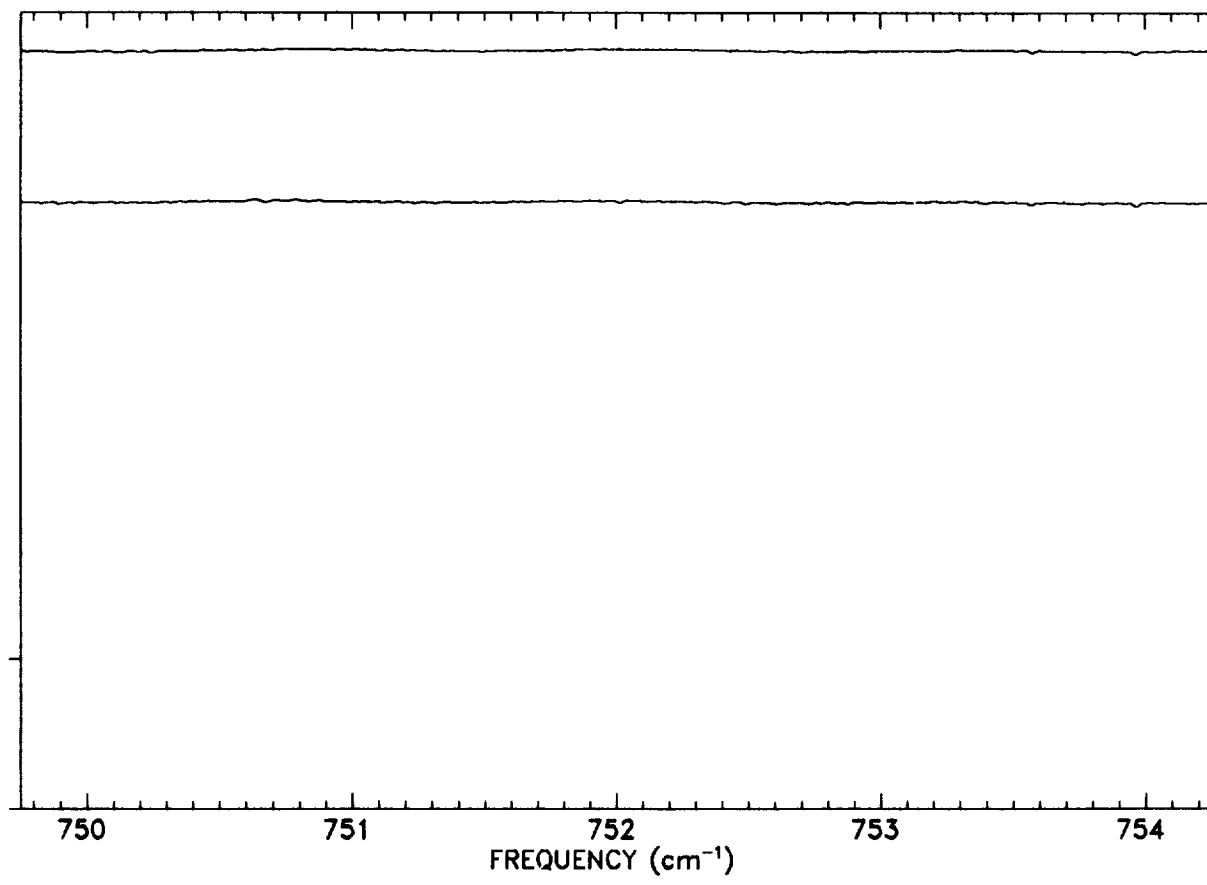


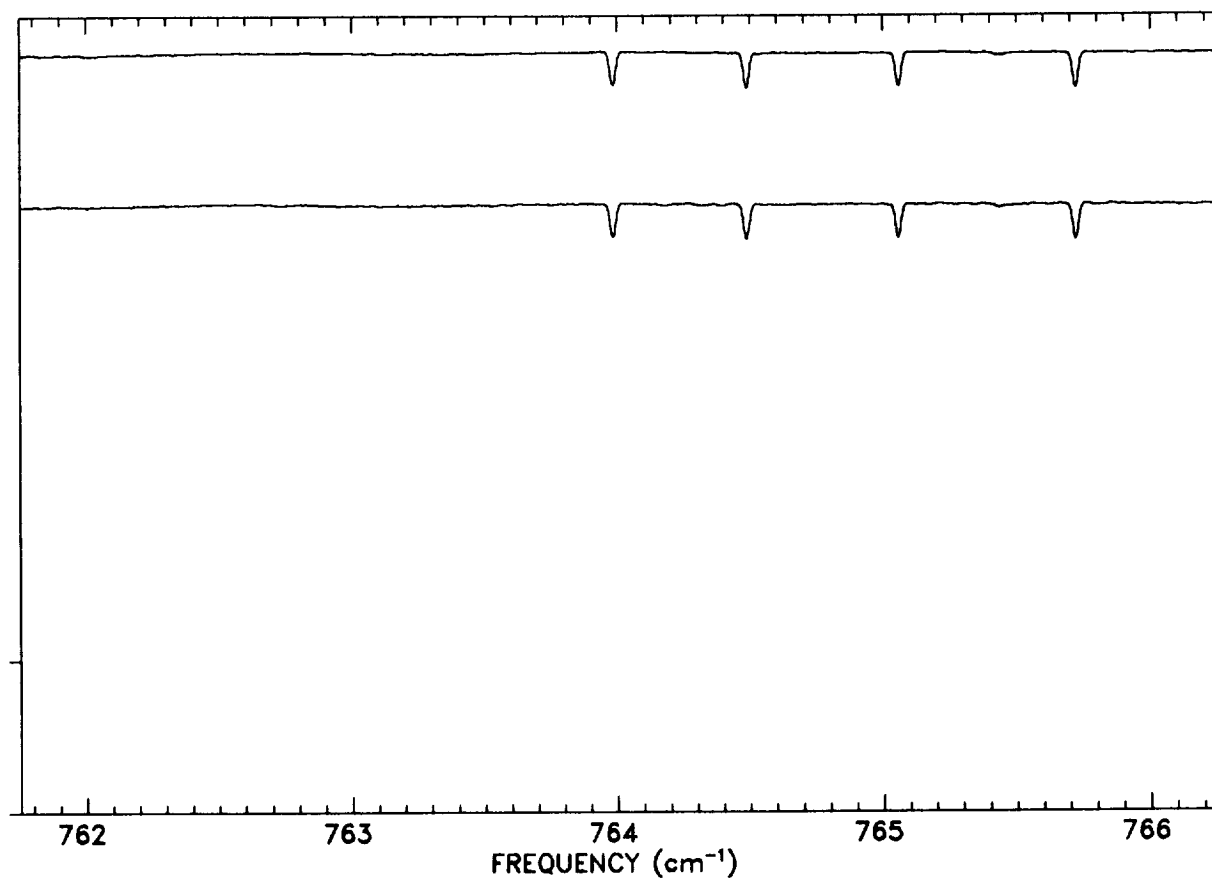
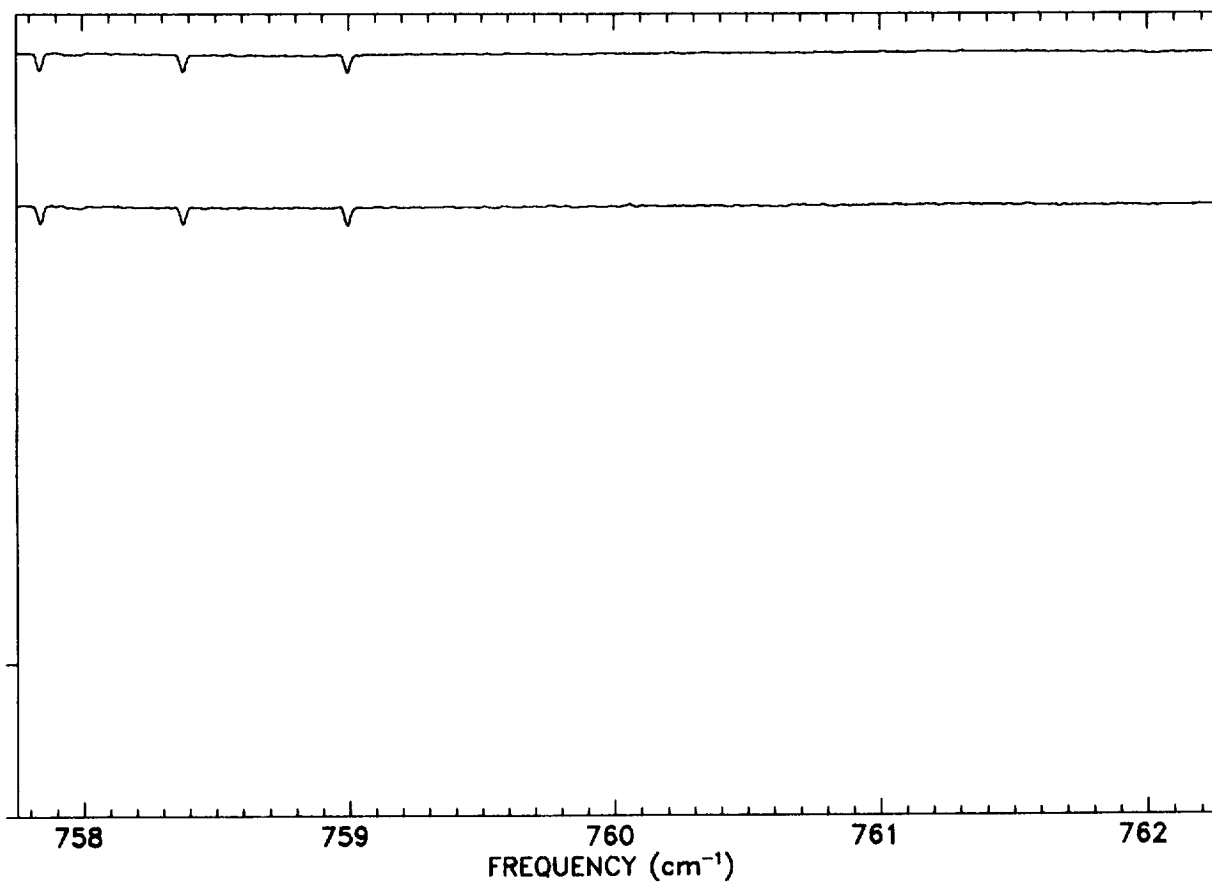


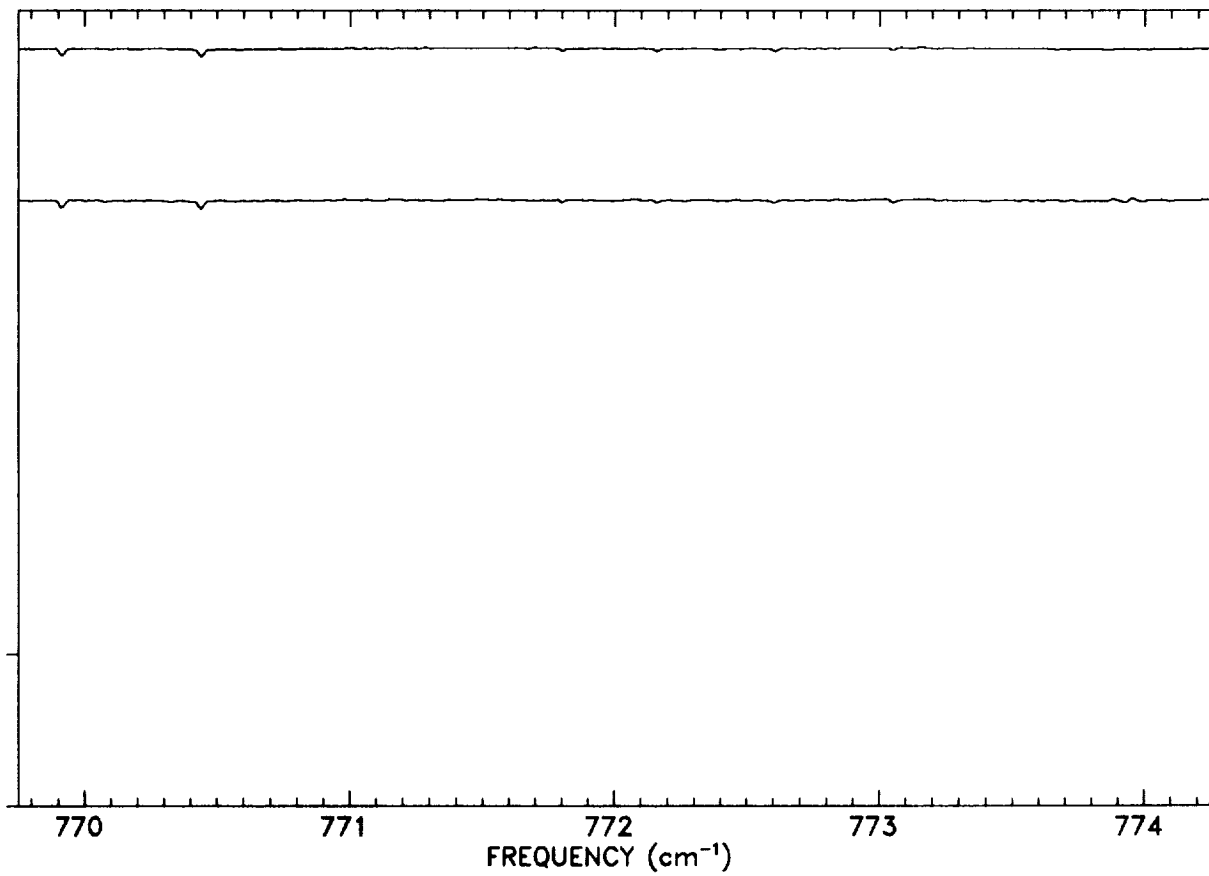
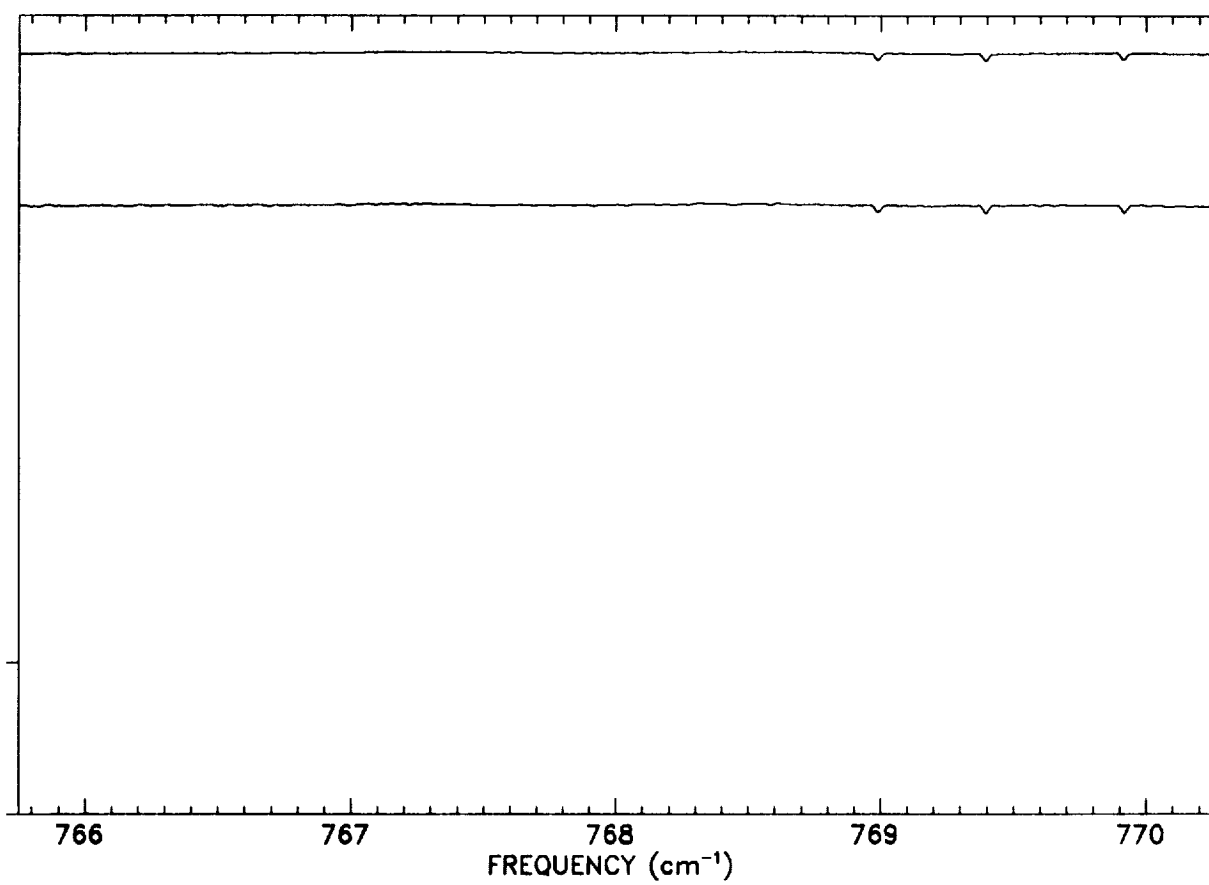


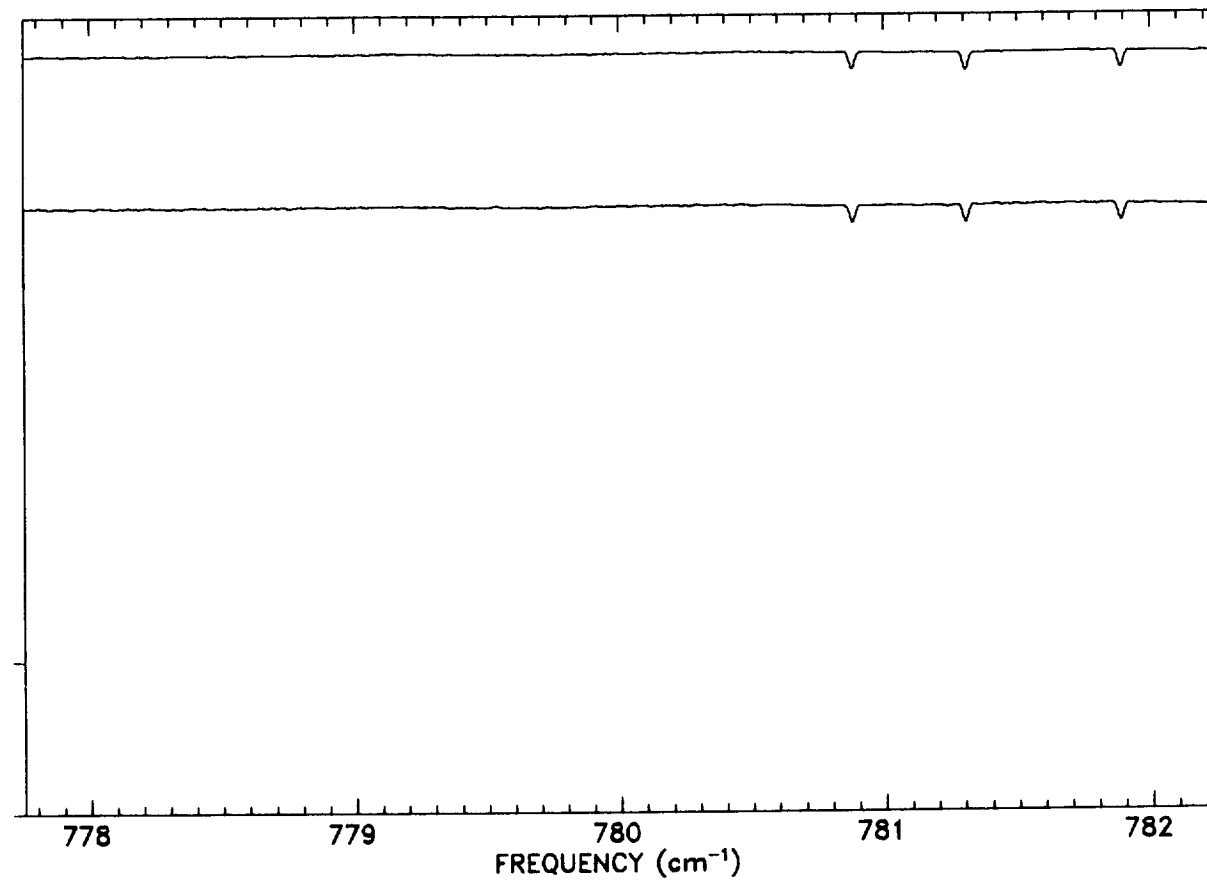
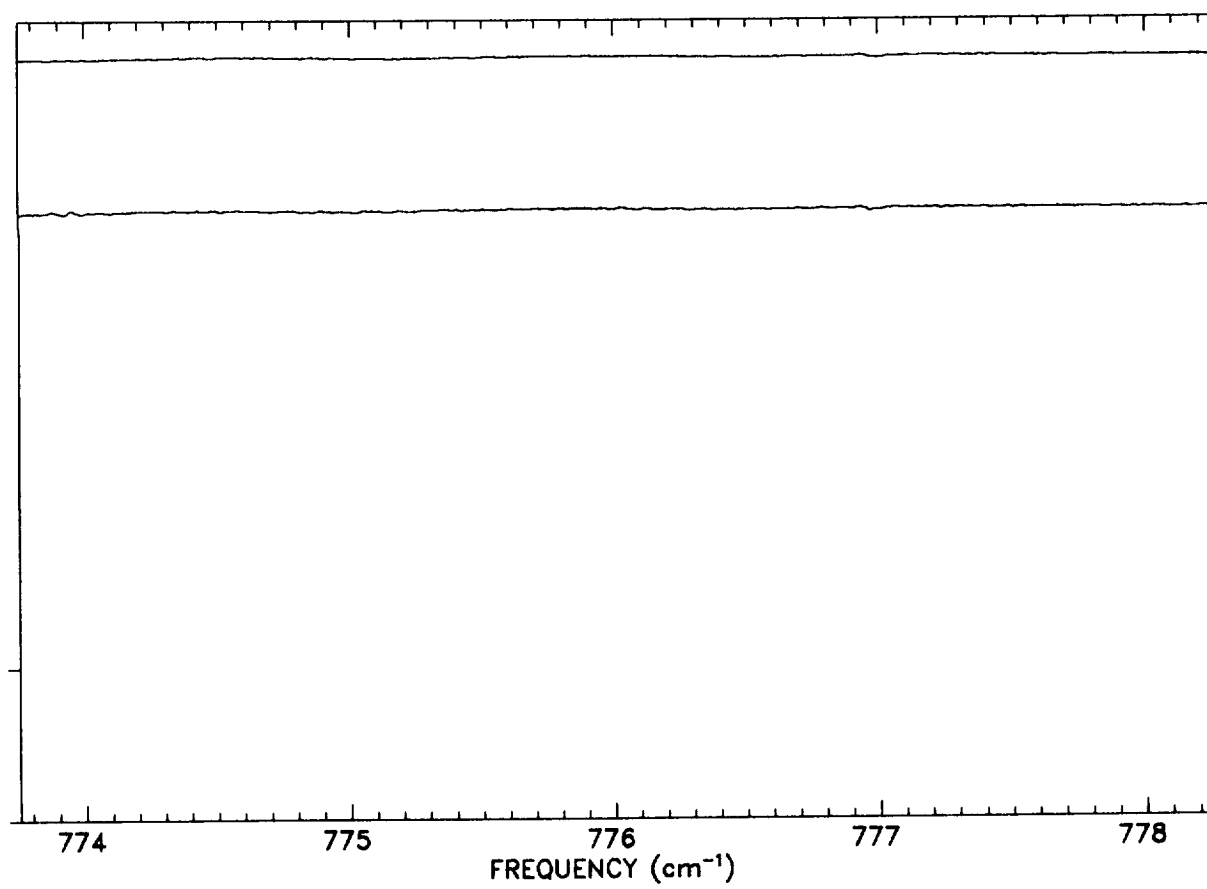


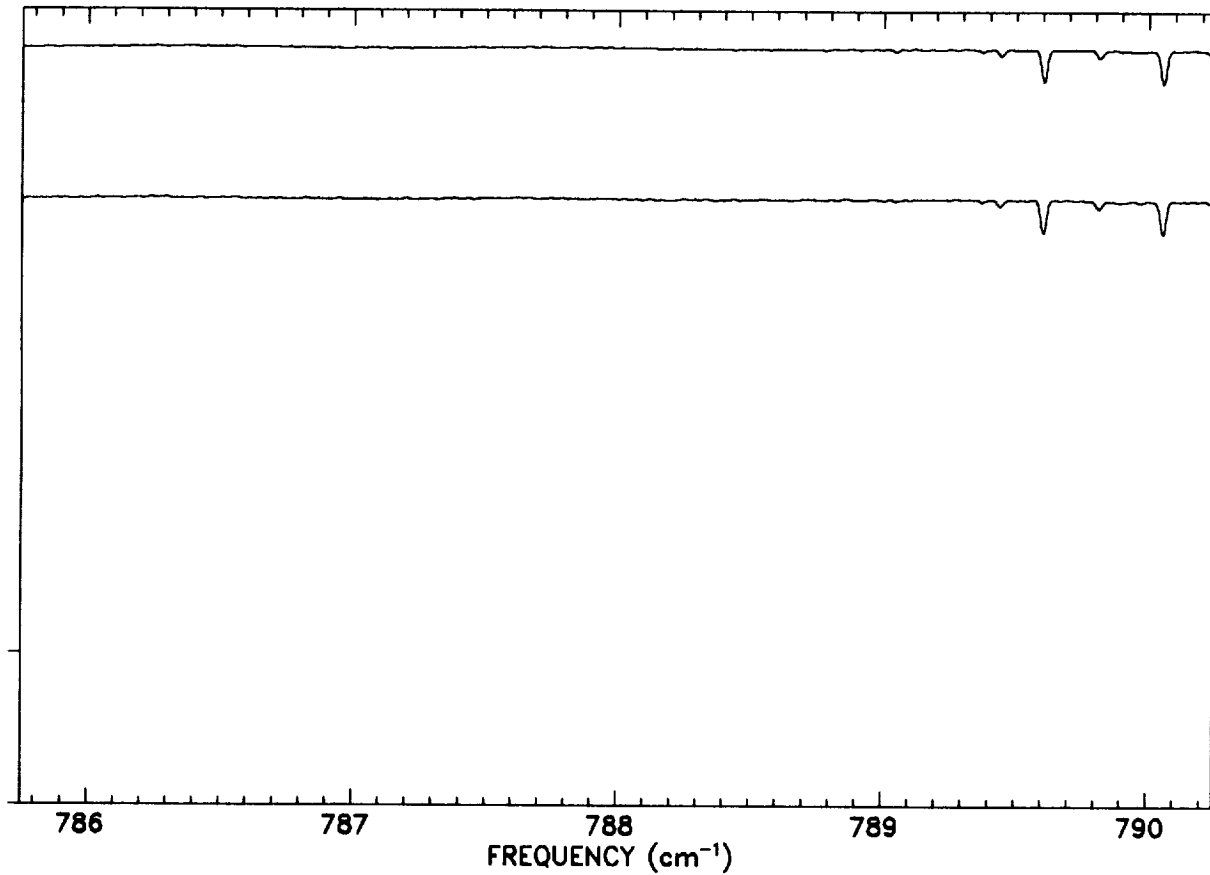
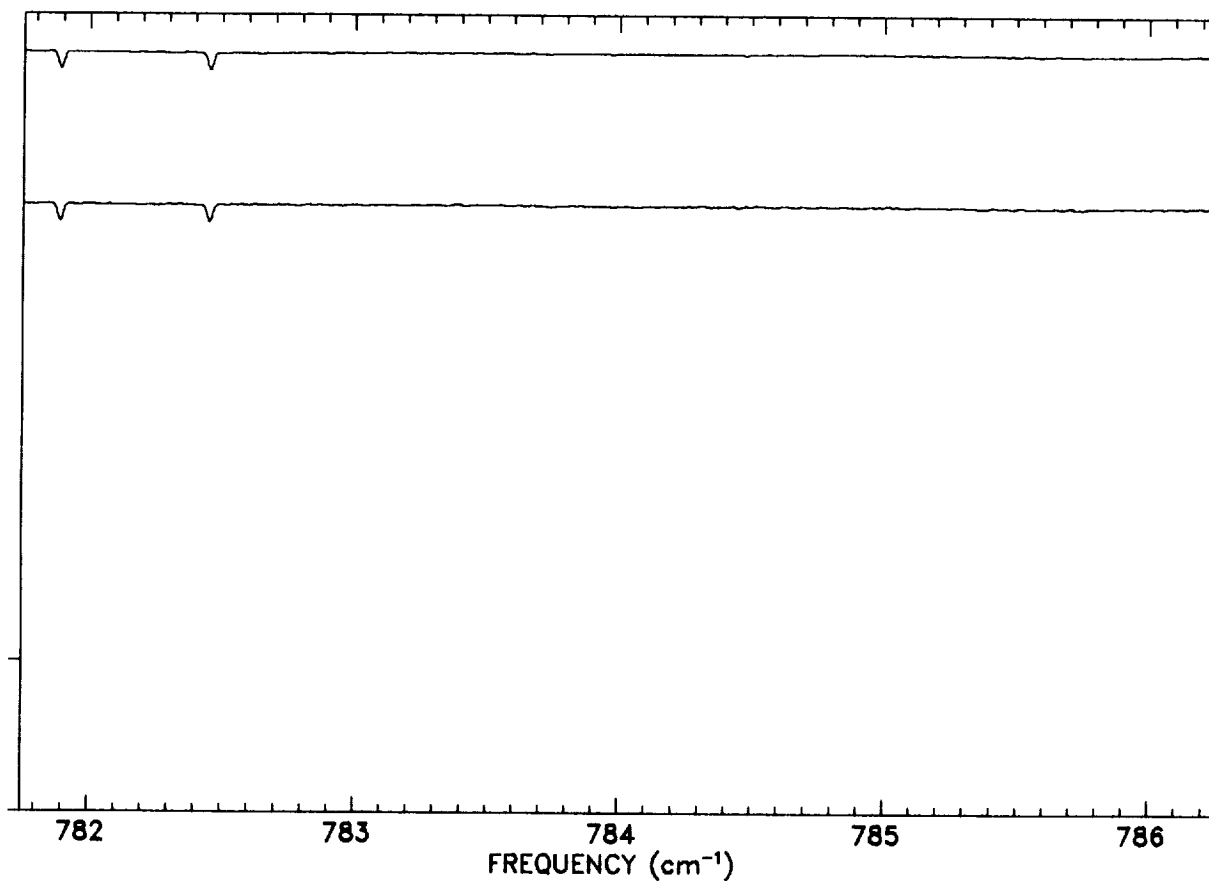


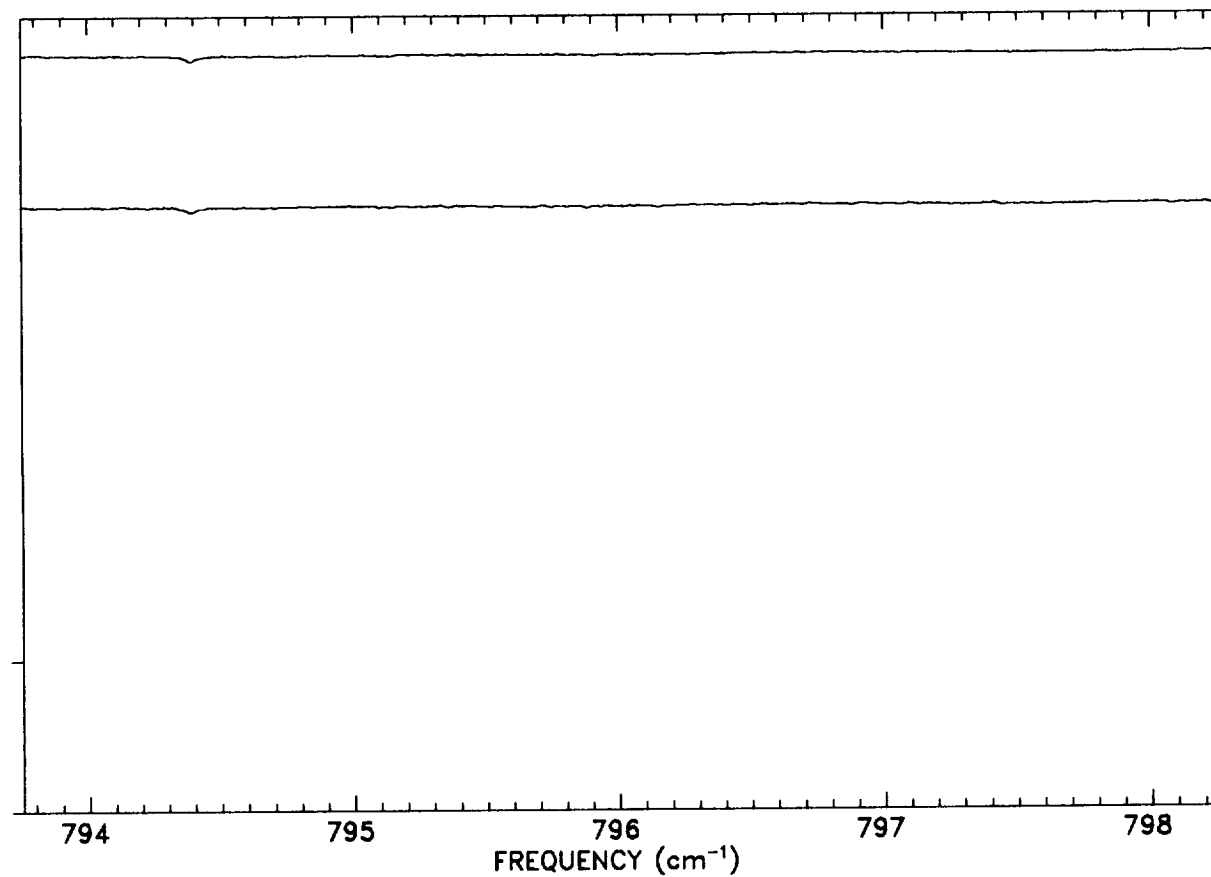
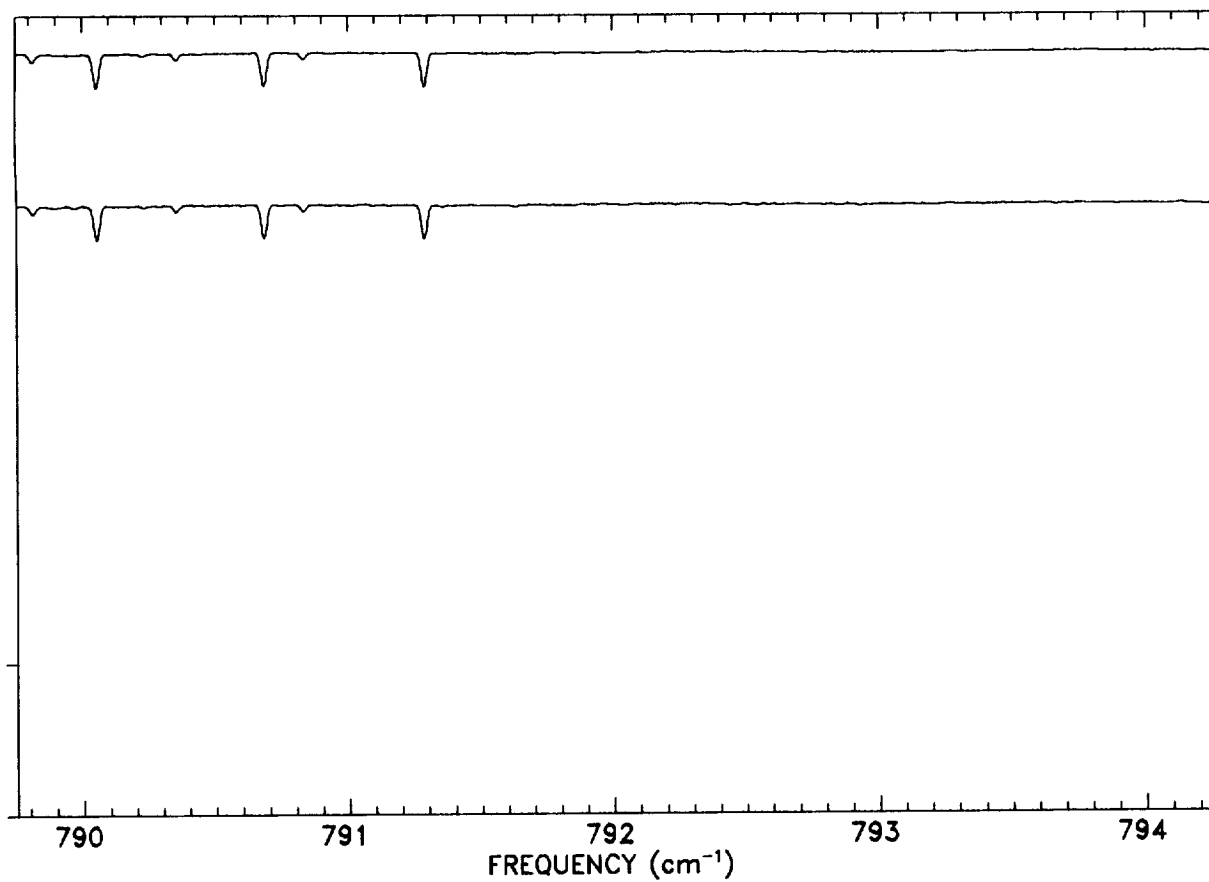


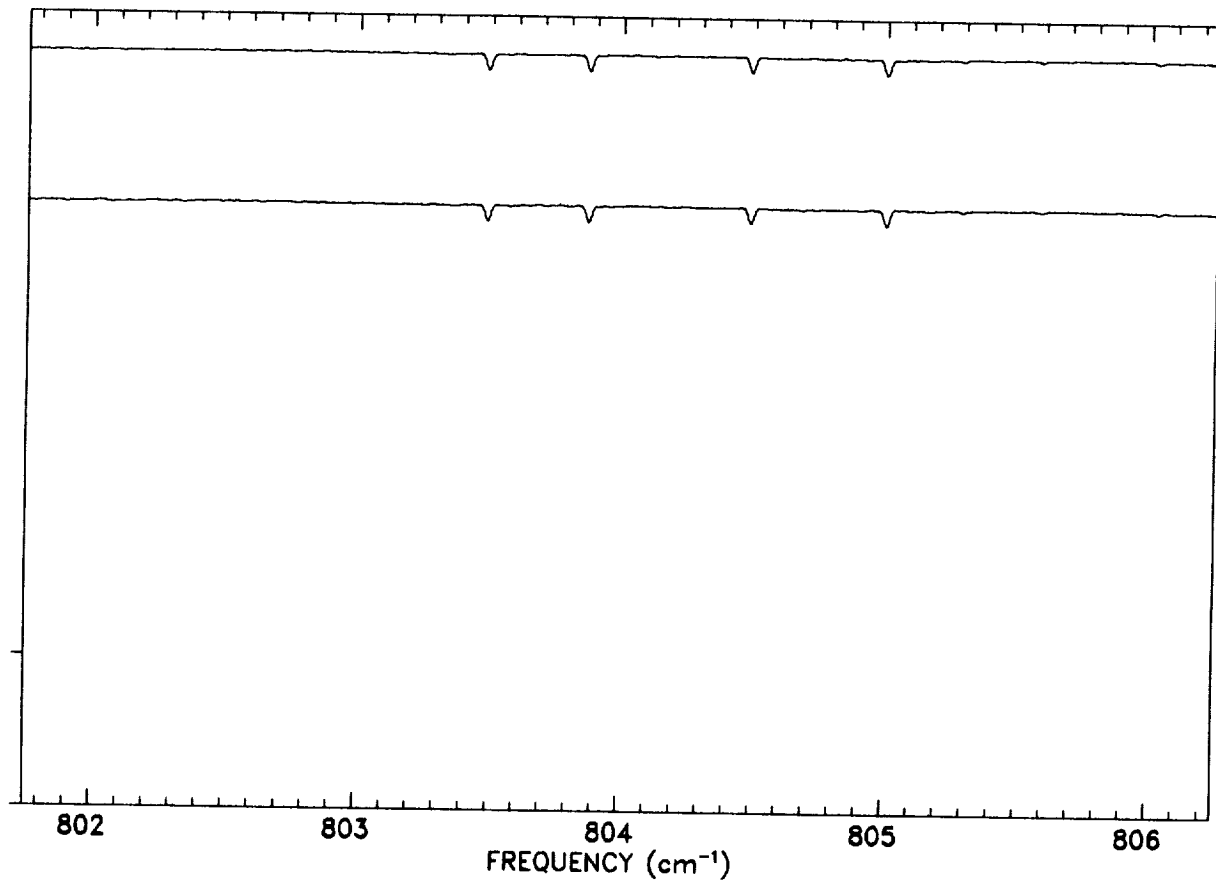
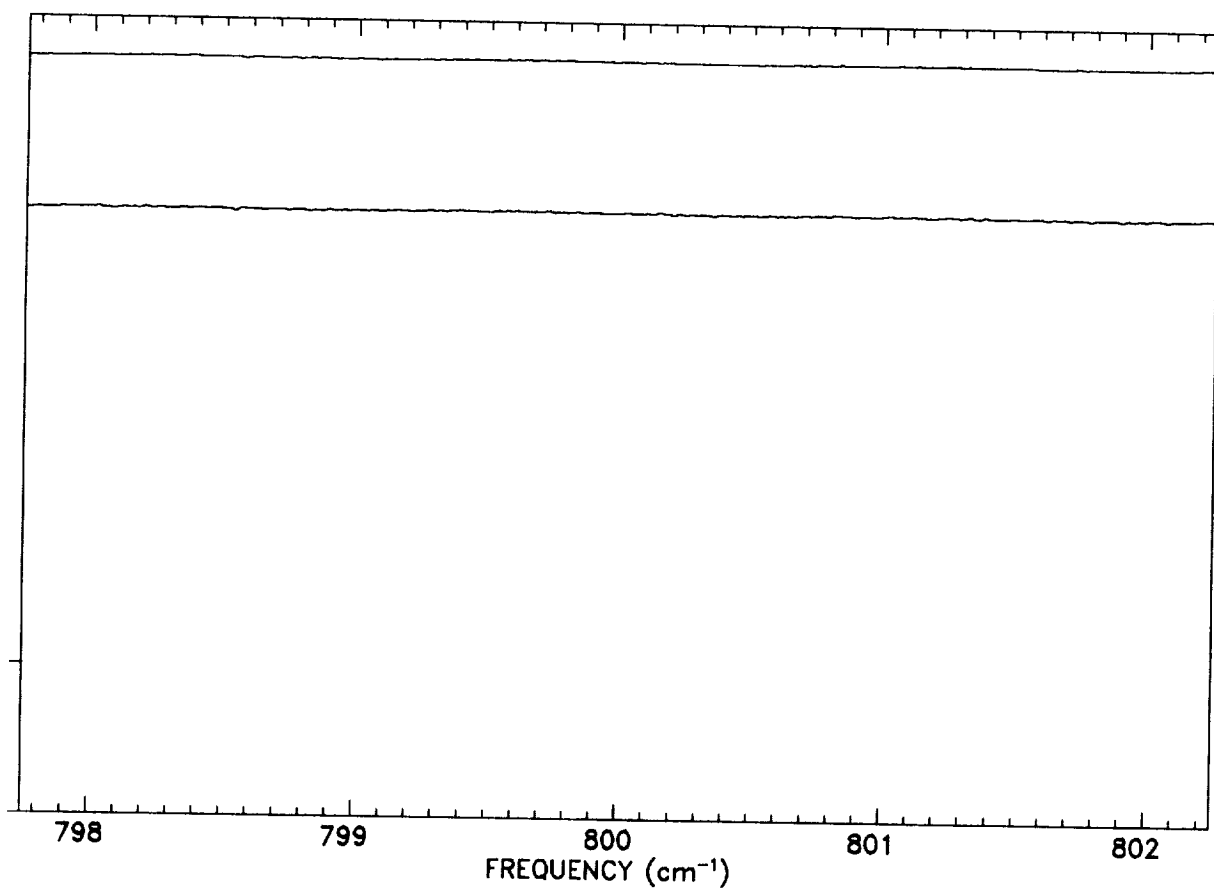


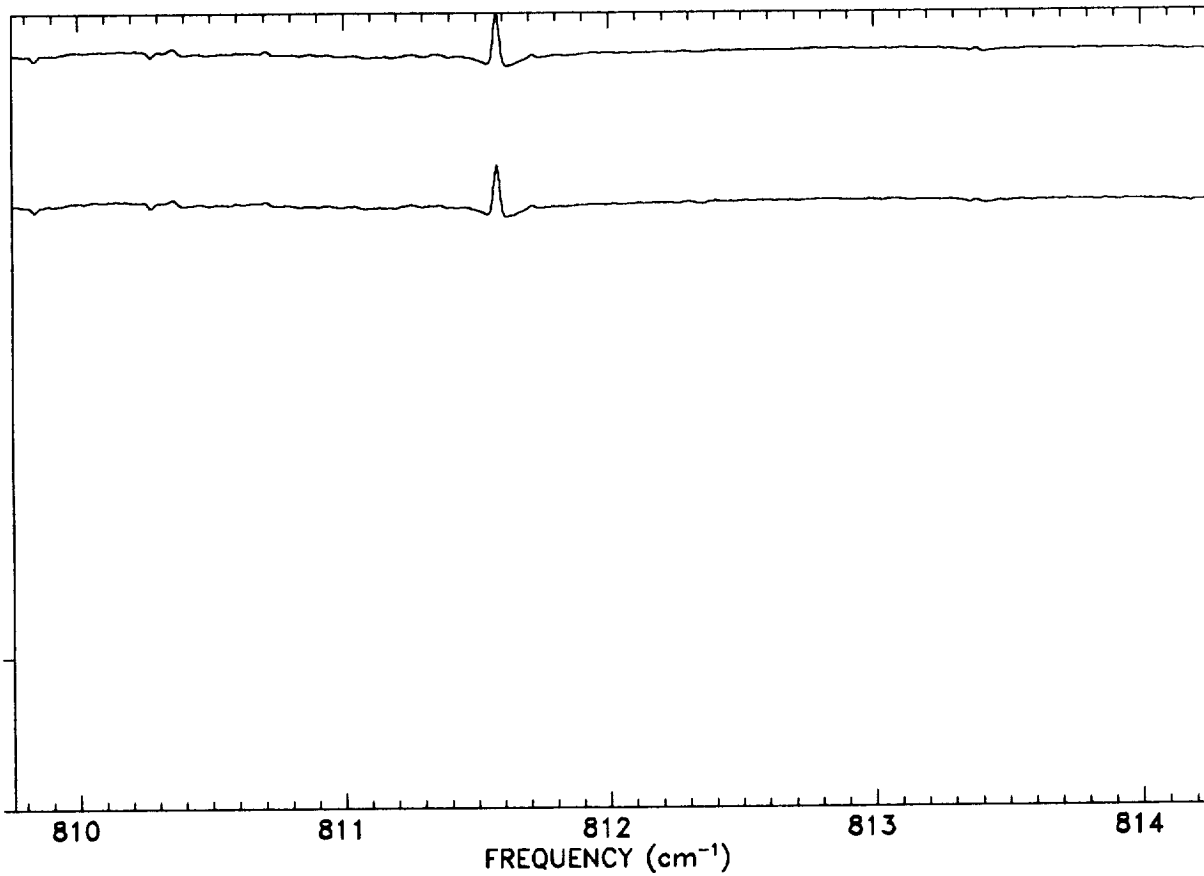
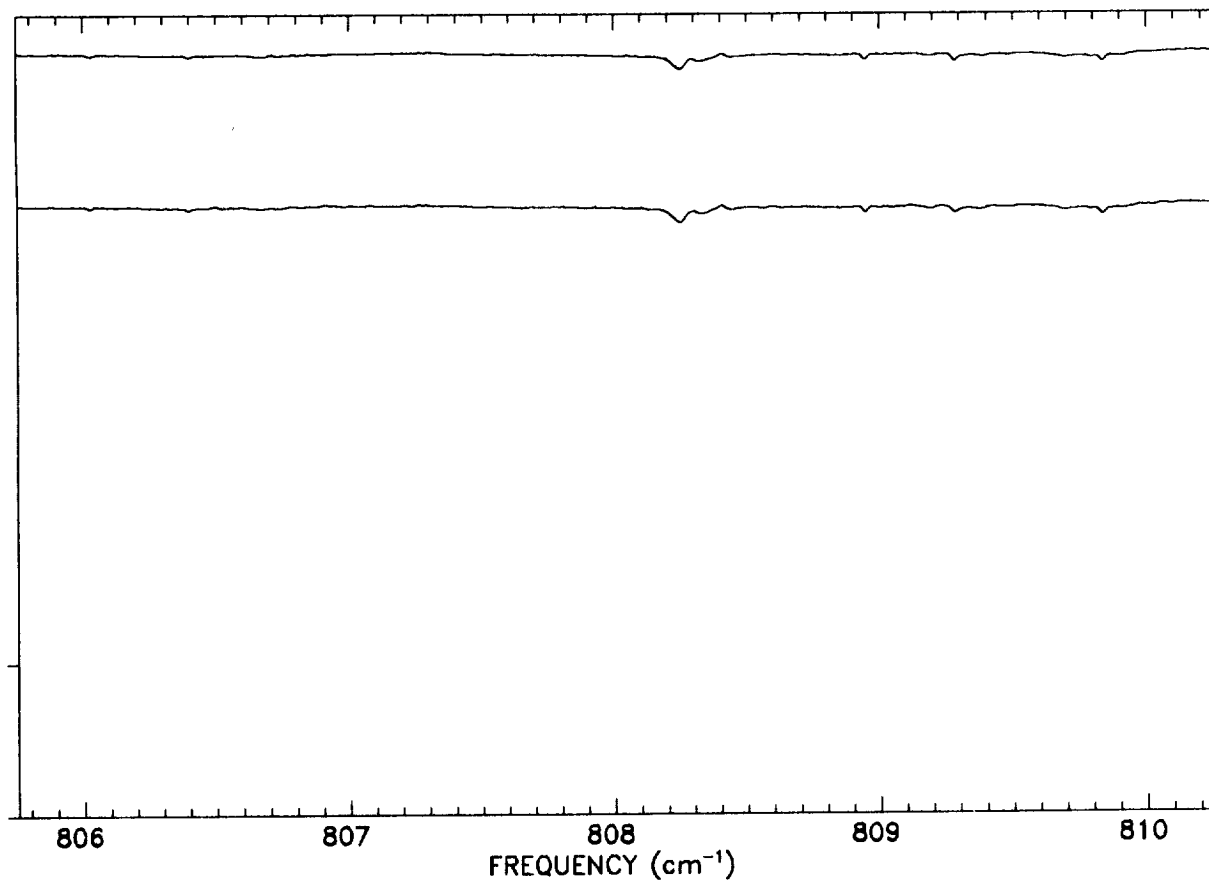


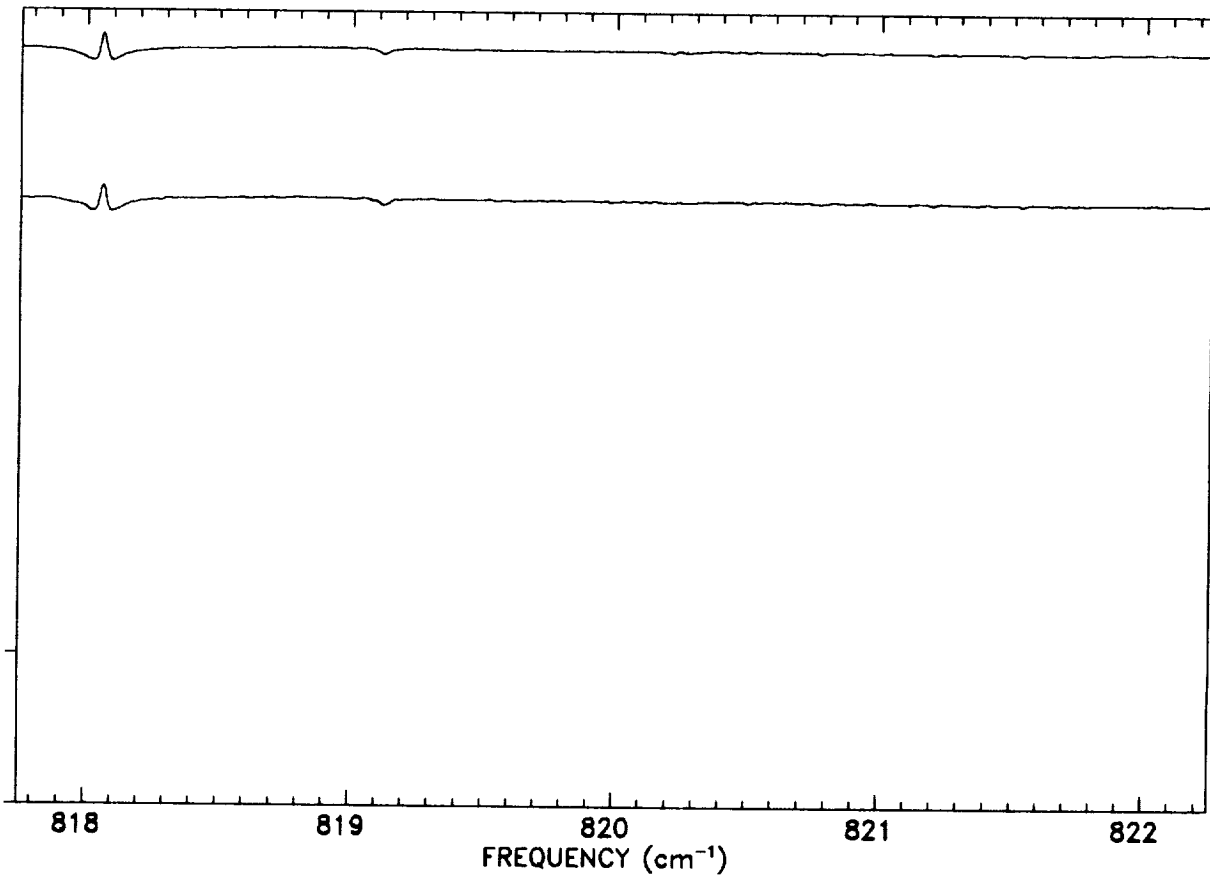
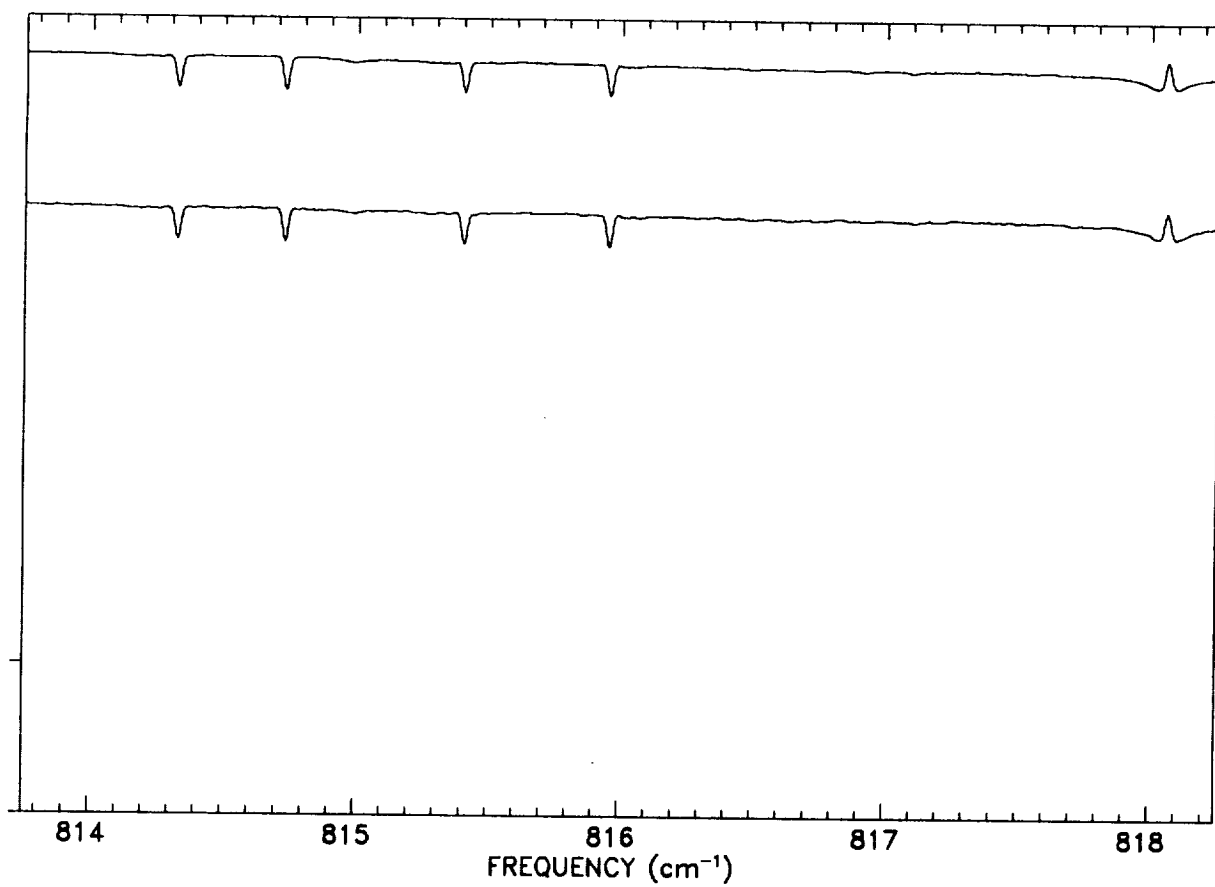


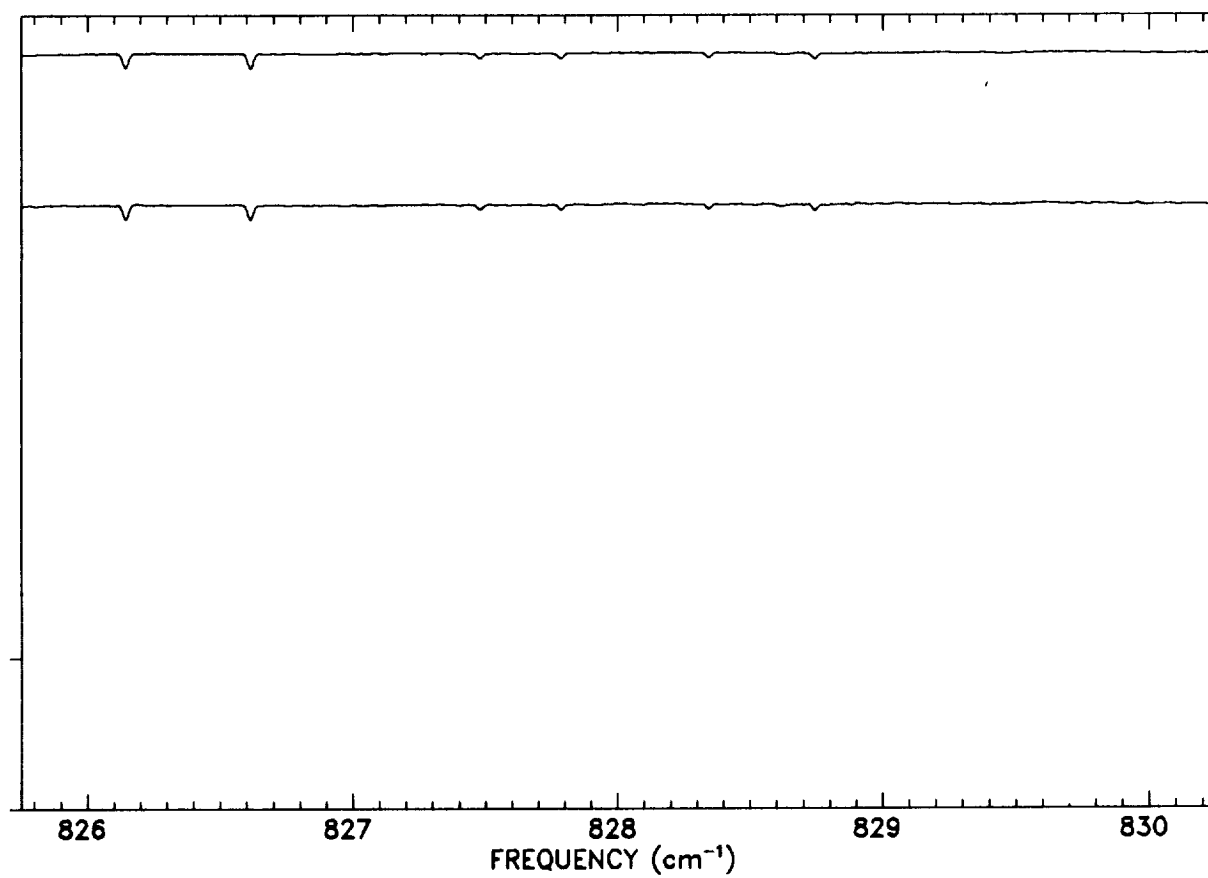
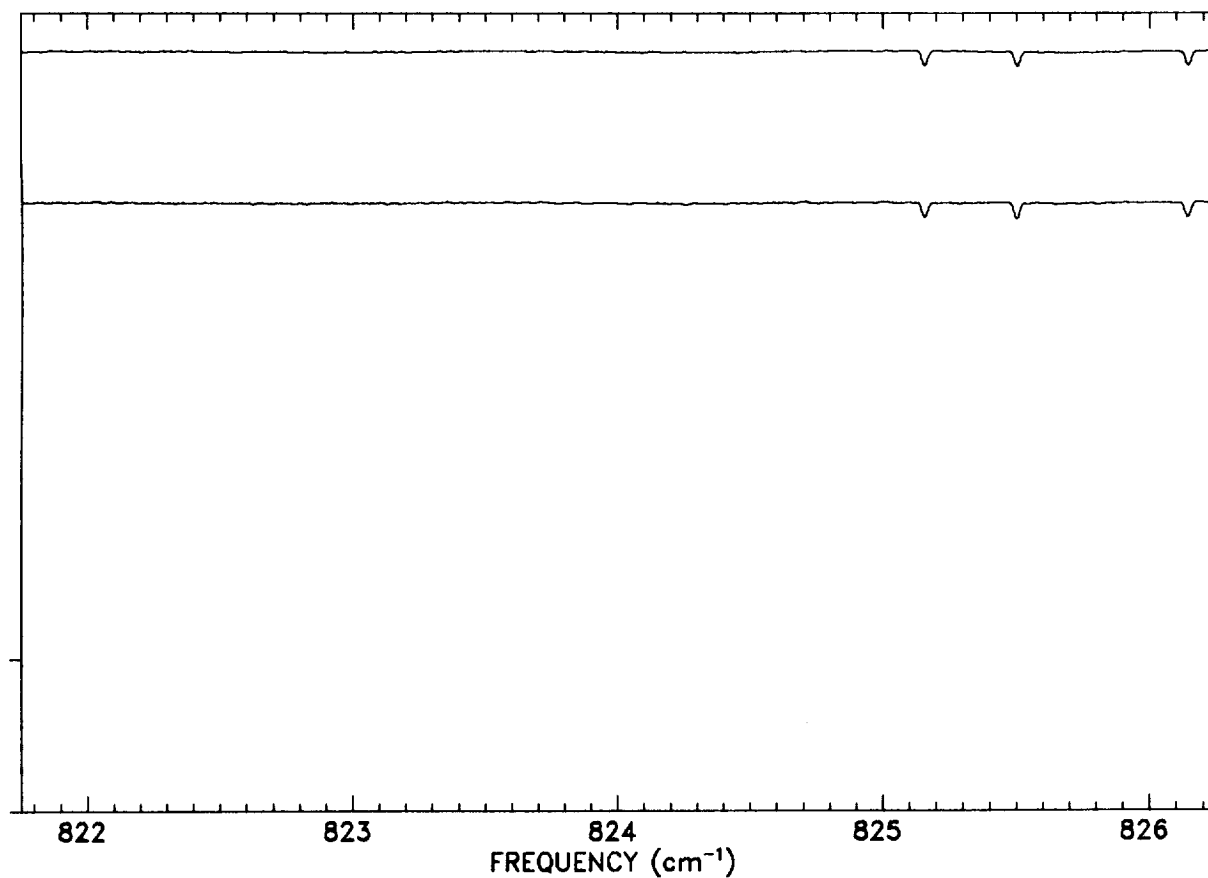


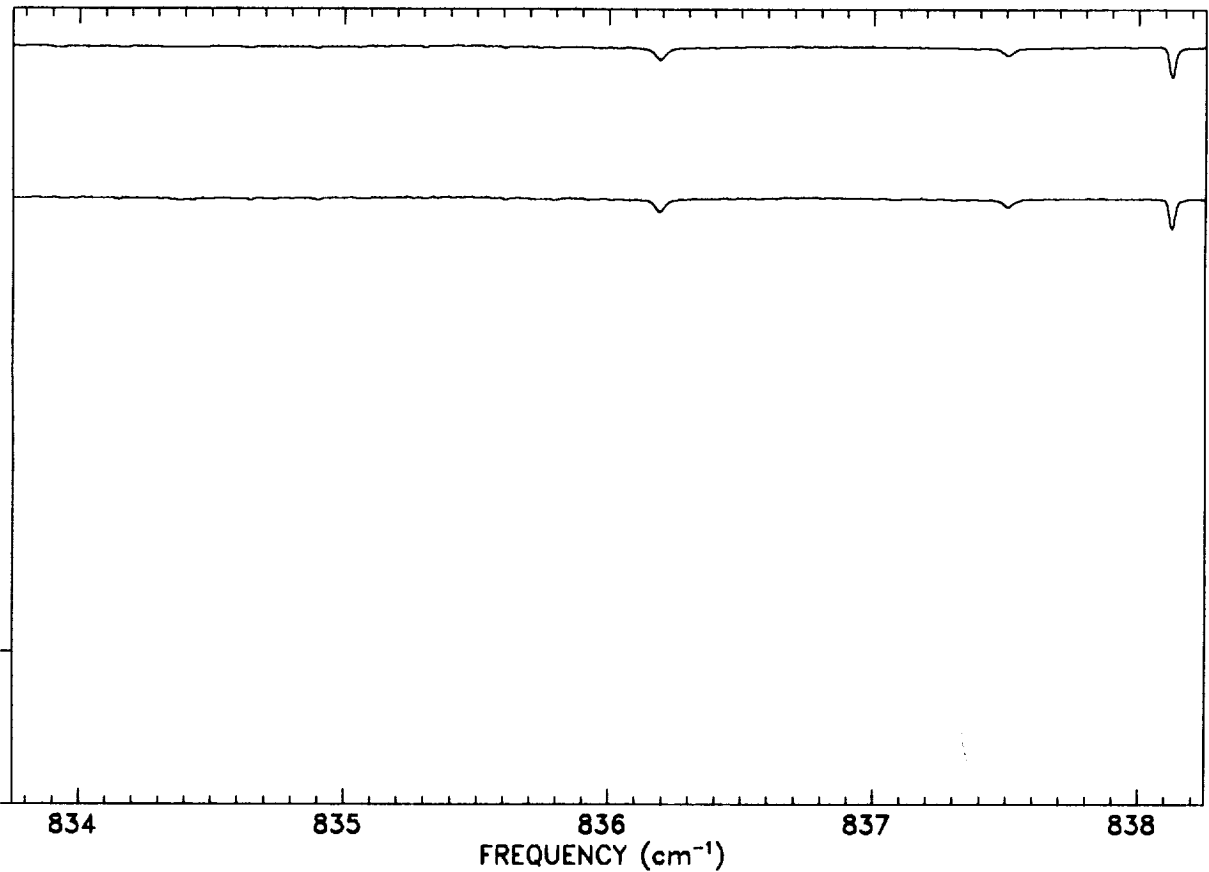
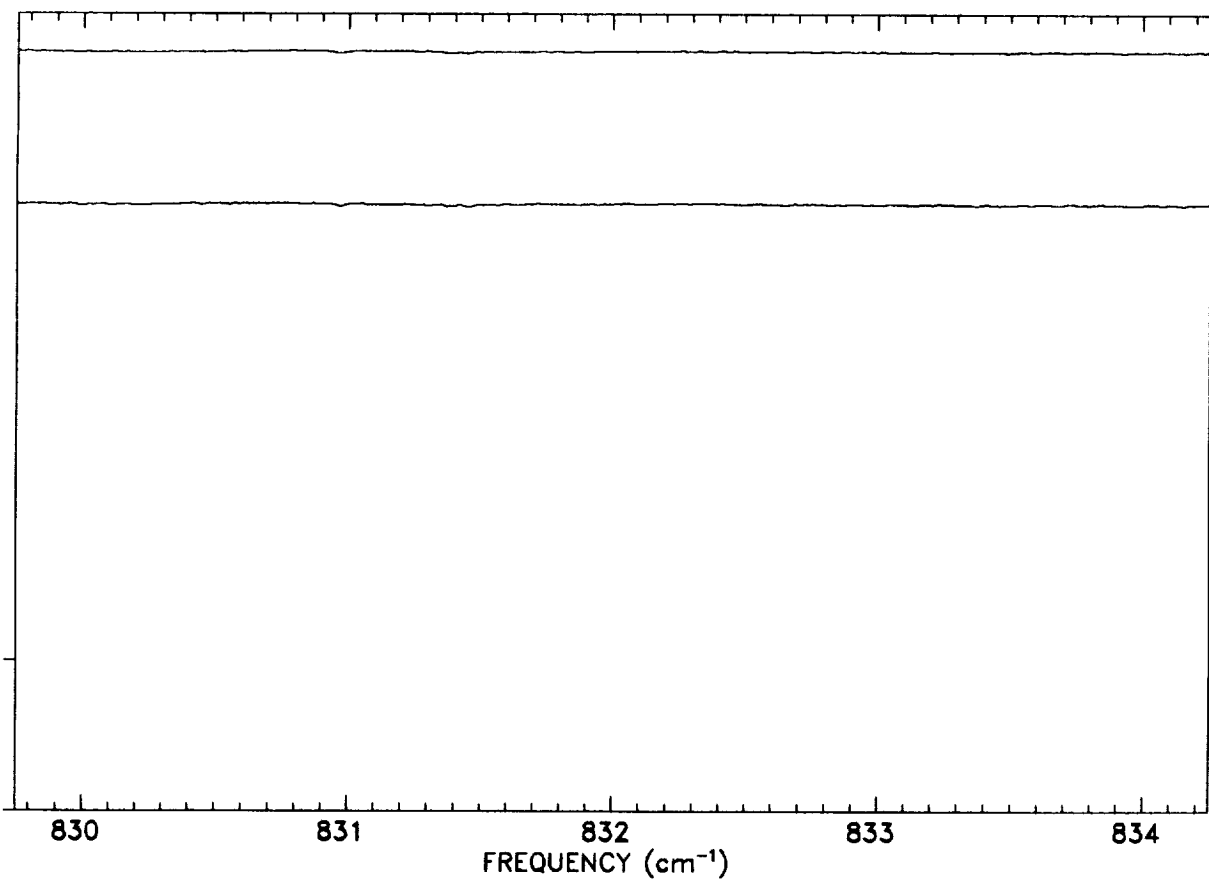


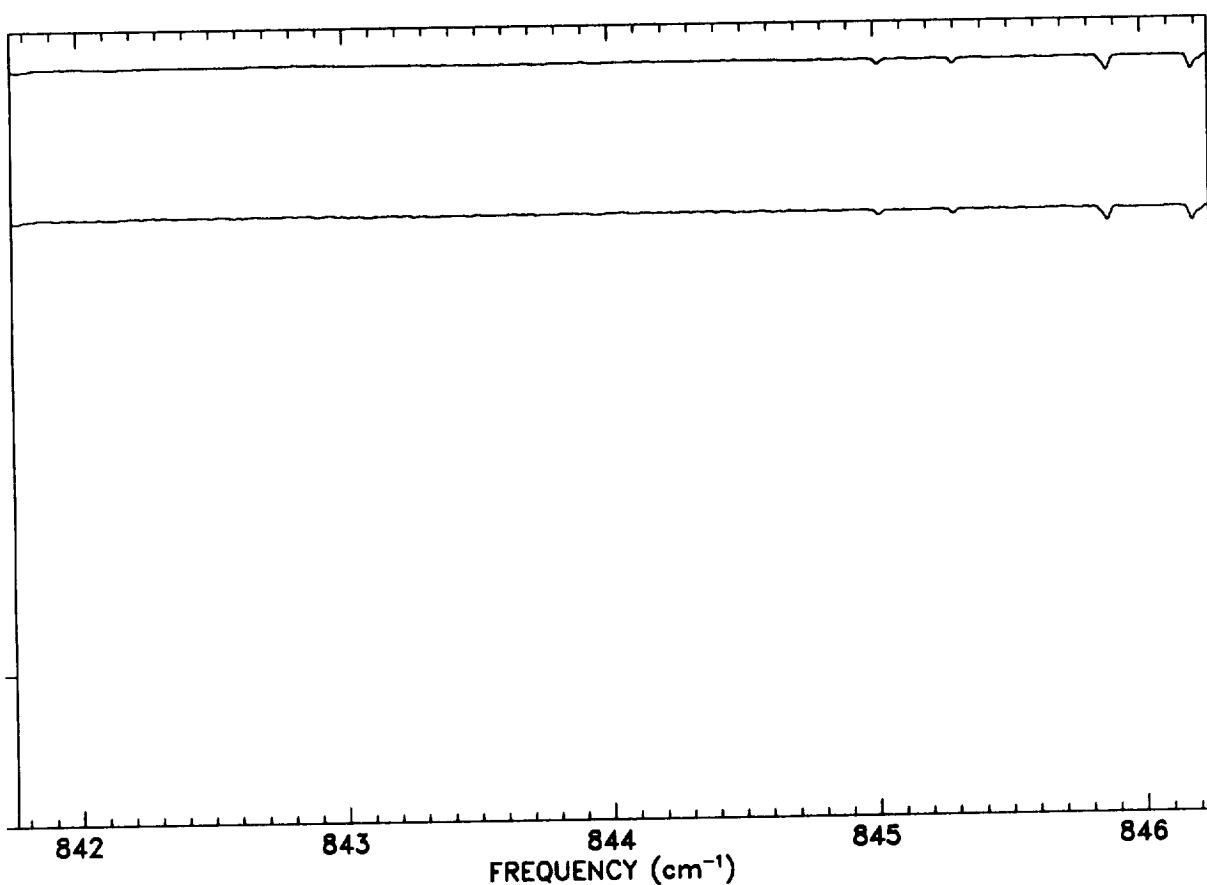
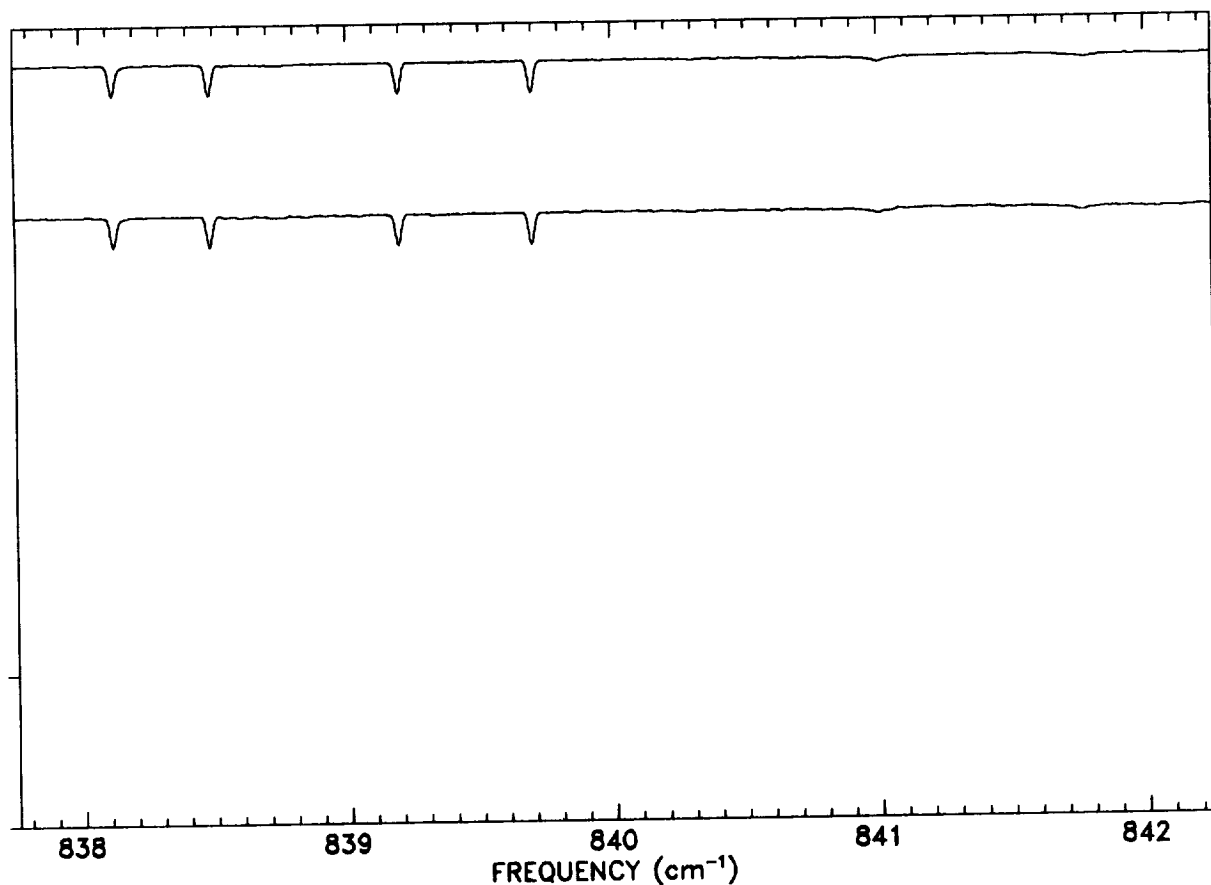


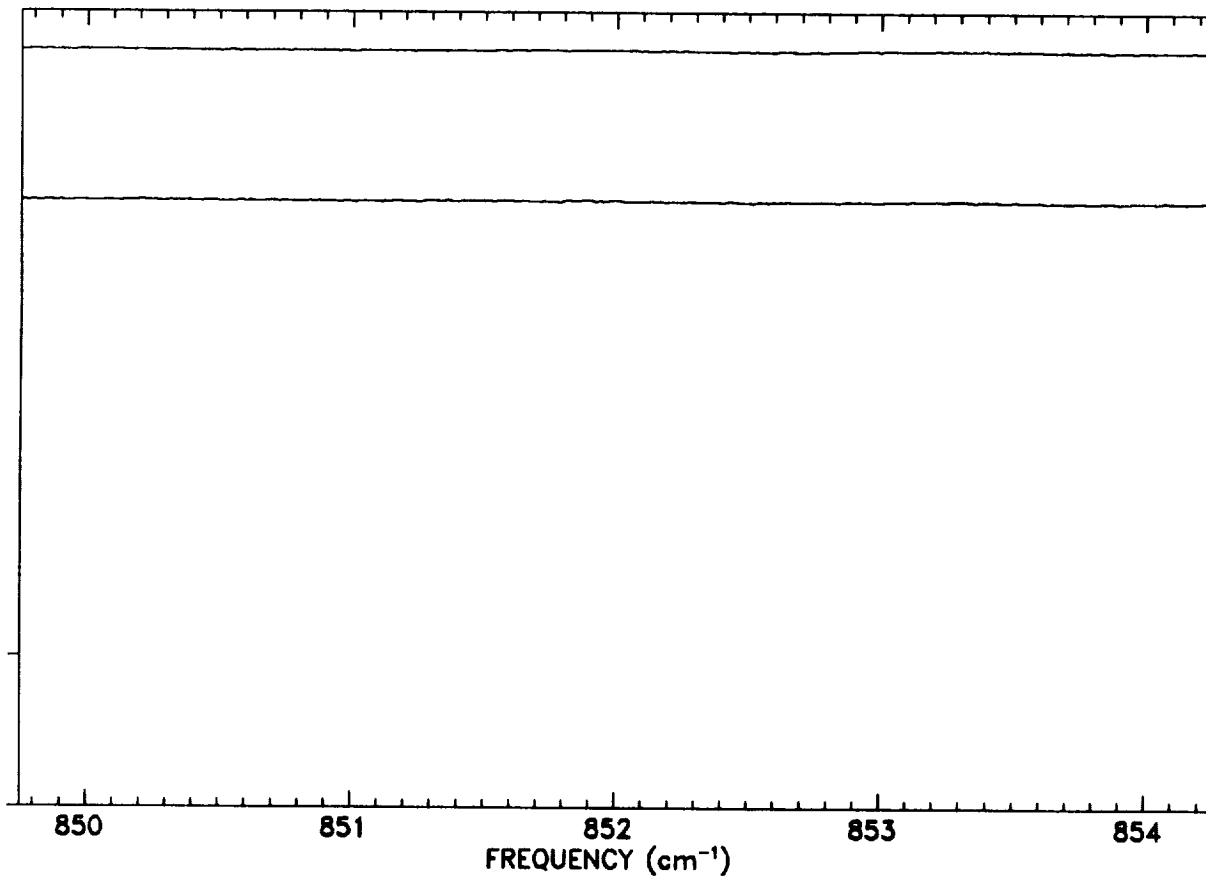
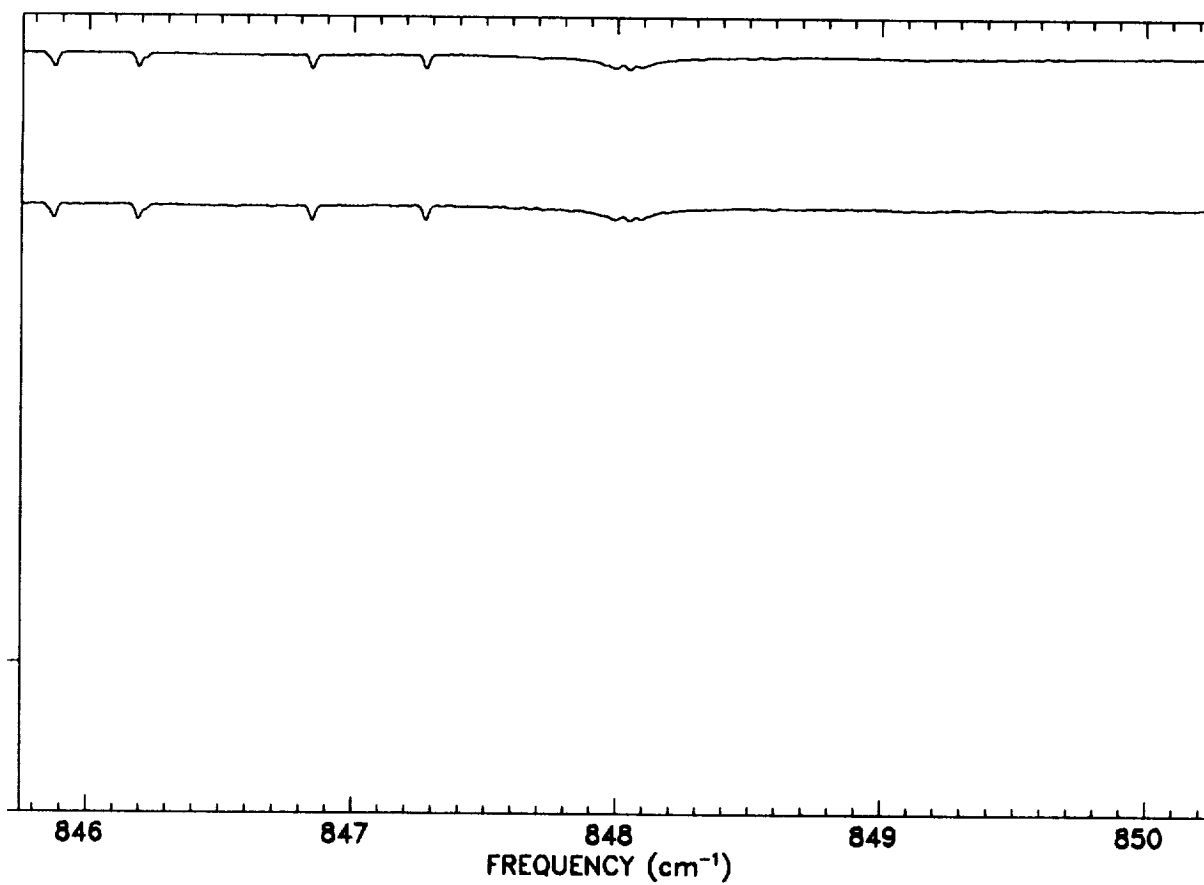


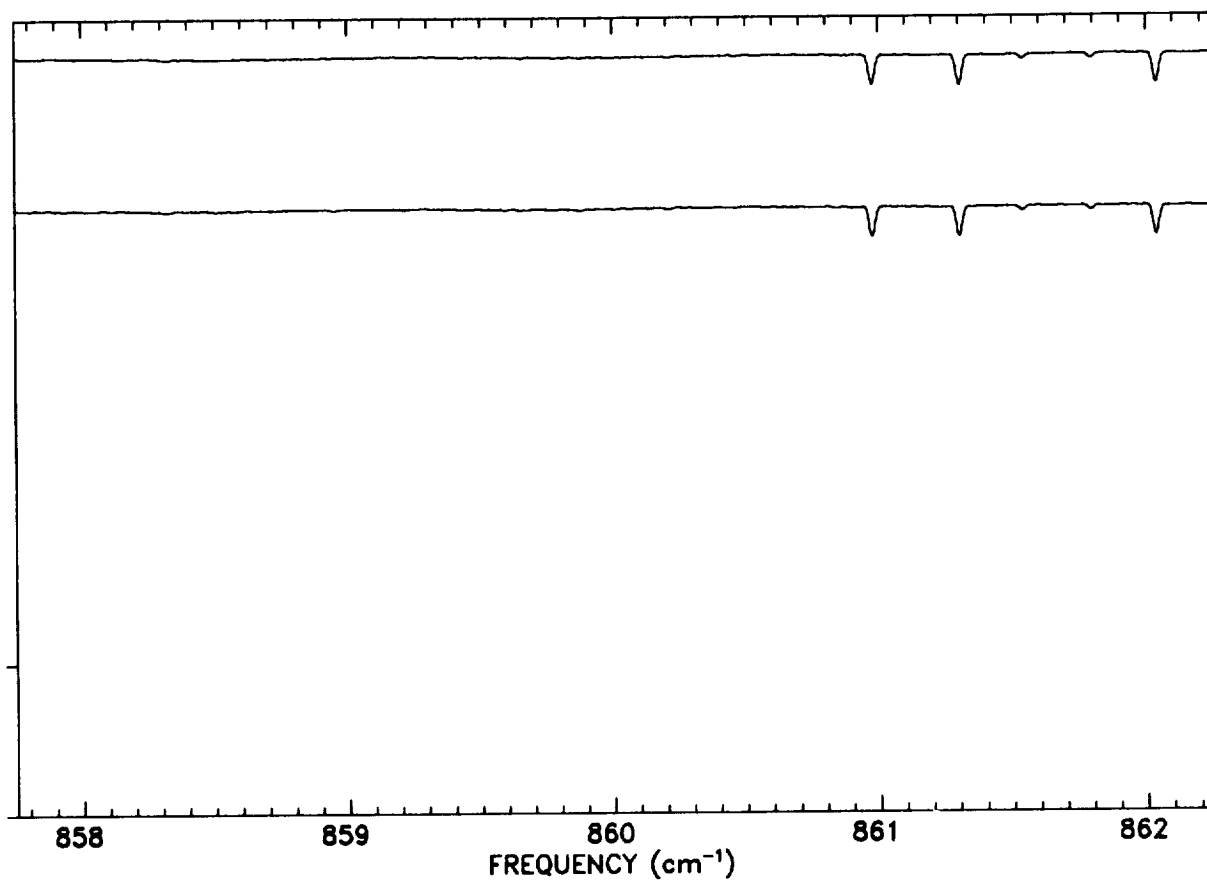
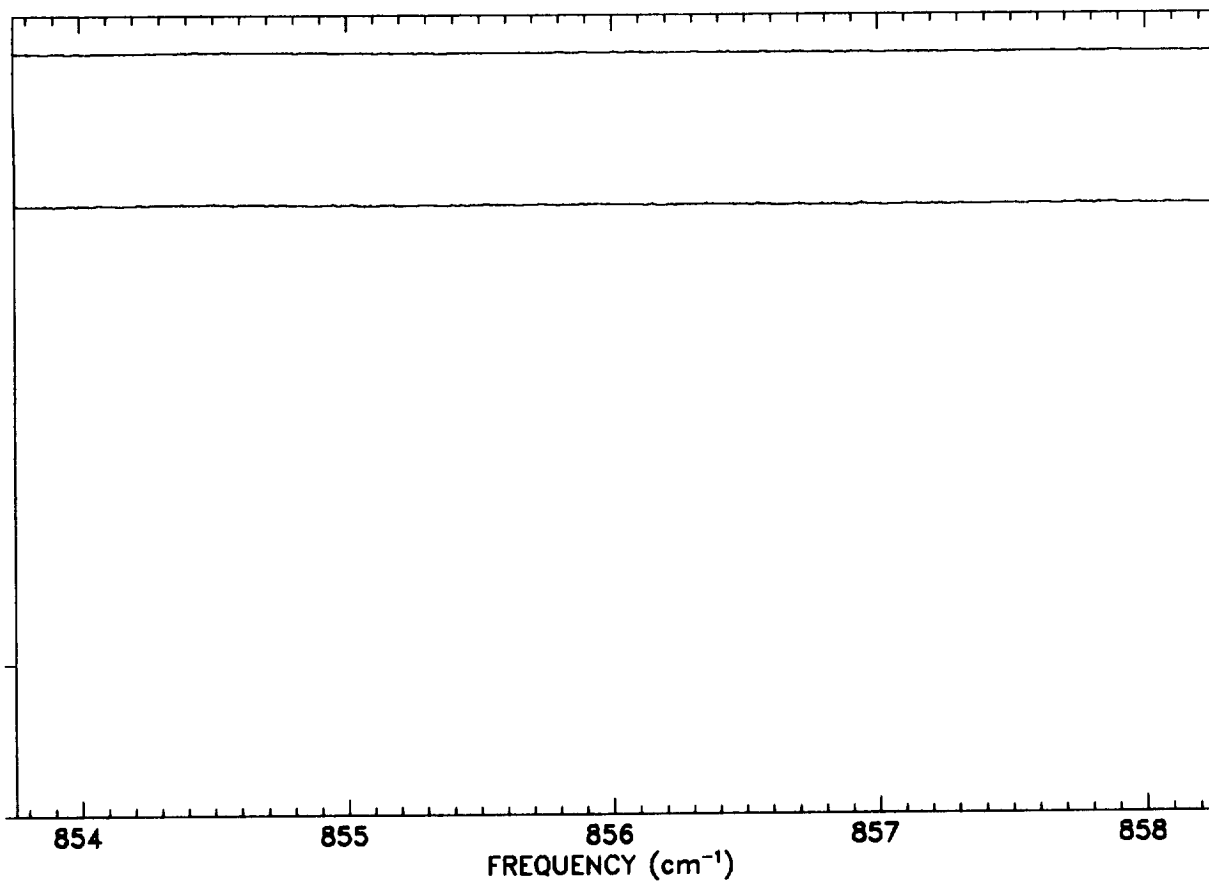


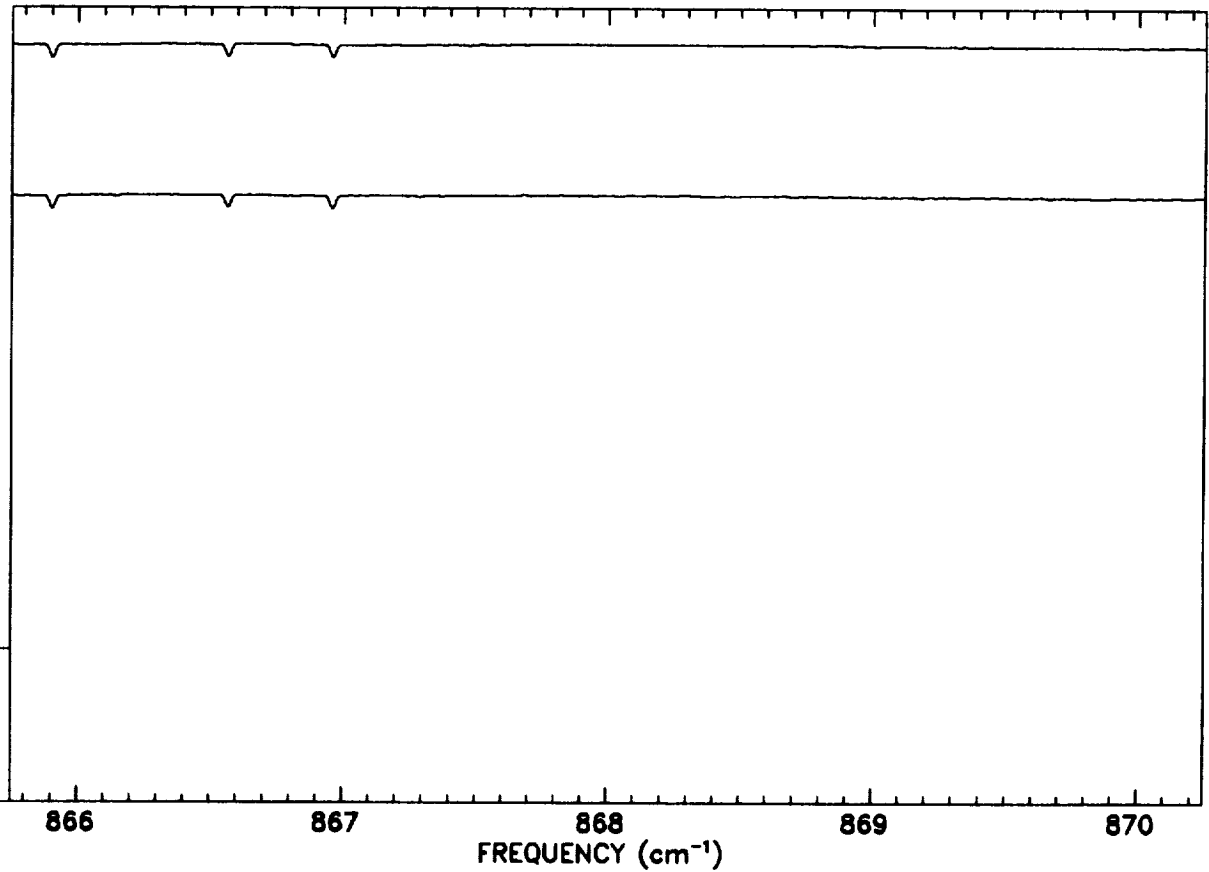
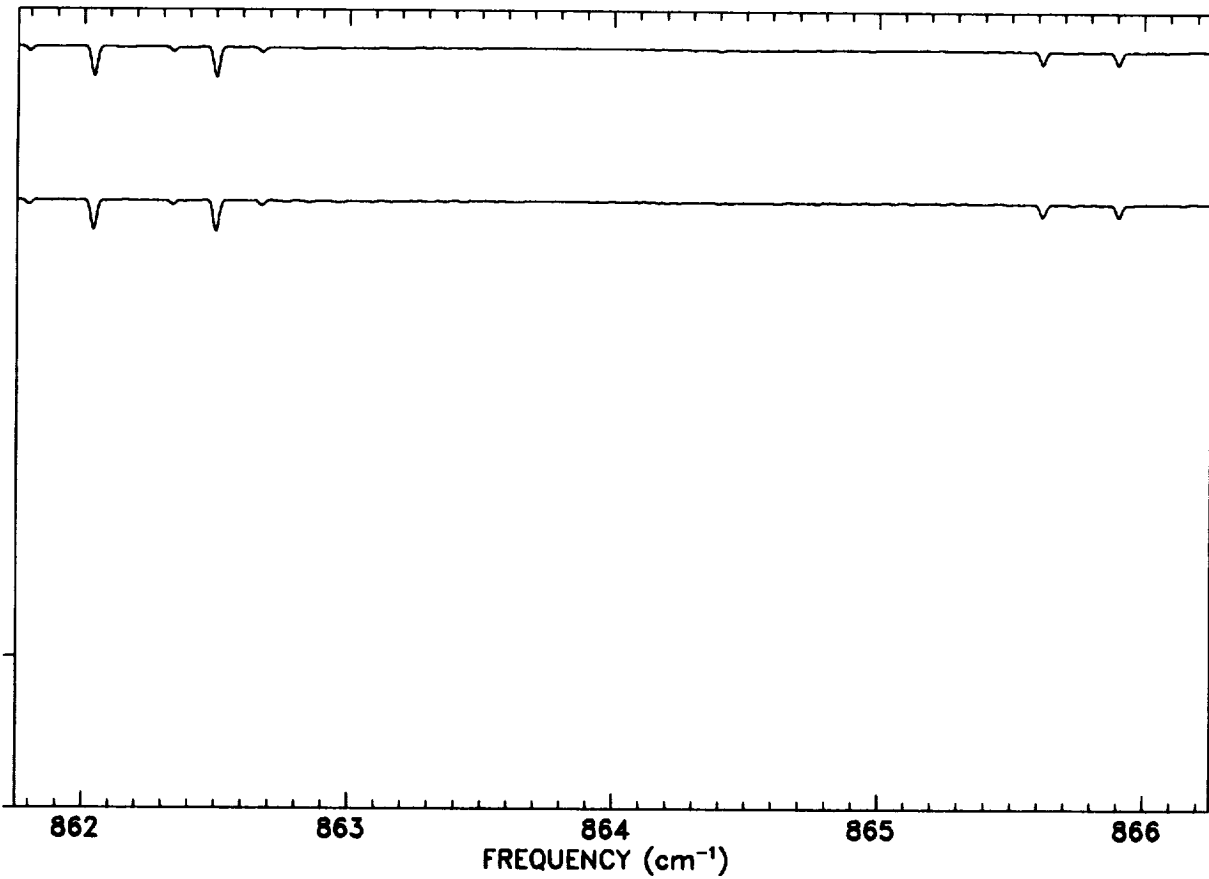


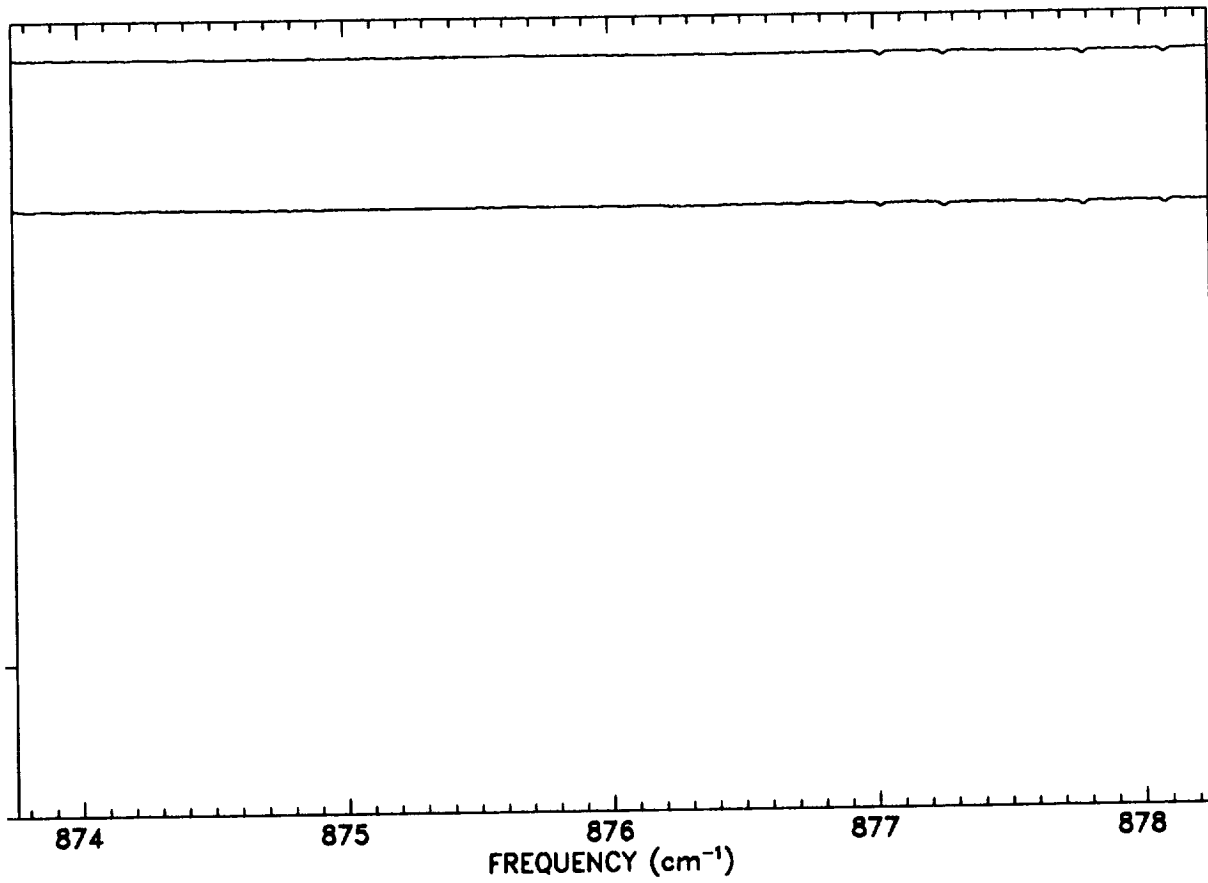
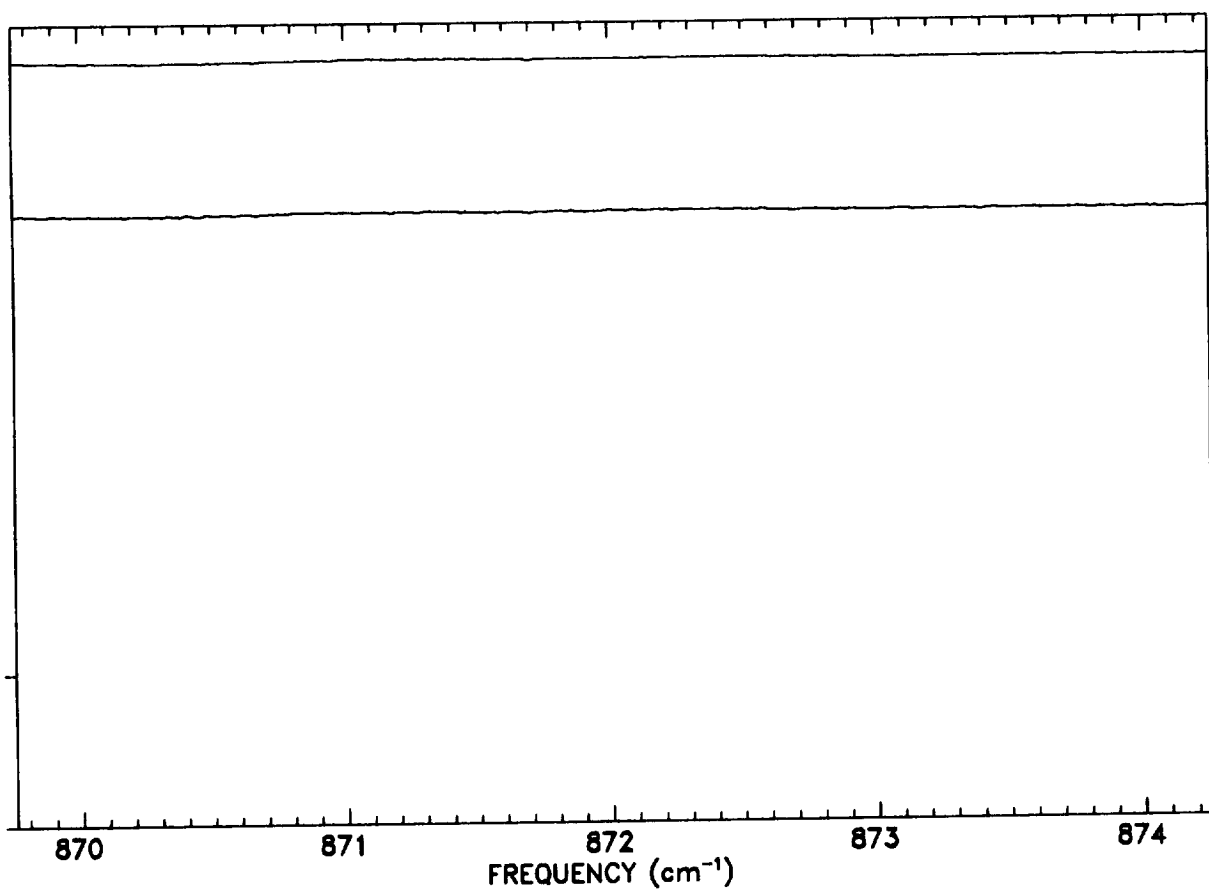


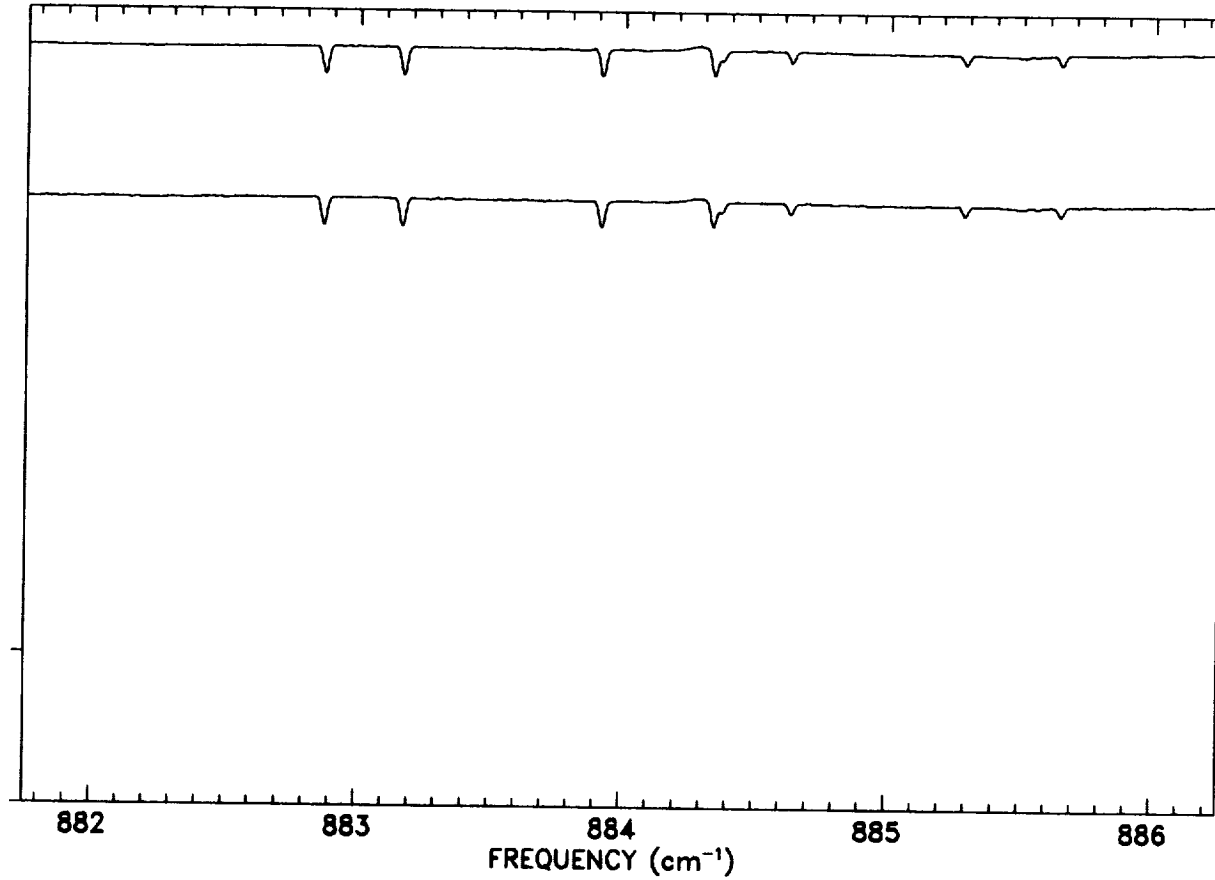
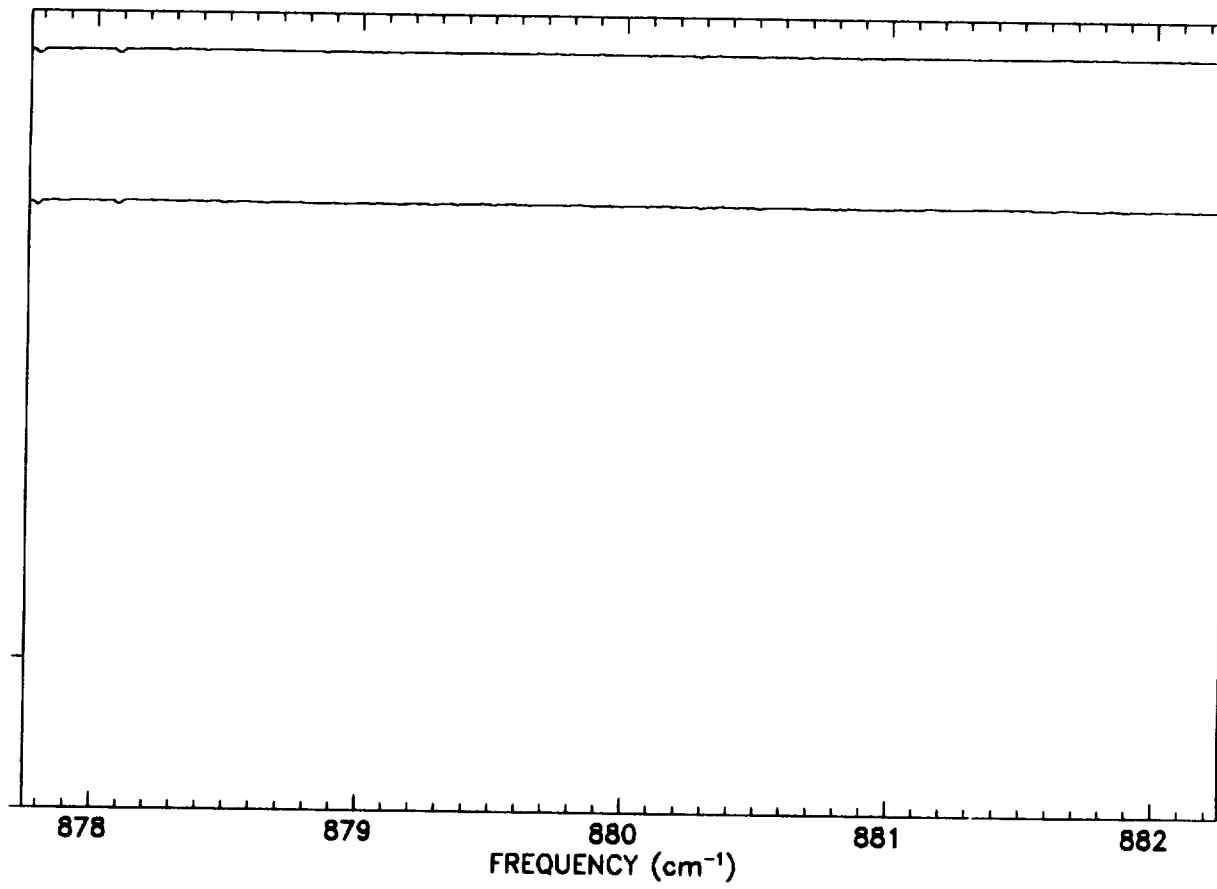


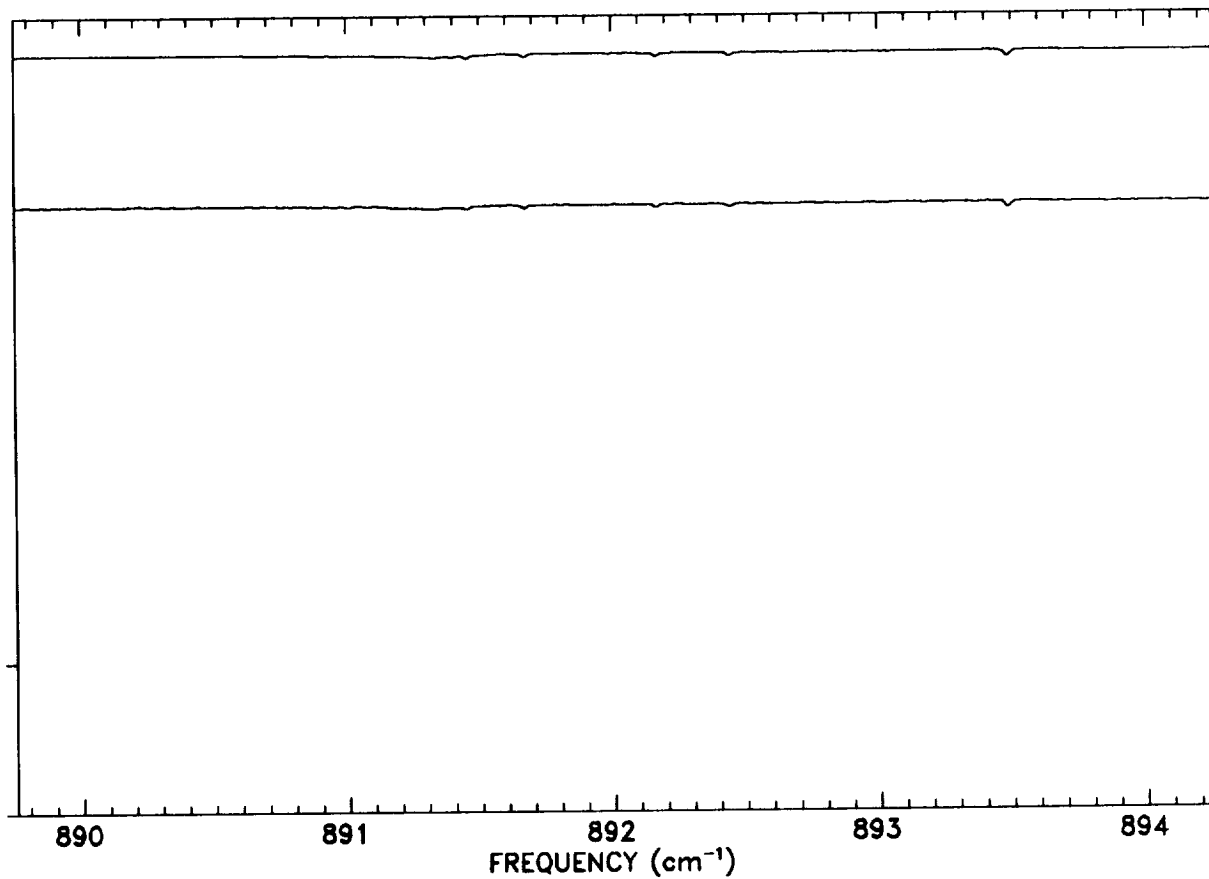
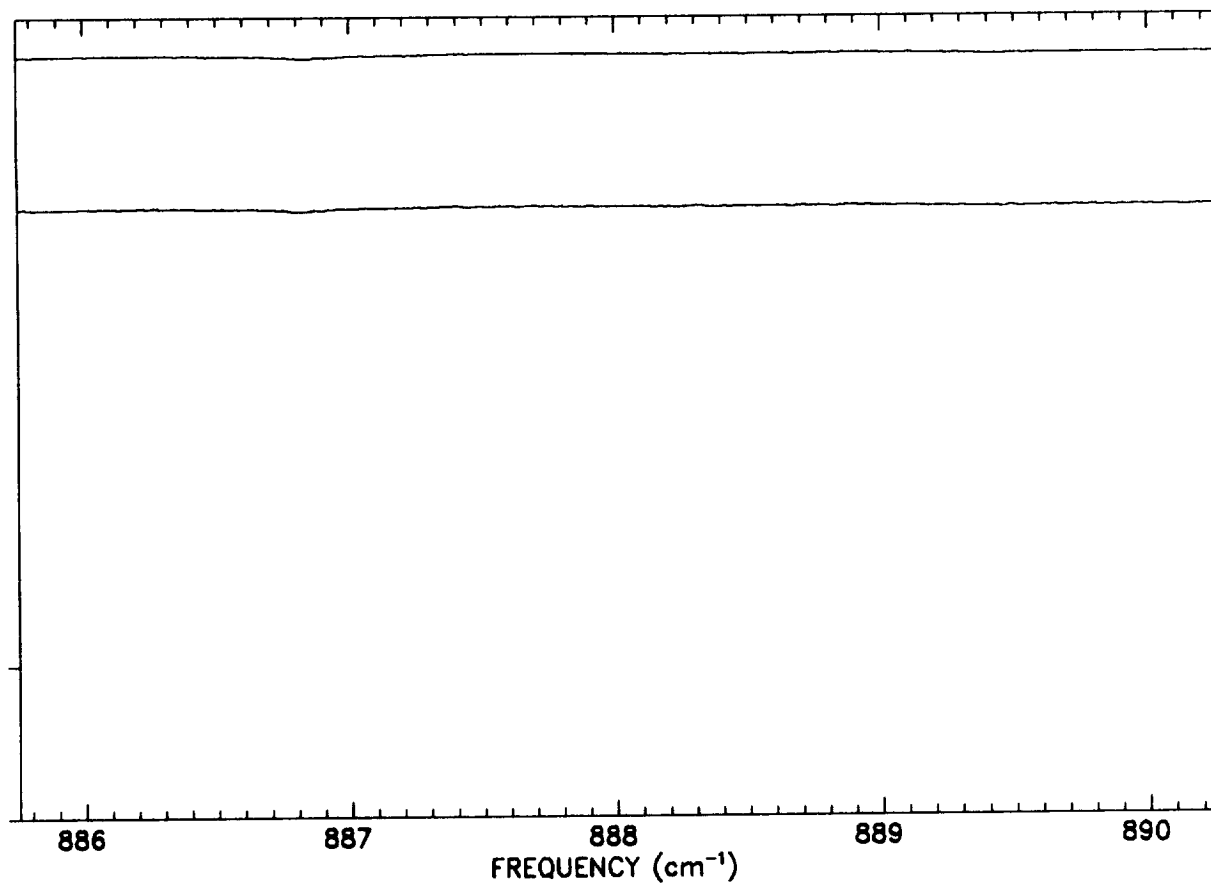


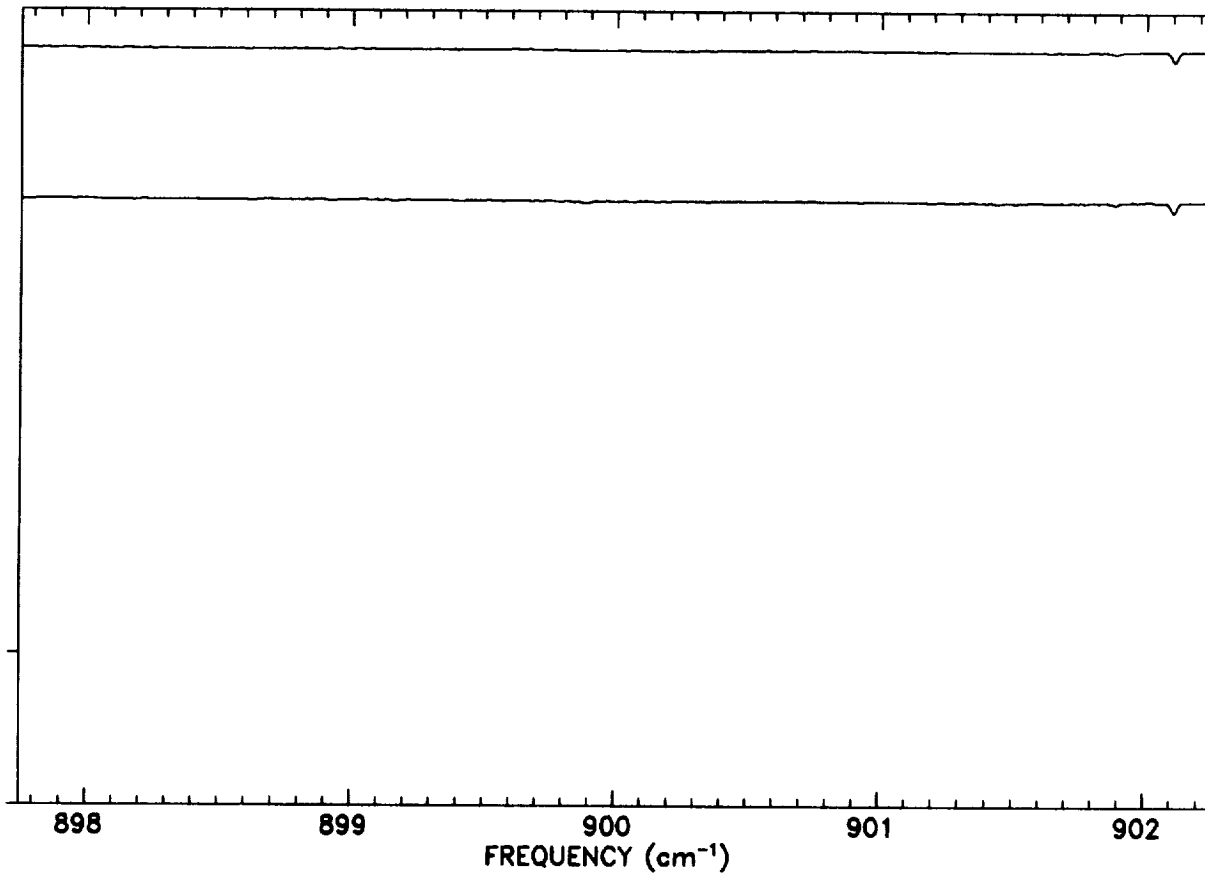
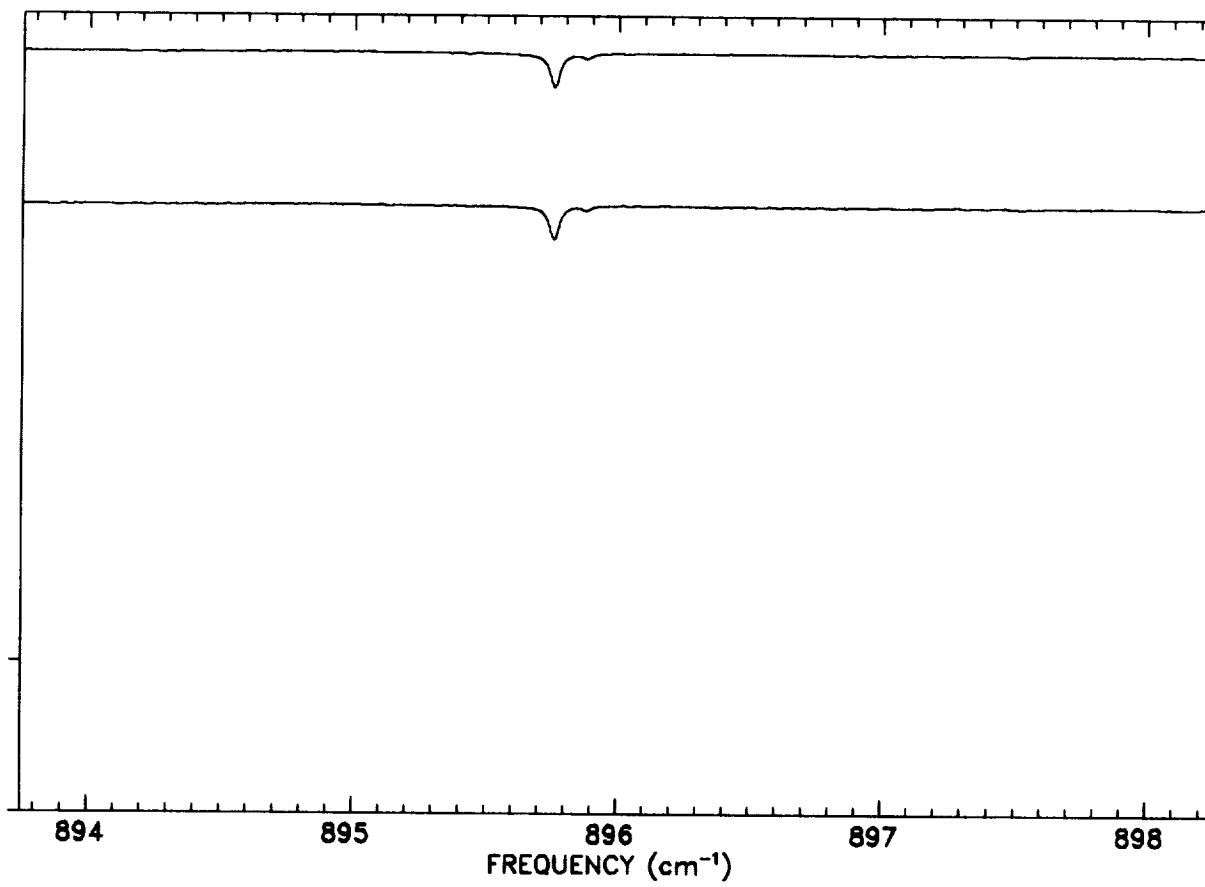


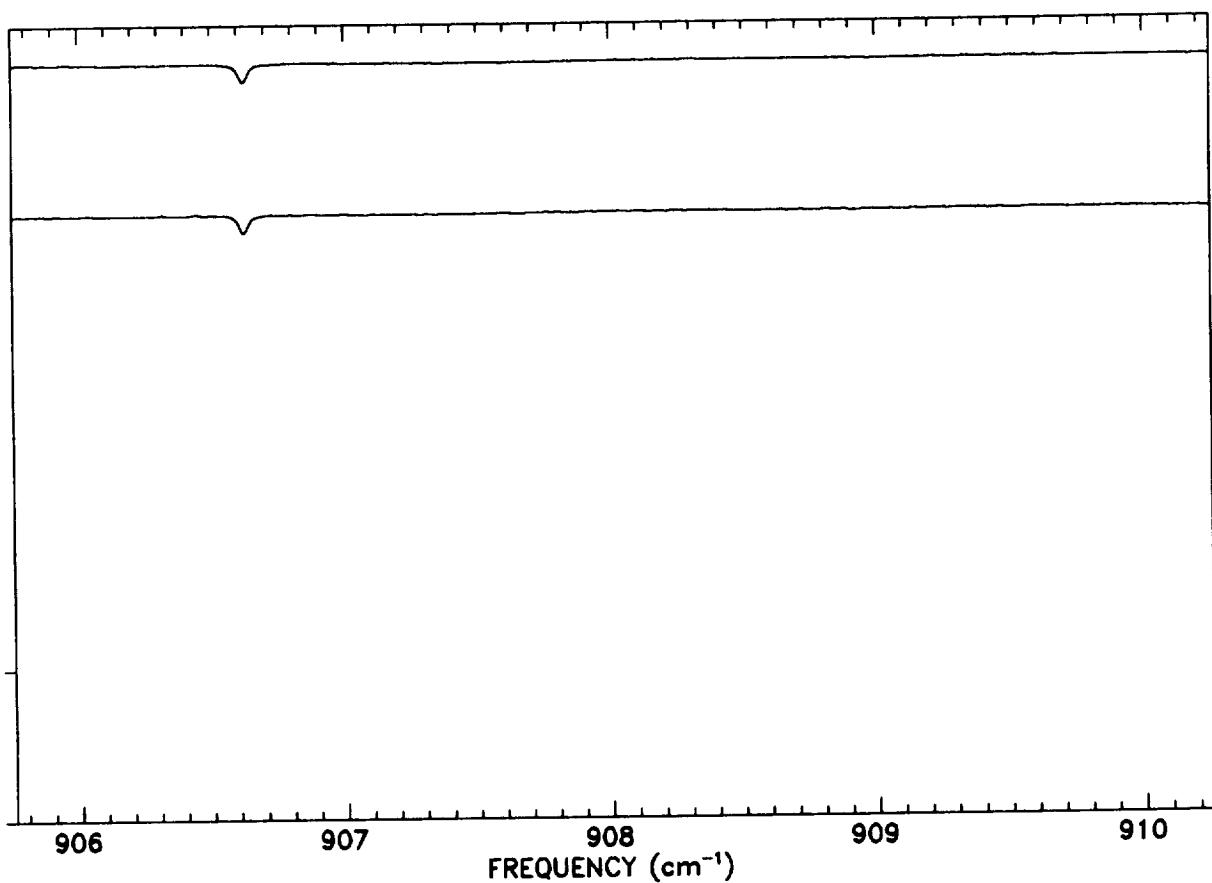
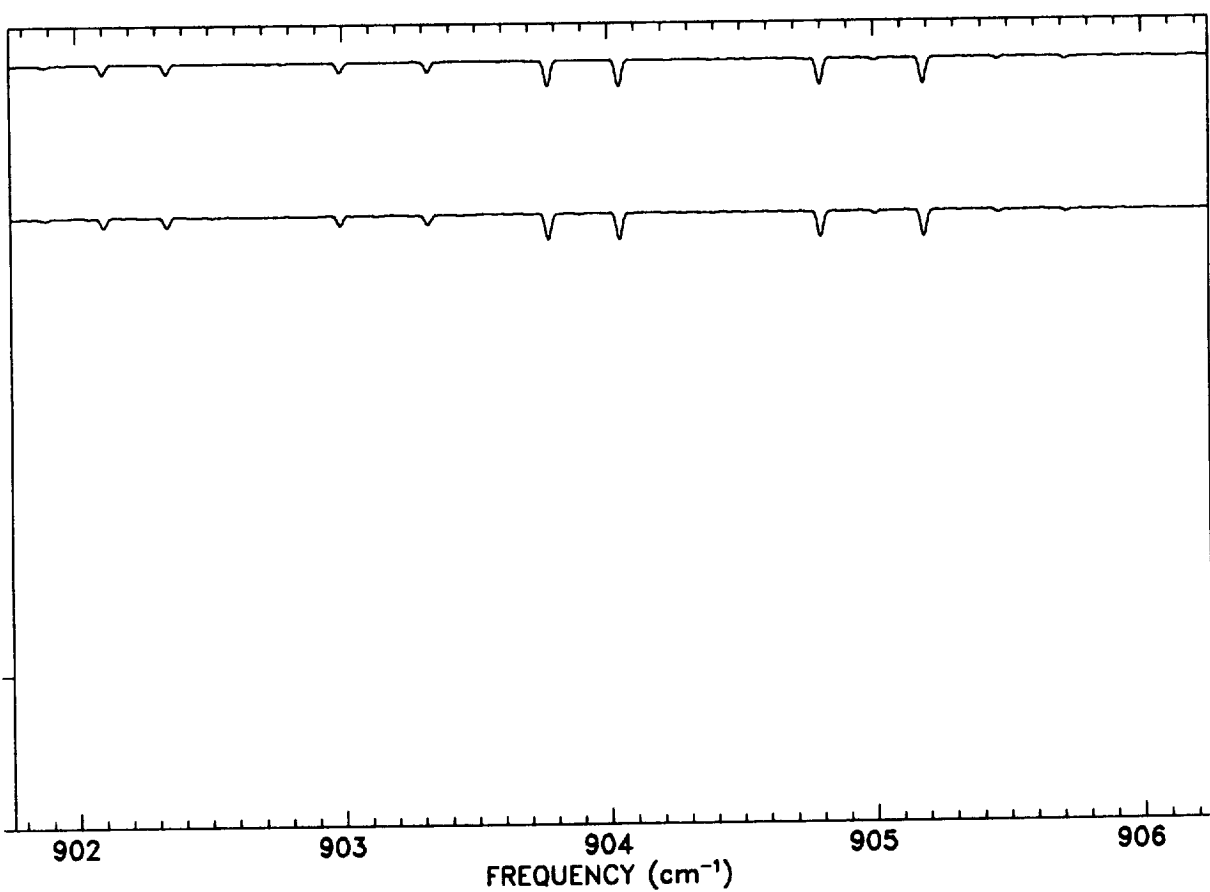


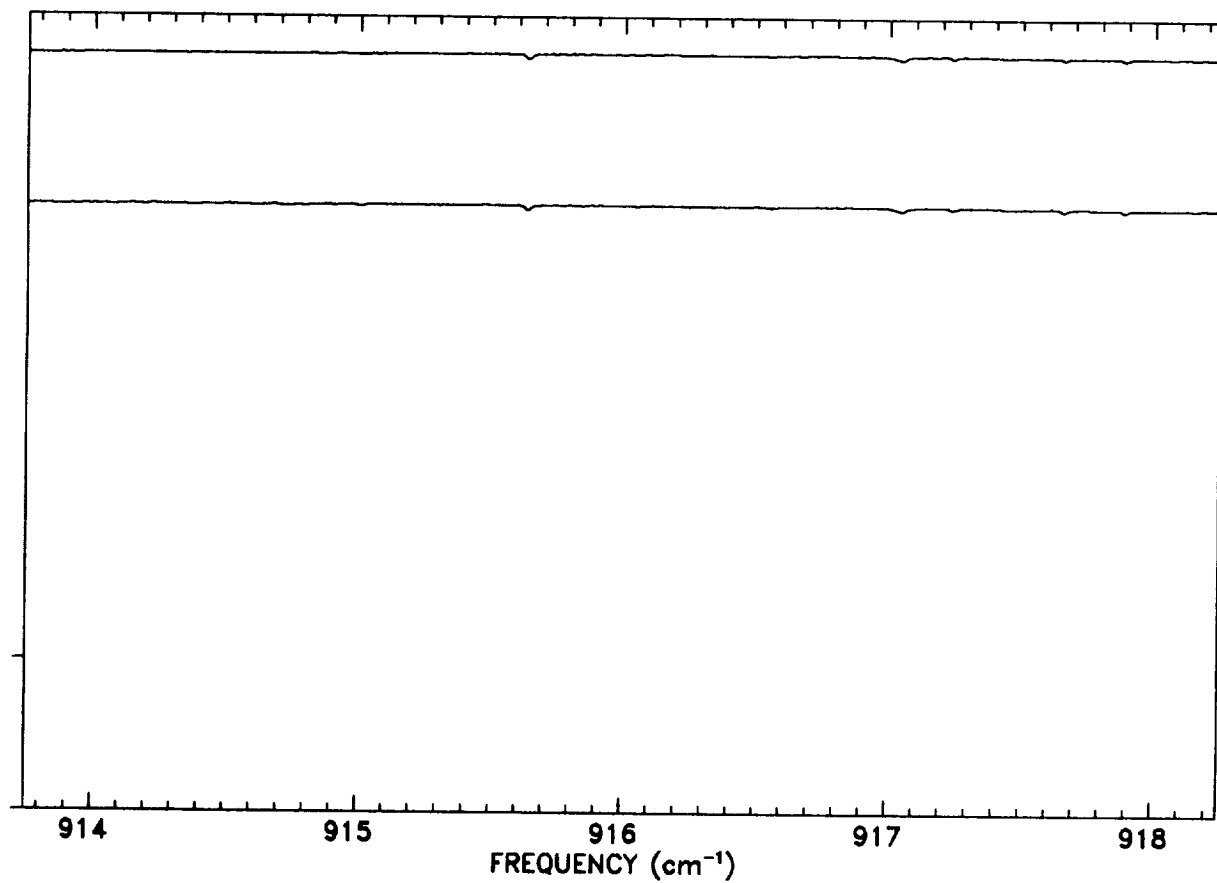
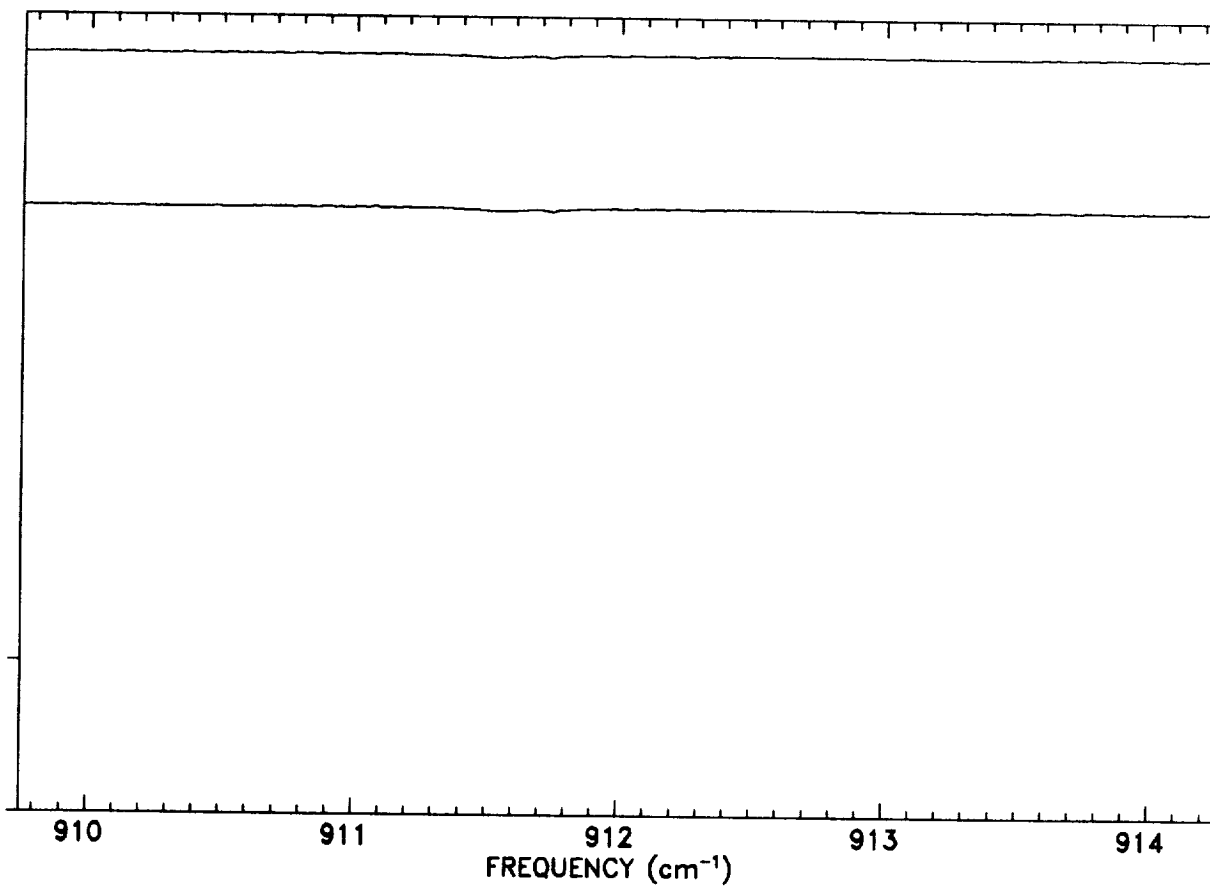


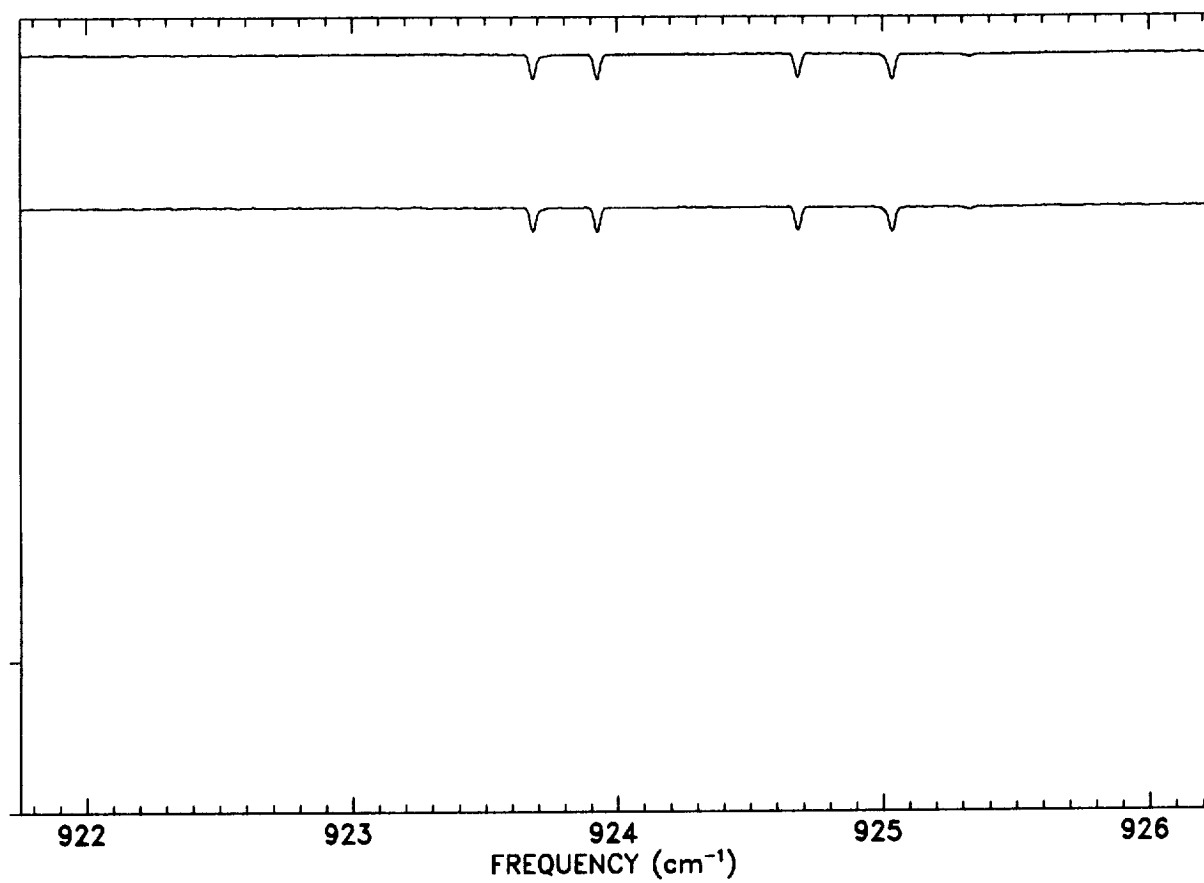
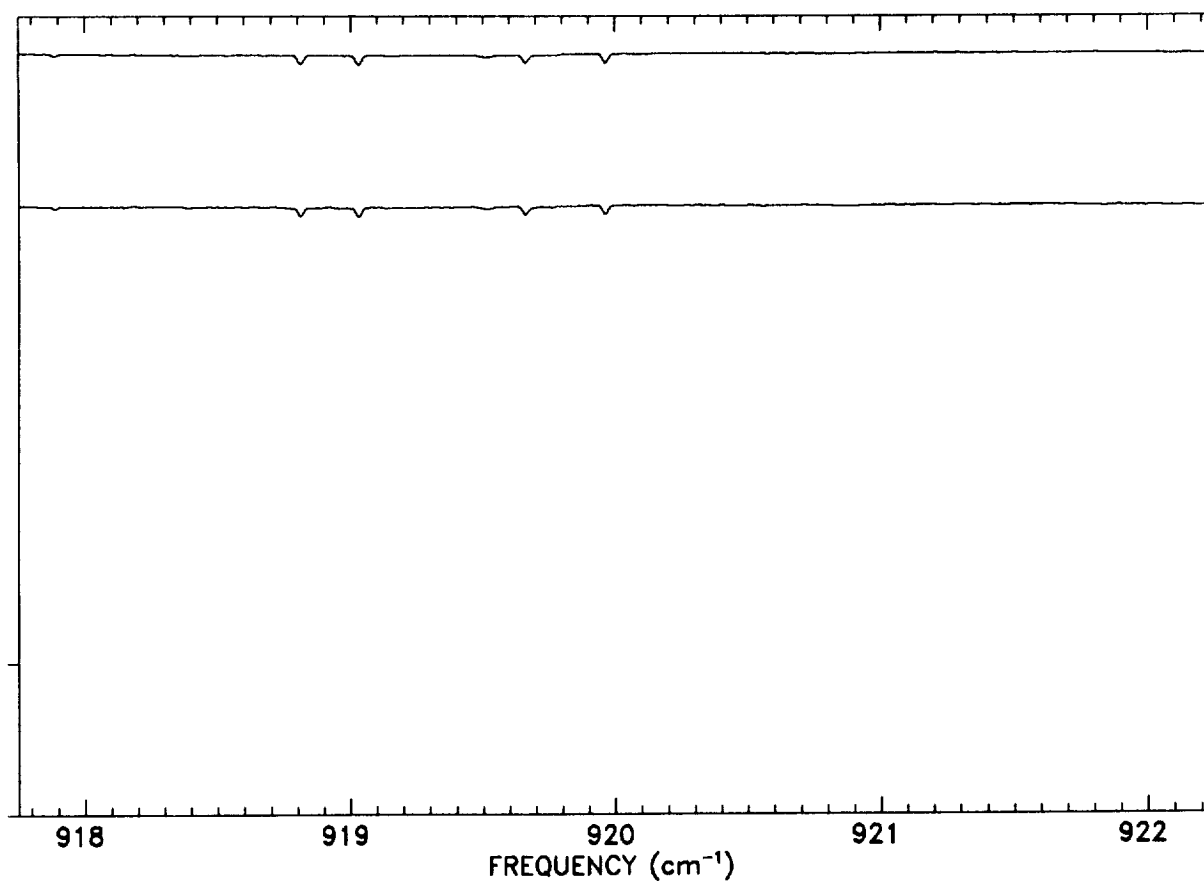


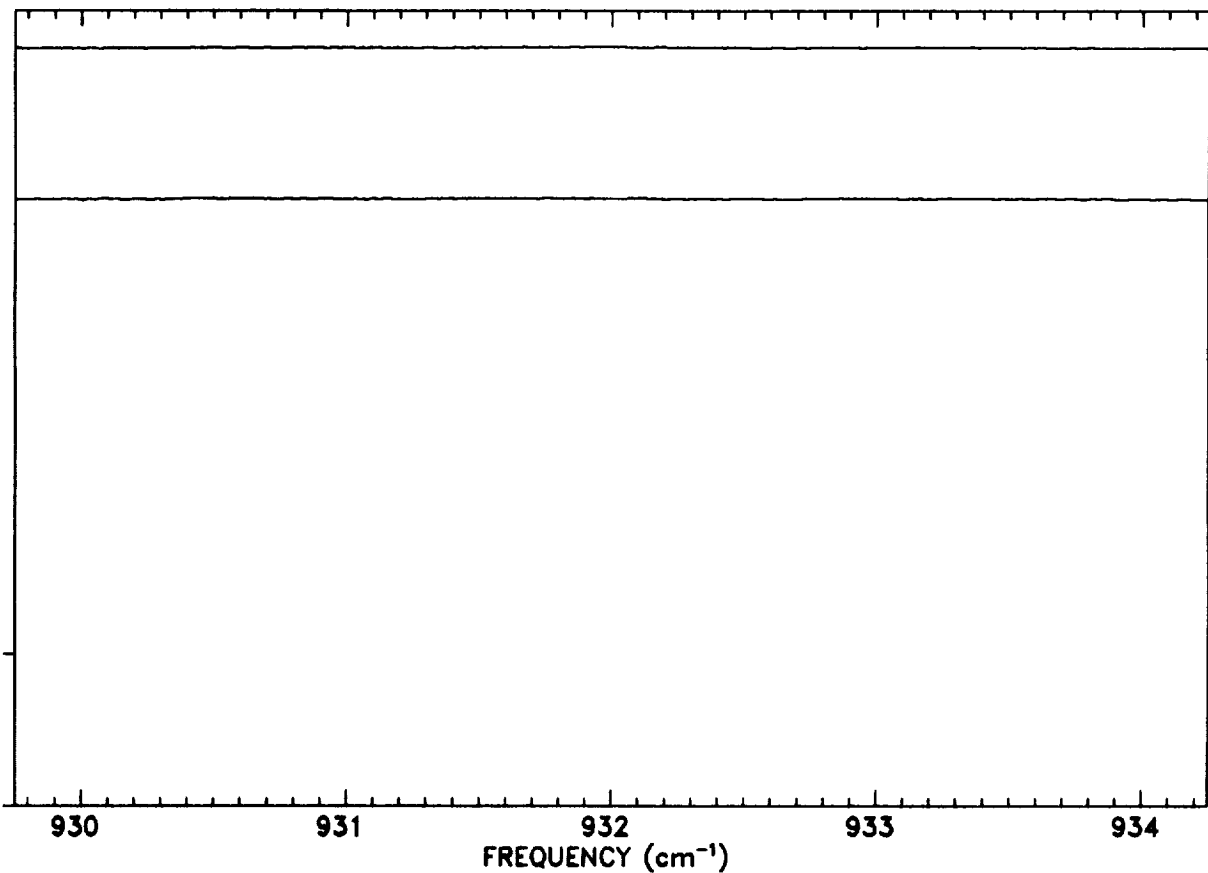
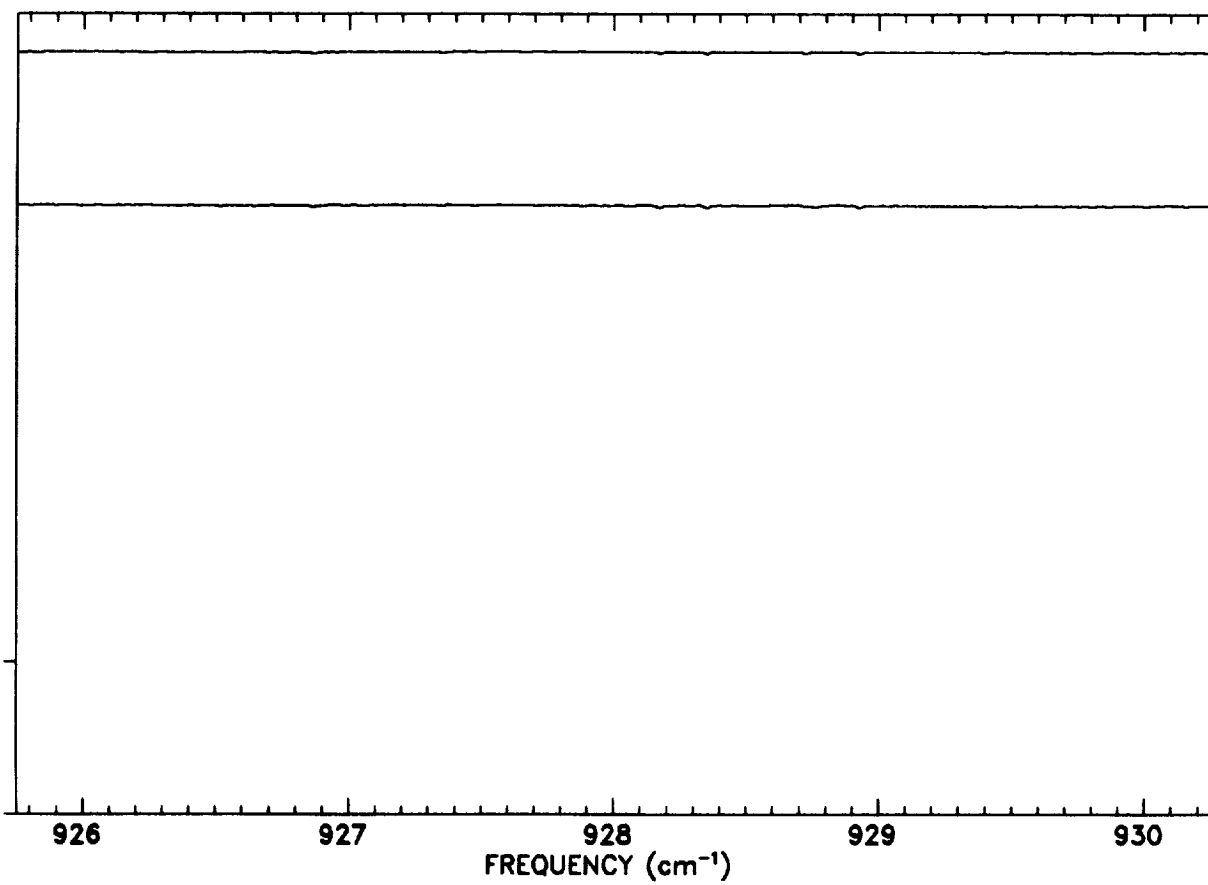


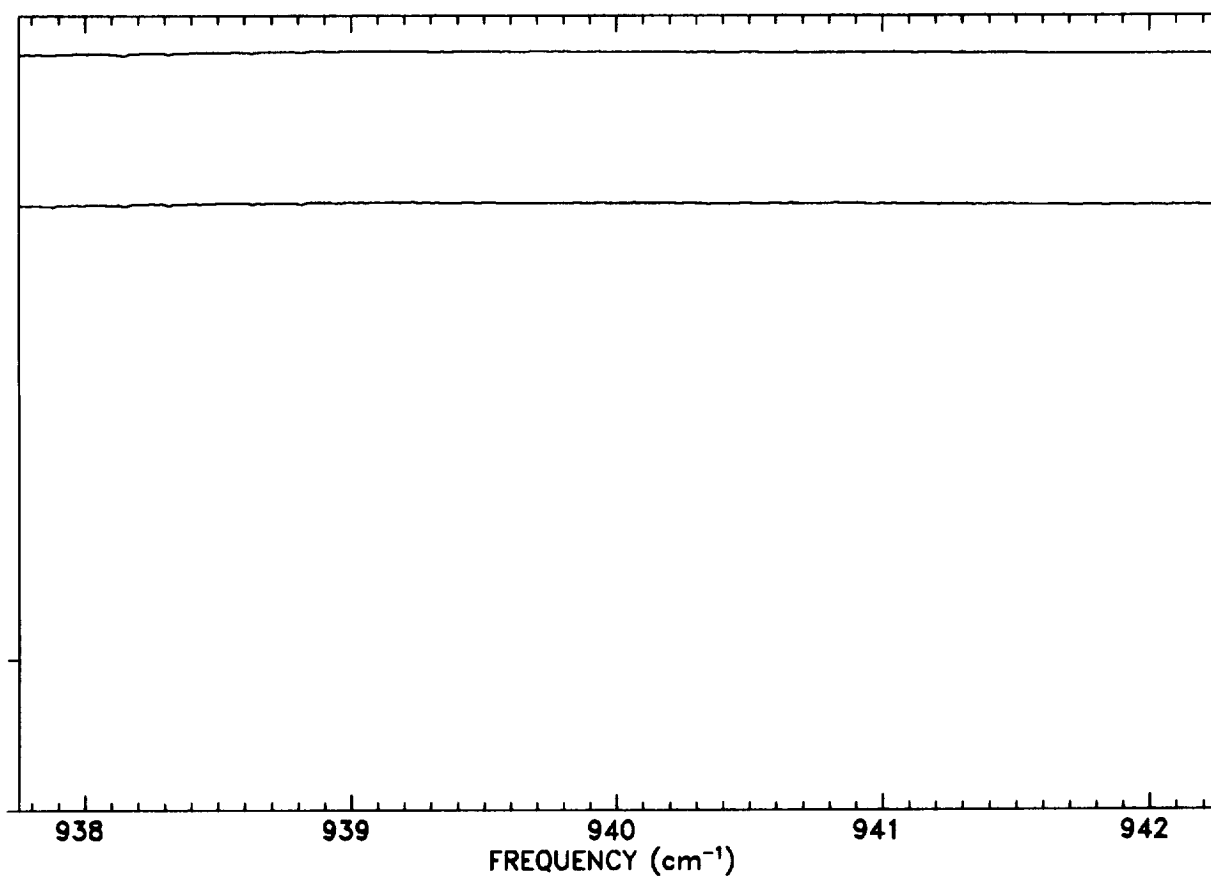
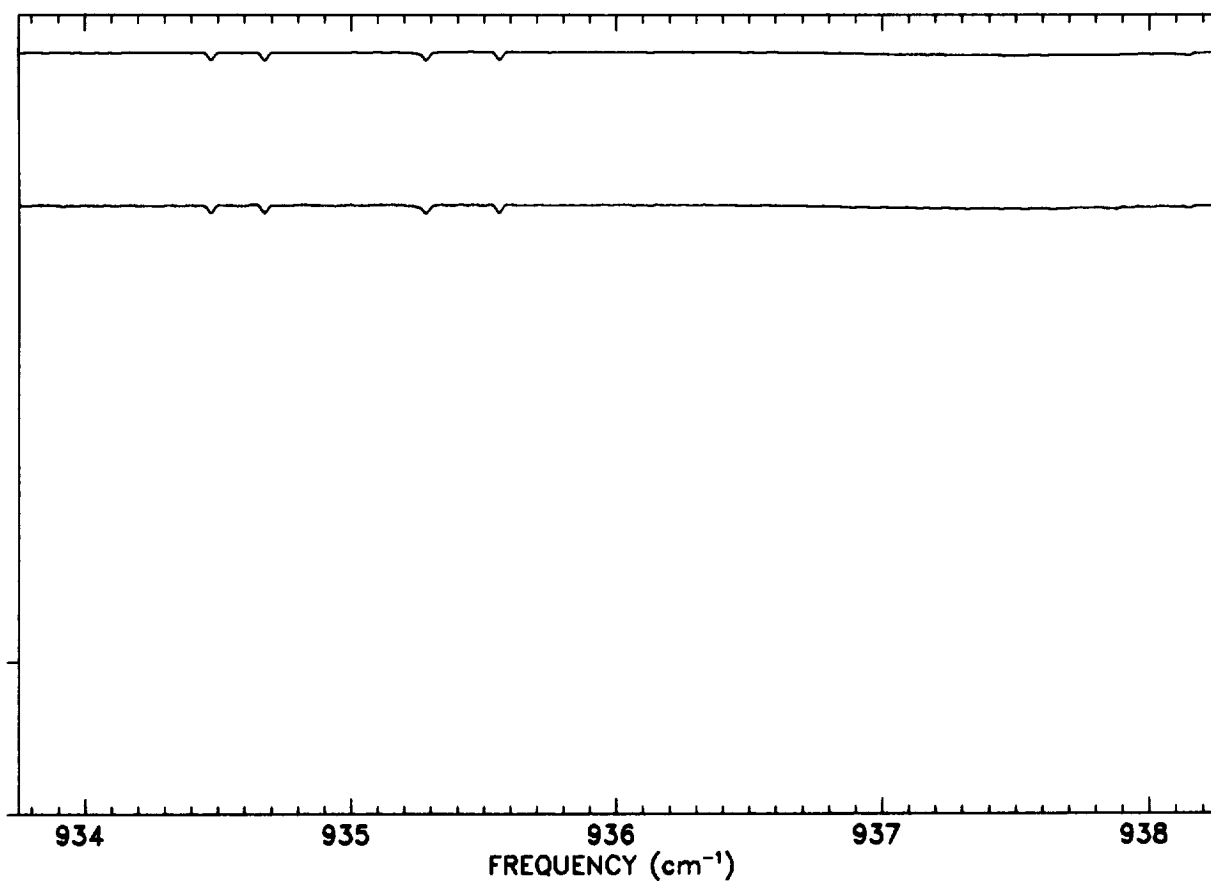


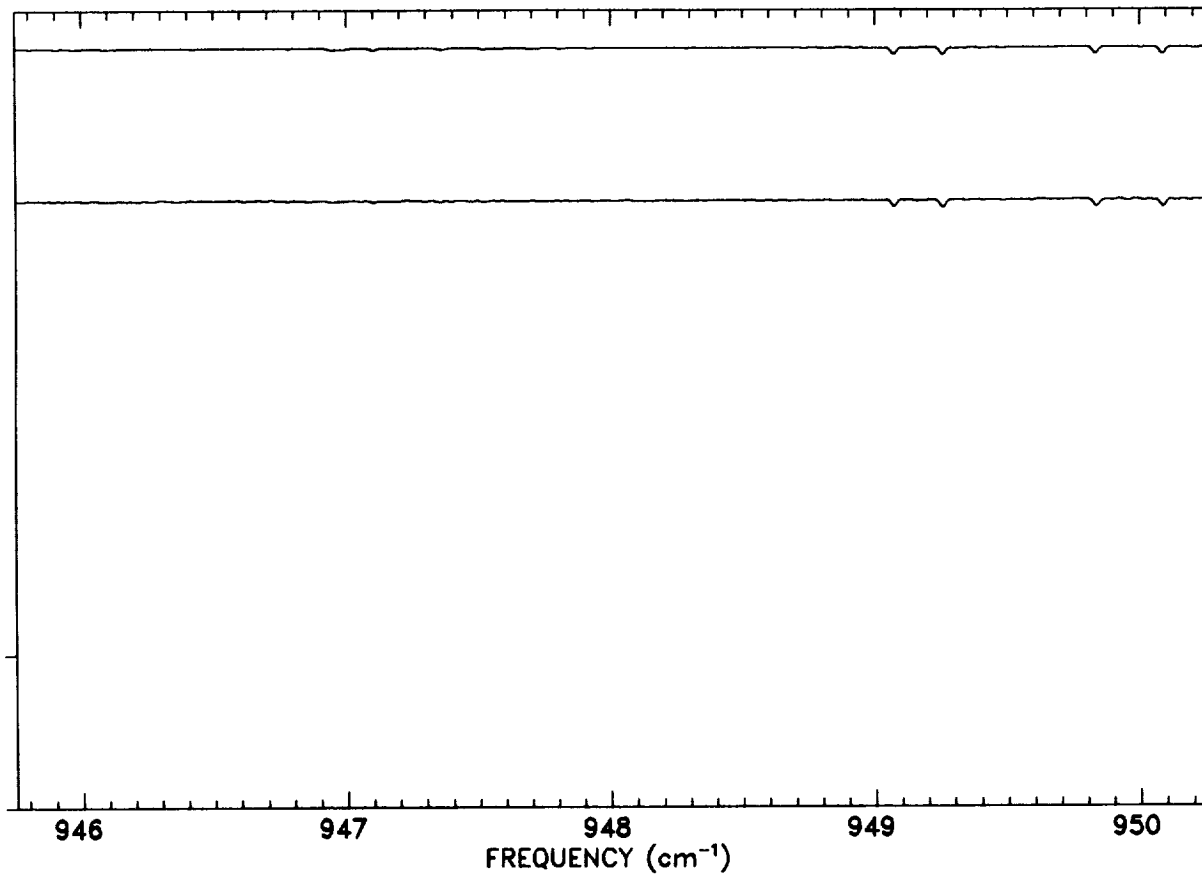
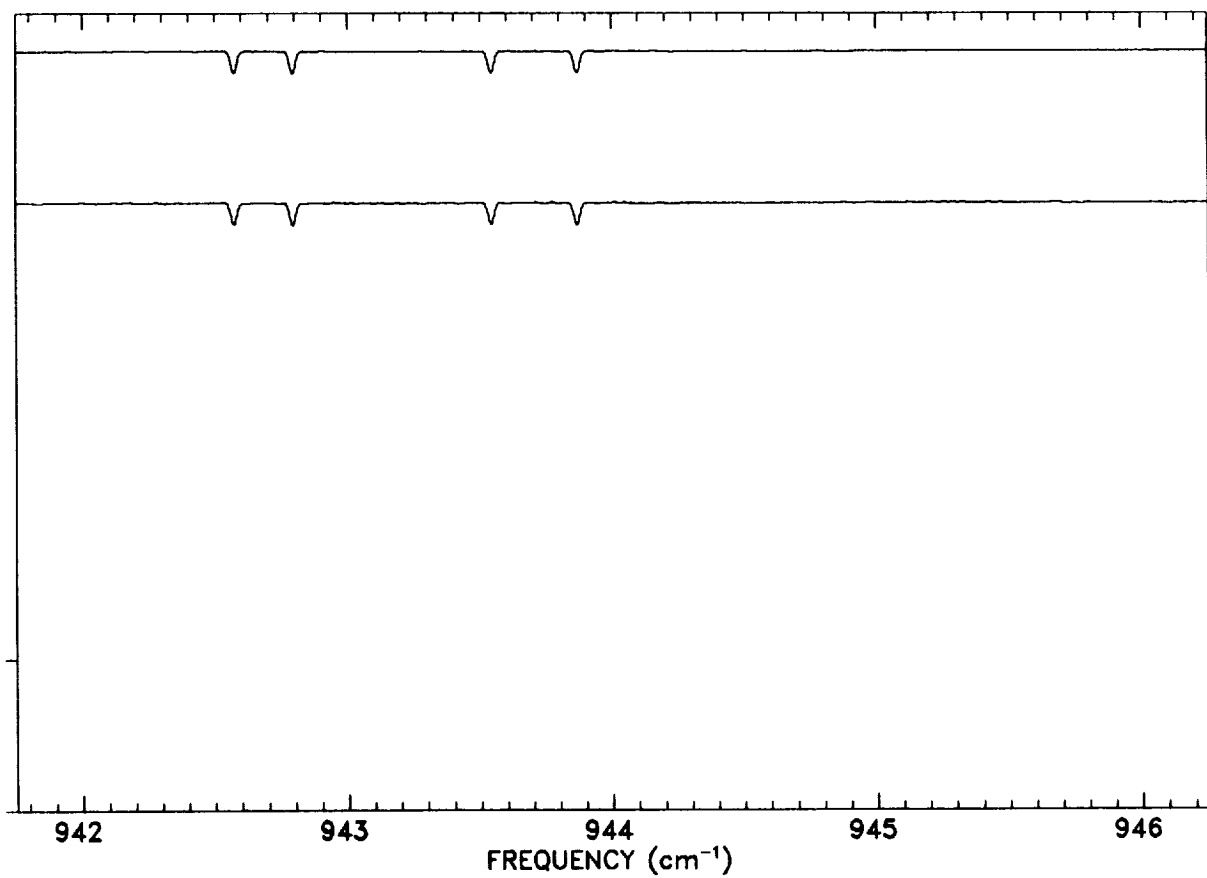


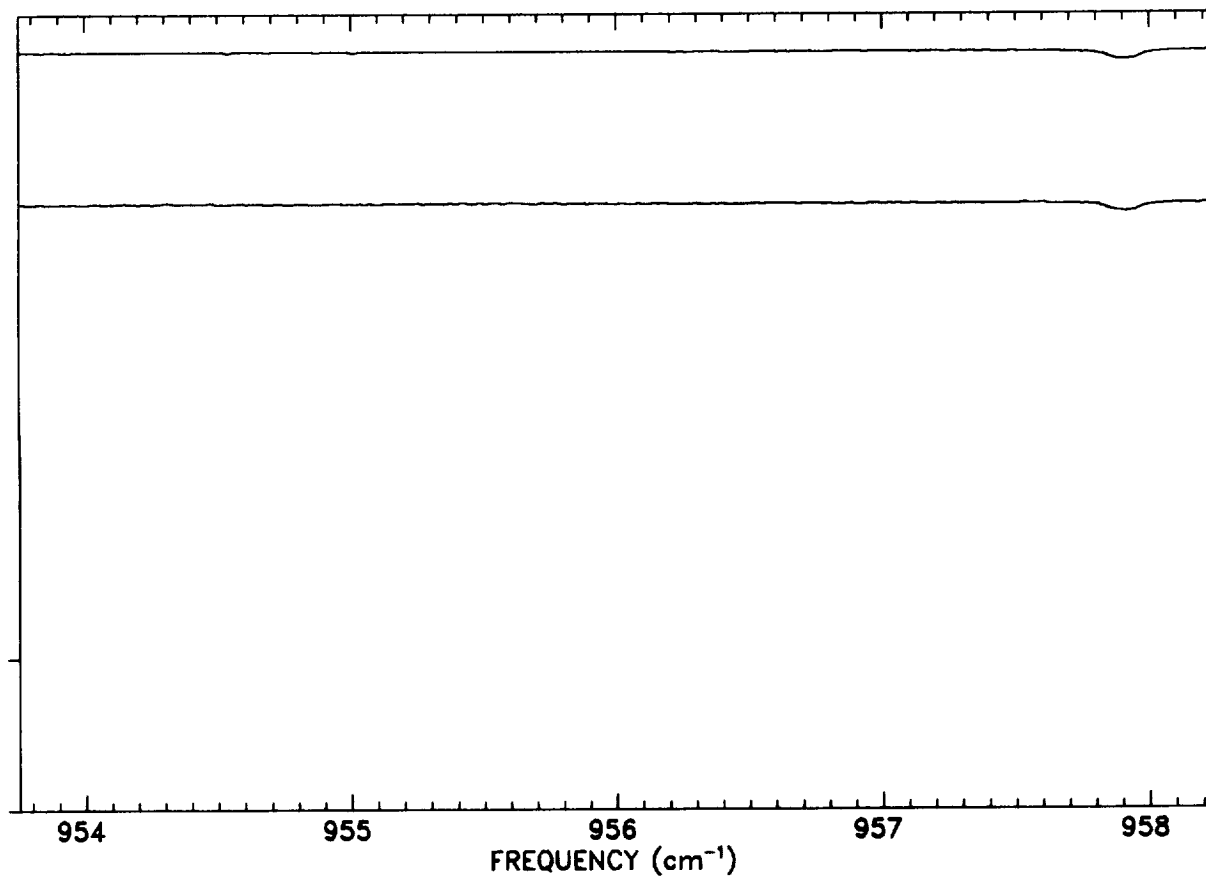
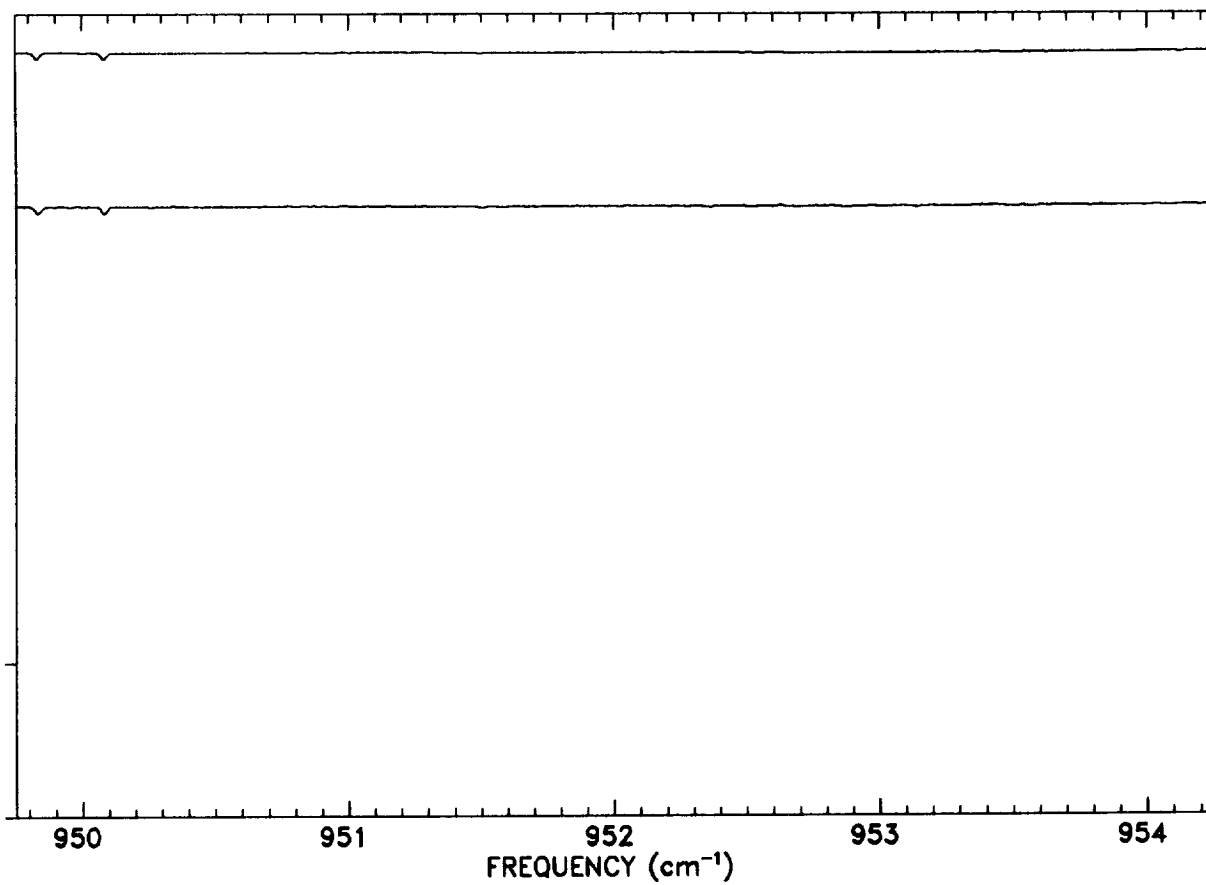


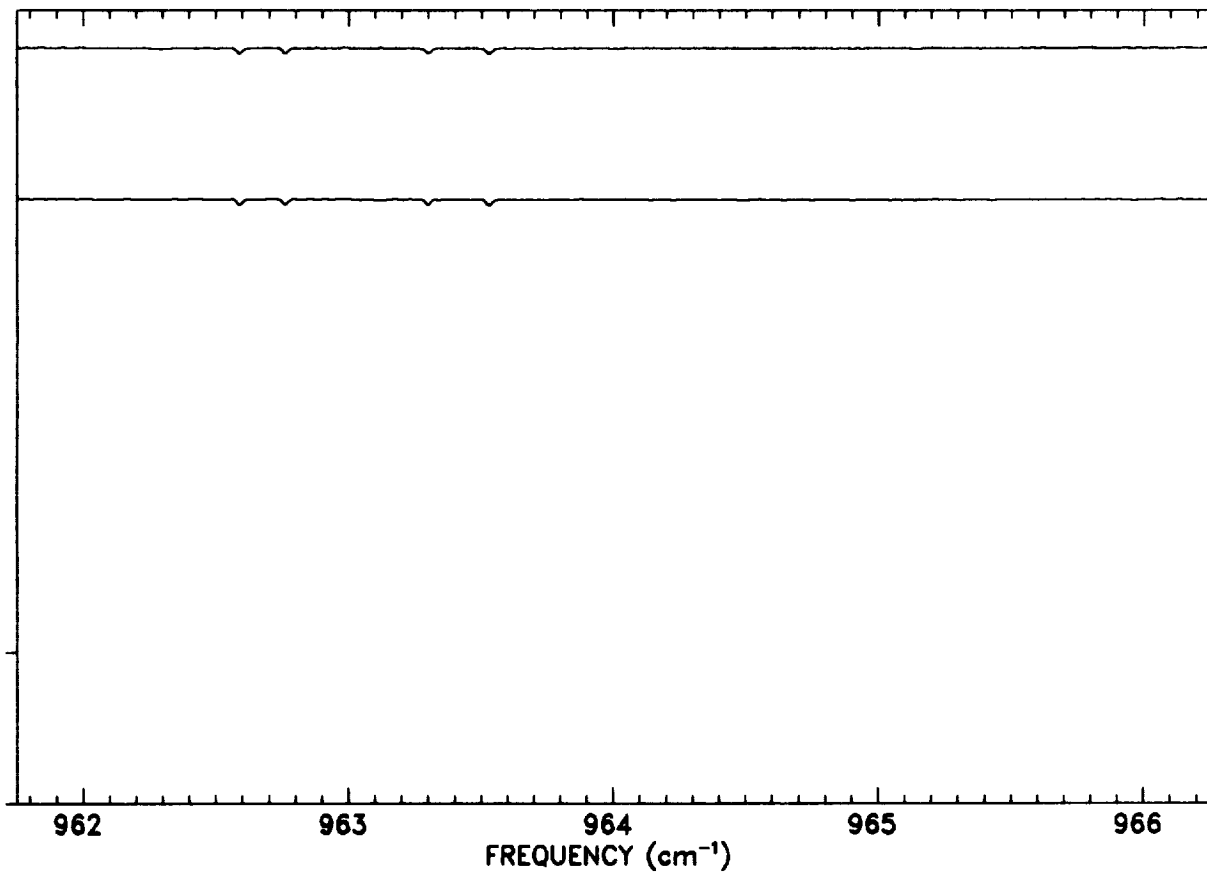
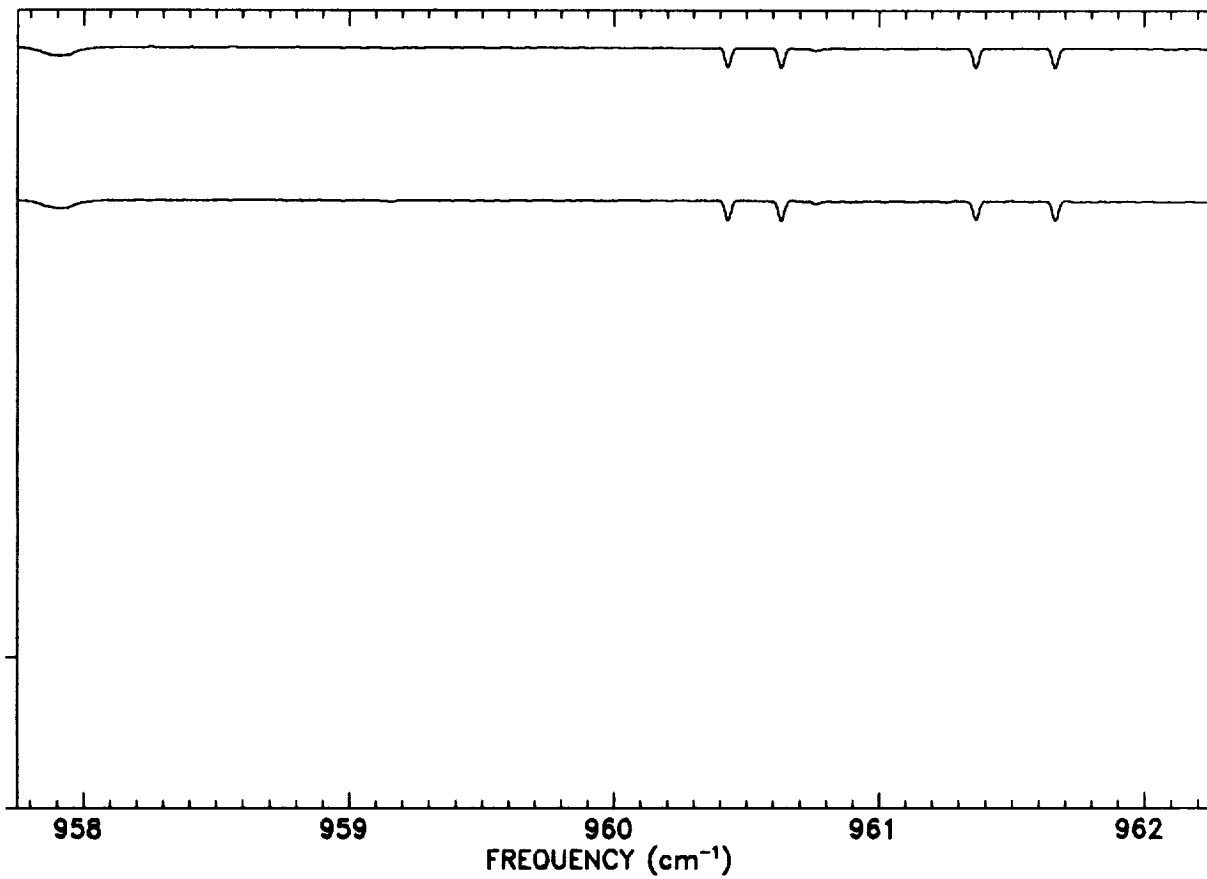


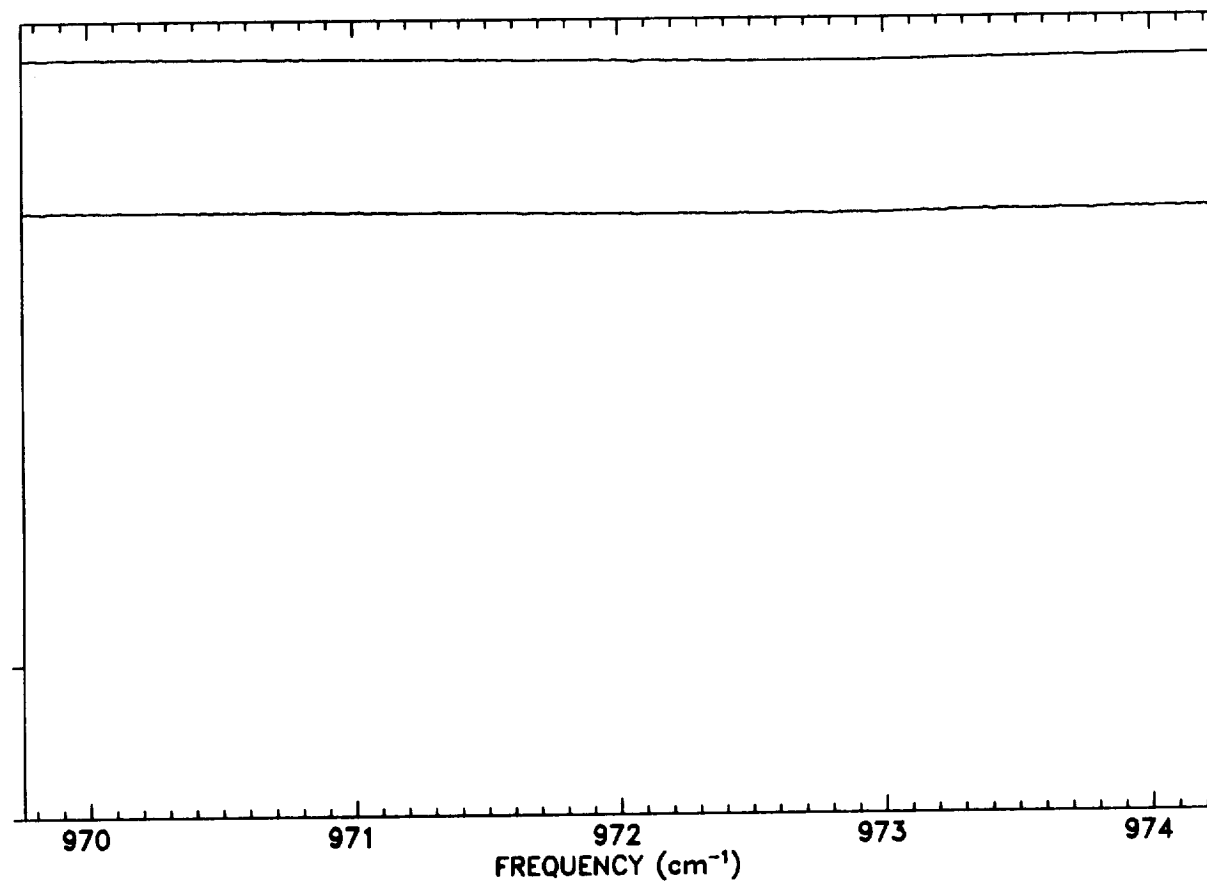
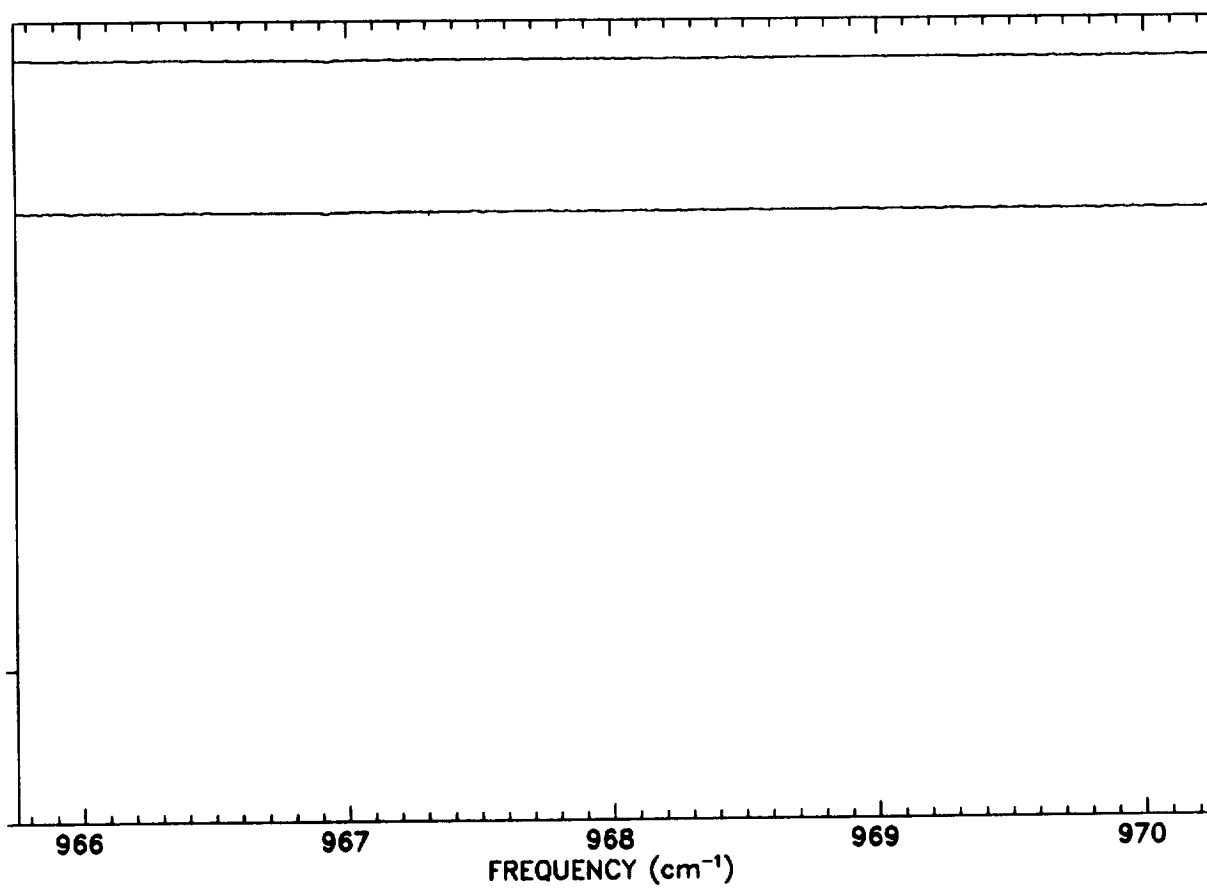


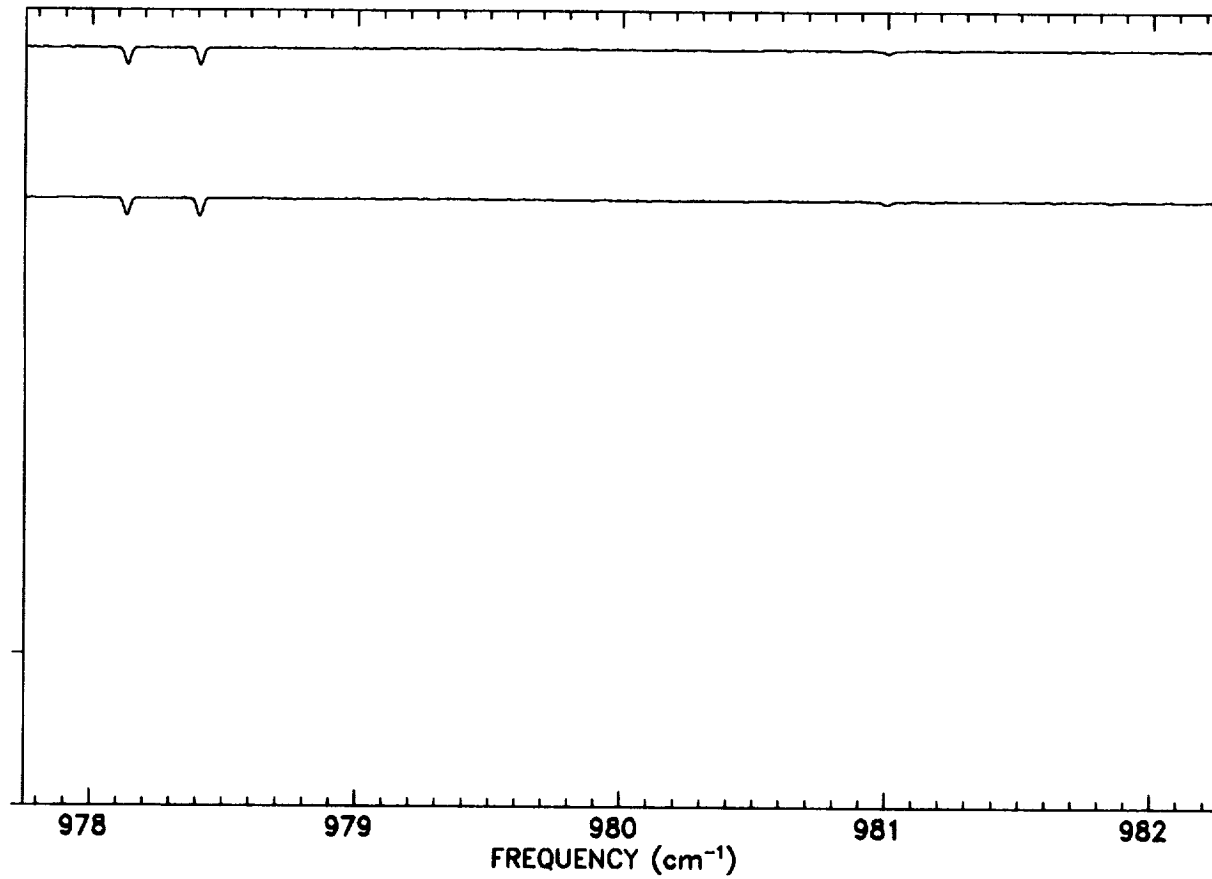
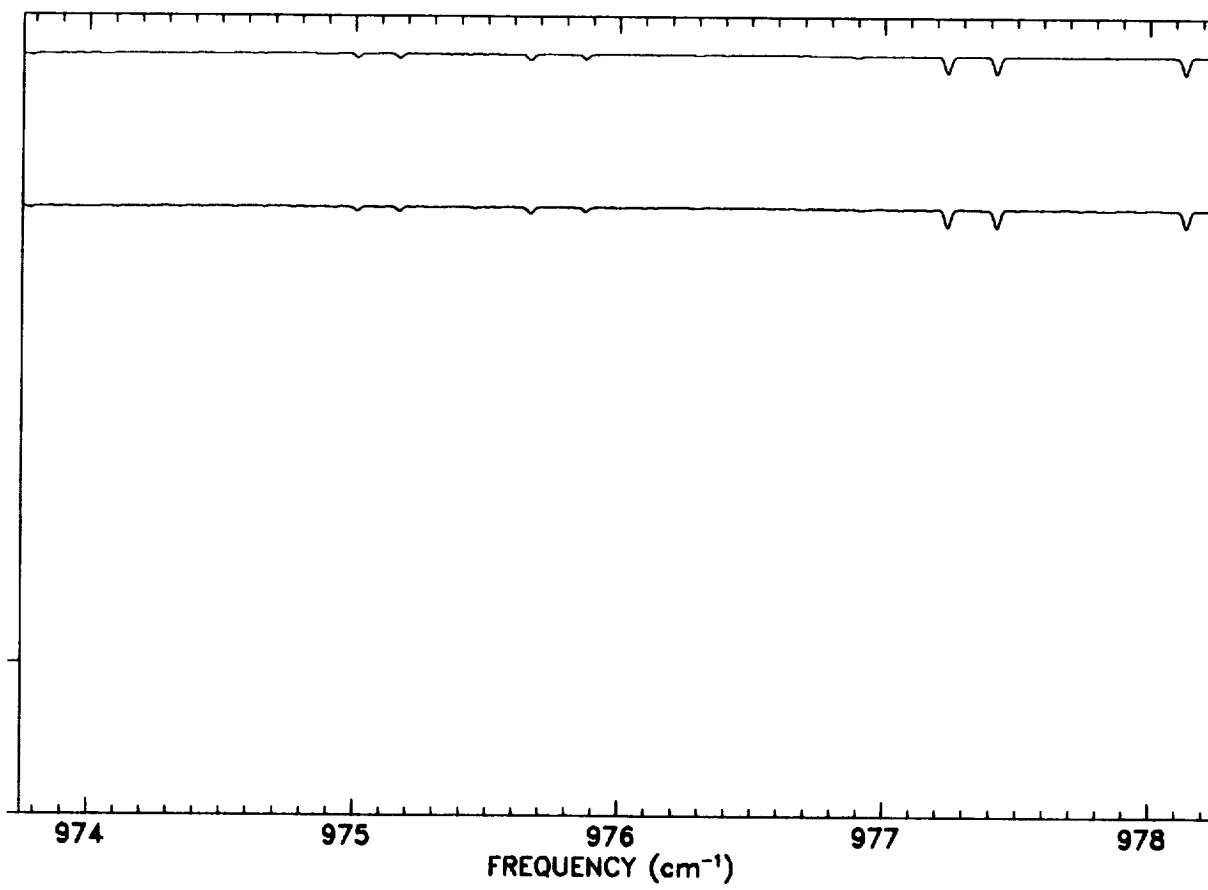


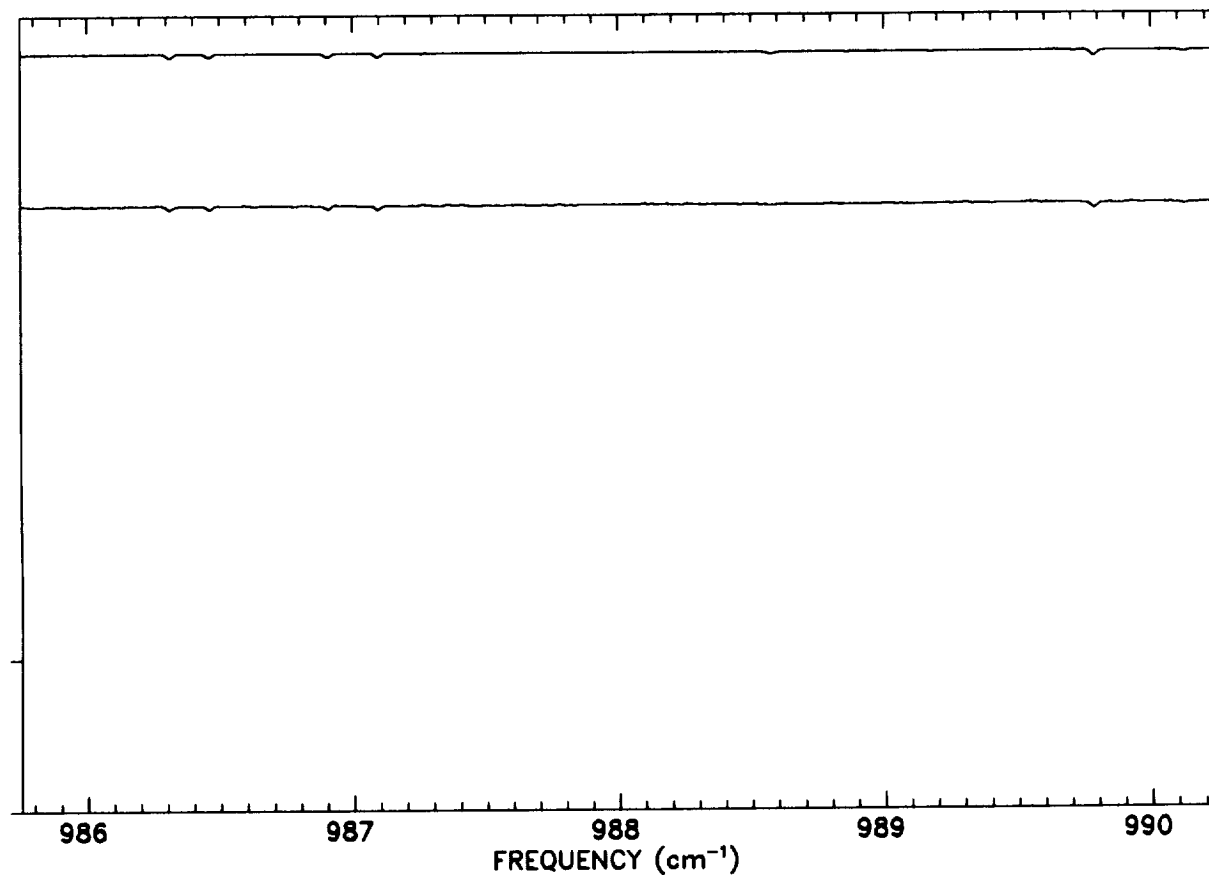
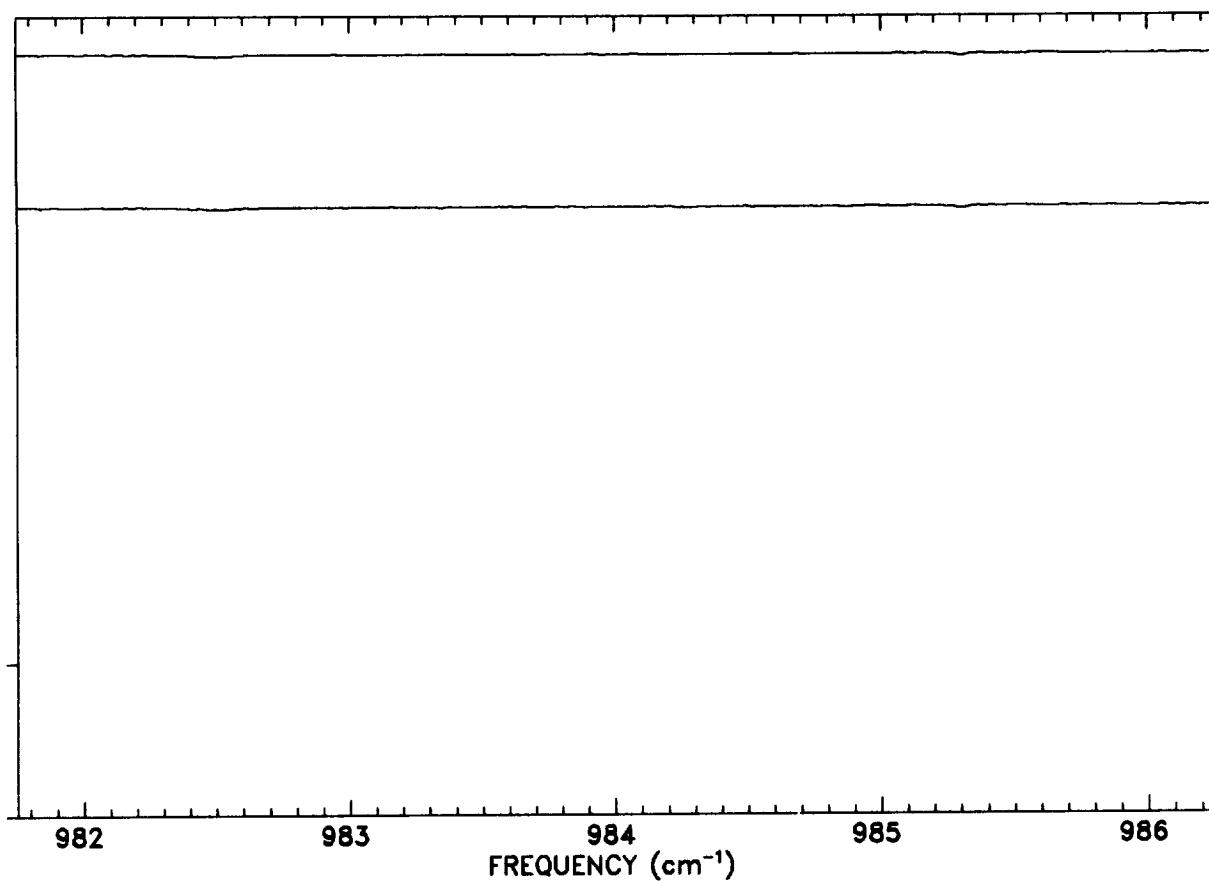


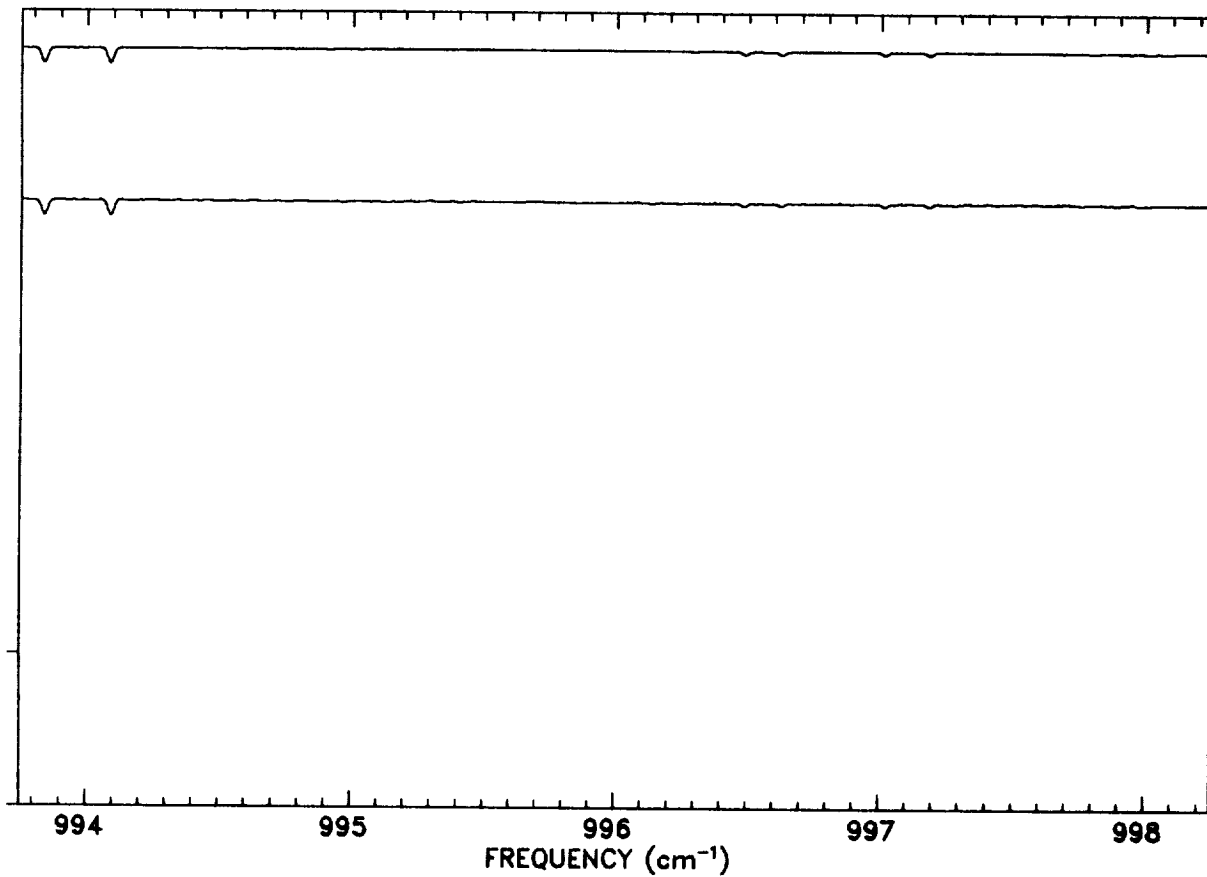
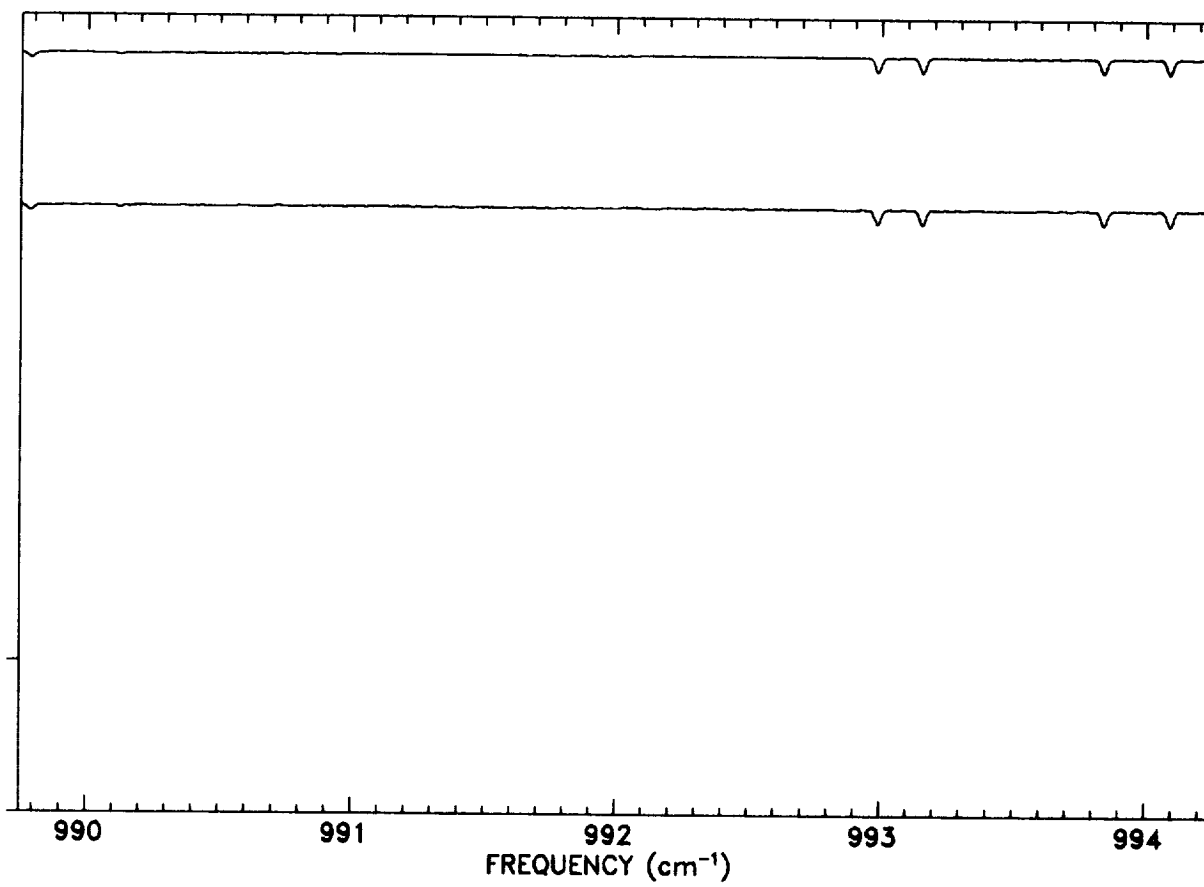


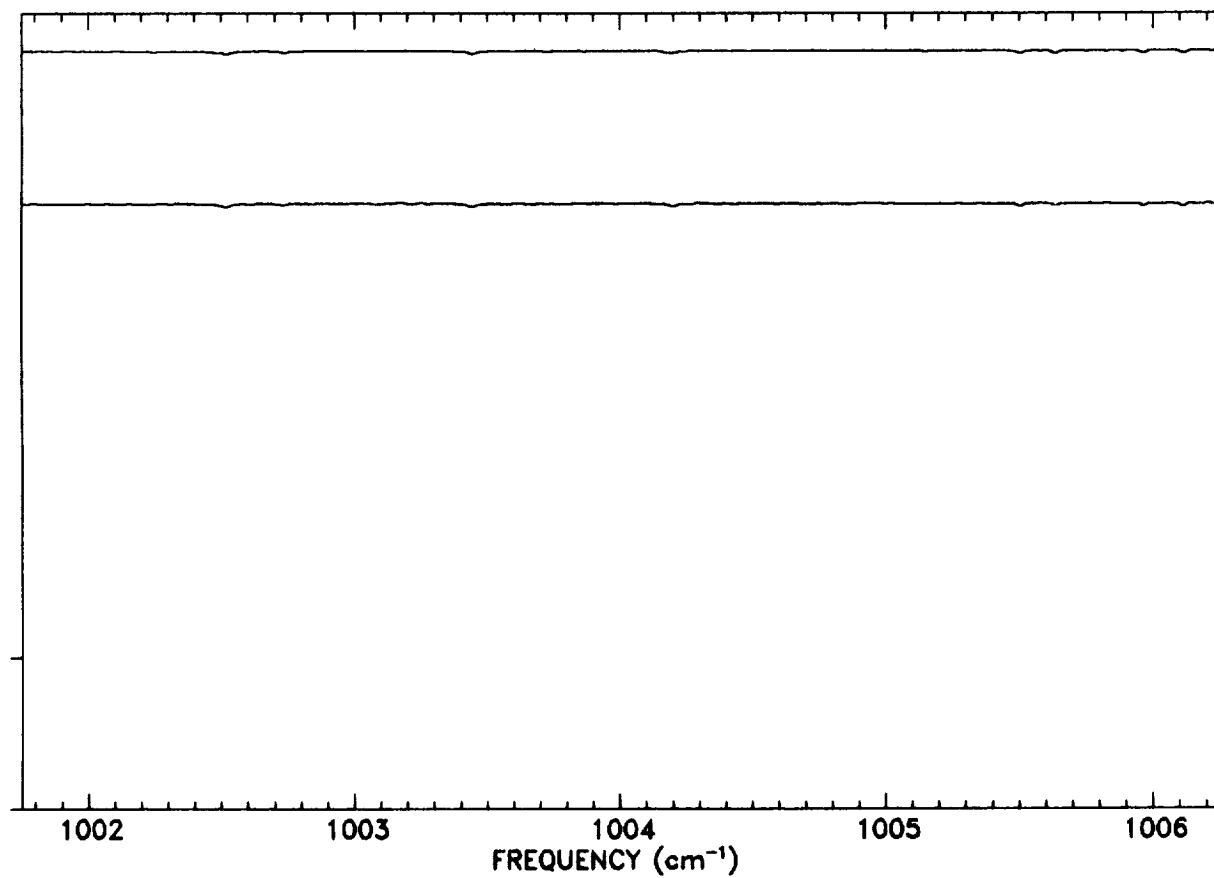
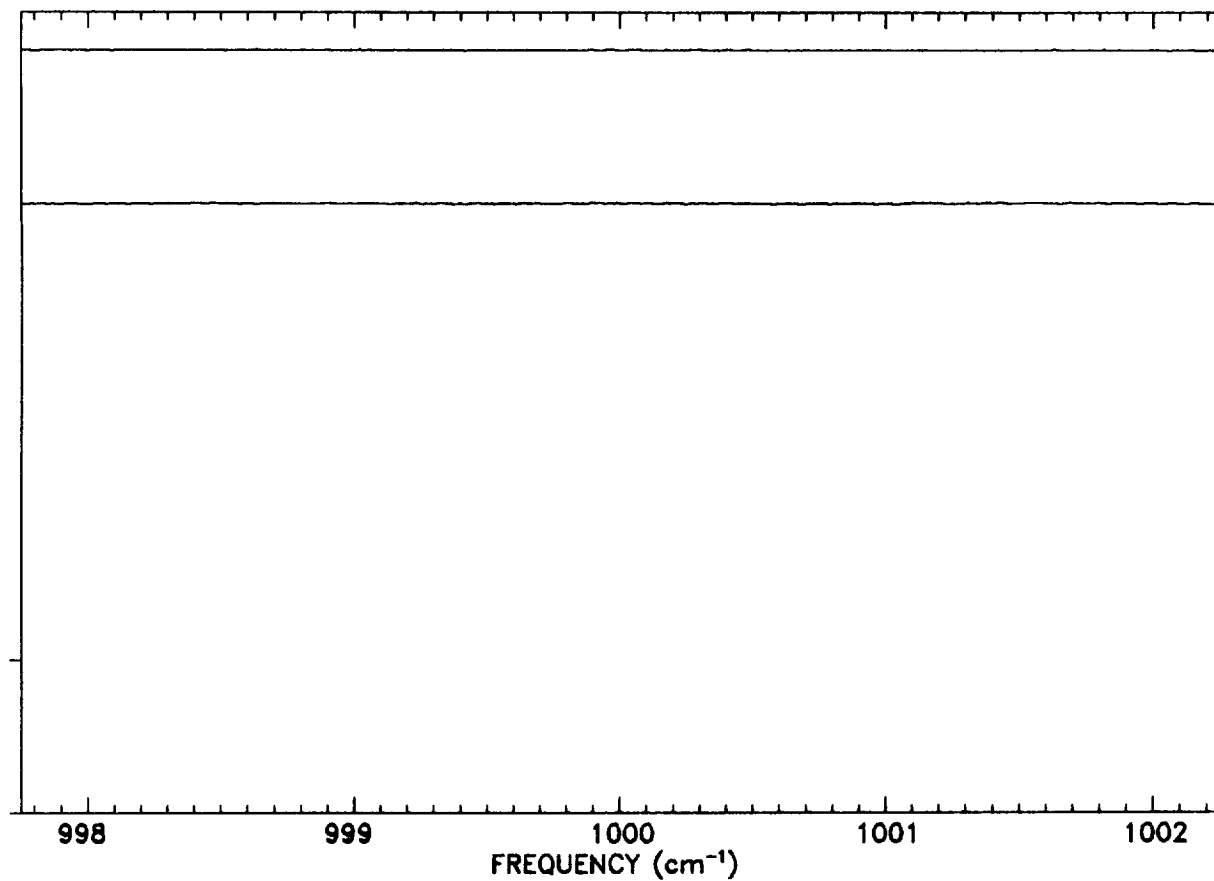


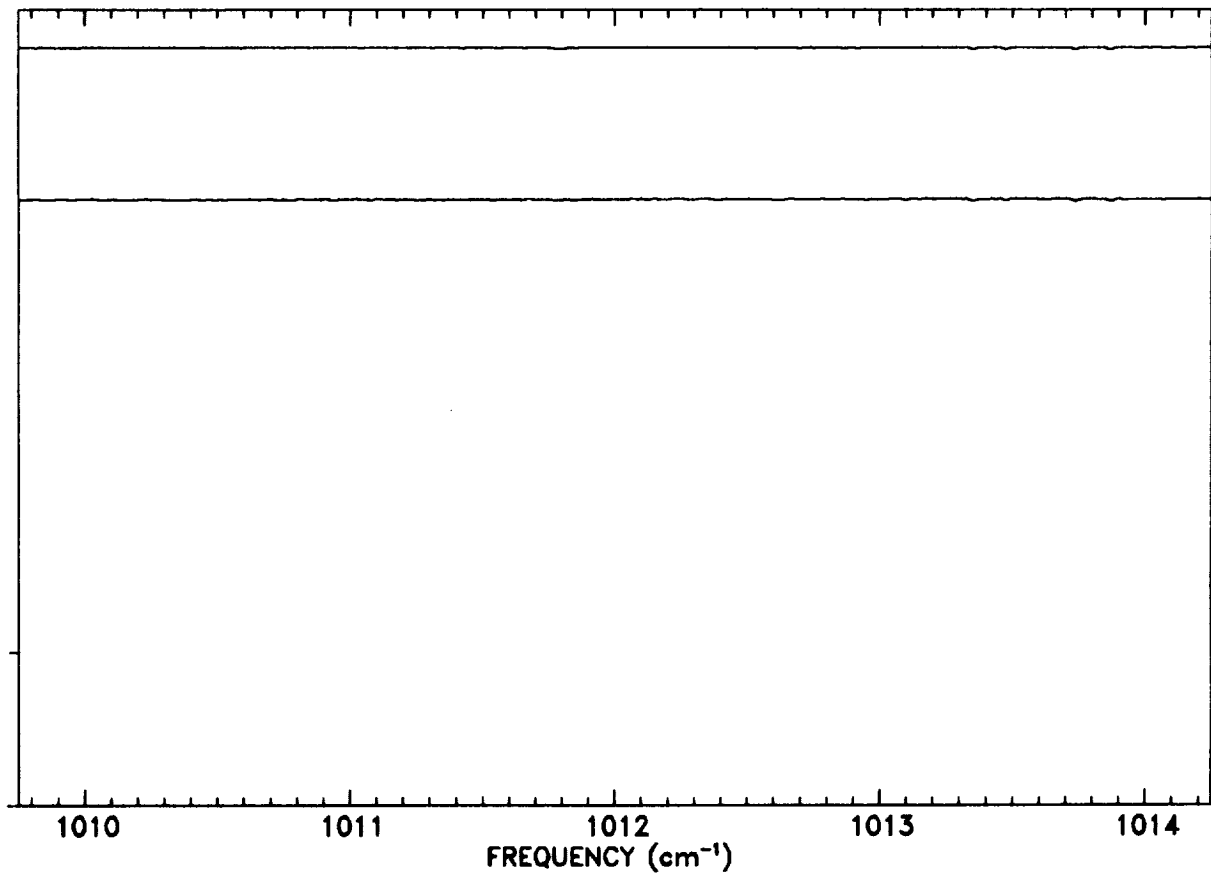
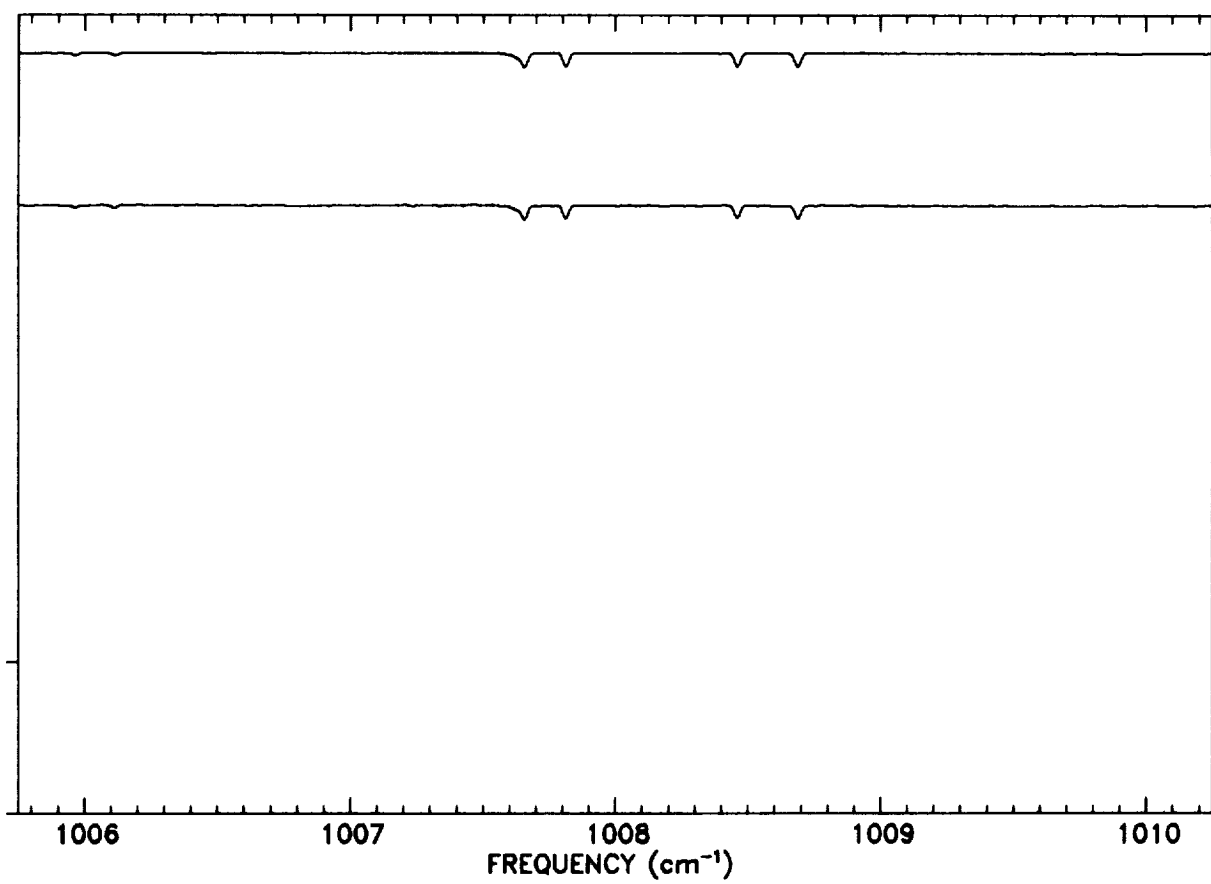


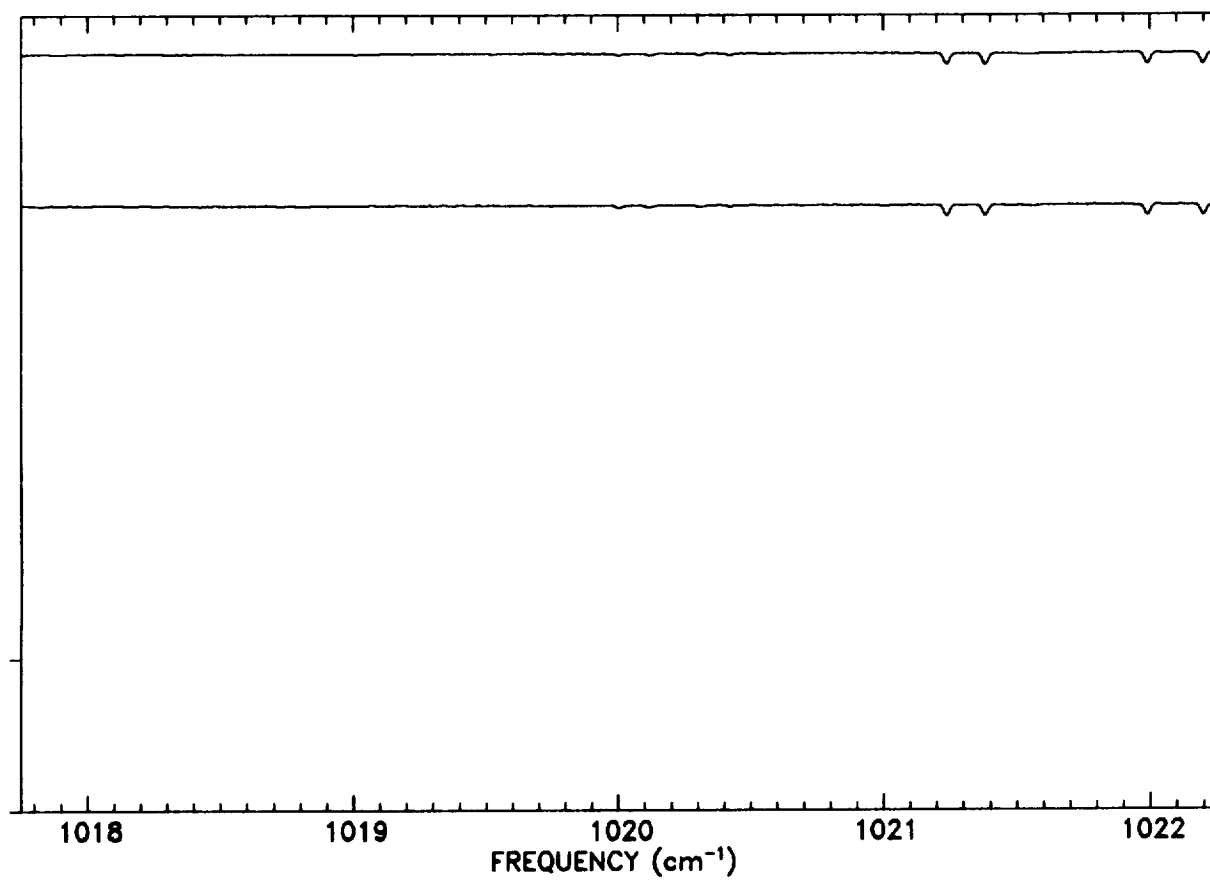
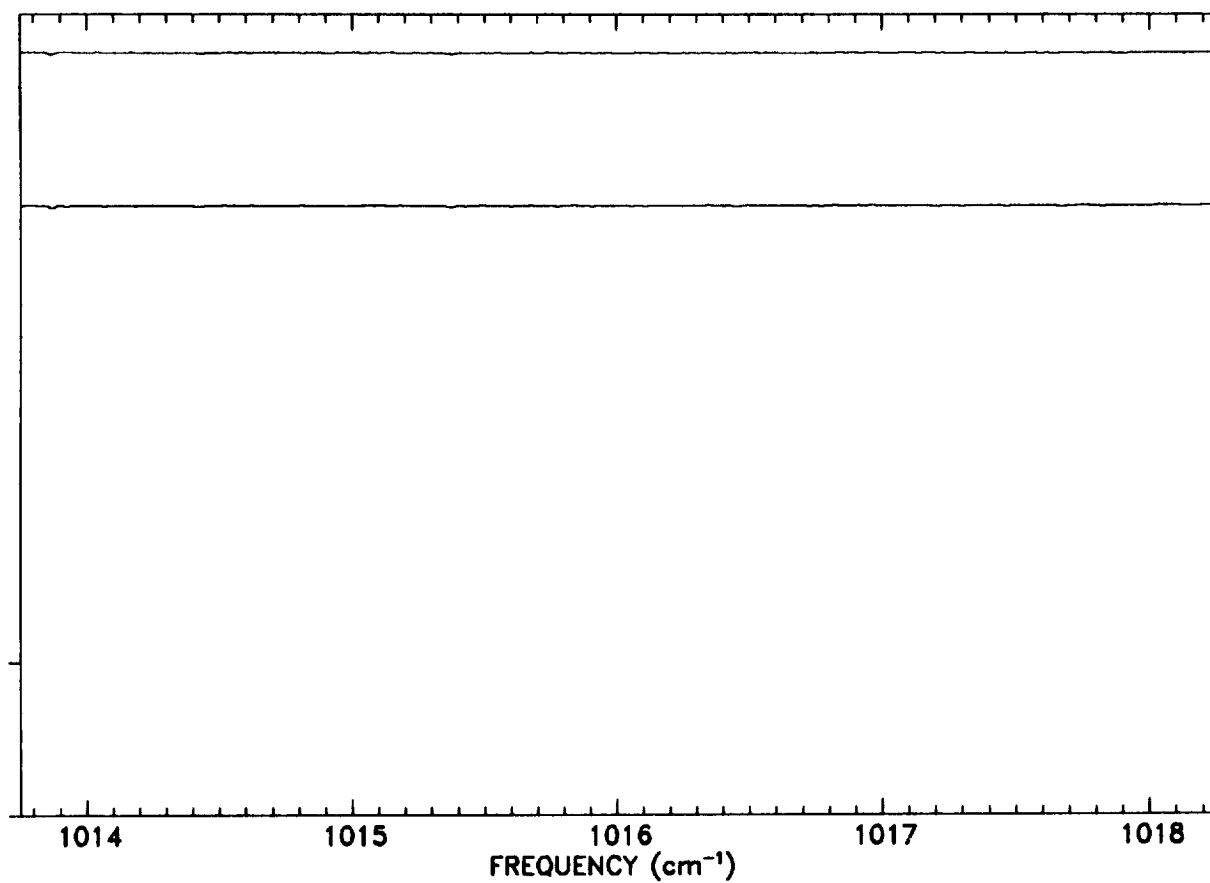


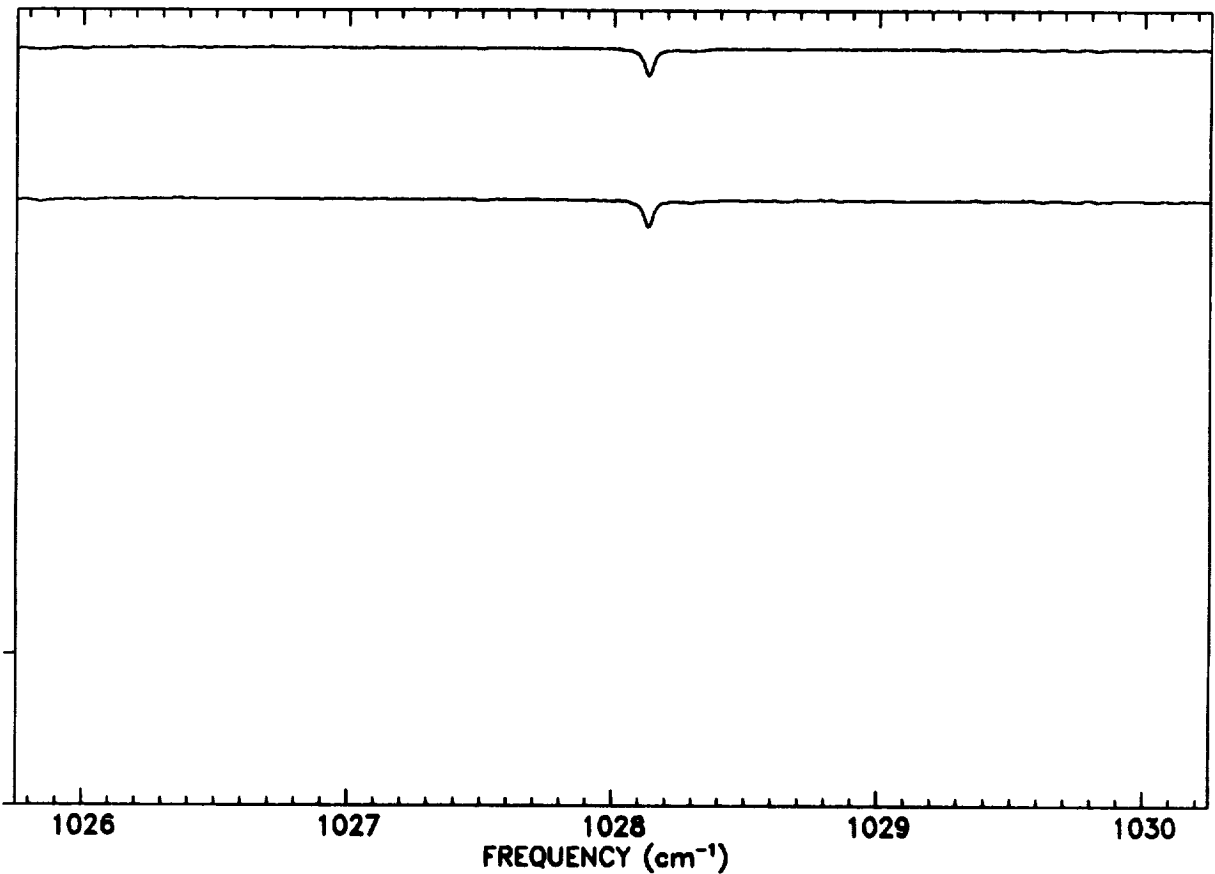
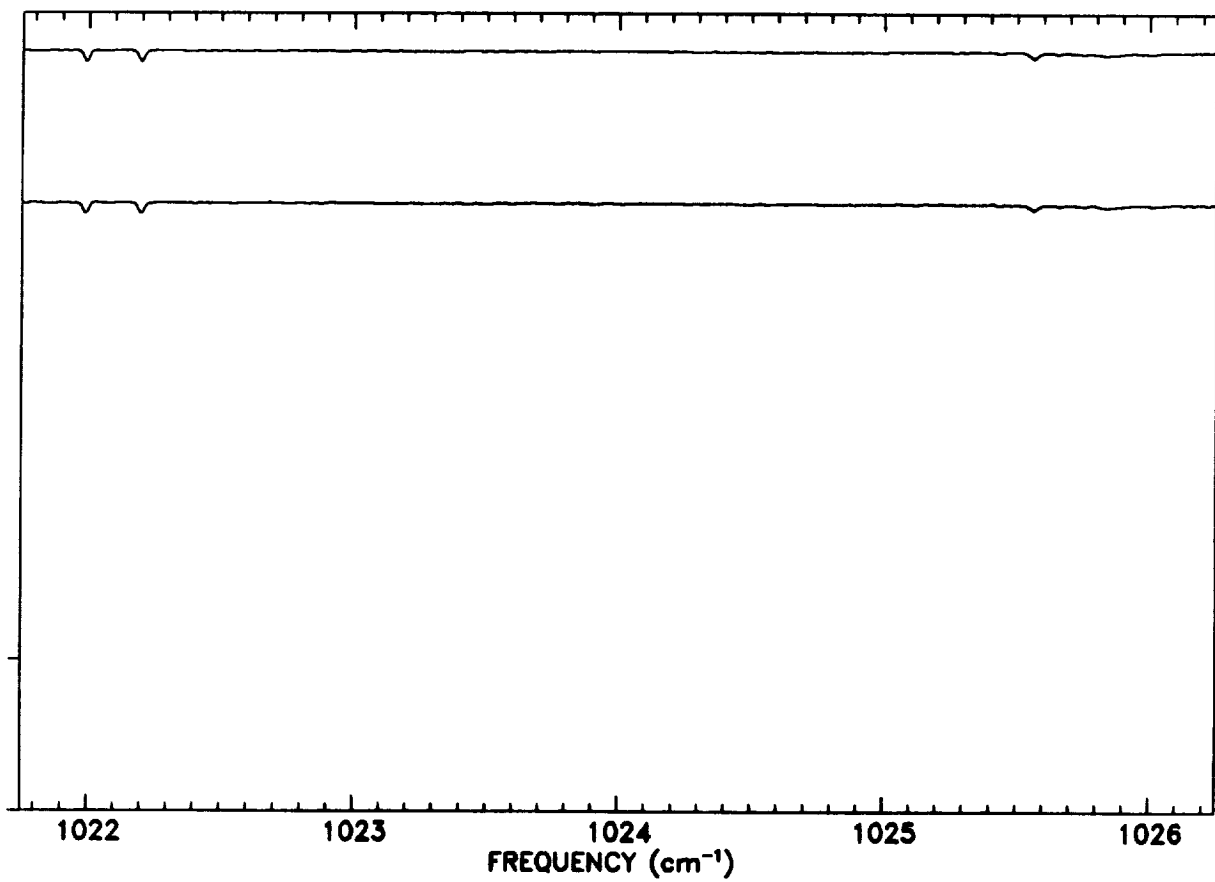


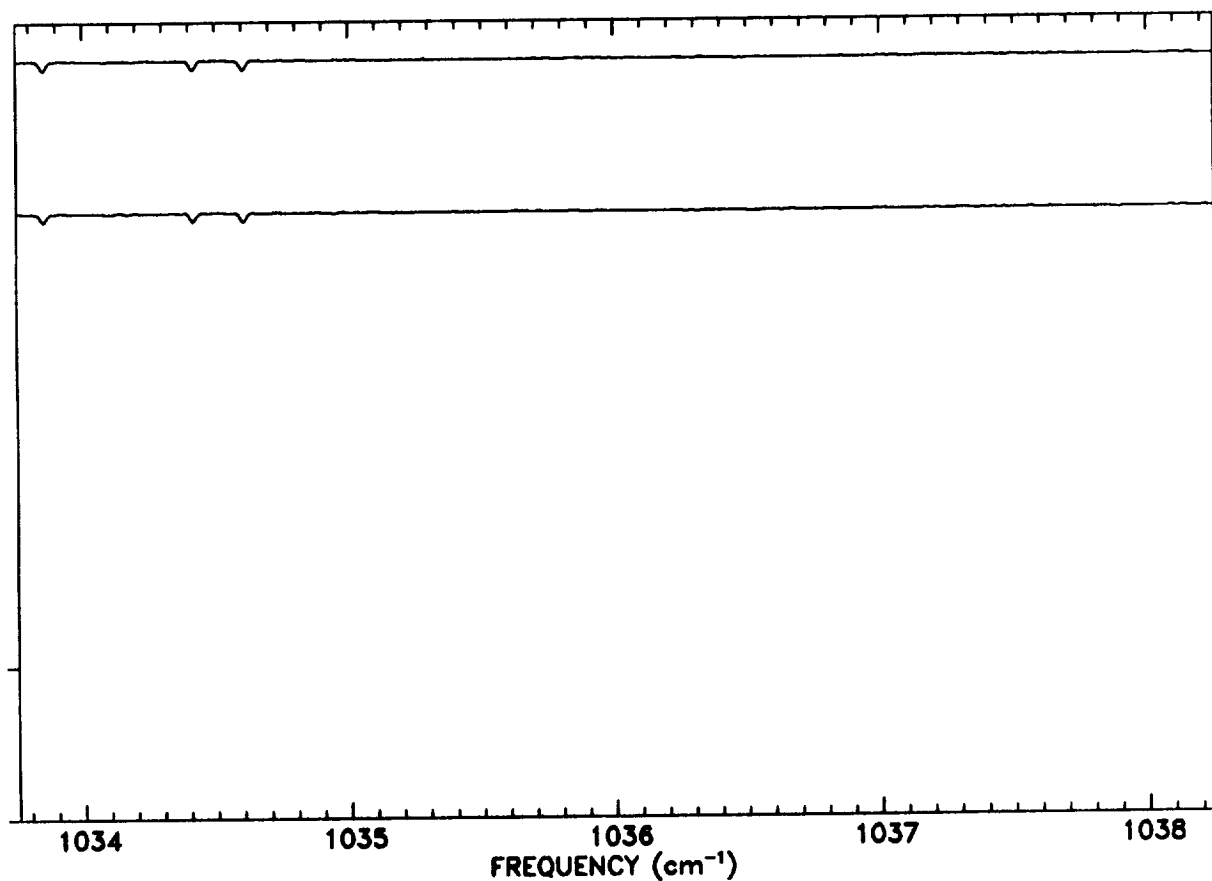
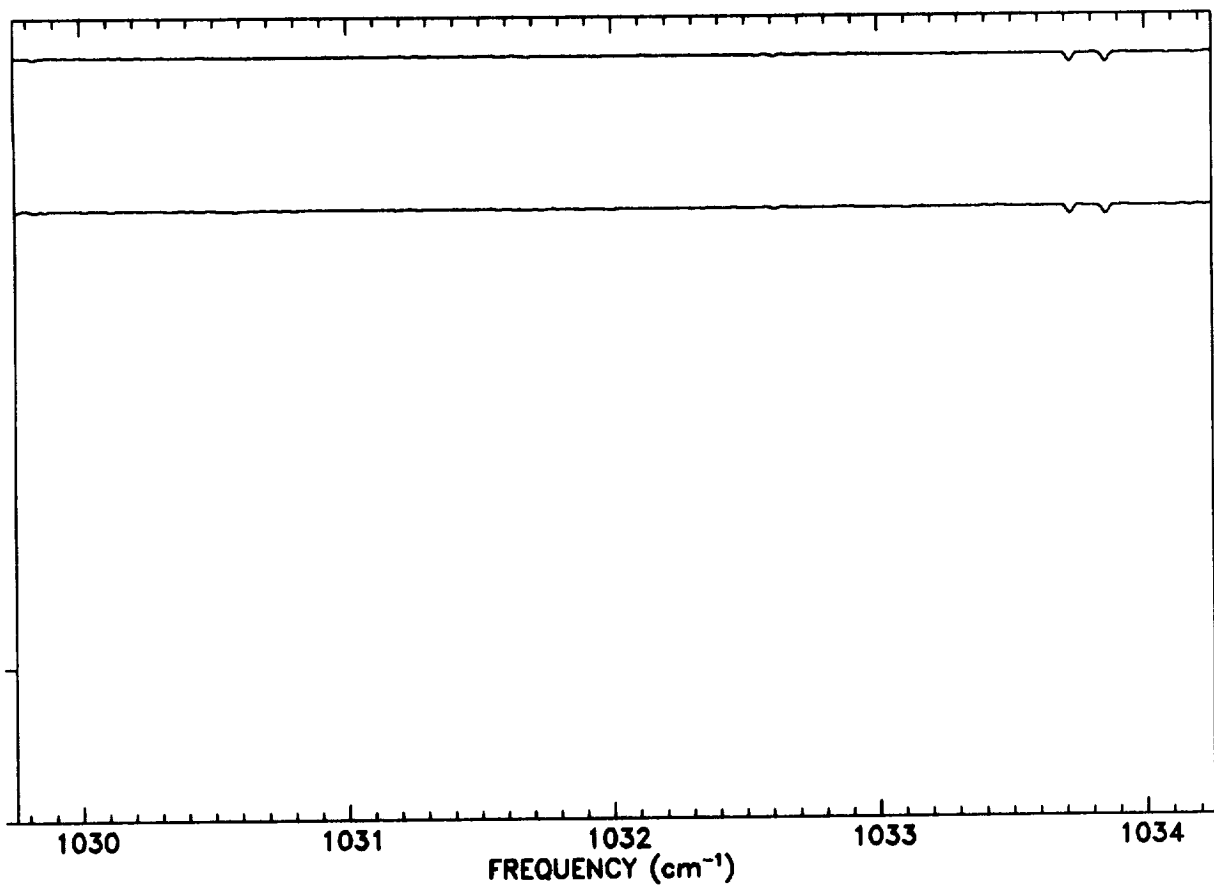


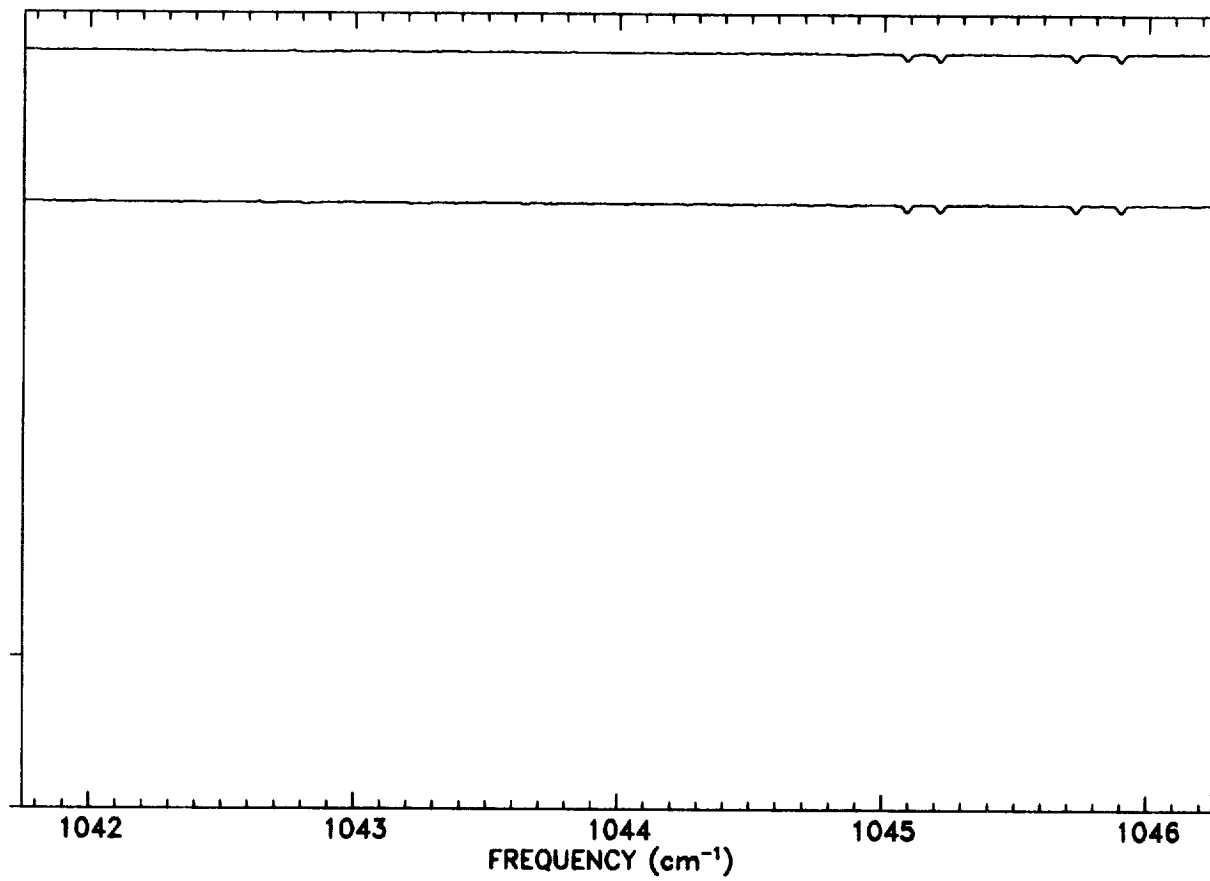
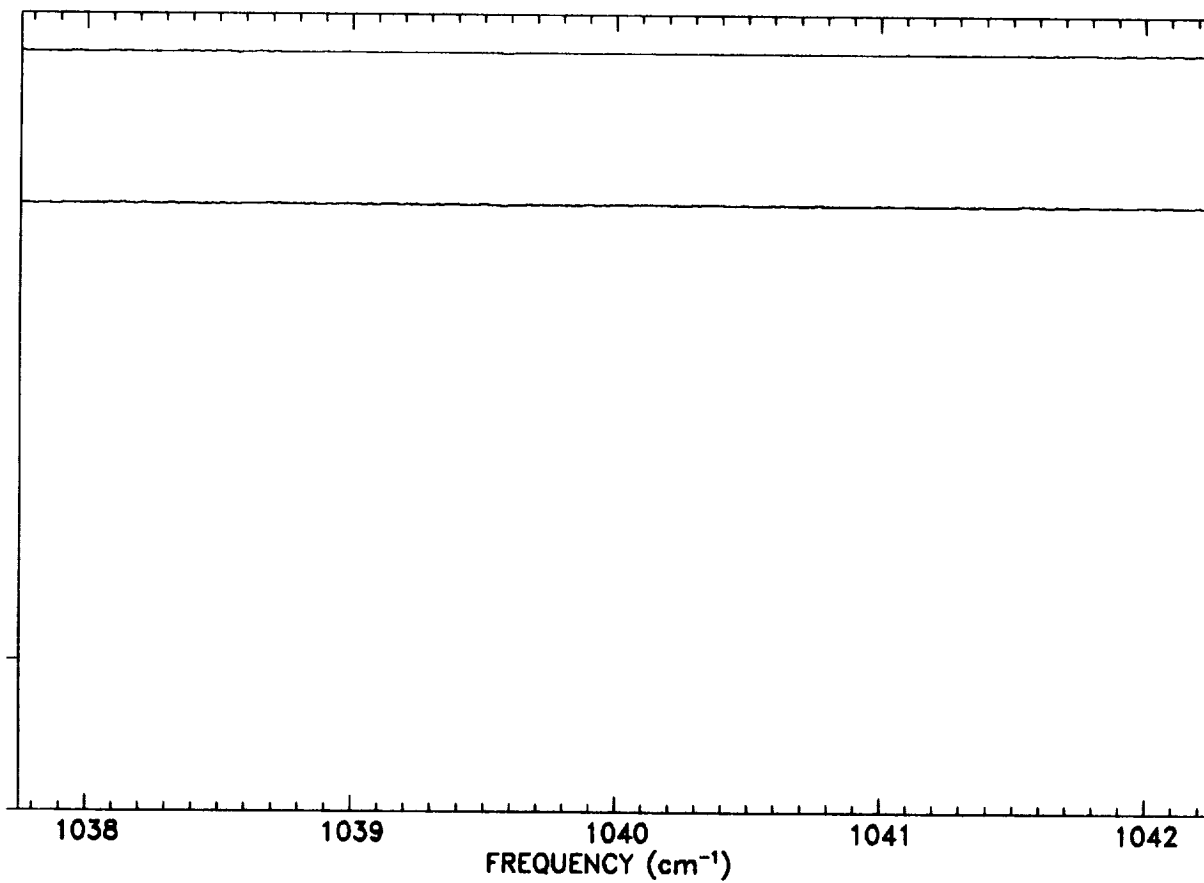


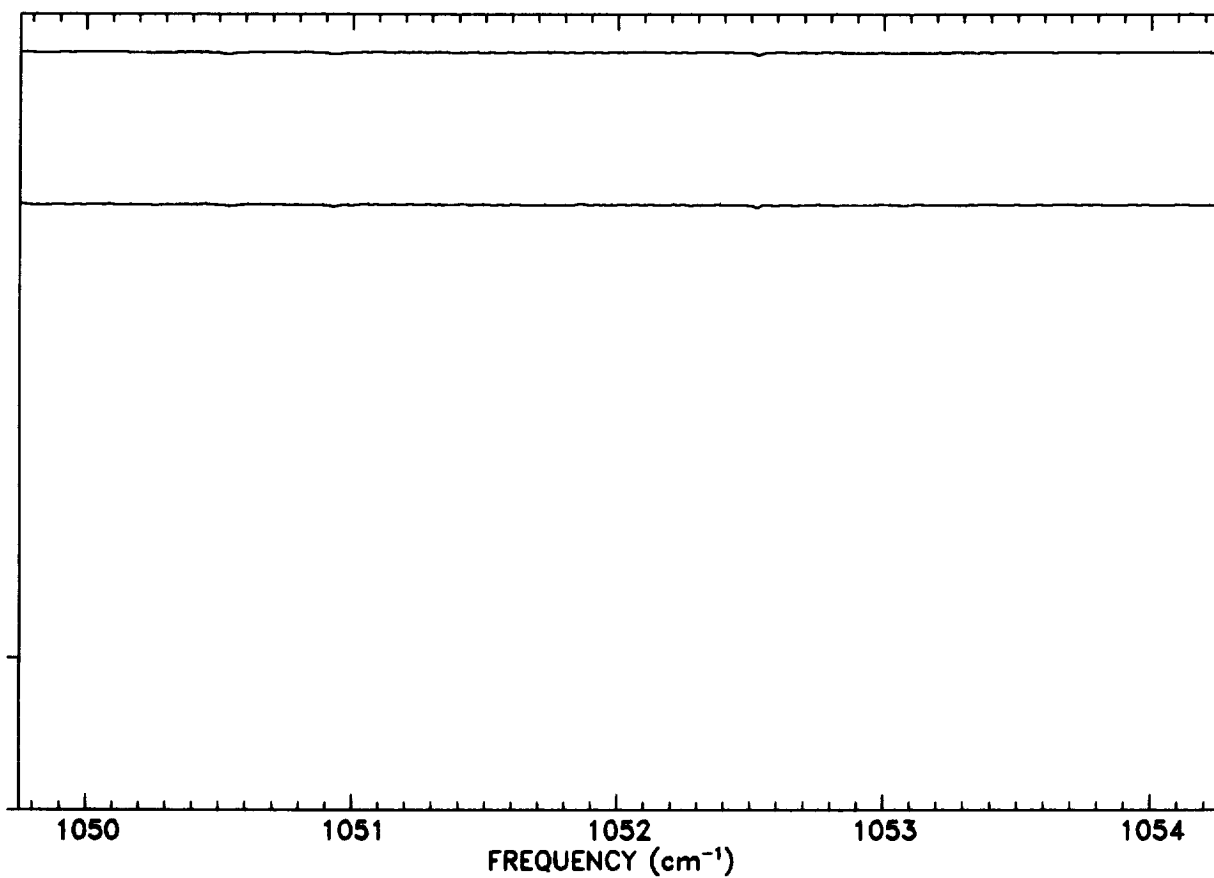
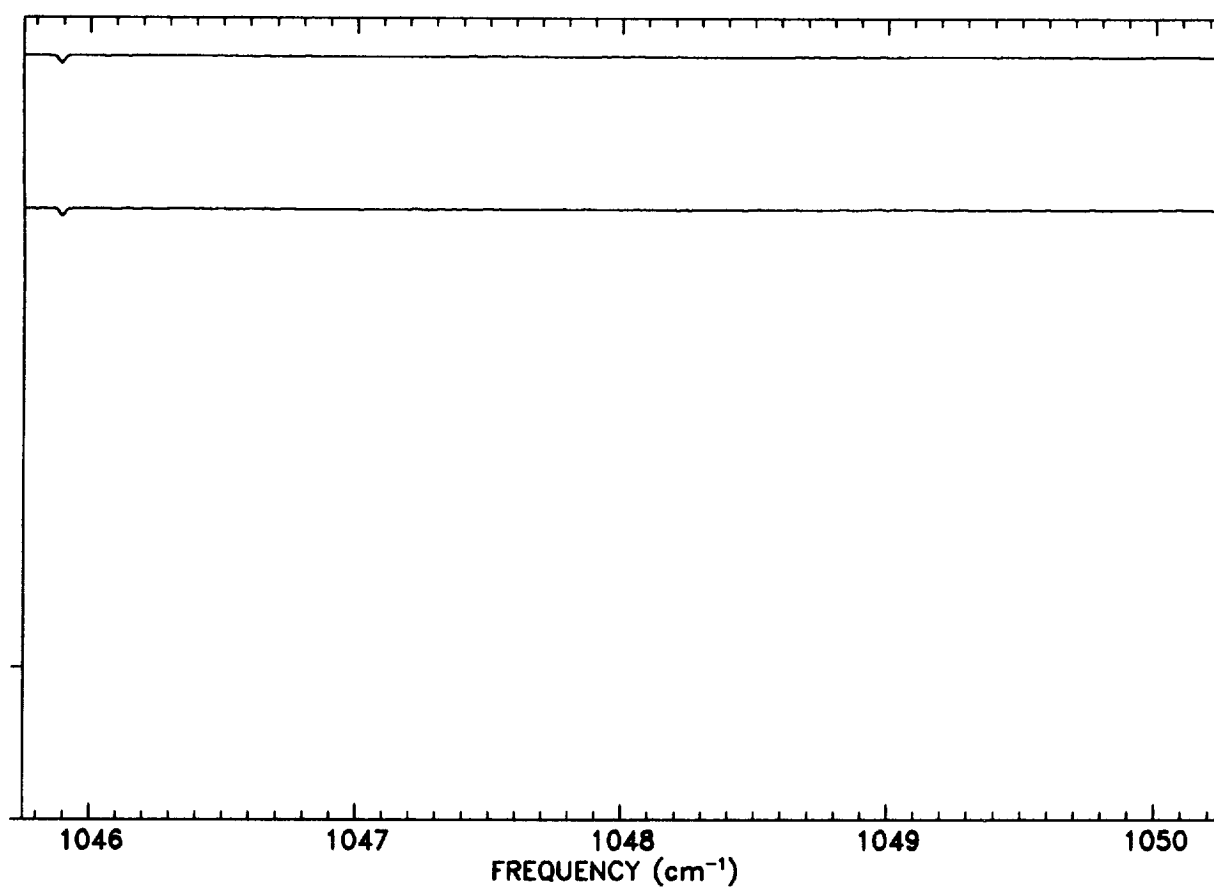


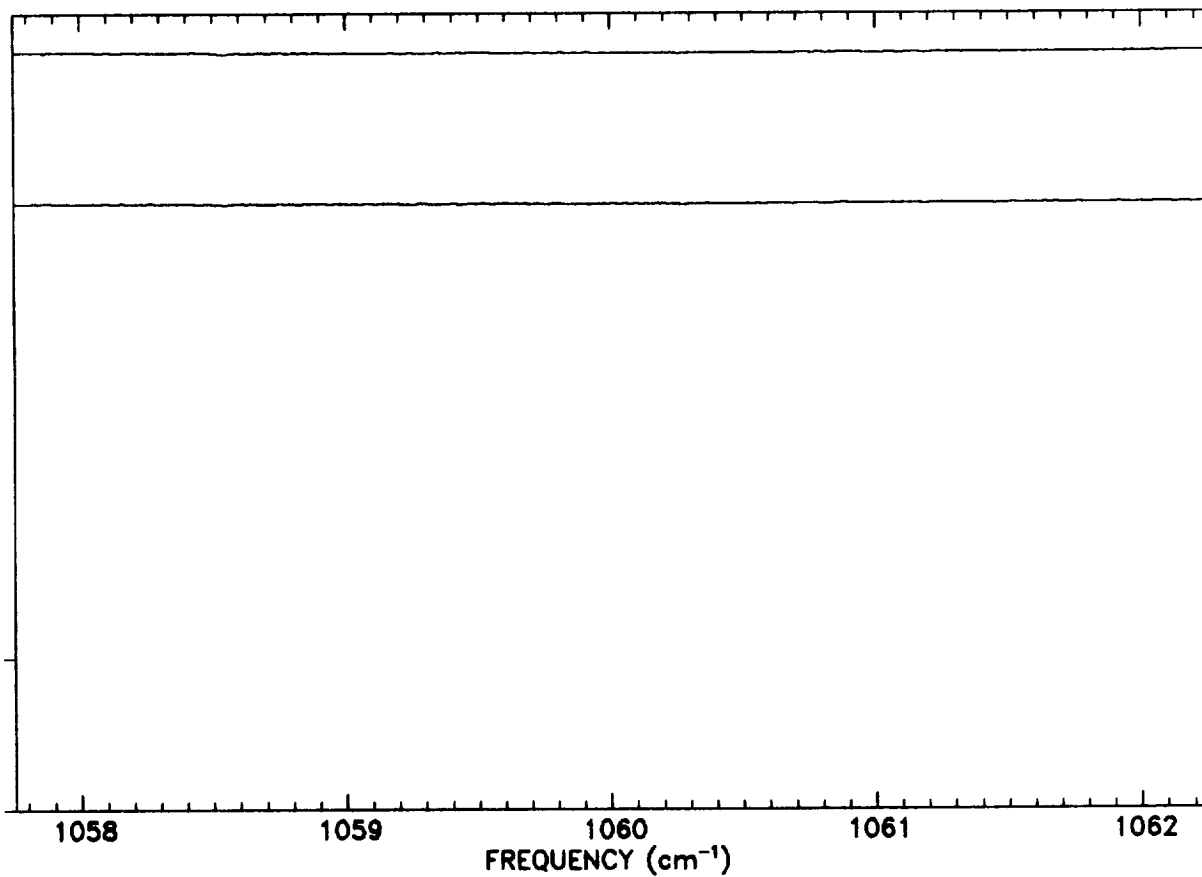
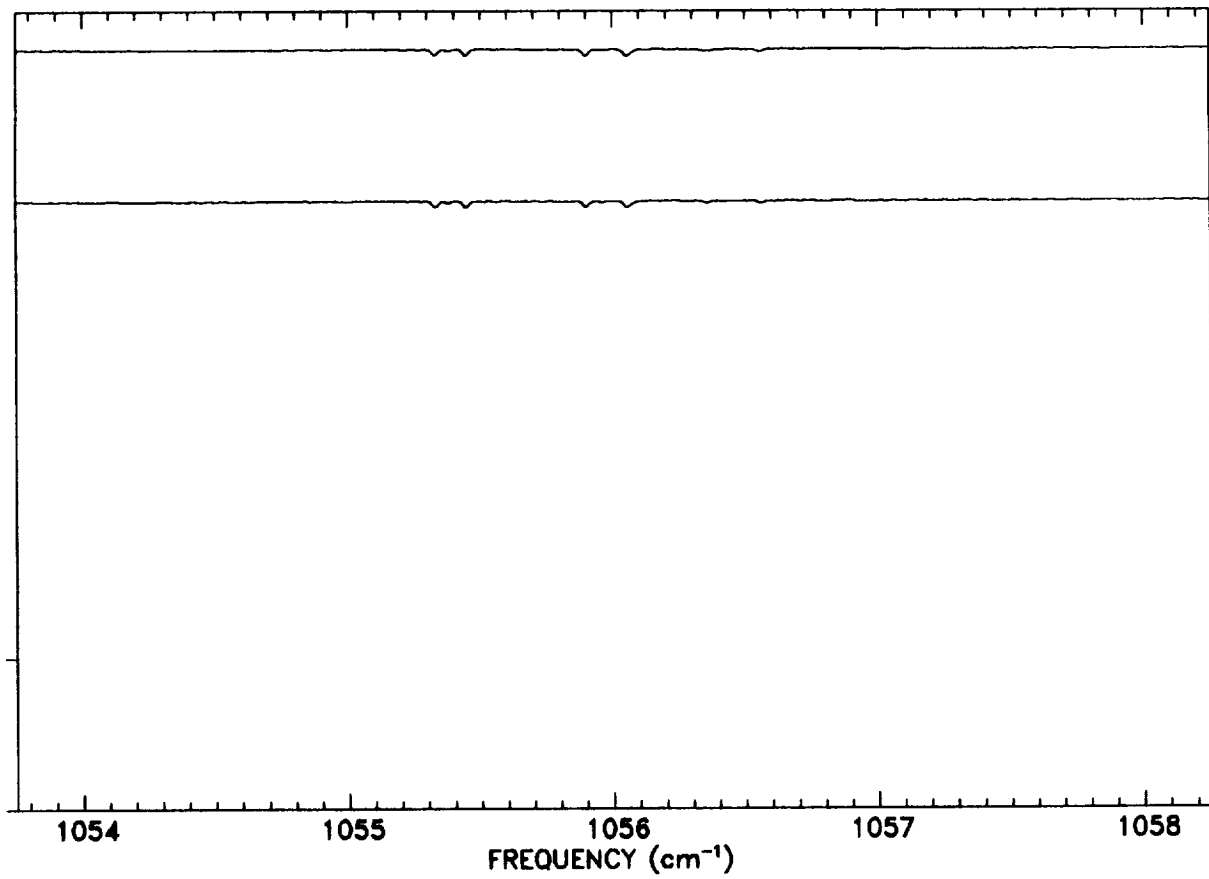


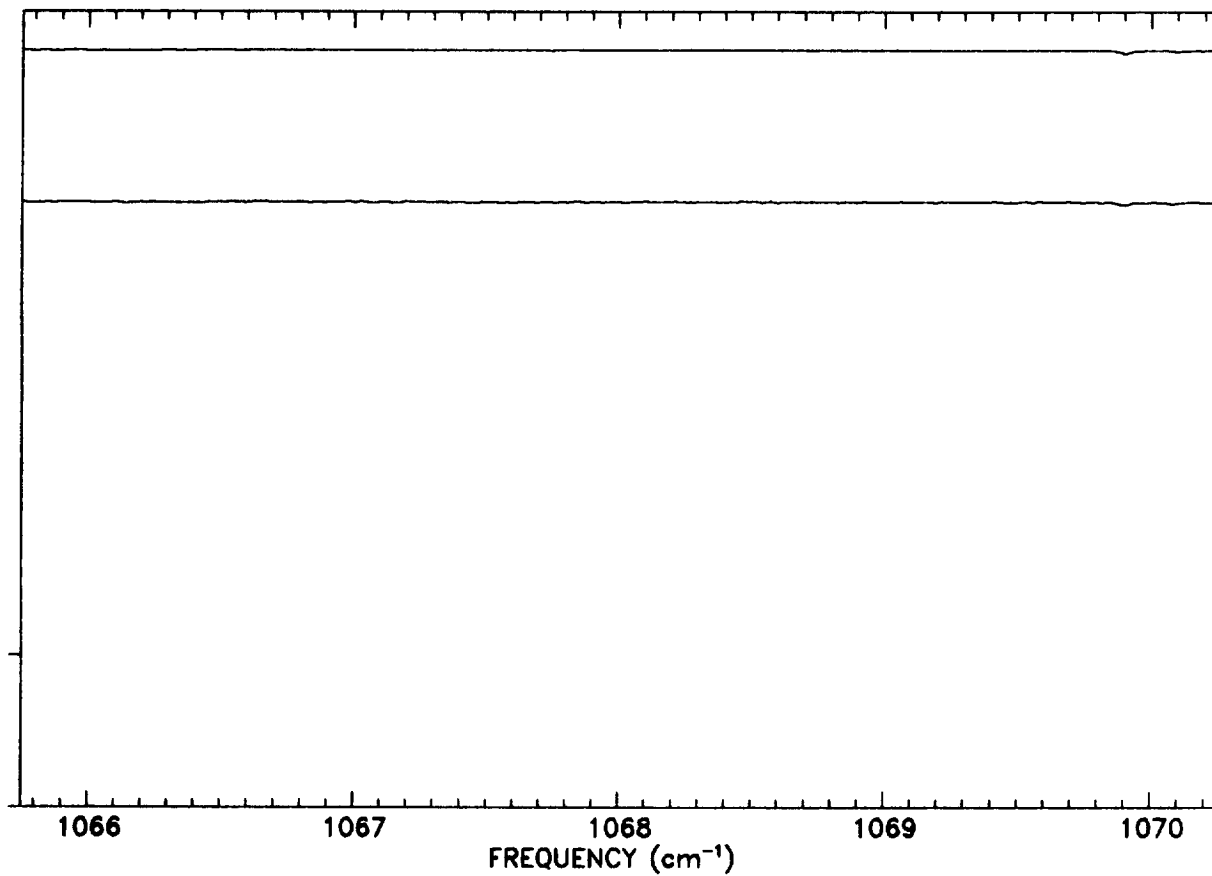
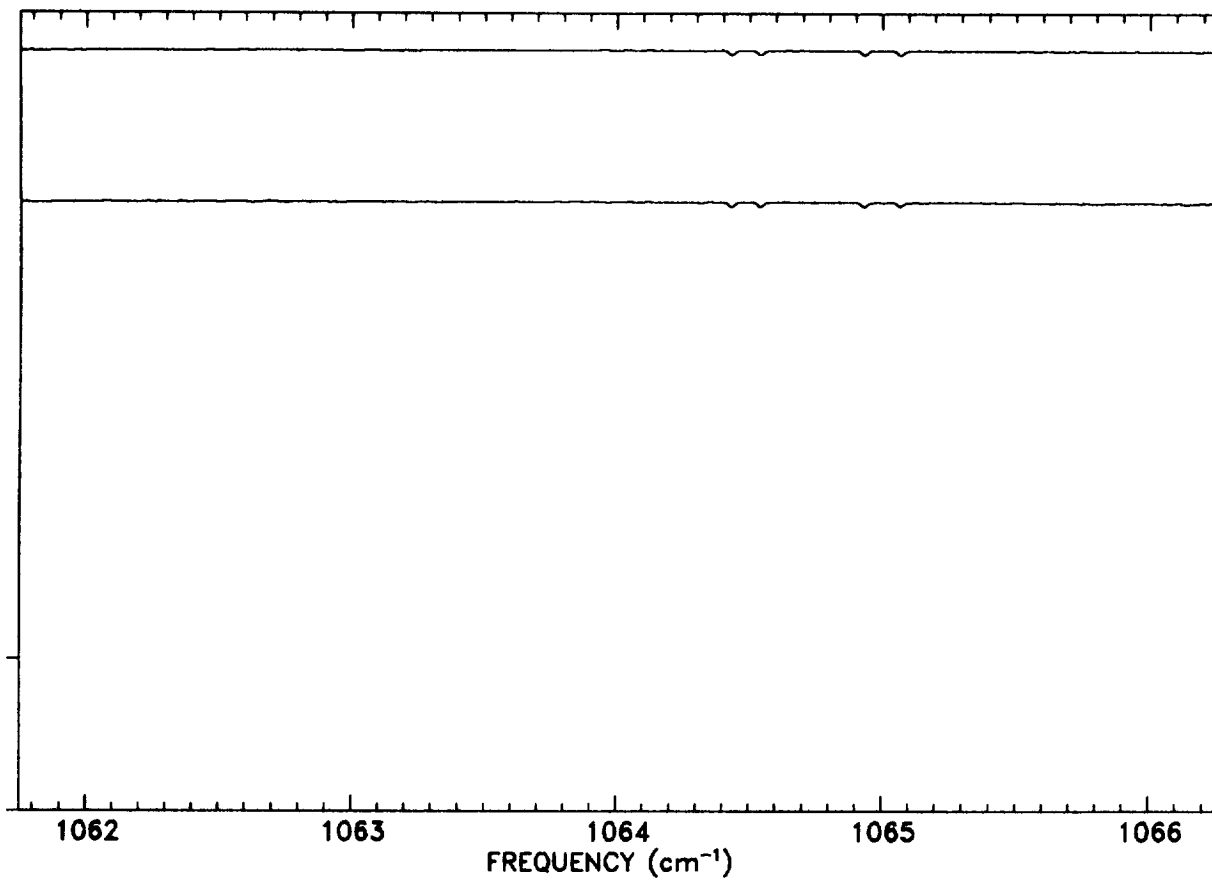


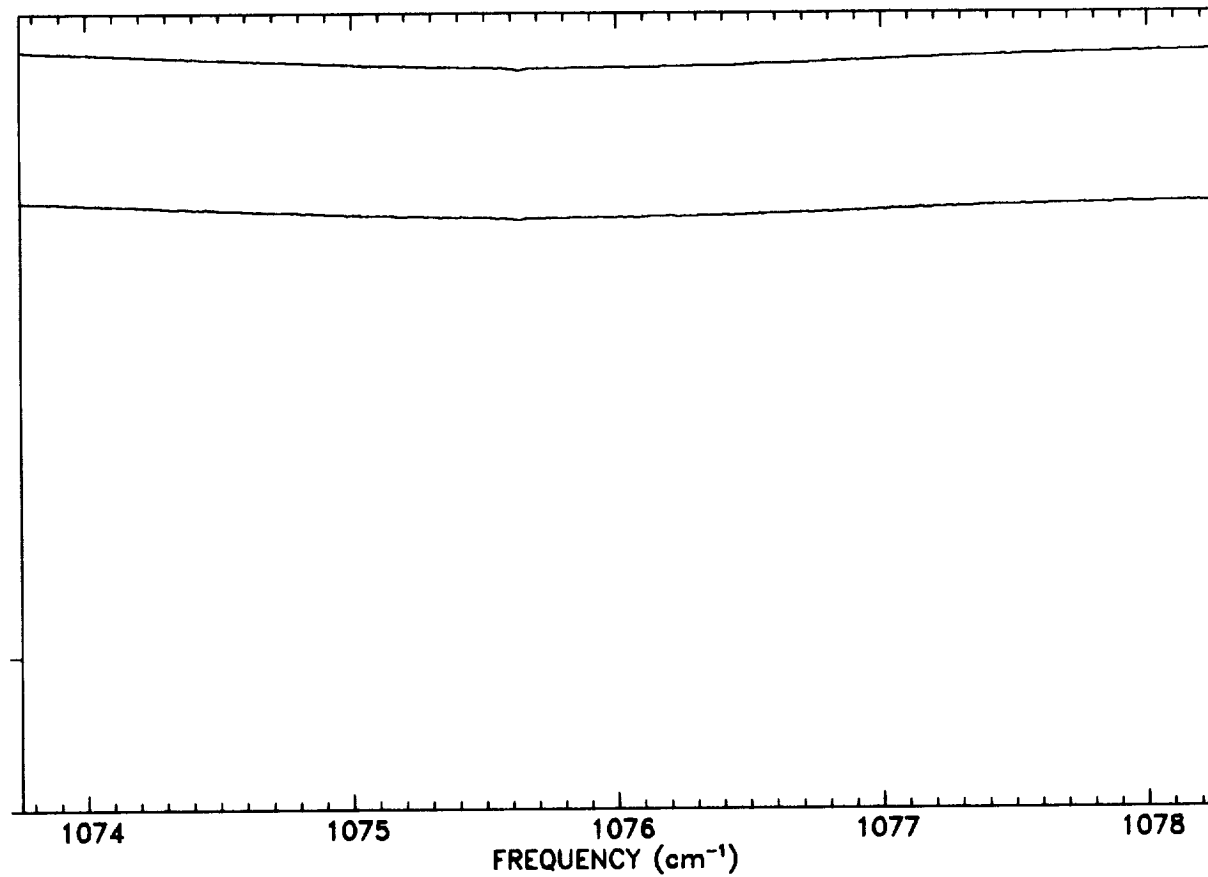
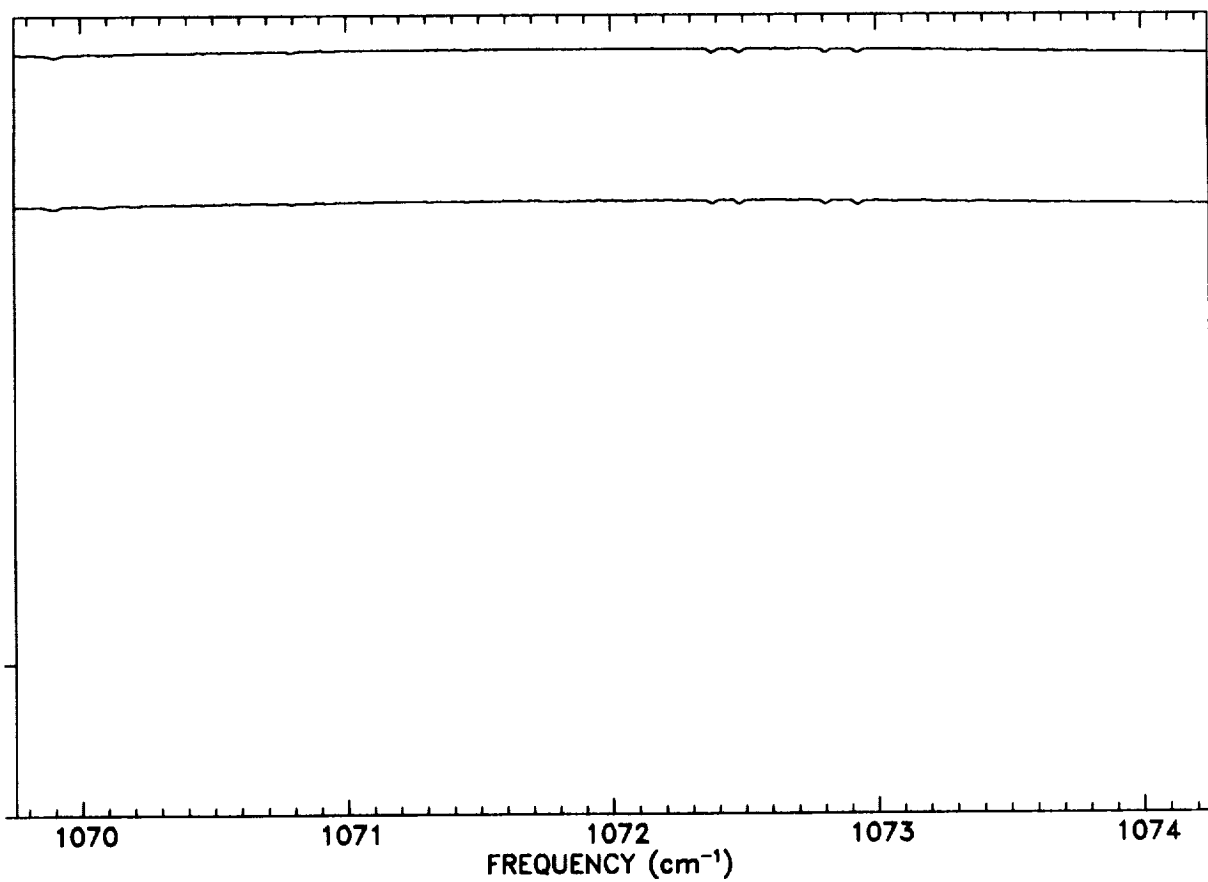


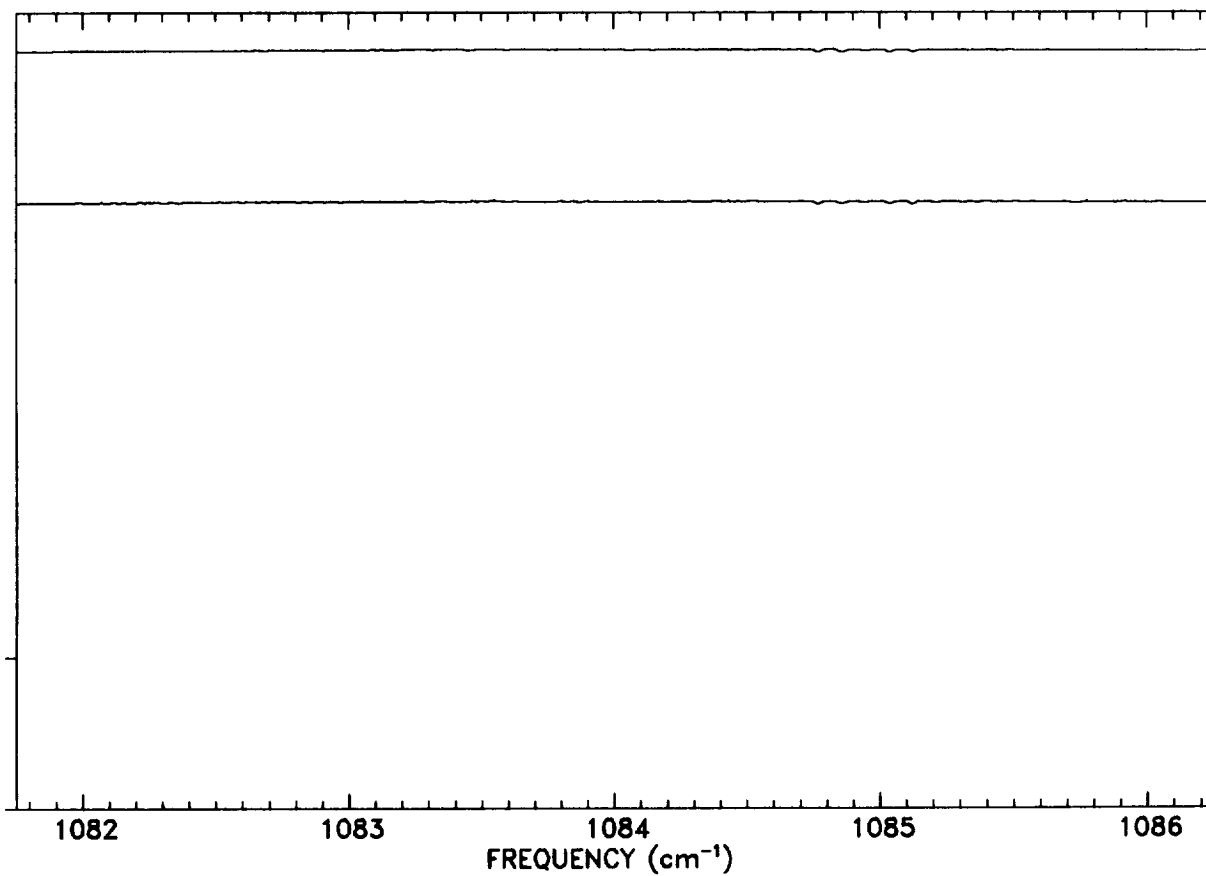
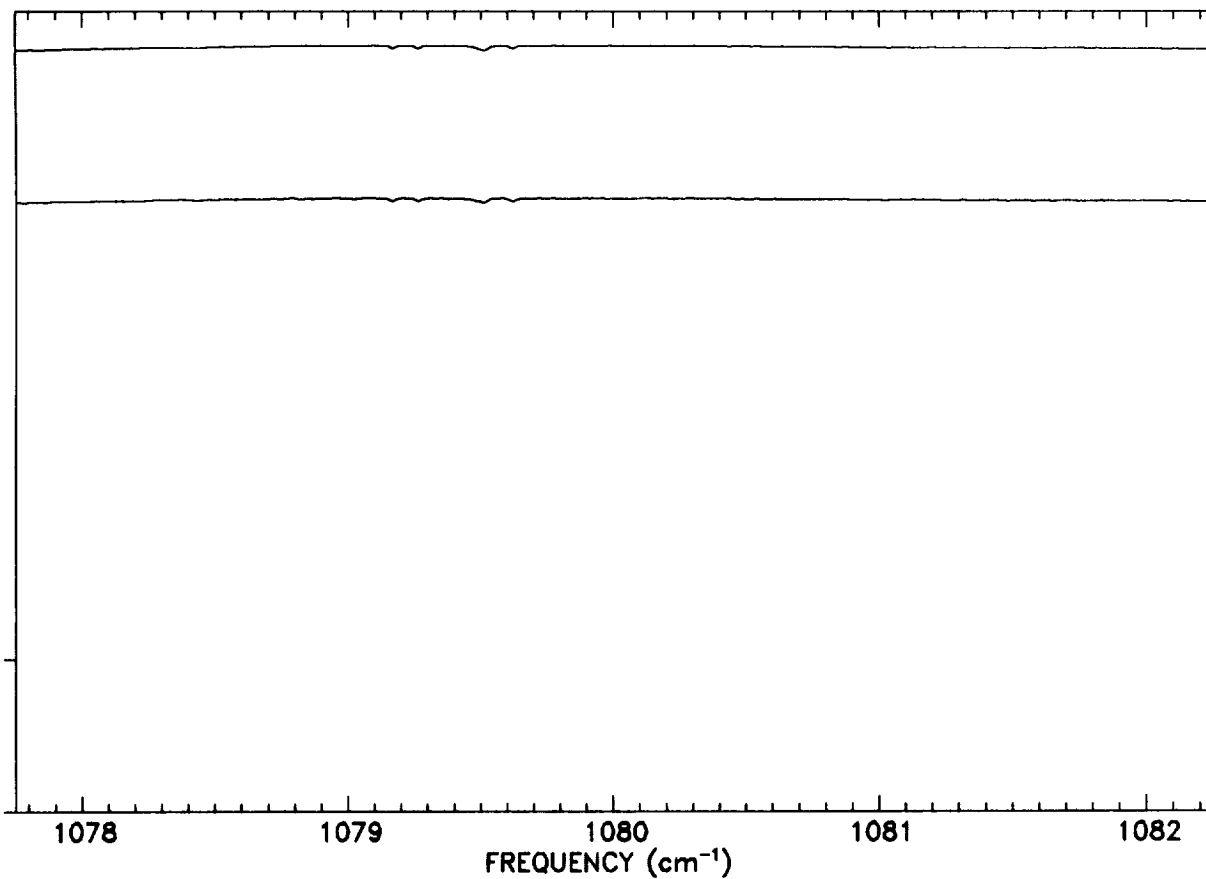


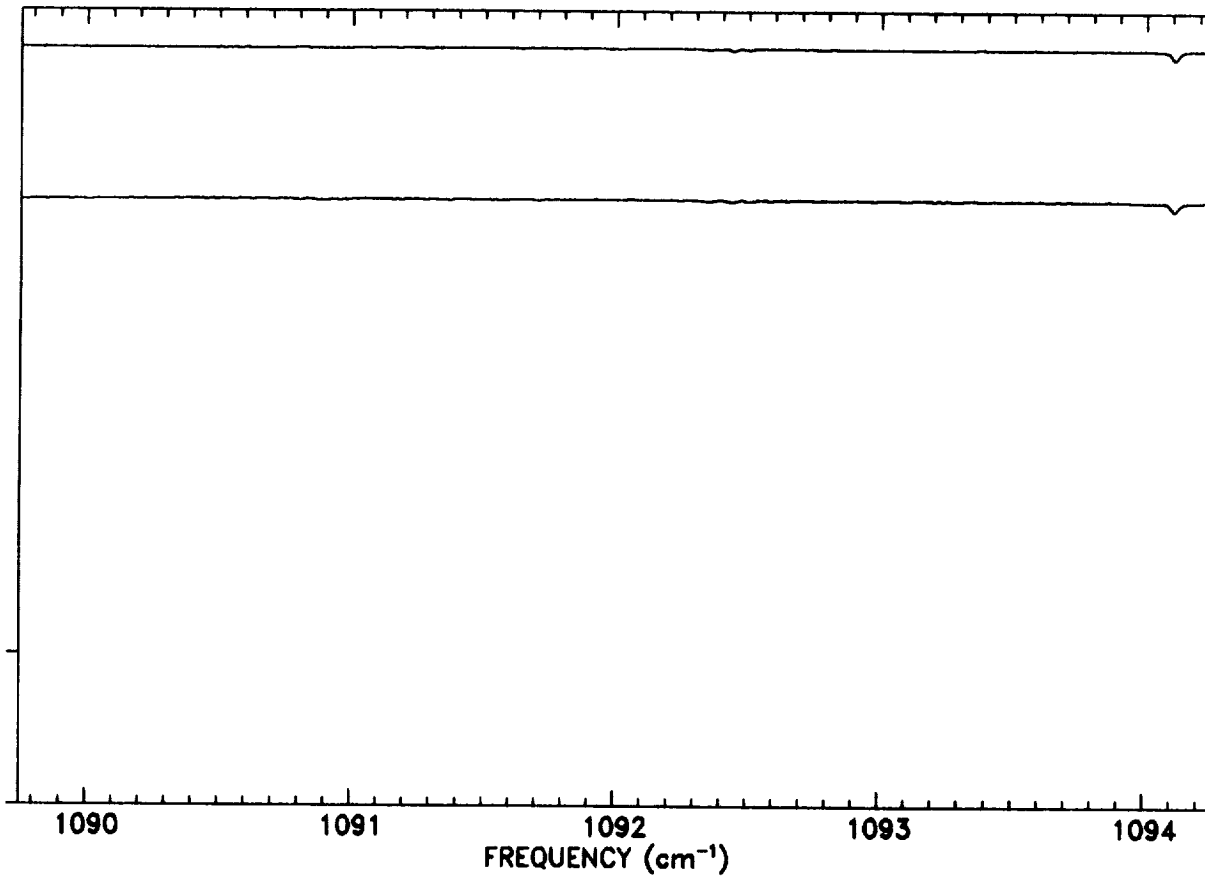
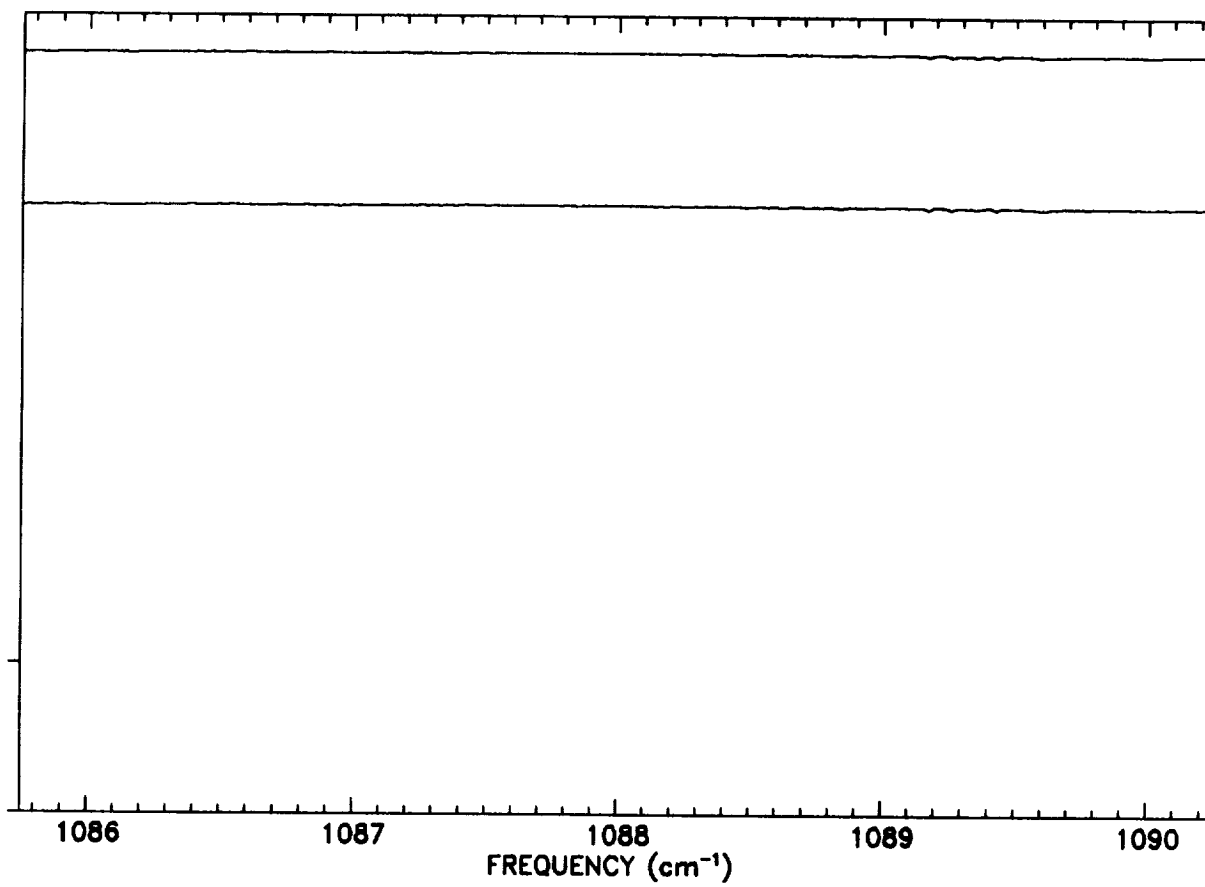


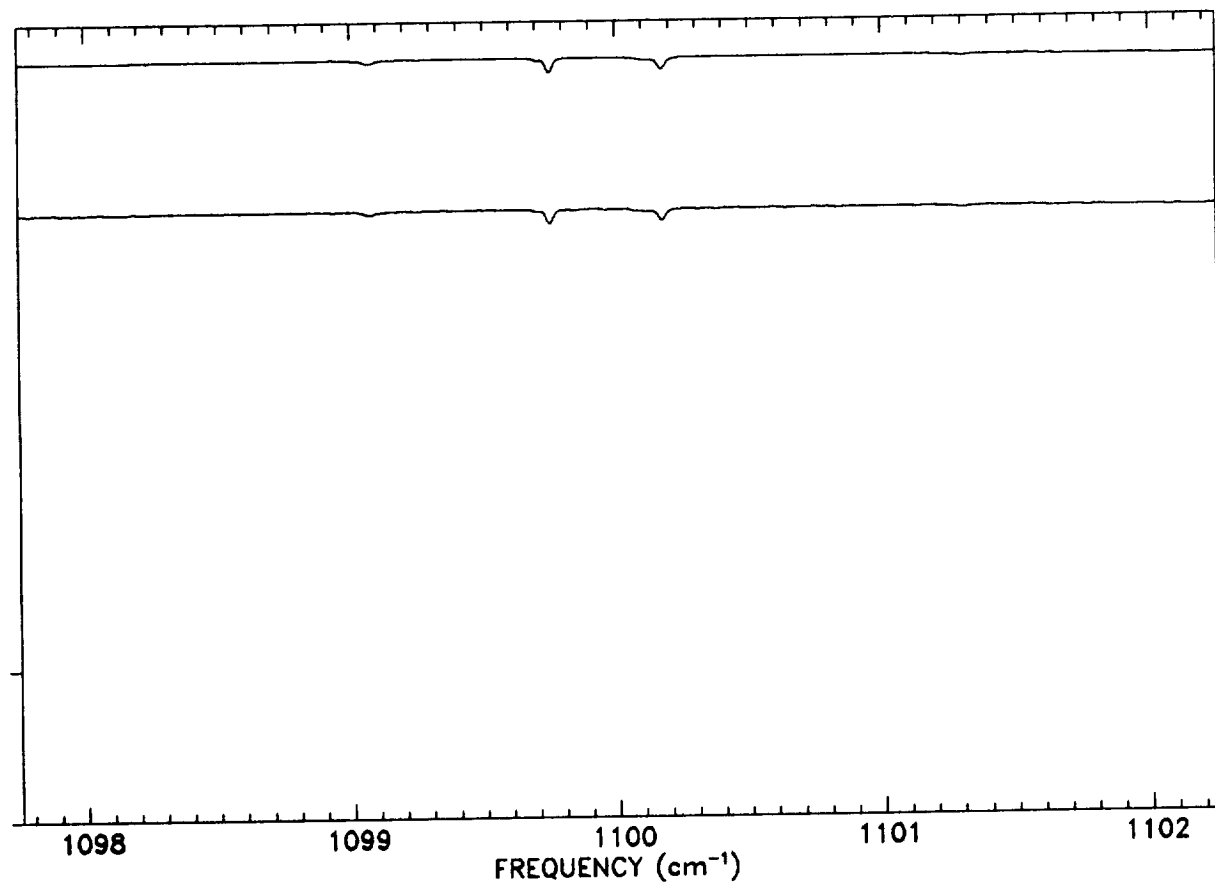
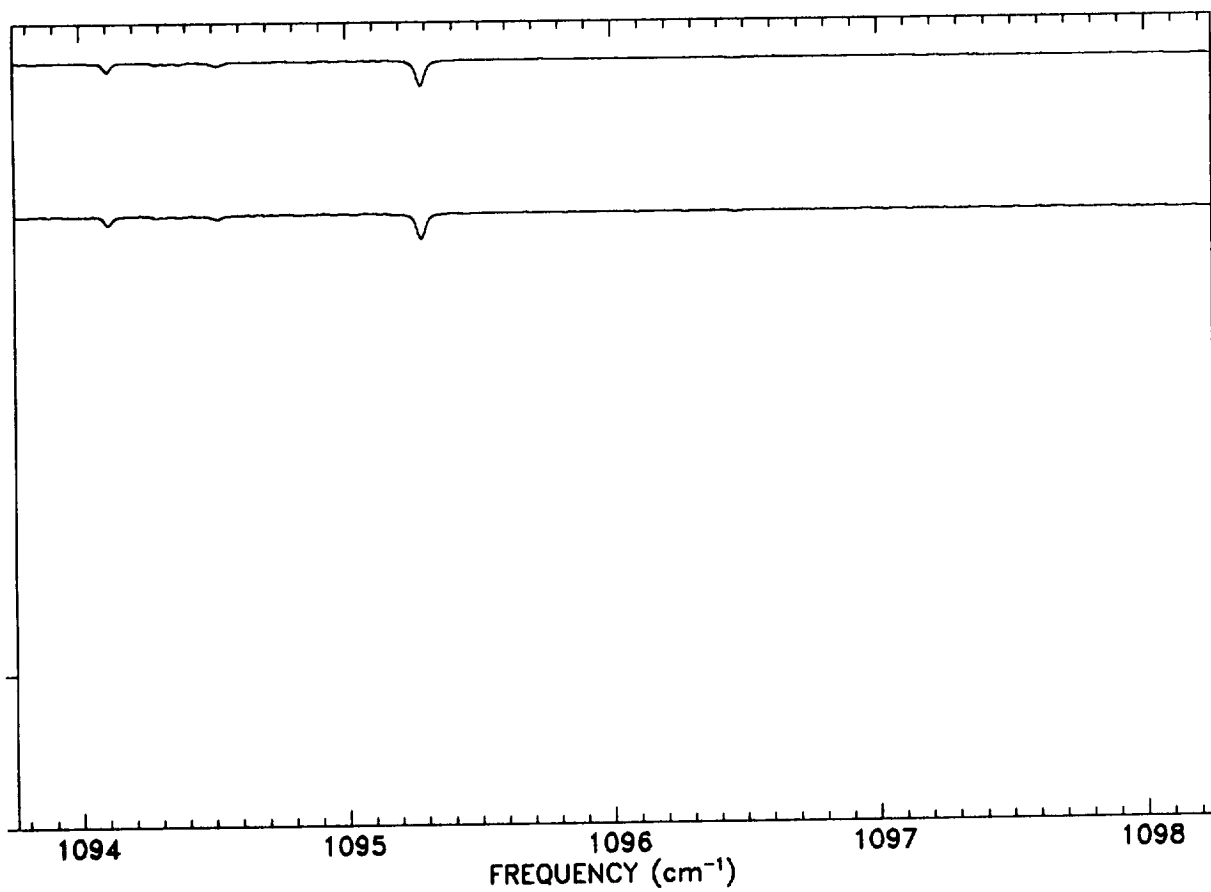


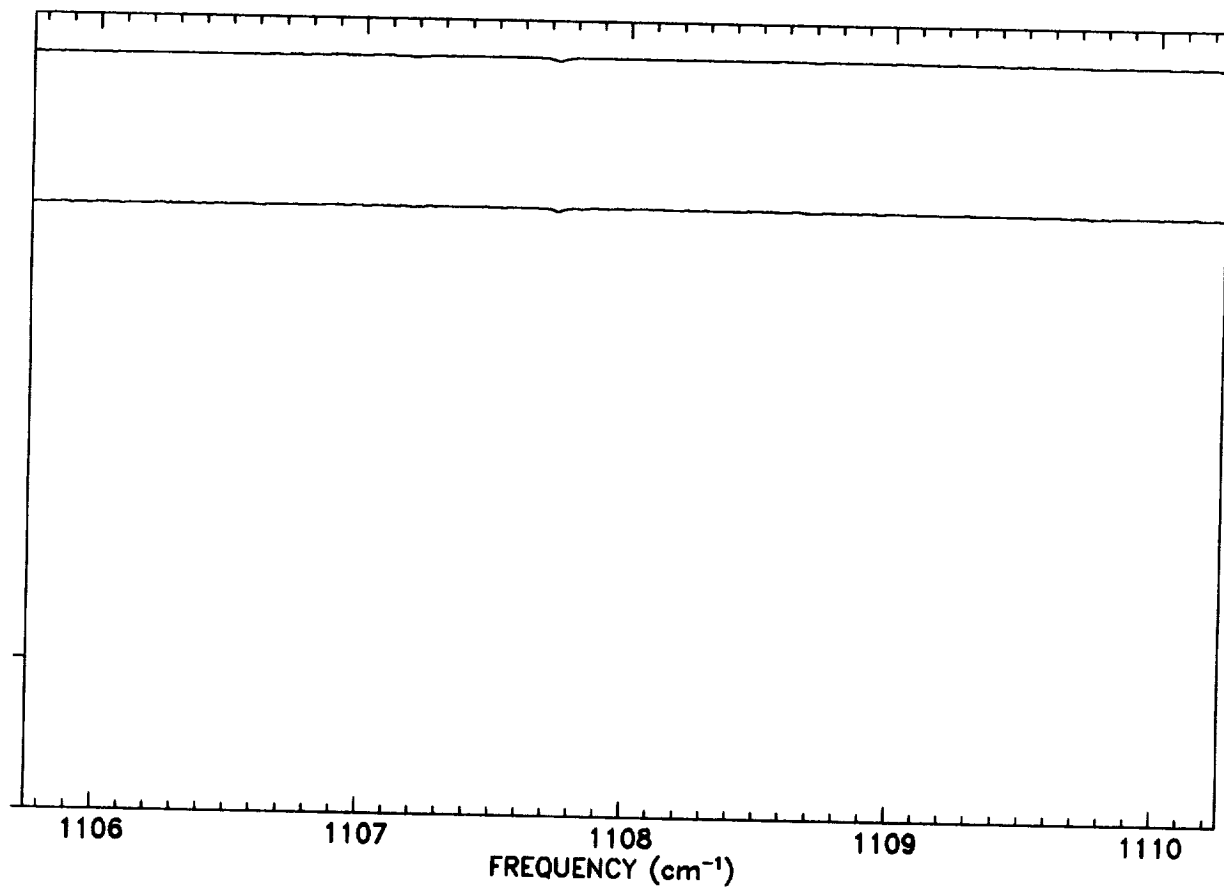
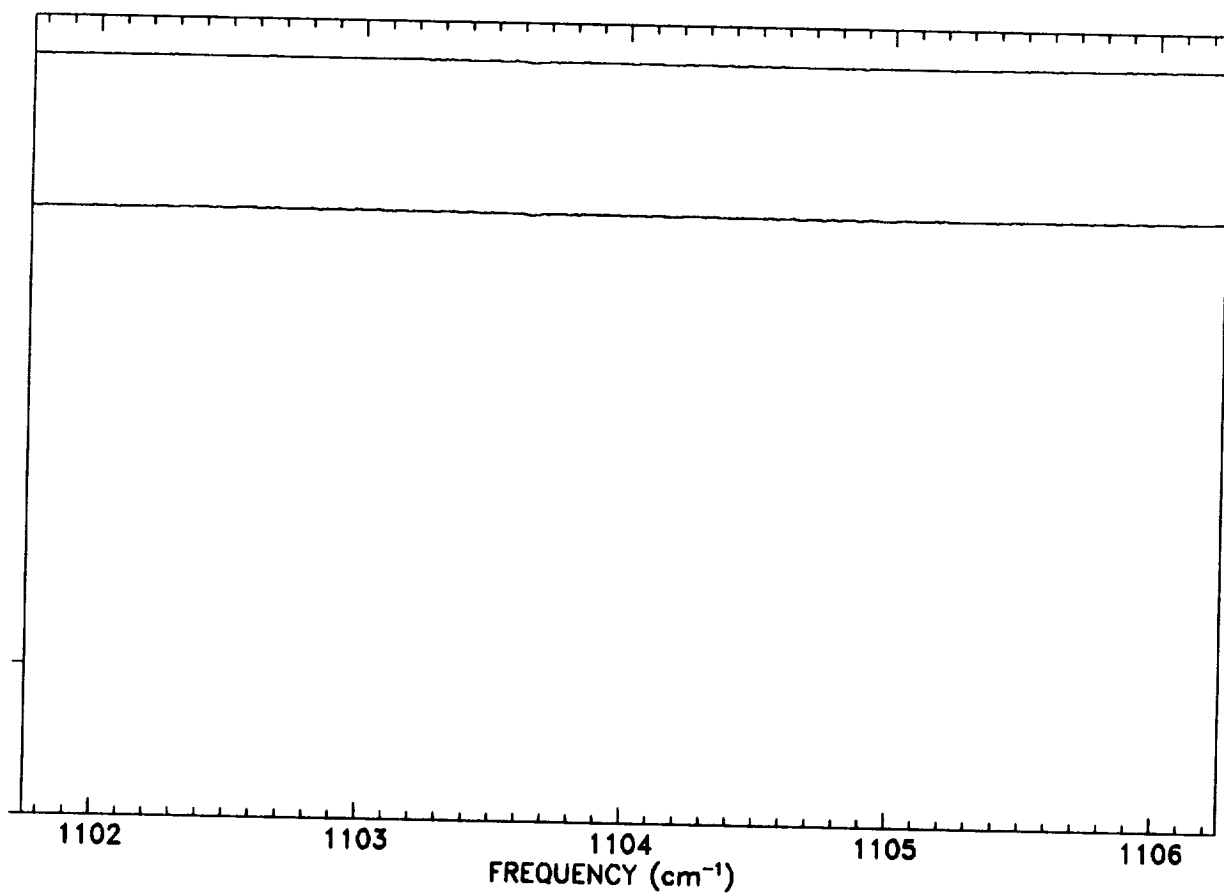


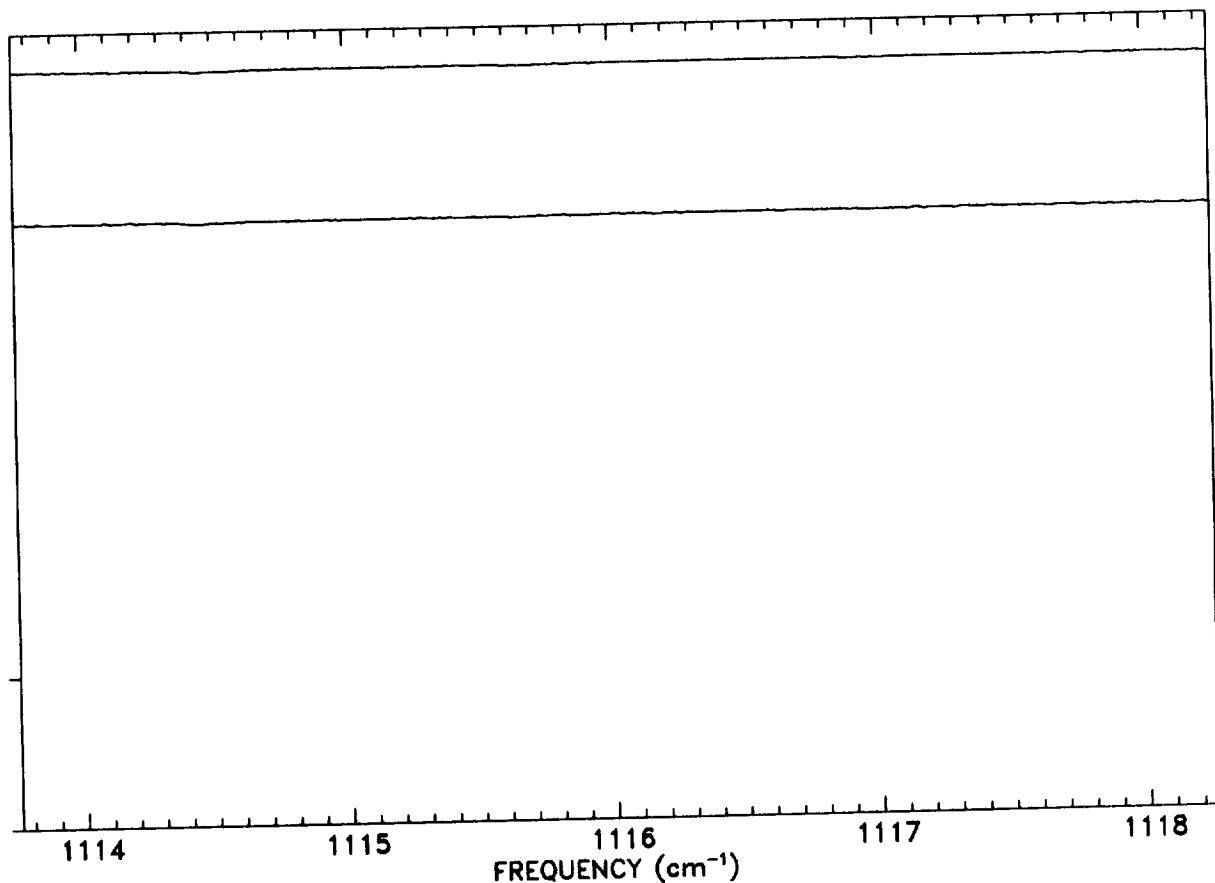
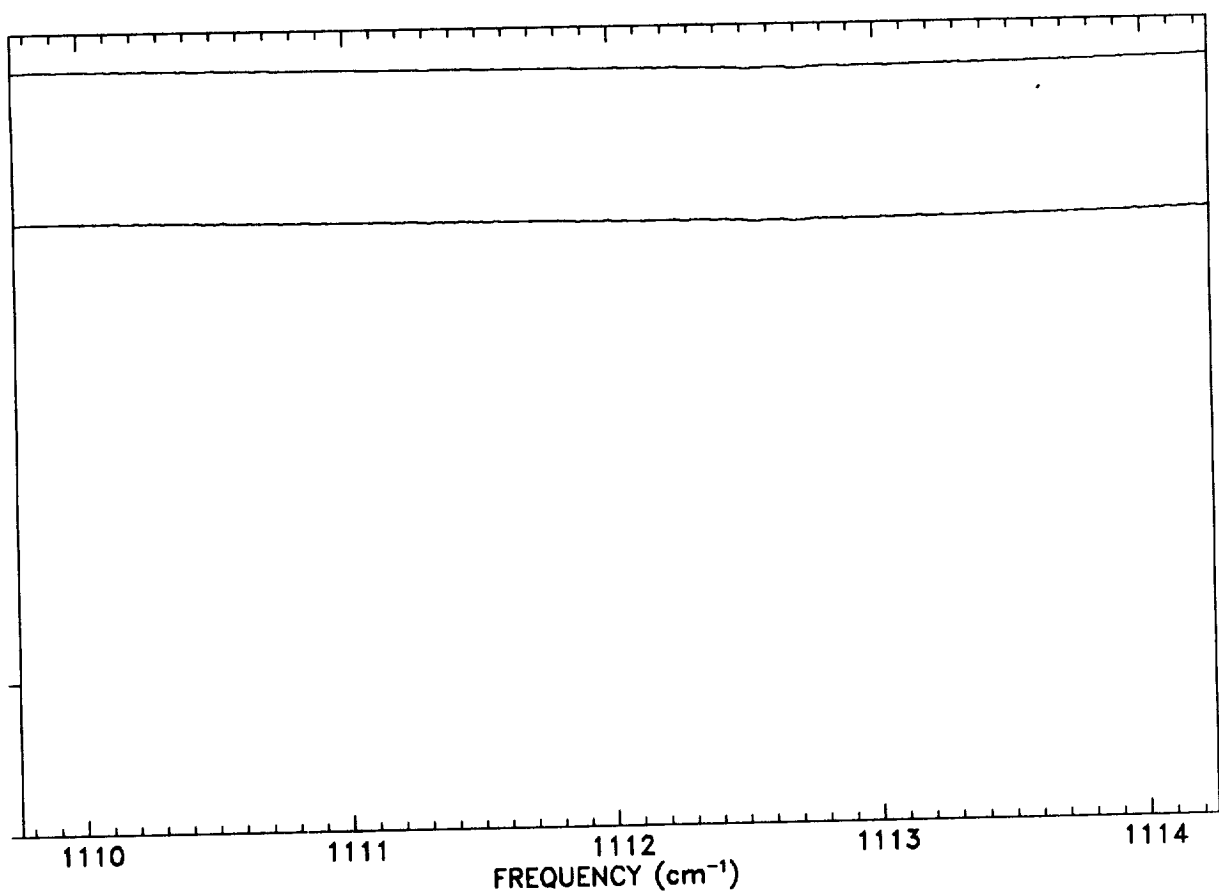


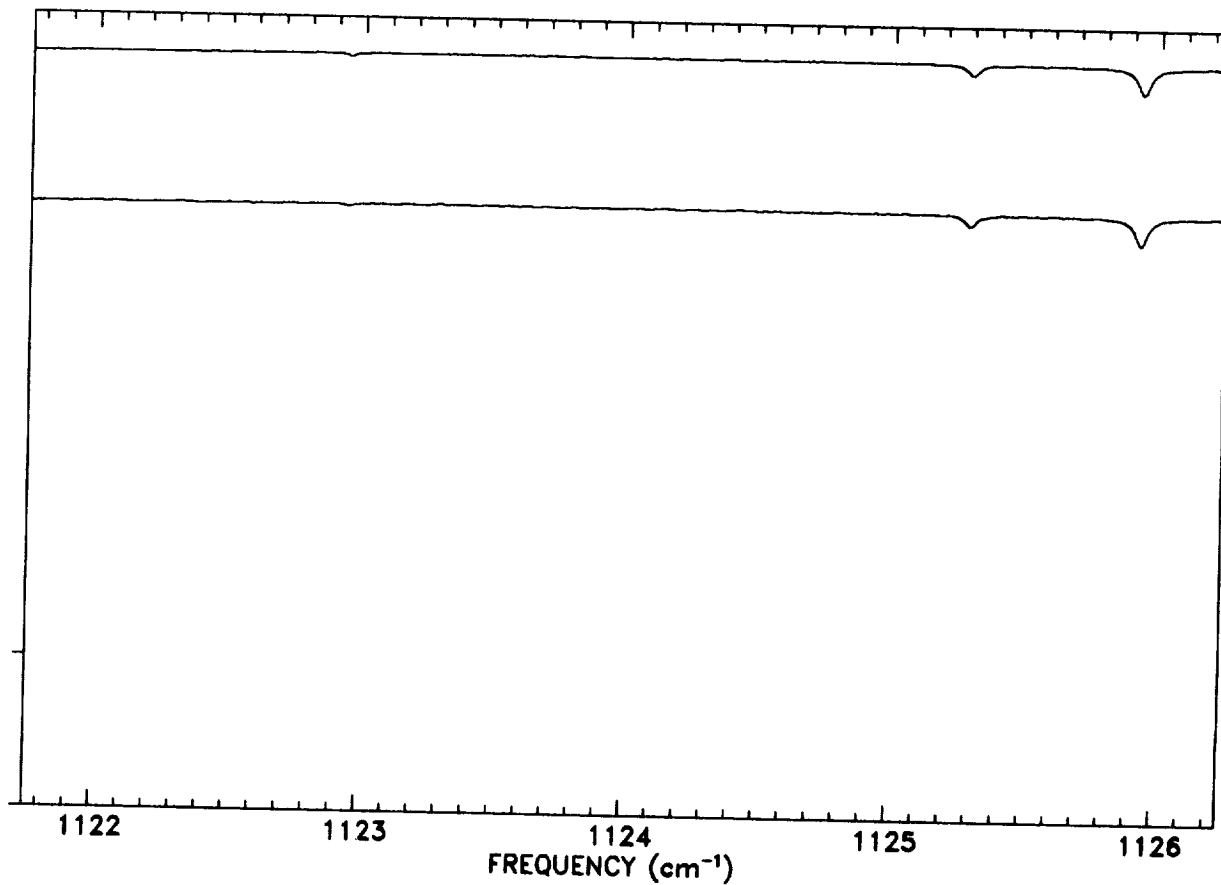
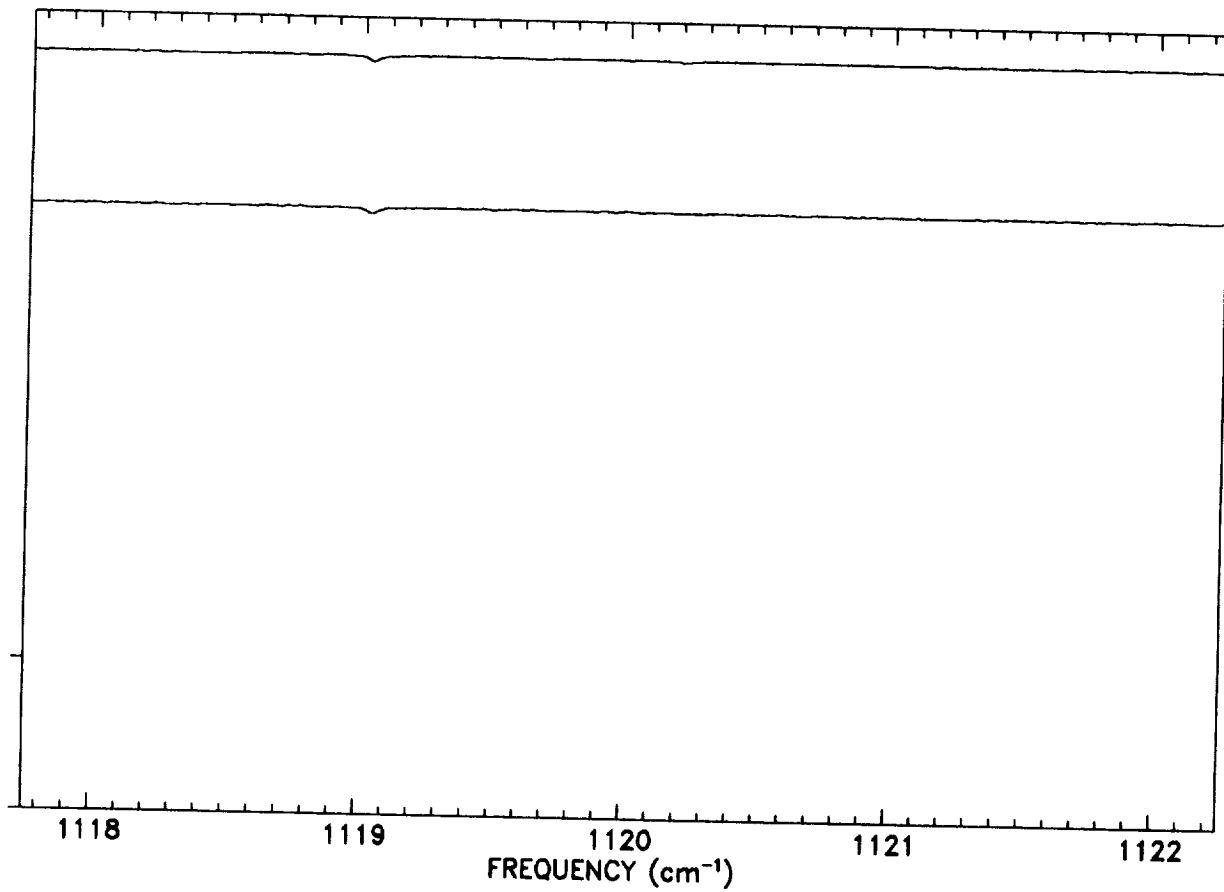


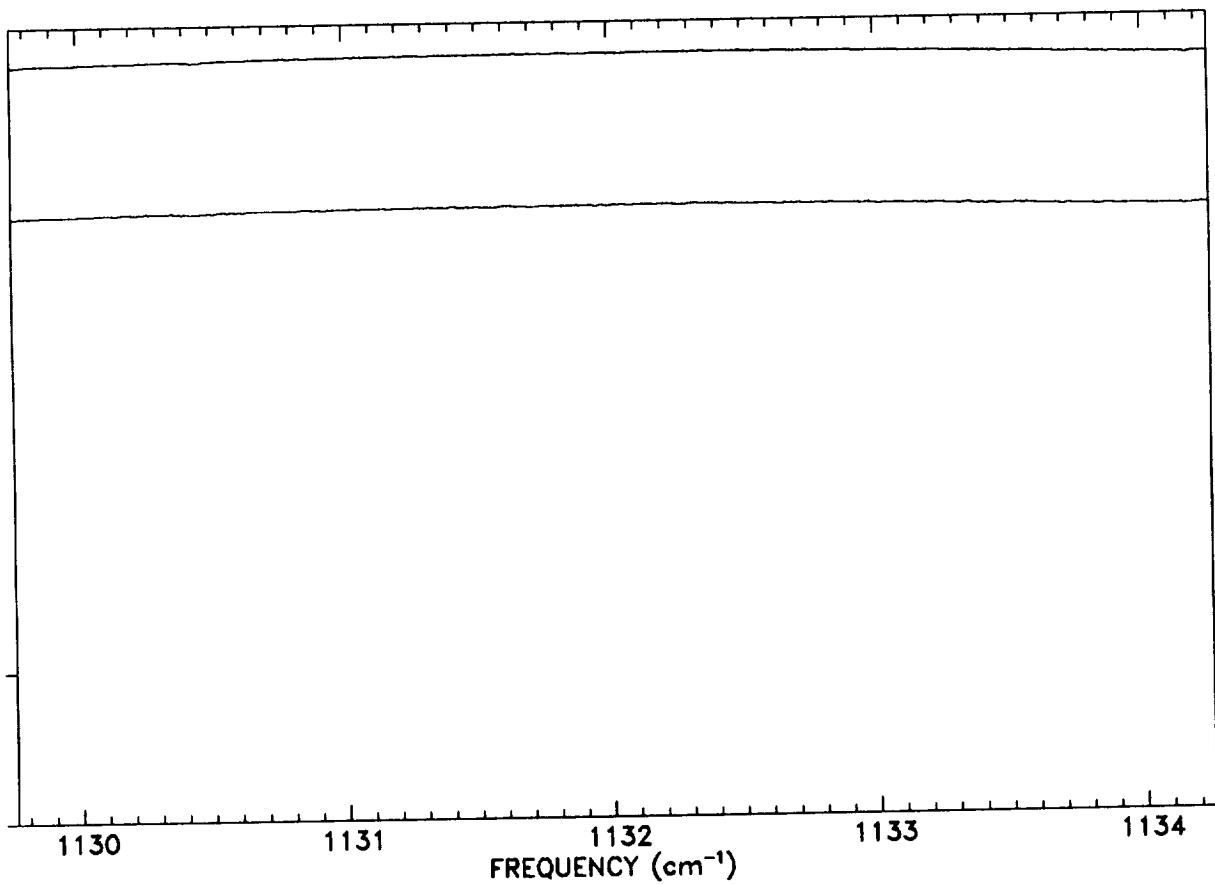
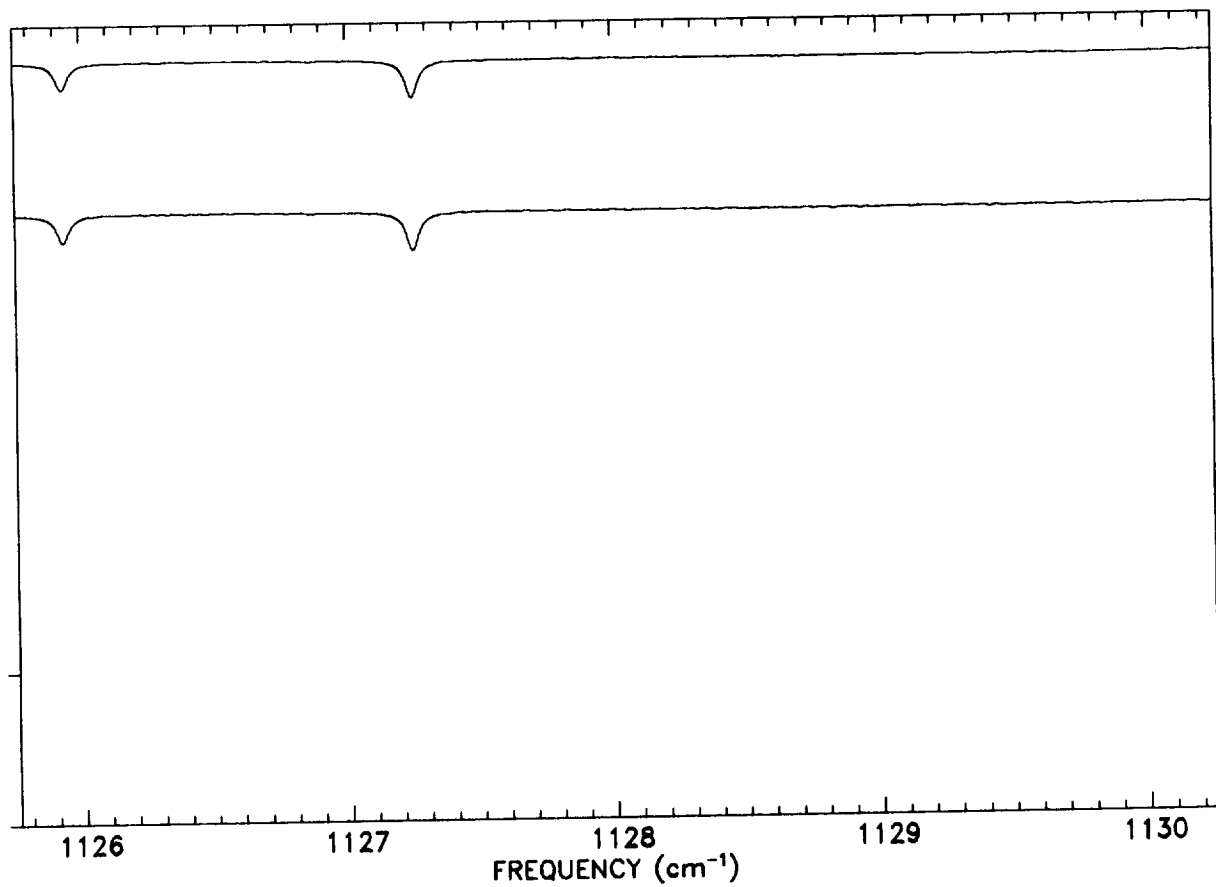


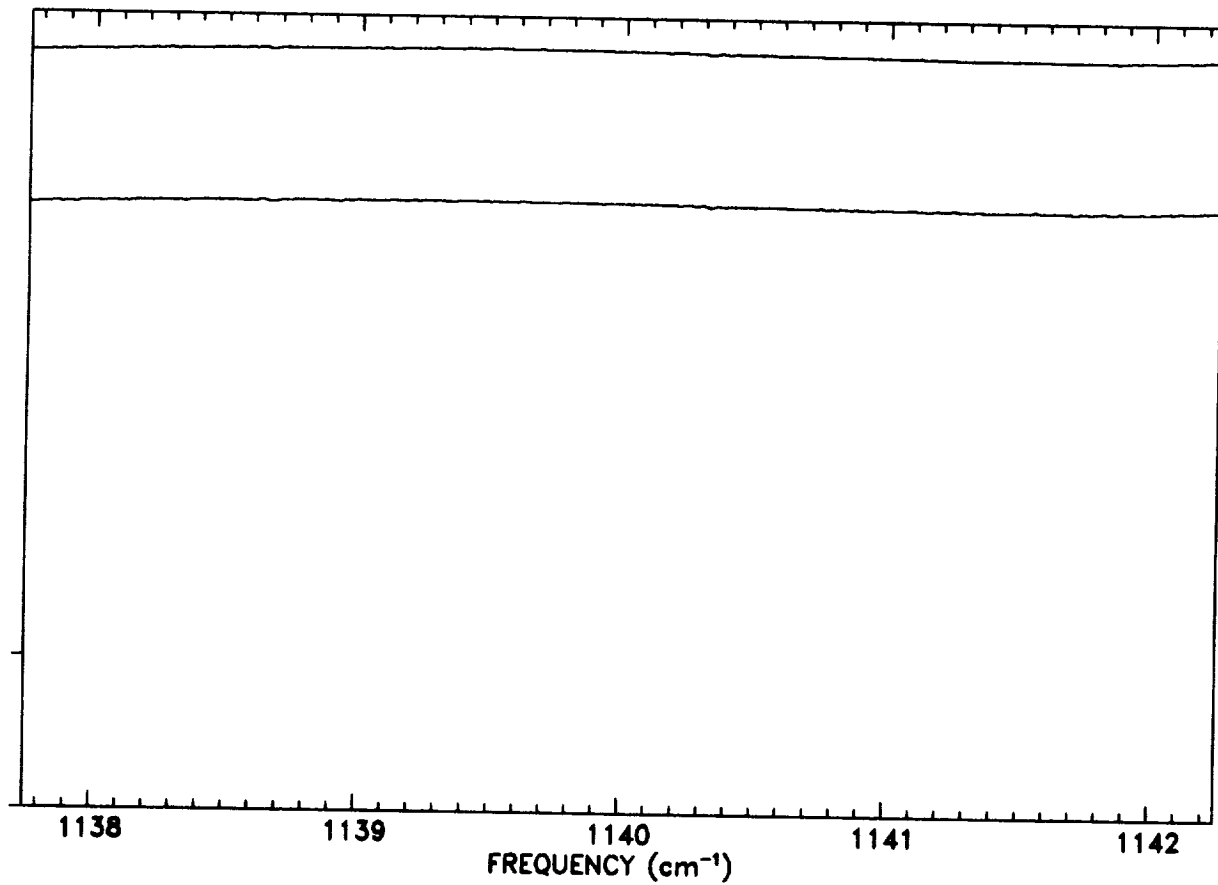
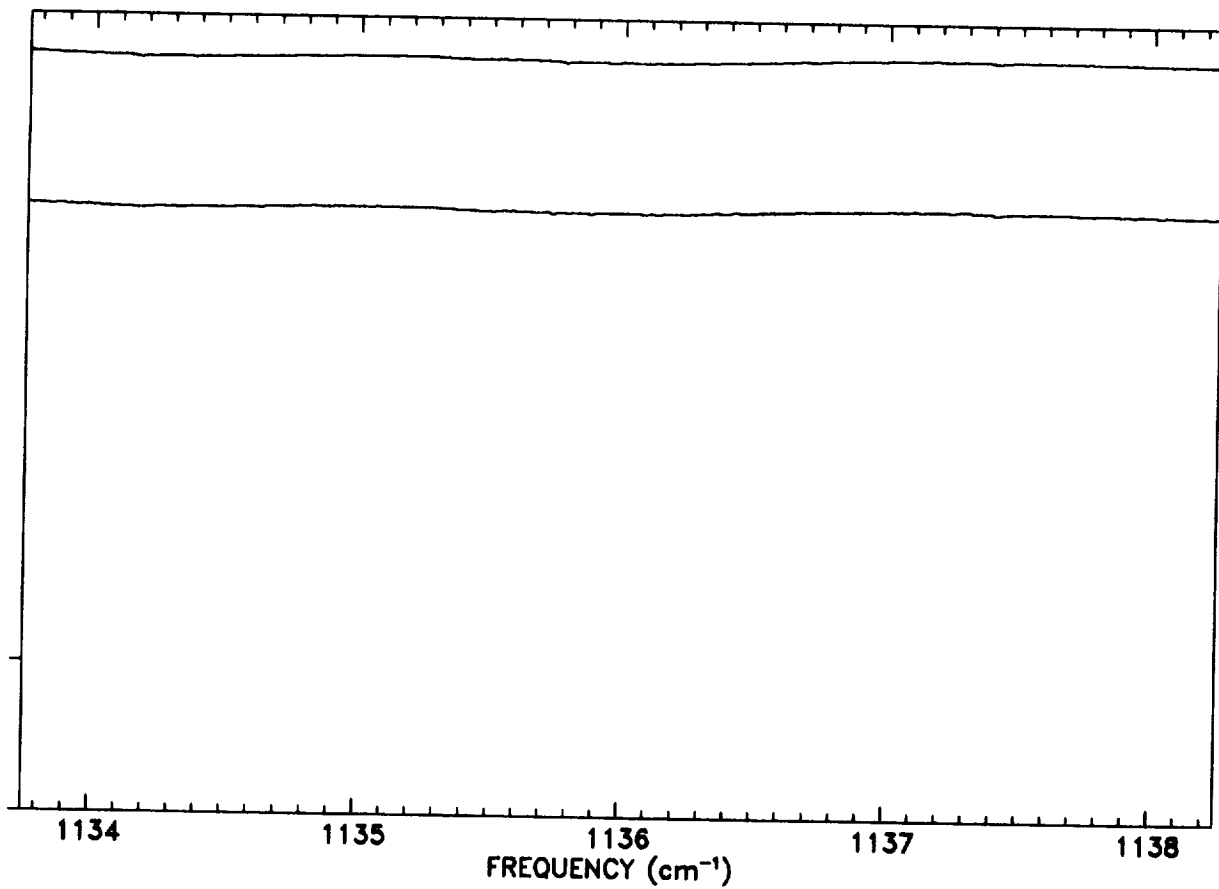


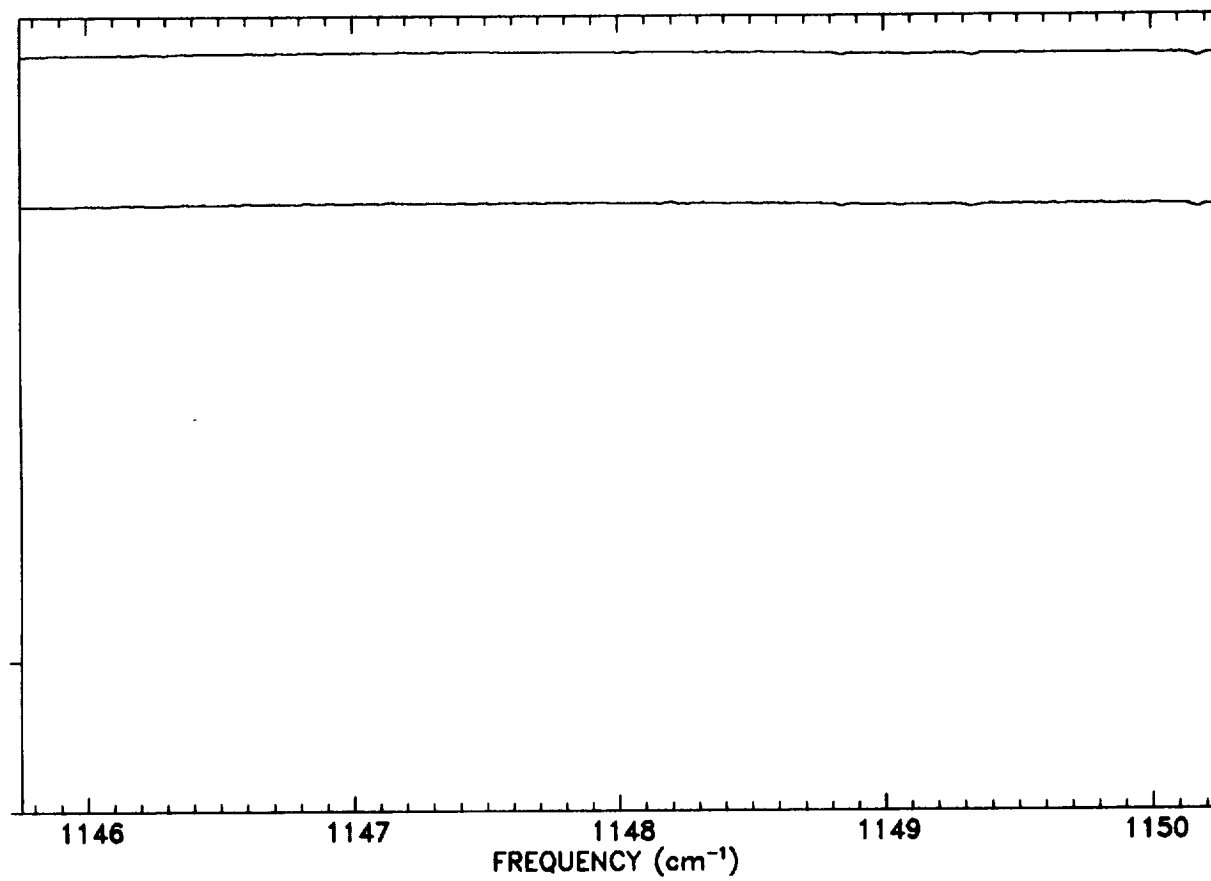
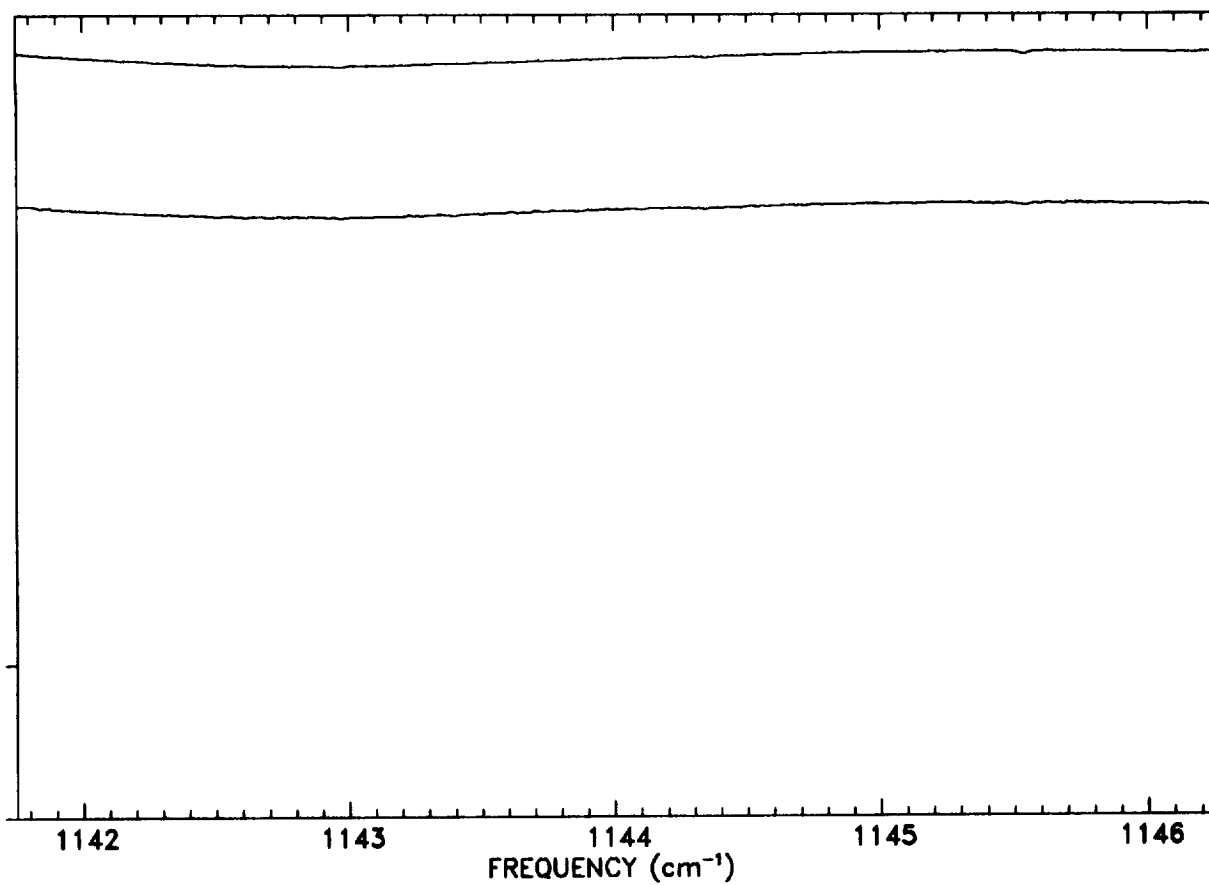


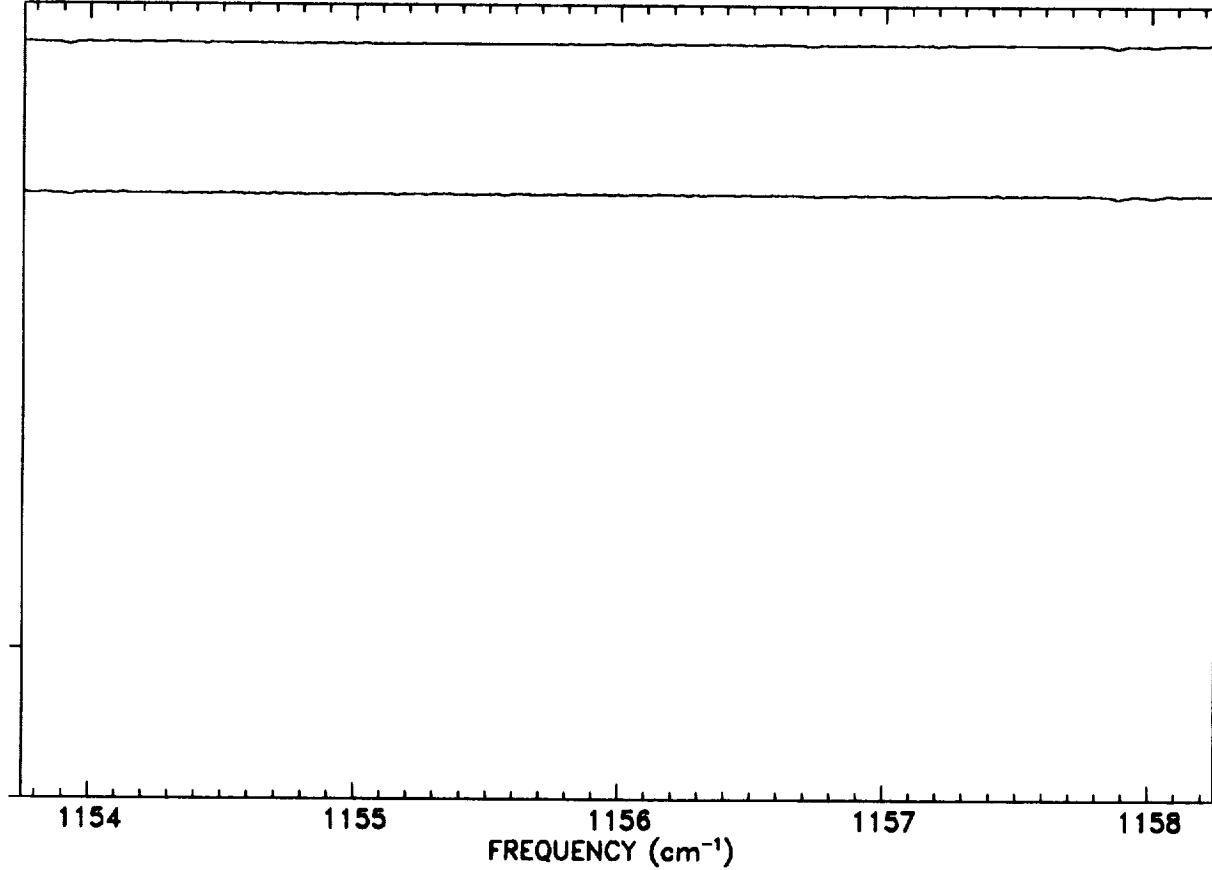
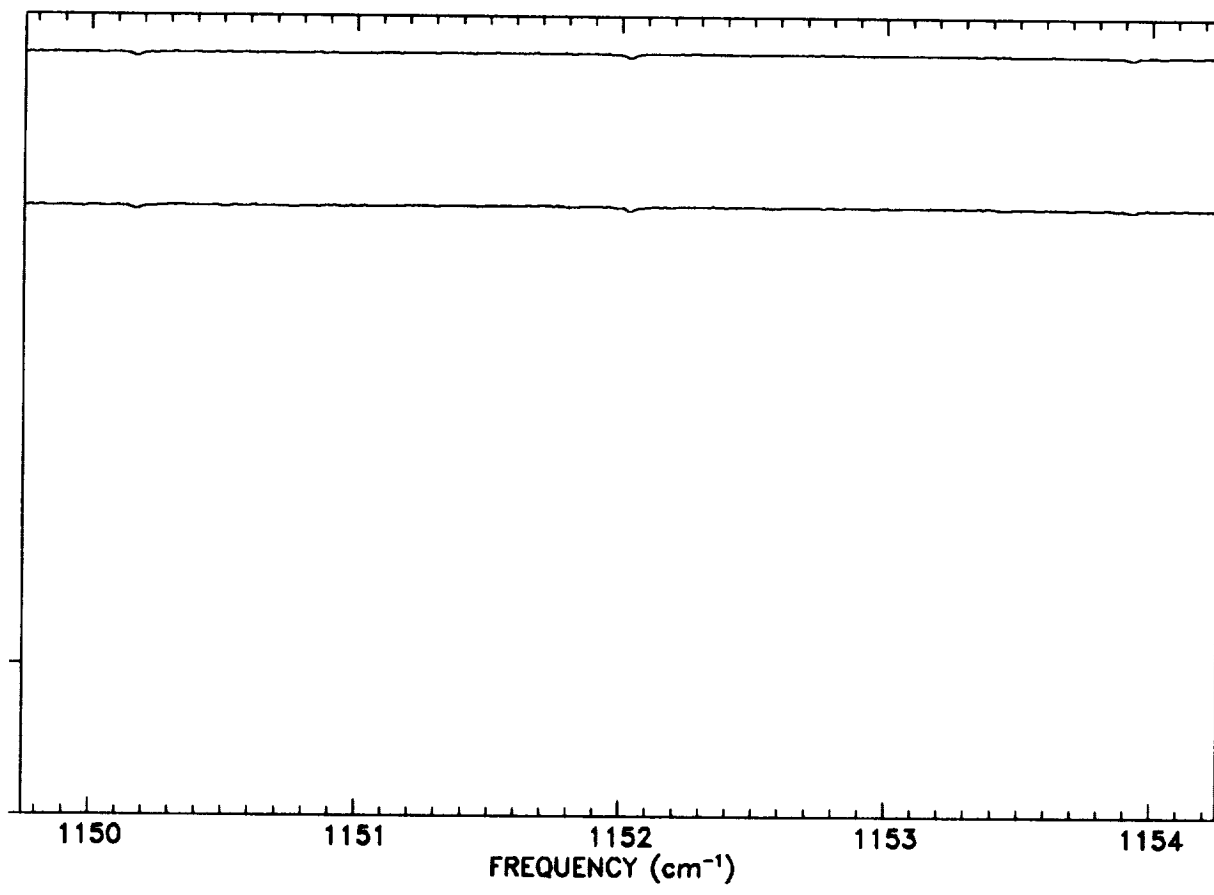


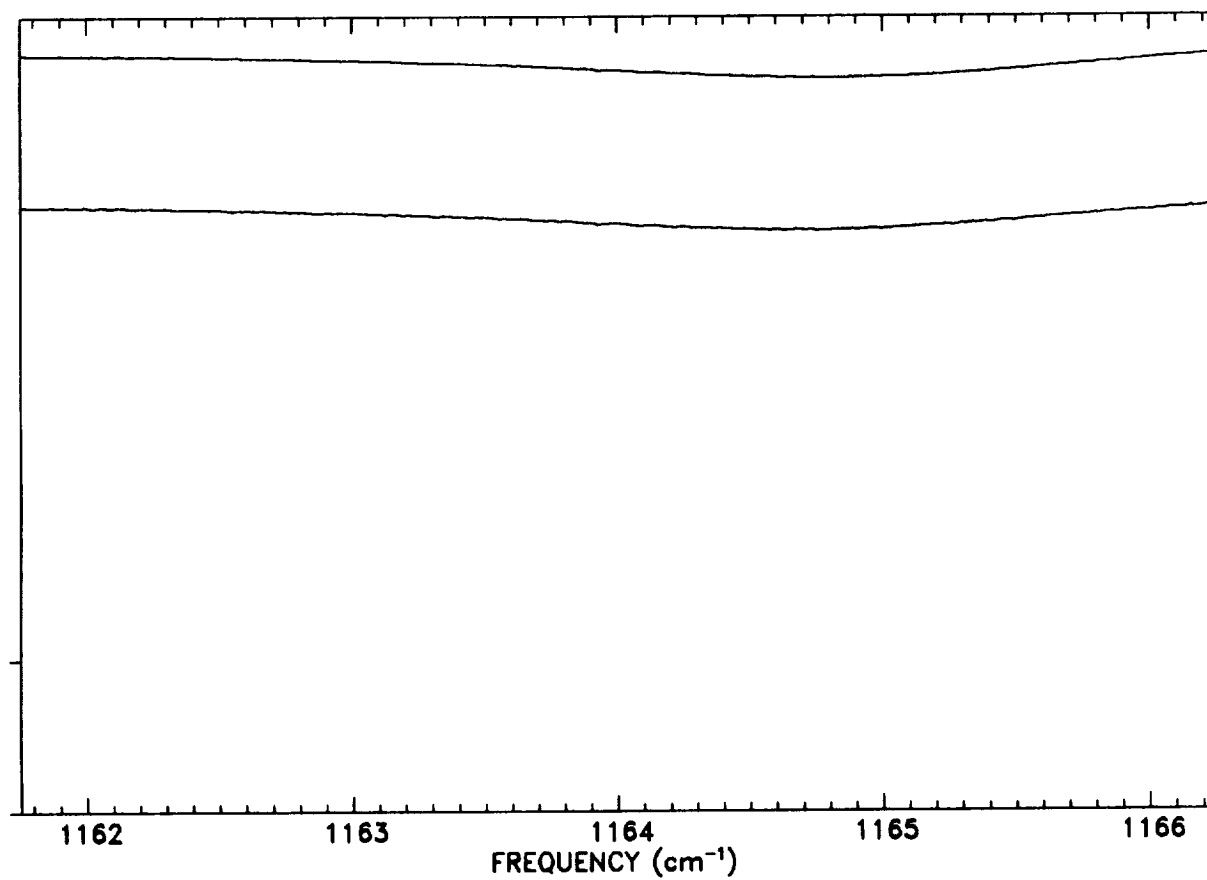
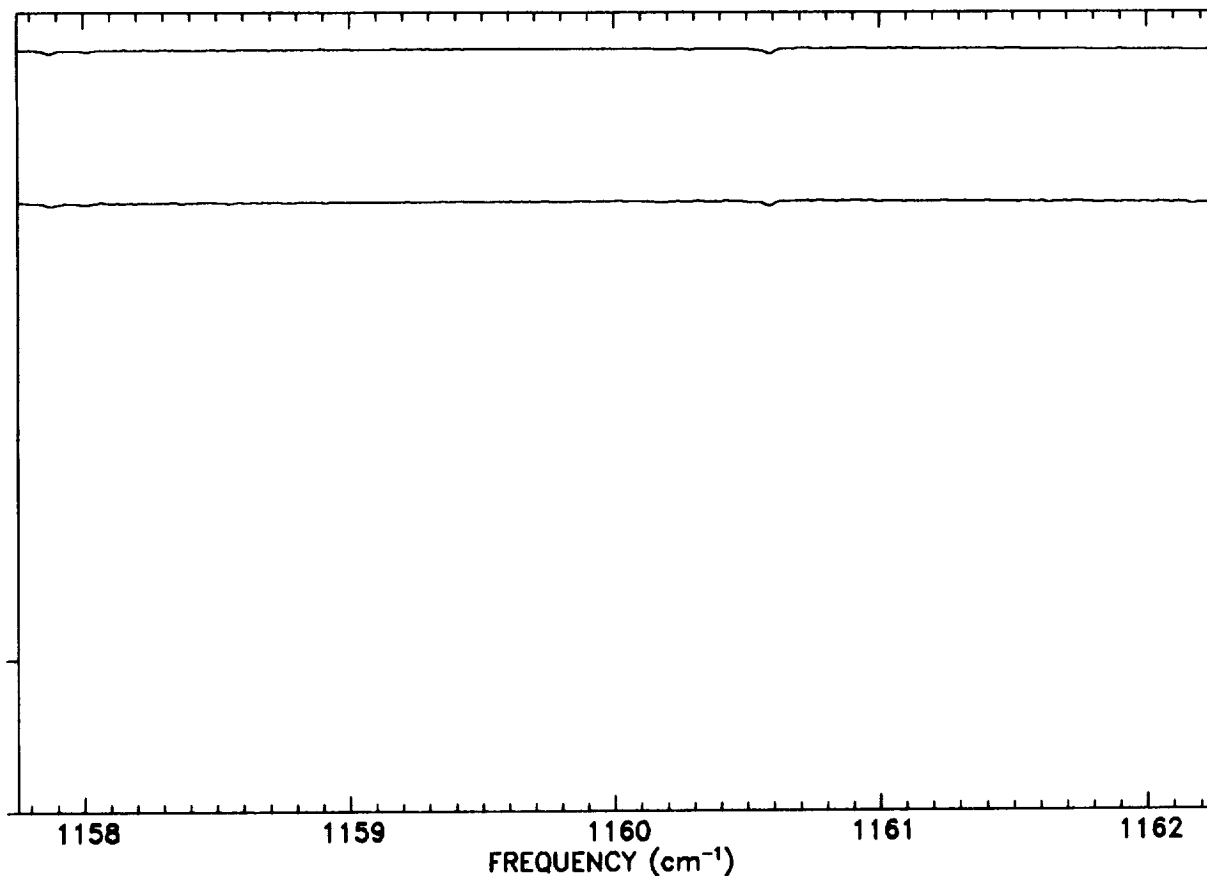


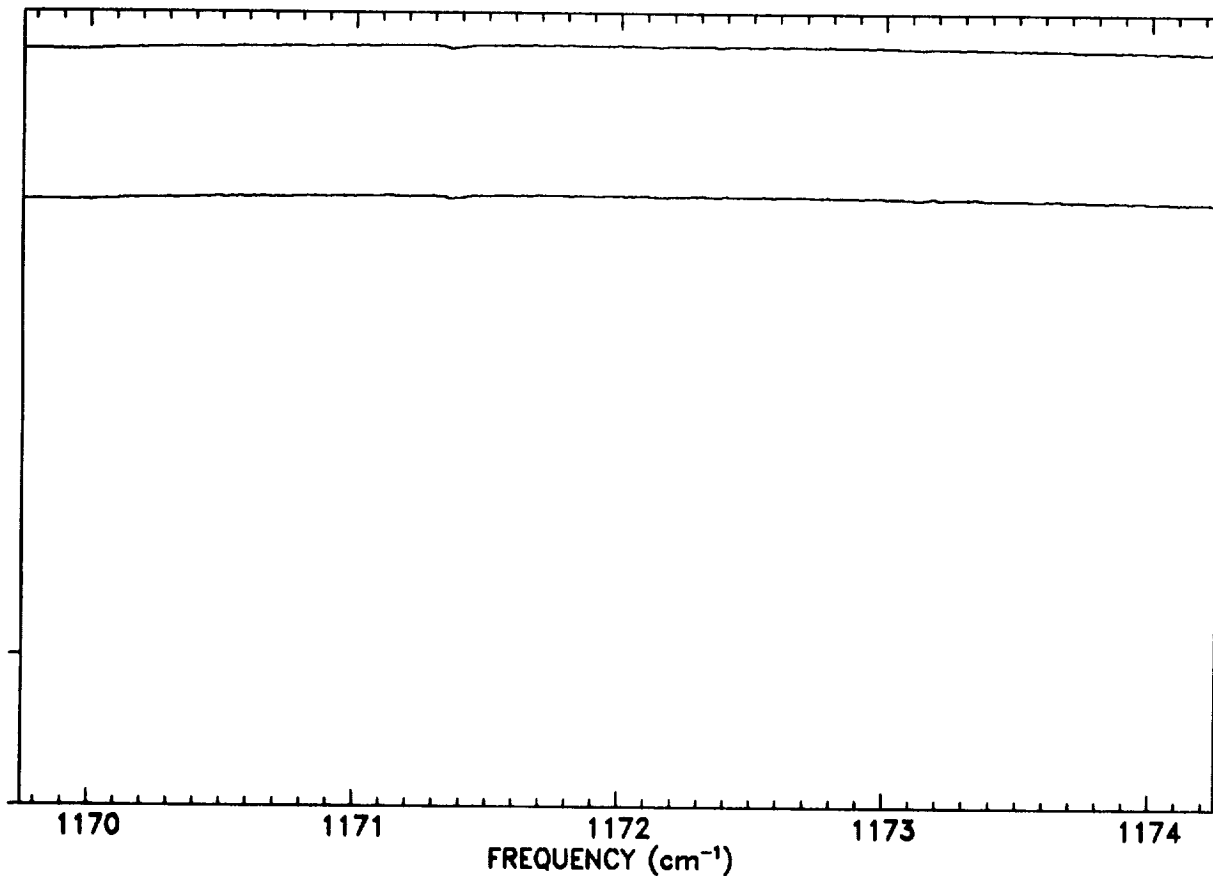
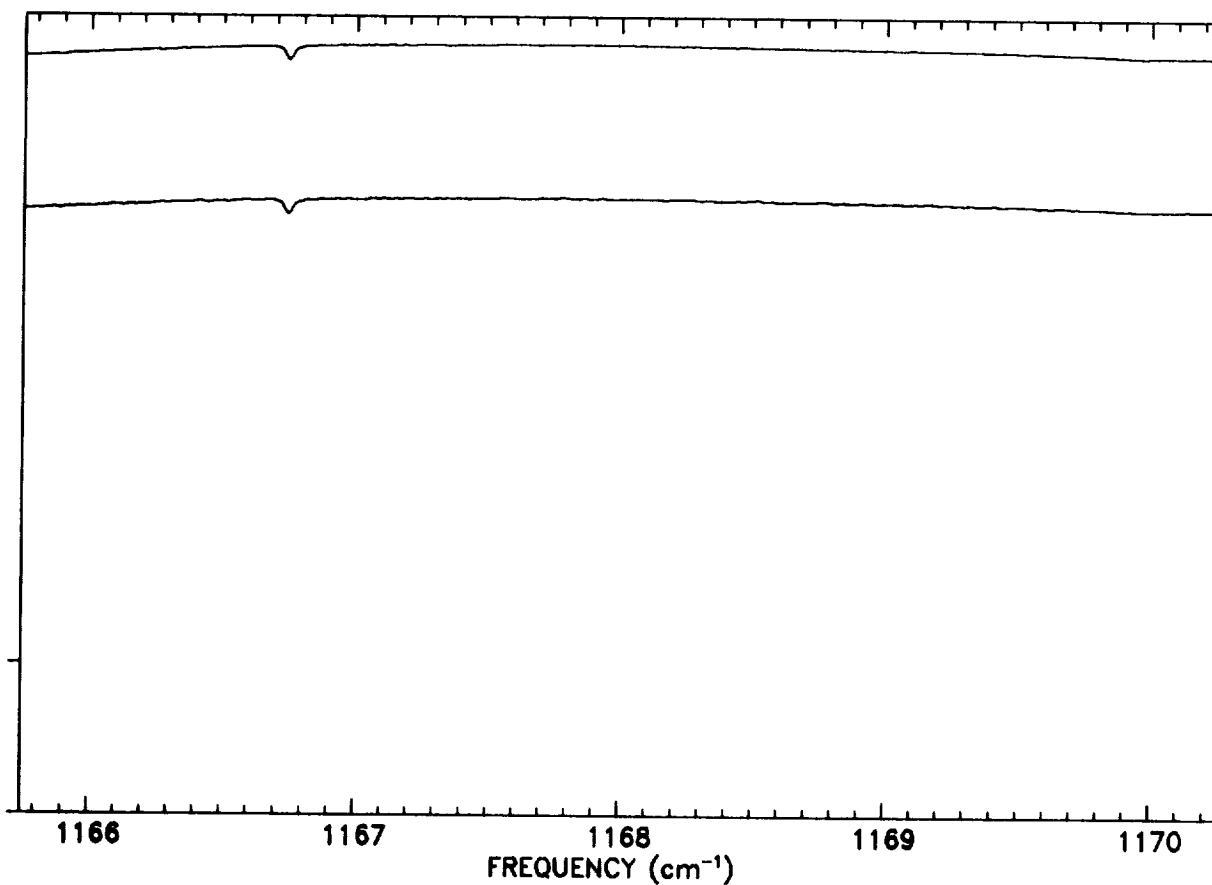


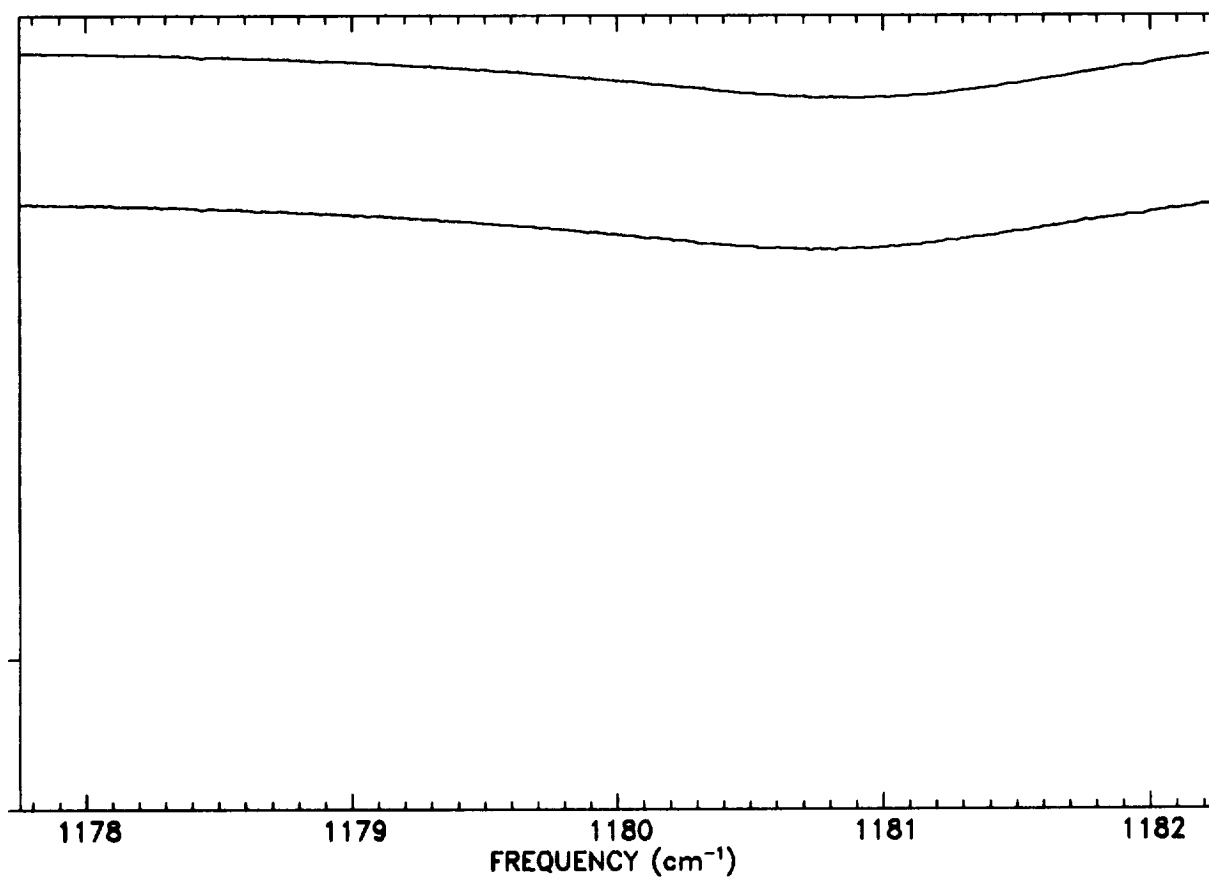
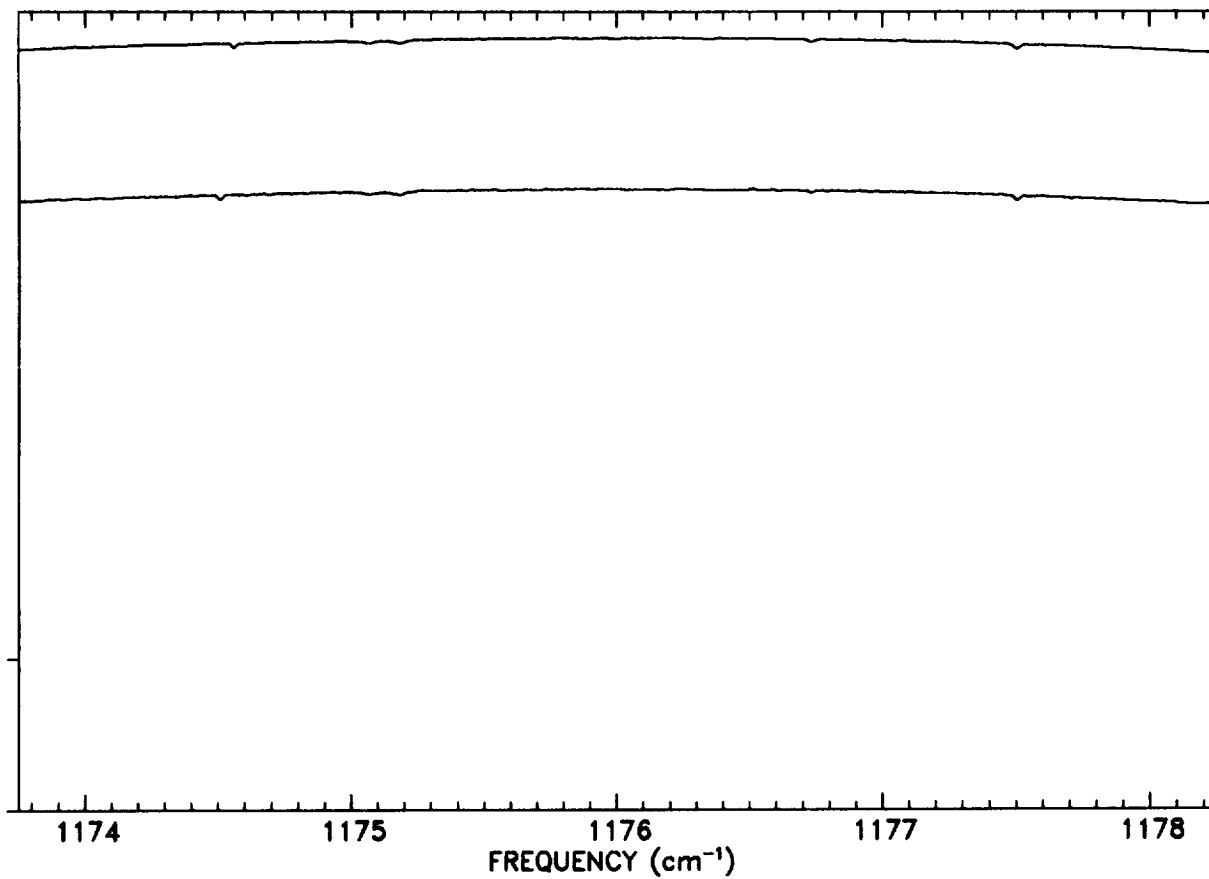


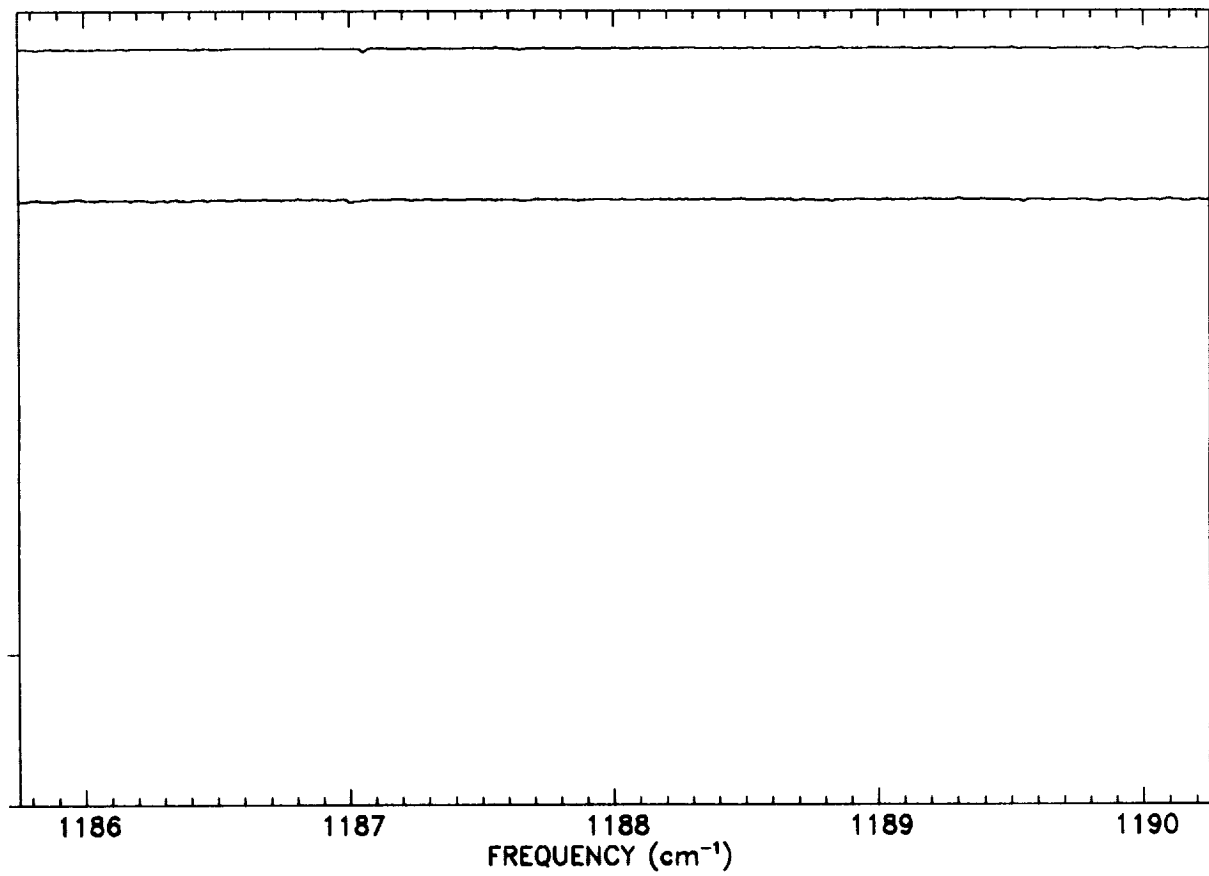
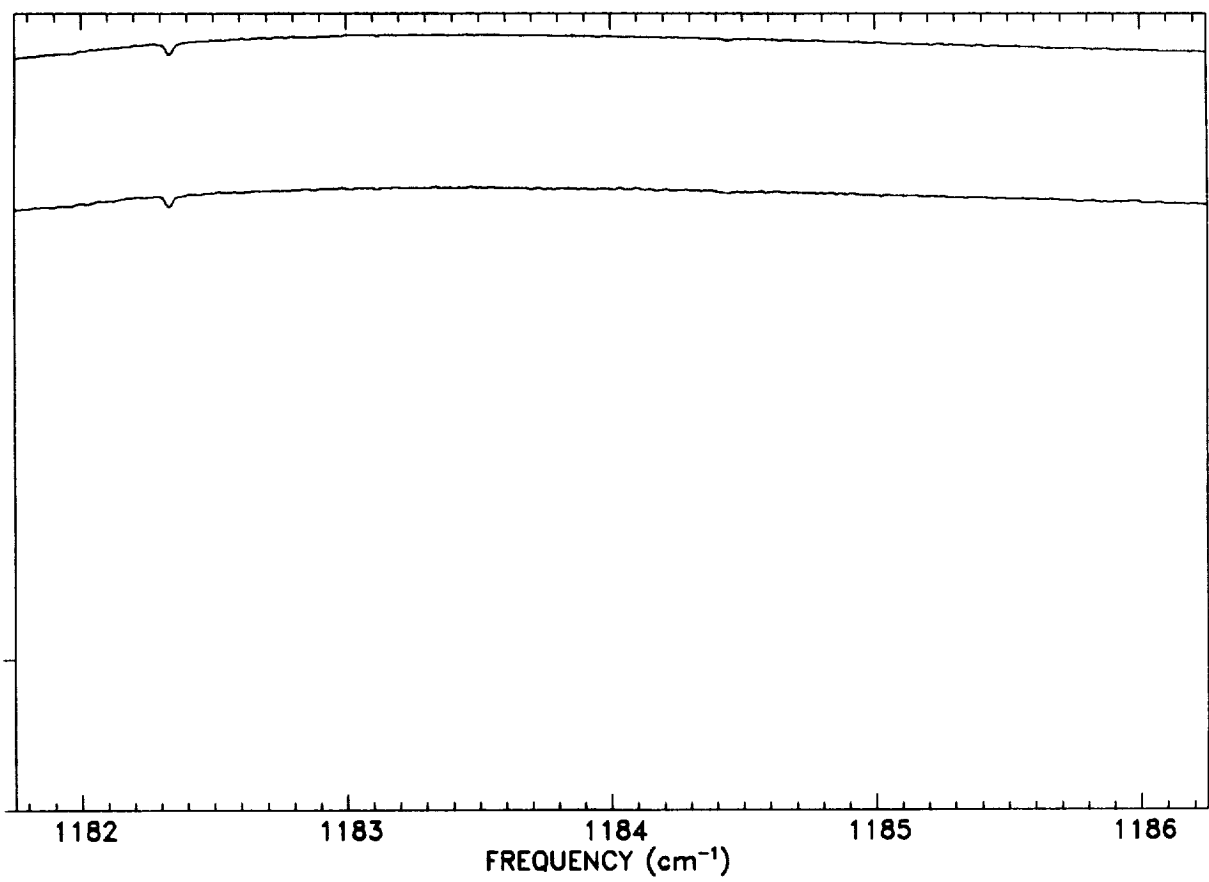


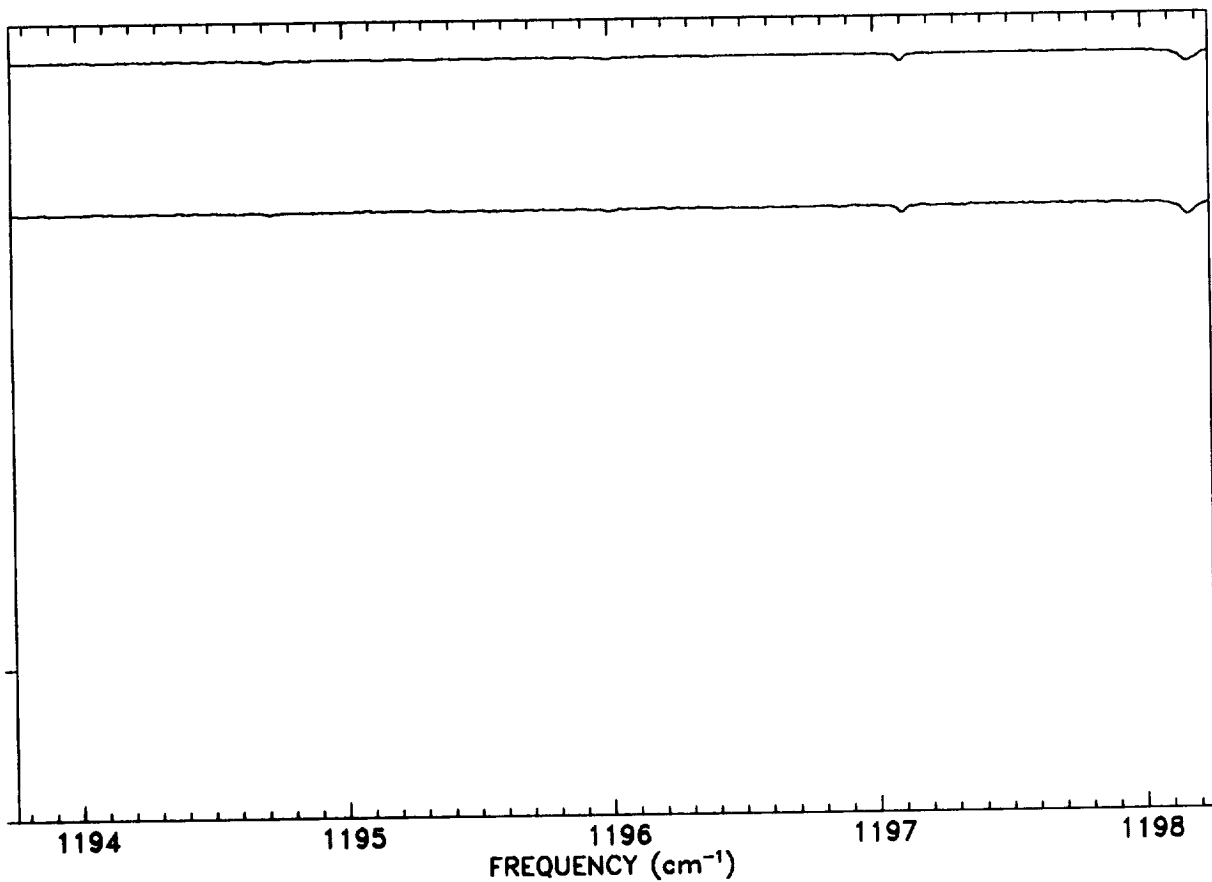
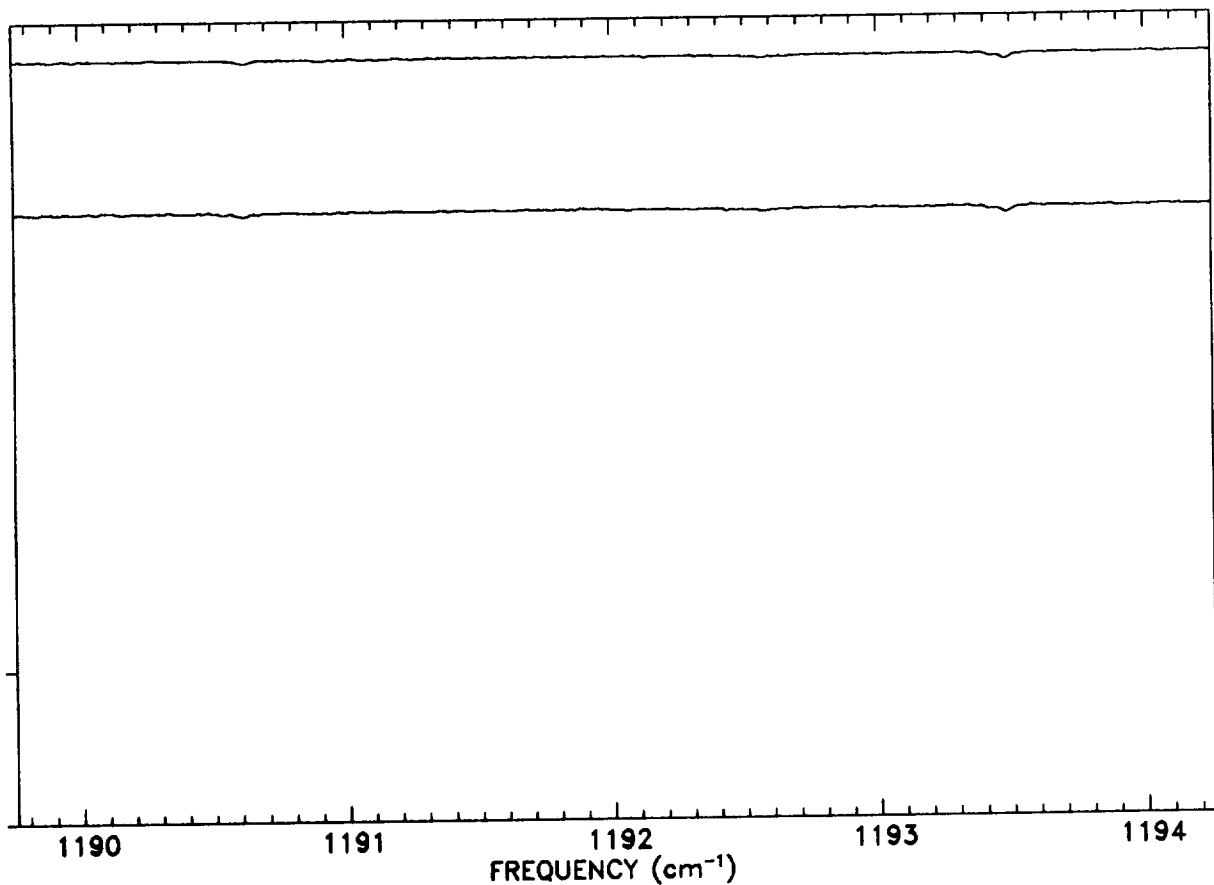


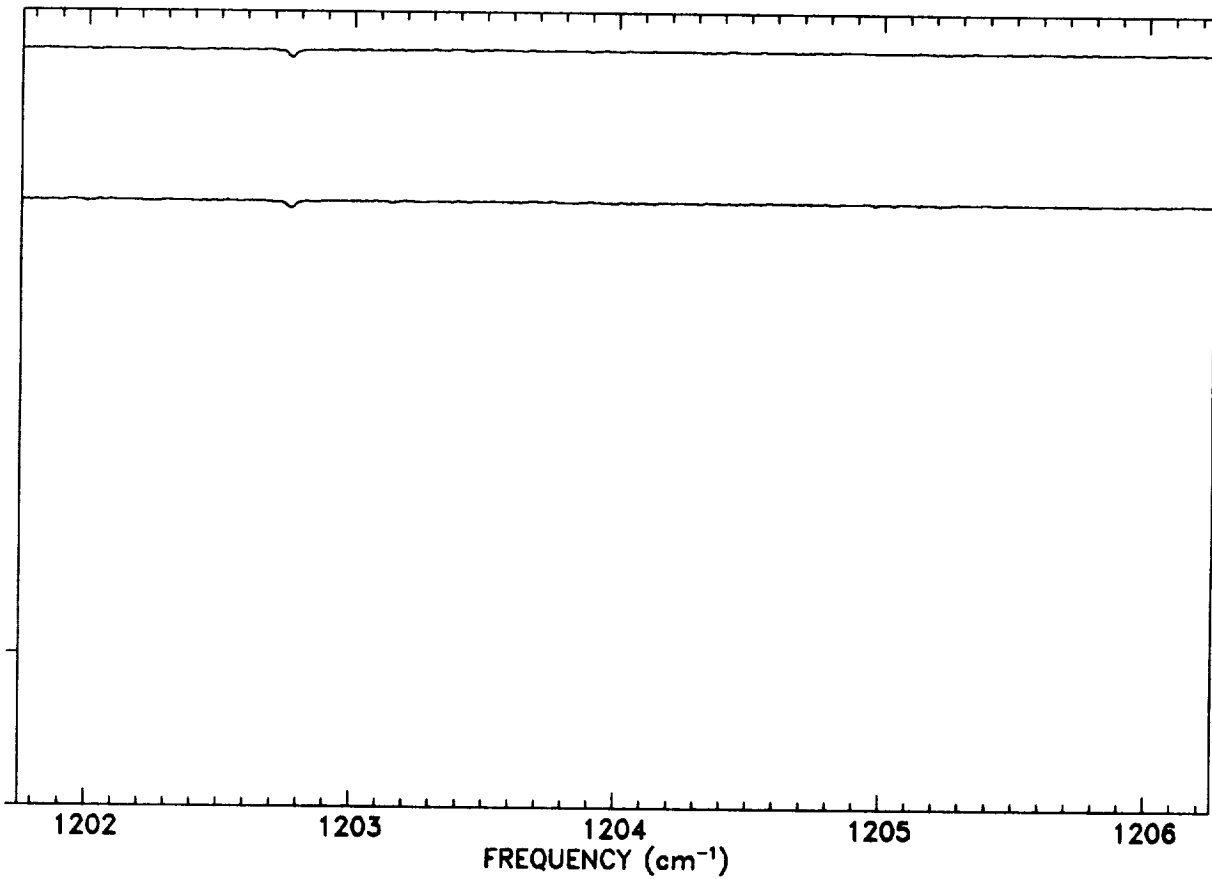
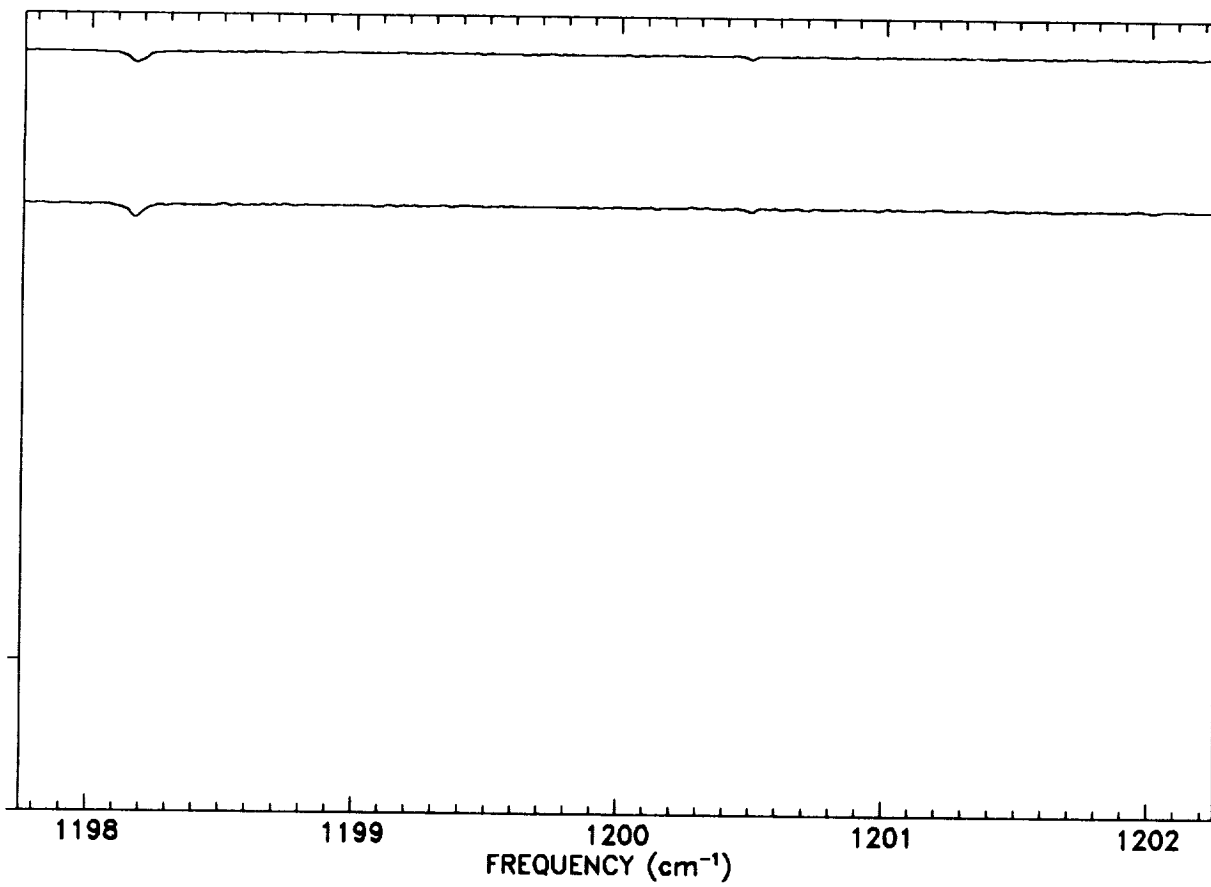


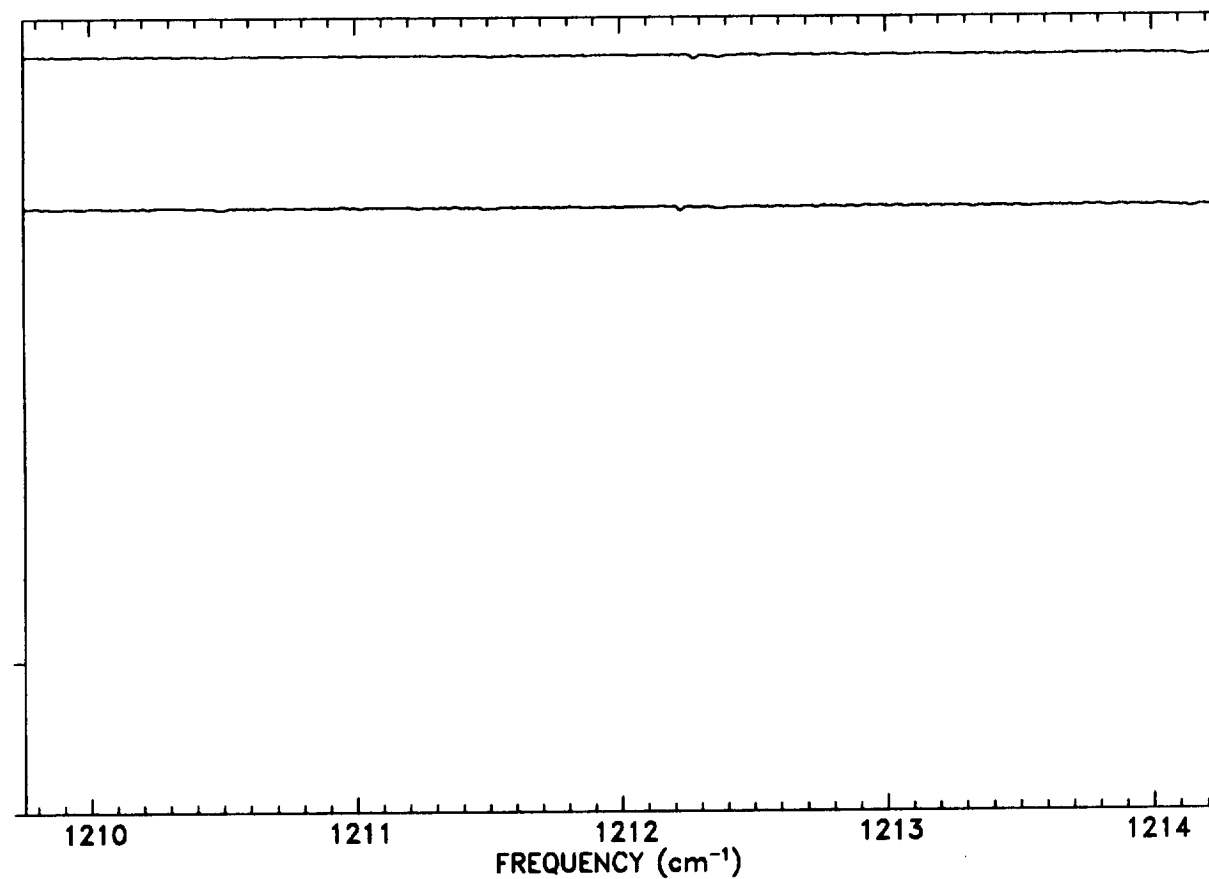
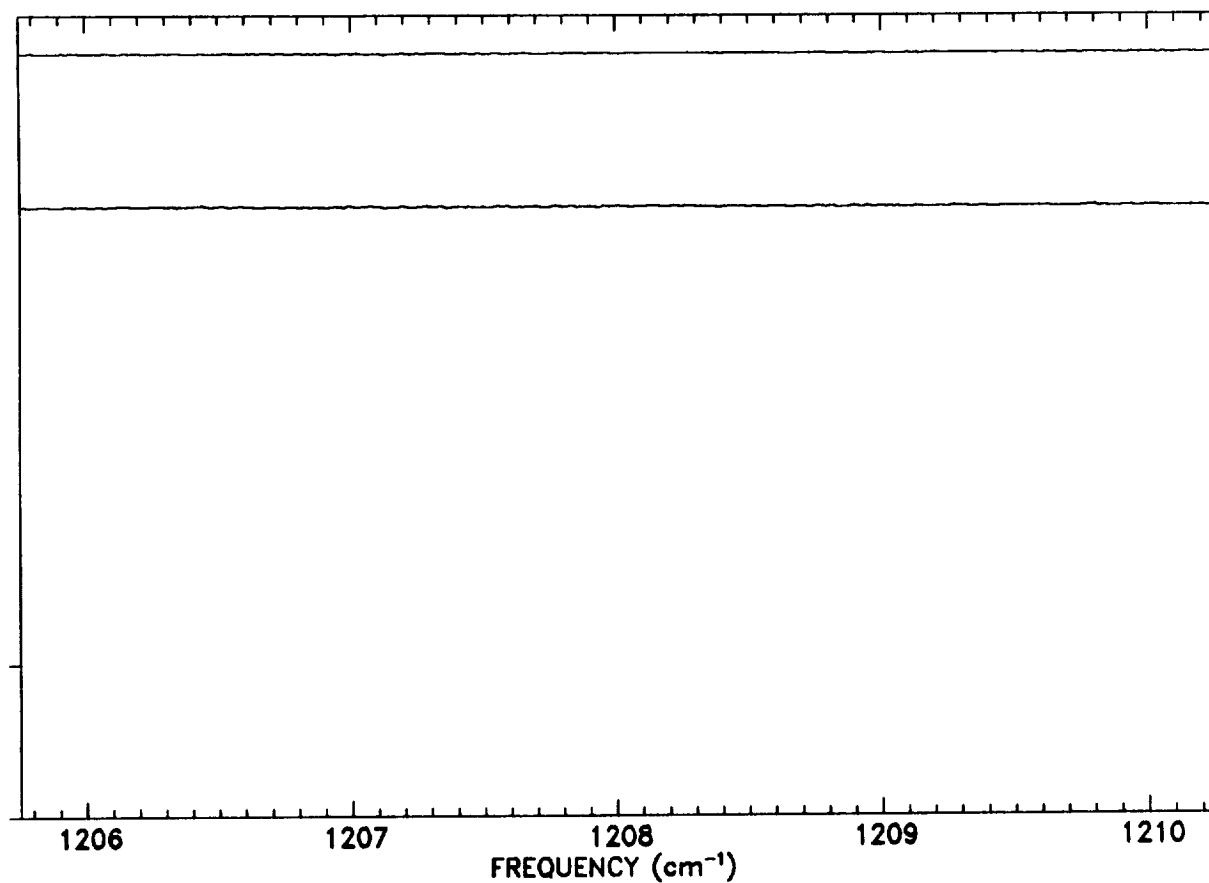


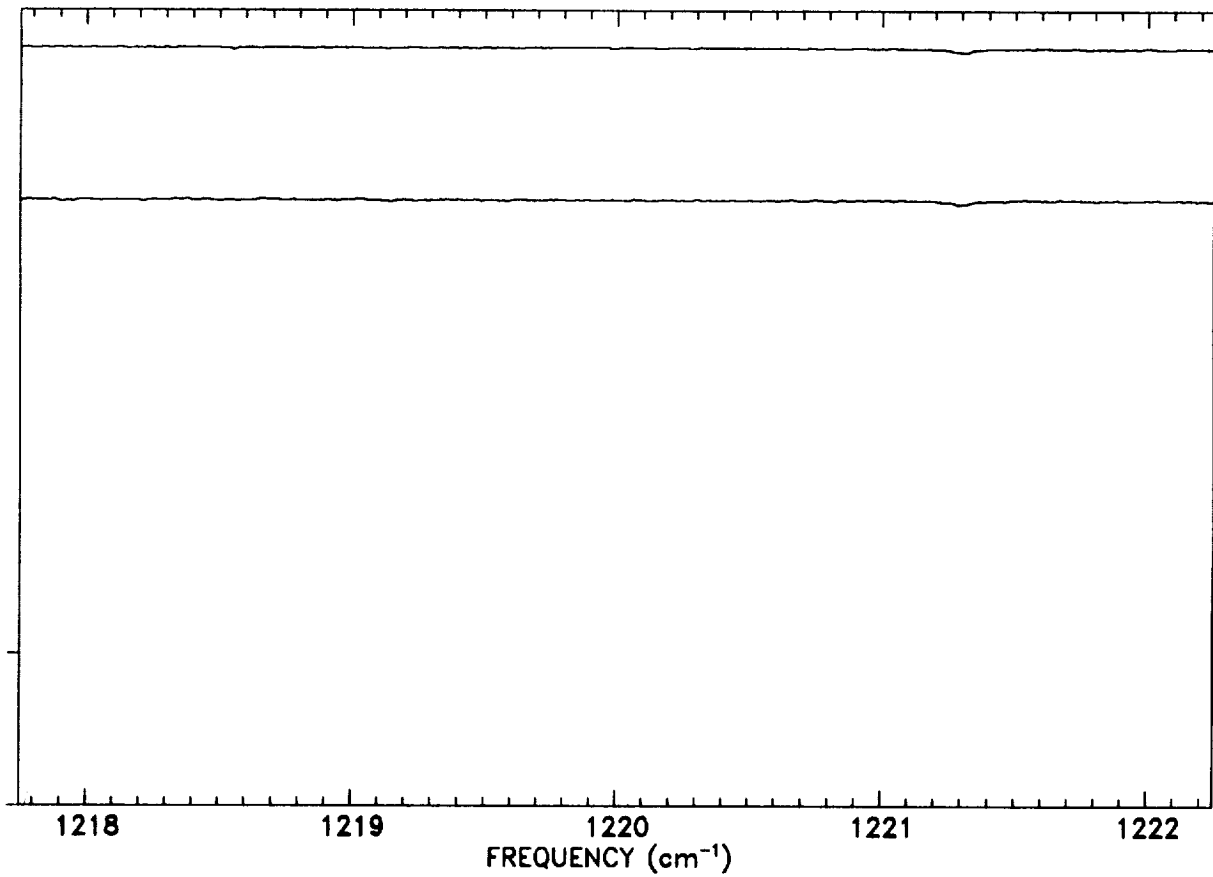
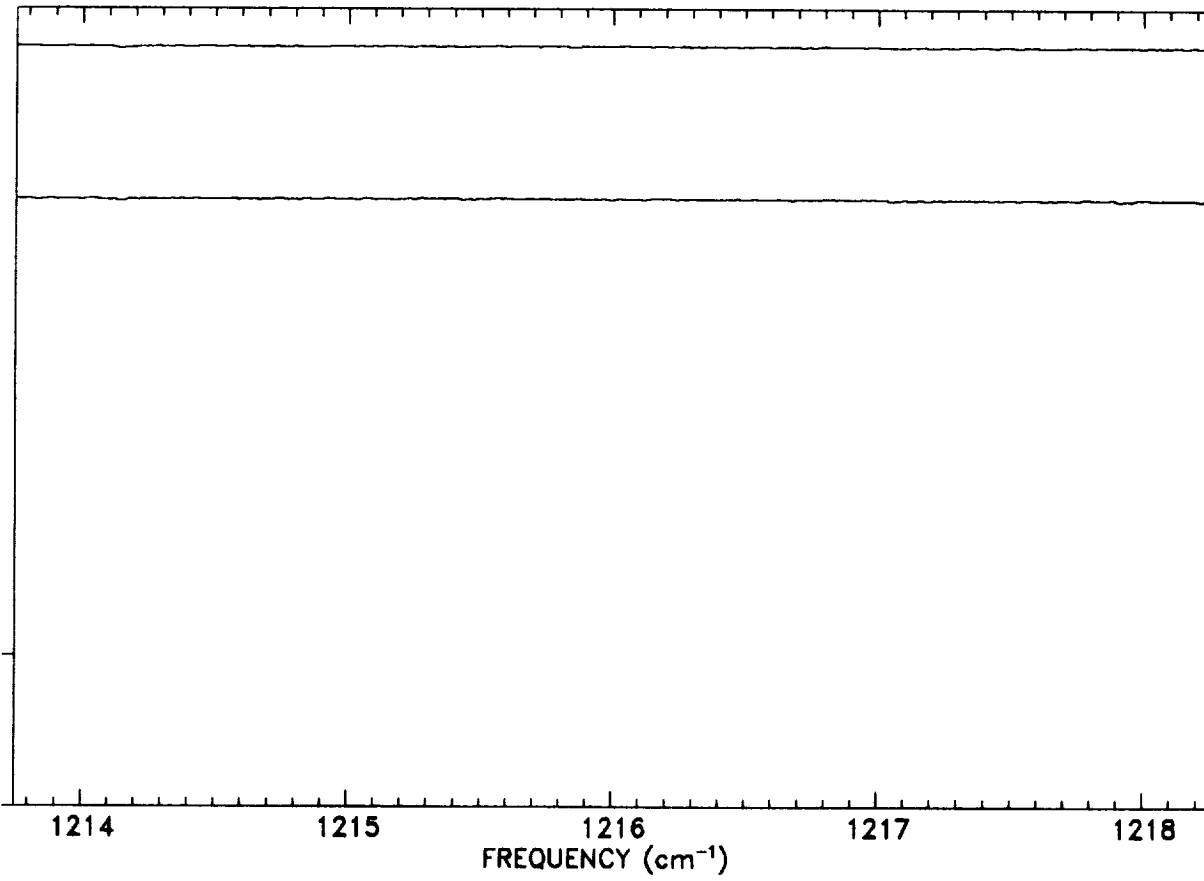


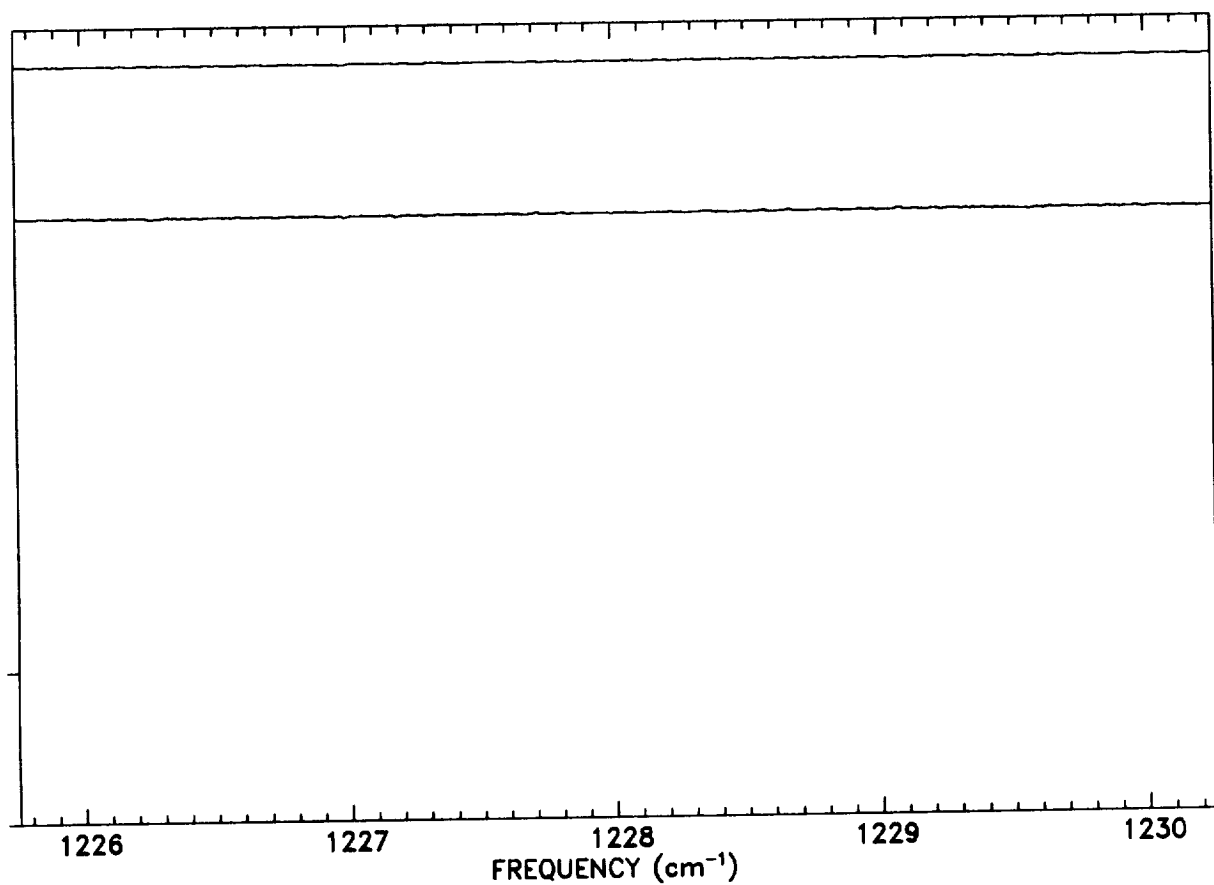
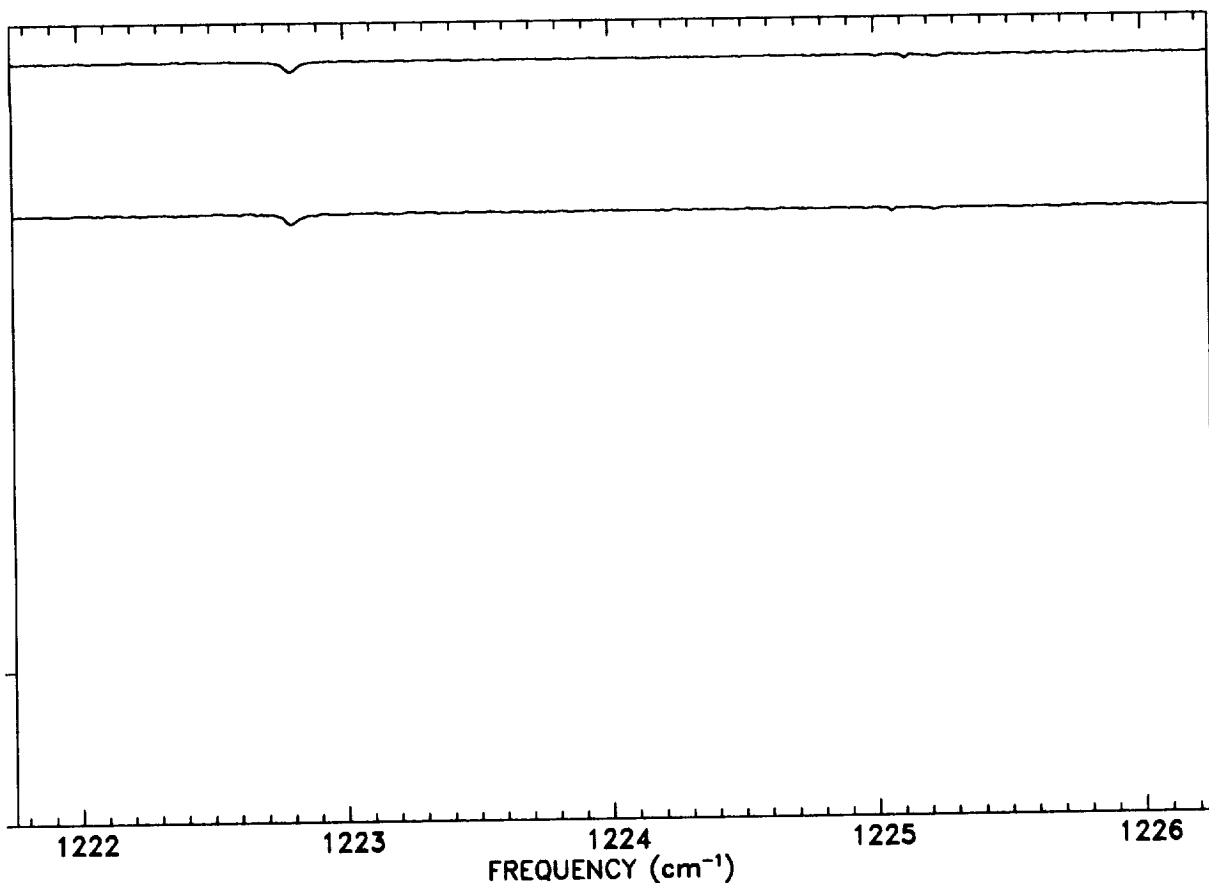


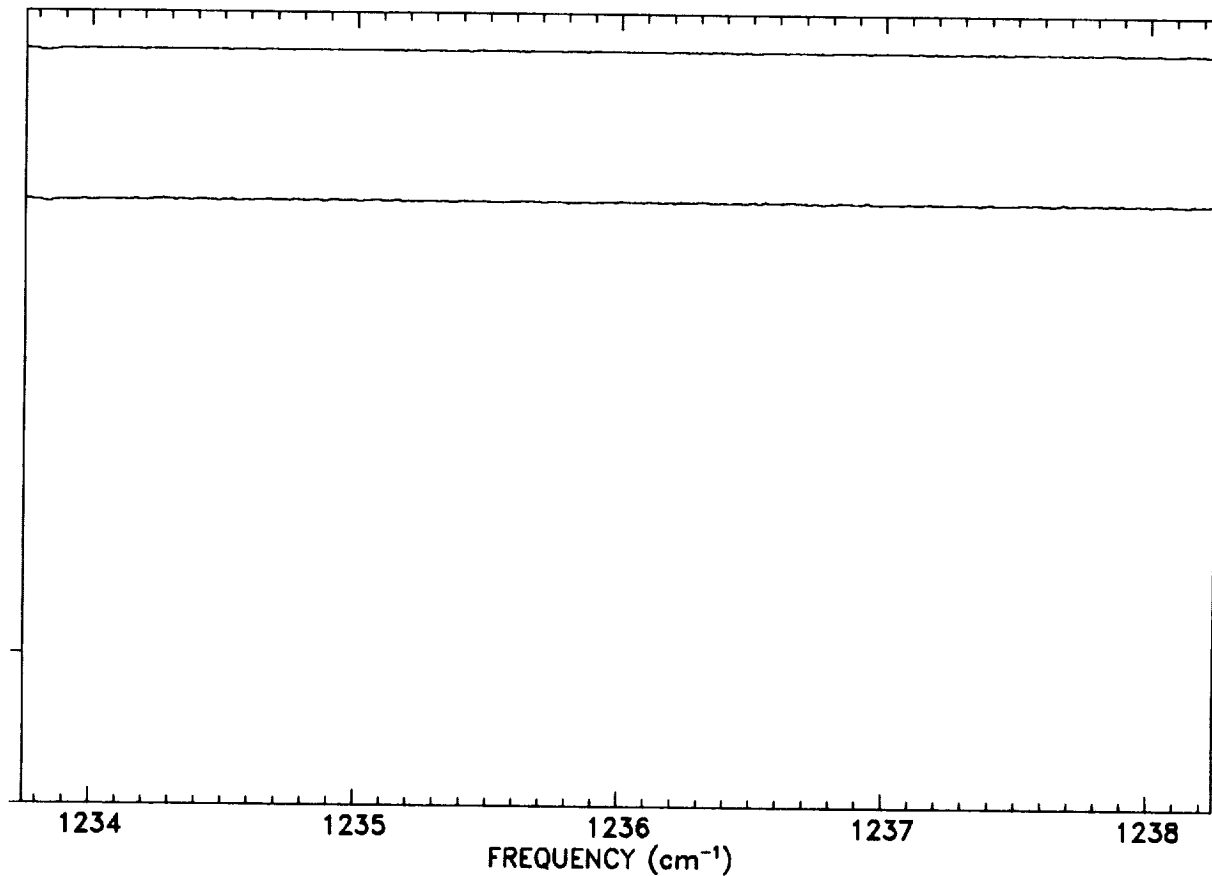
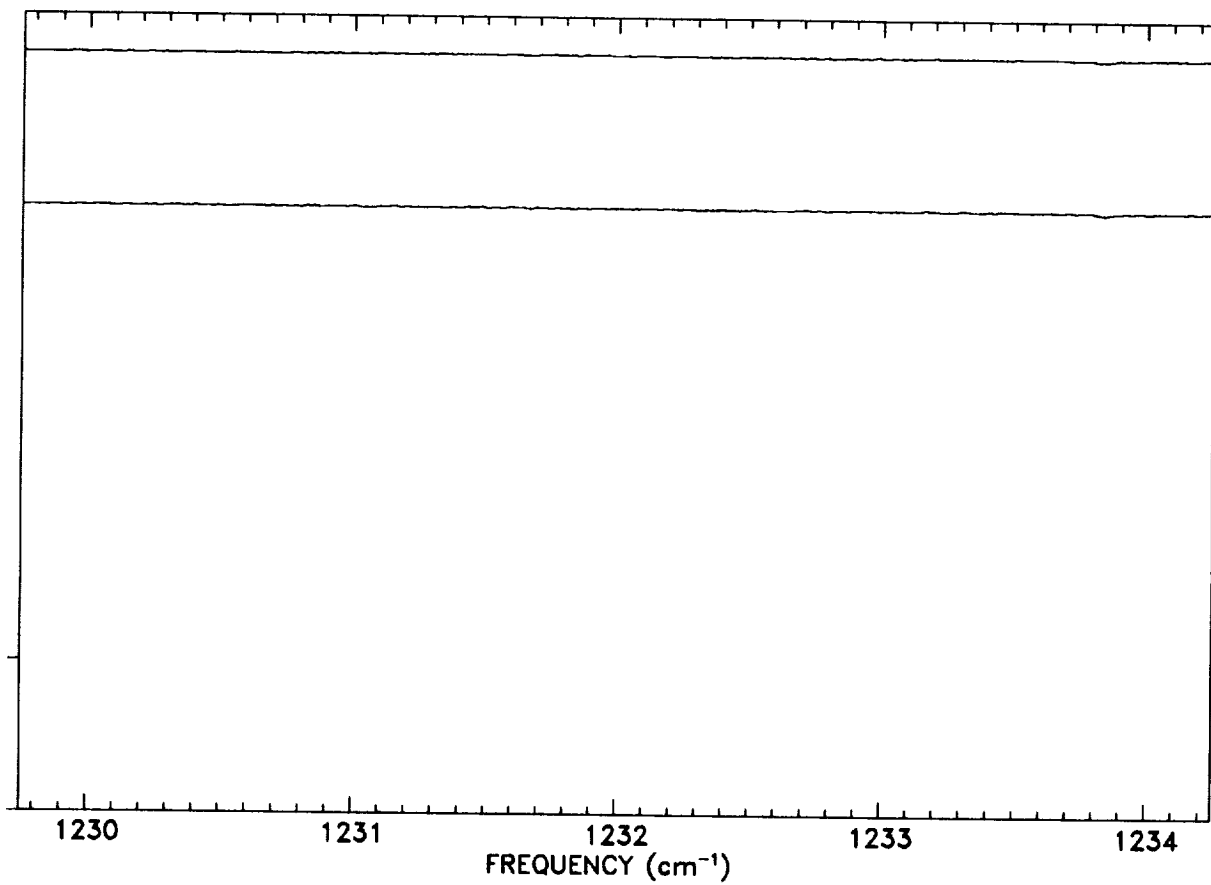


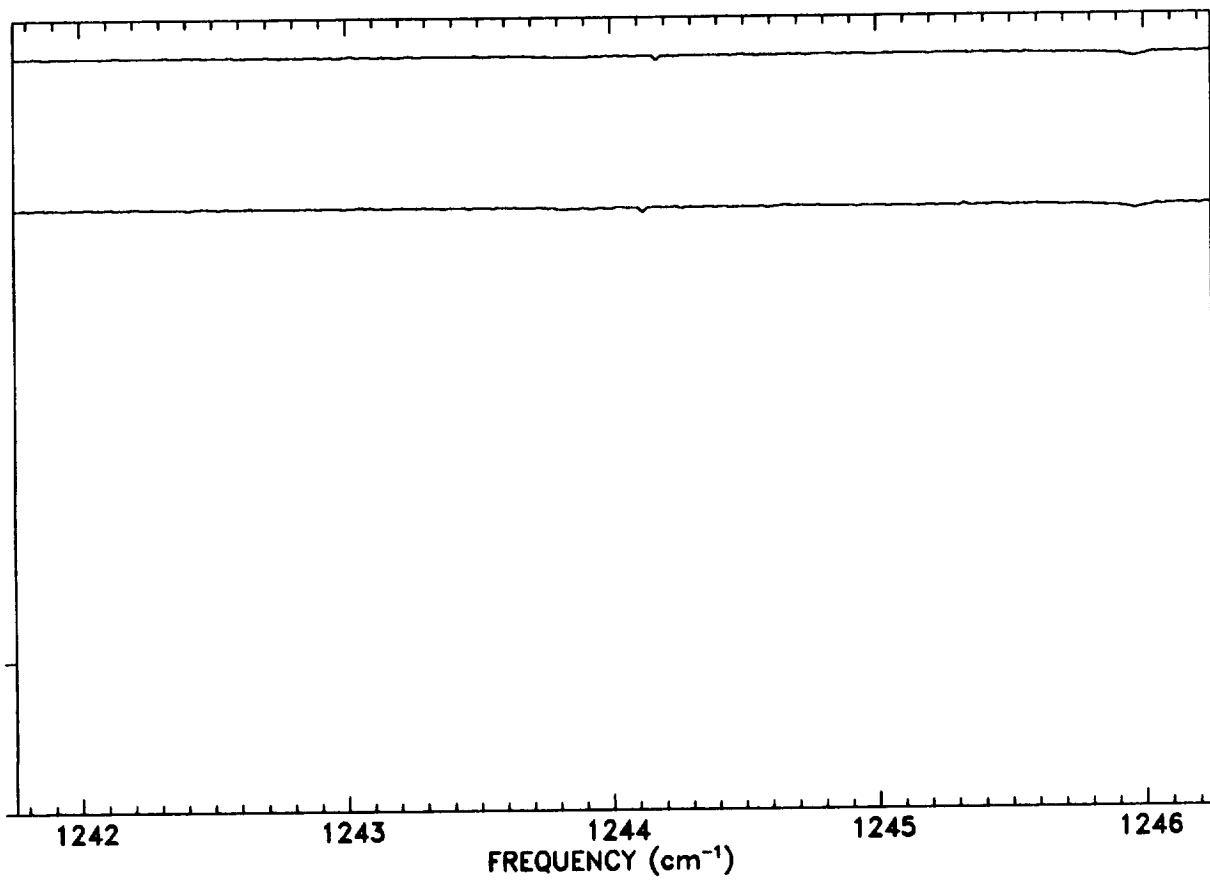
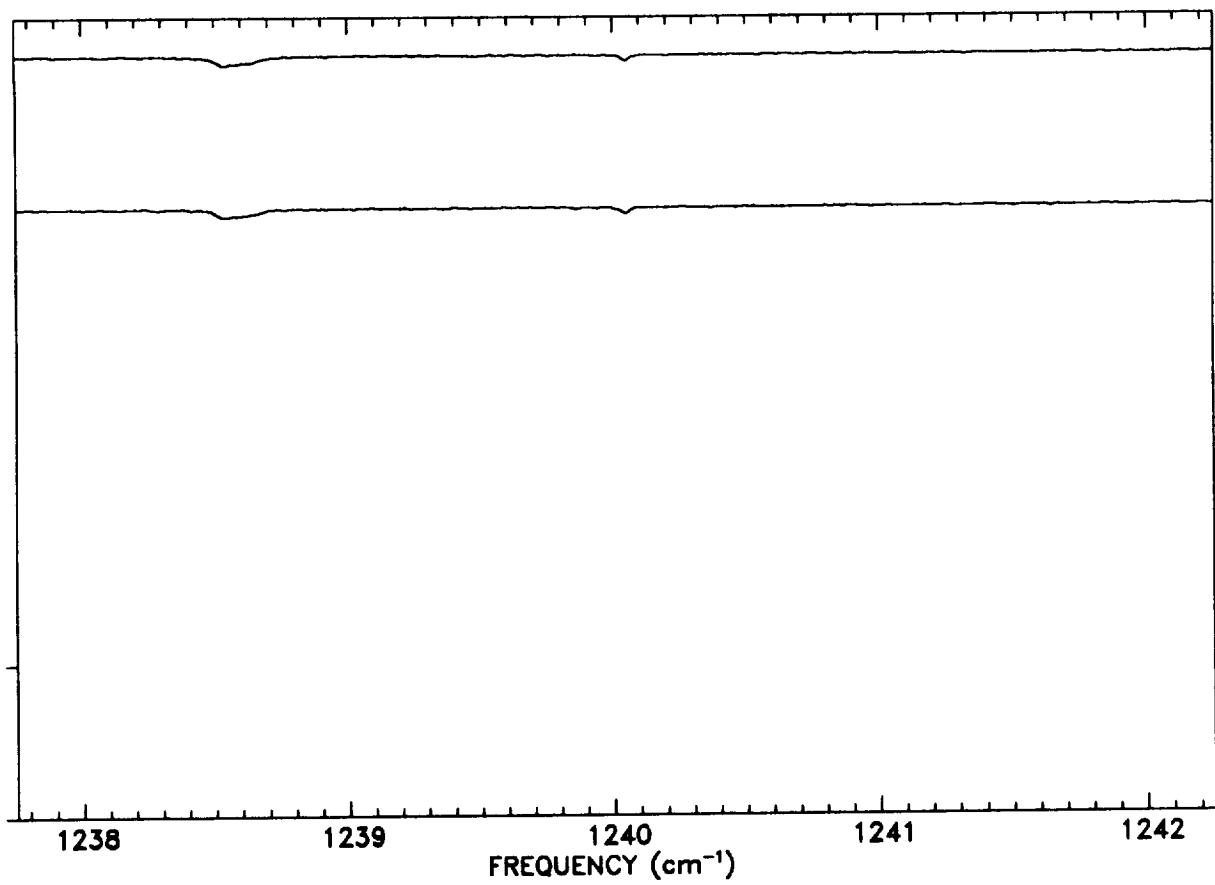


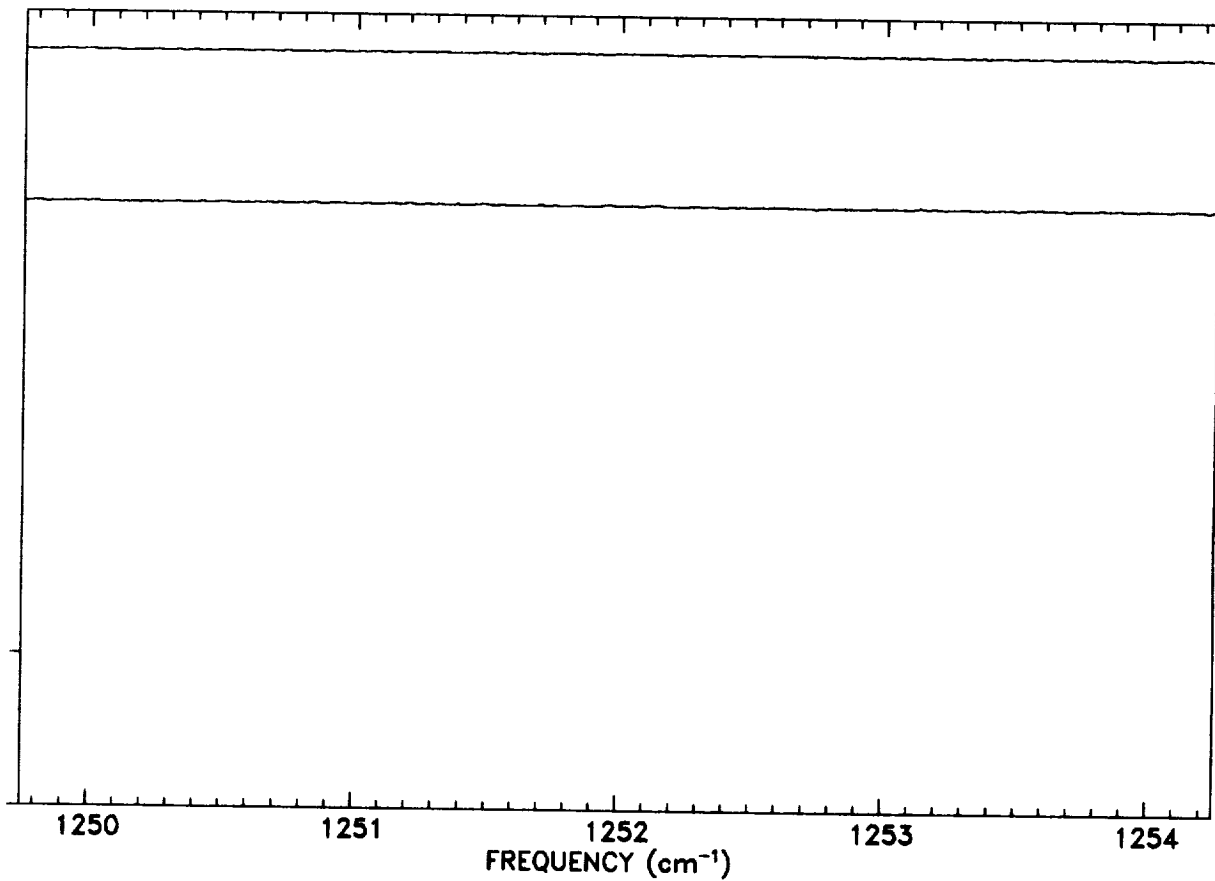
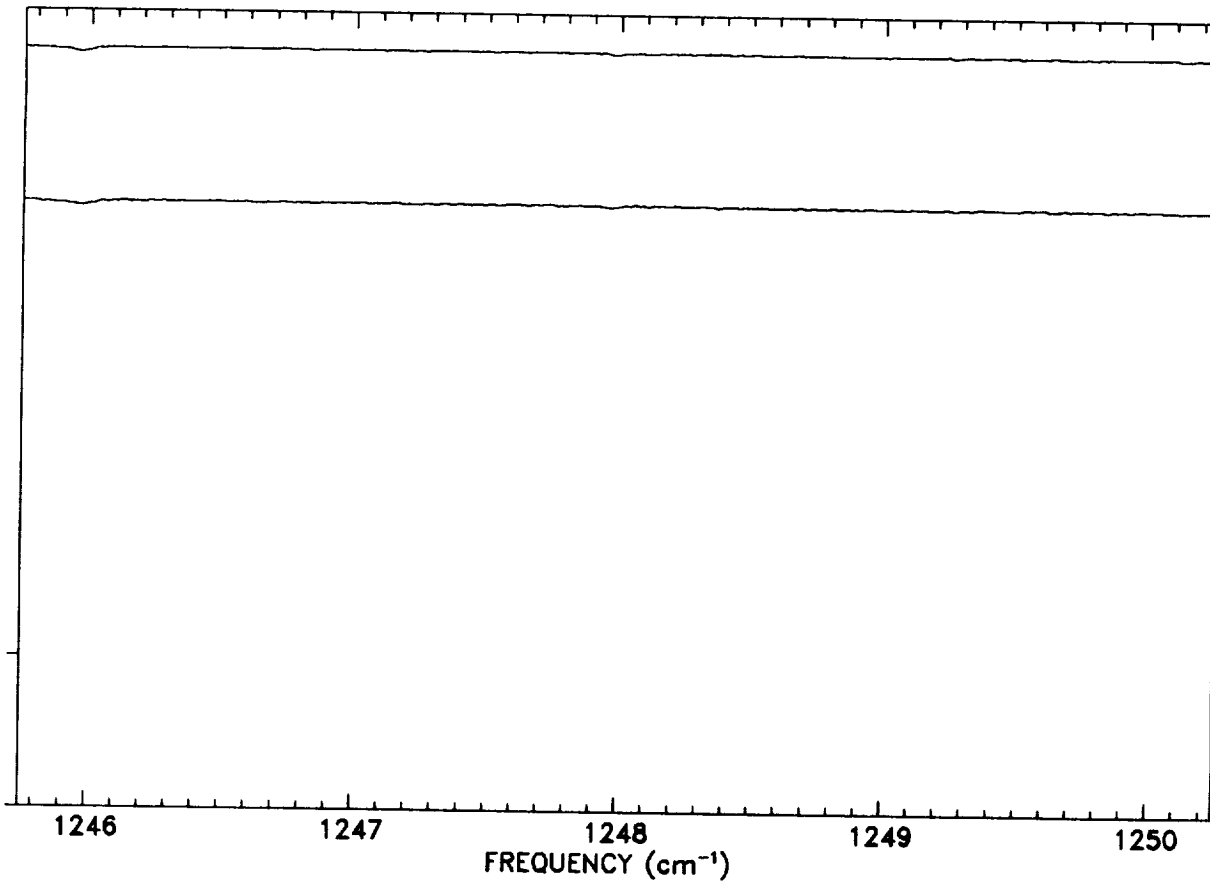


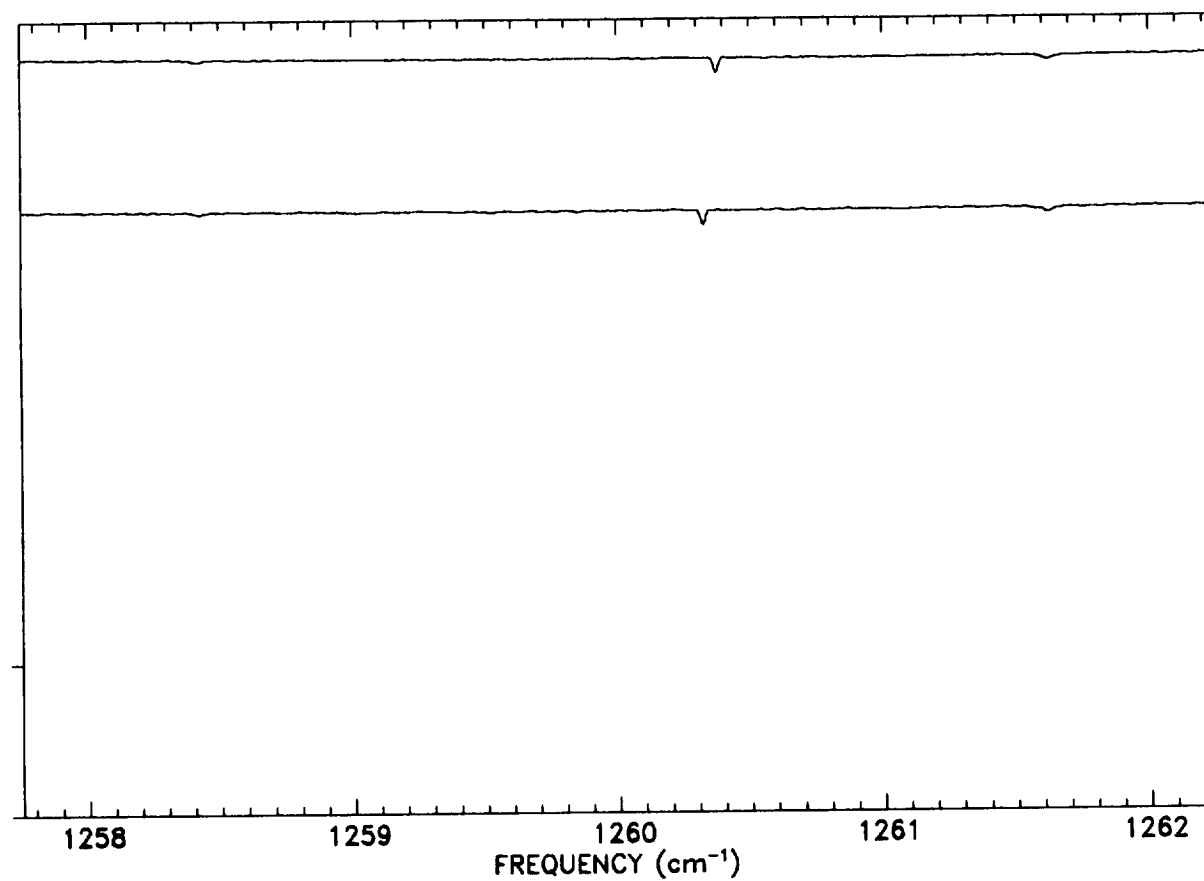
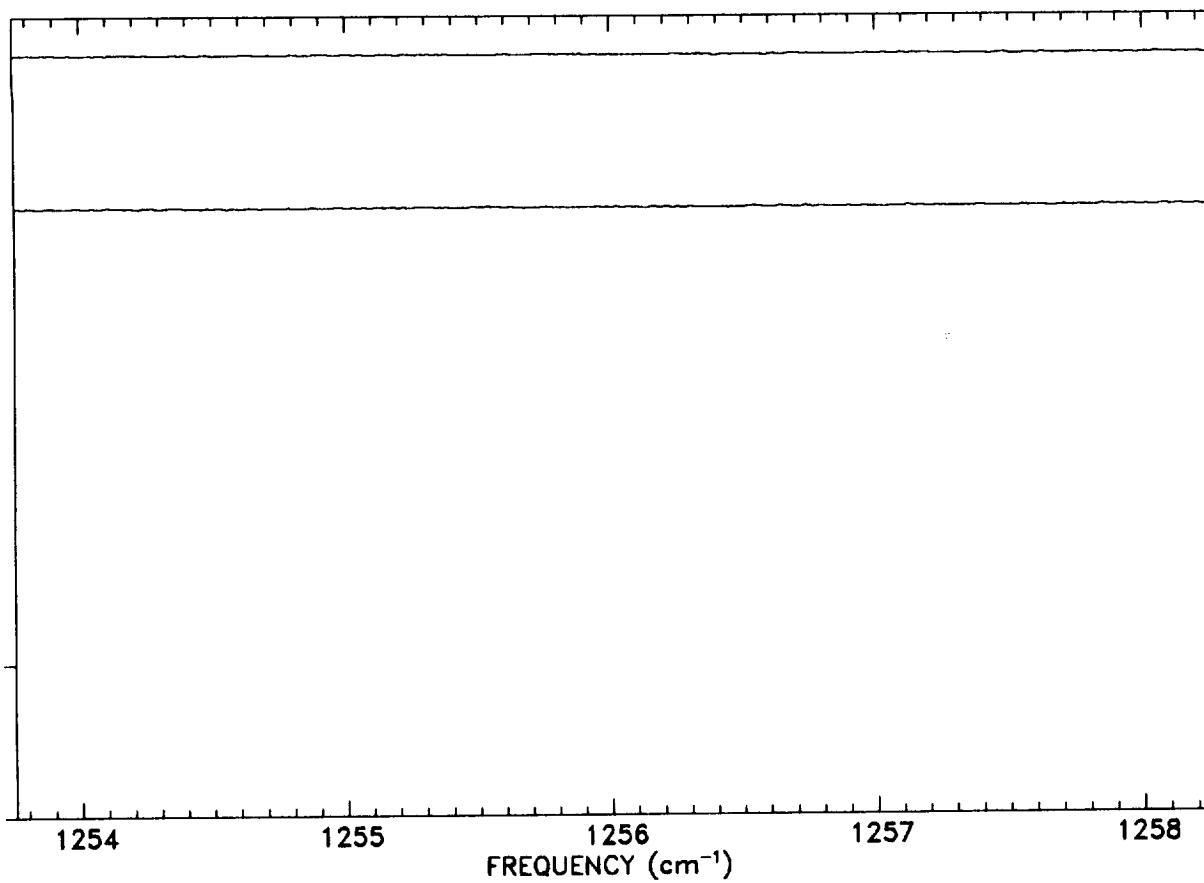


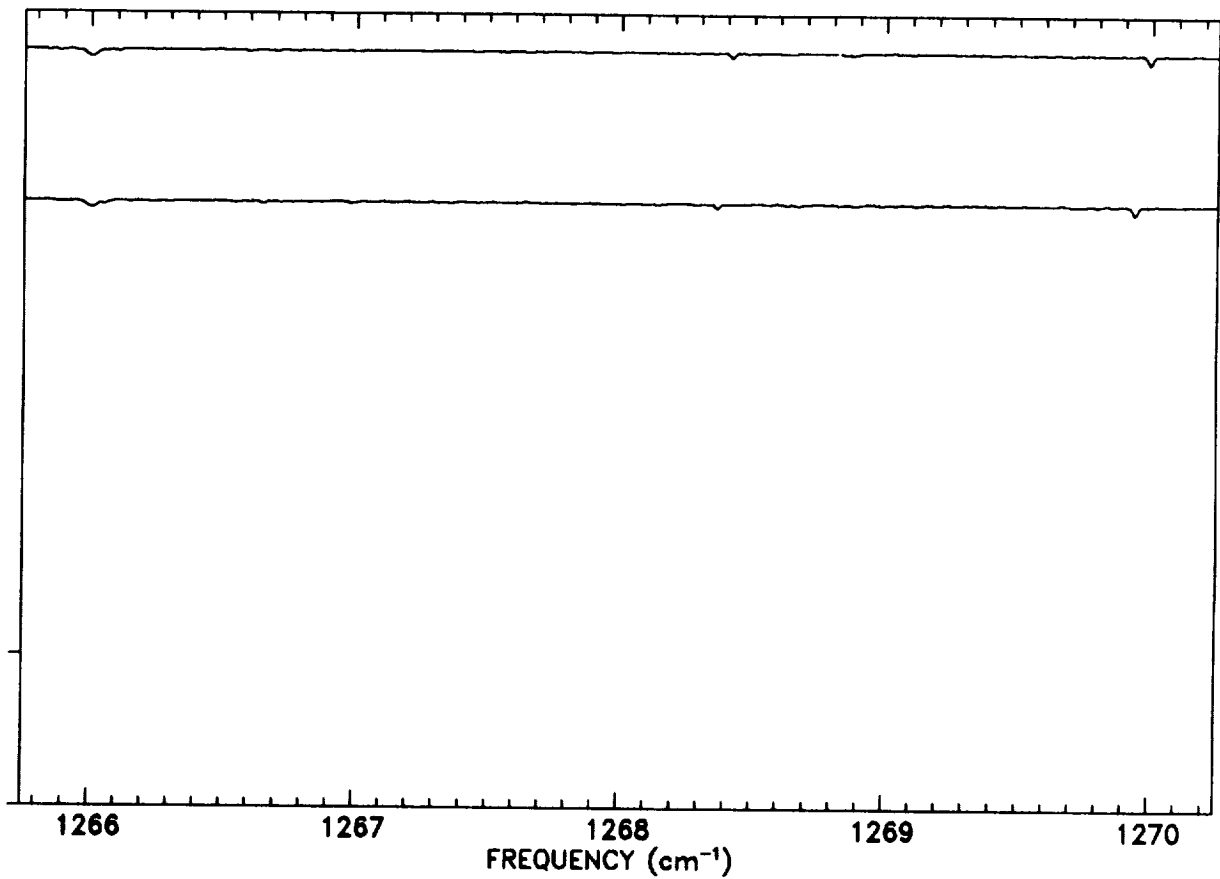
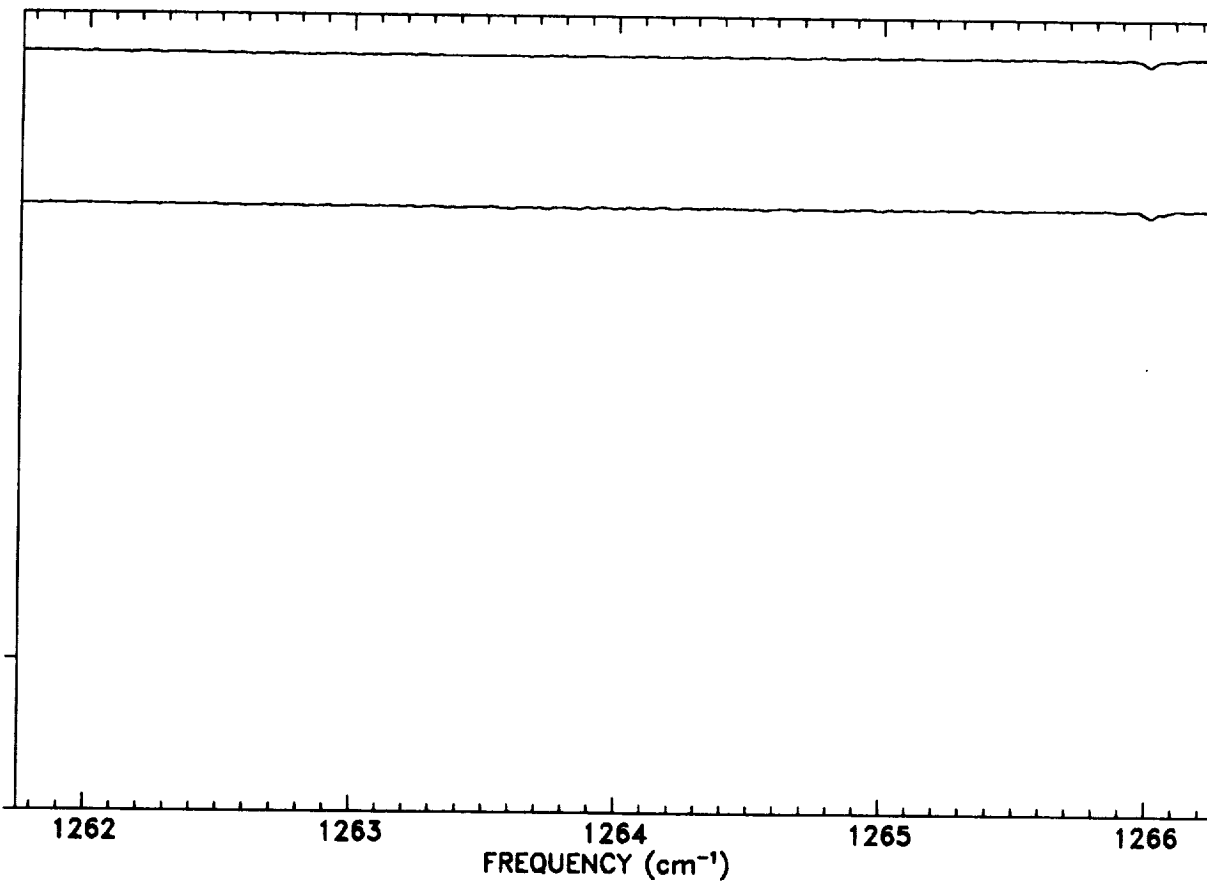


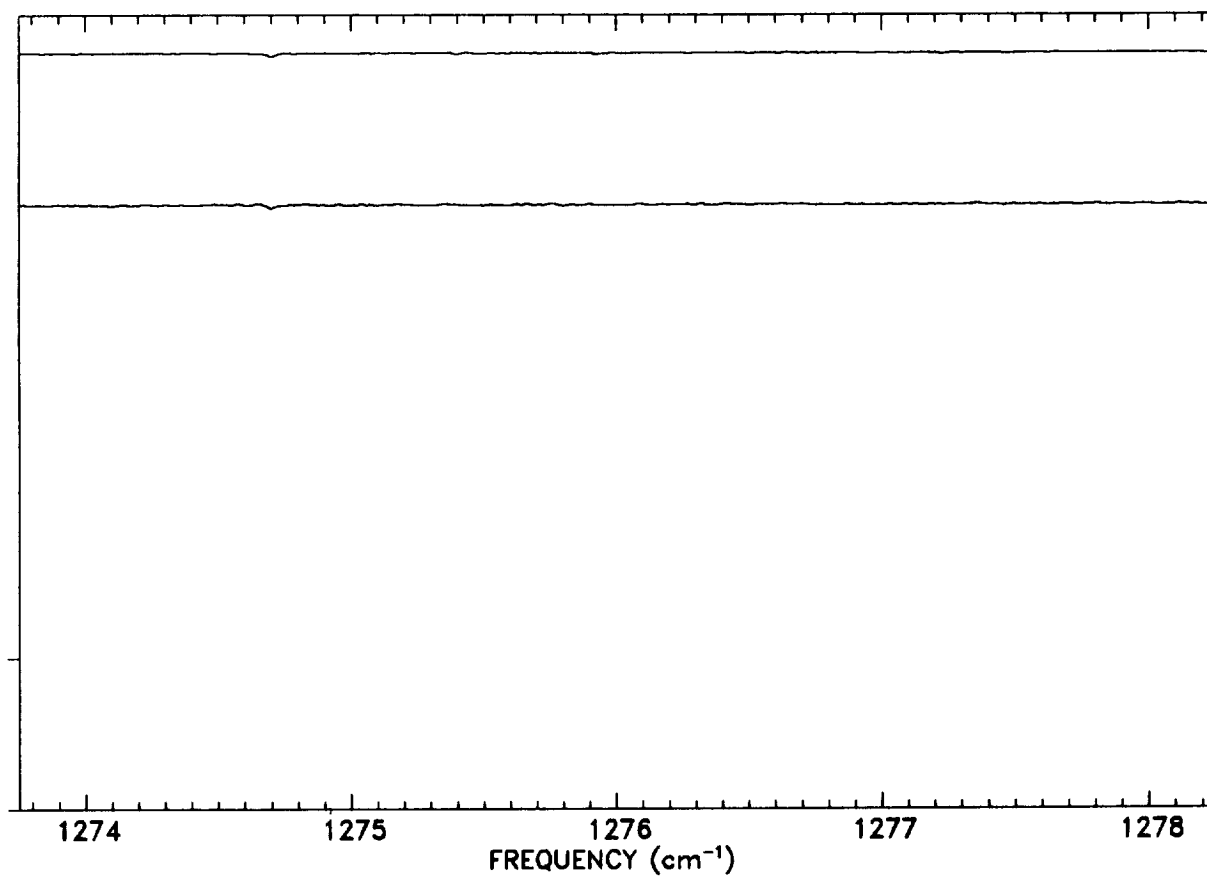
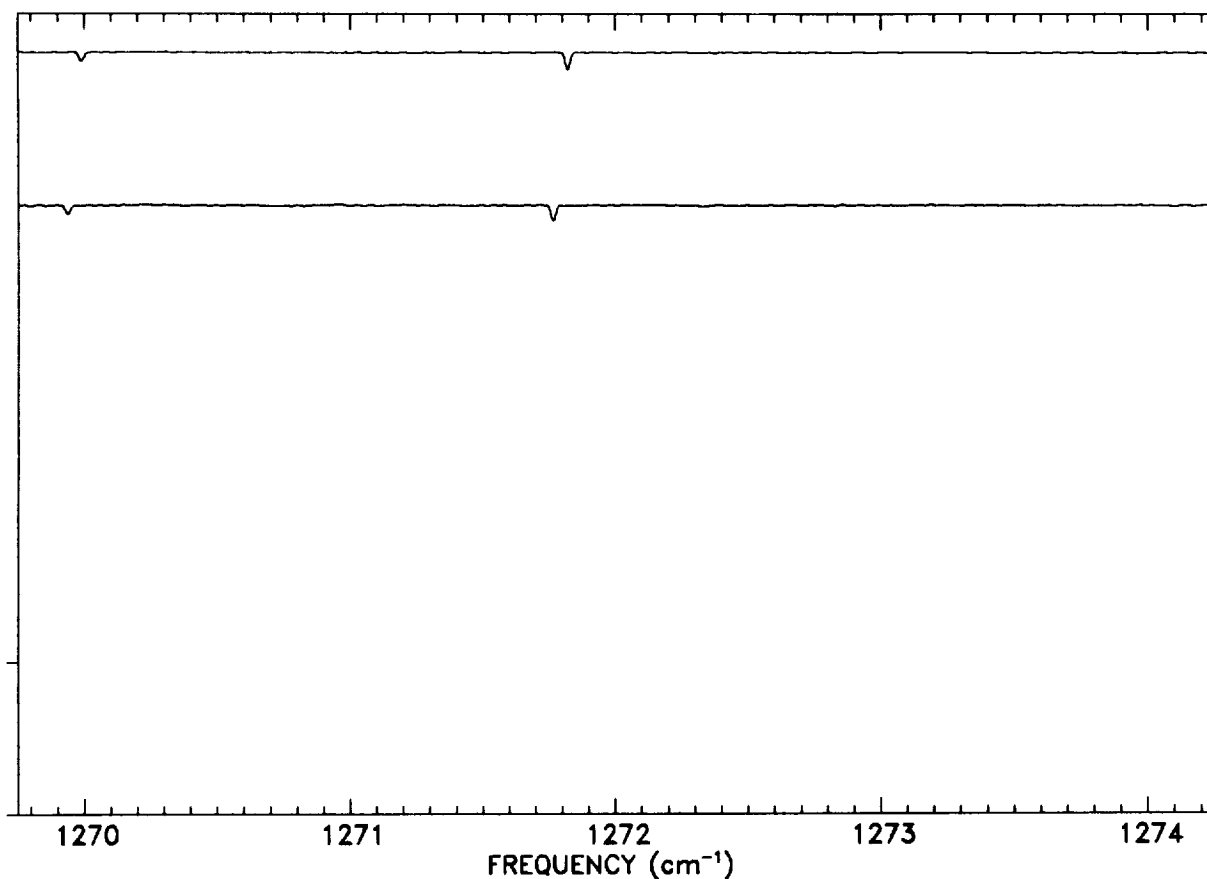


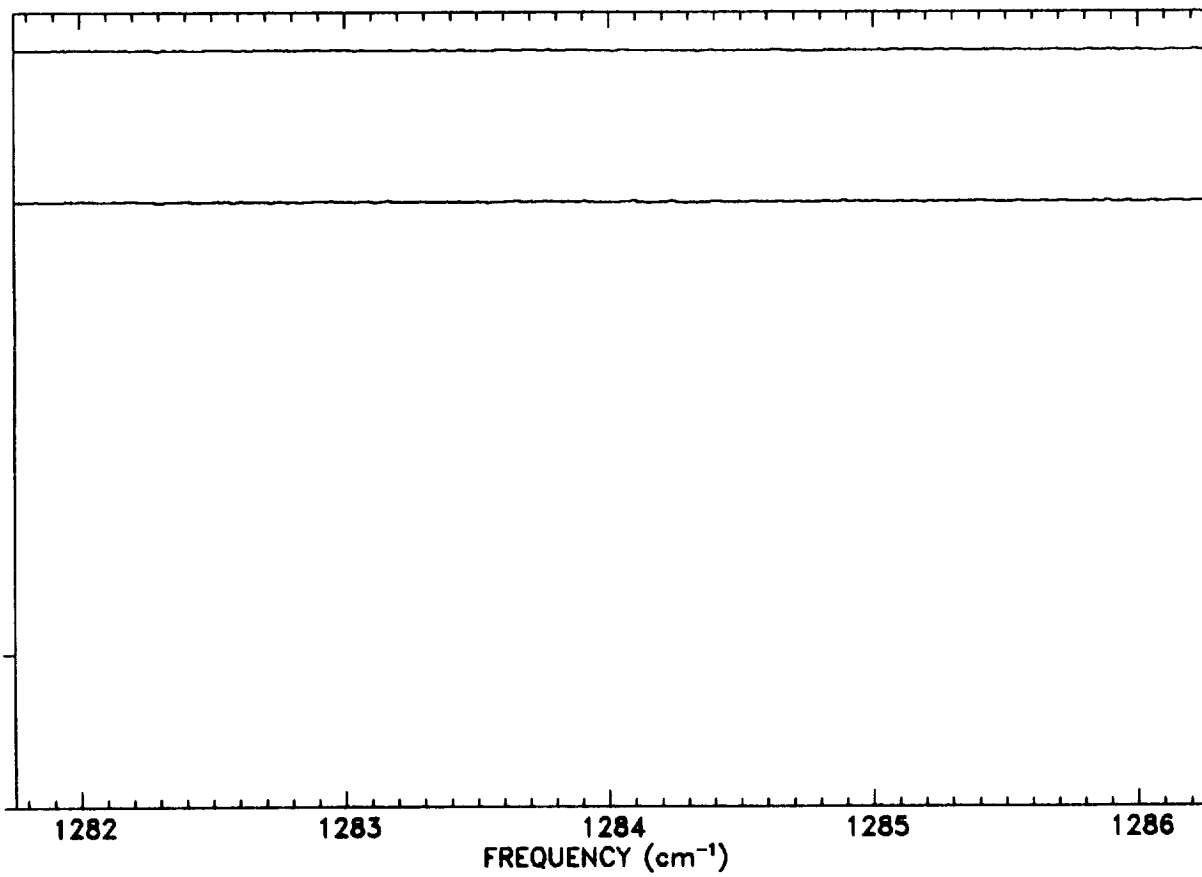
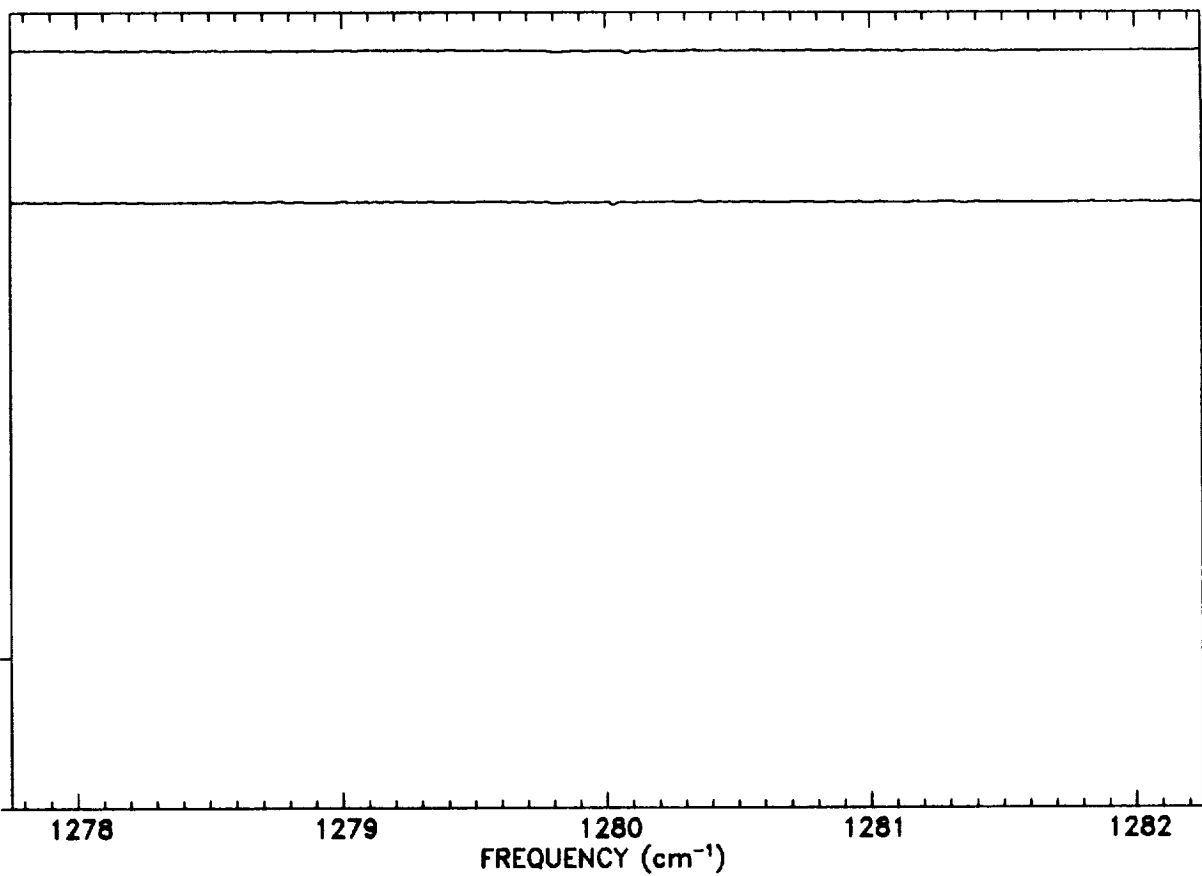


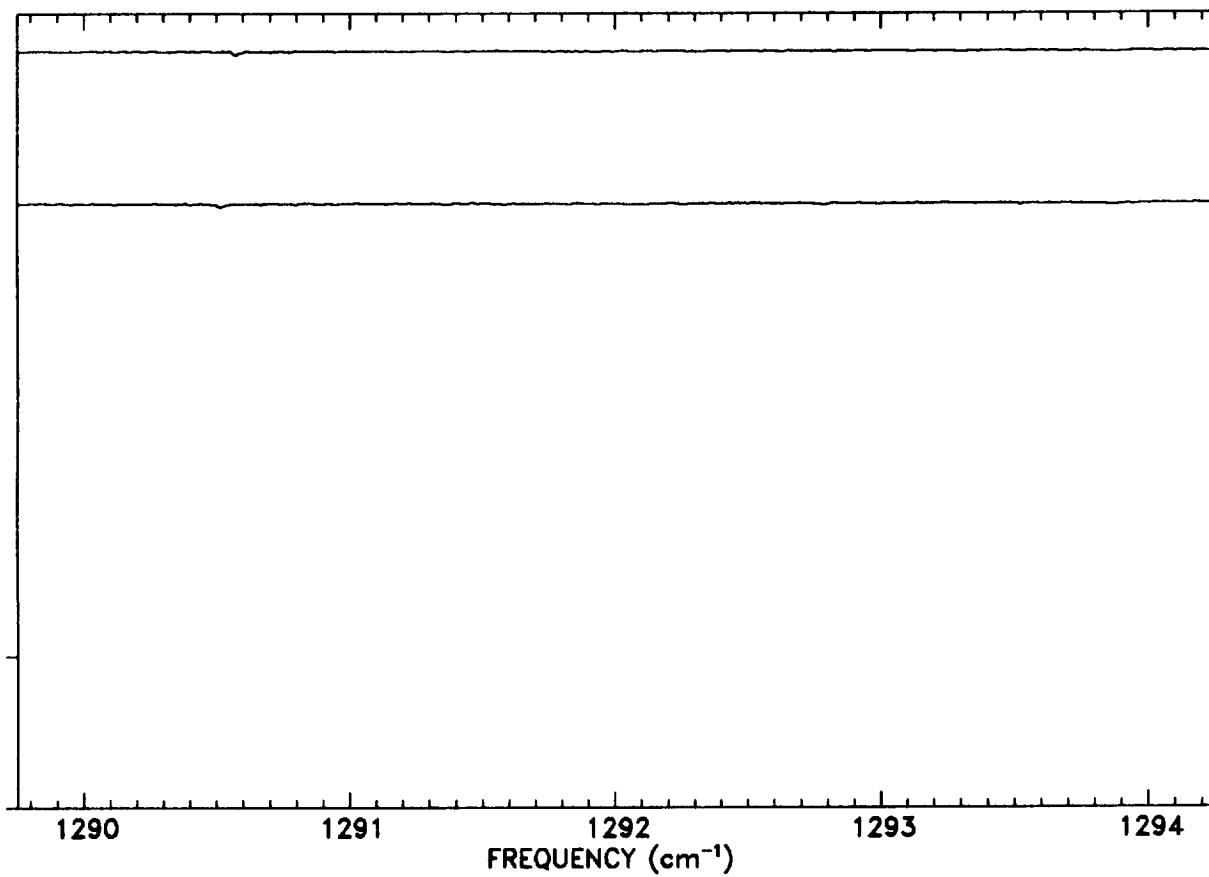
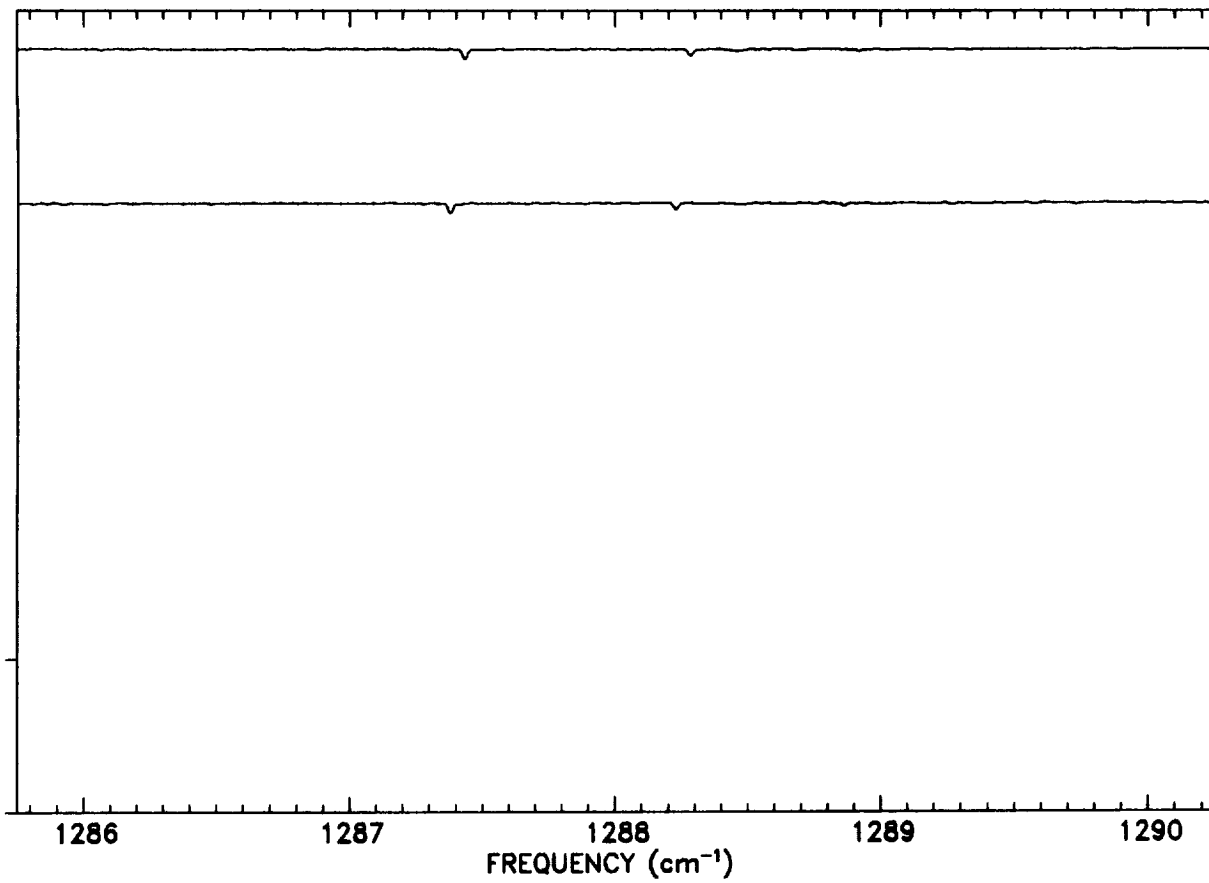


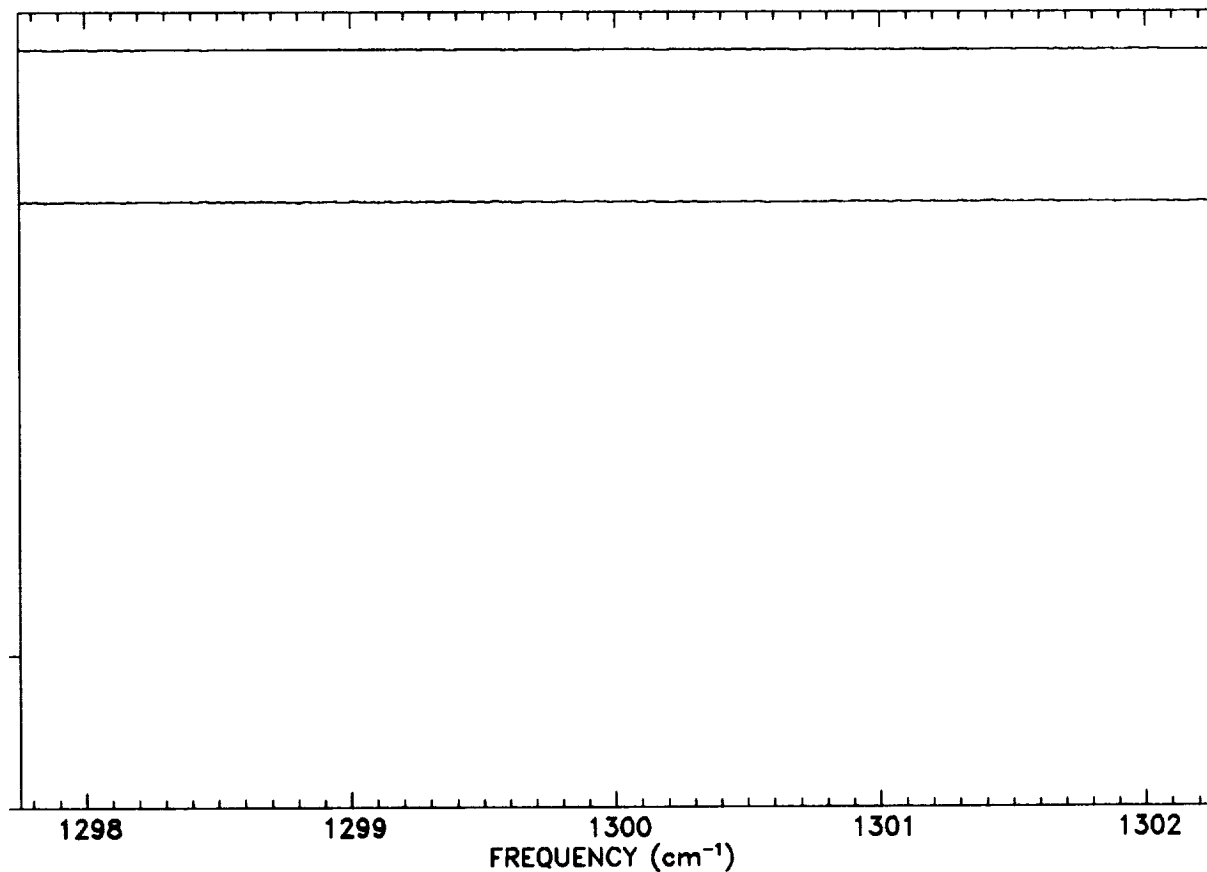
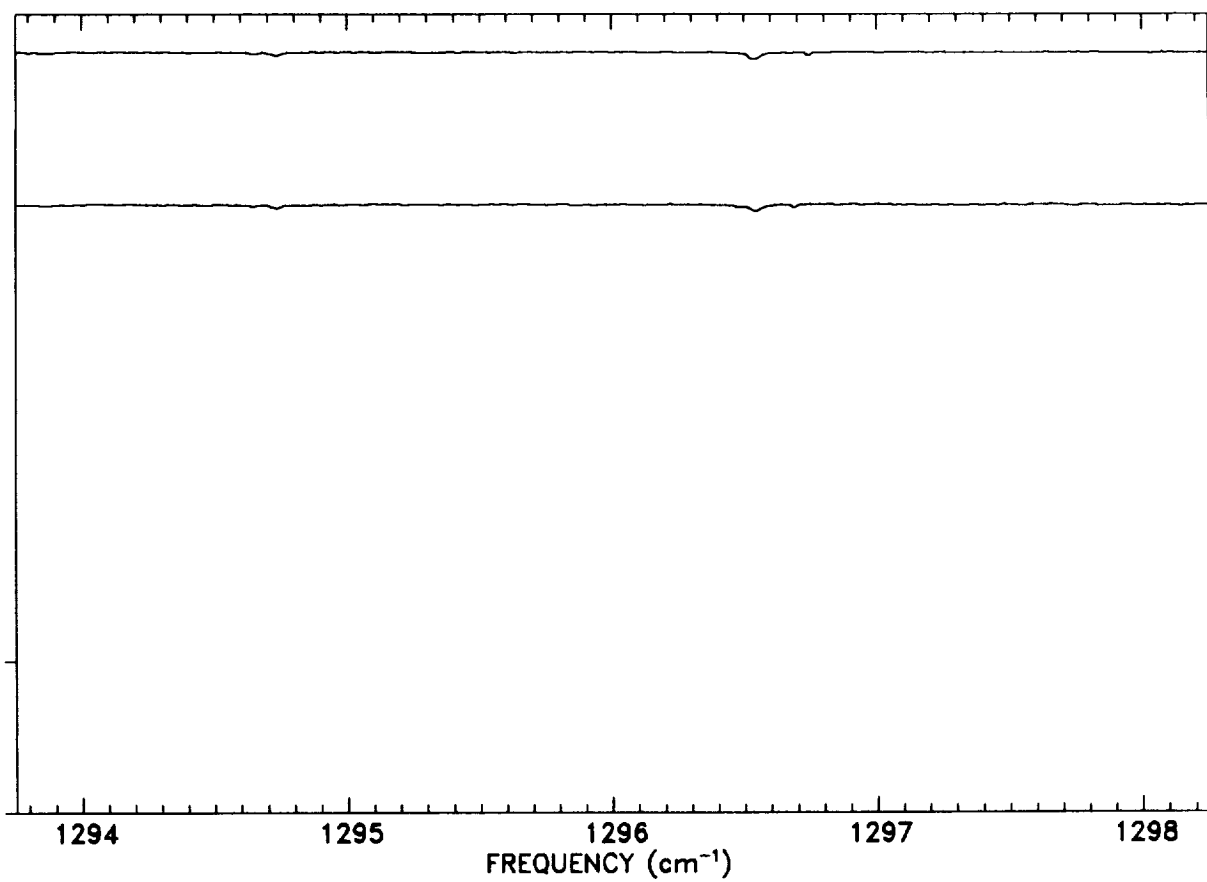


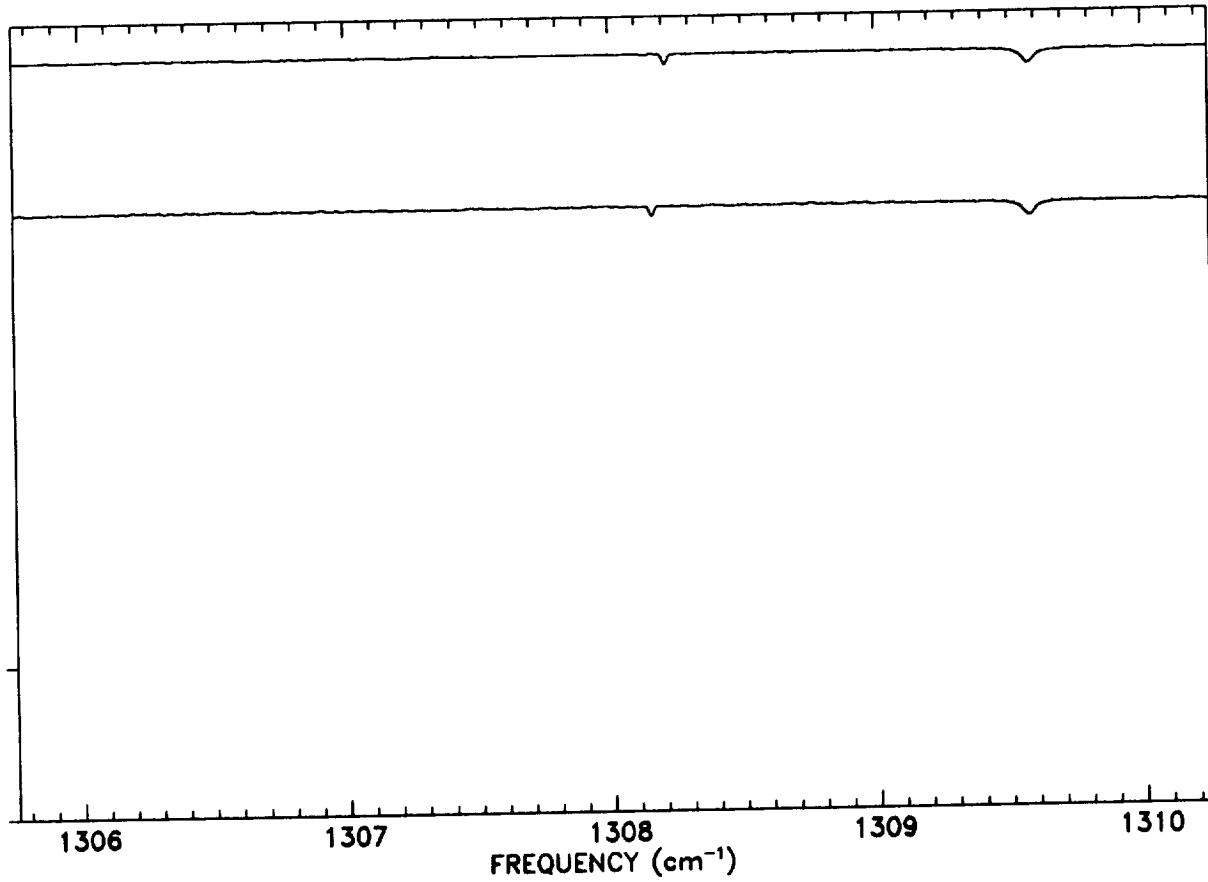
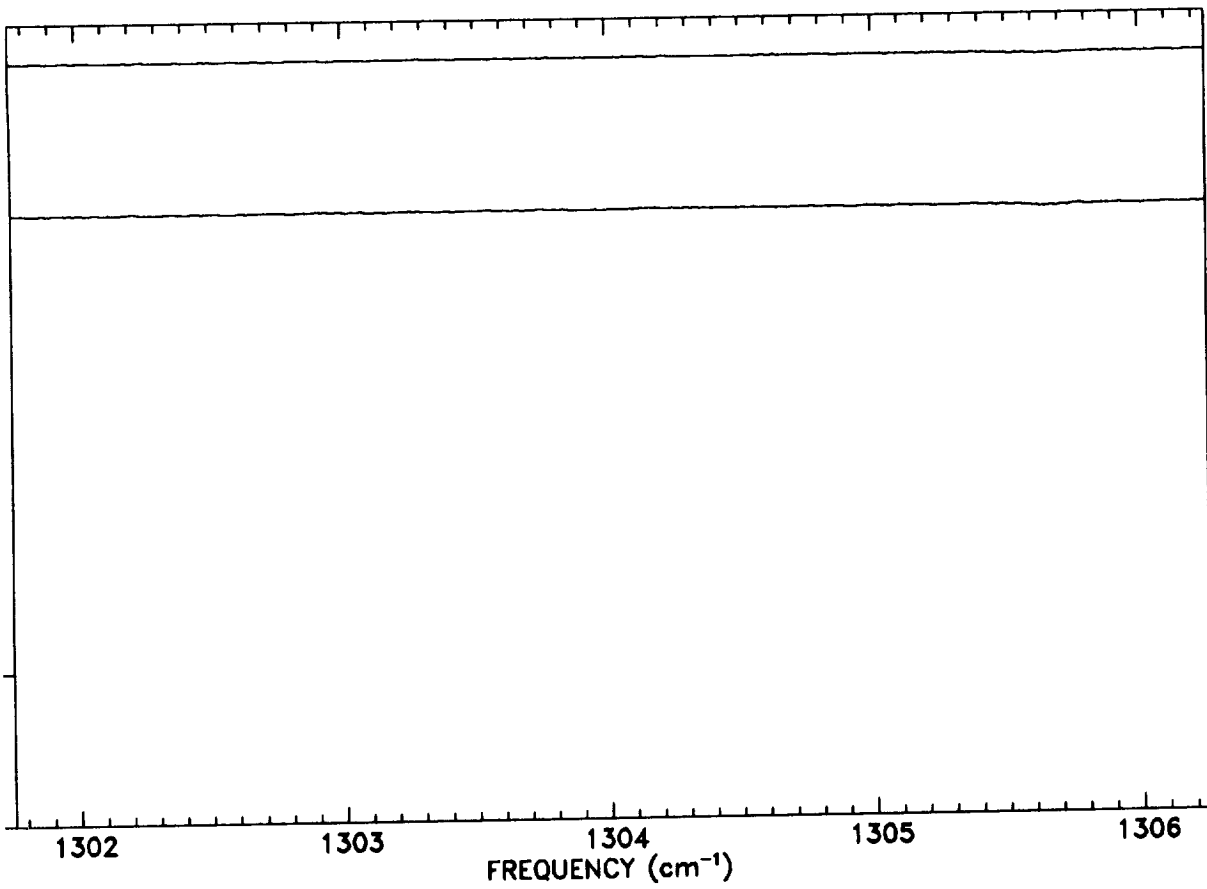


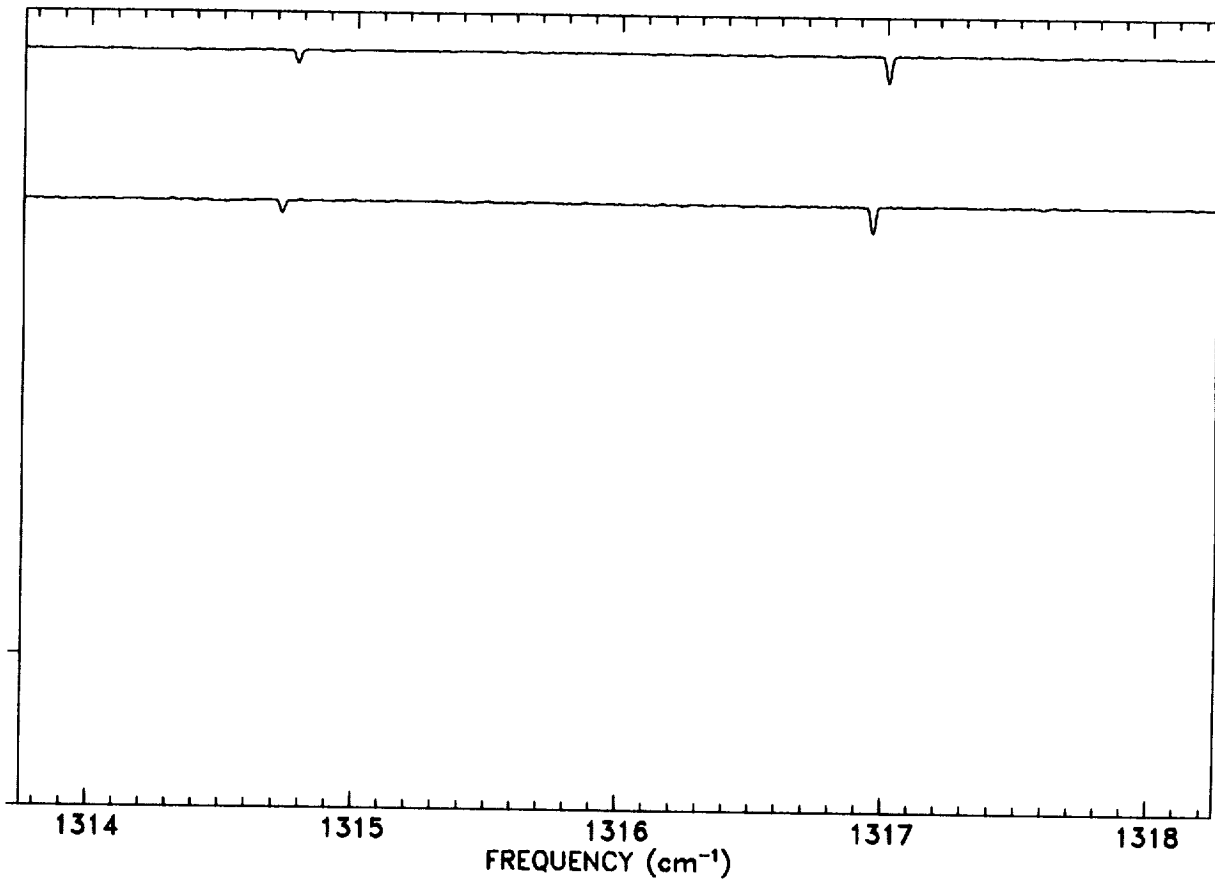
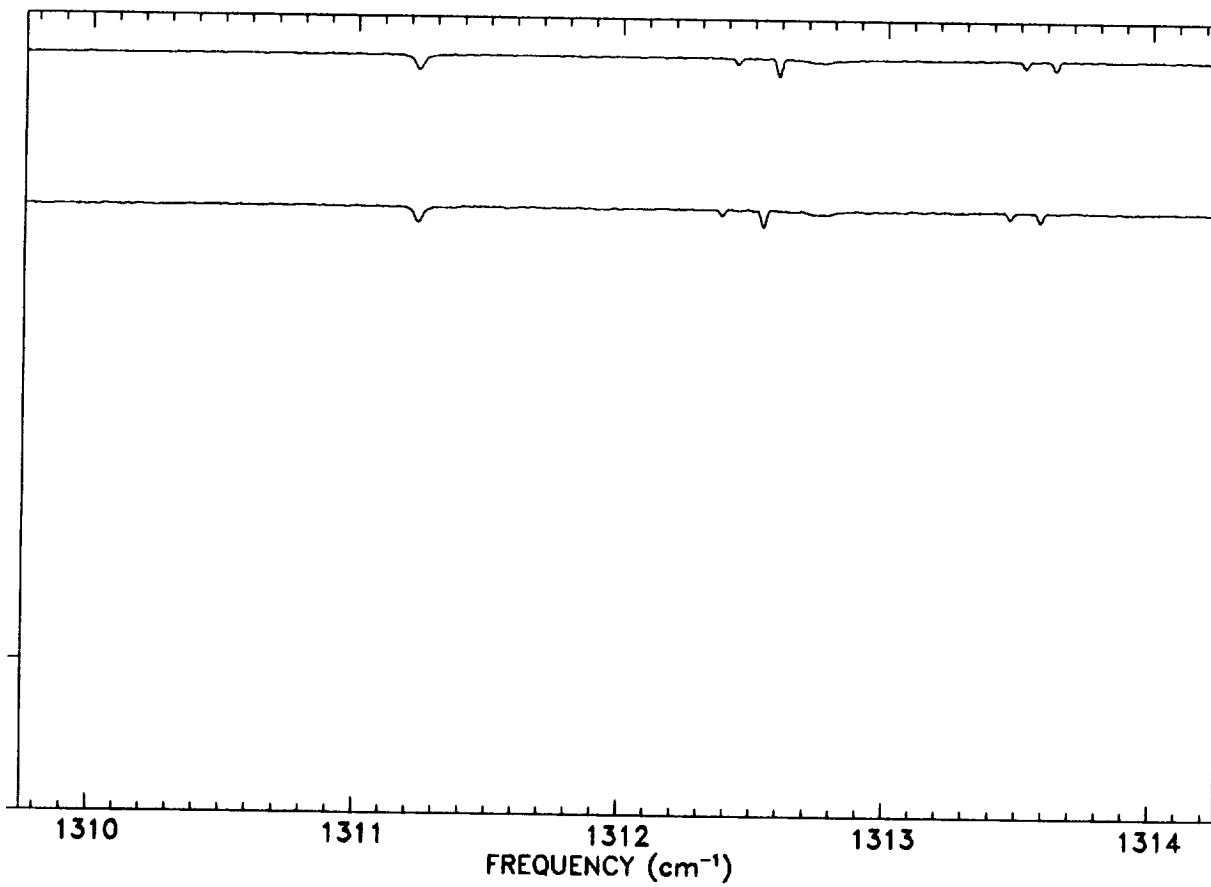


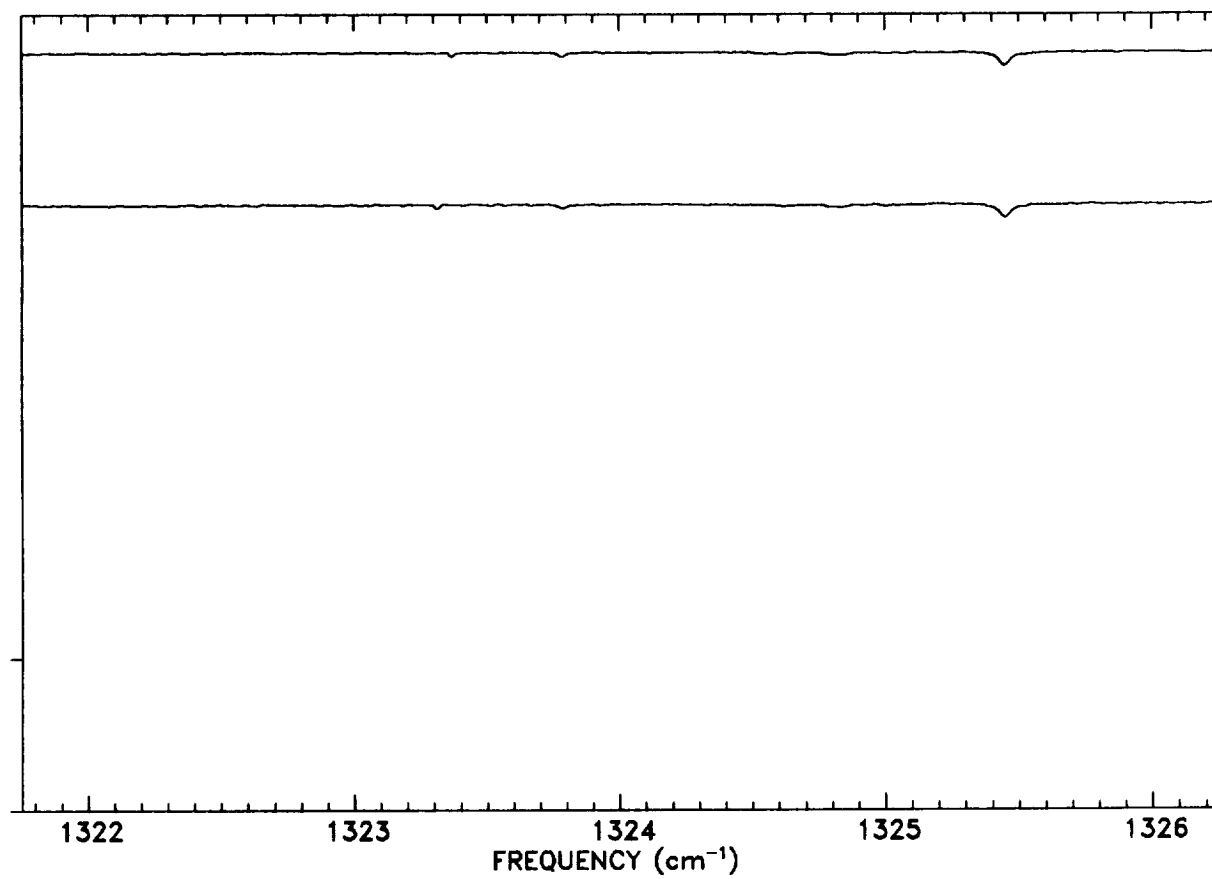
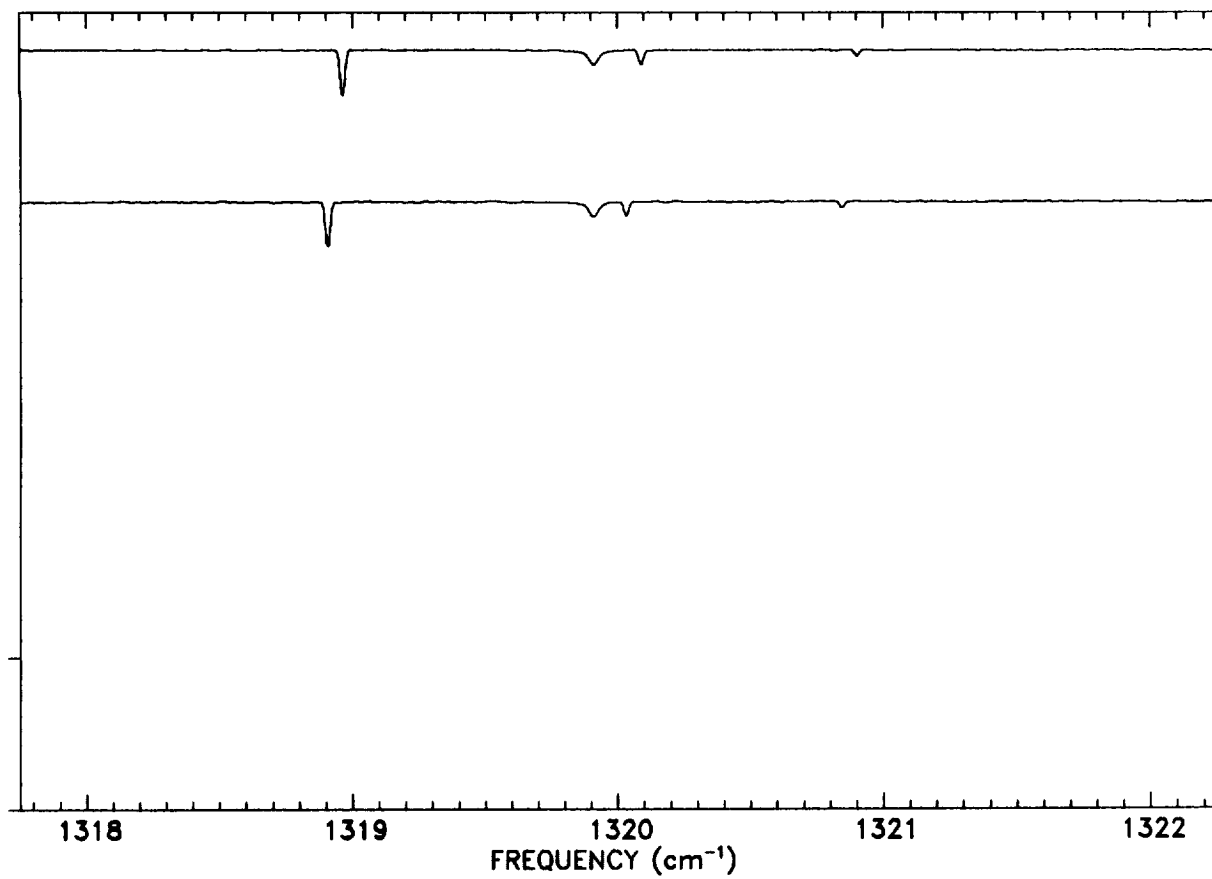


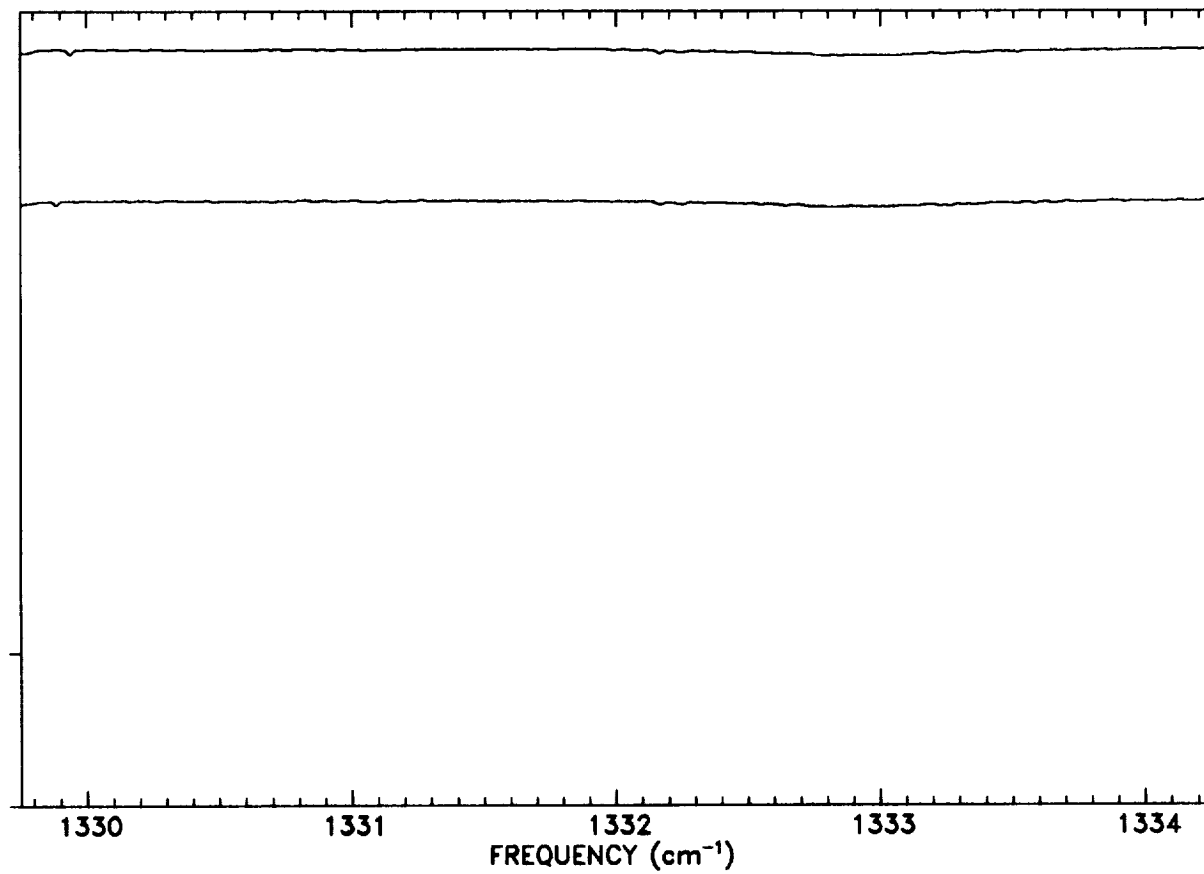
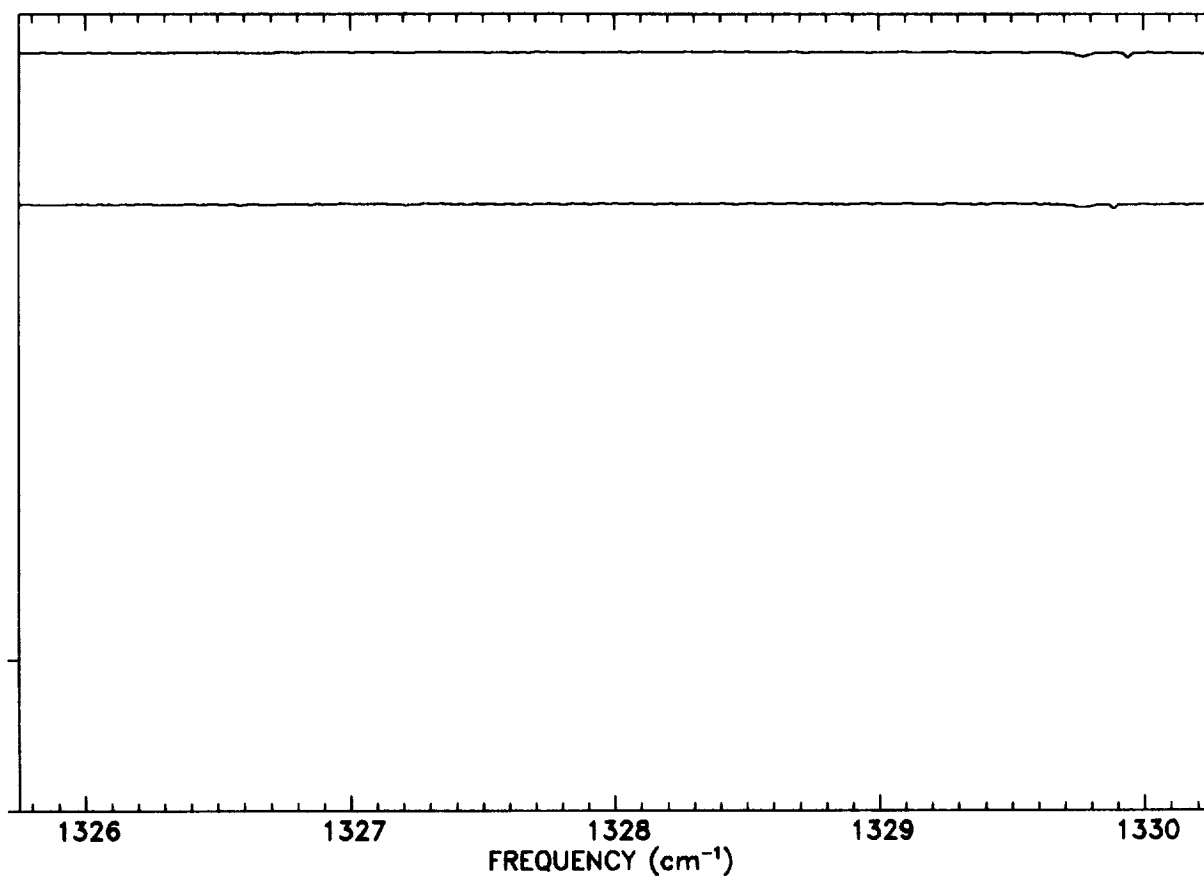


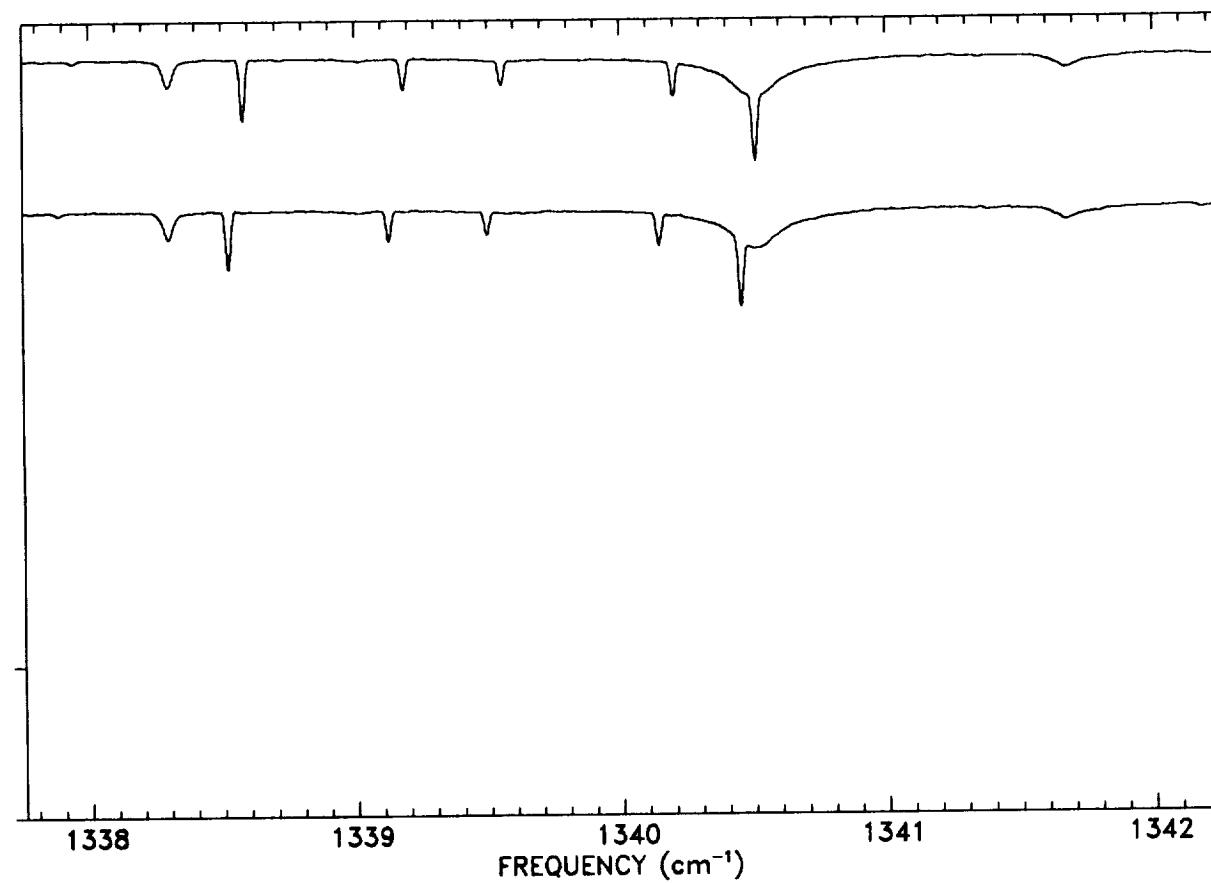
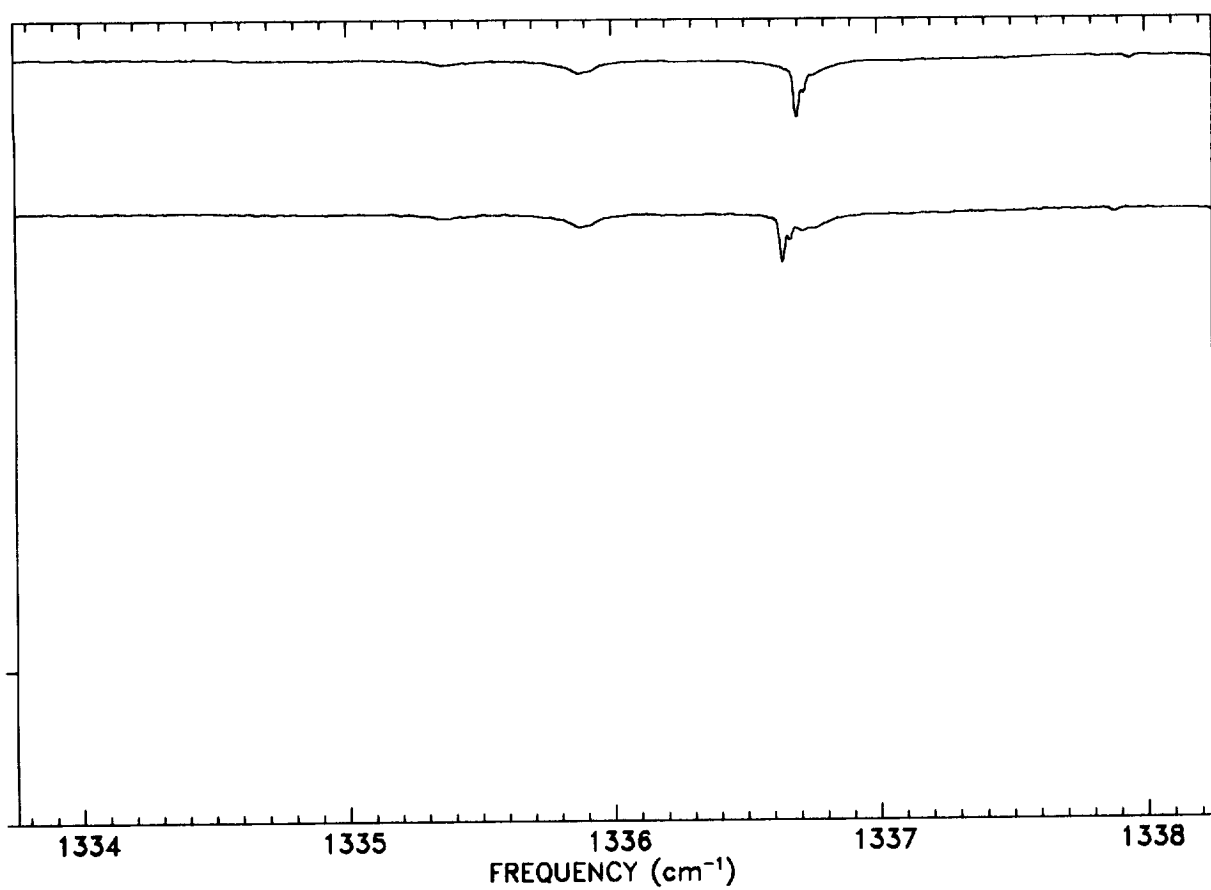


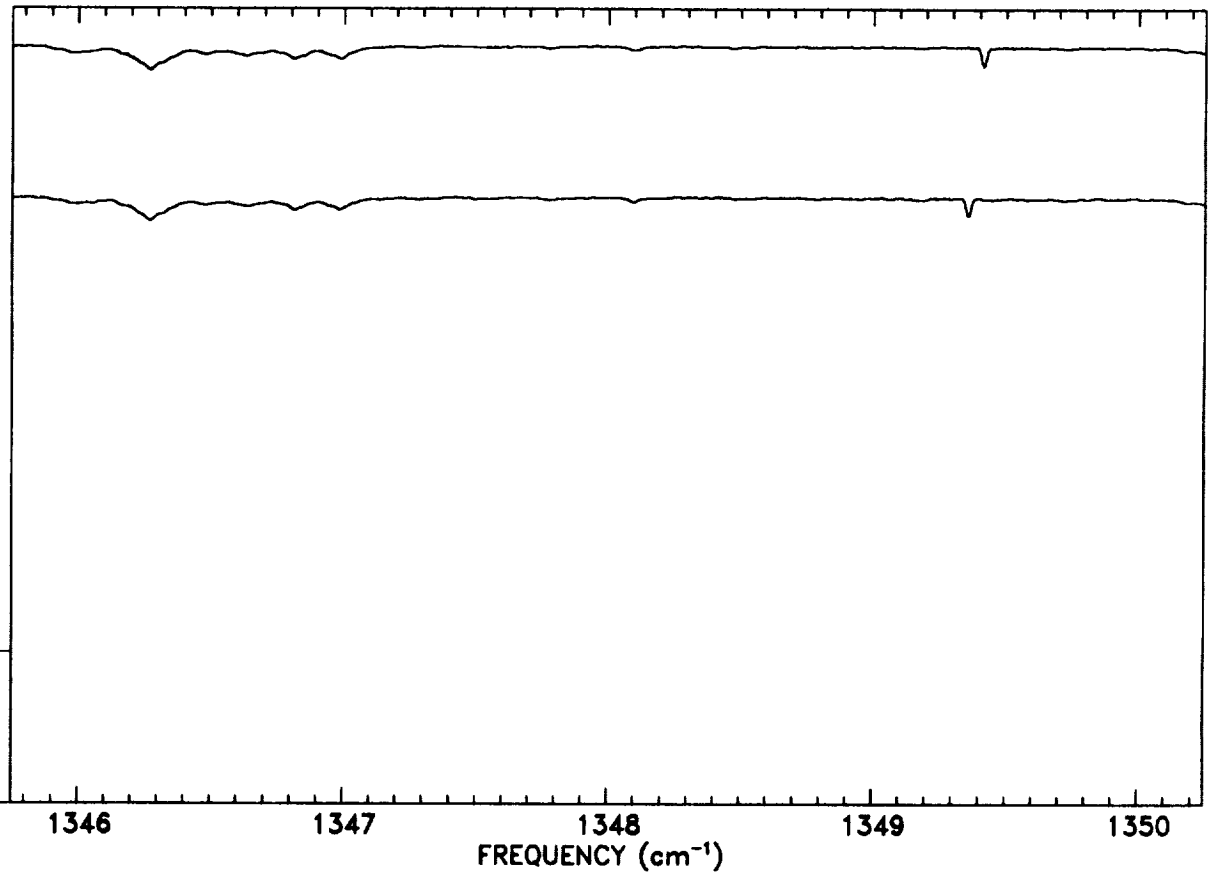
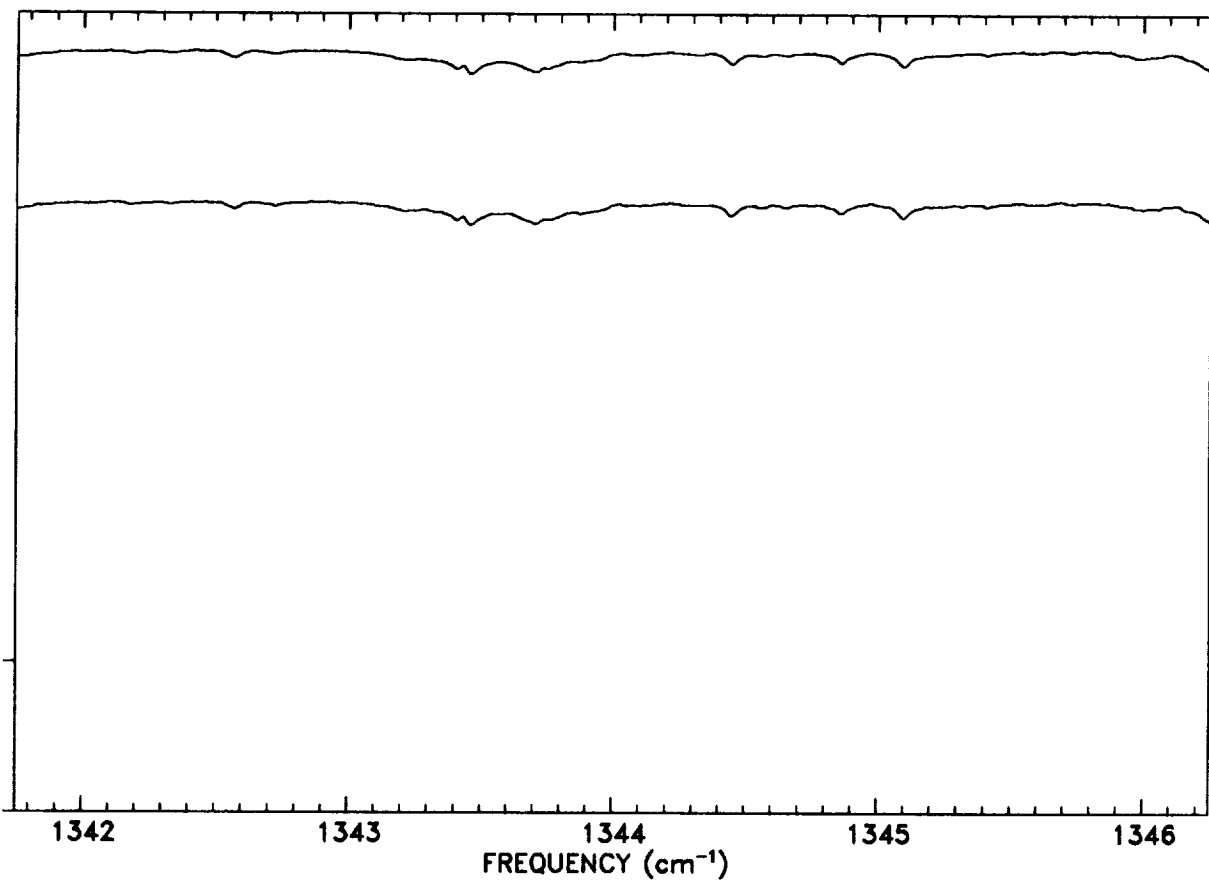


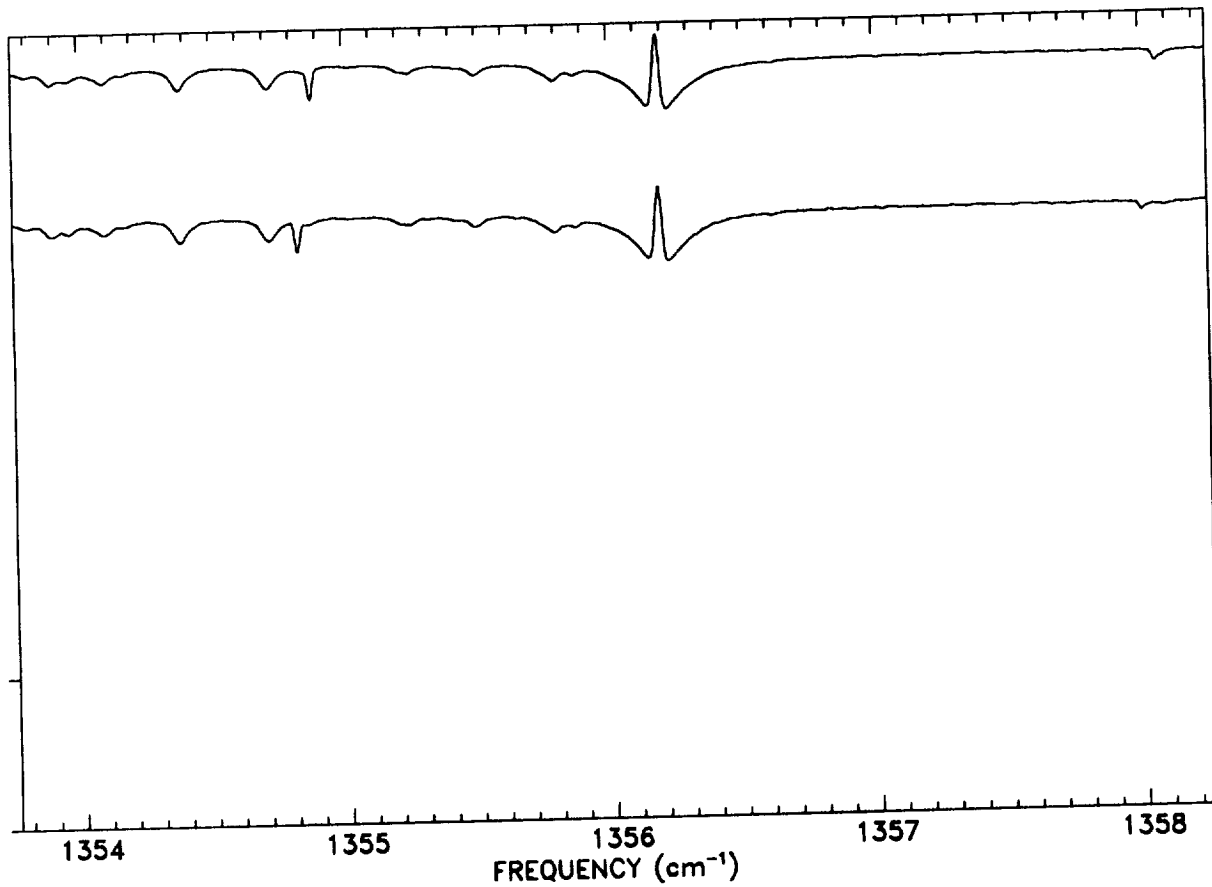
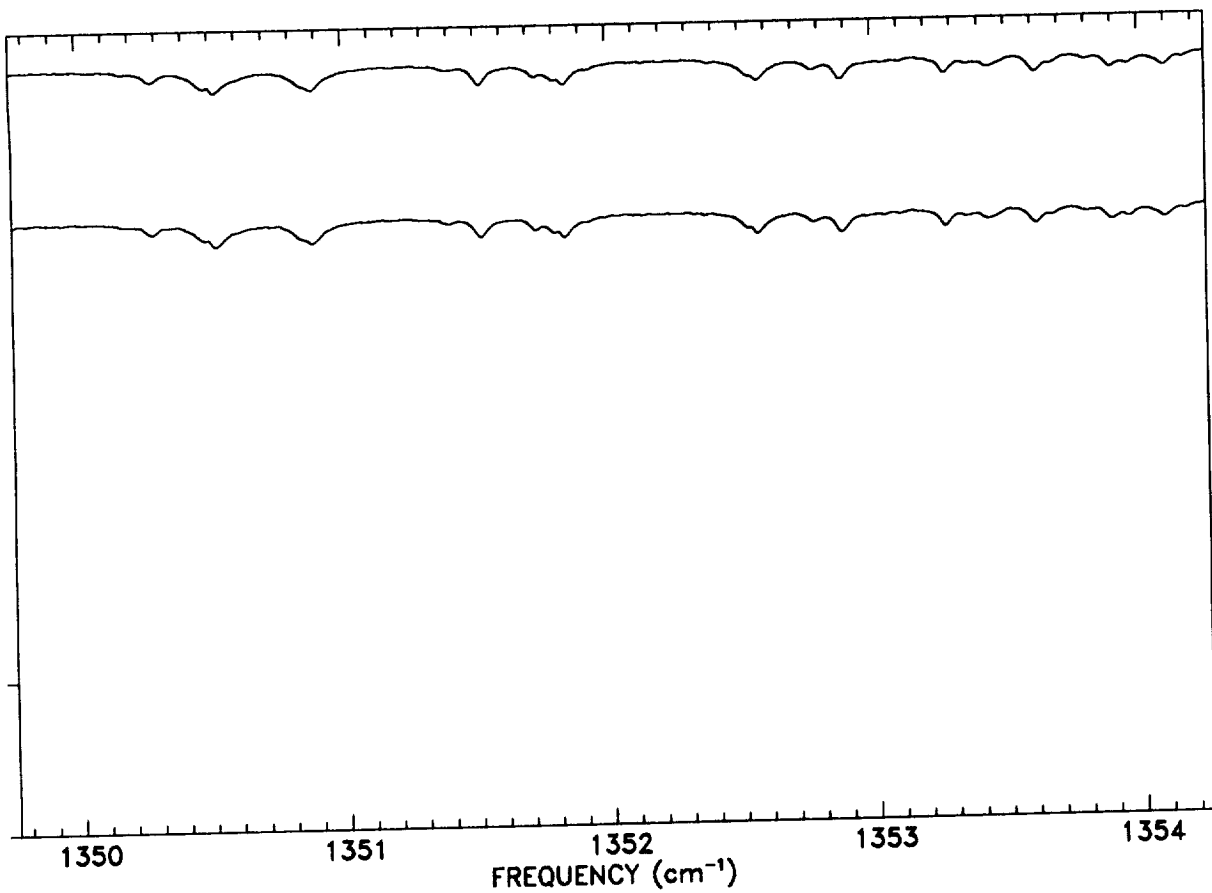


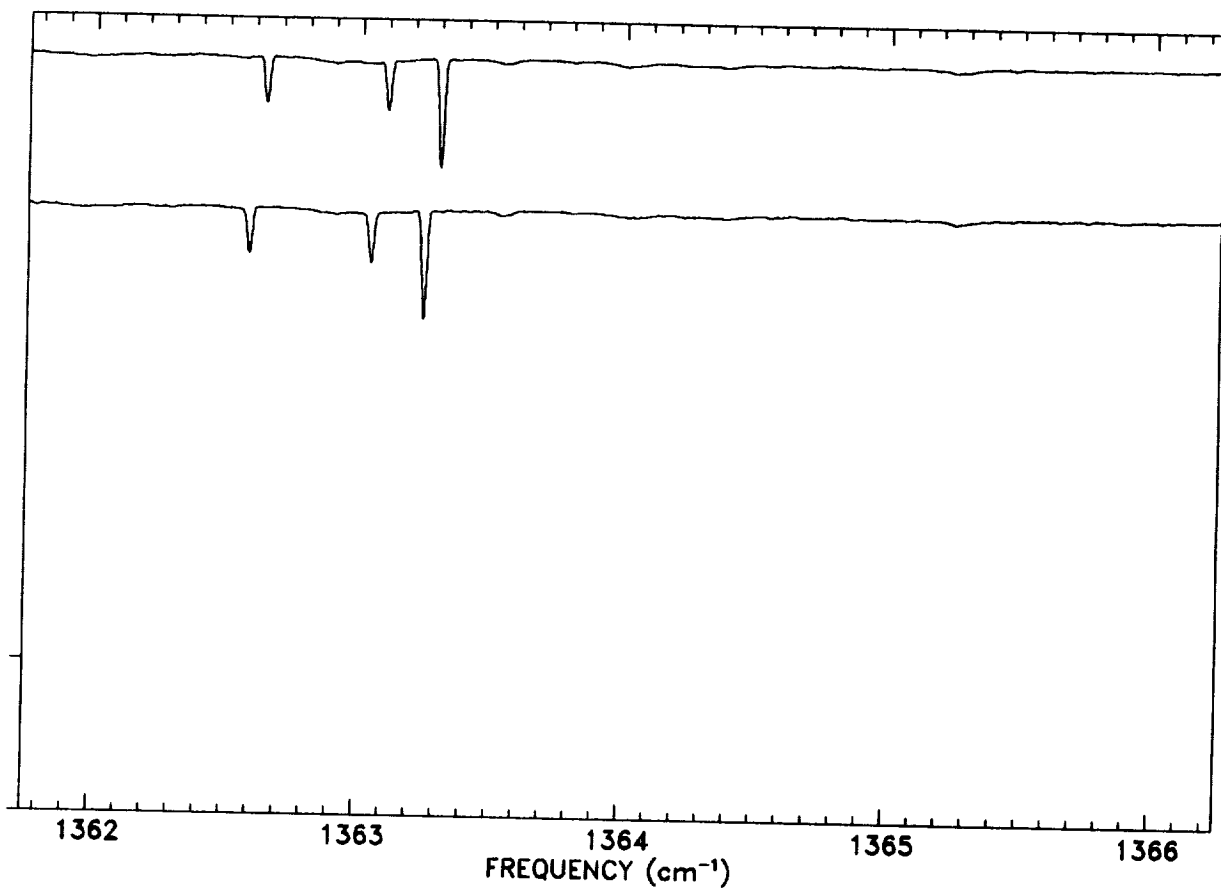
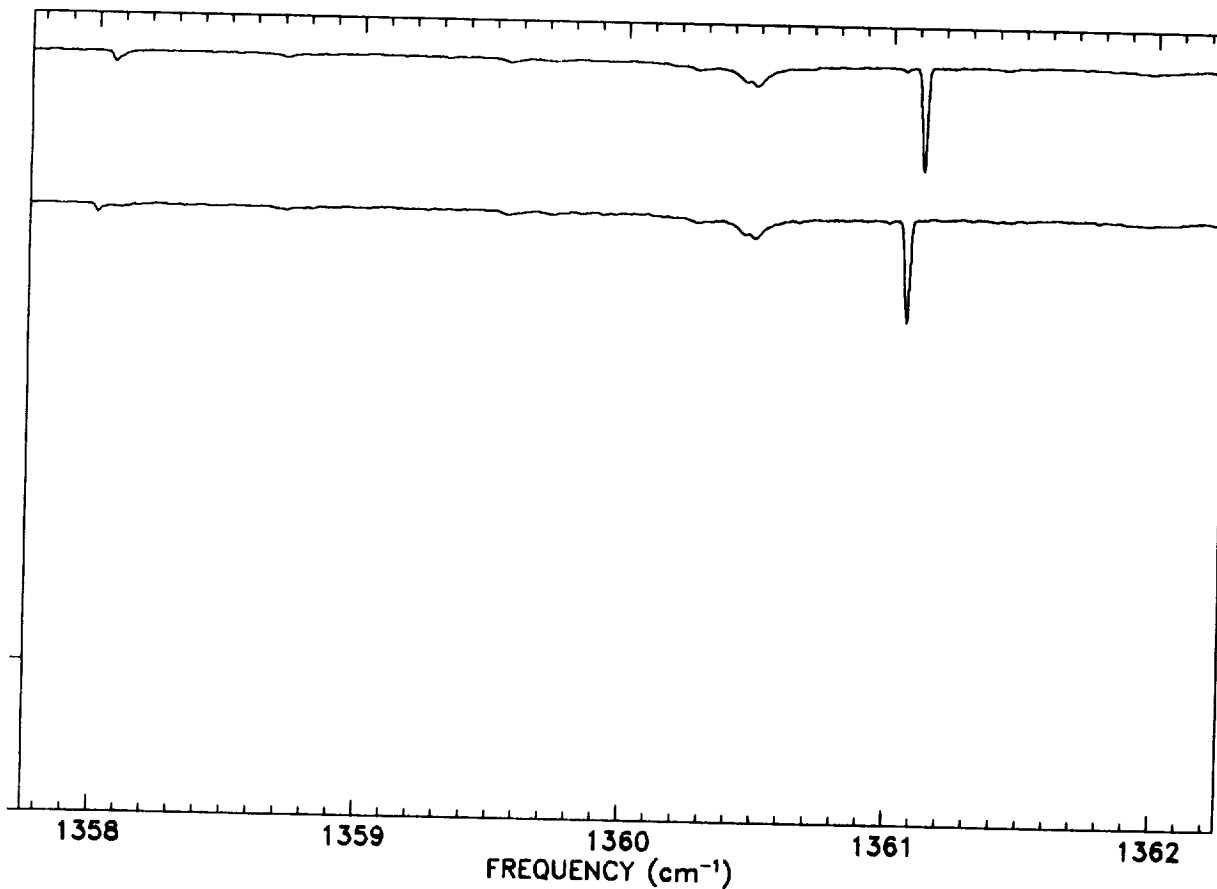


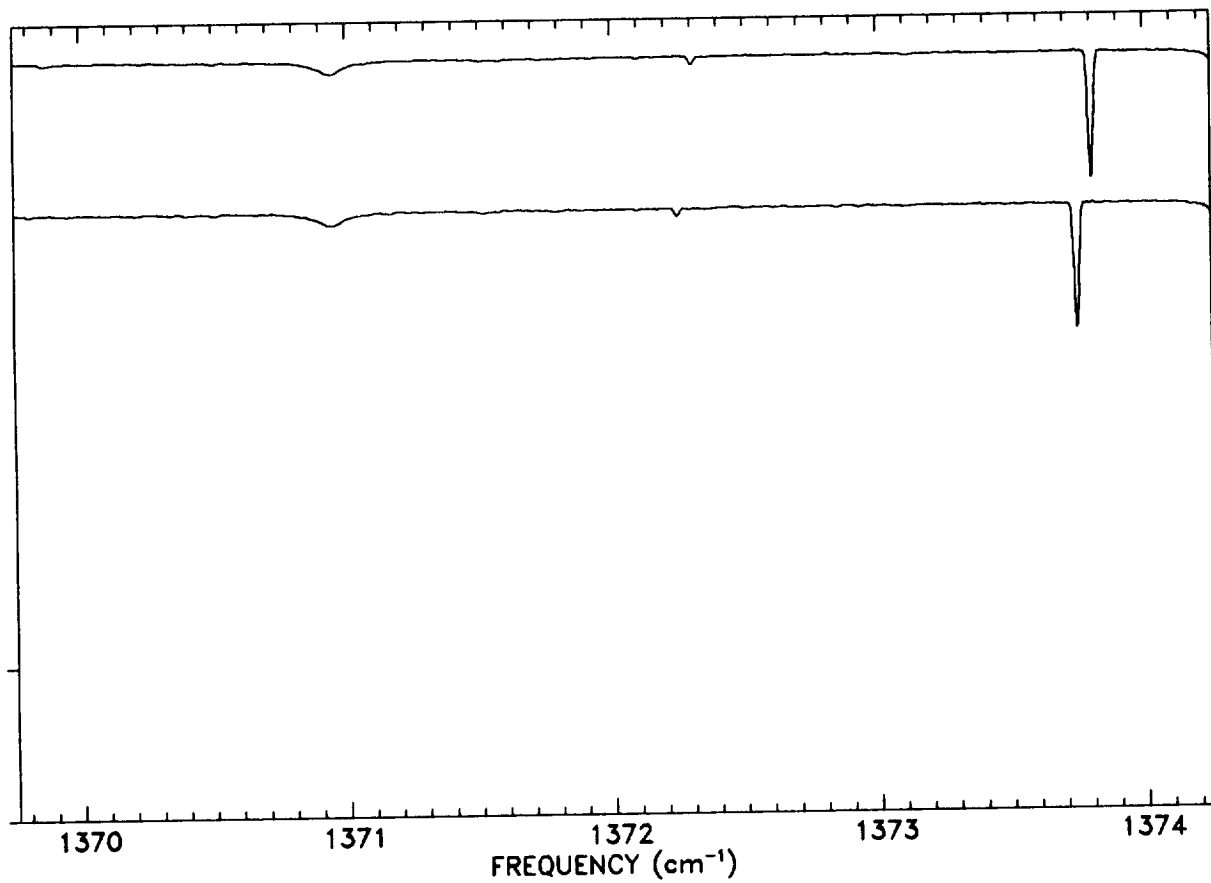
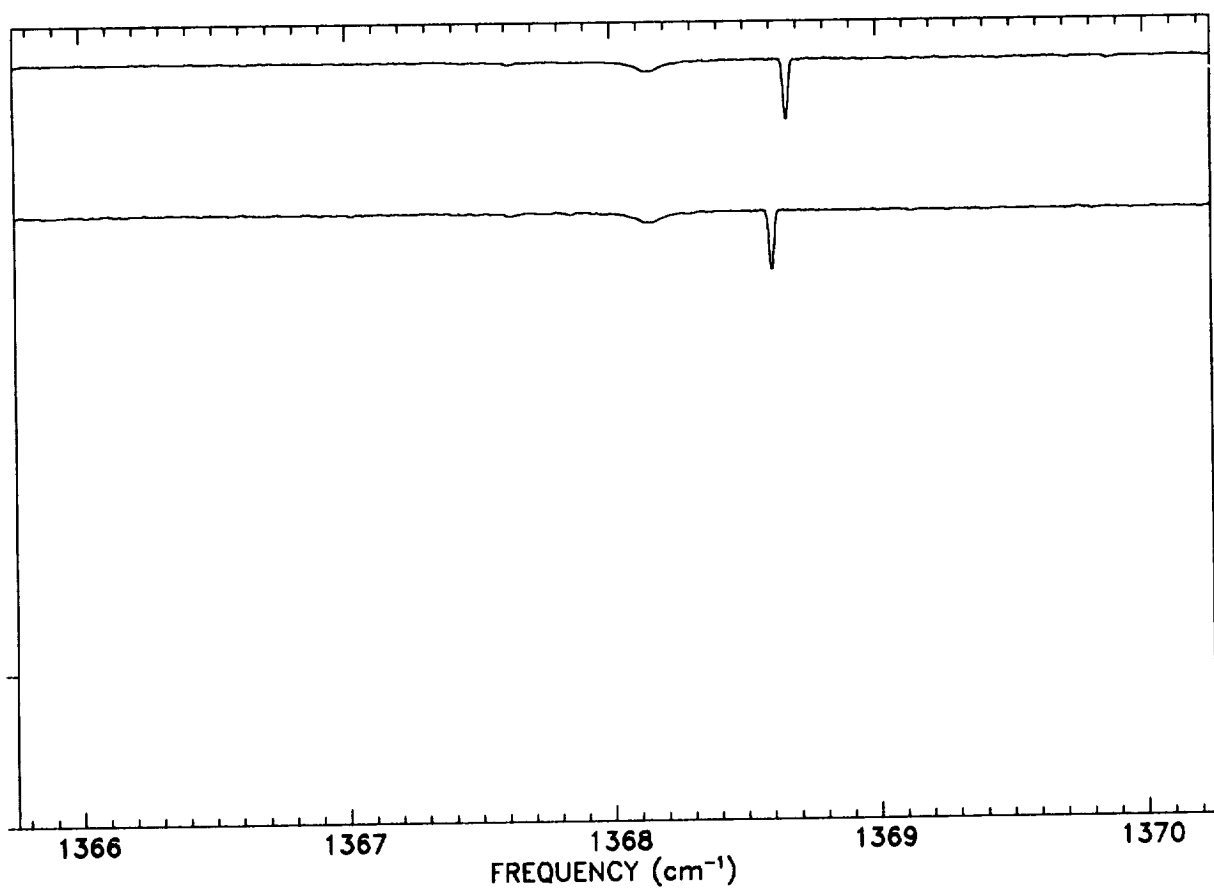


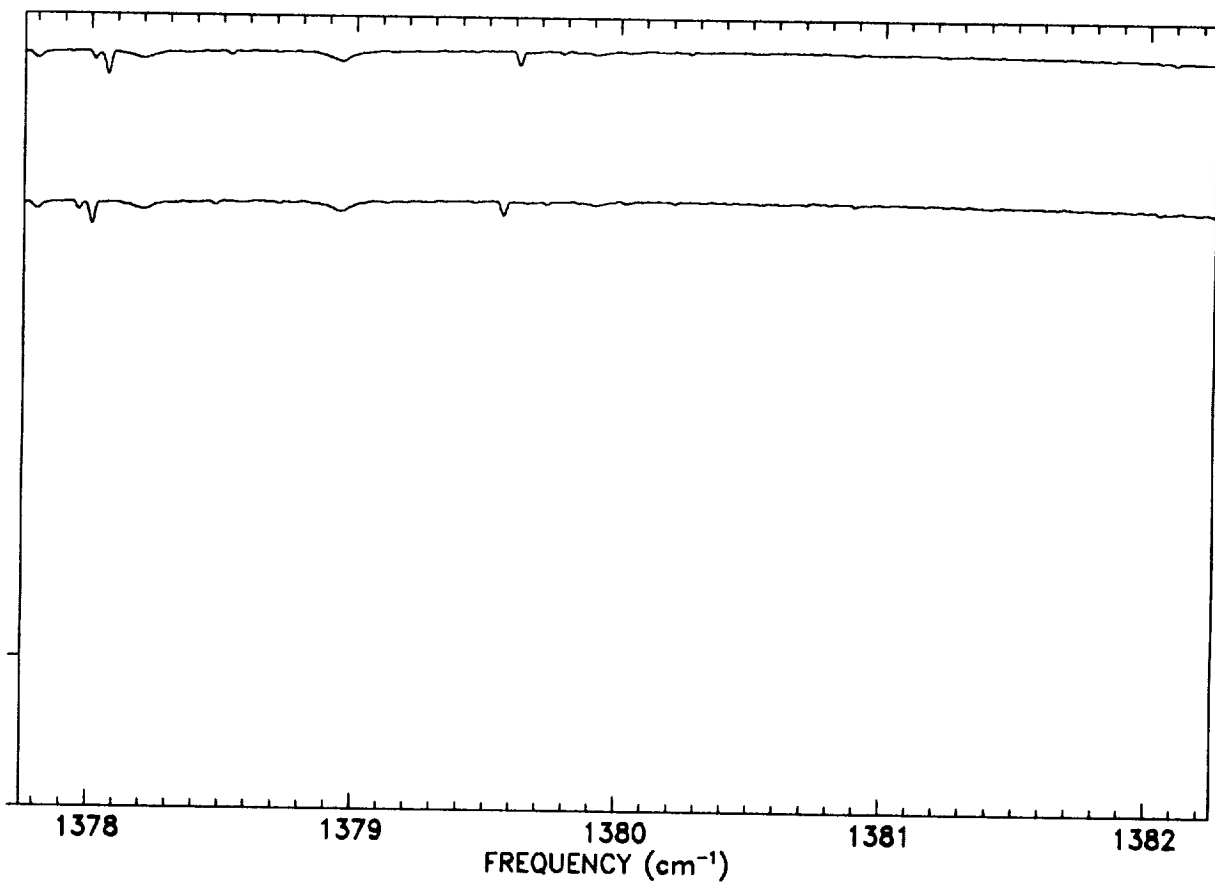
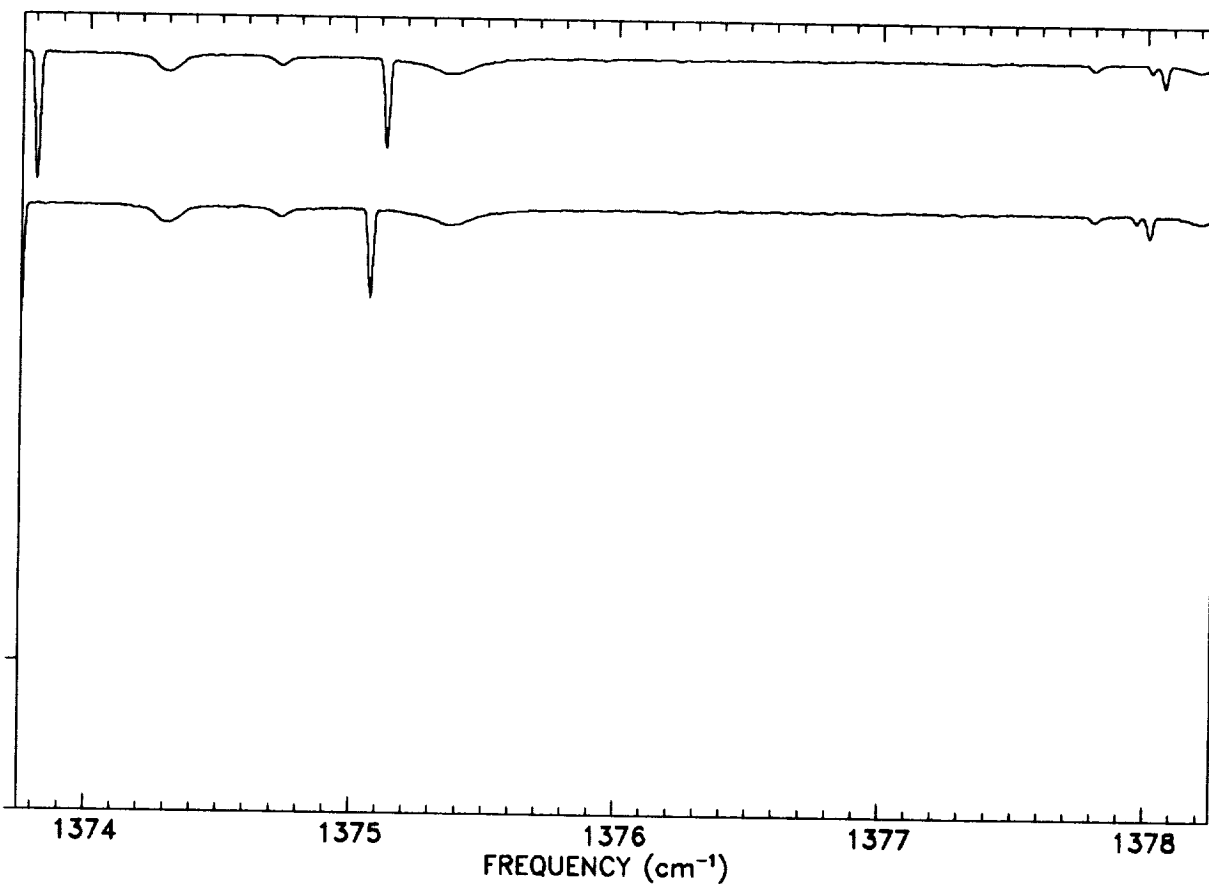


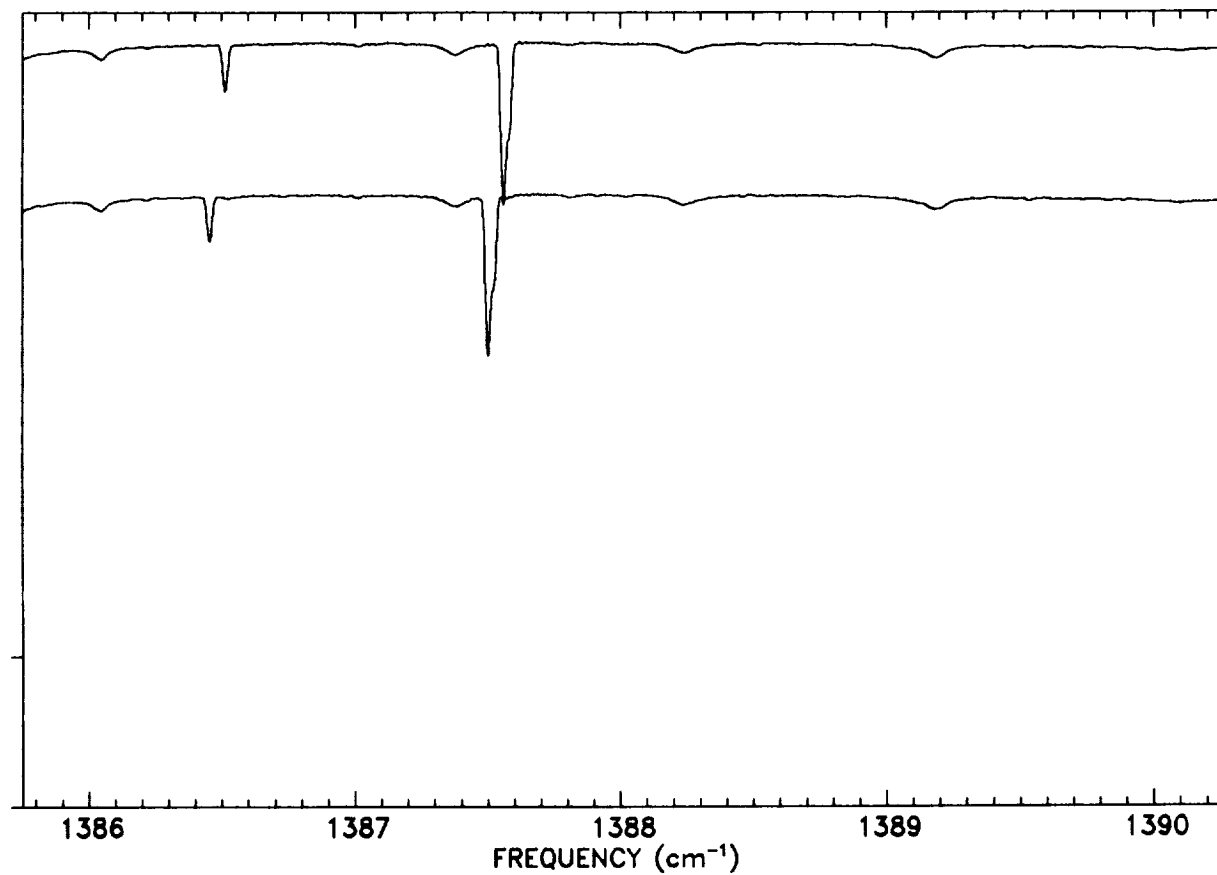
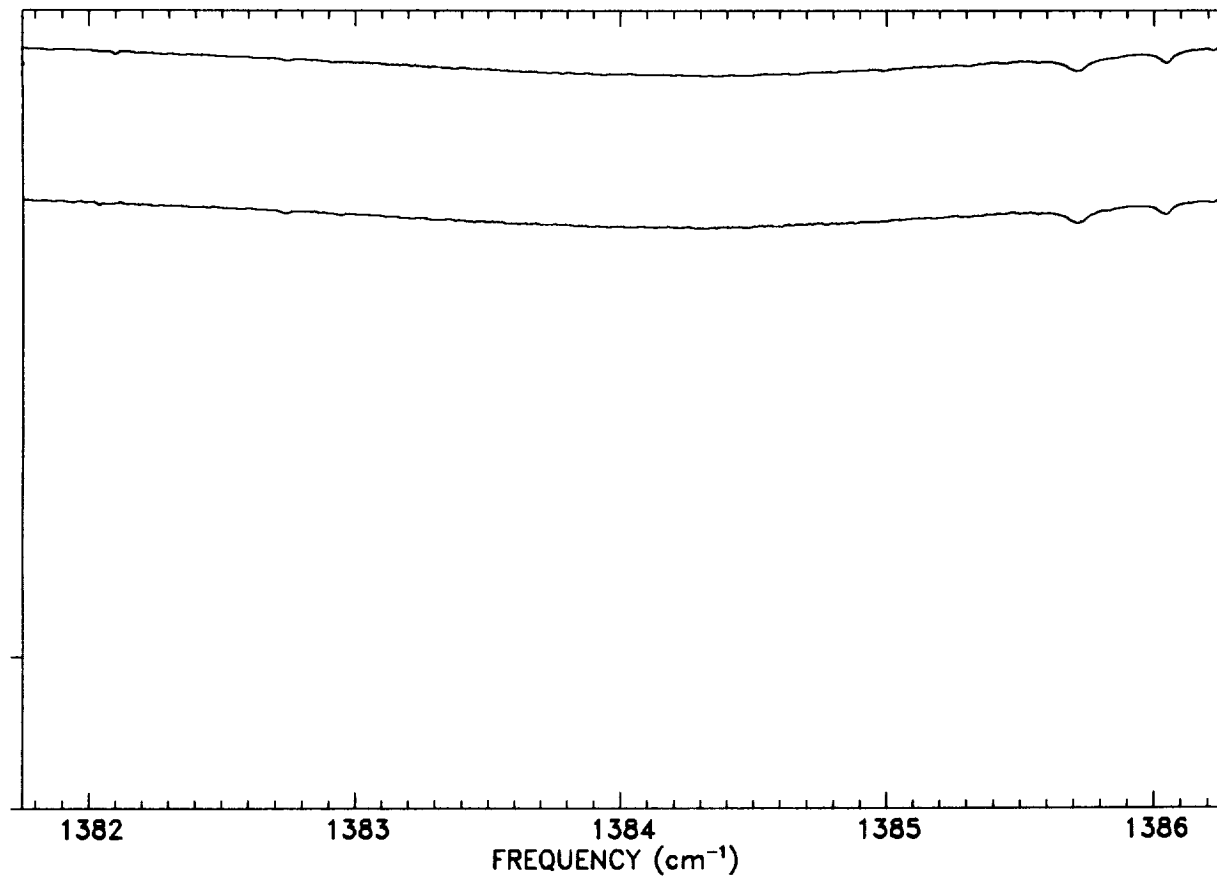


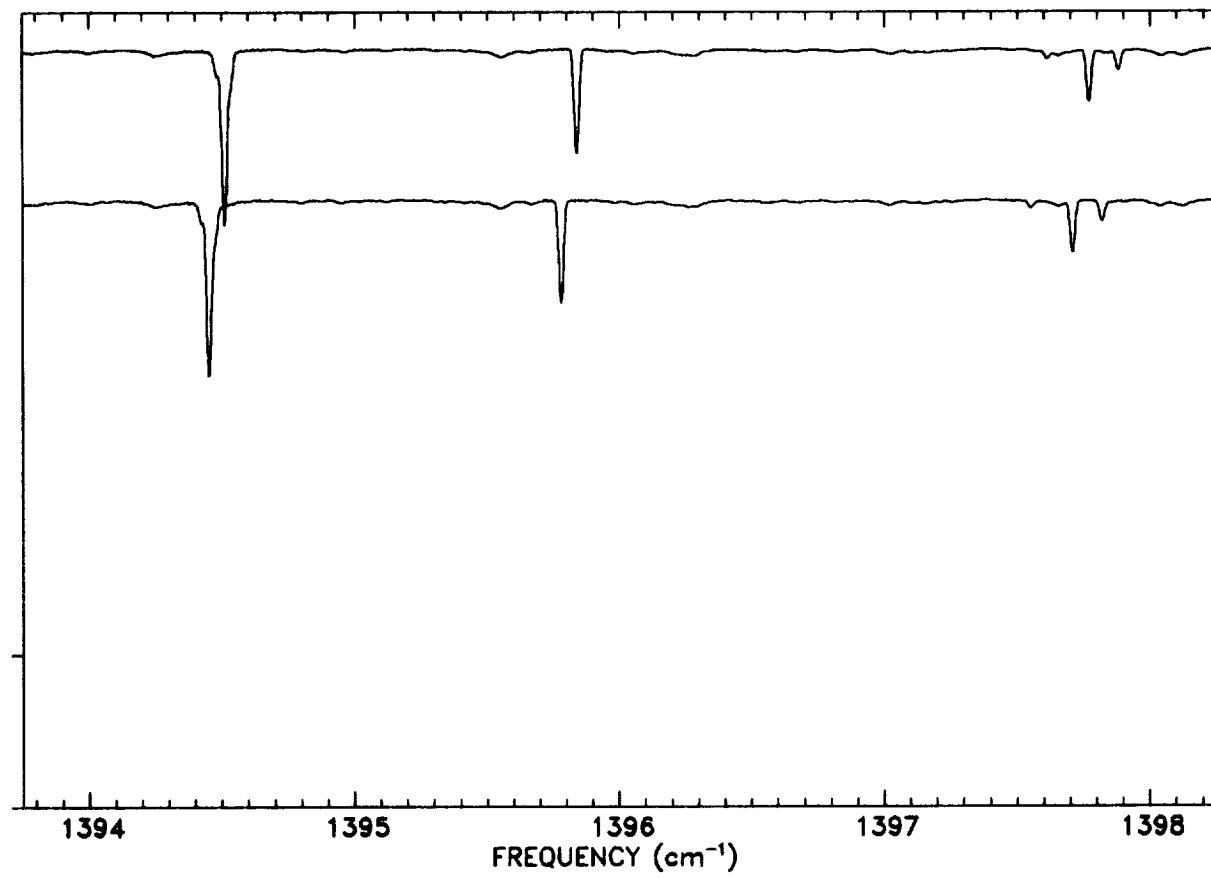
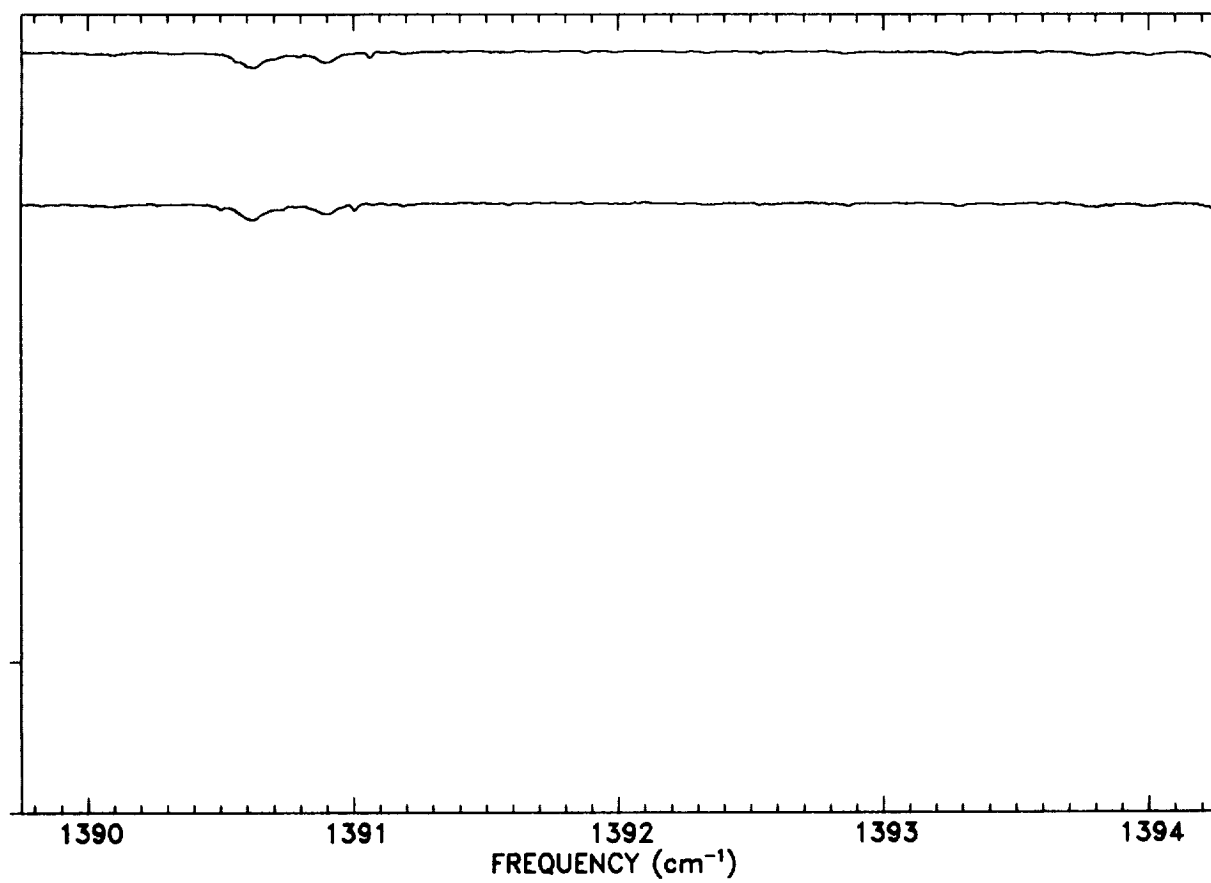


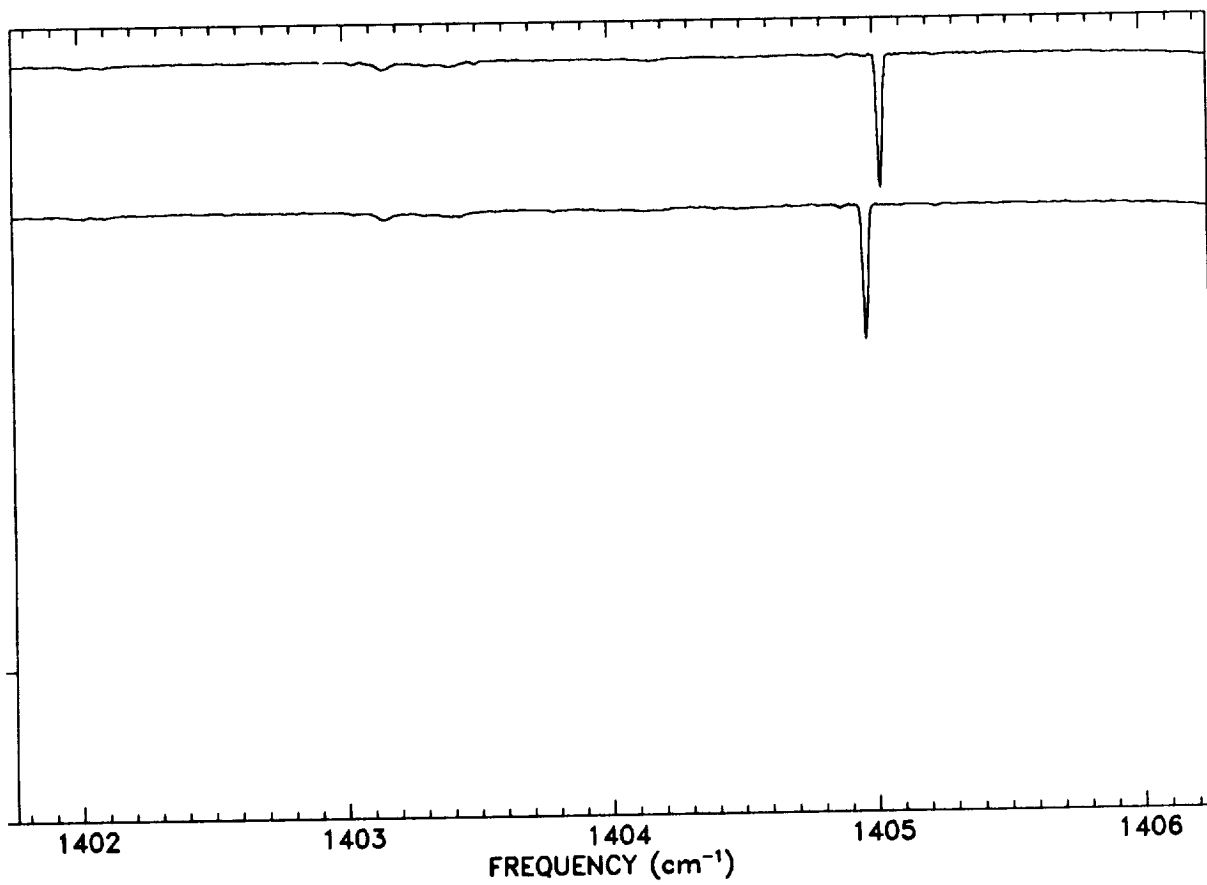
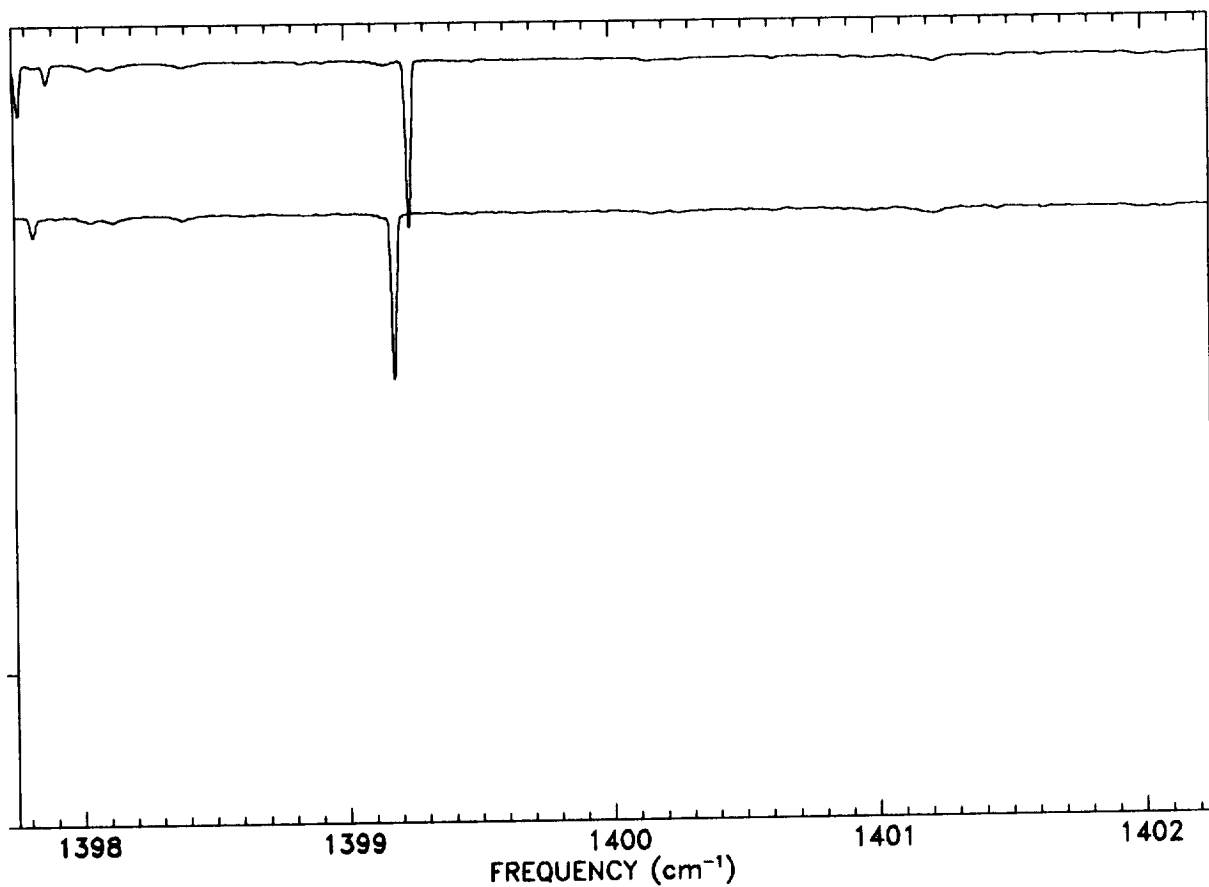


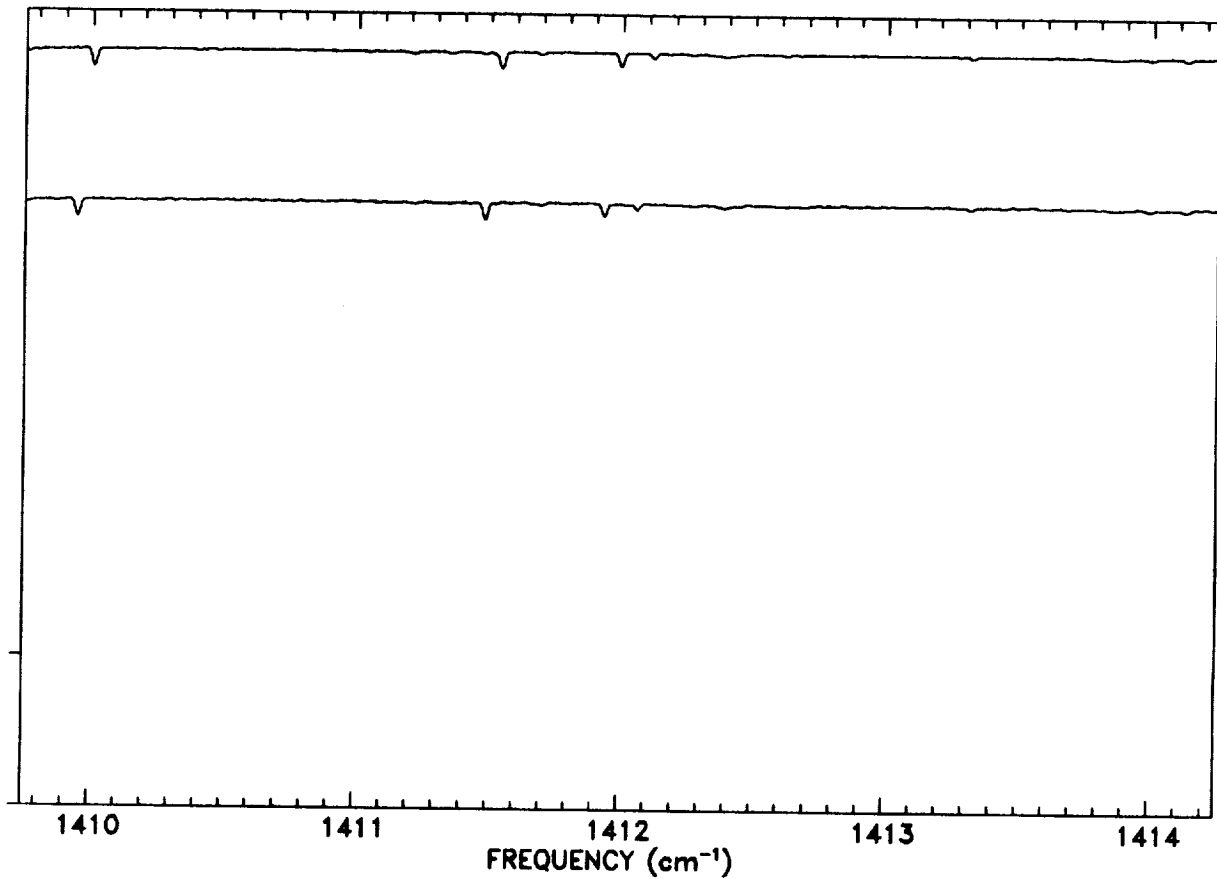
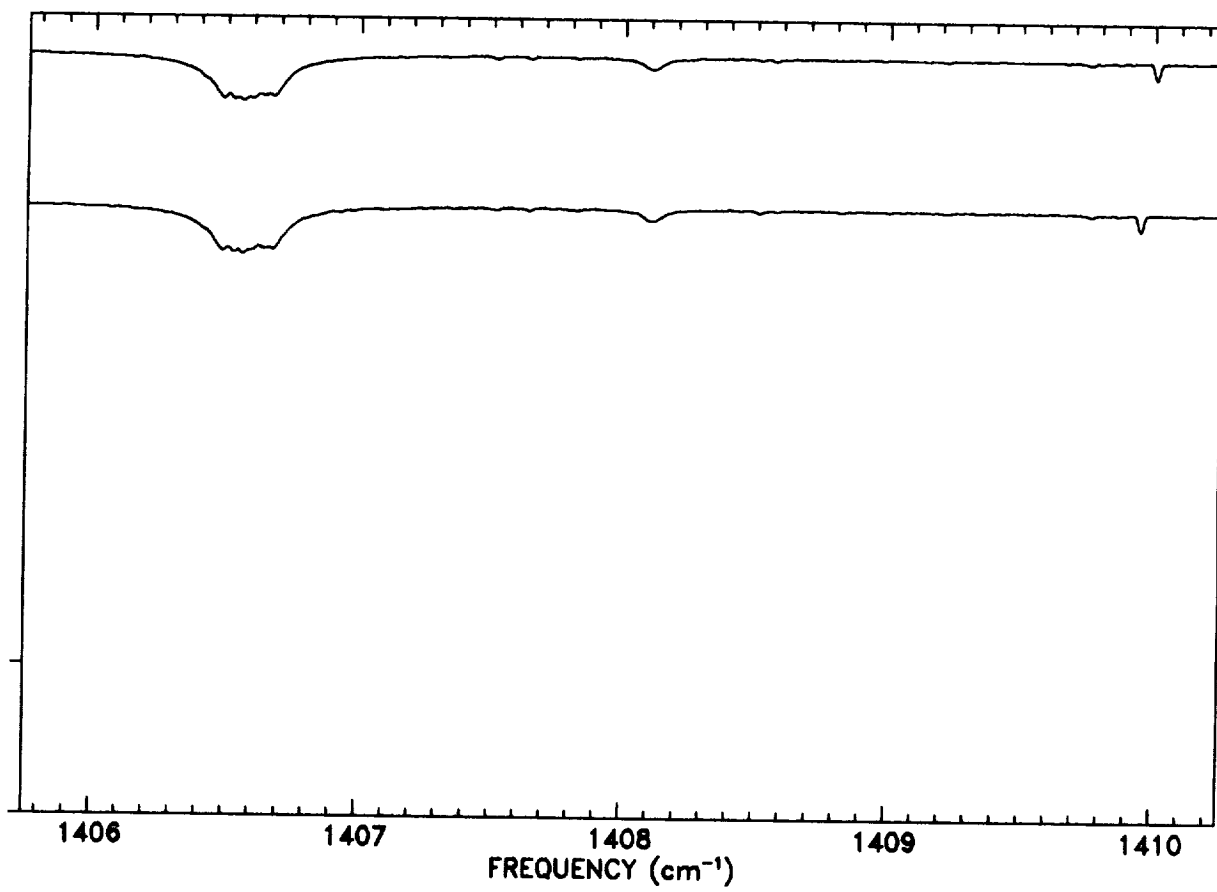


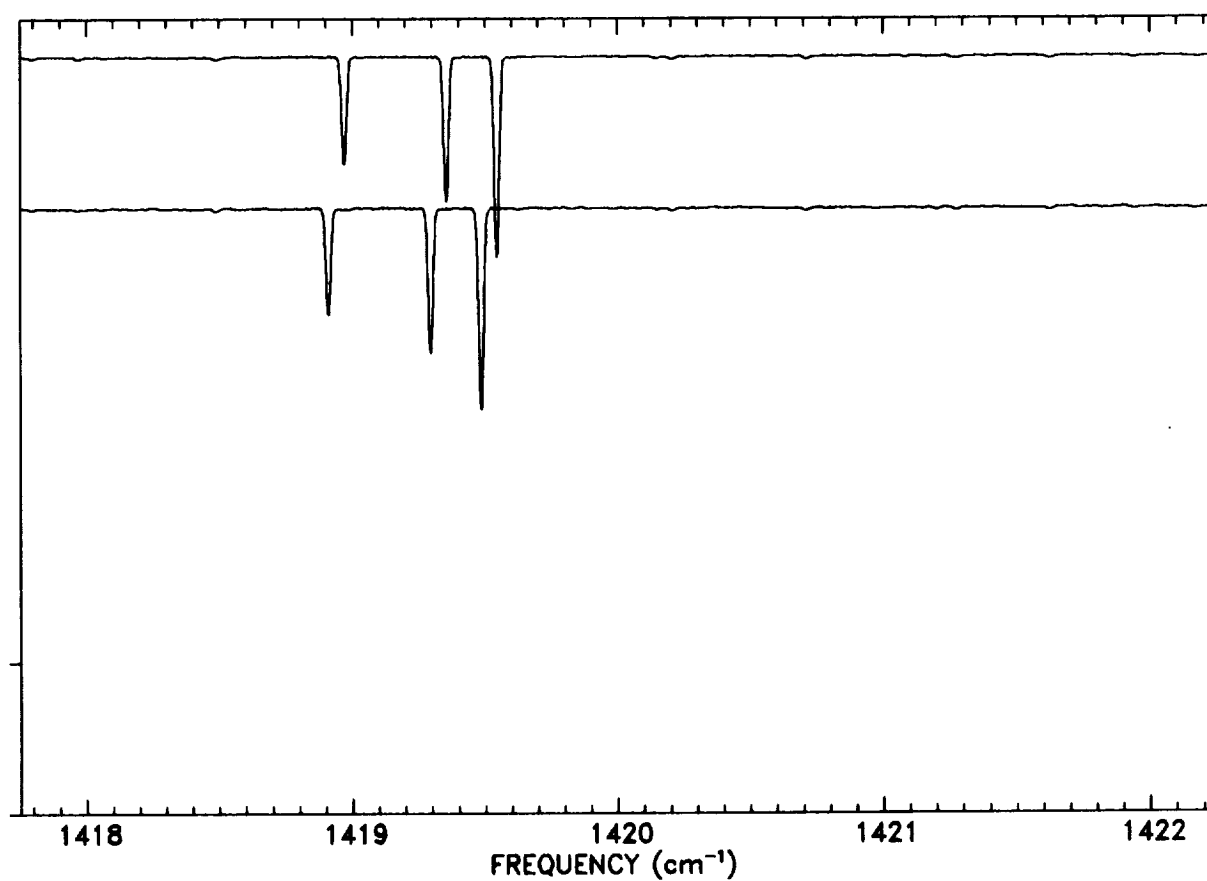
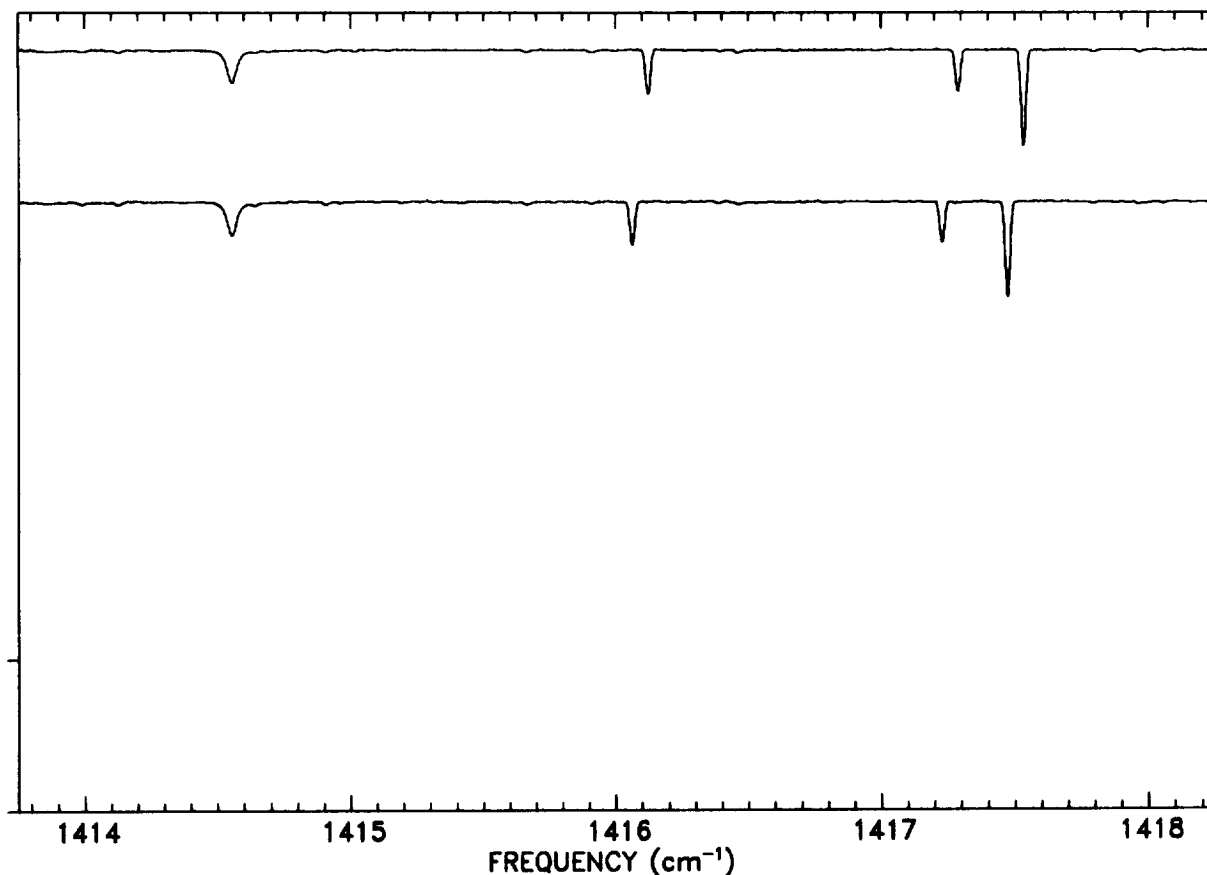


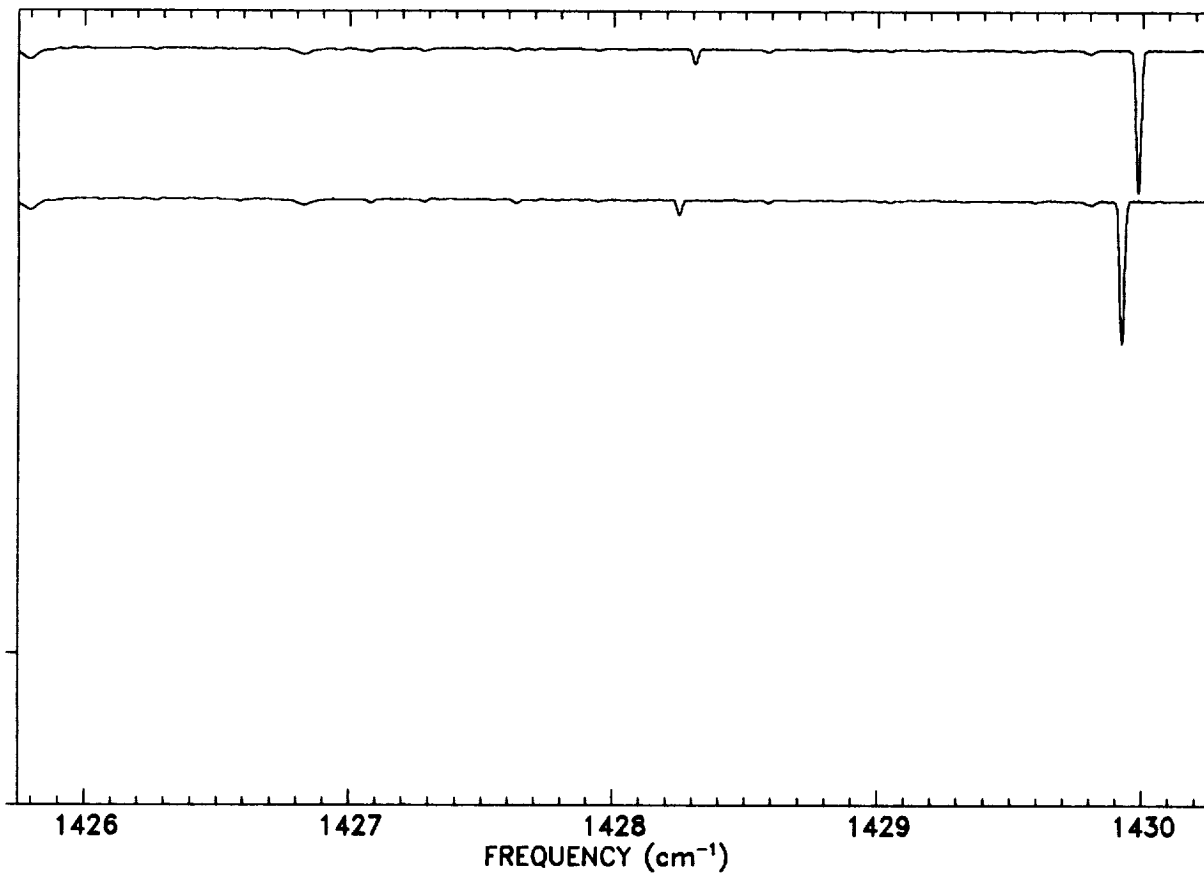
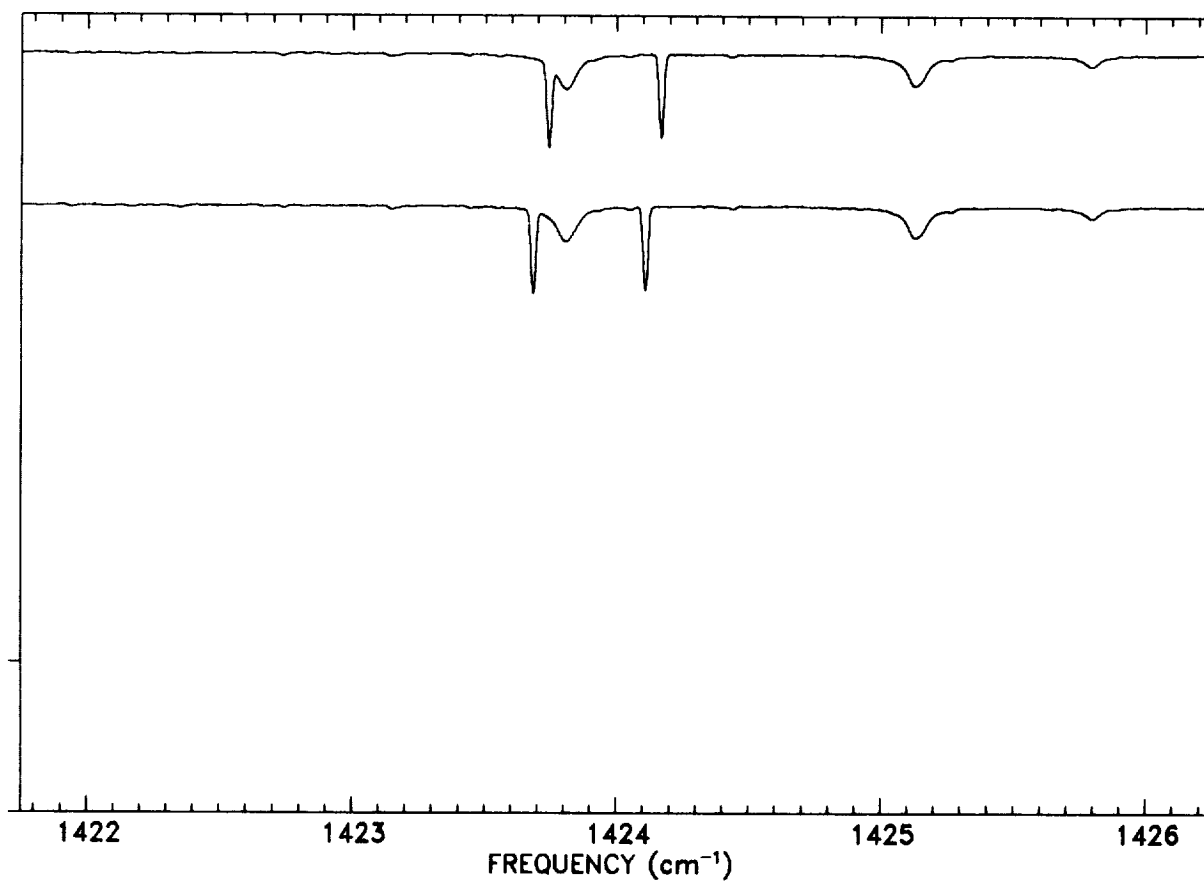


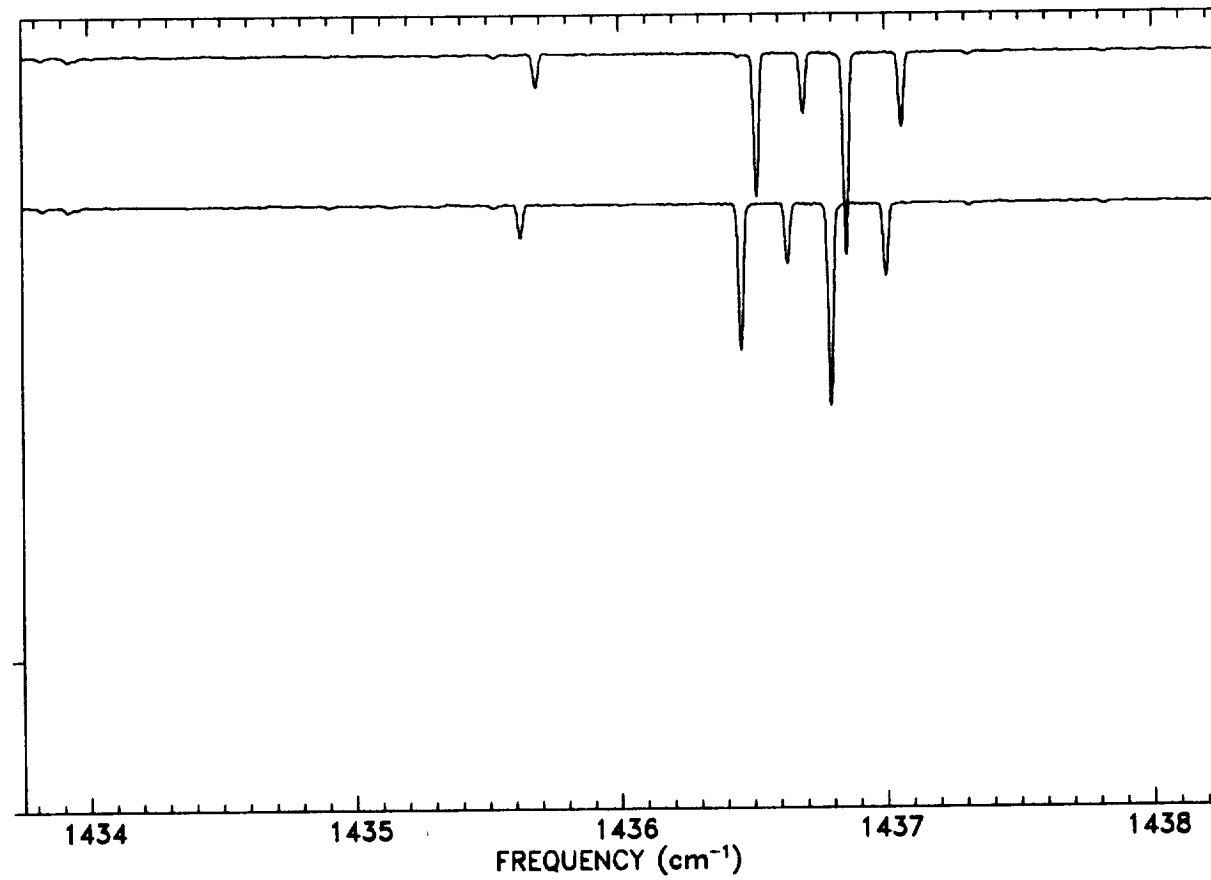
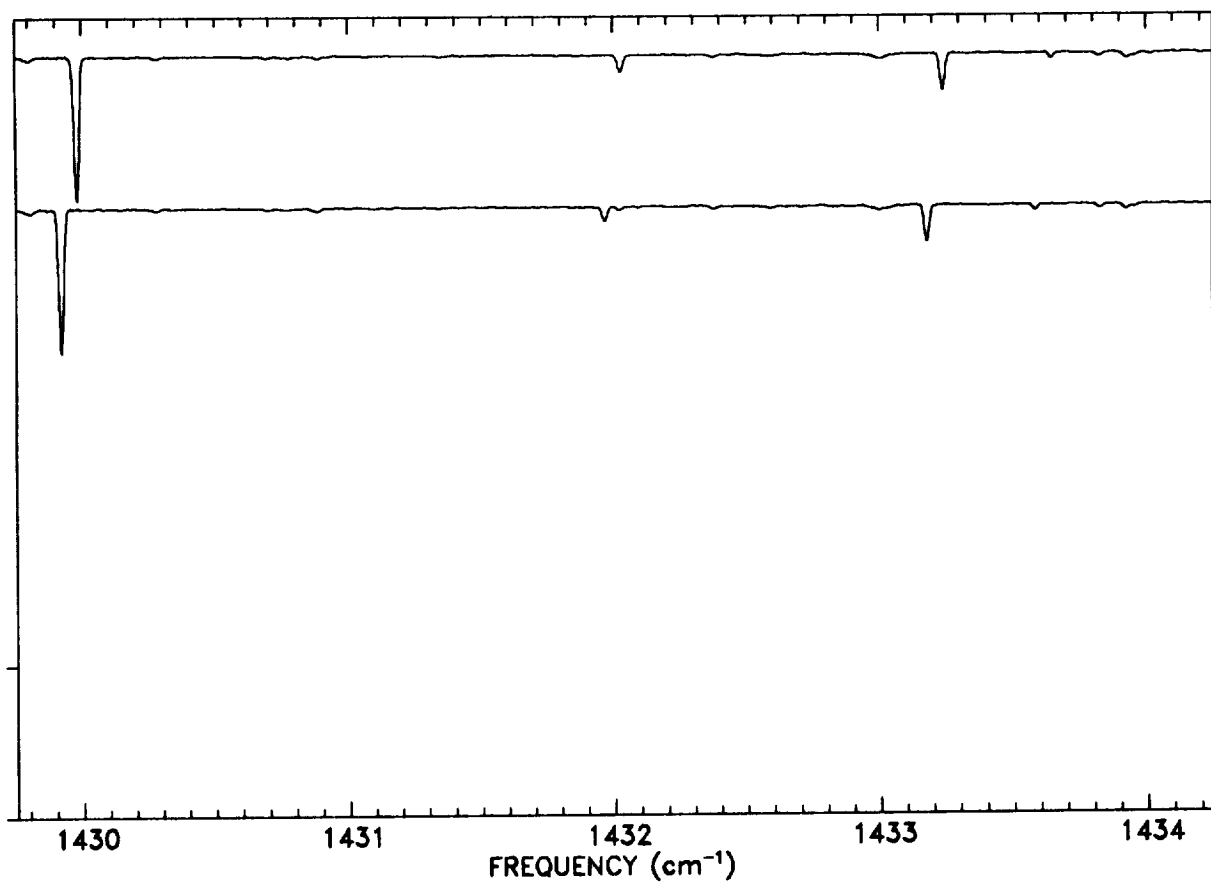


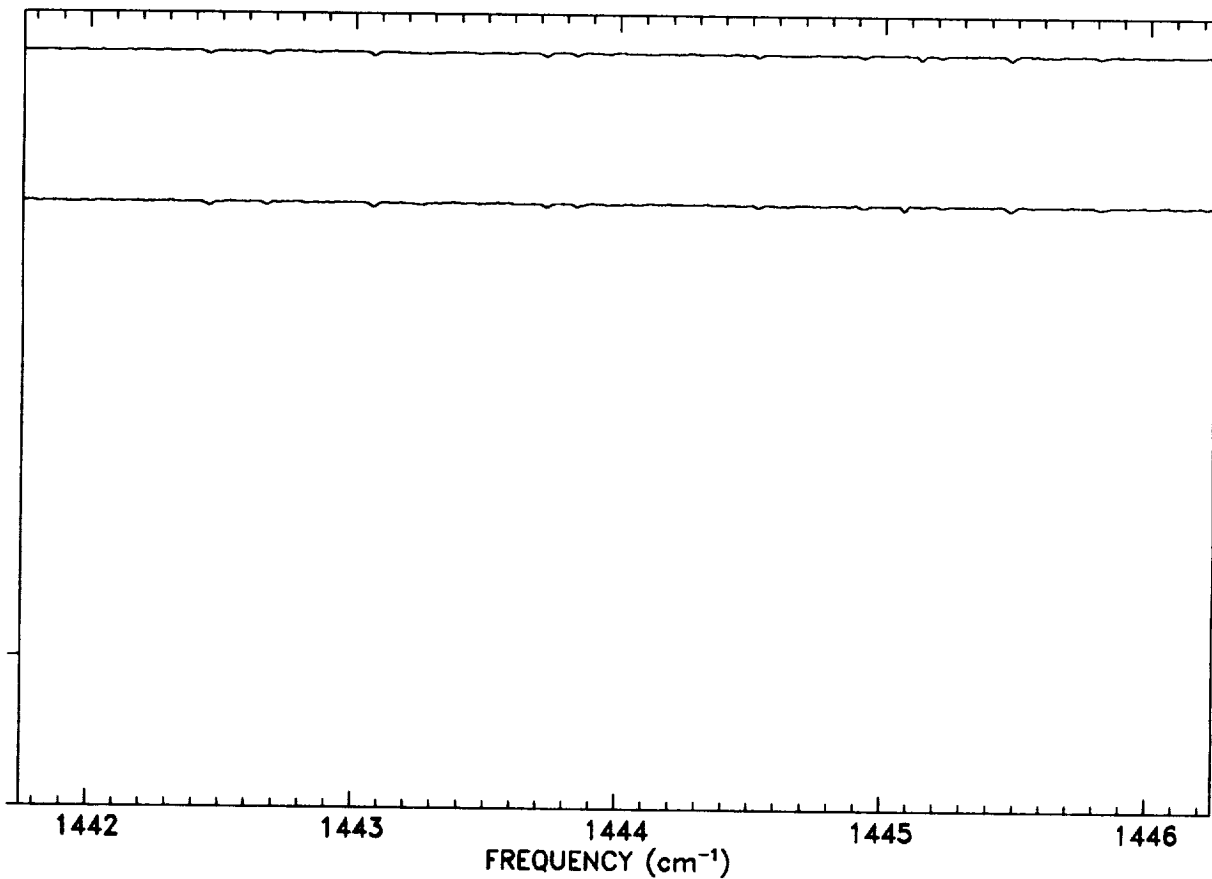
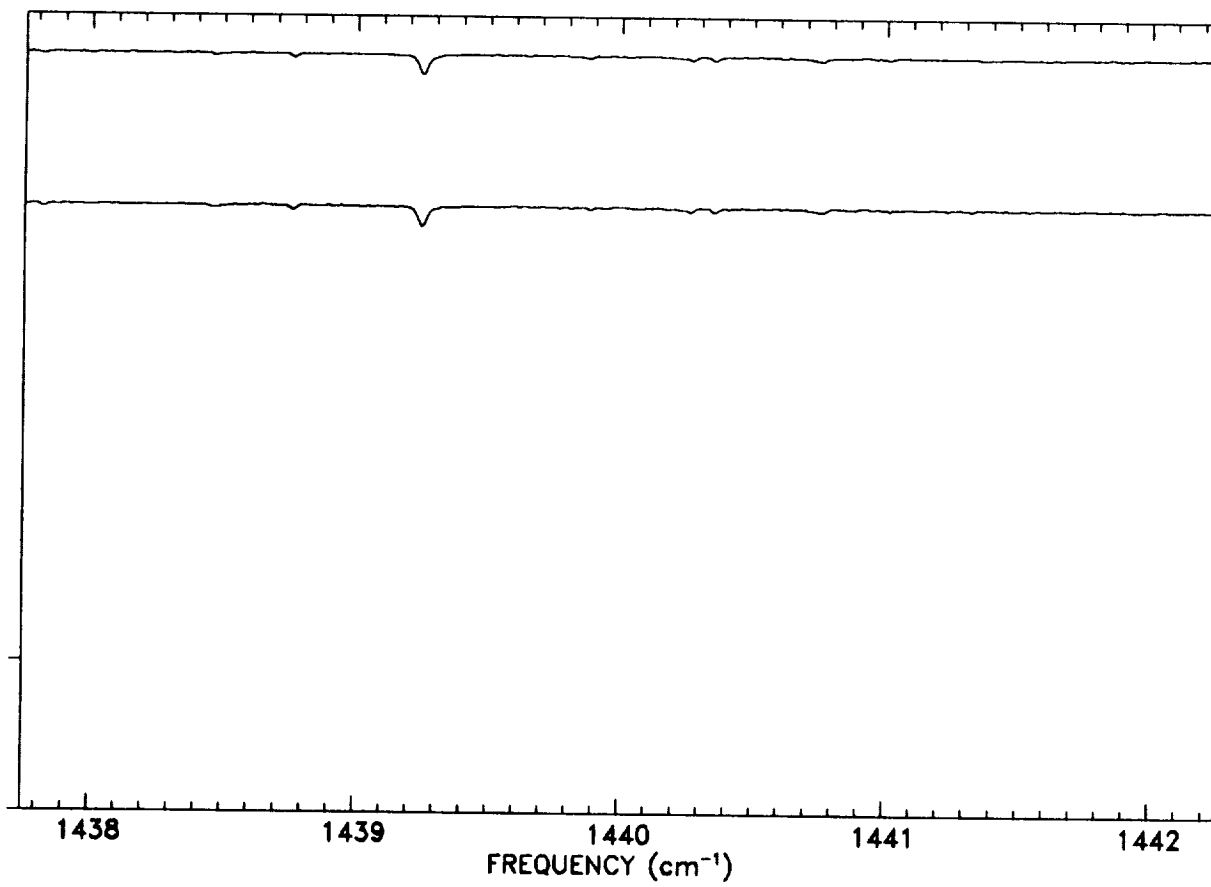


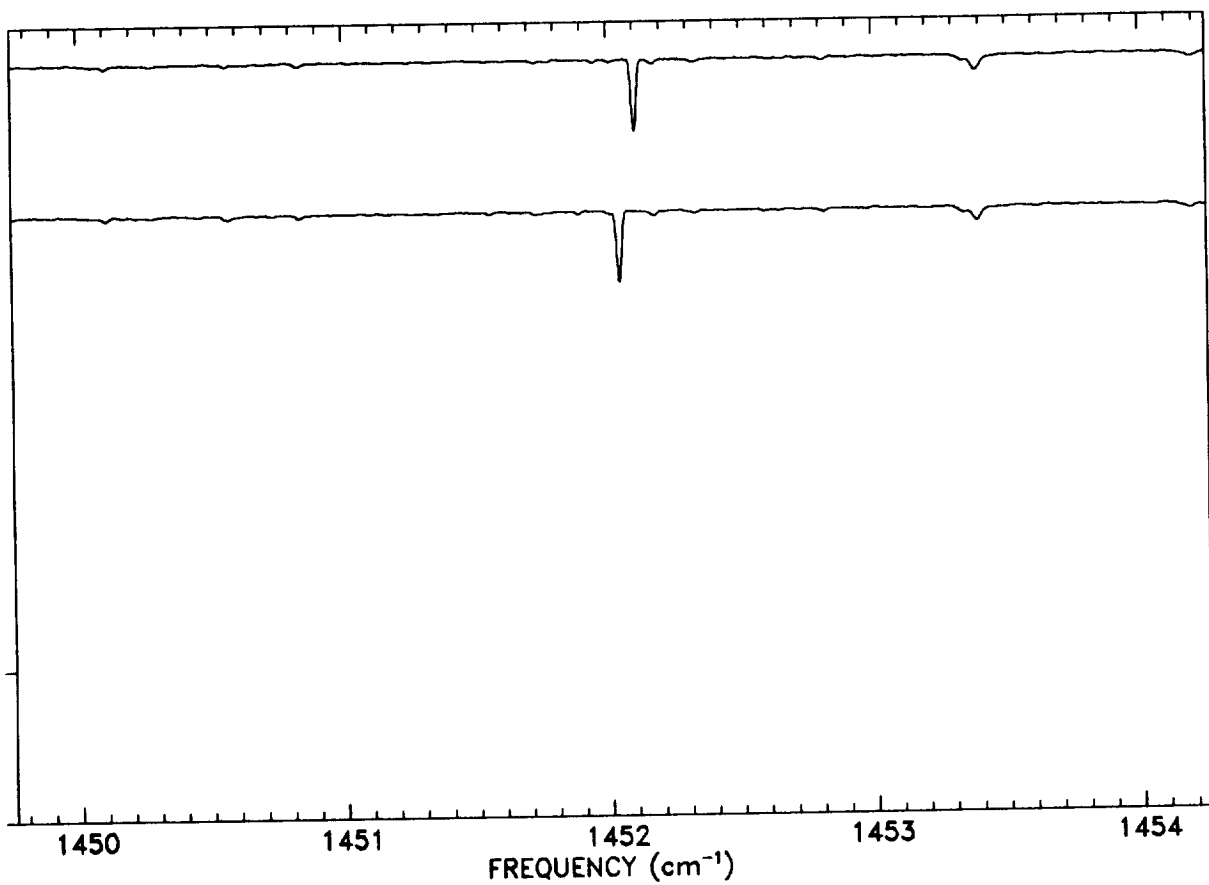
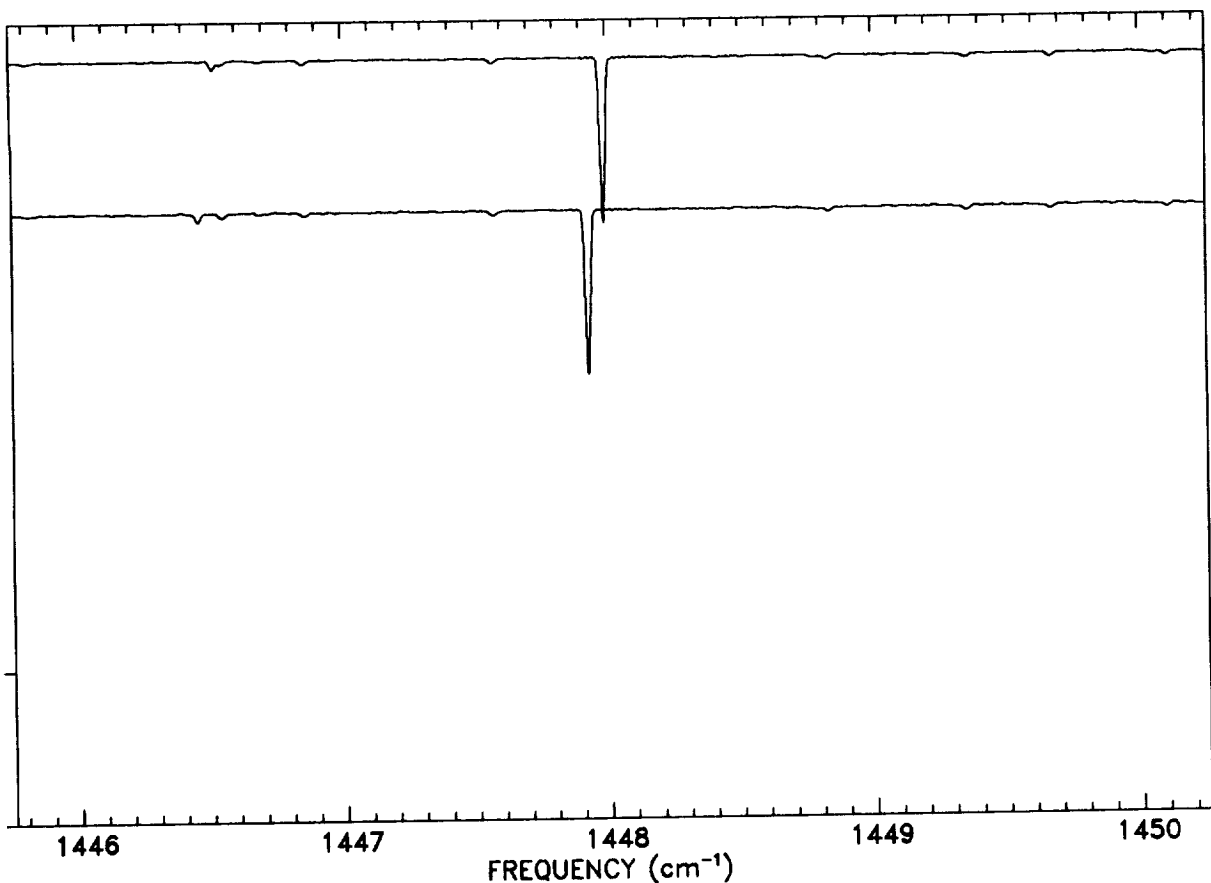


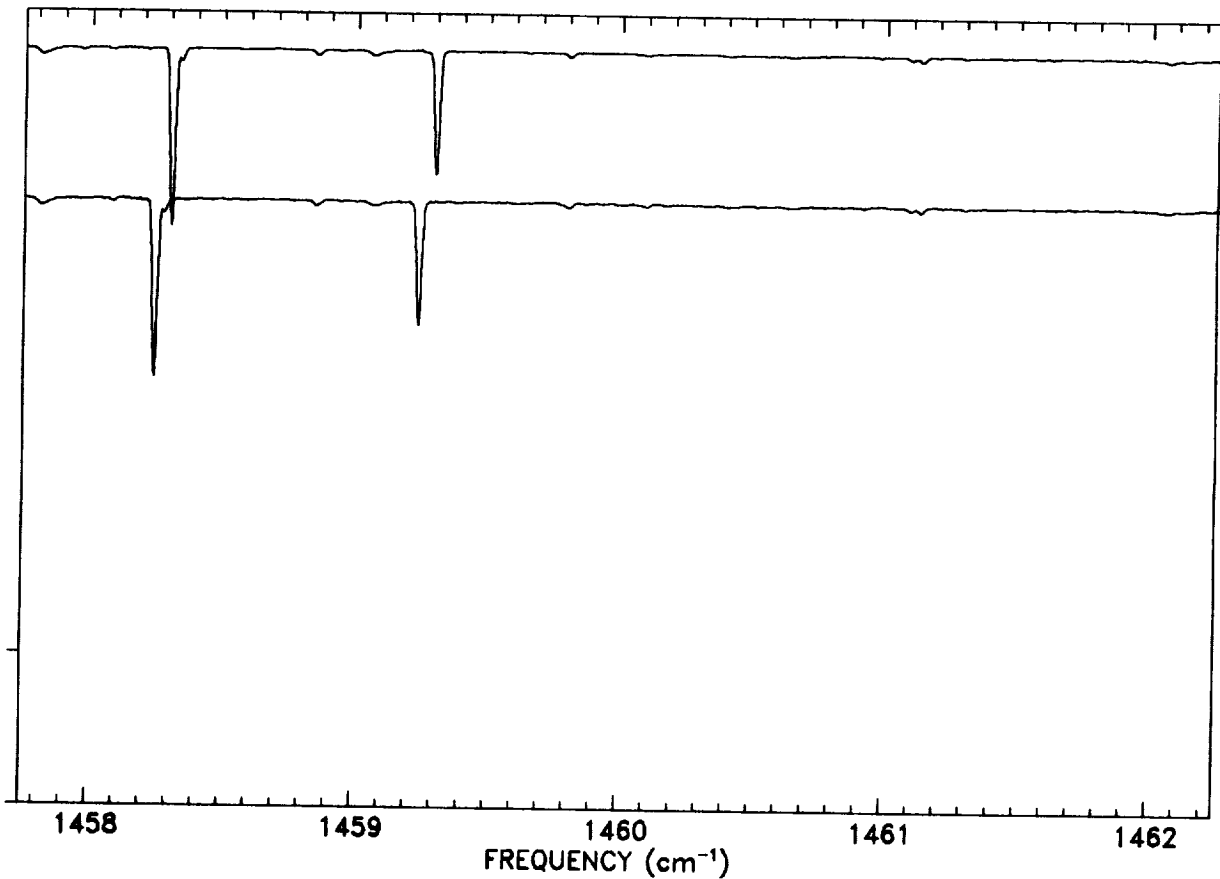
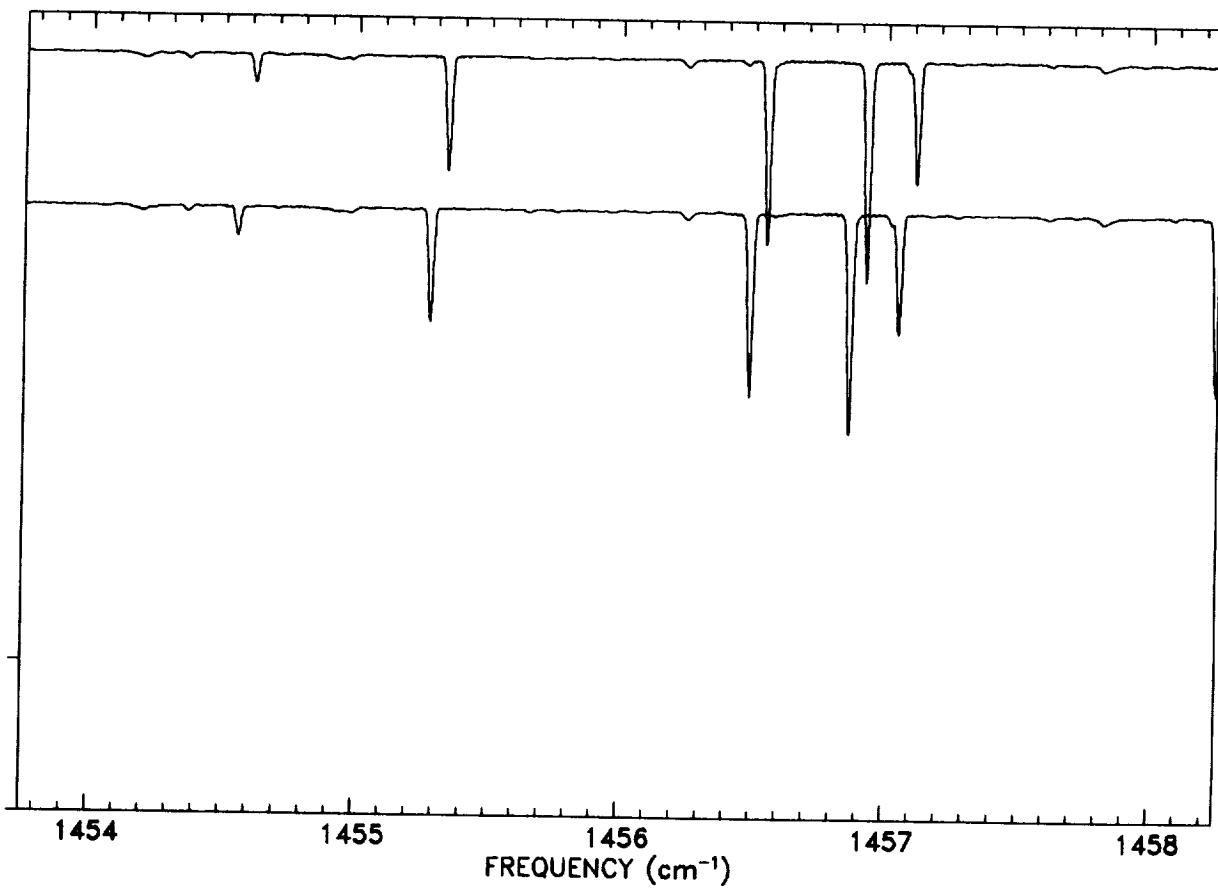


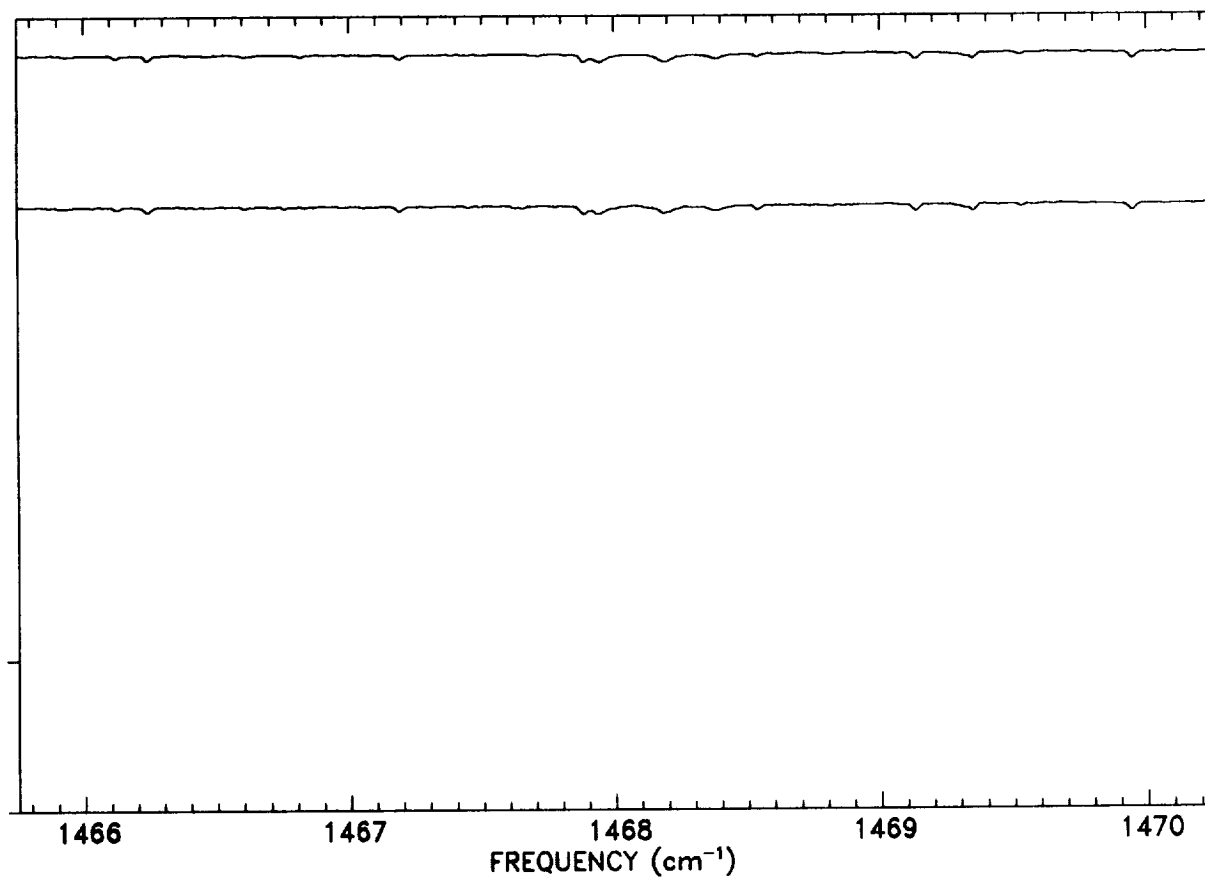
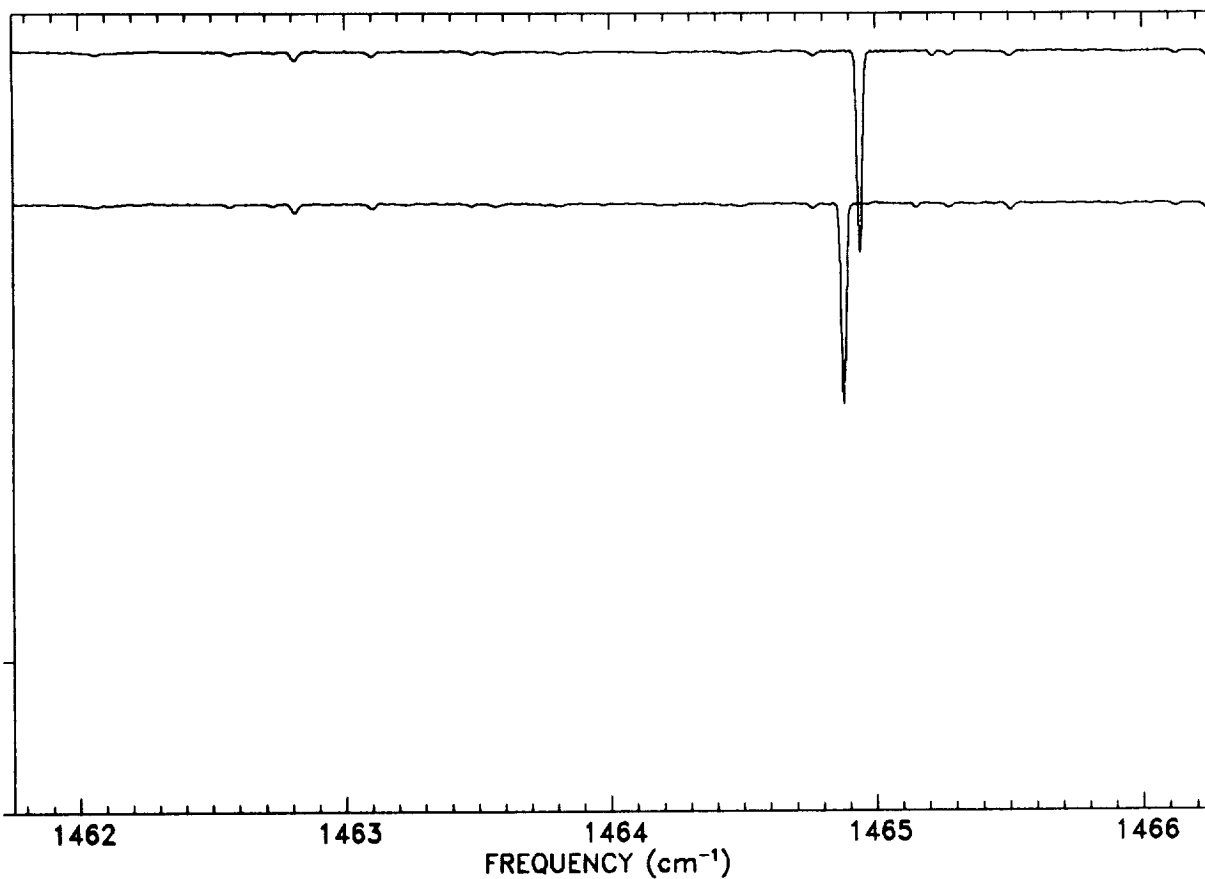


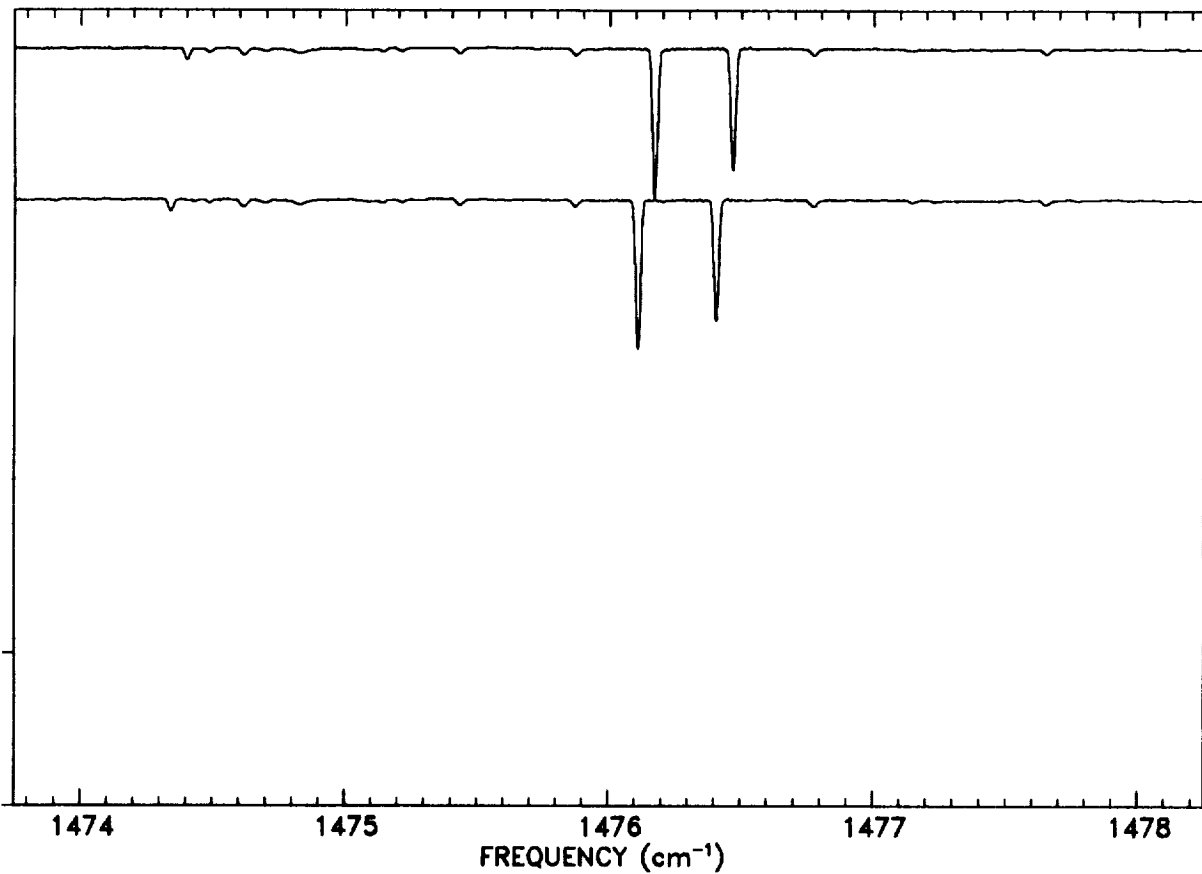
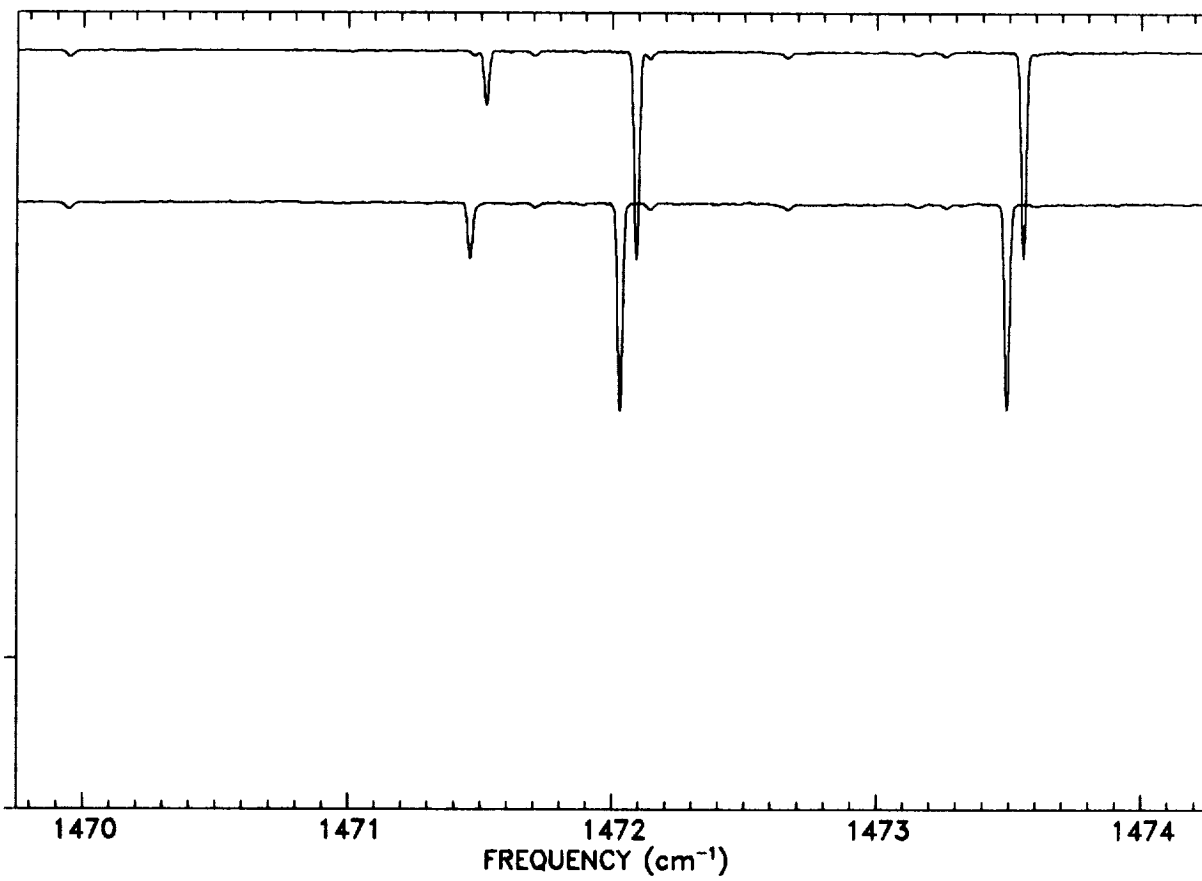


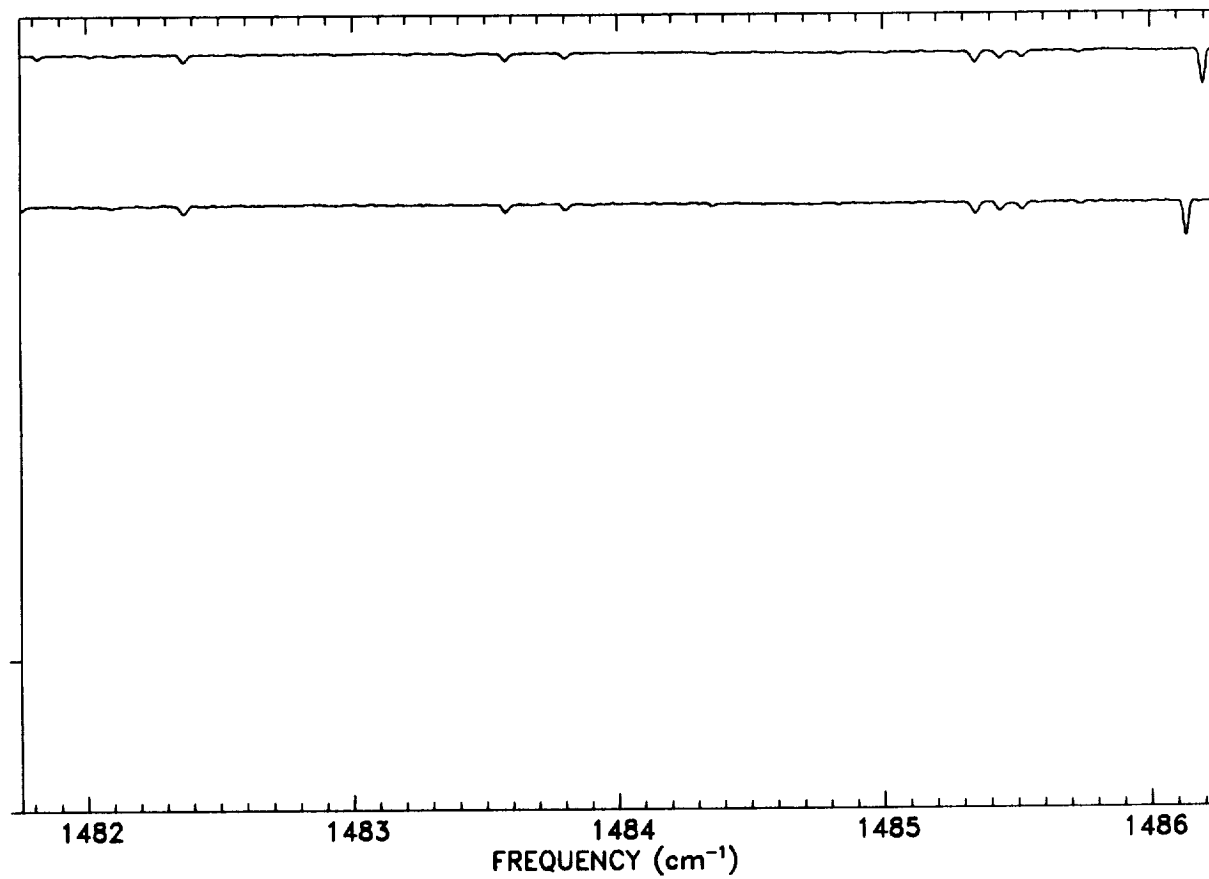
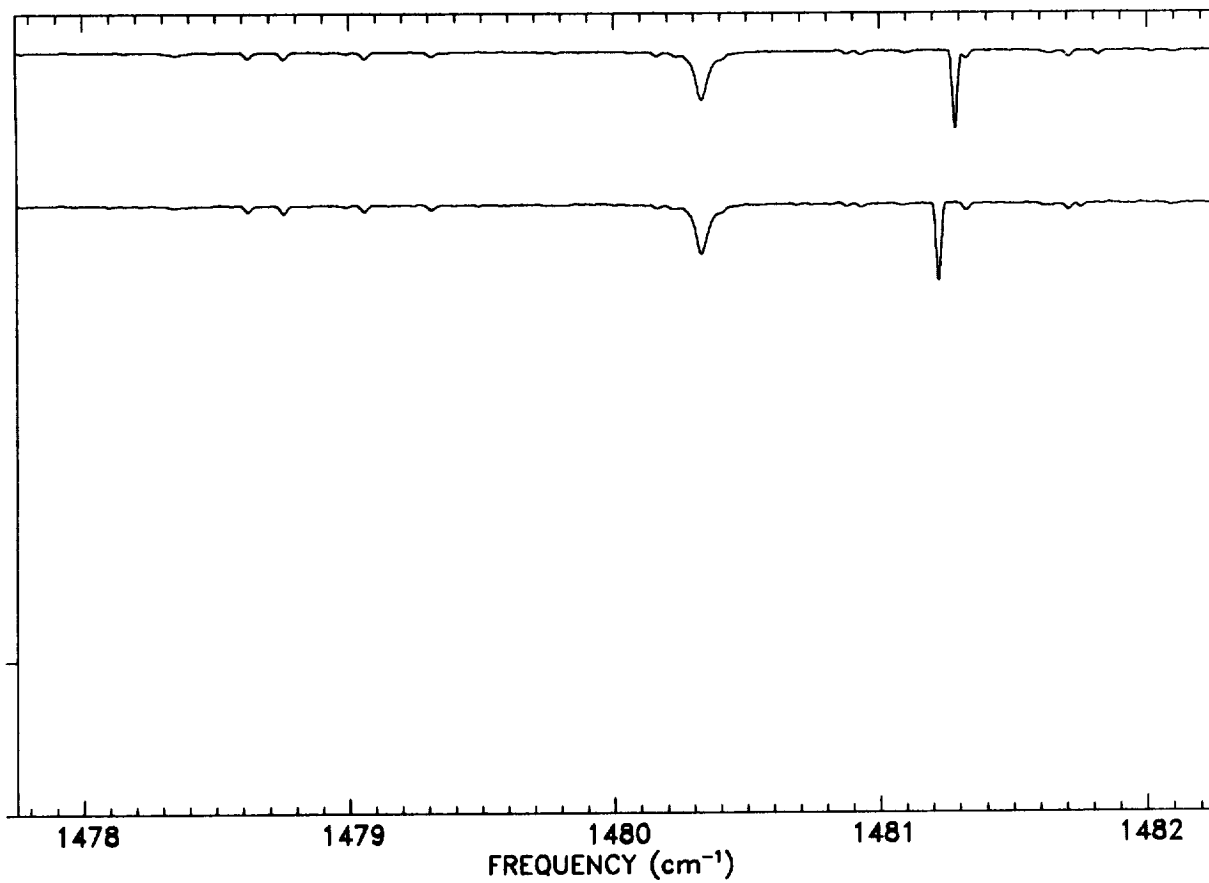


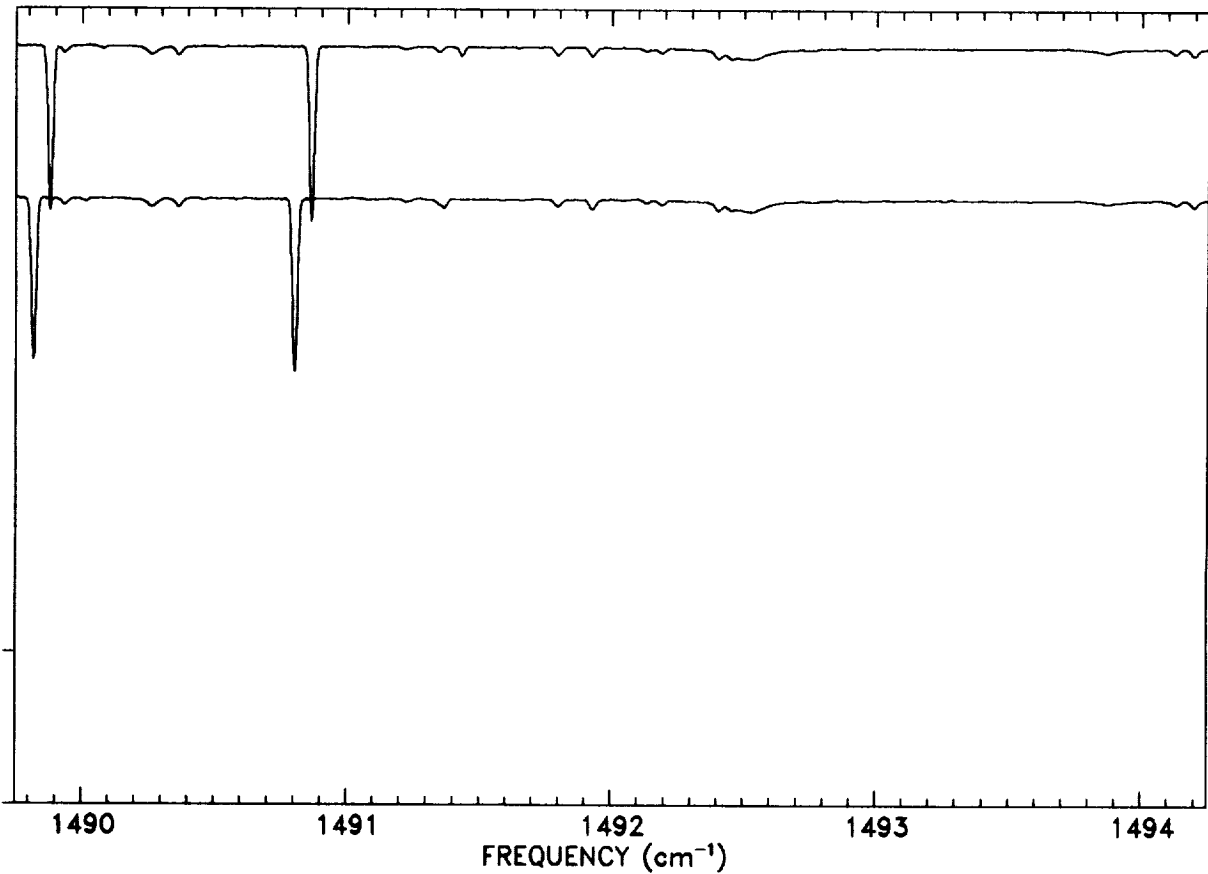
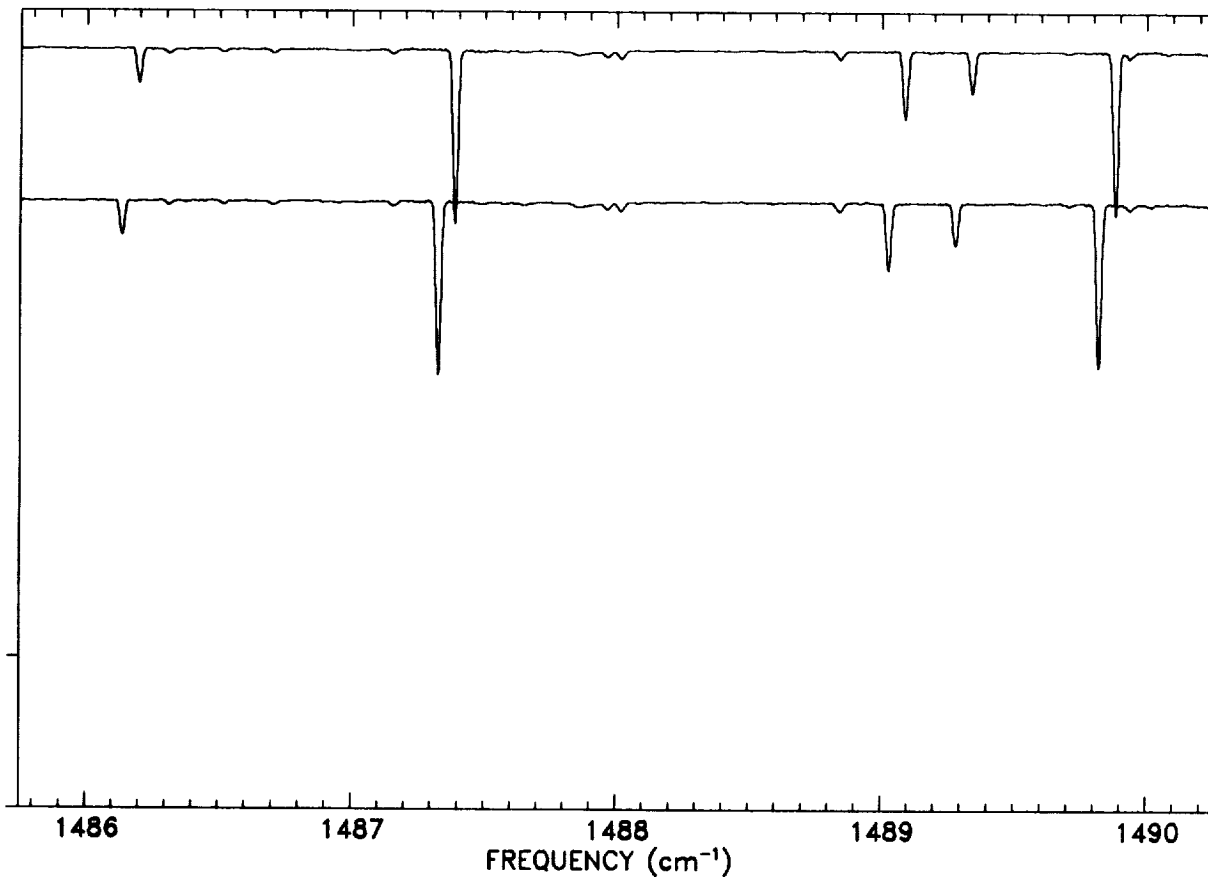


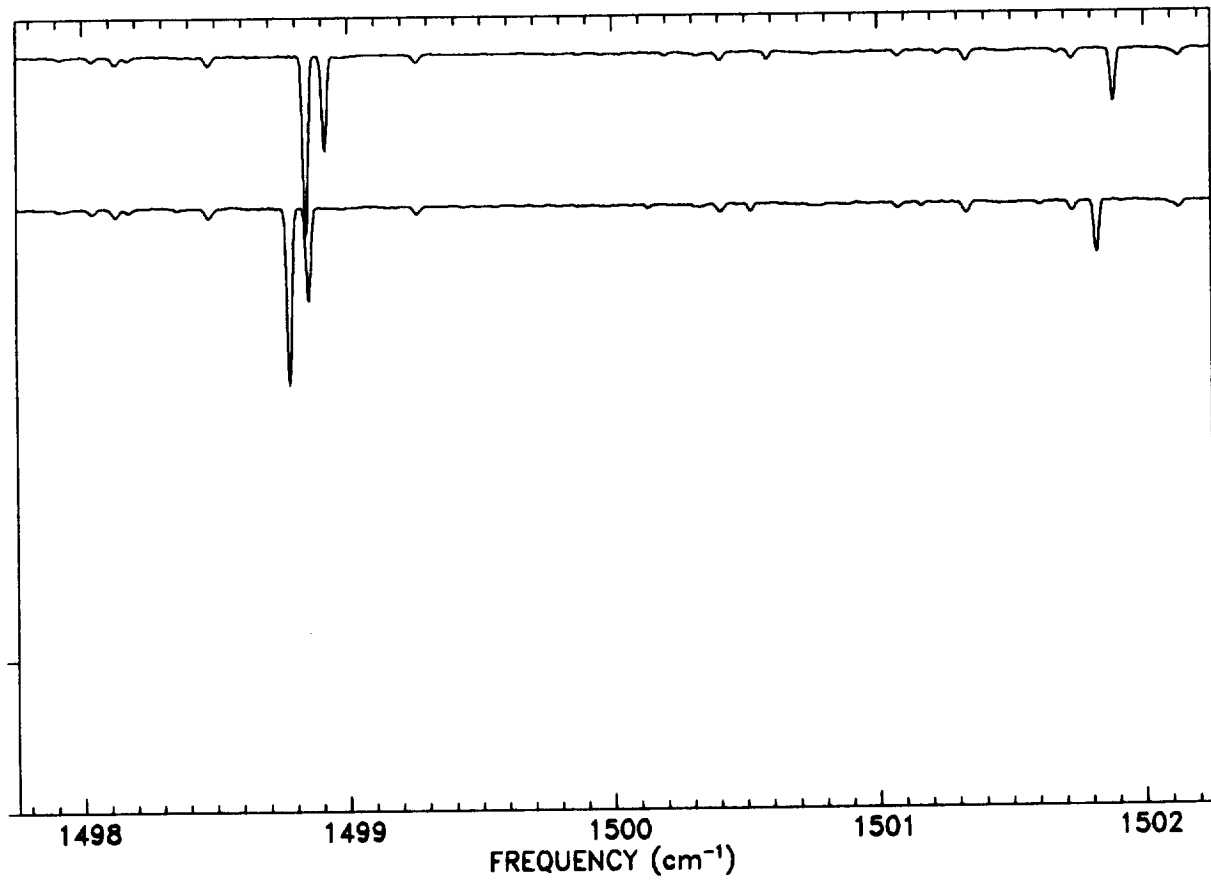
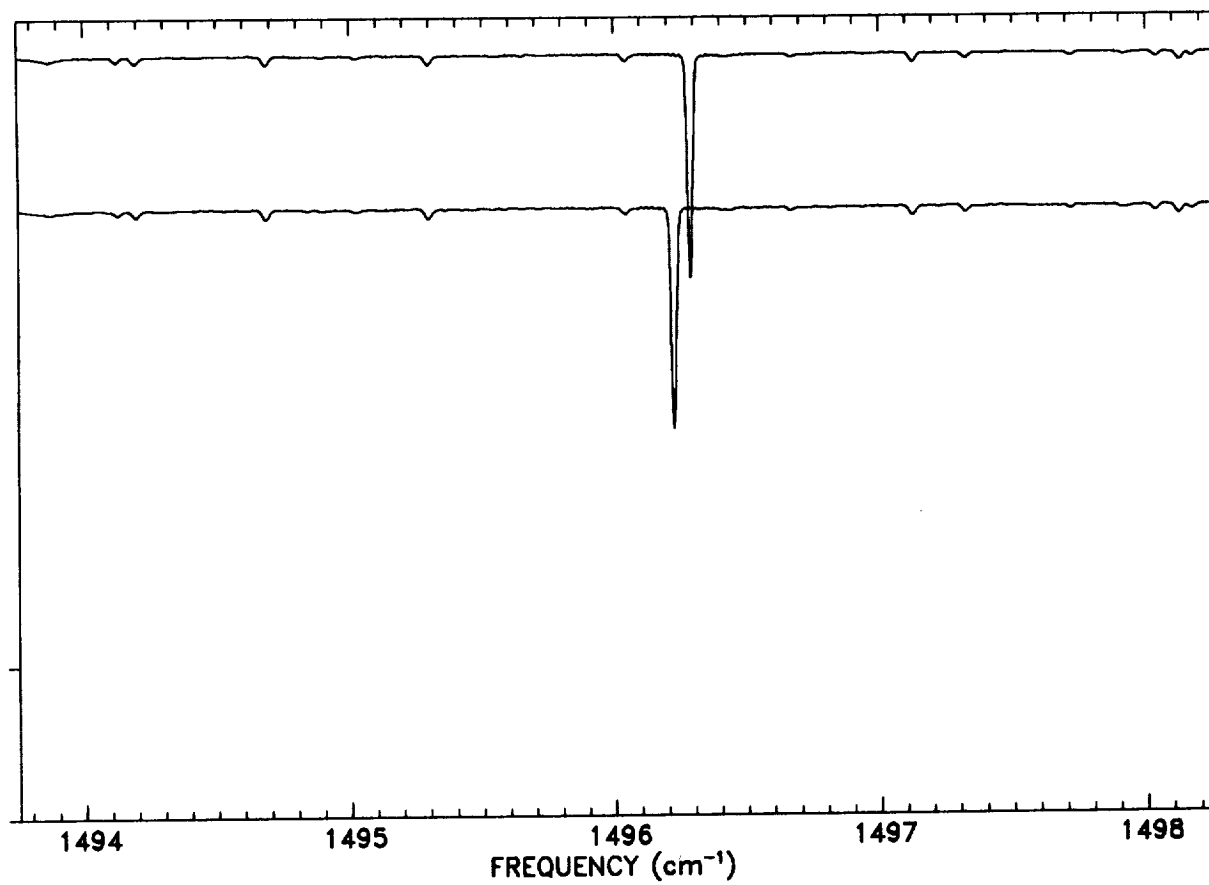


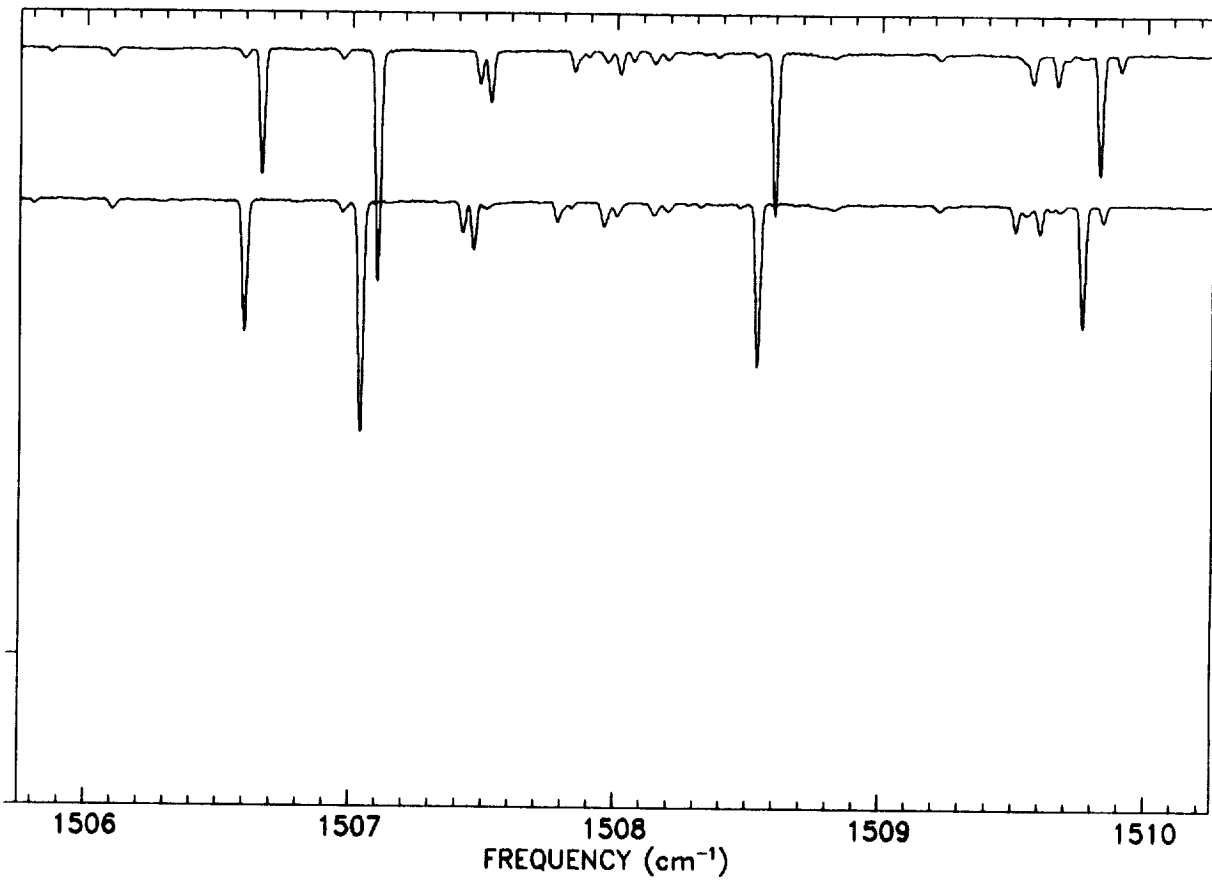
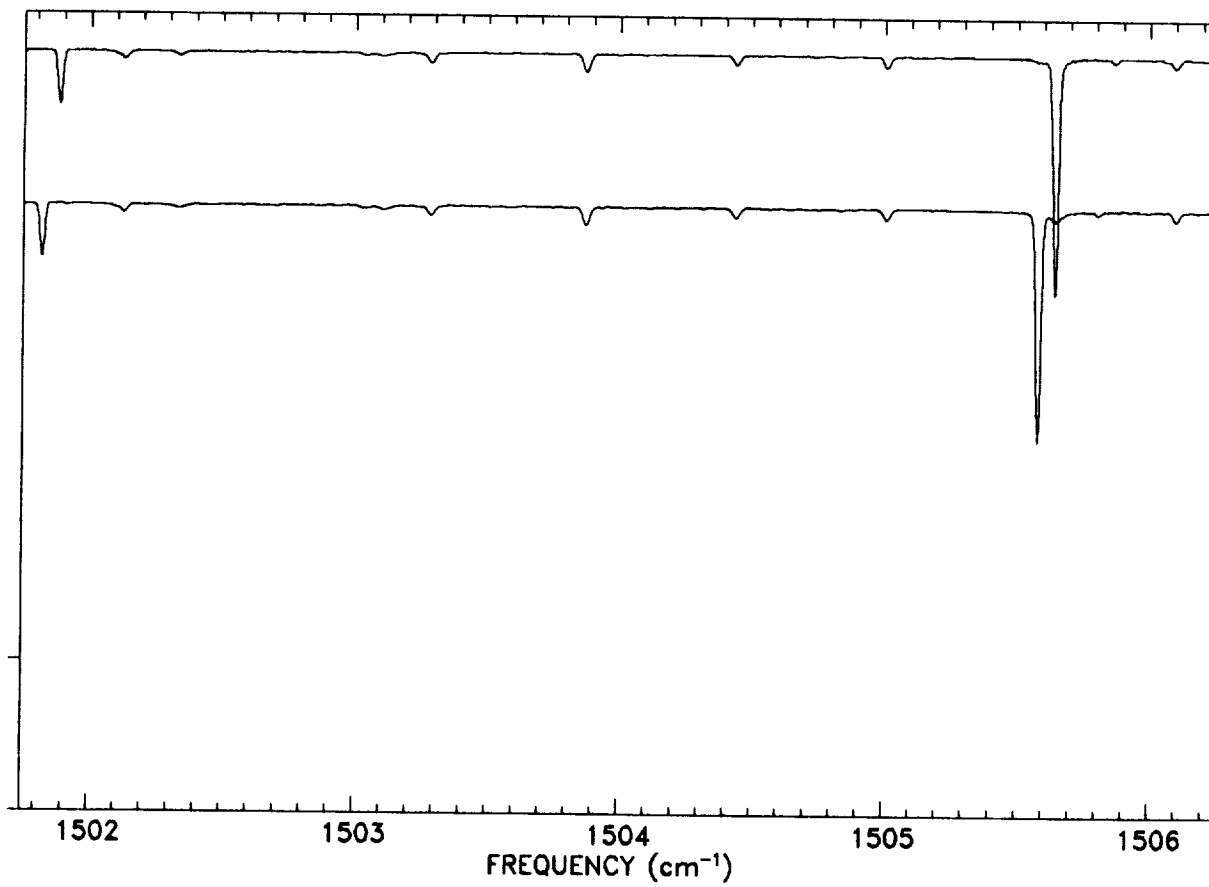


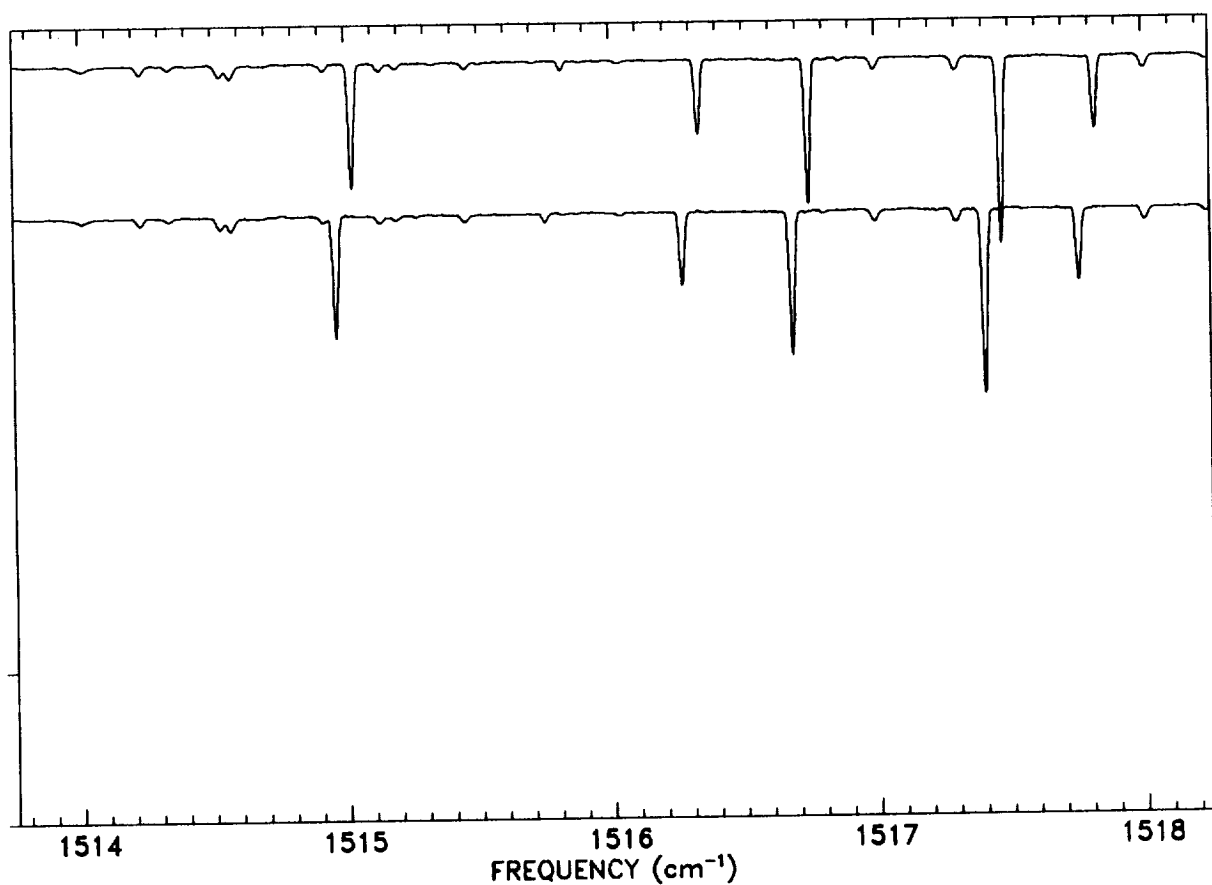
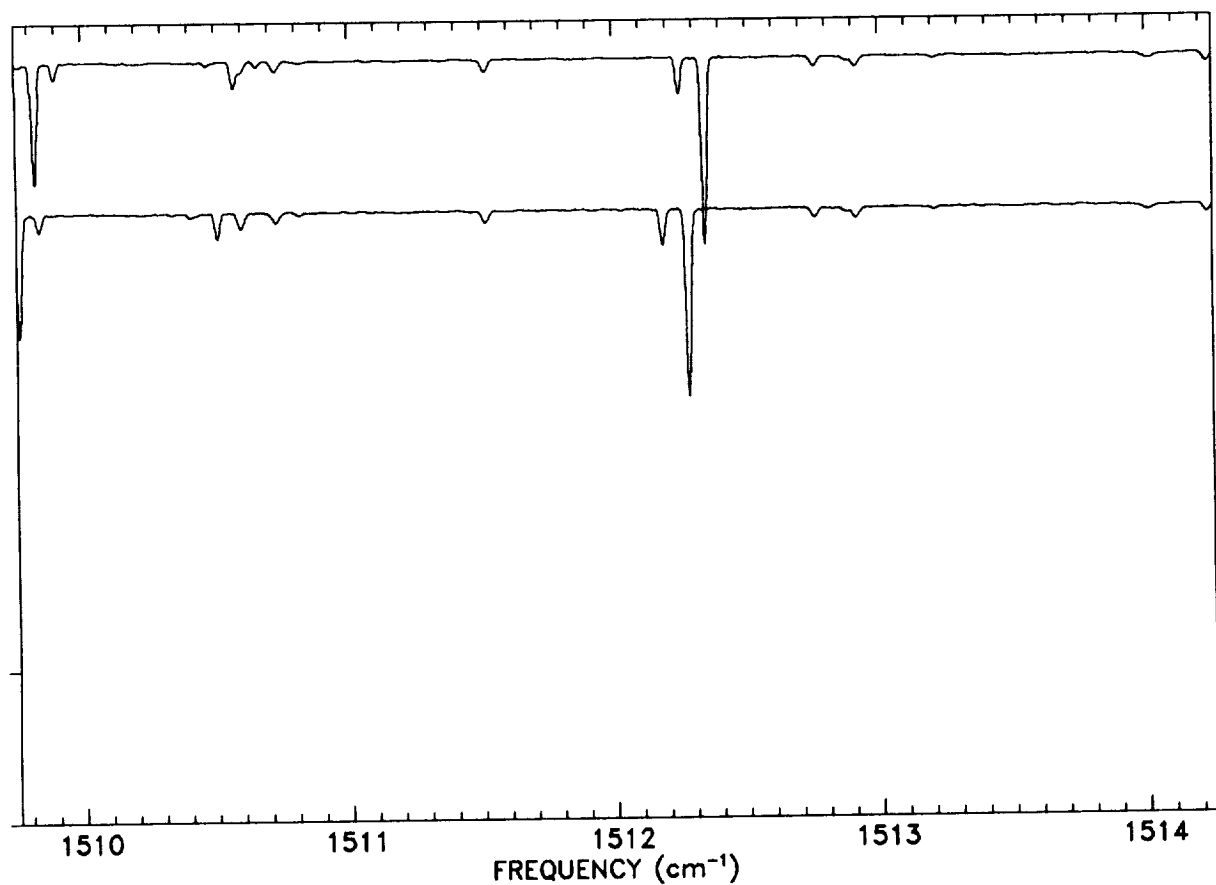


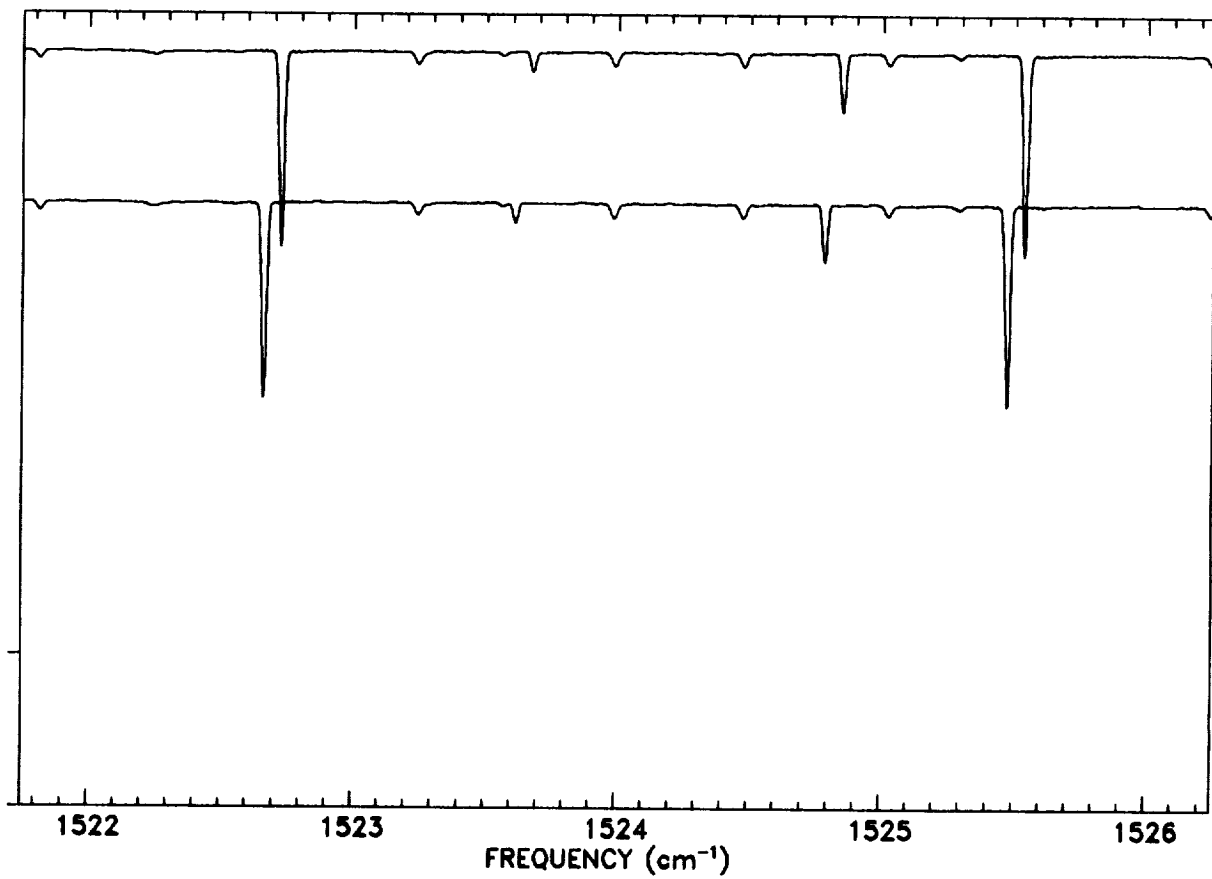
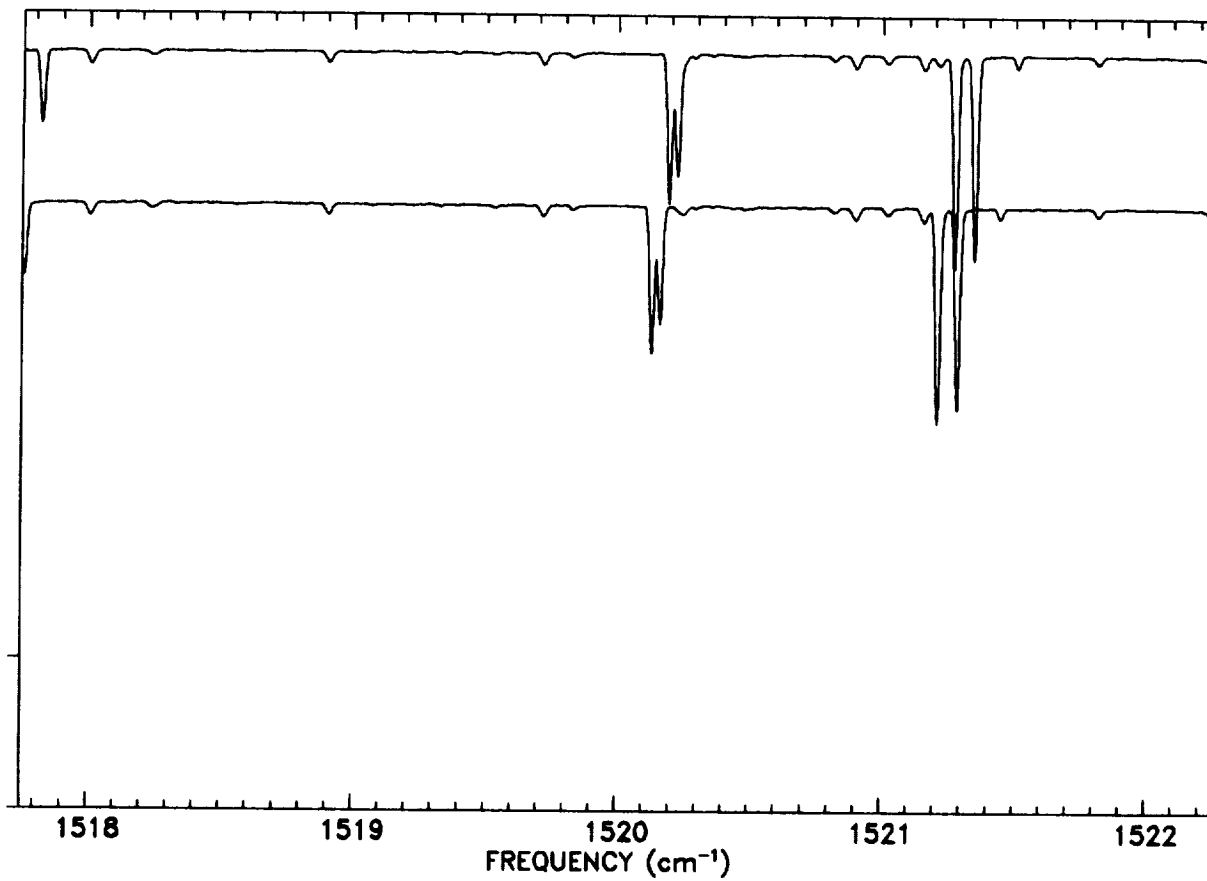


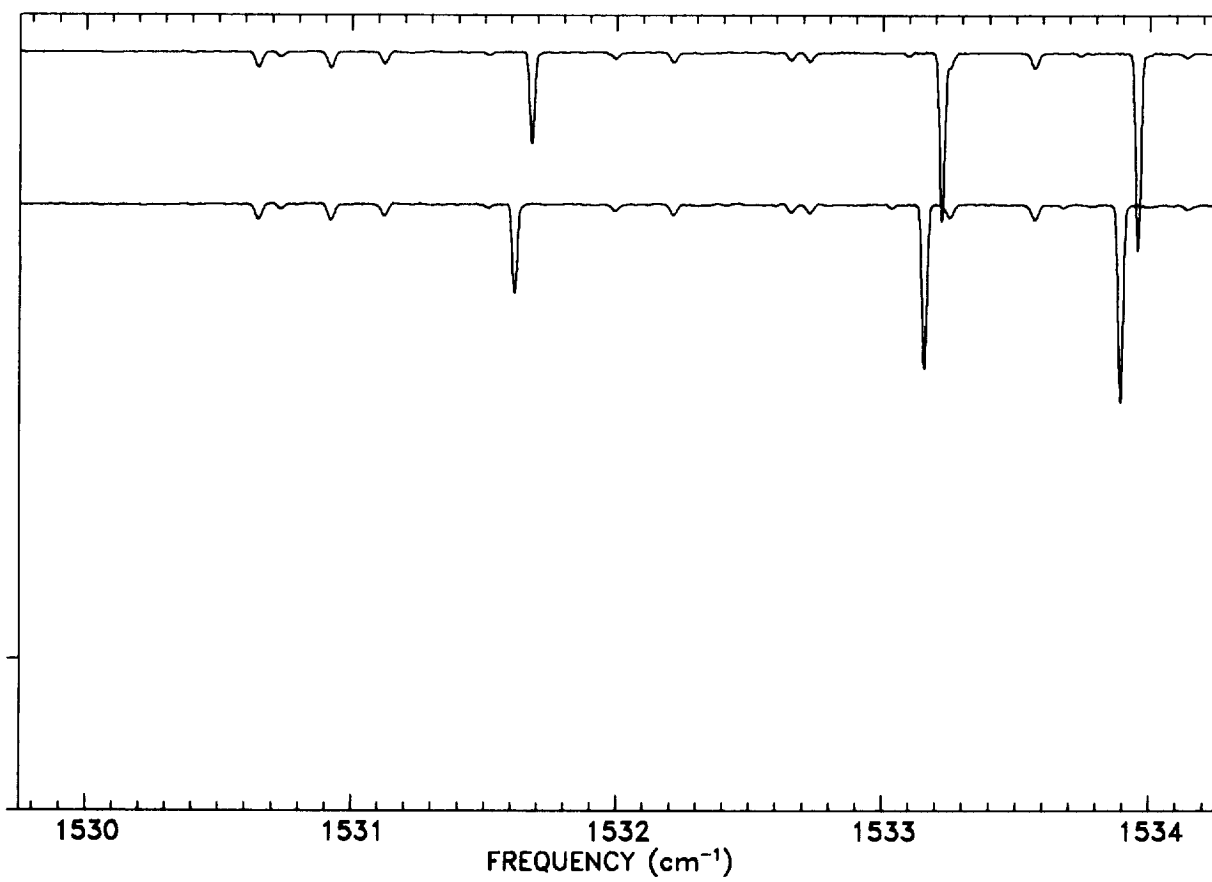
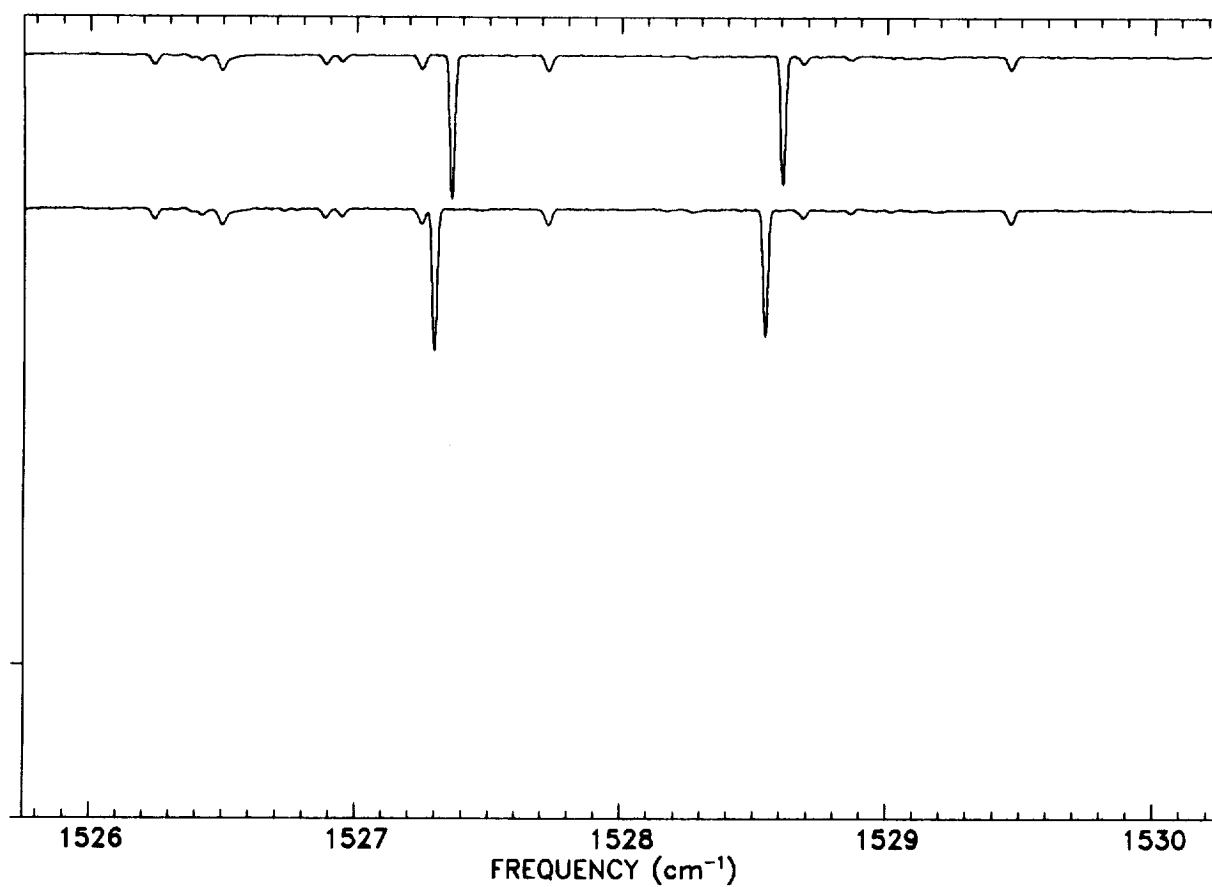


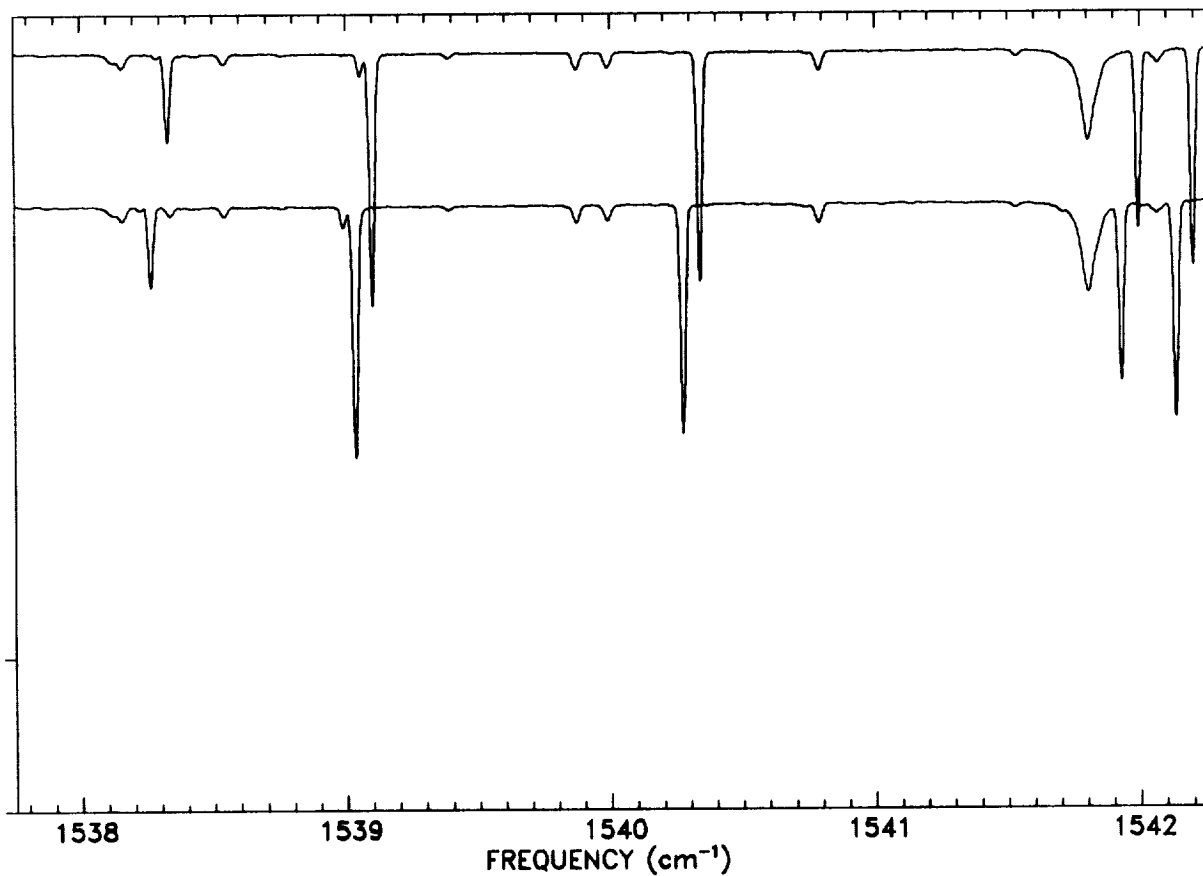
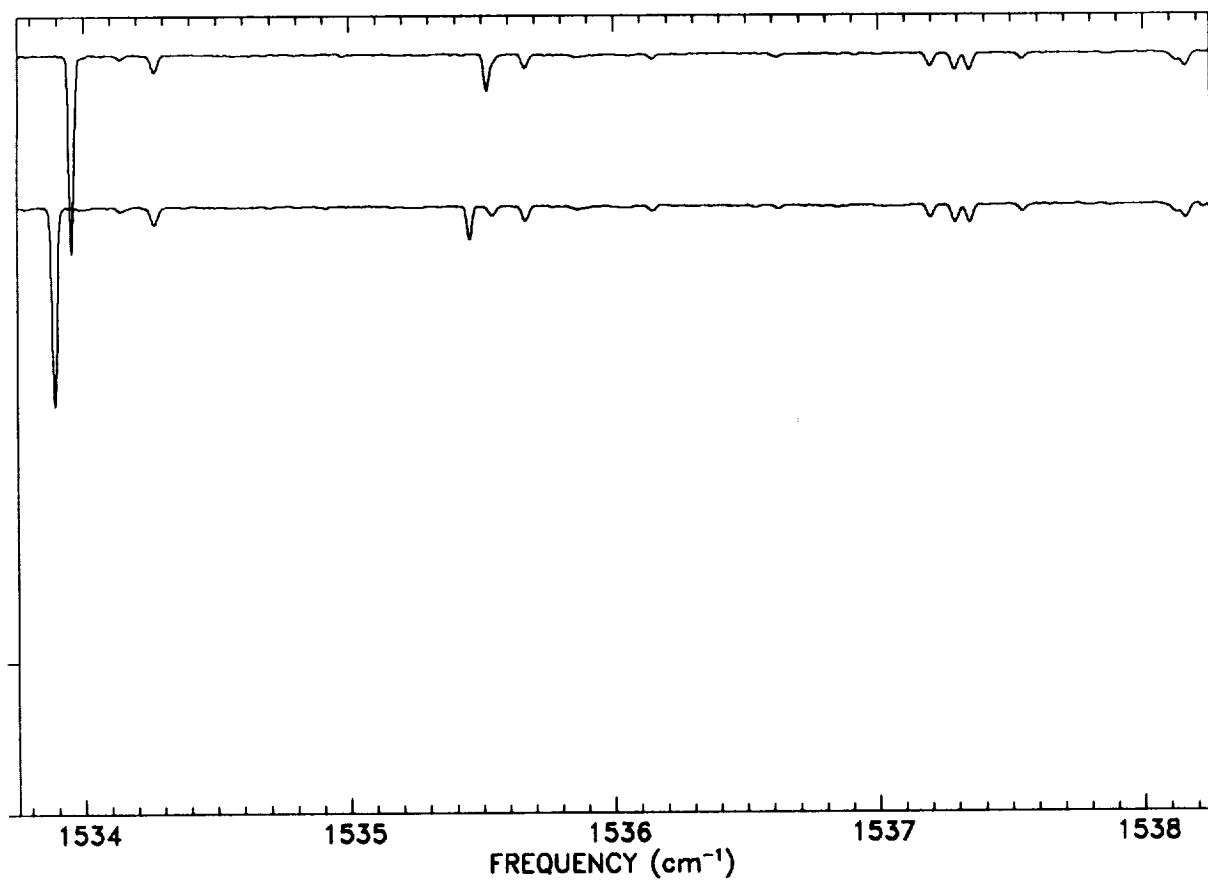


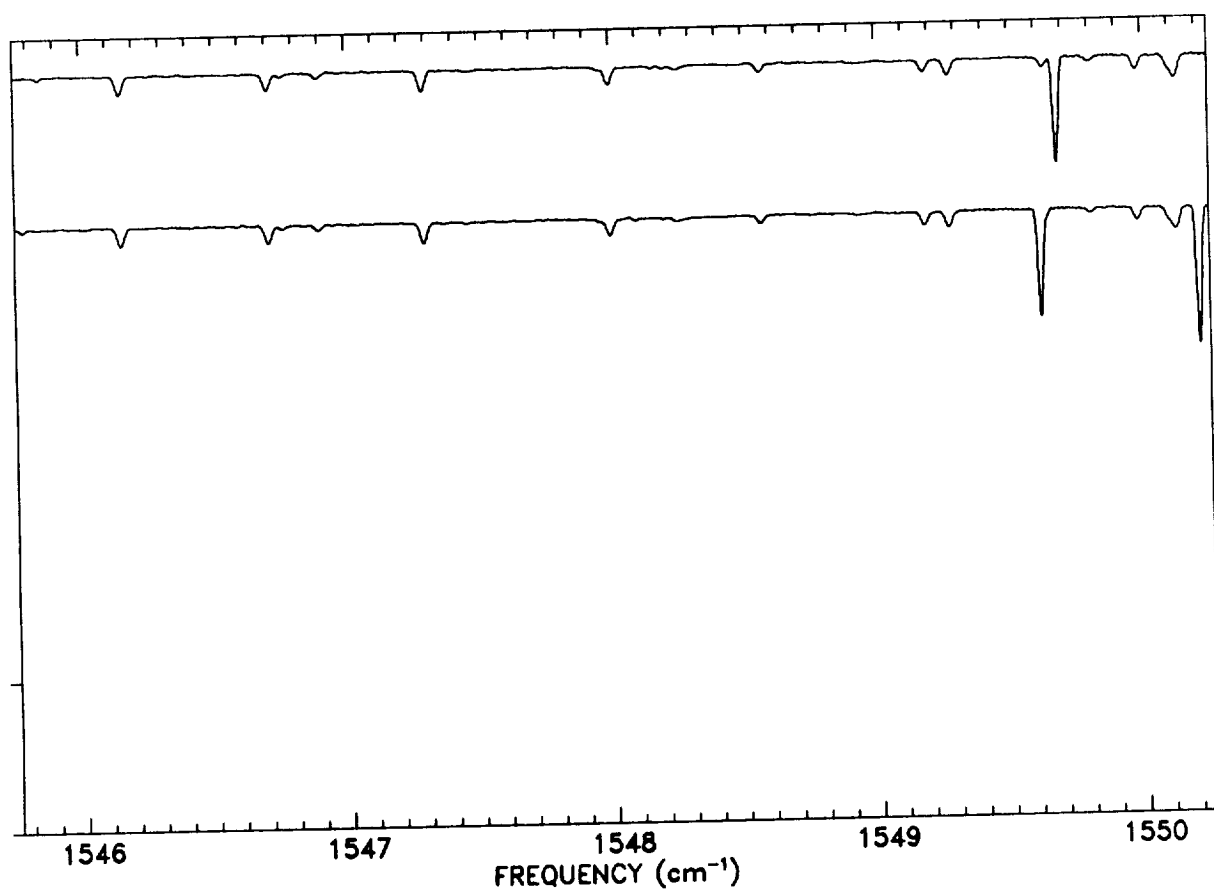
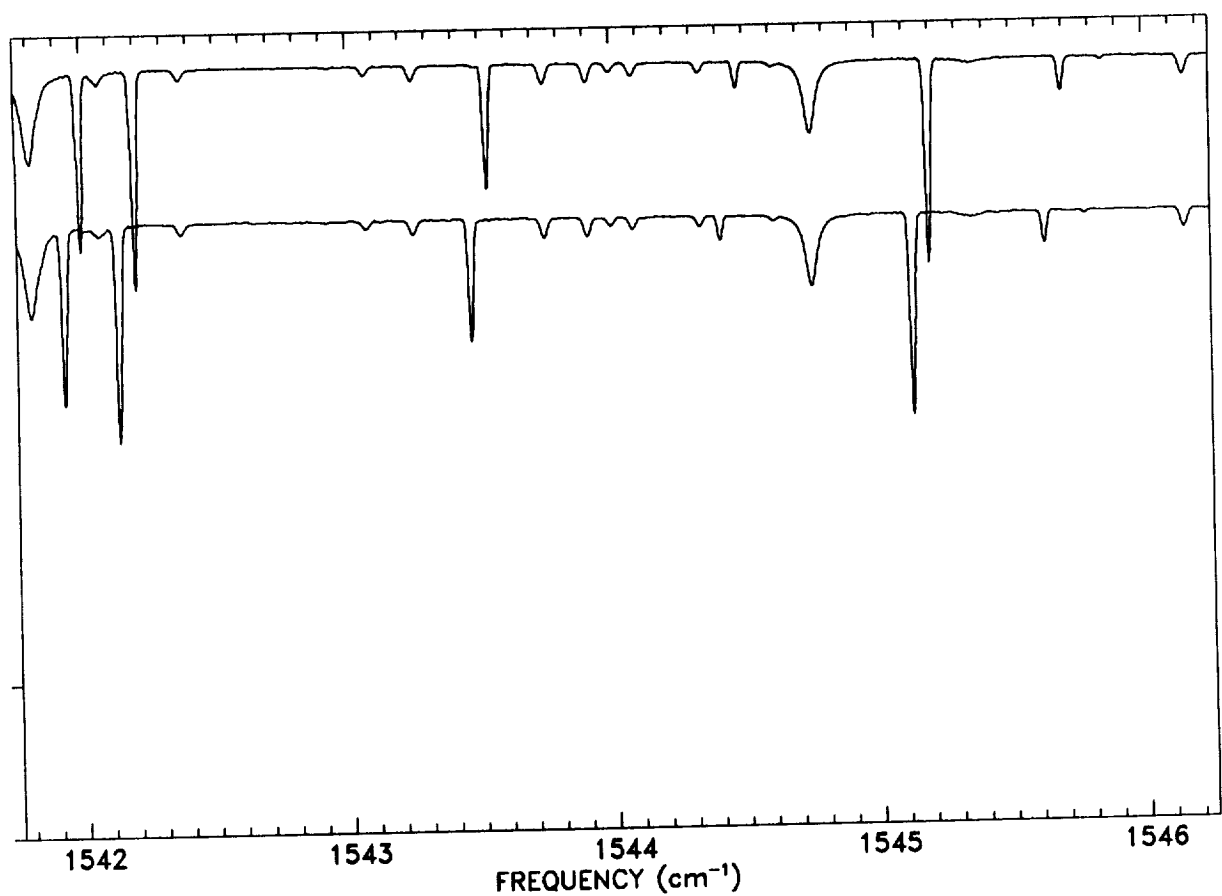


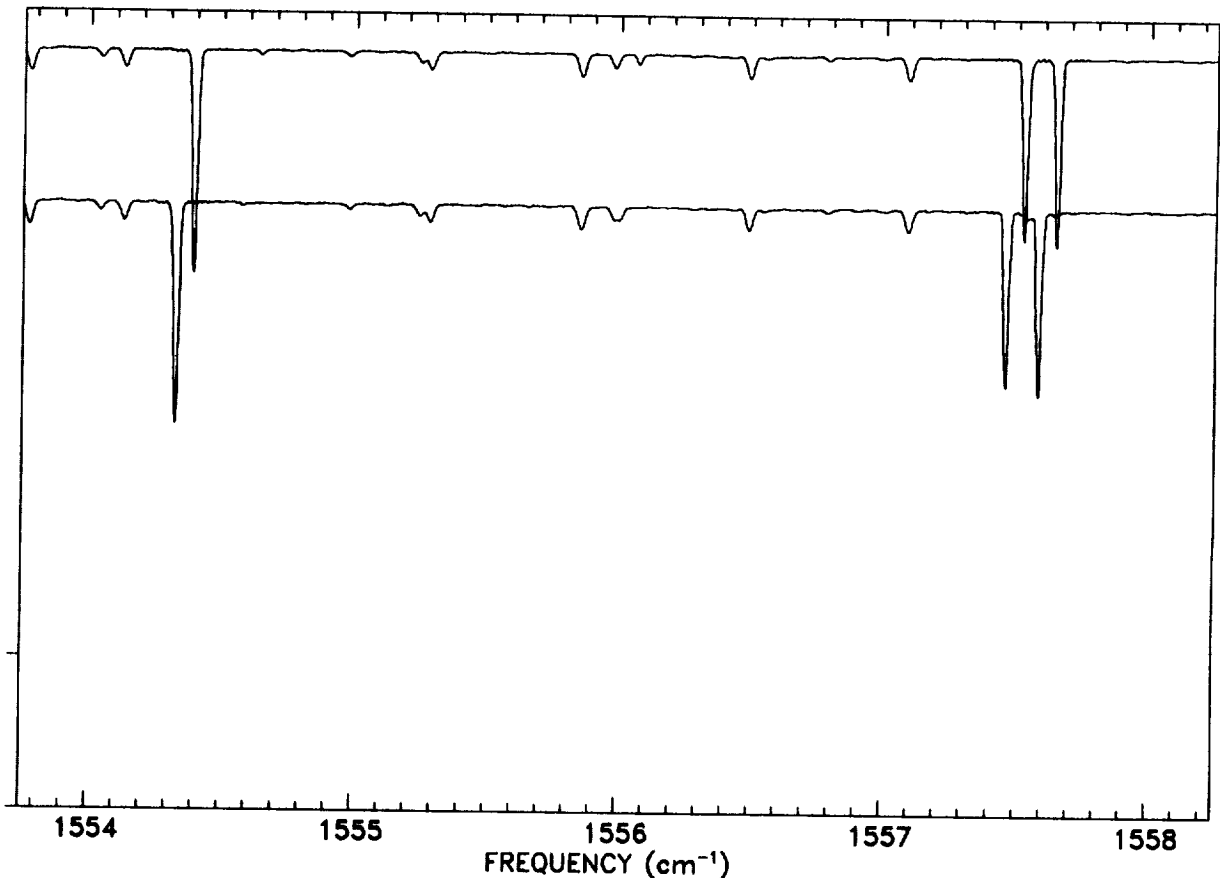
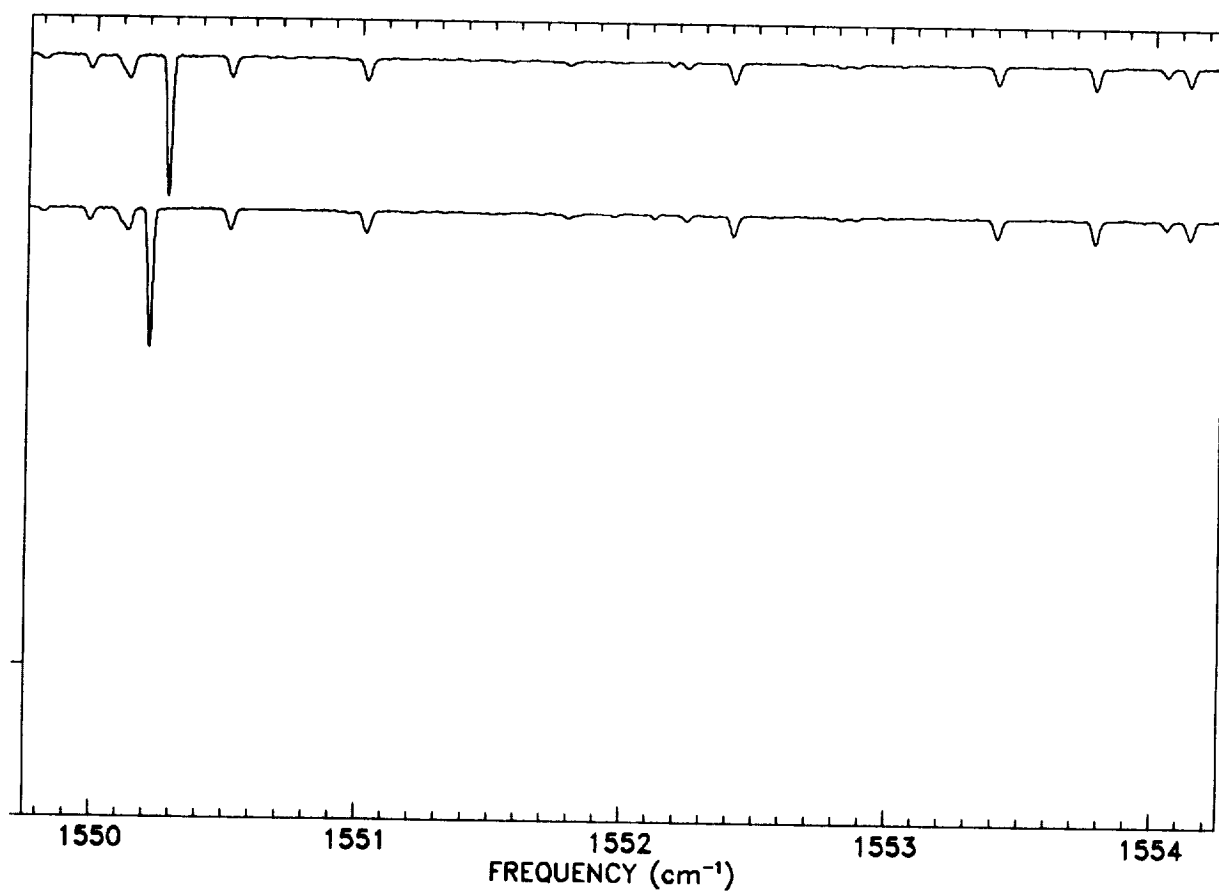


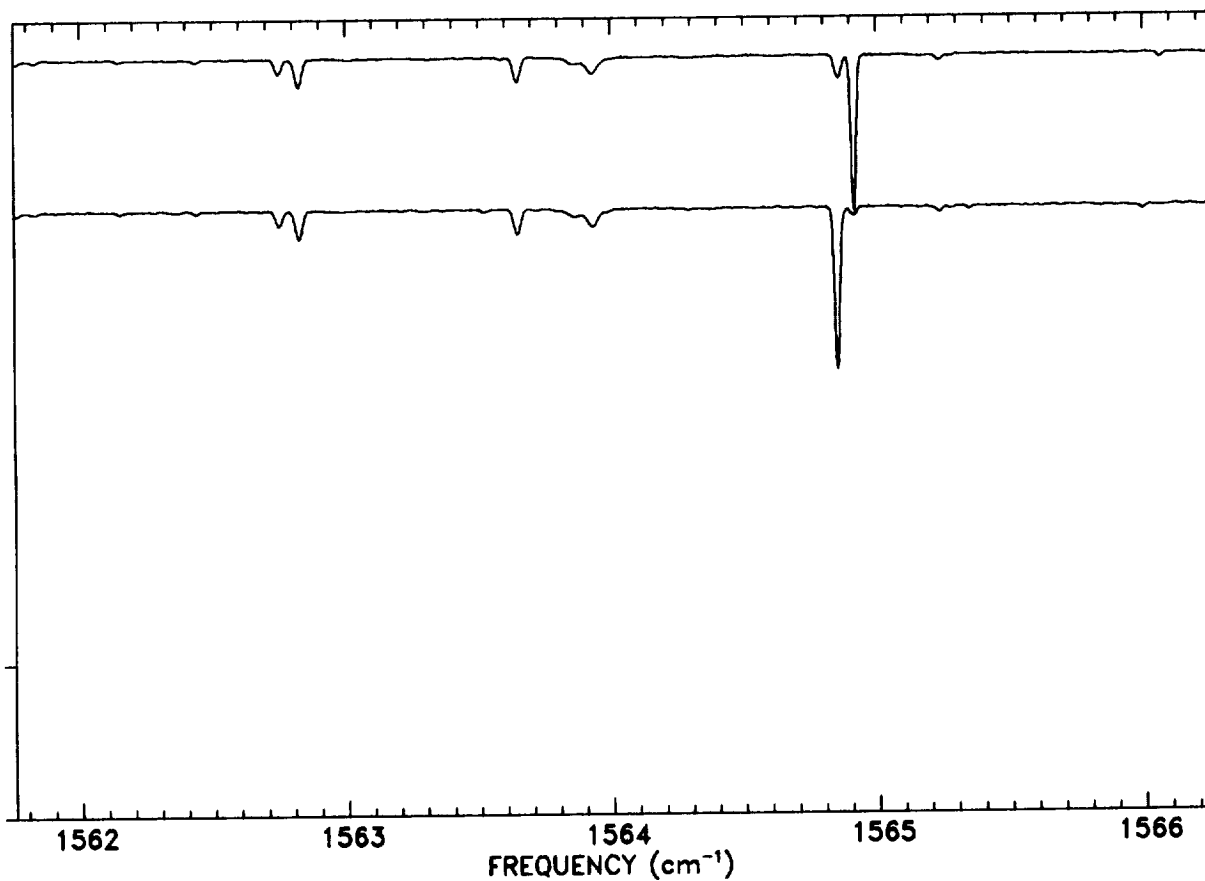
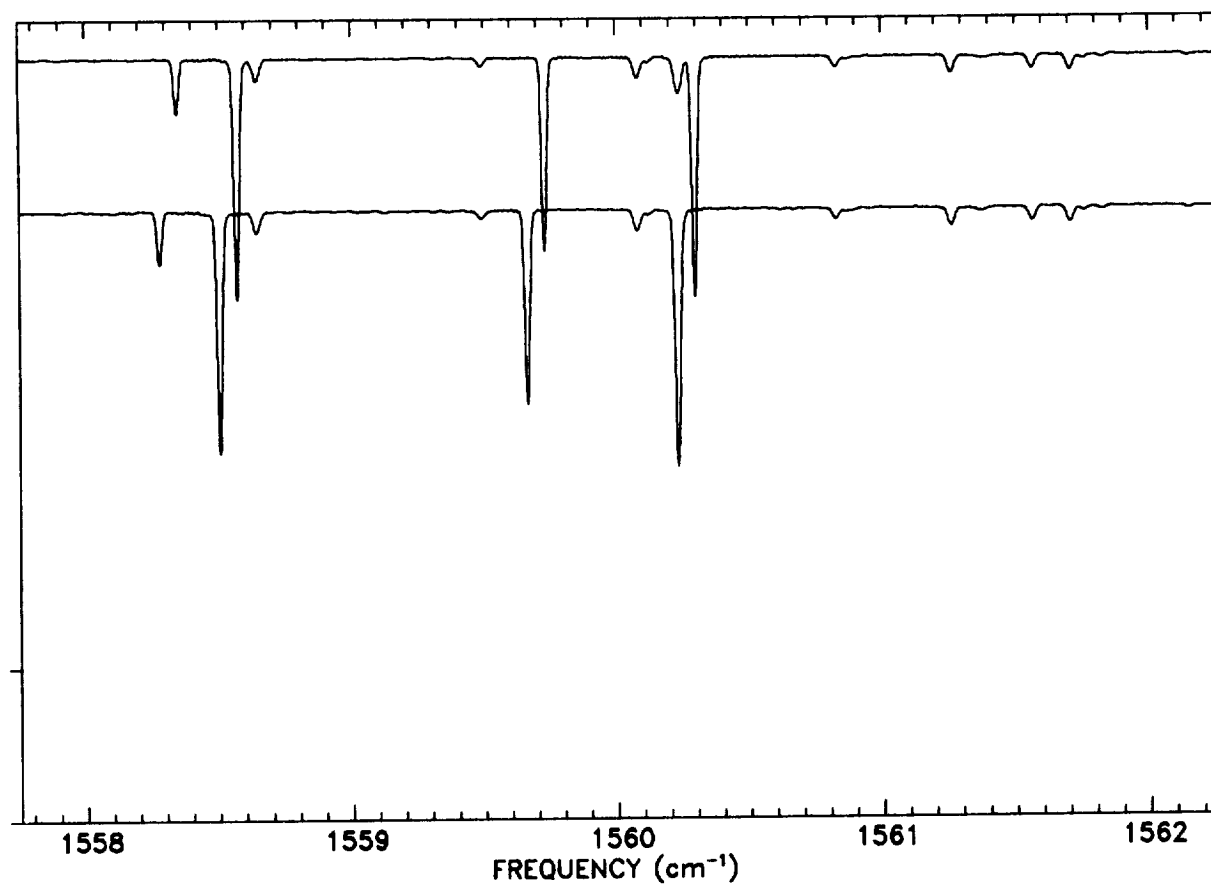


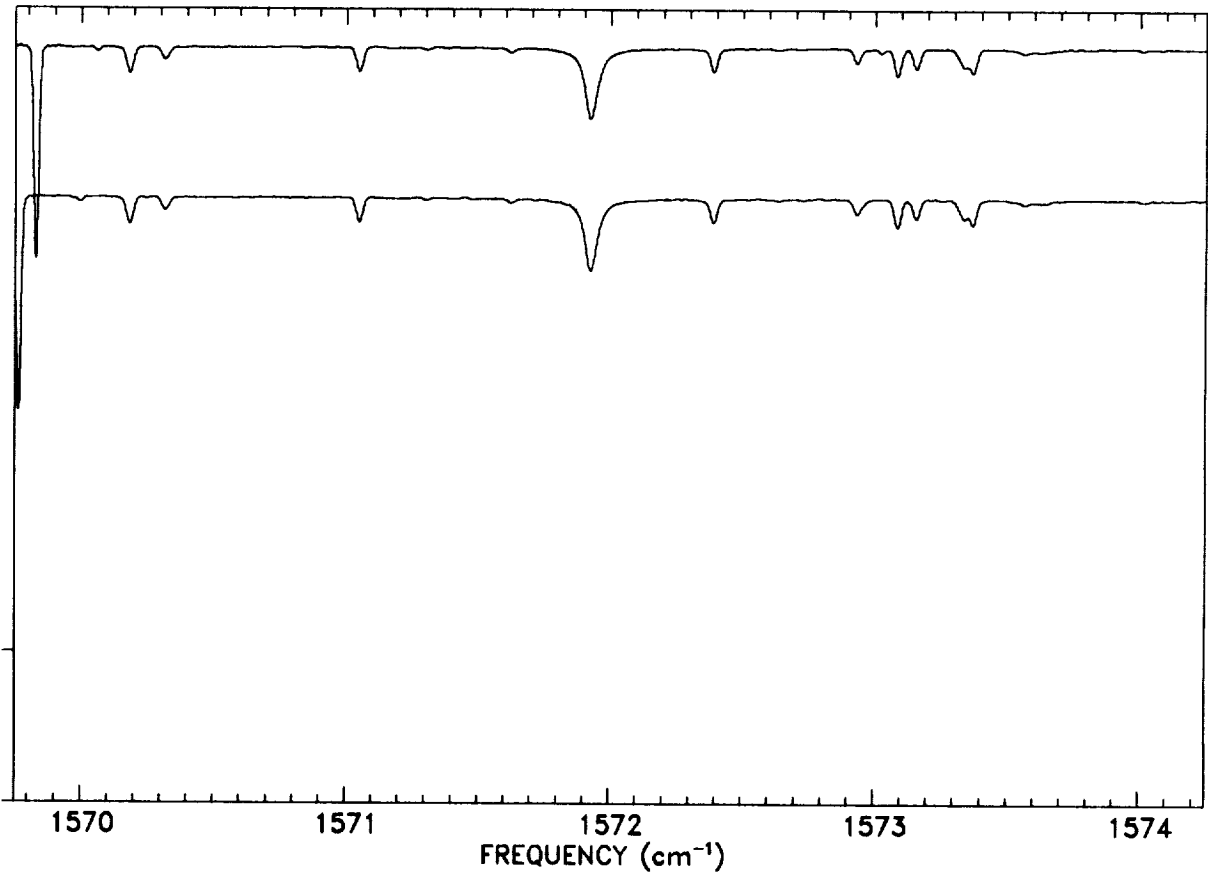
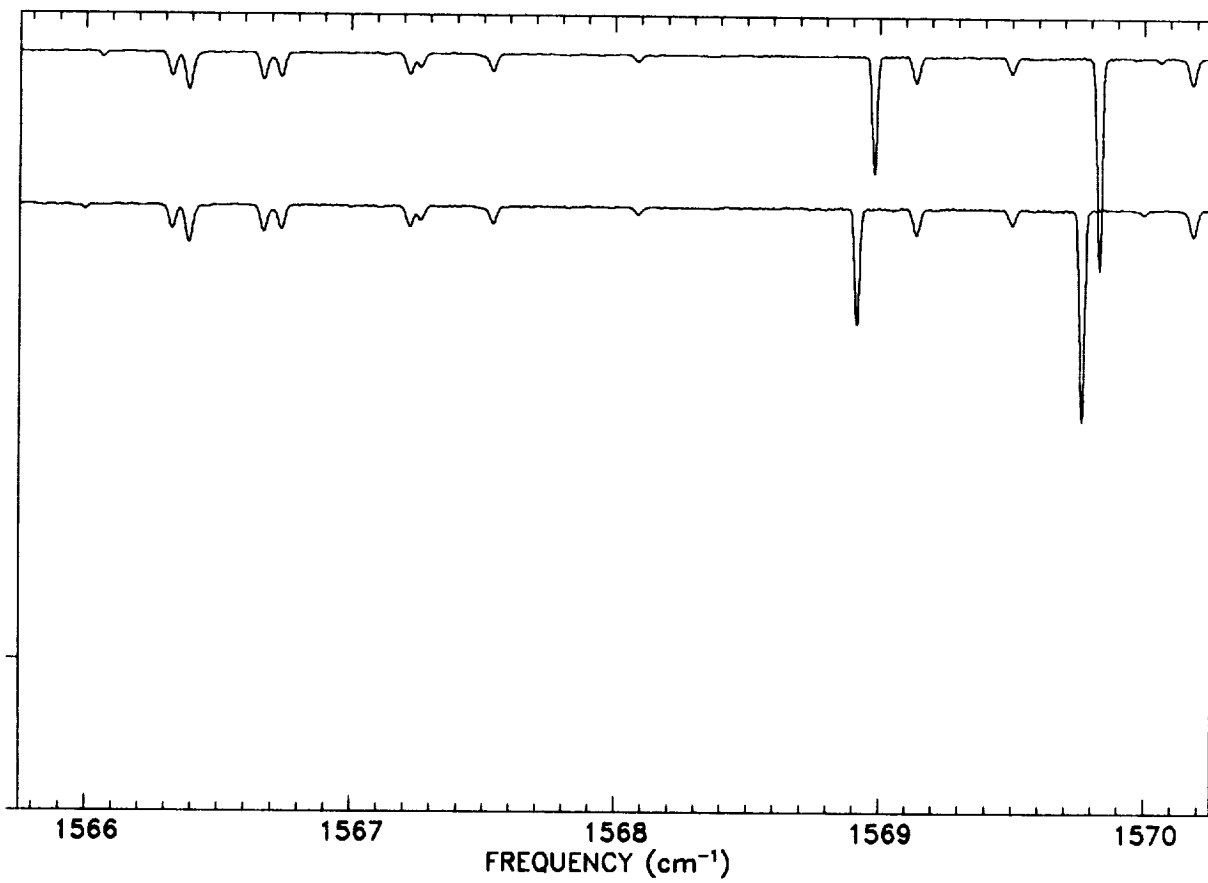


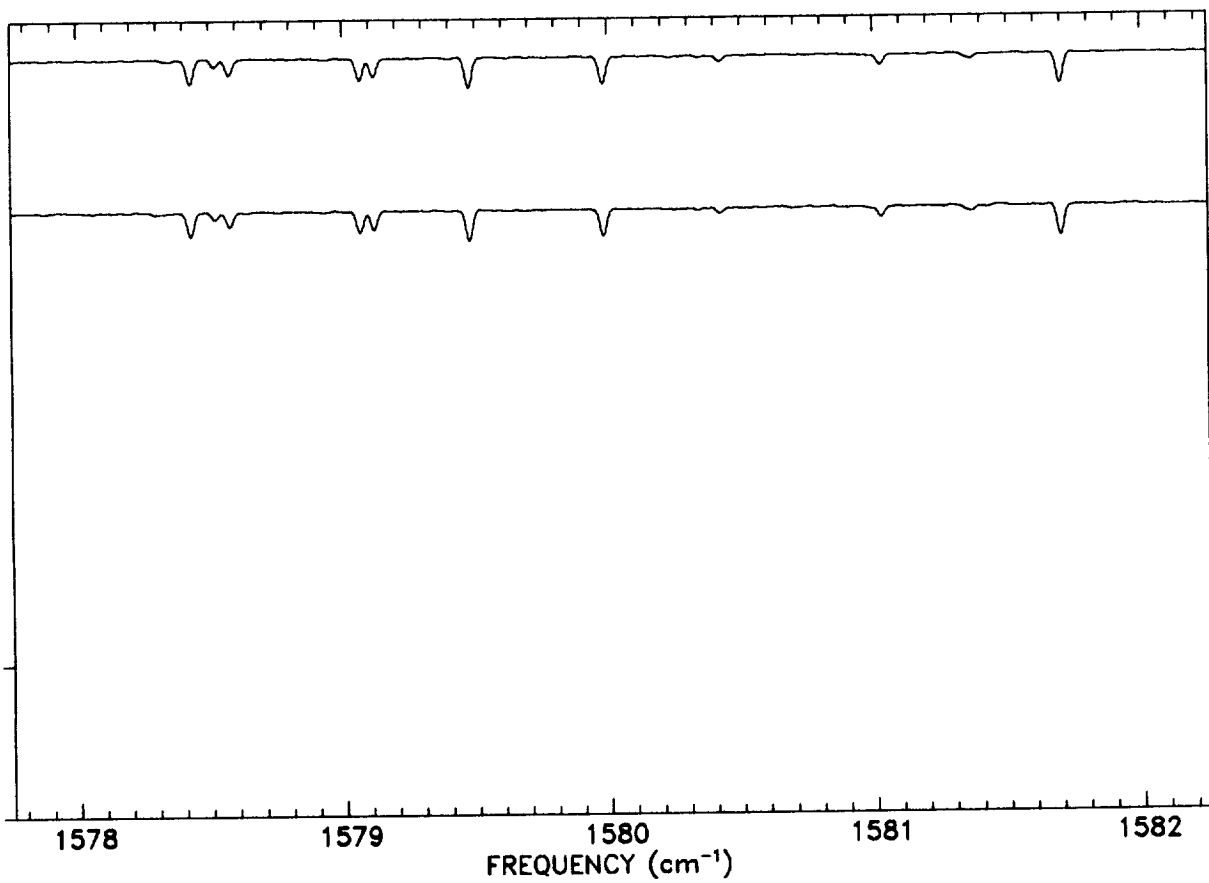
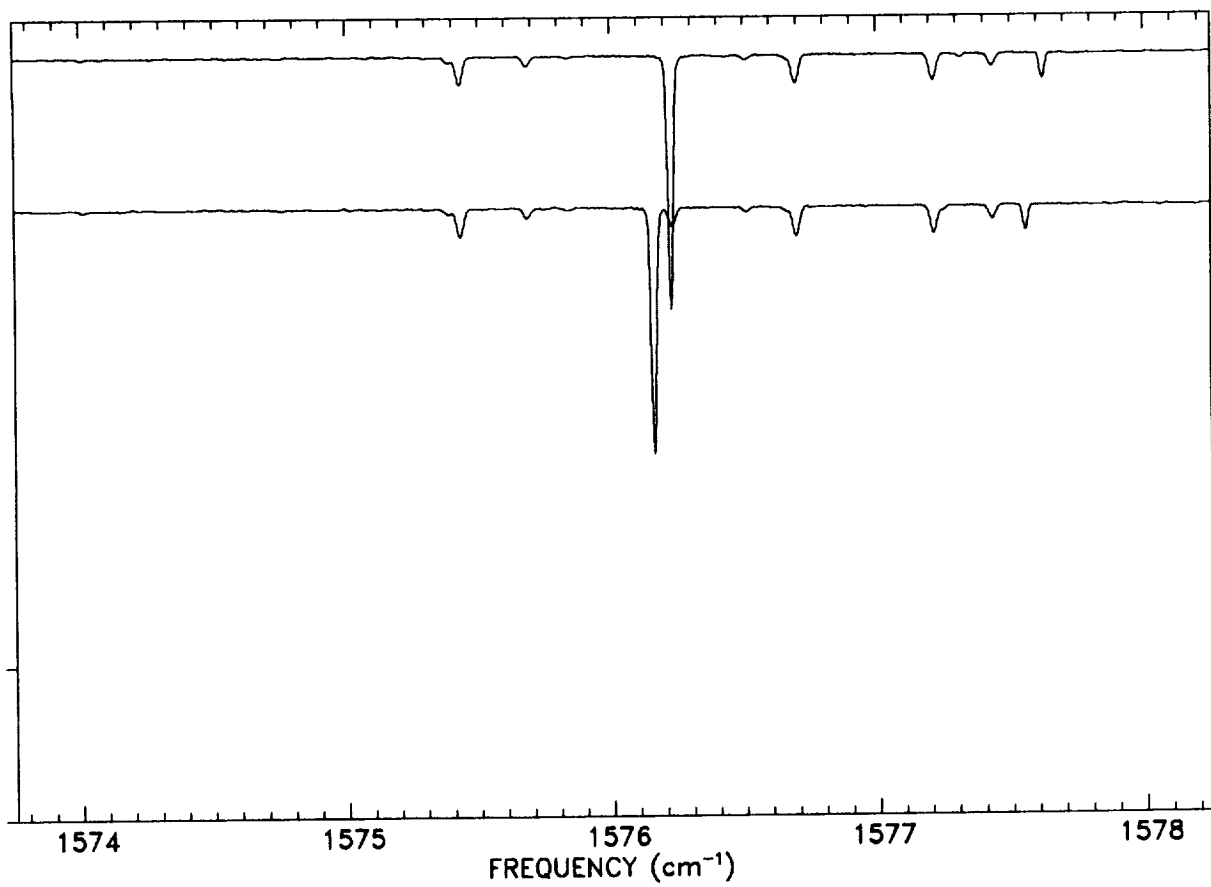


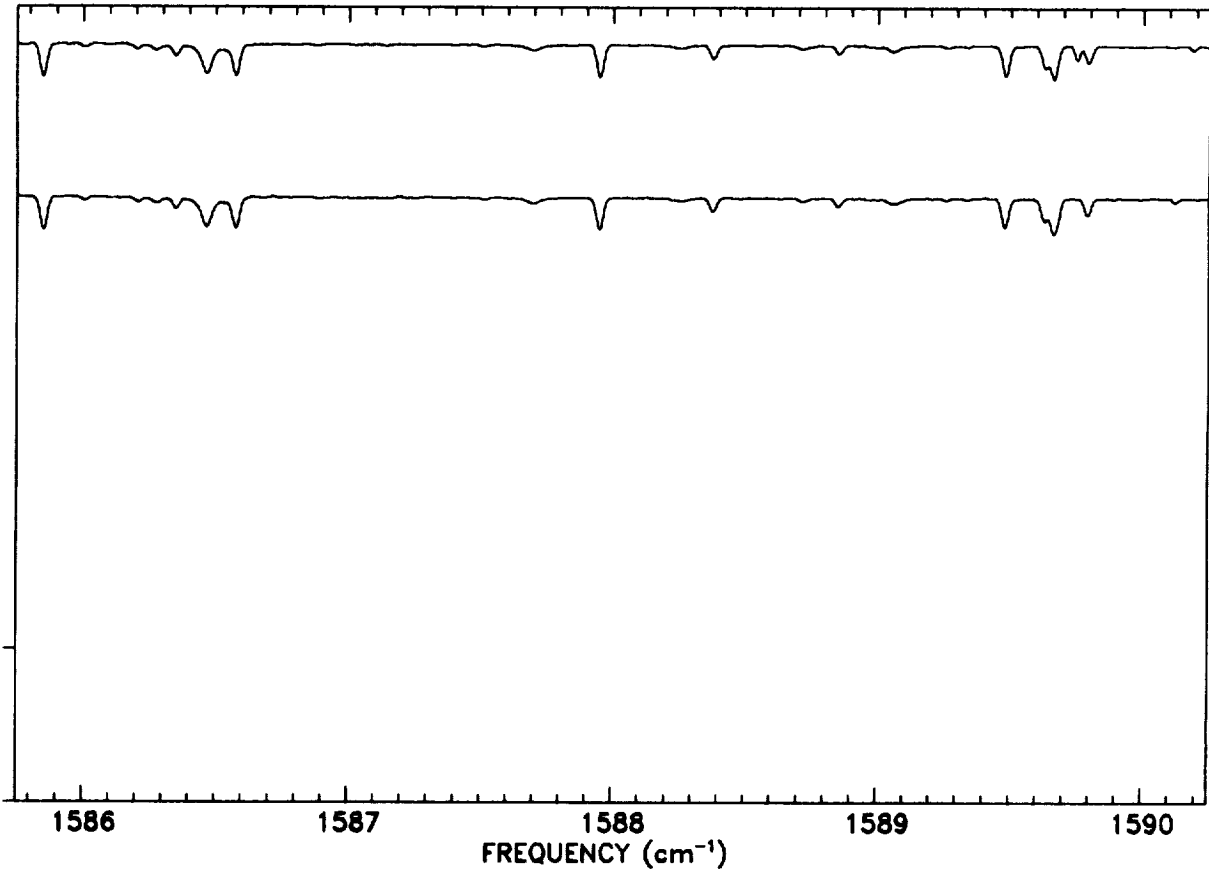
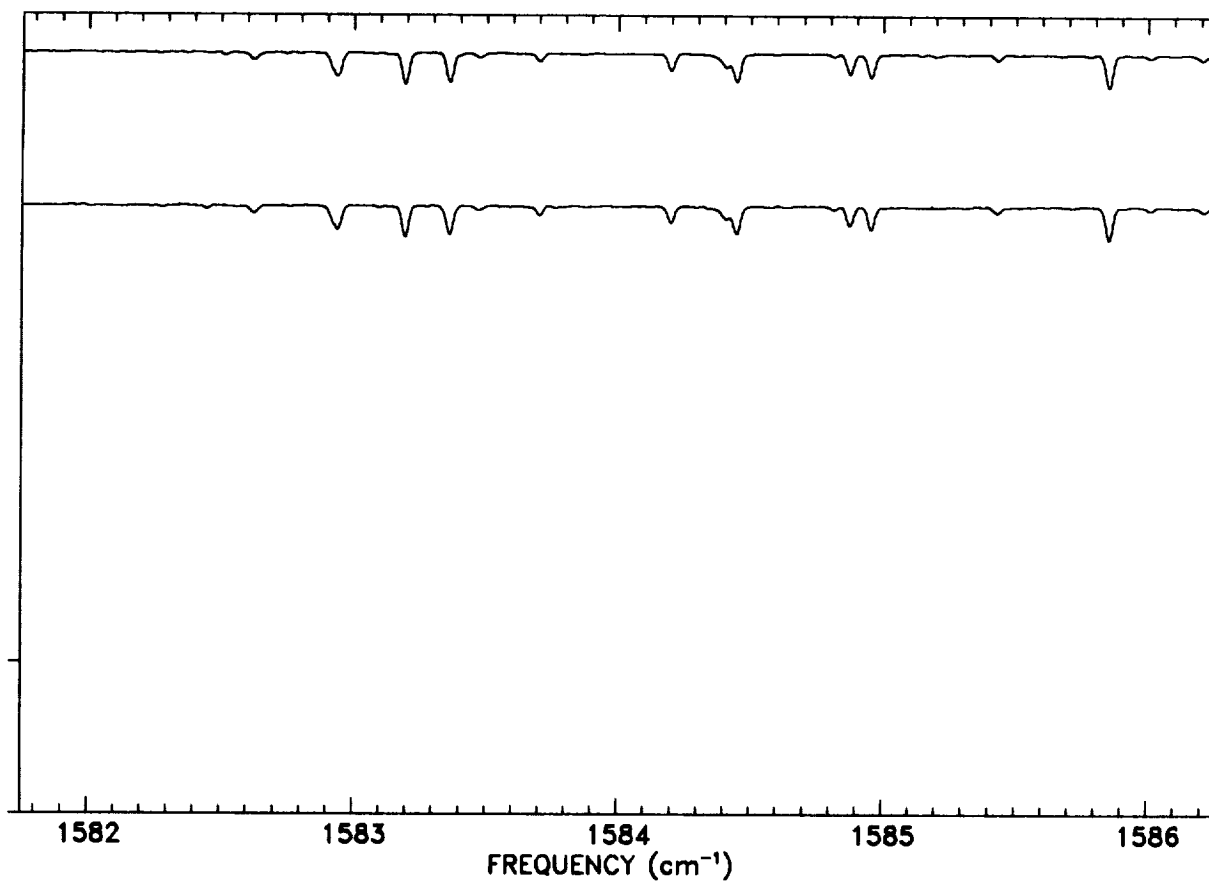


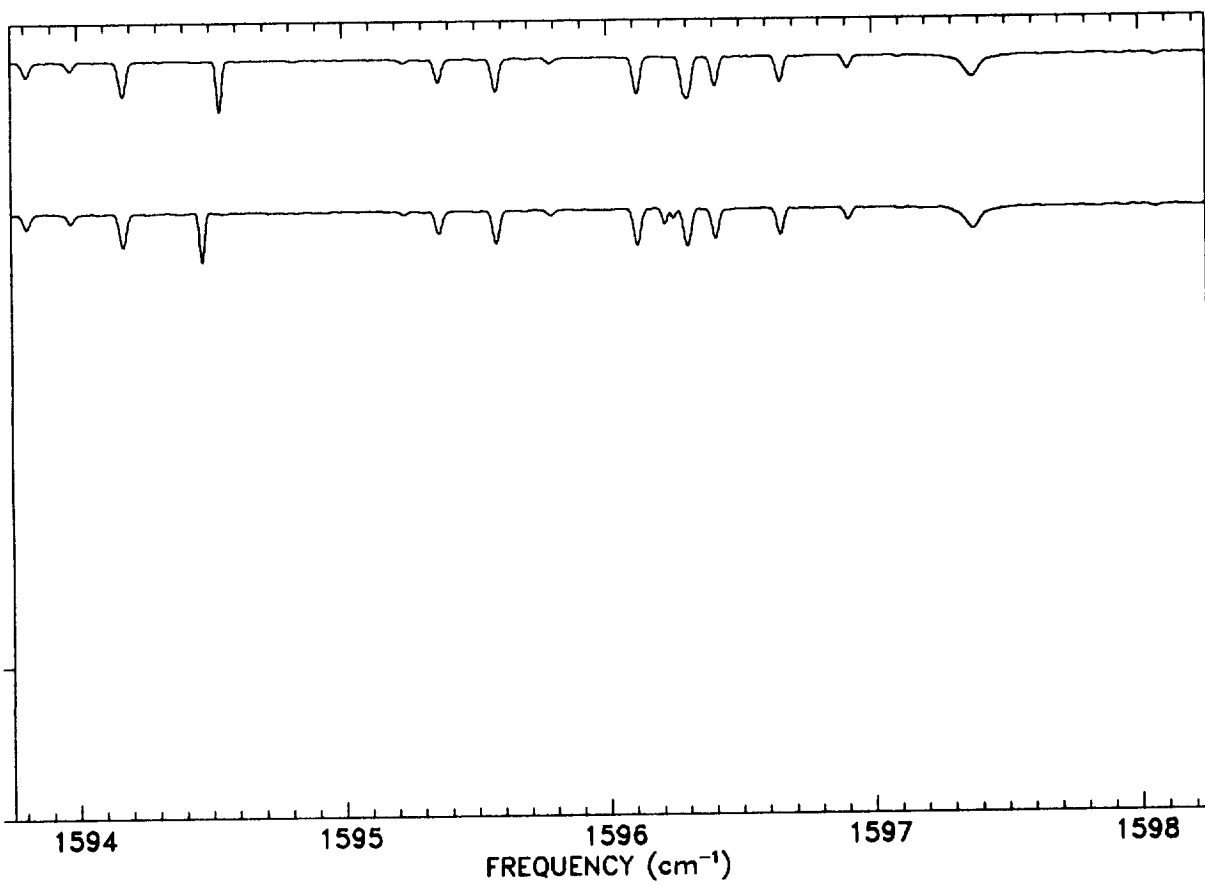
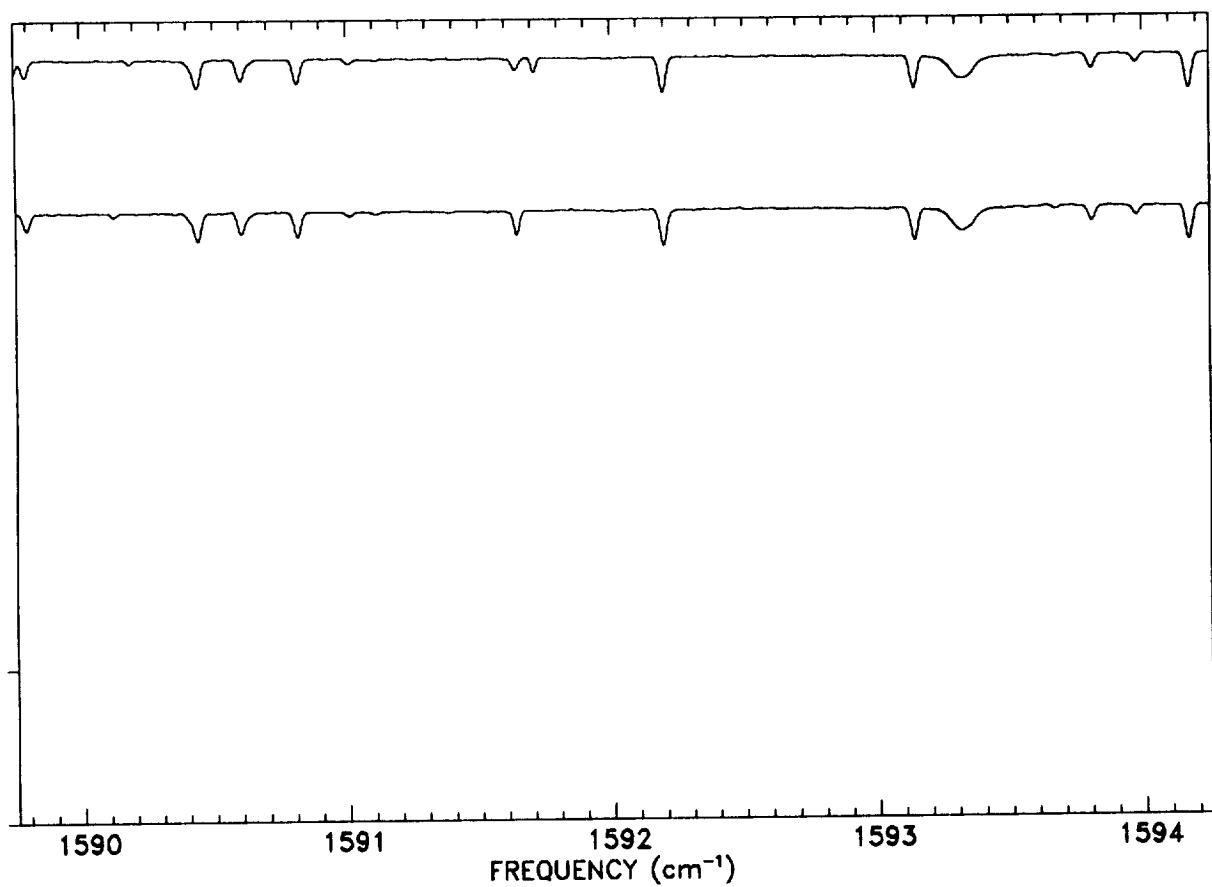


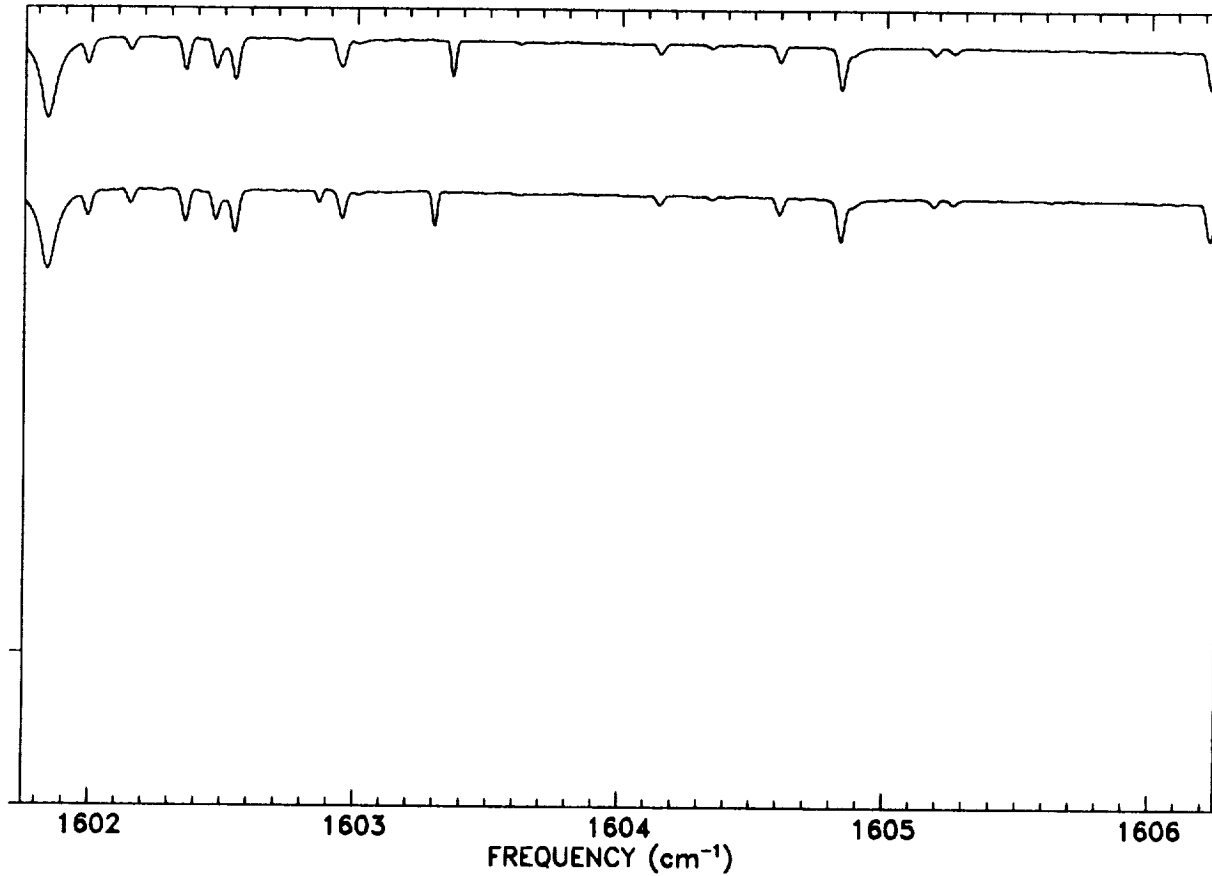
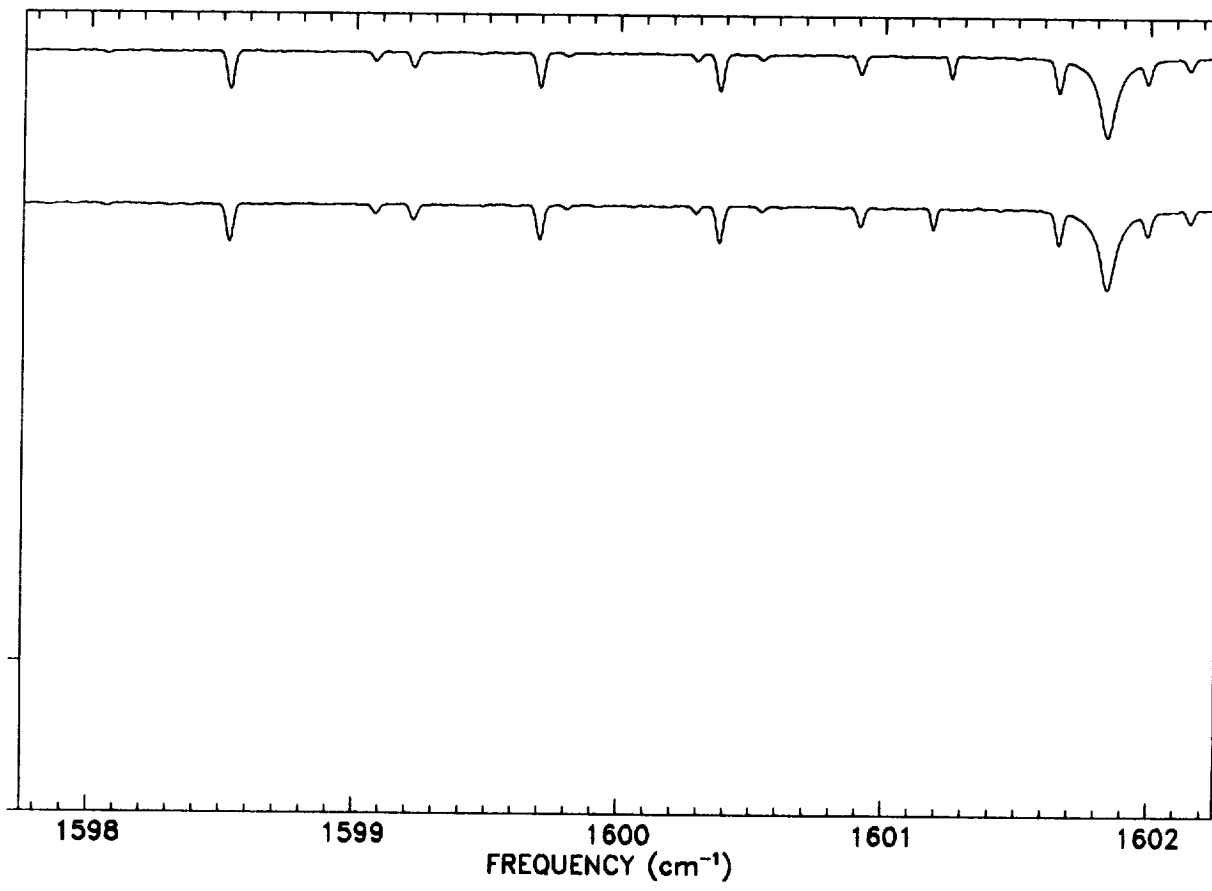


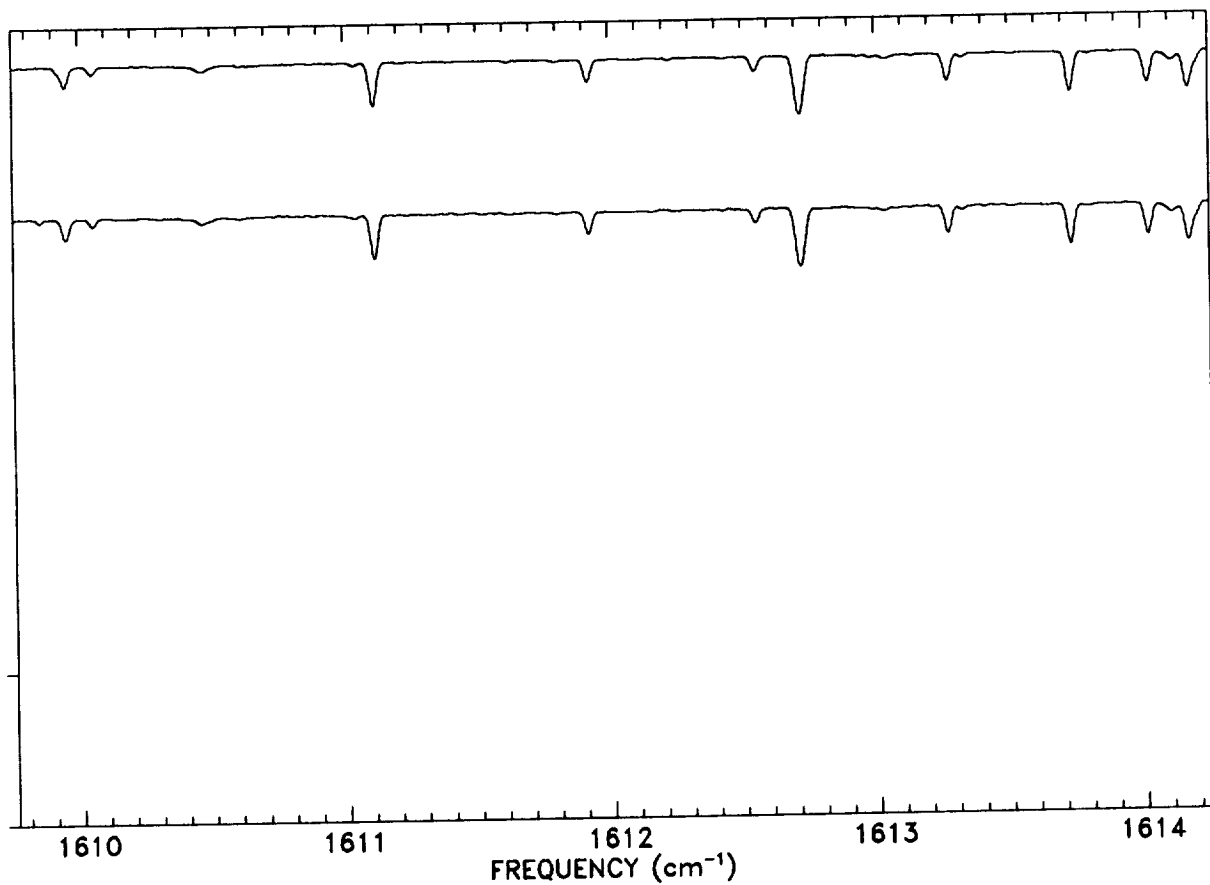
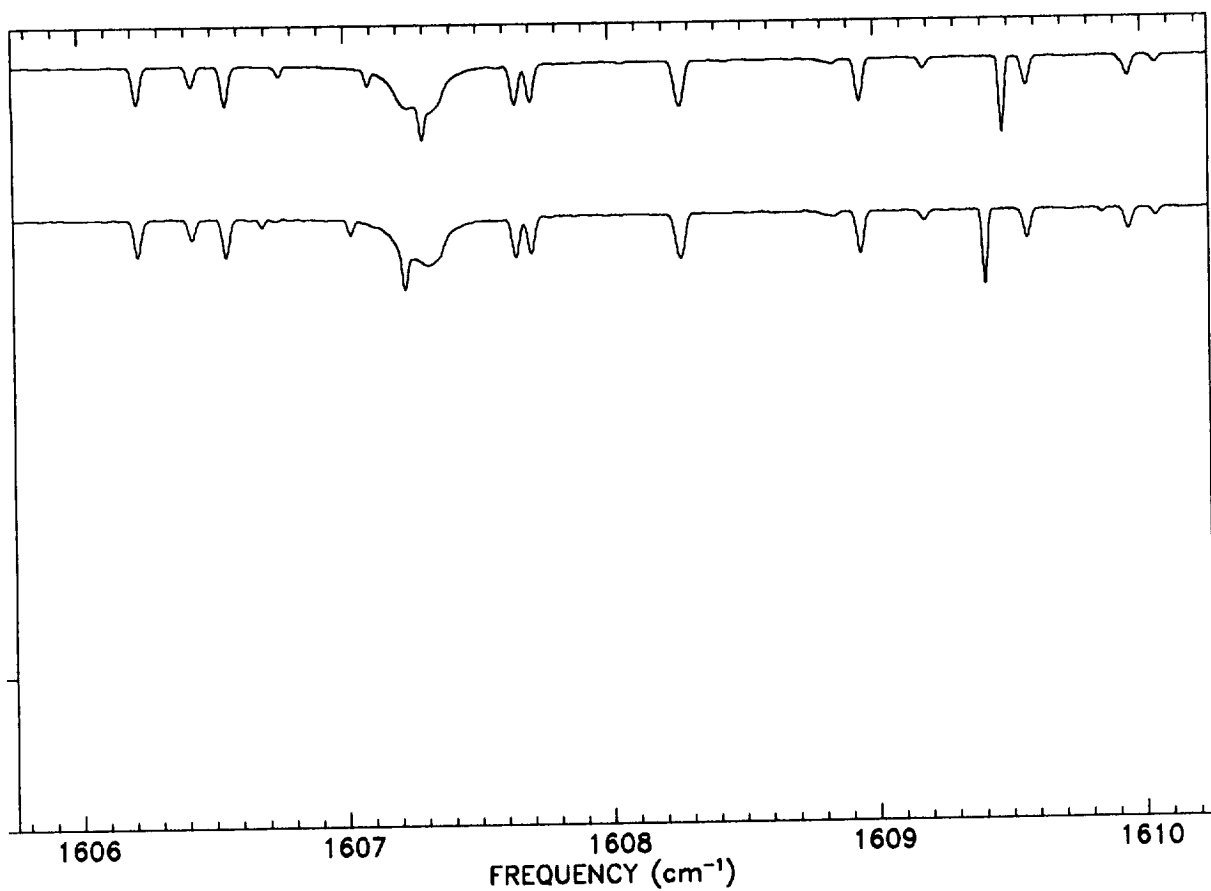


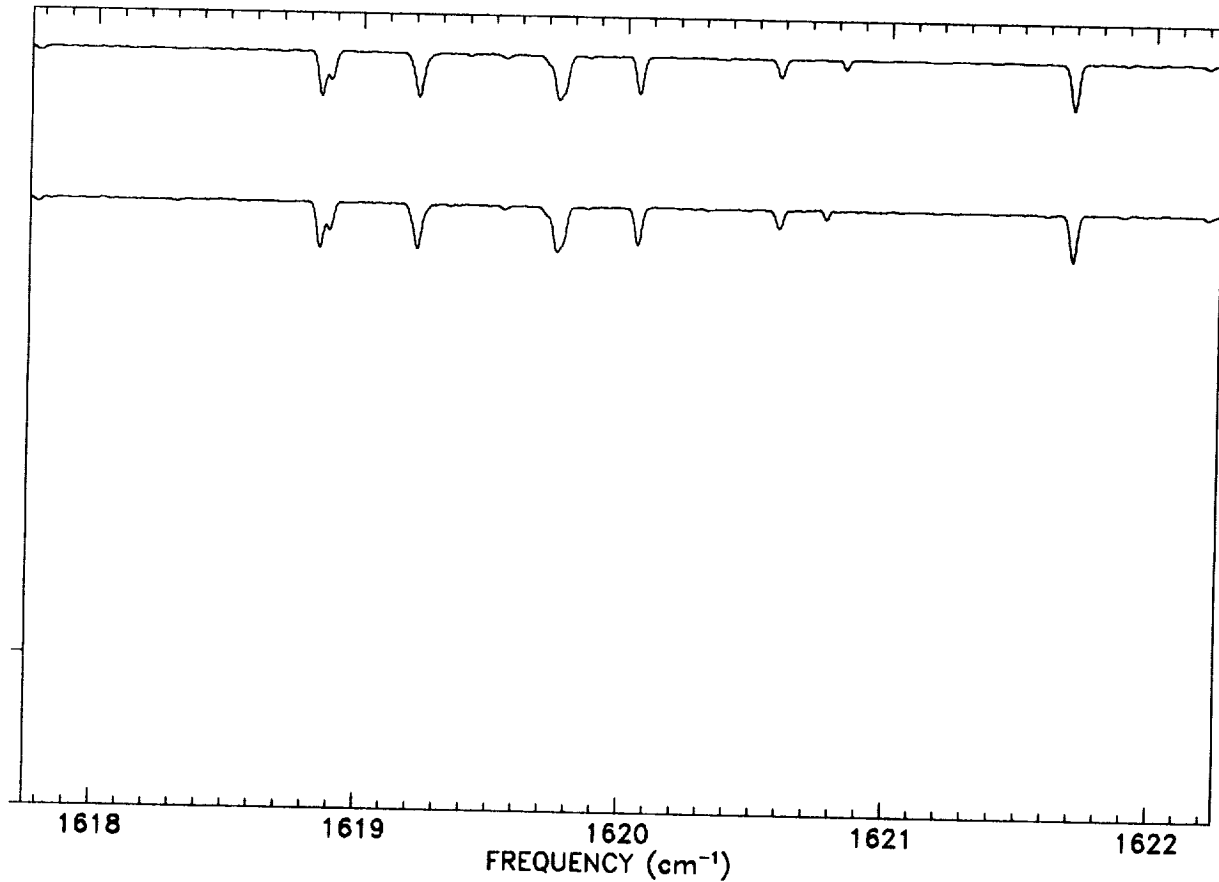
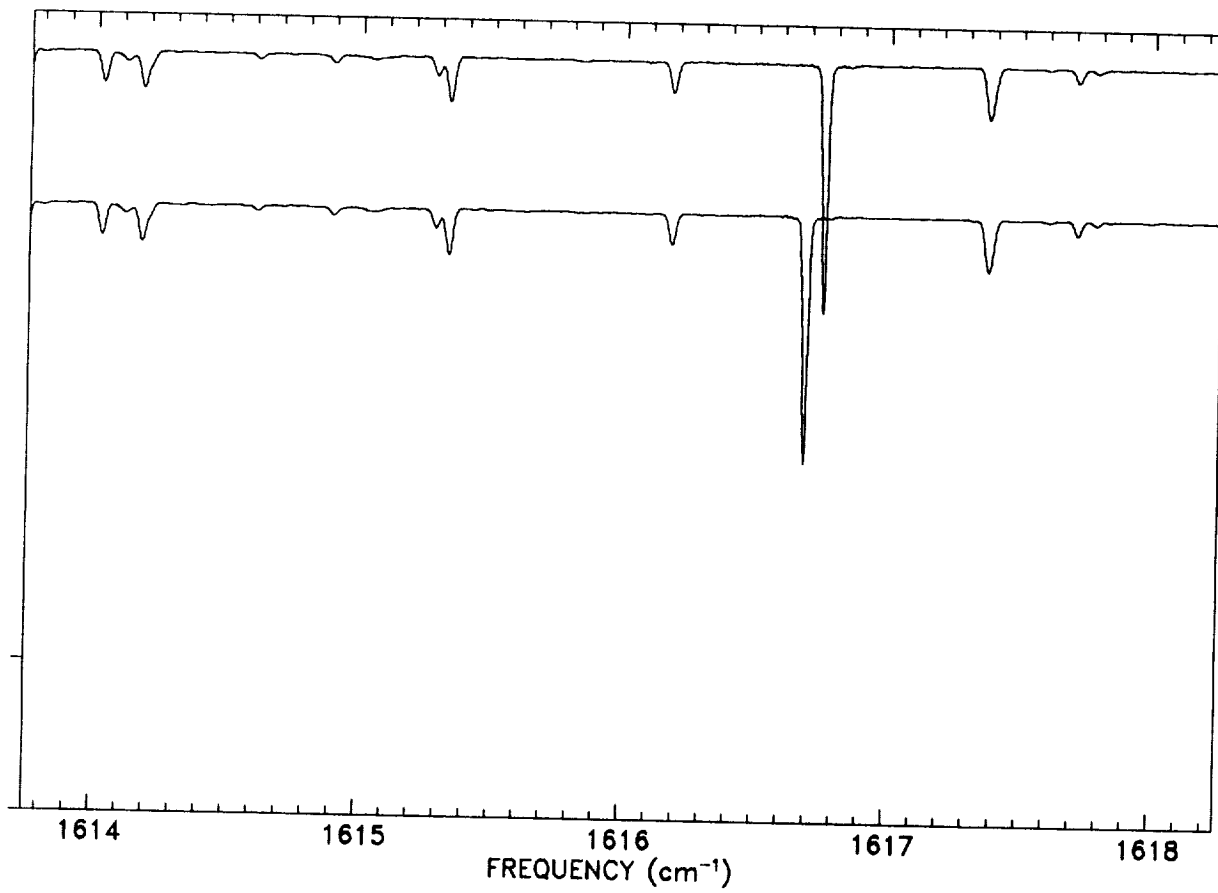


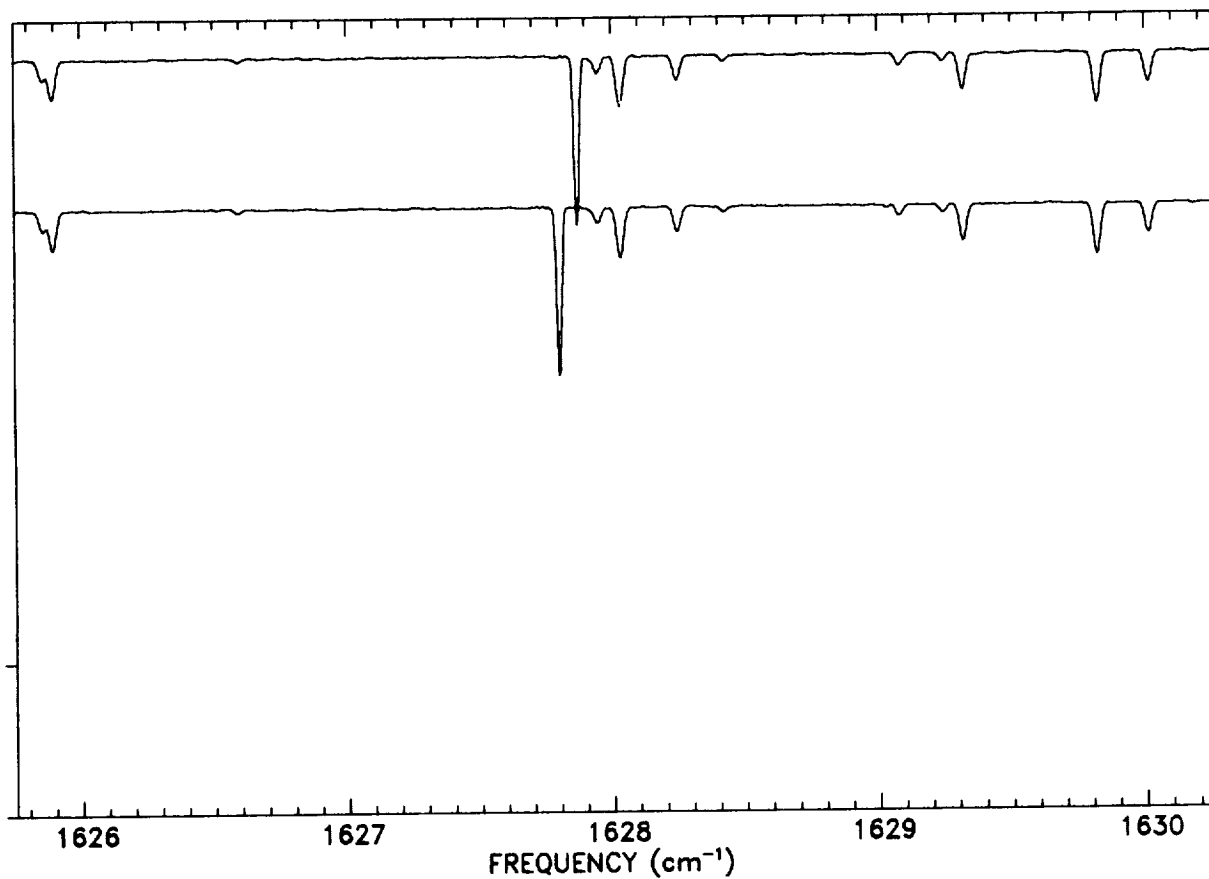
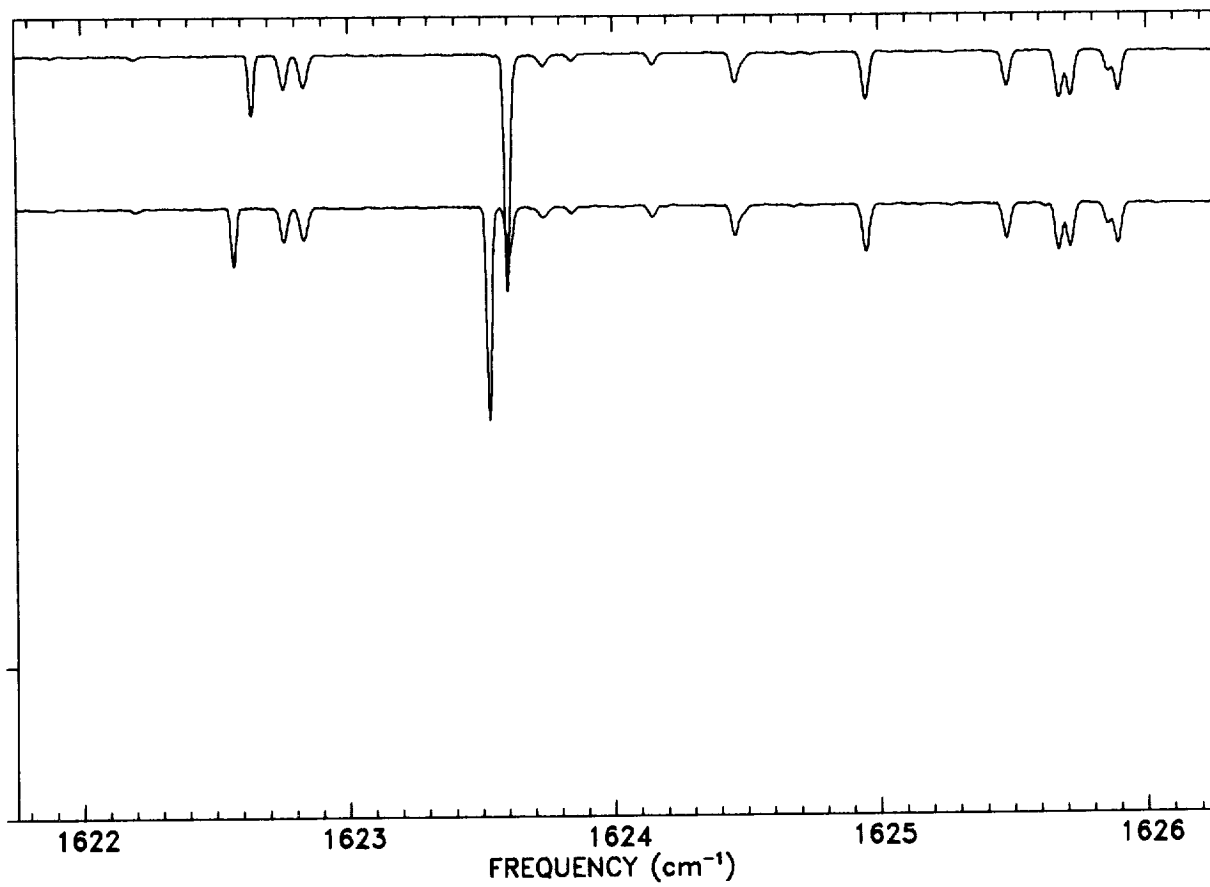


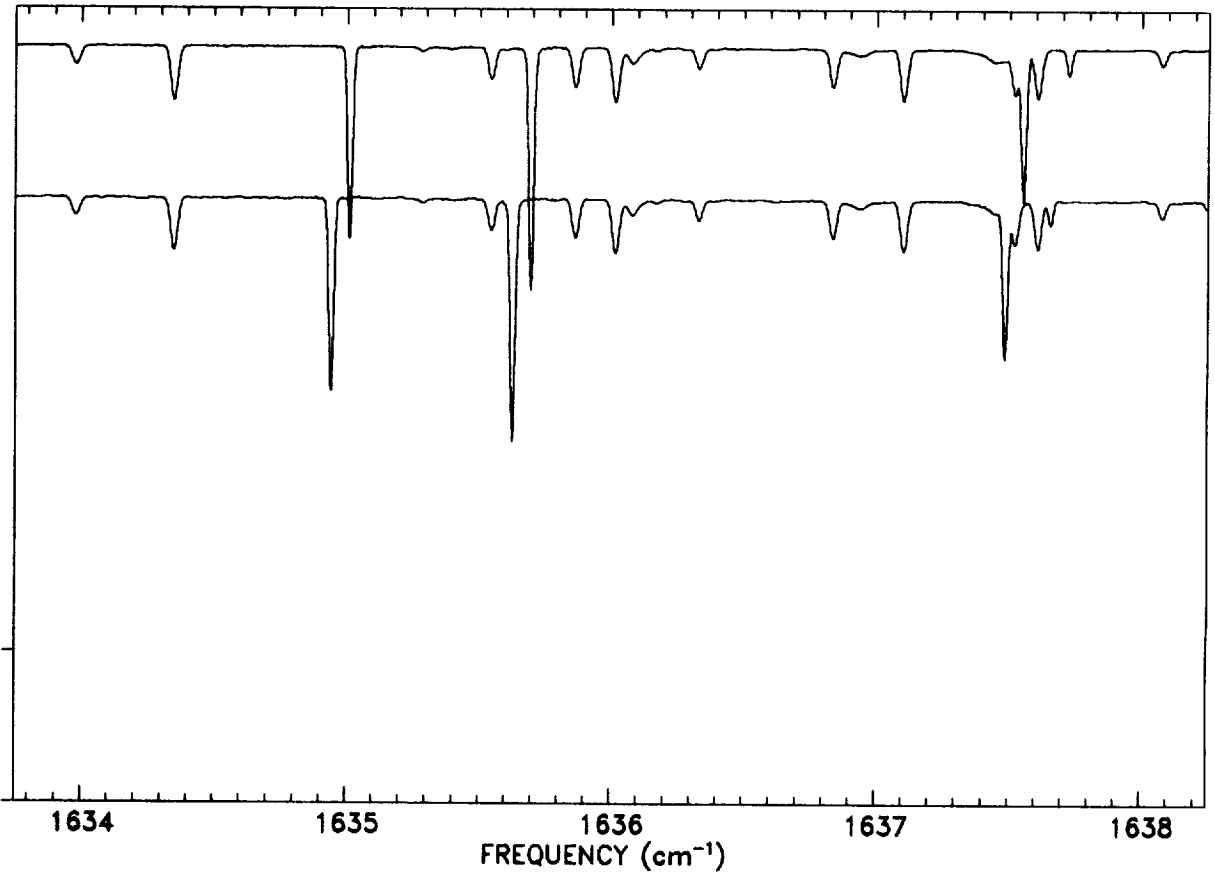
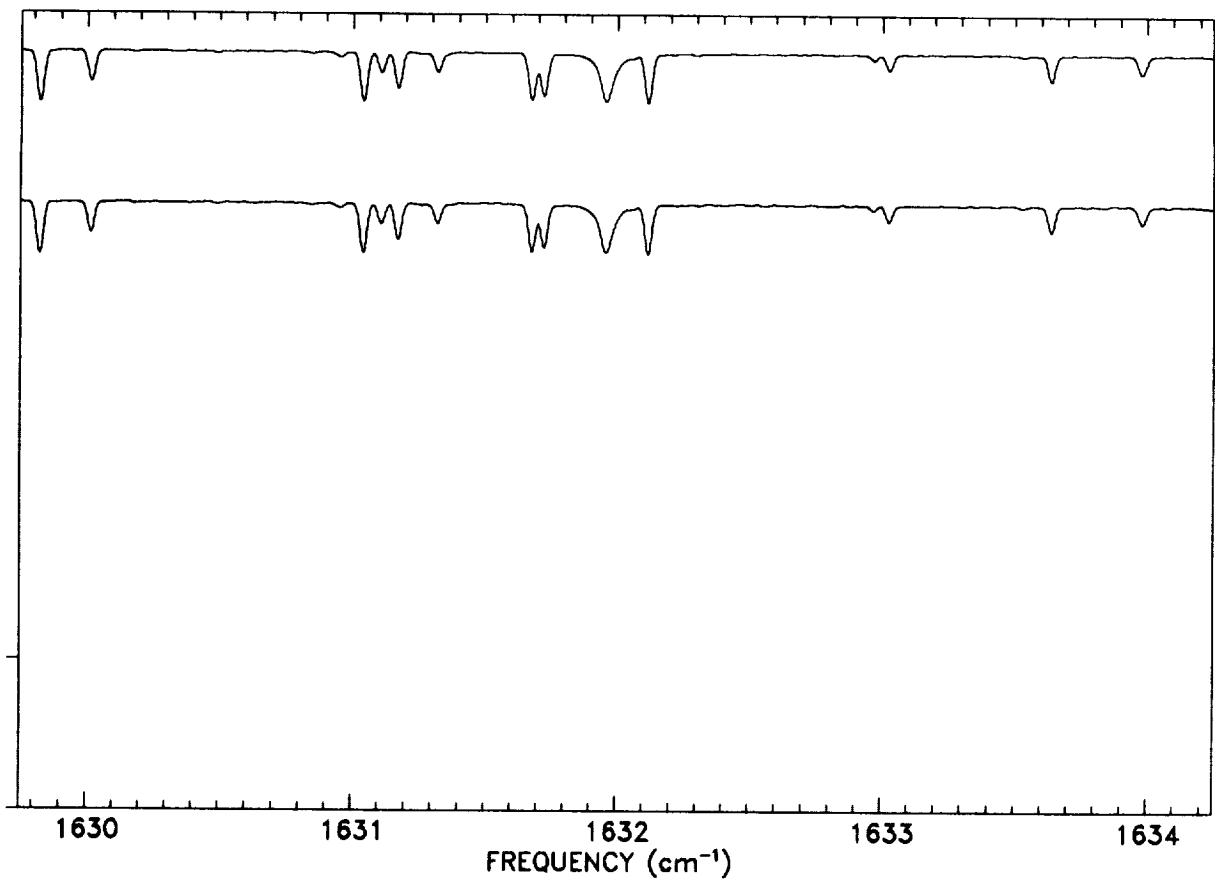


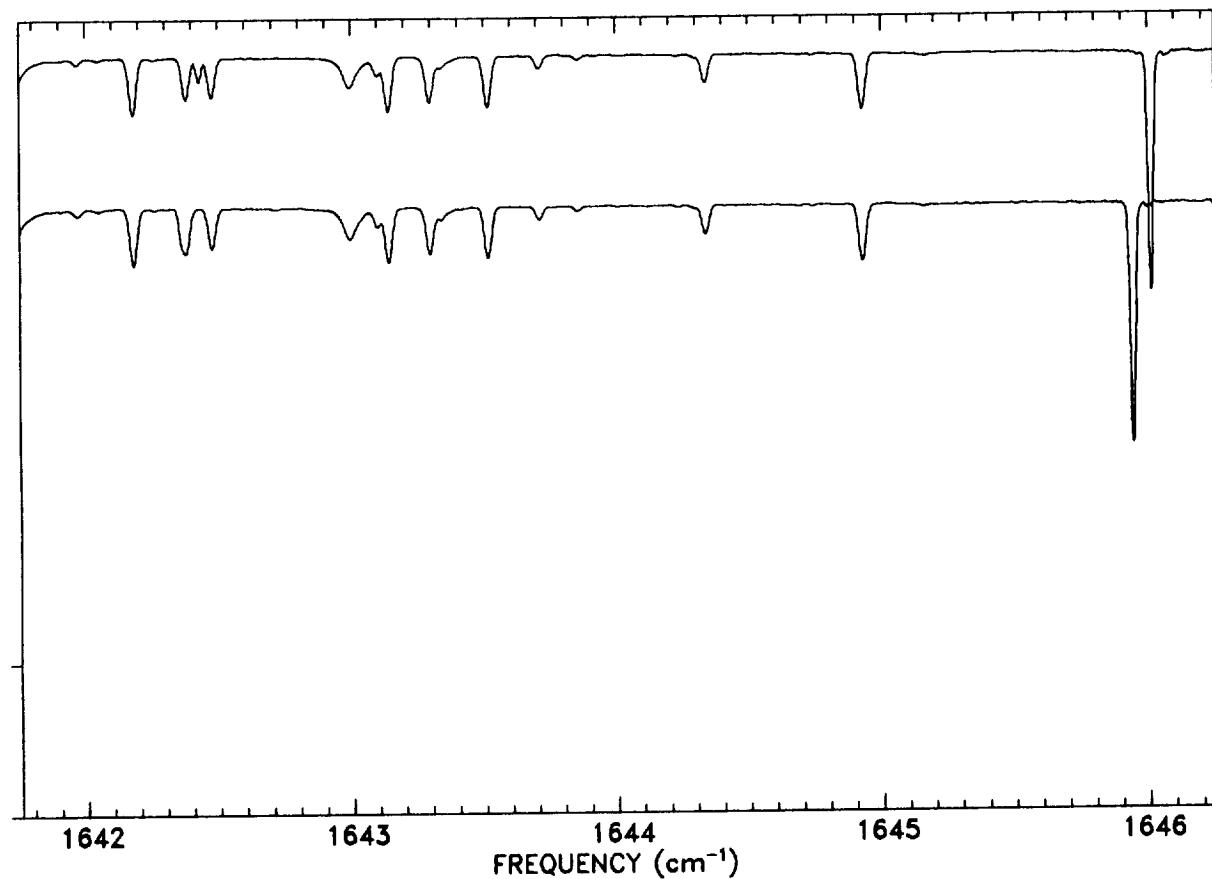
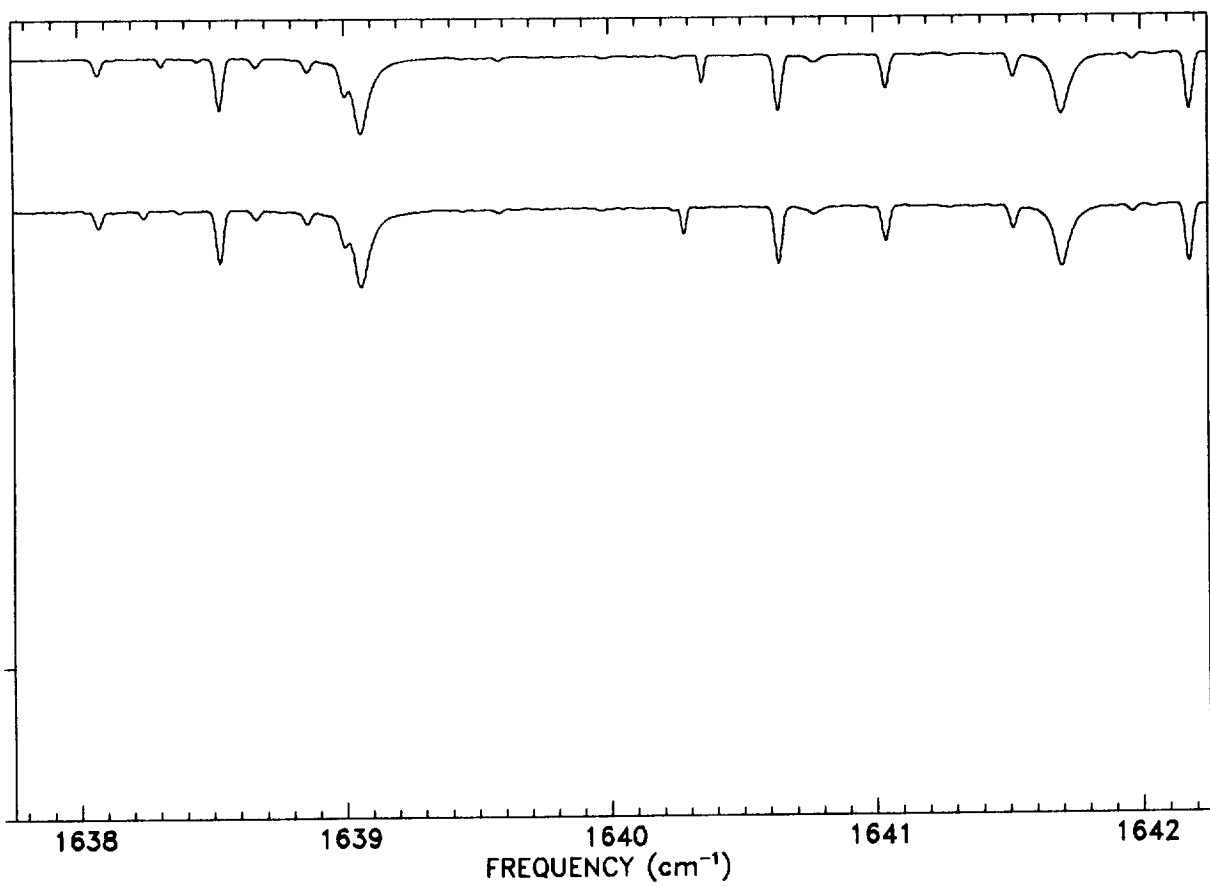


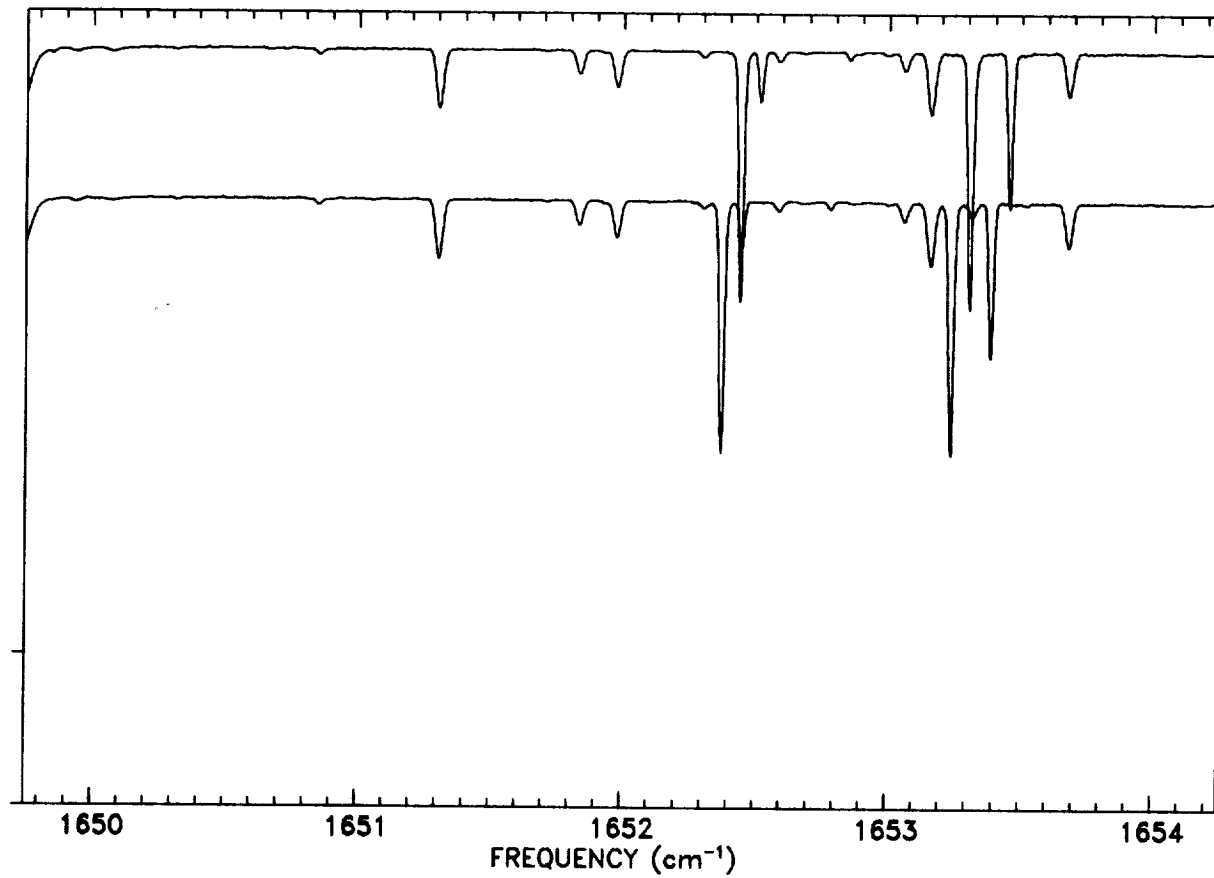
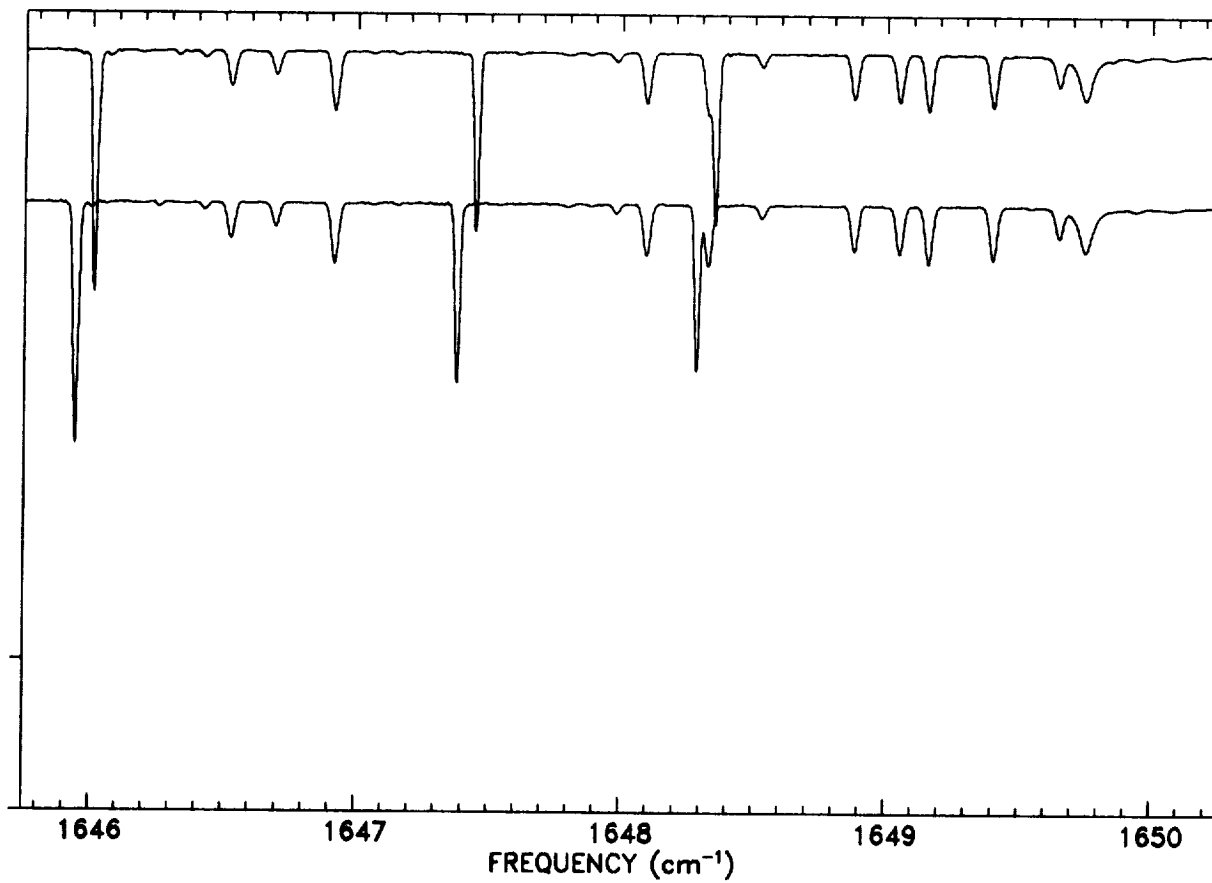


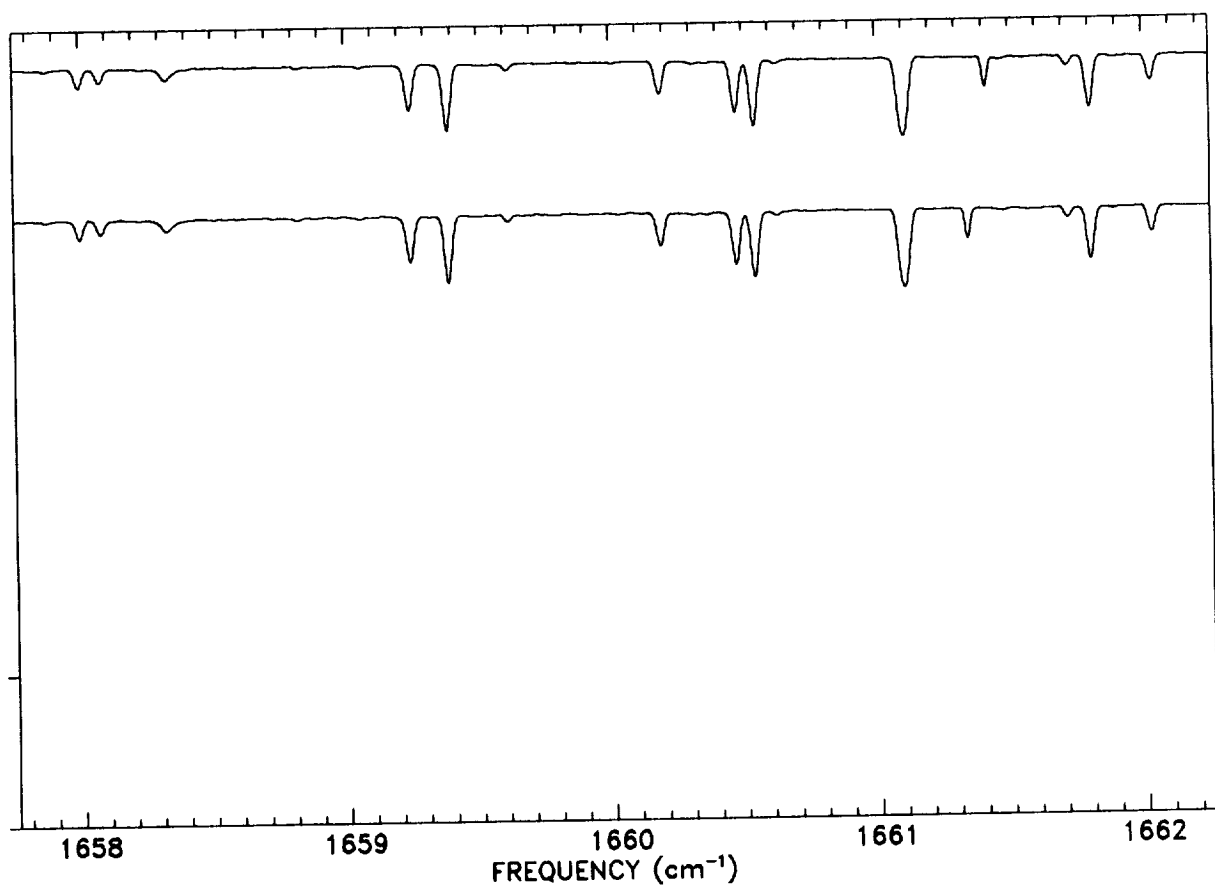
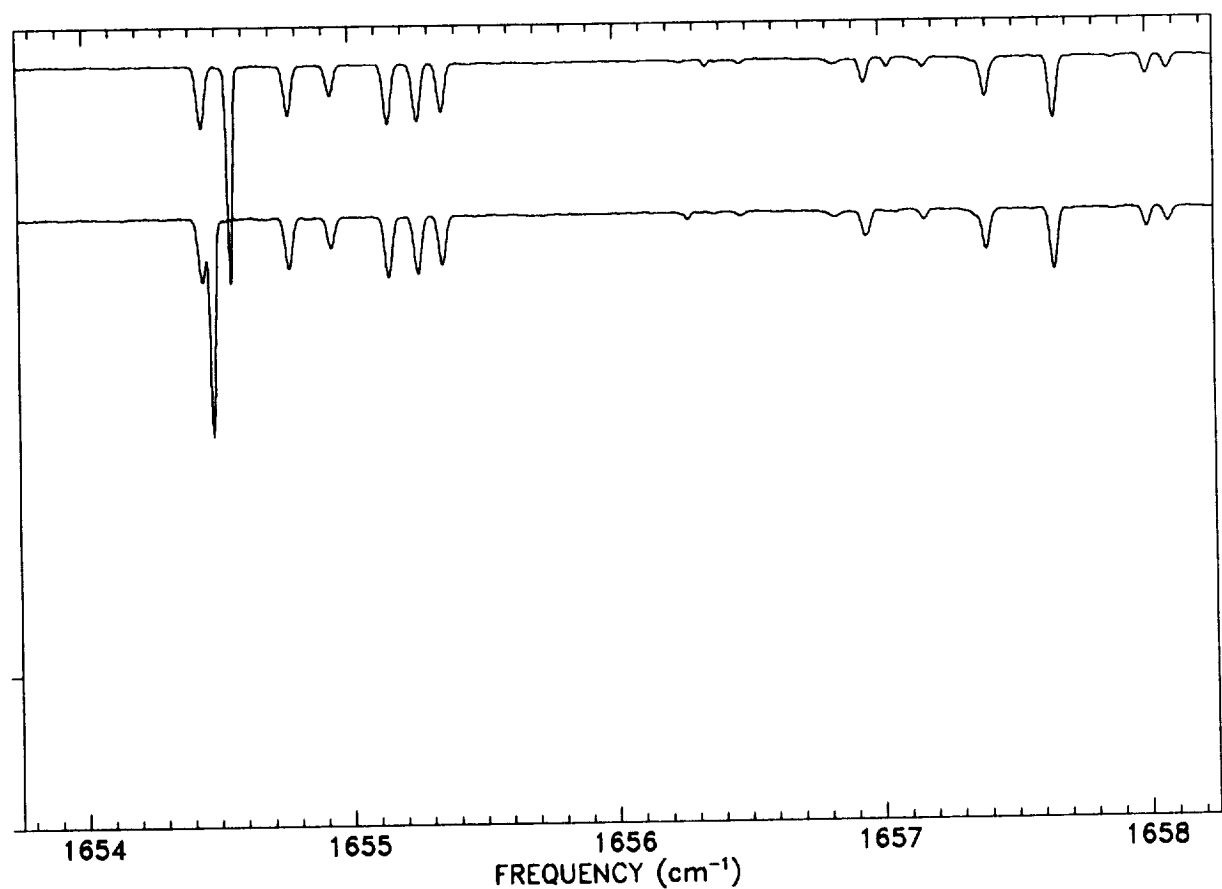


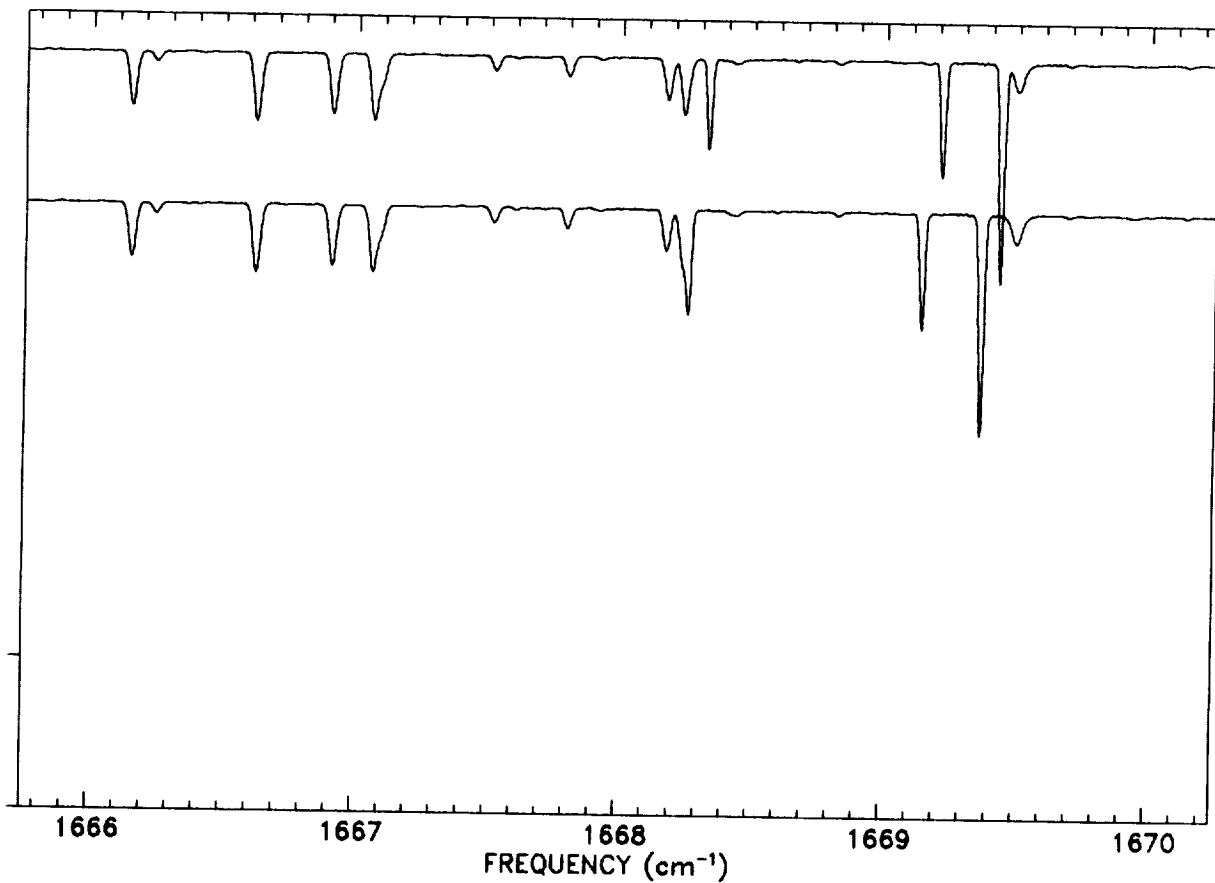
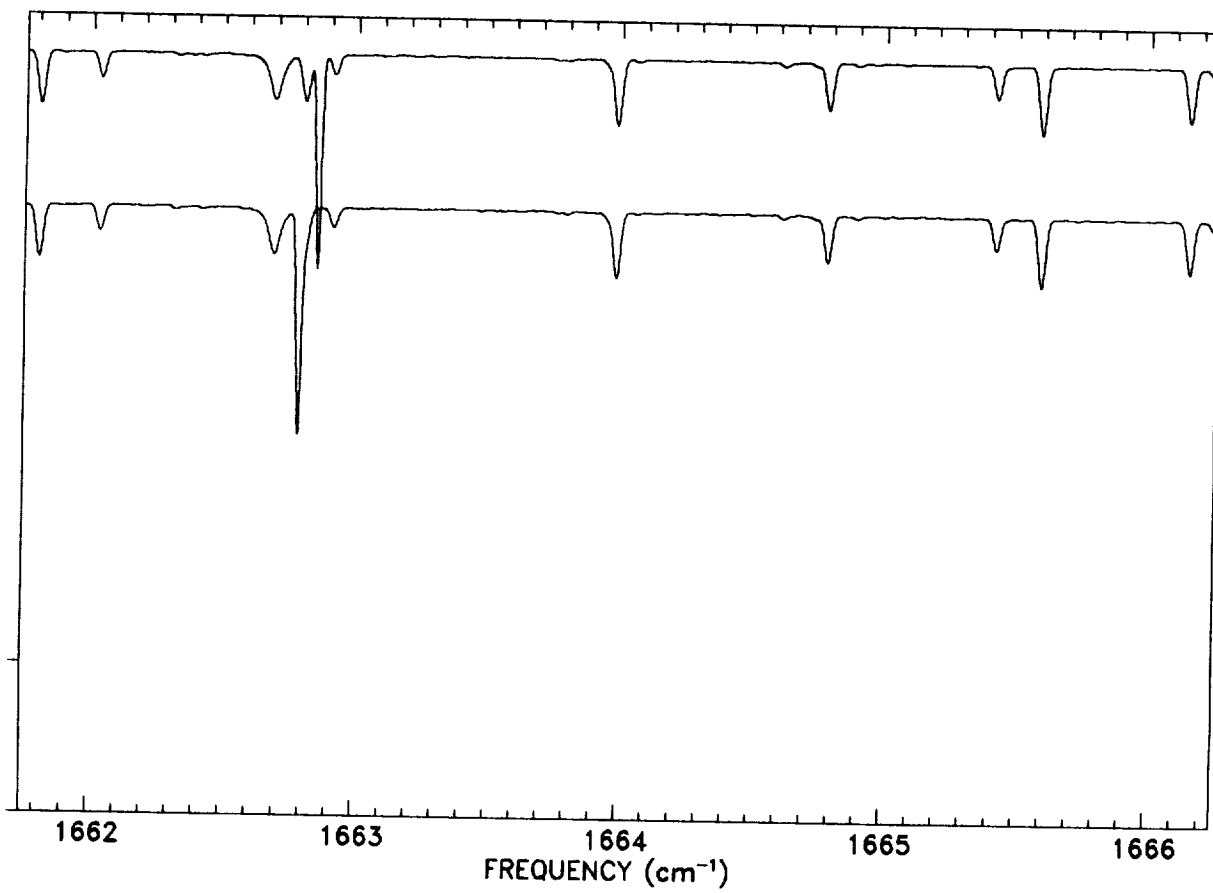


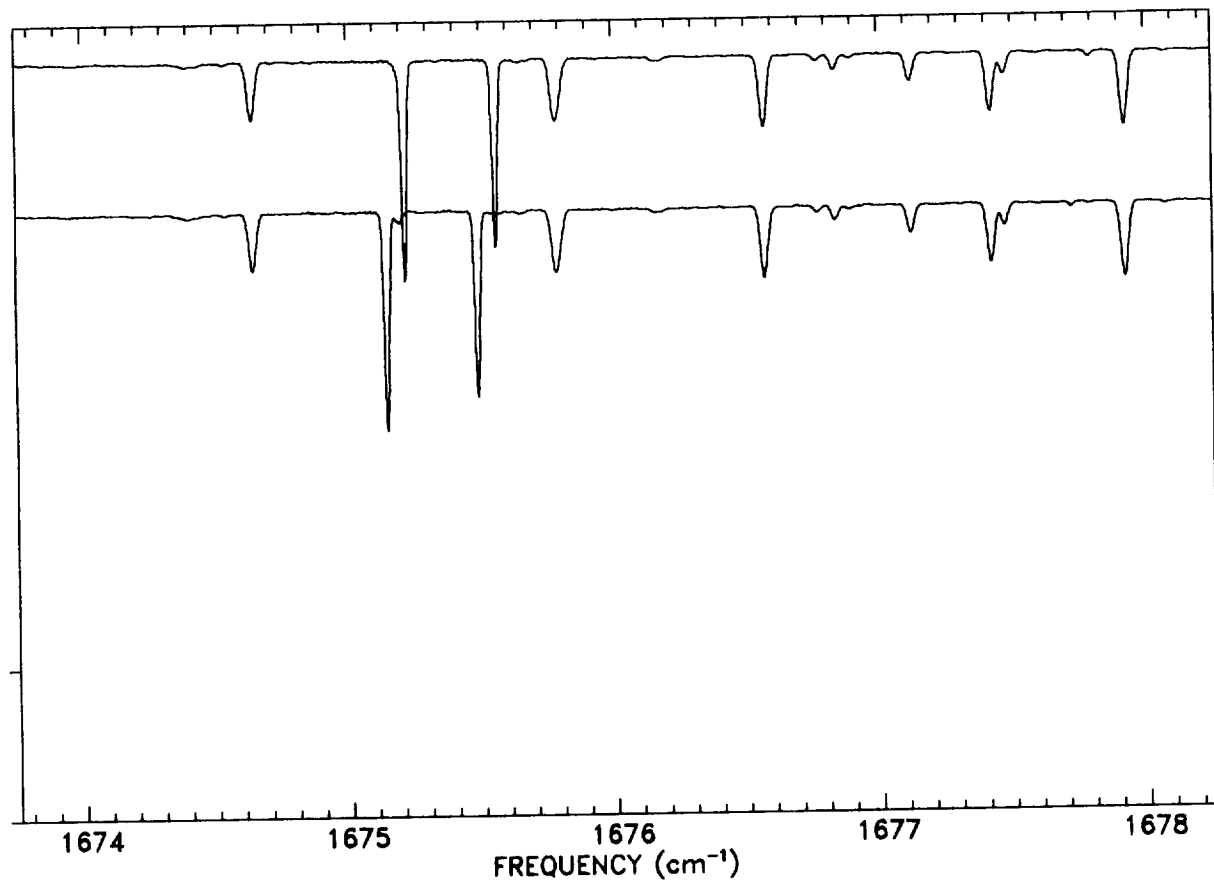
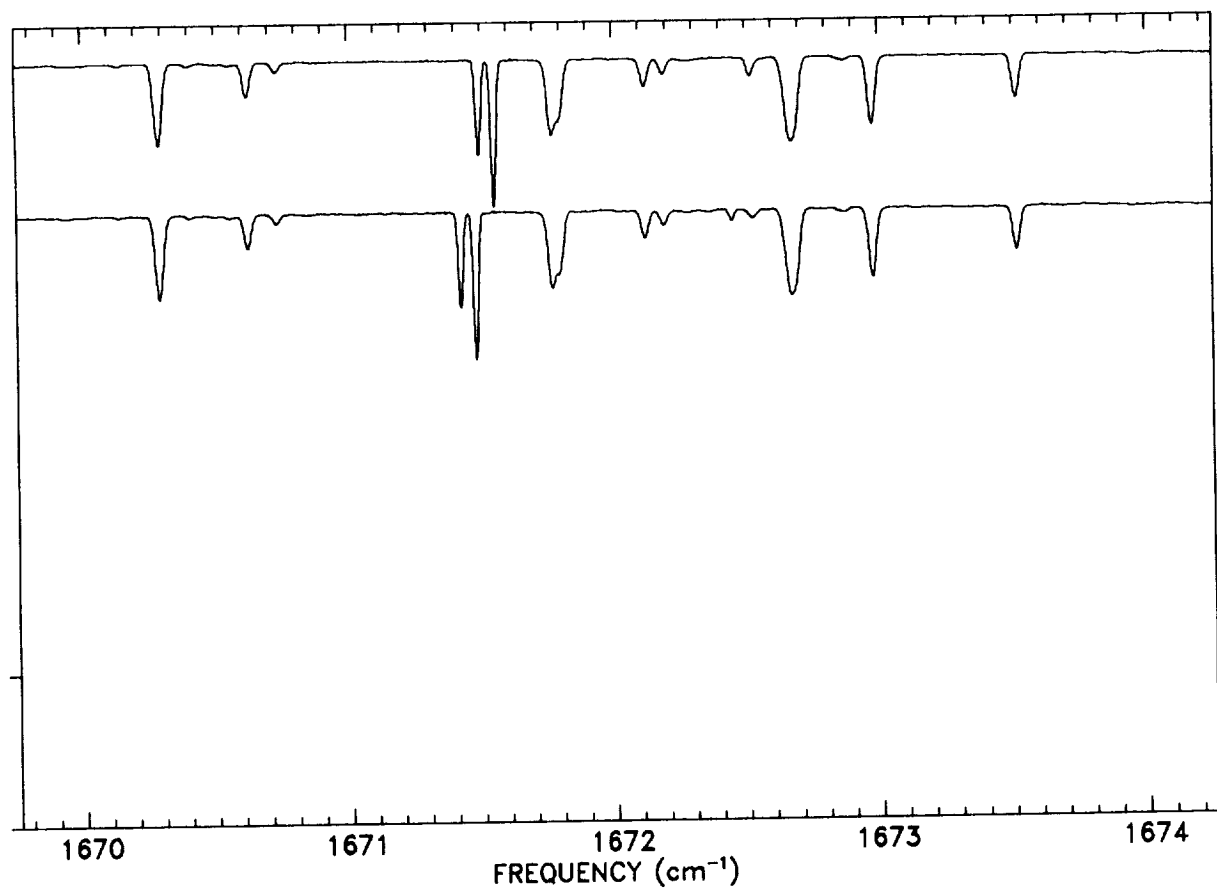


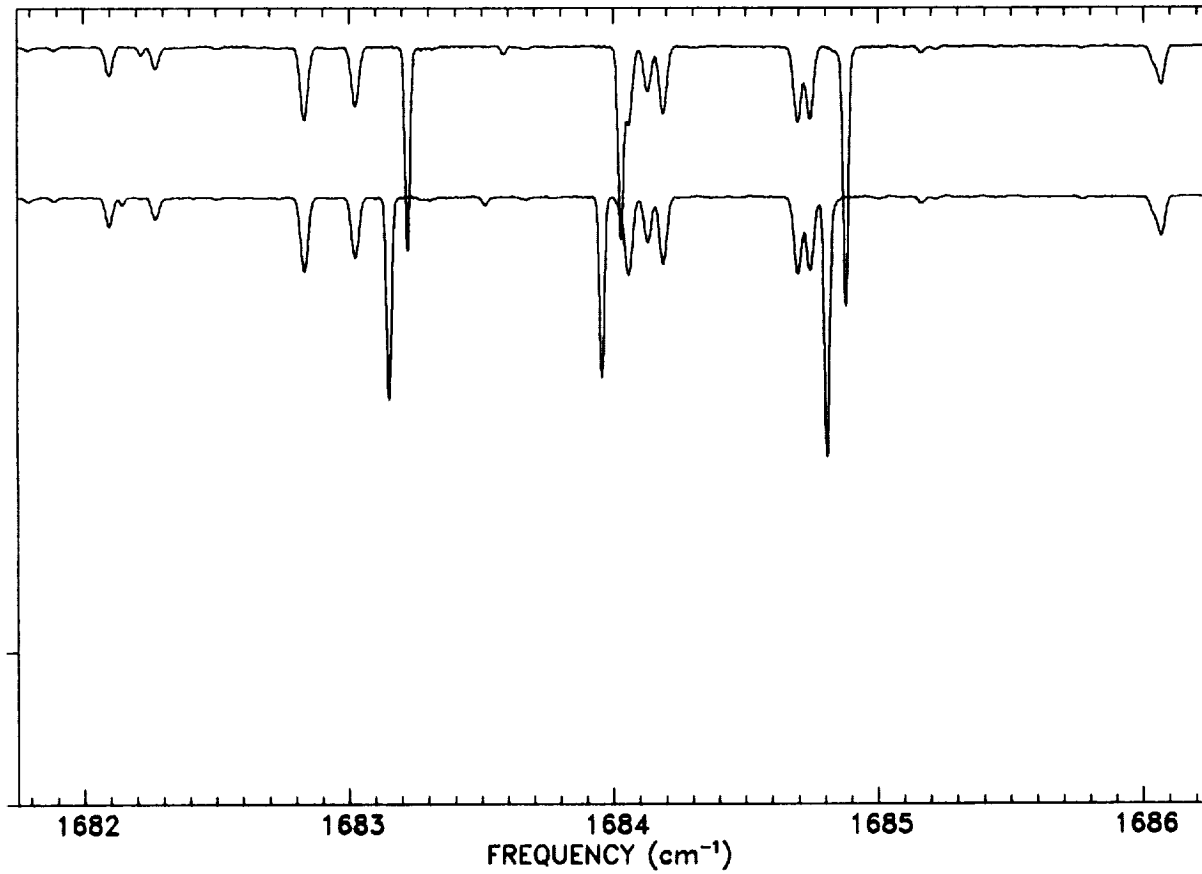
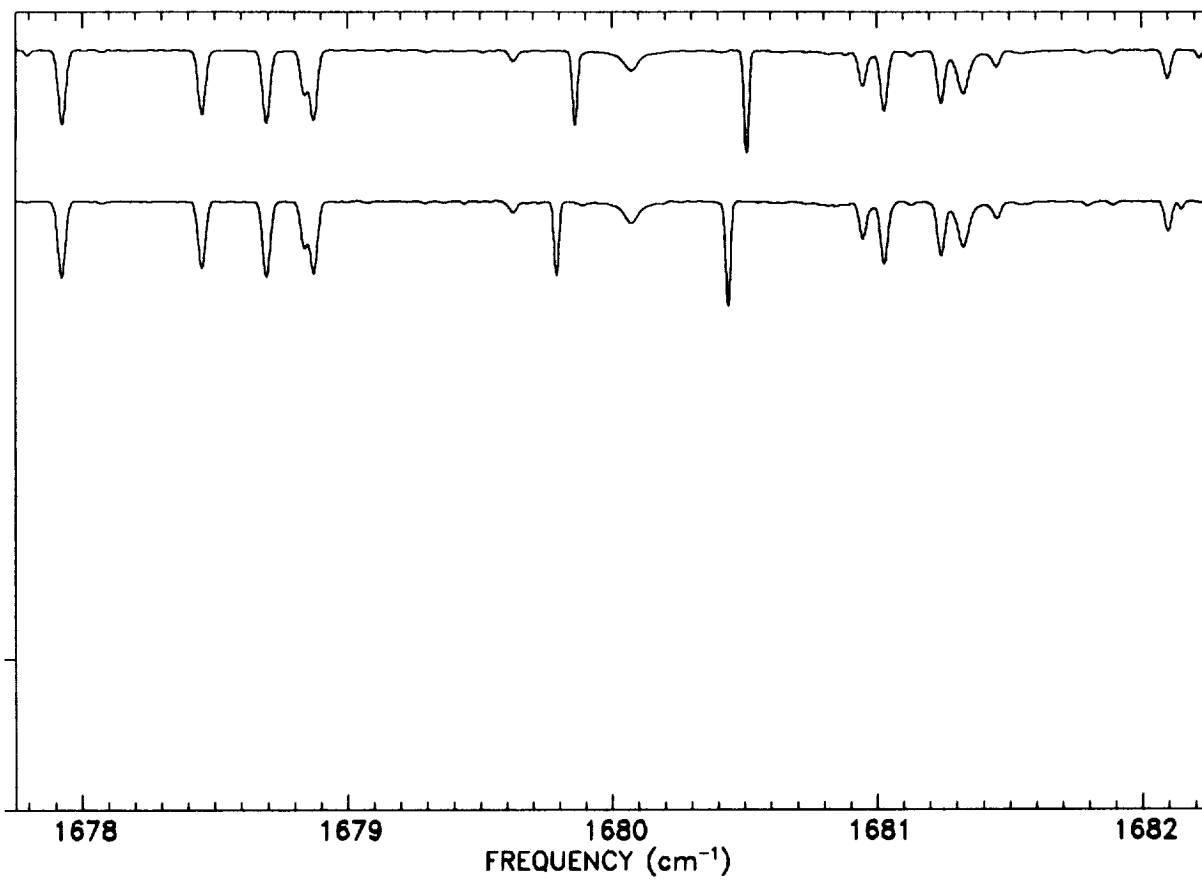


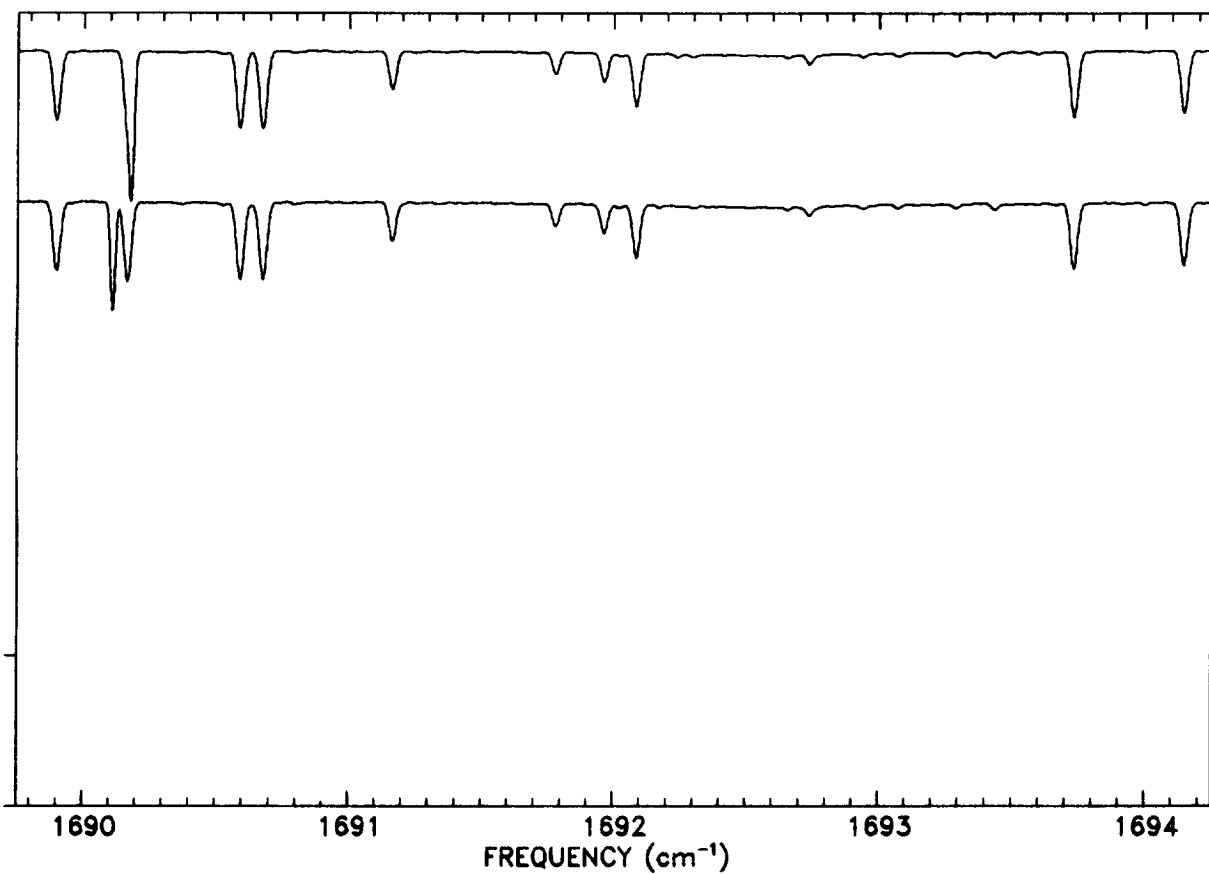
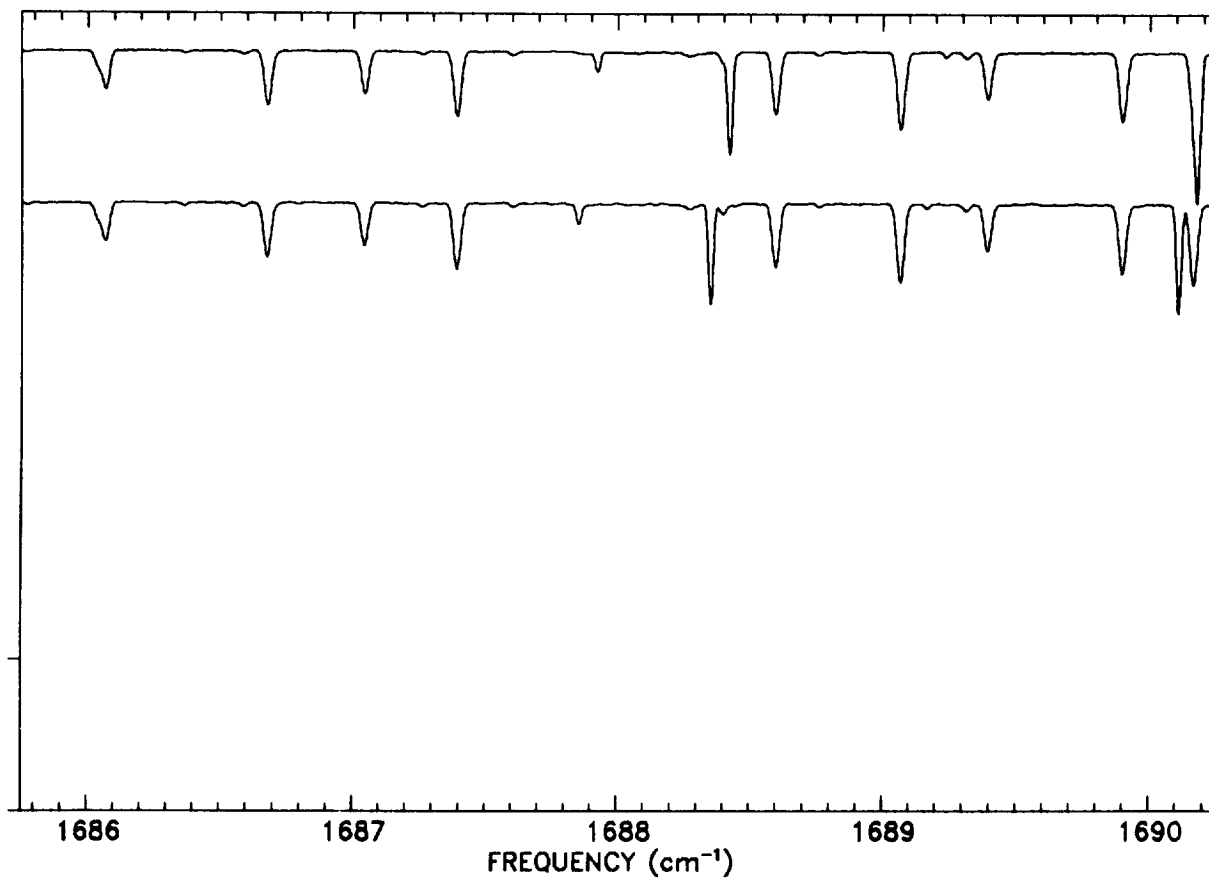


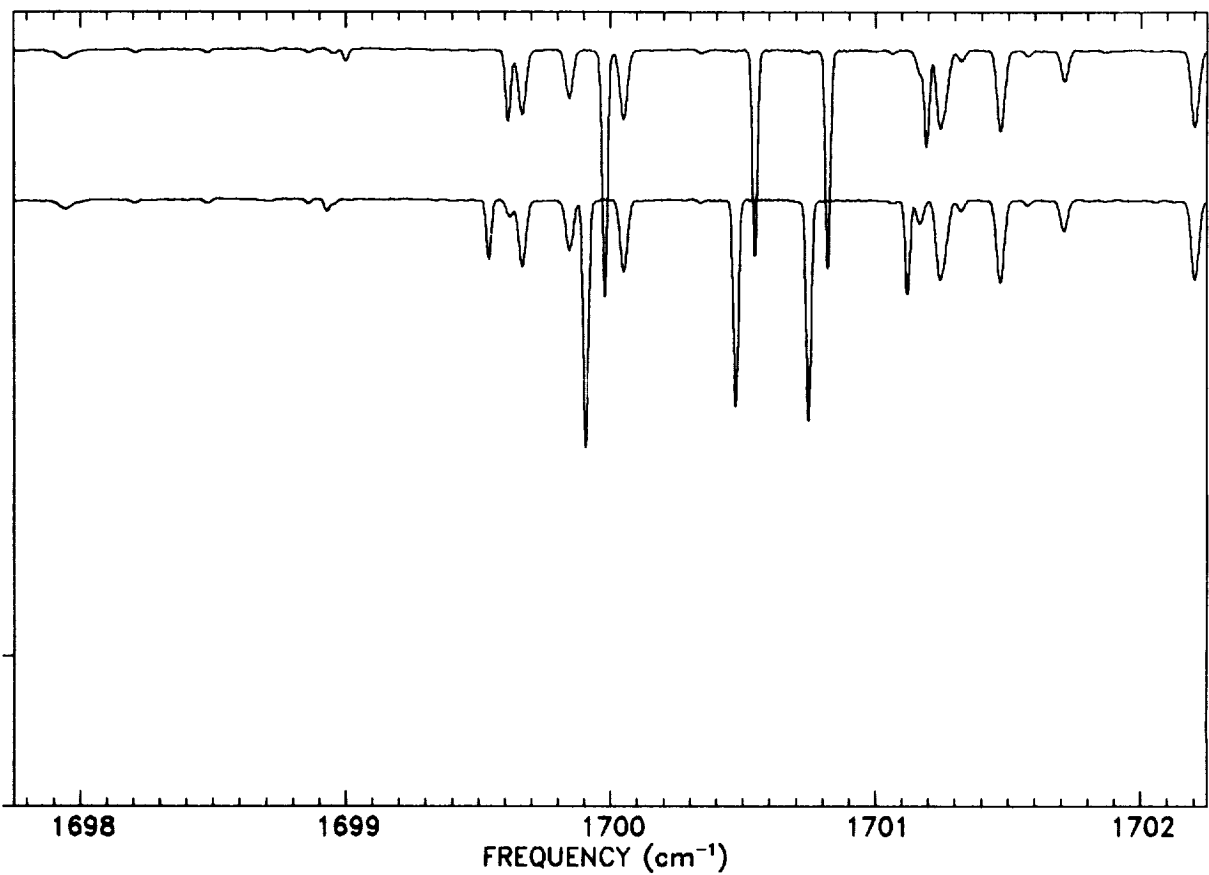
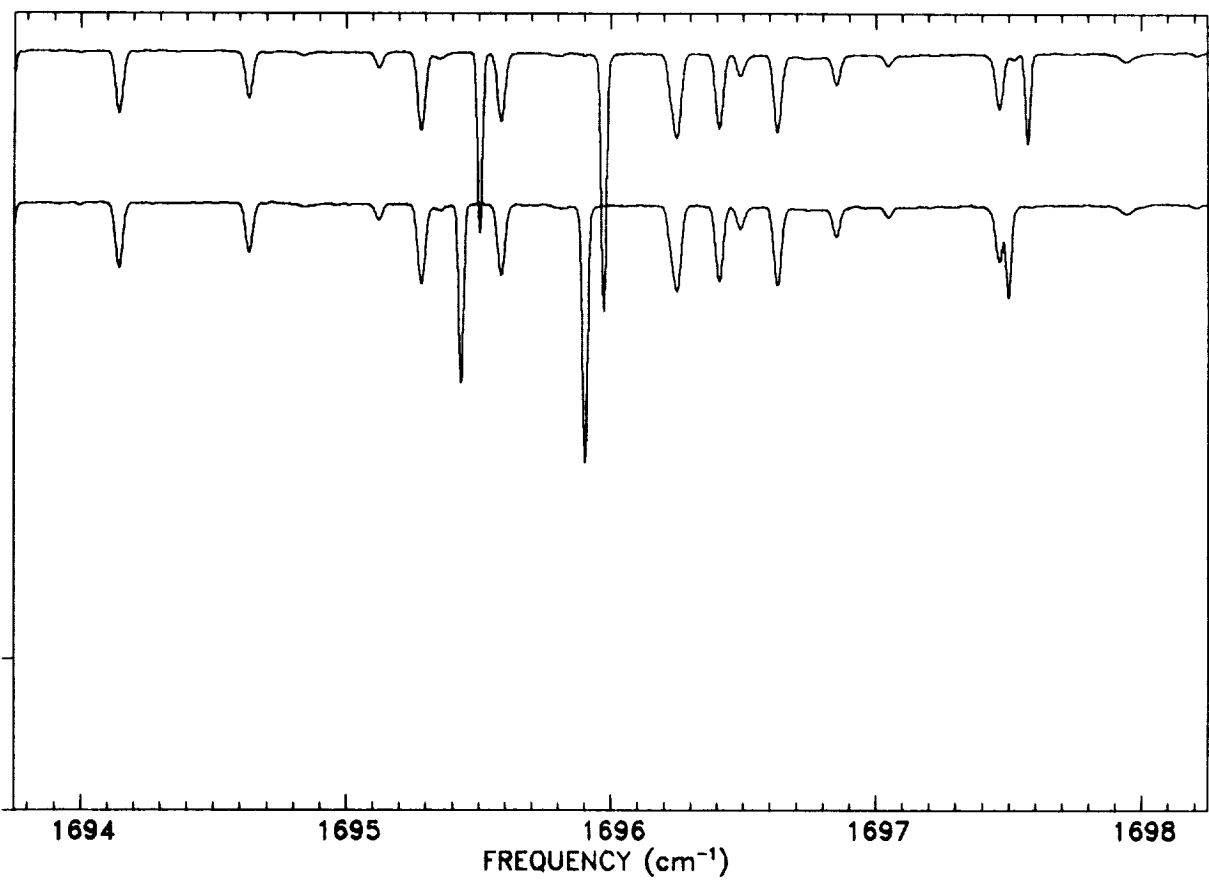


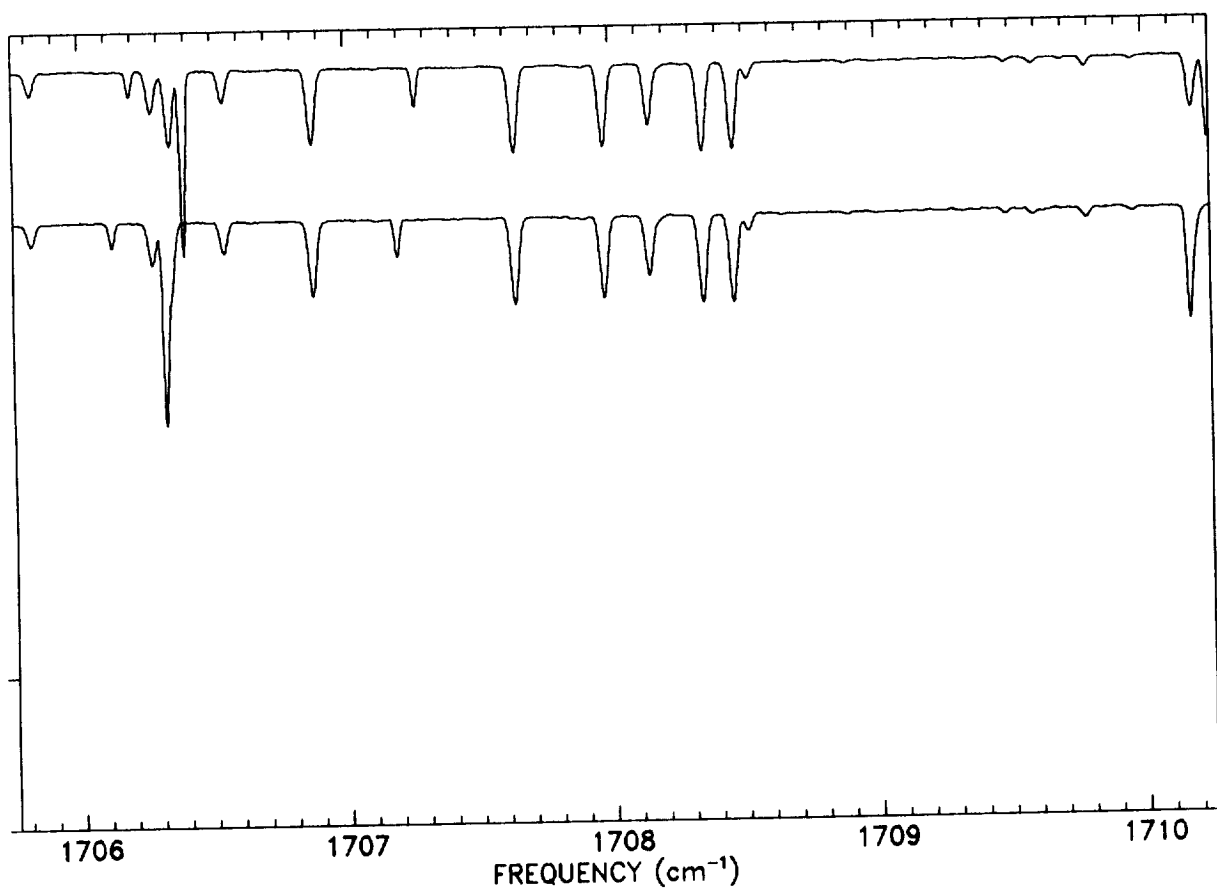
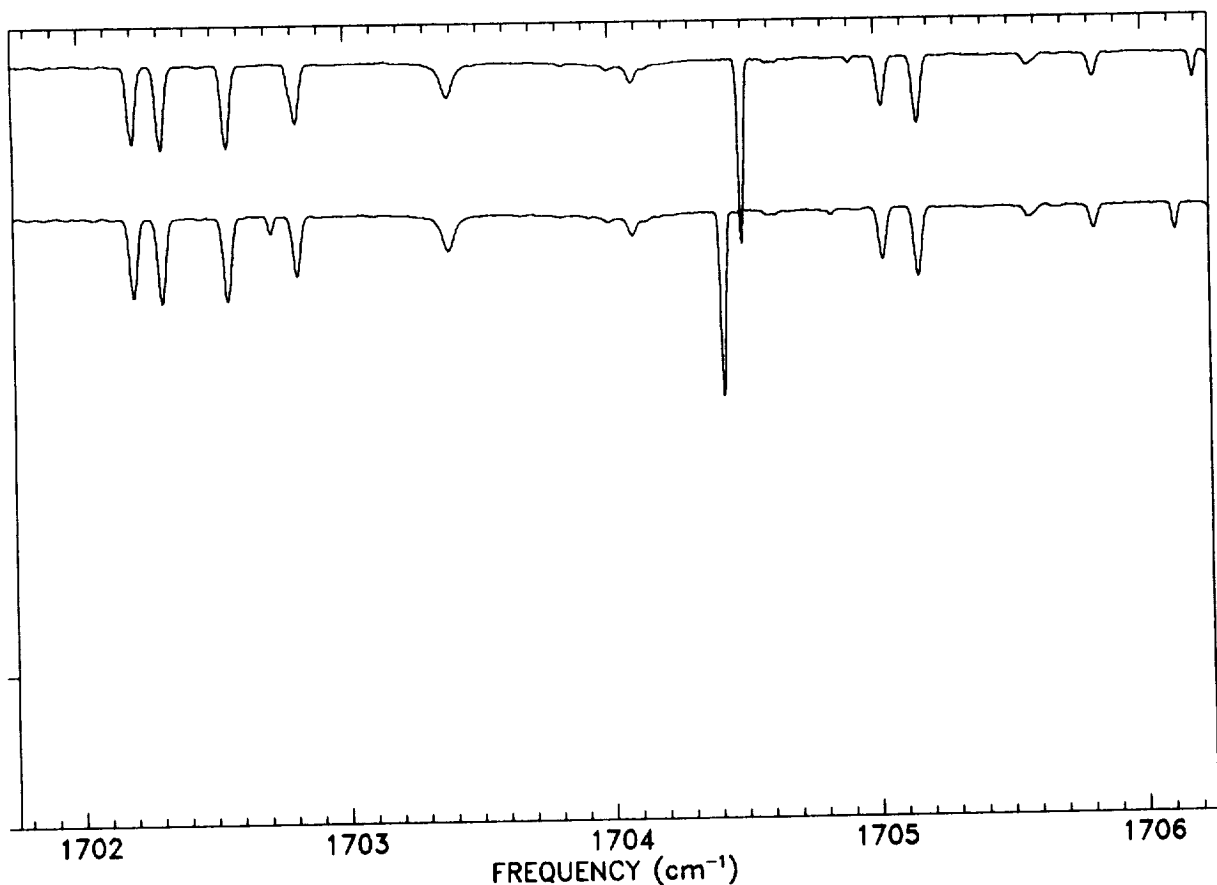


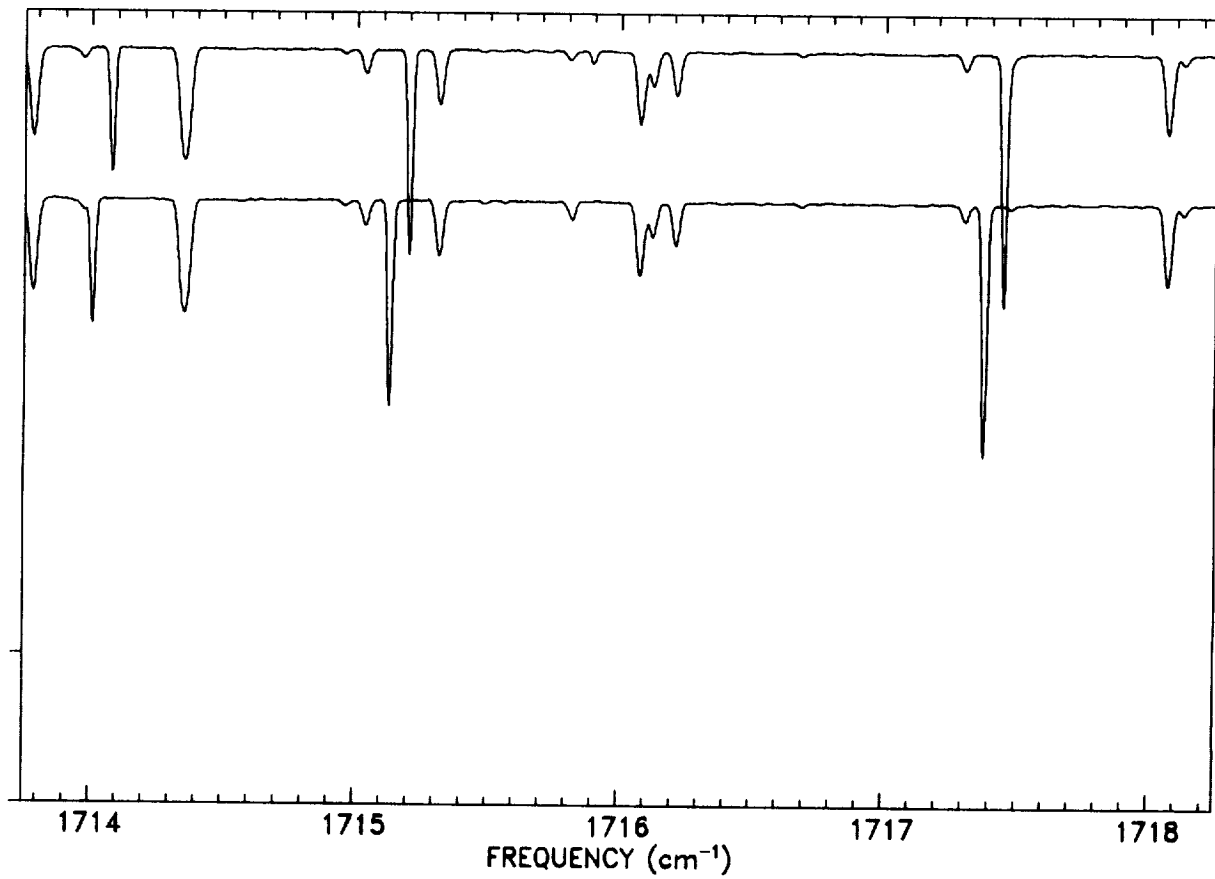
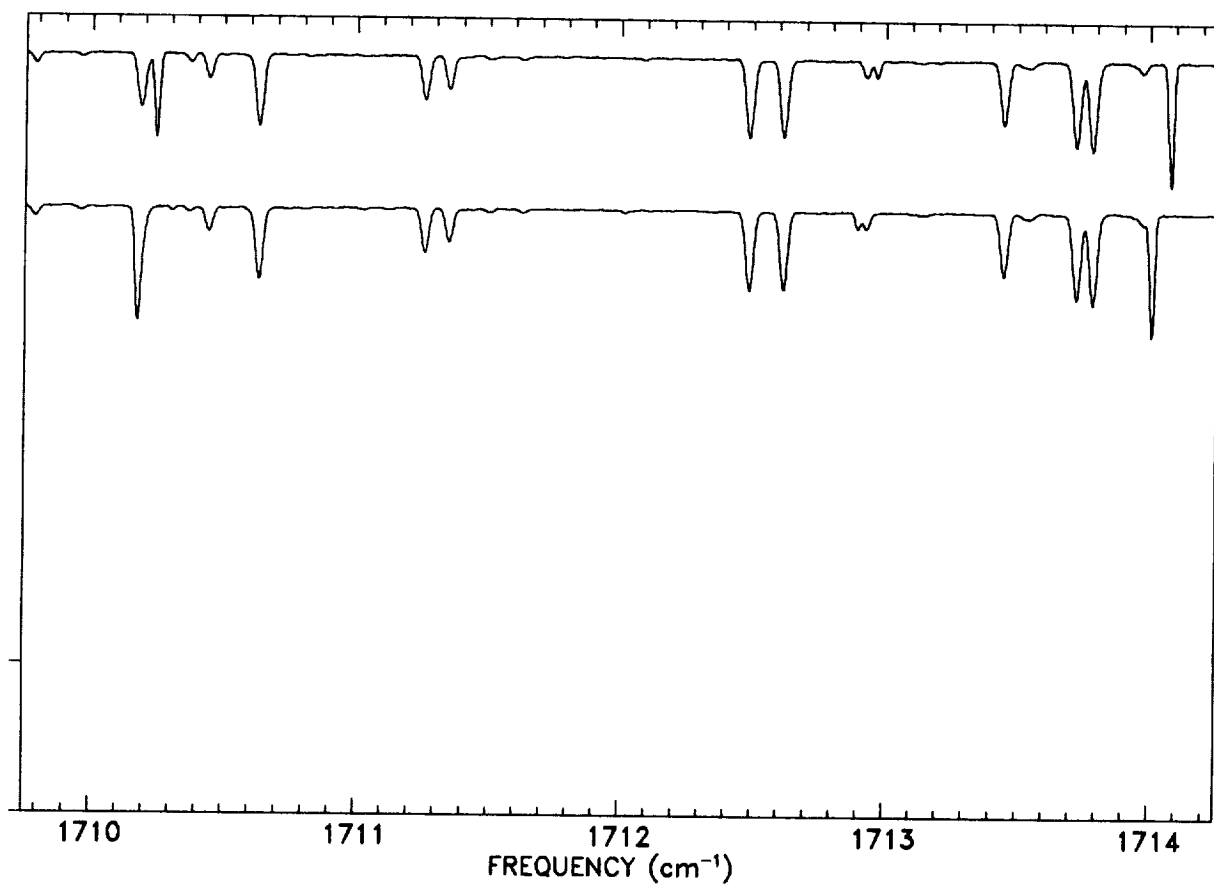


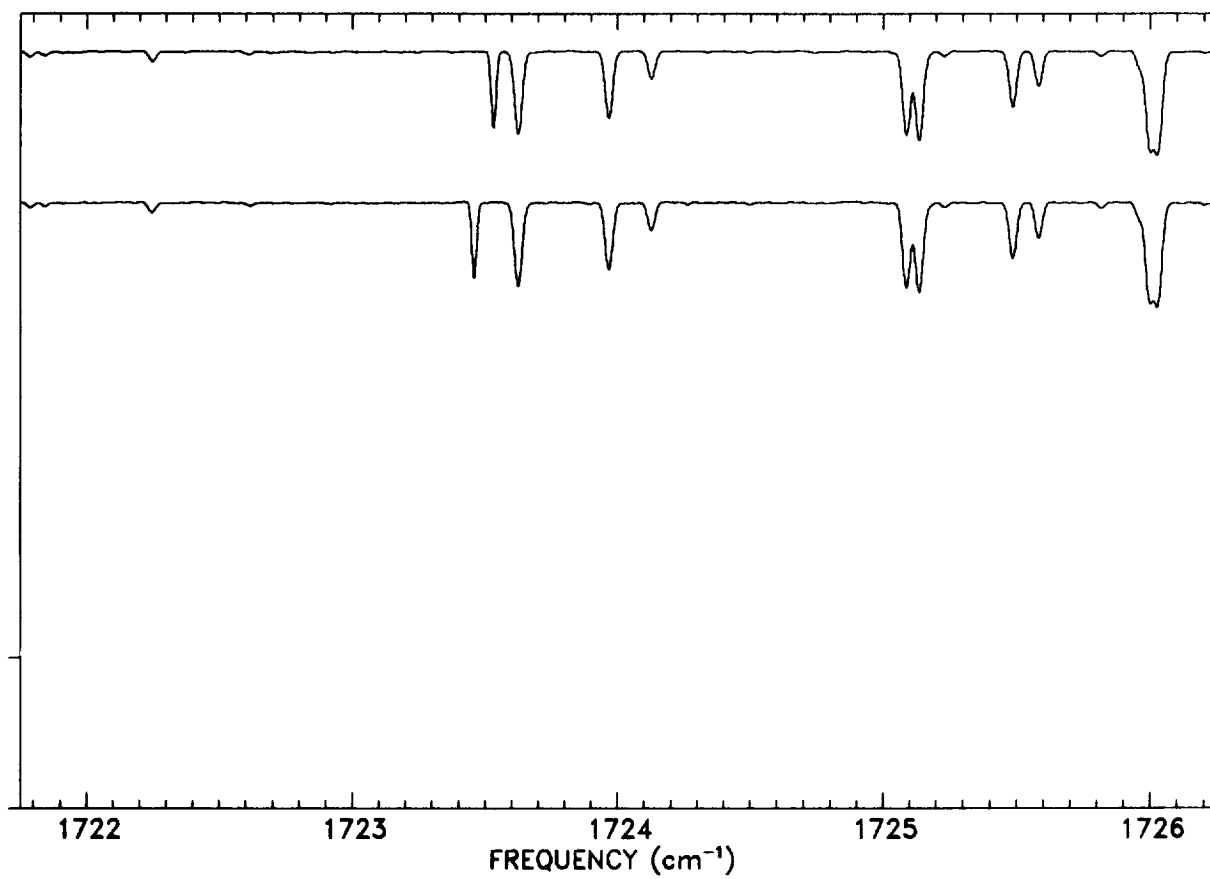
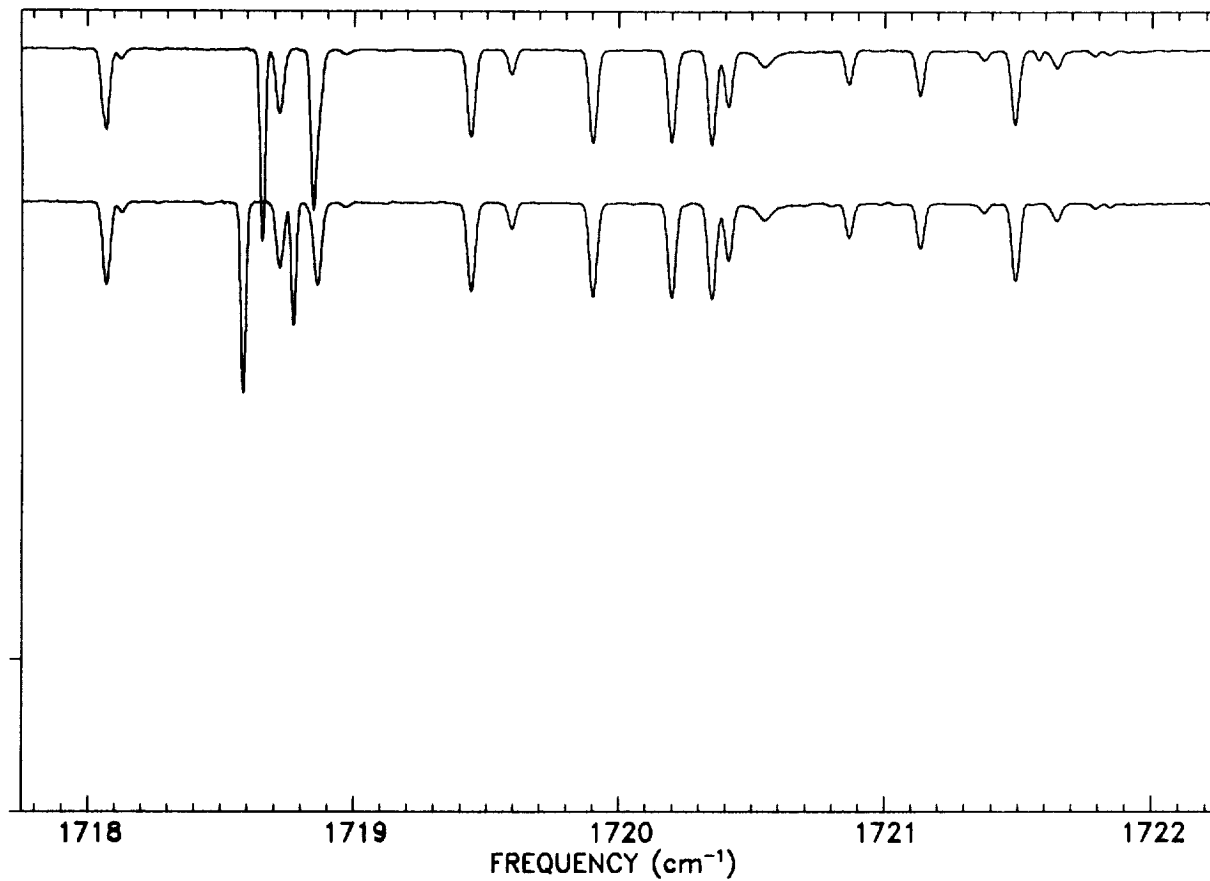


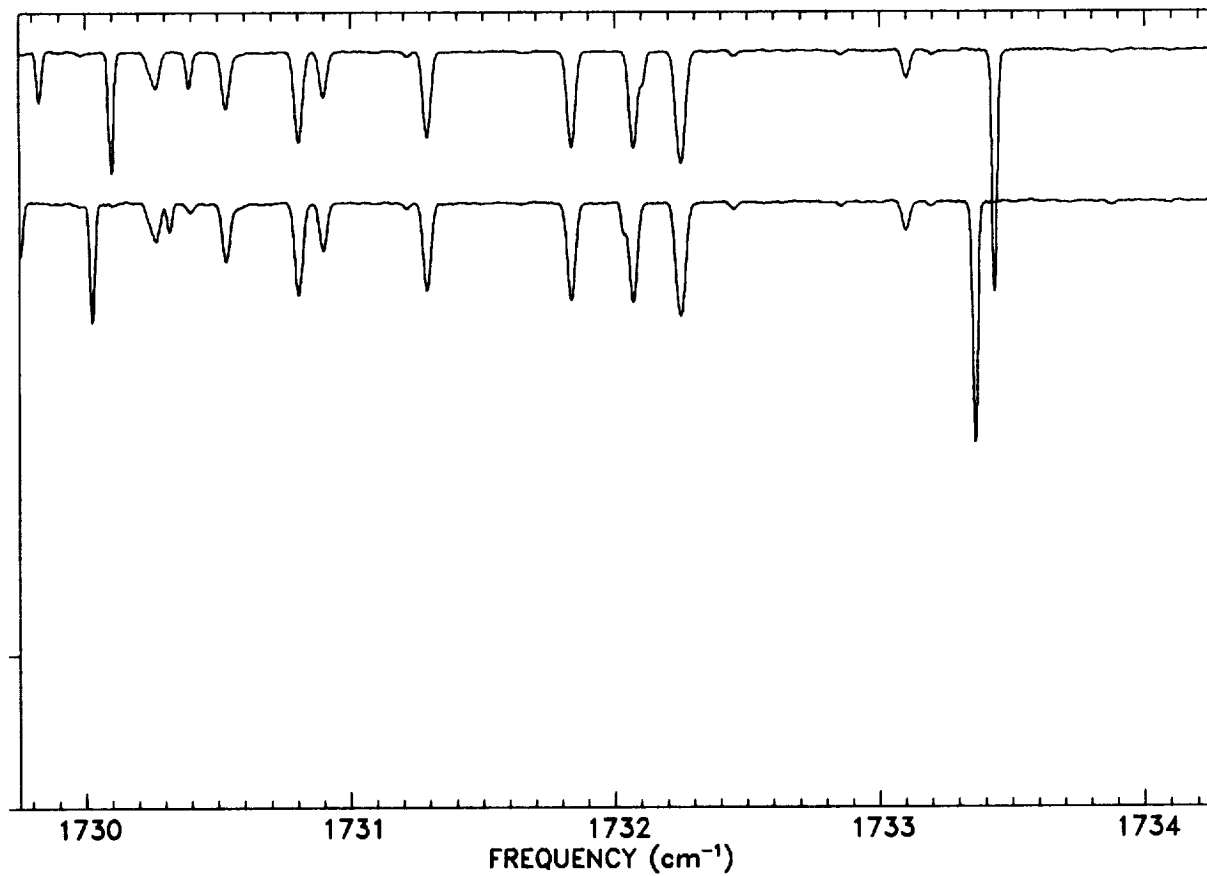
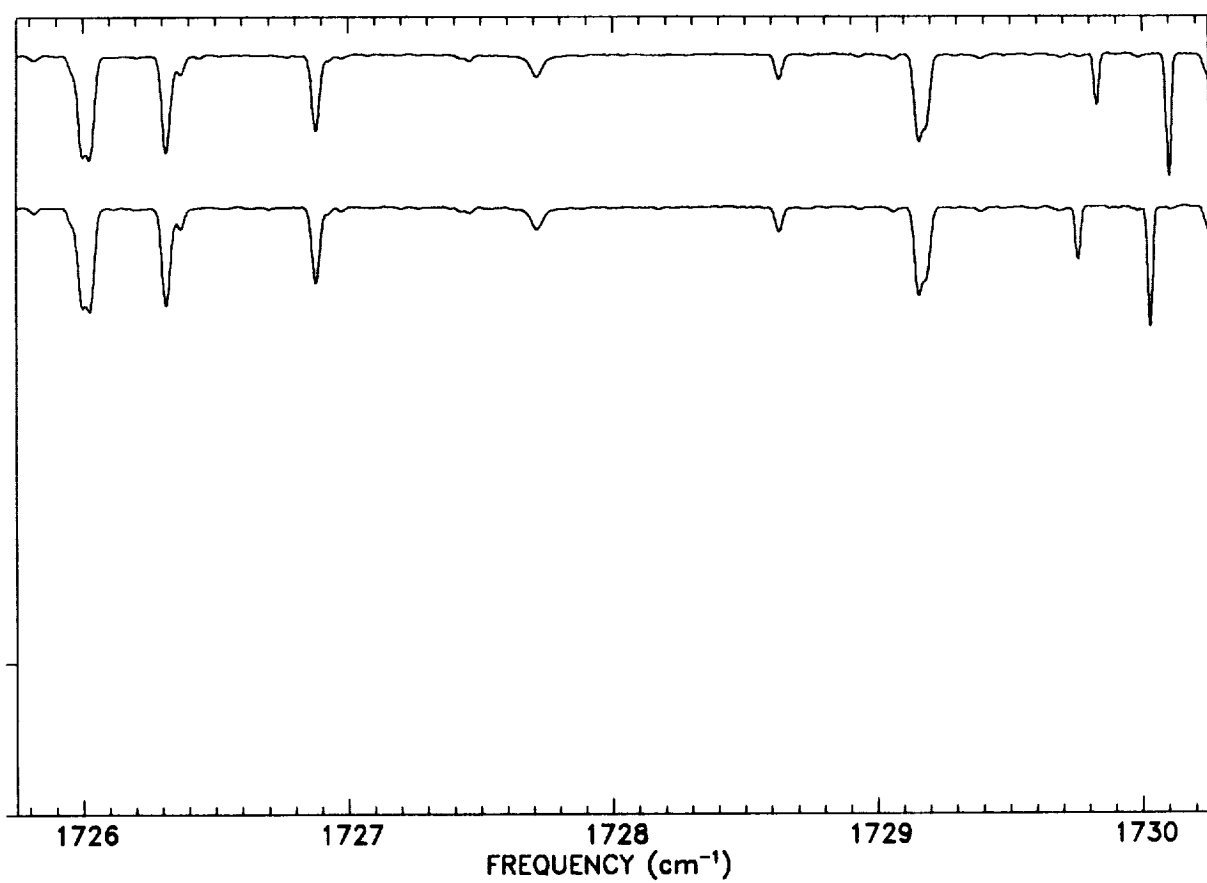


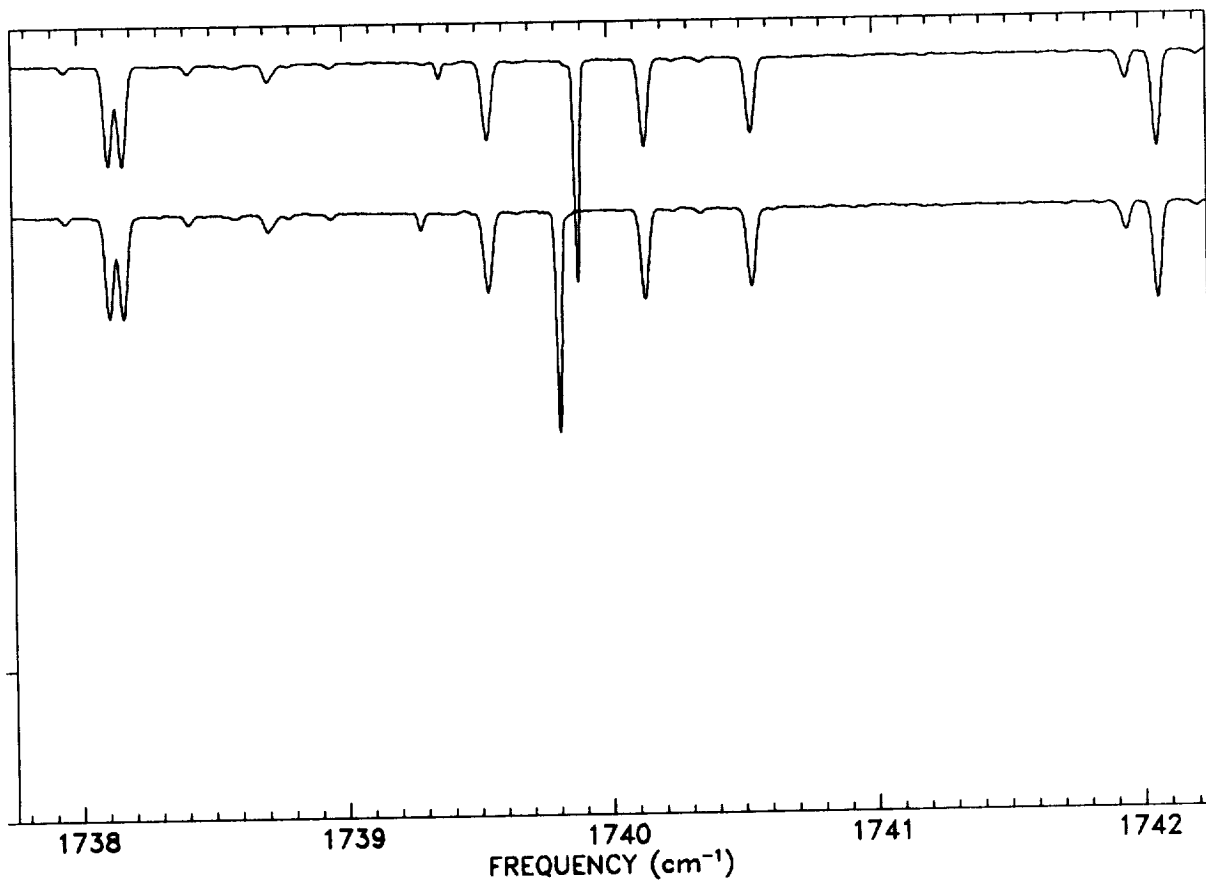
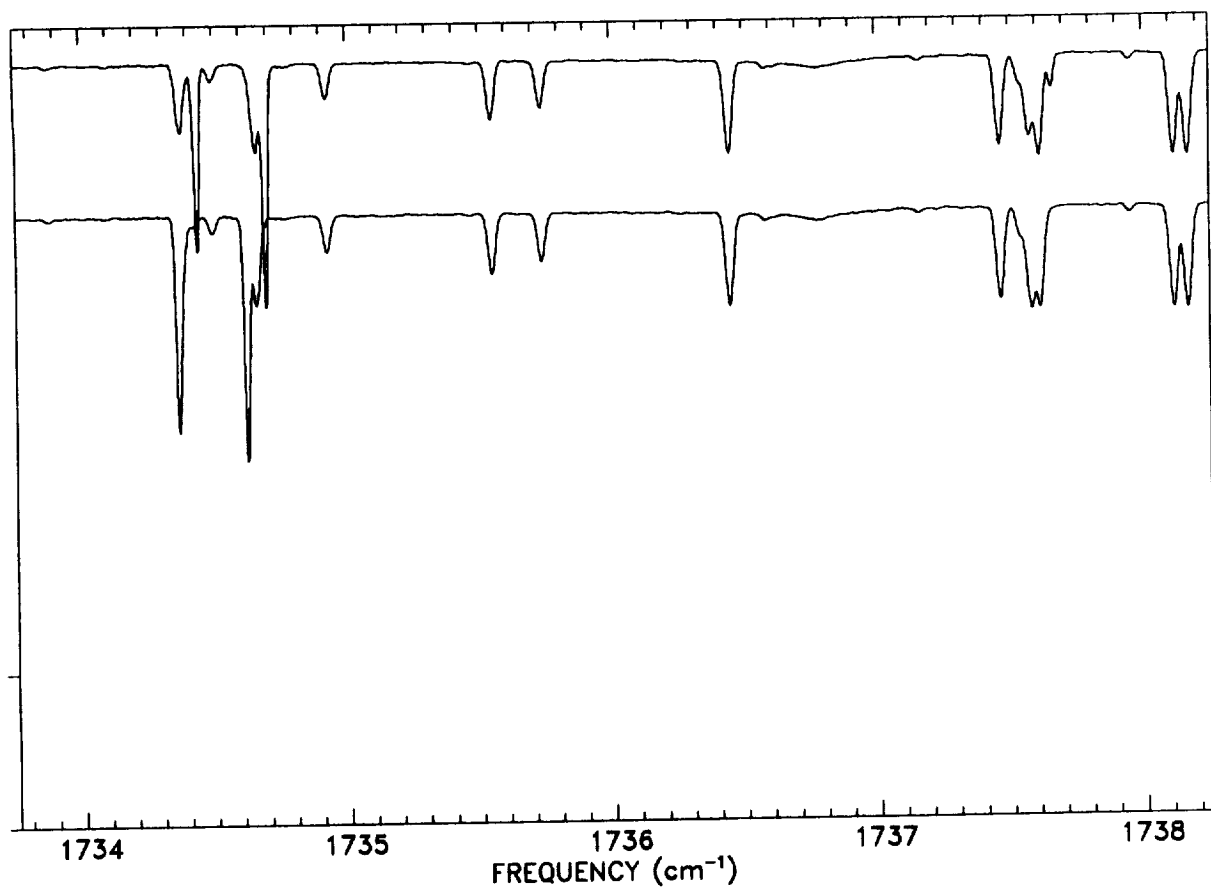


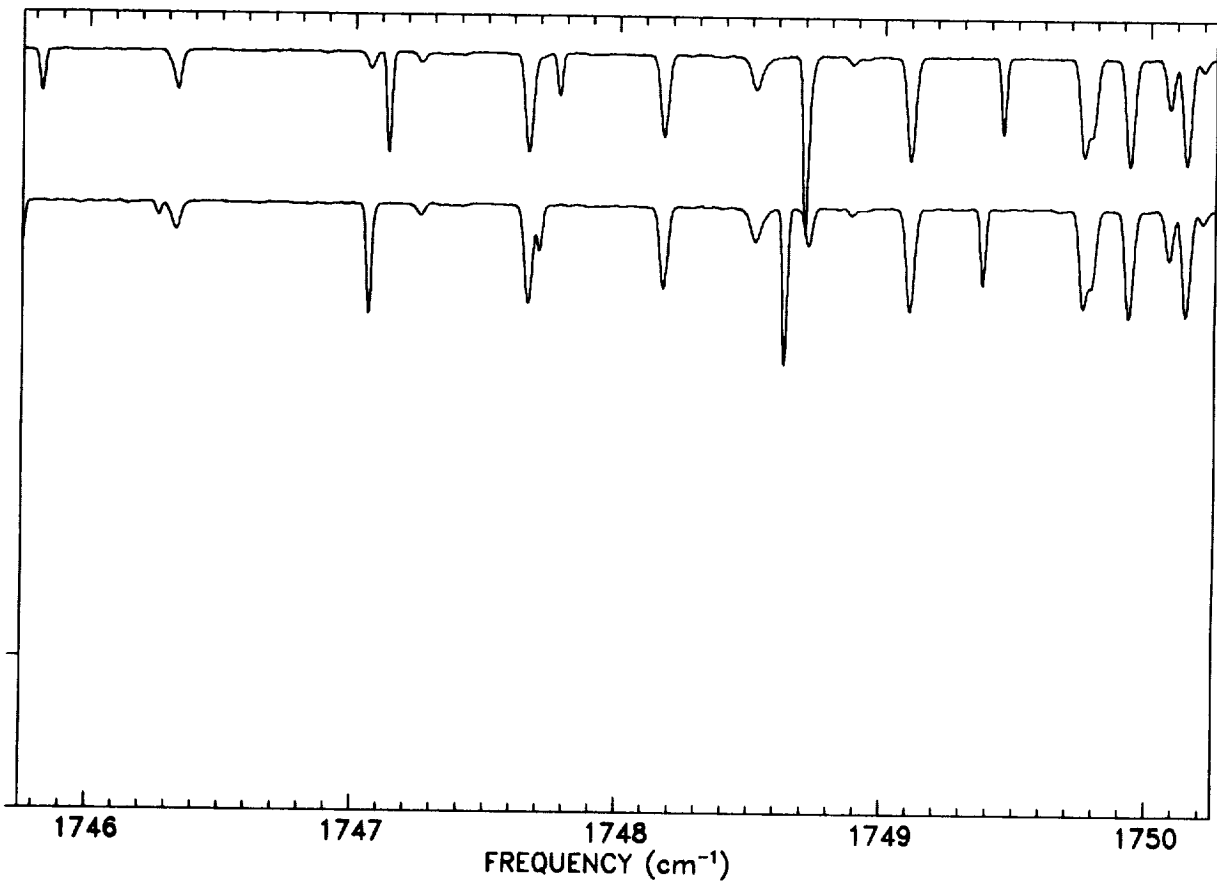
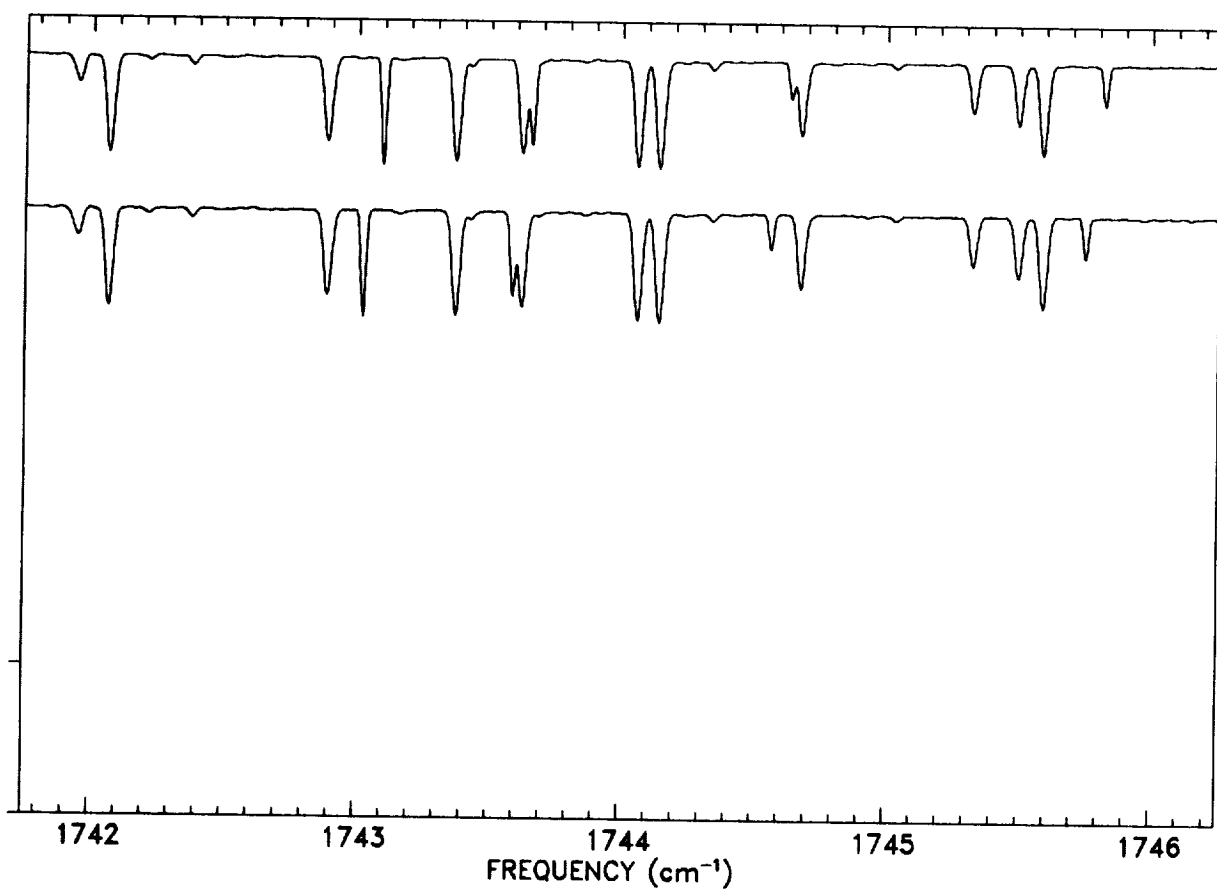


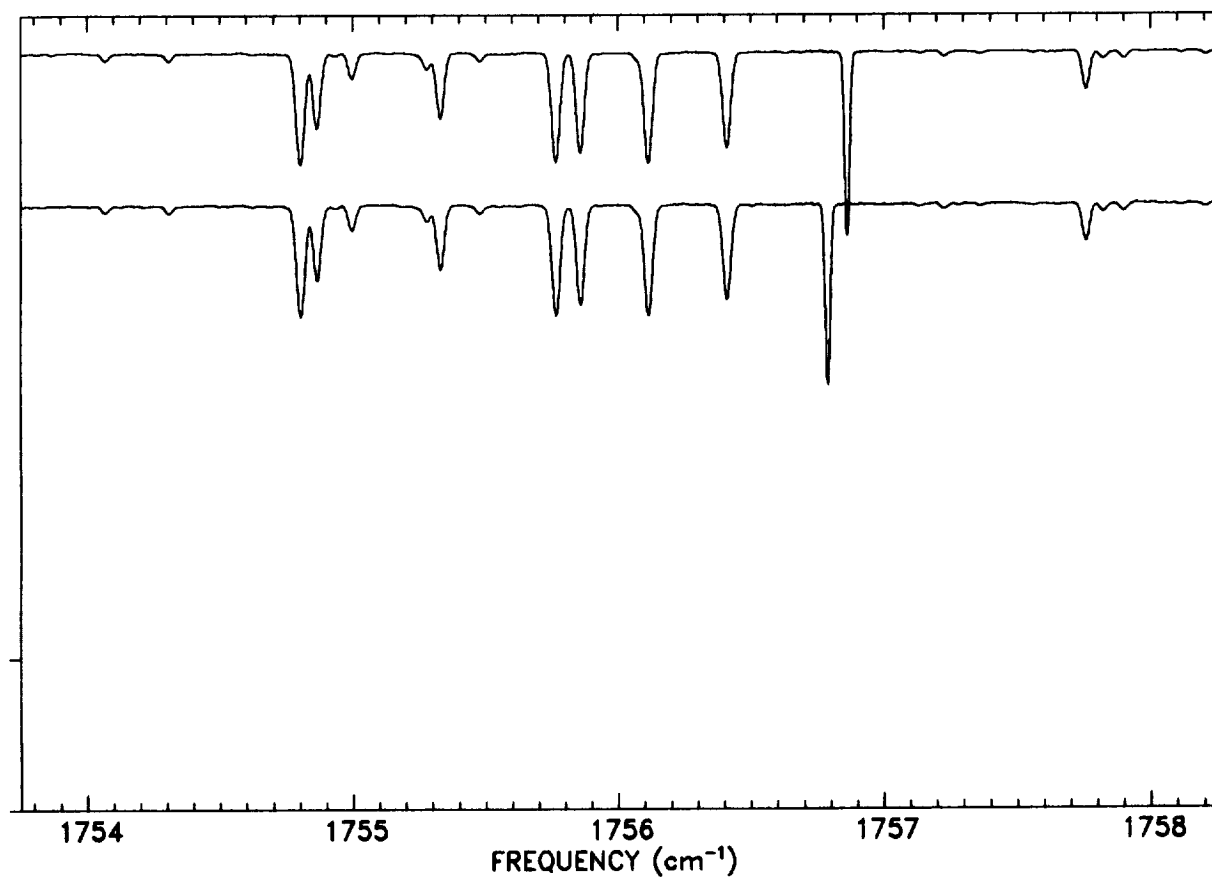
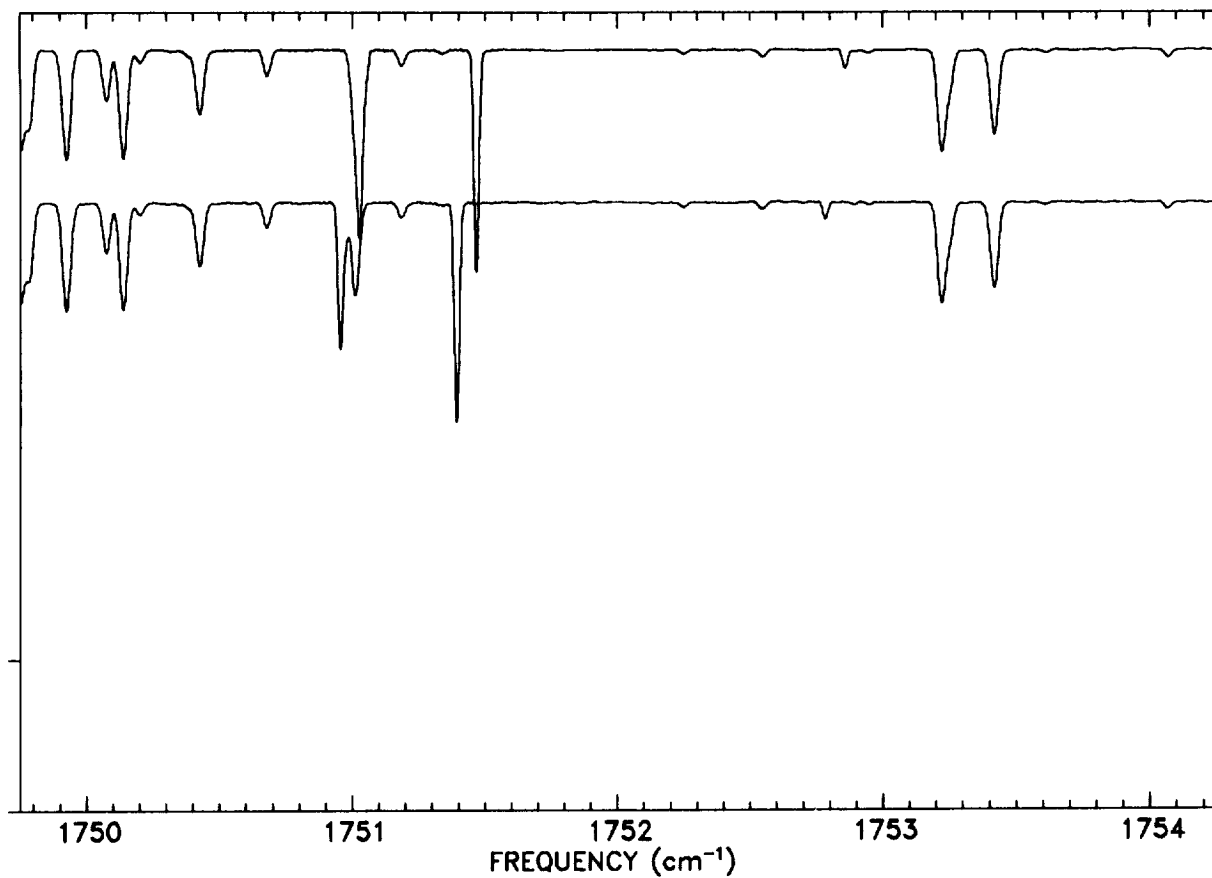


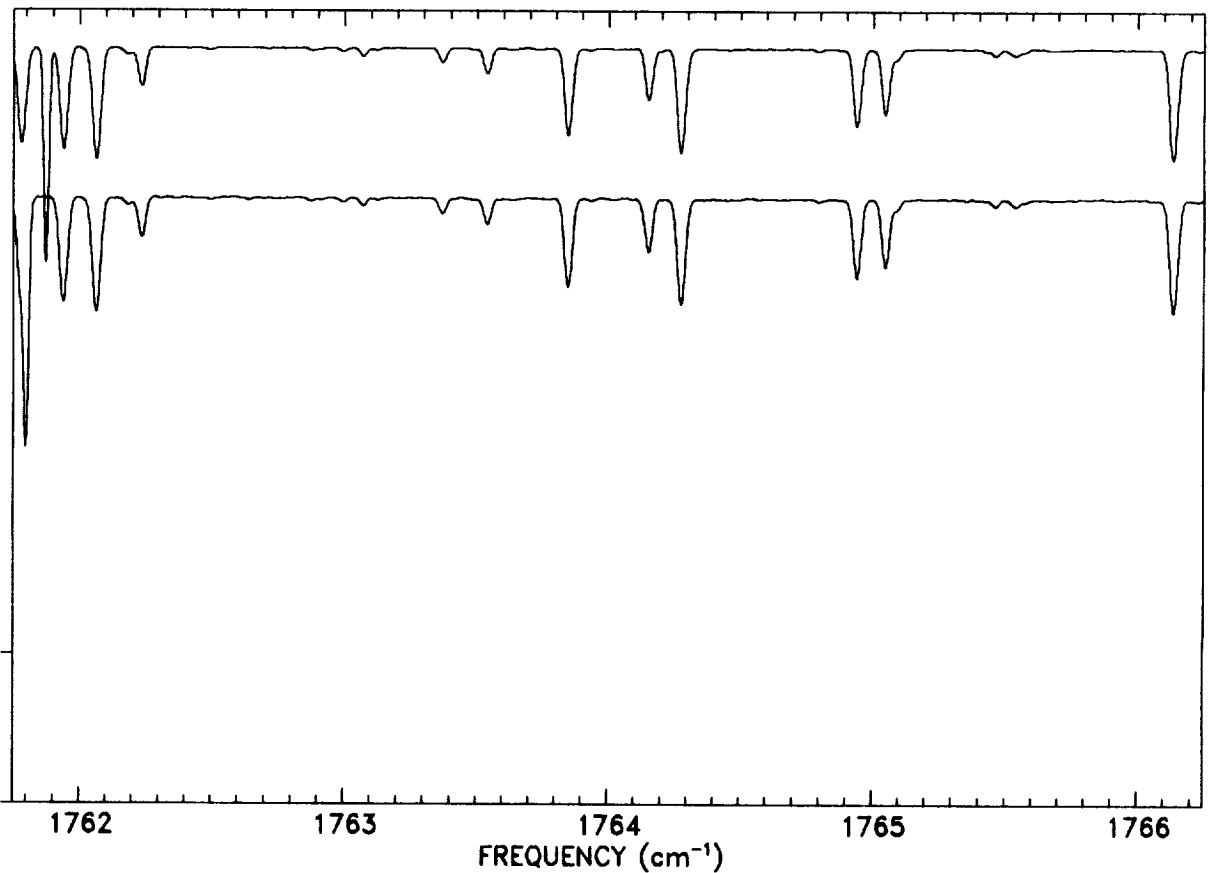
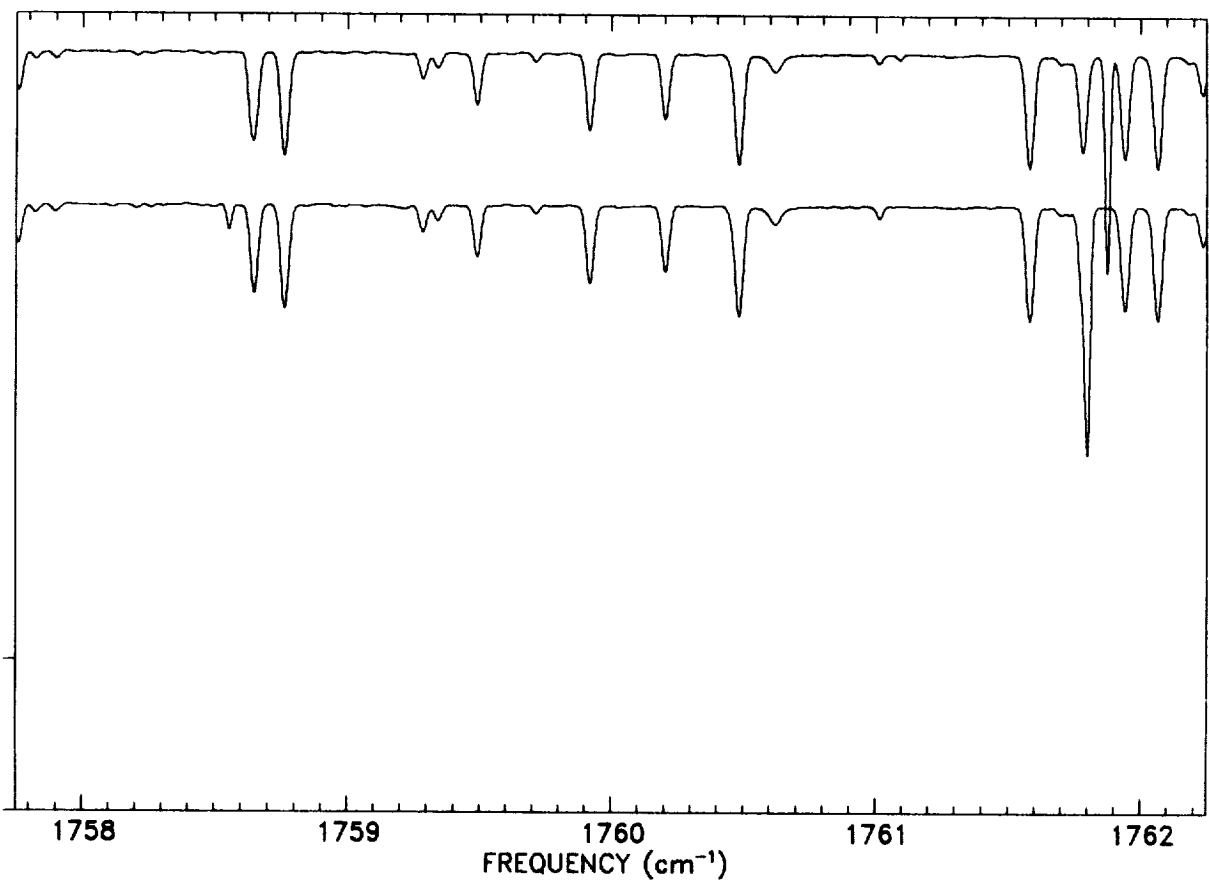


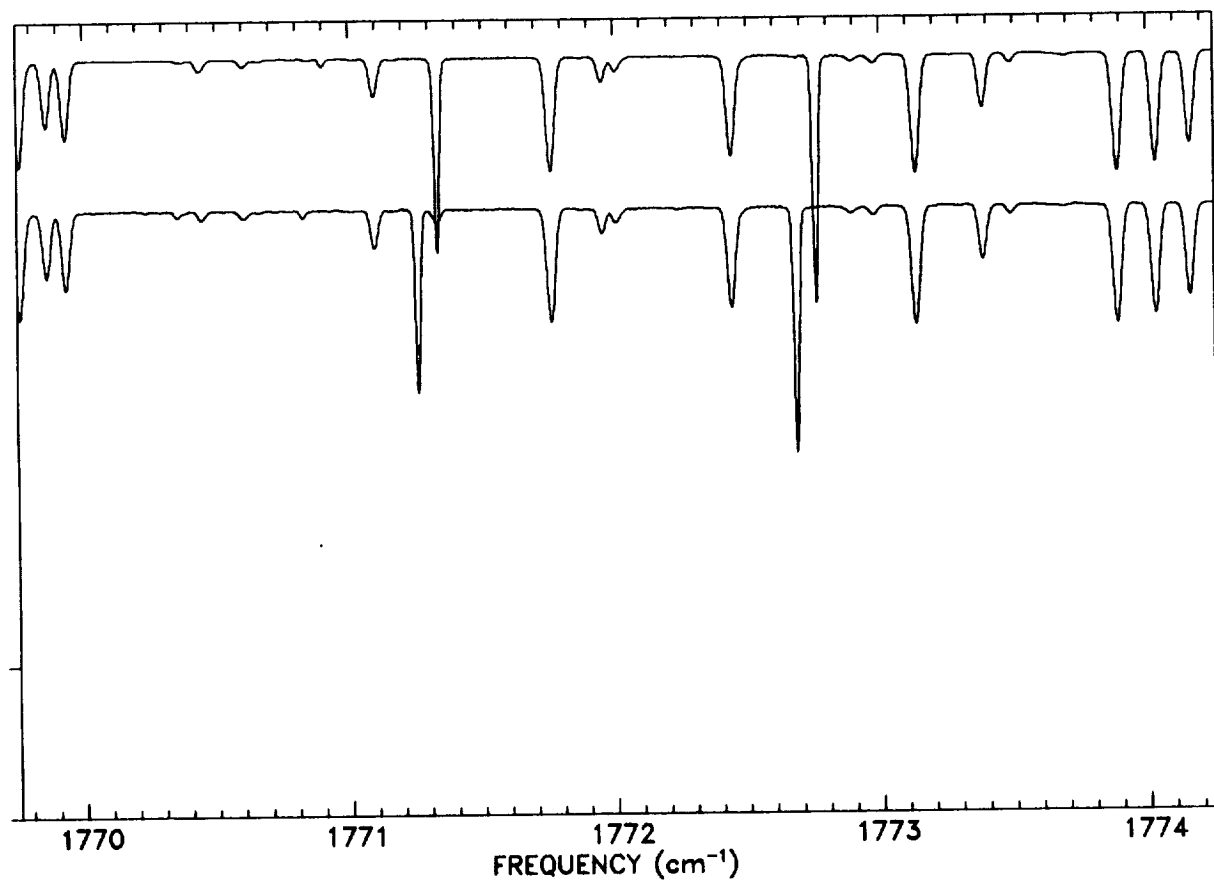
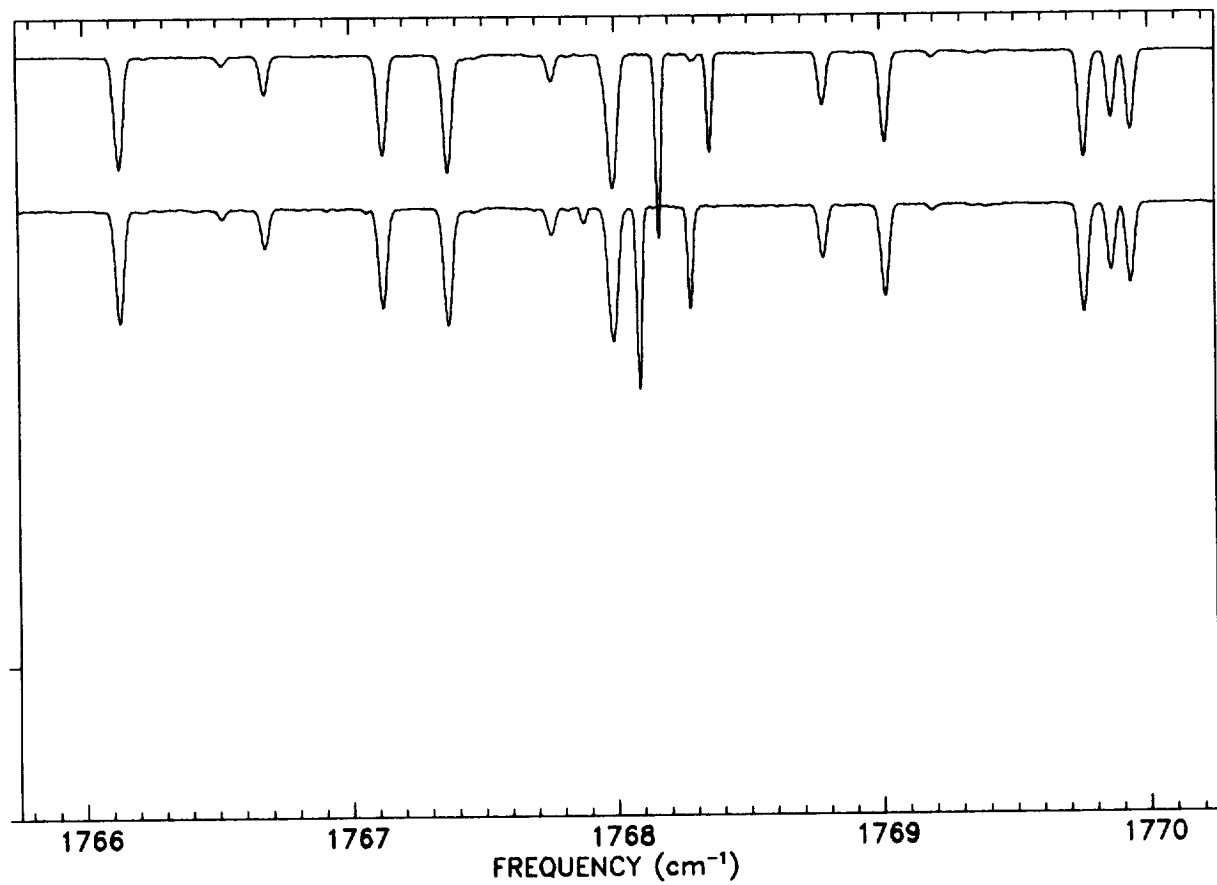


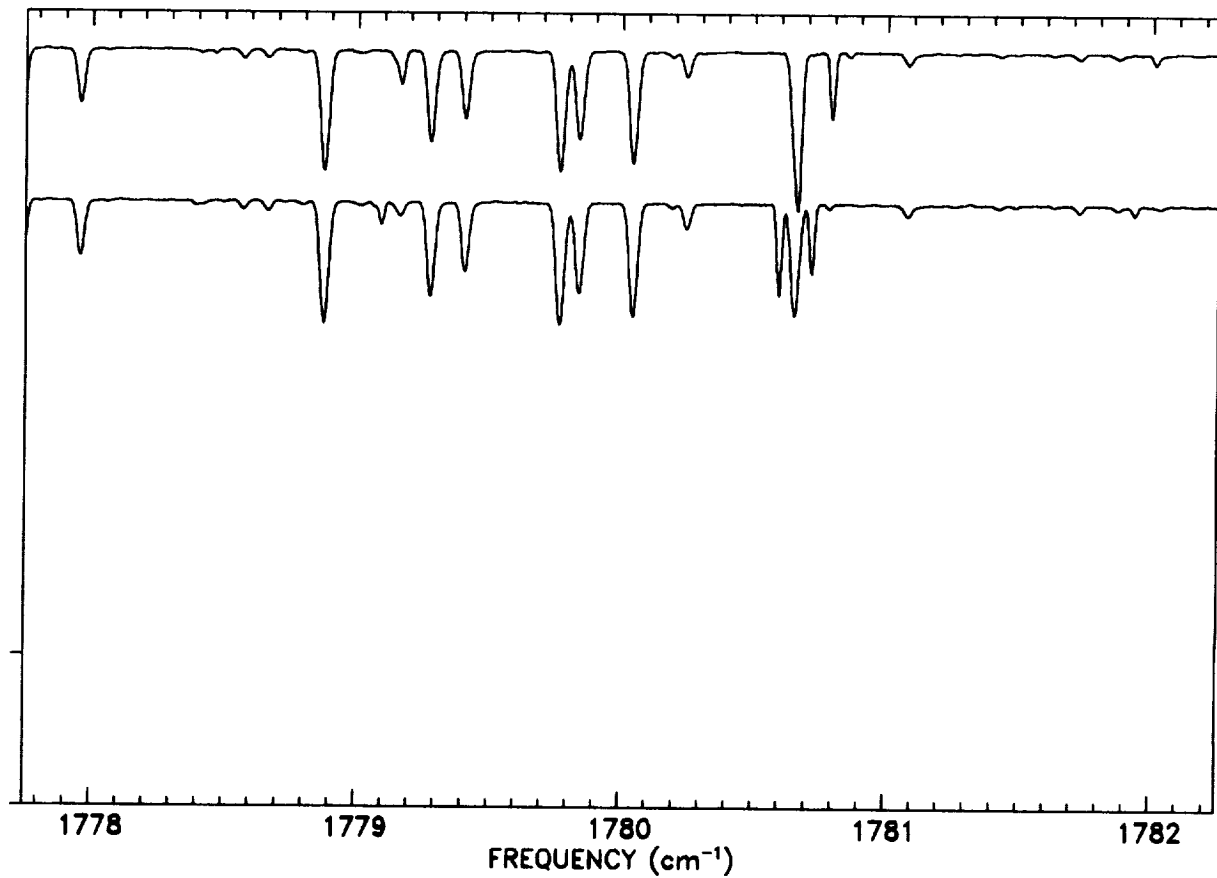
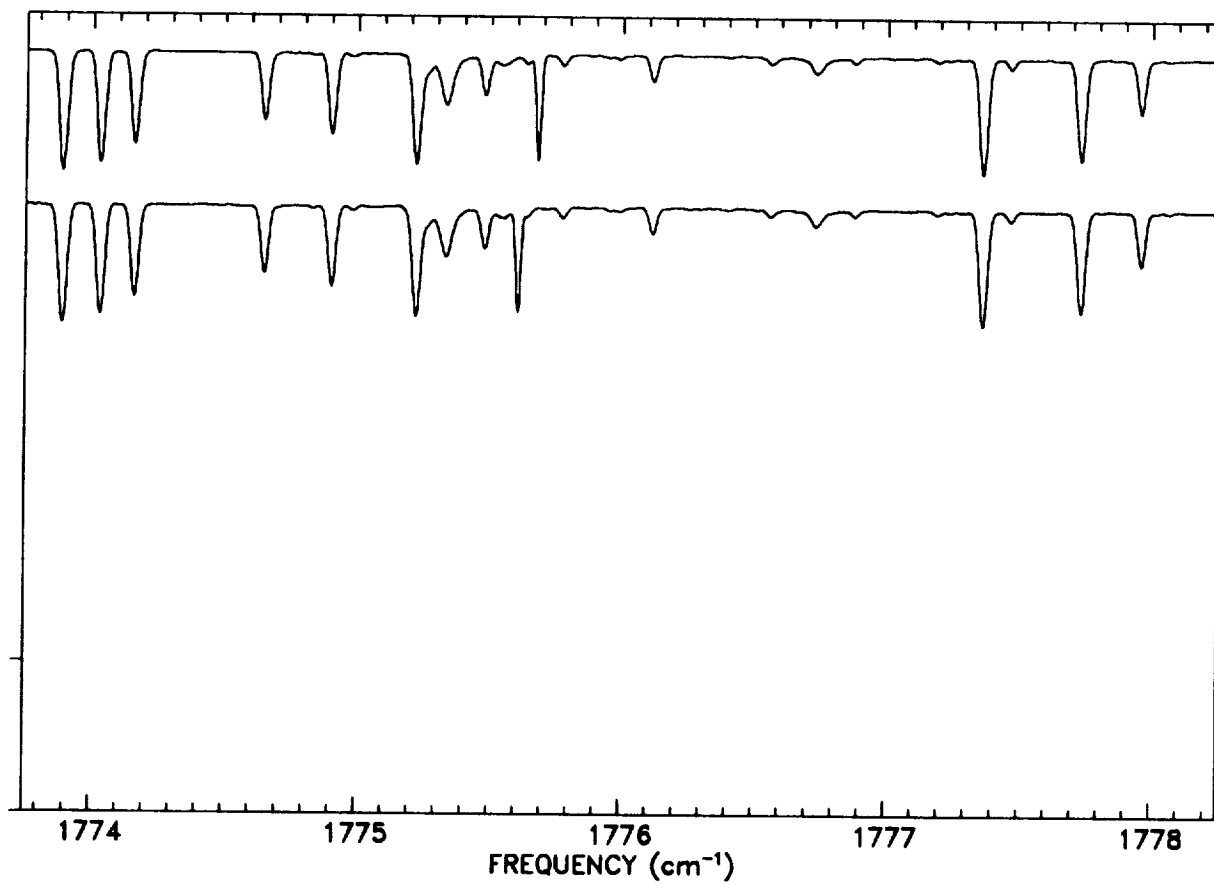


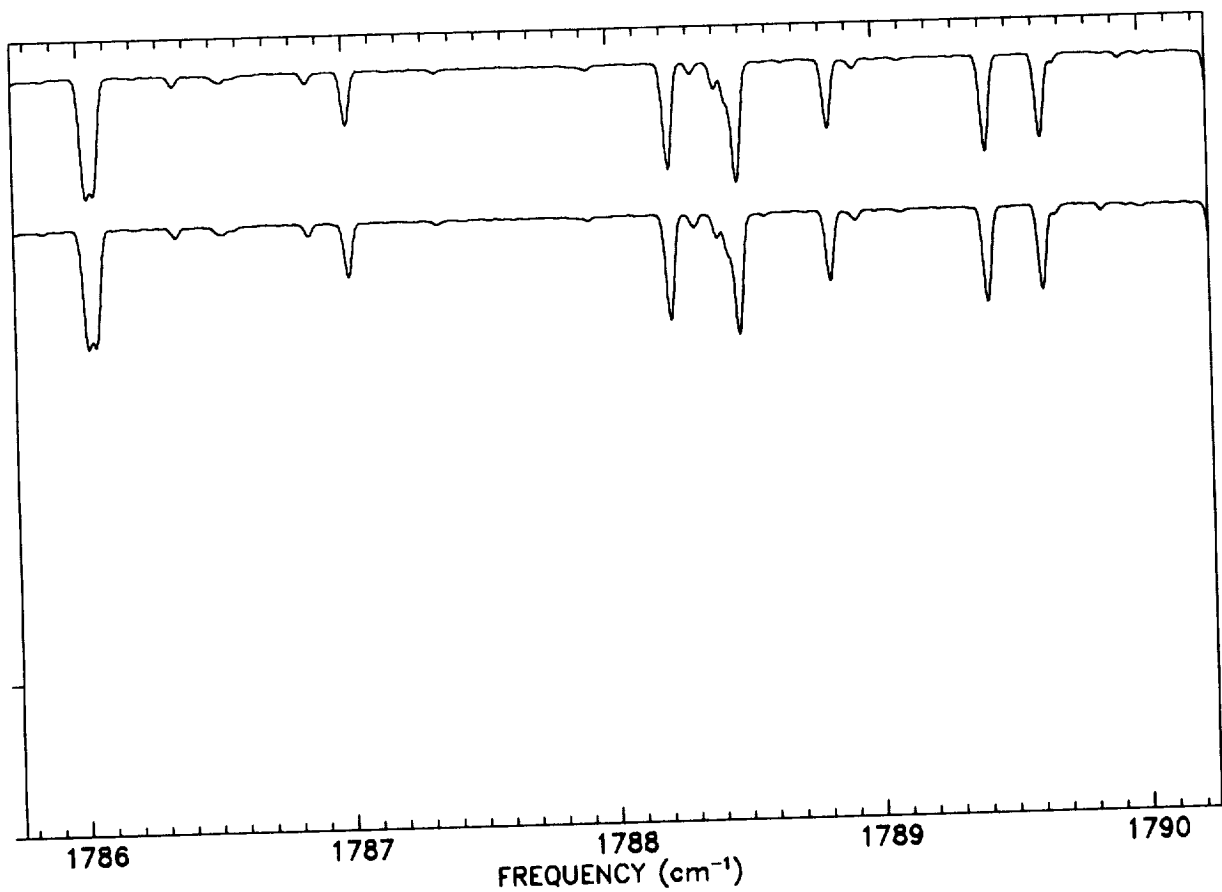
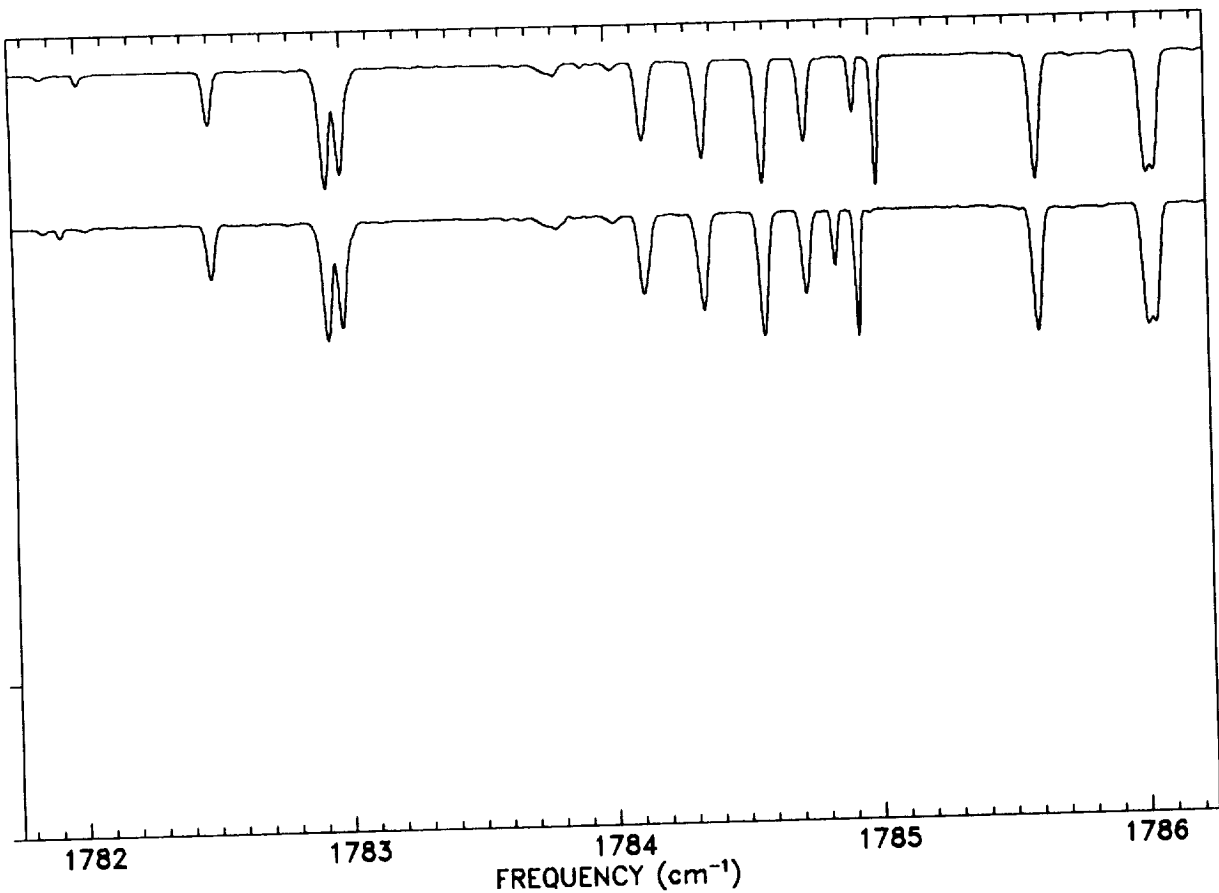


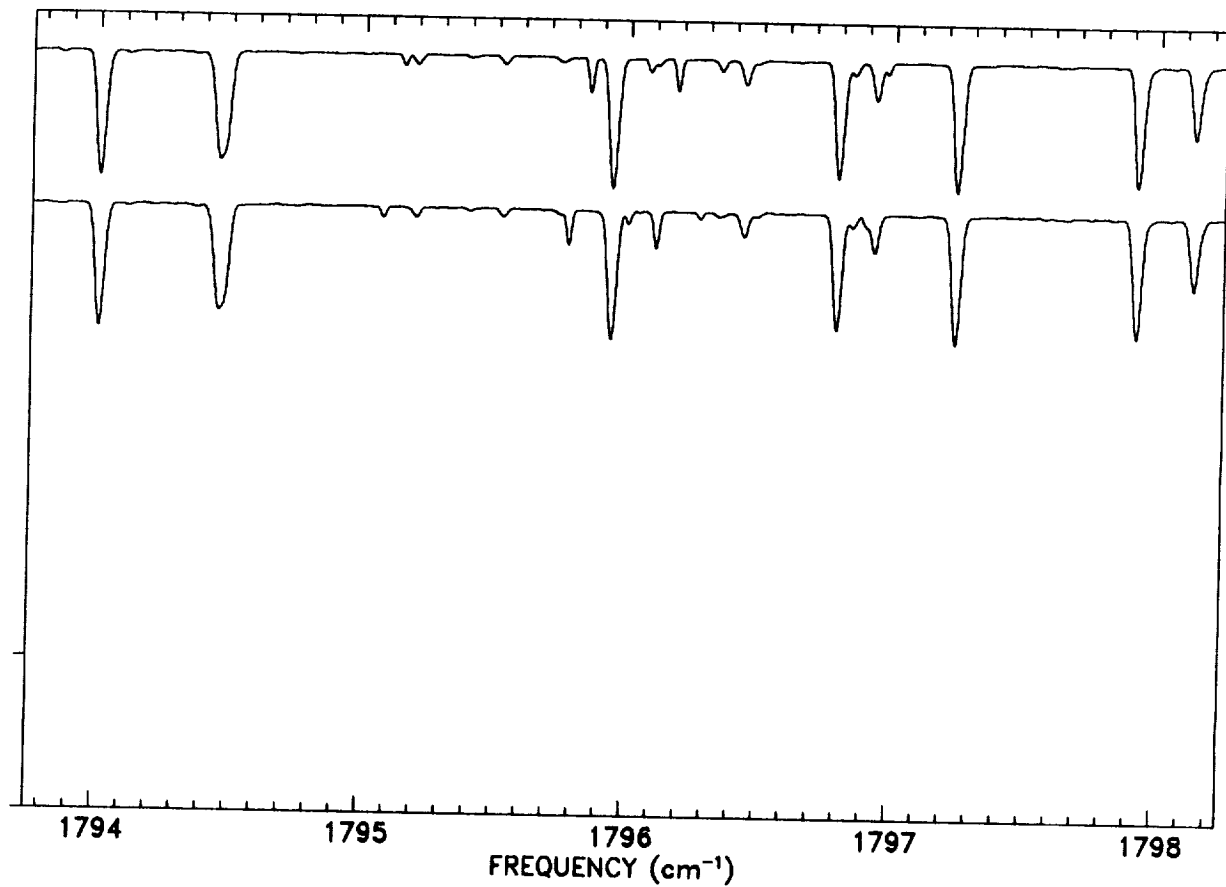
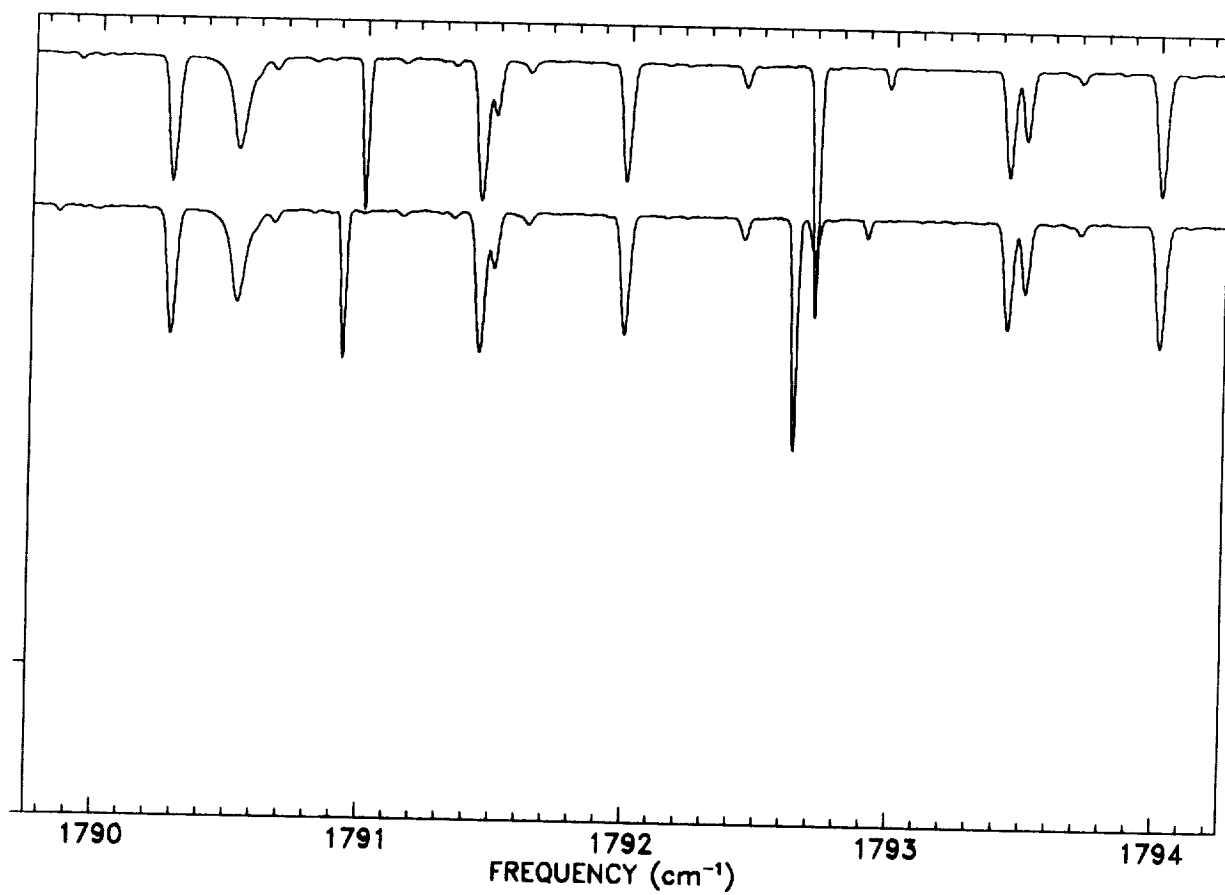


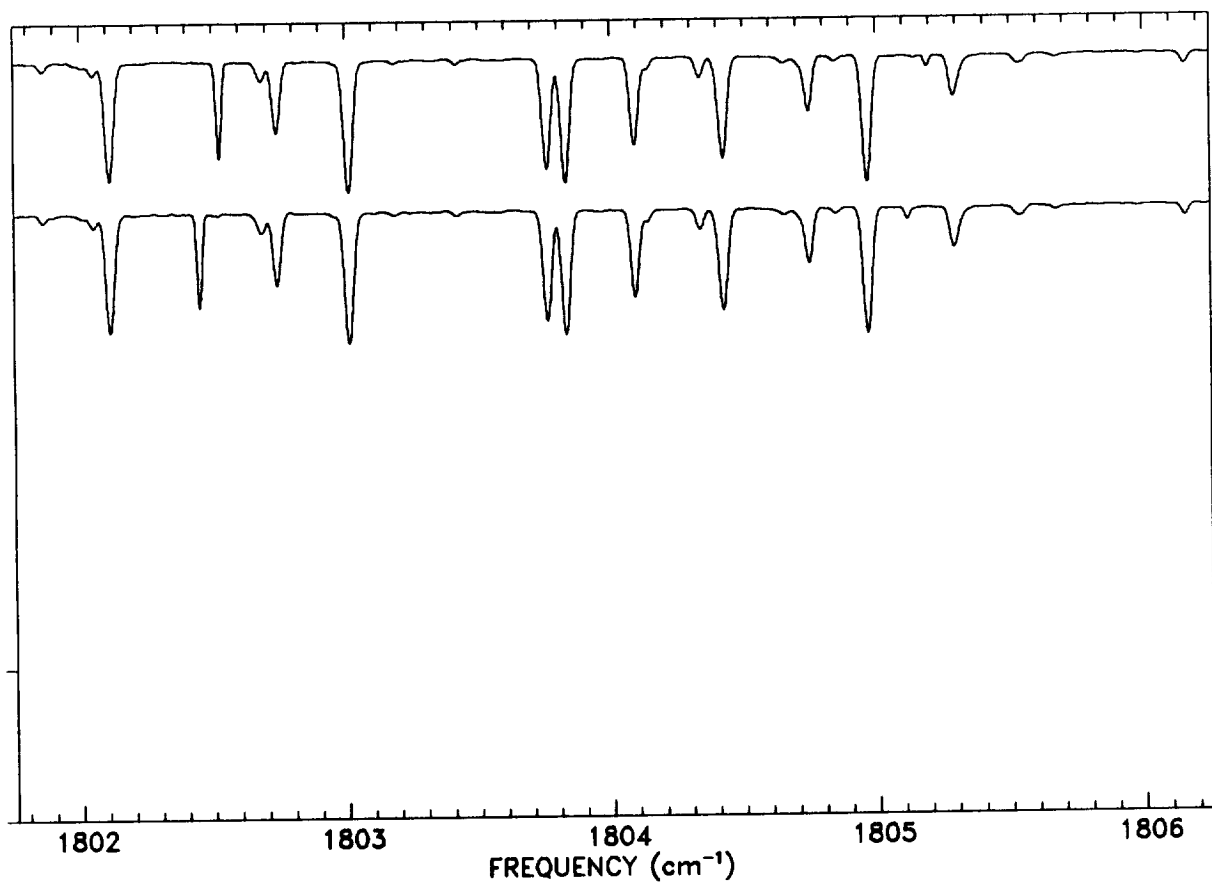
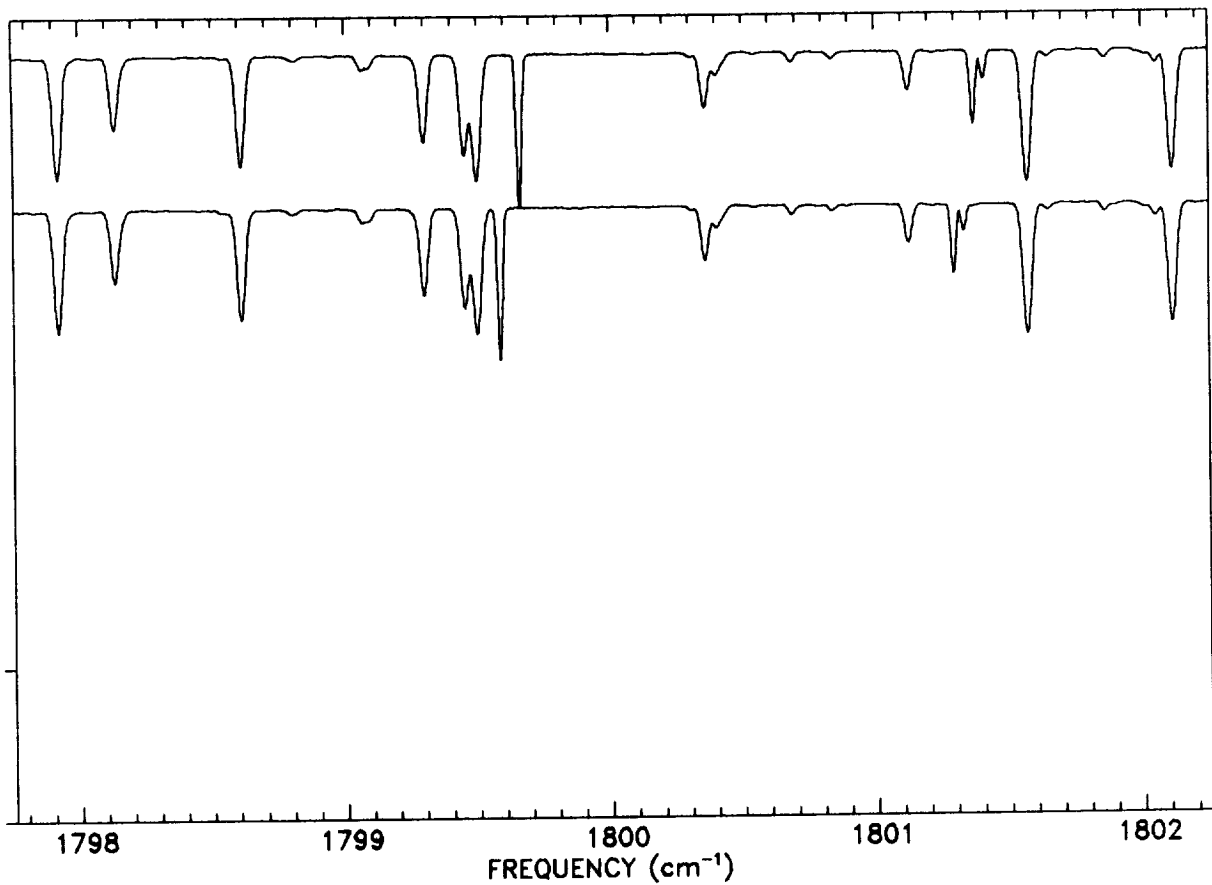


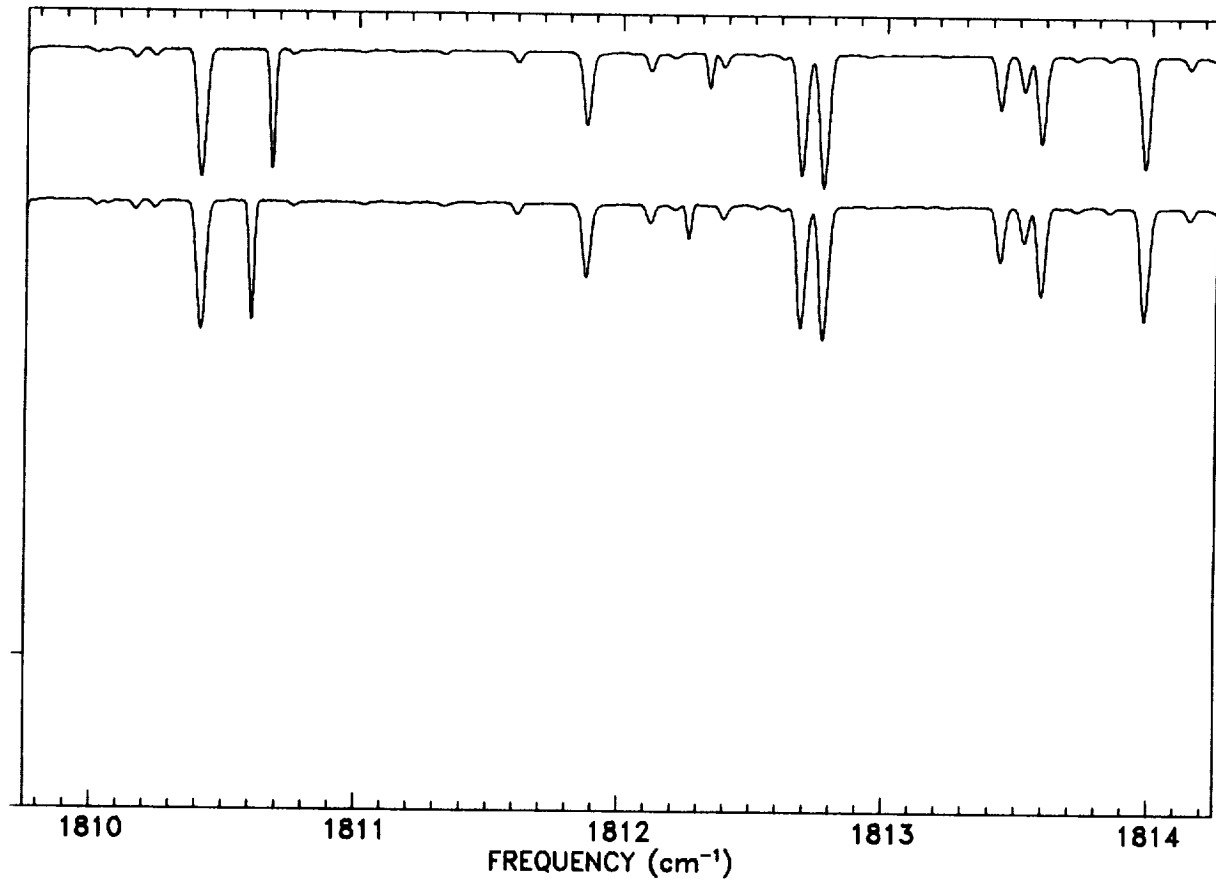
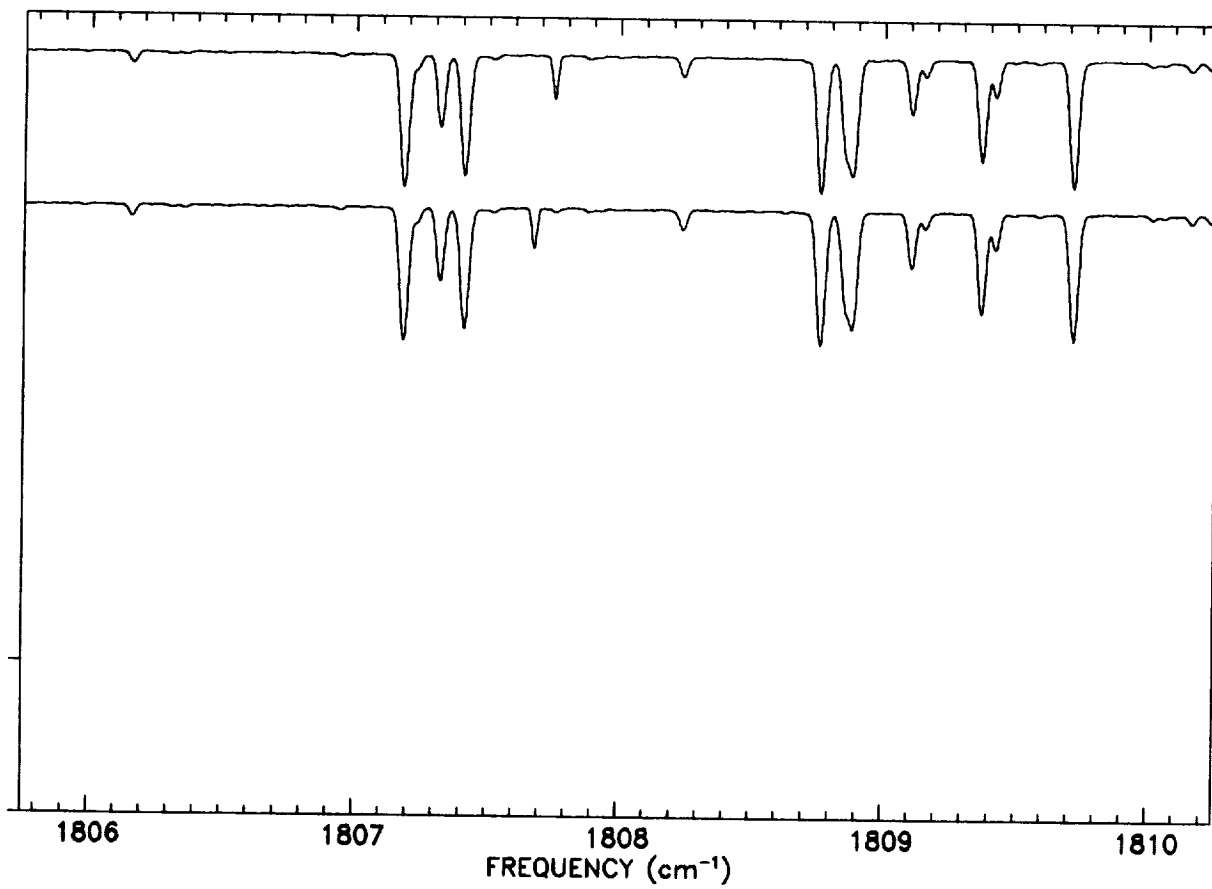


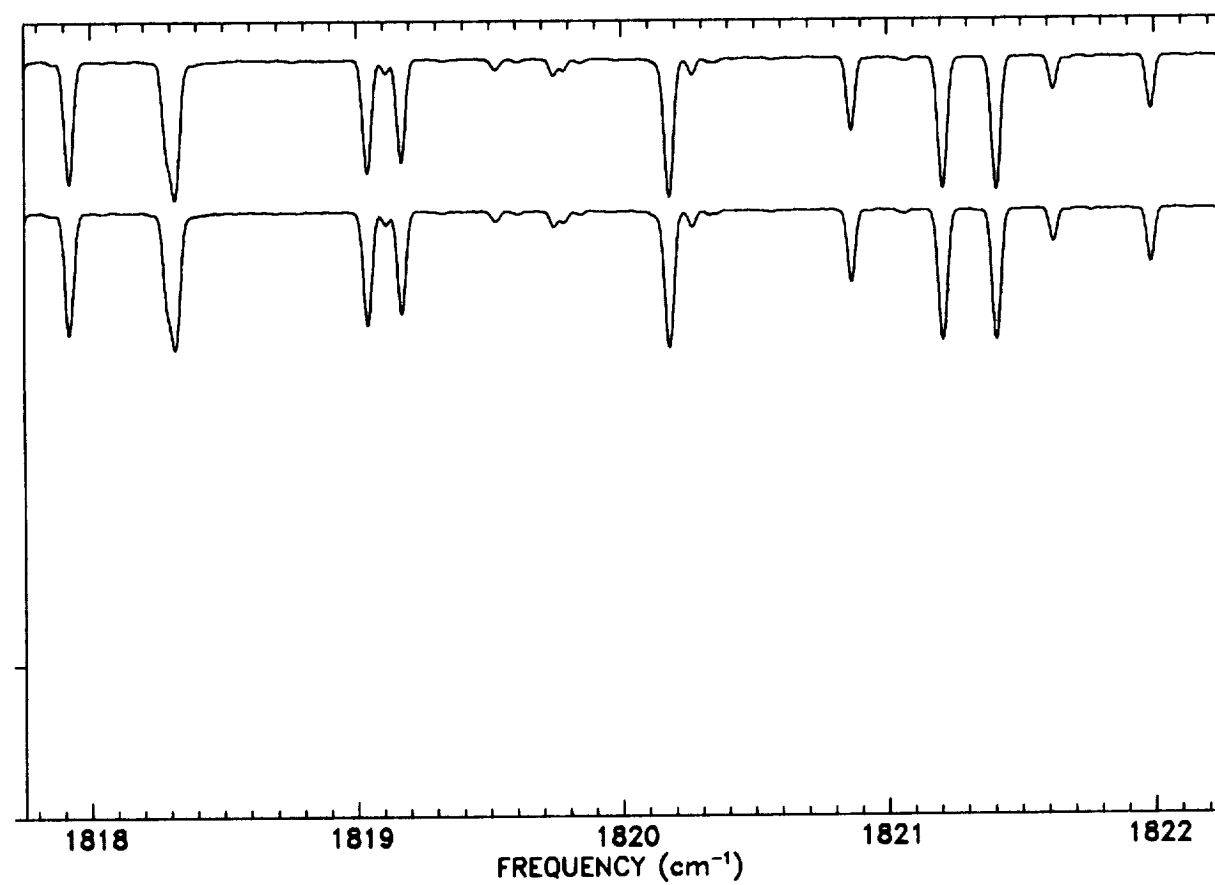
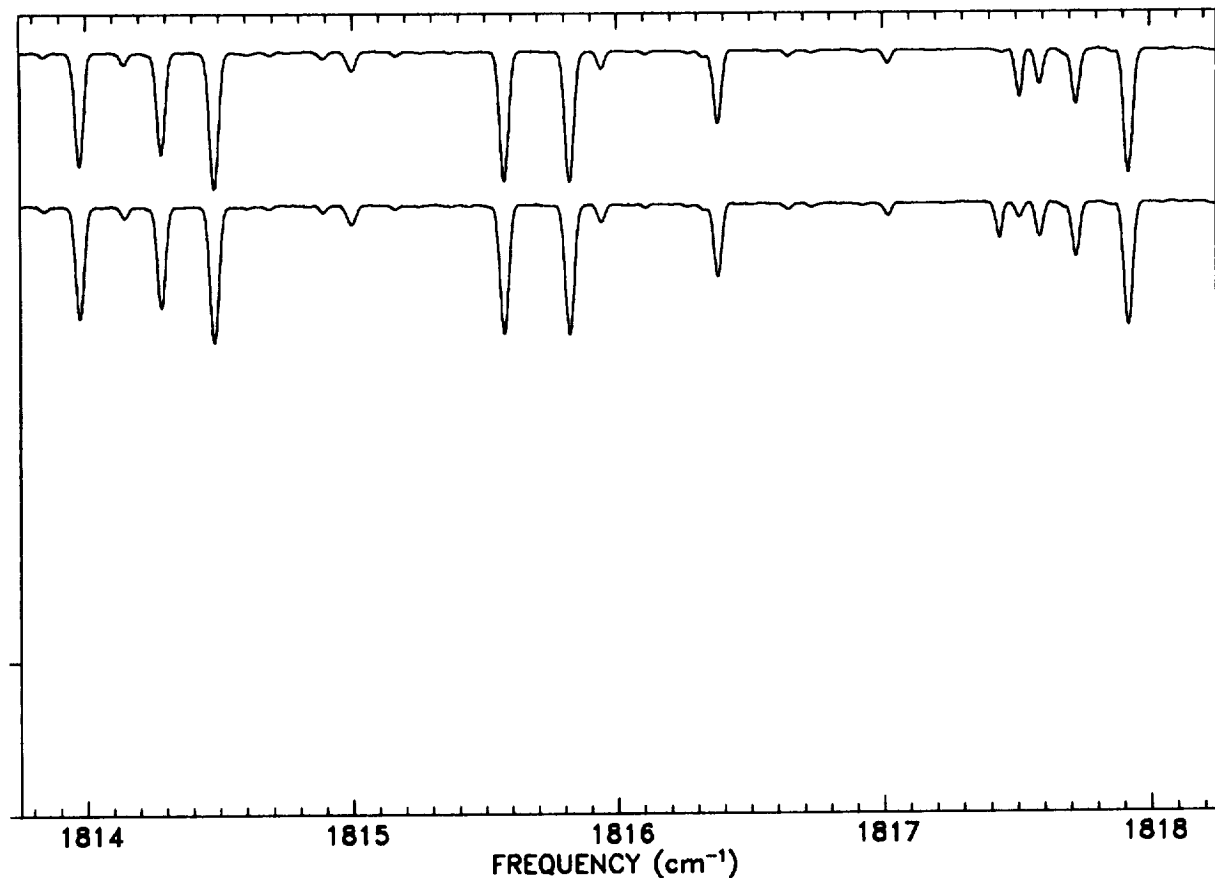


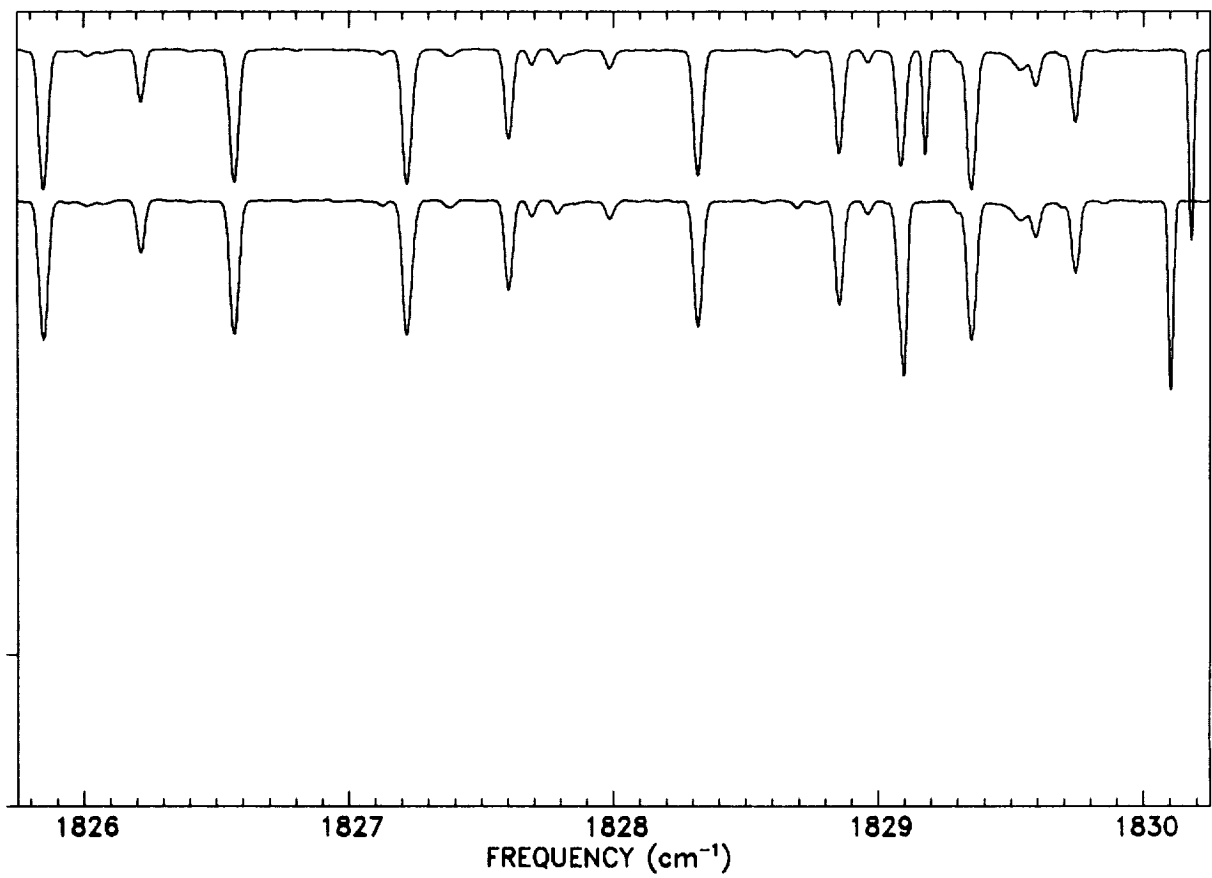
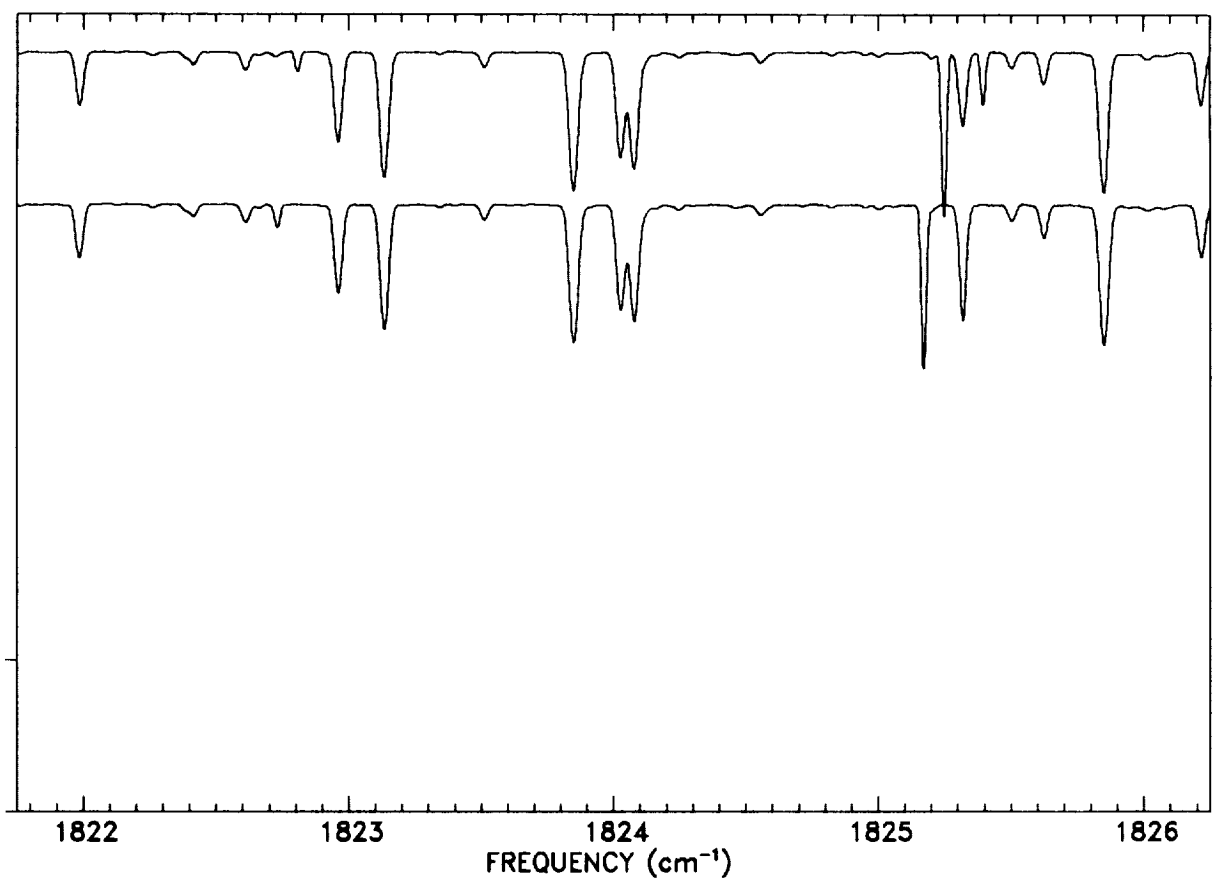


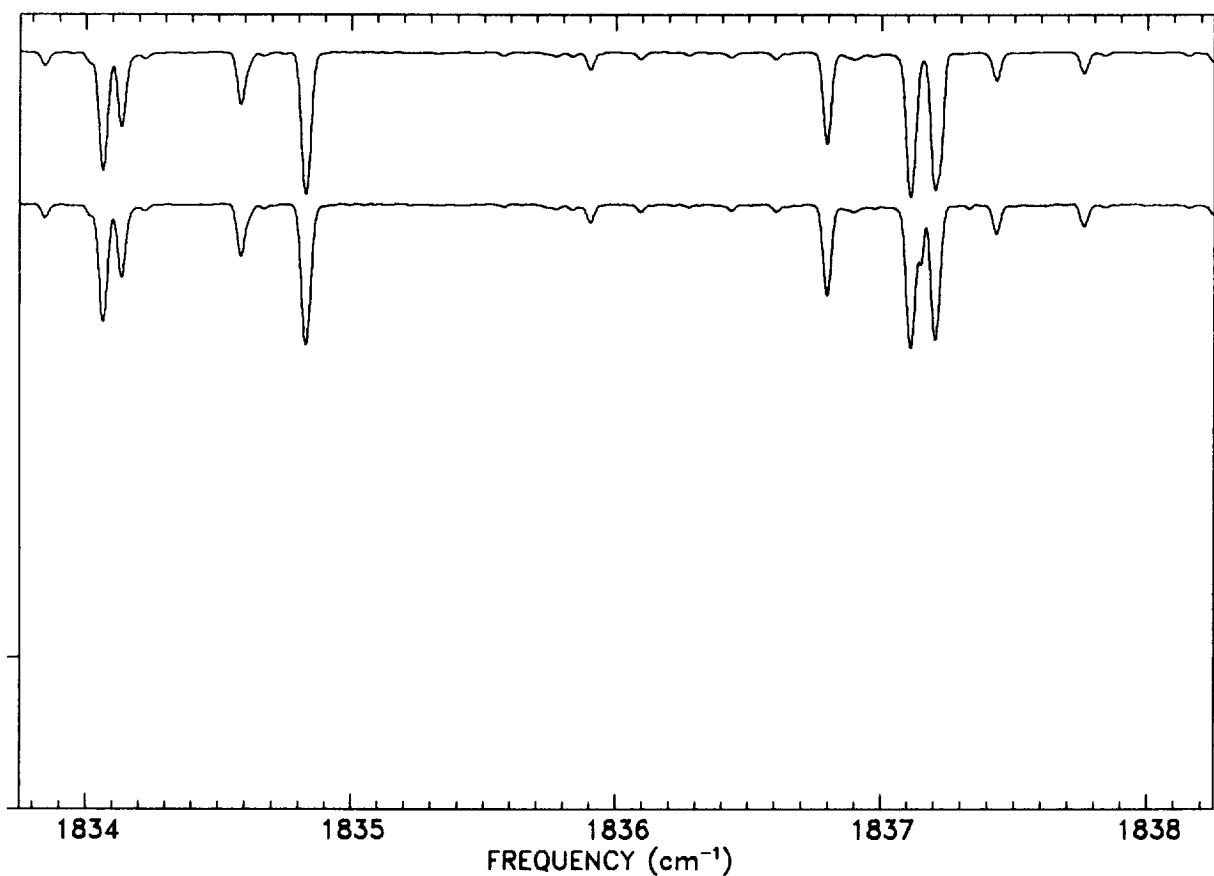
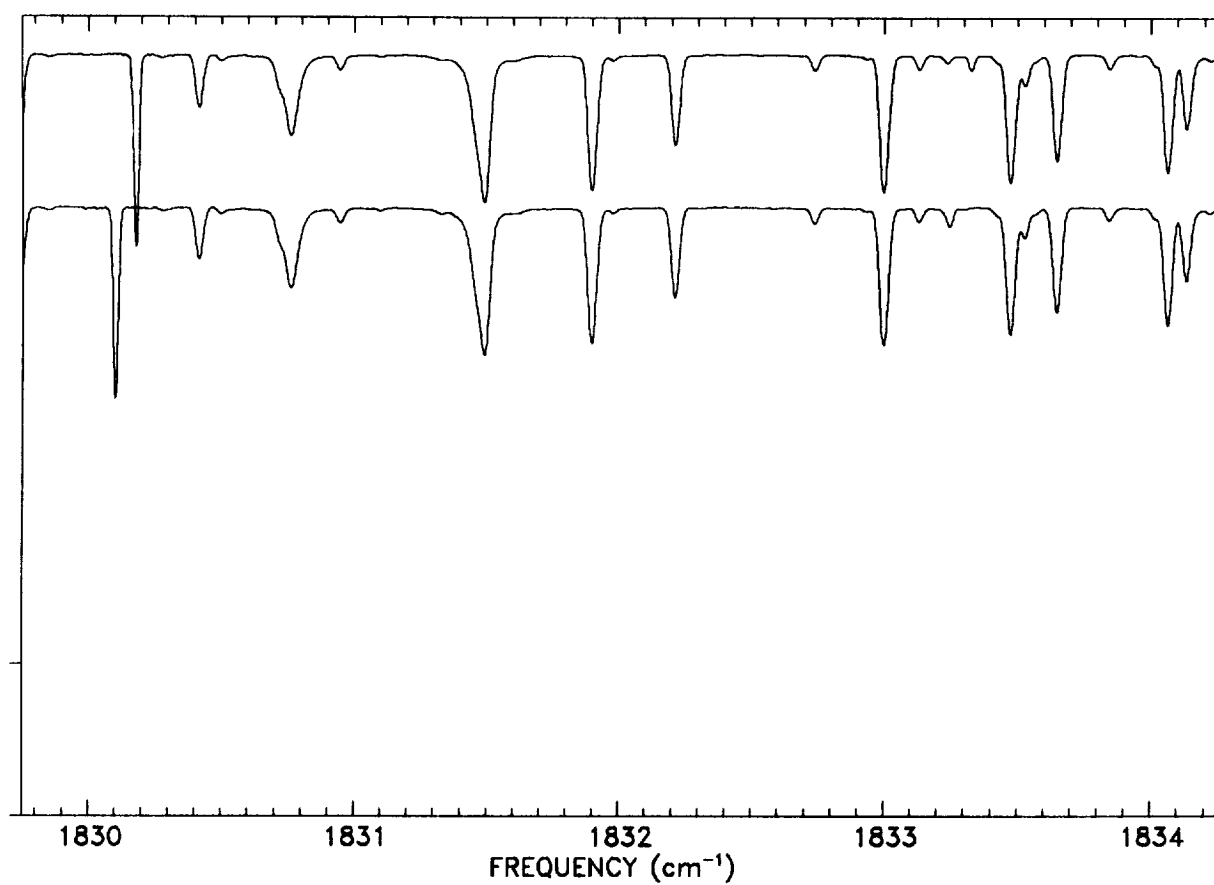


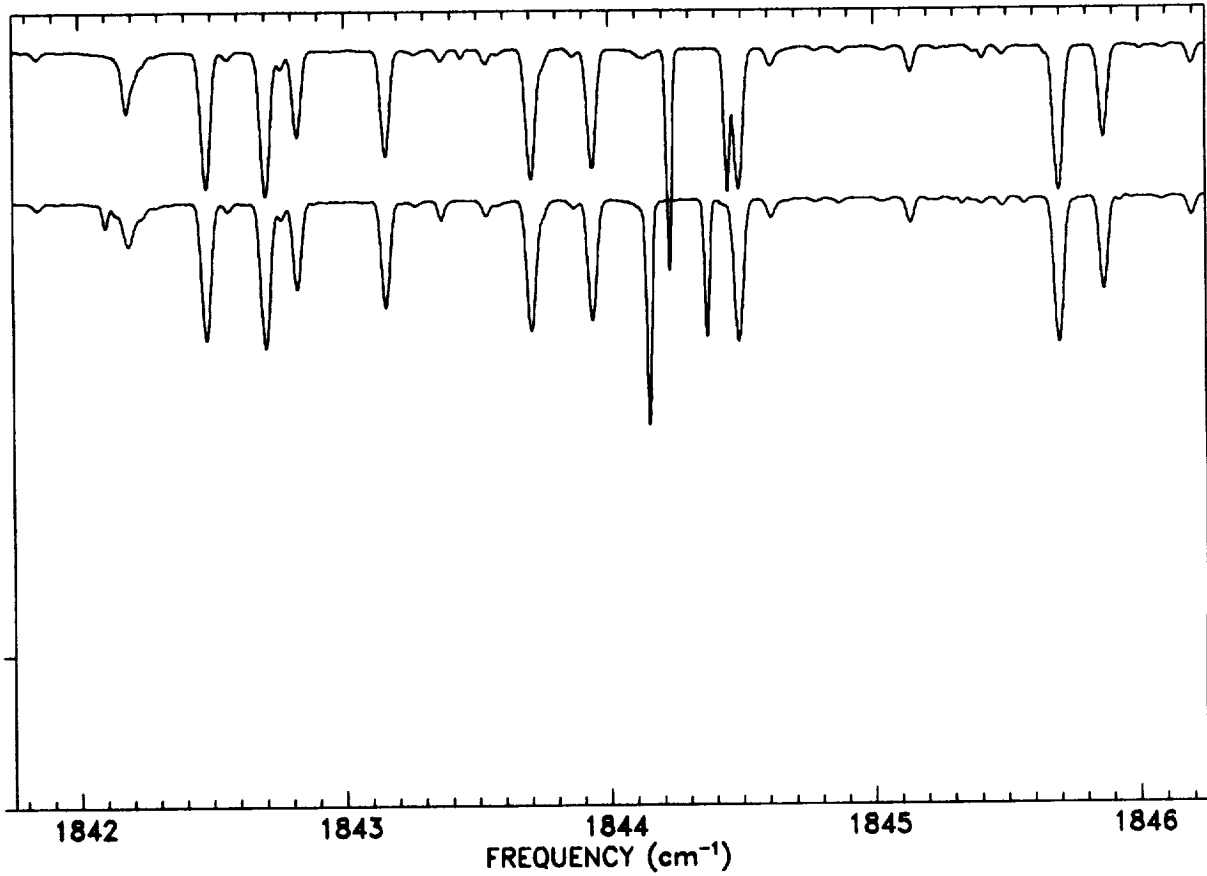
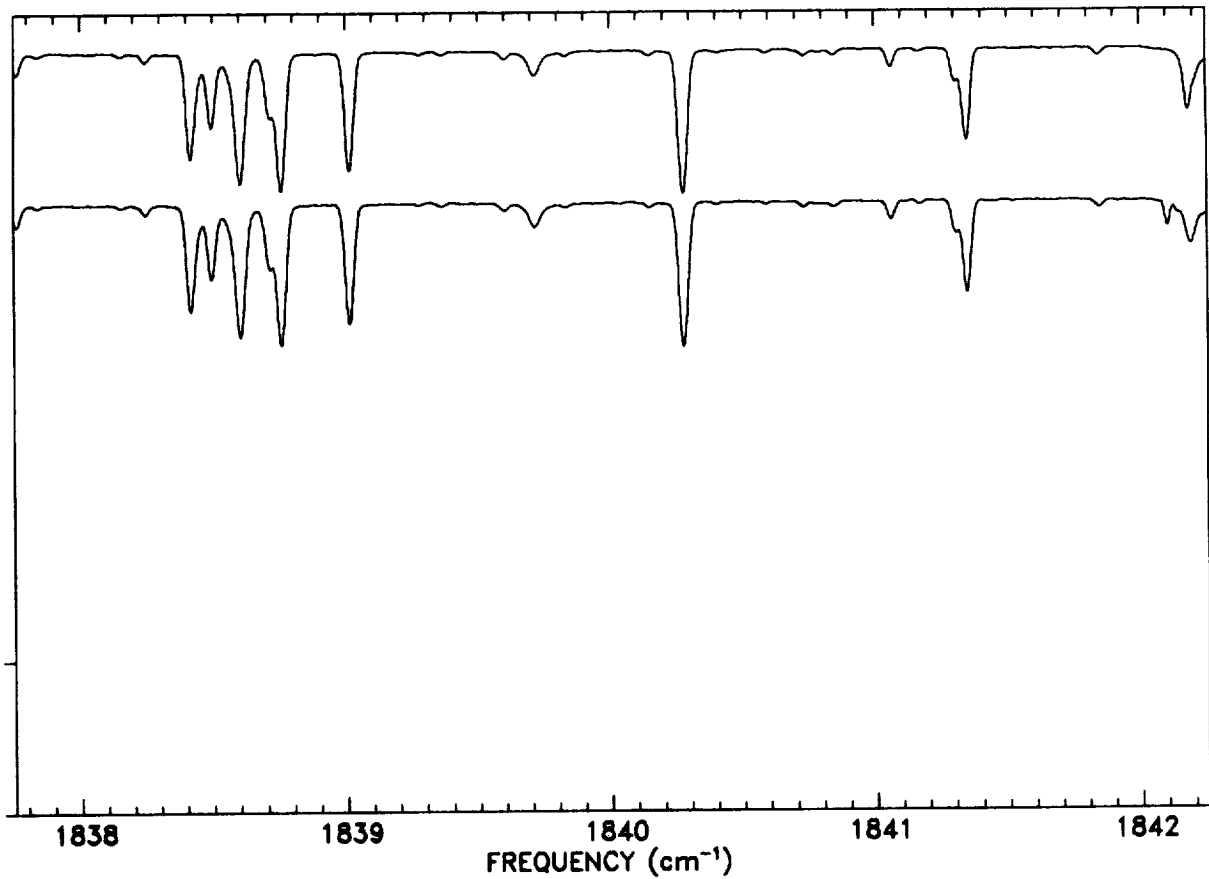


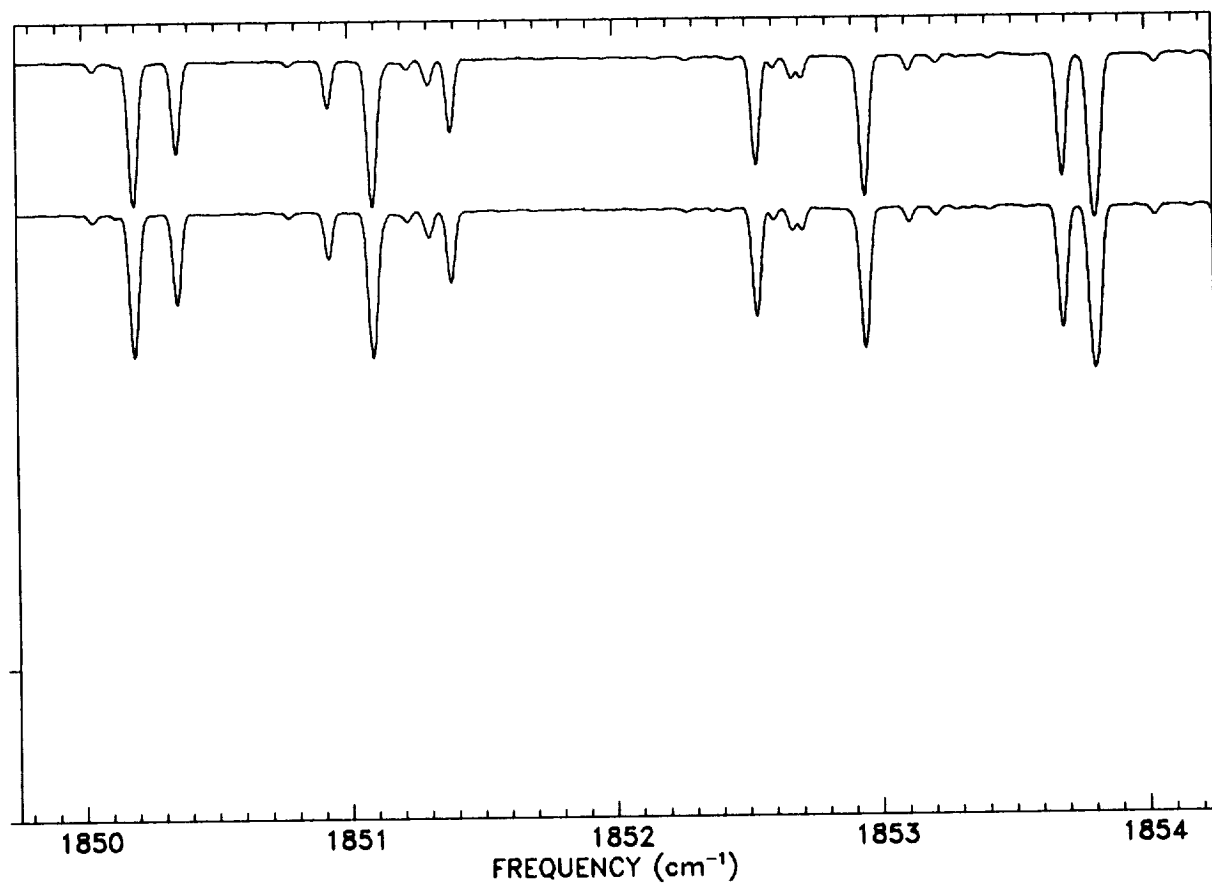
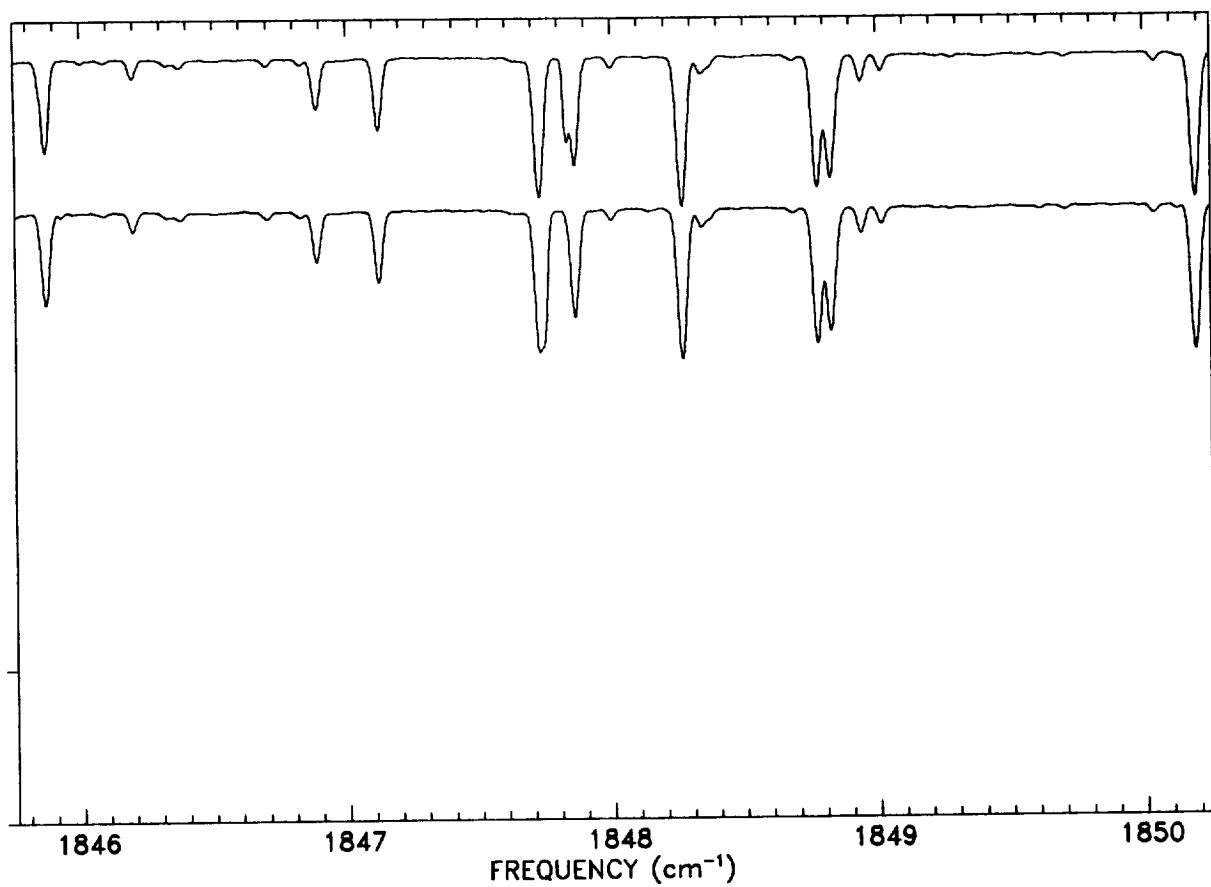


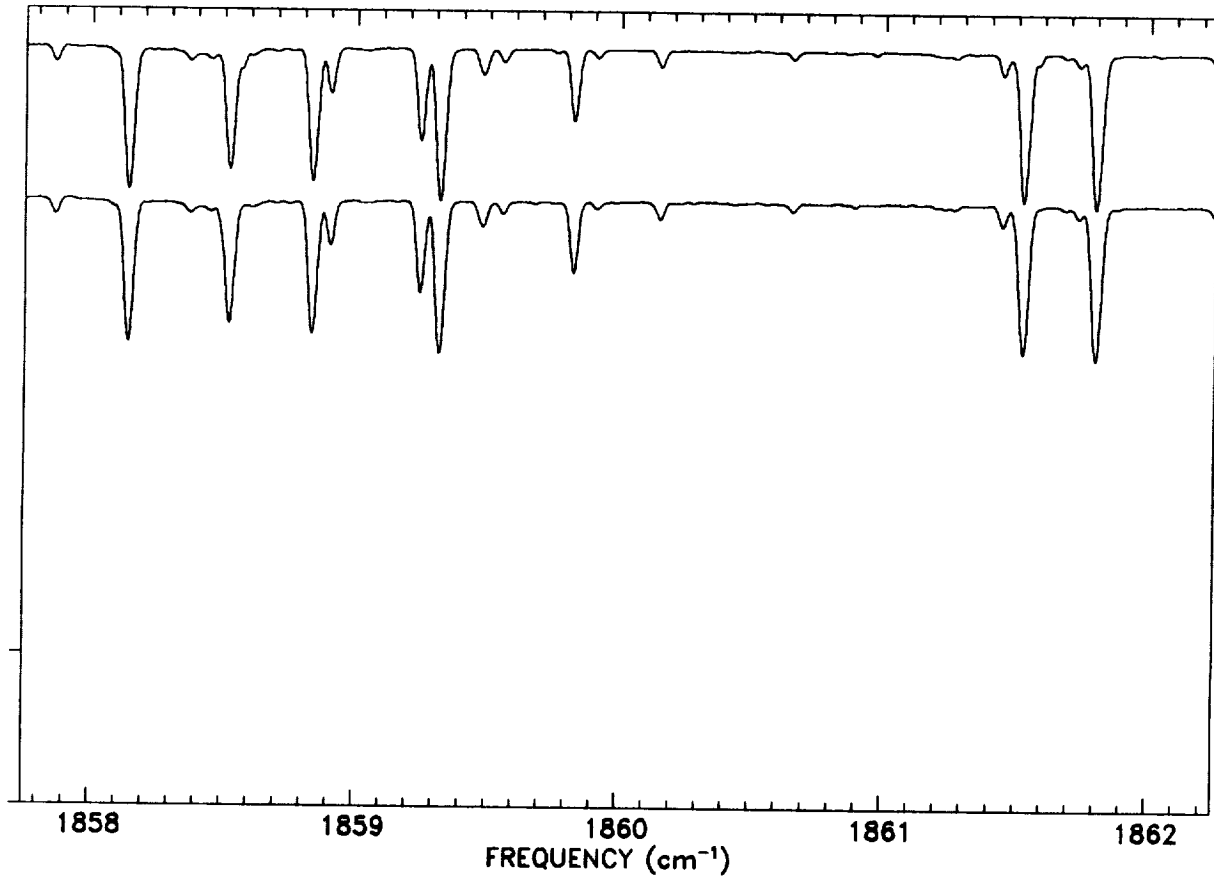
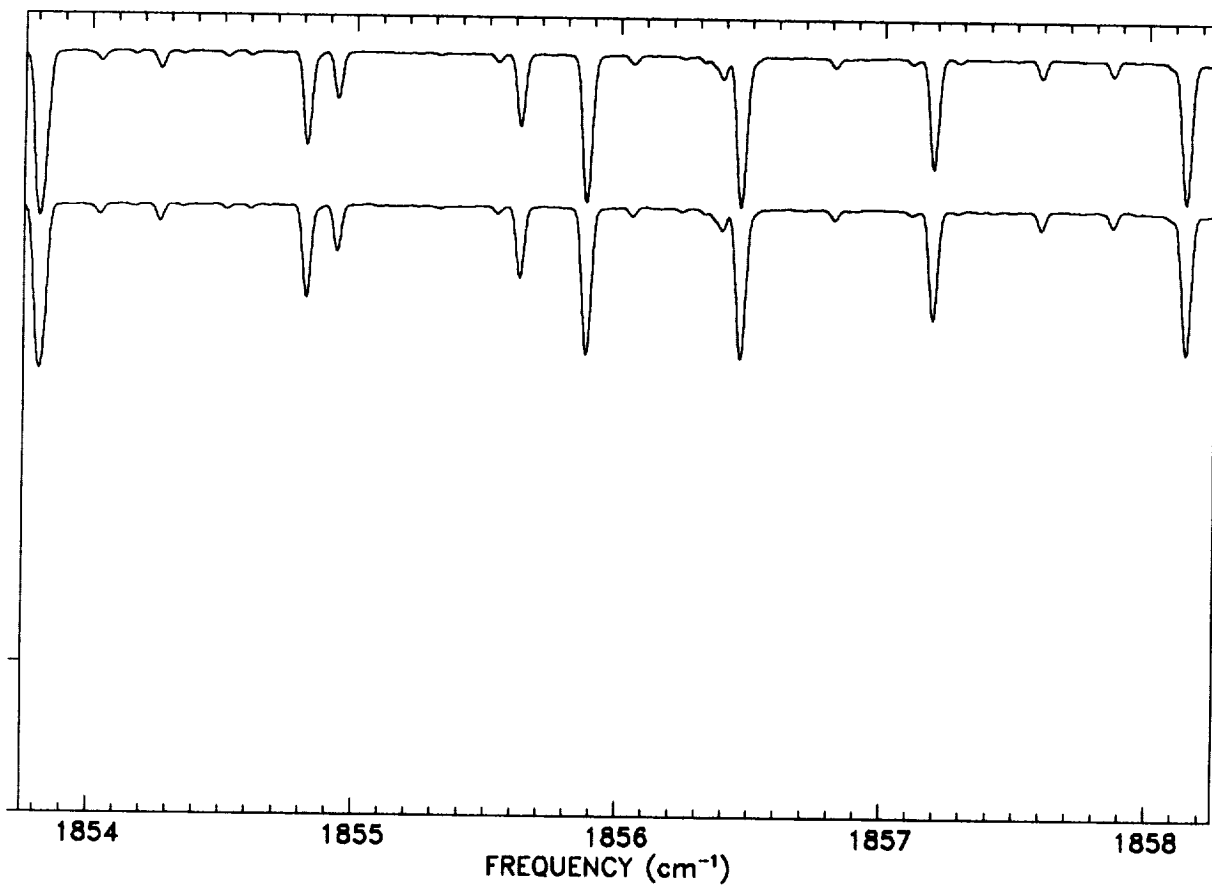


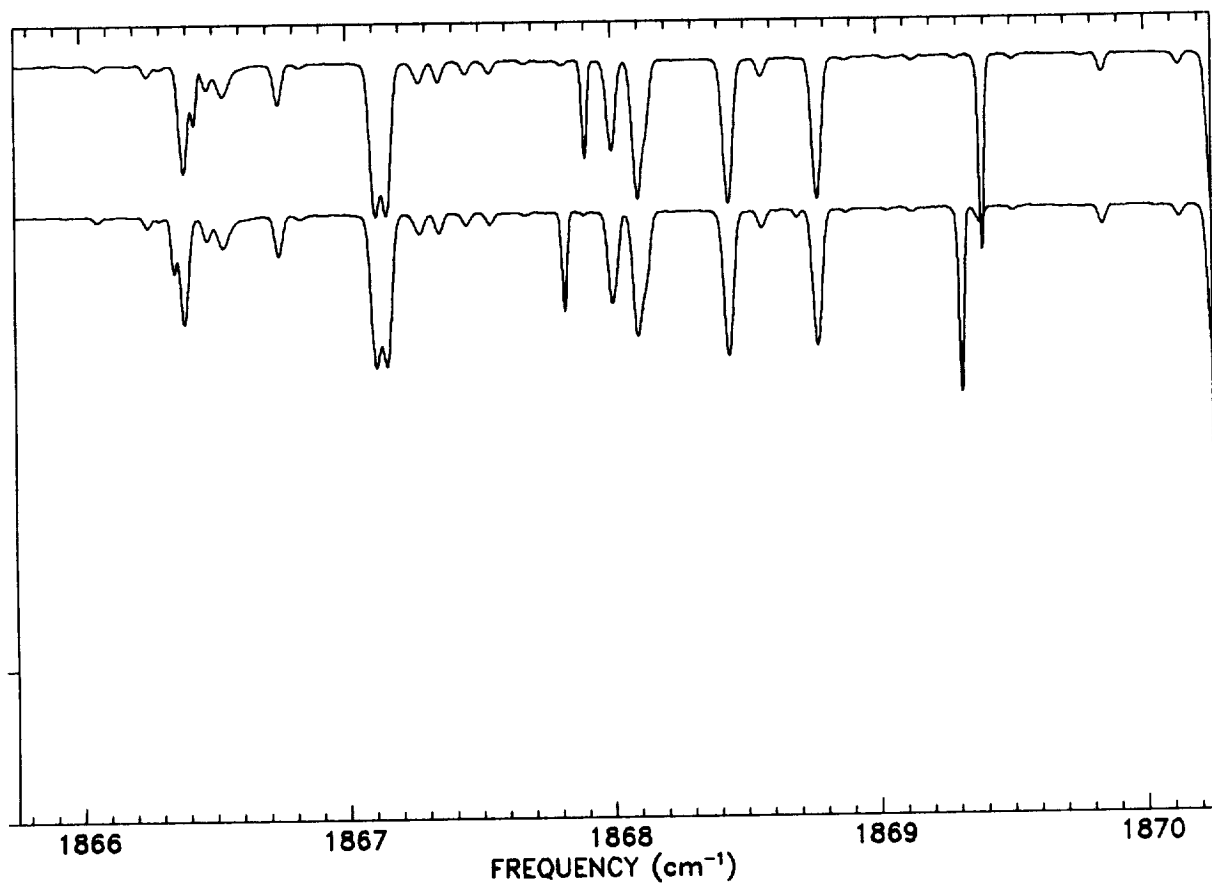
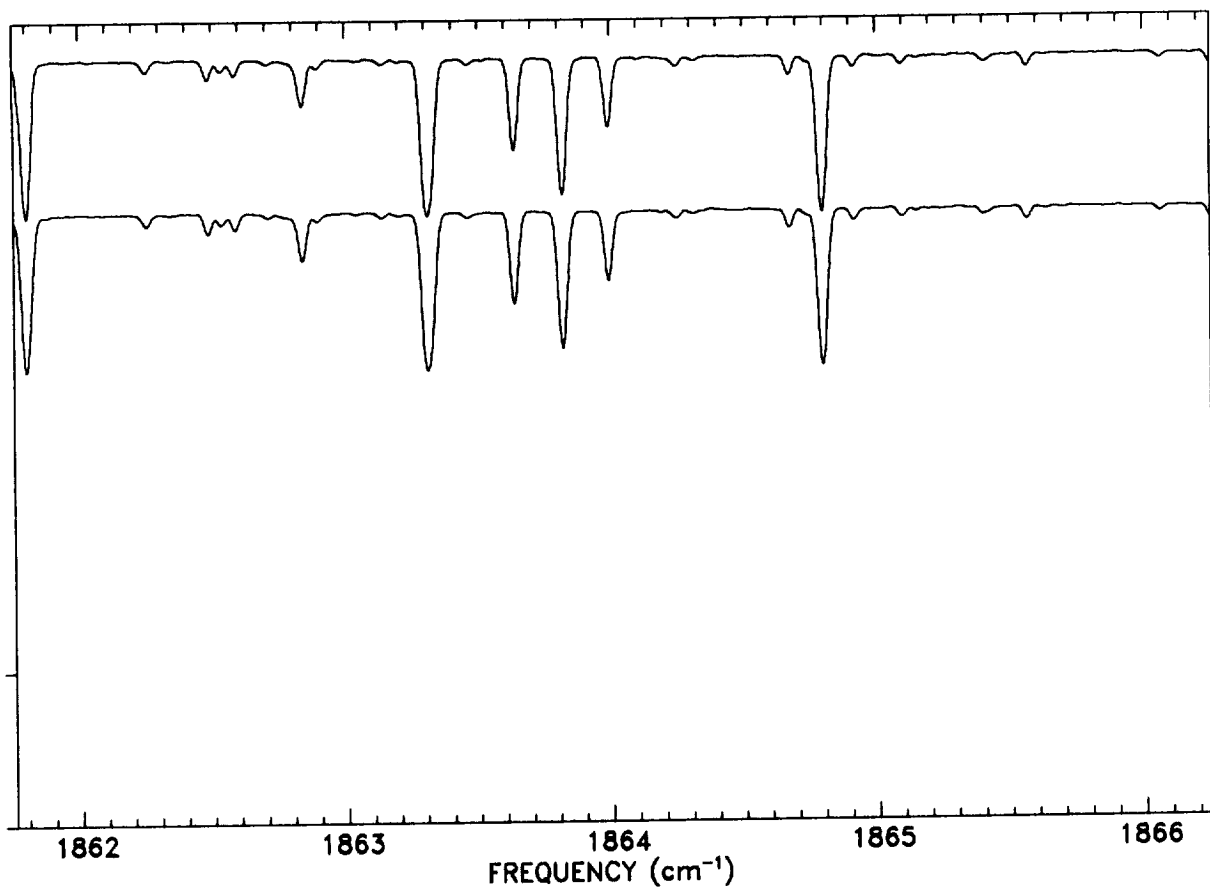


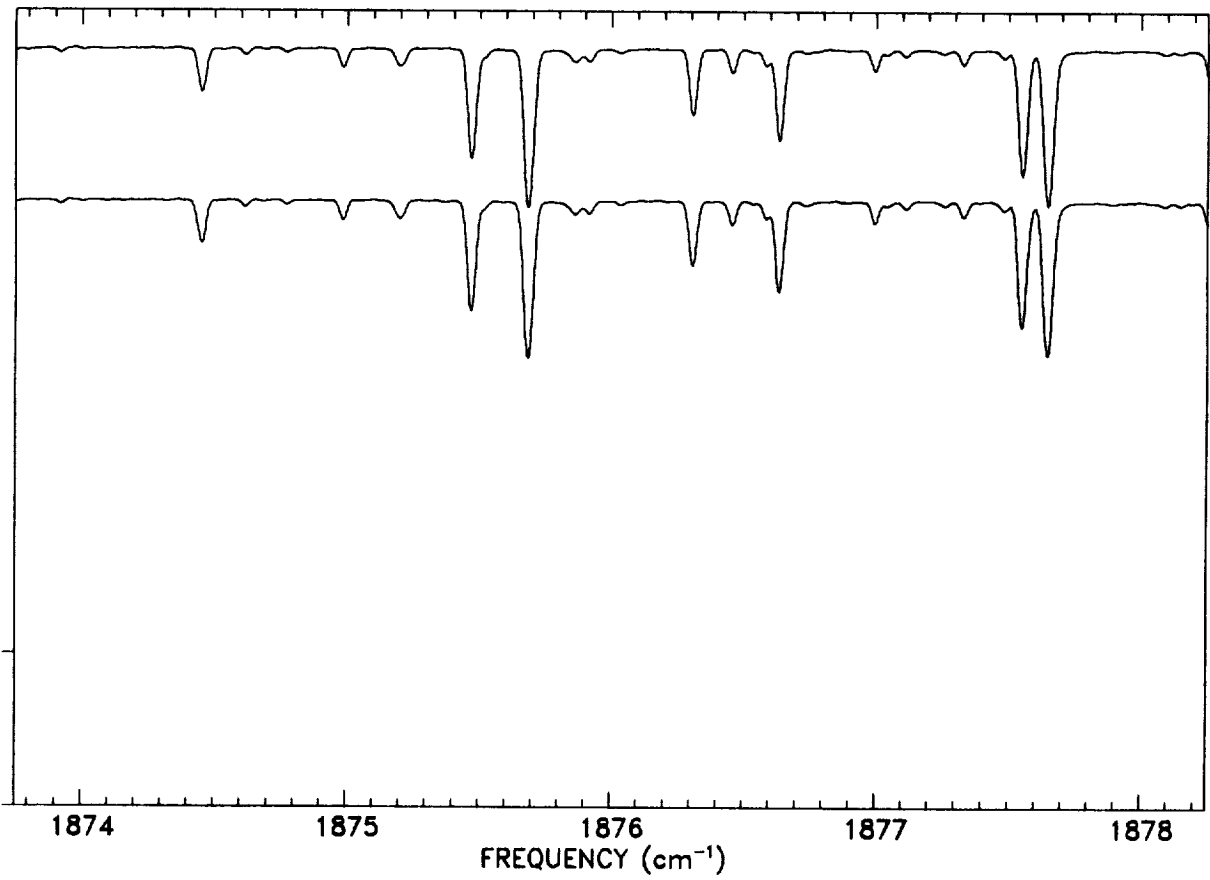
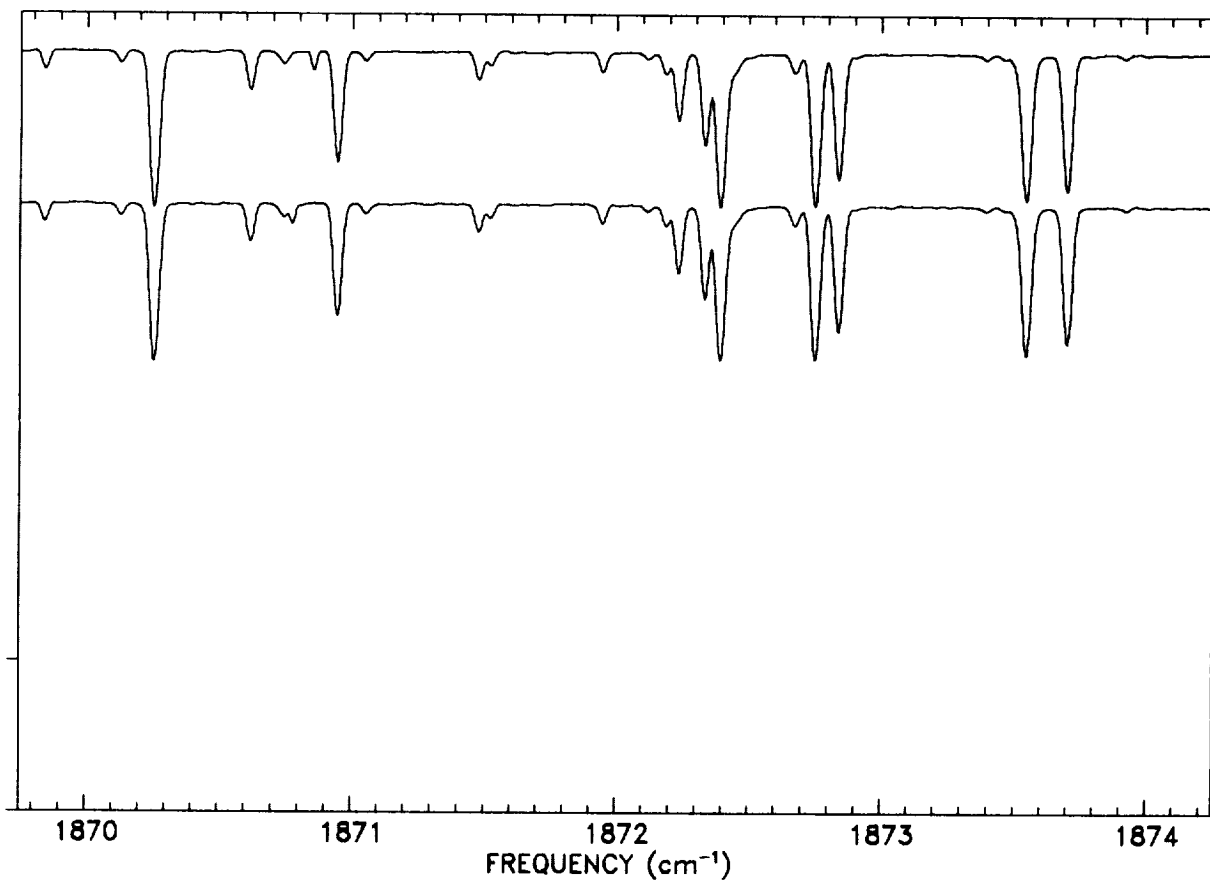


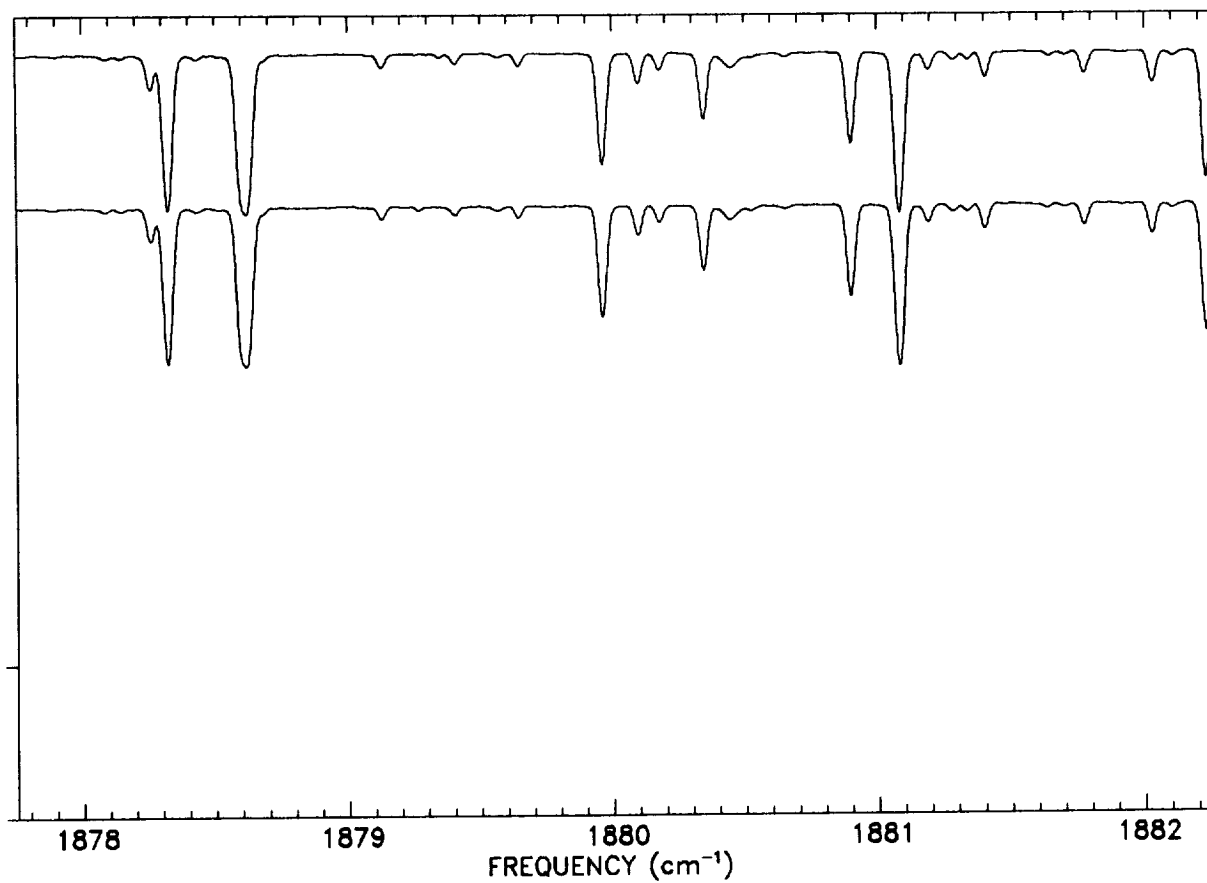






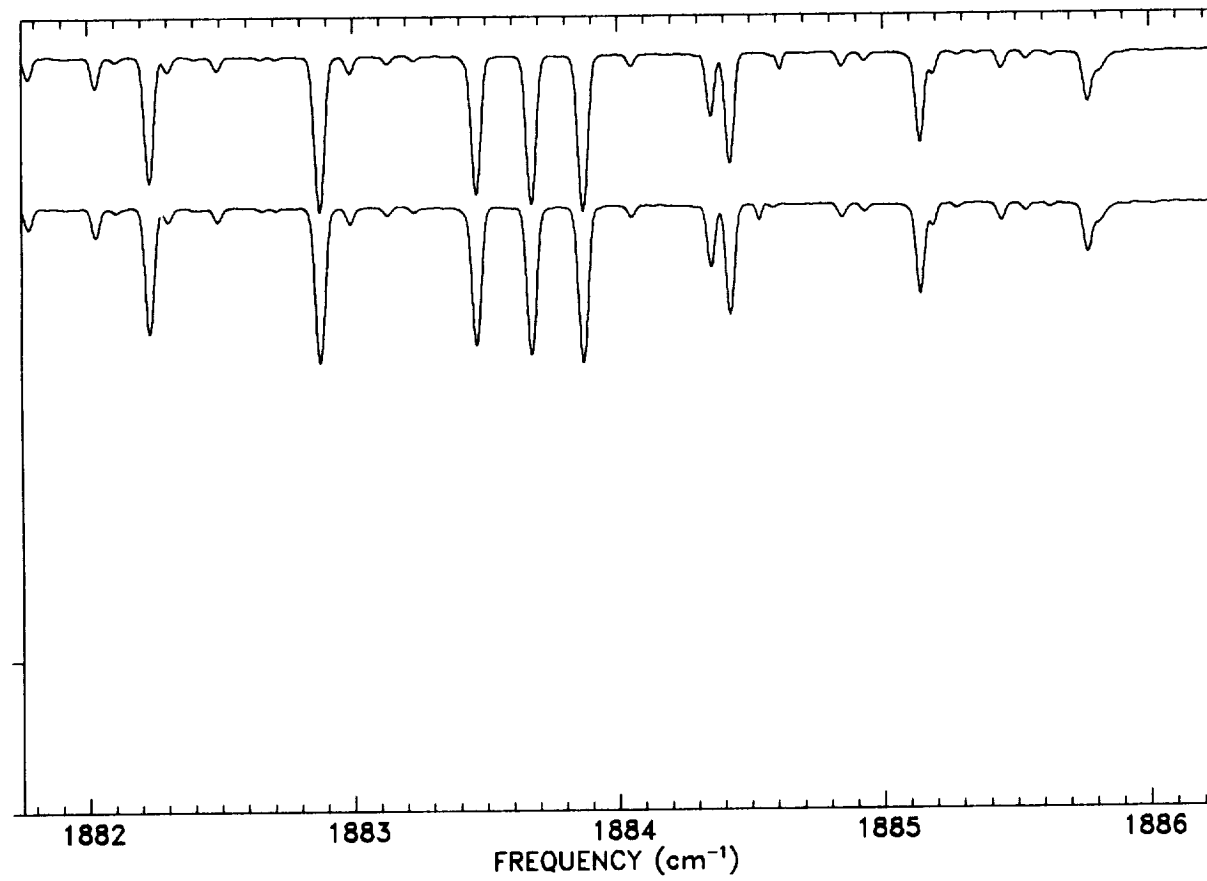






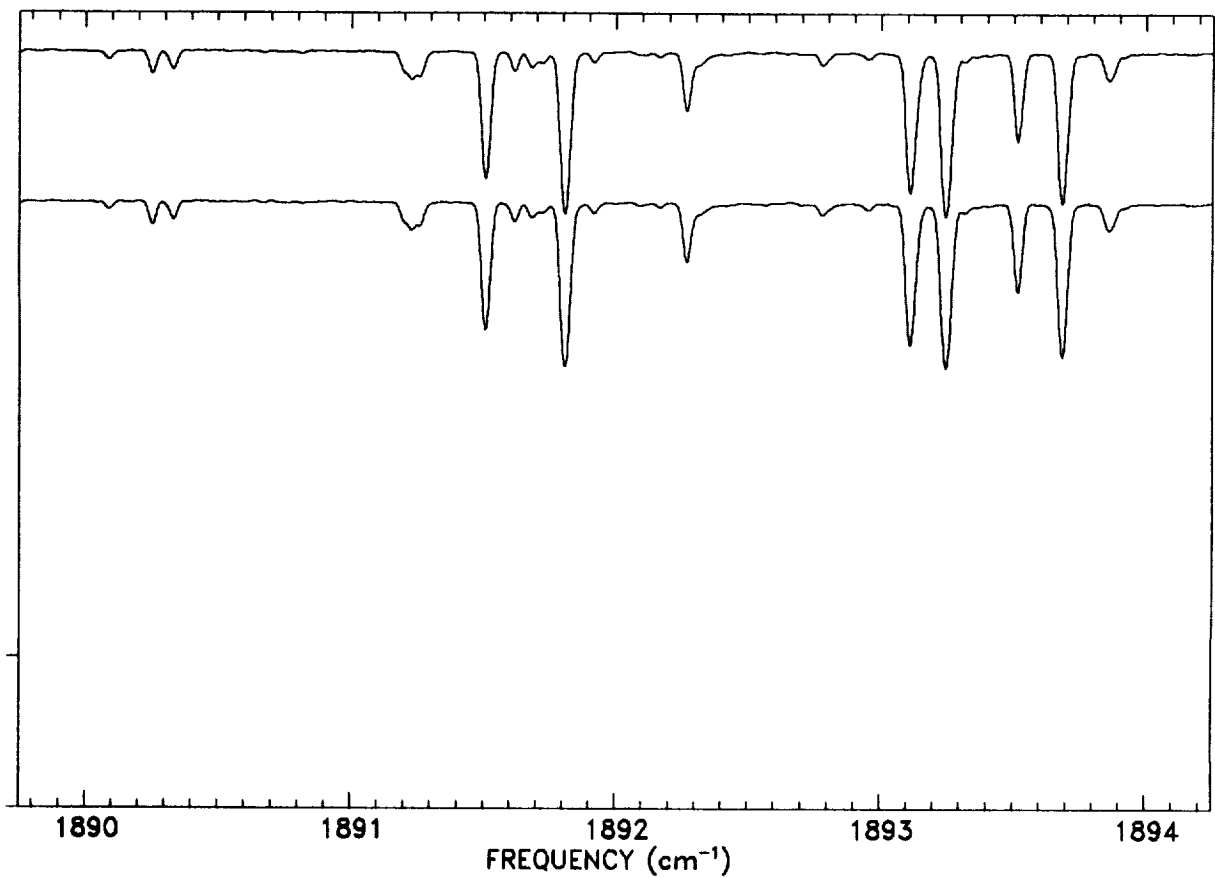
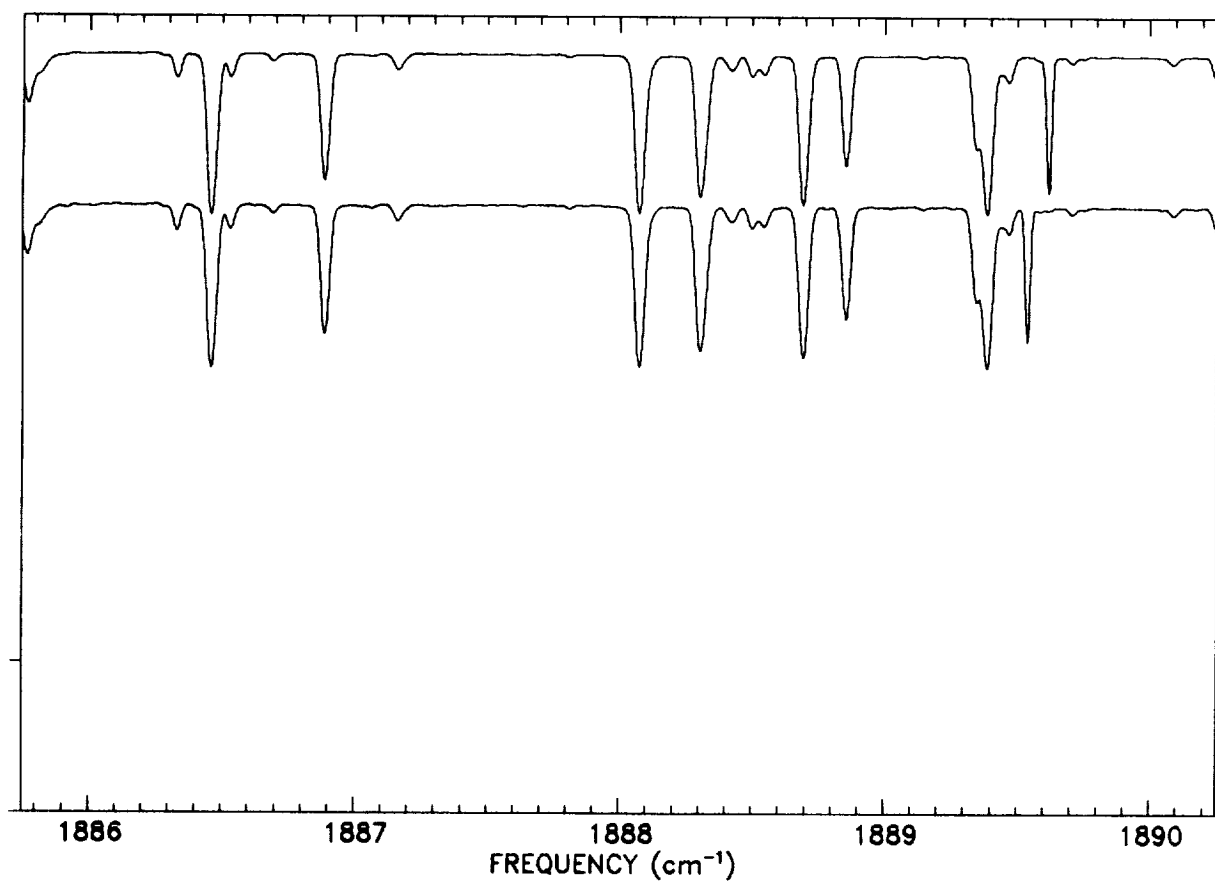
1878 1879 1880 1881 1882

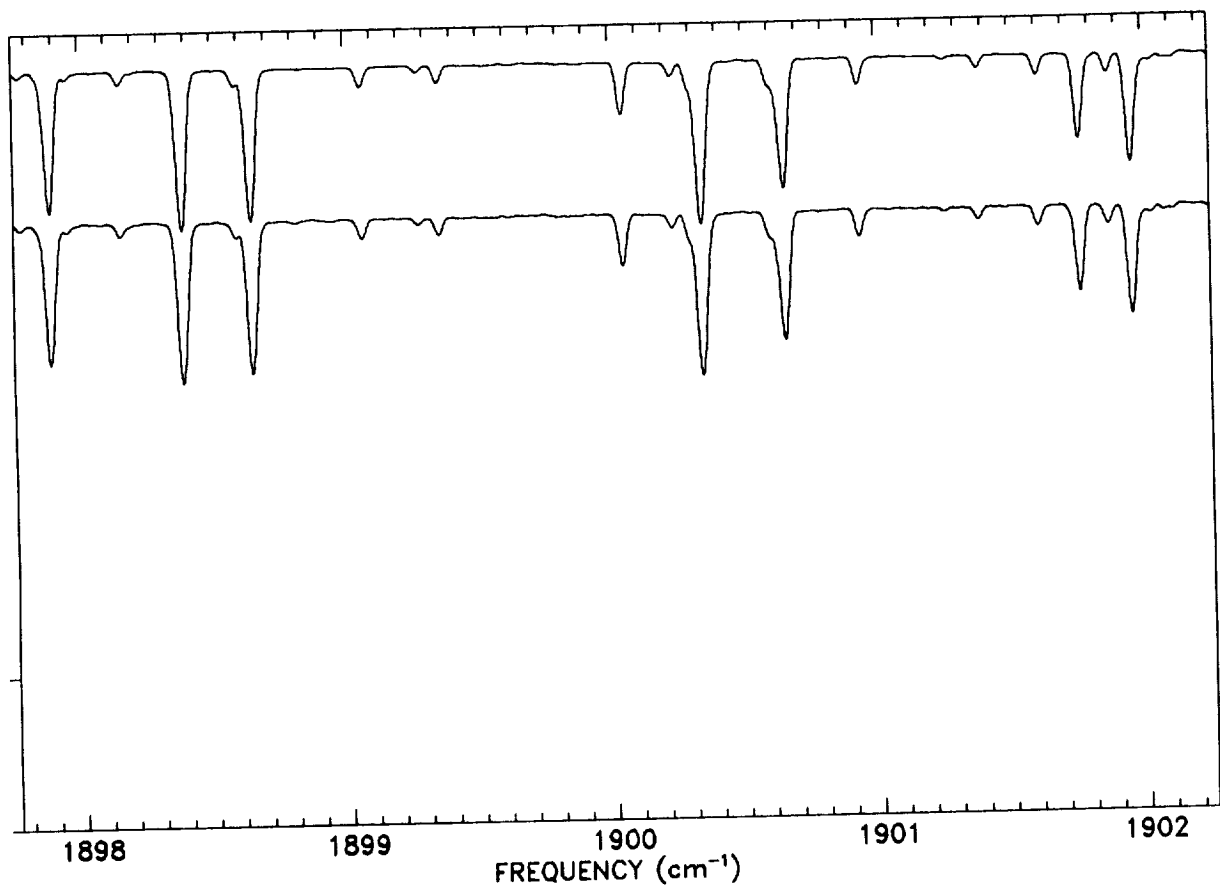
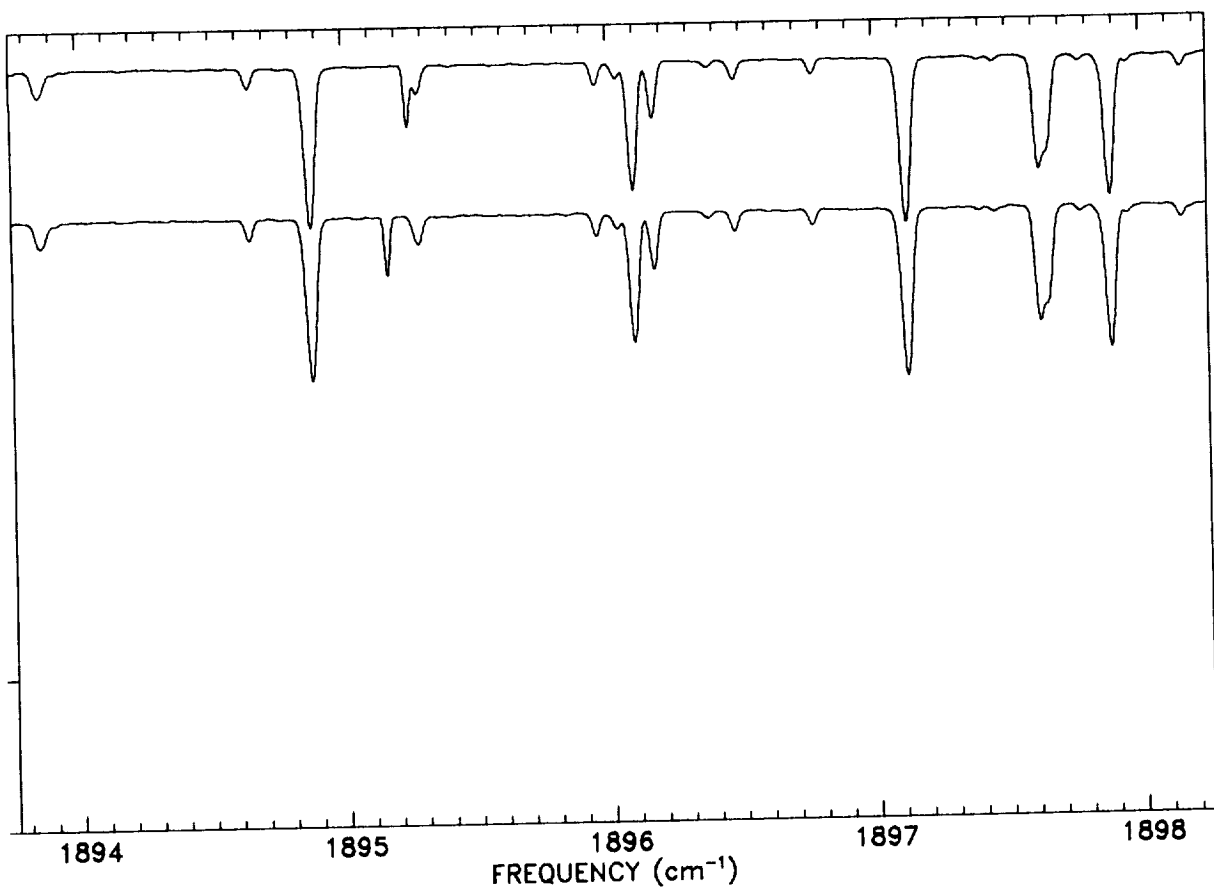
FREQUENCY (cm^{-1})

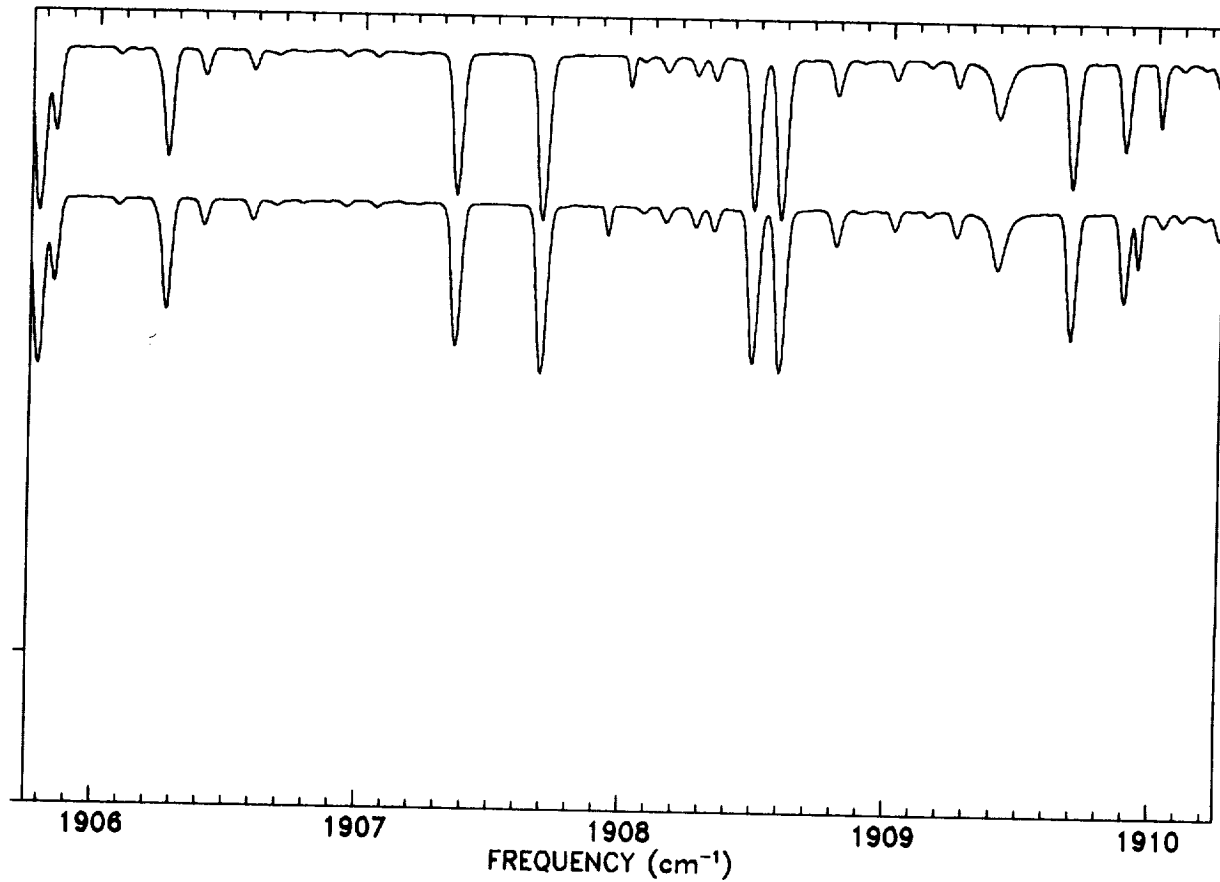
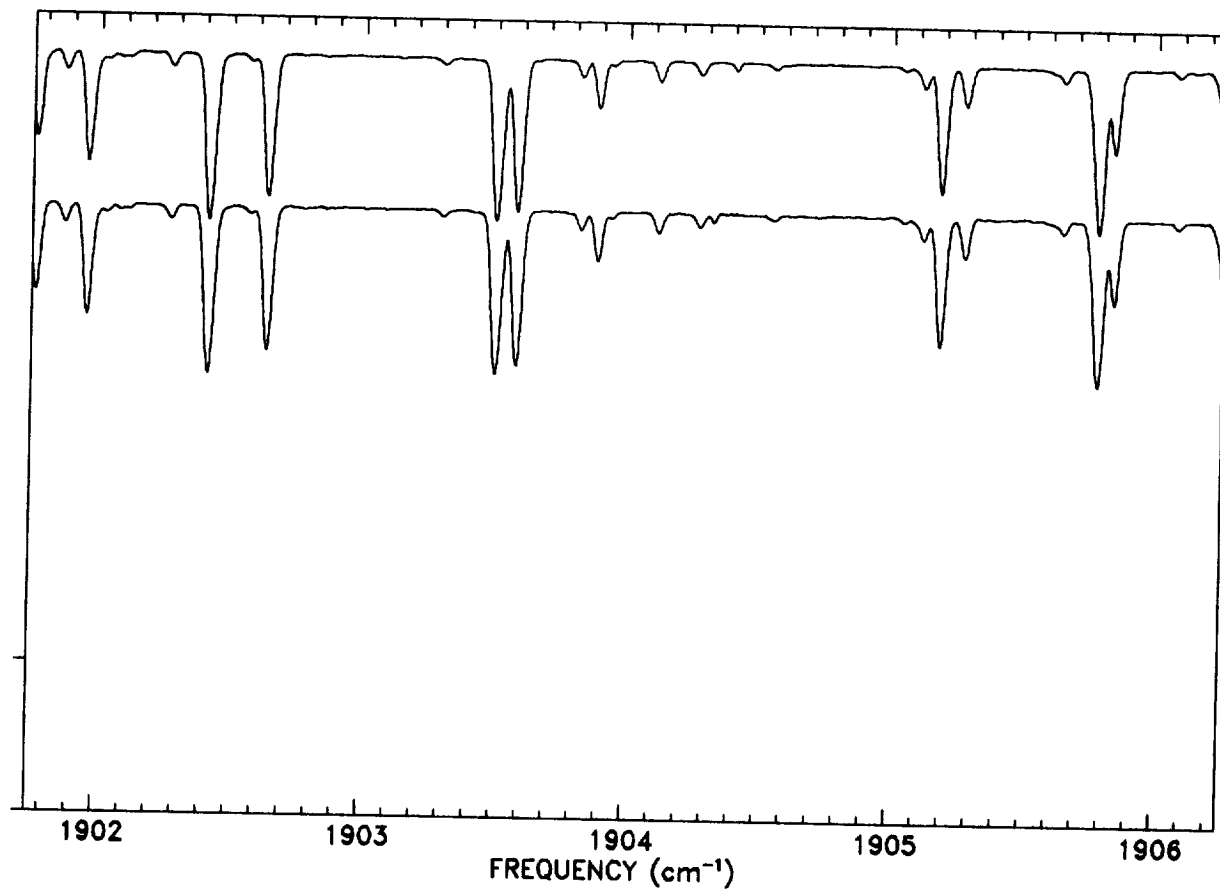


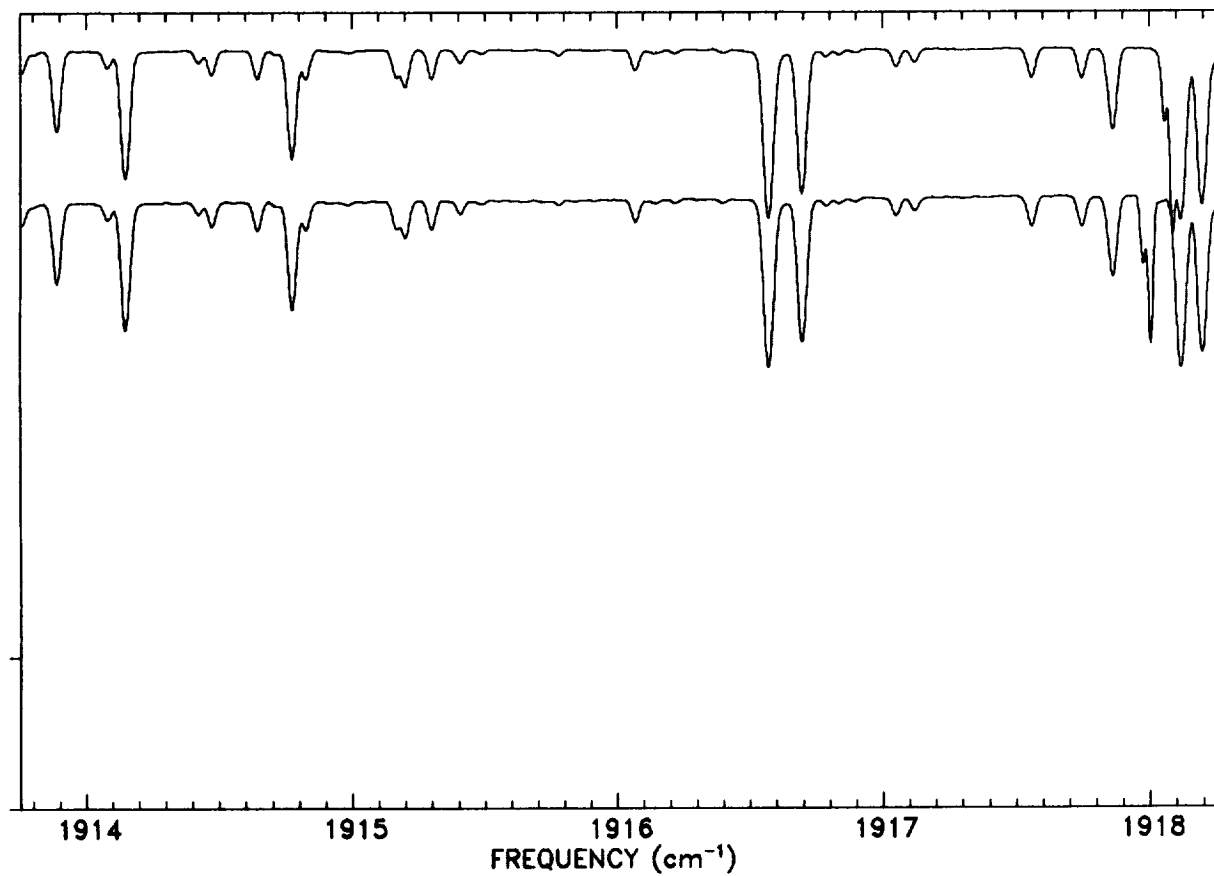
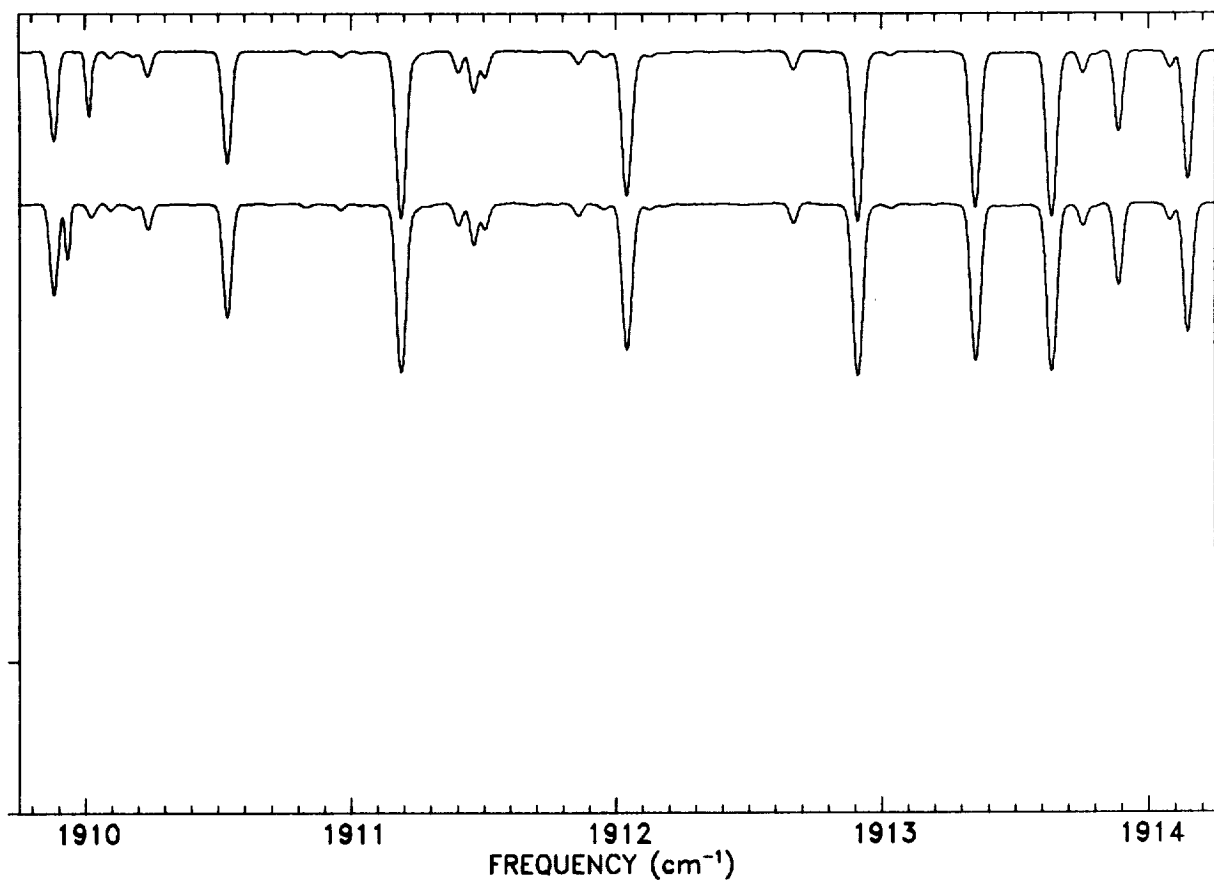
1882 1883 1884 1885 1886

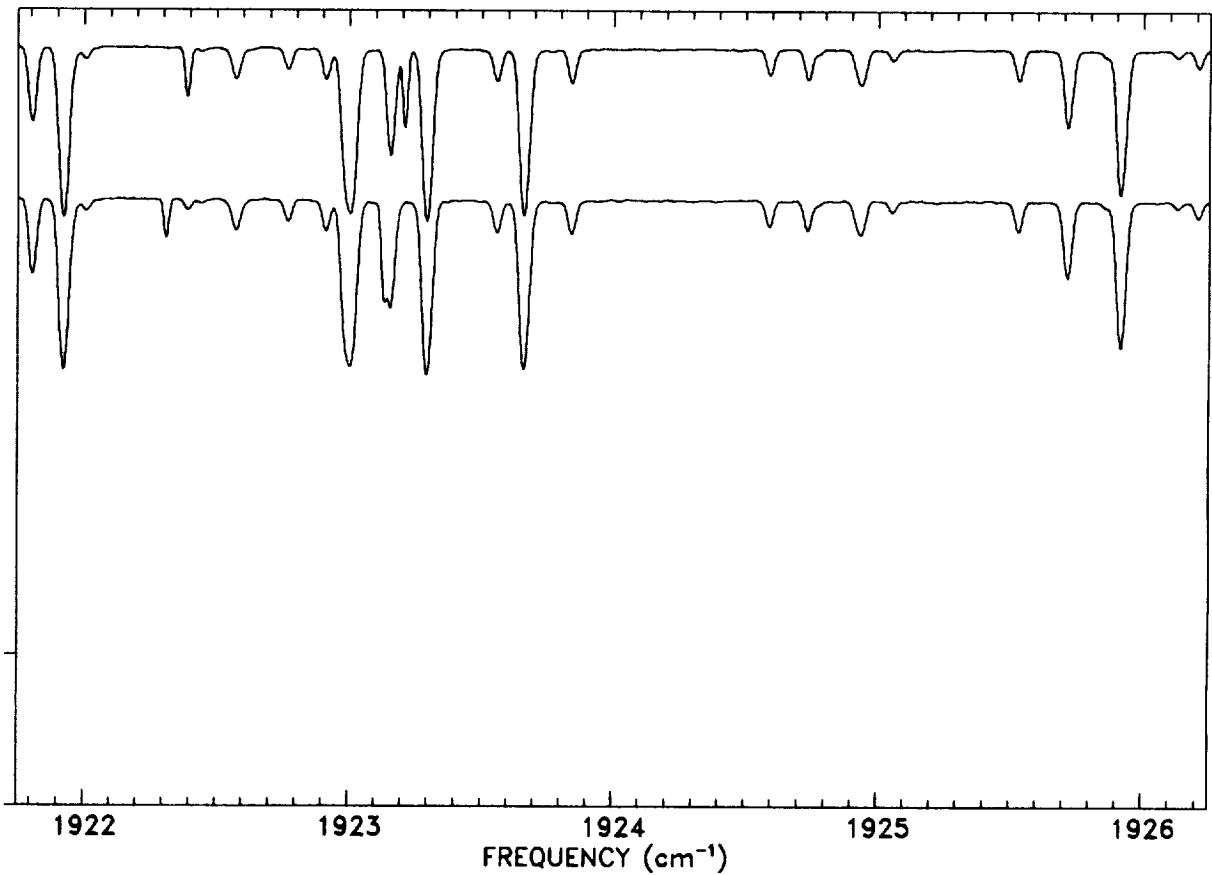
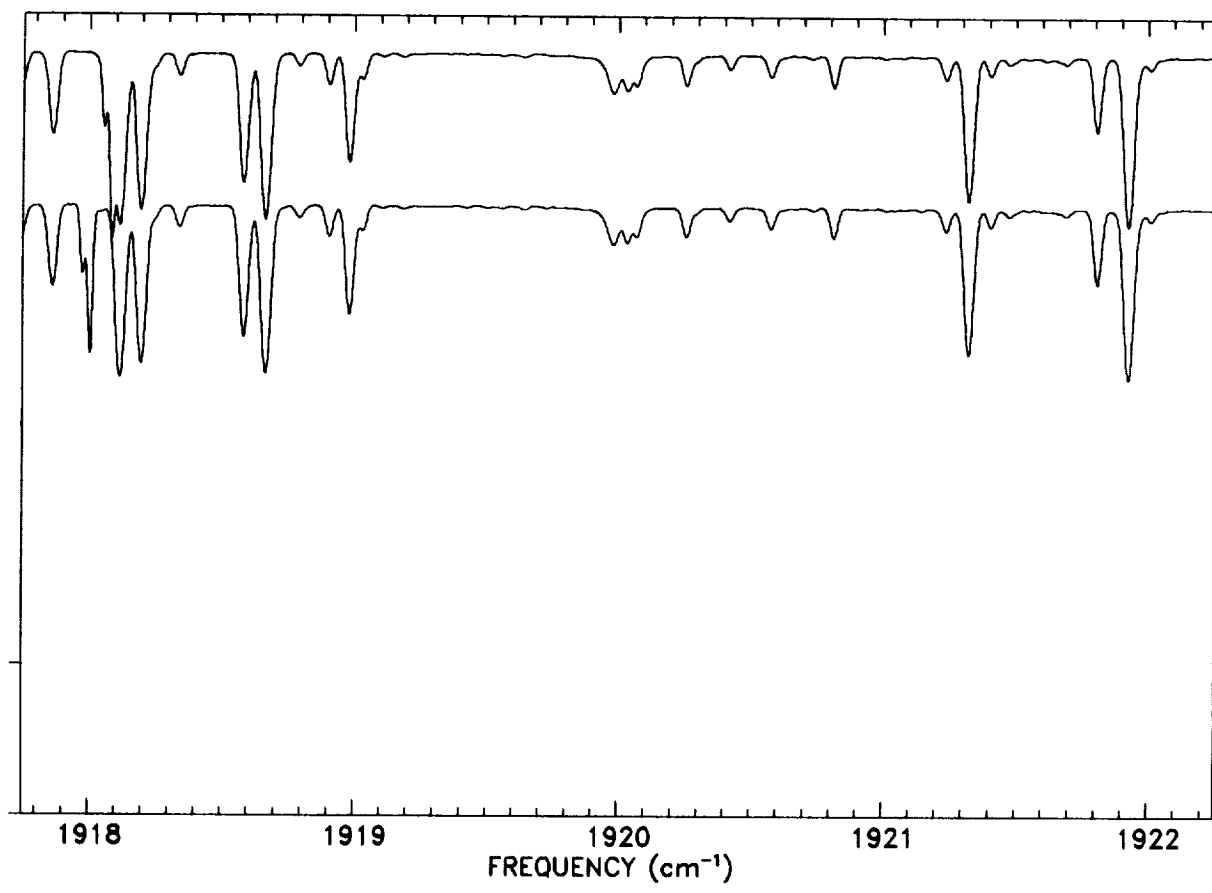
FREQUENCY (cm^{-1})

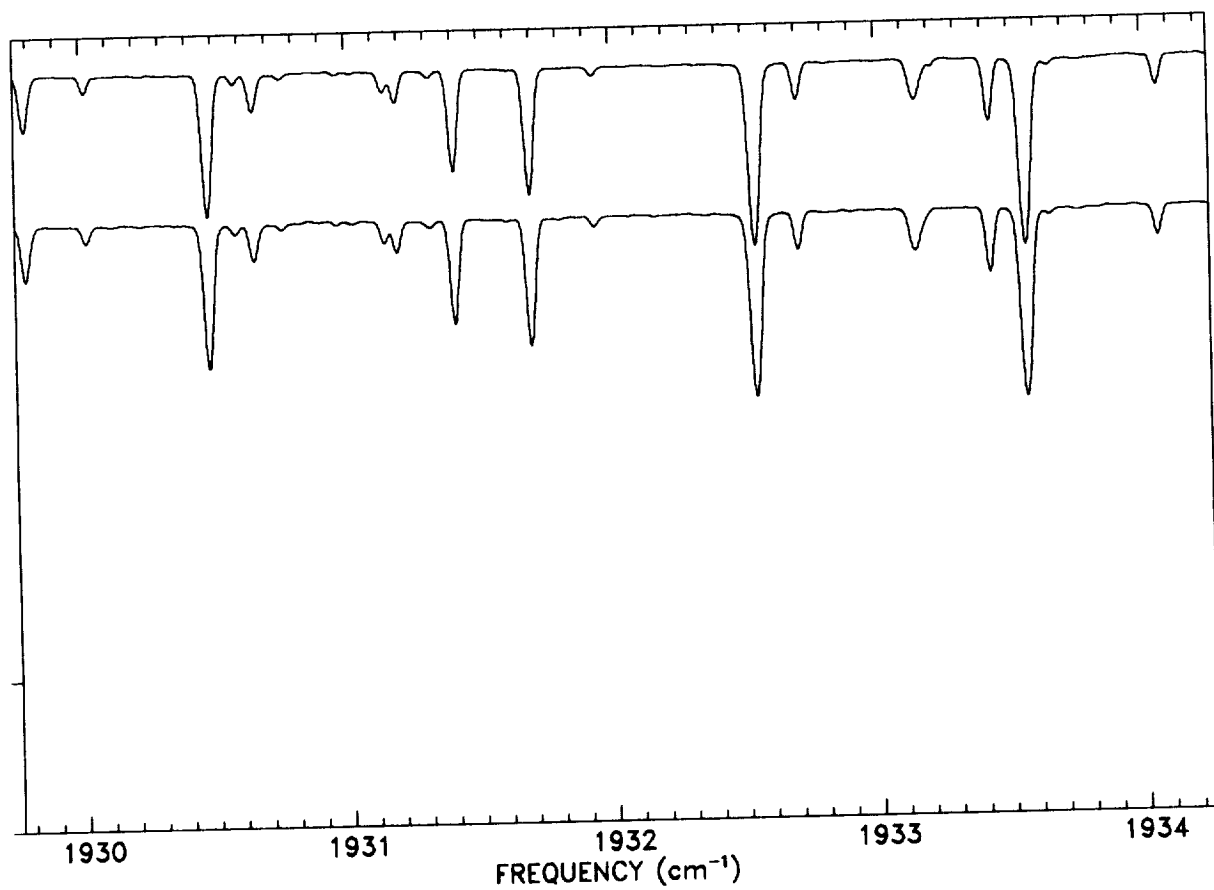
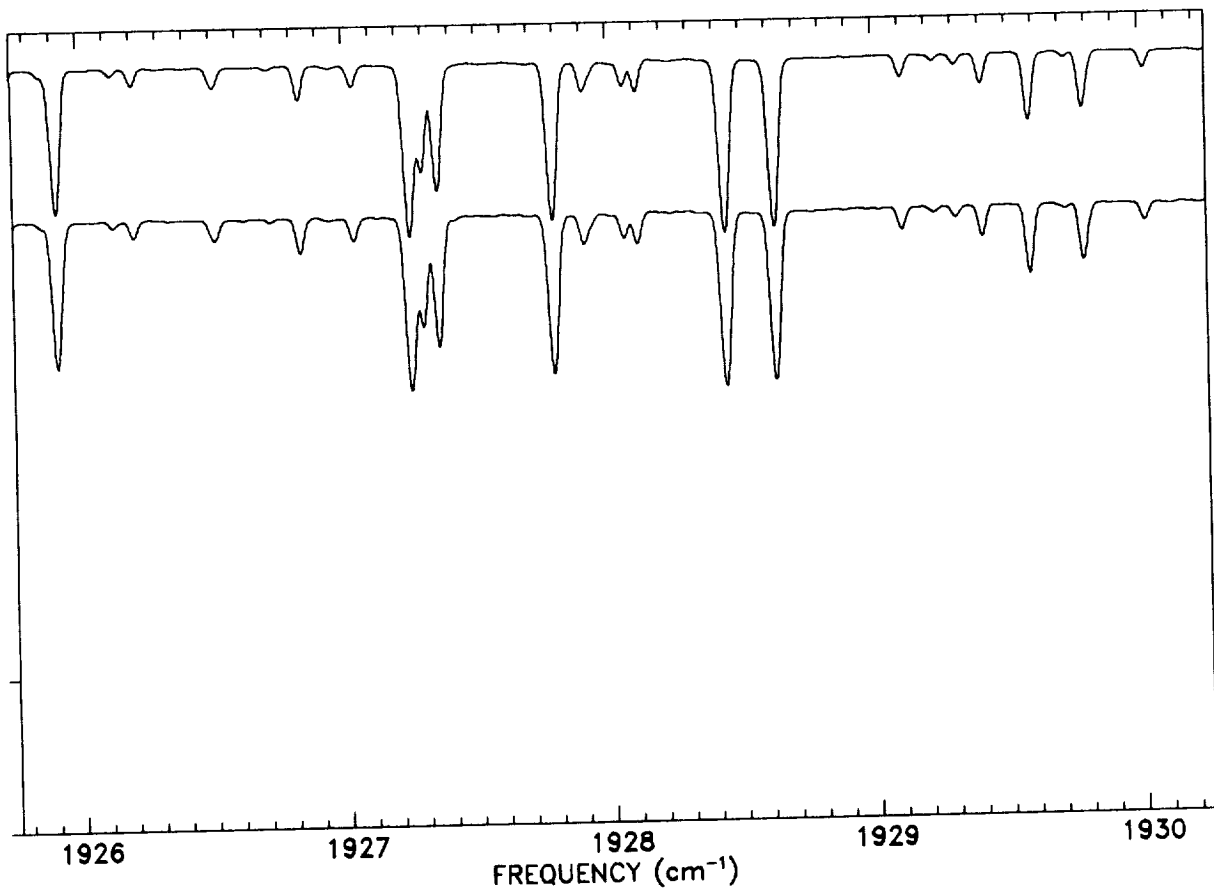


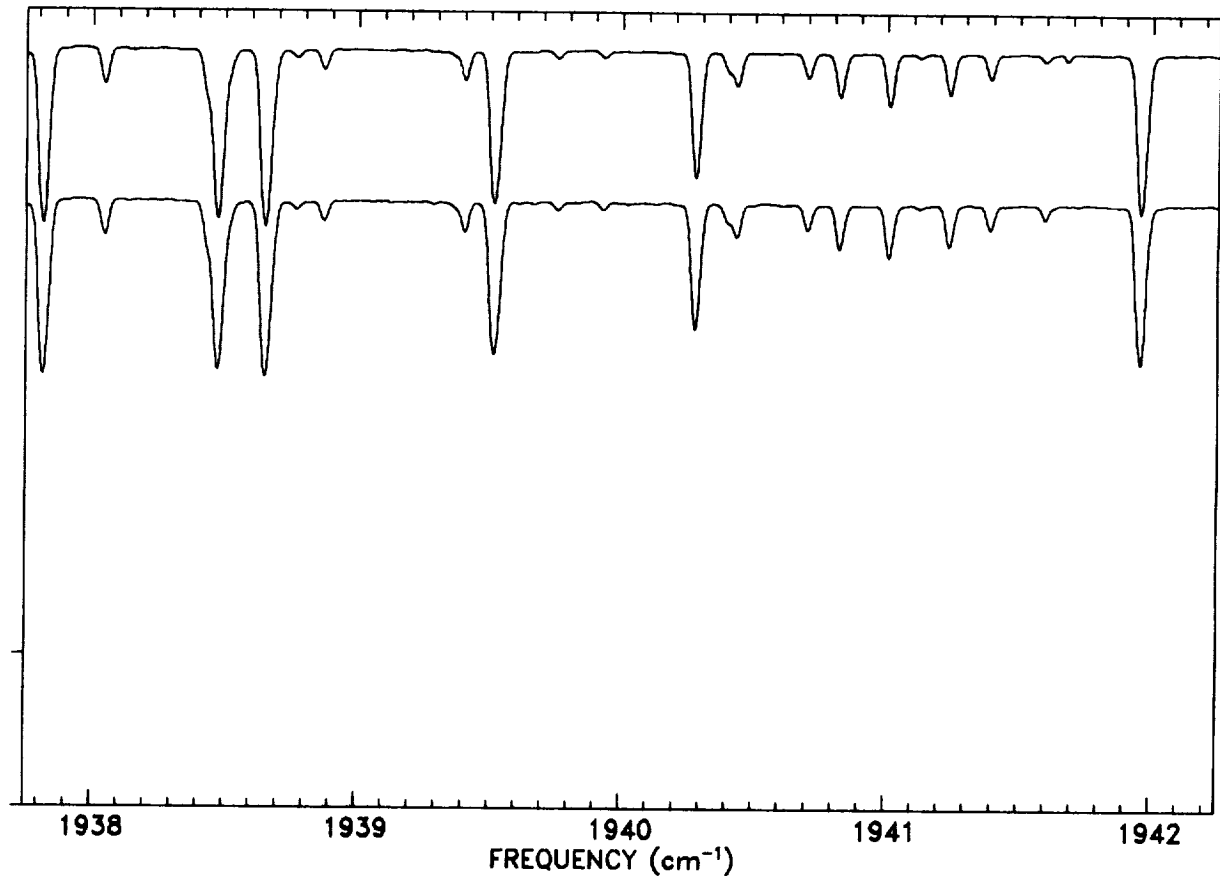
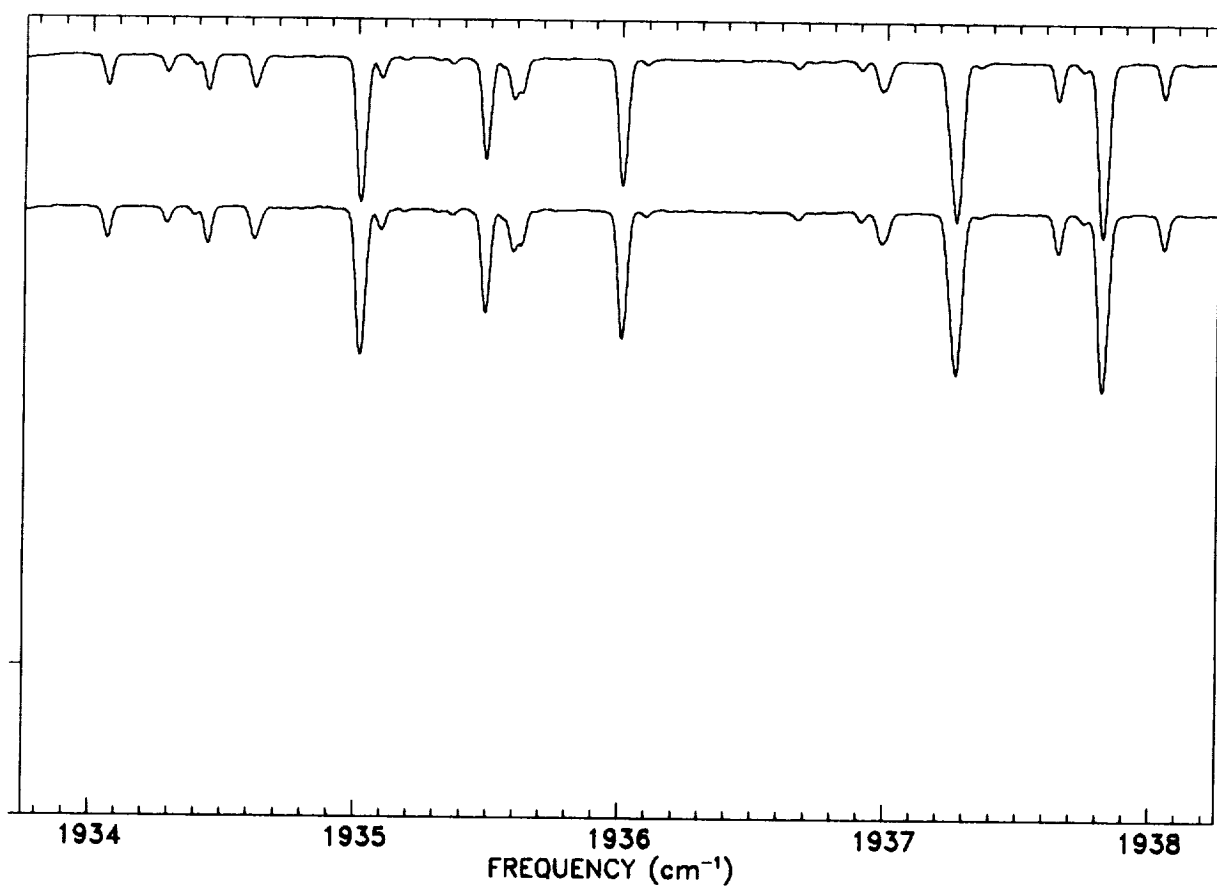


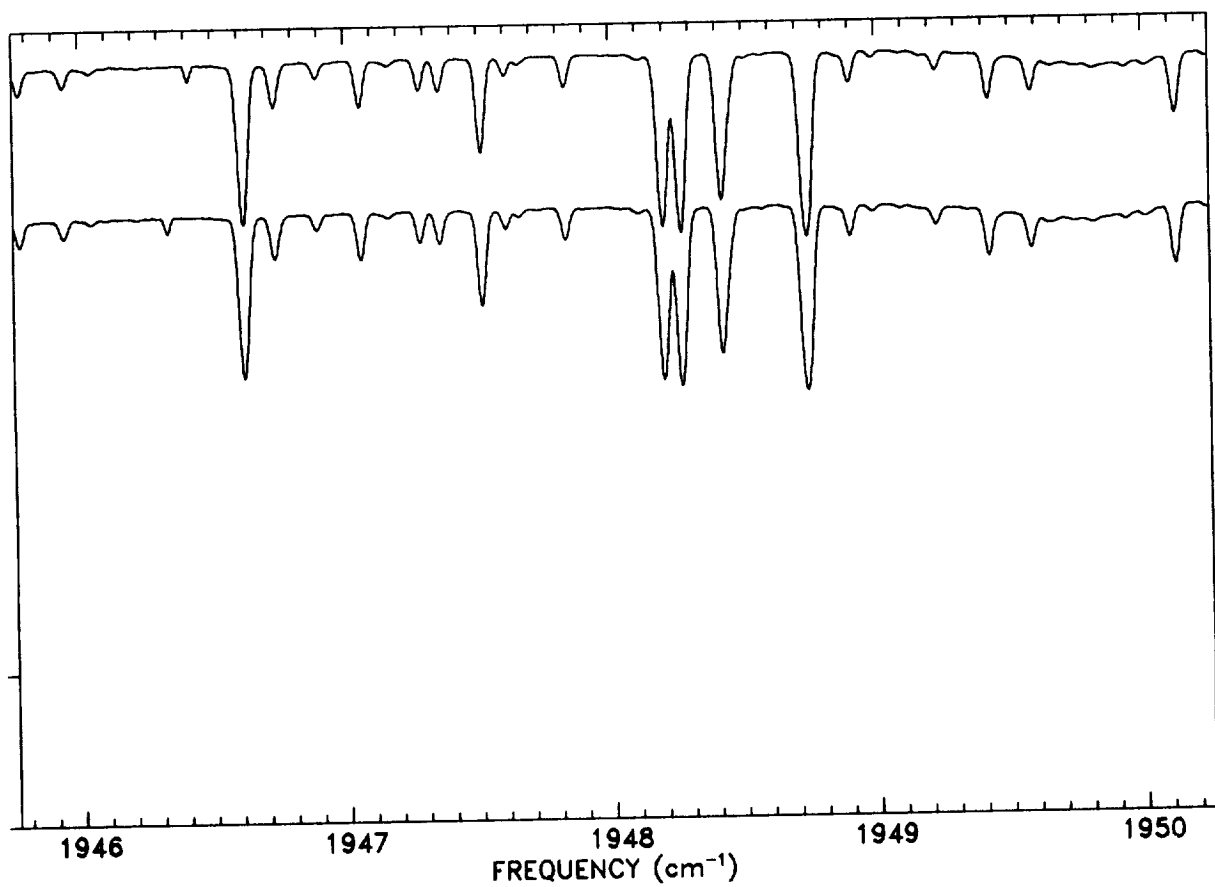
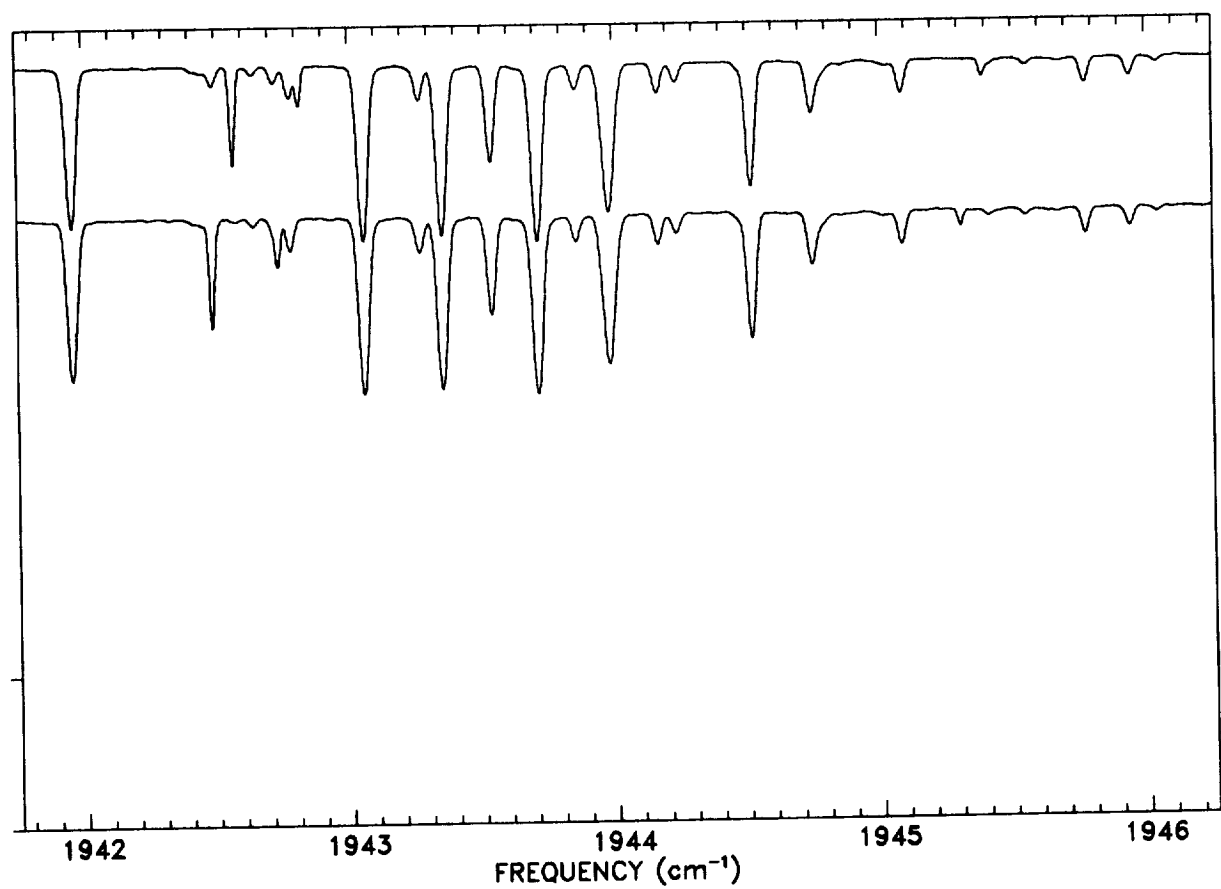


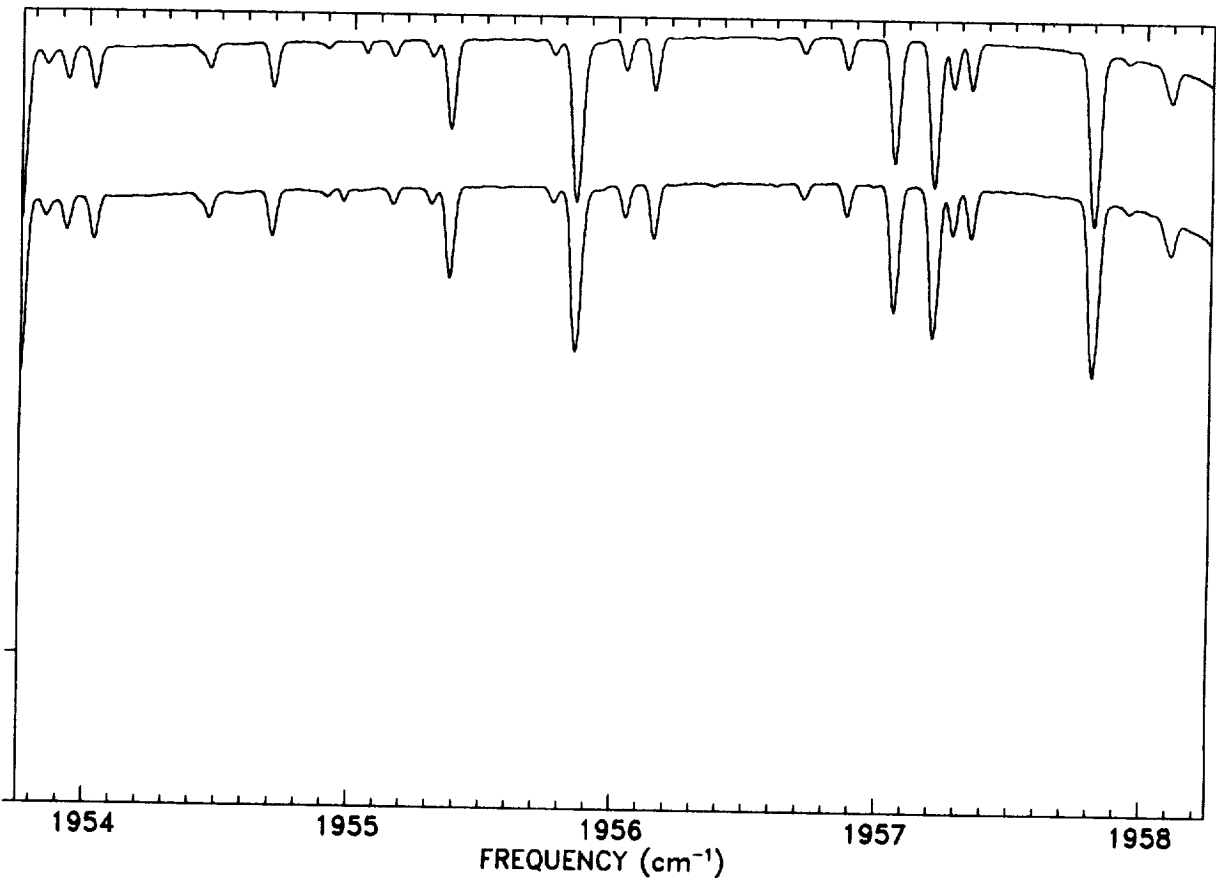
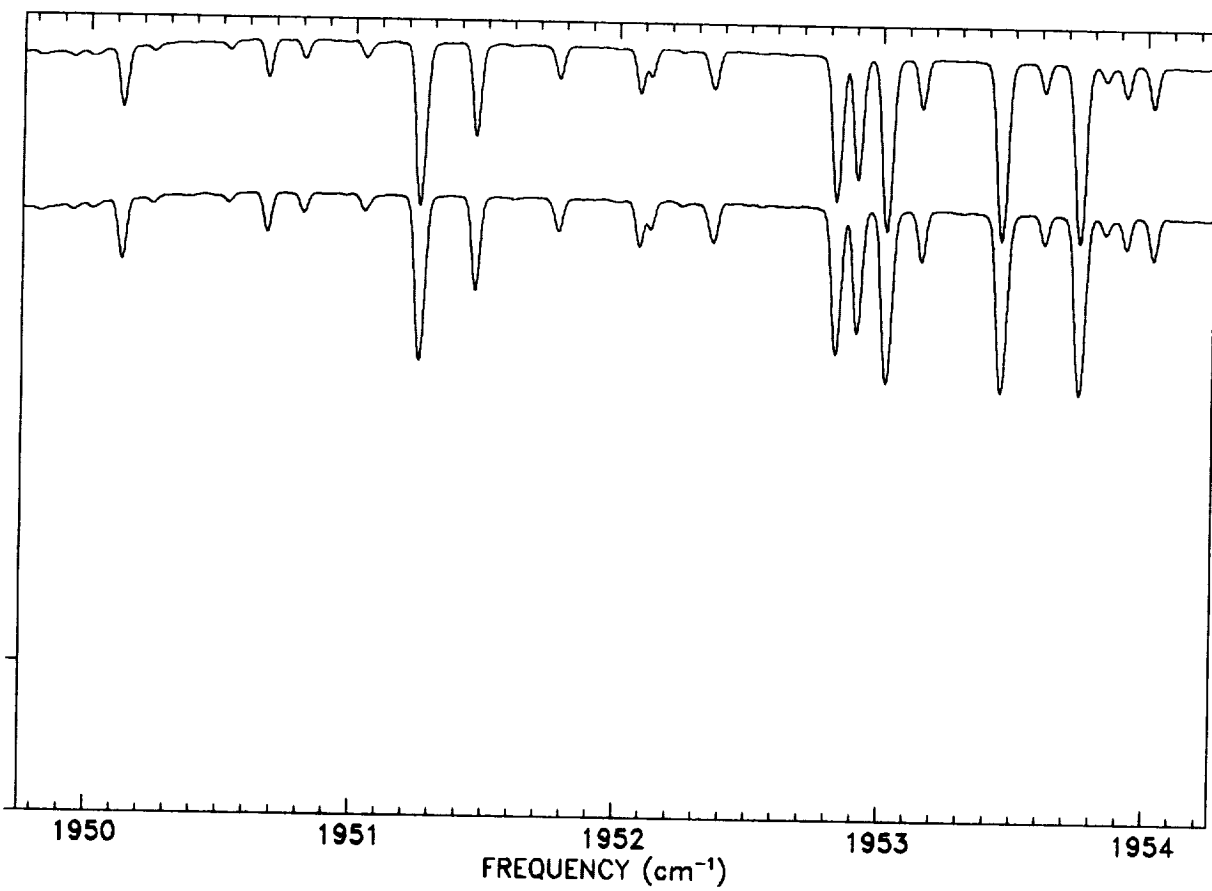


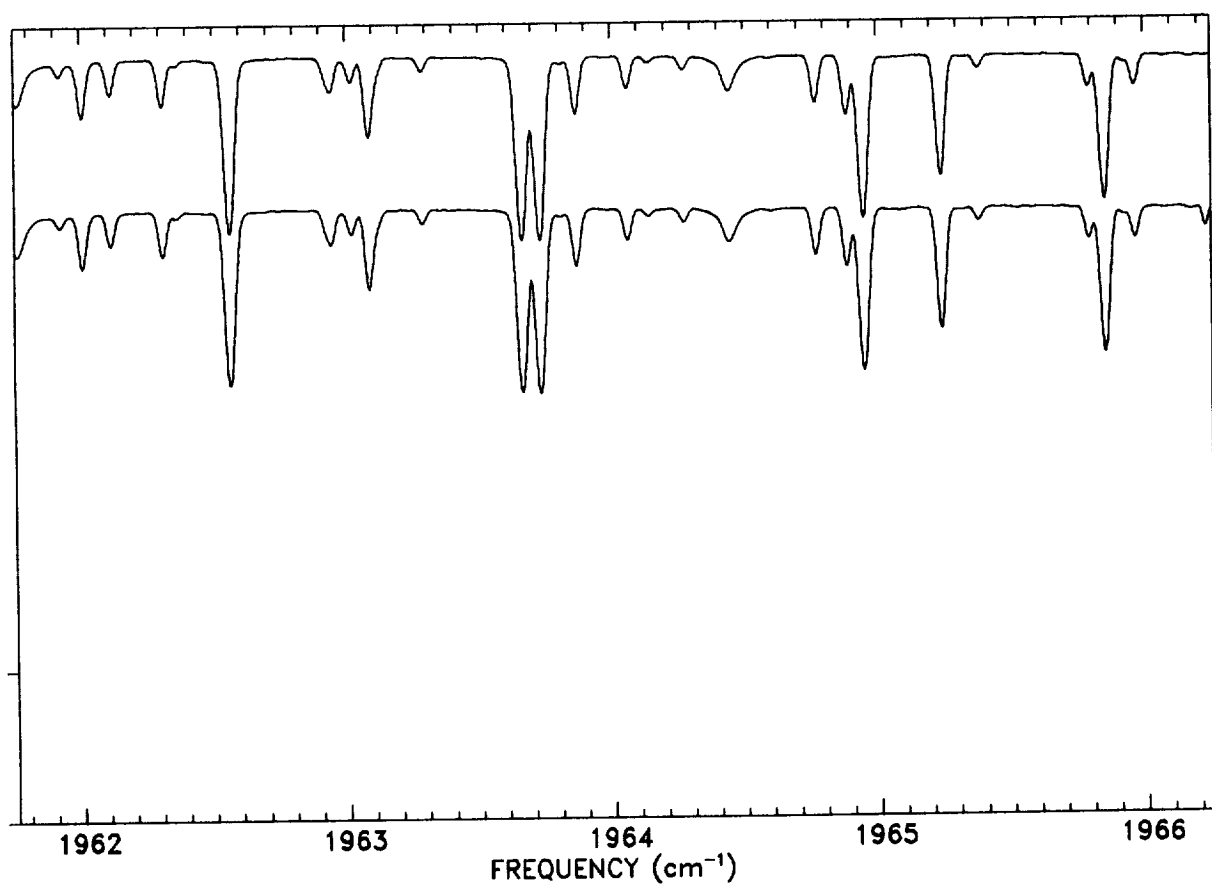
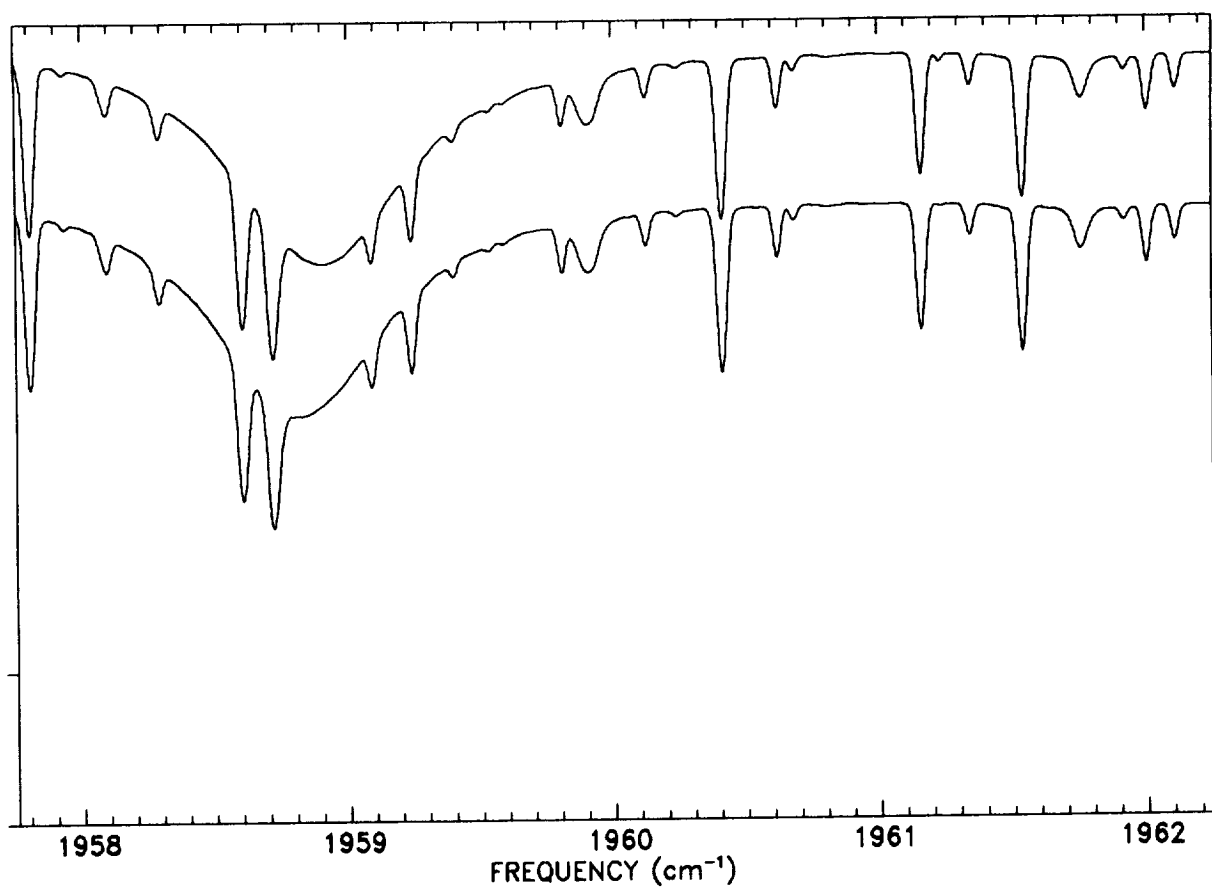


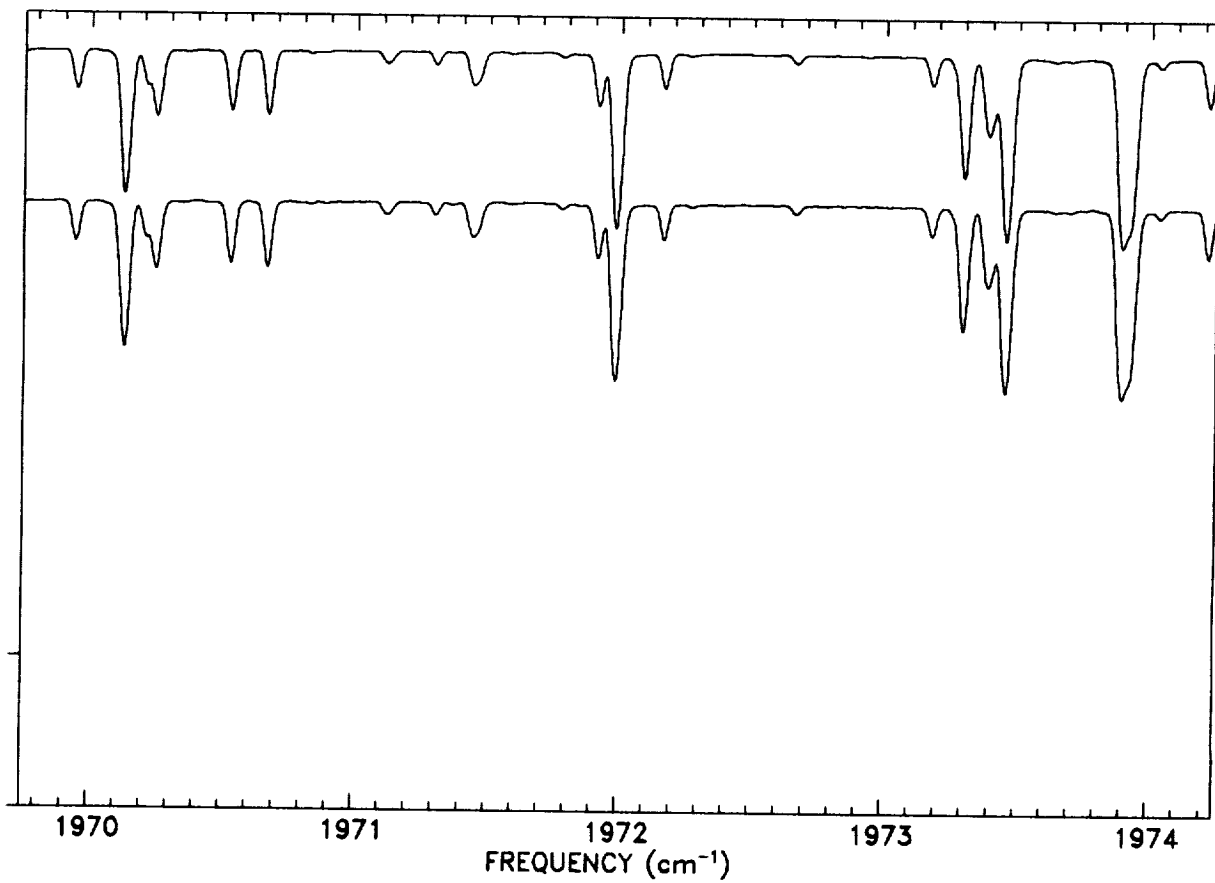
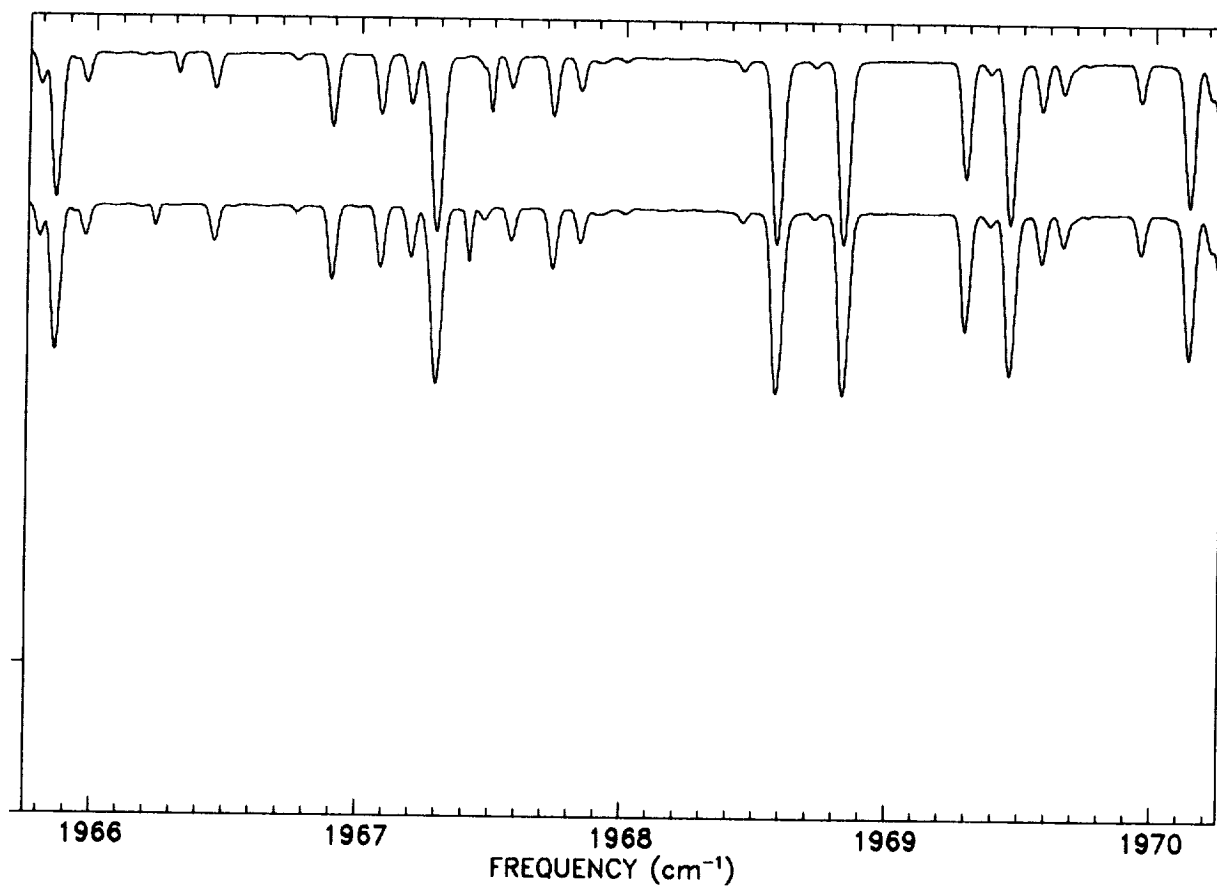


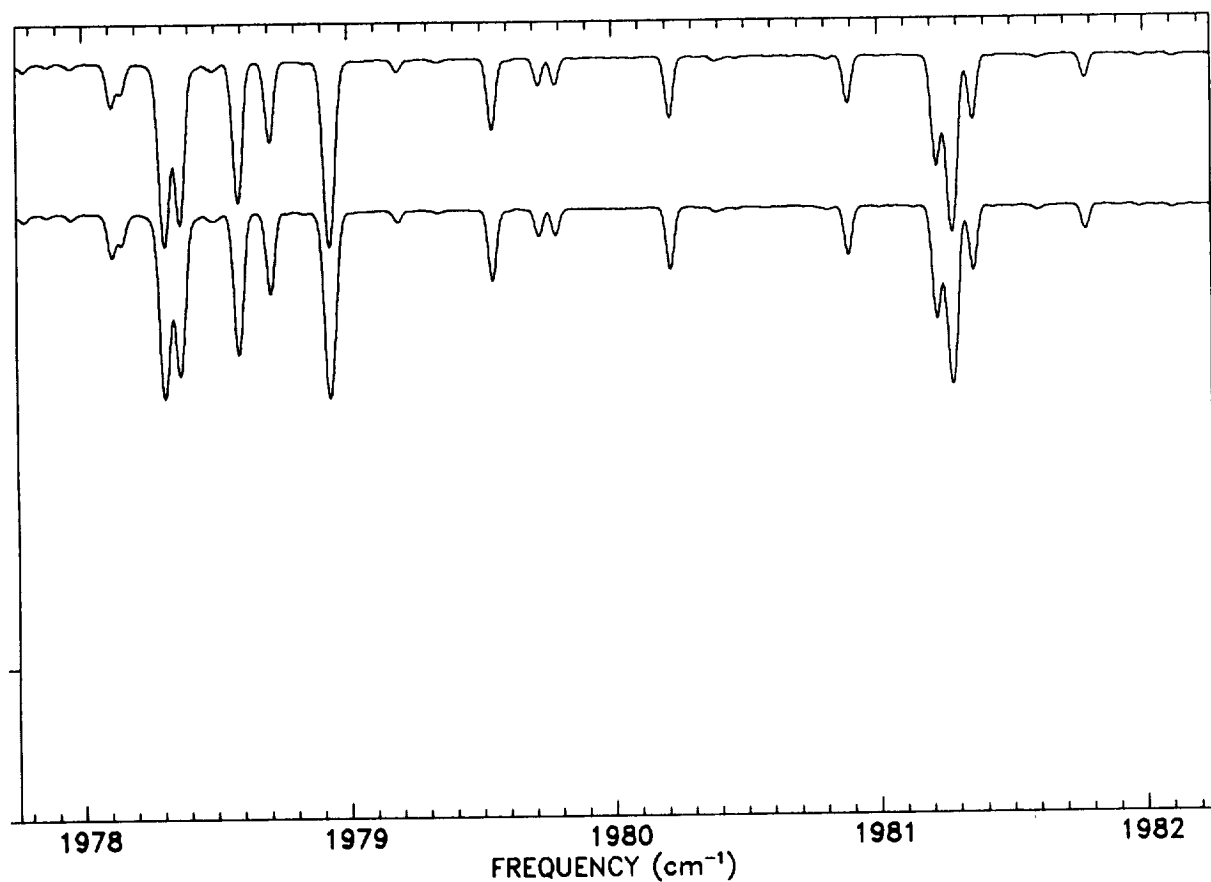
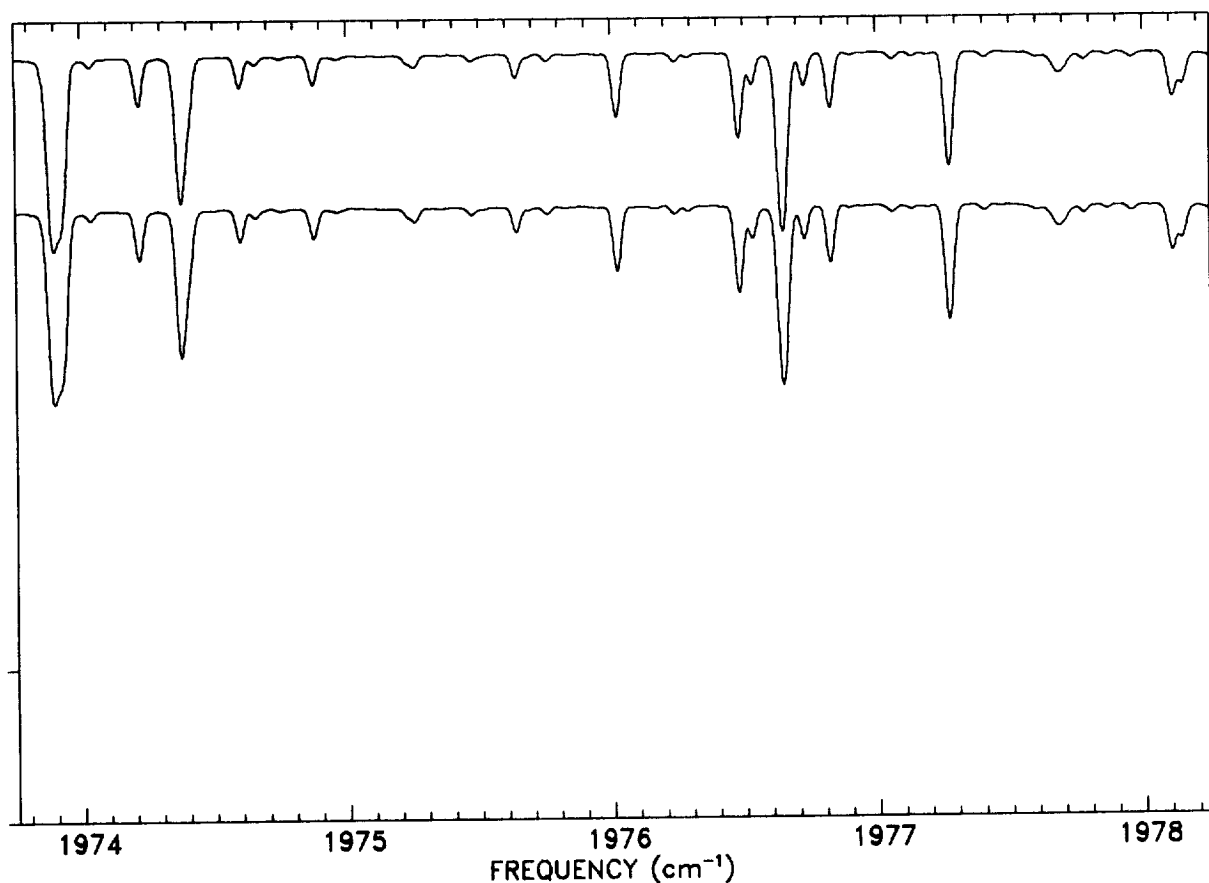


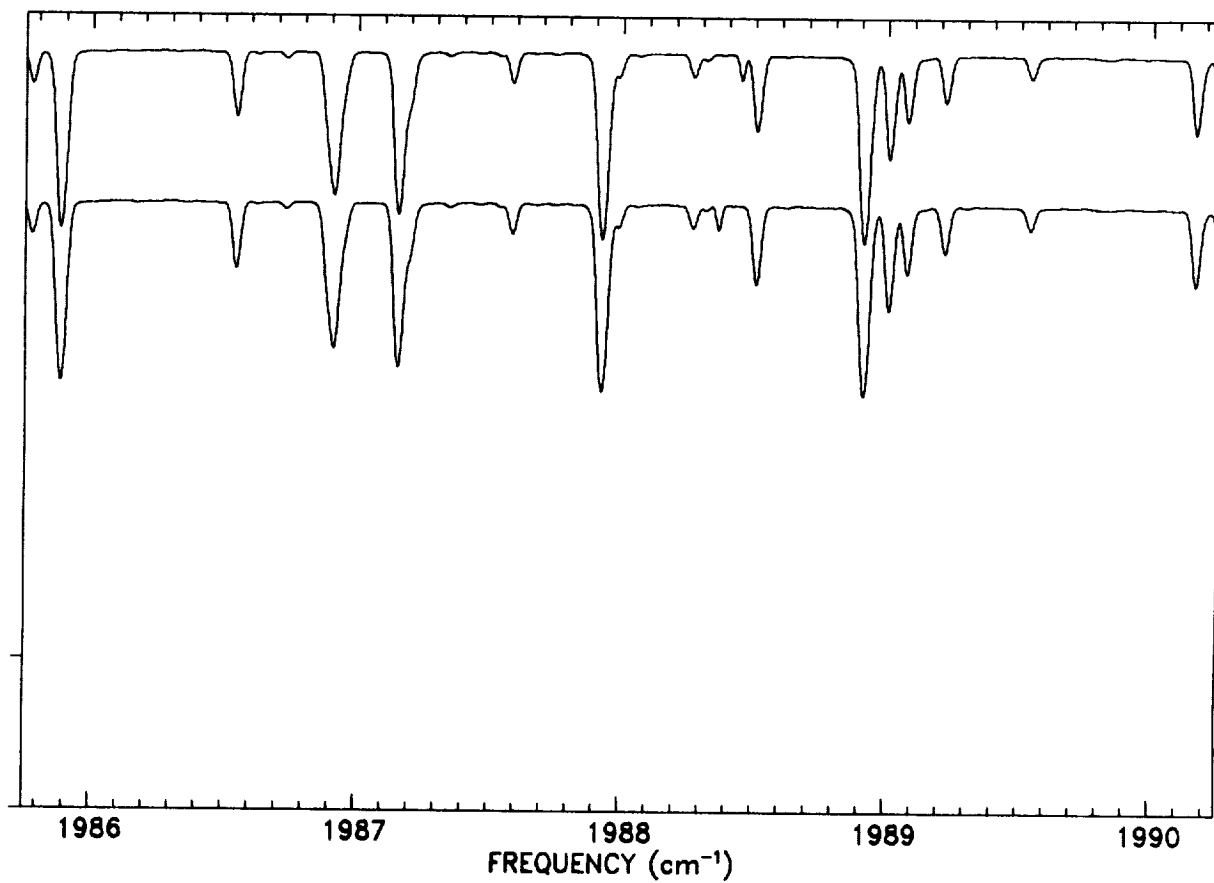
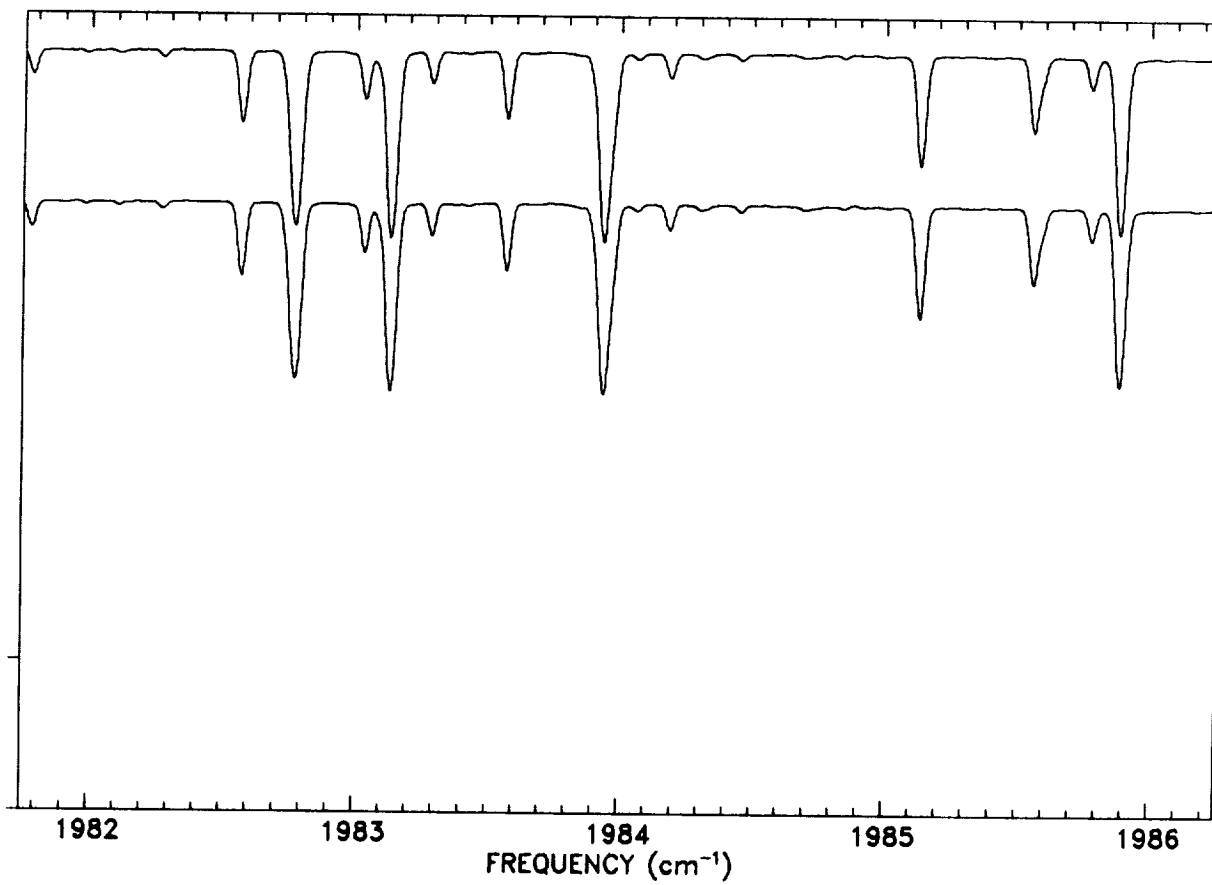


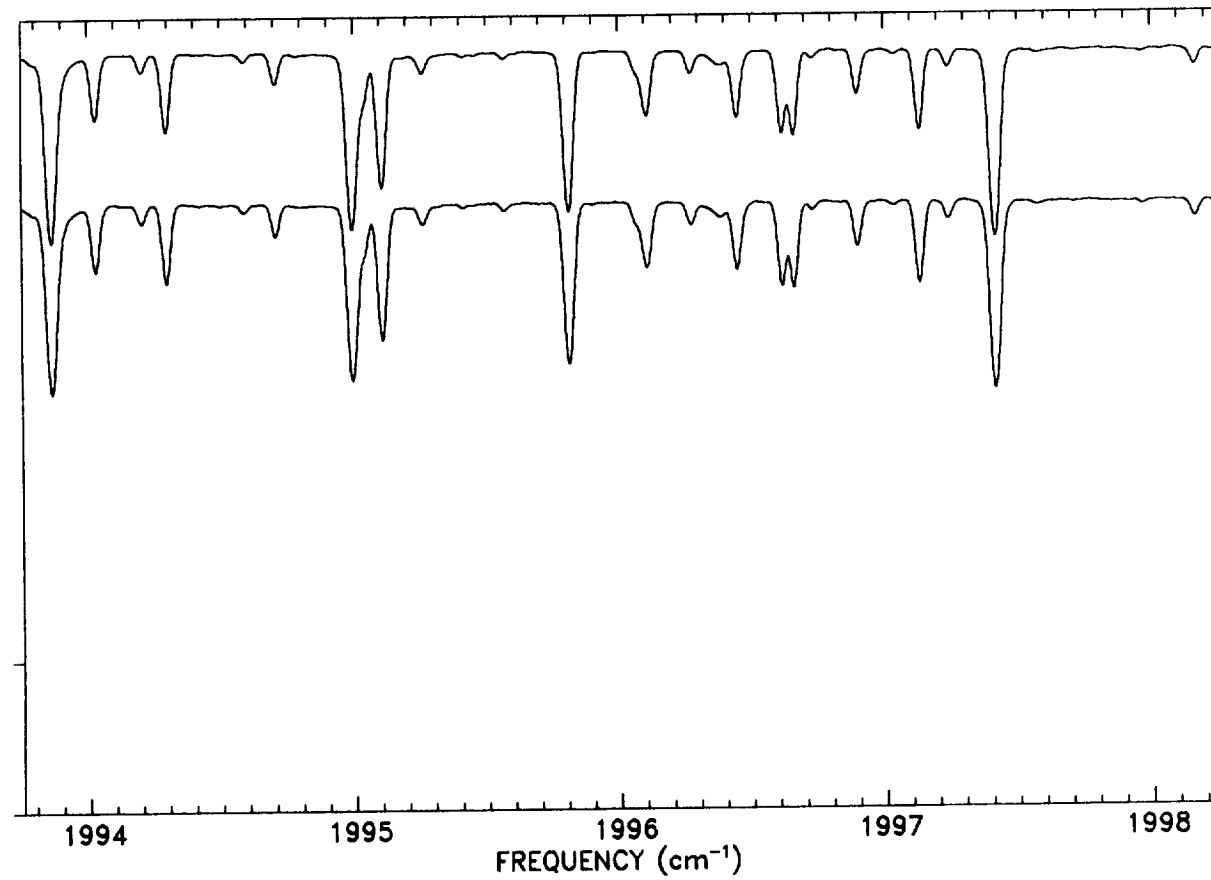
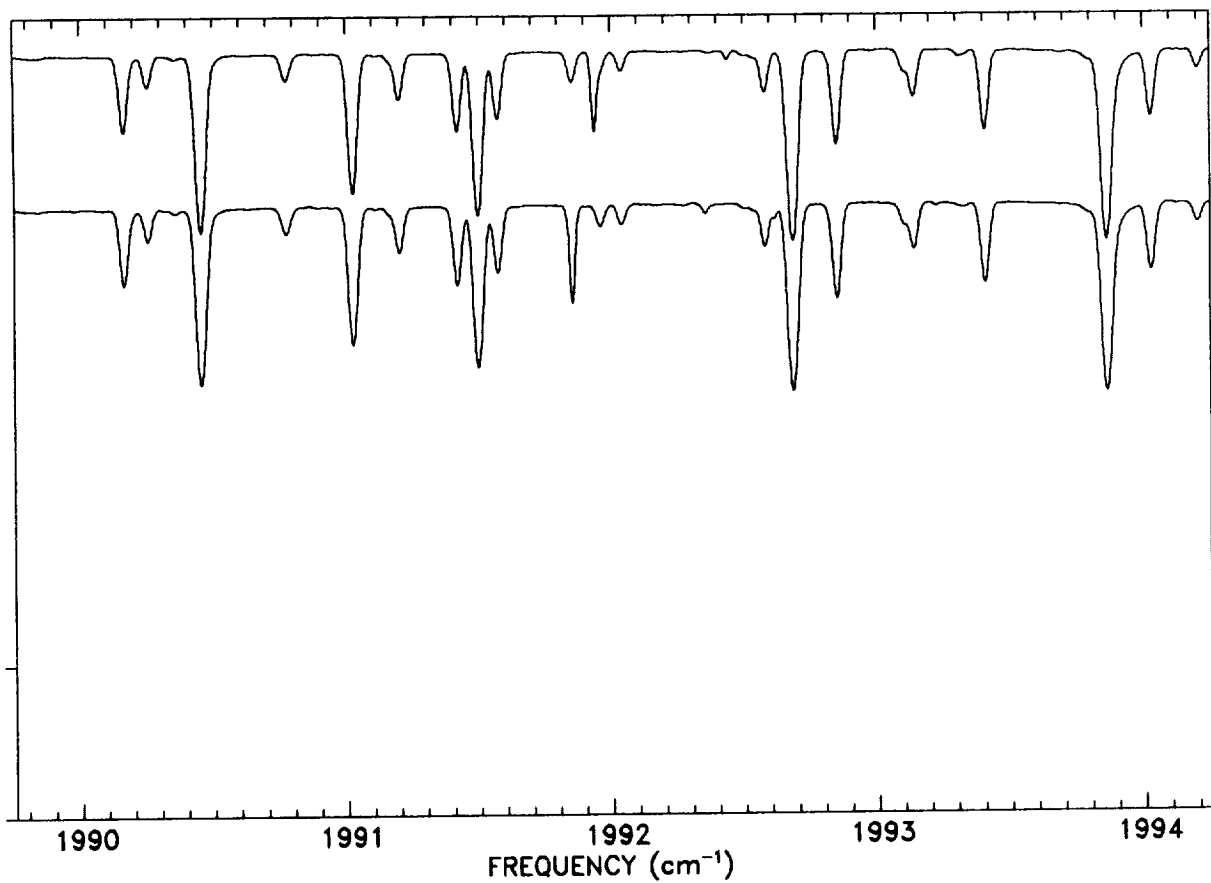


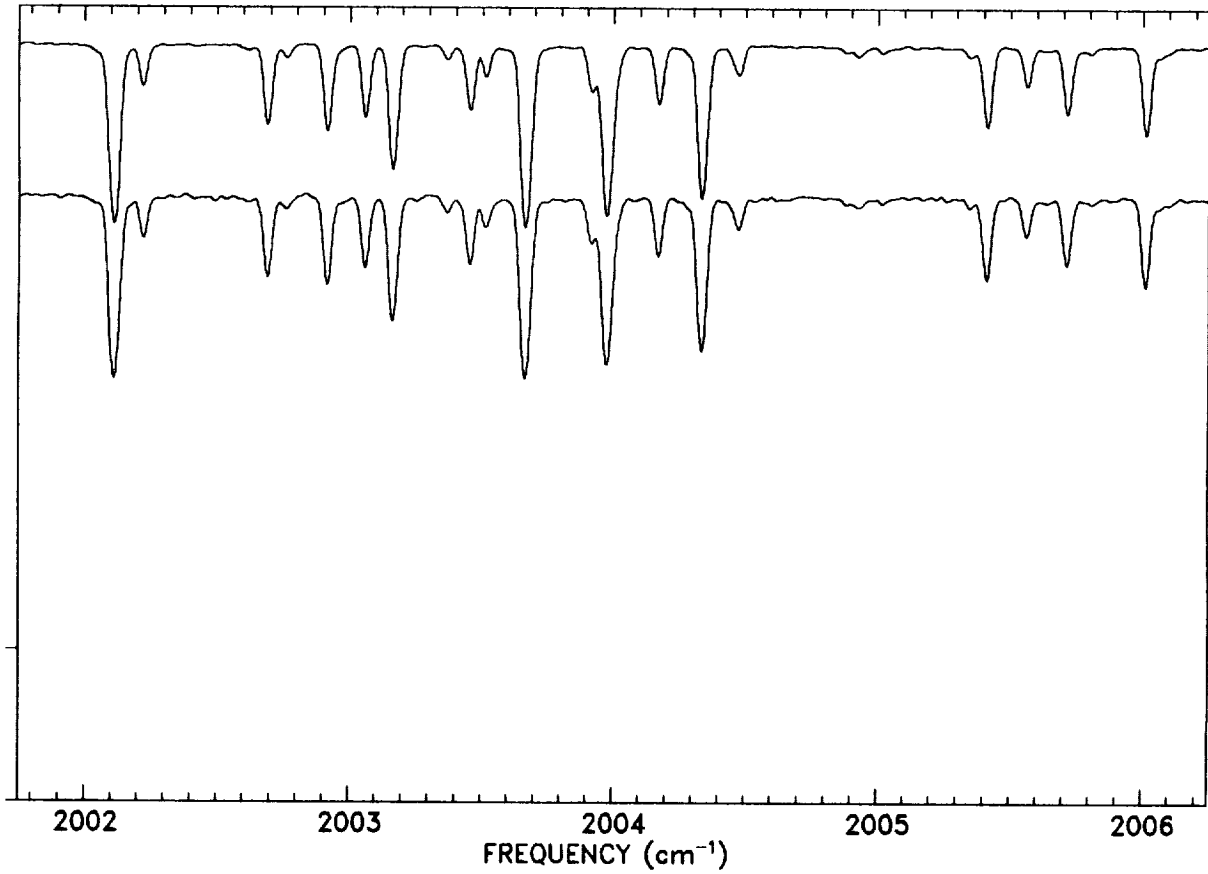
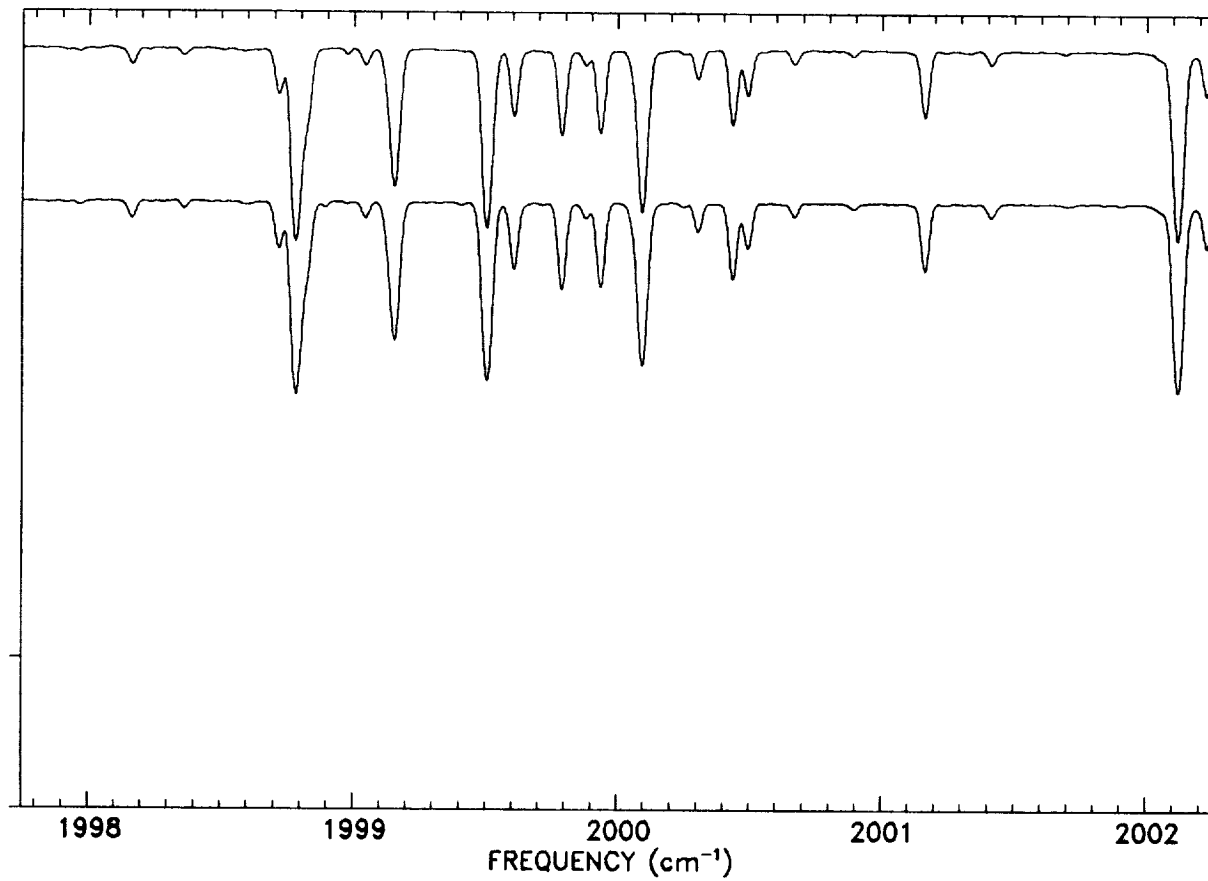


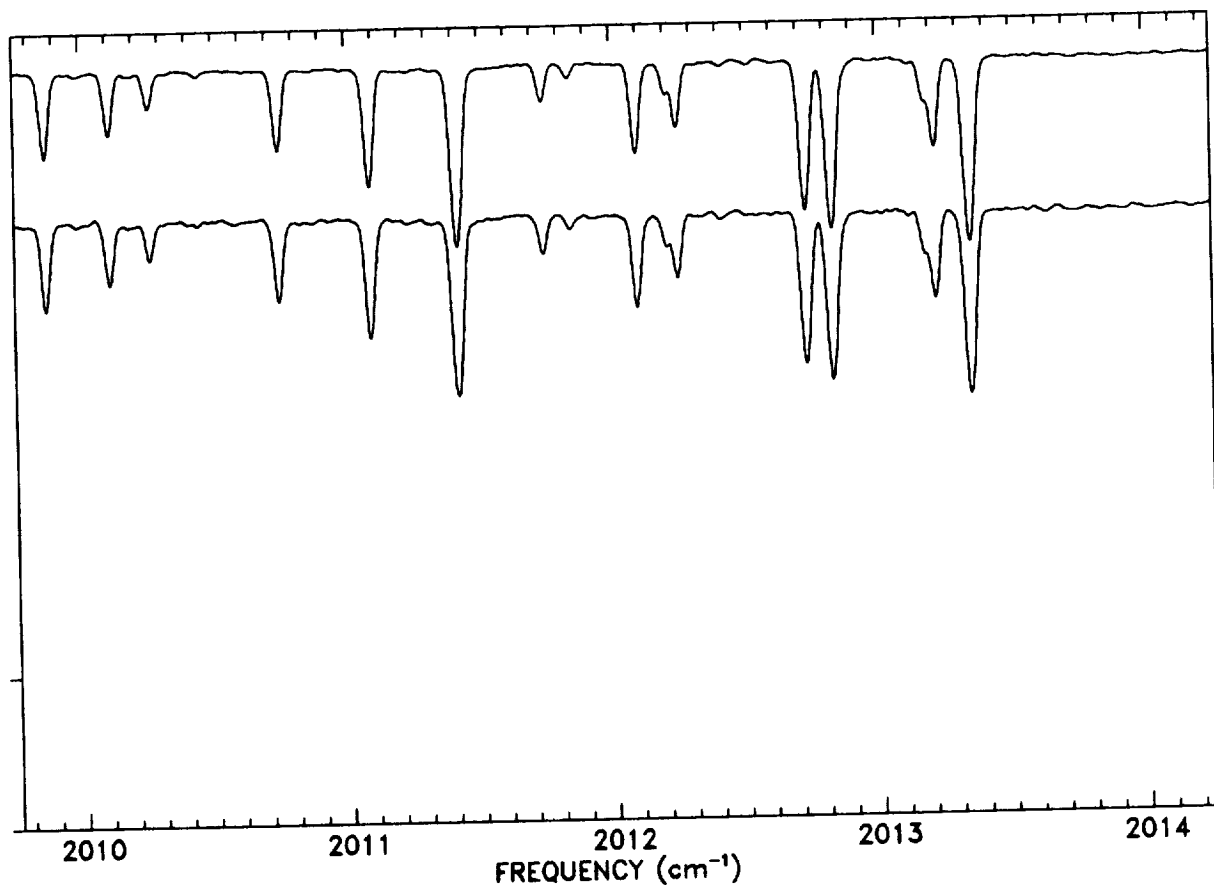
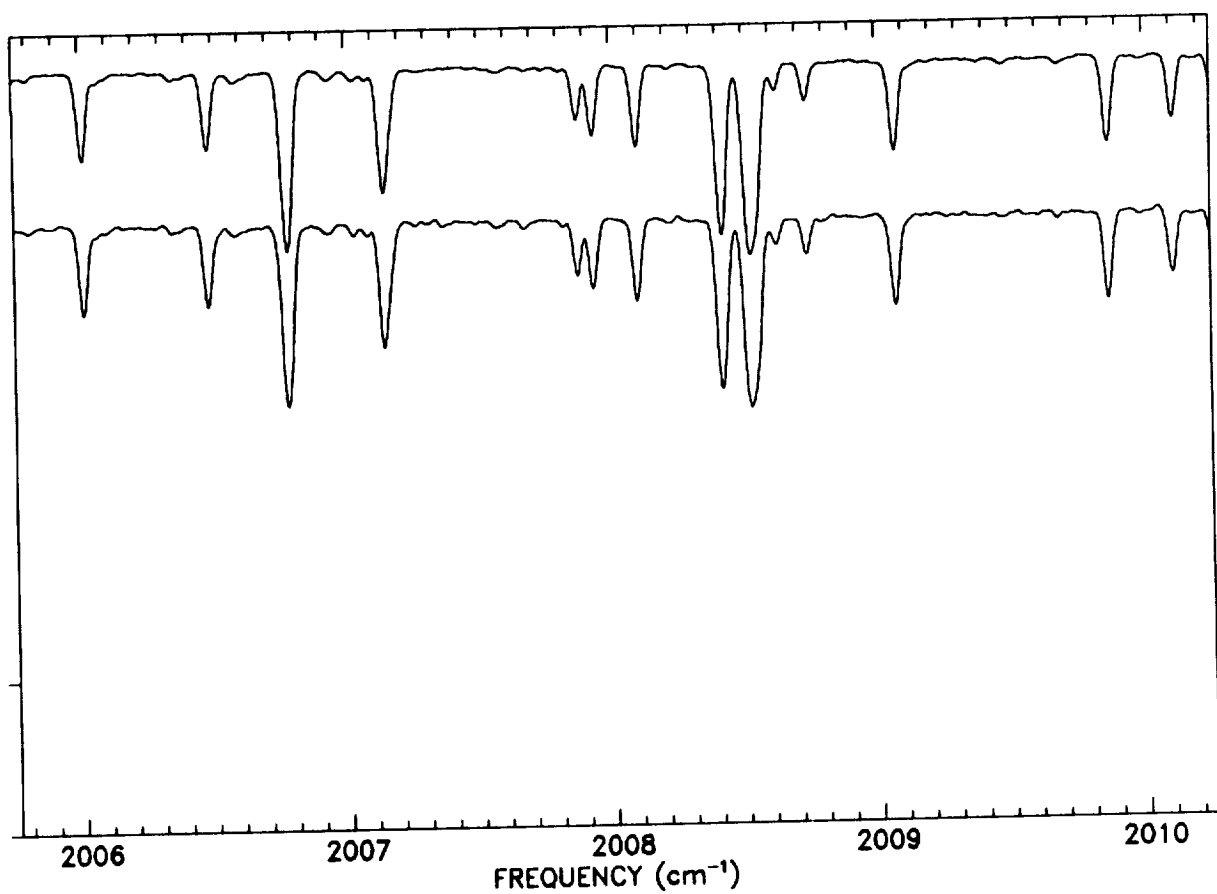


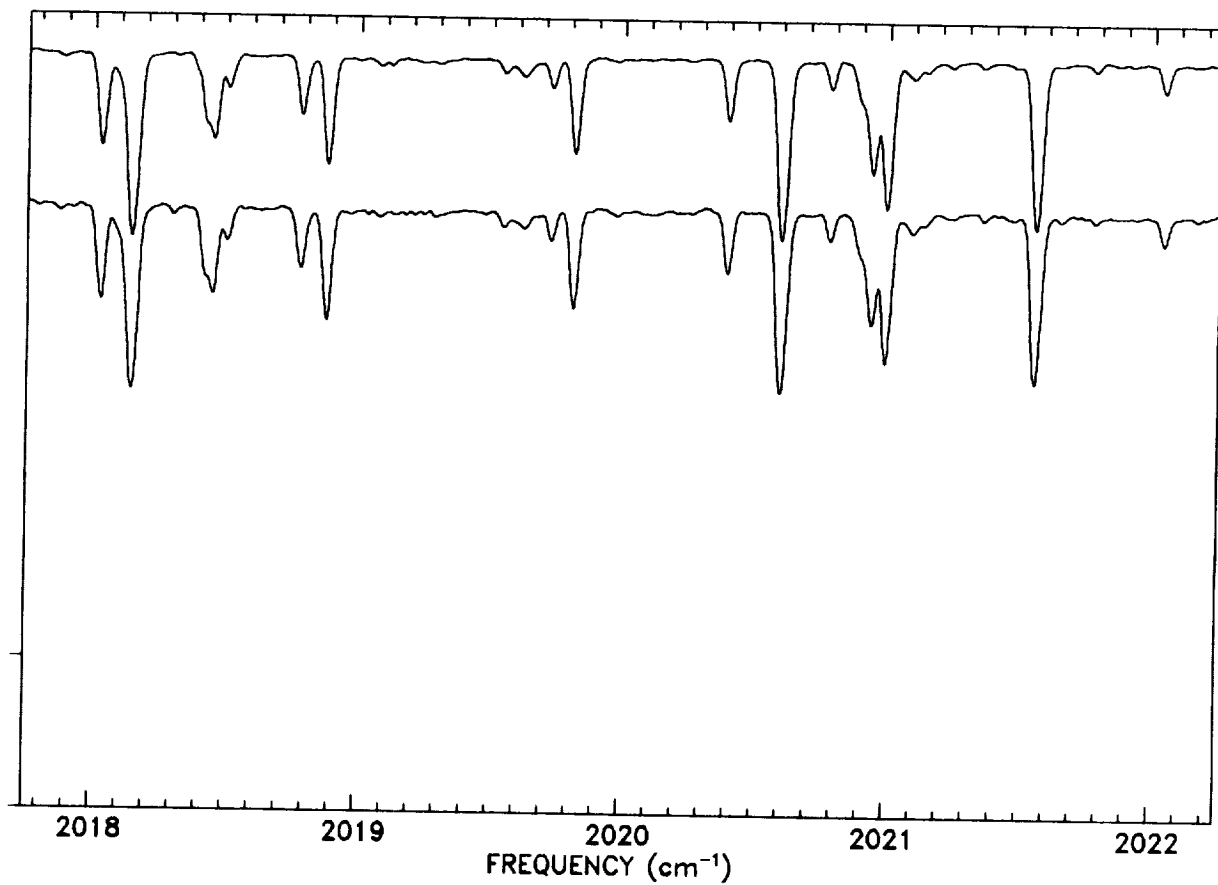
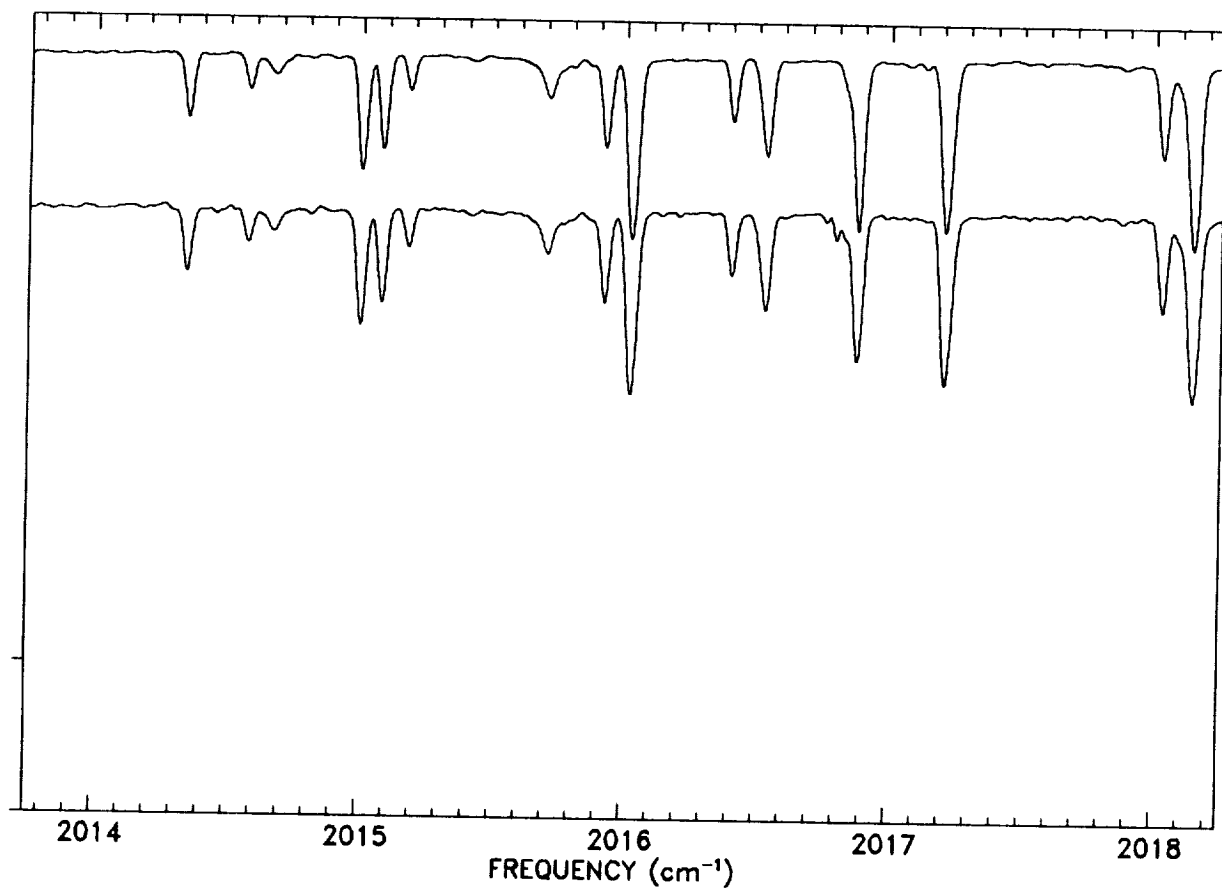


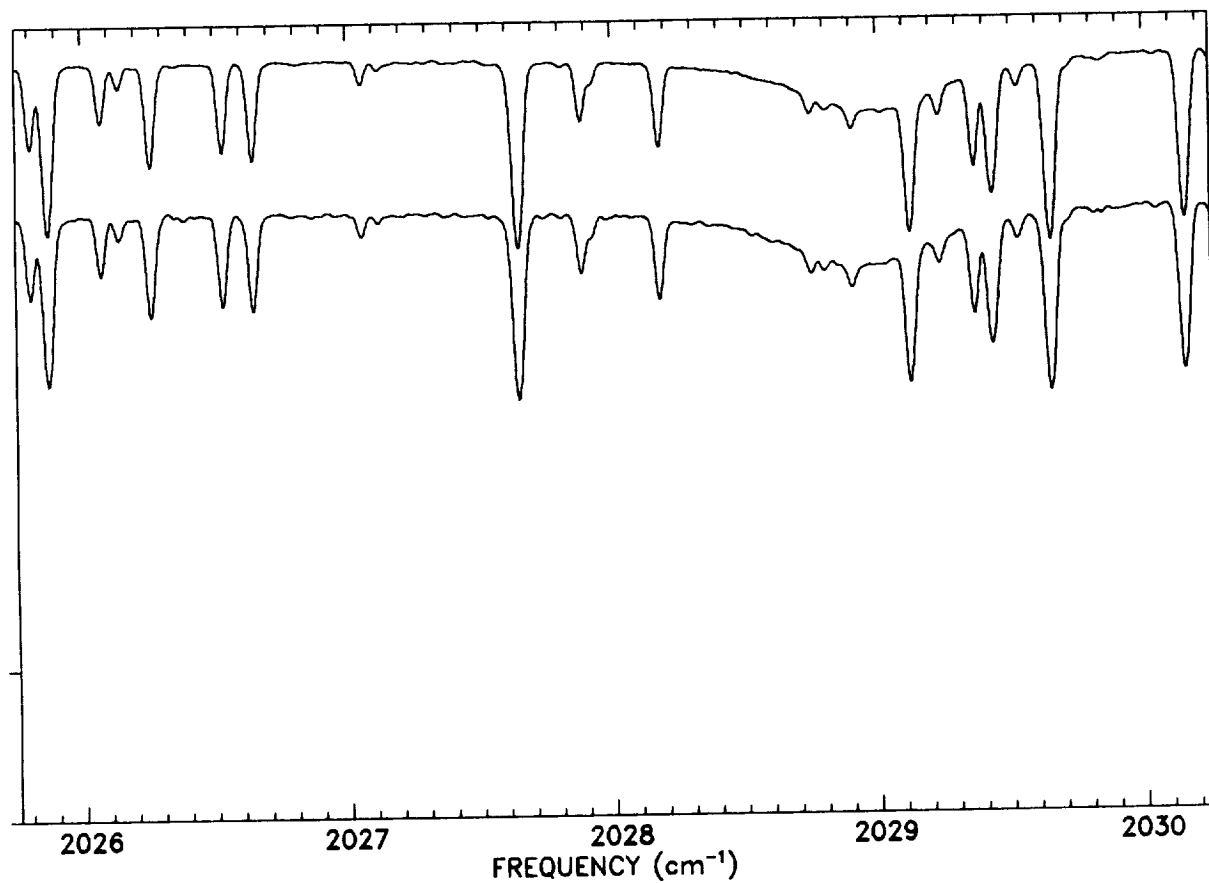
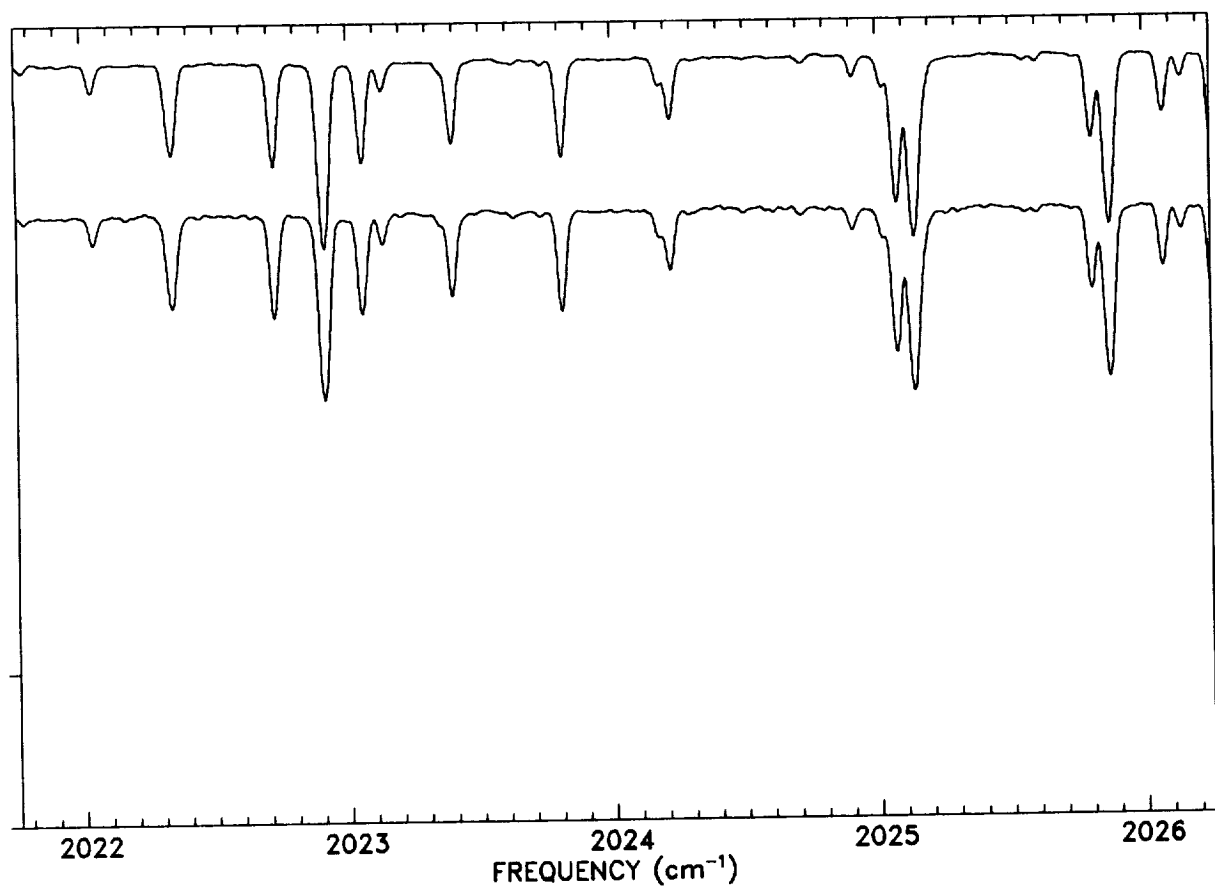


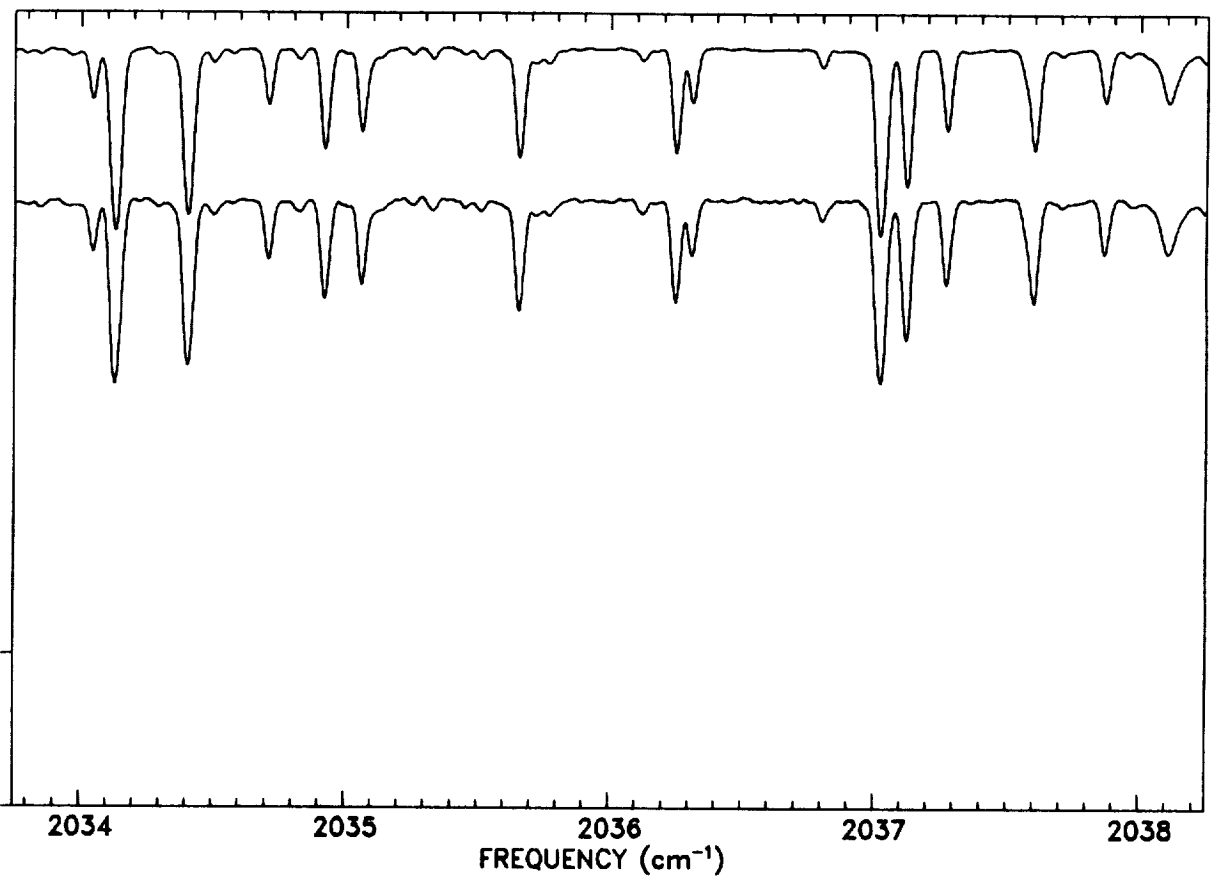
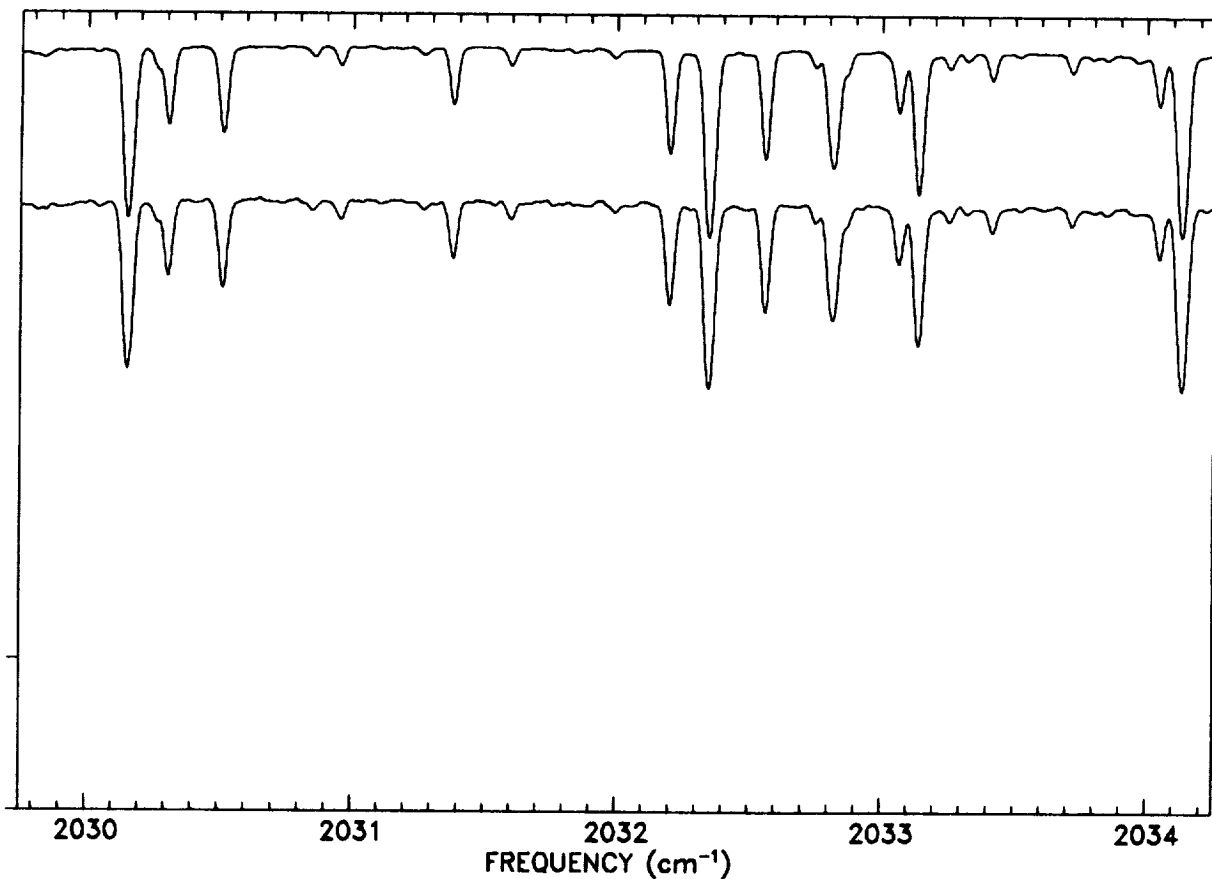


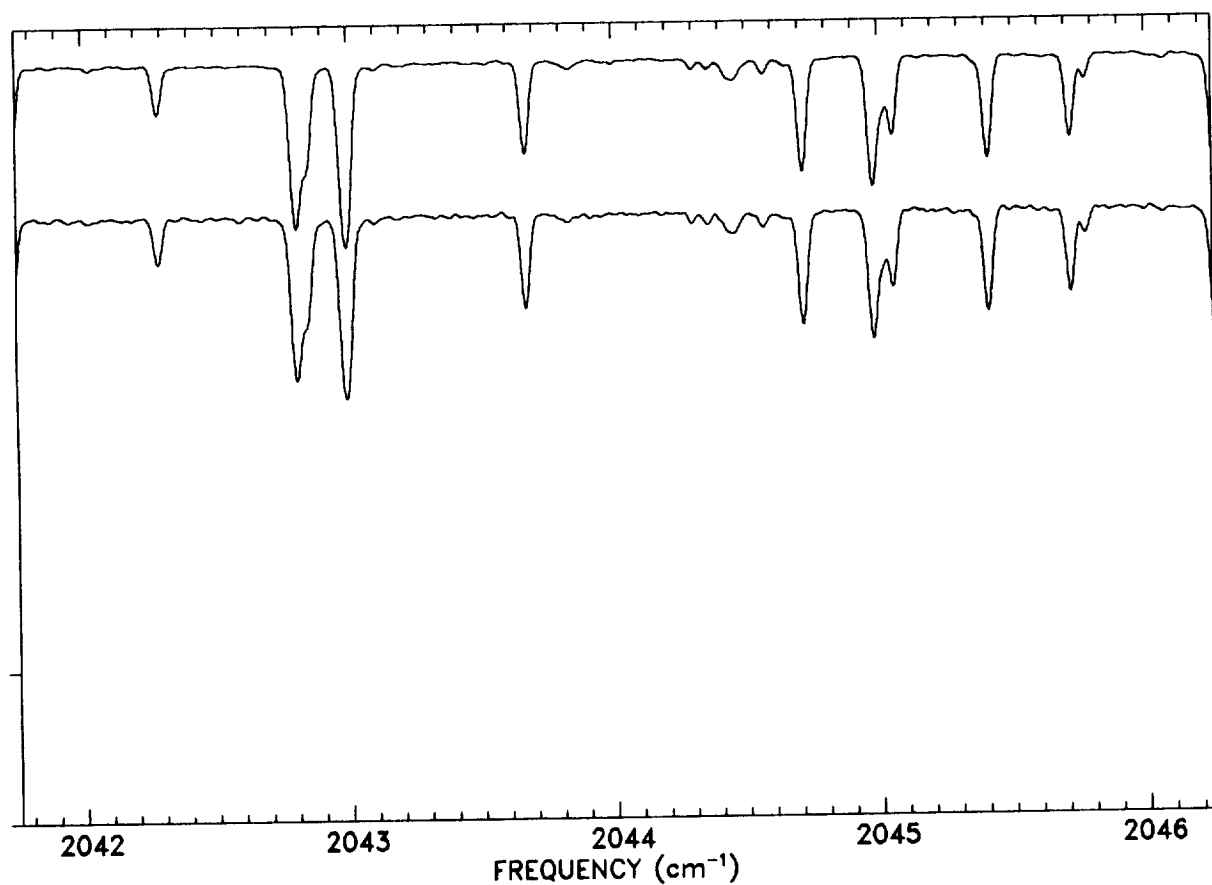
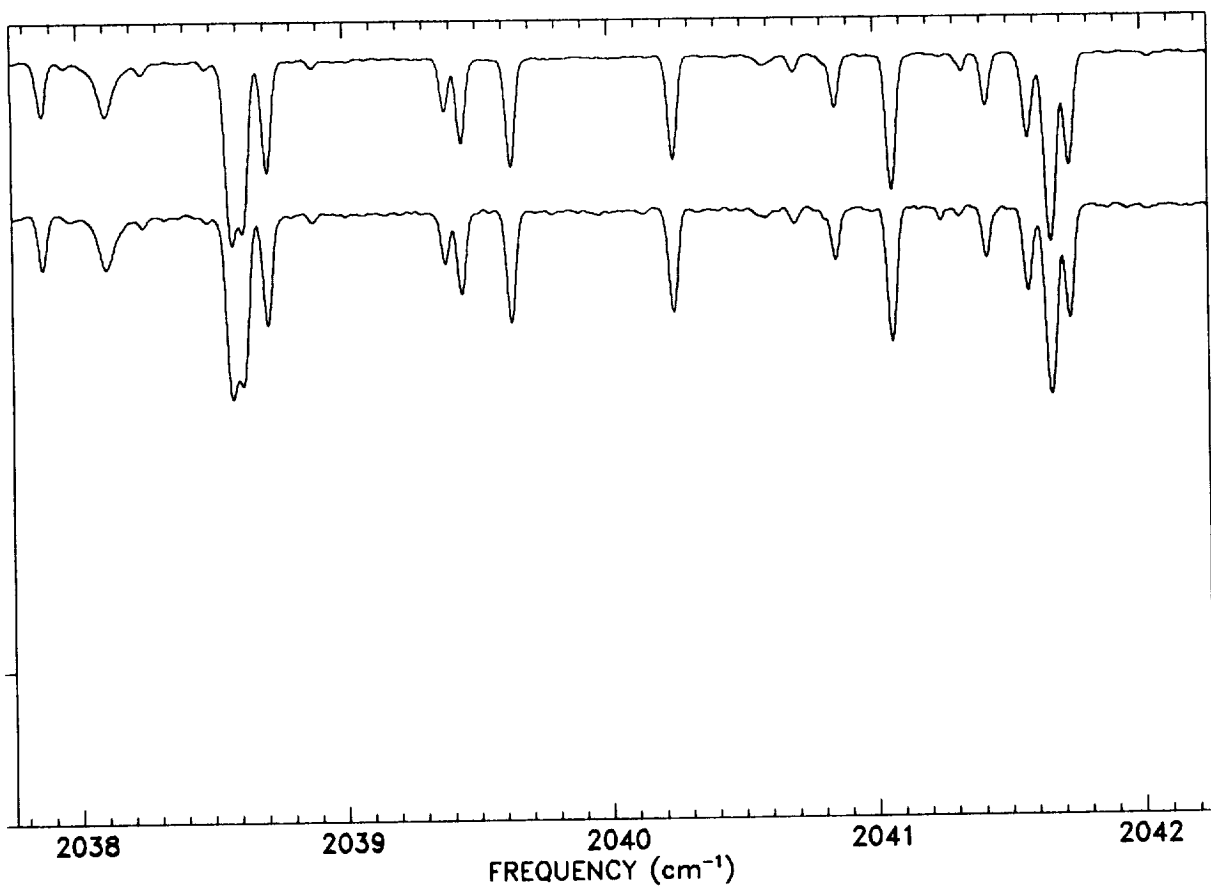


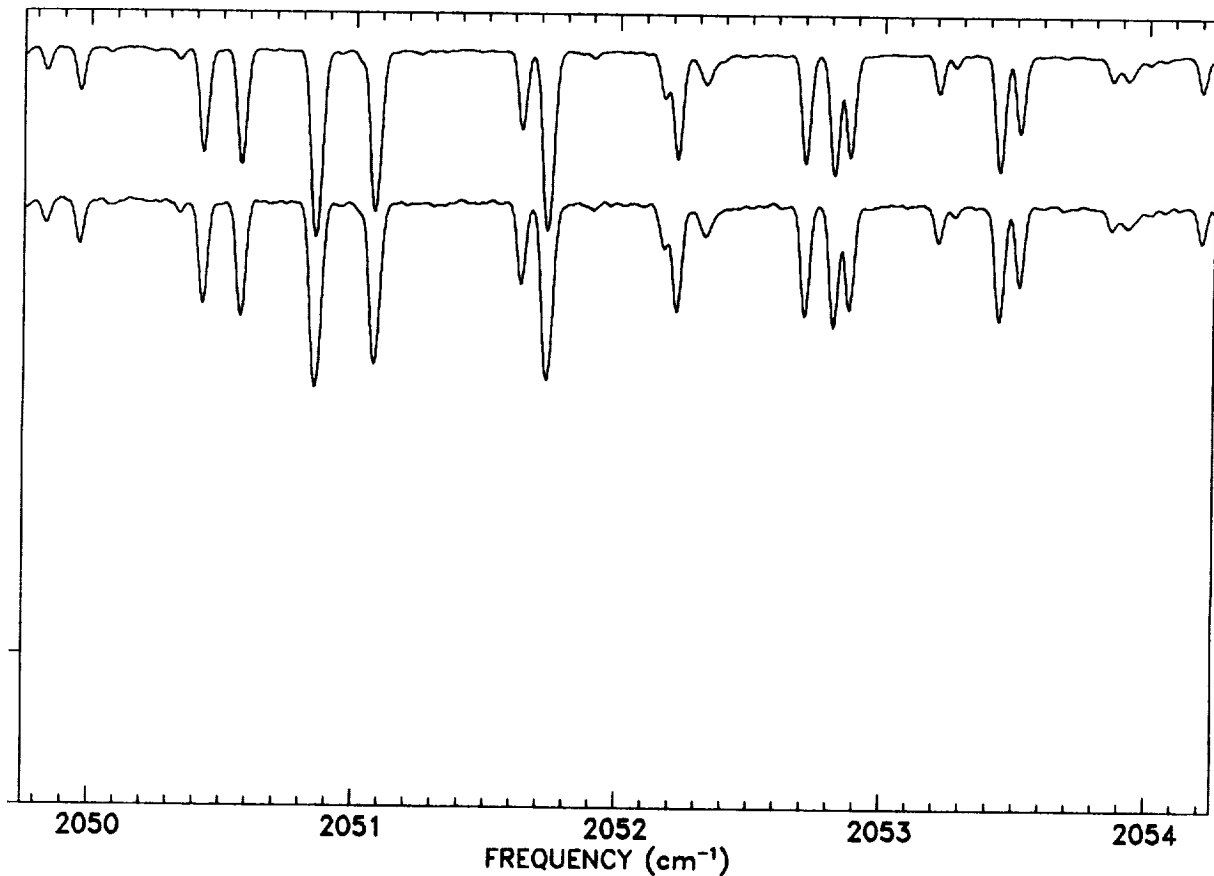
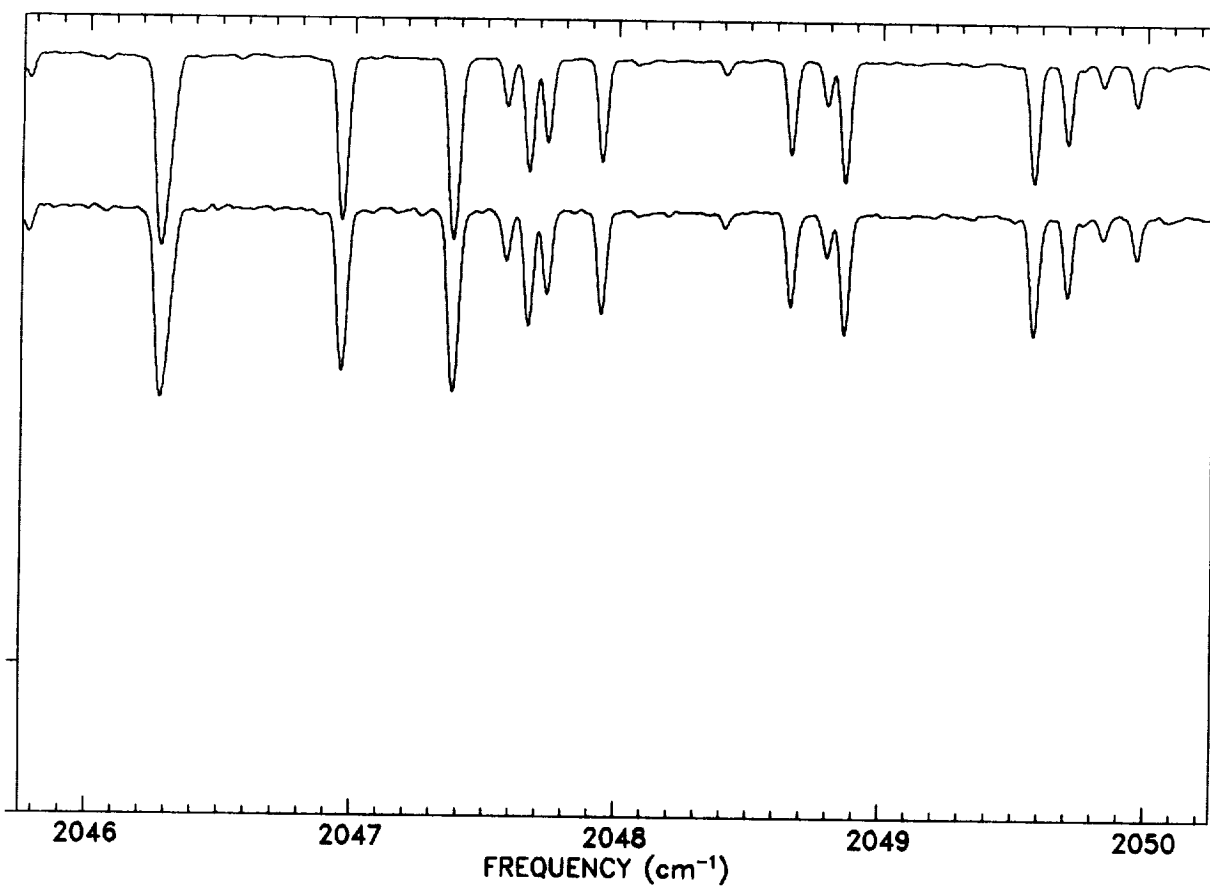


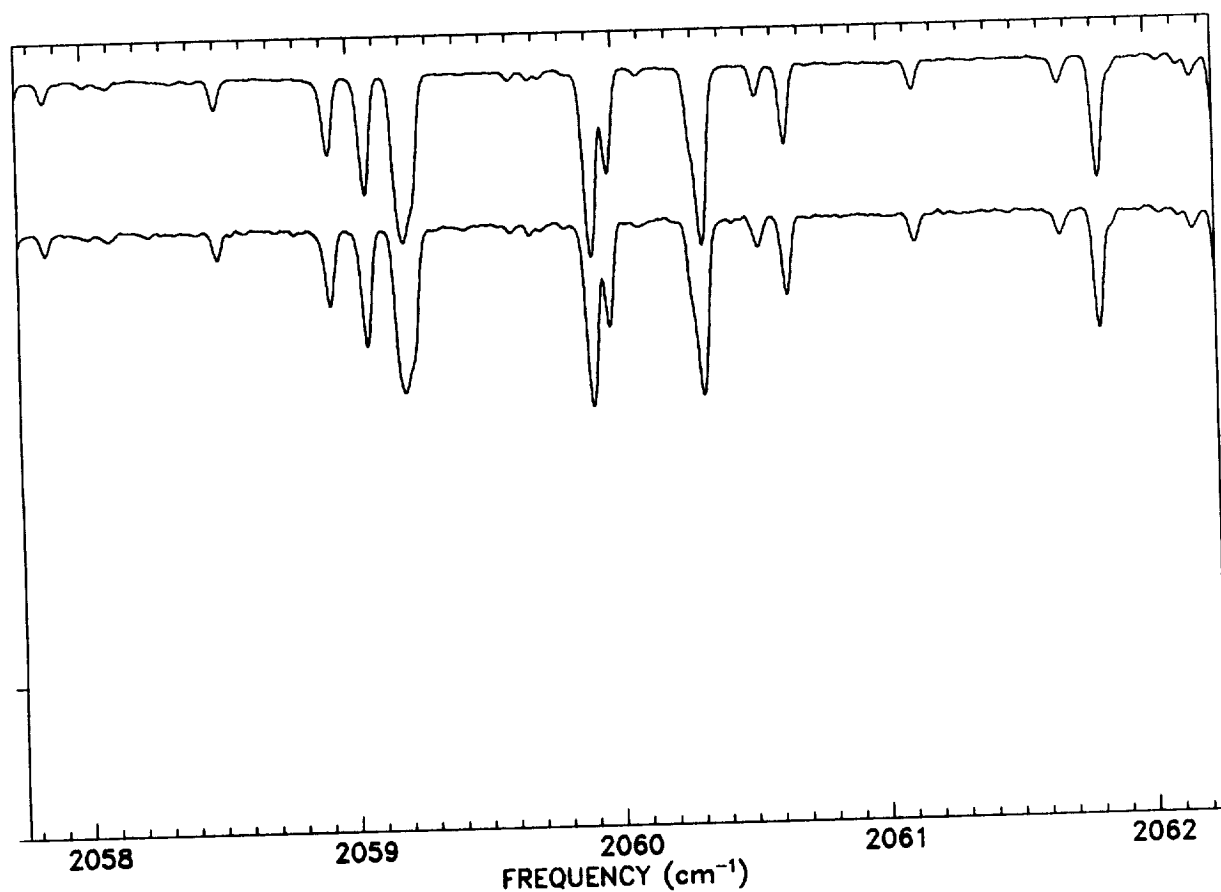
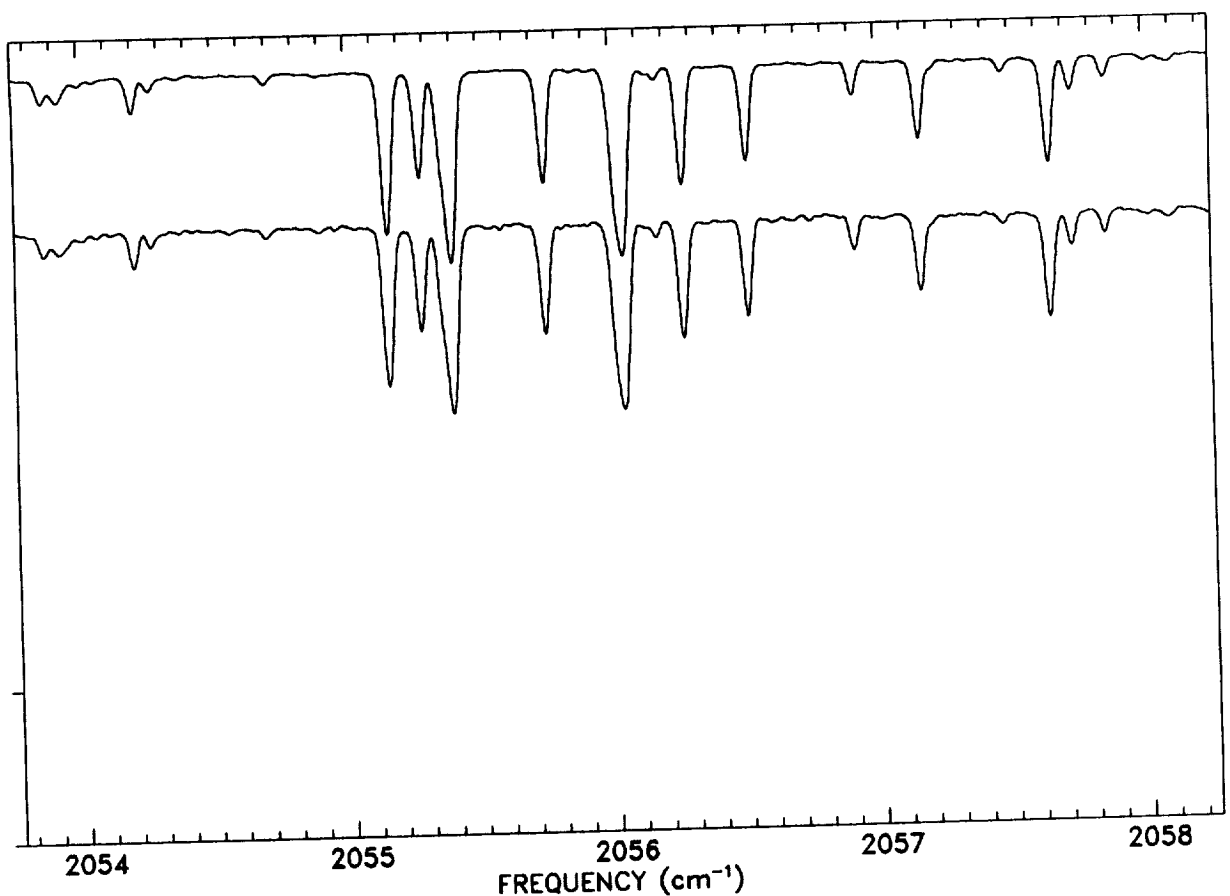


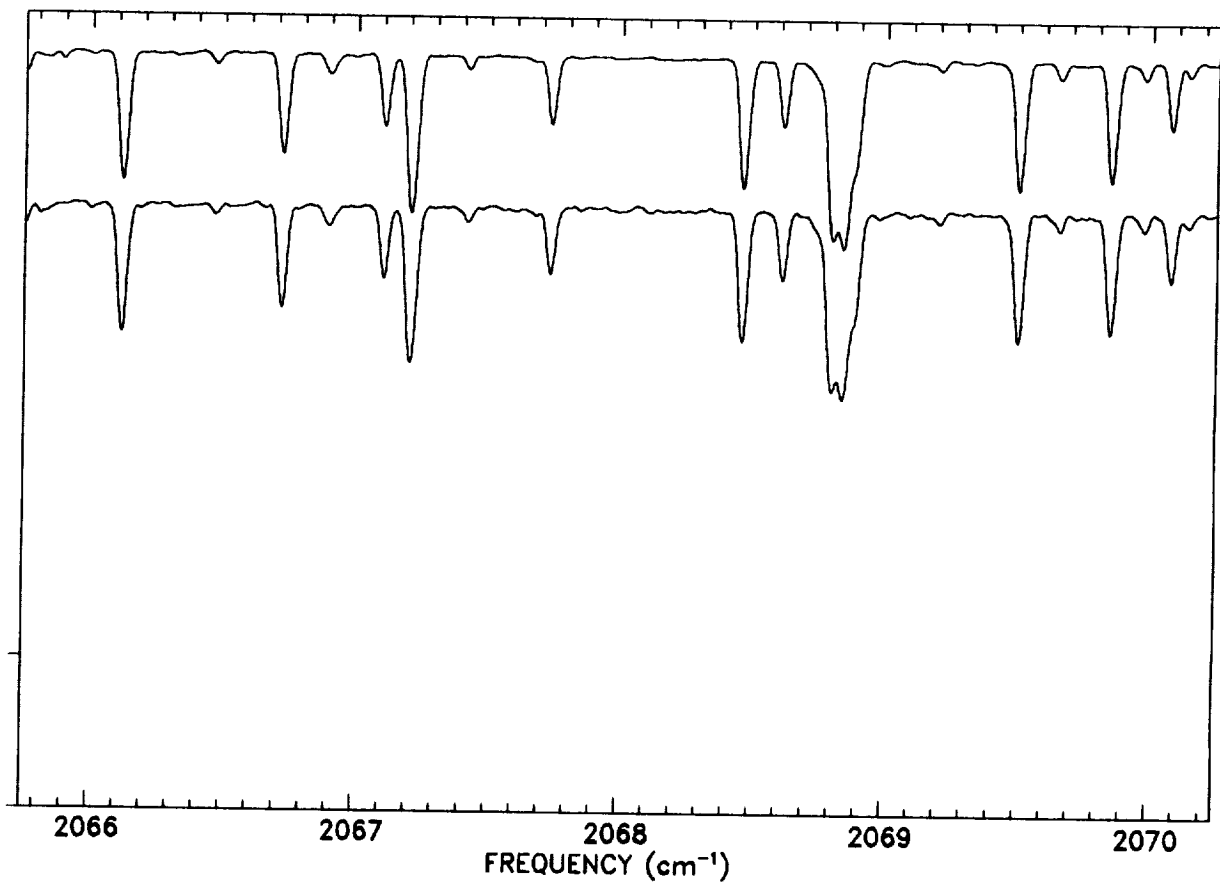
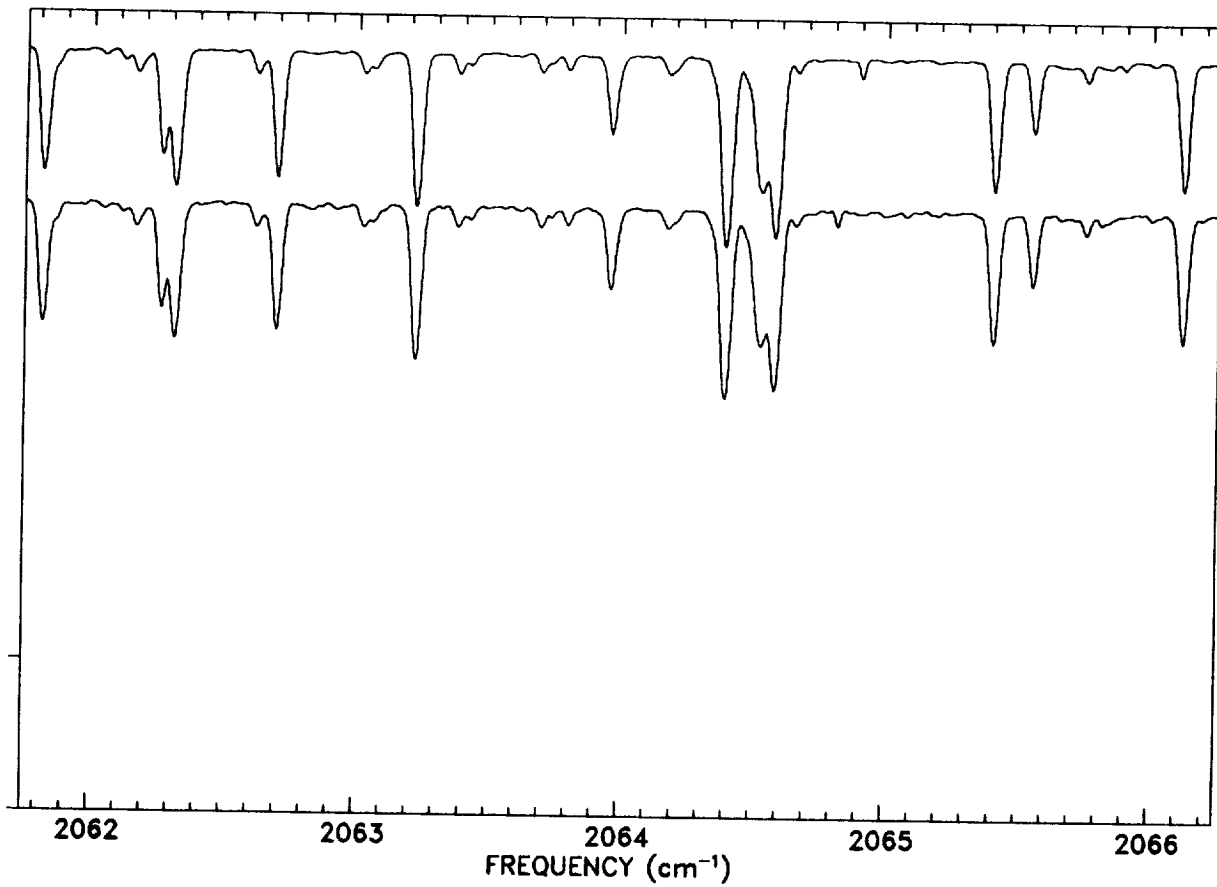


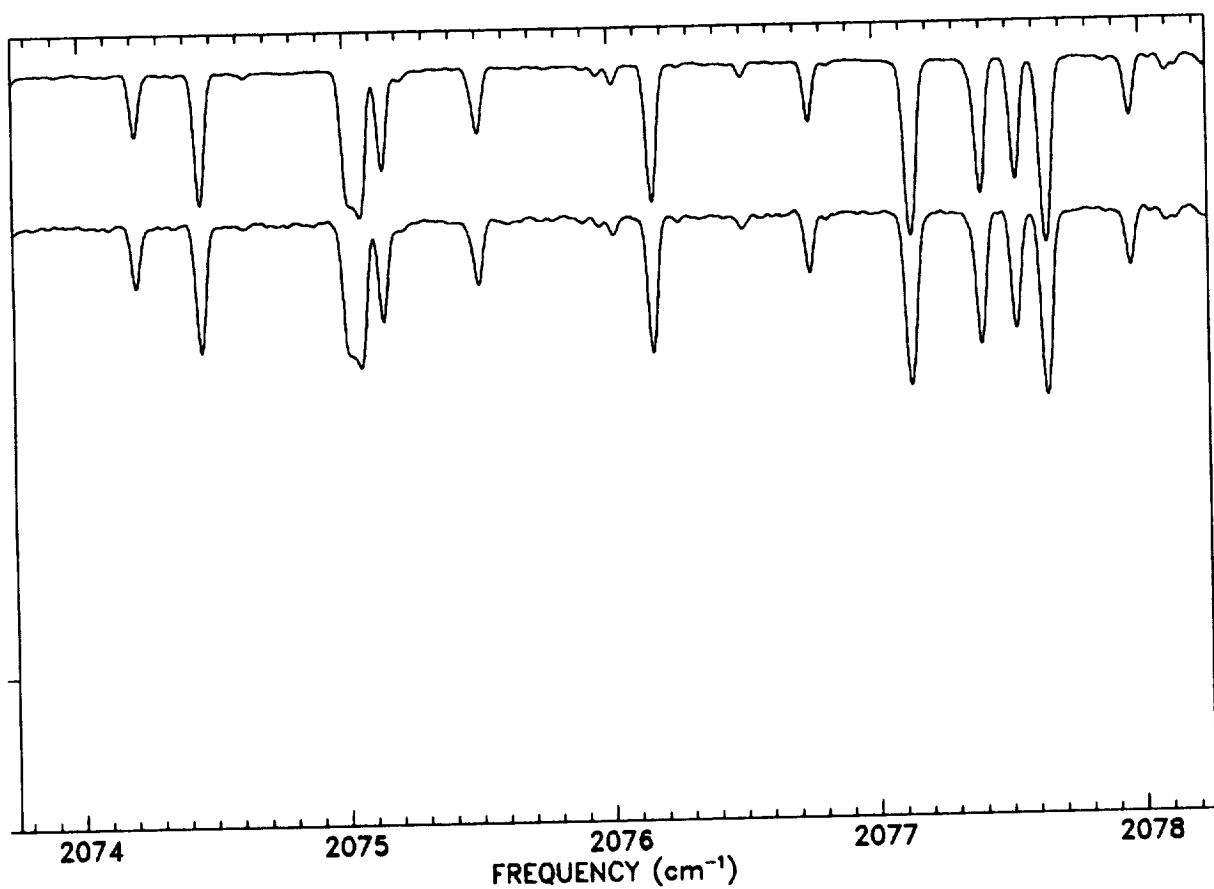
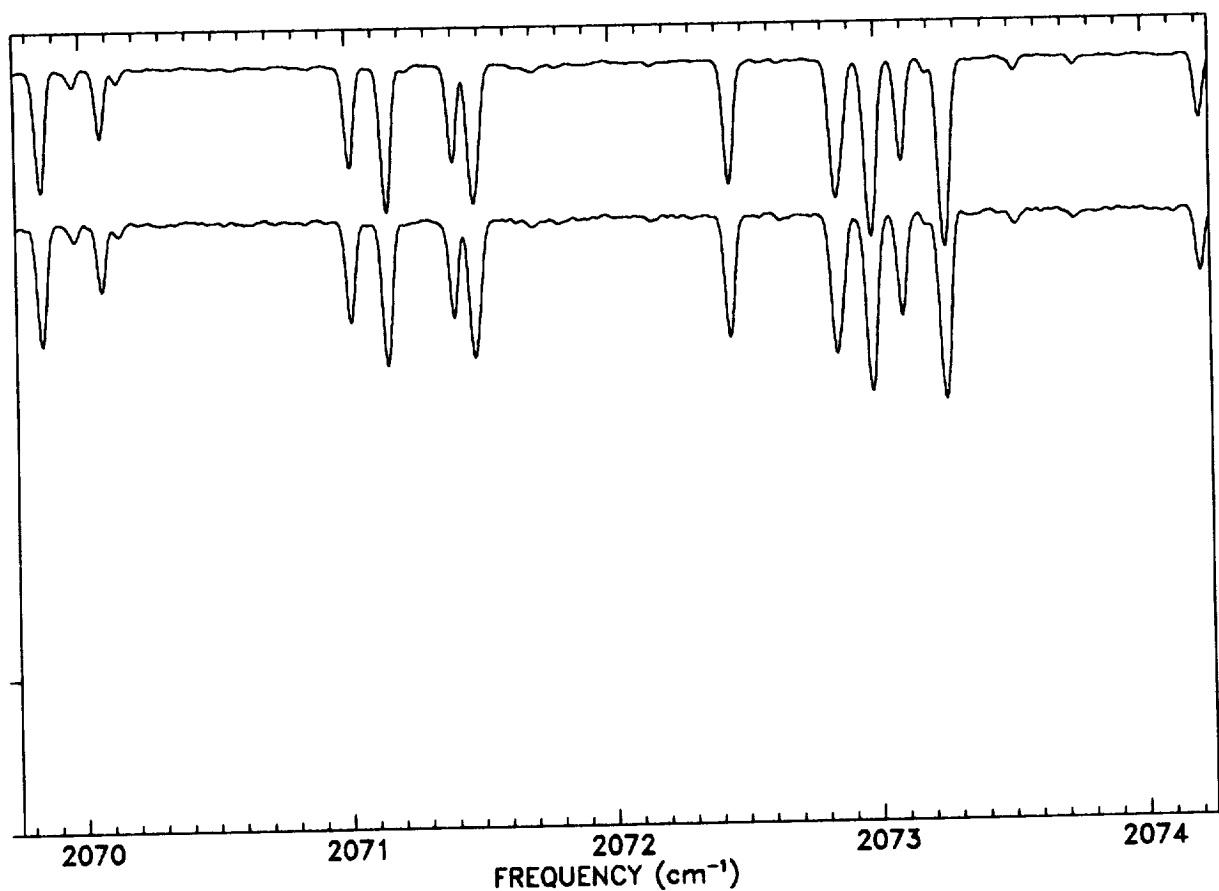


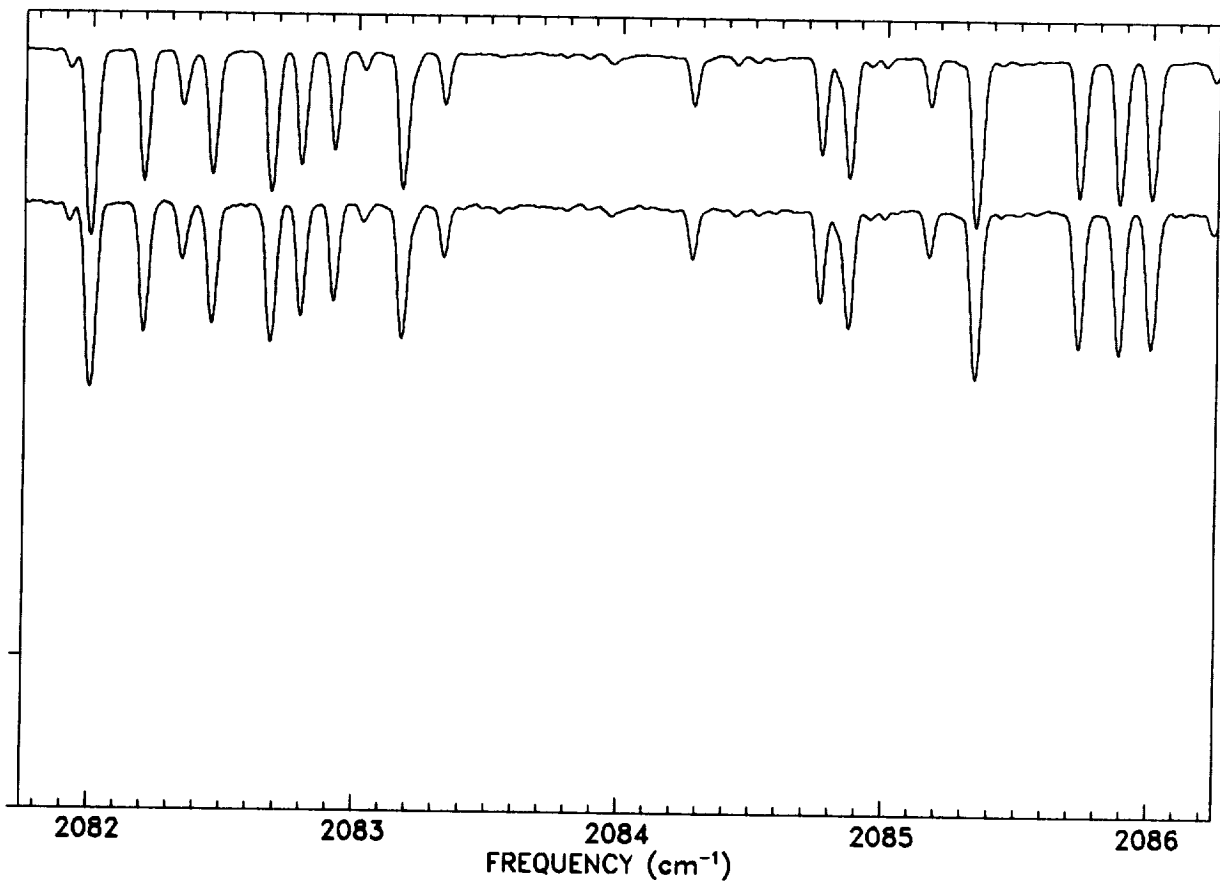
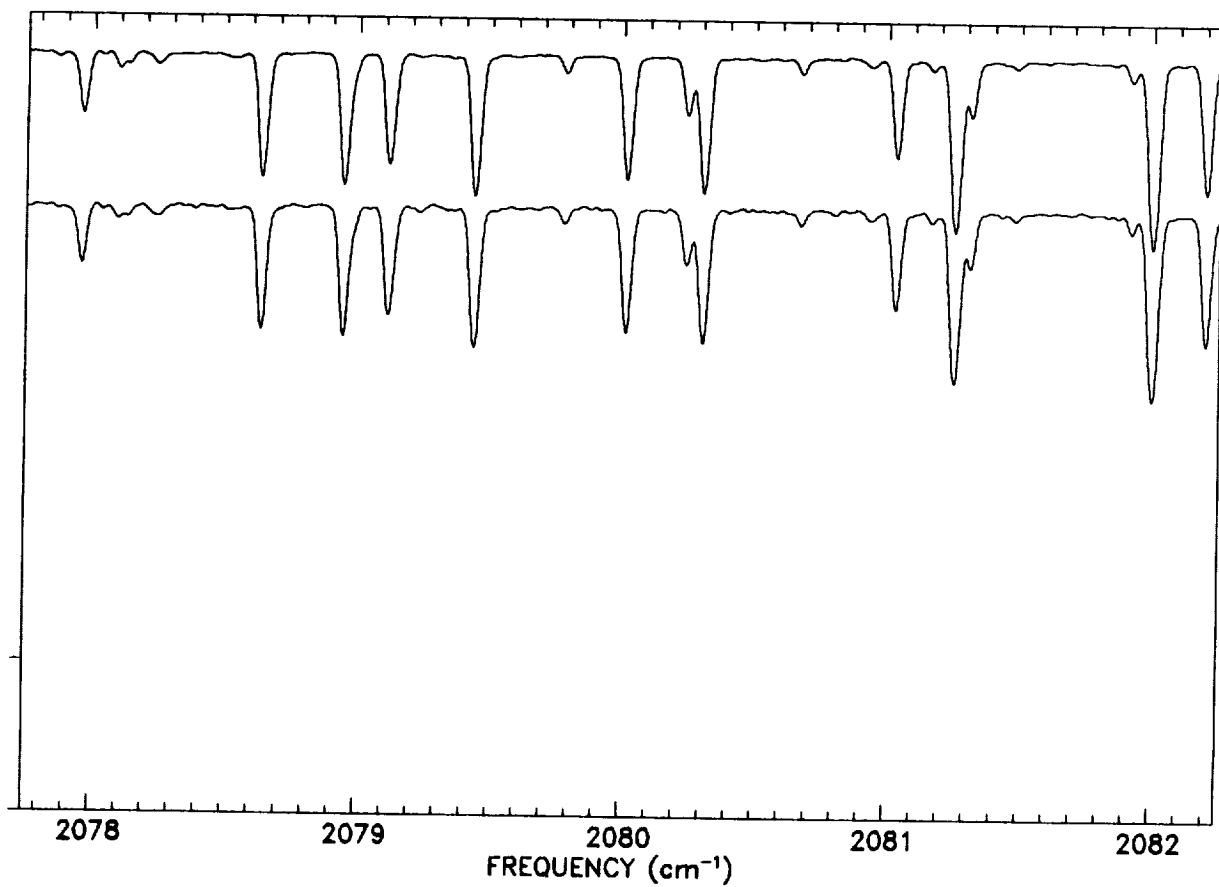


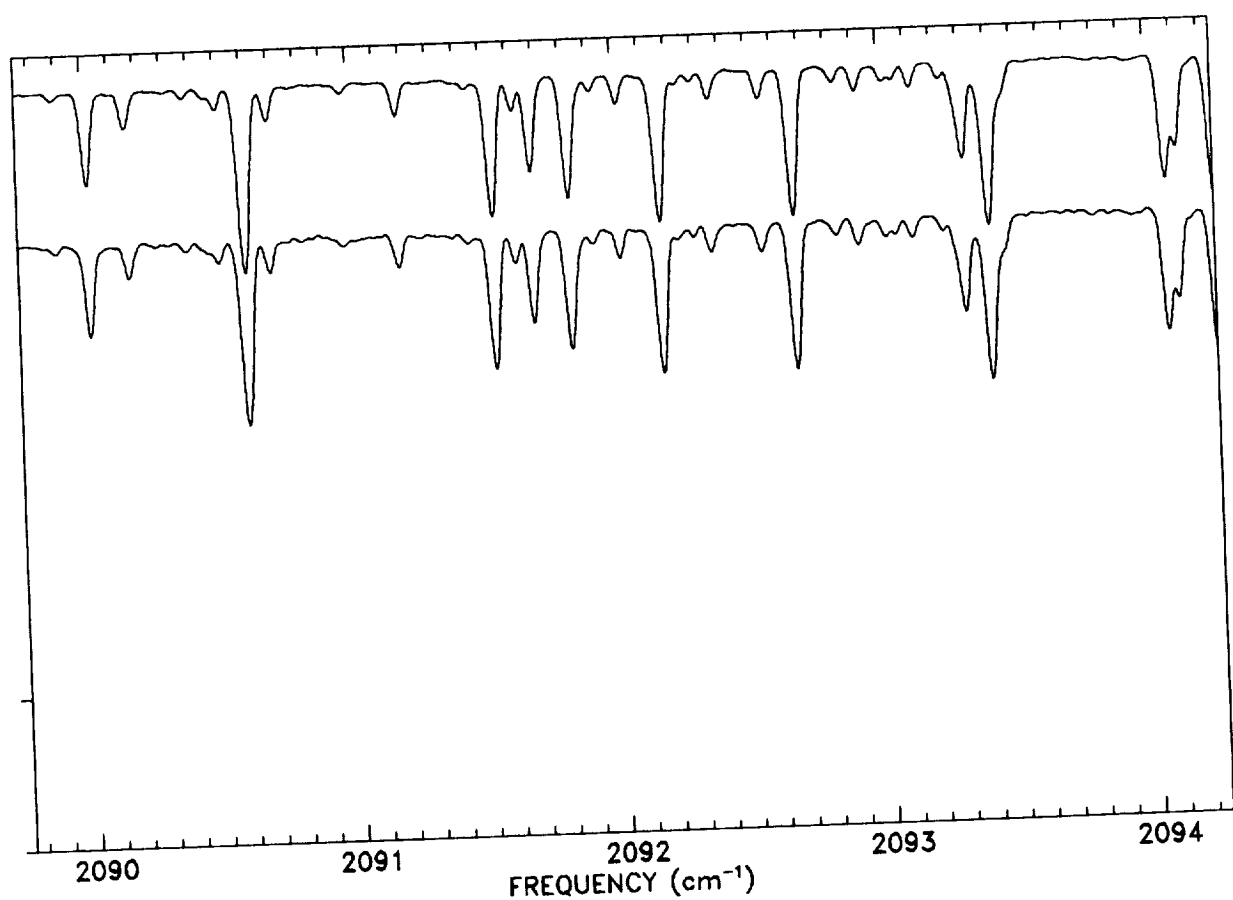
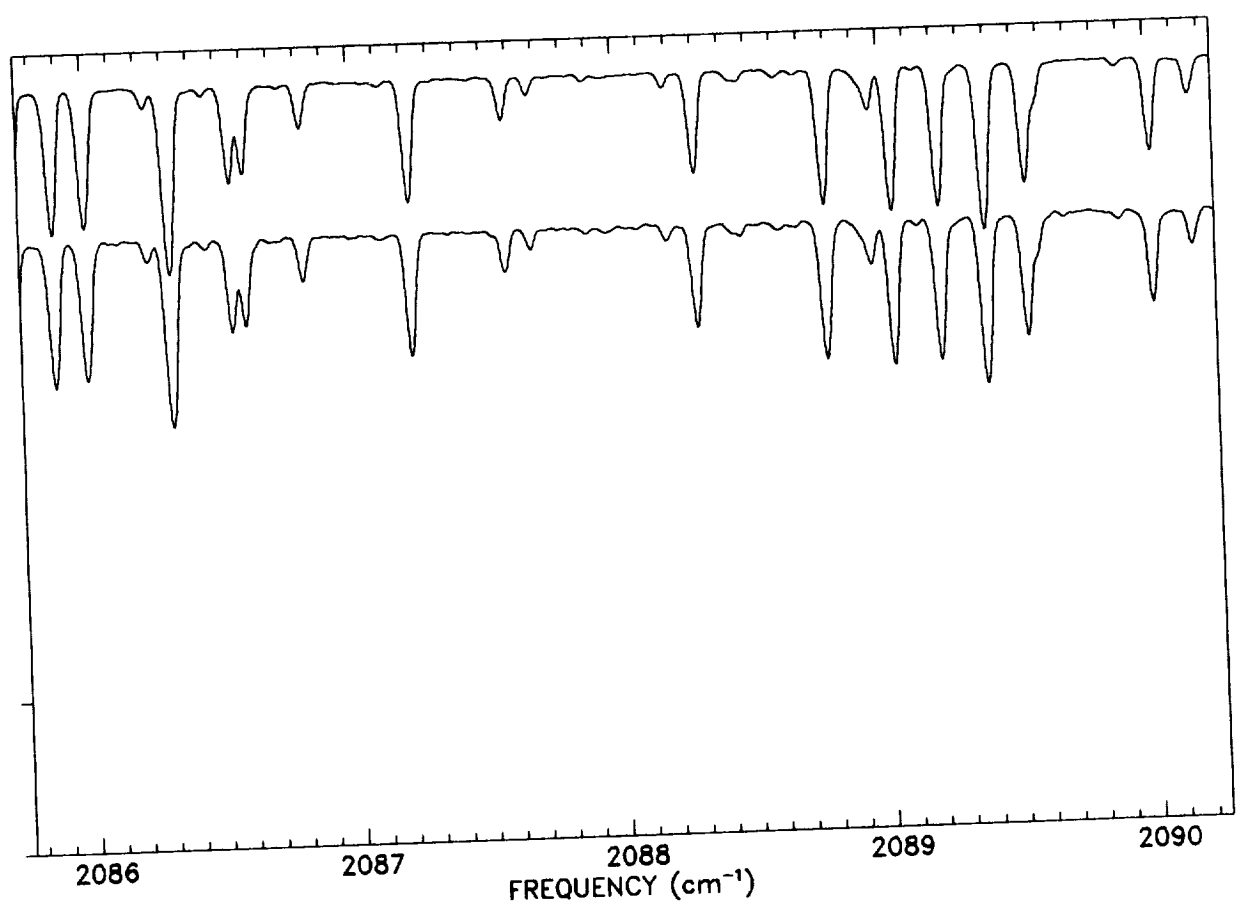




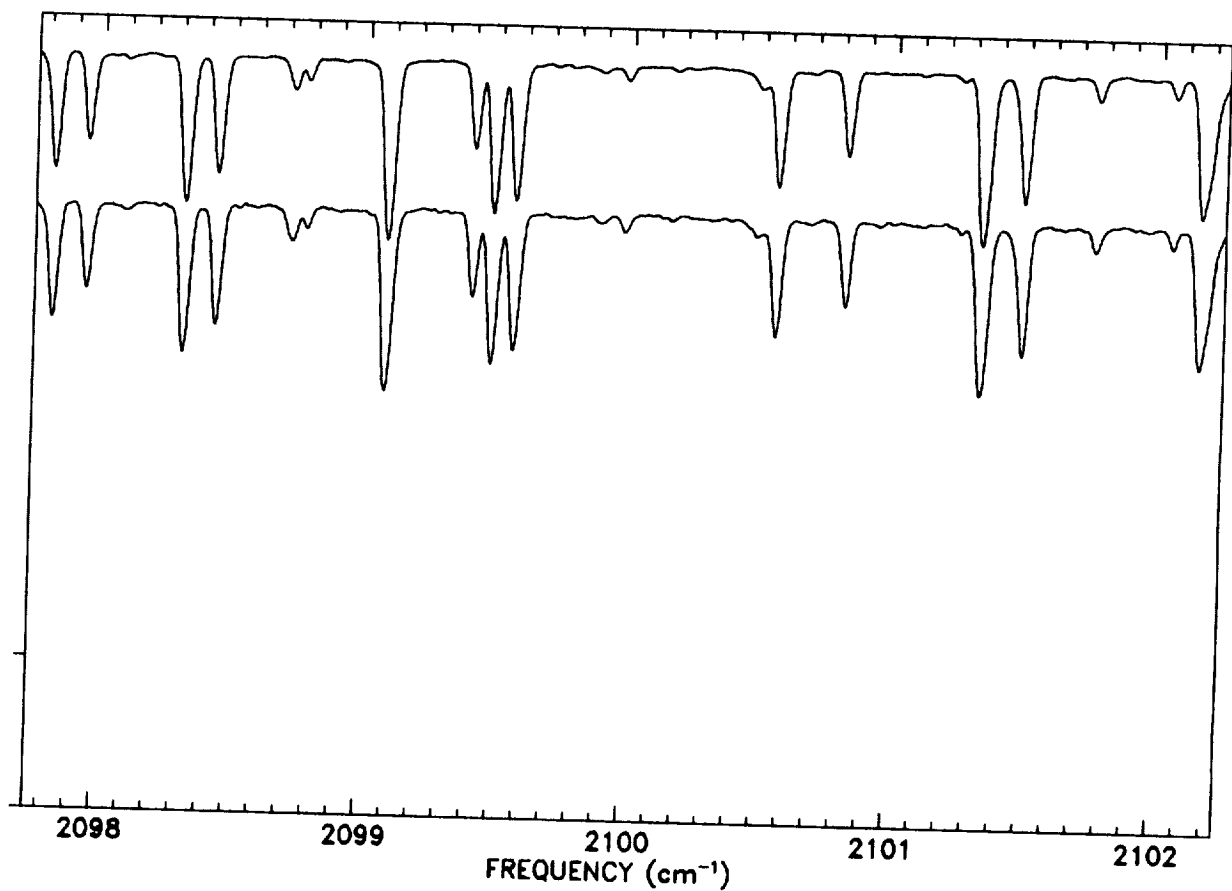
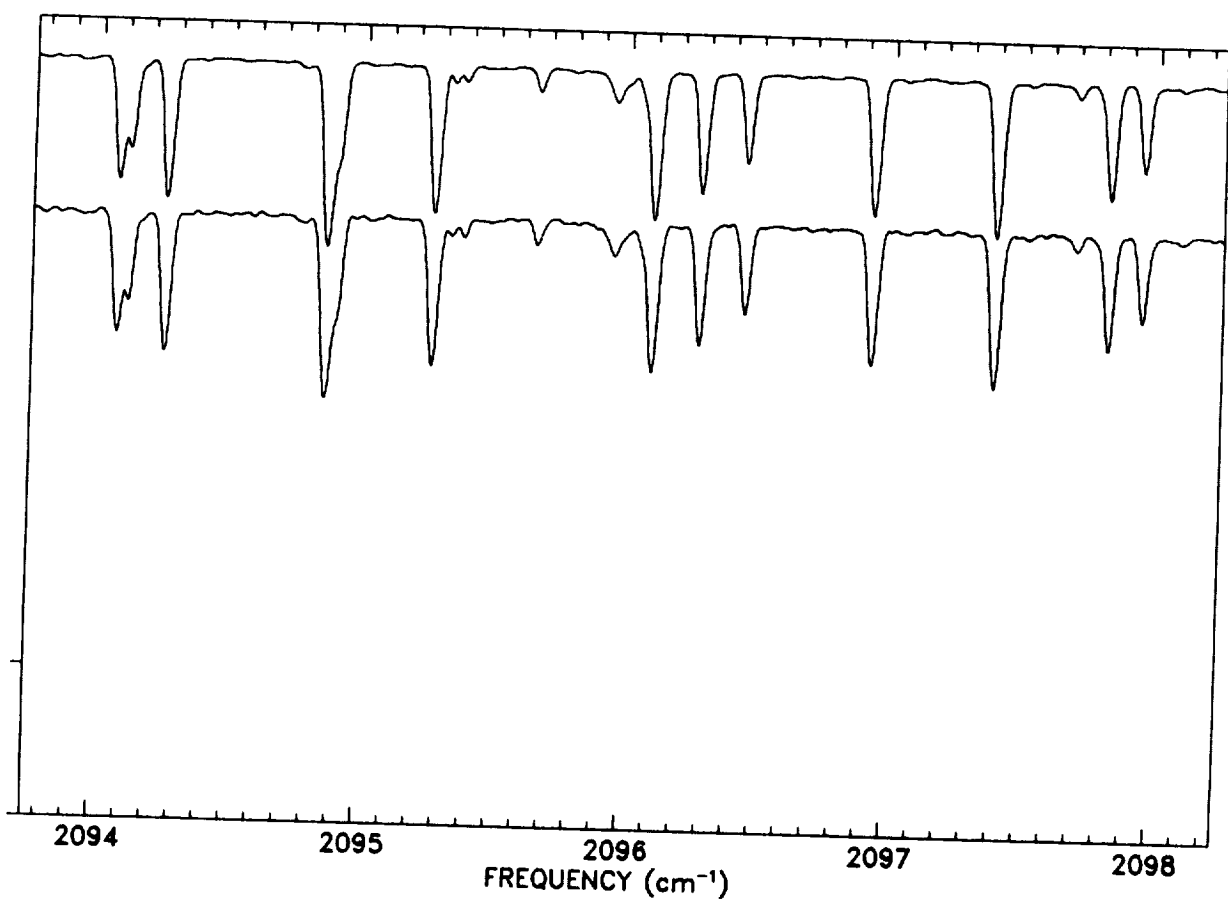


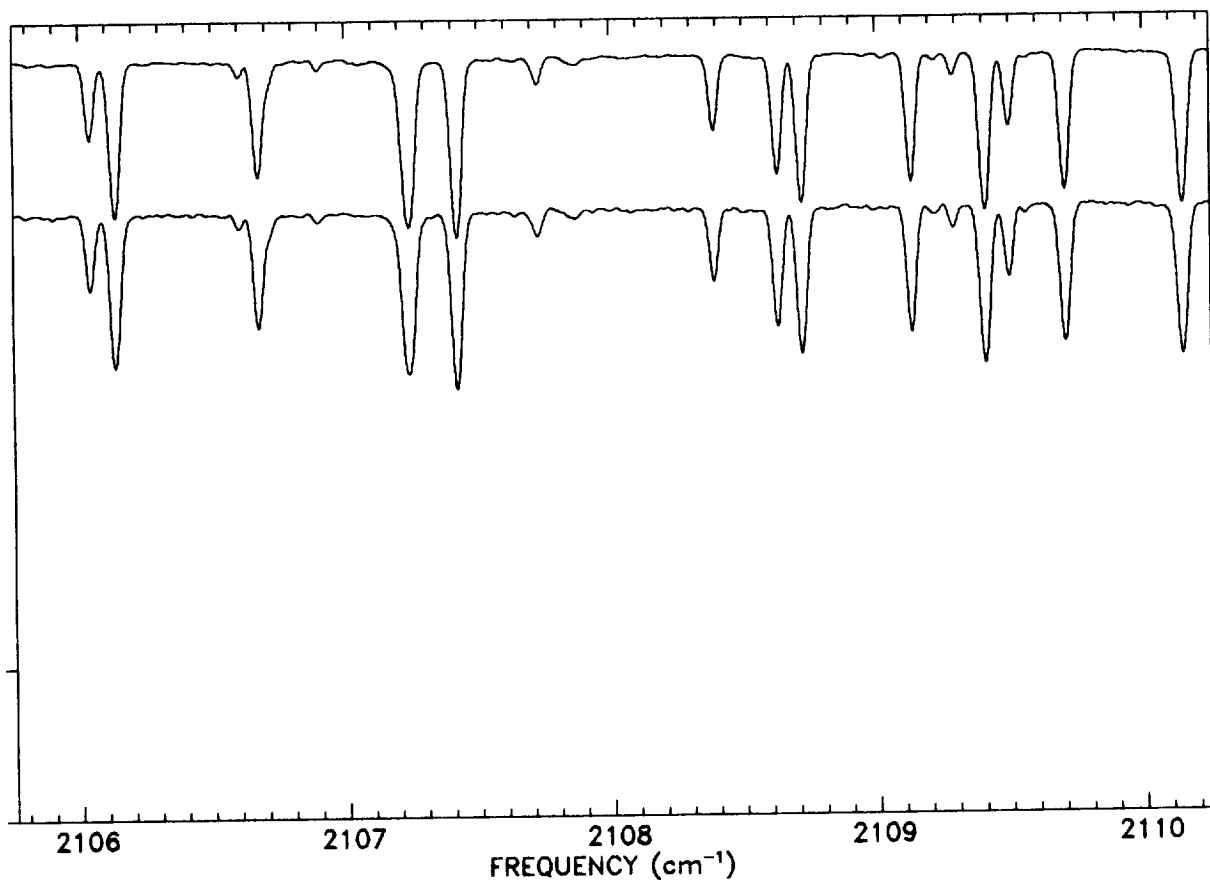
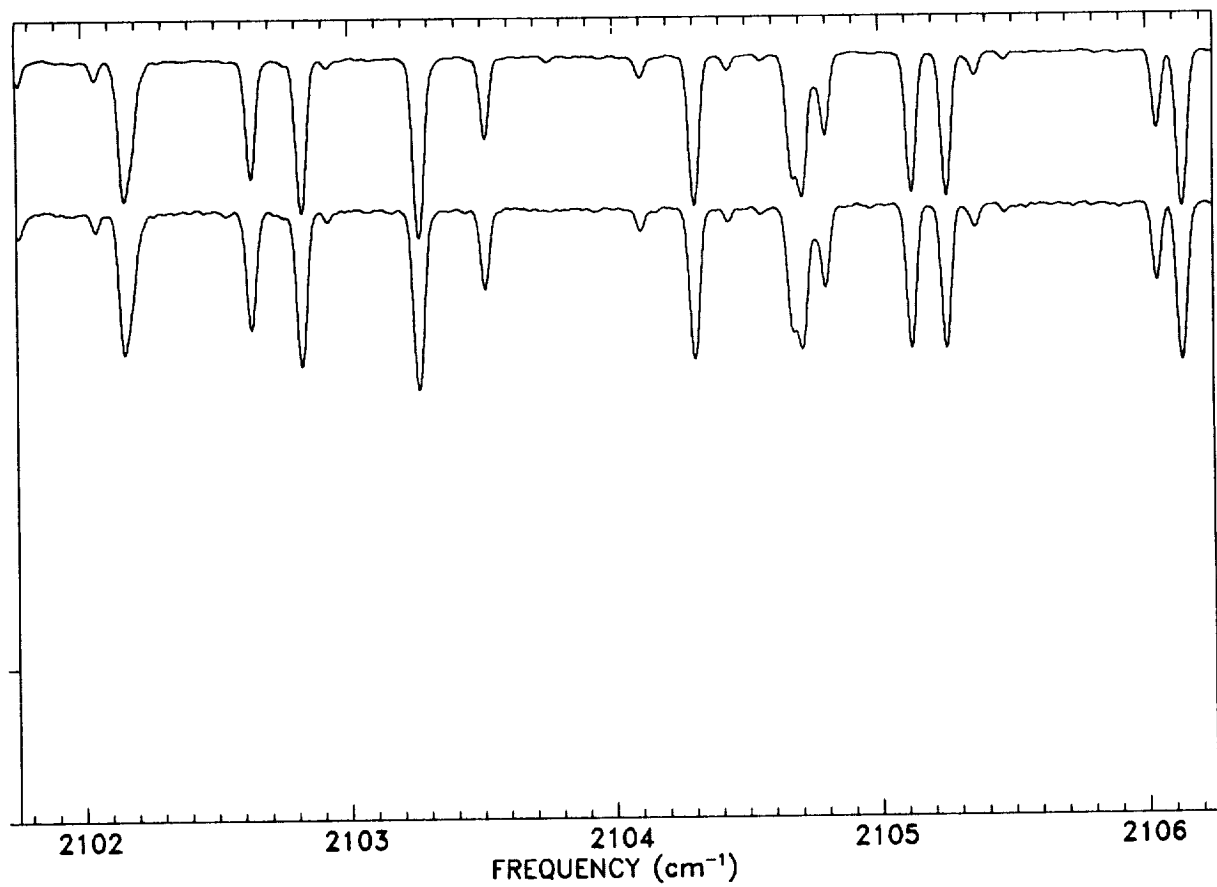


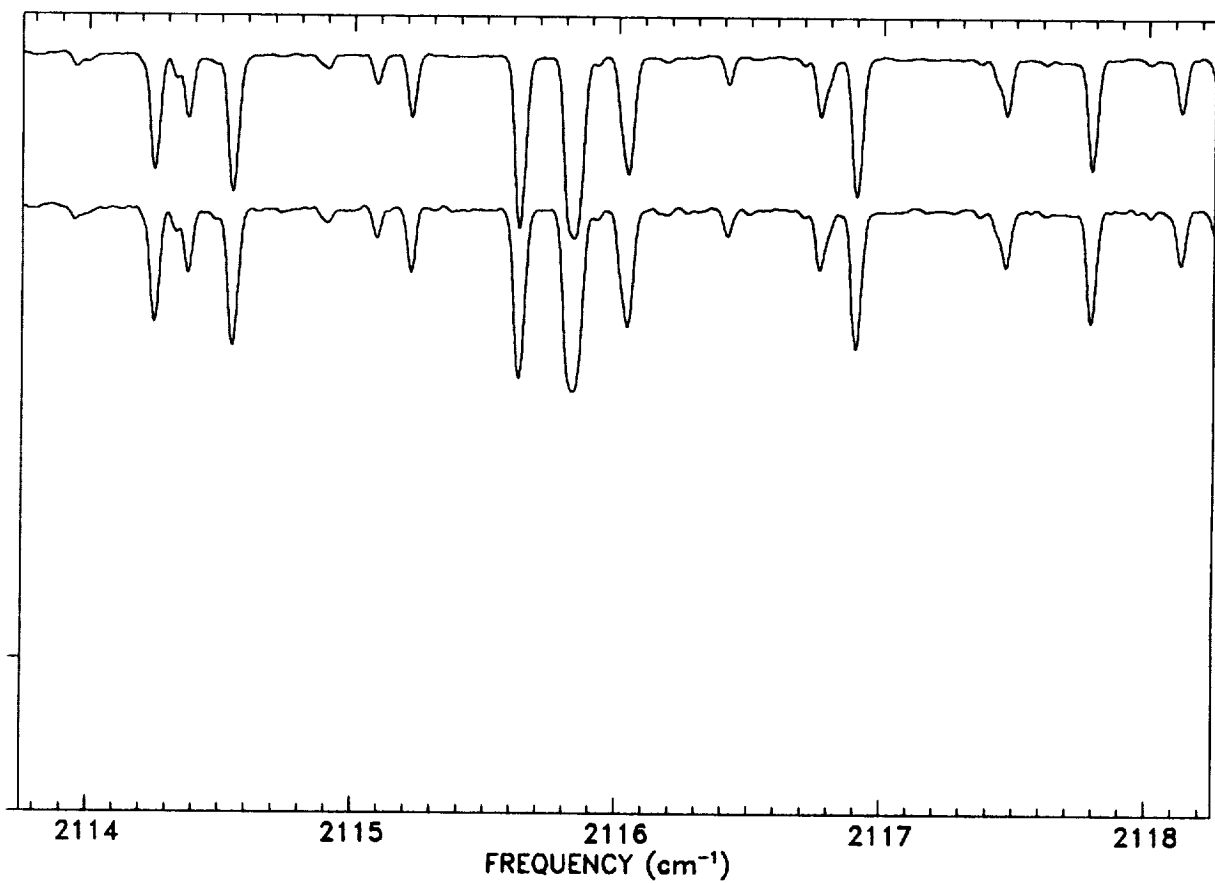
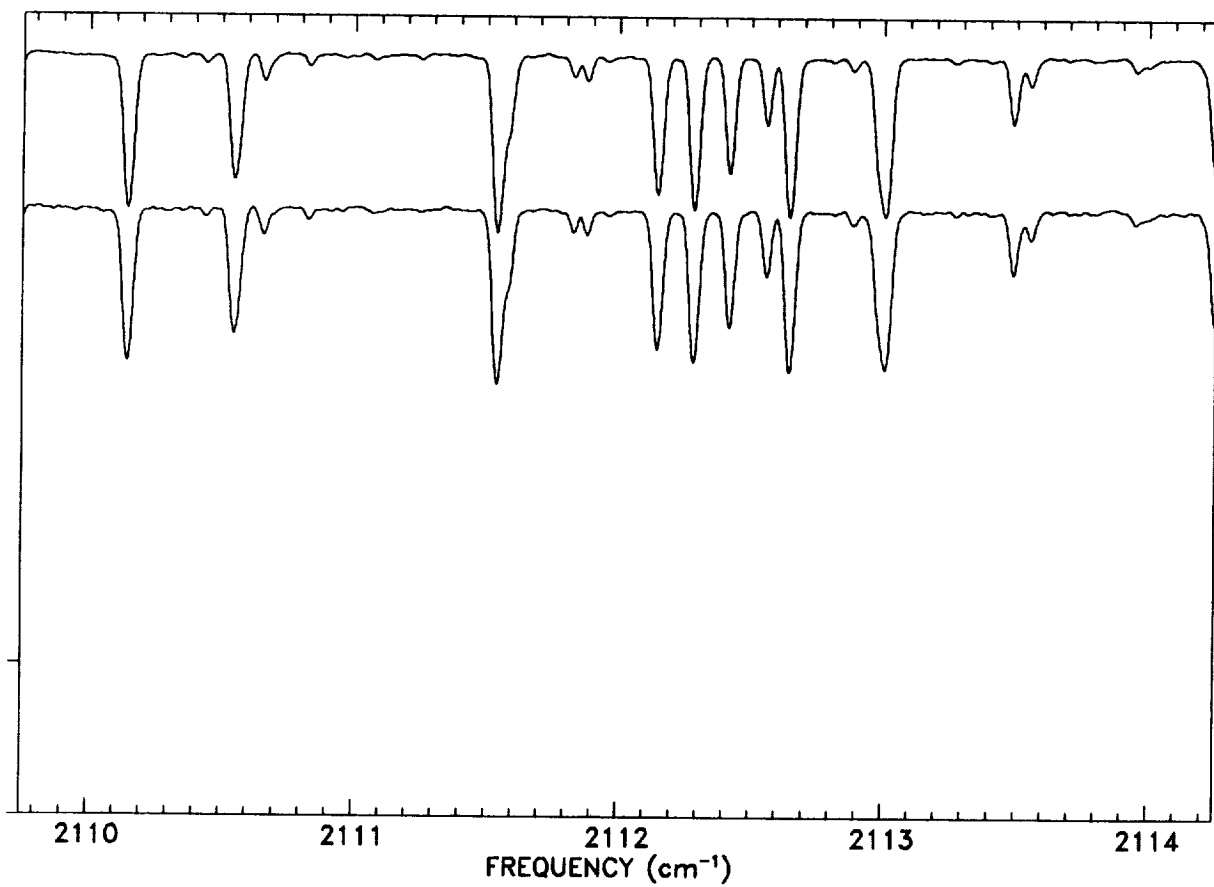


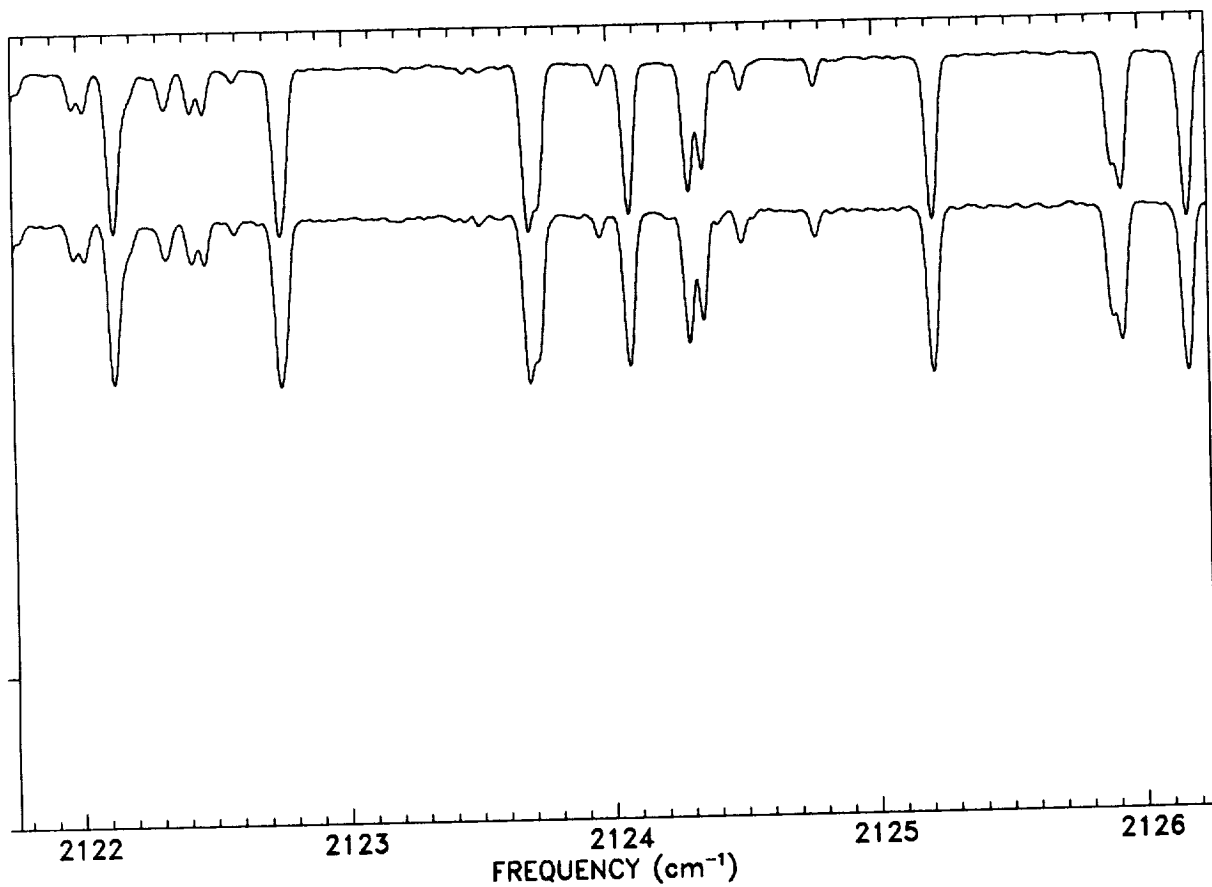
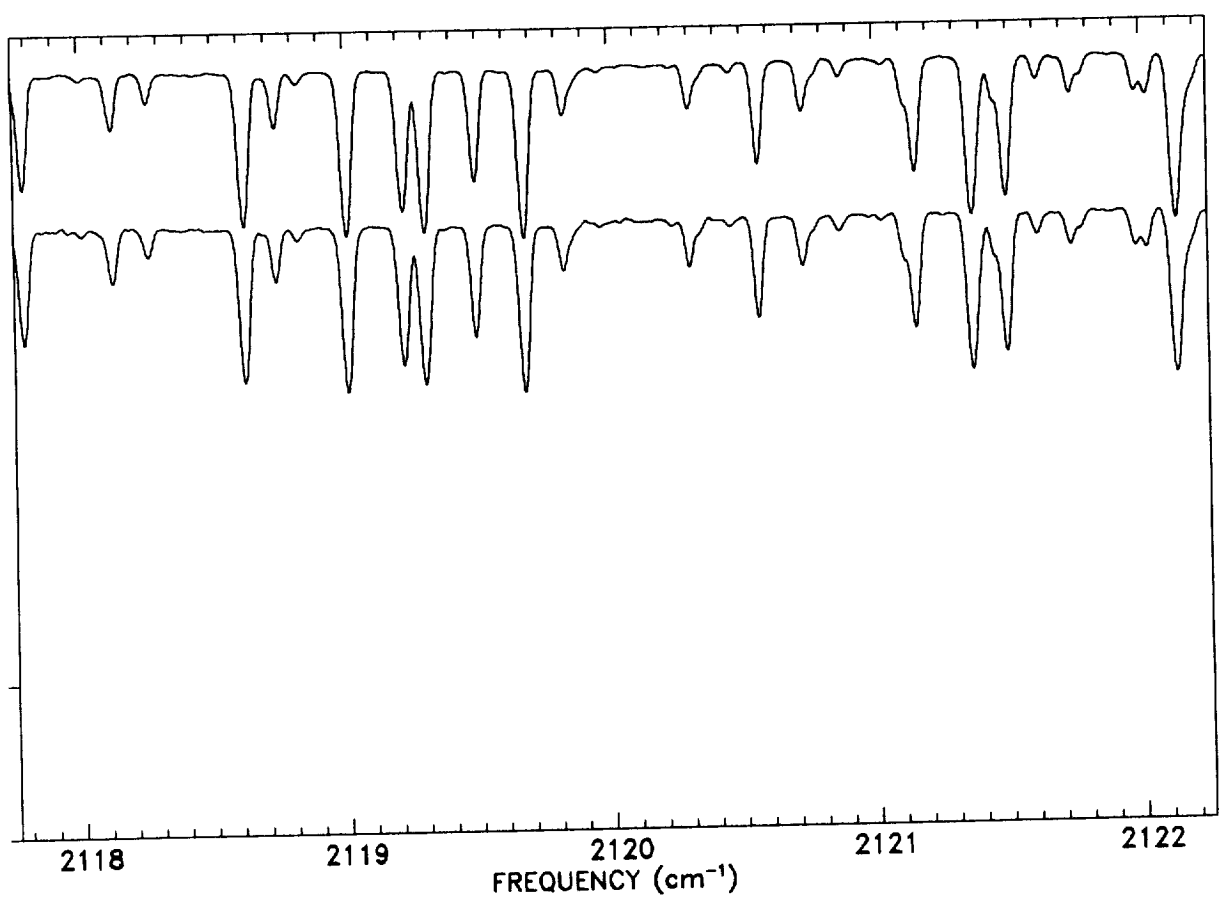


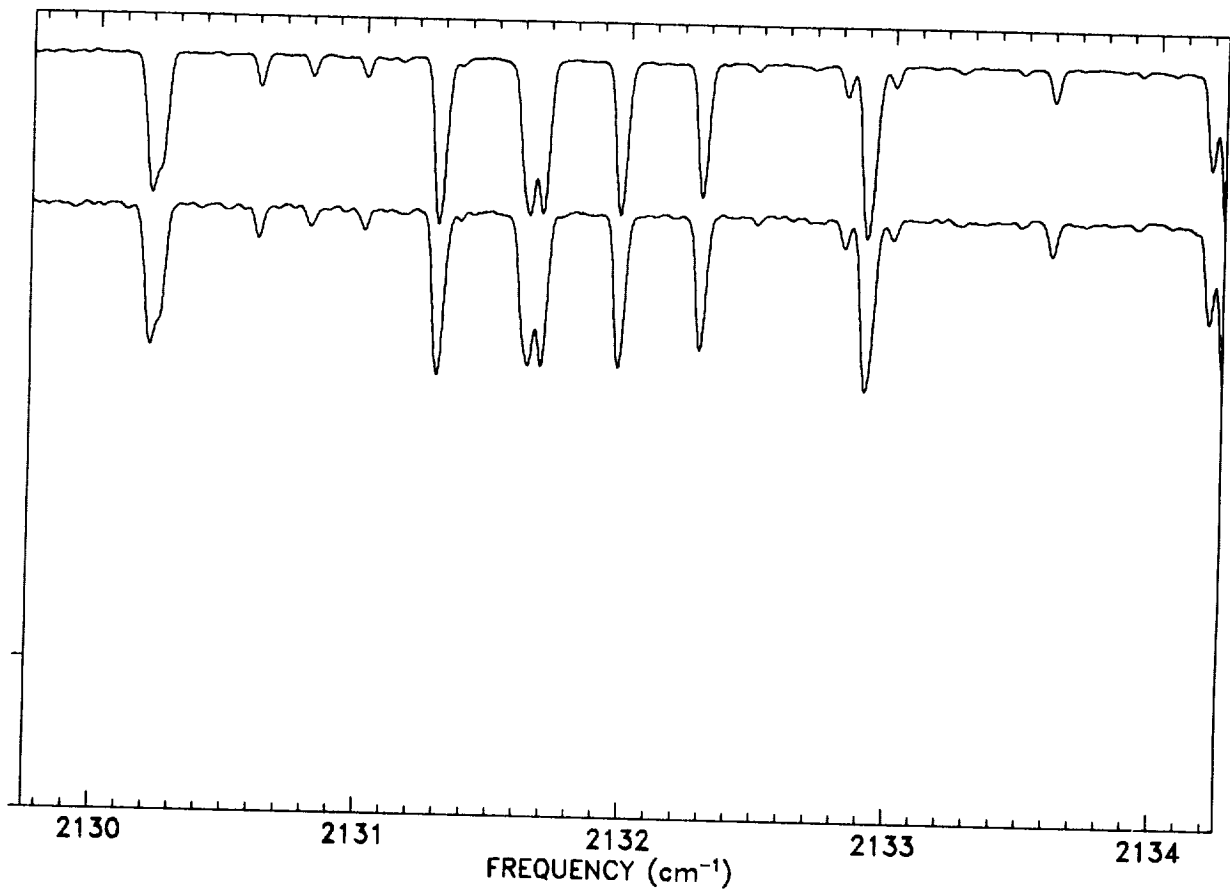
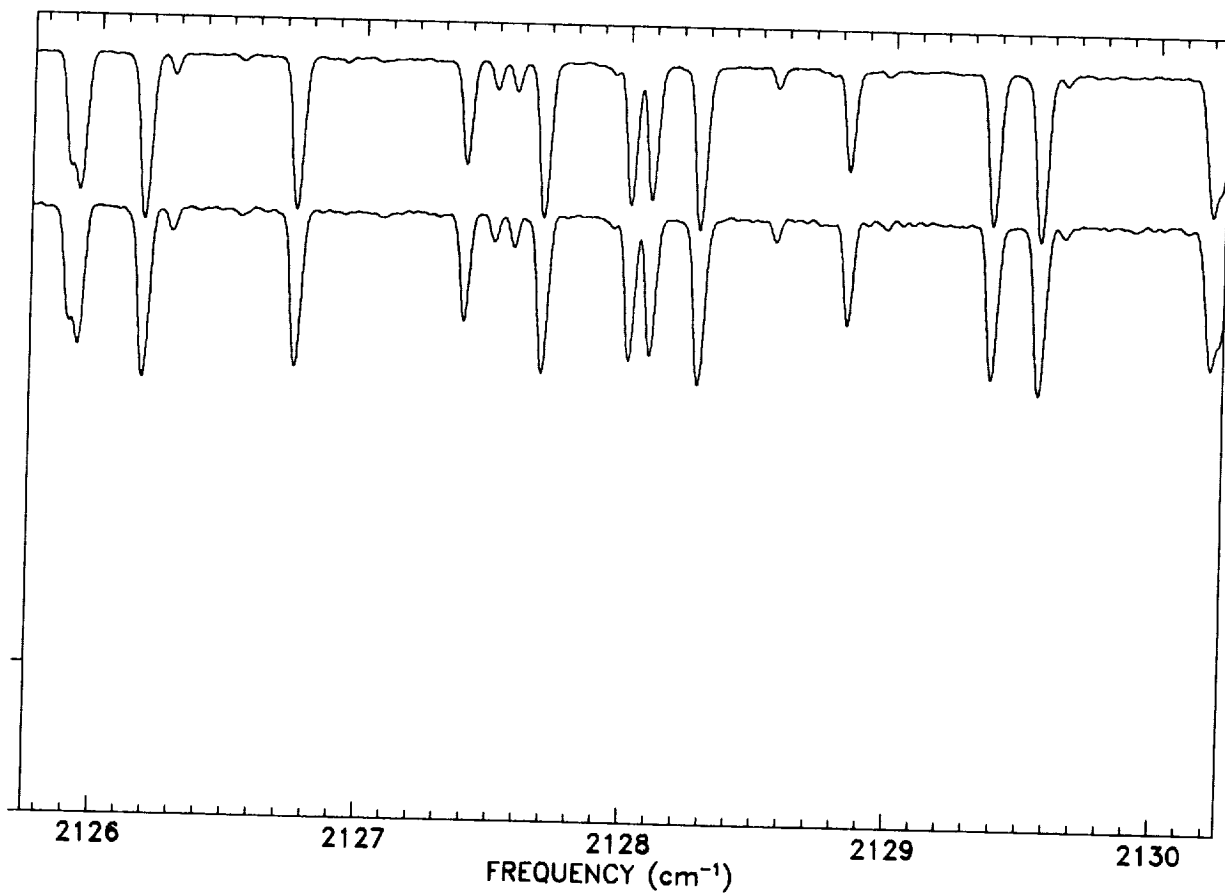
C - 3

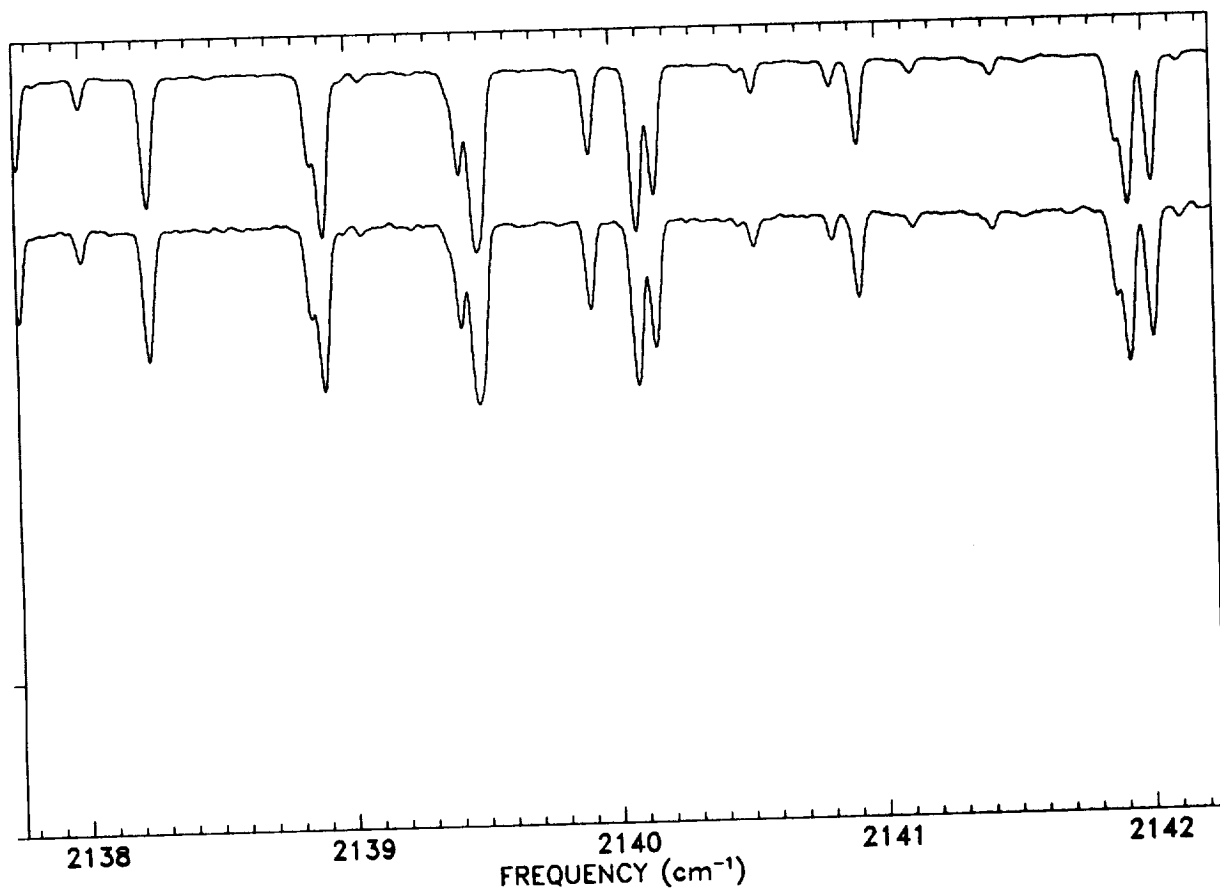
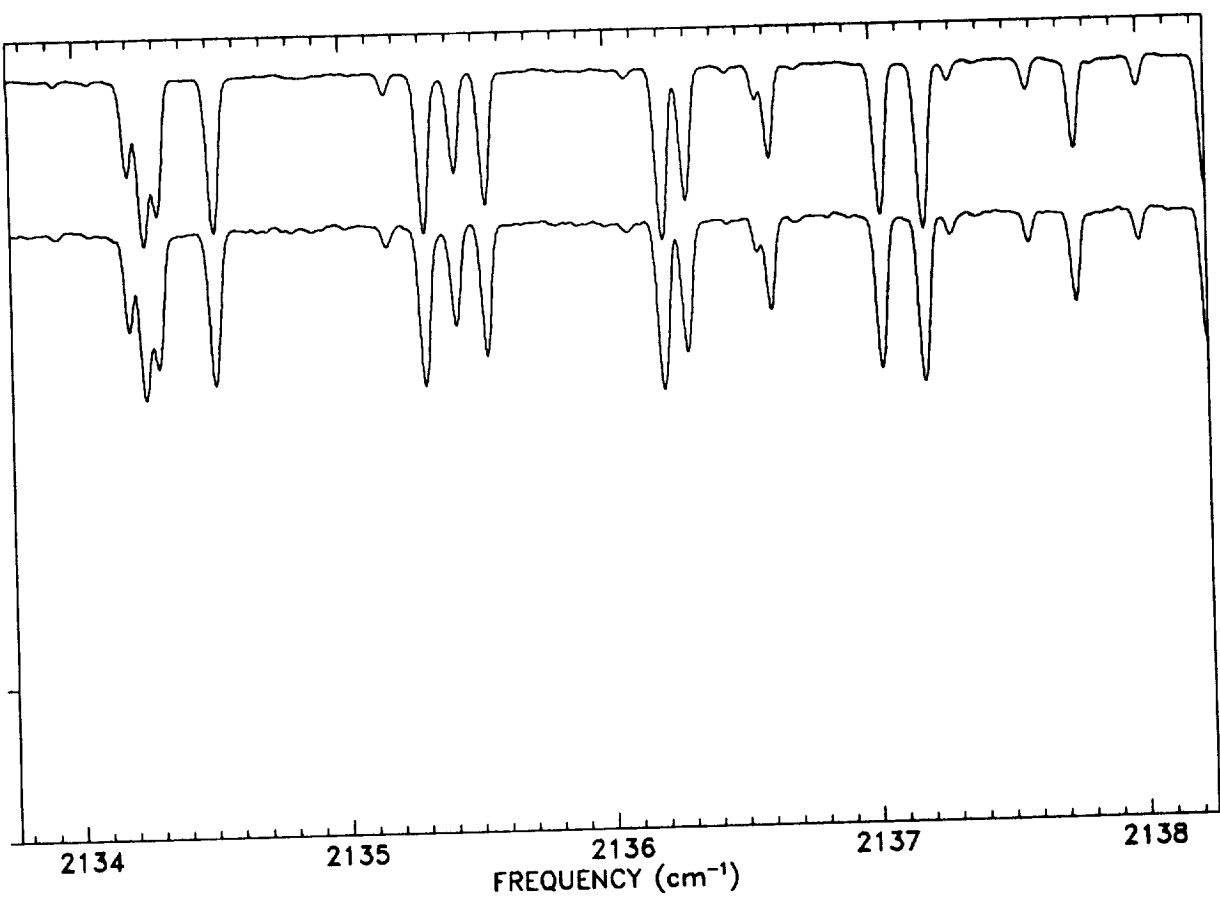


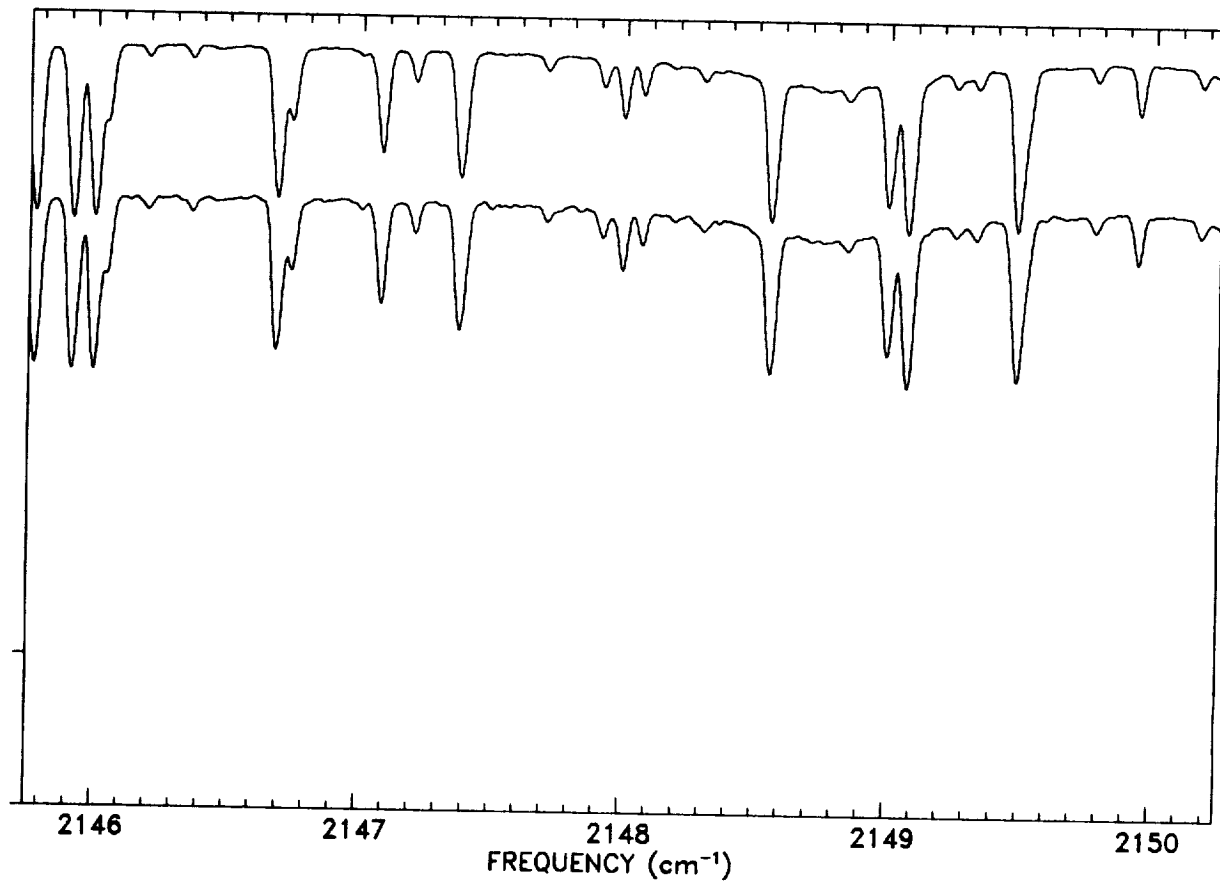
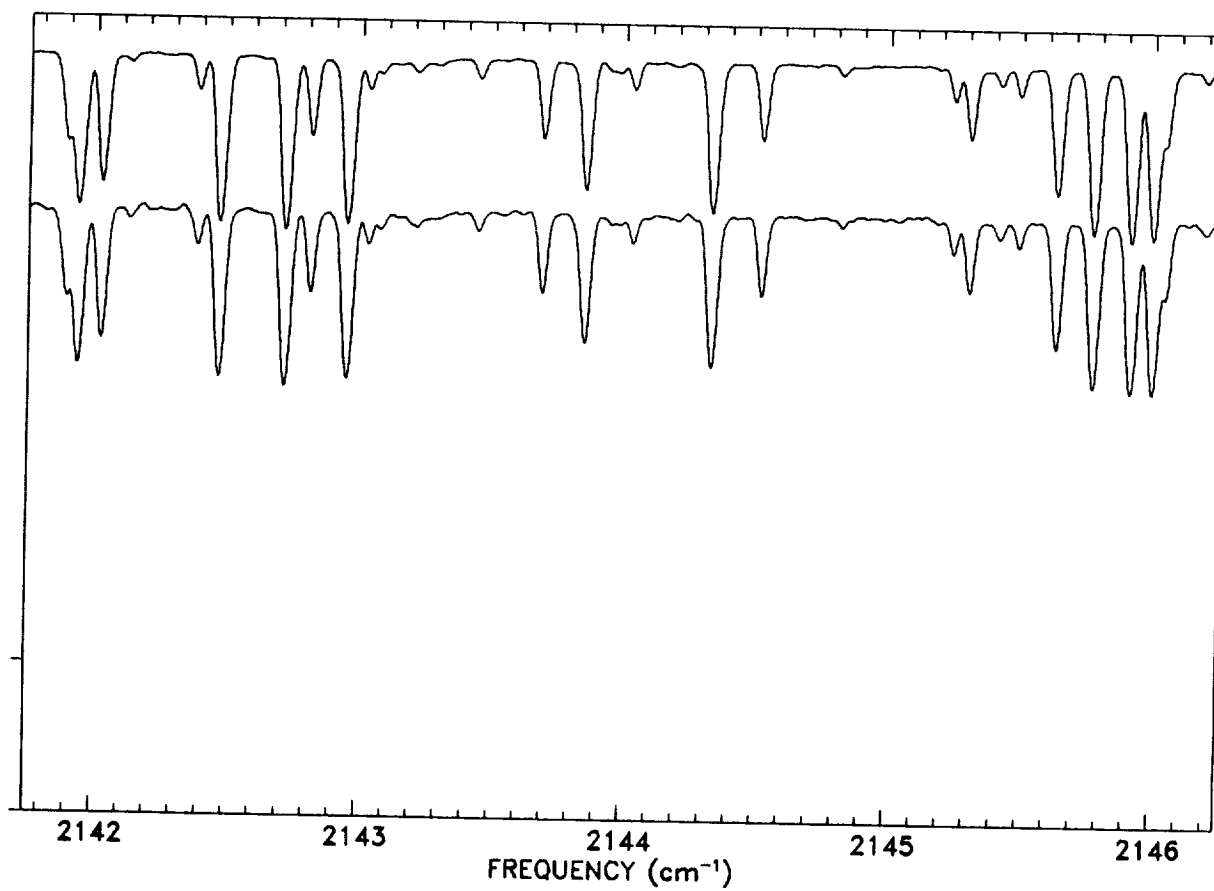


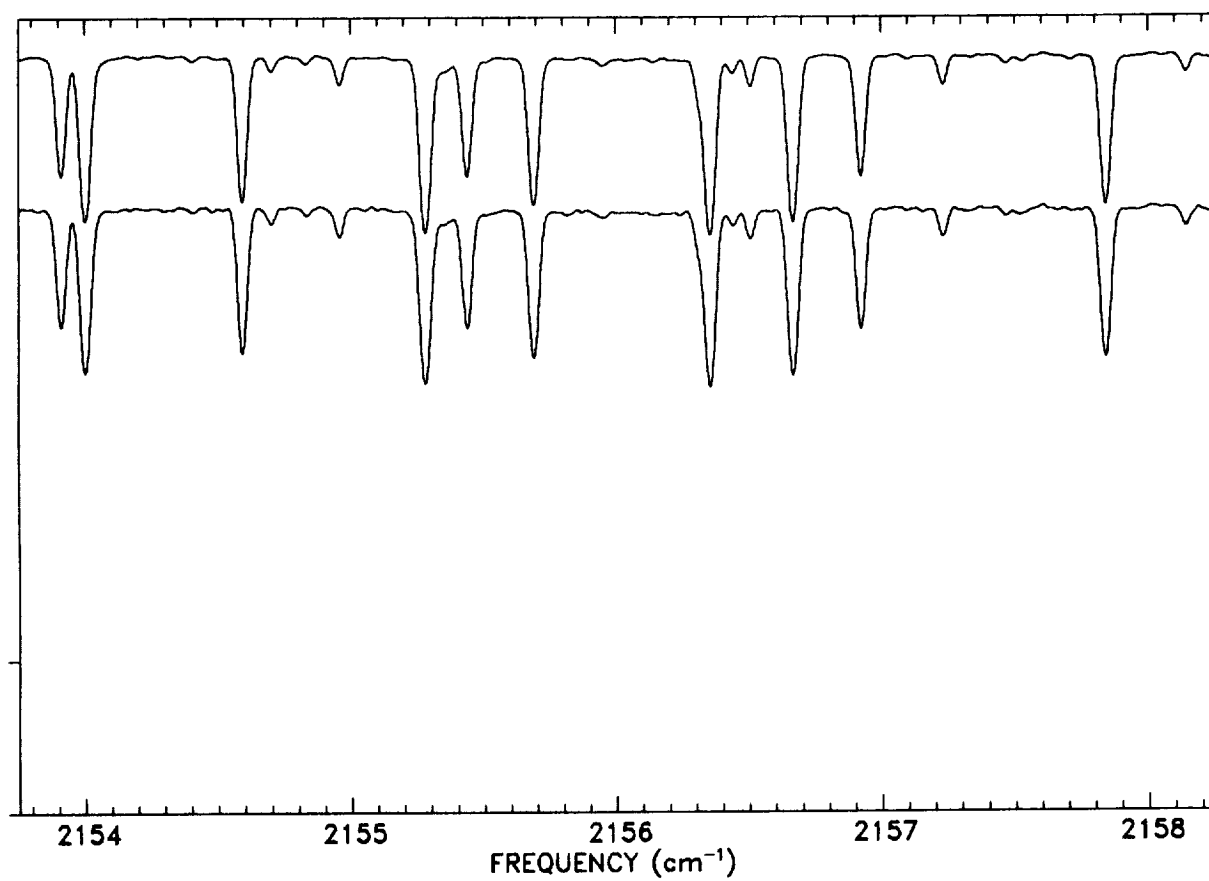
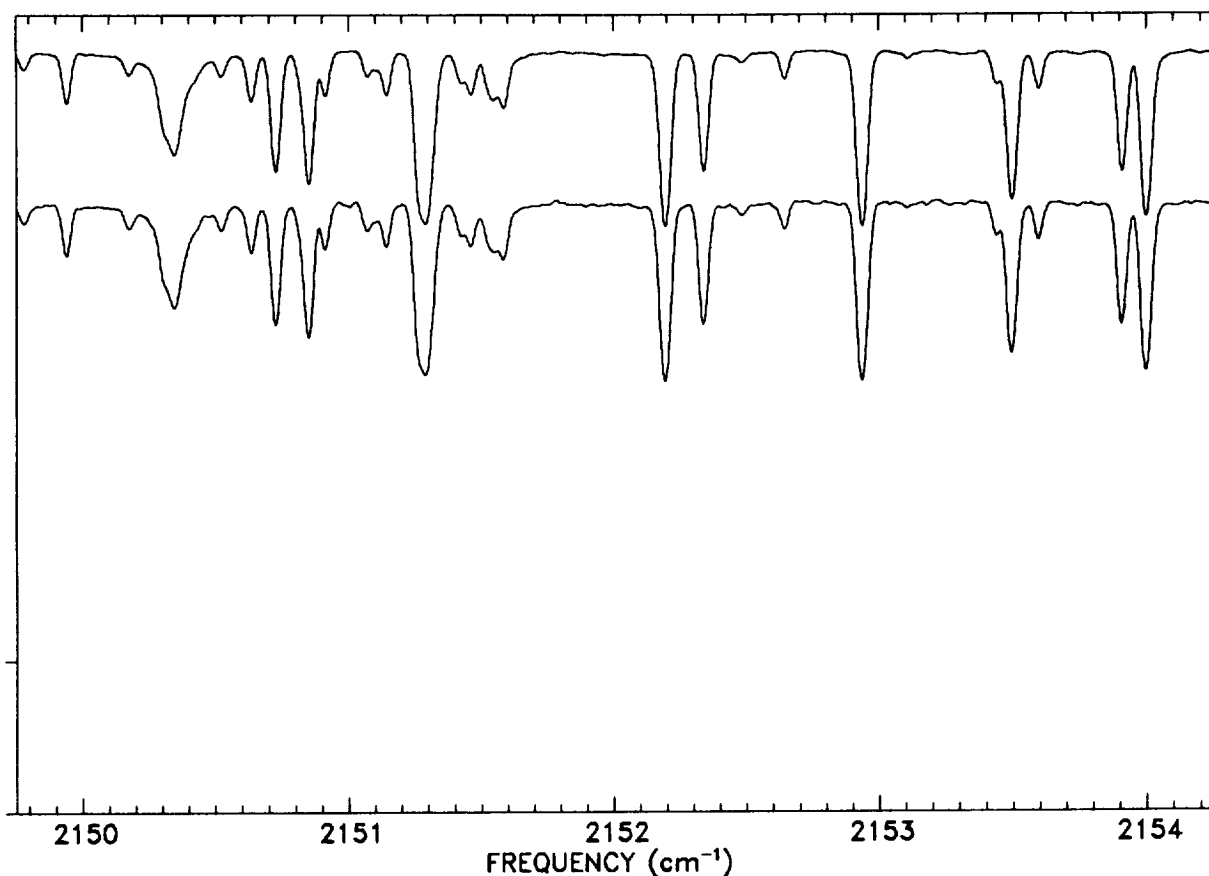


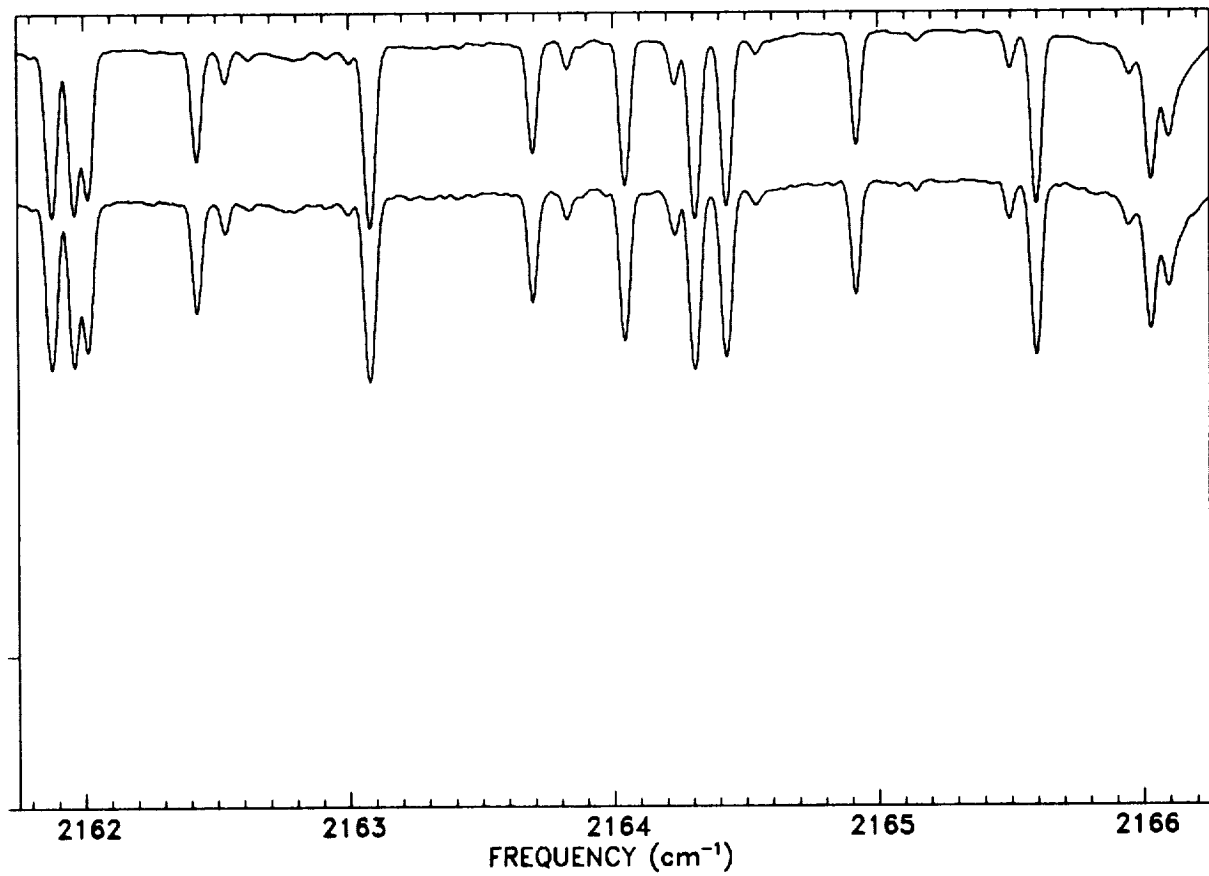
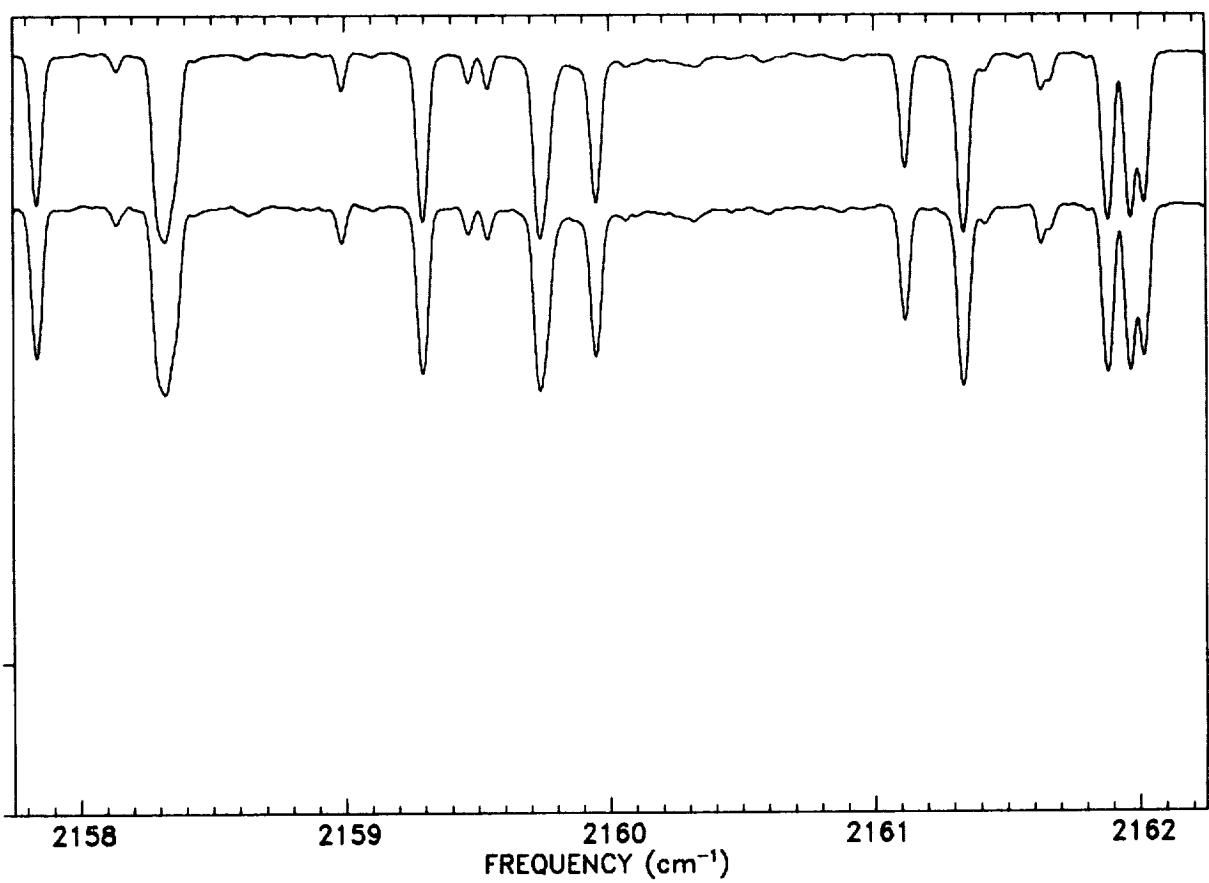


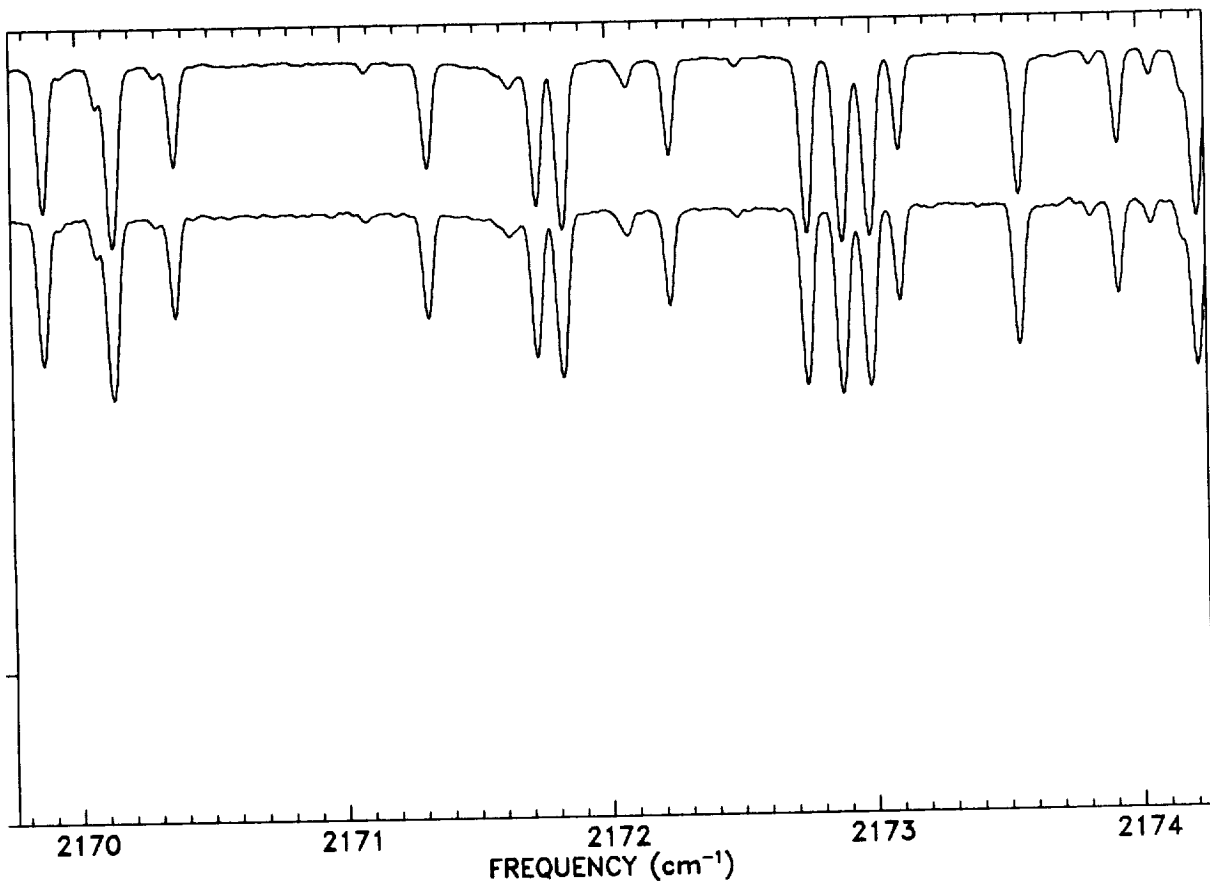
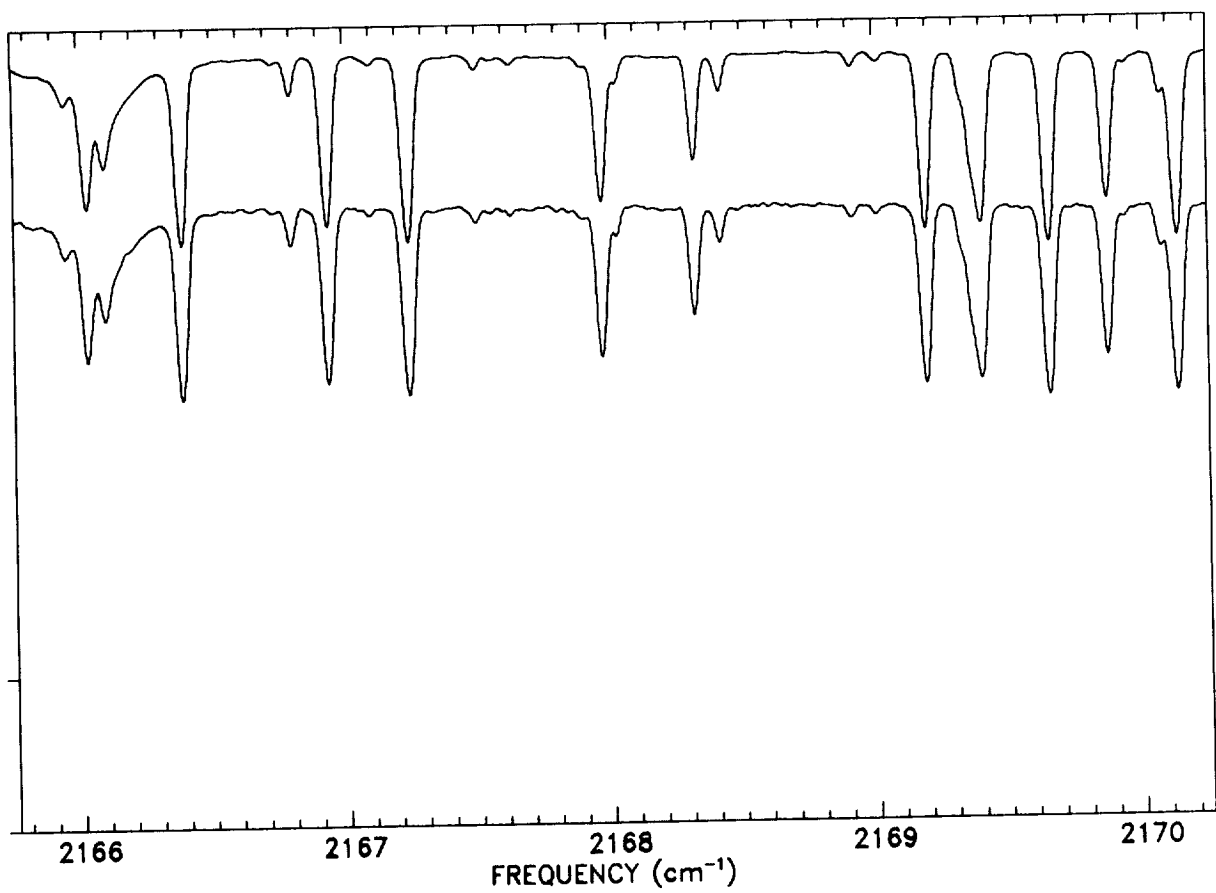


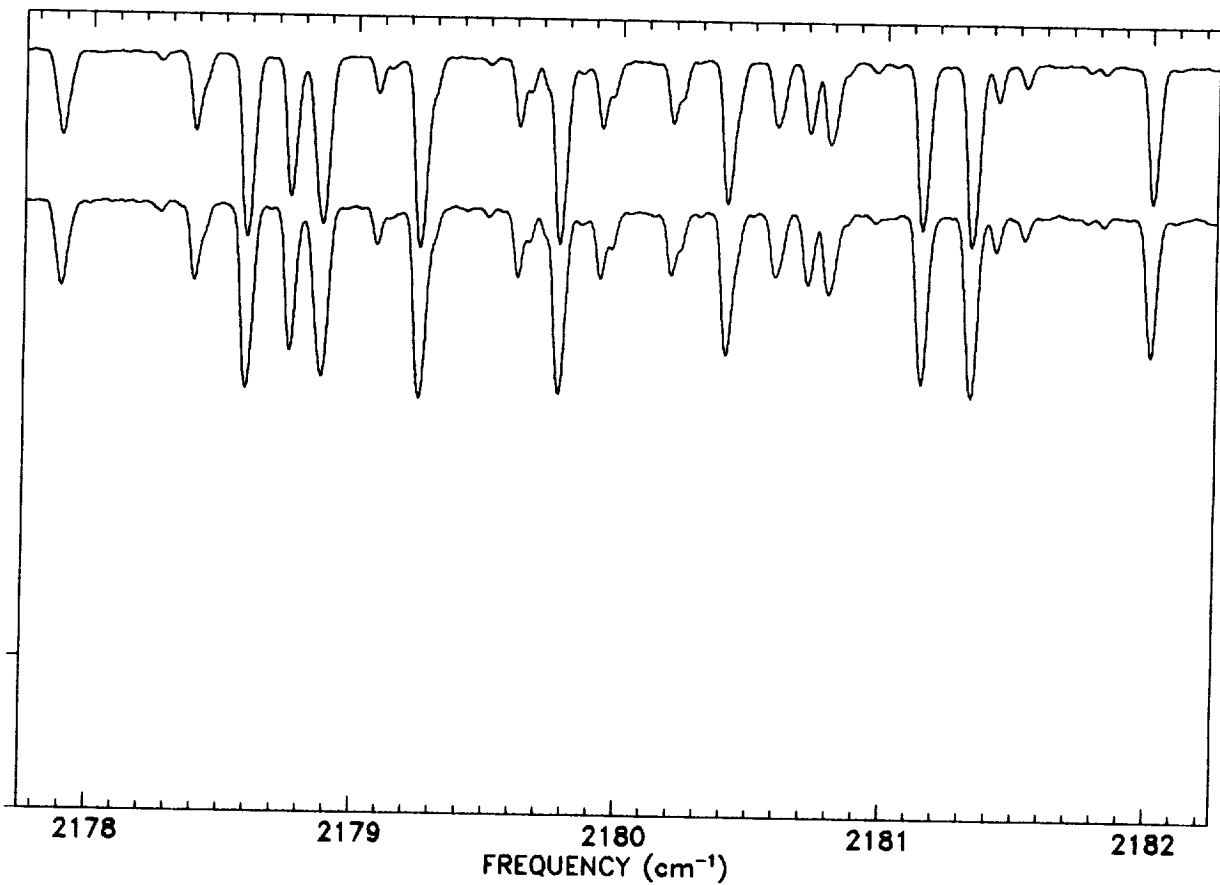
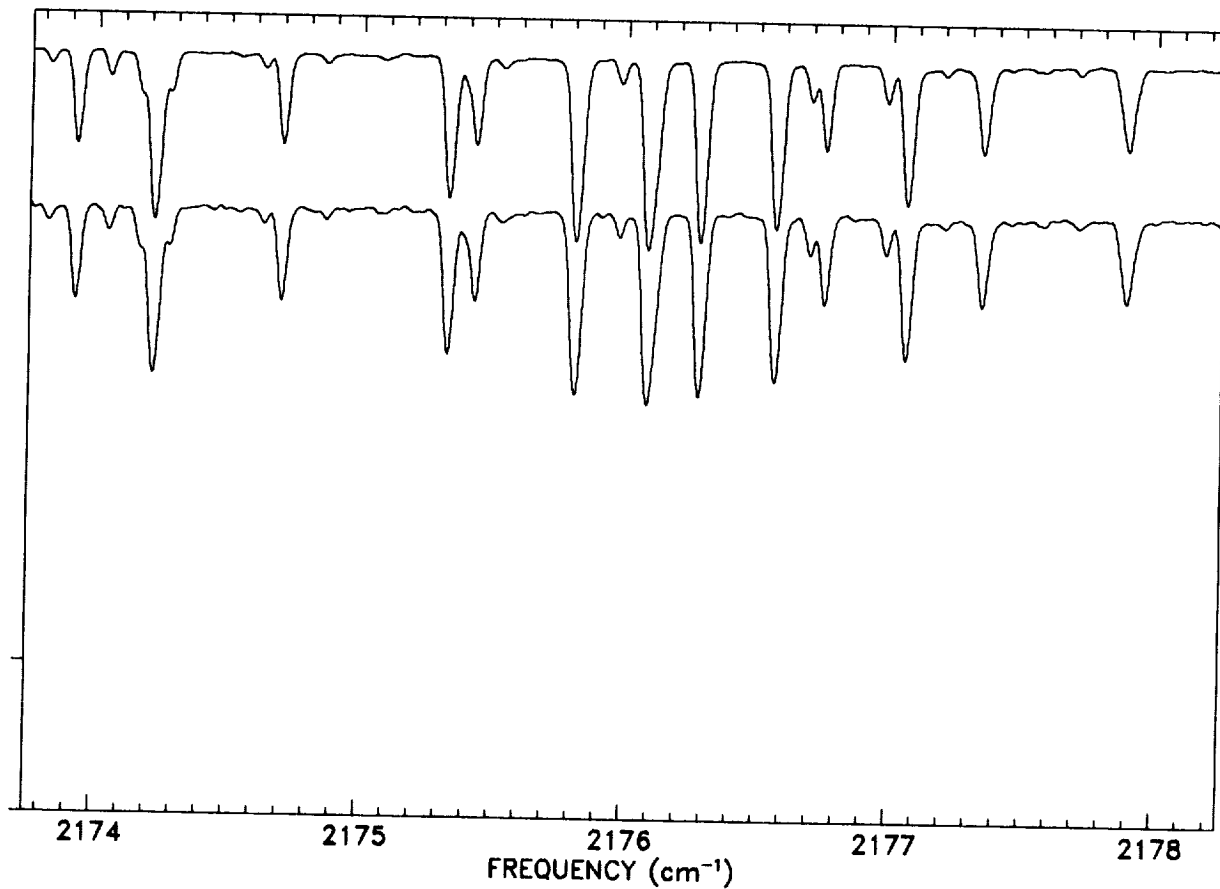


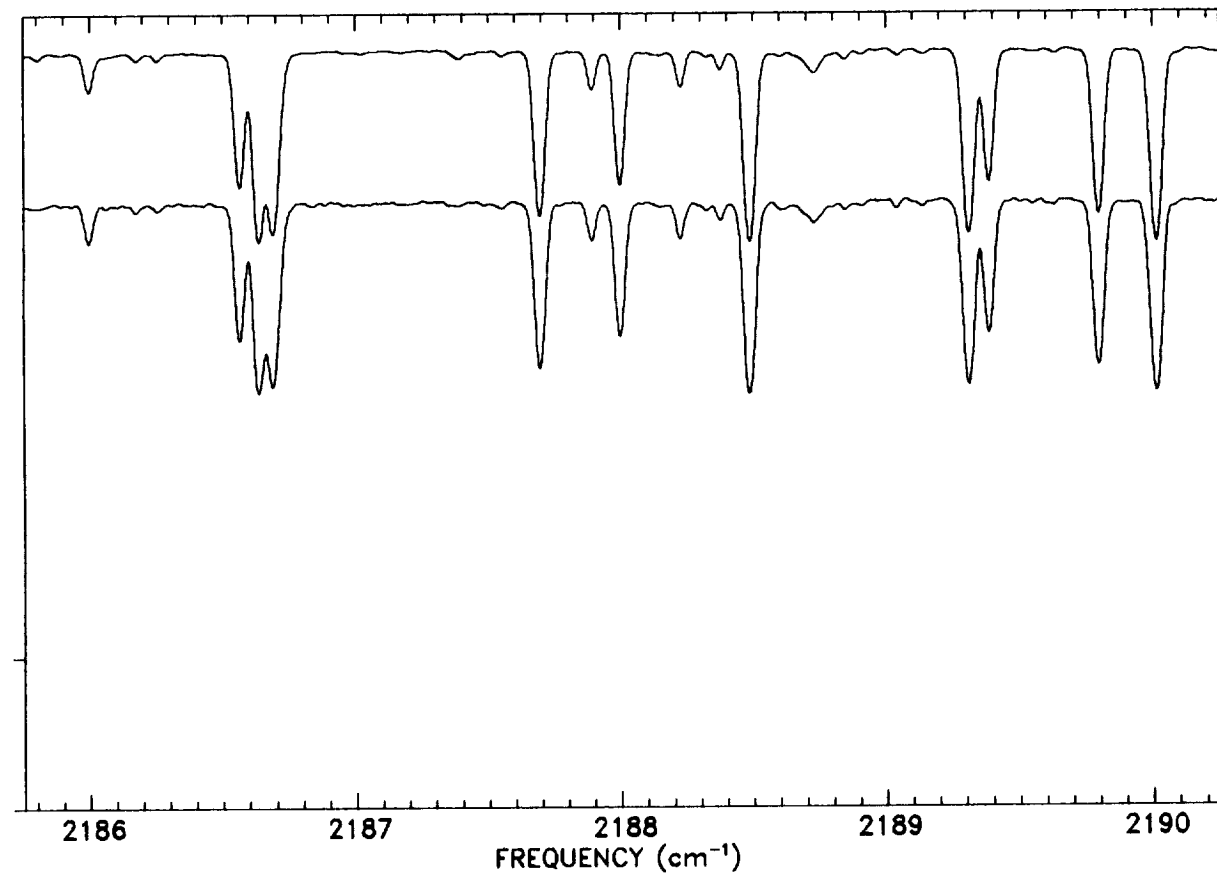
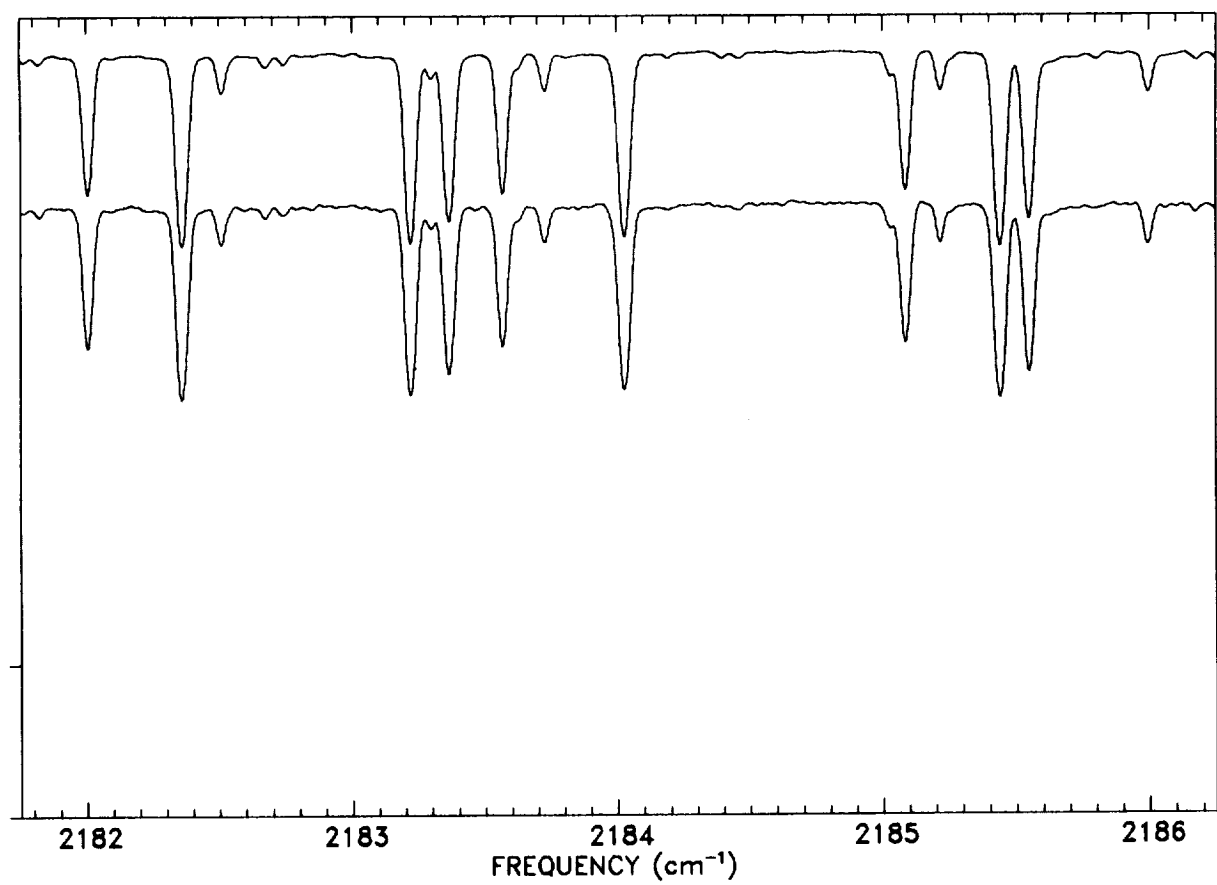


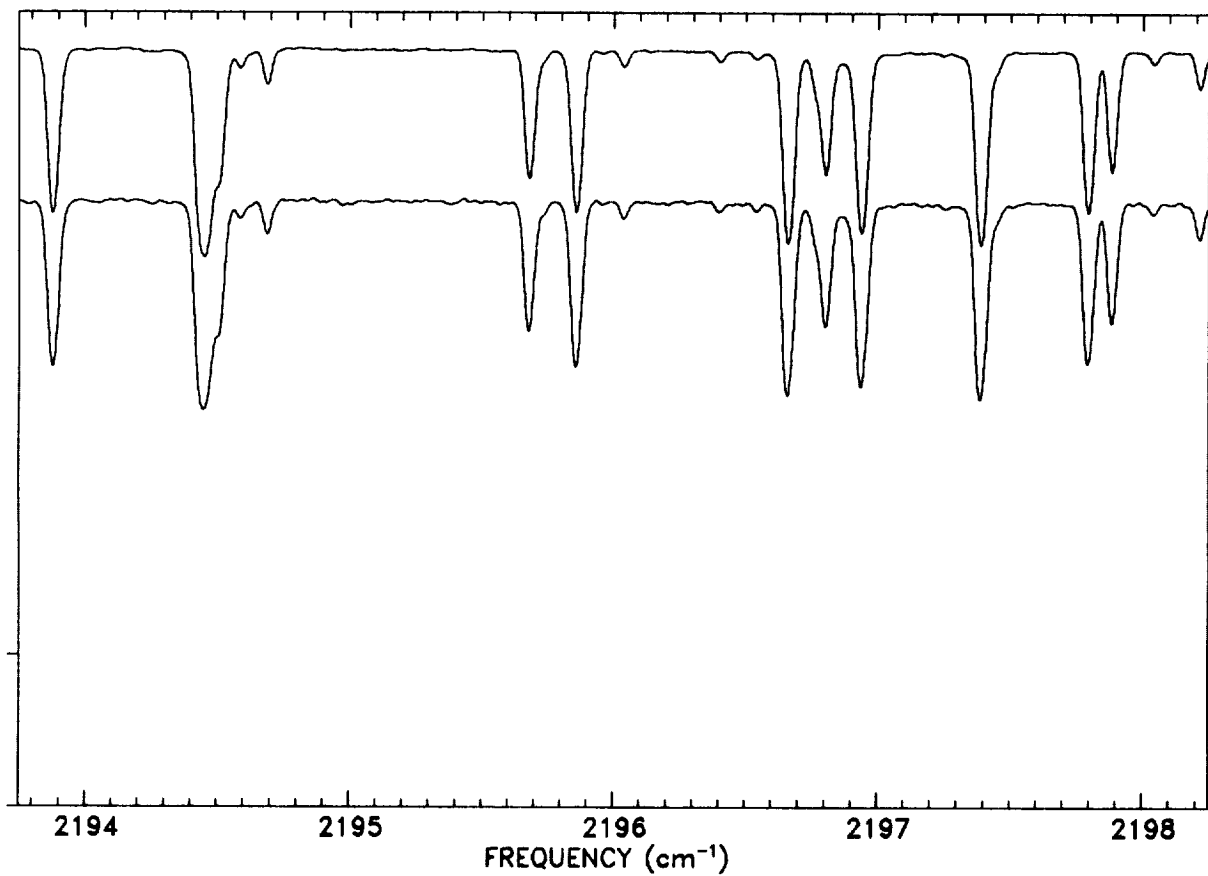
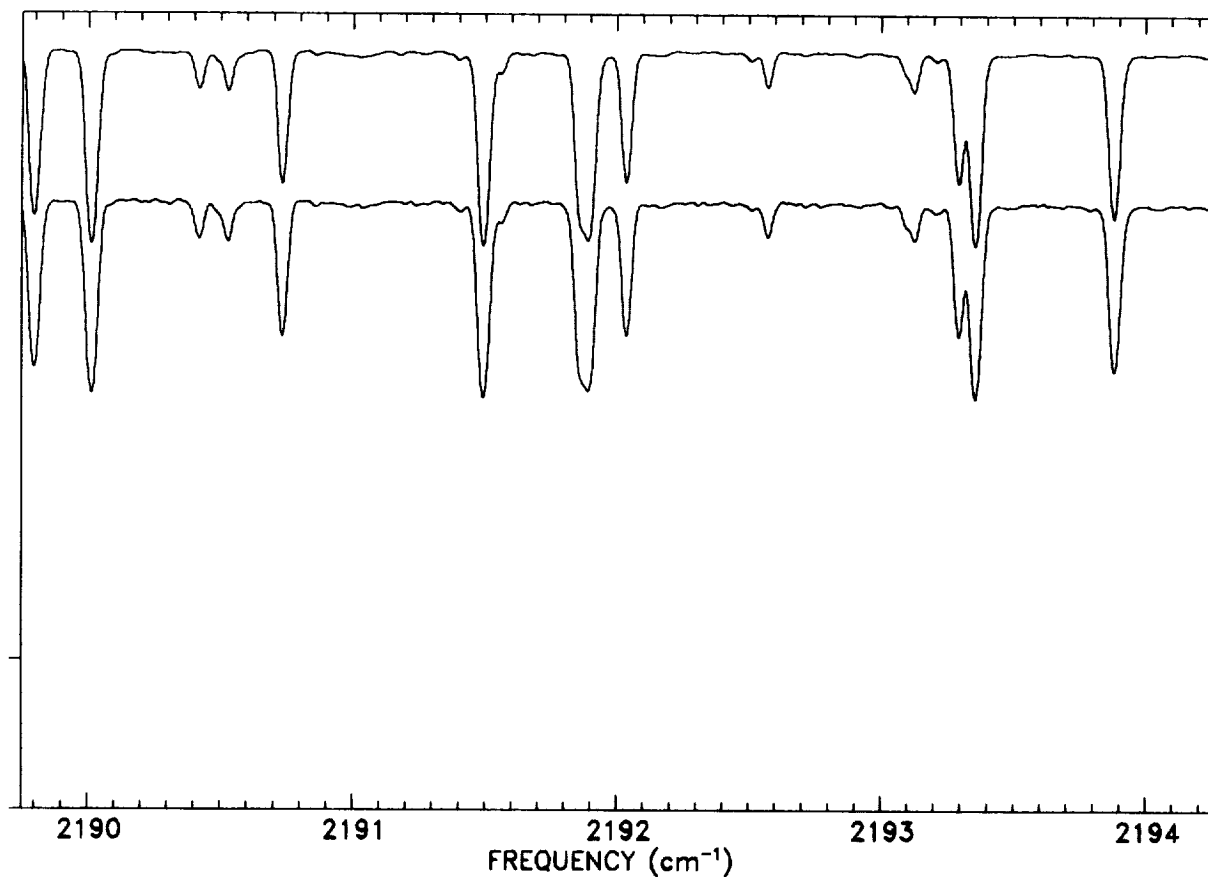


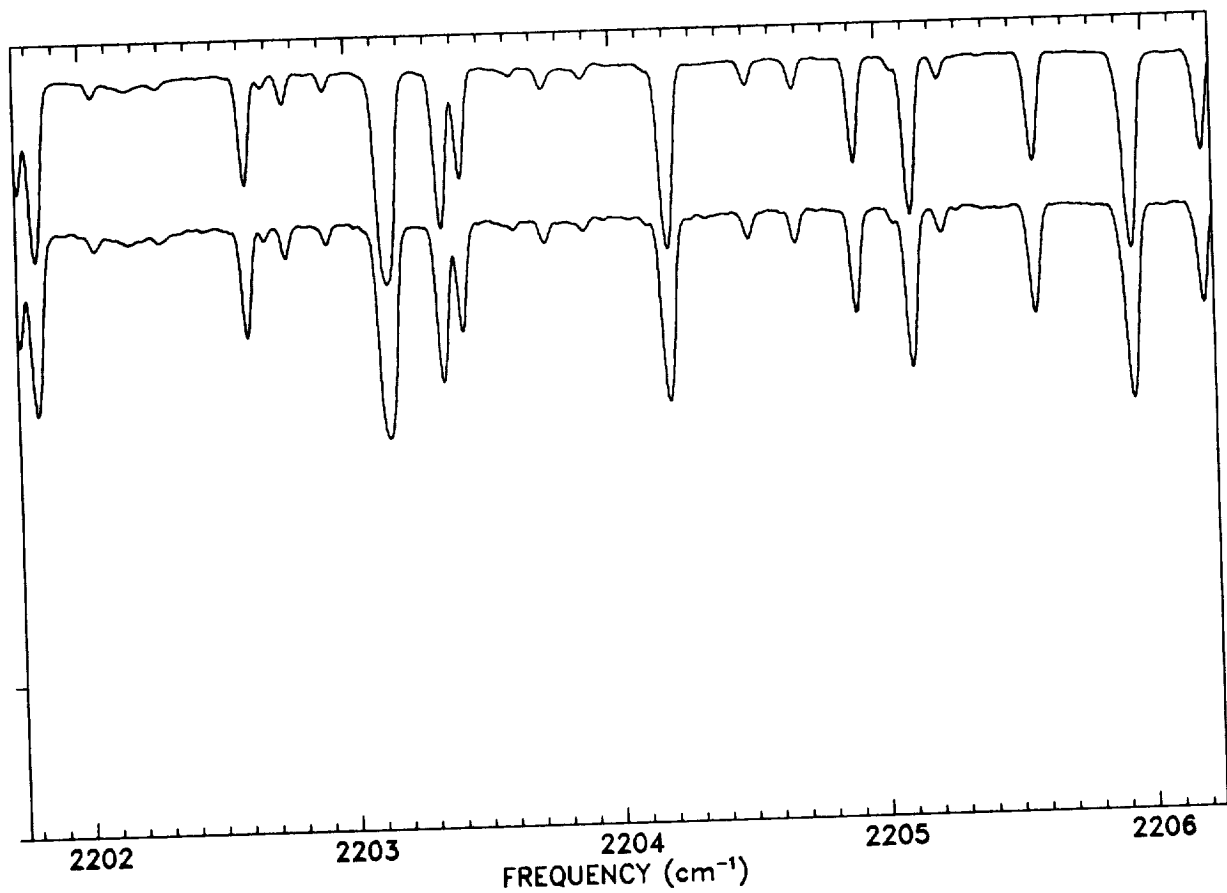
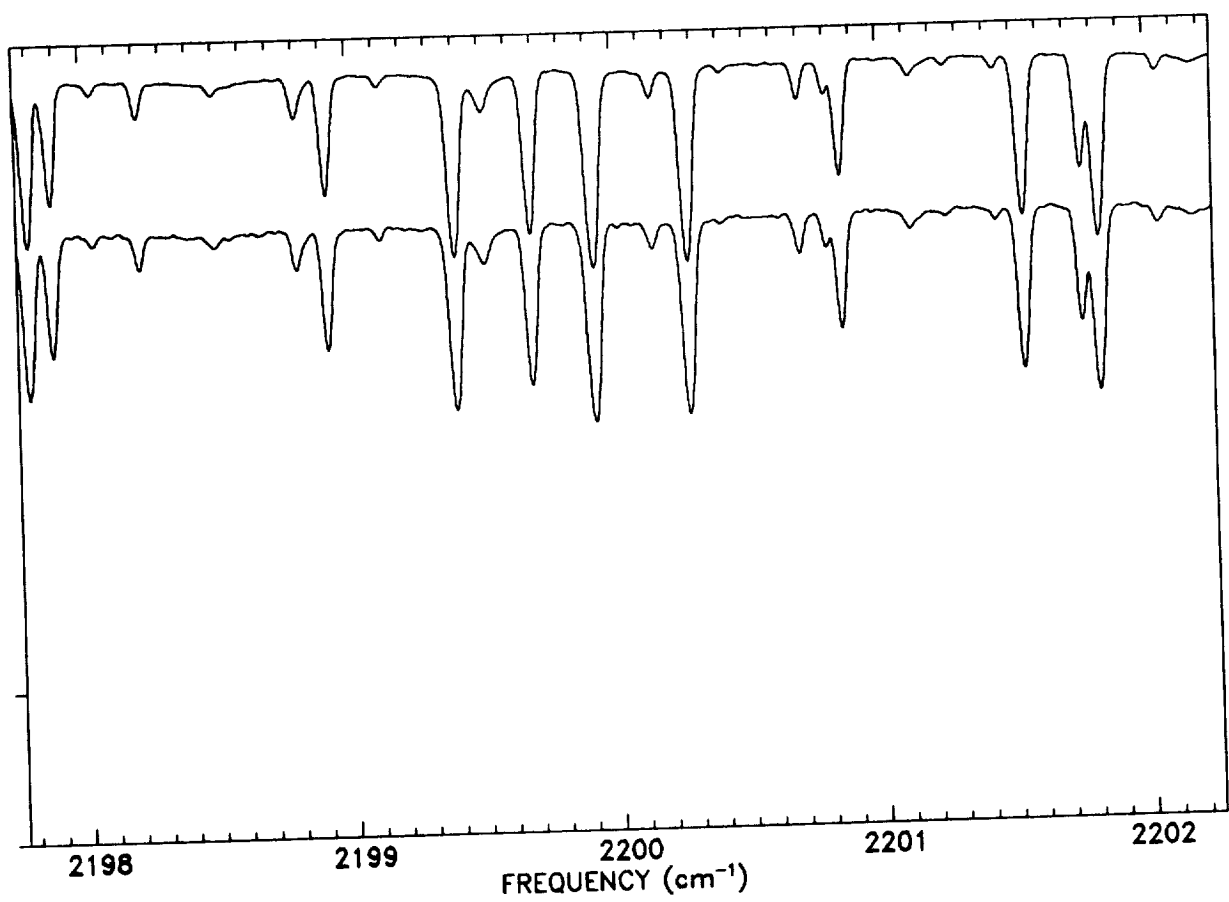


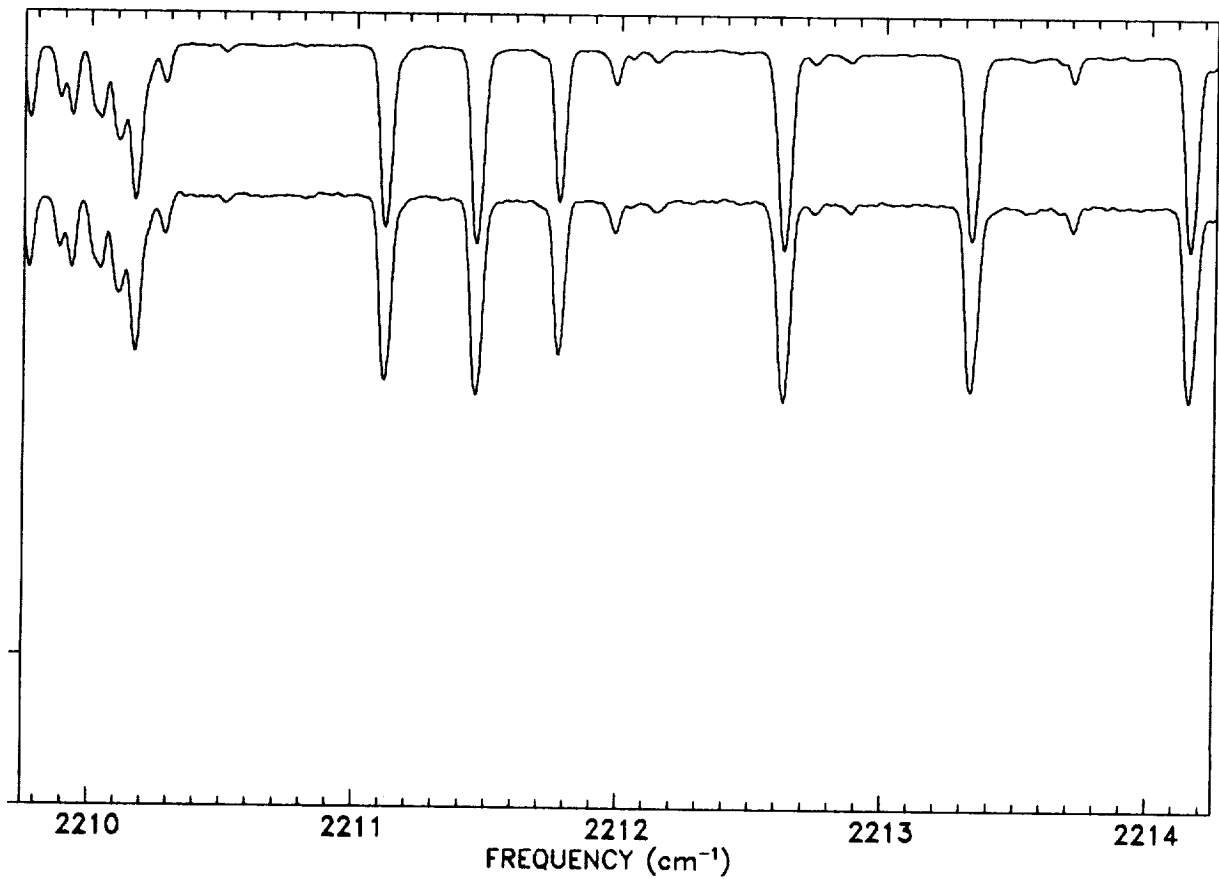
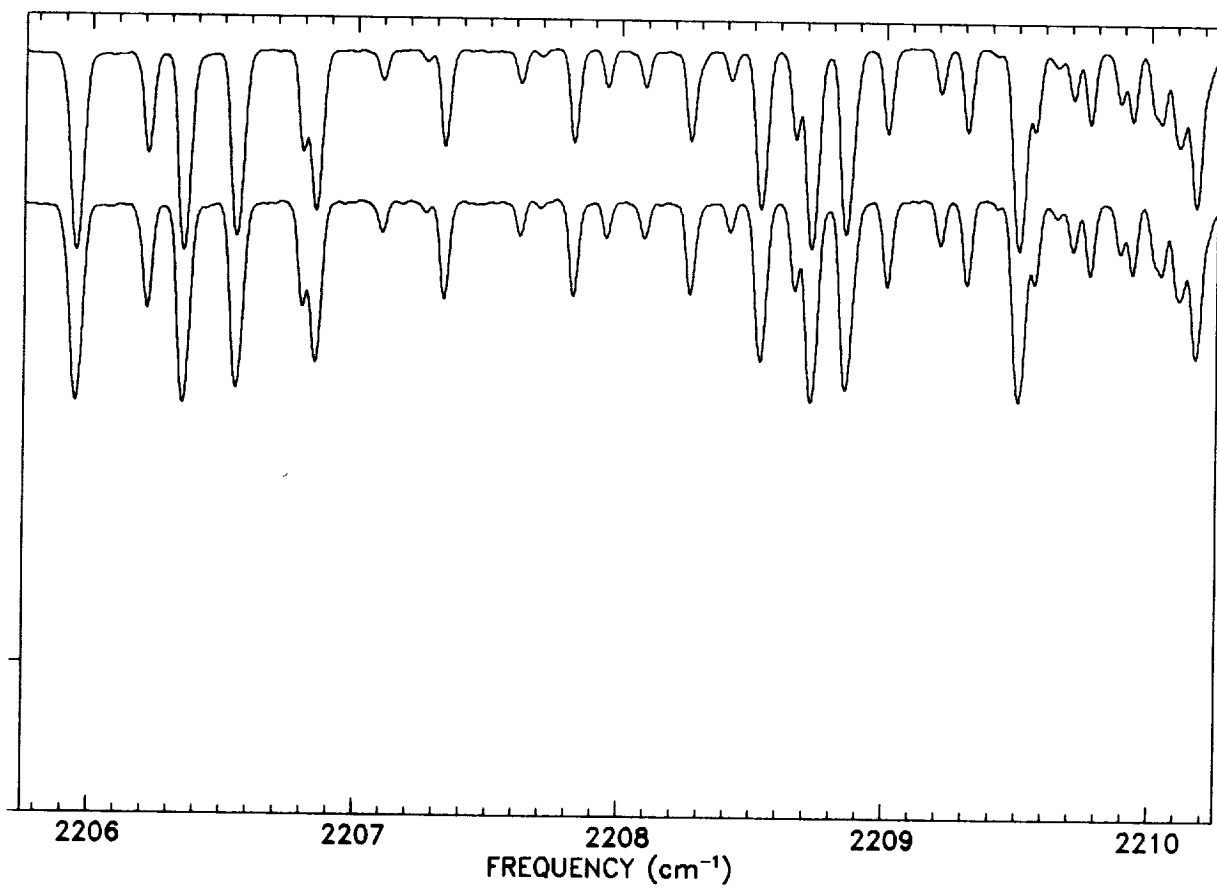


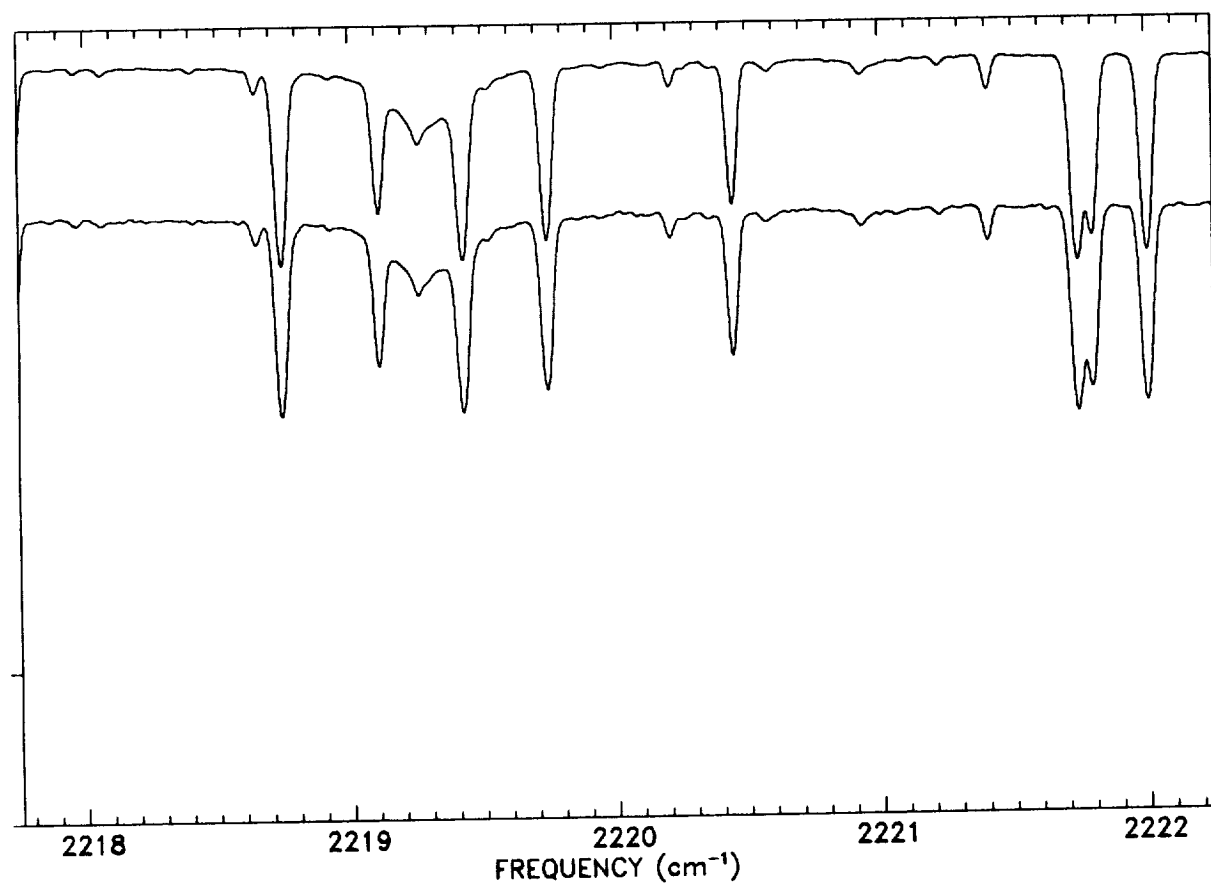
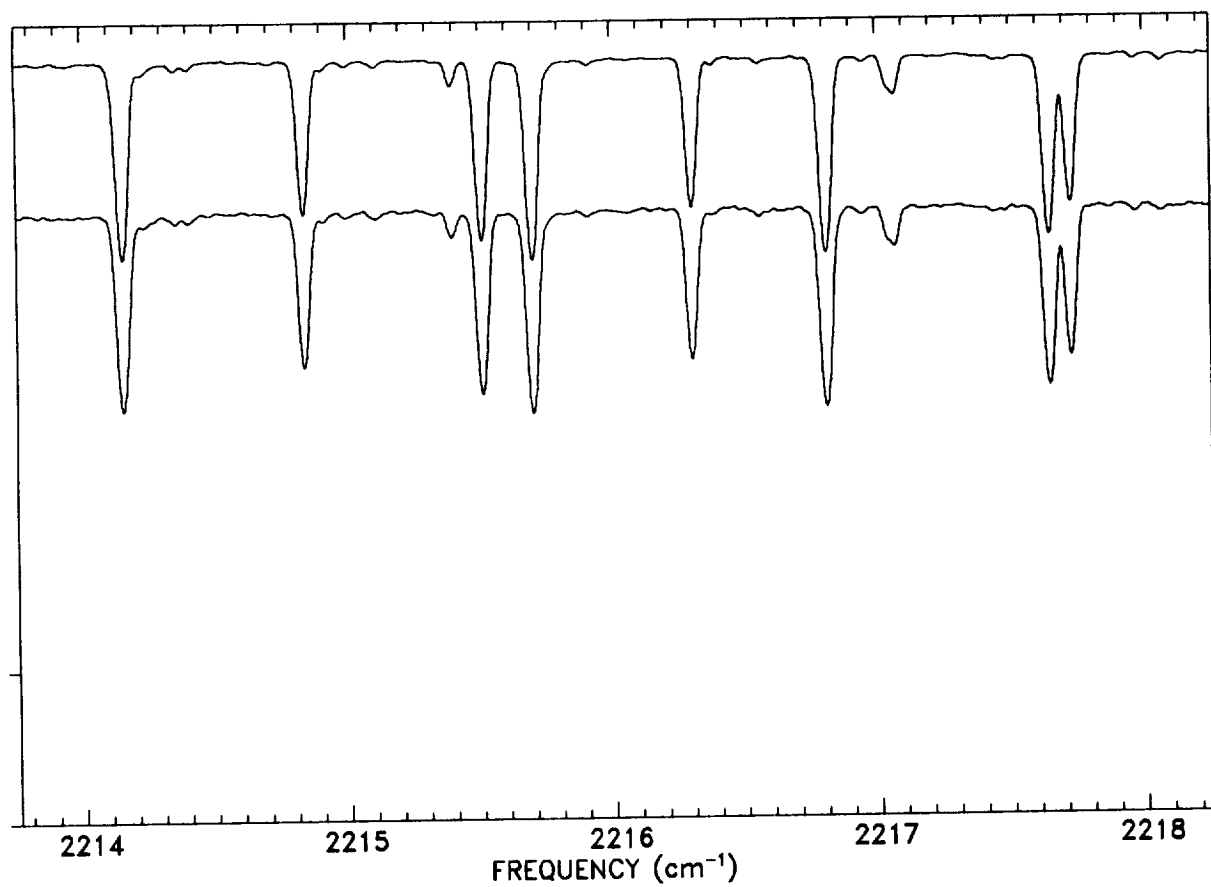


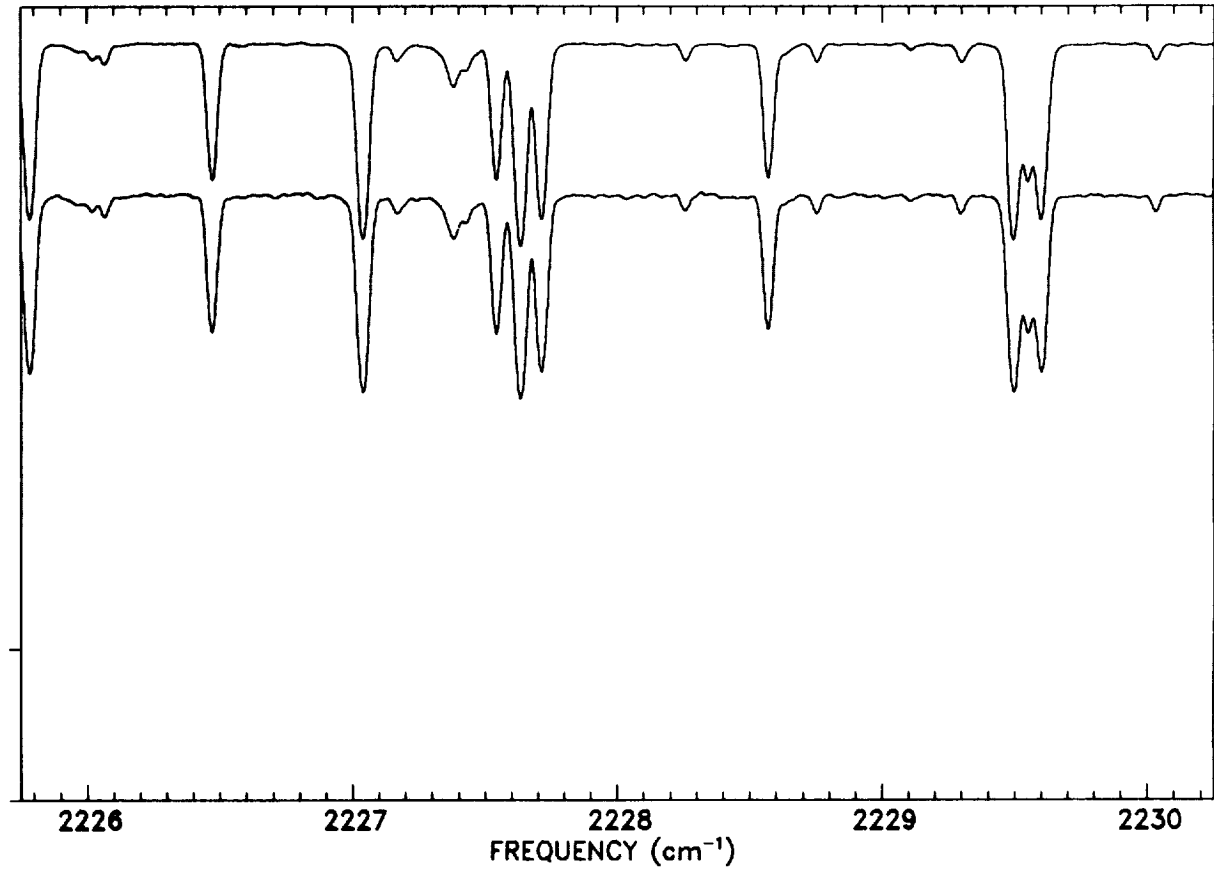
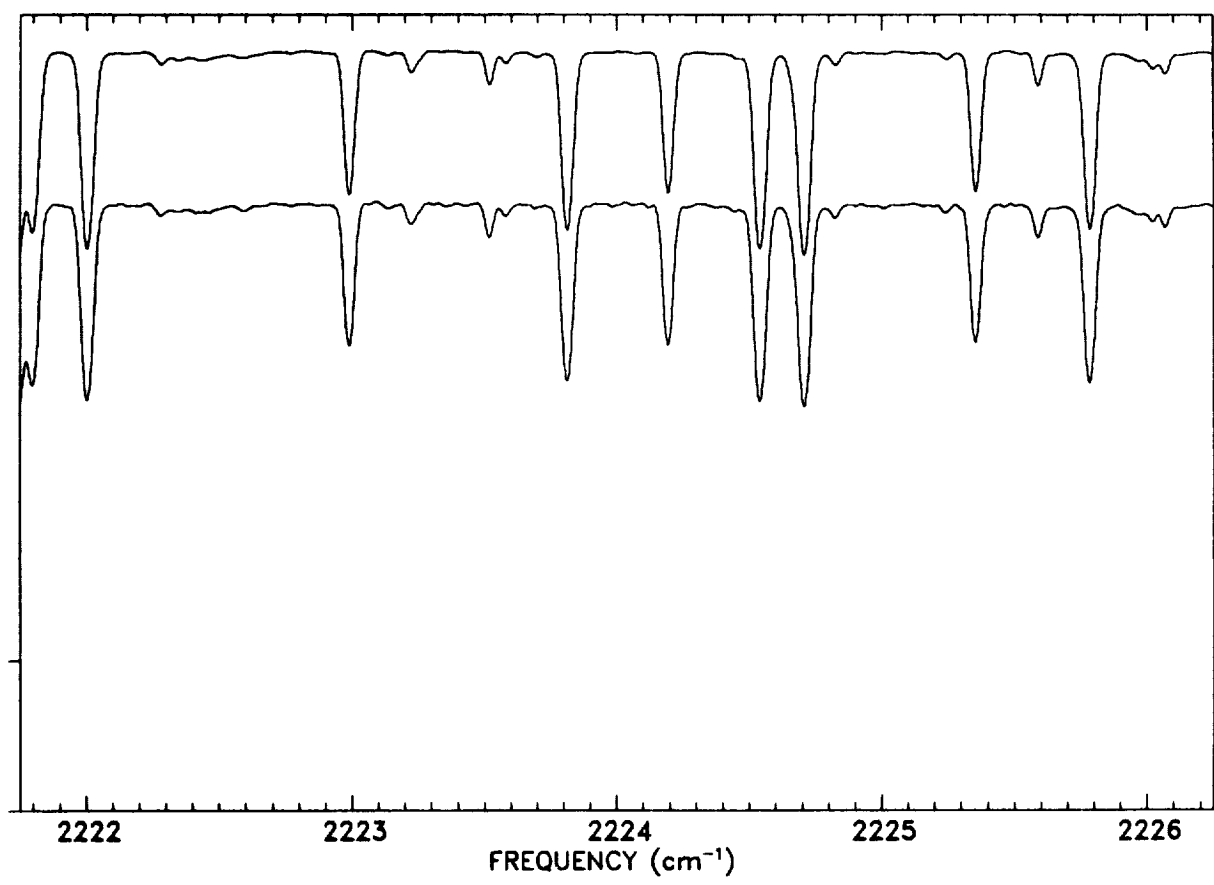


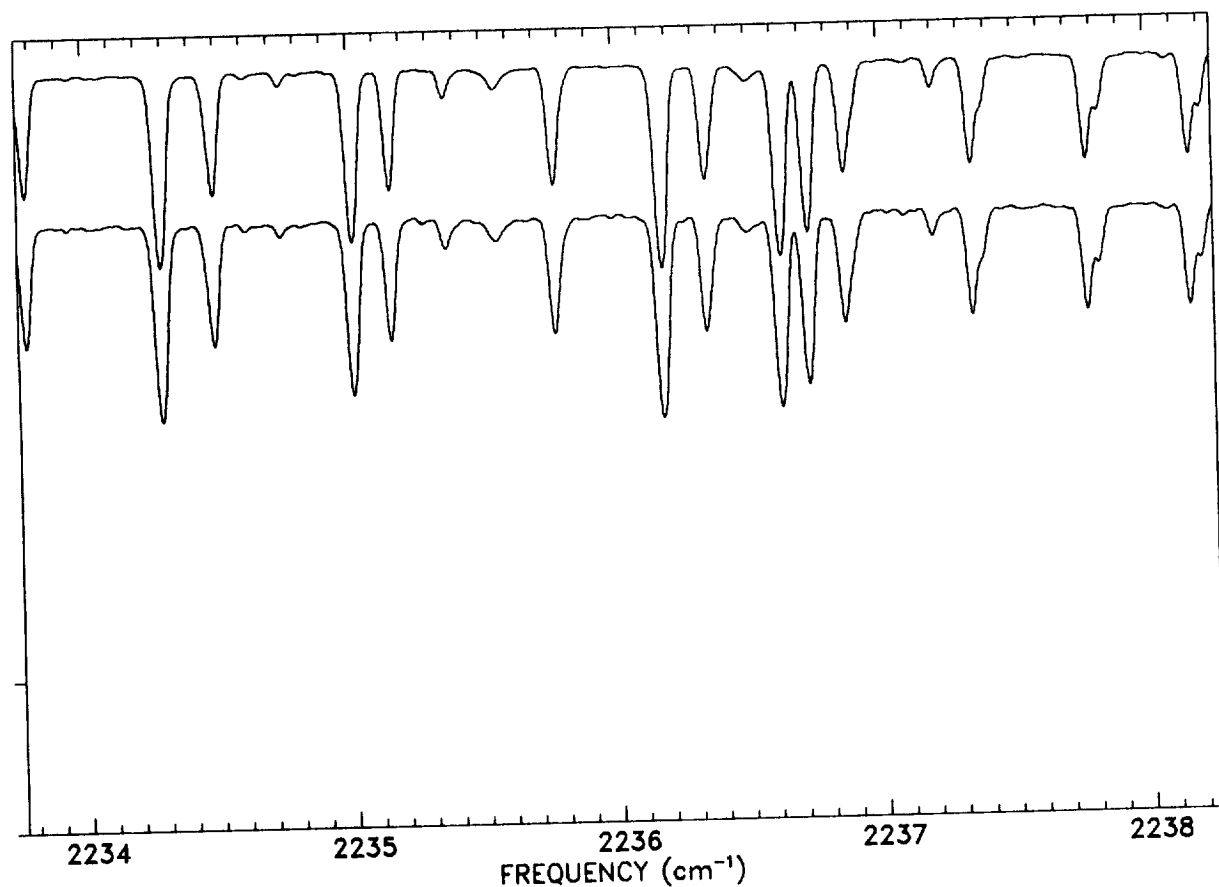
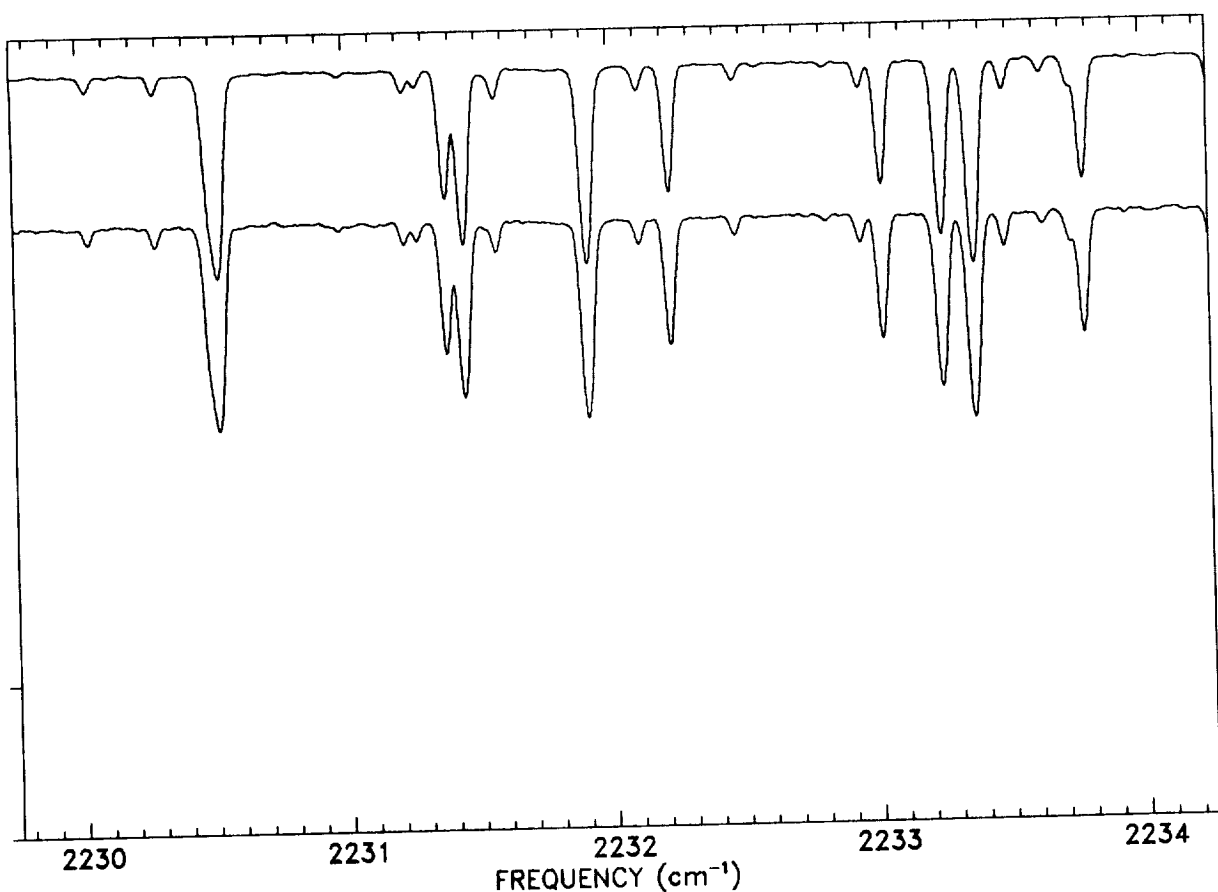


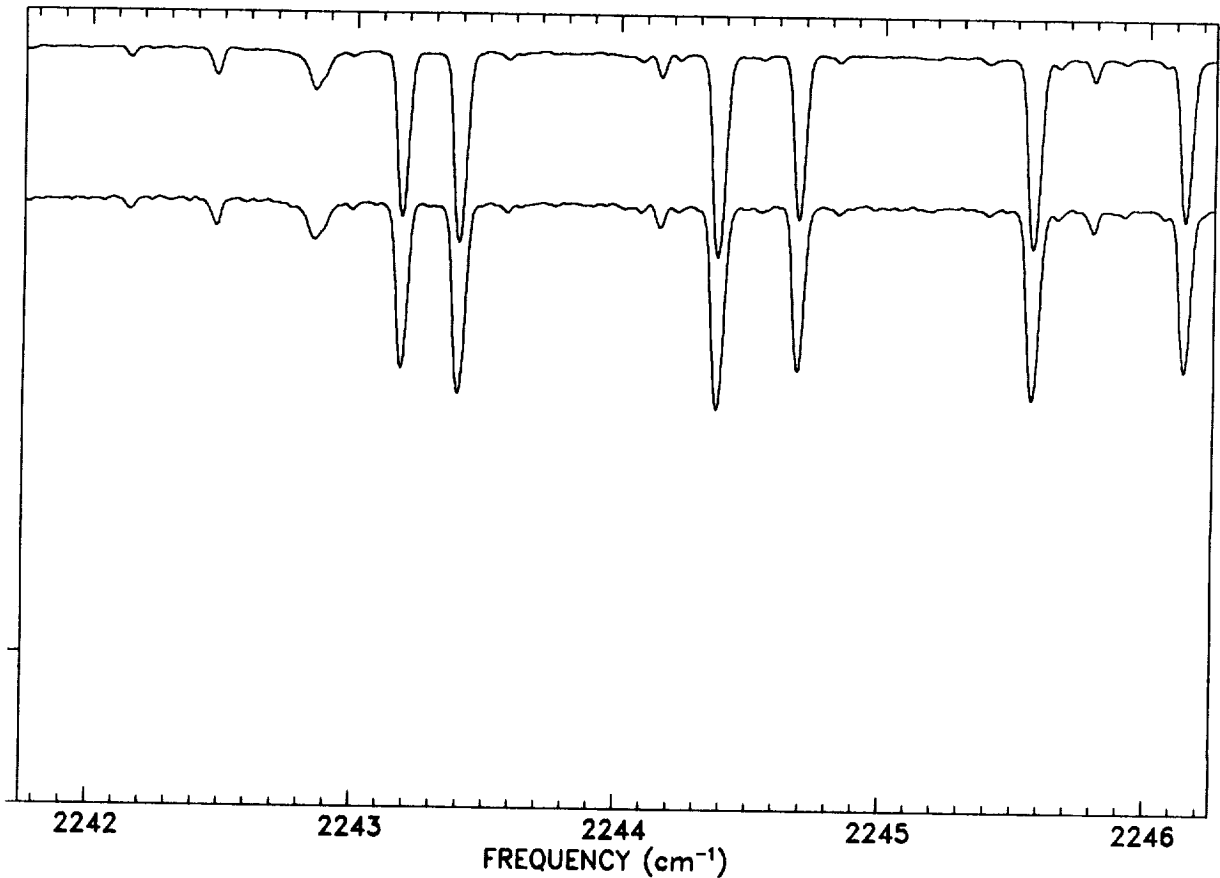
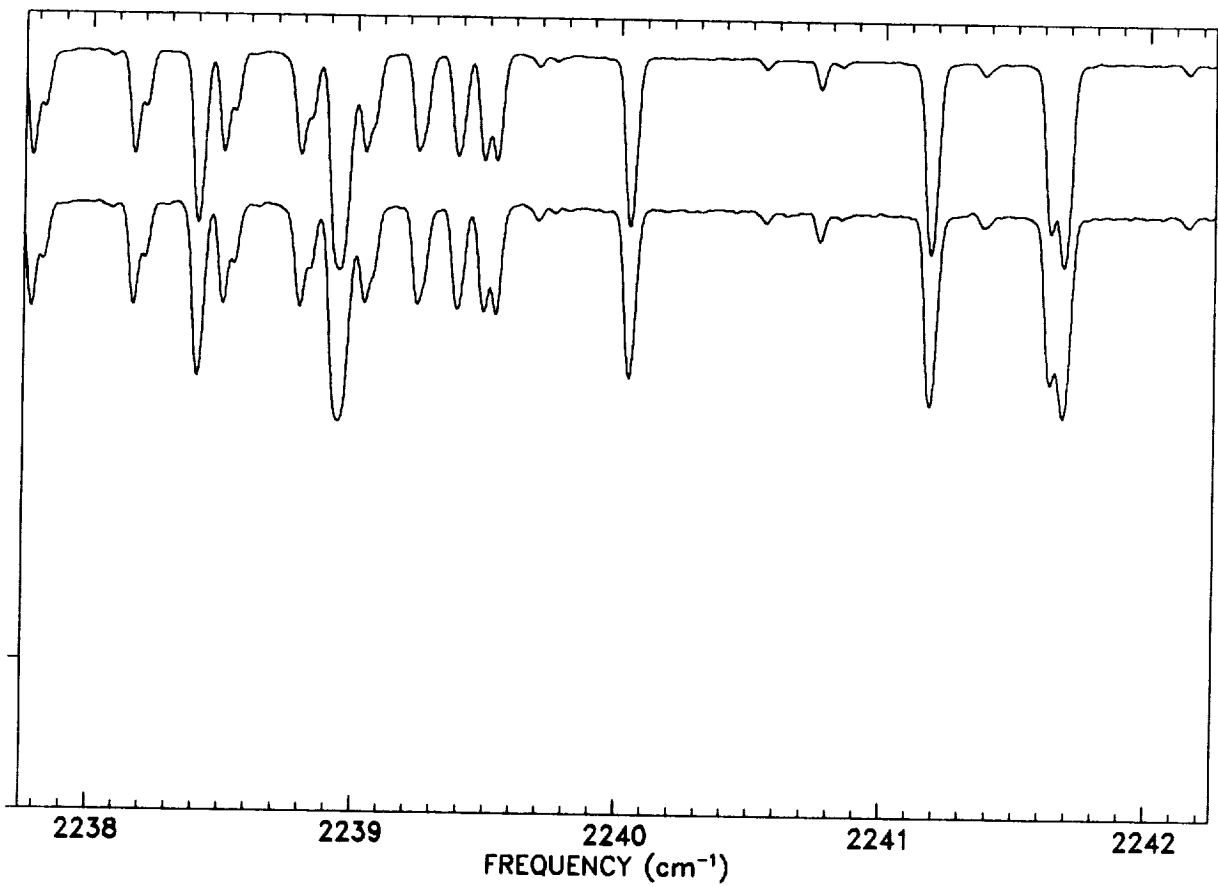


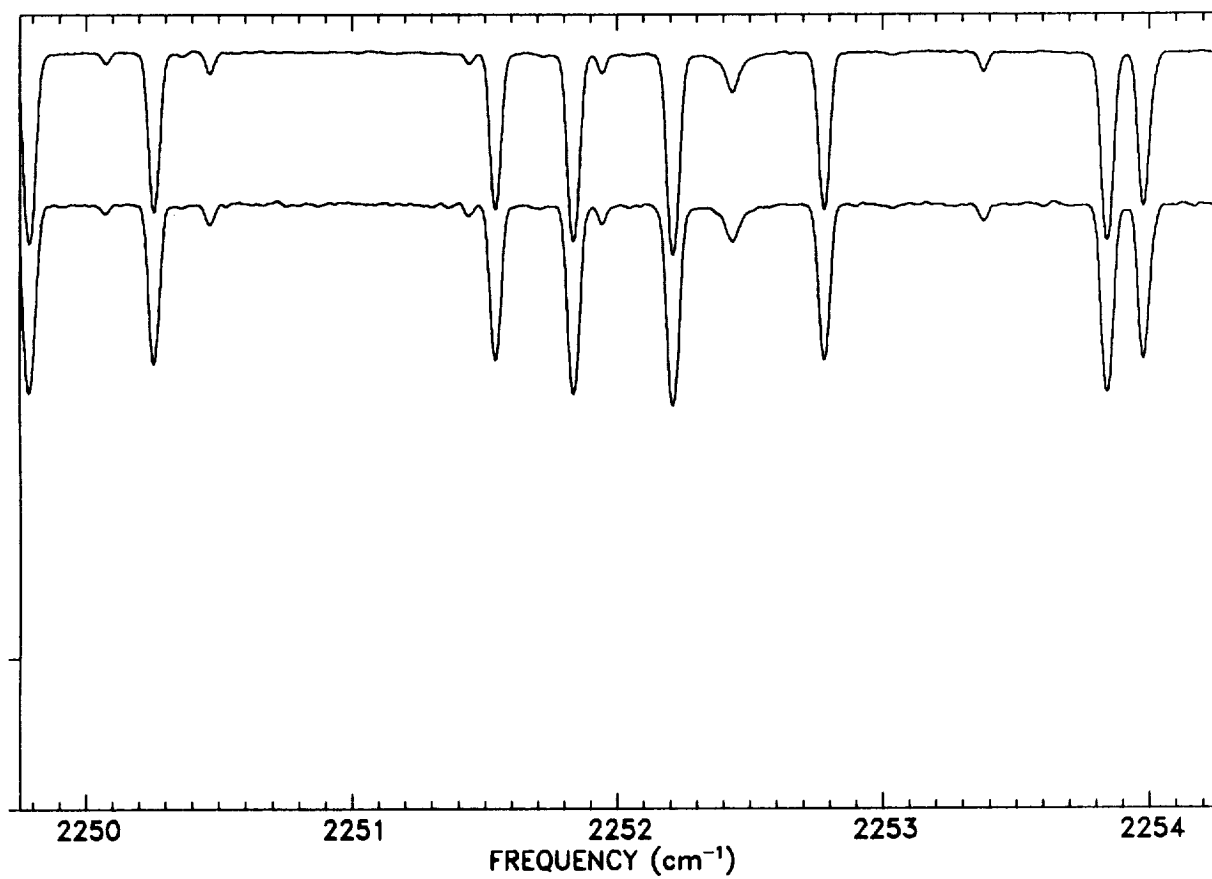
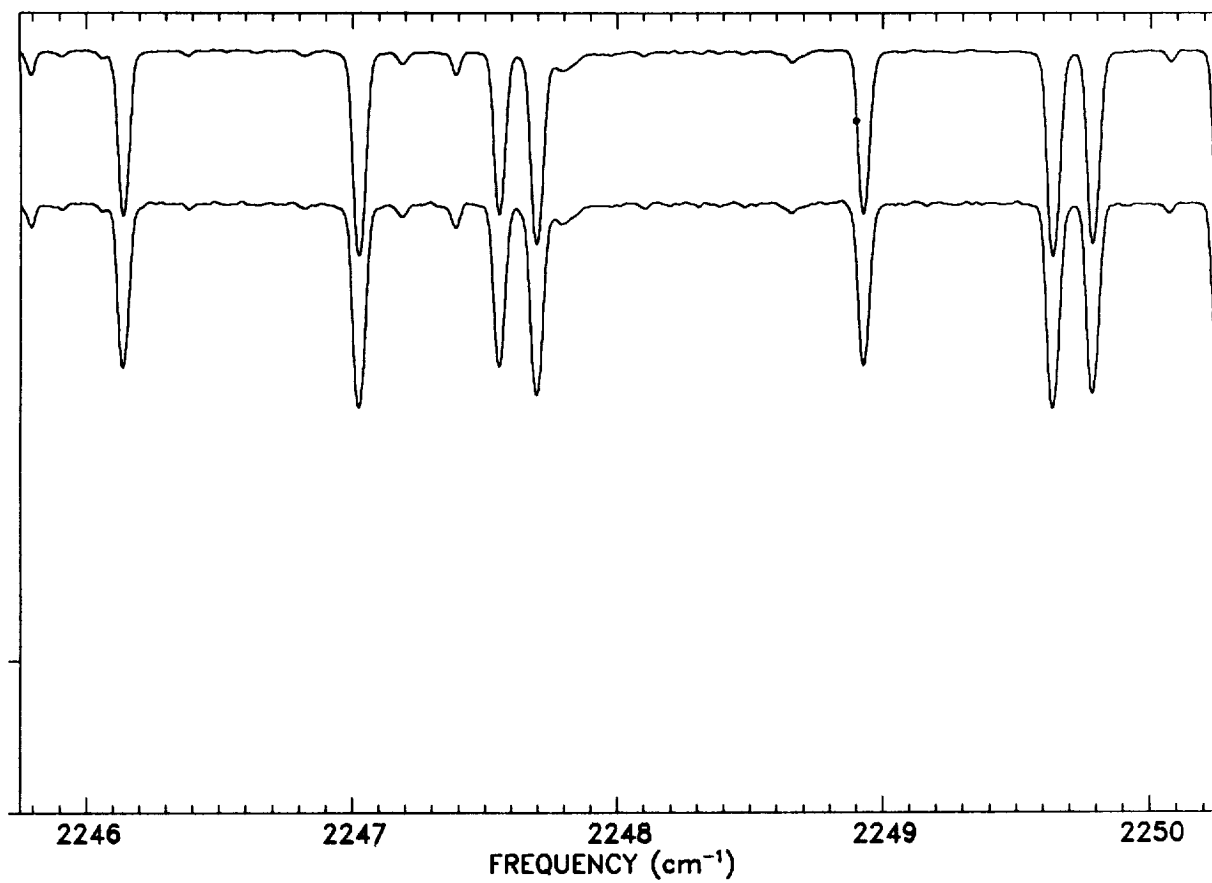


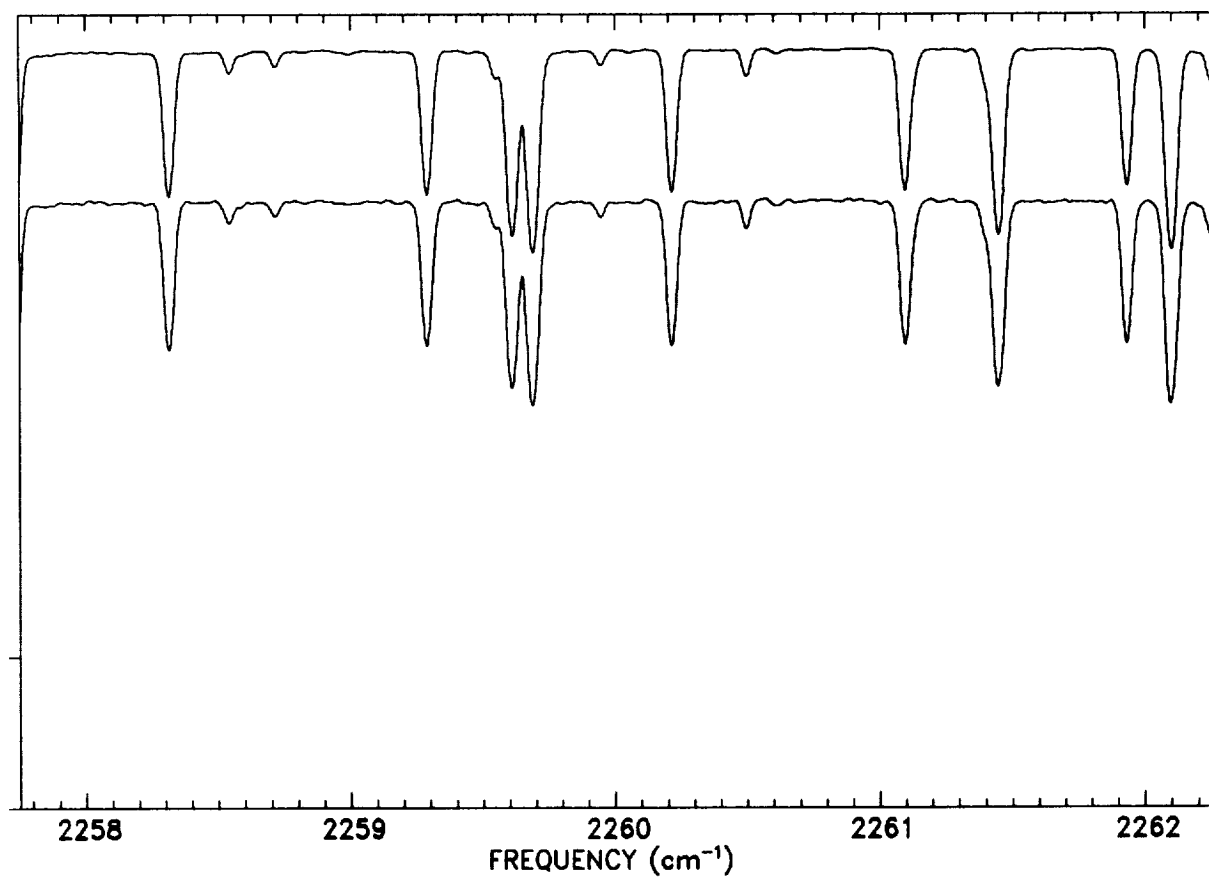
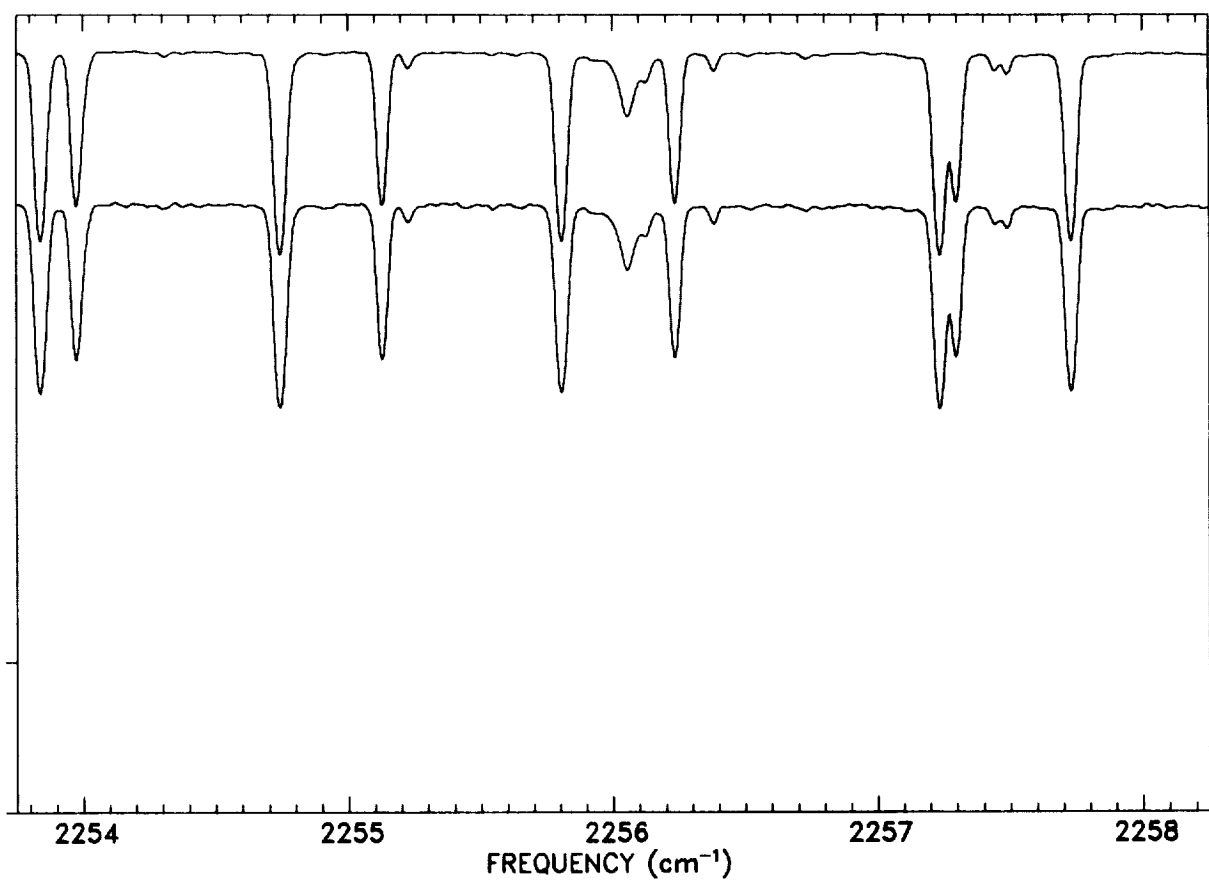


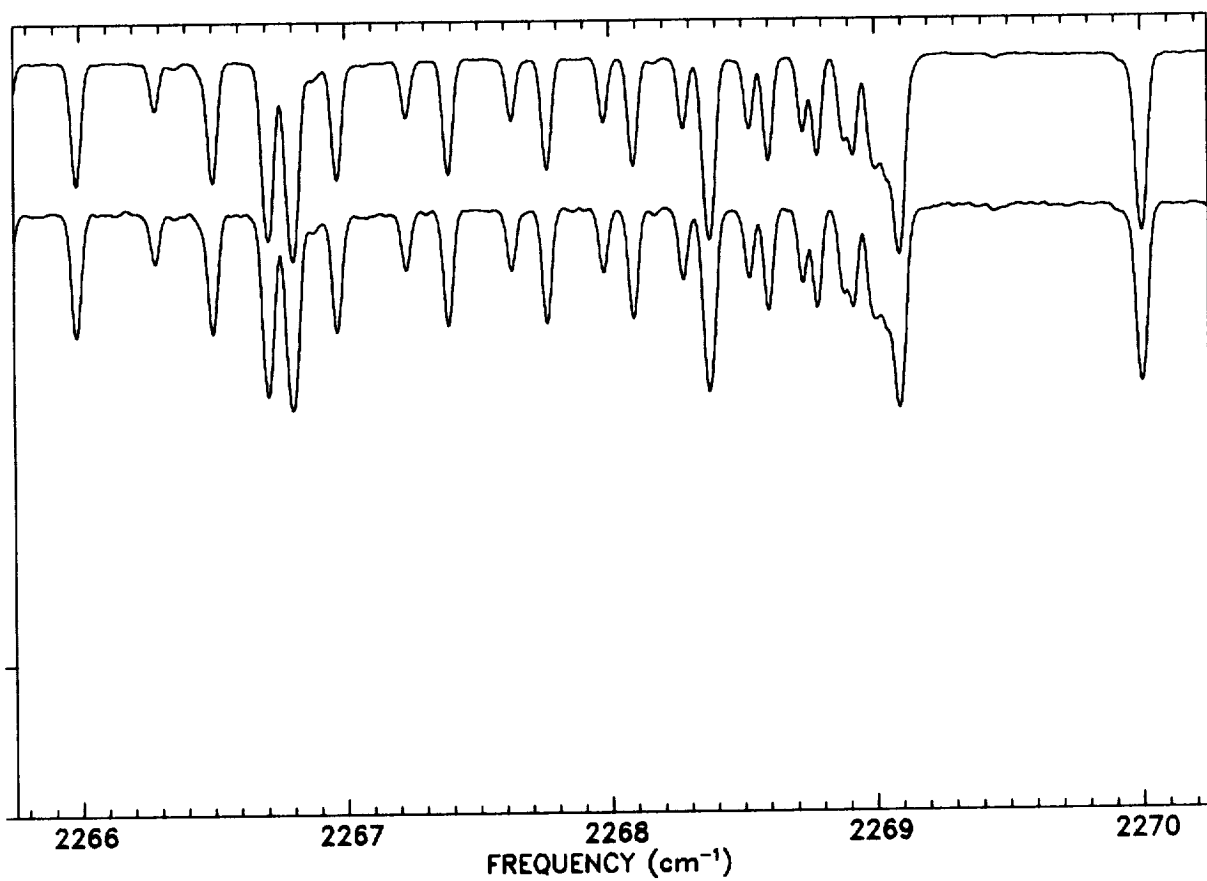
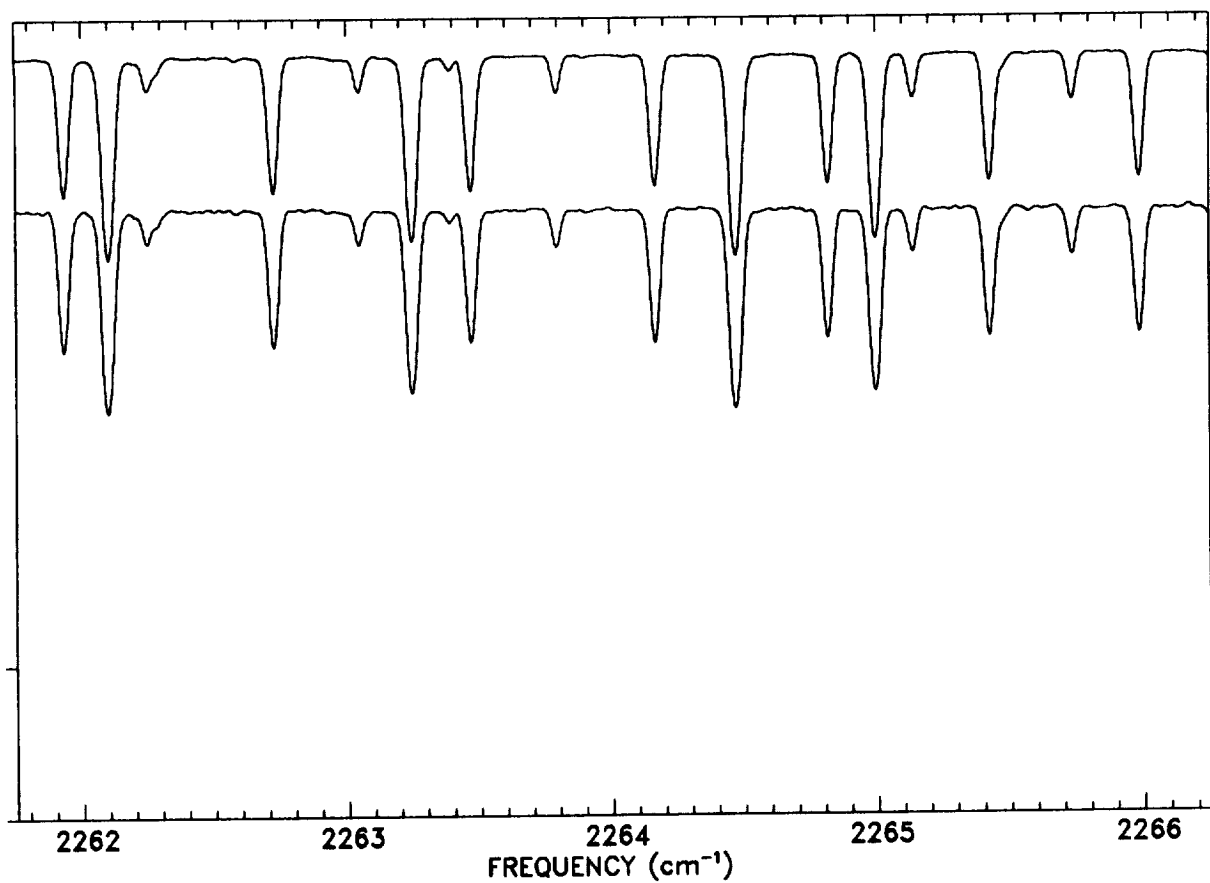


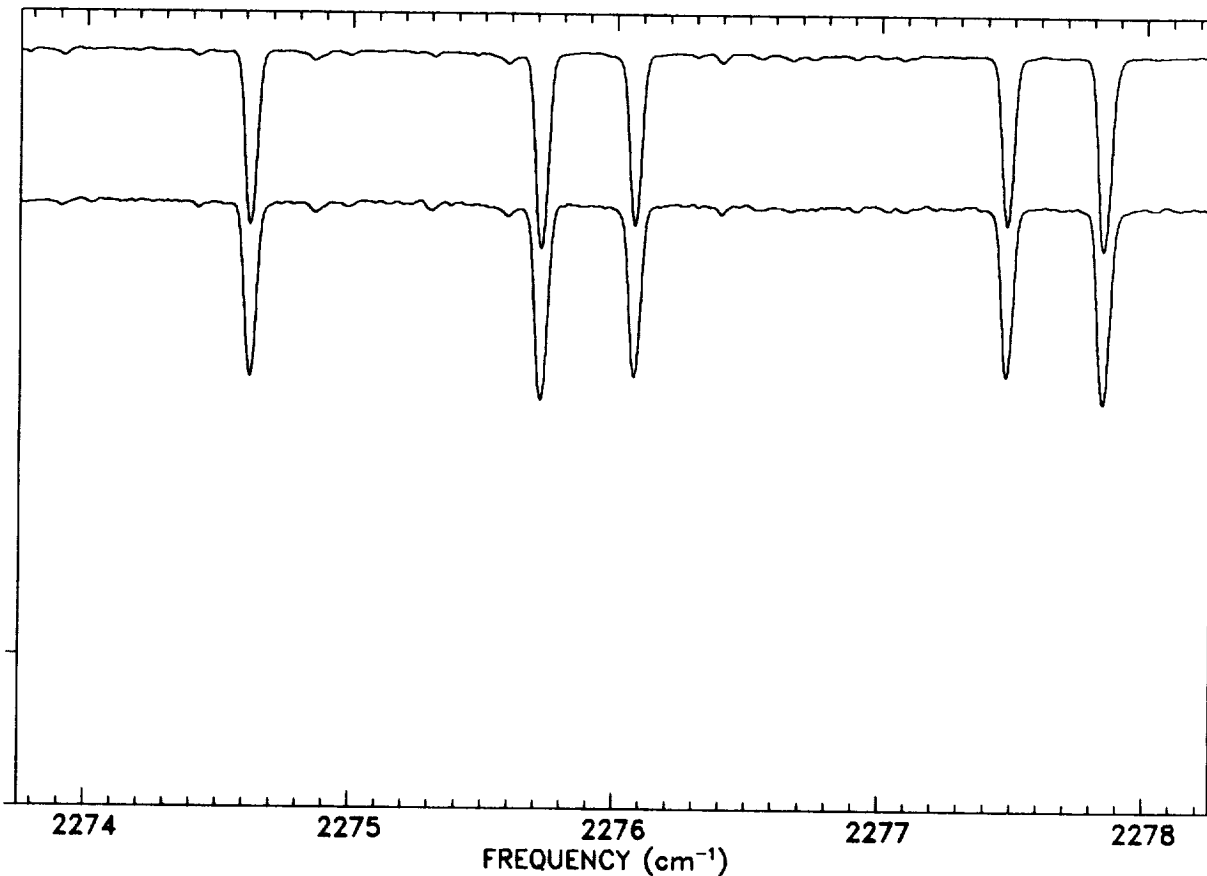
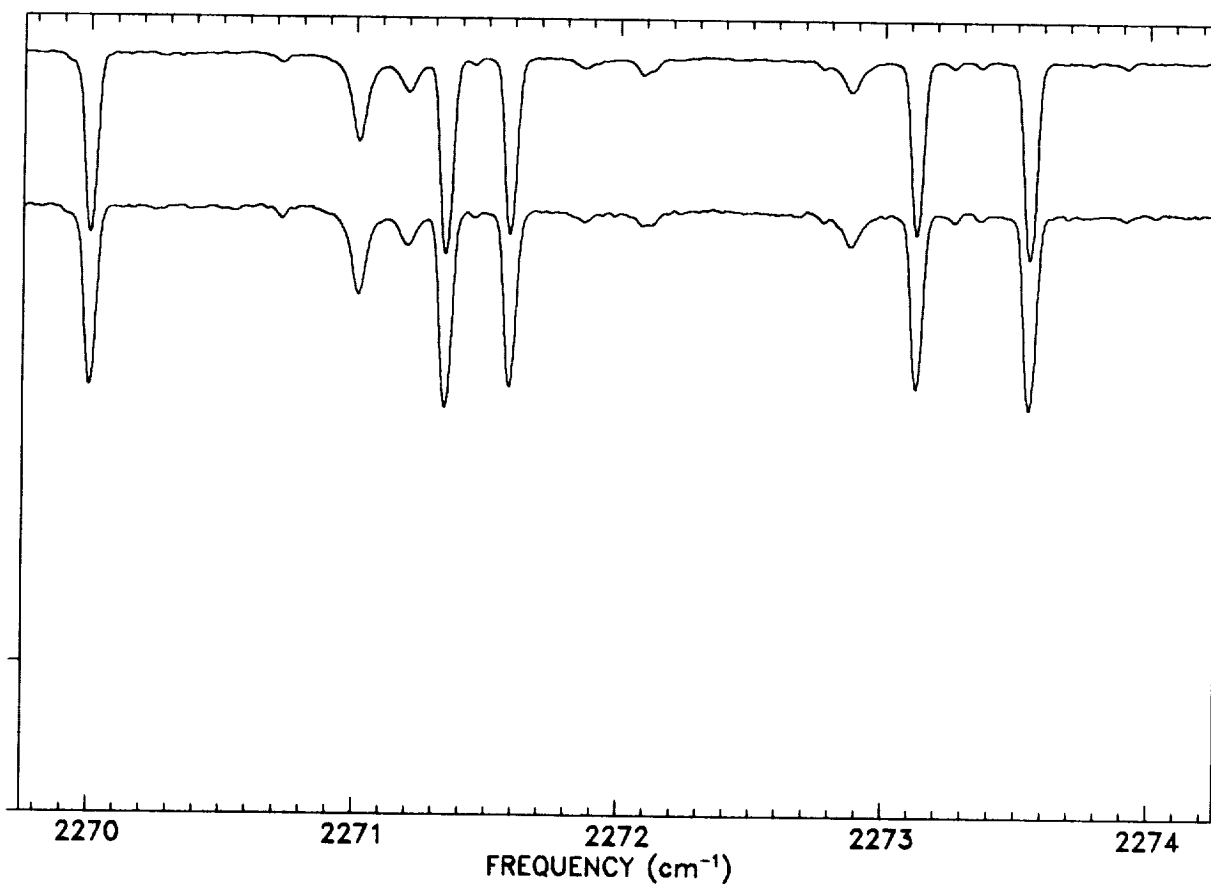


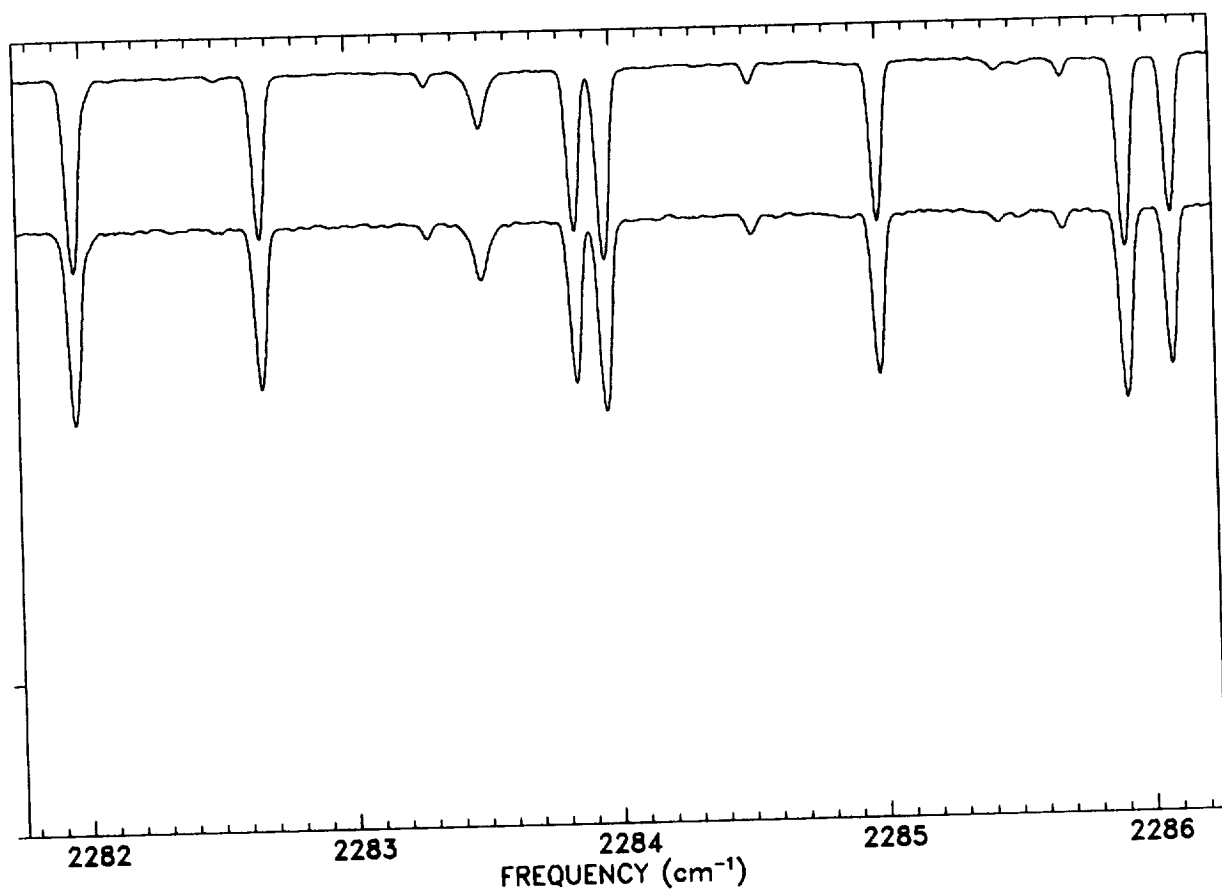
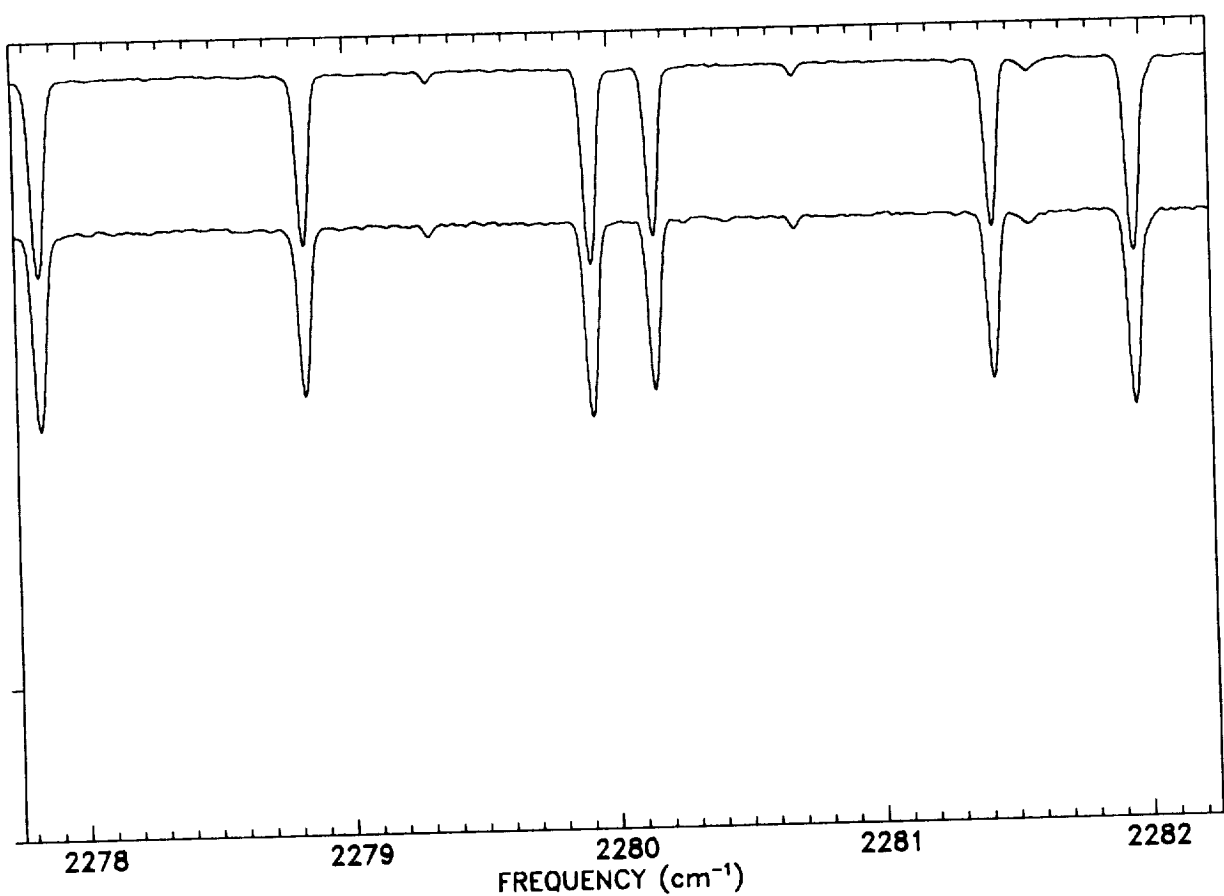


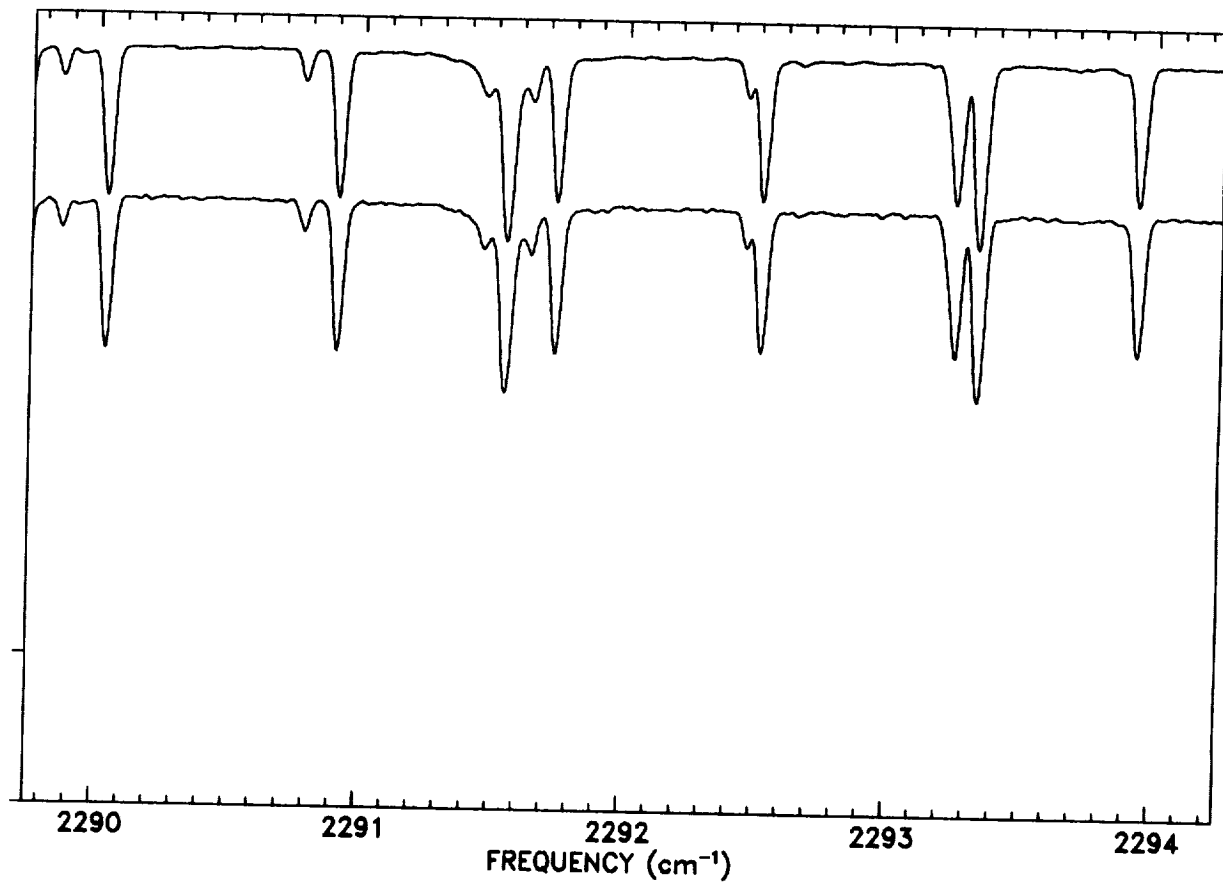
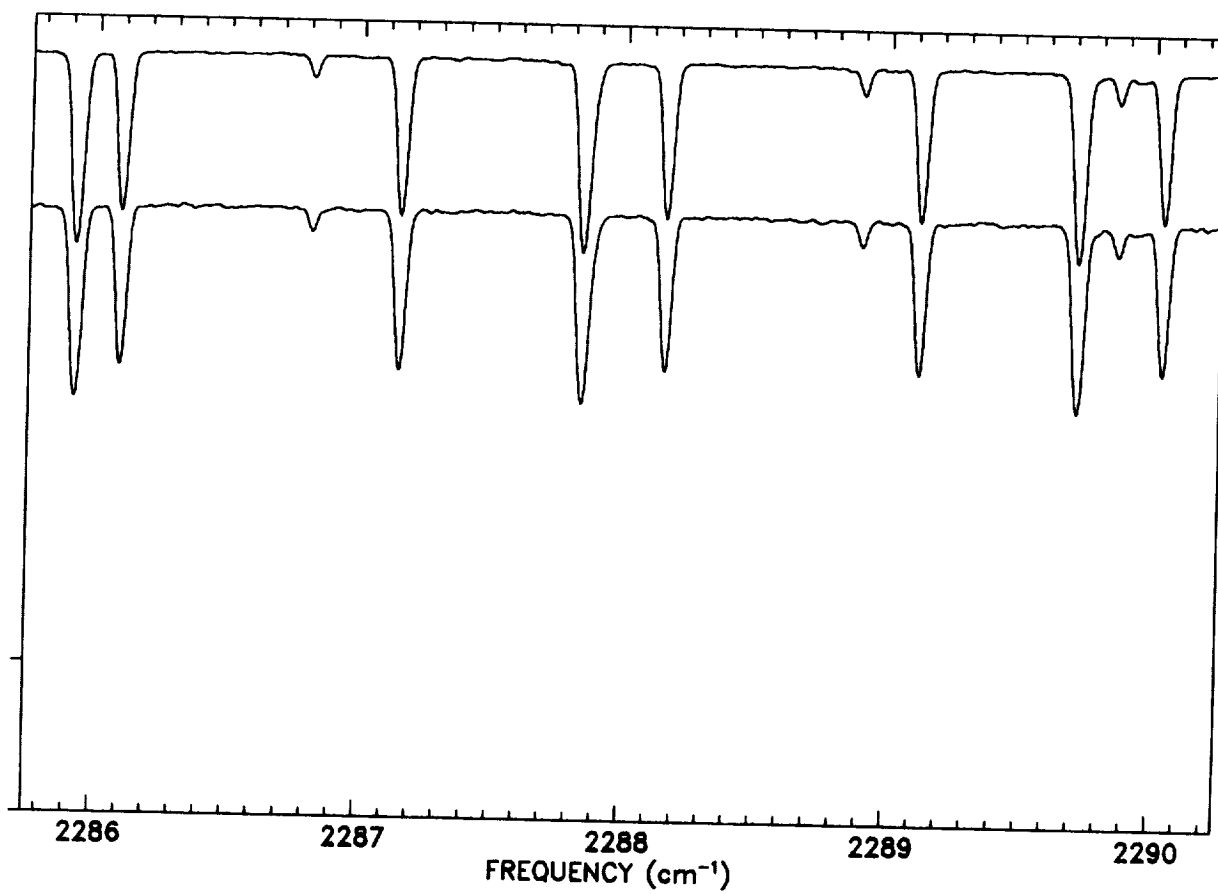


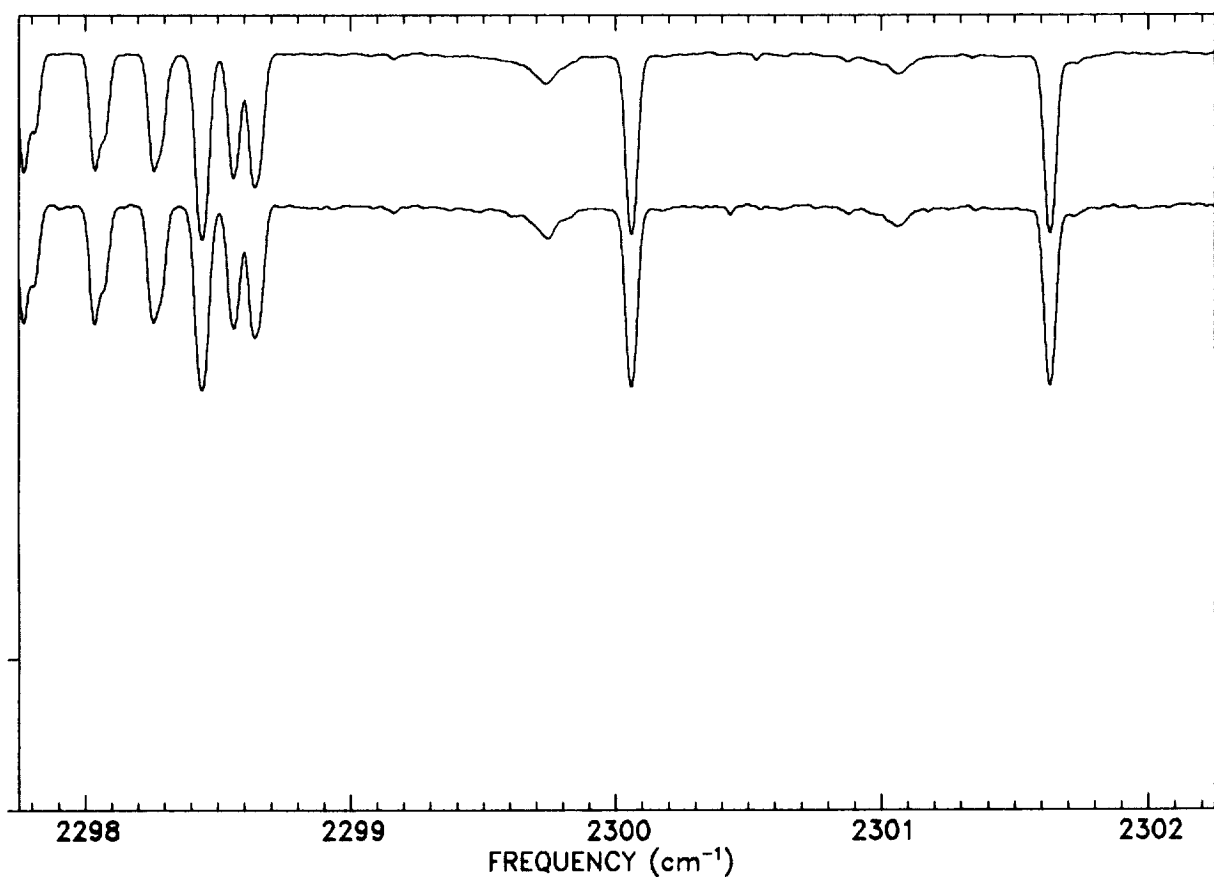
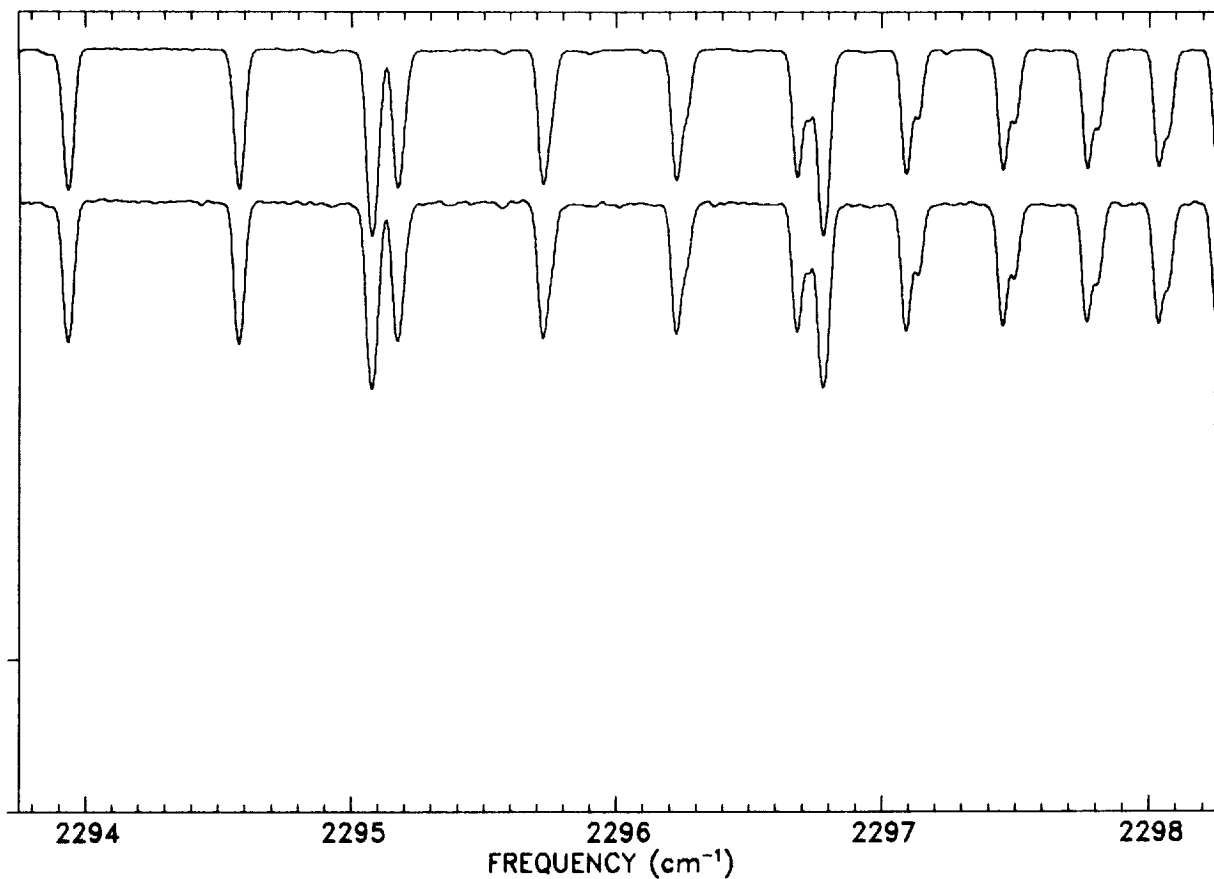


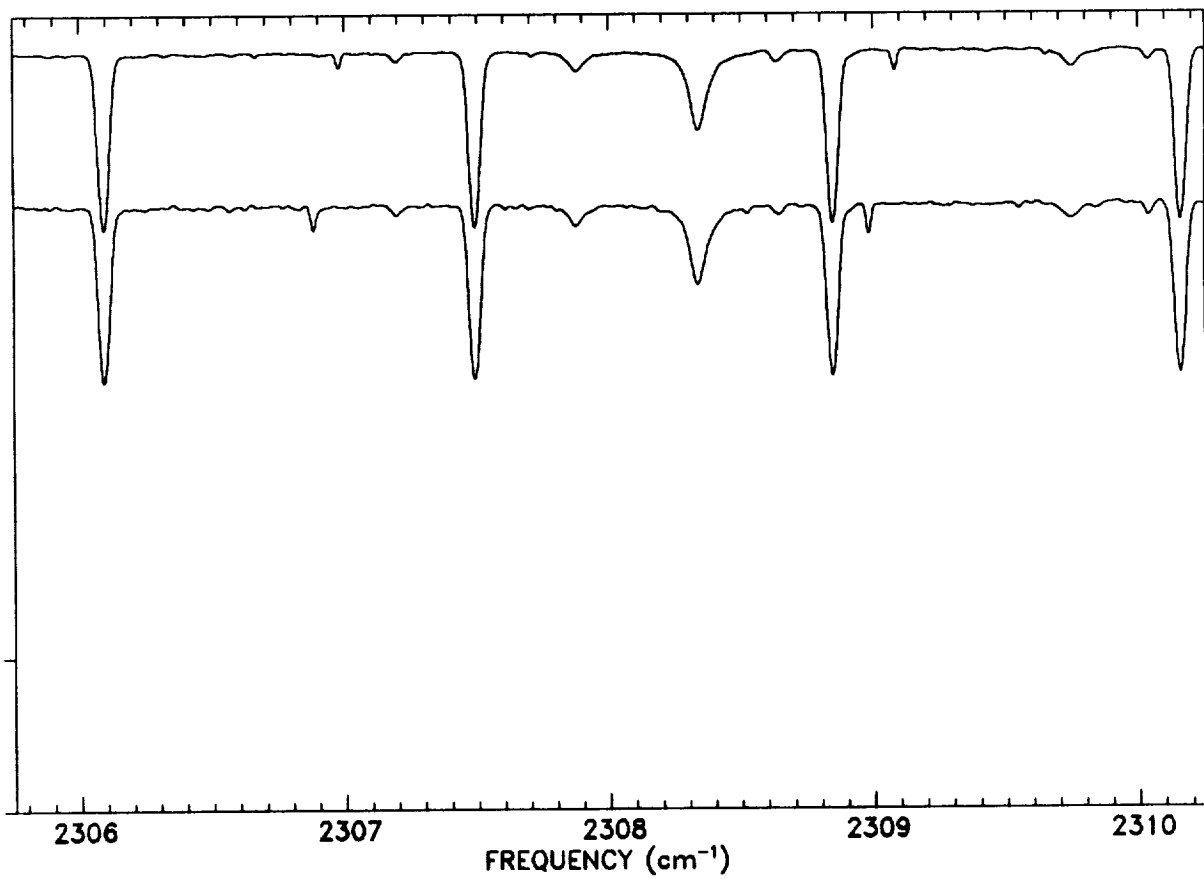
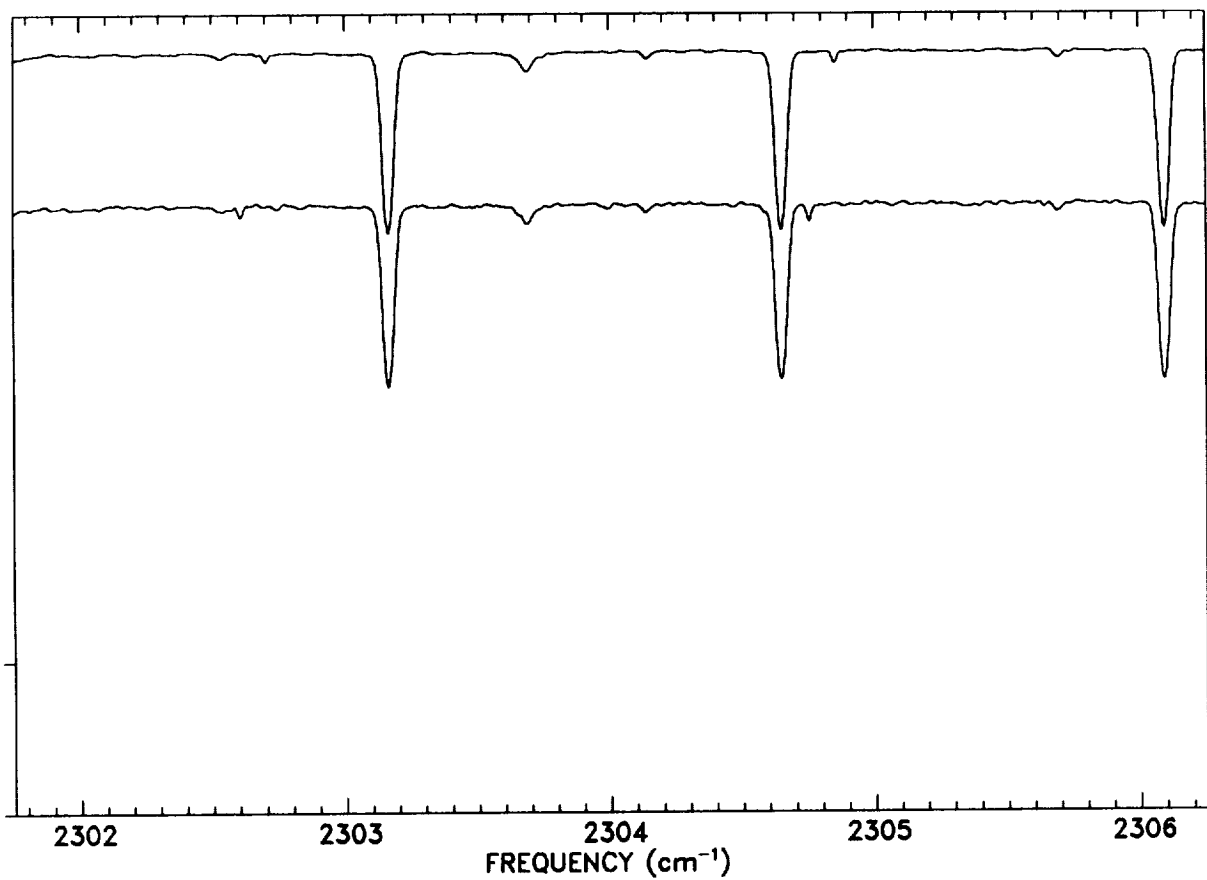


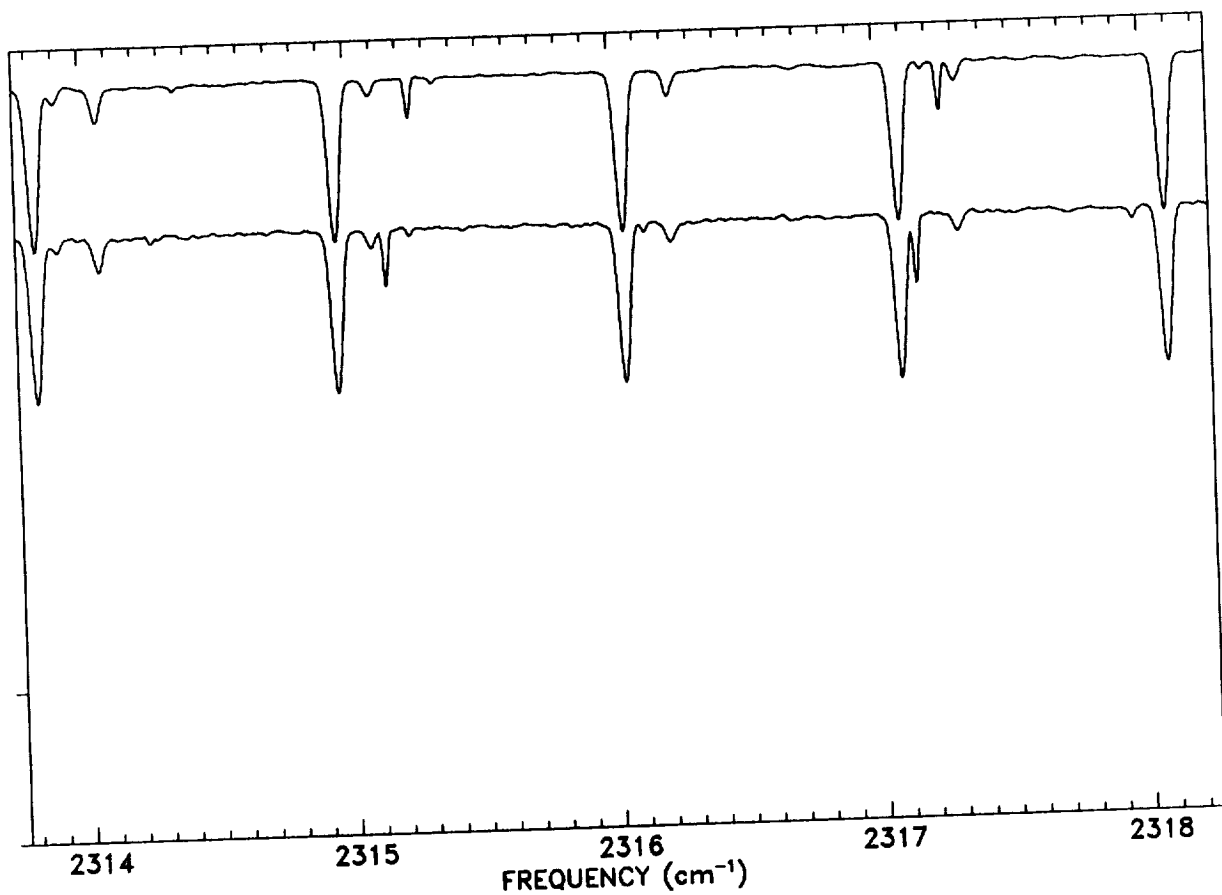
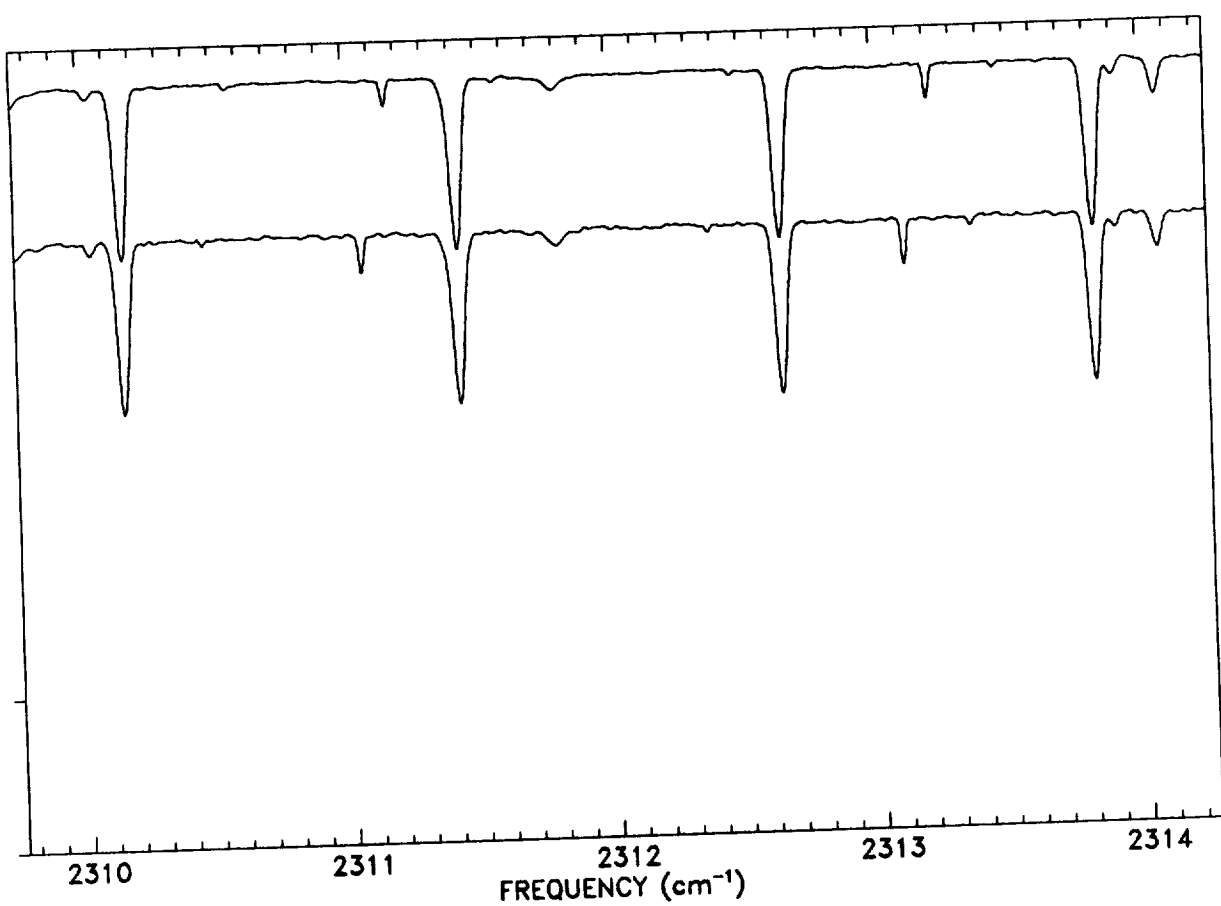


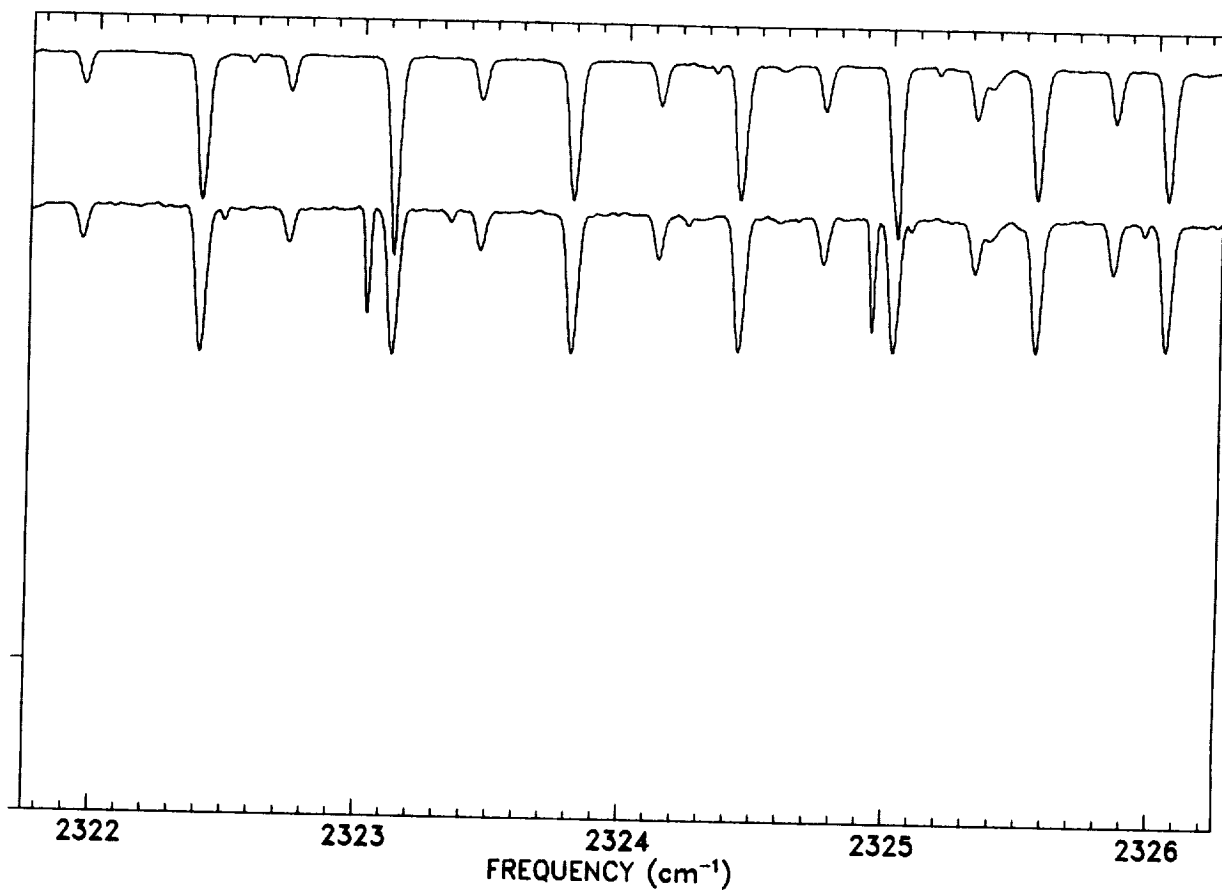
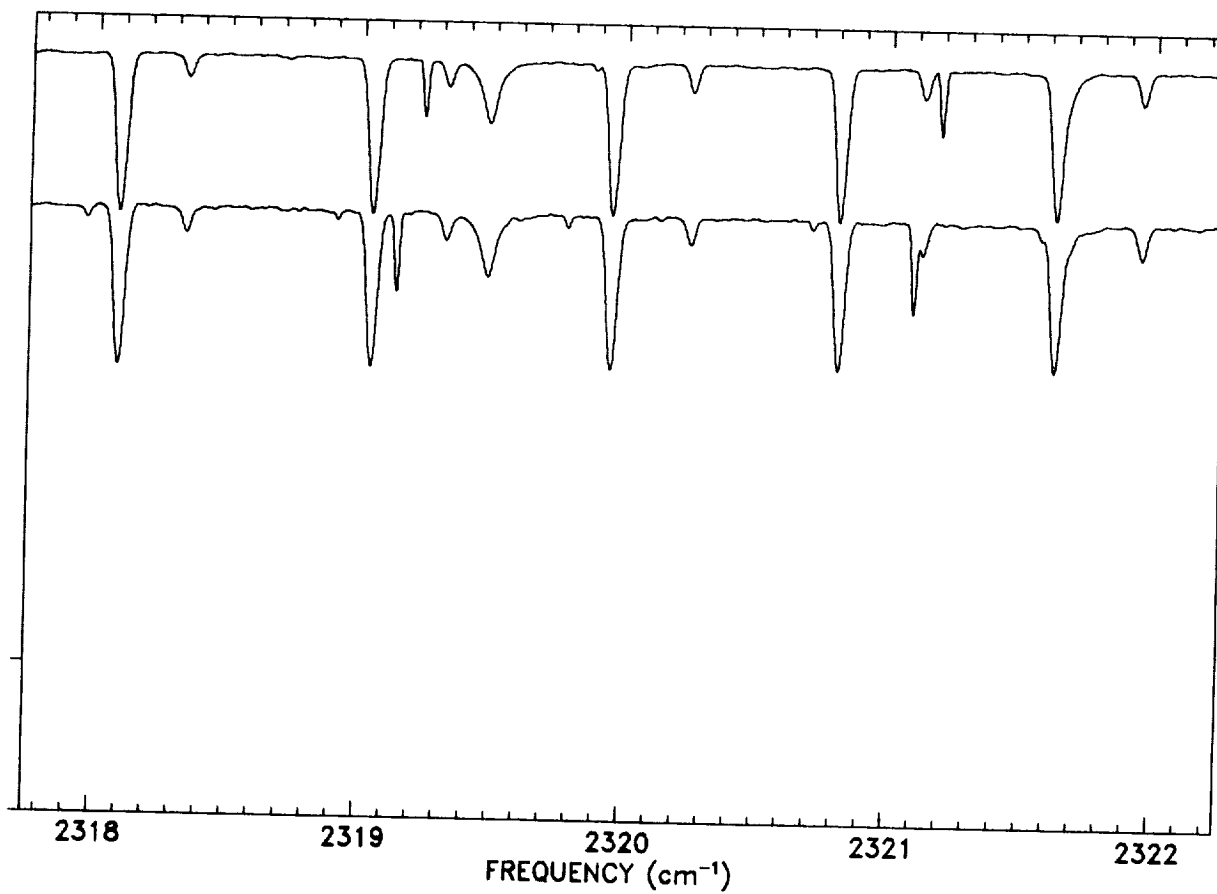


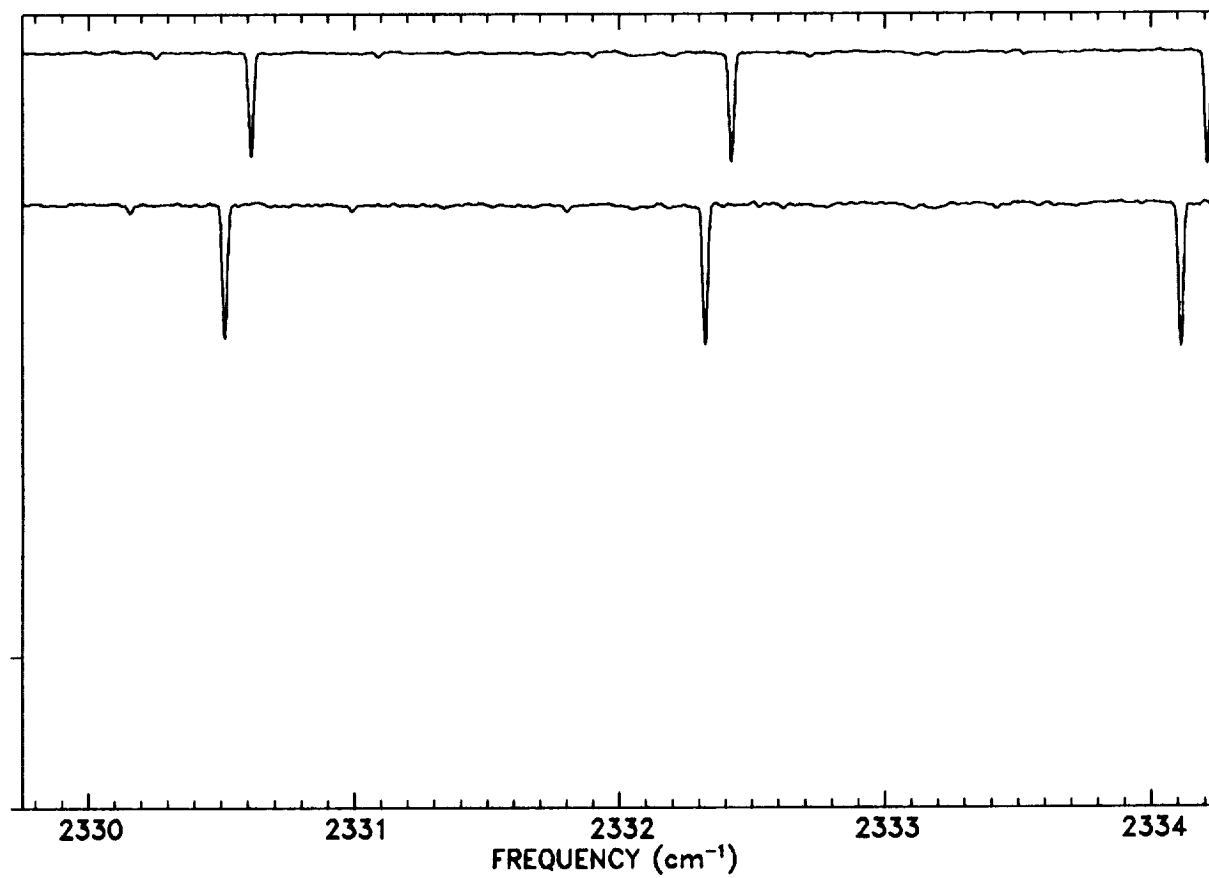
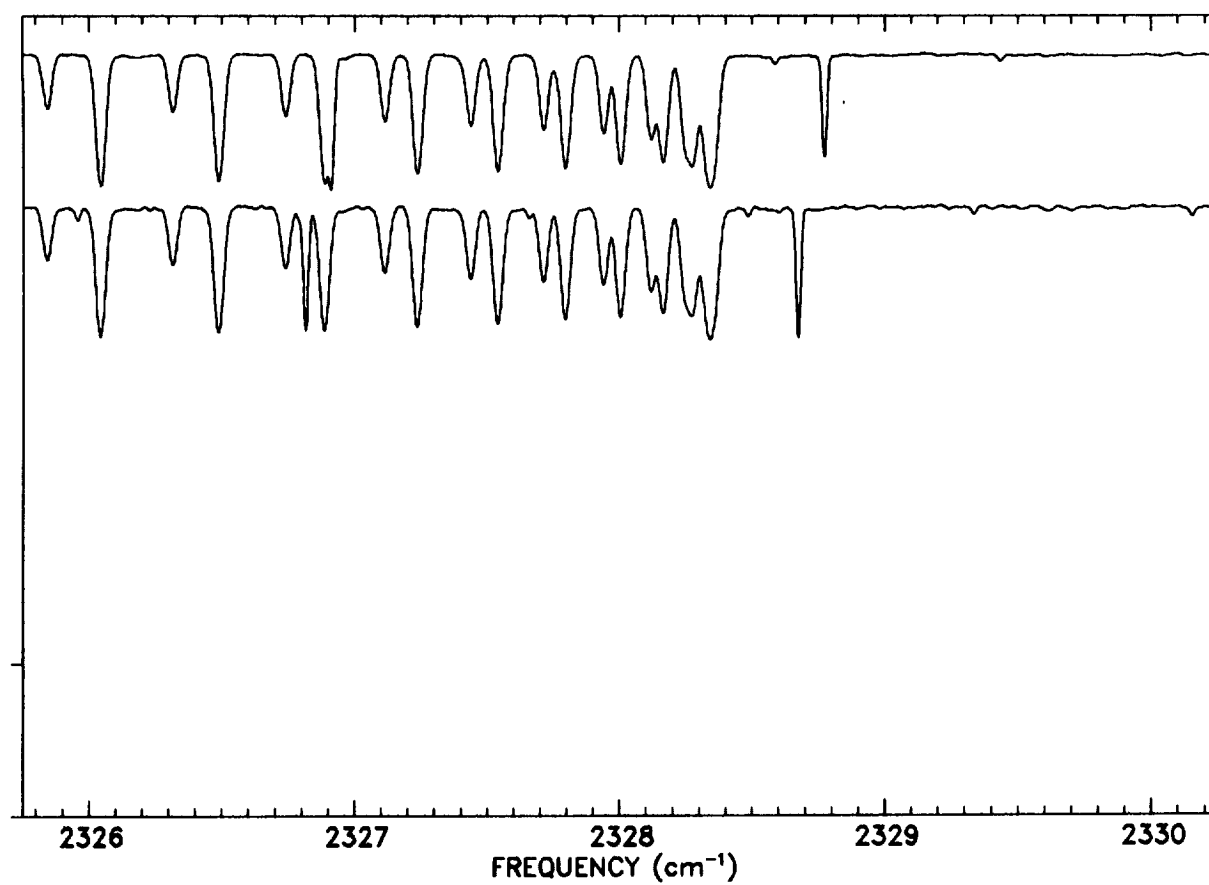


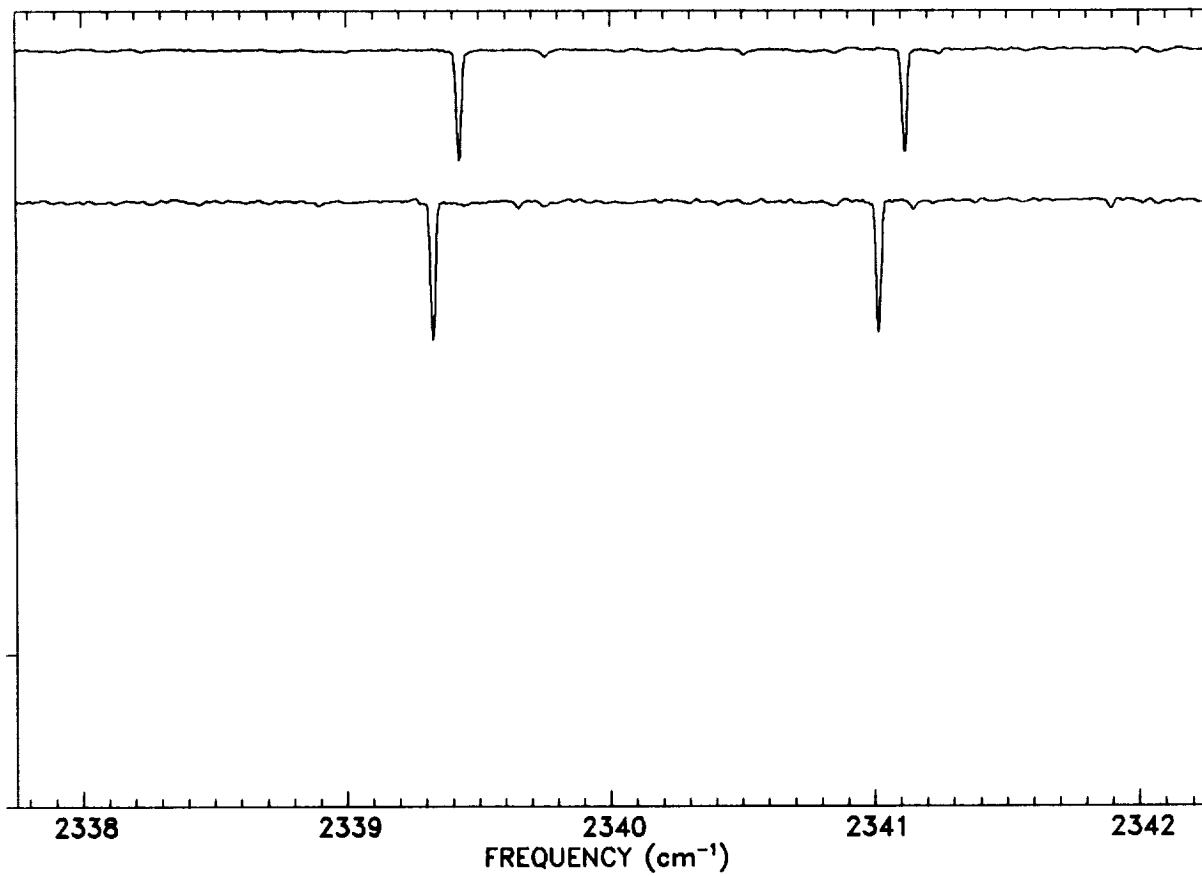
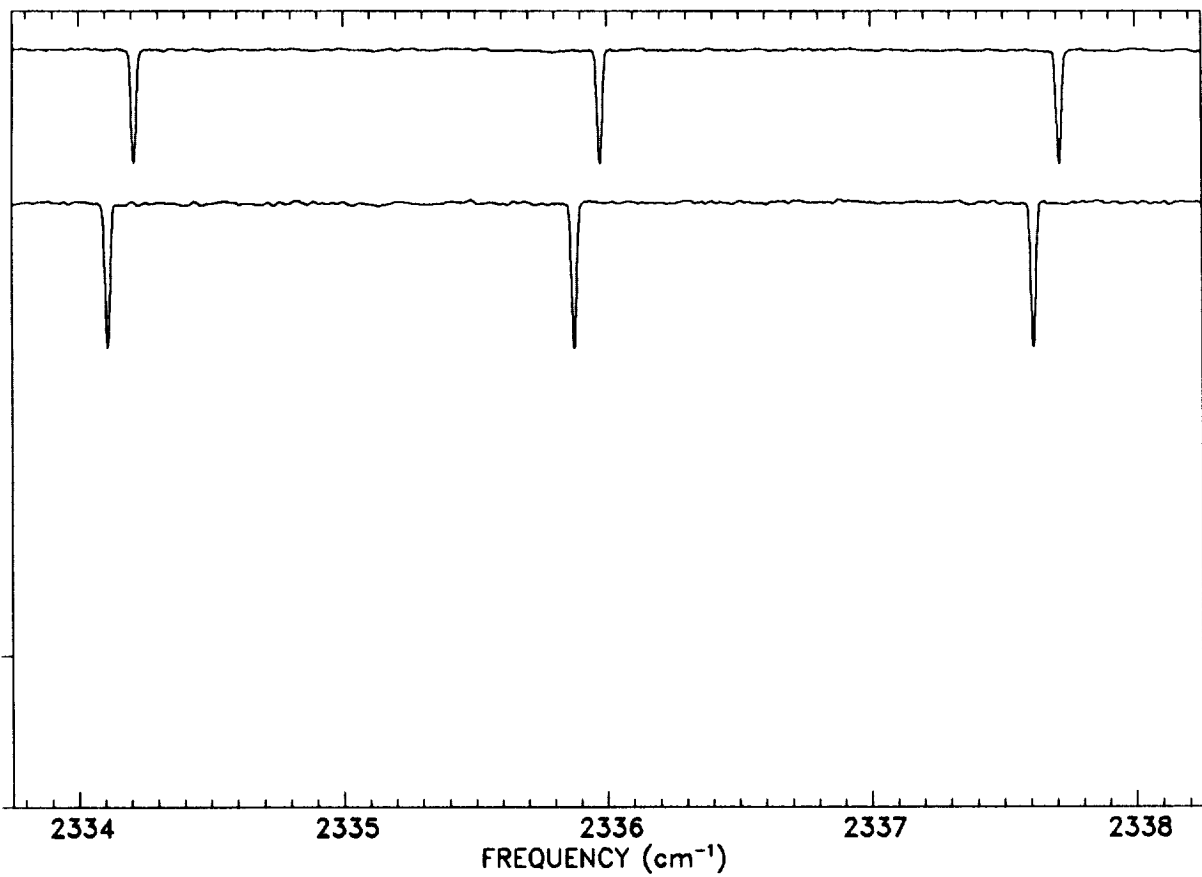


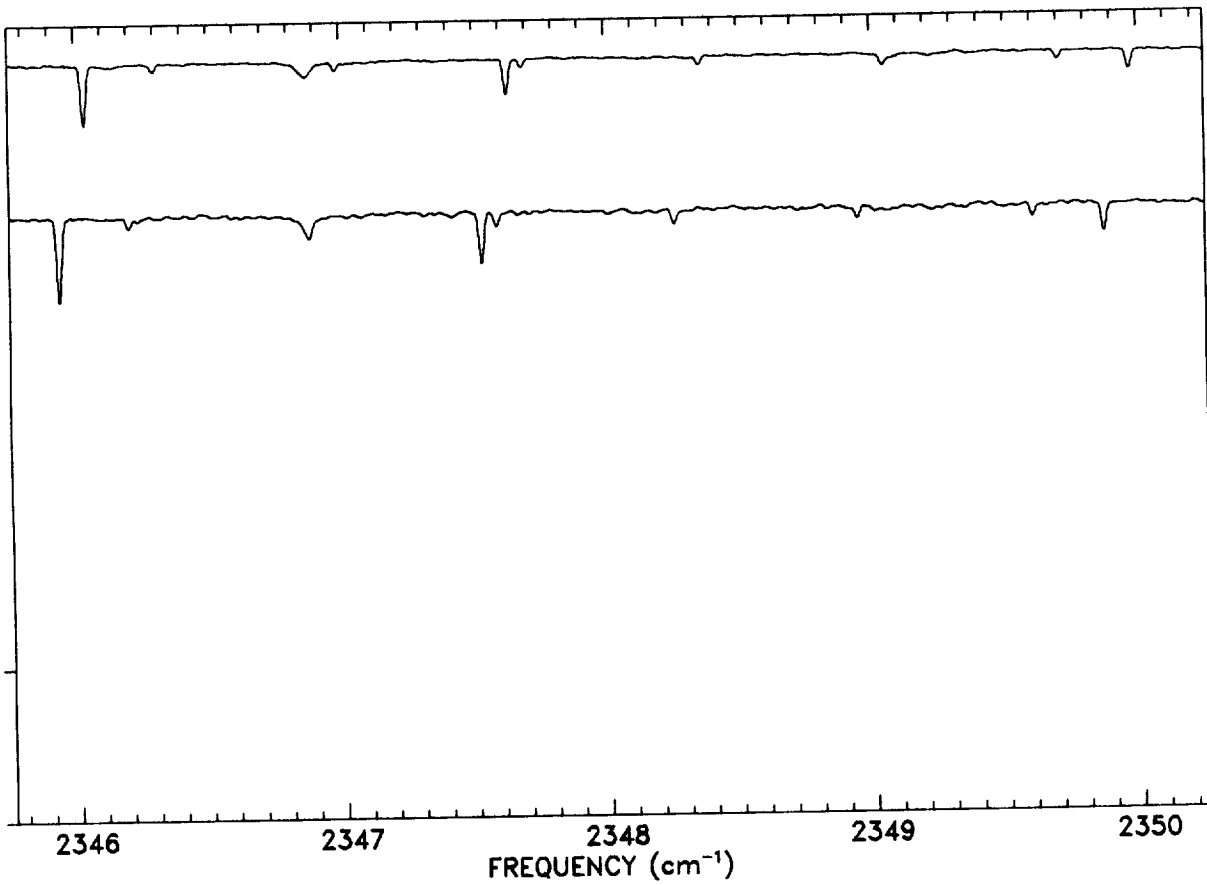
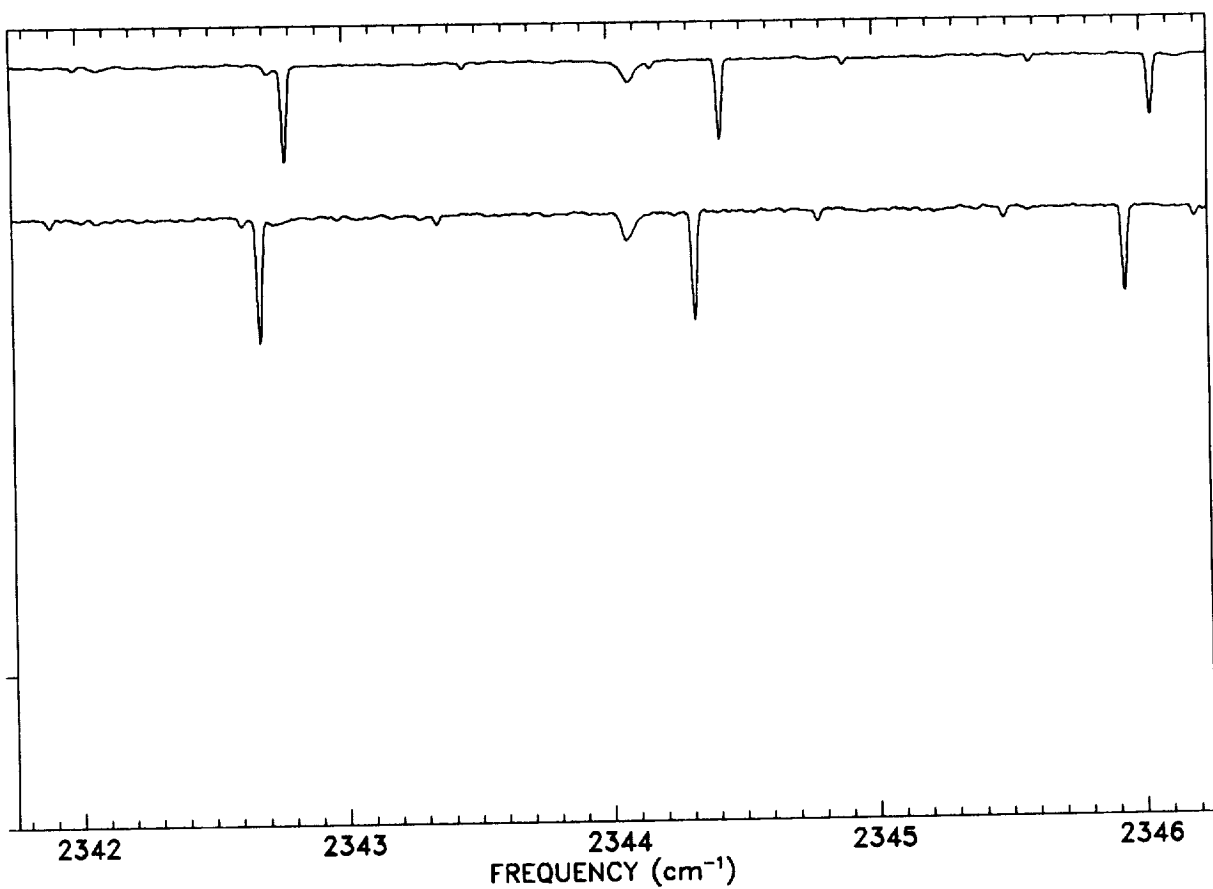


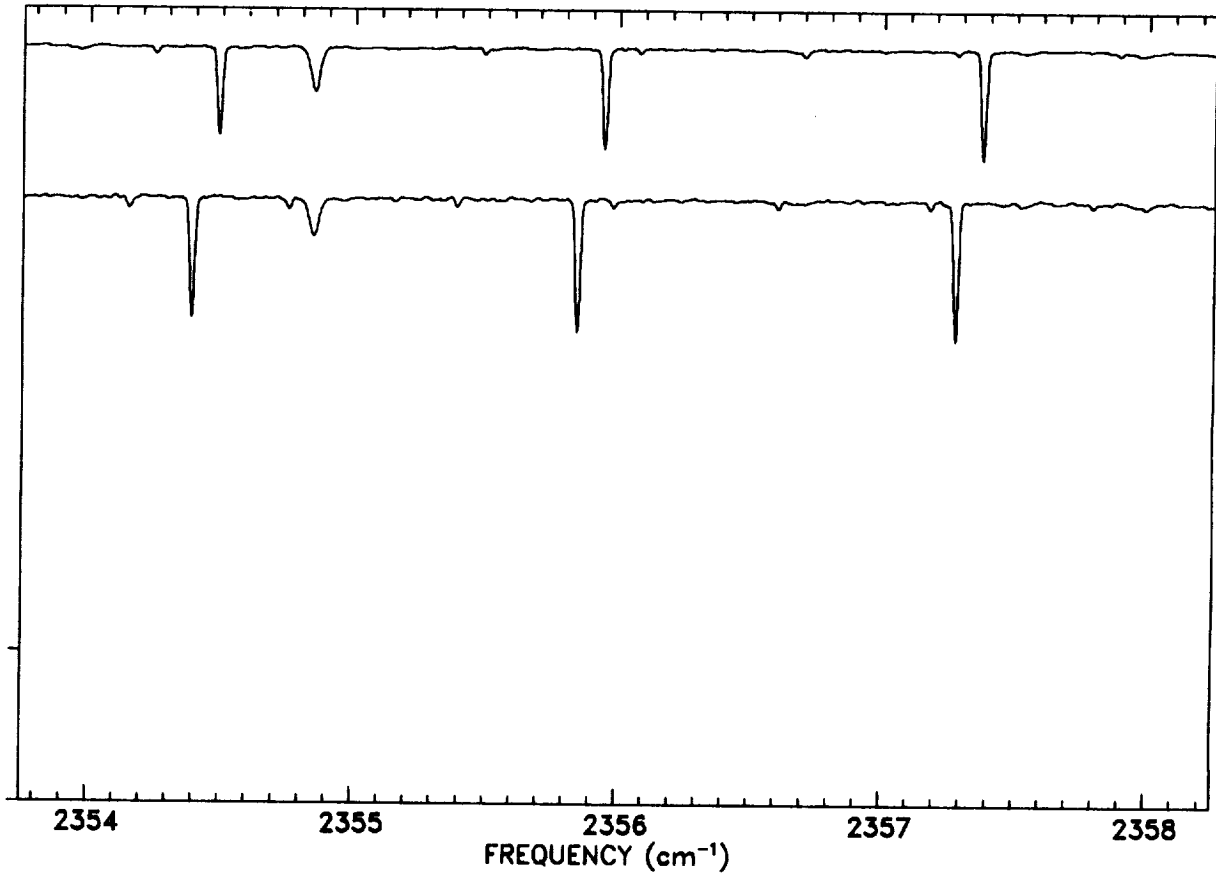
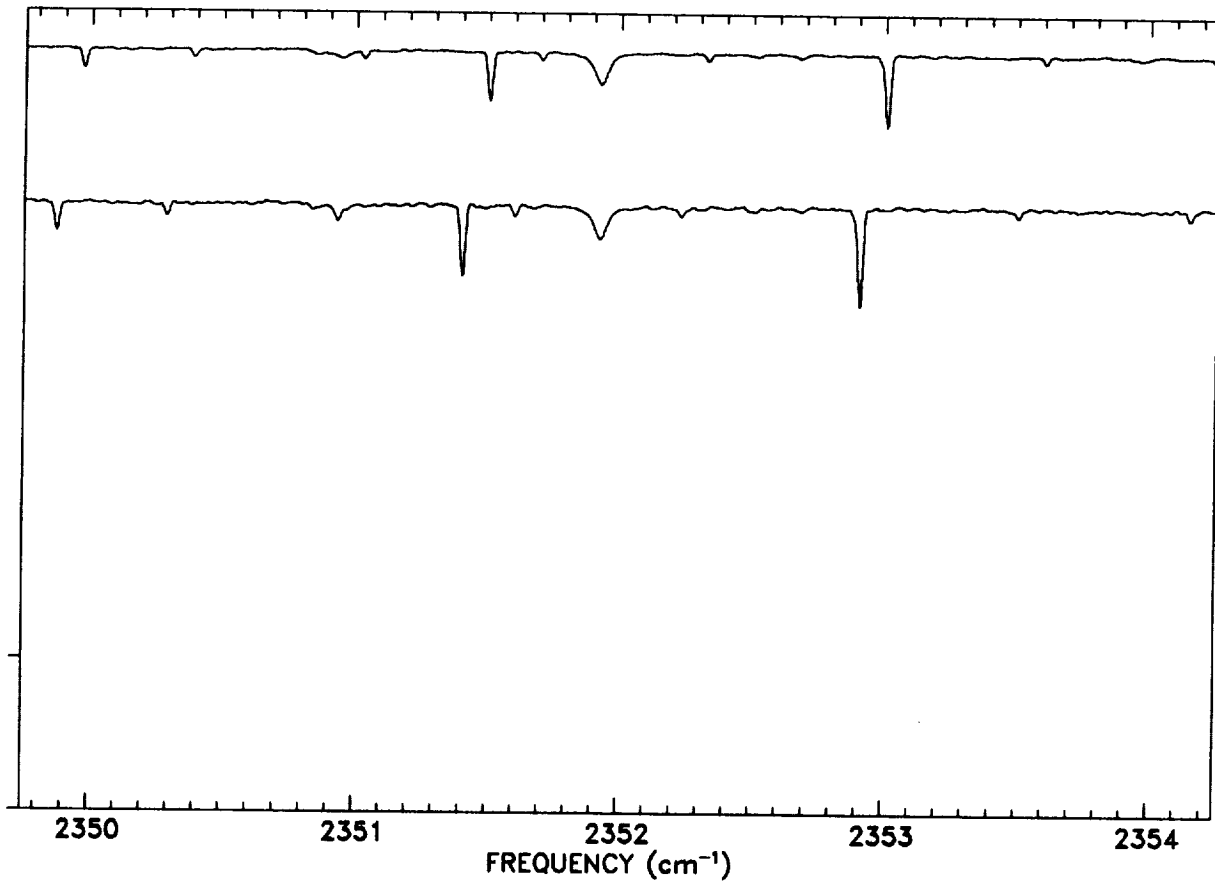


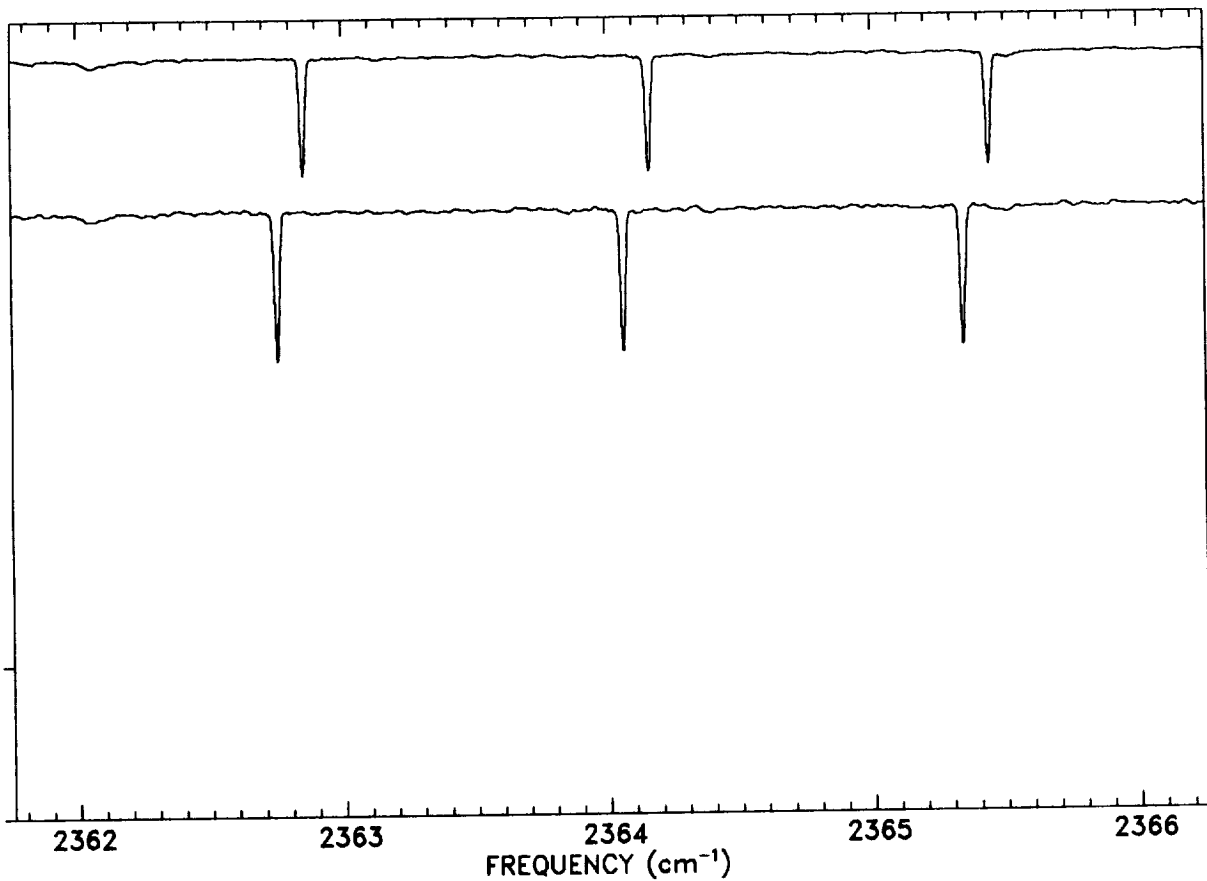
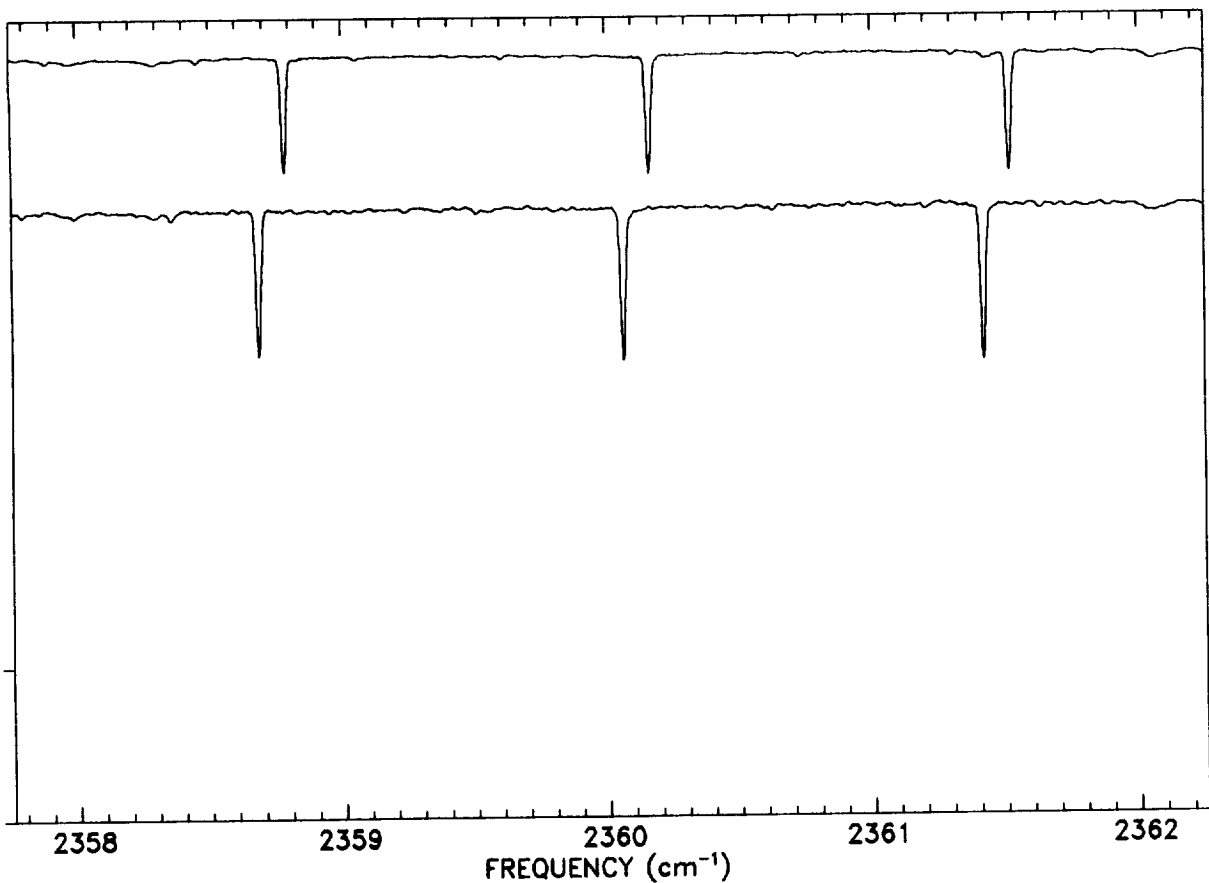


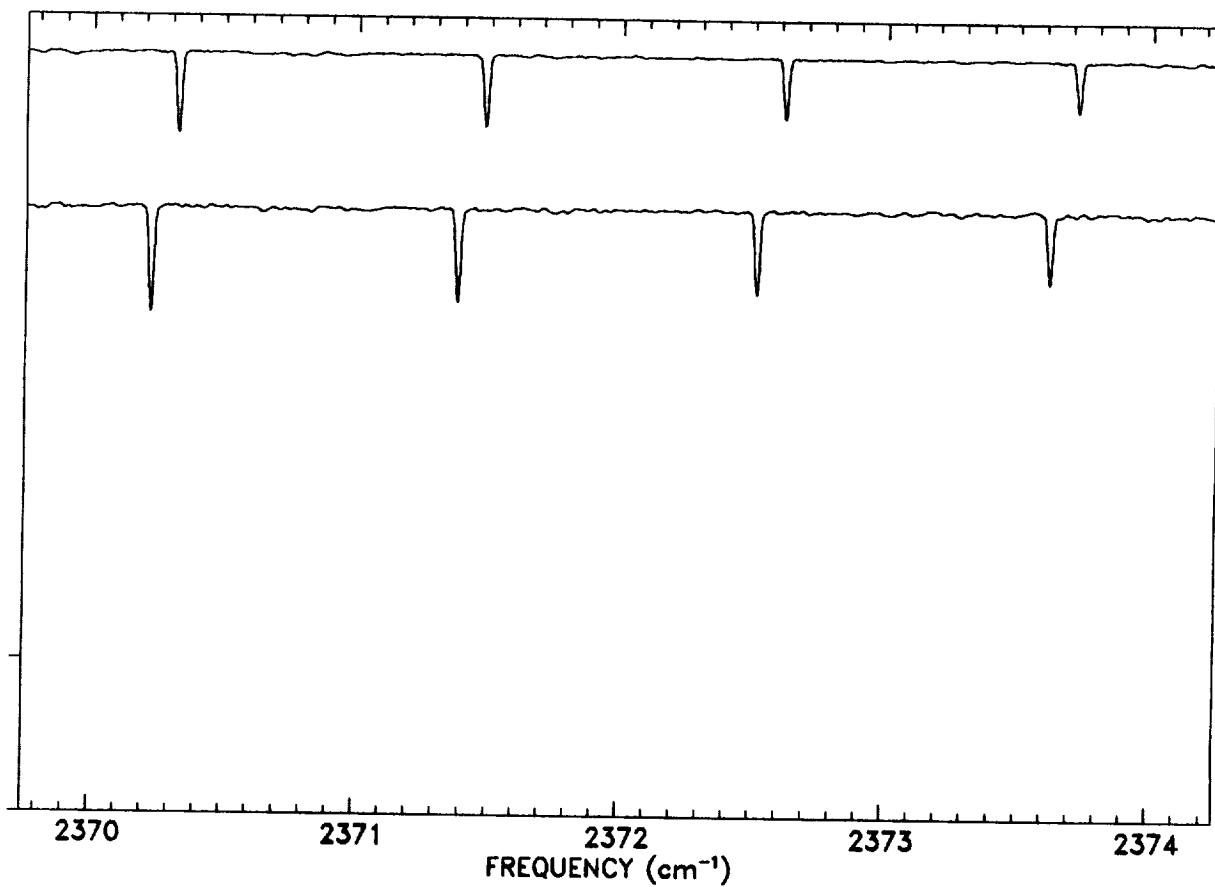
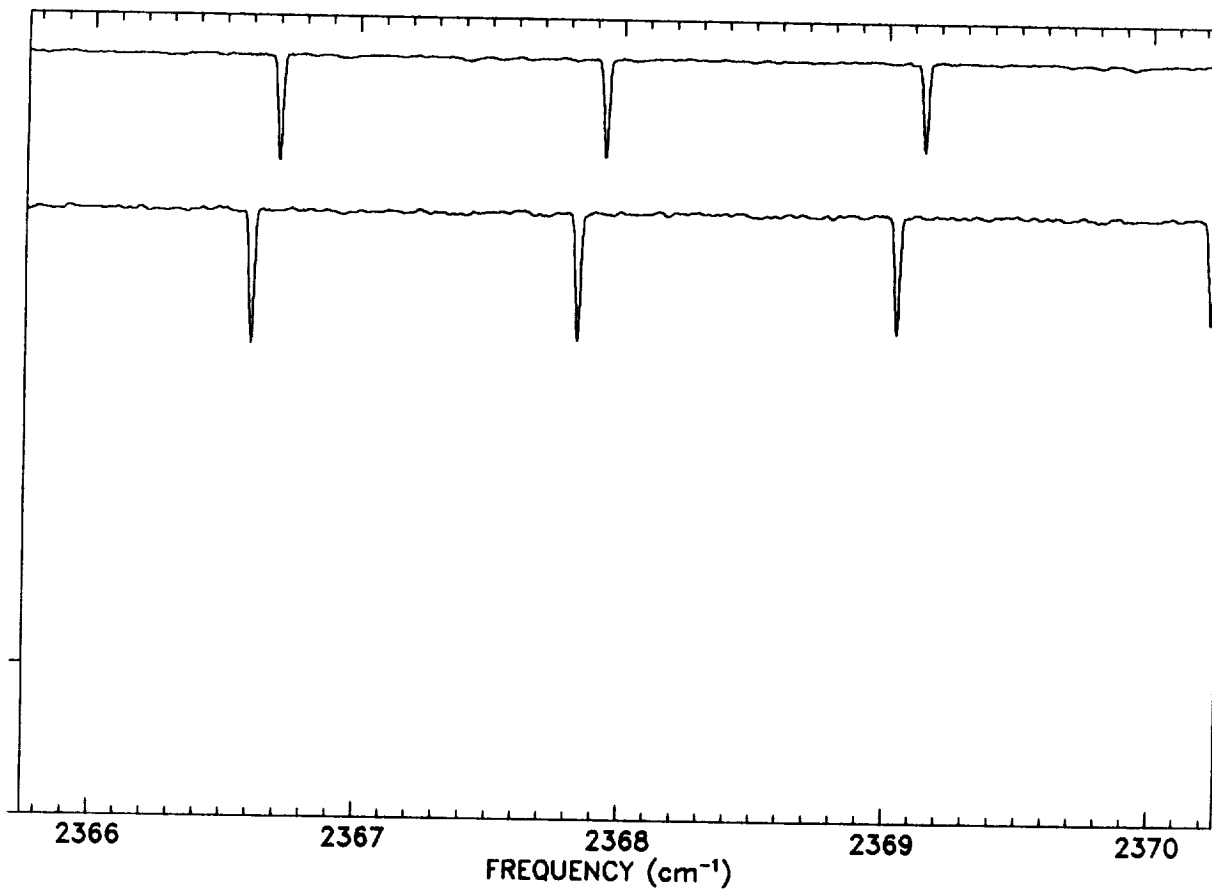


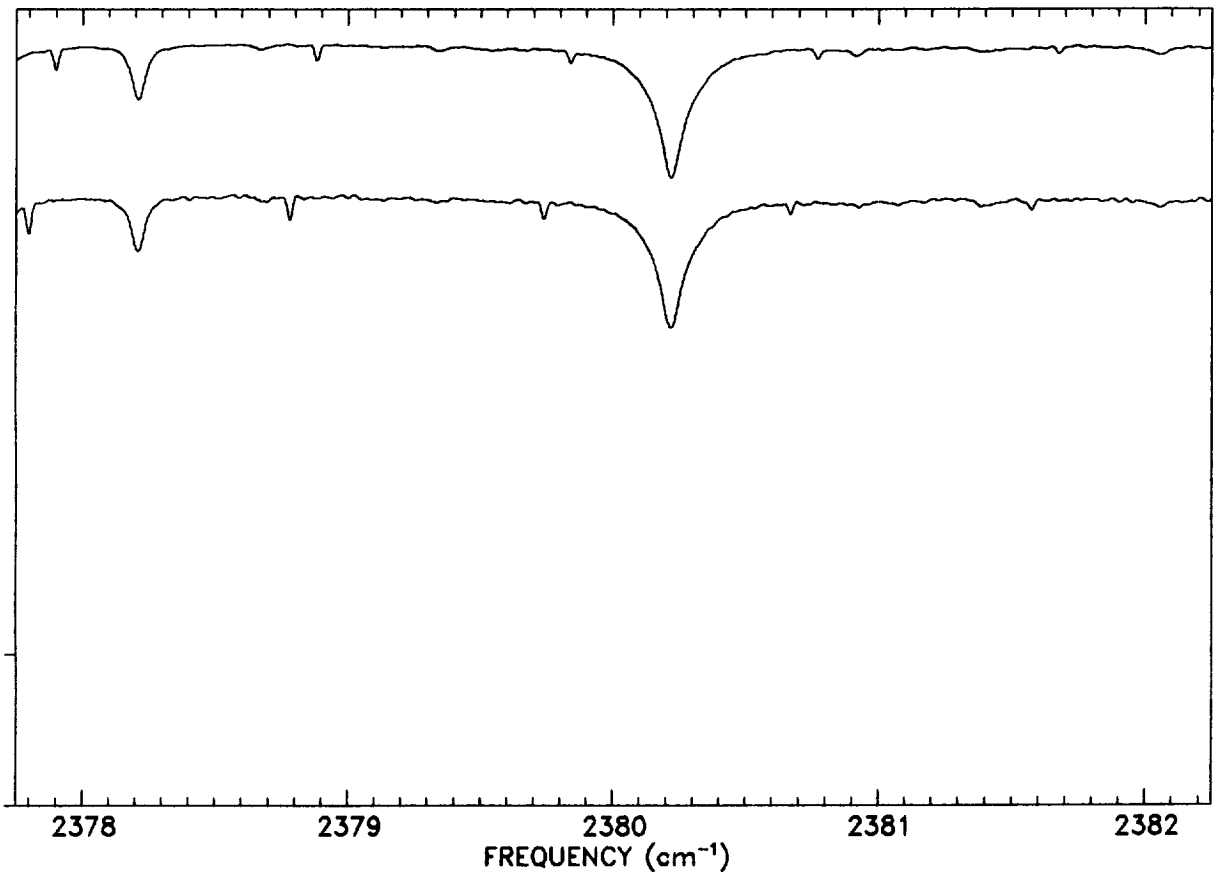
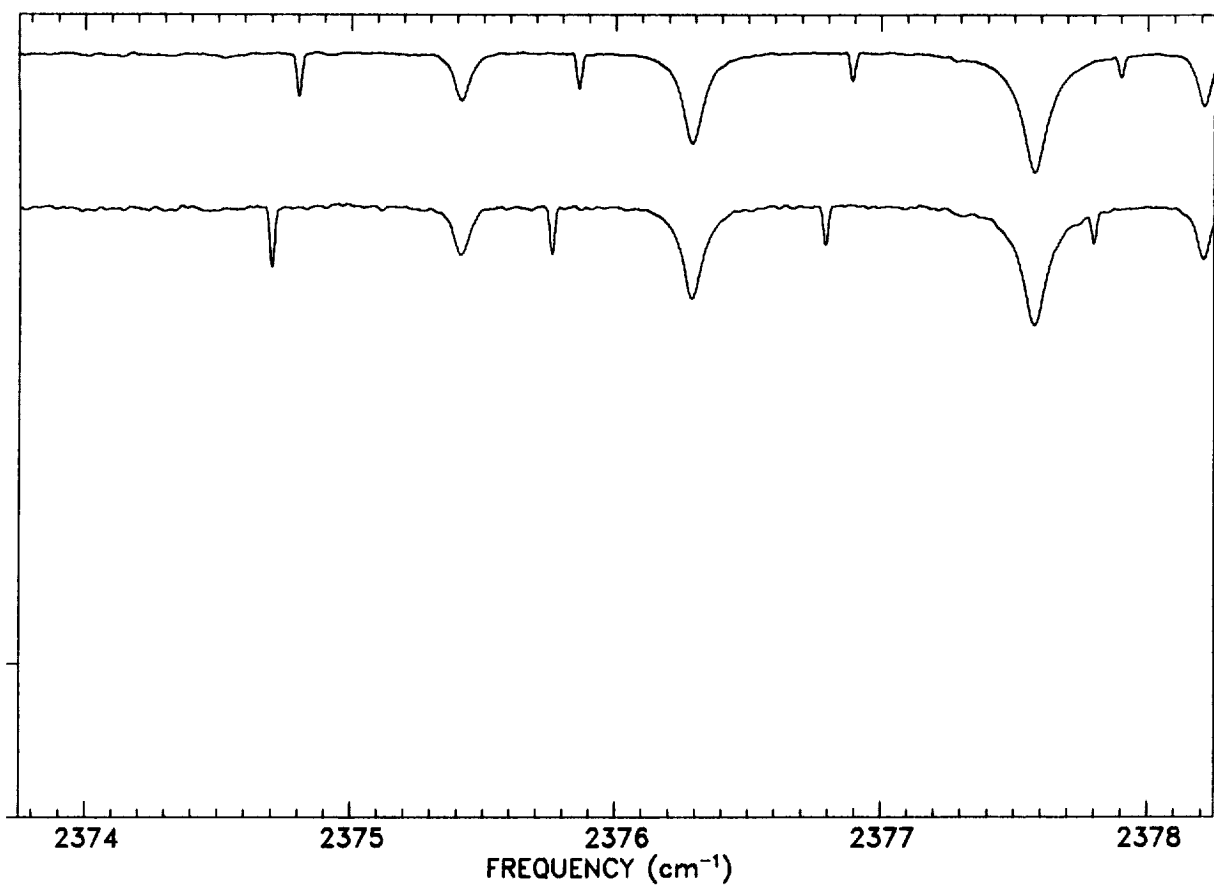


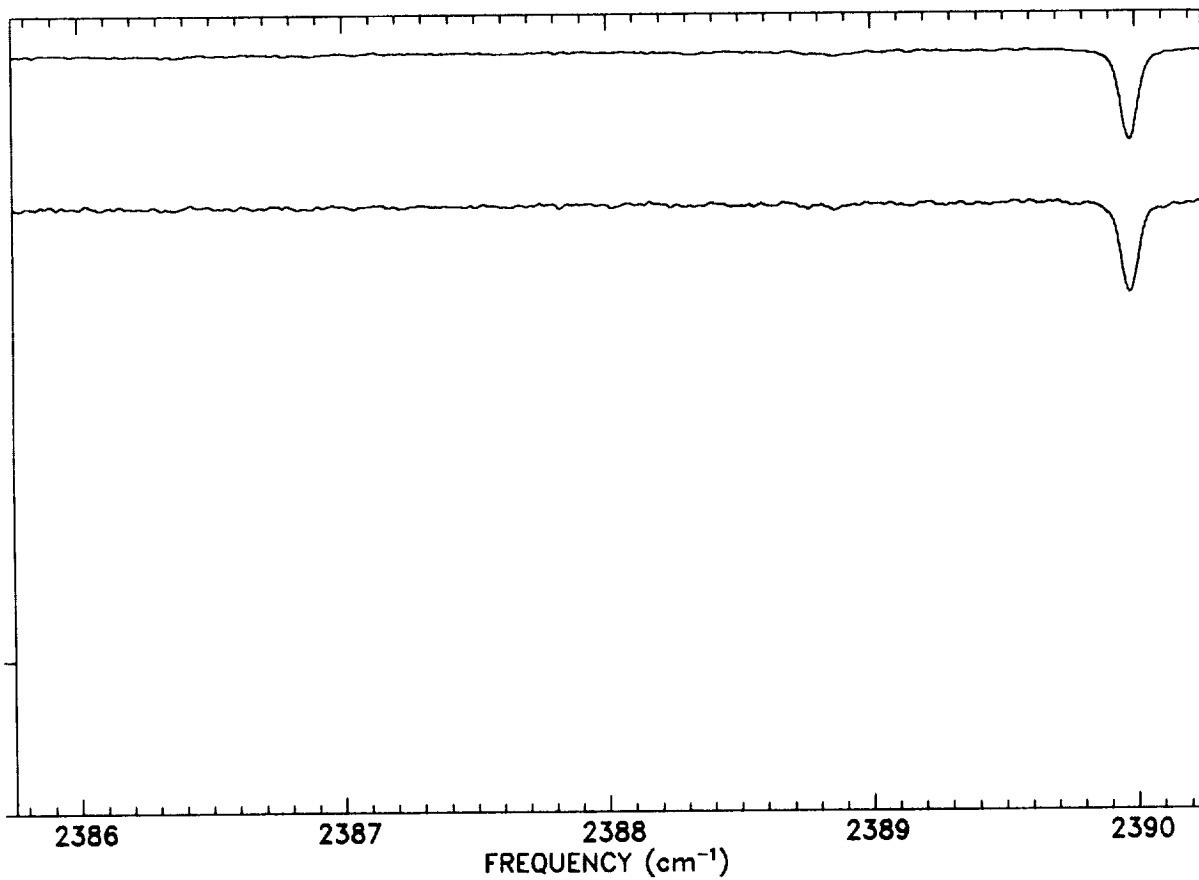
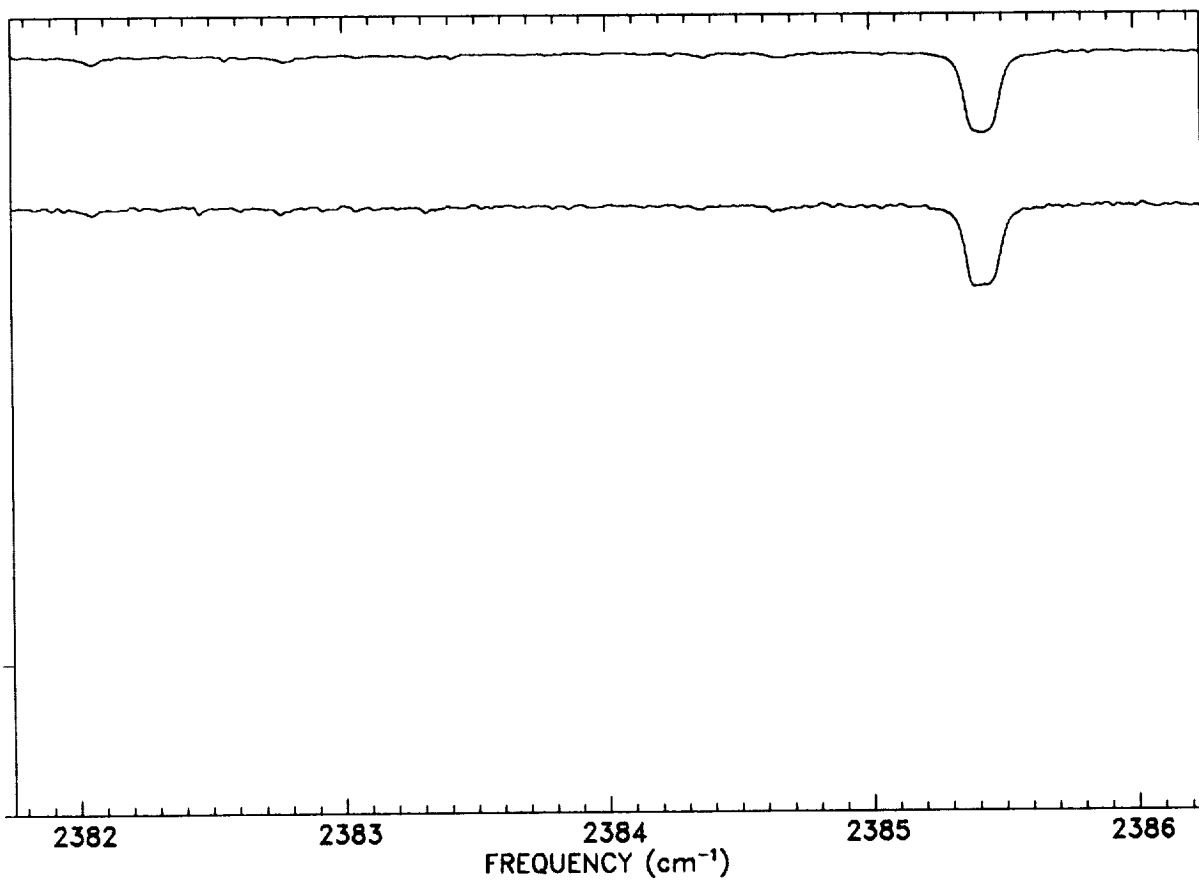


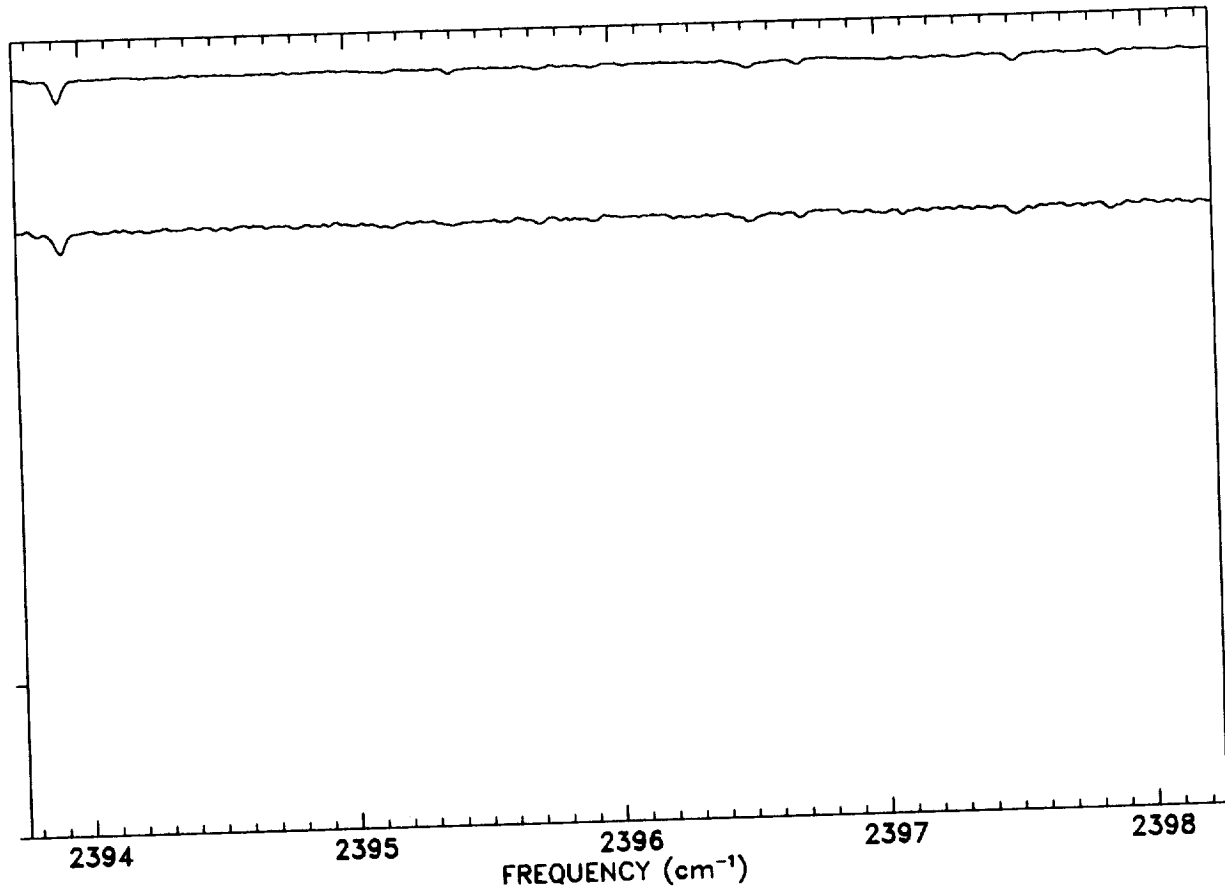
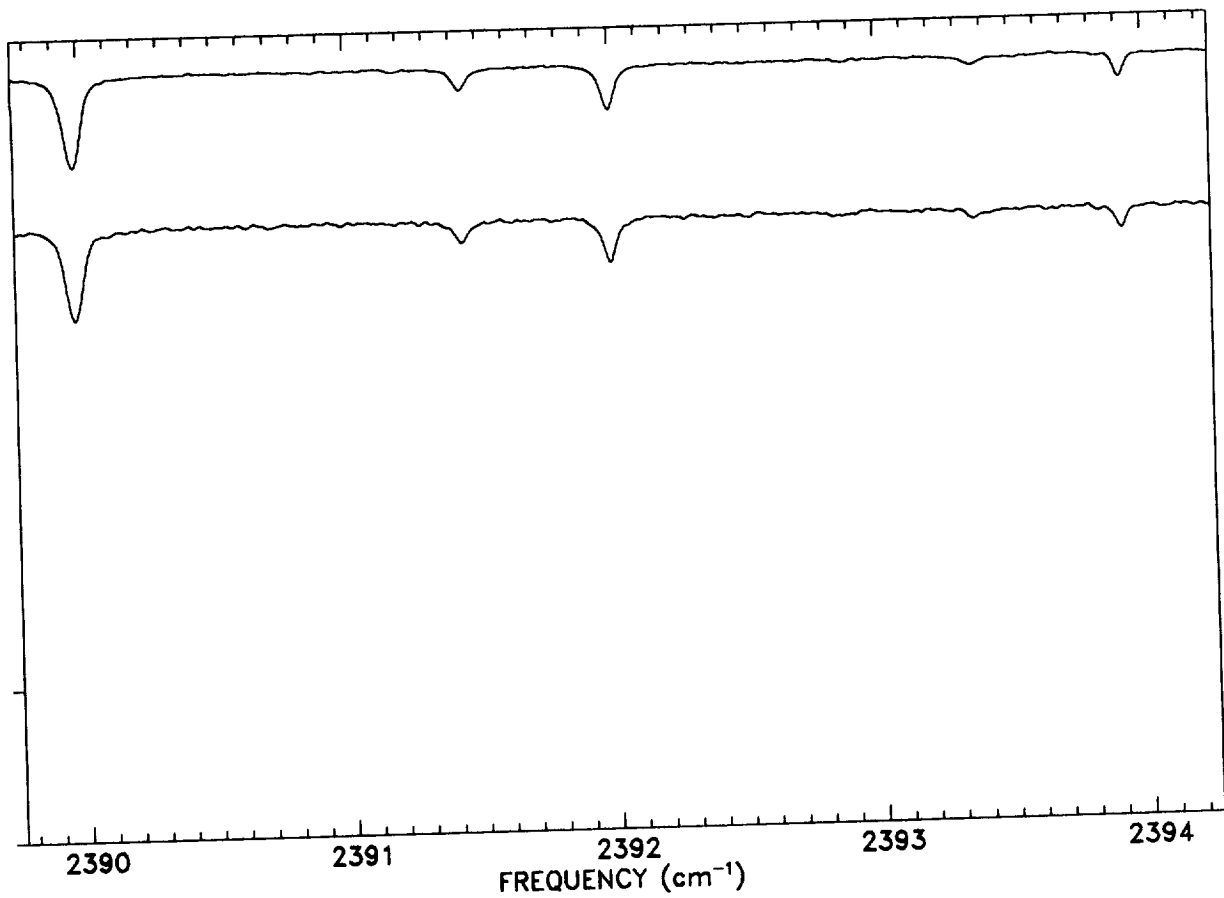


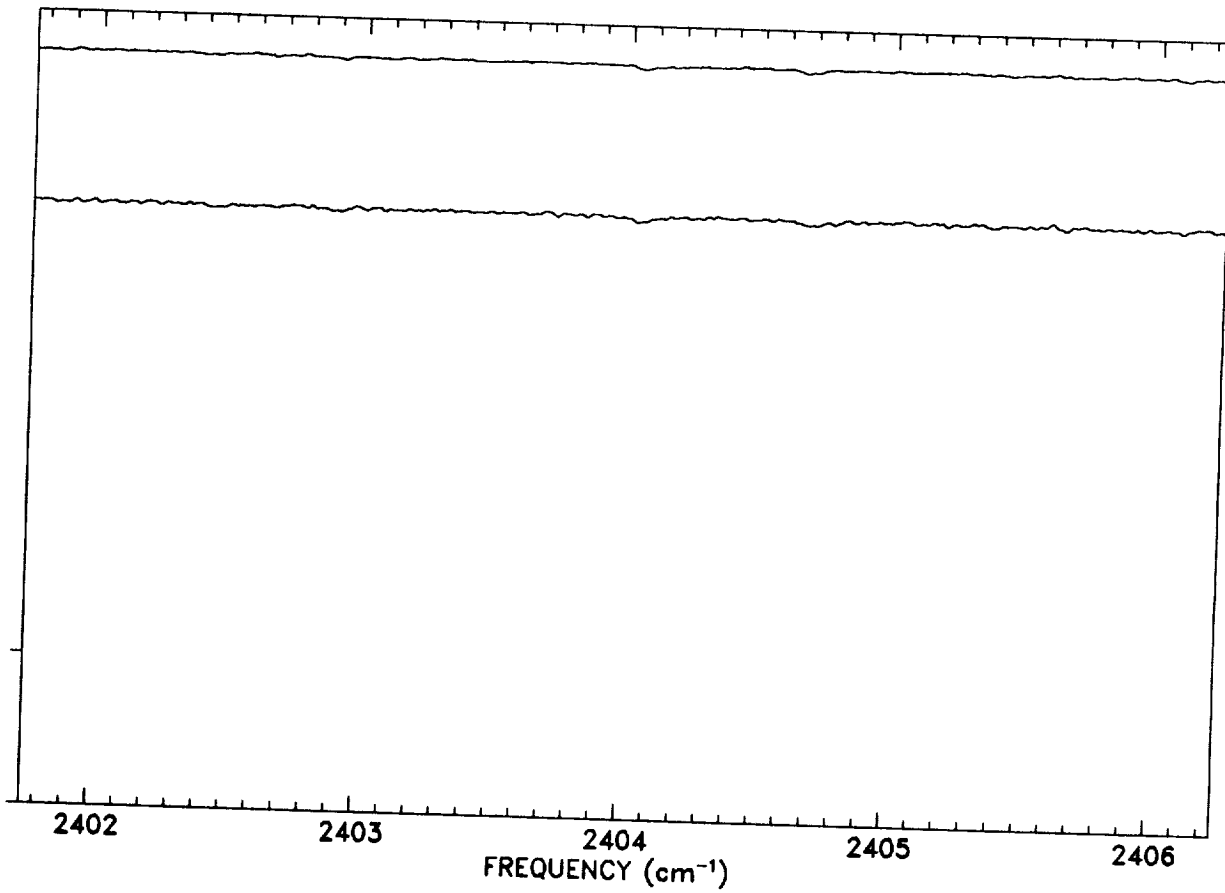
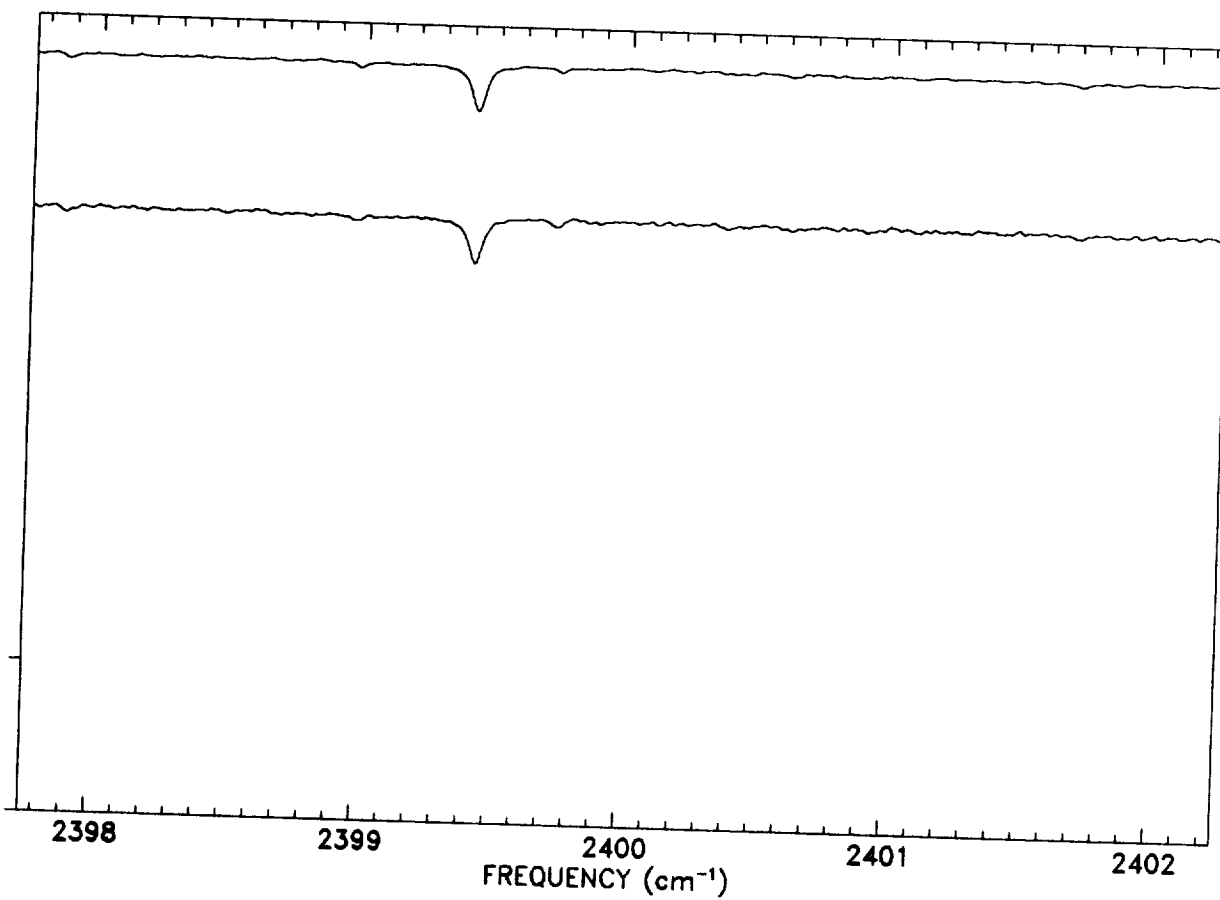


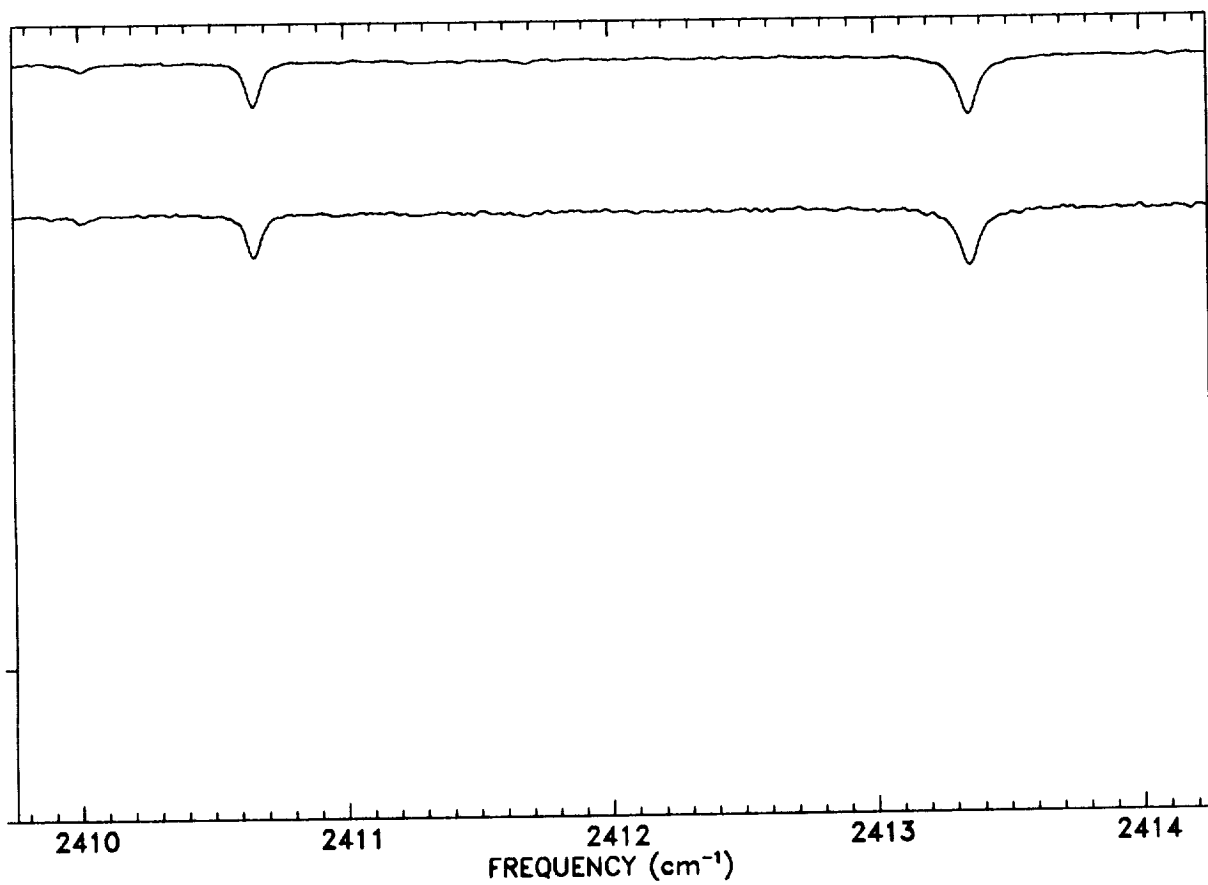
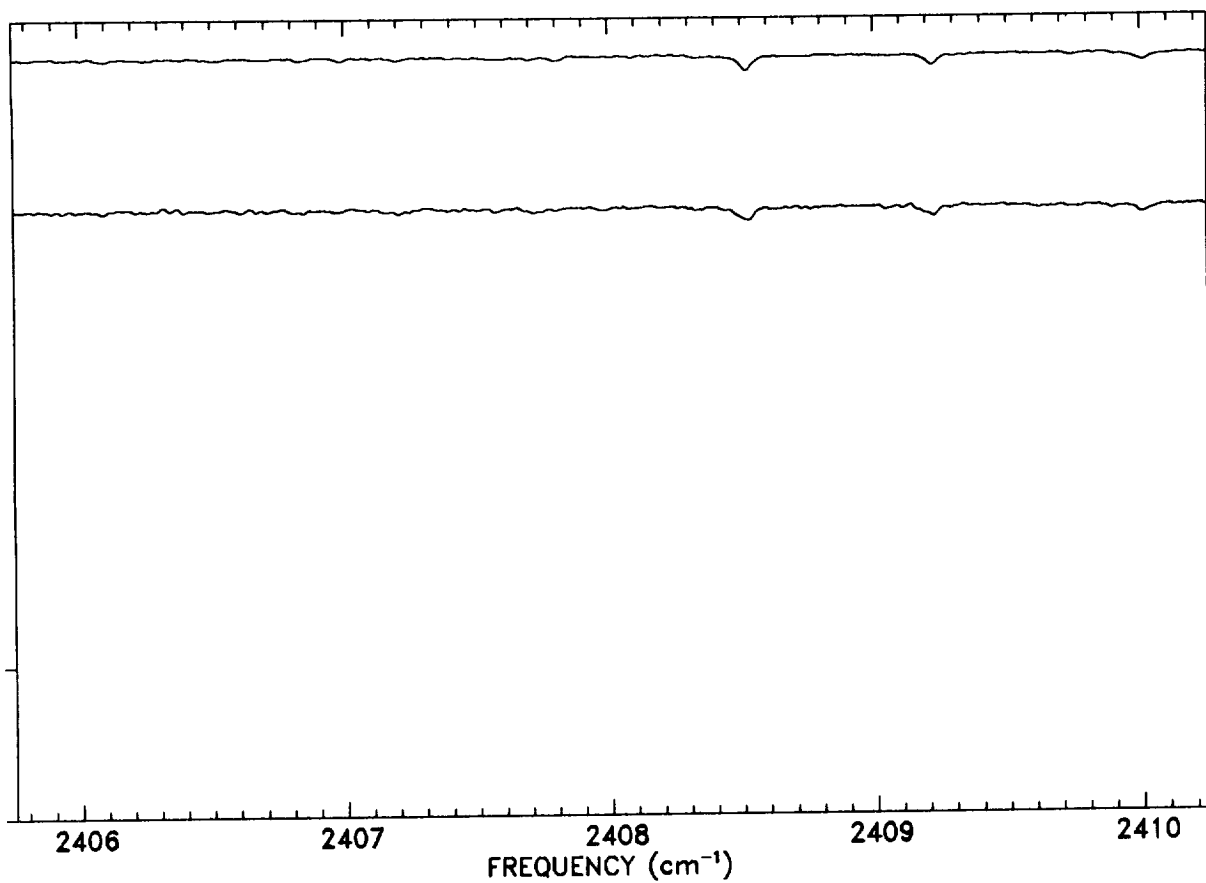


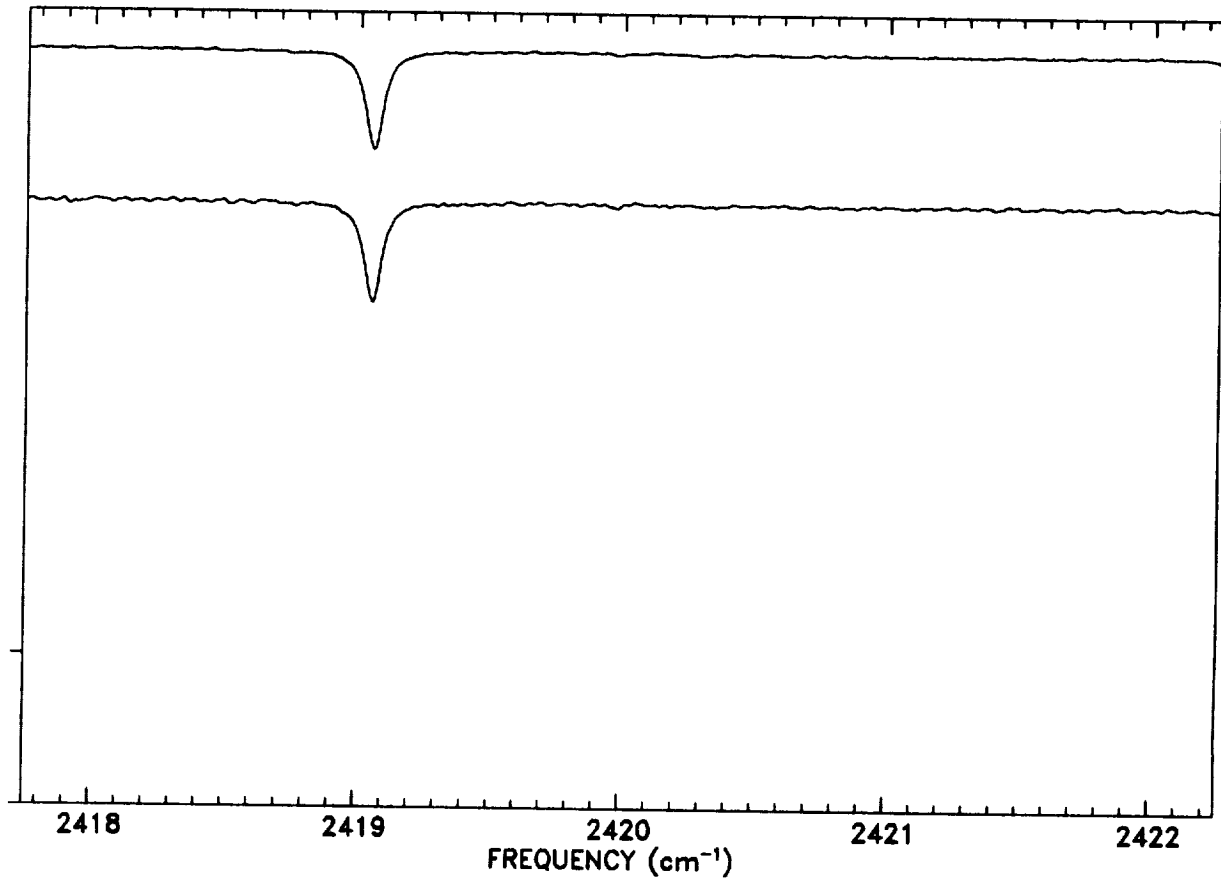
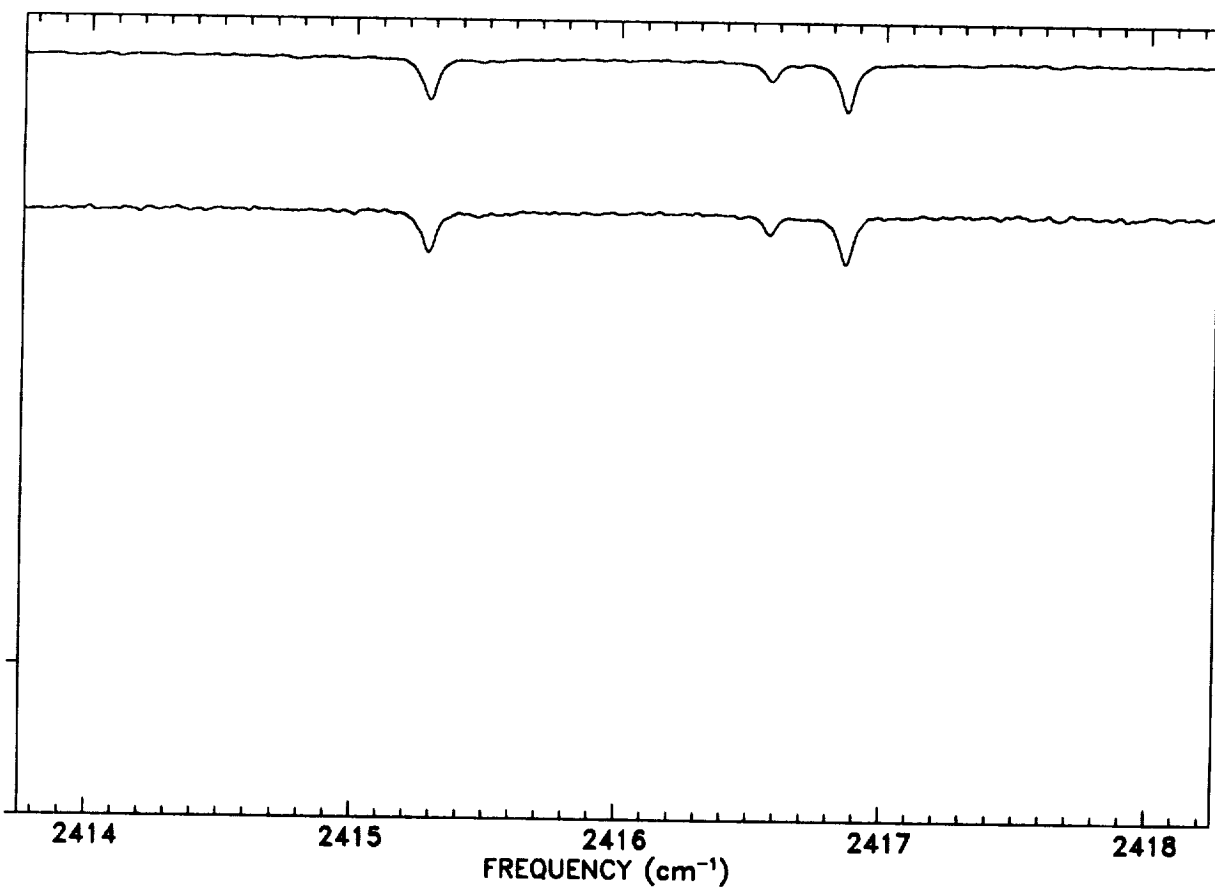


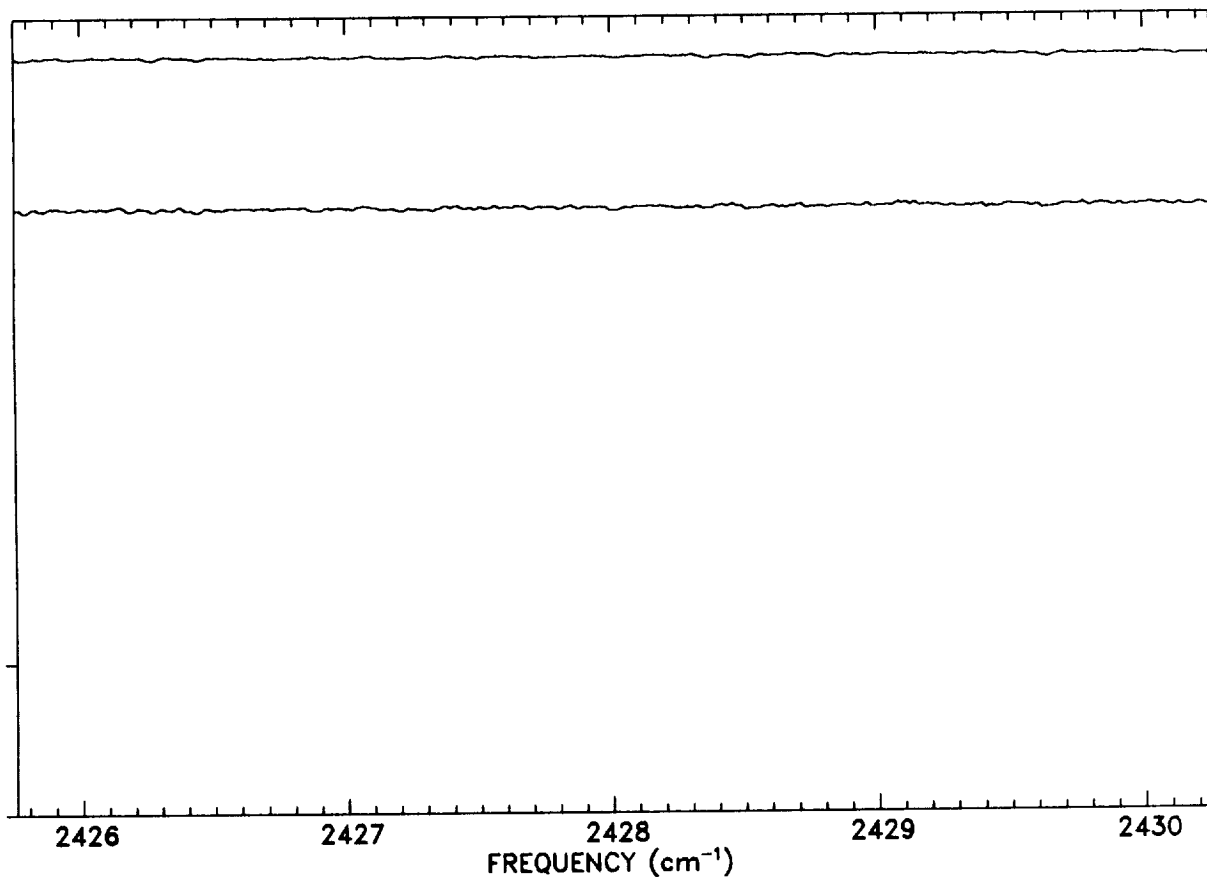
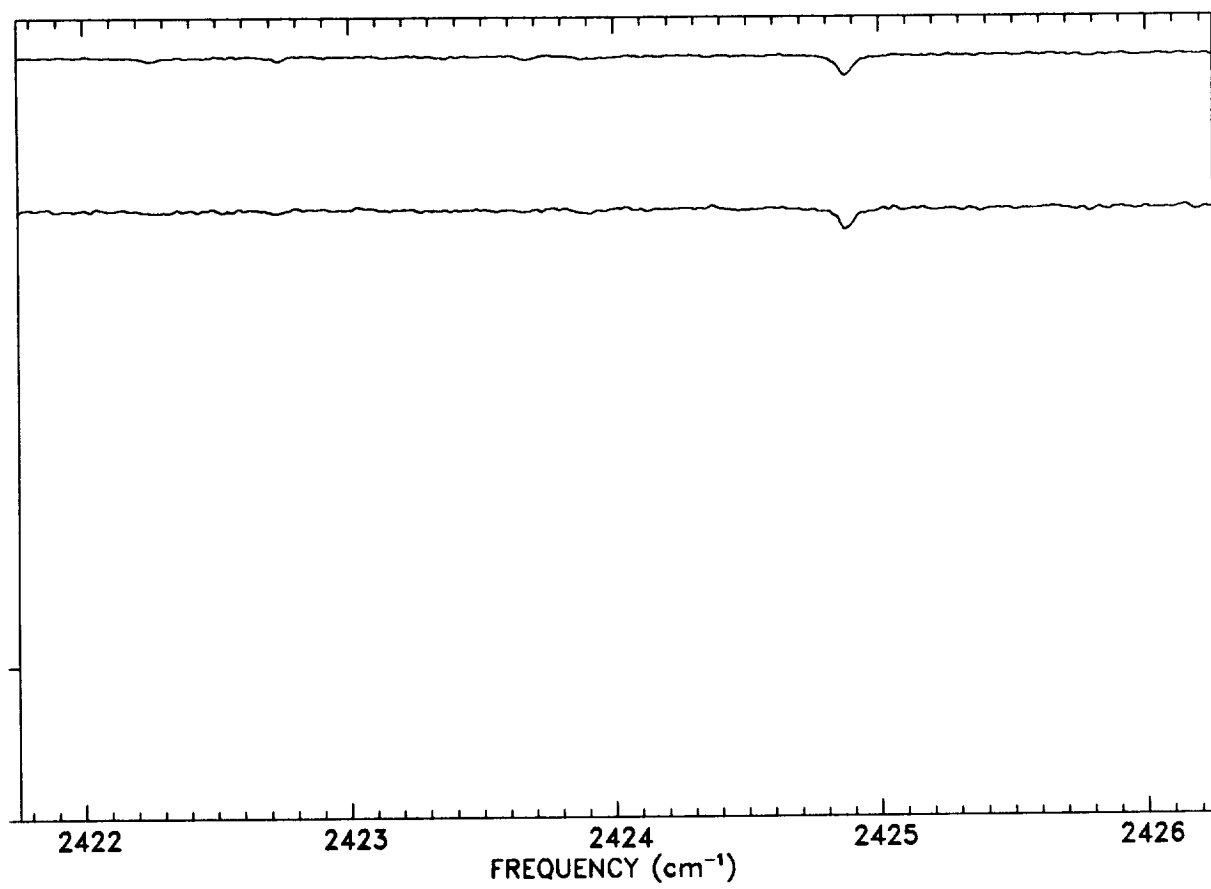


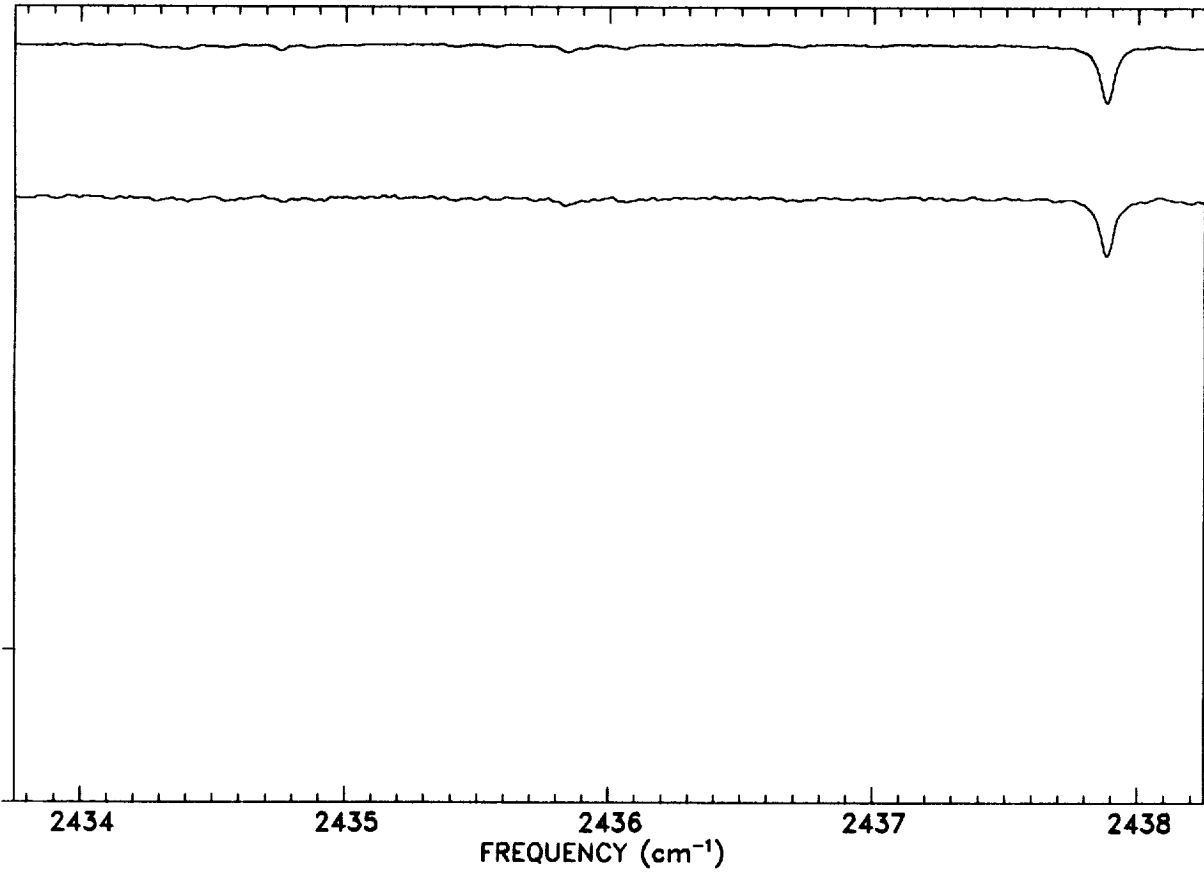
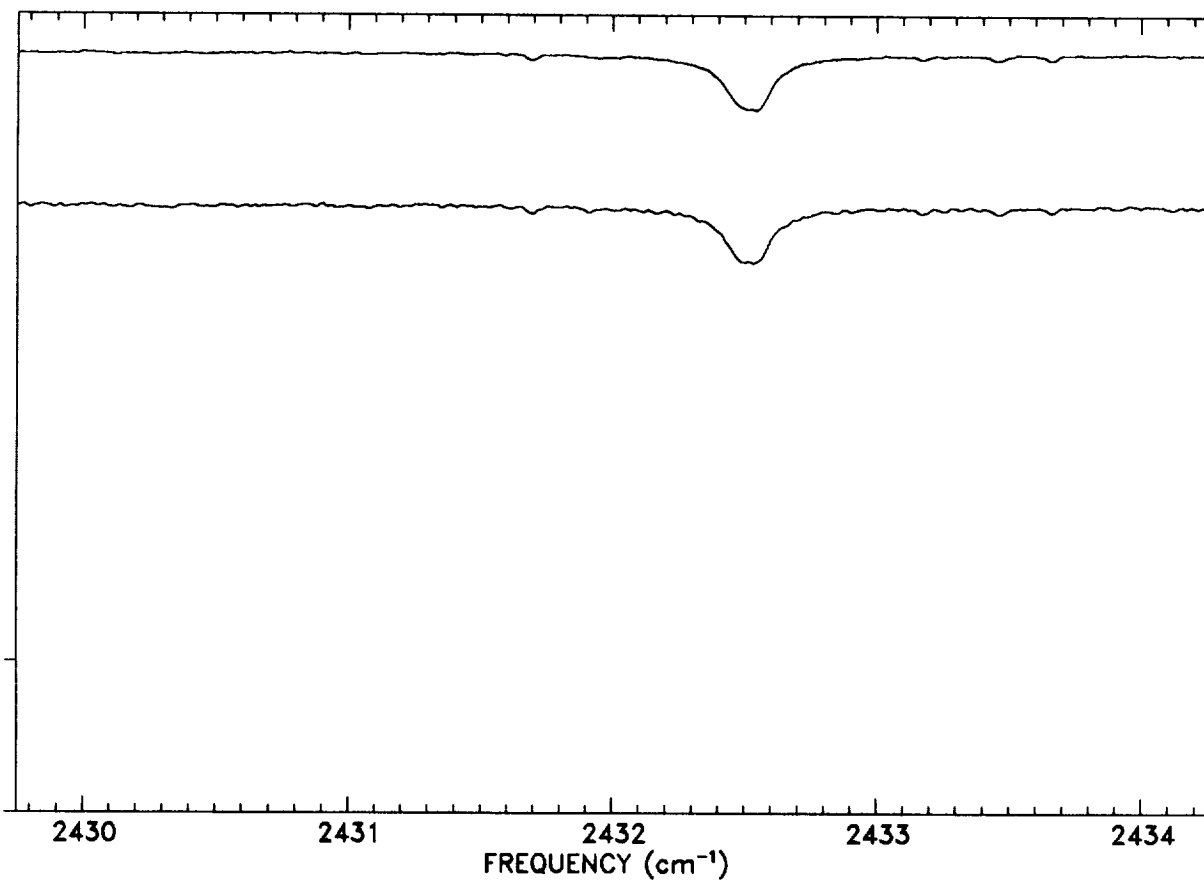


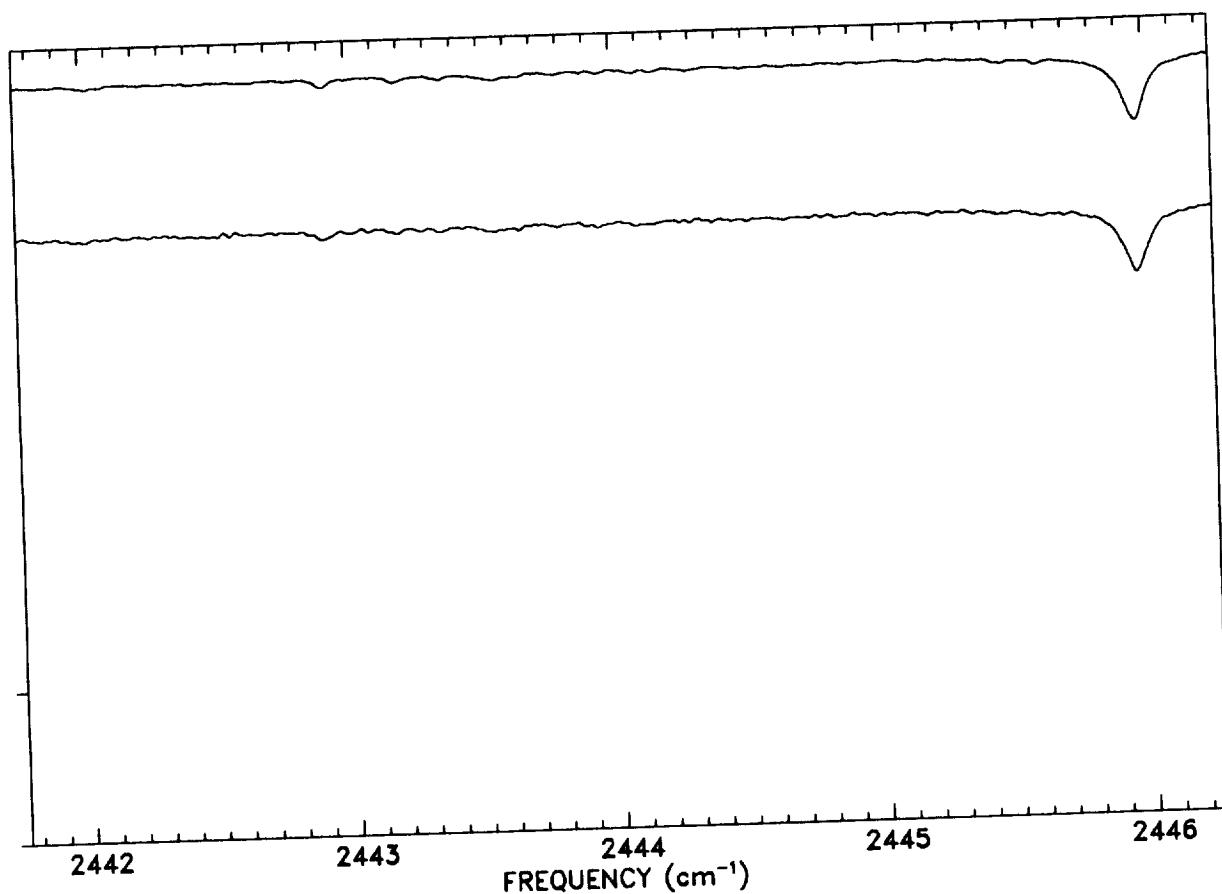
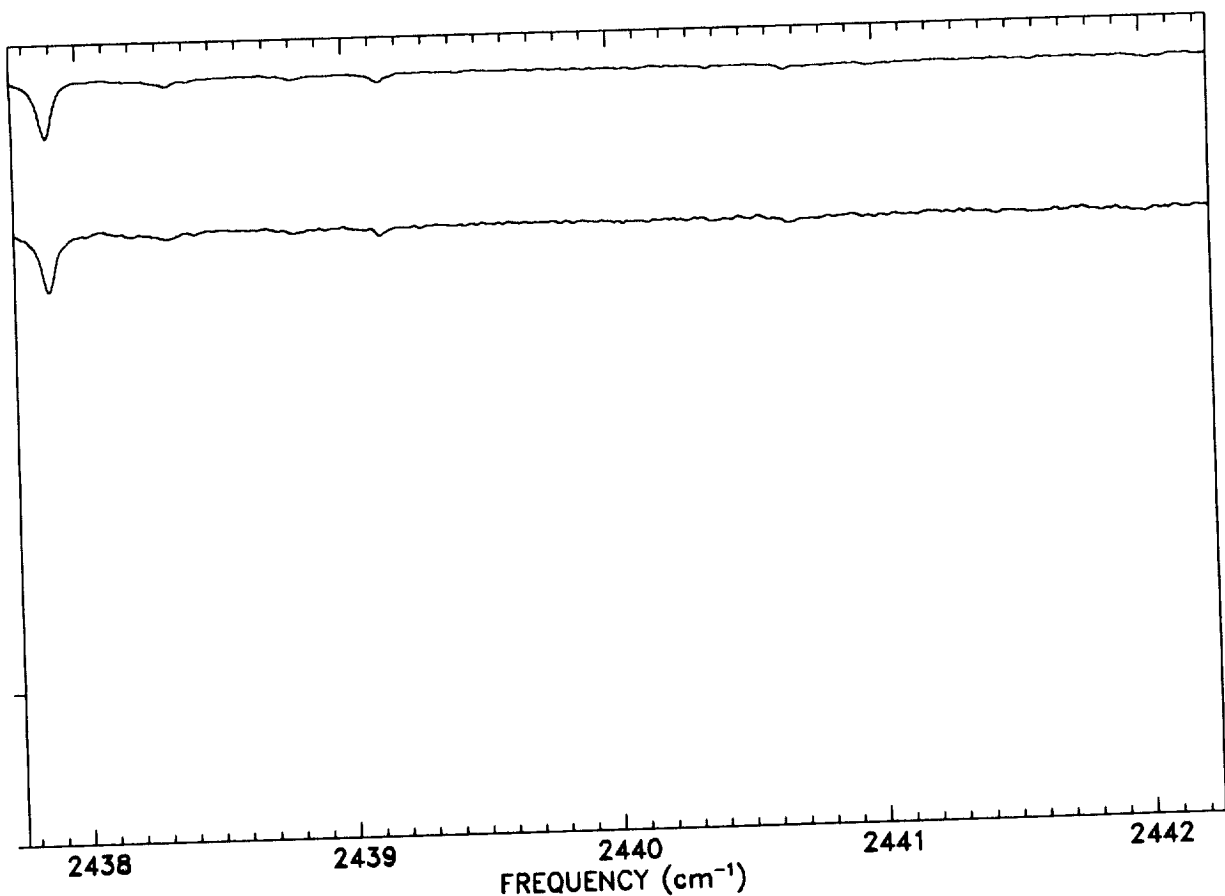


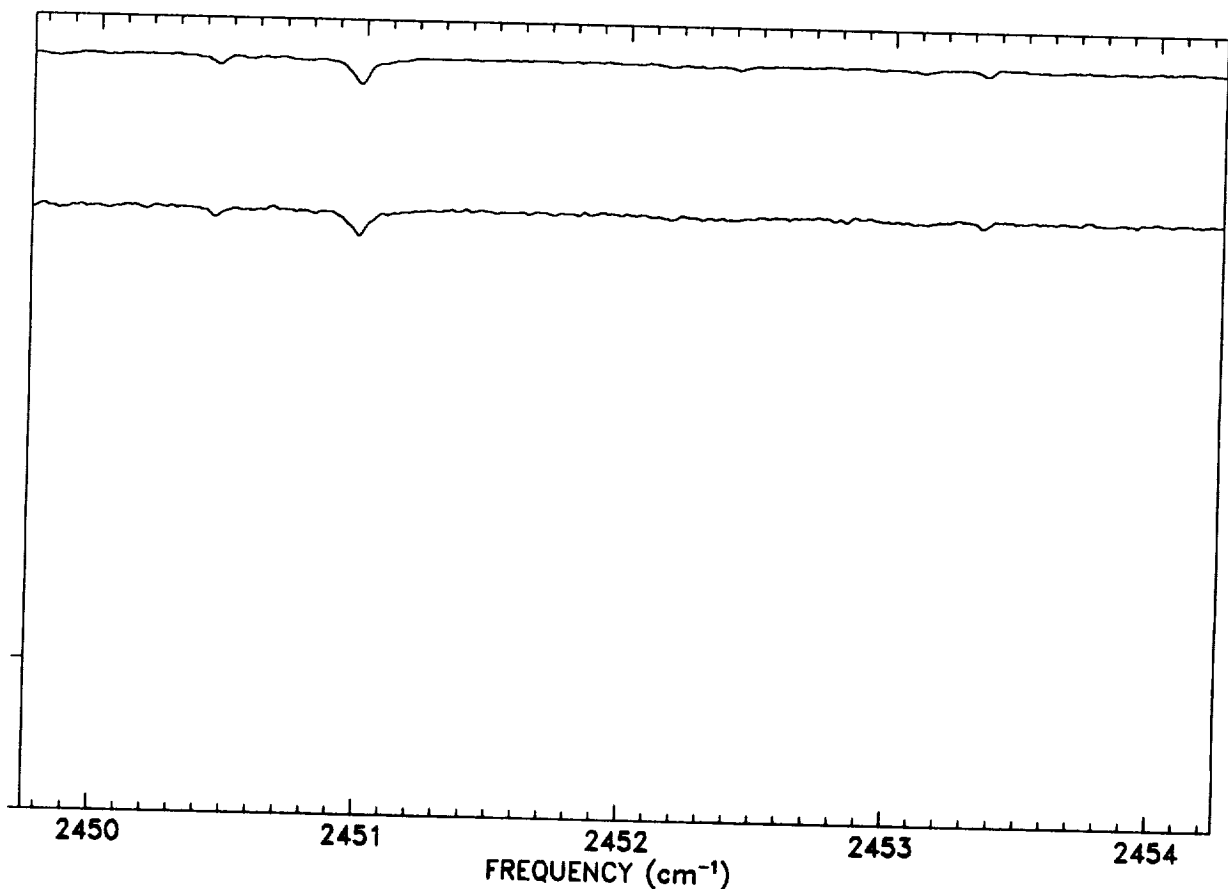
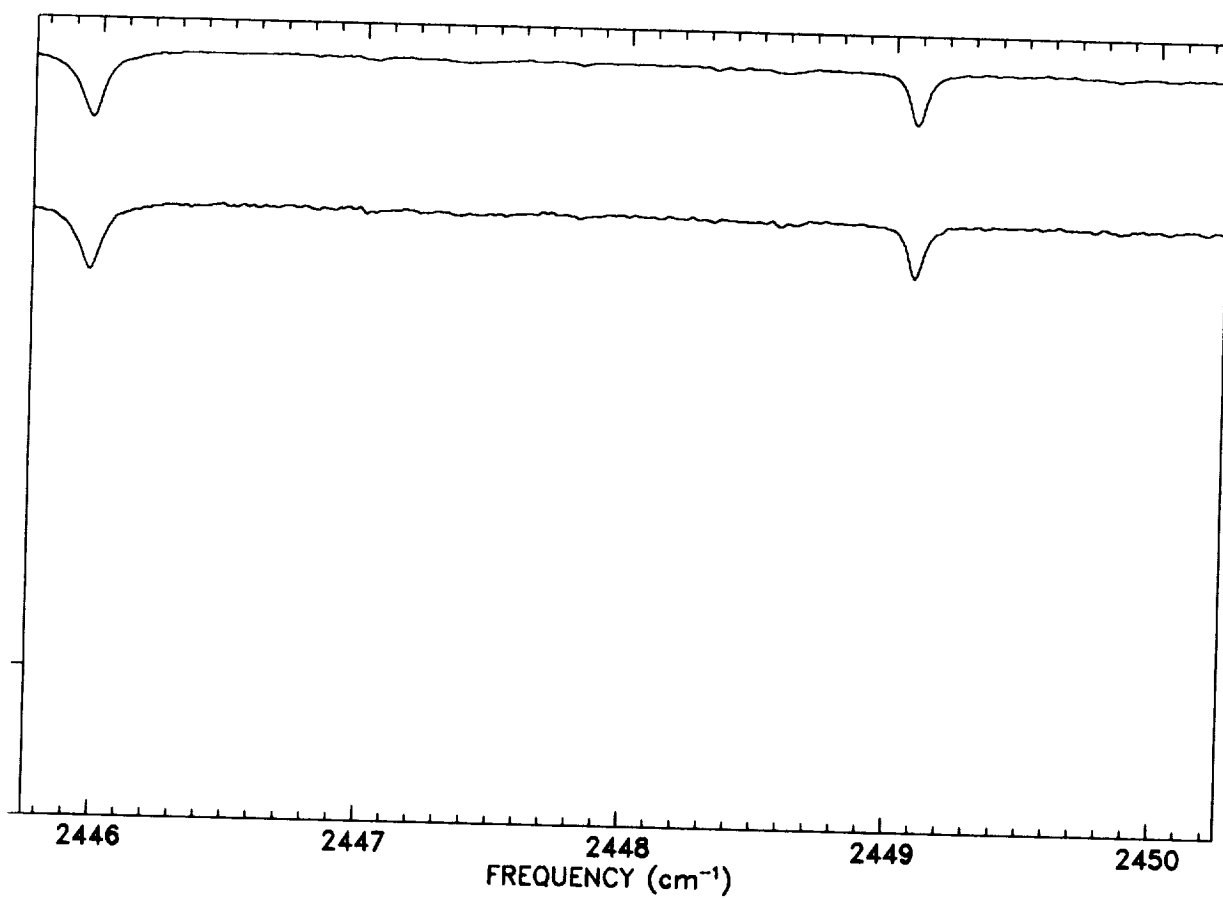


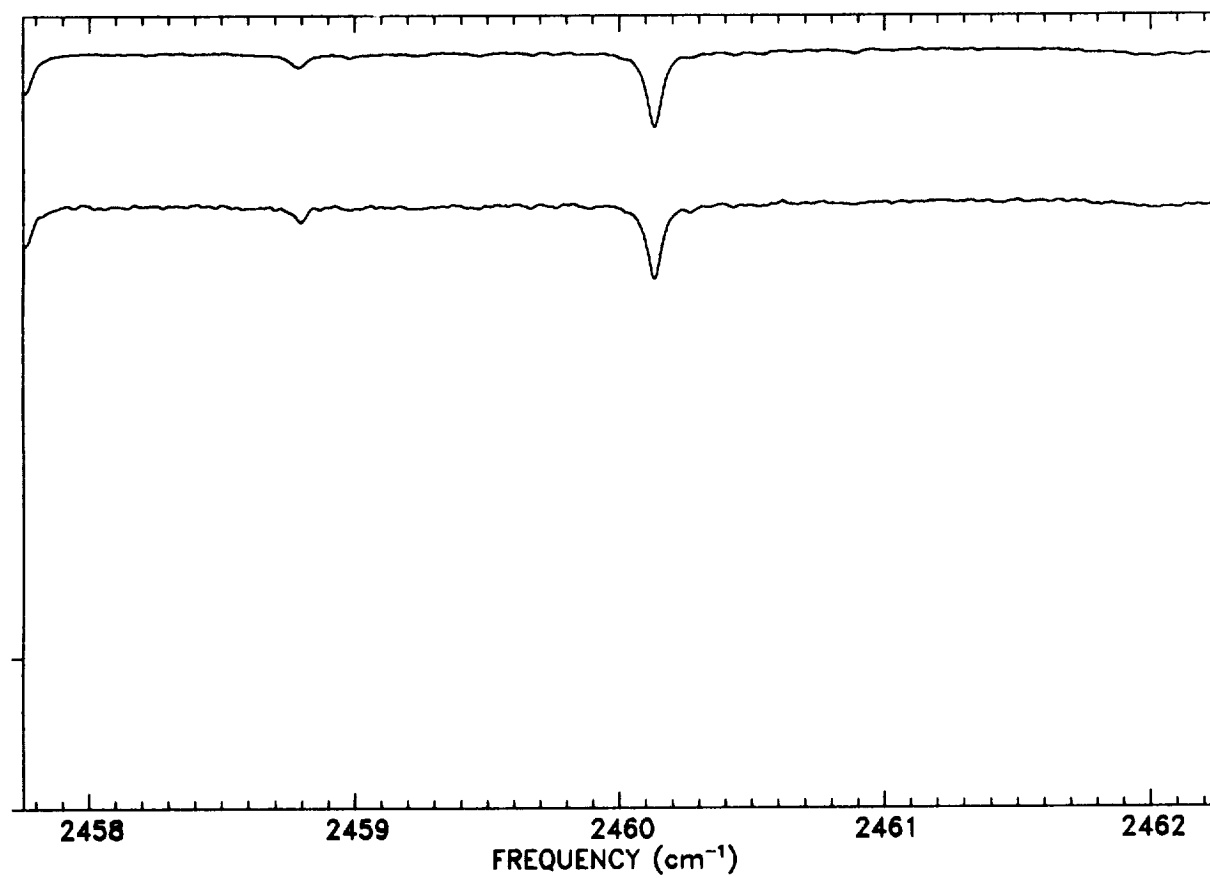
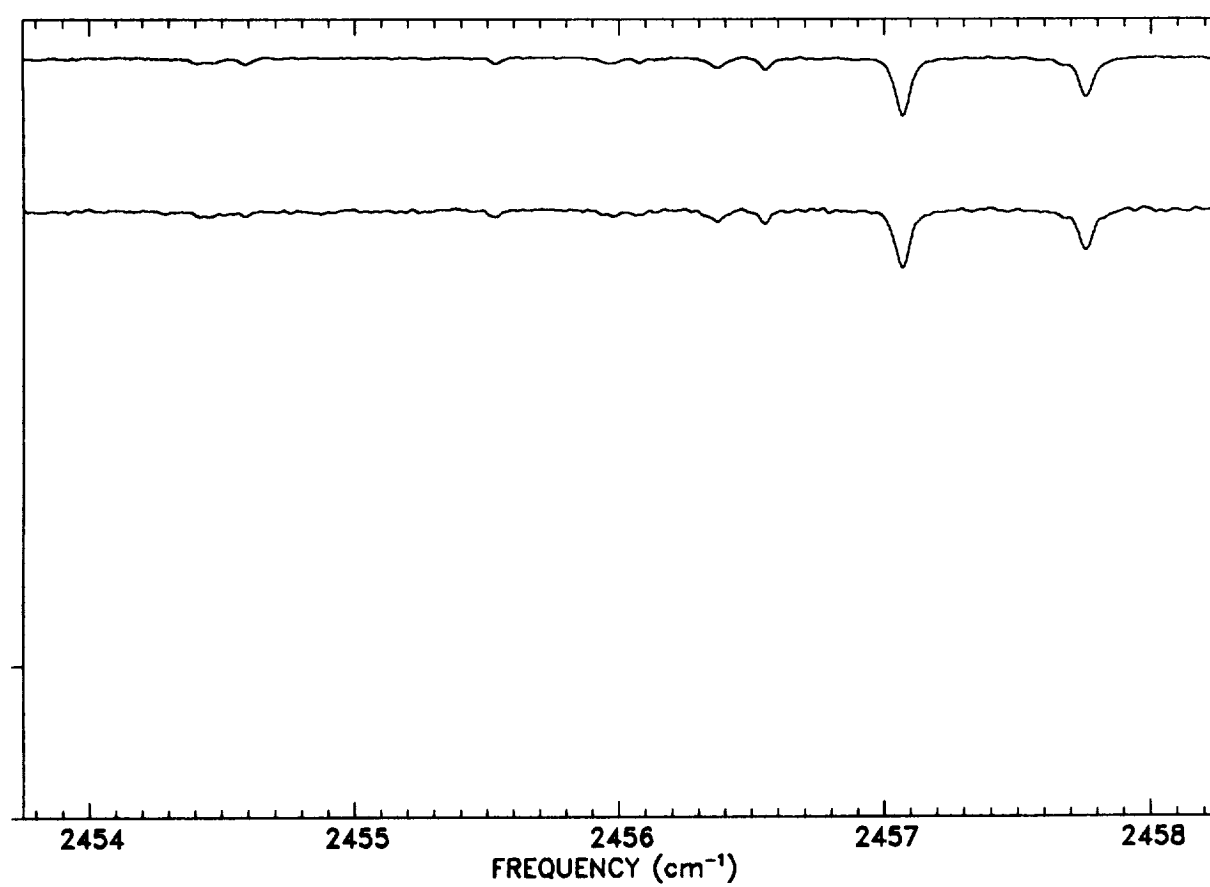


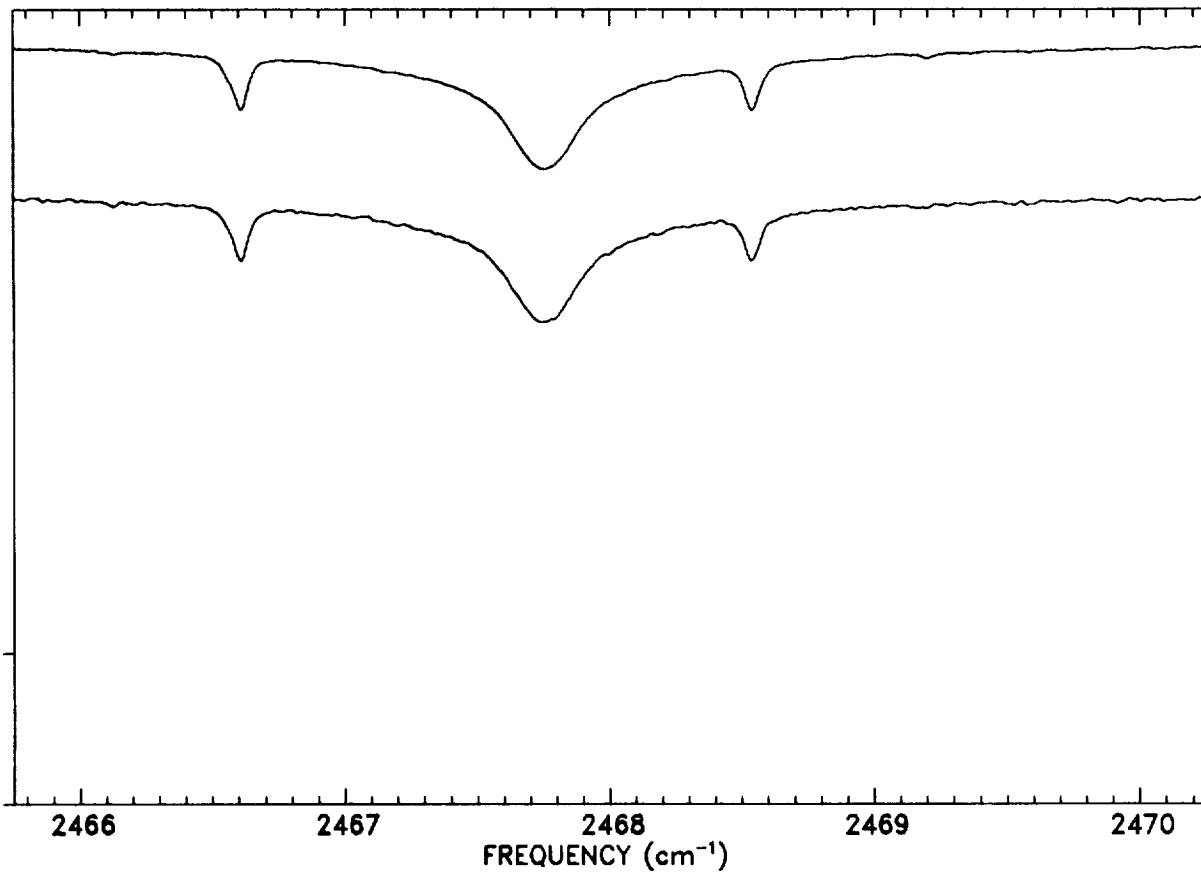
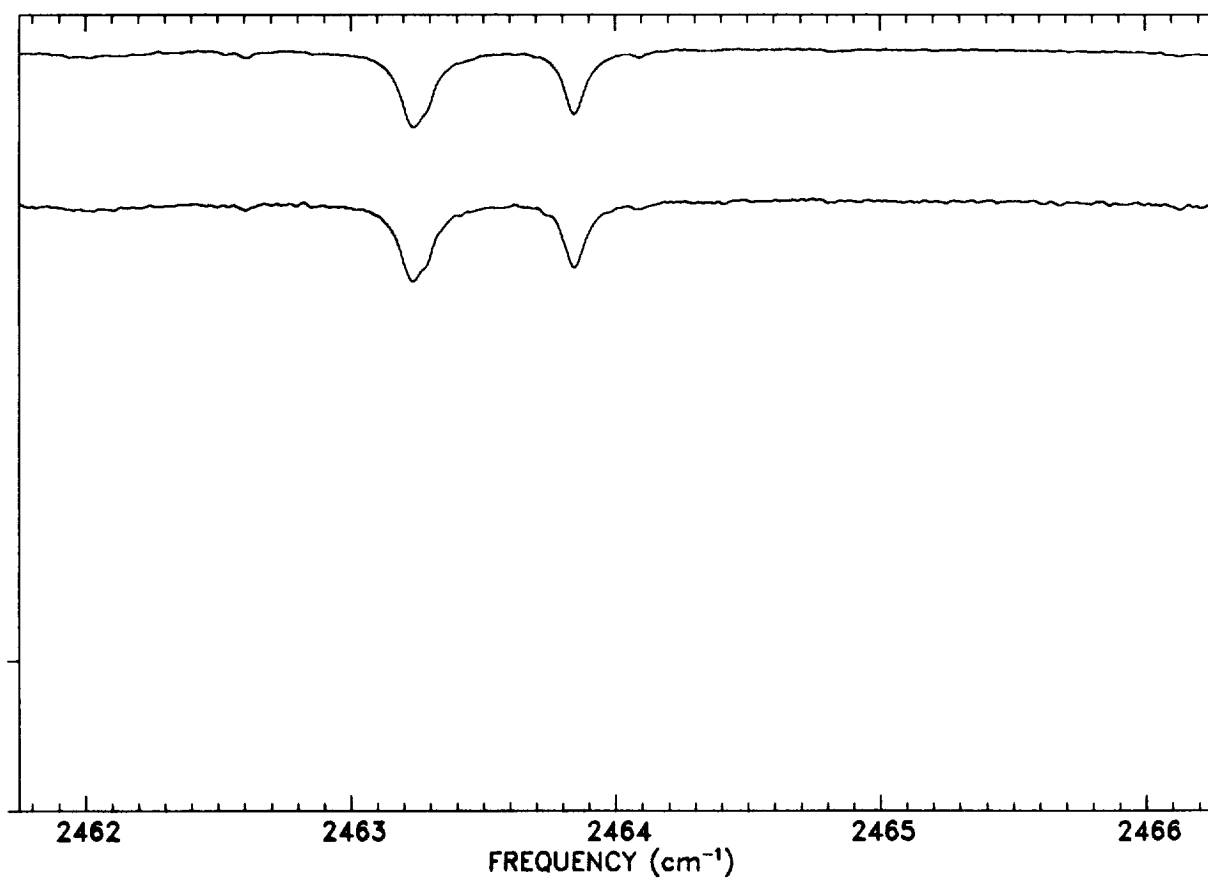


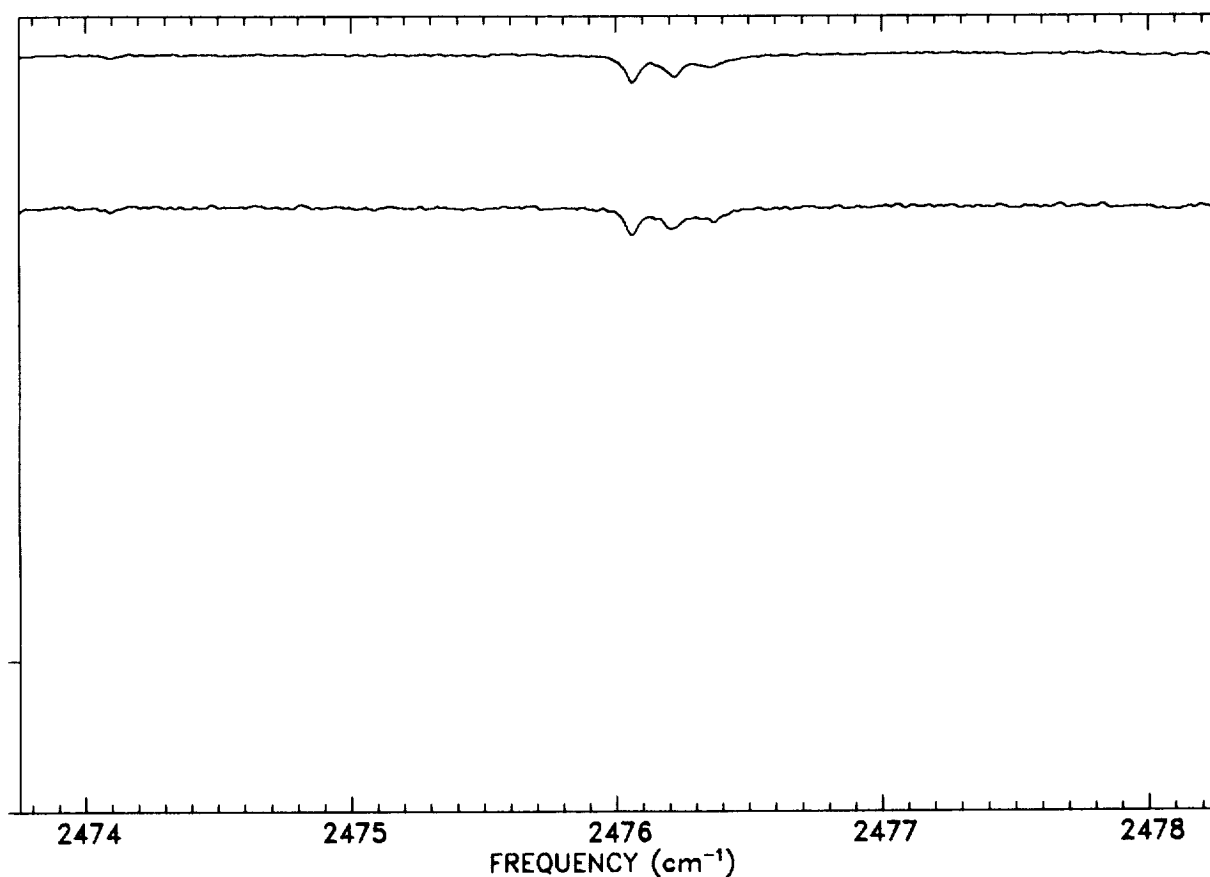
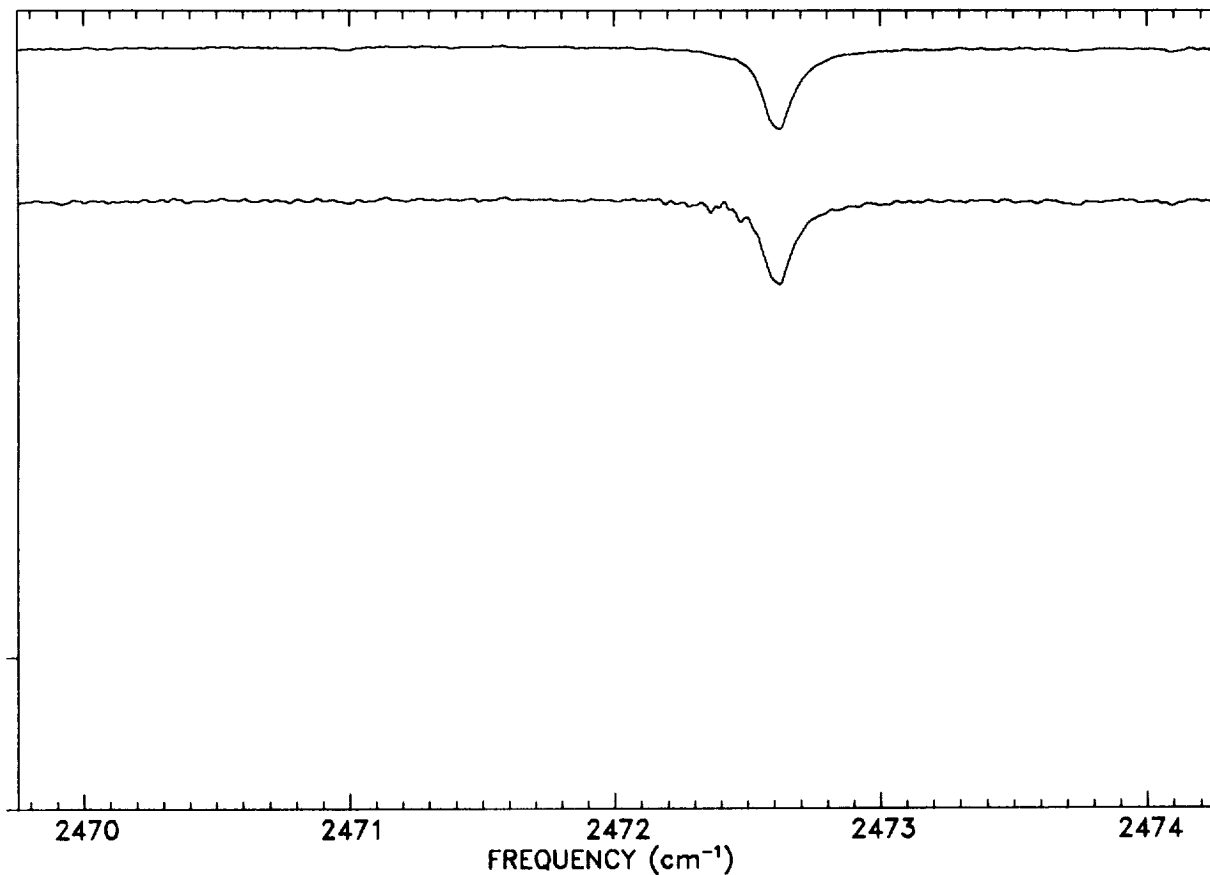


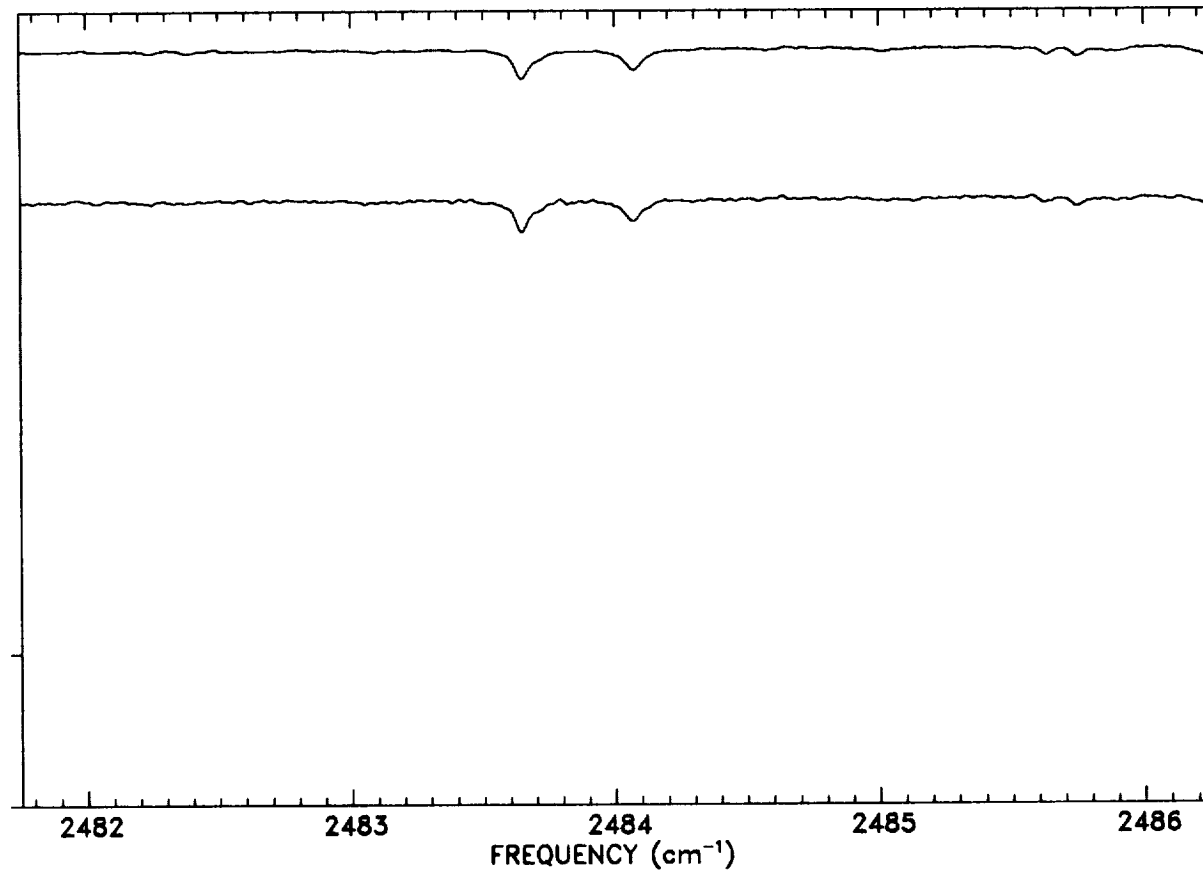
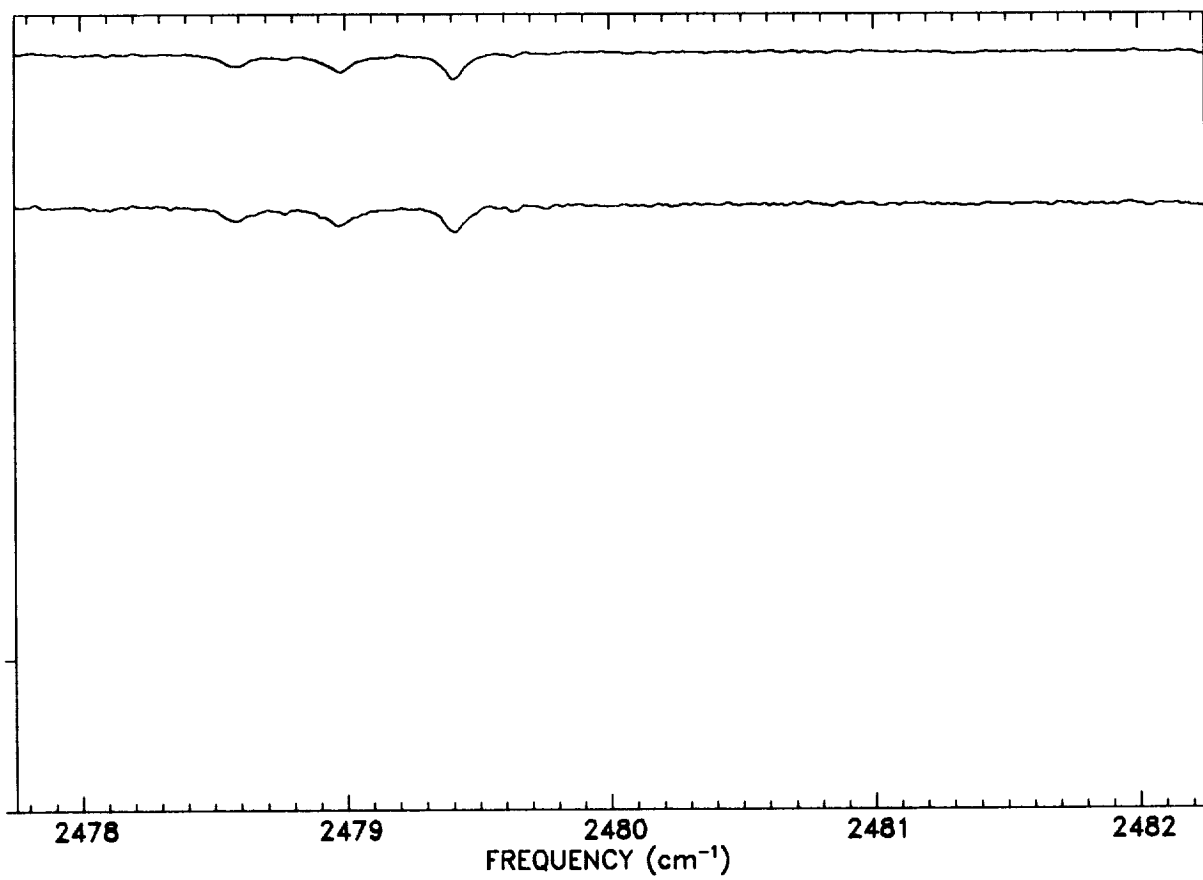


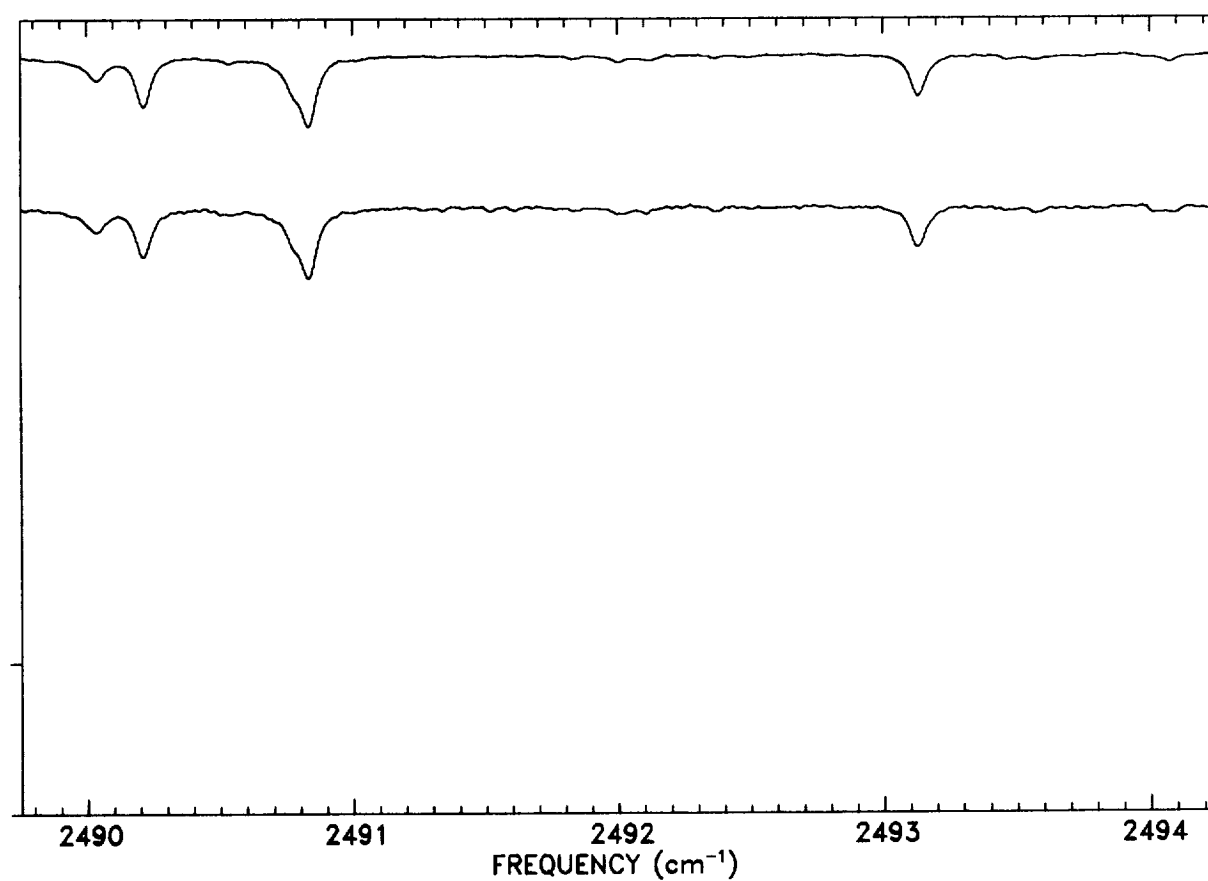
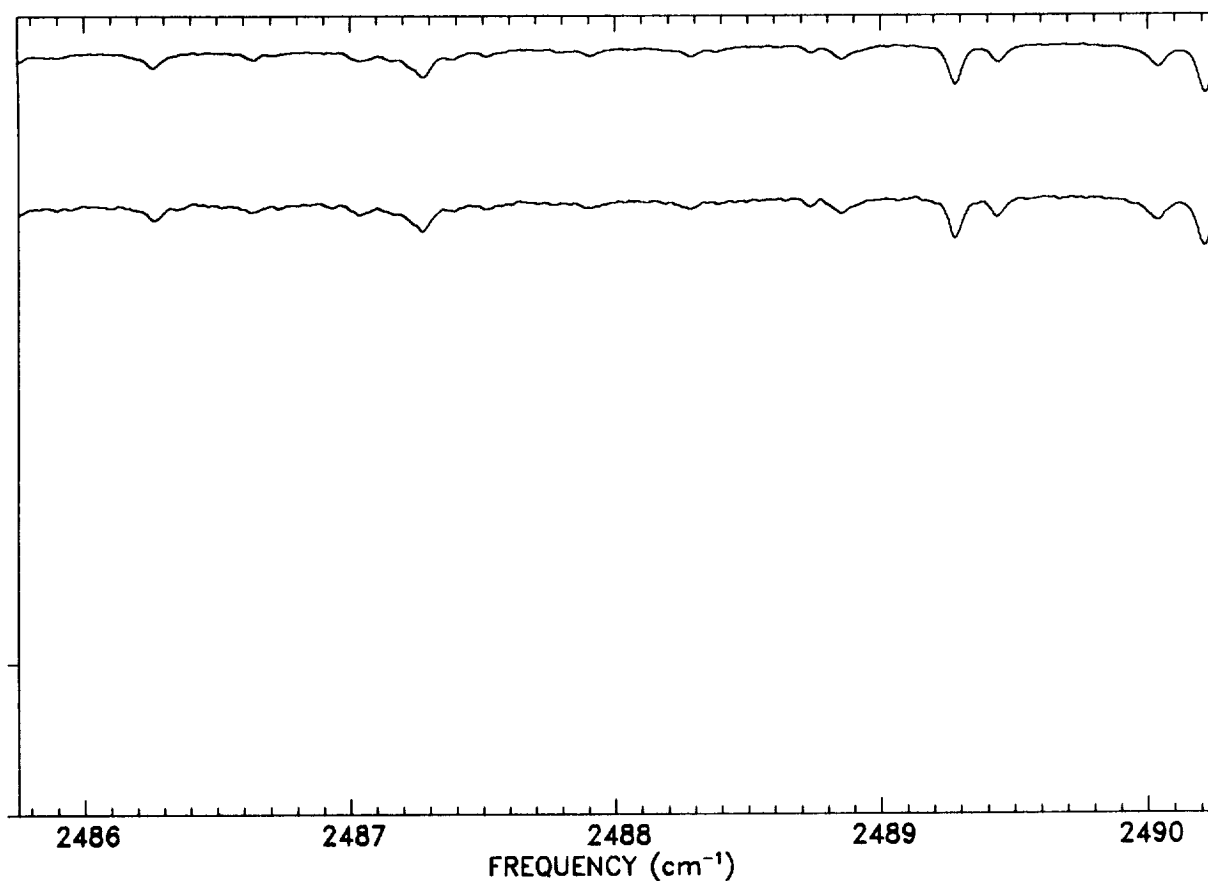


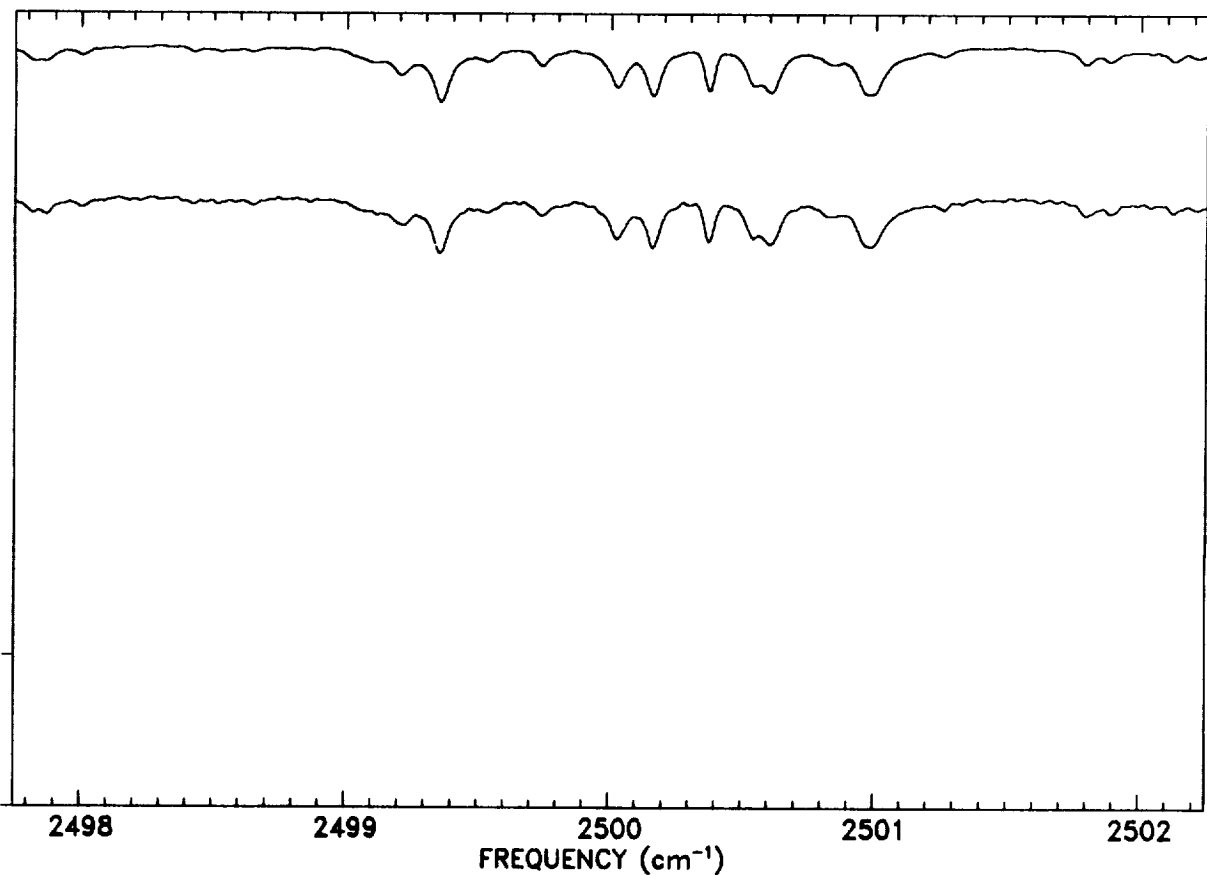
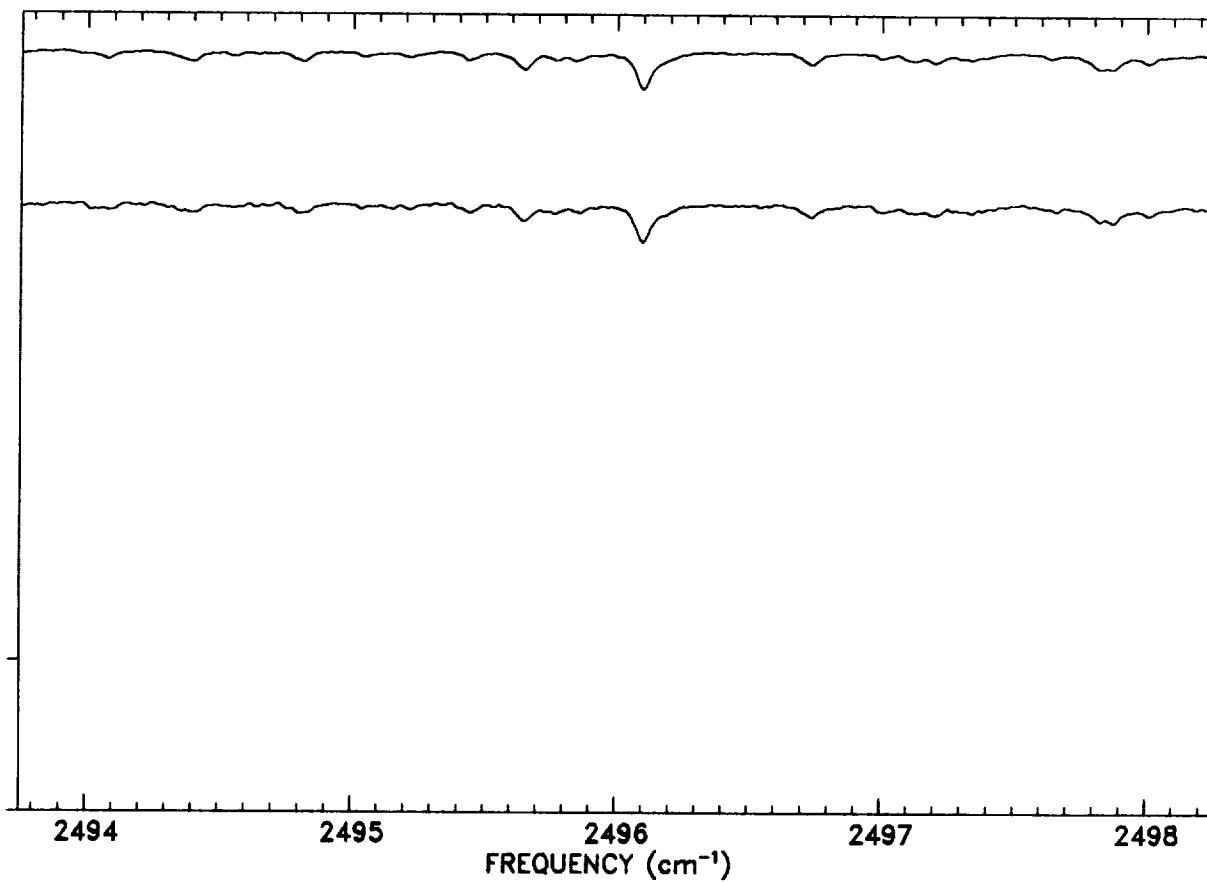


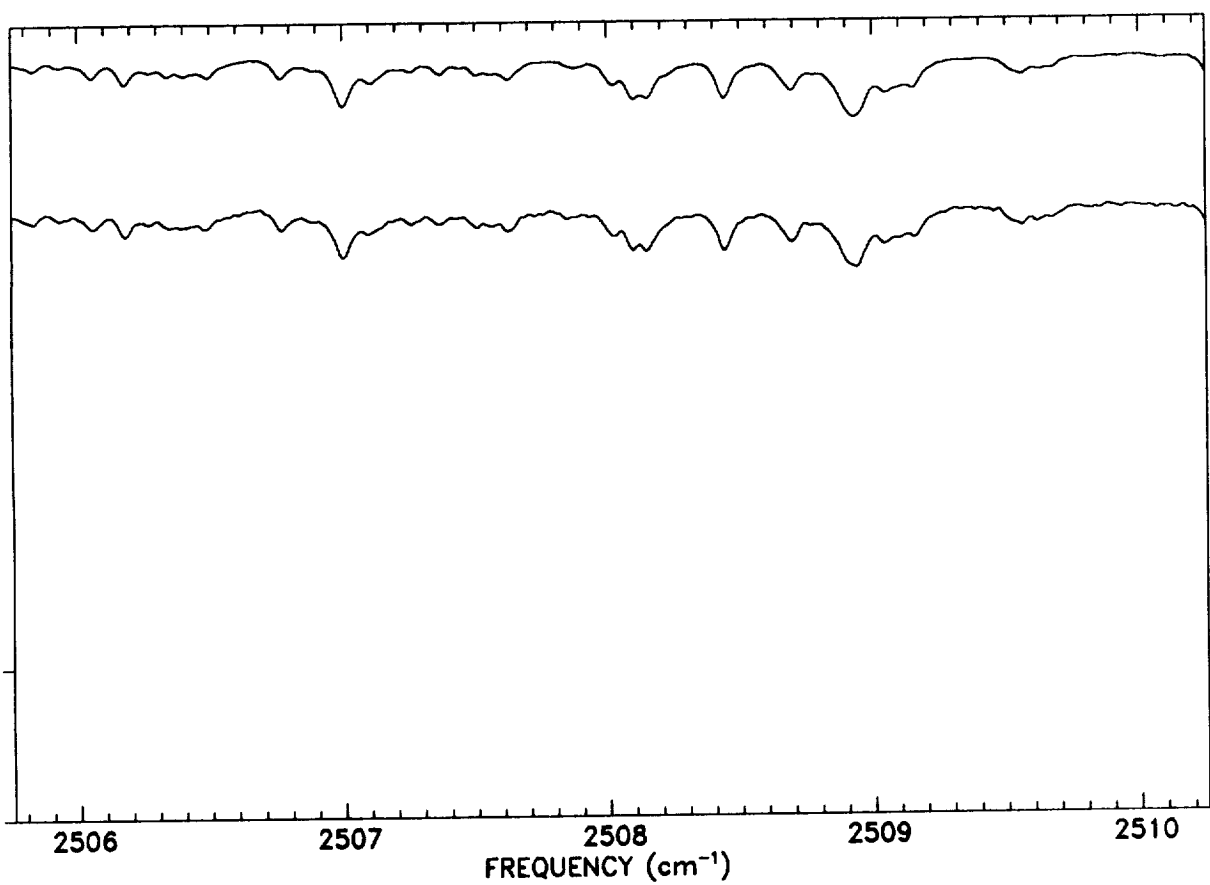
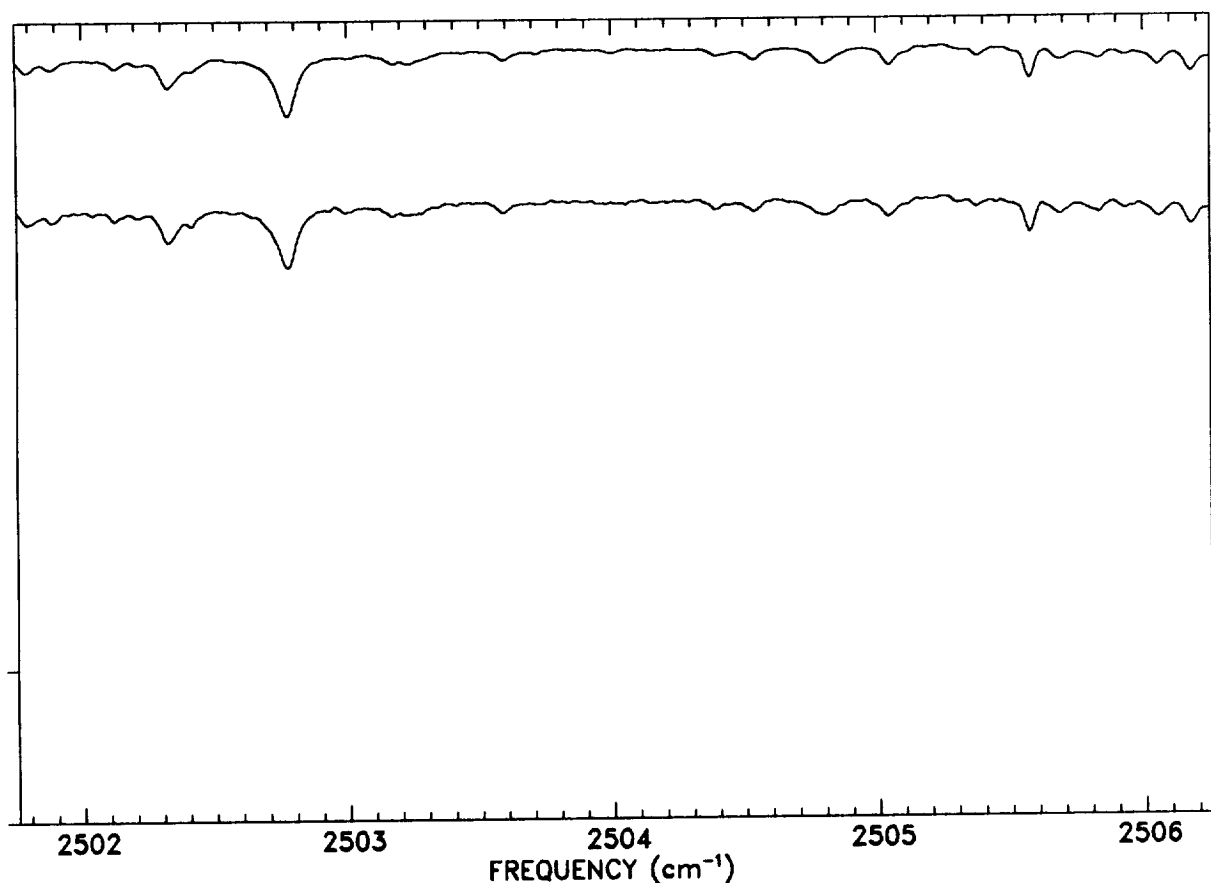


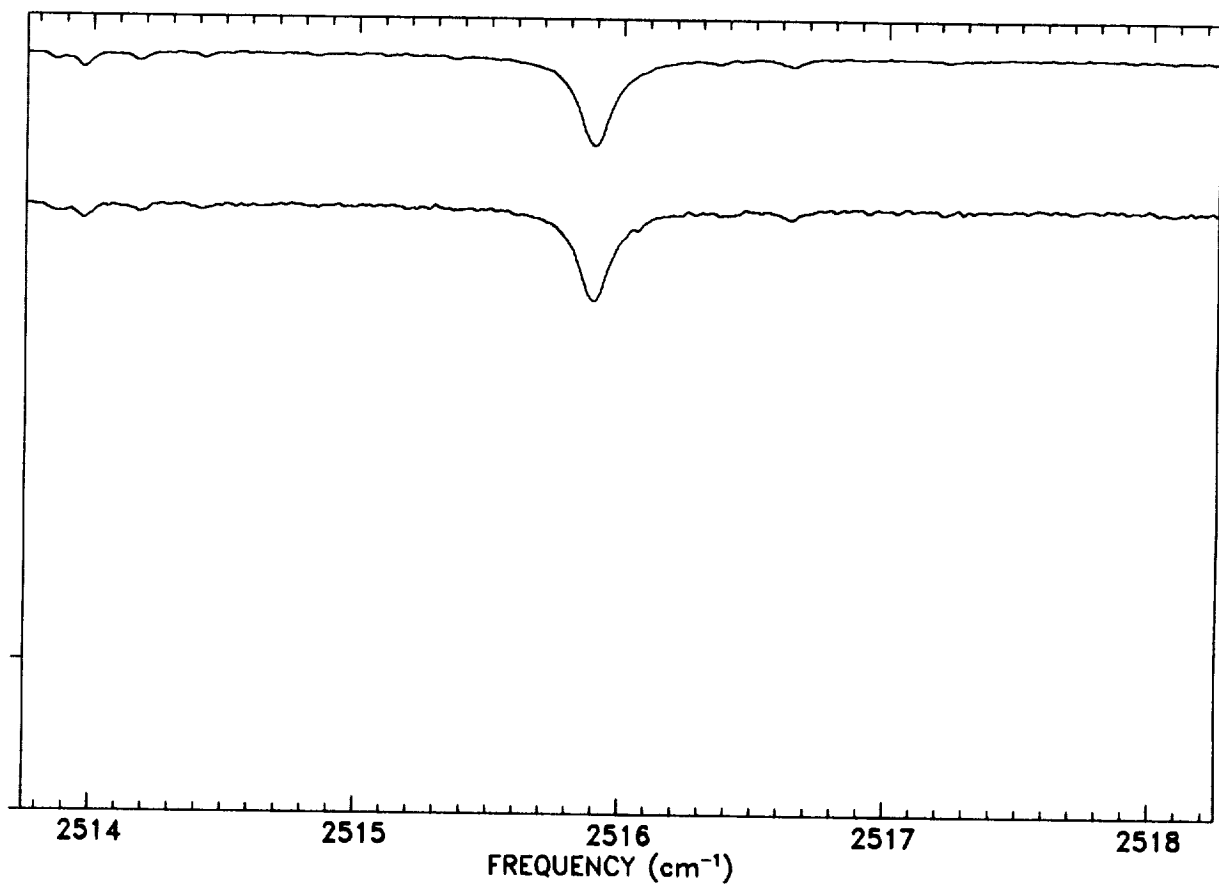
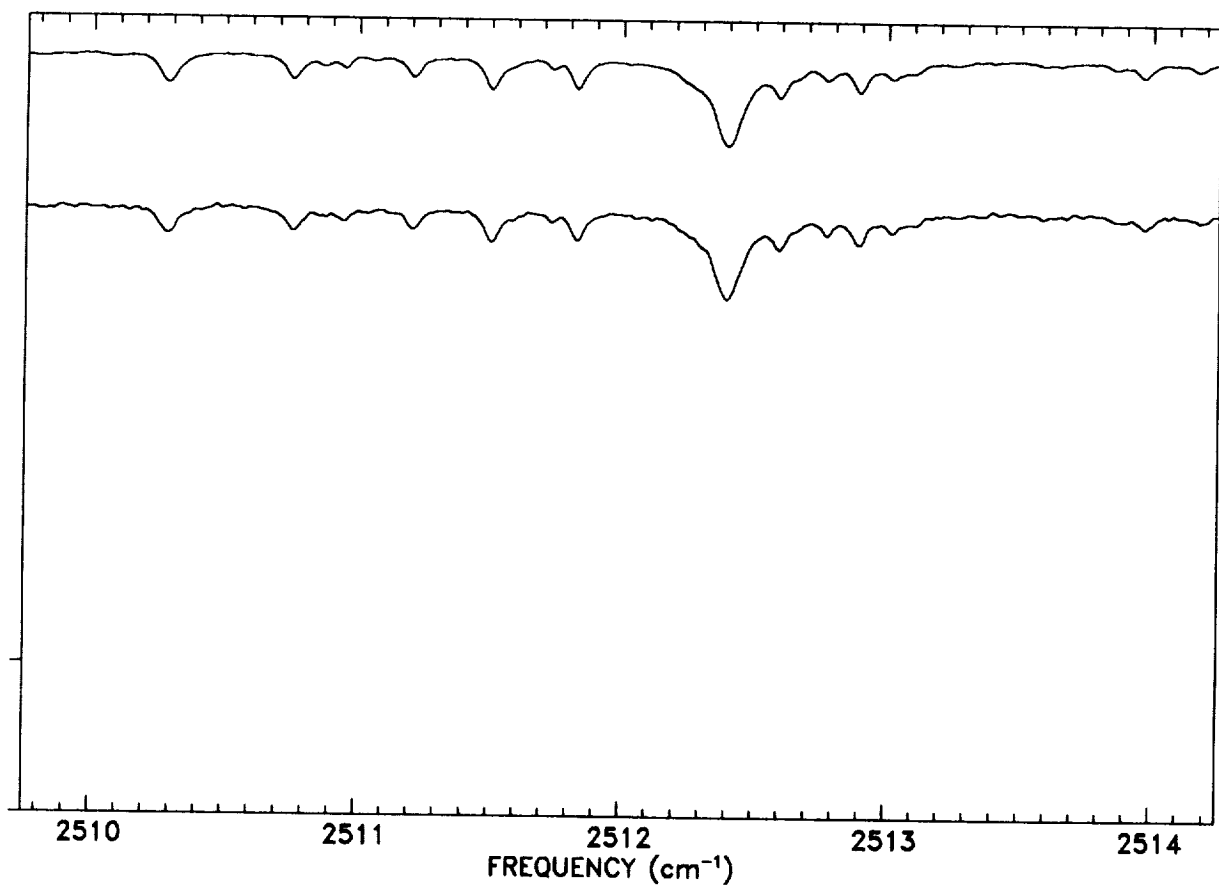


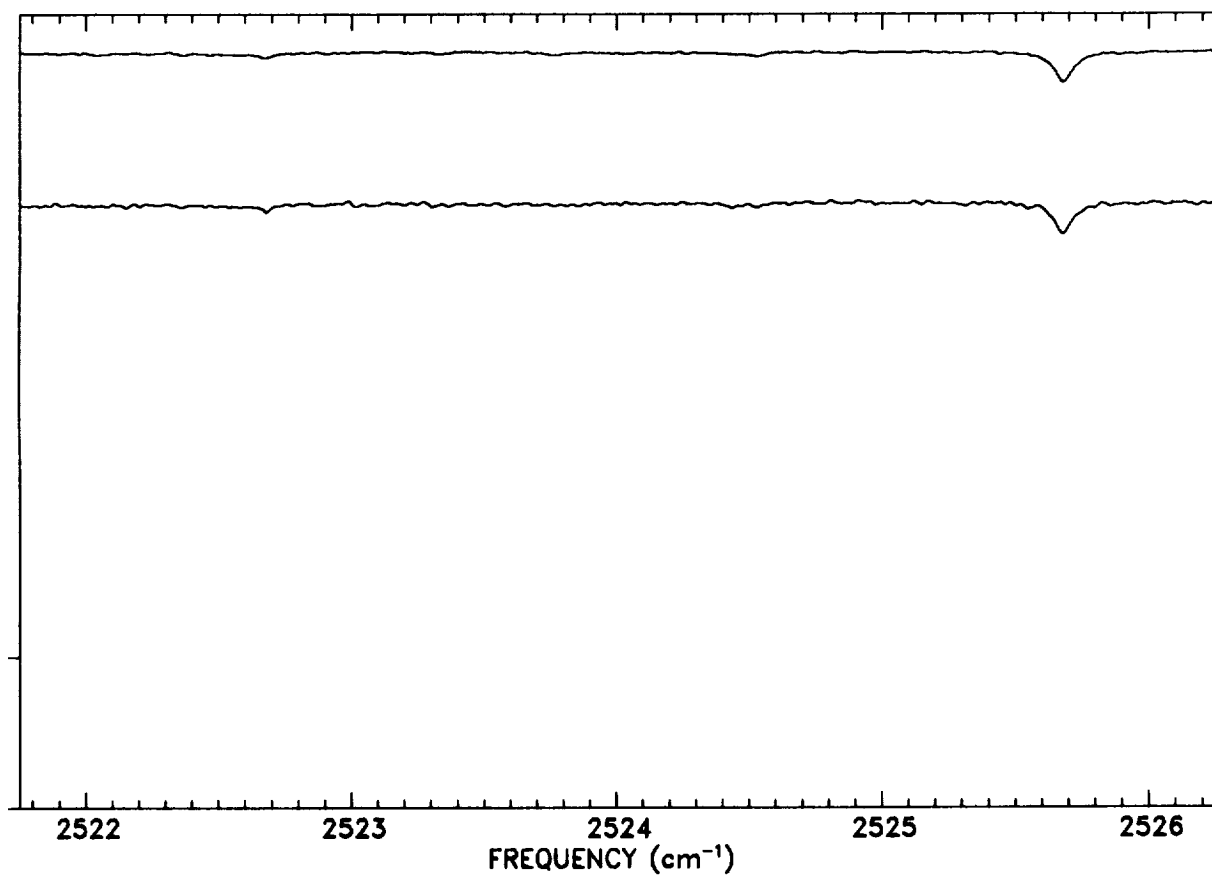
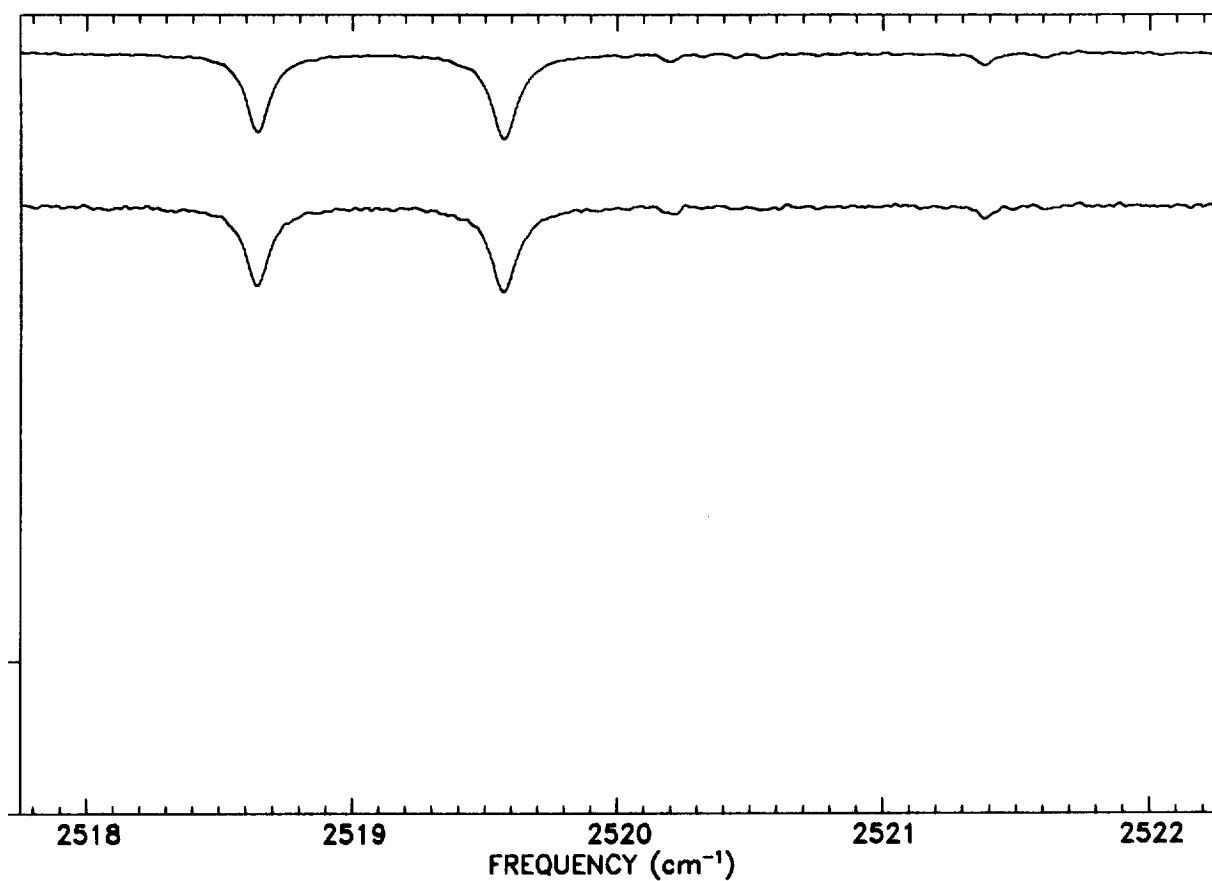


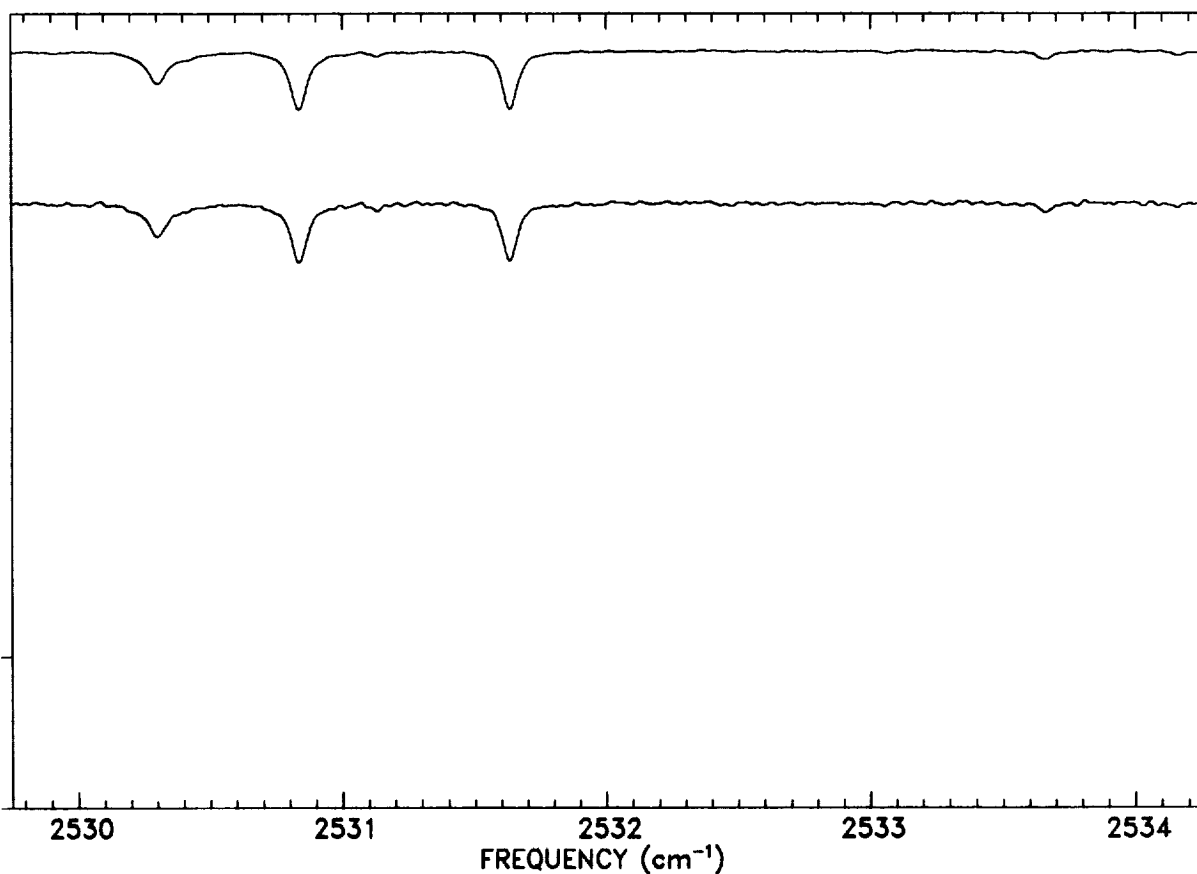
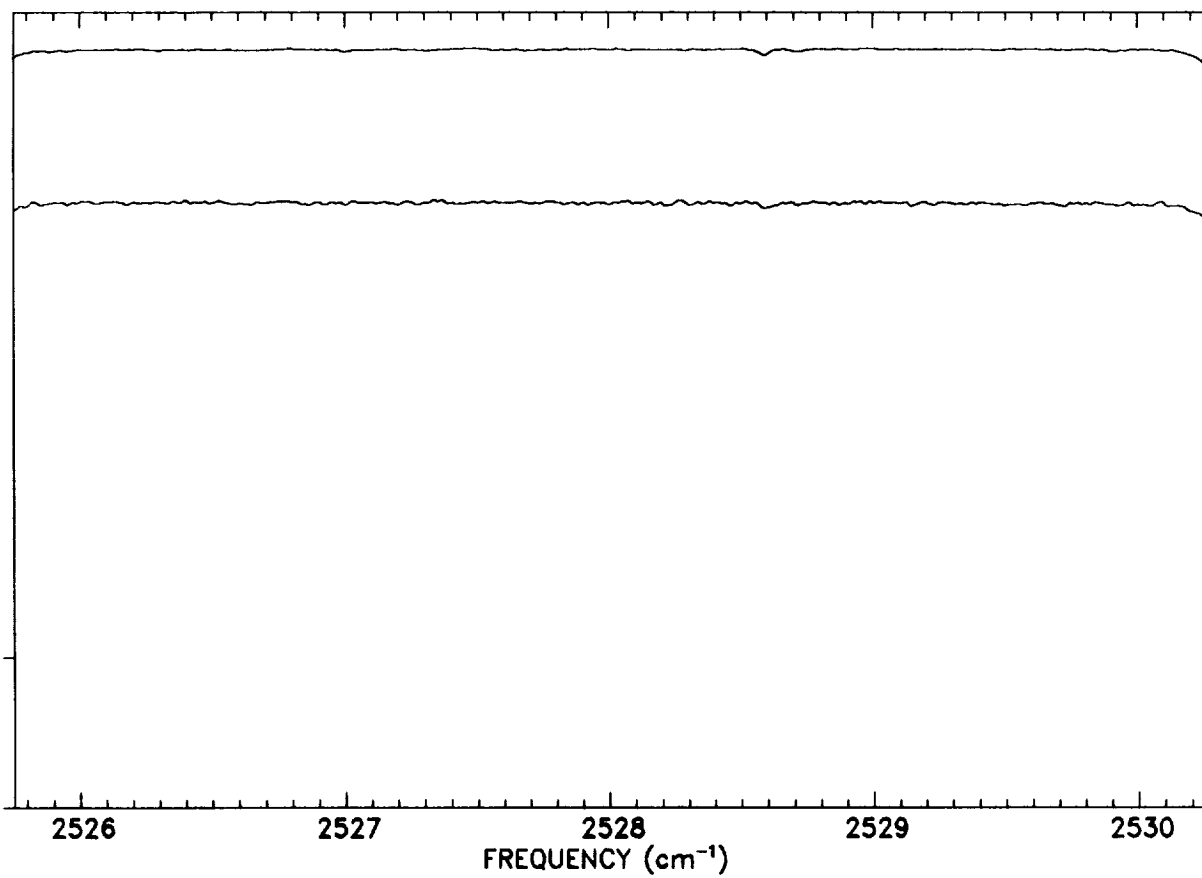


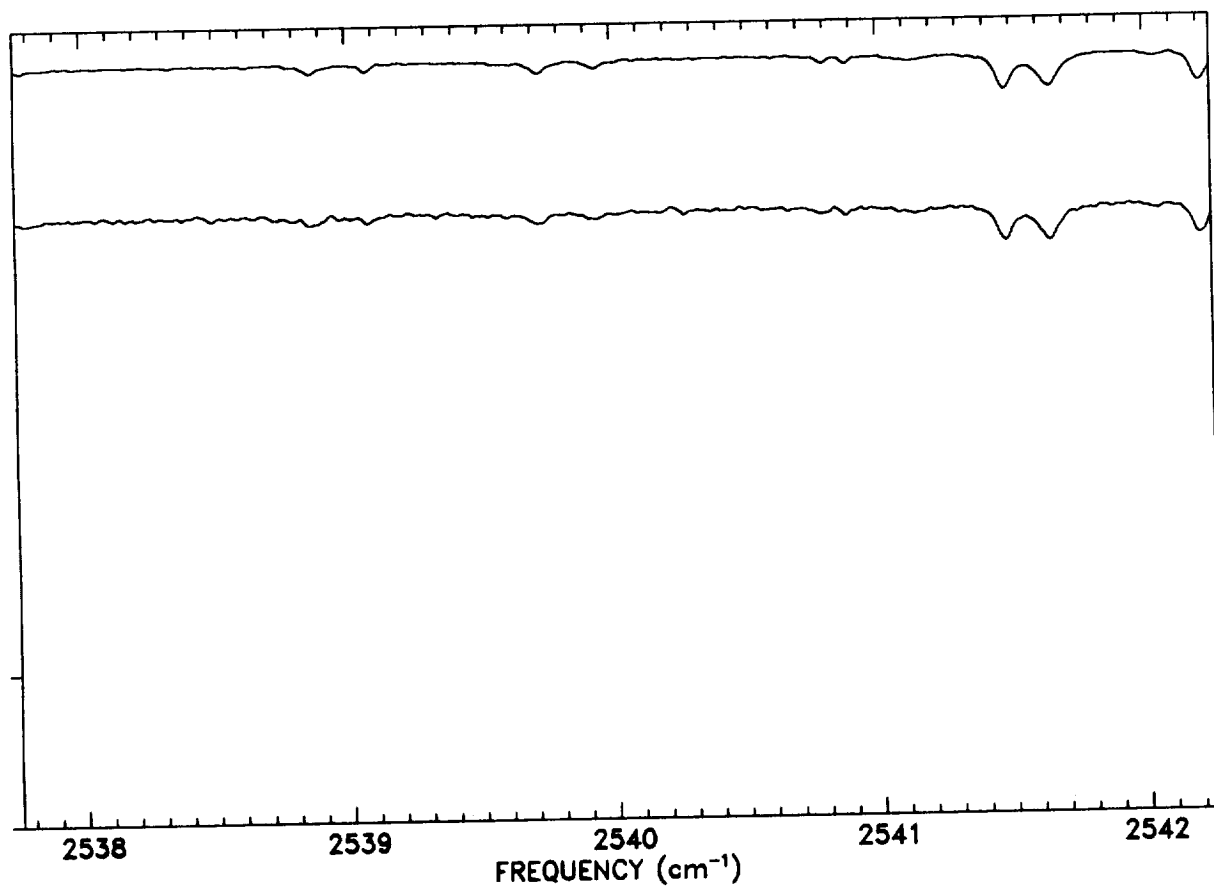
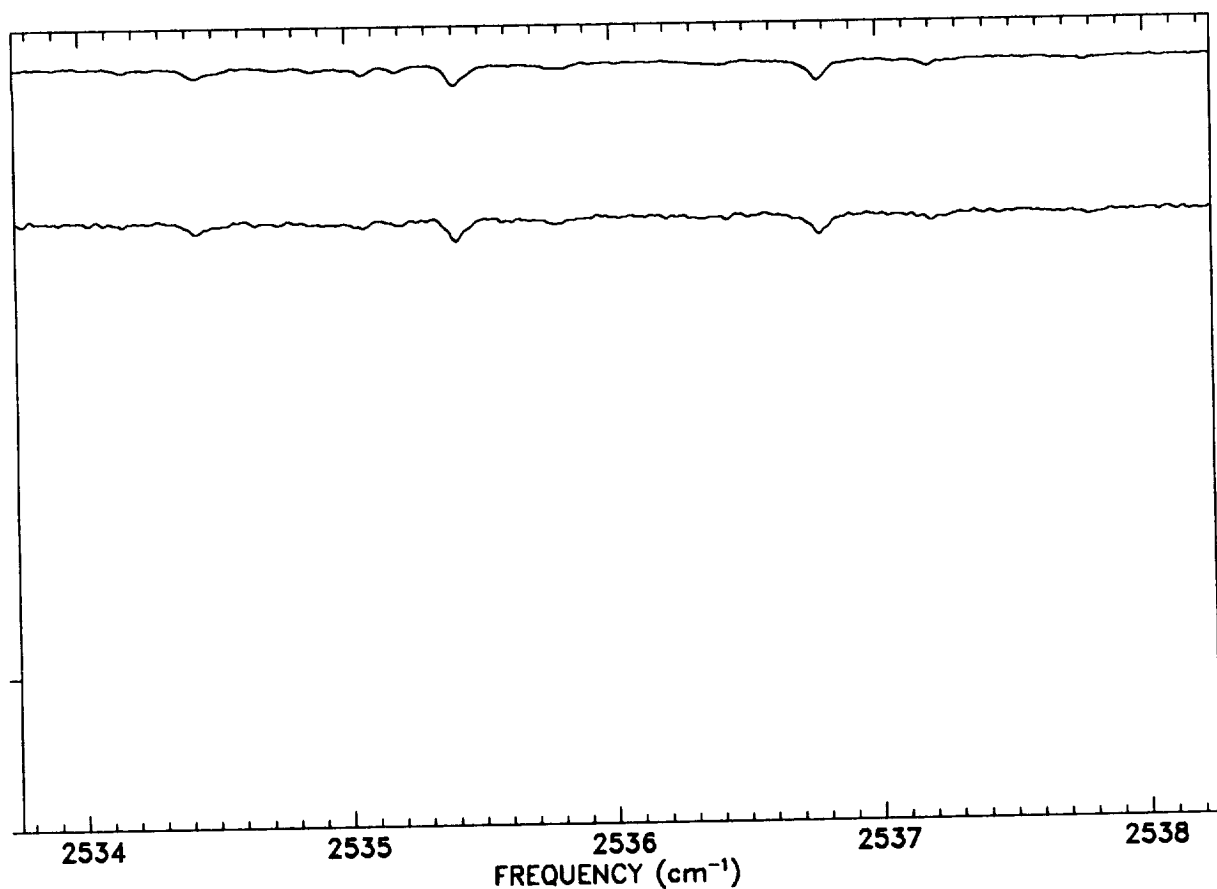


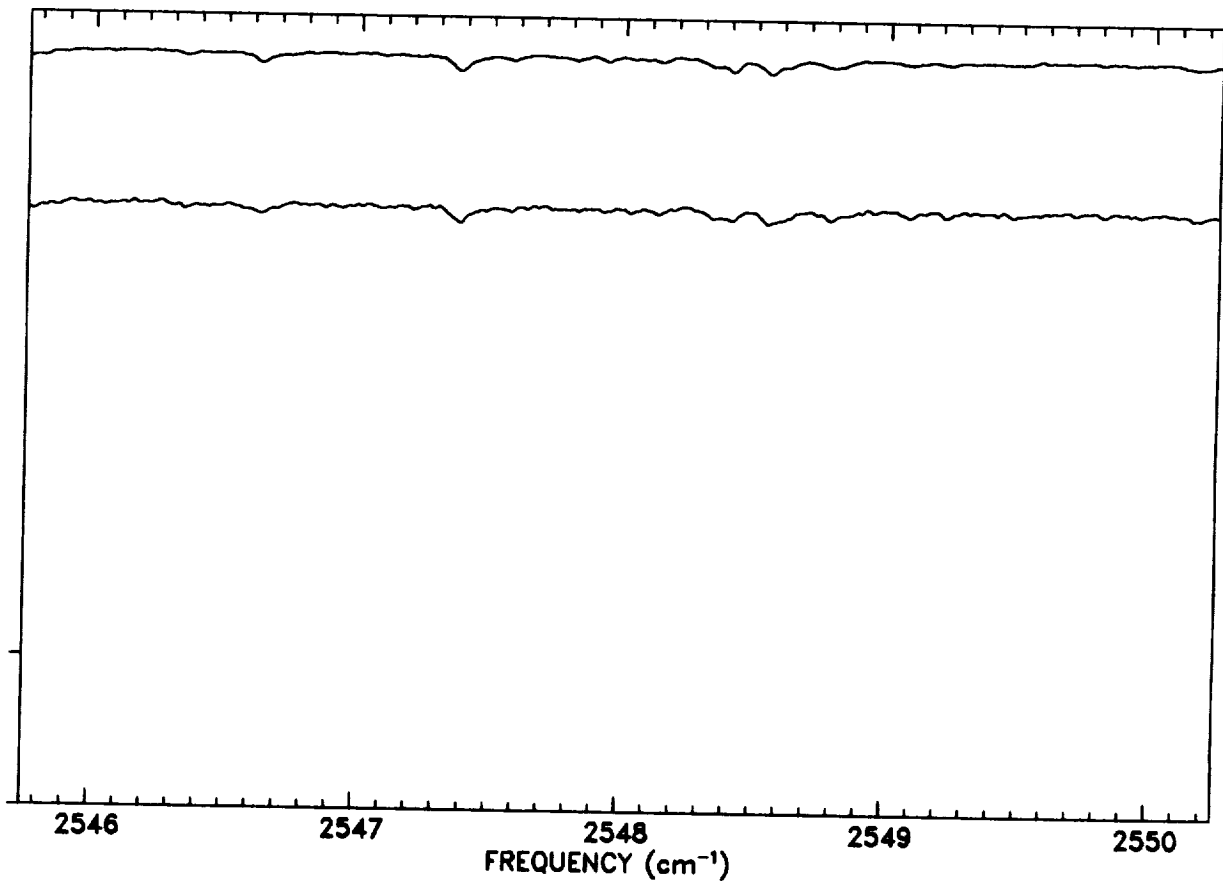
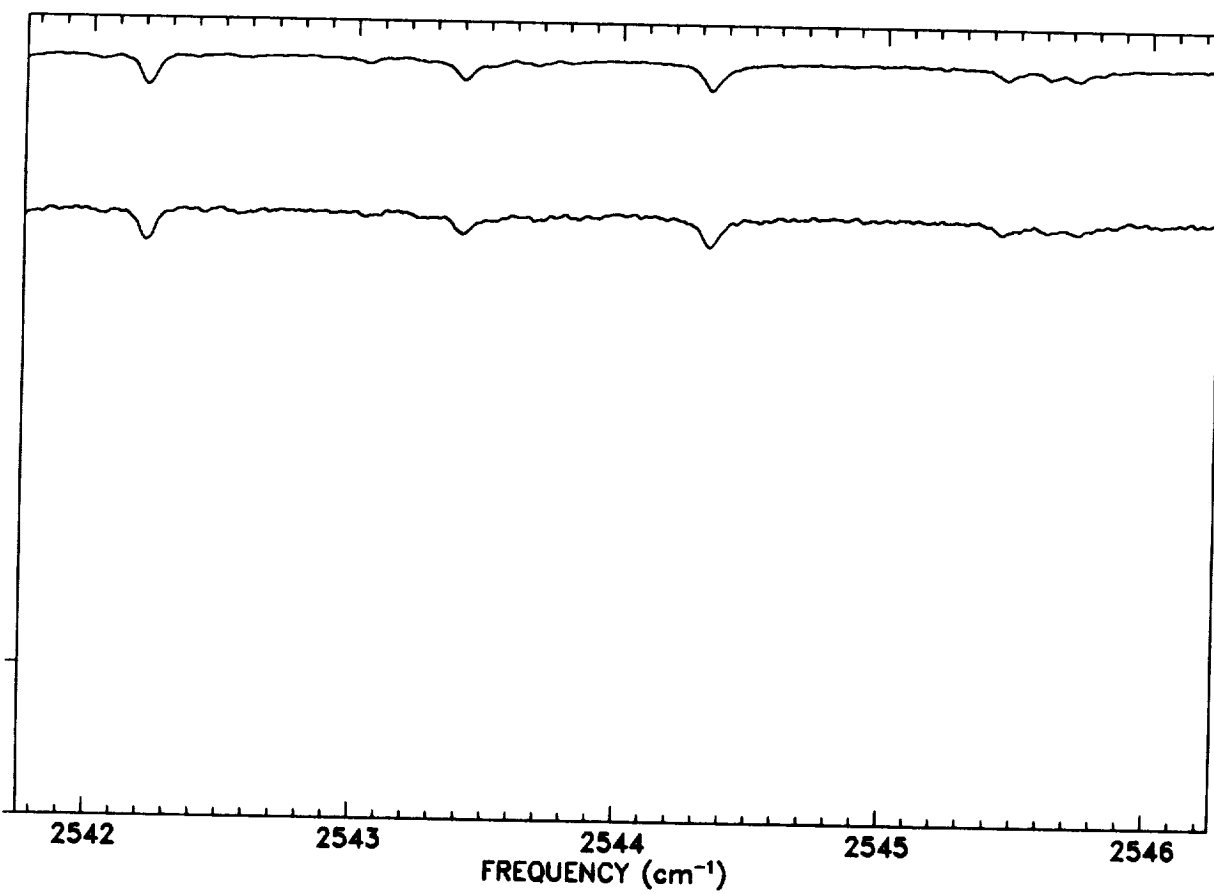


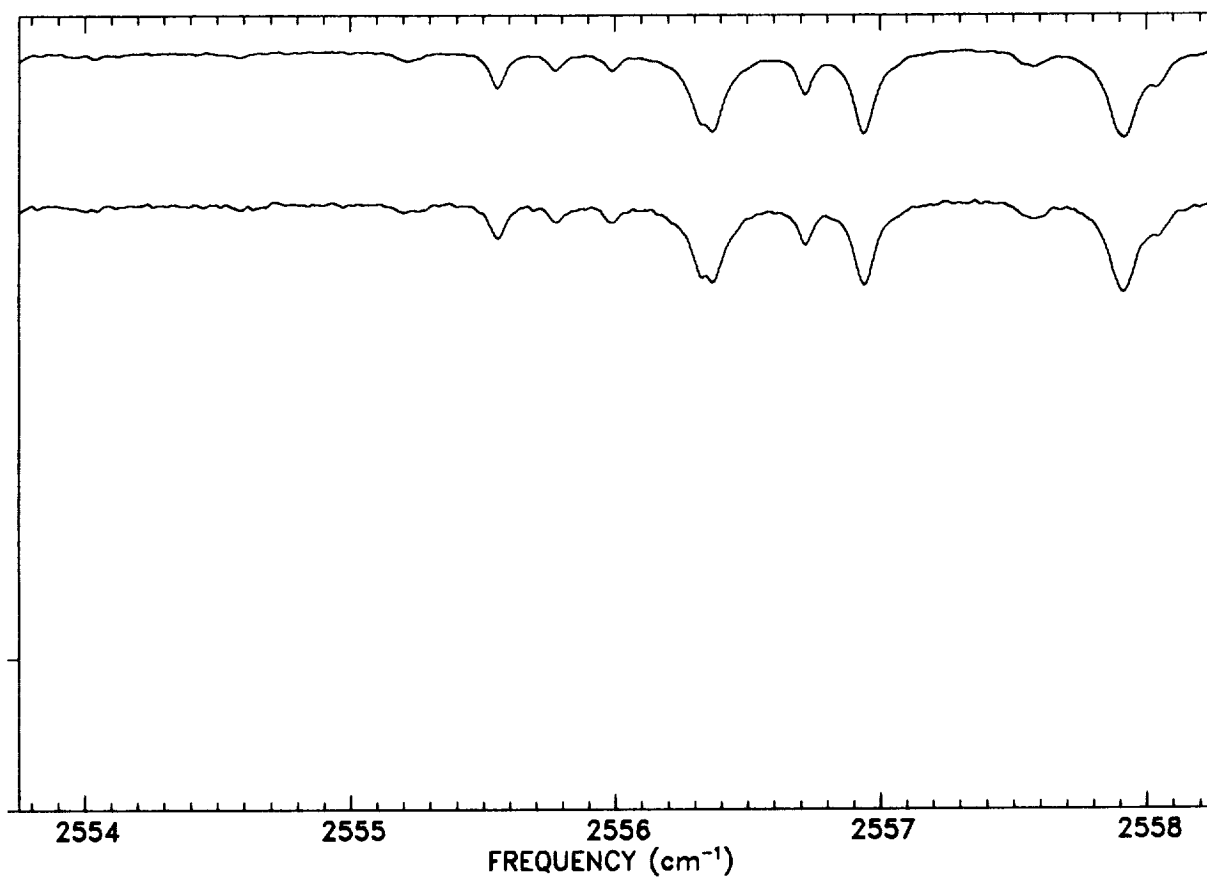
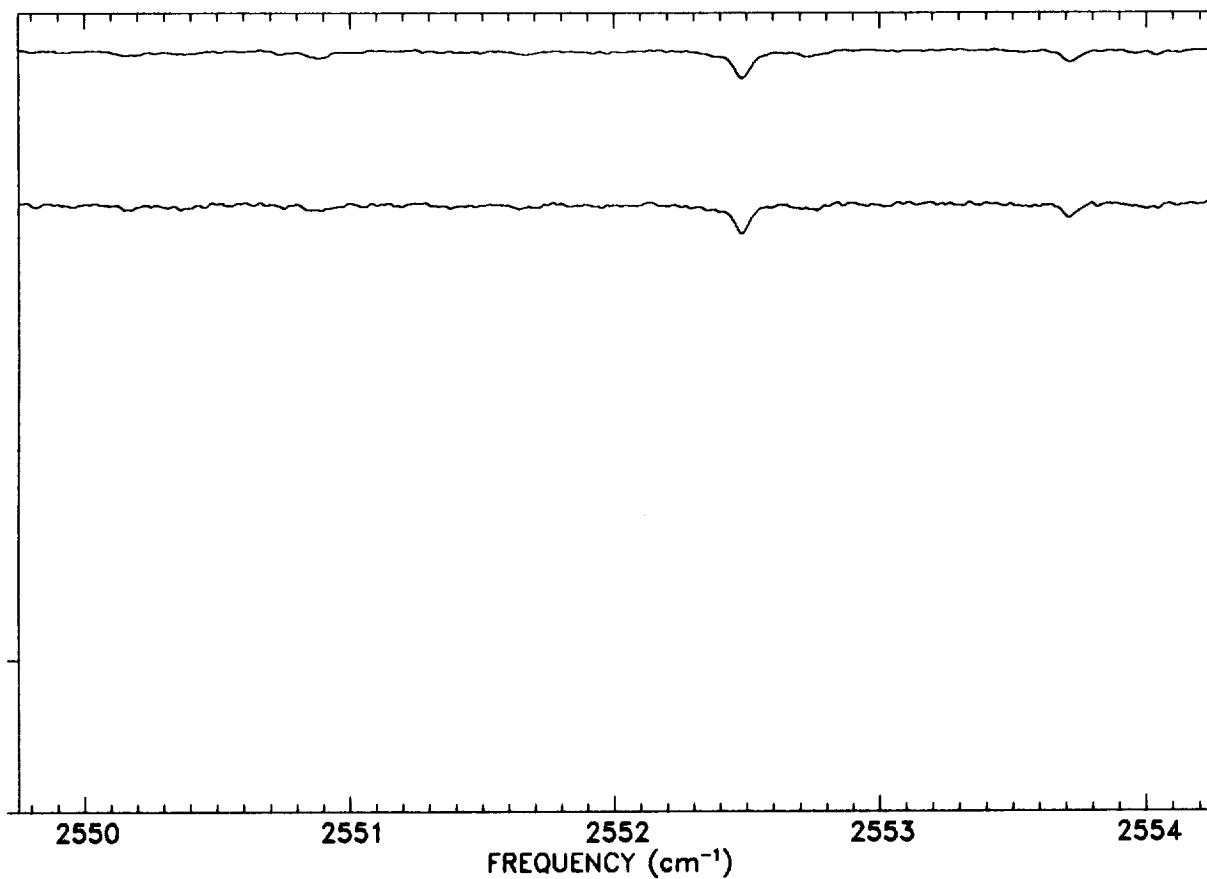


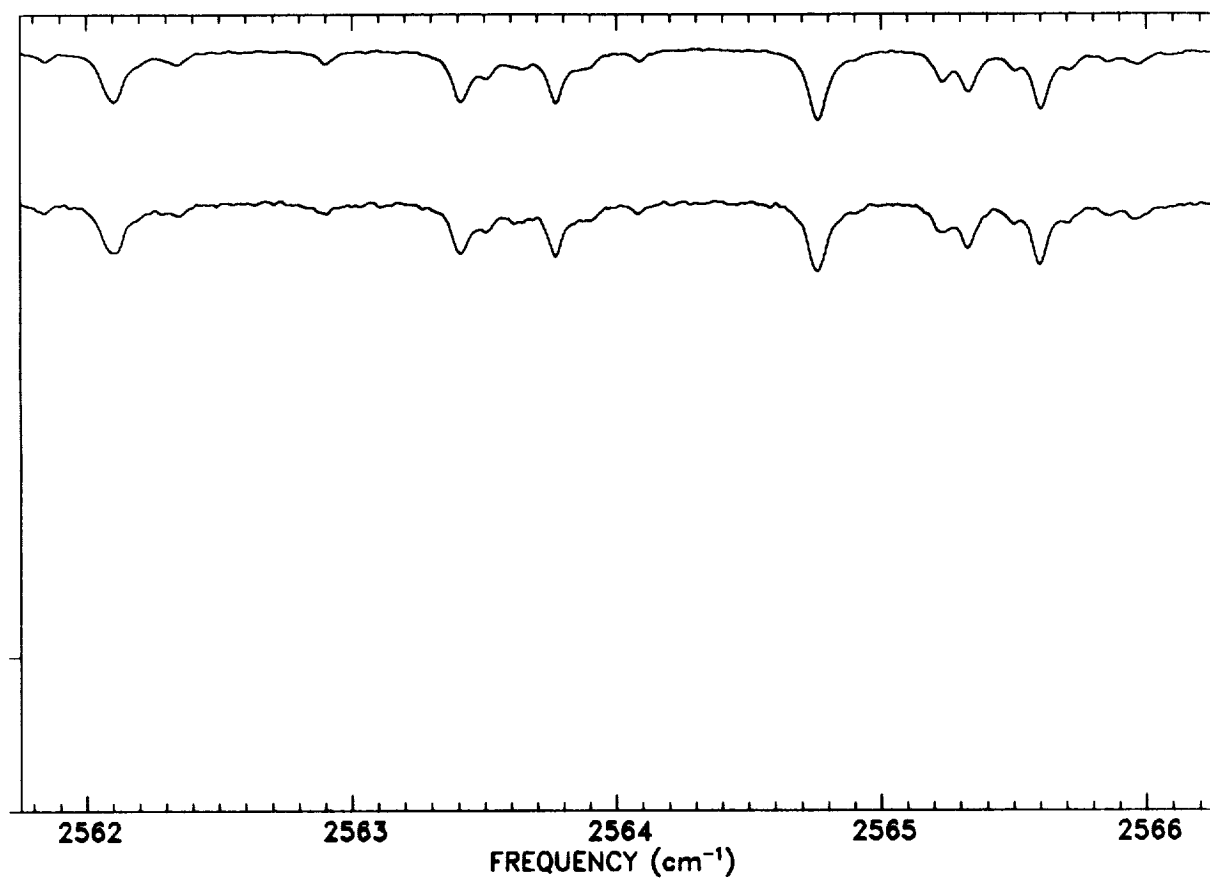
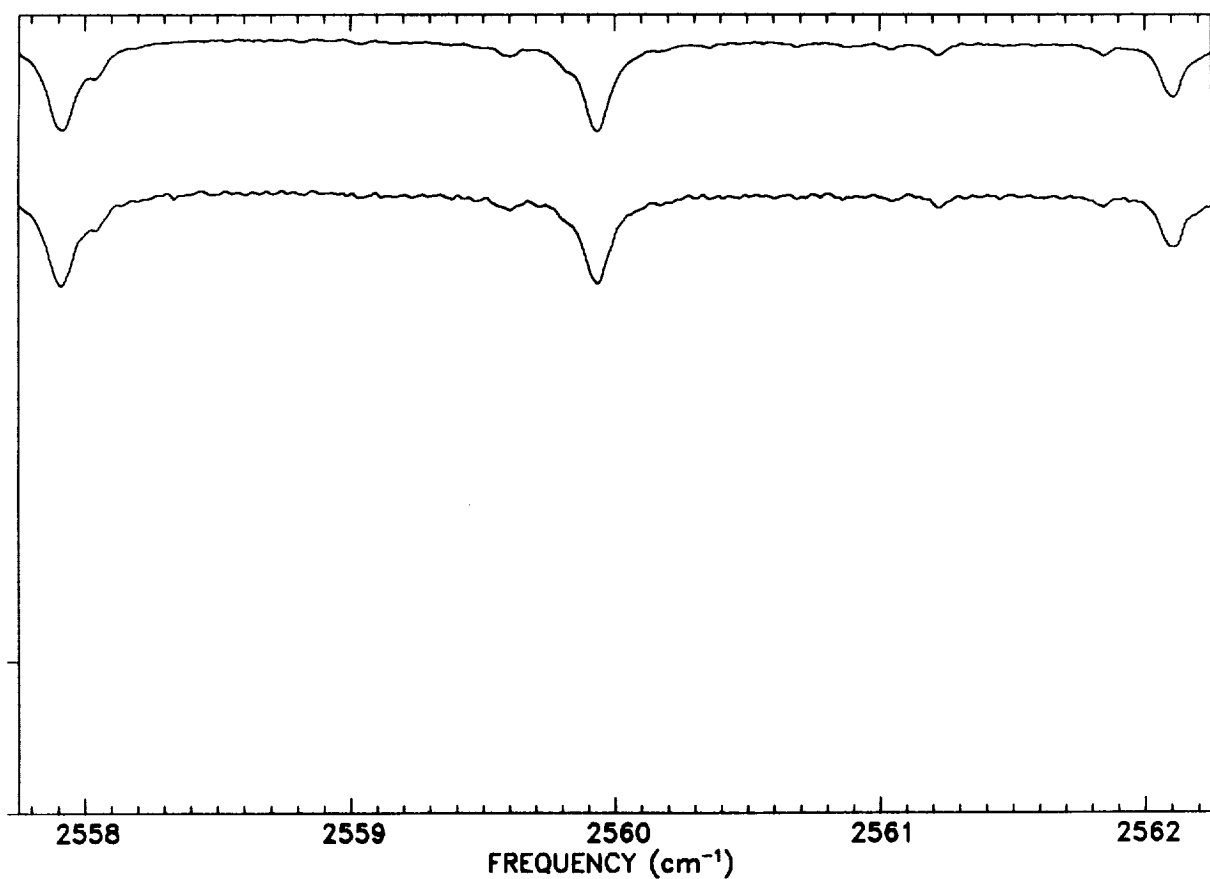


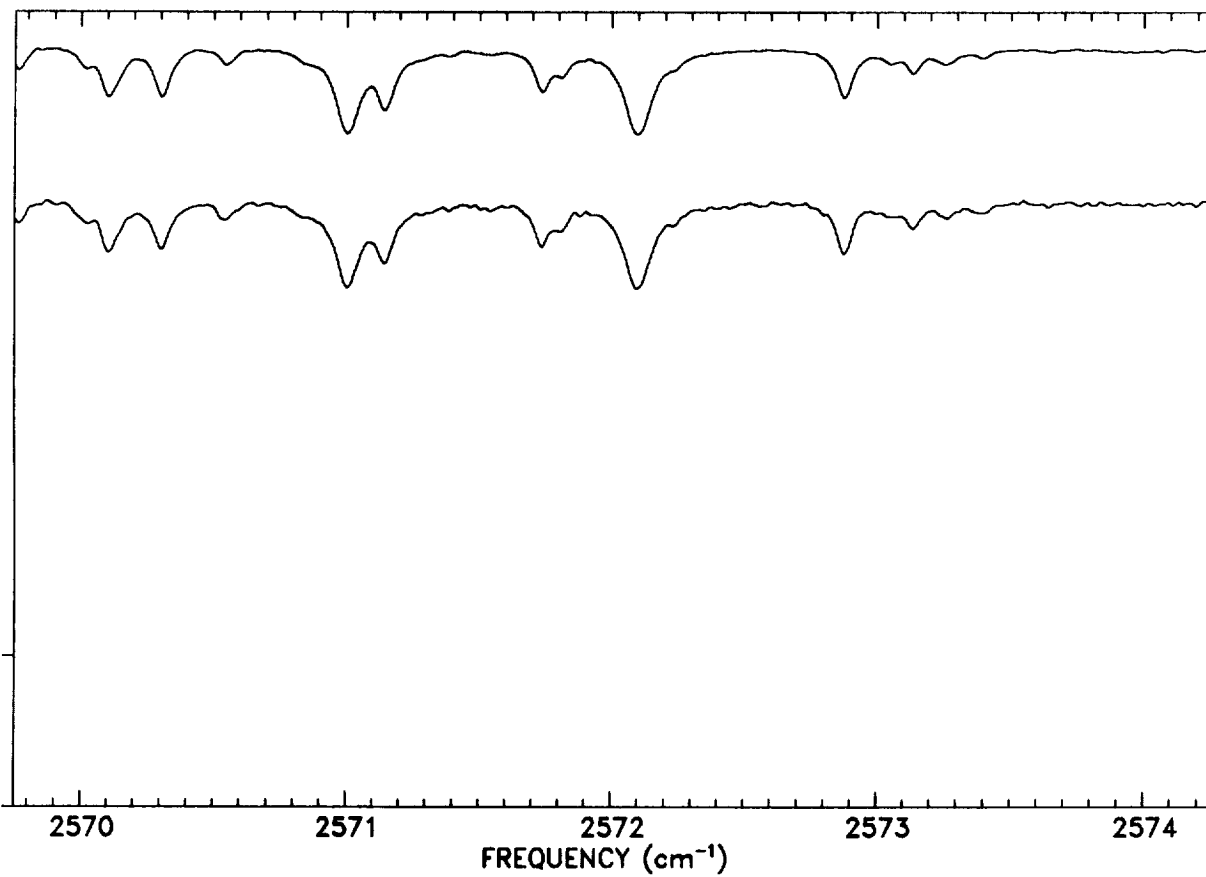
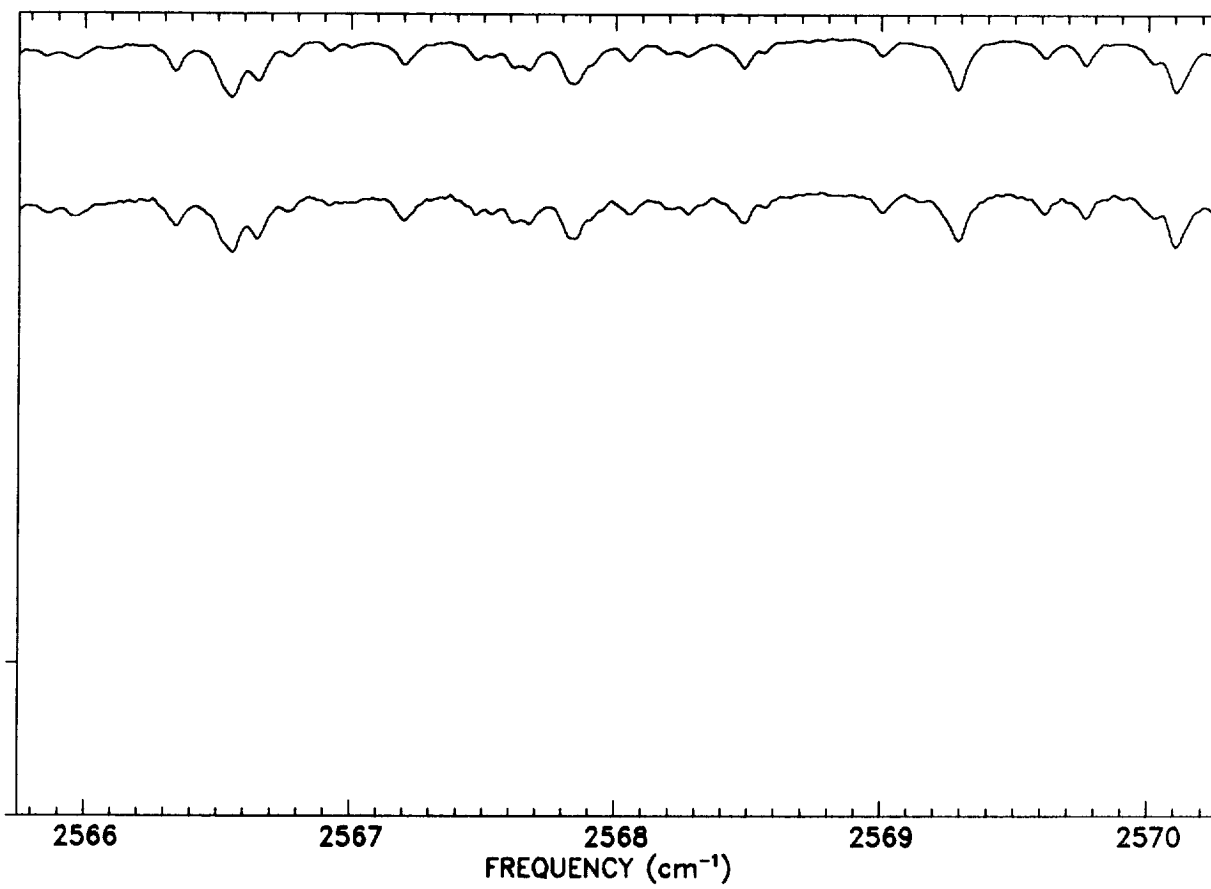


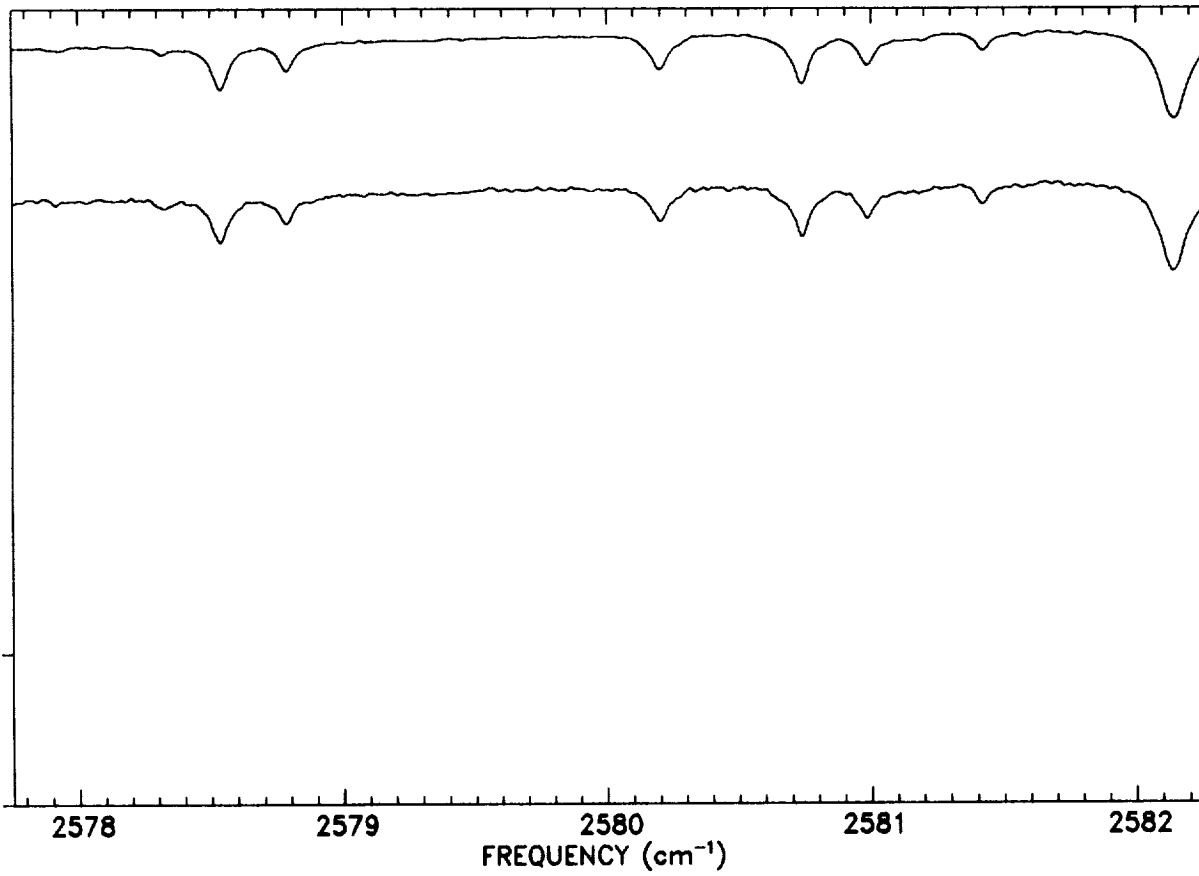
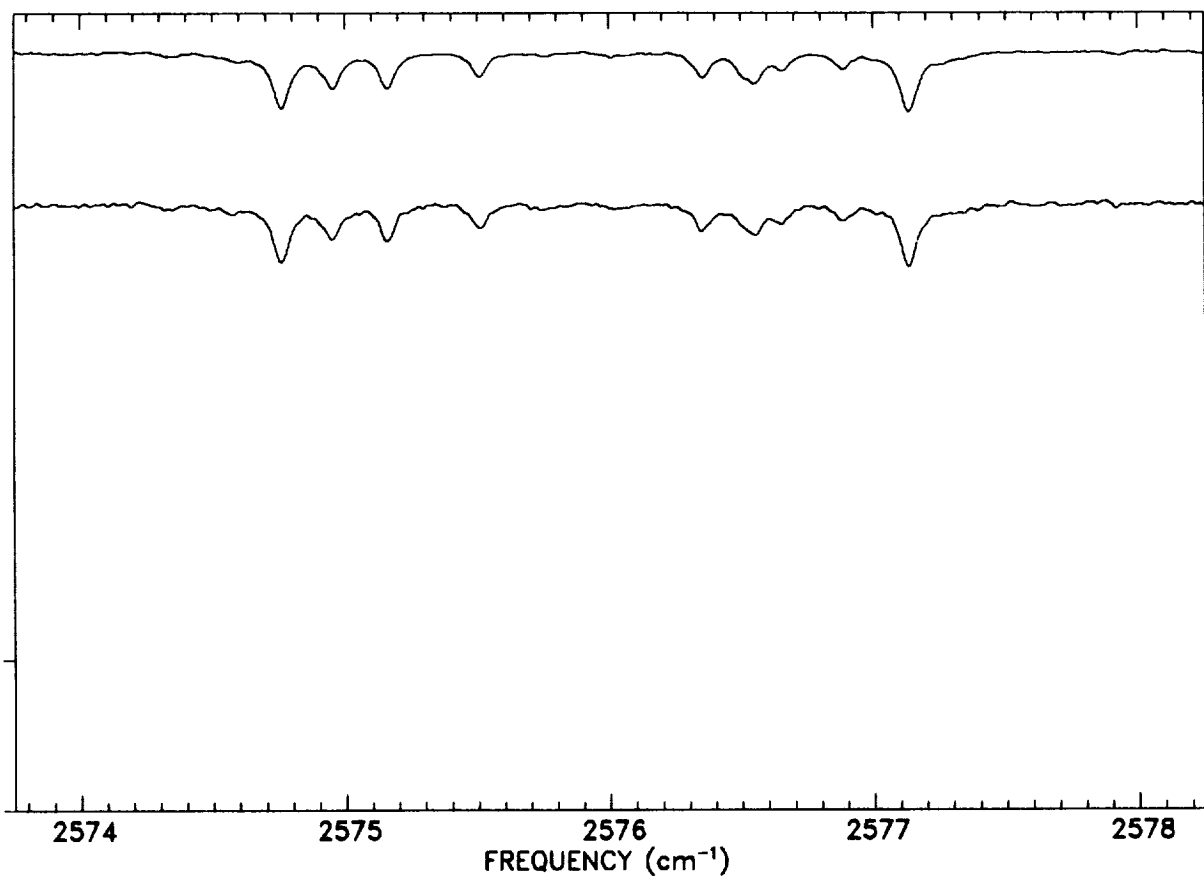


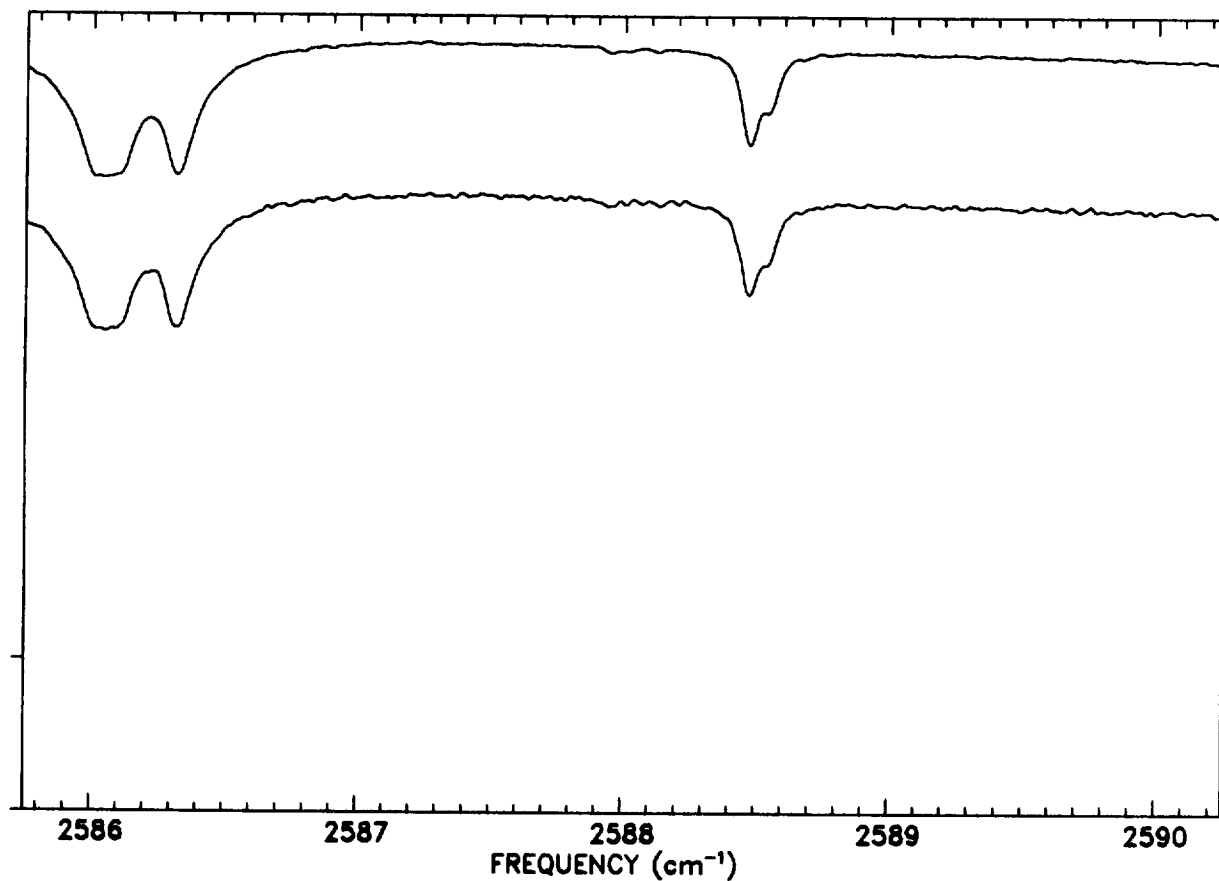
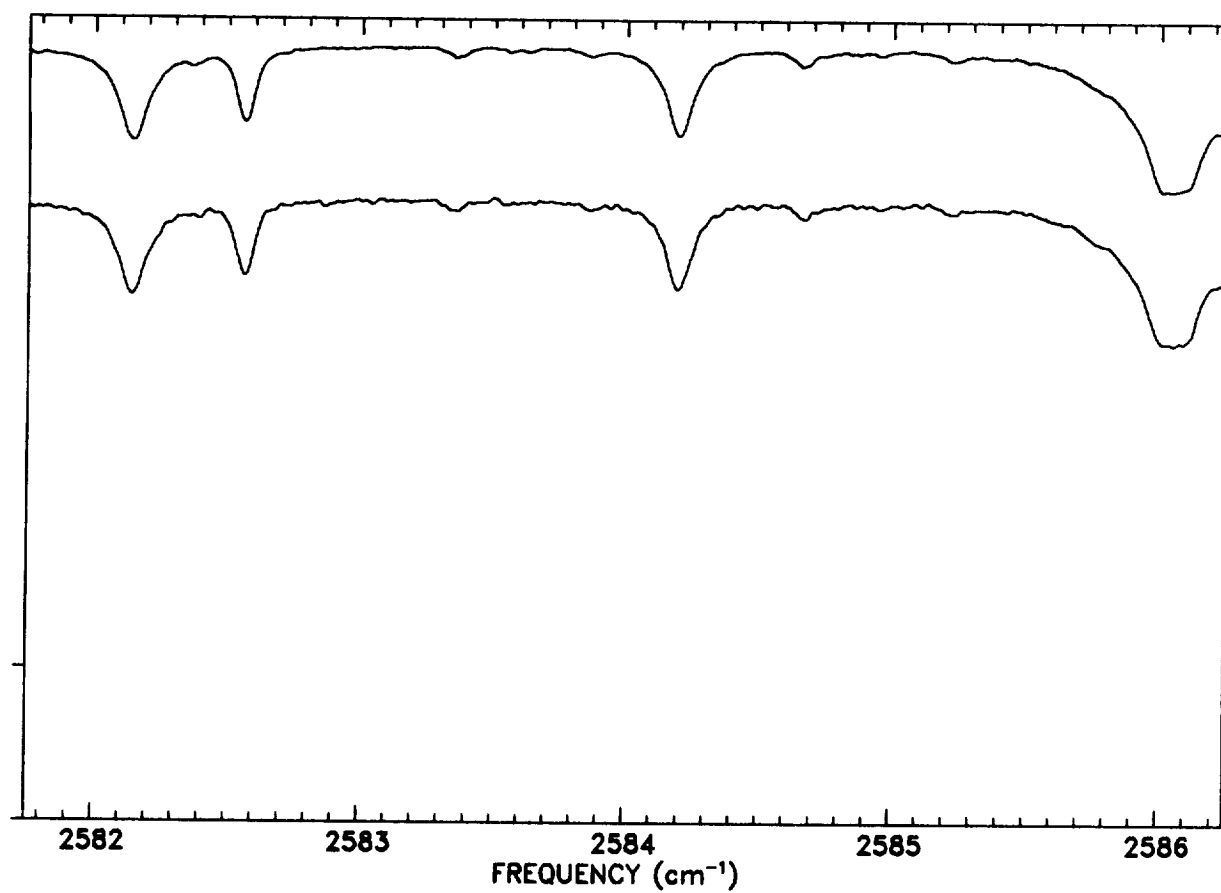


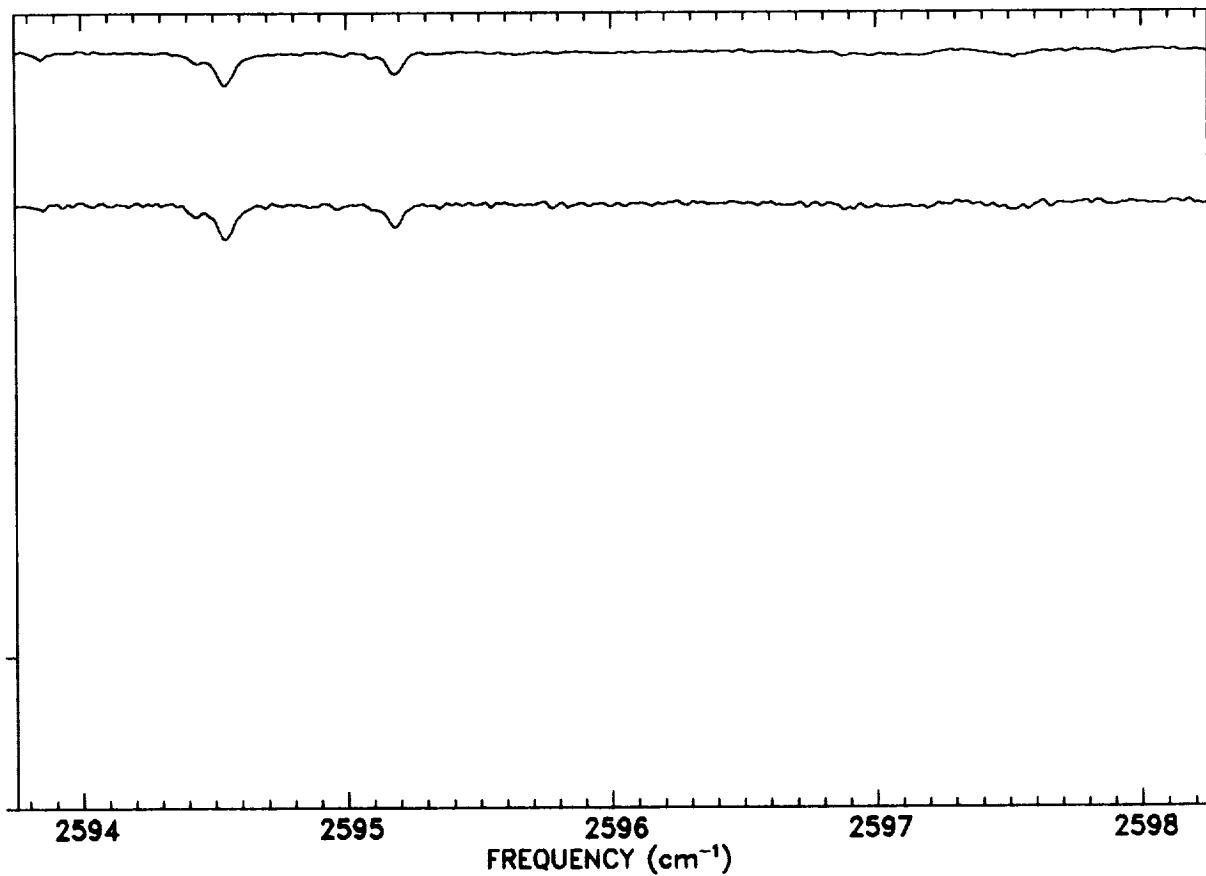
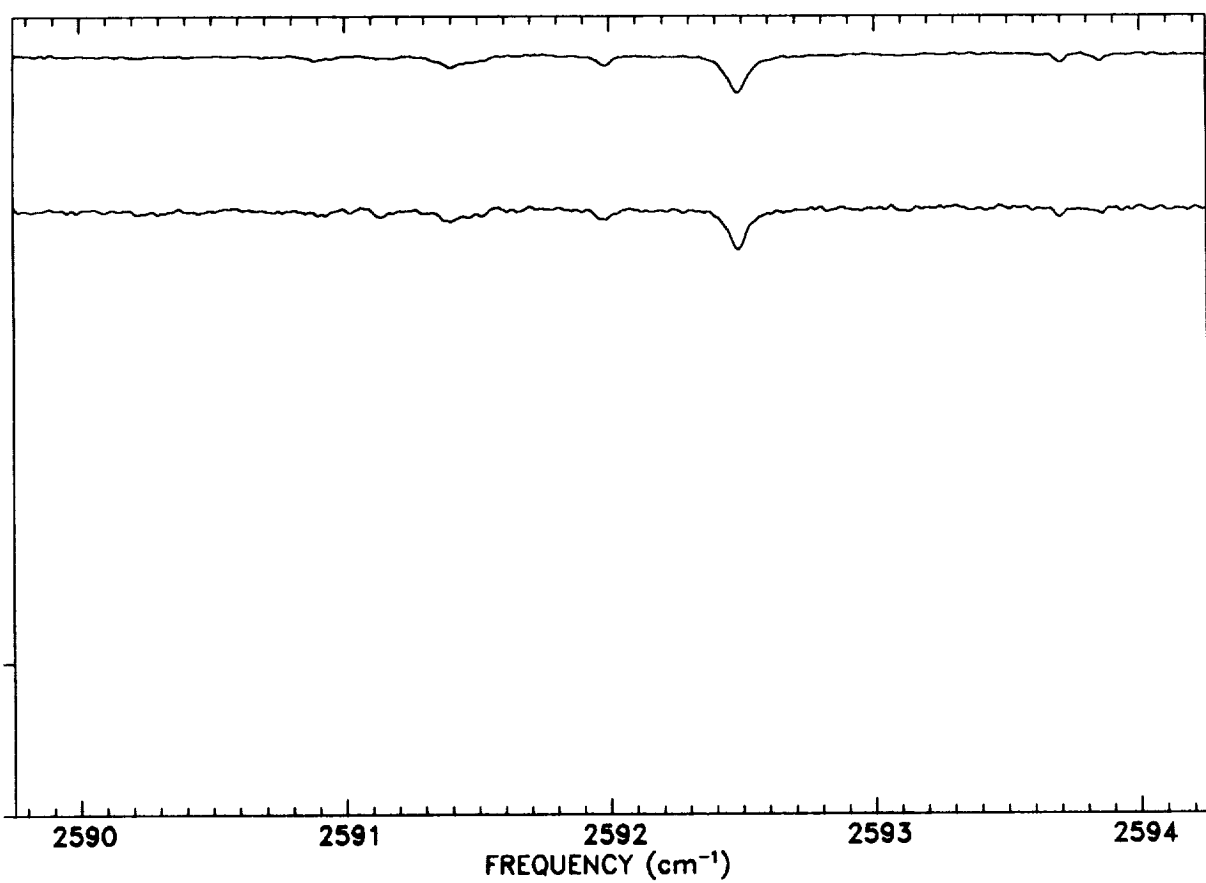


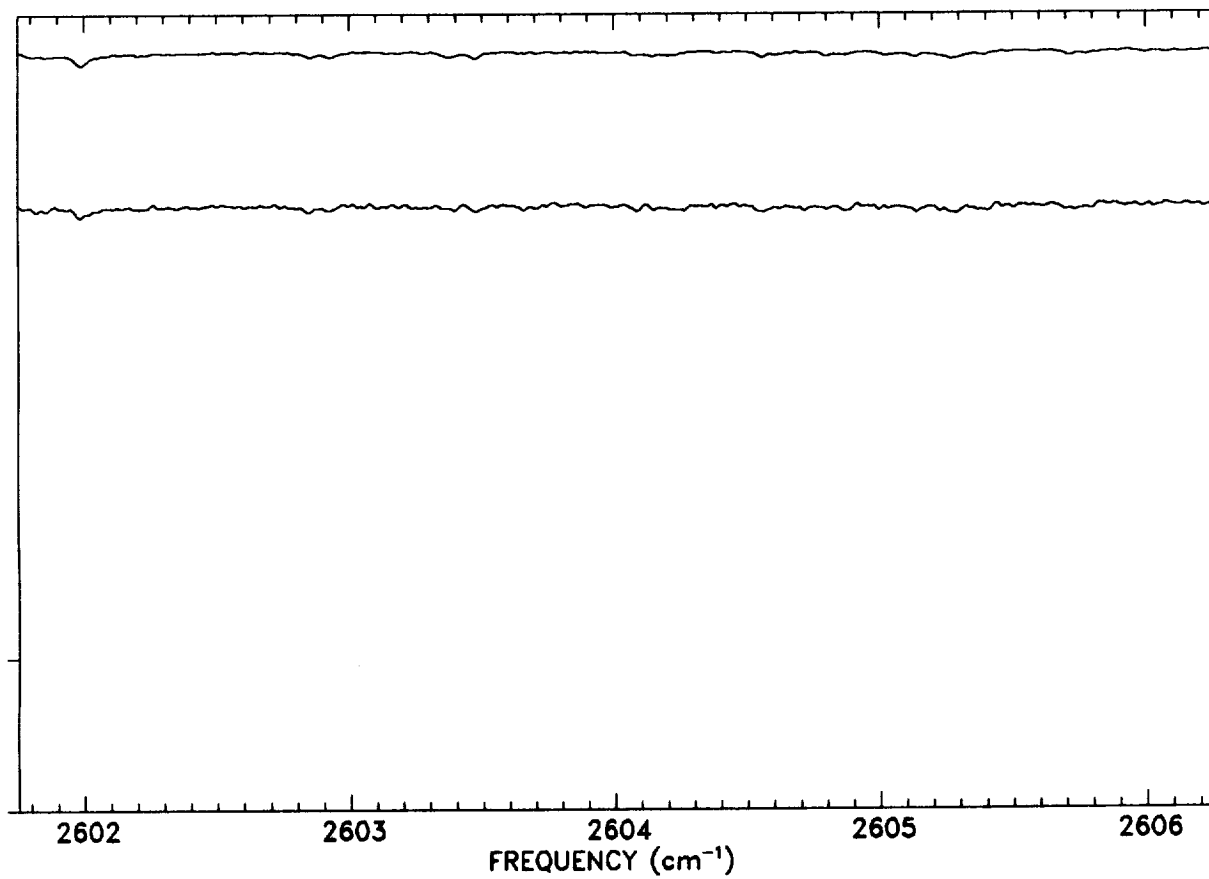
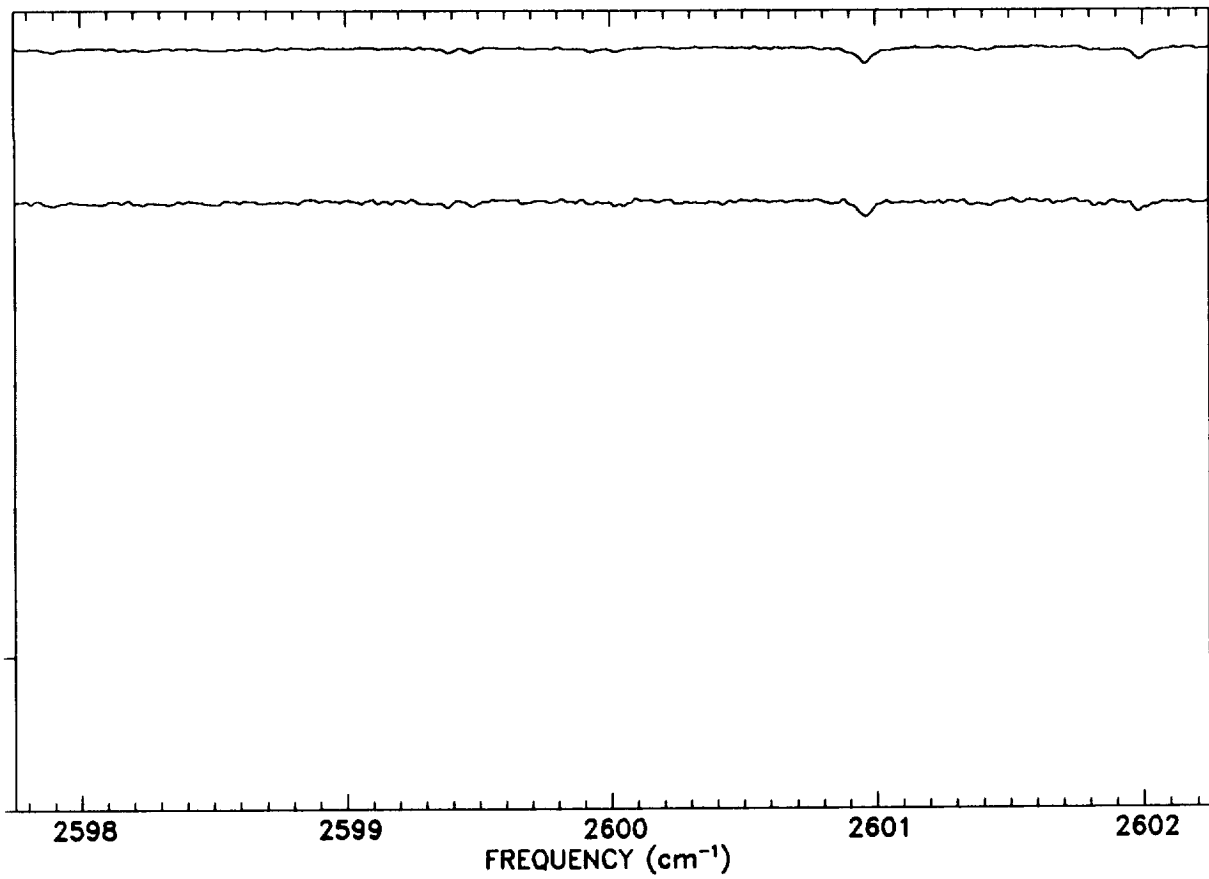


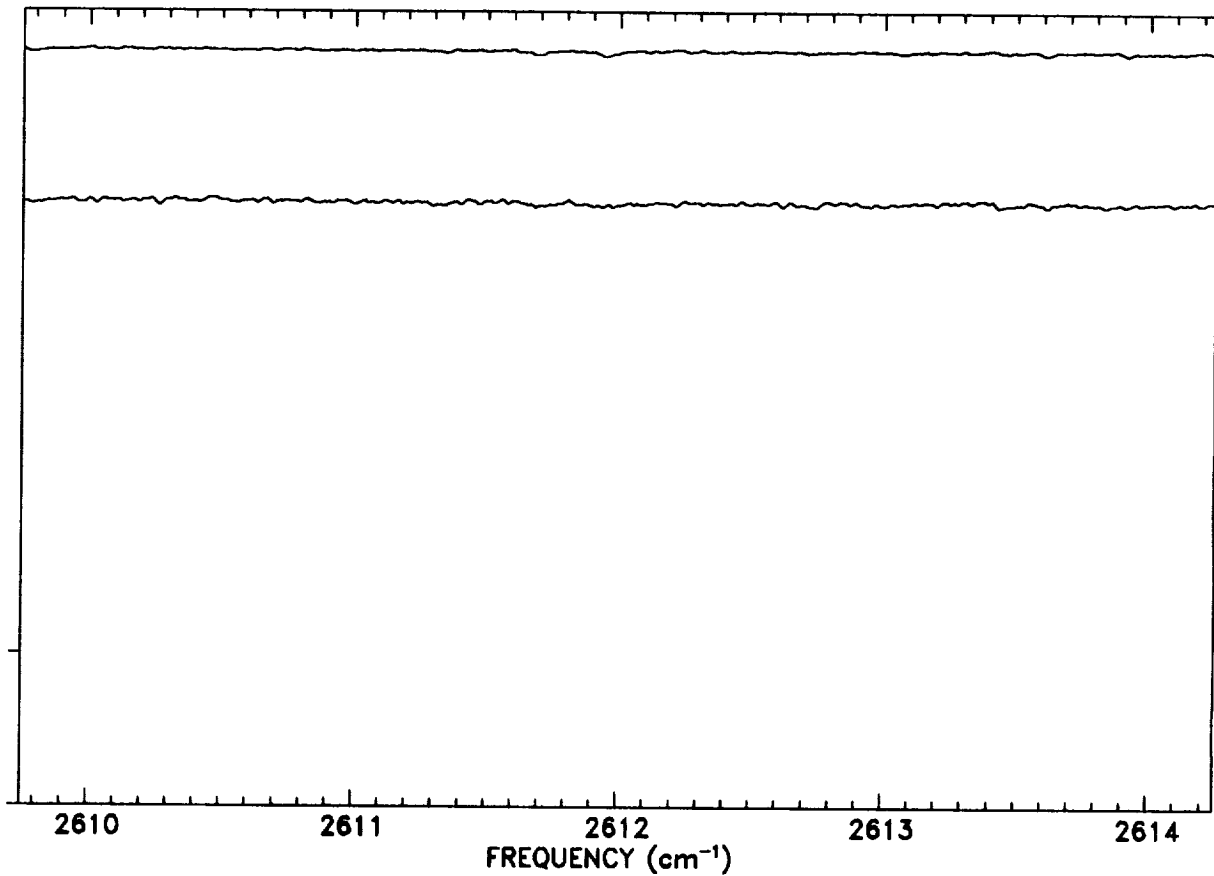
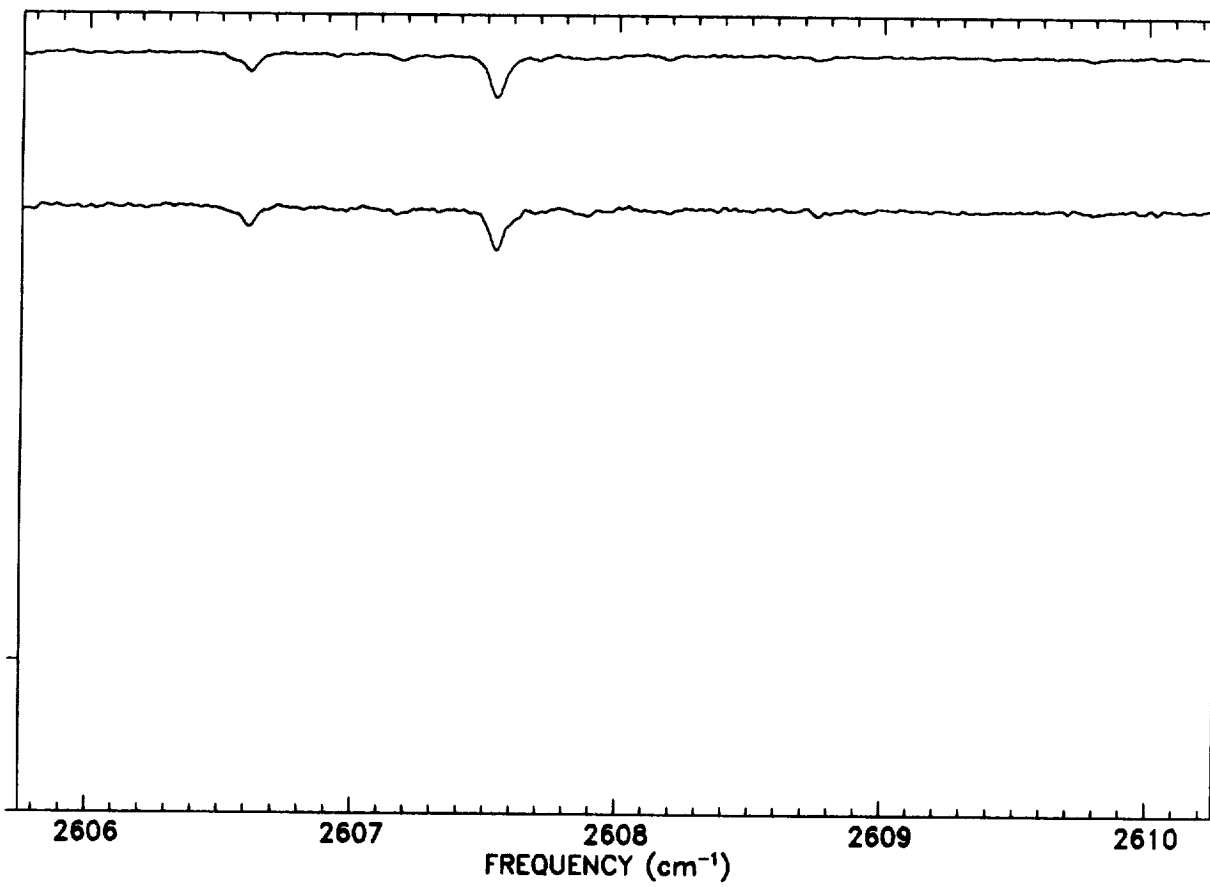


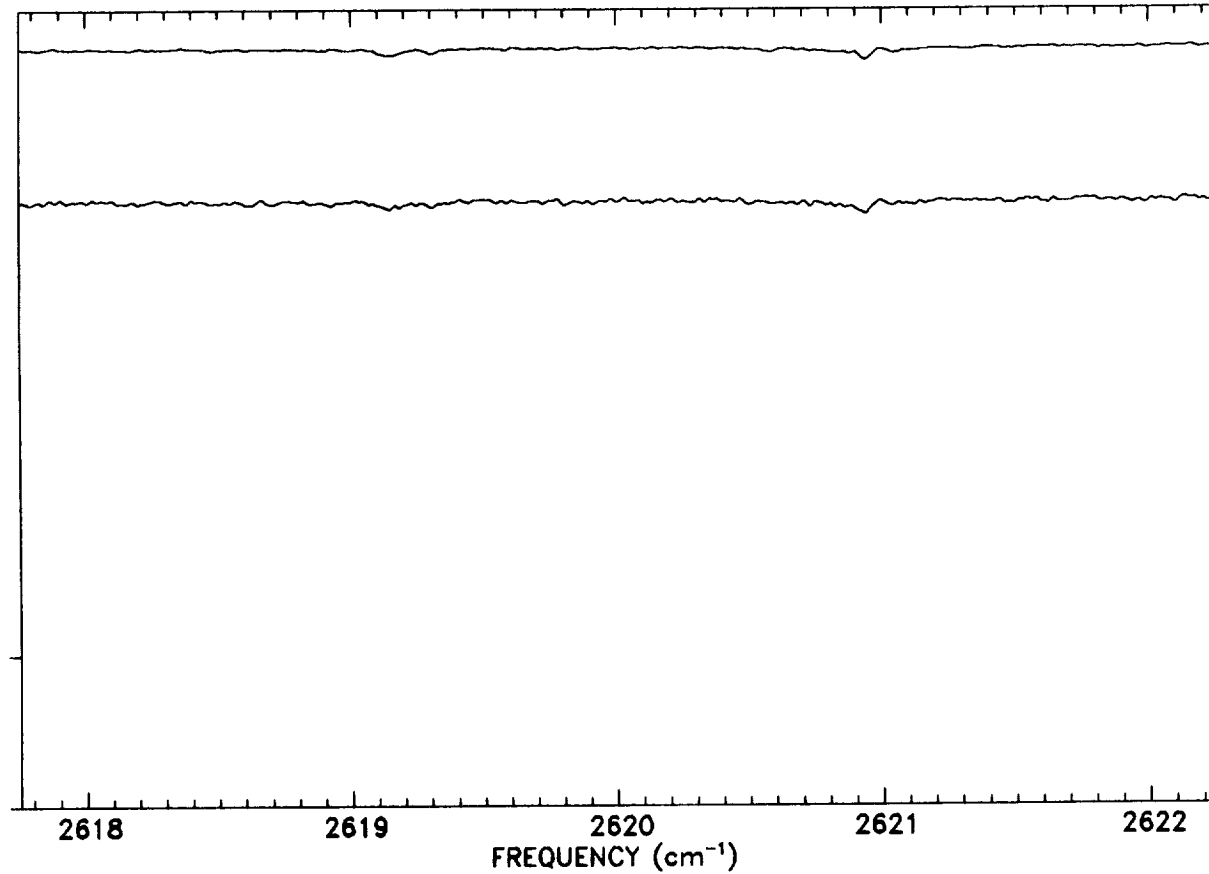
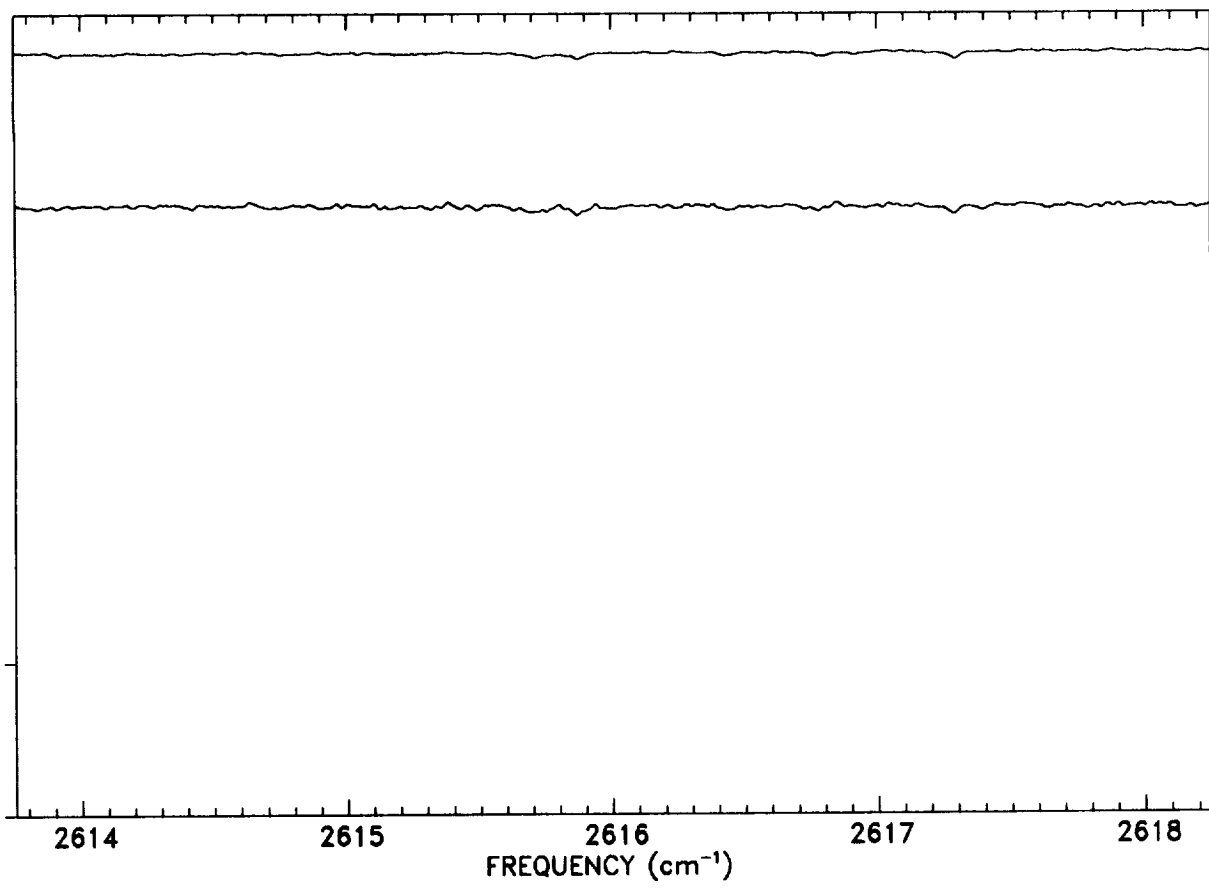


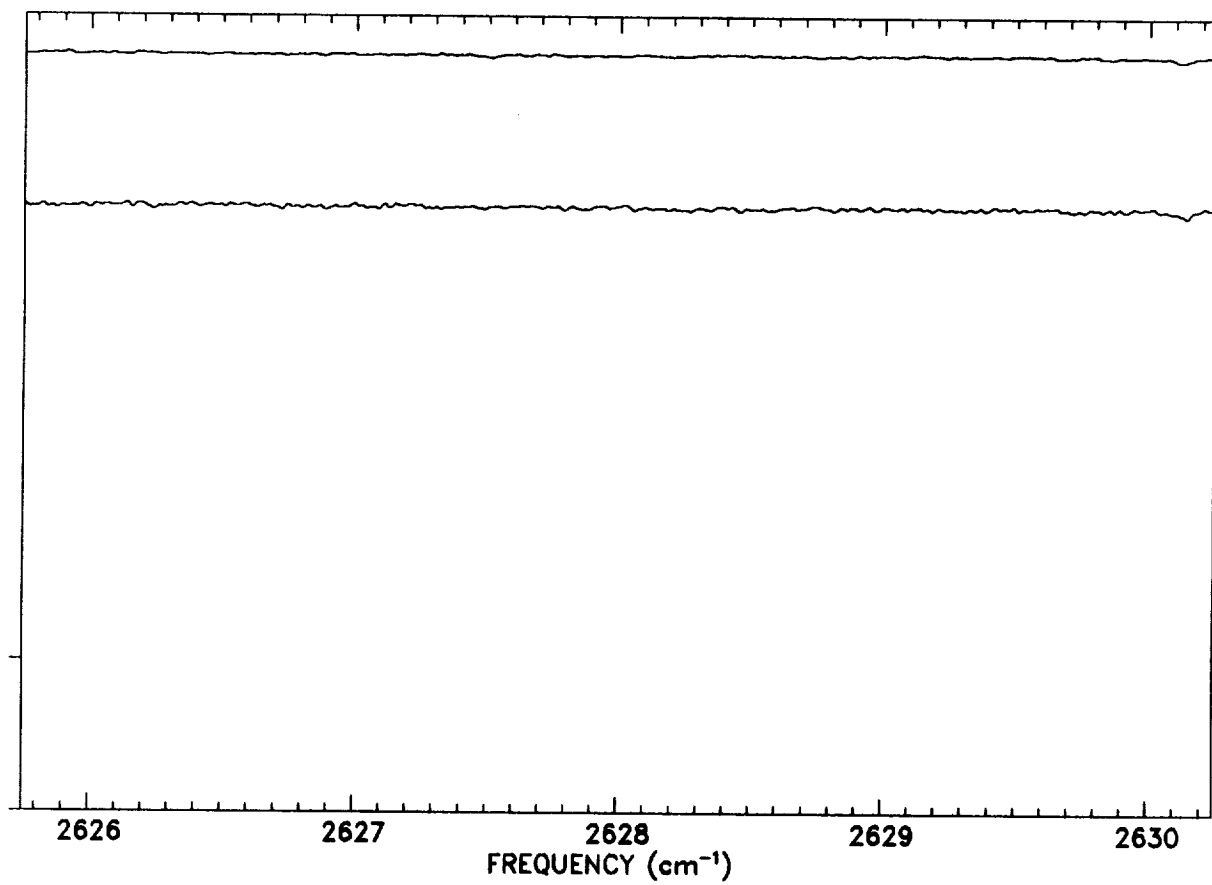
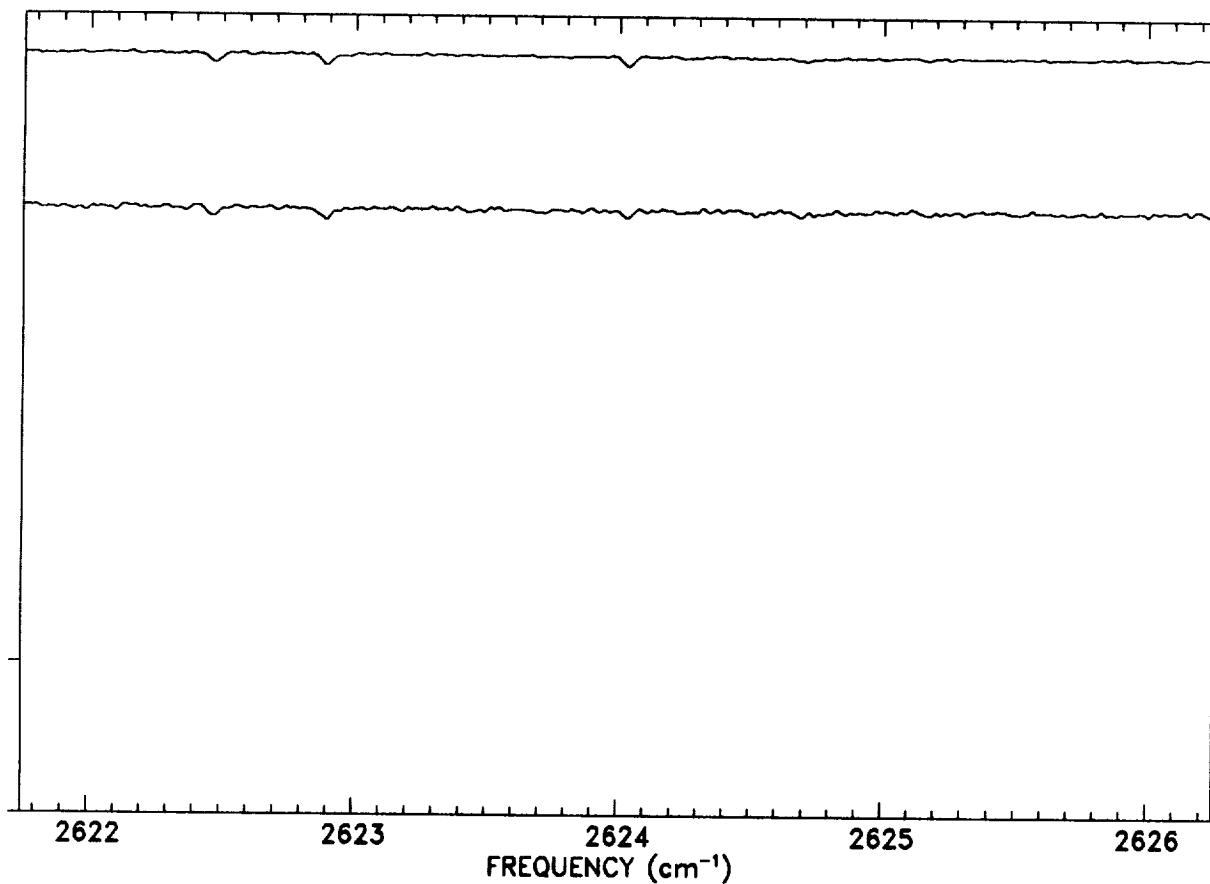


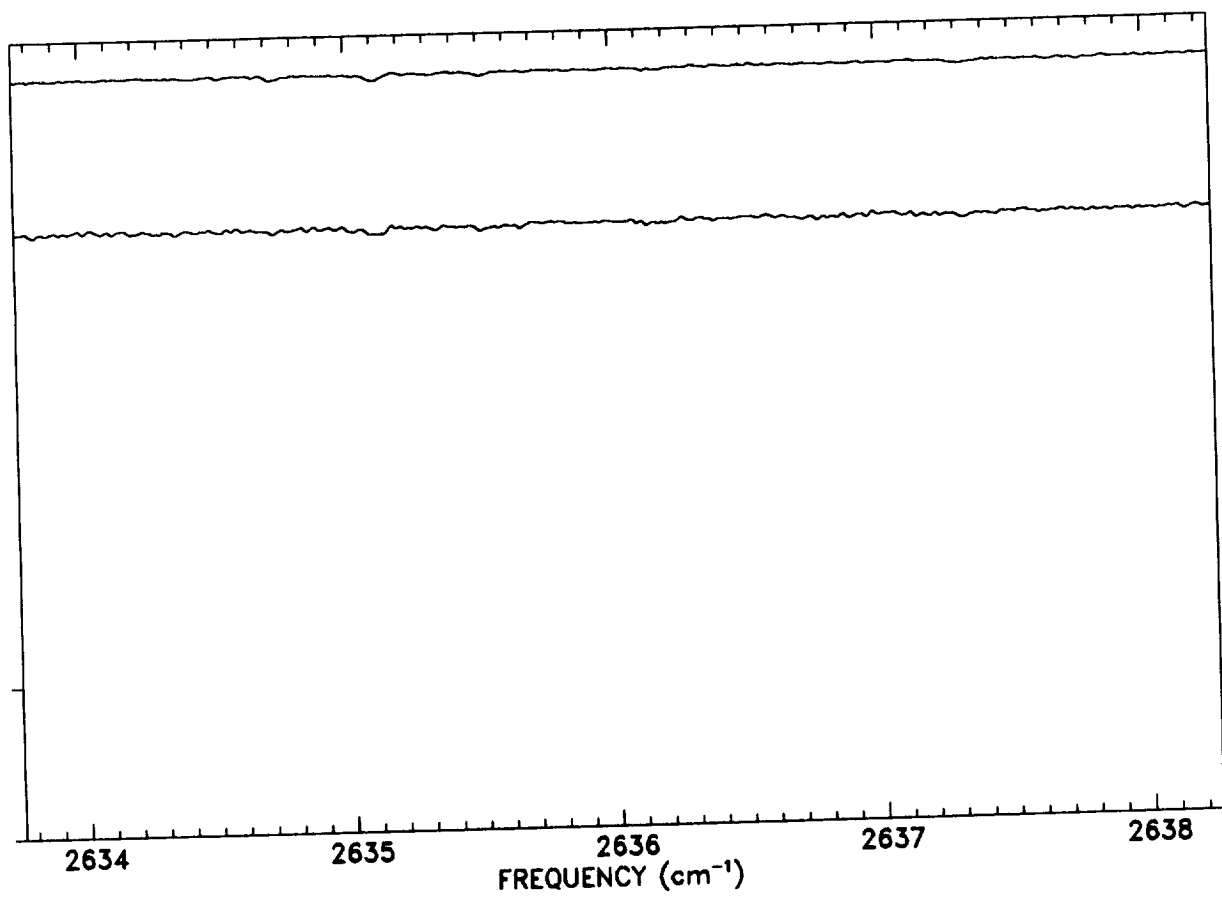
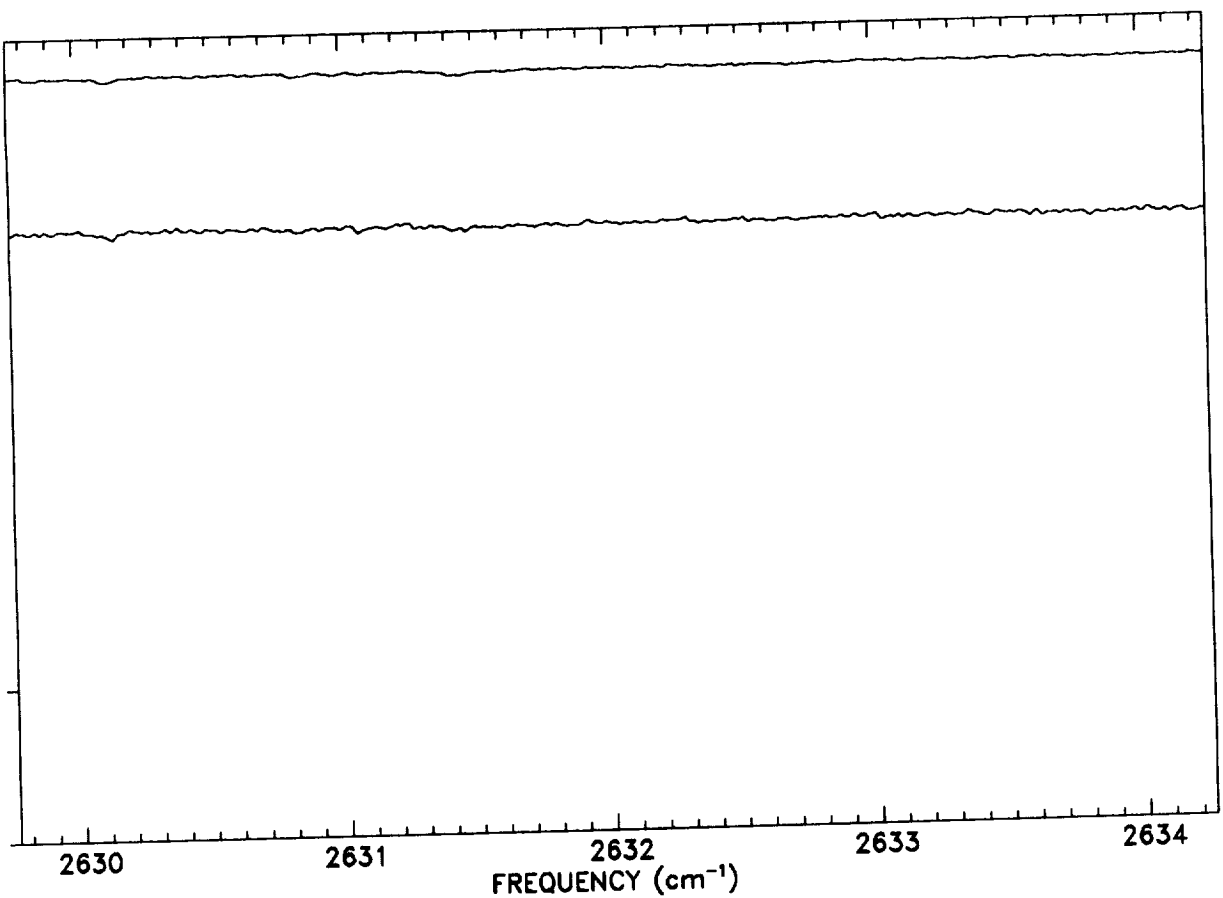


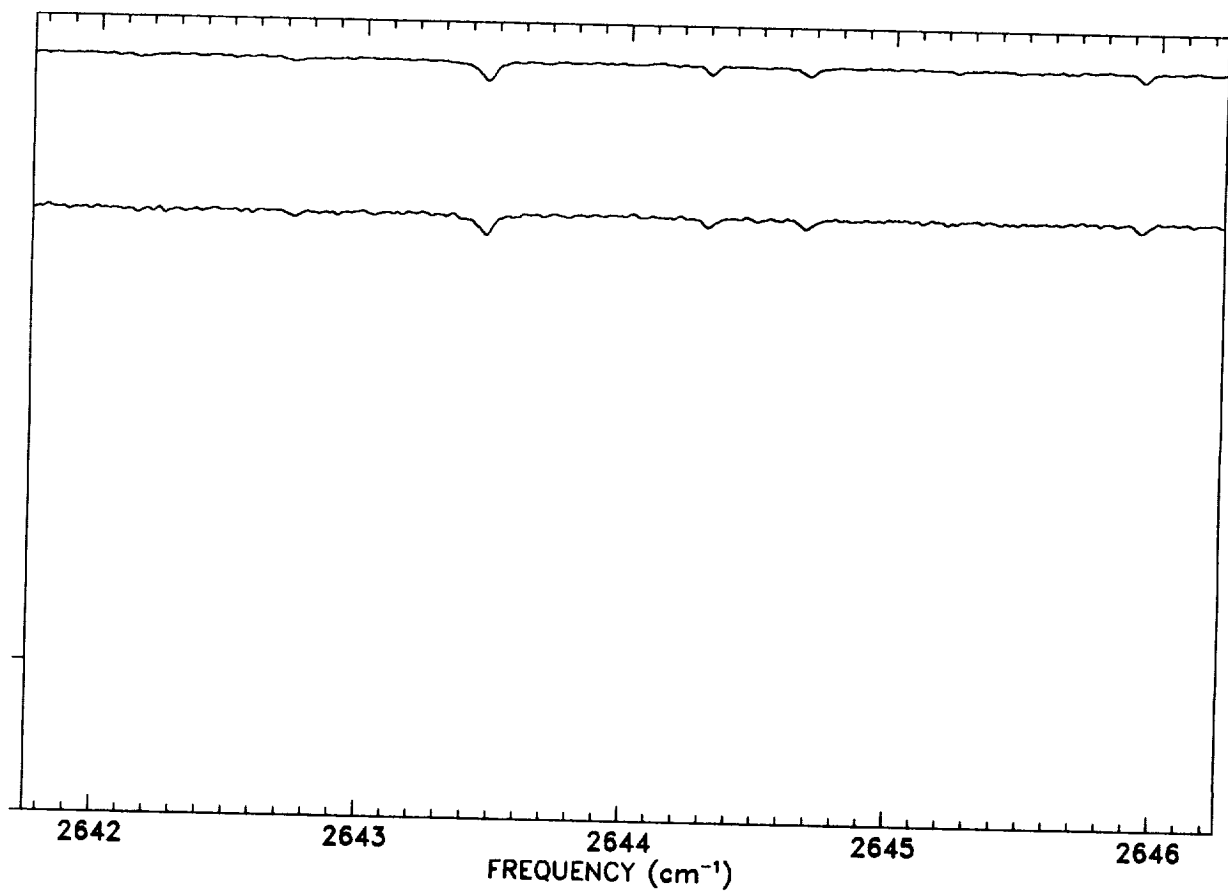
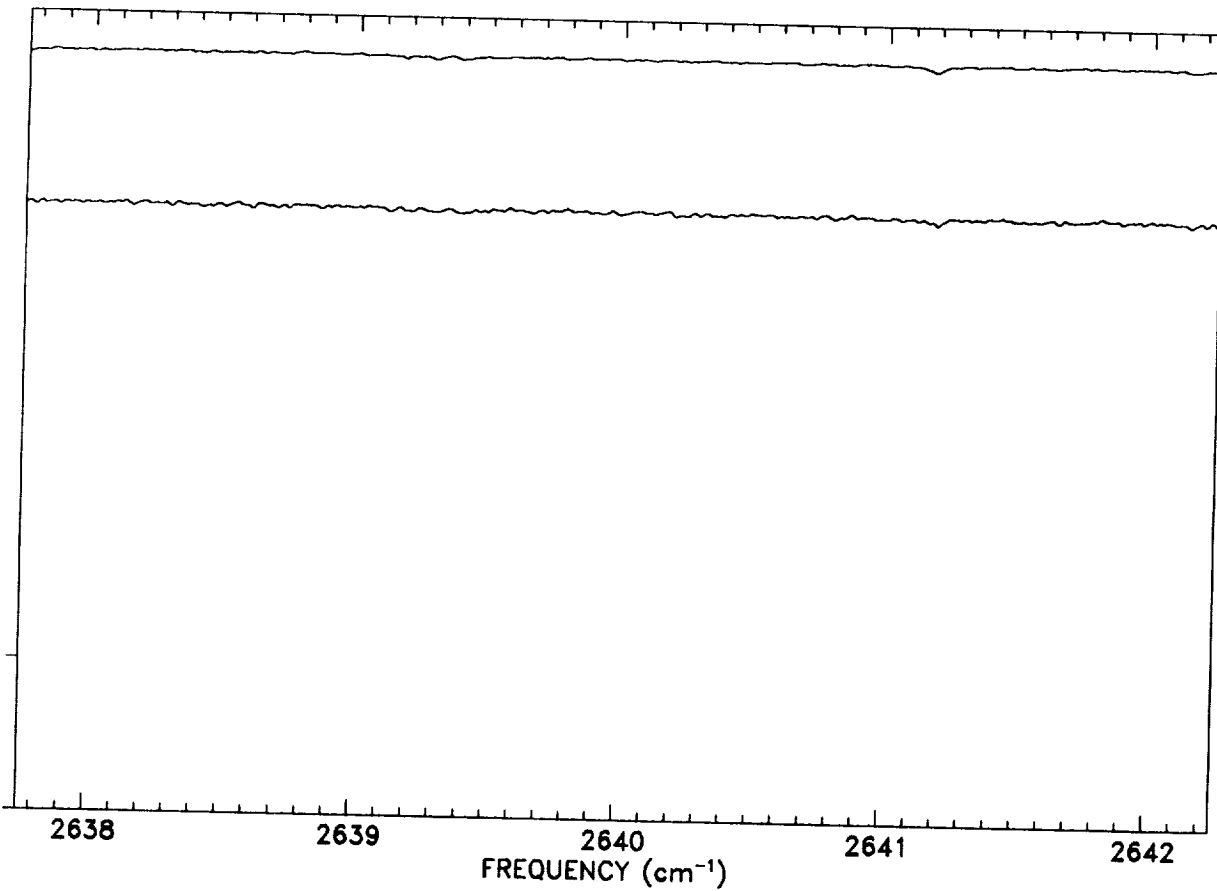


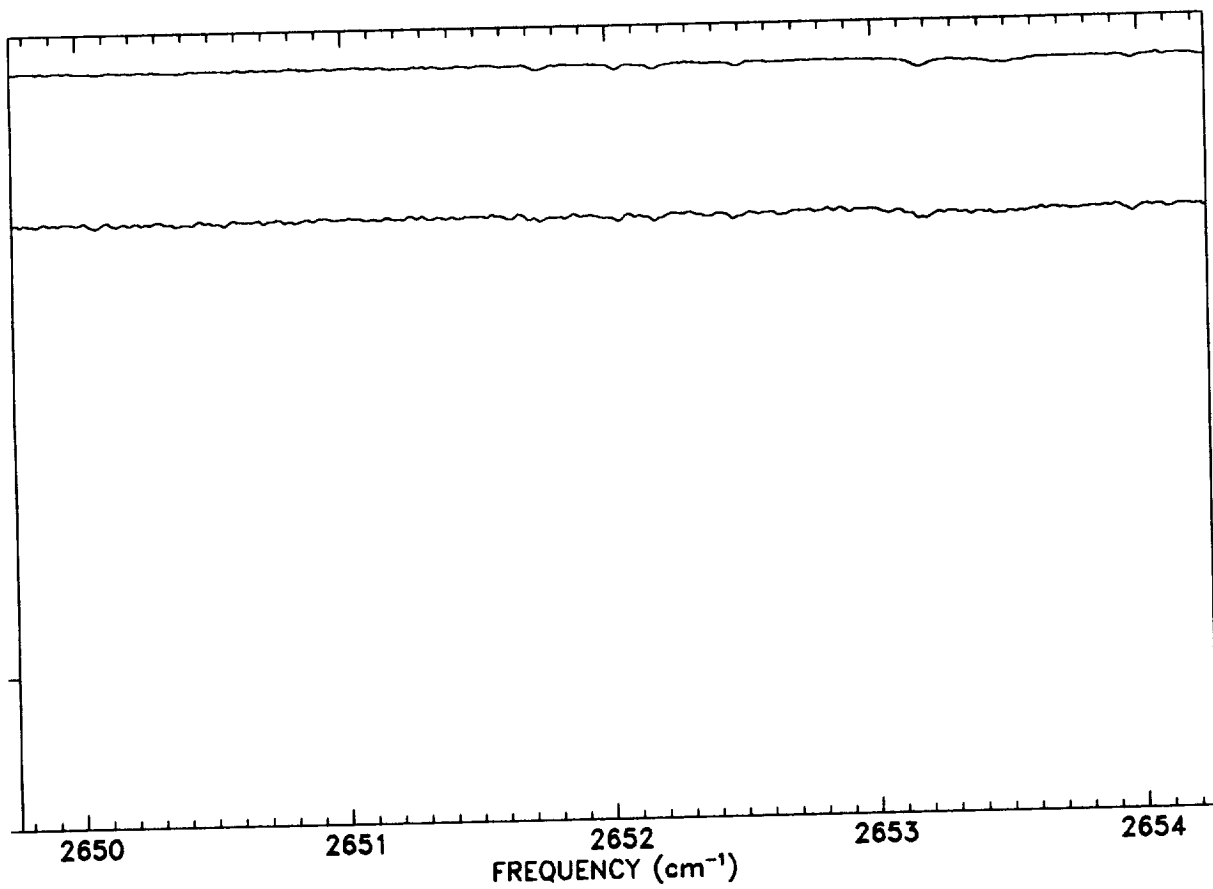
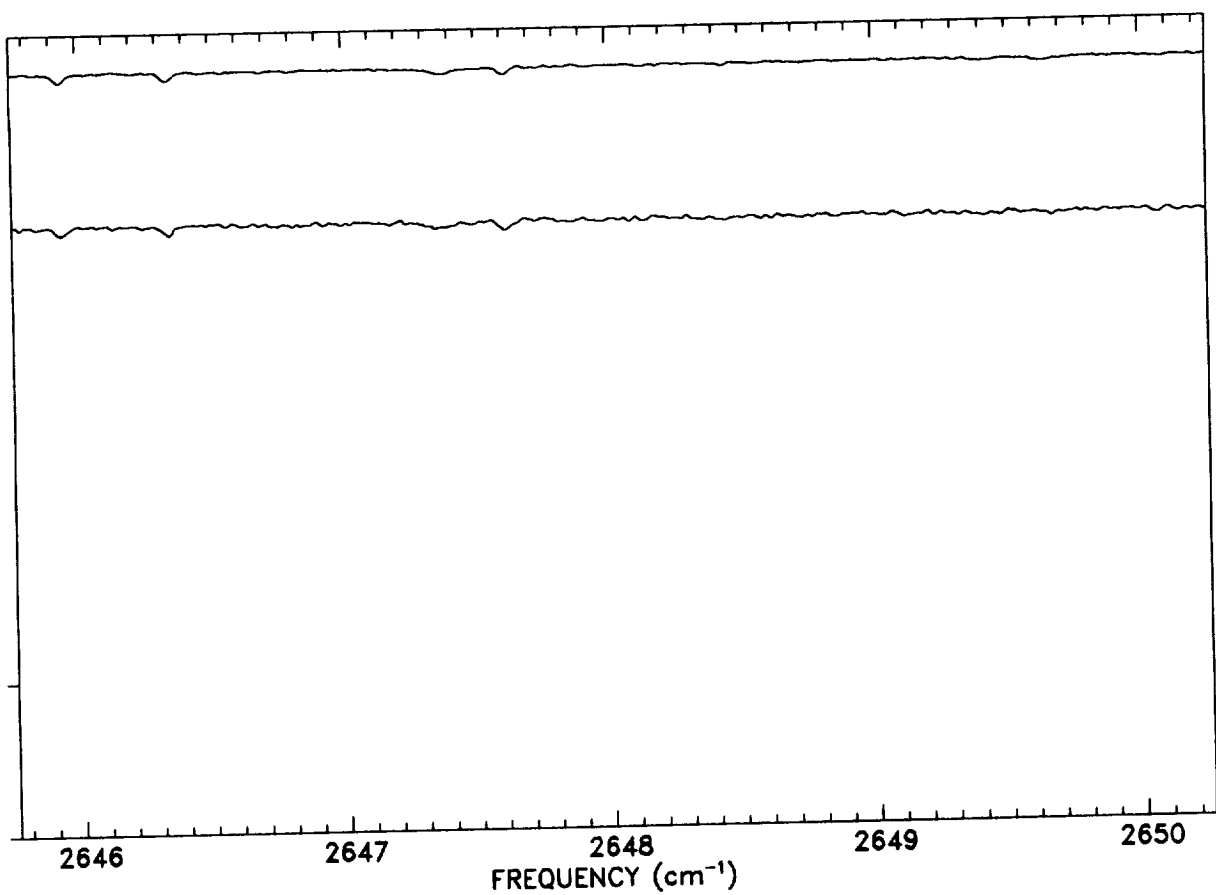


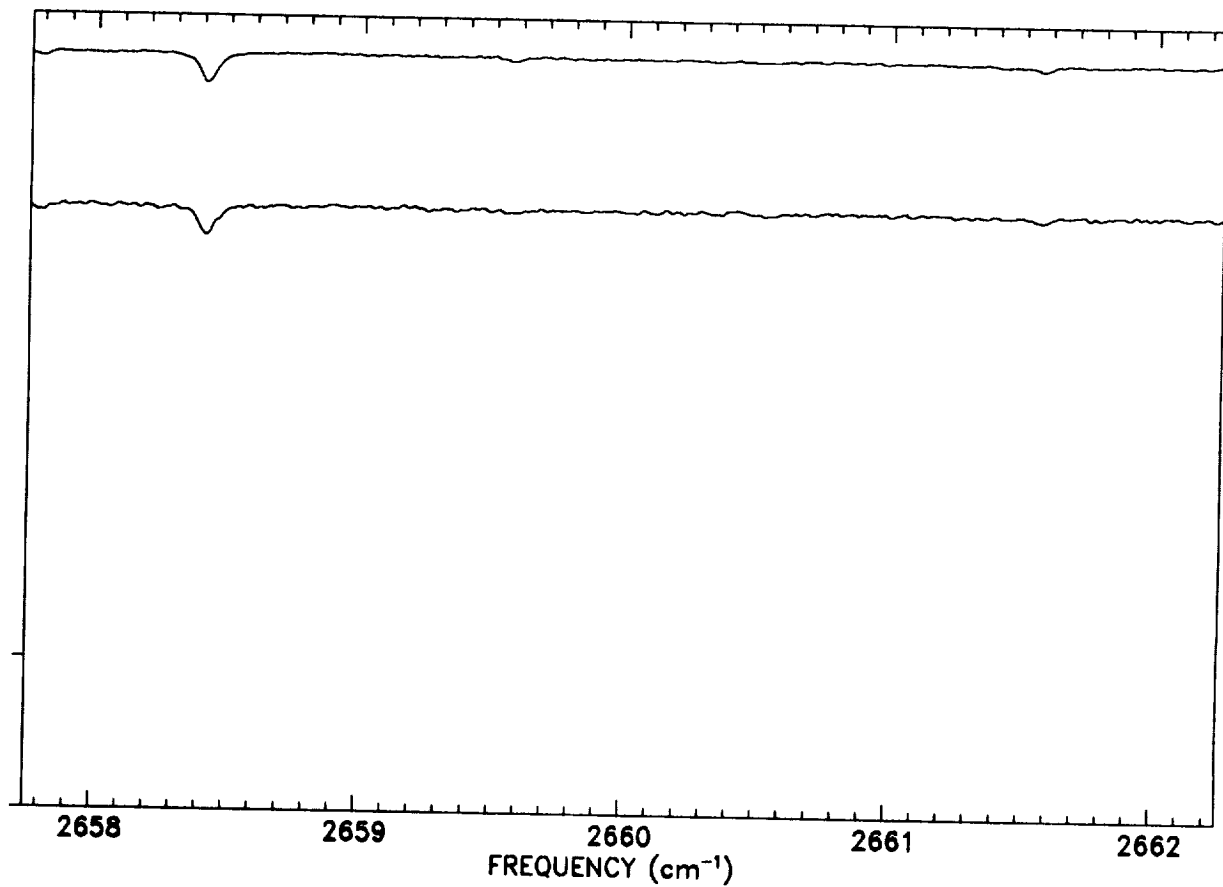
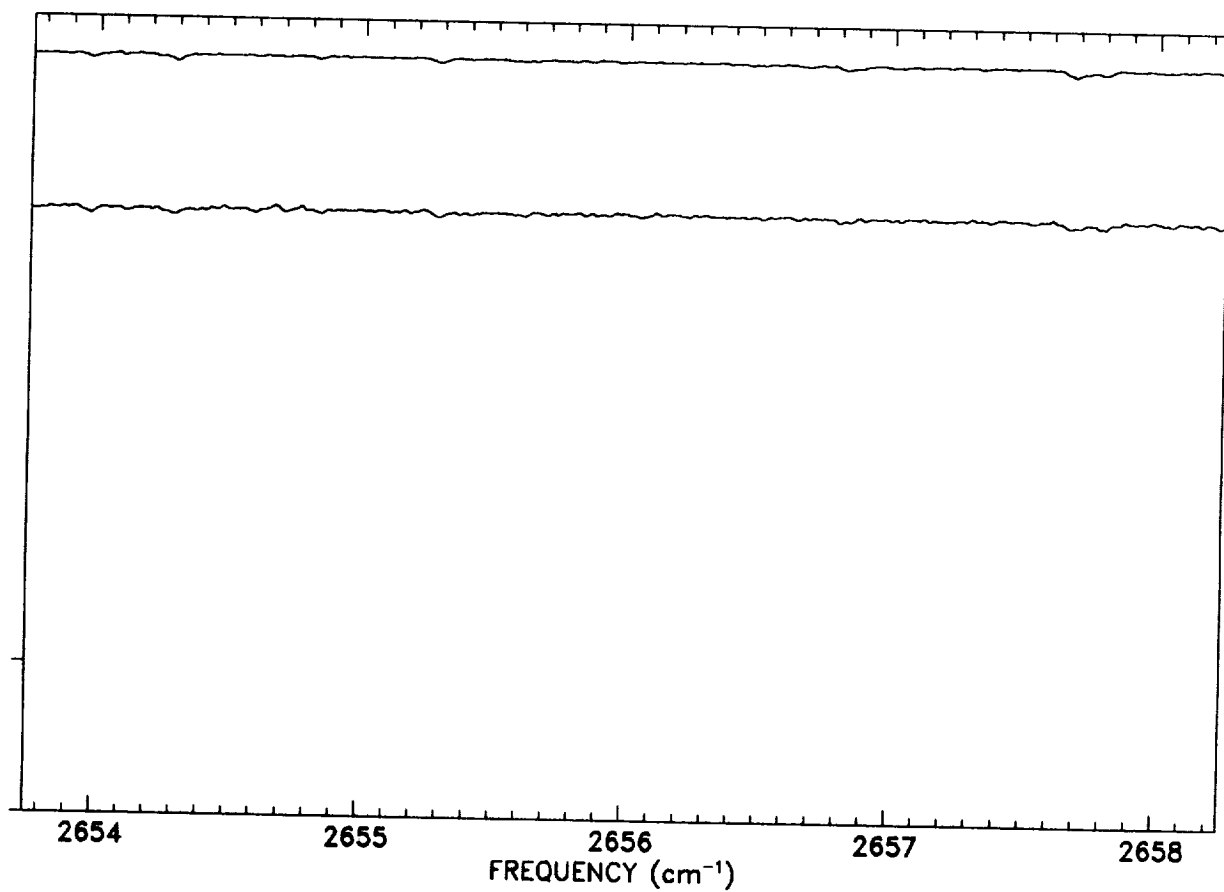


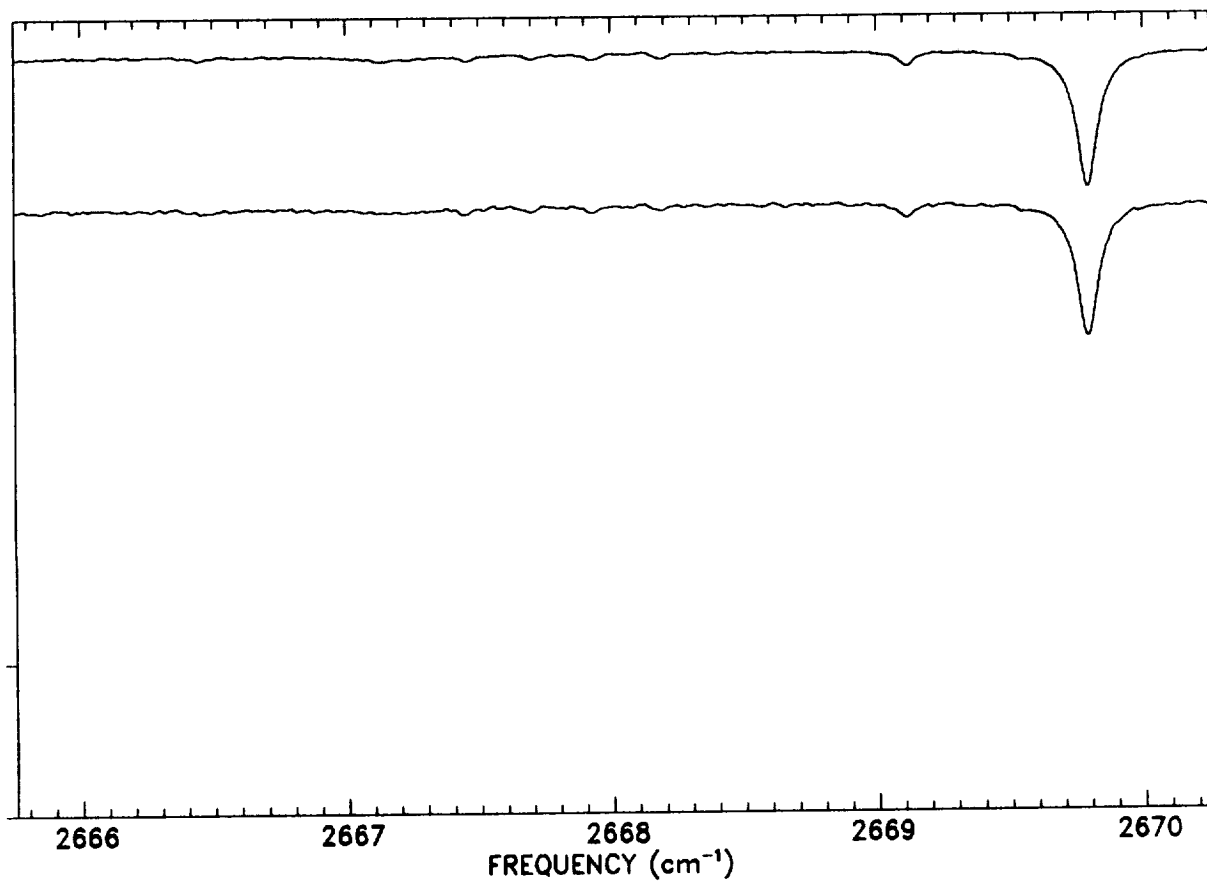
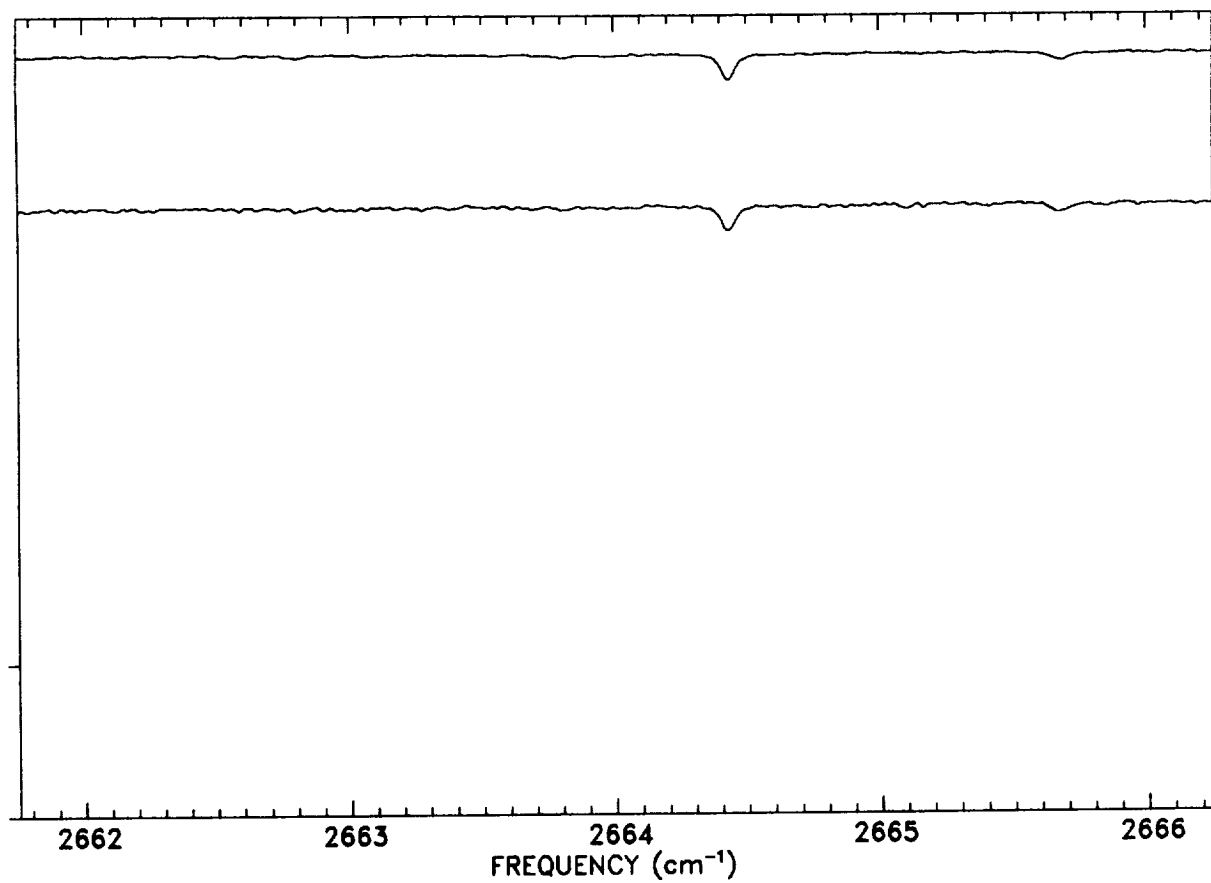


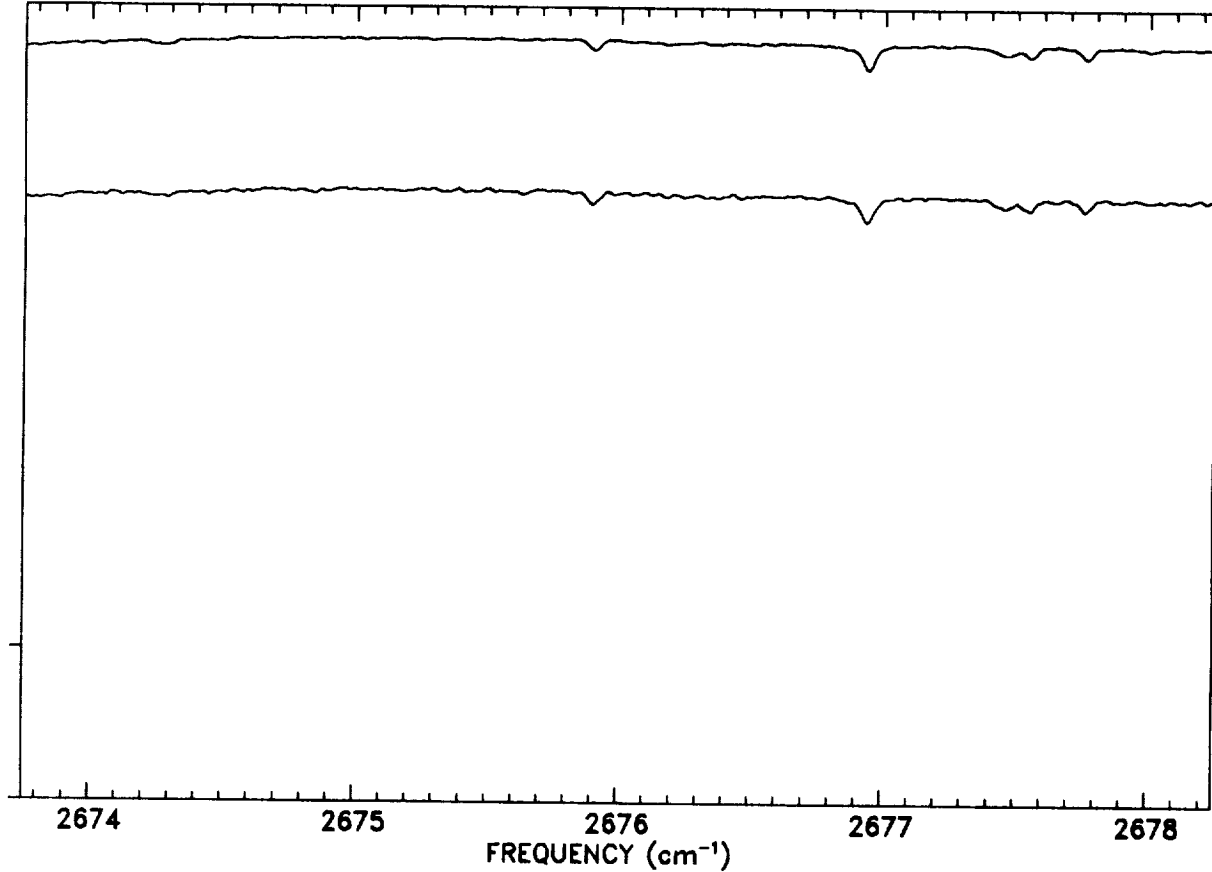
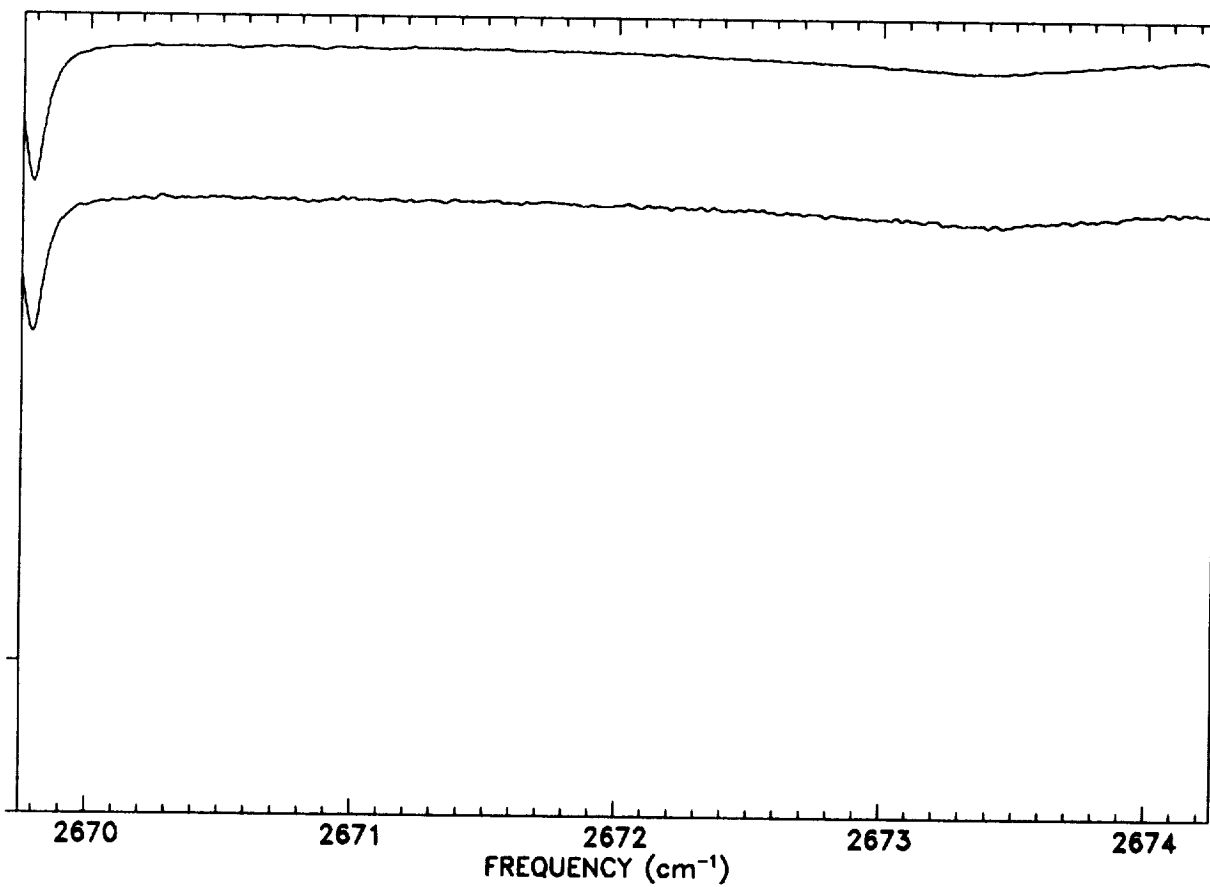


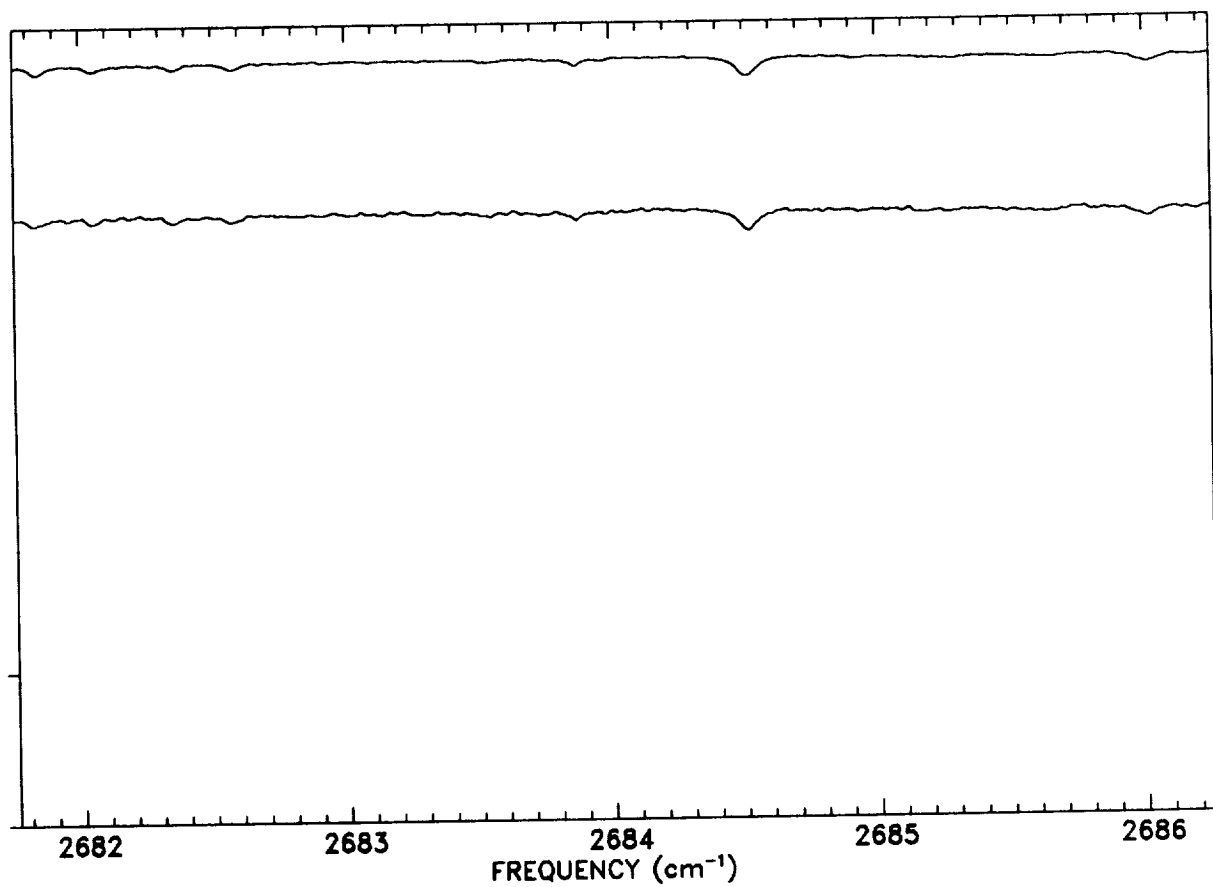
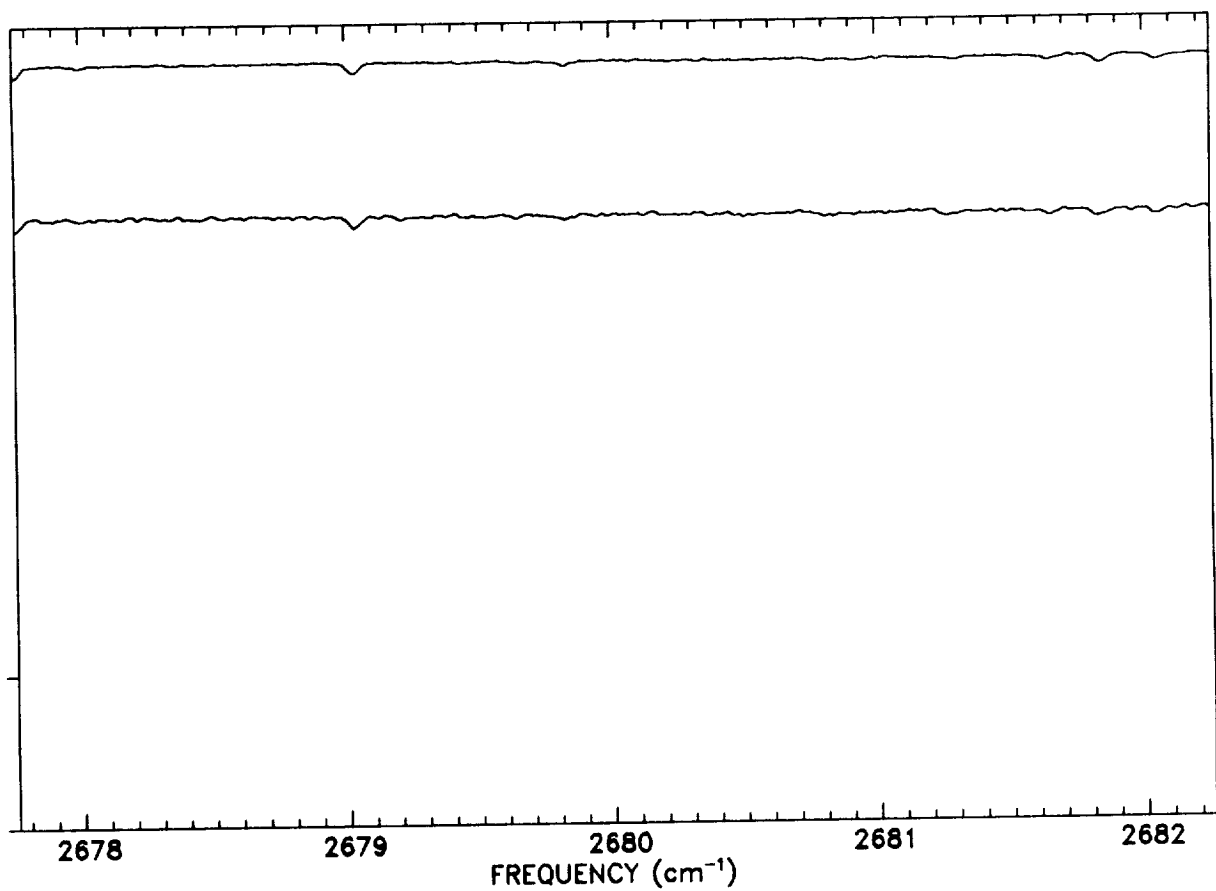


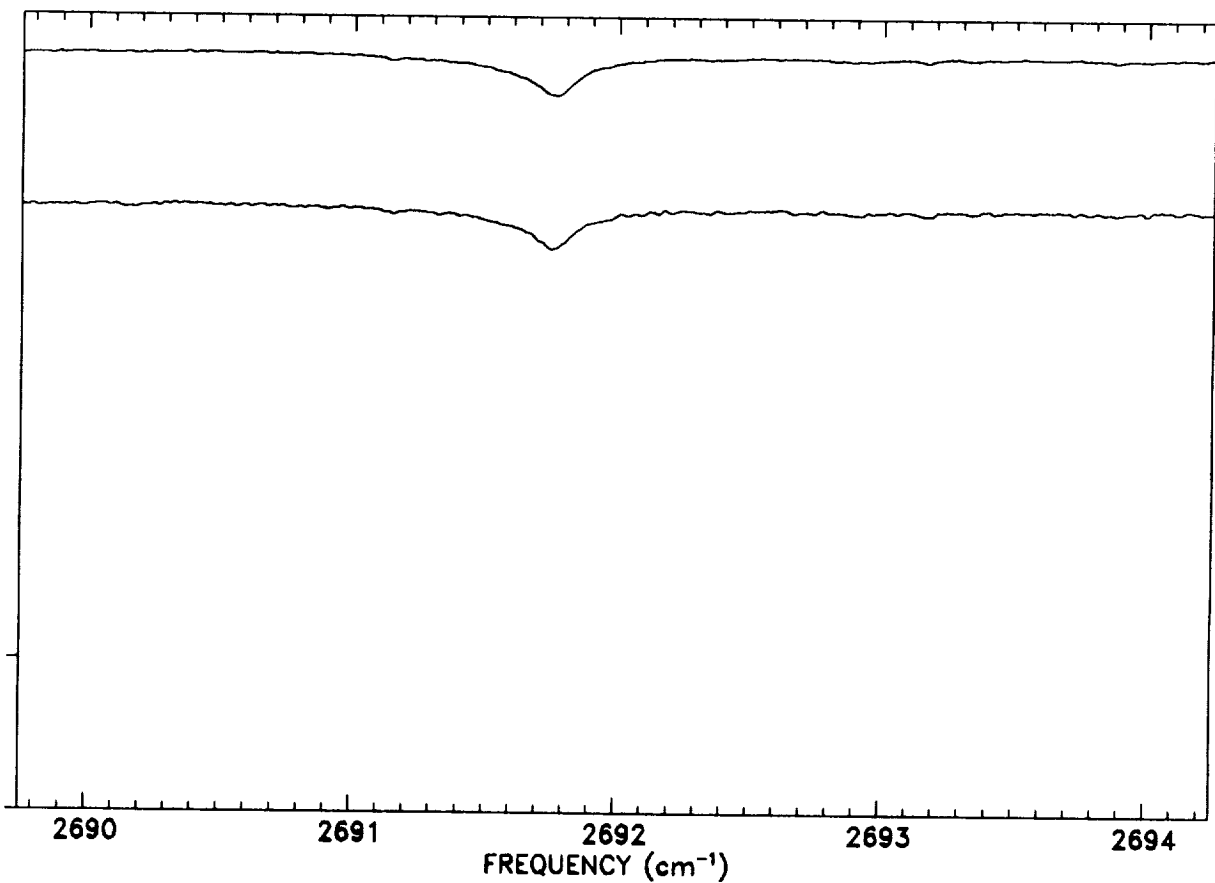
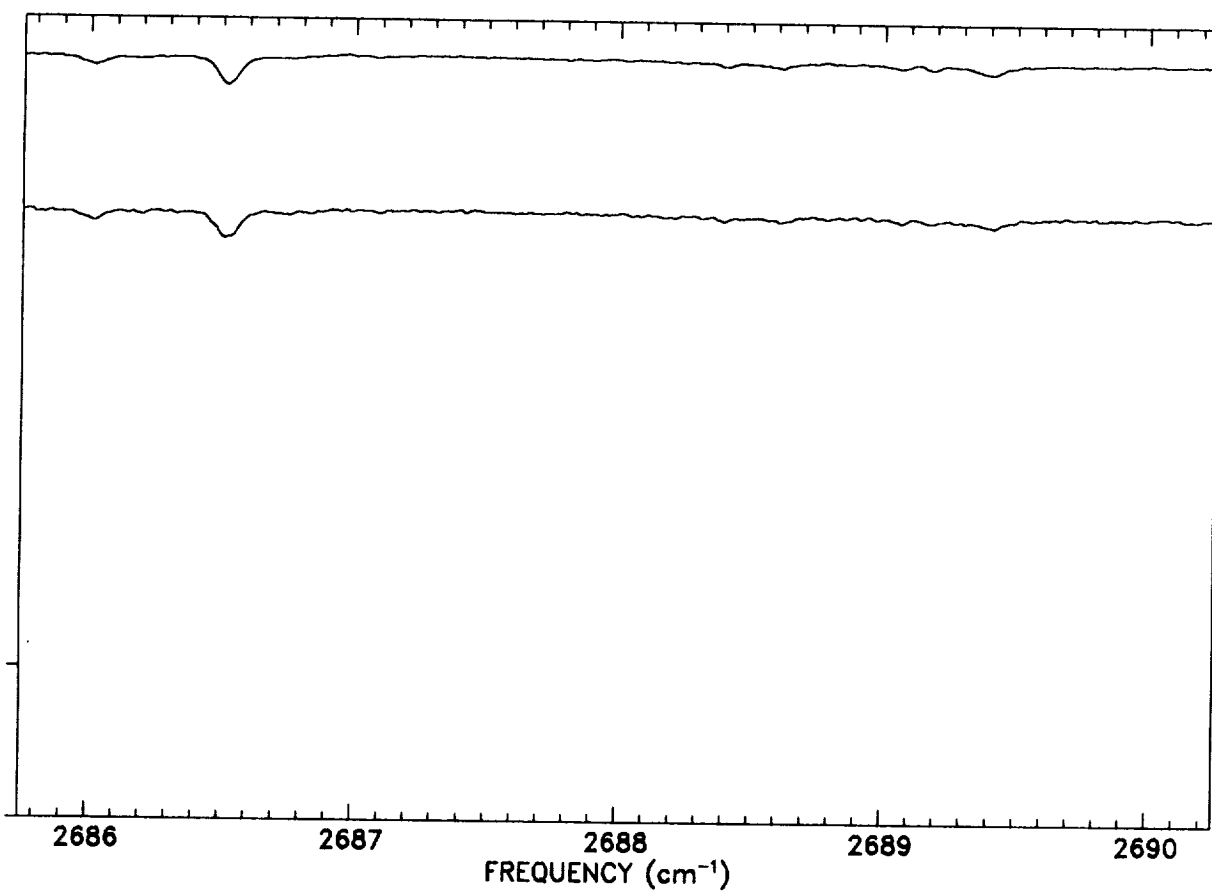


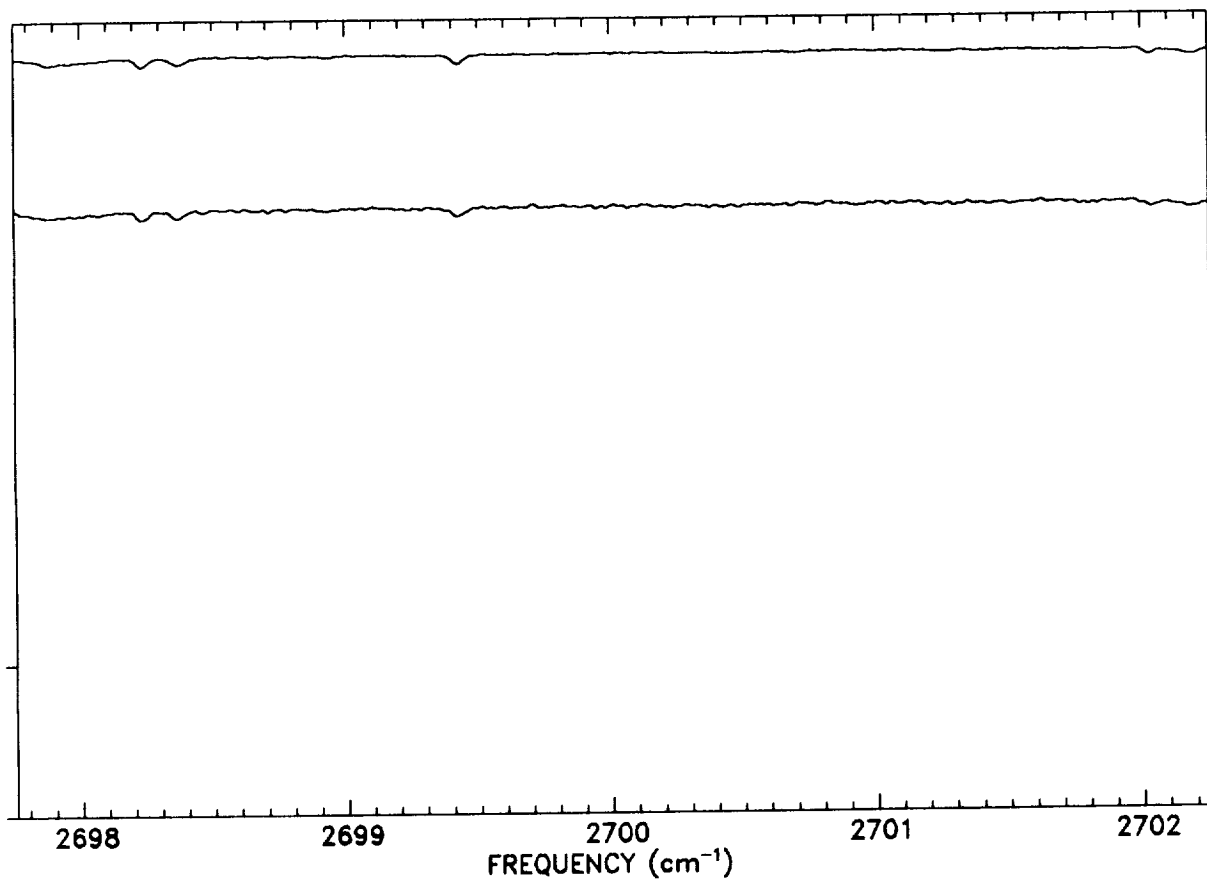
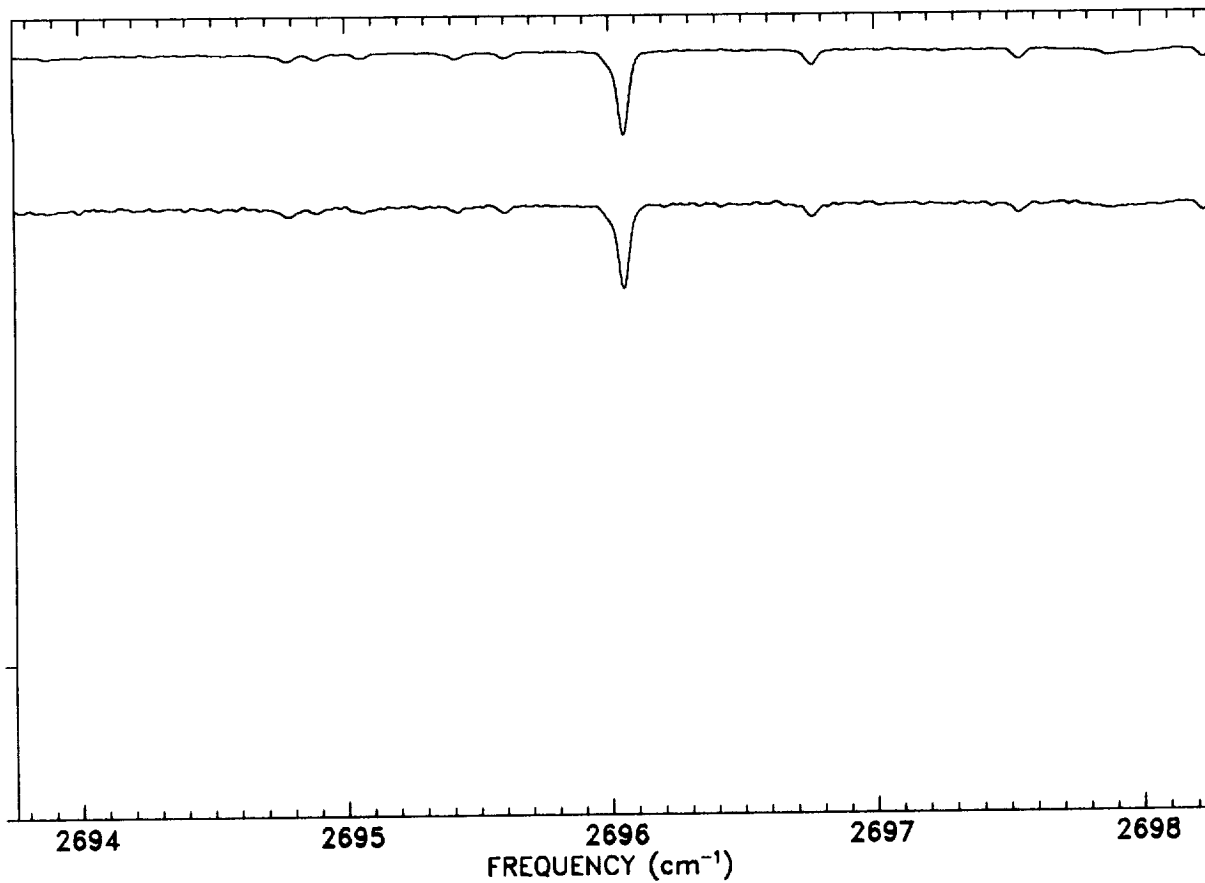


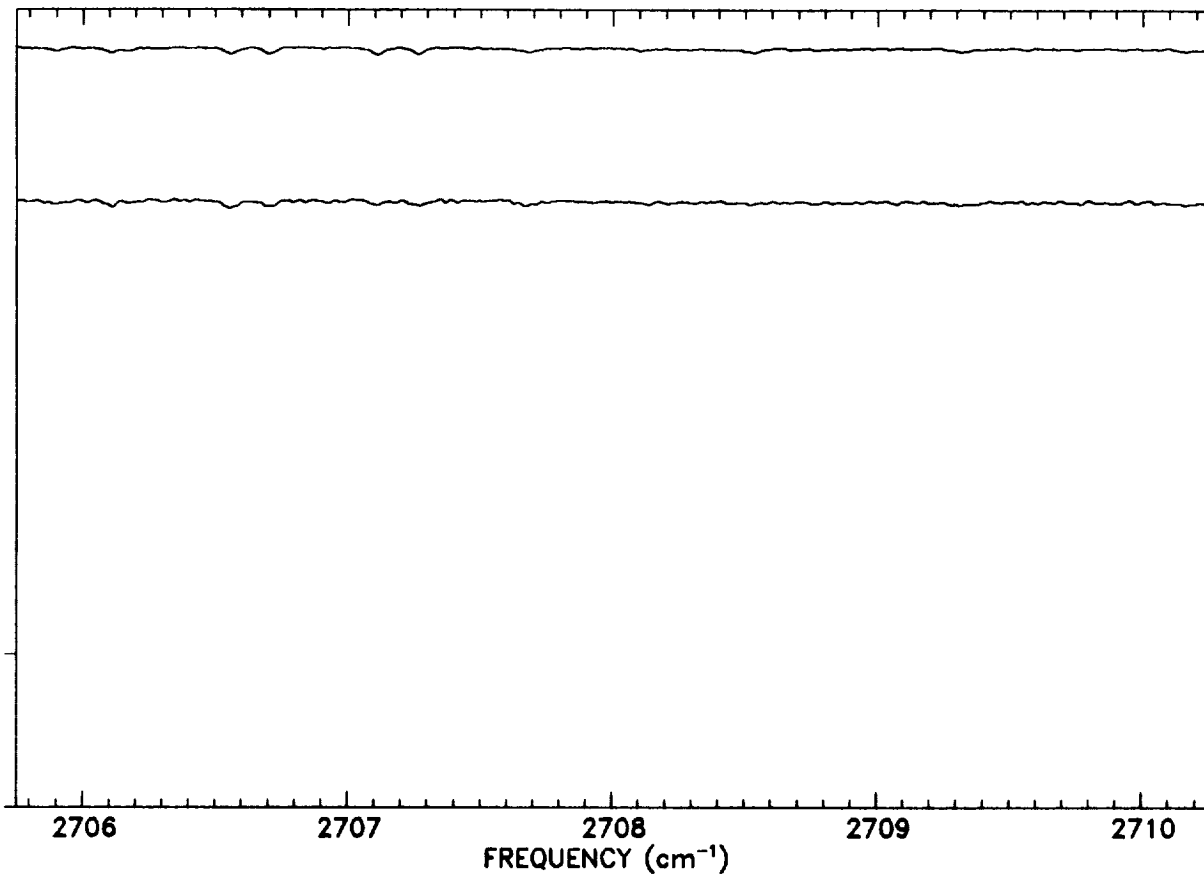
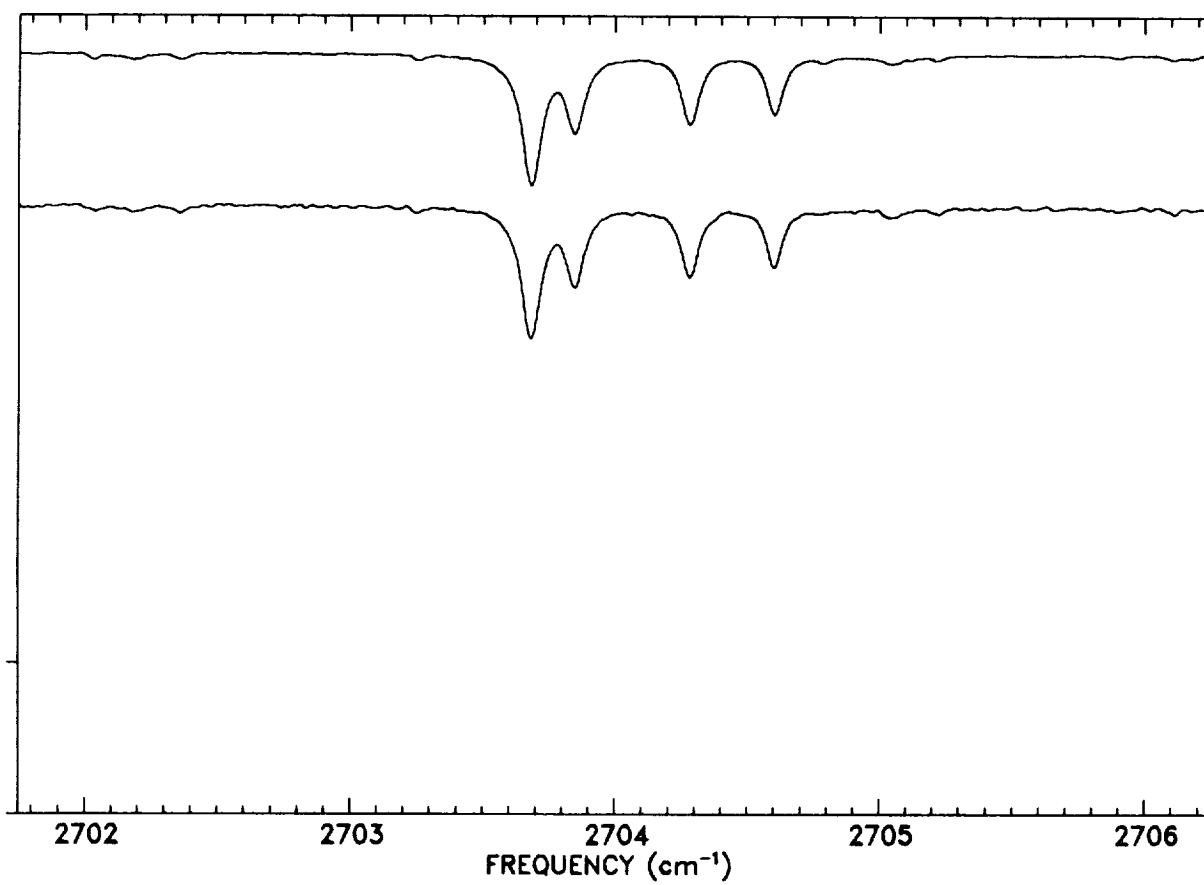


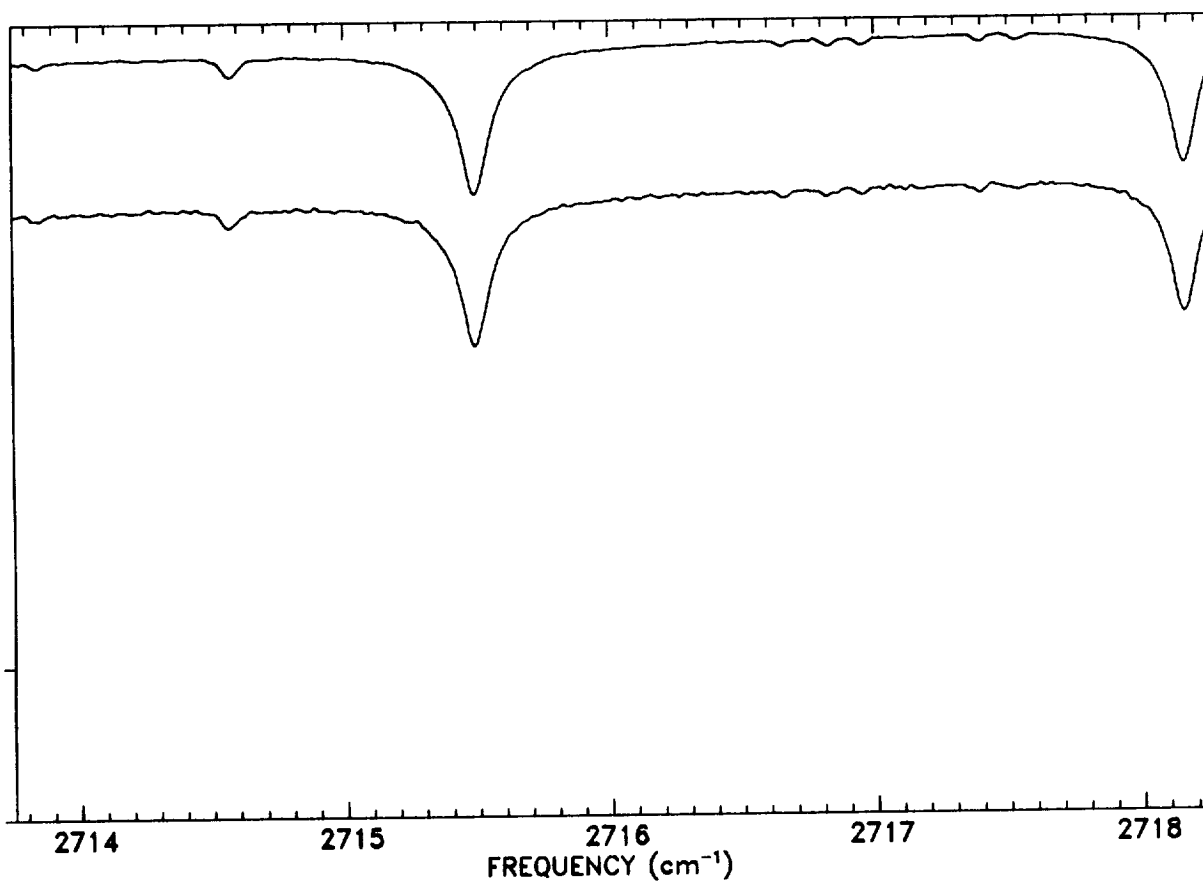
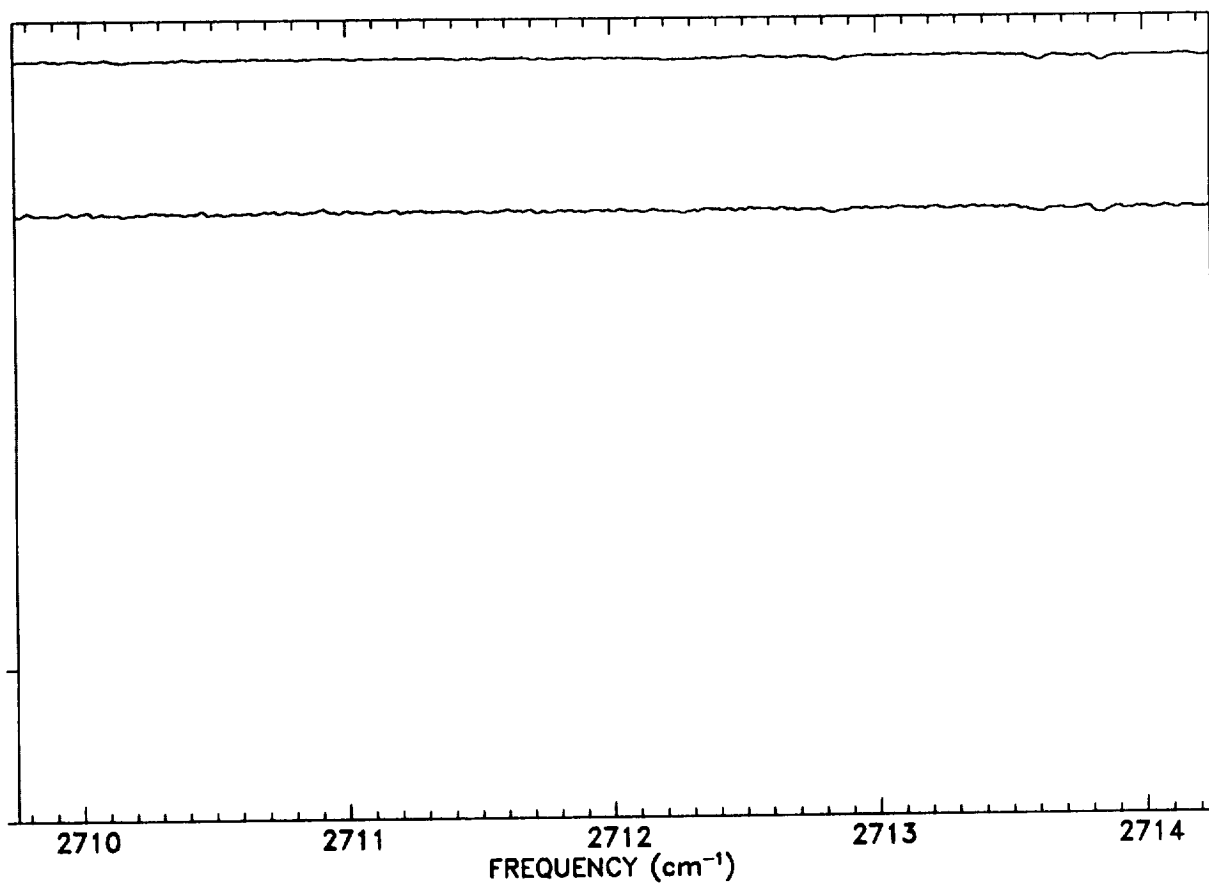


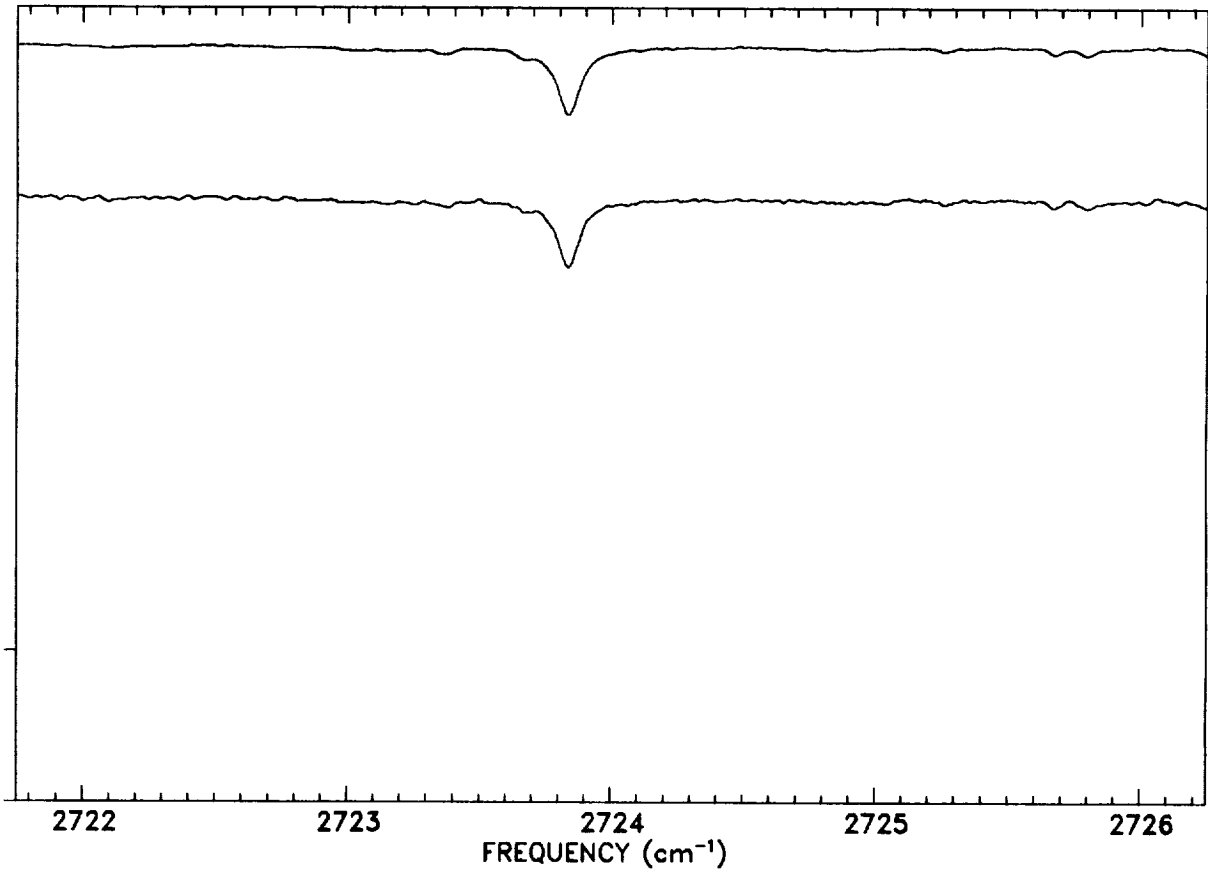
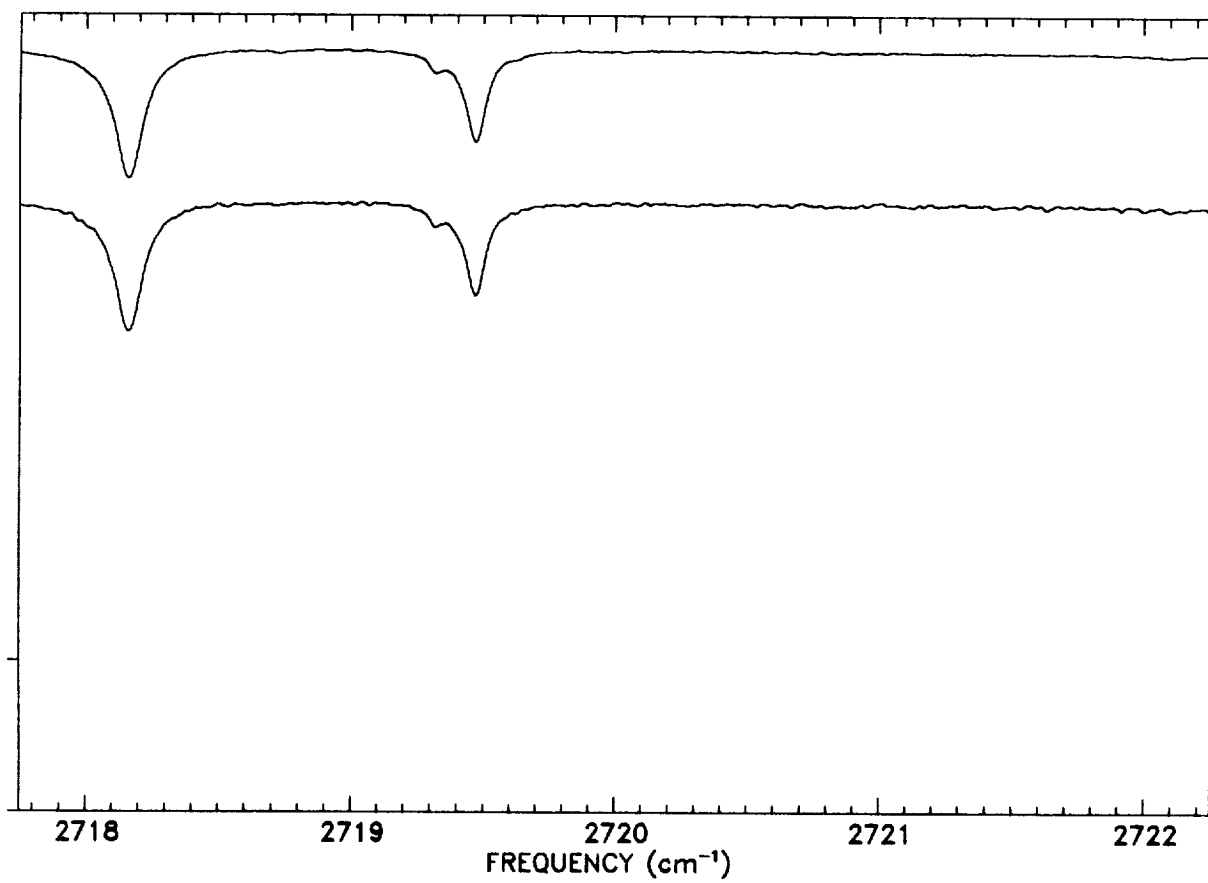


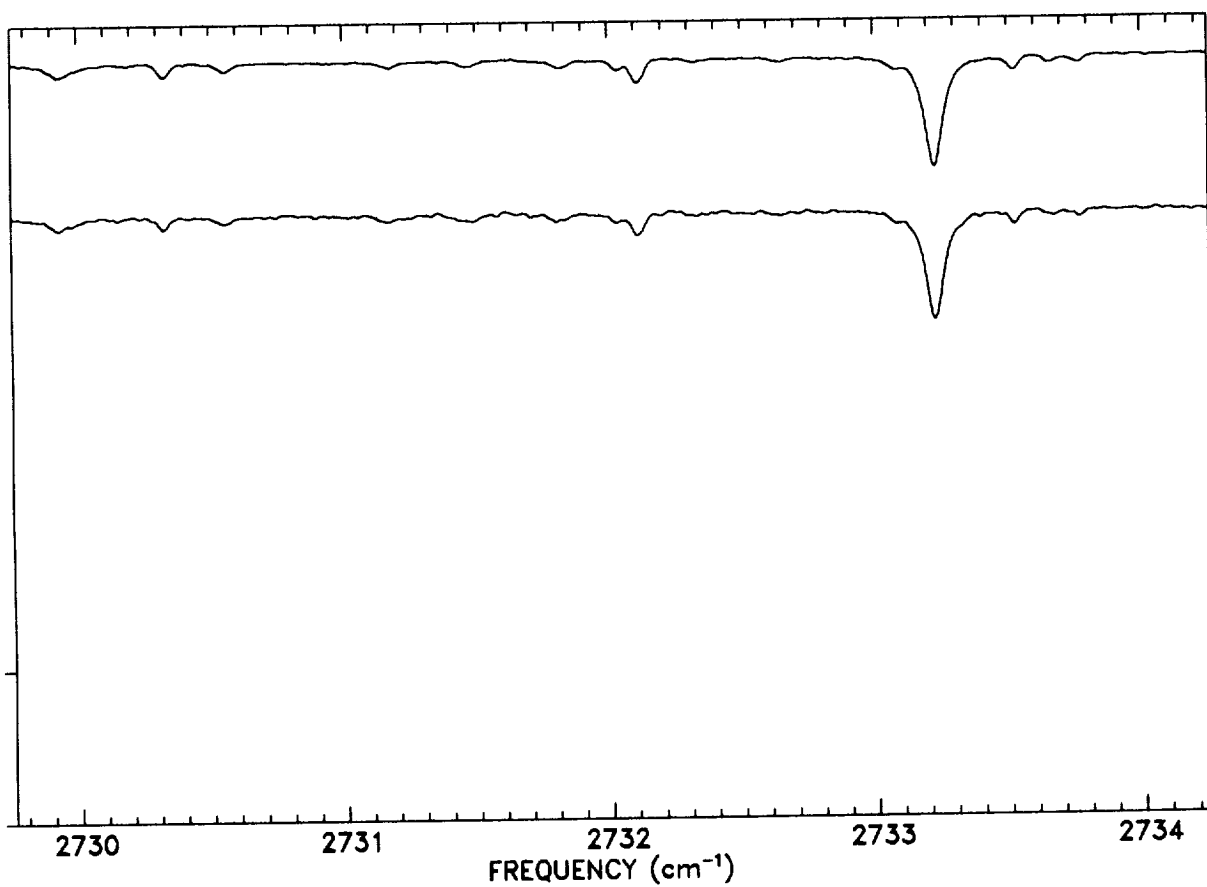
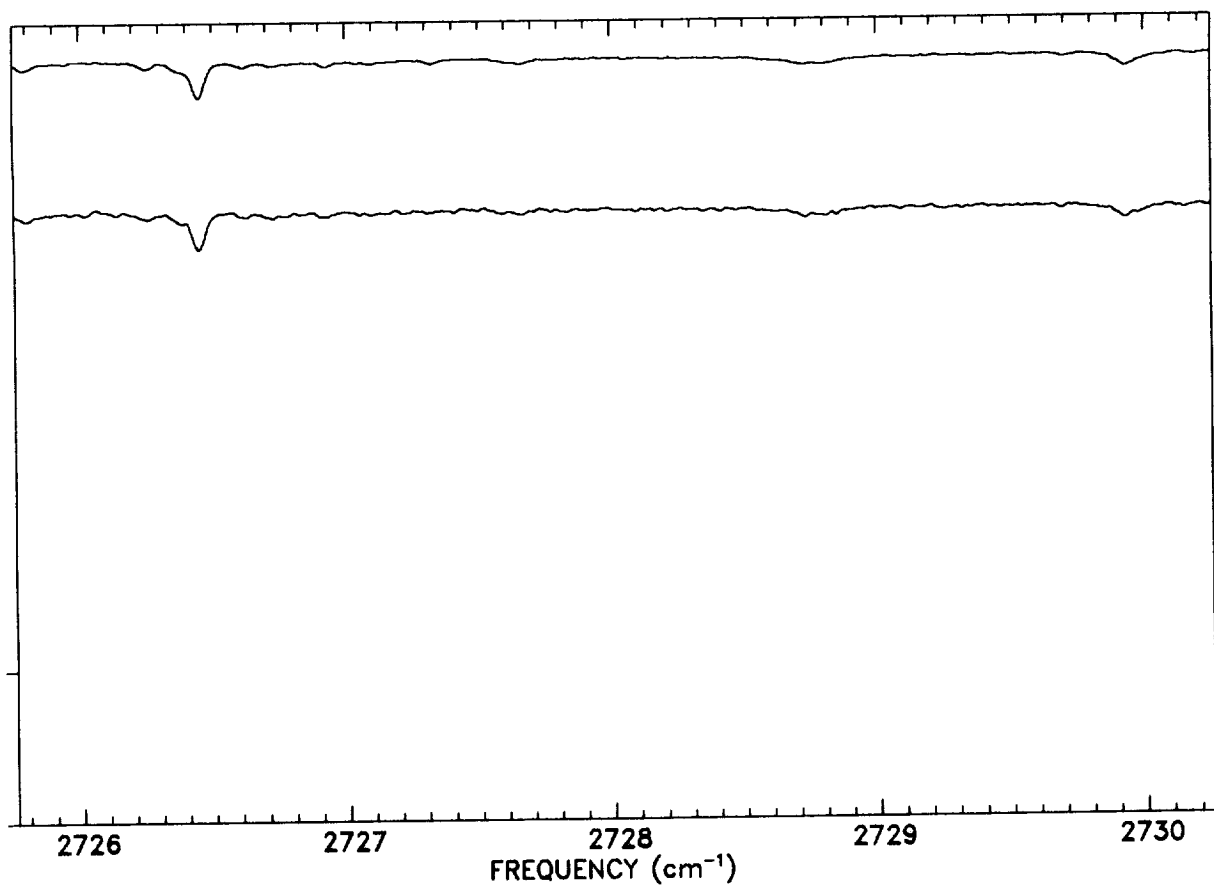


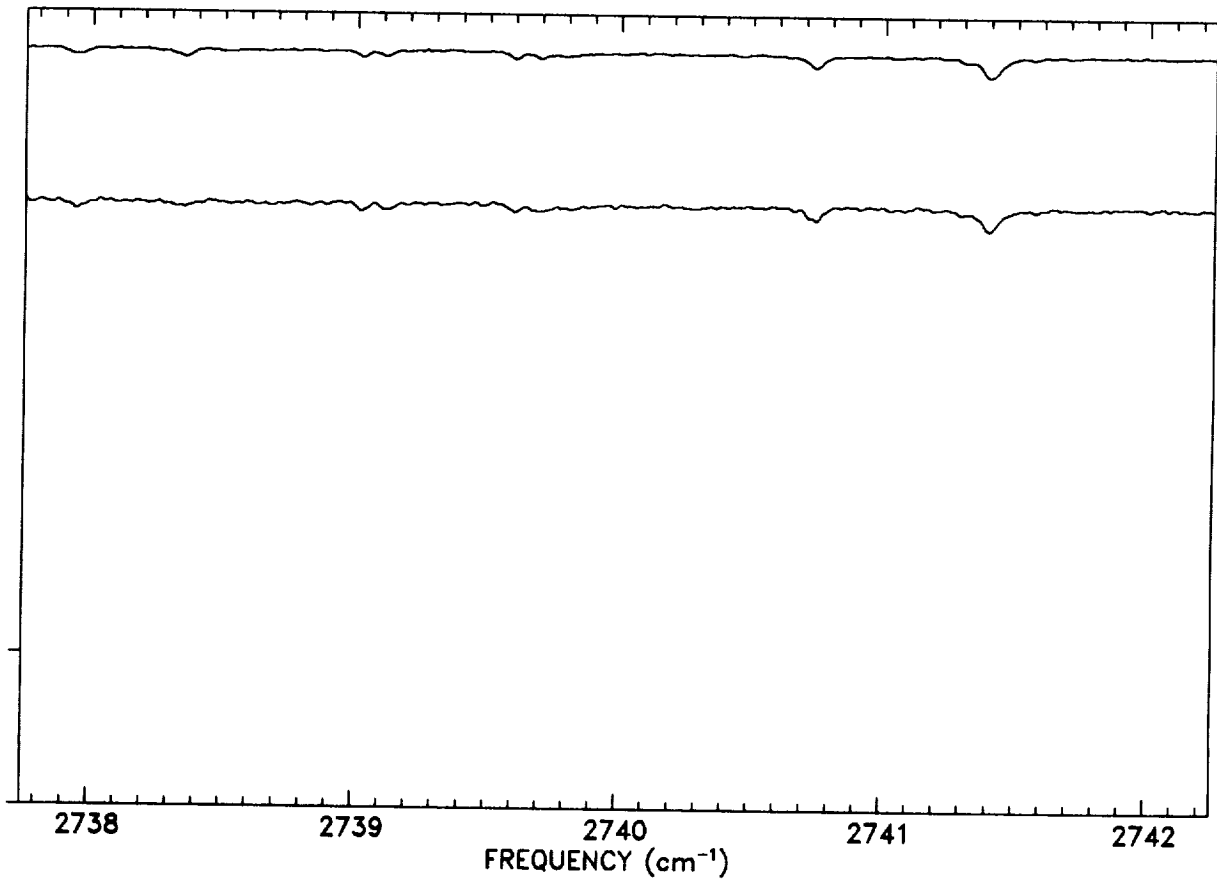
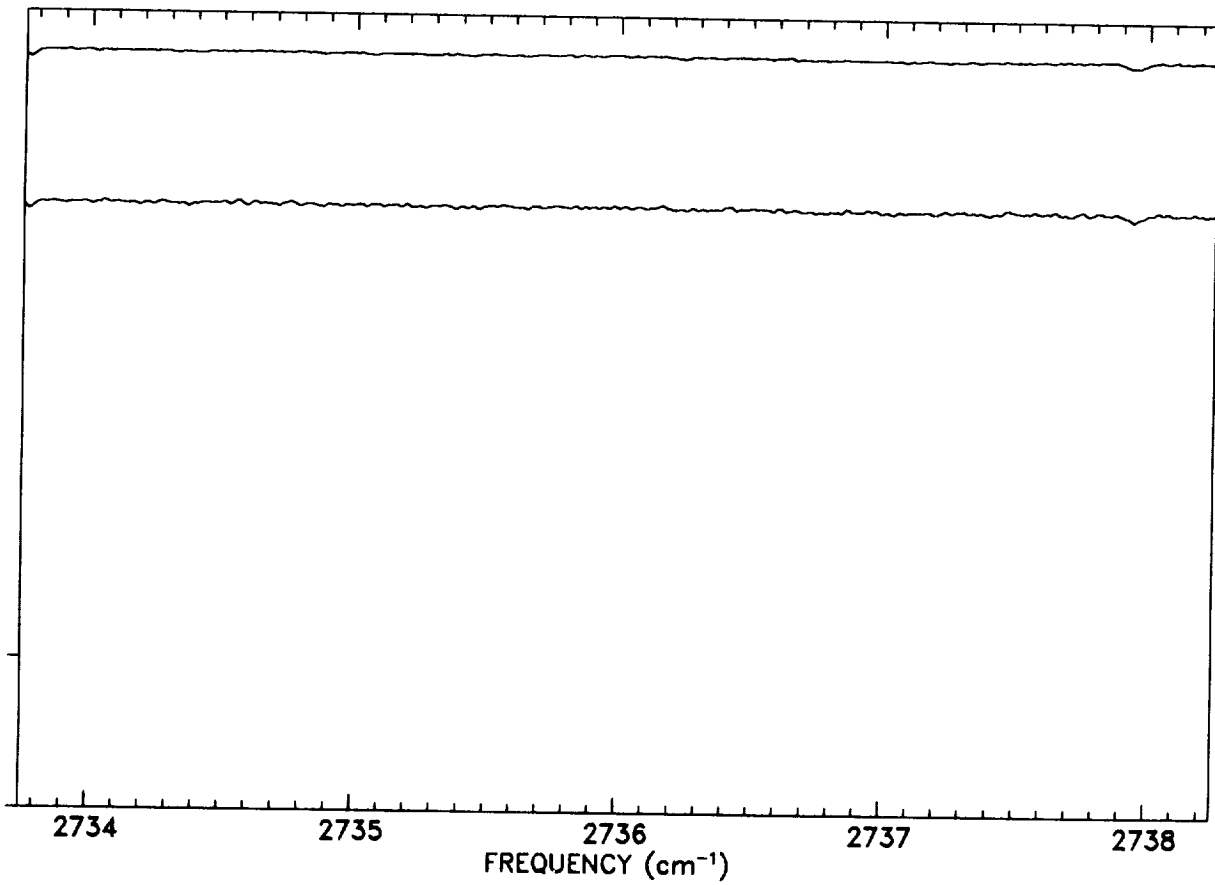


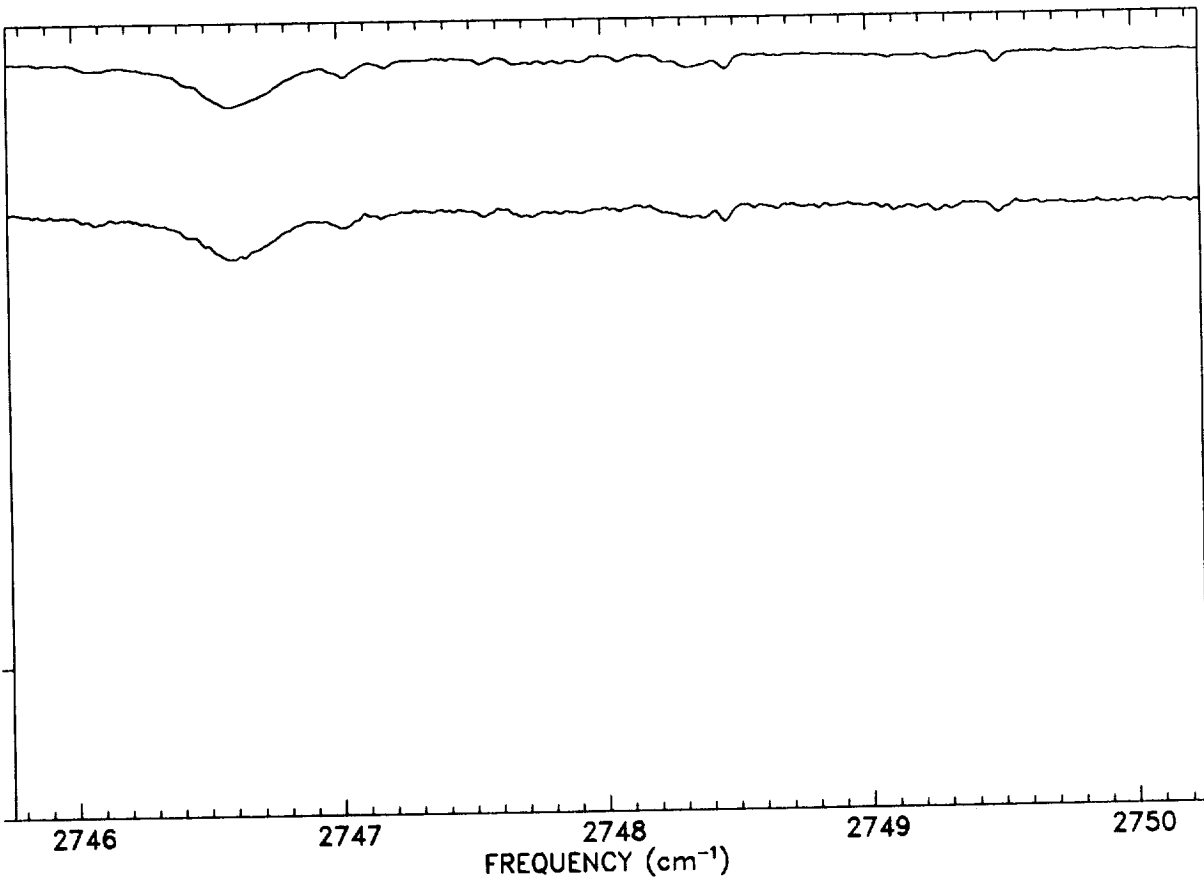
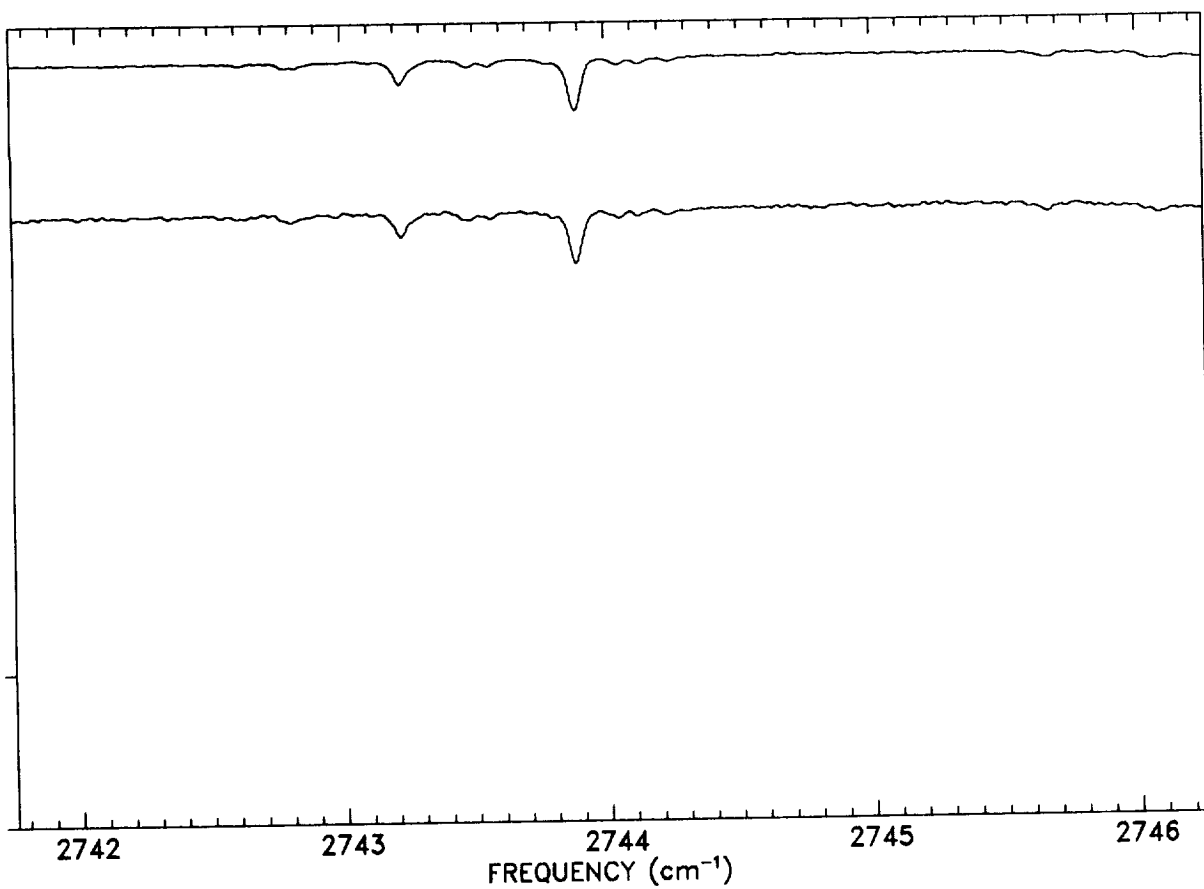


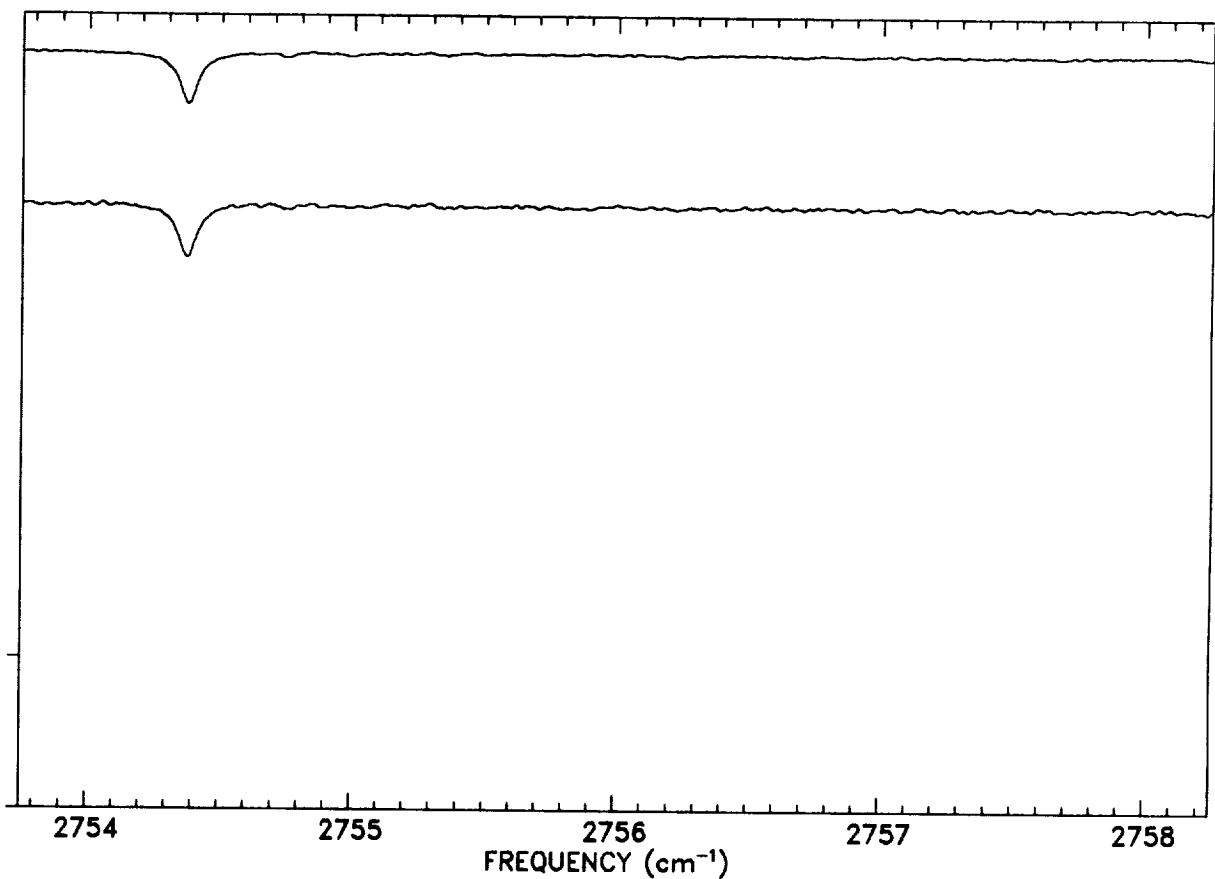
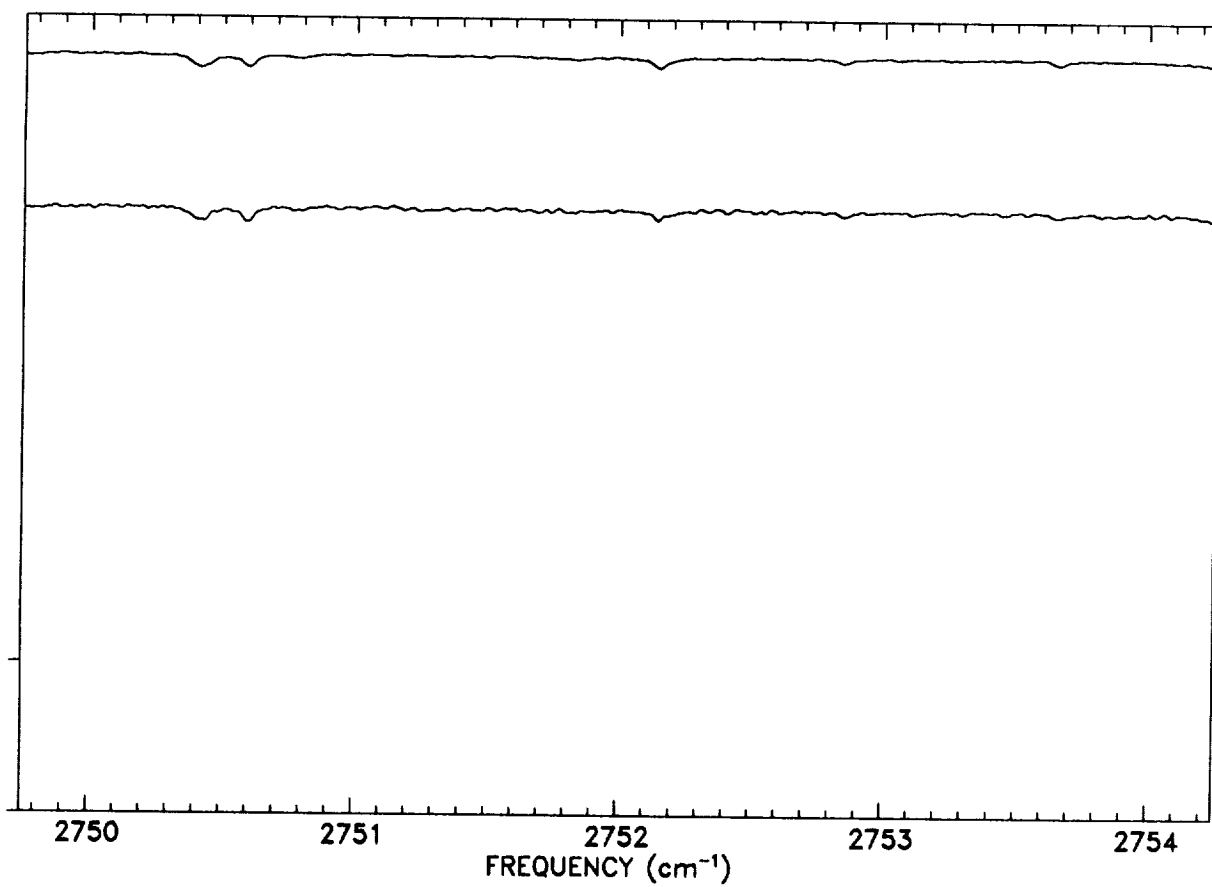


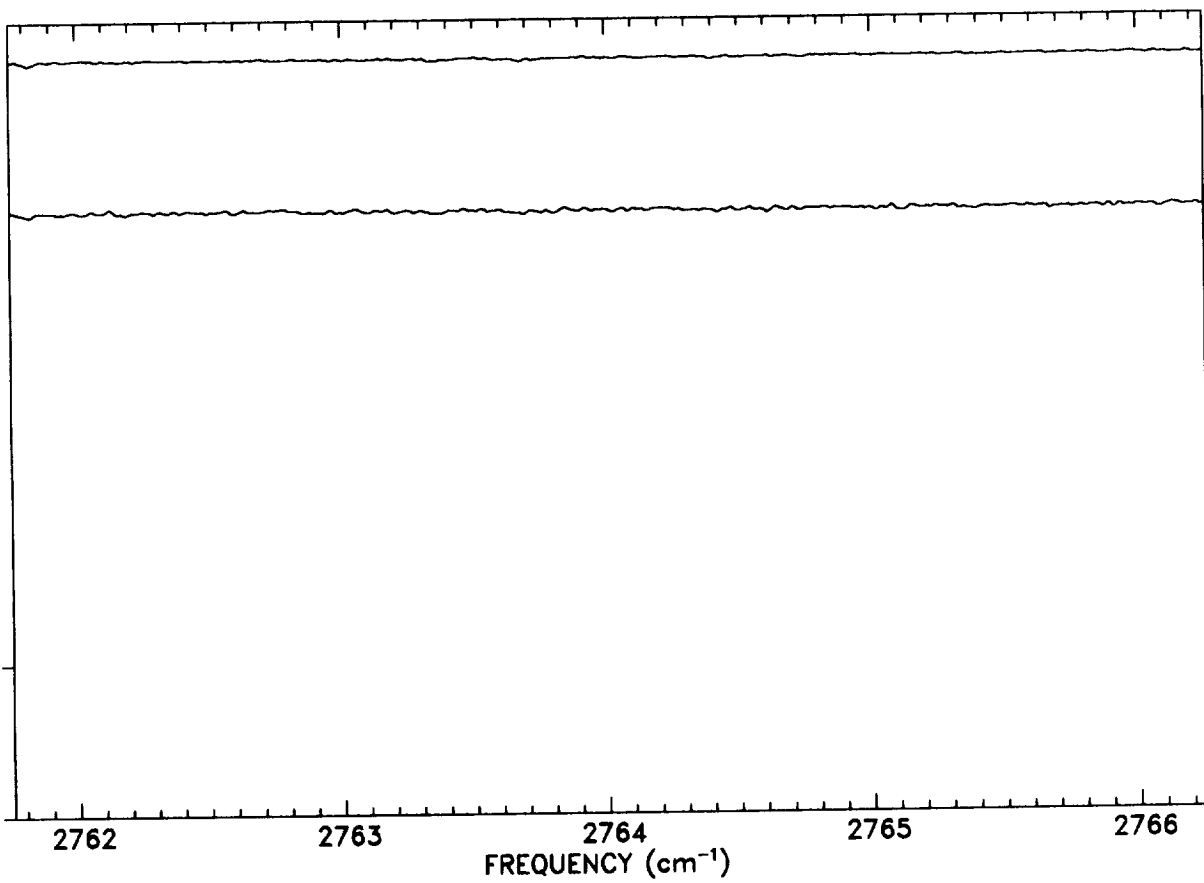
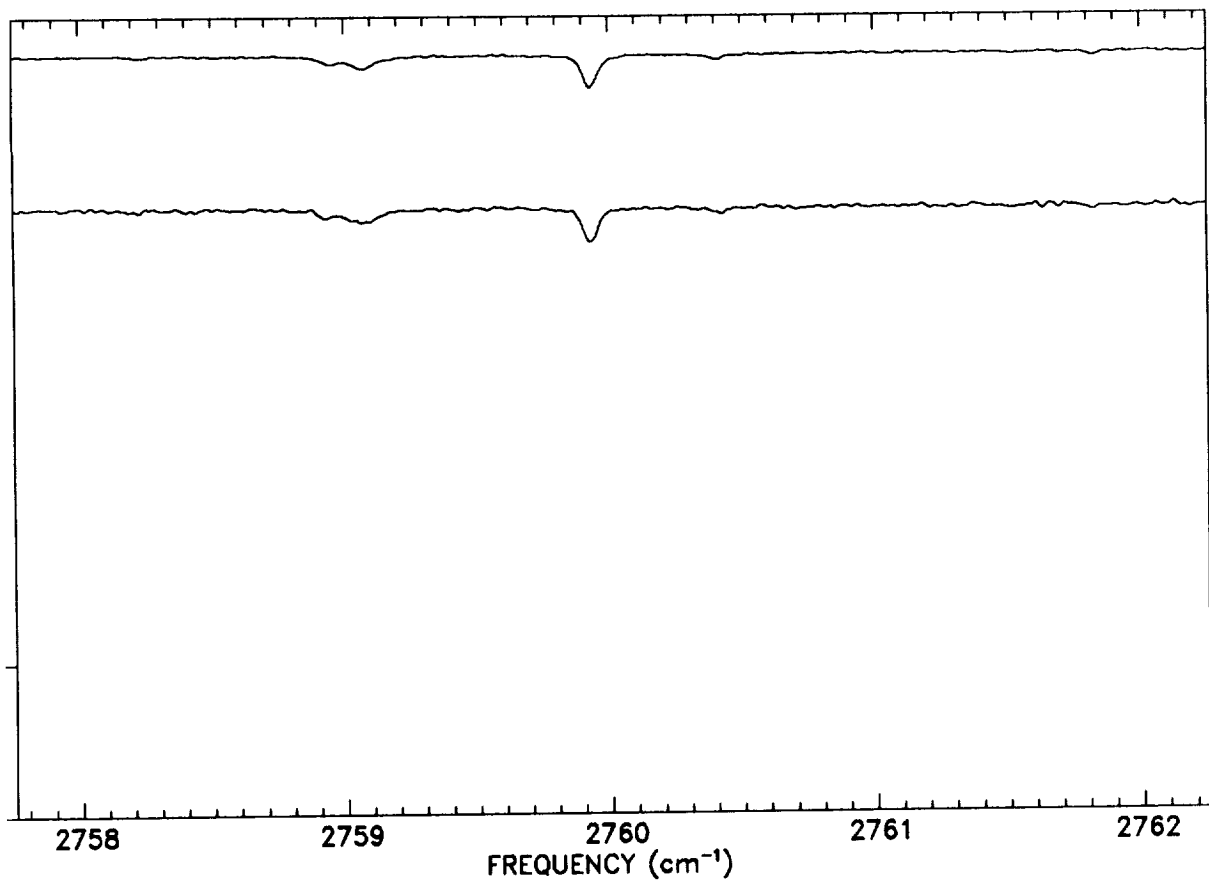


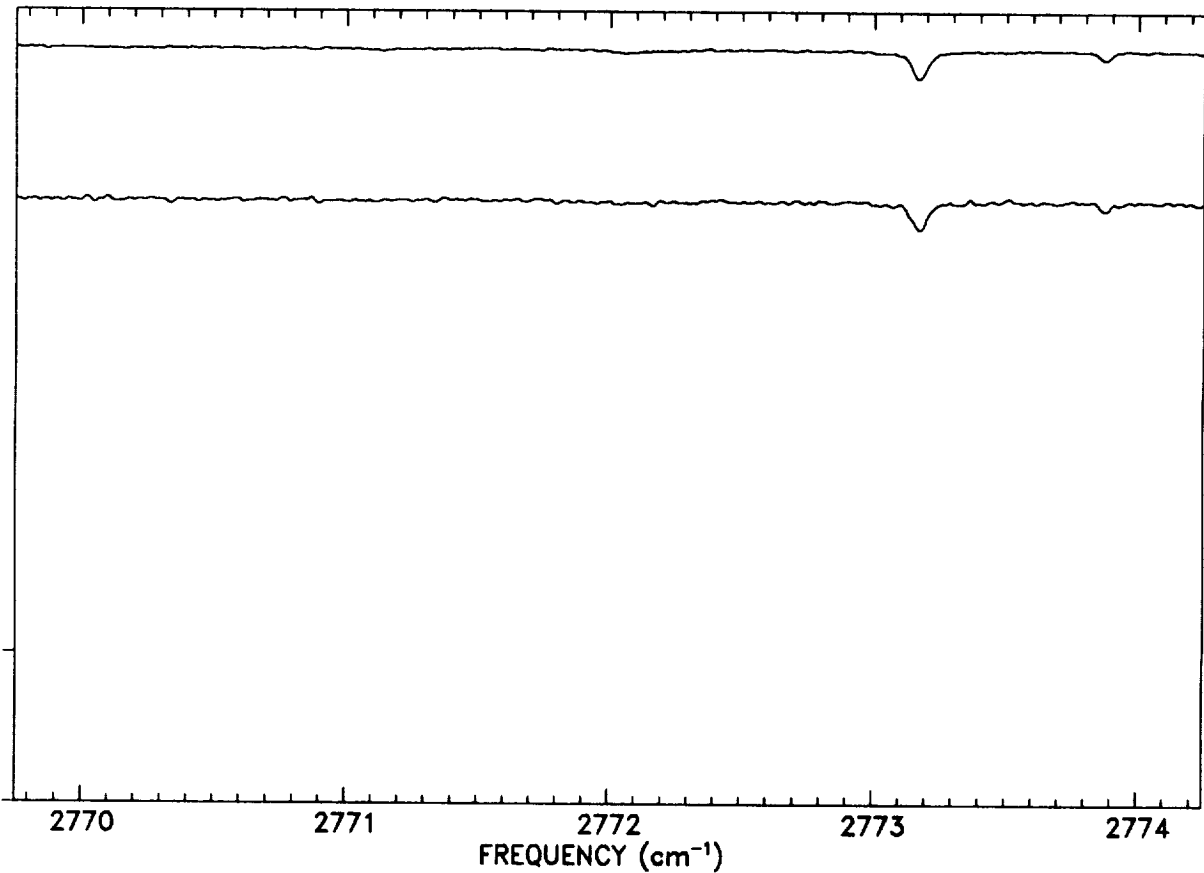
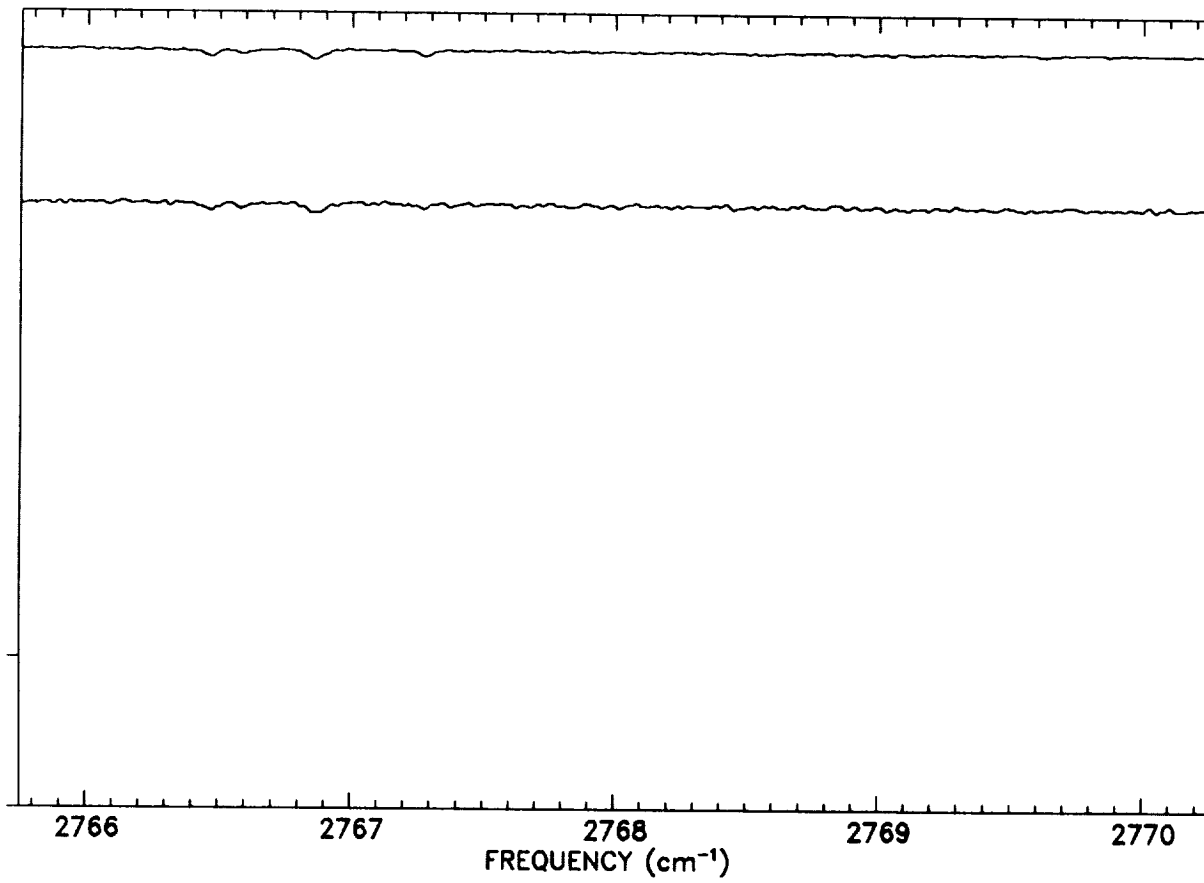


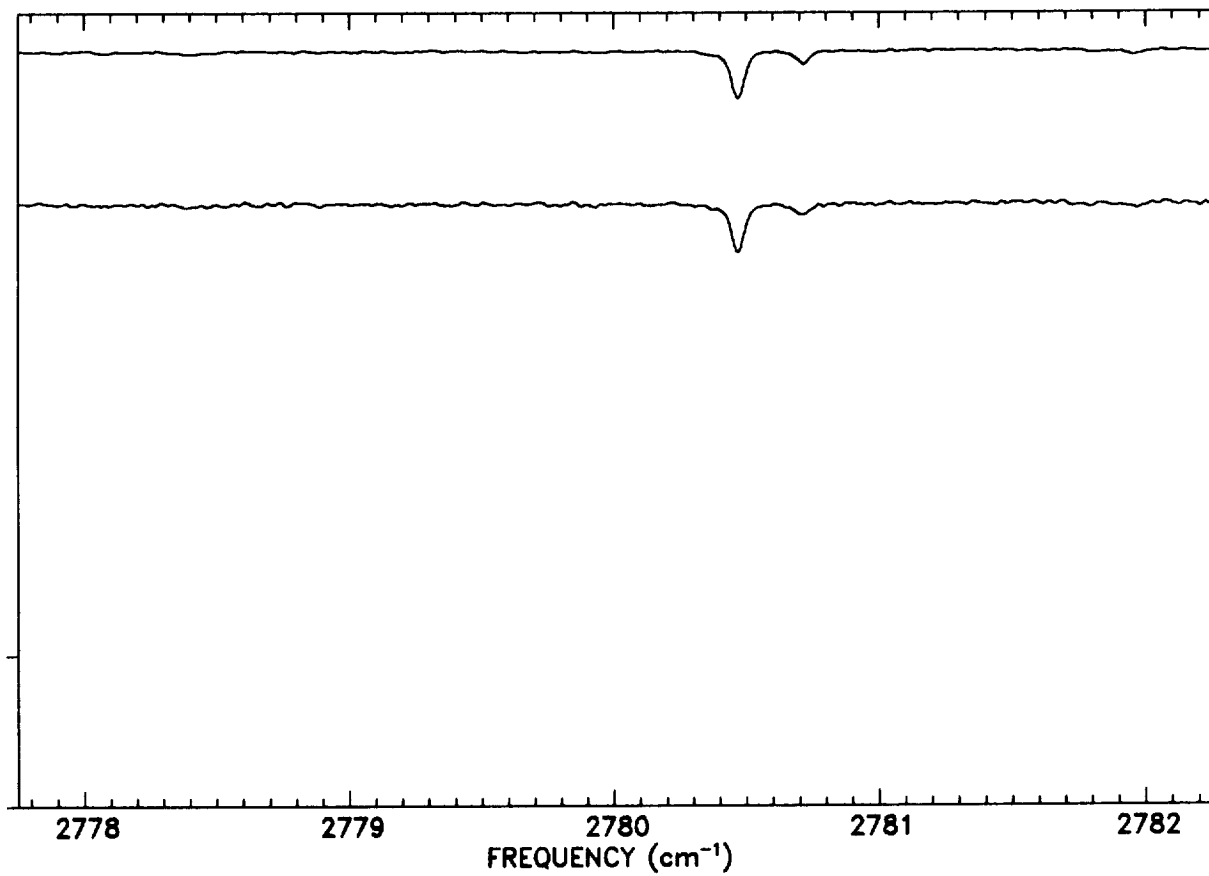
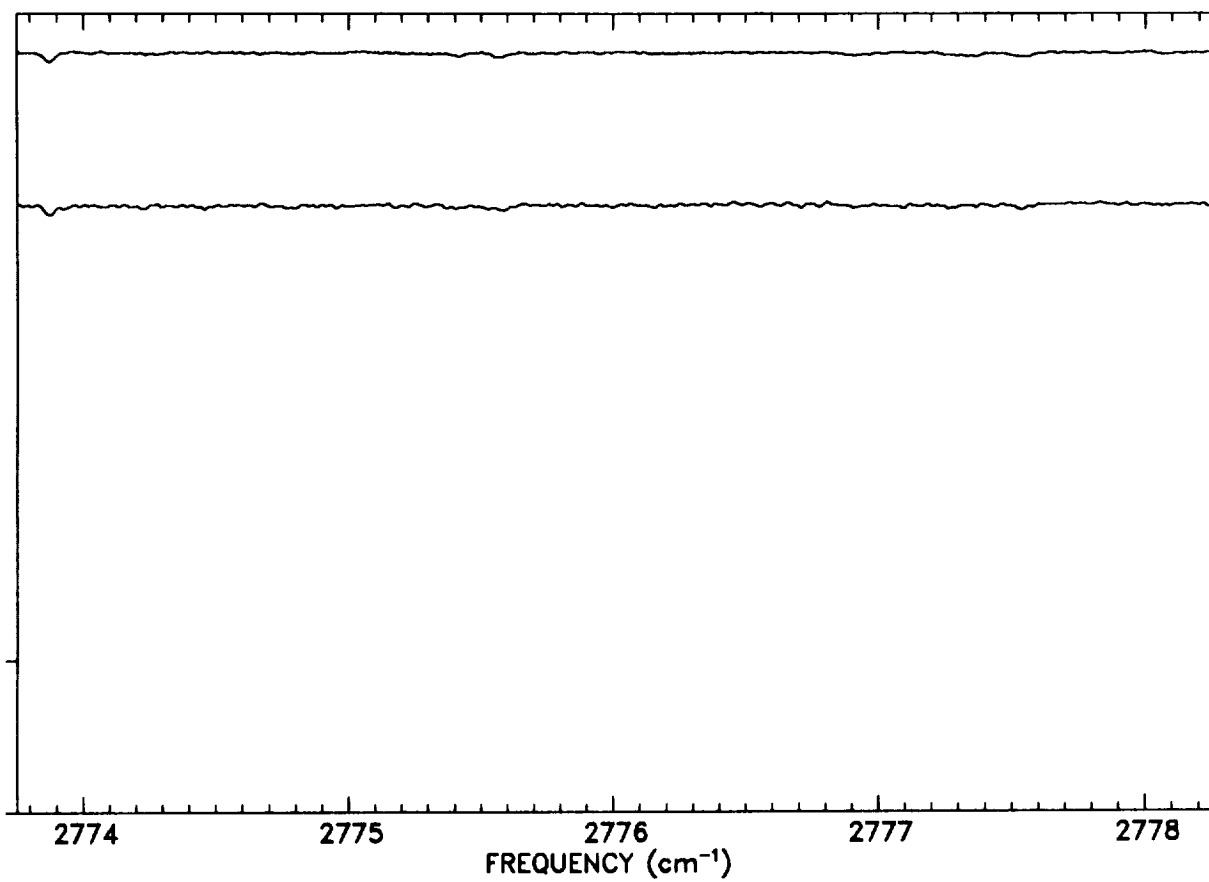


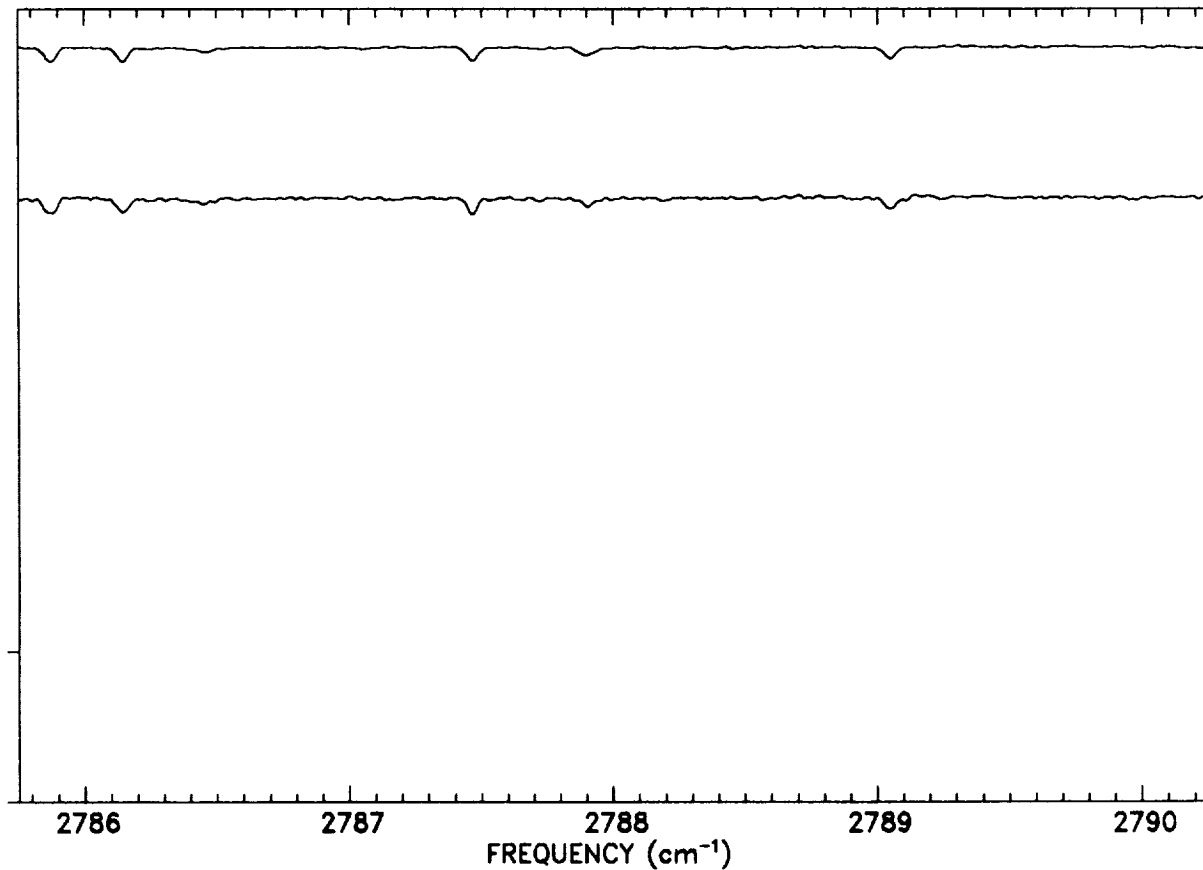
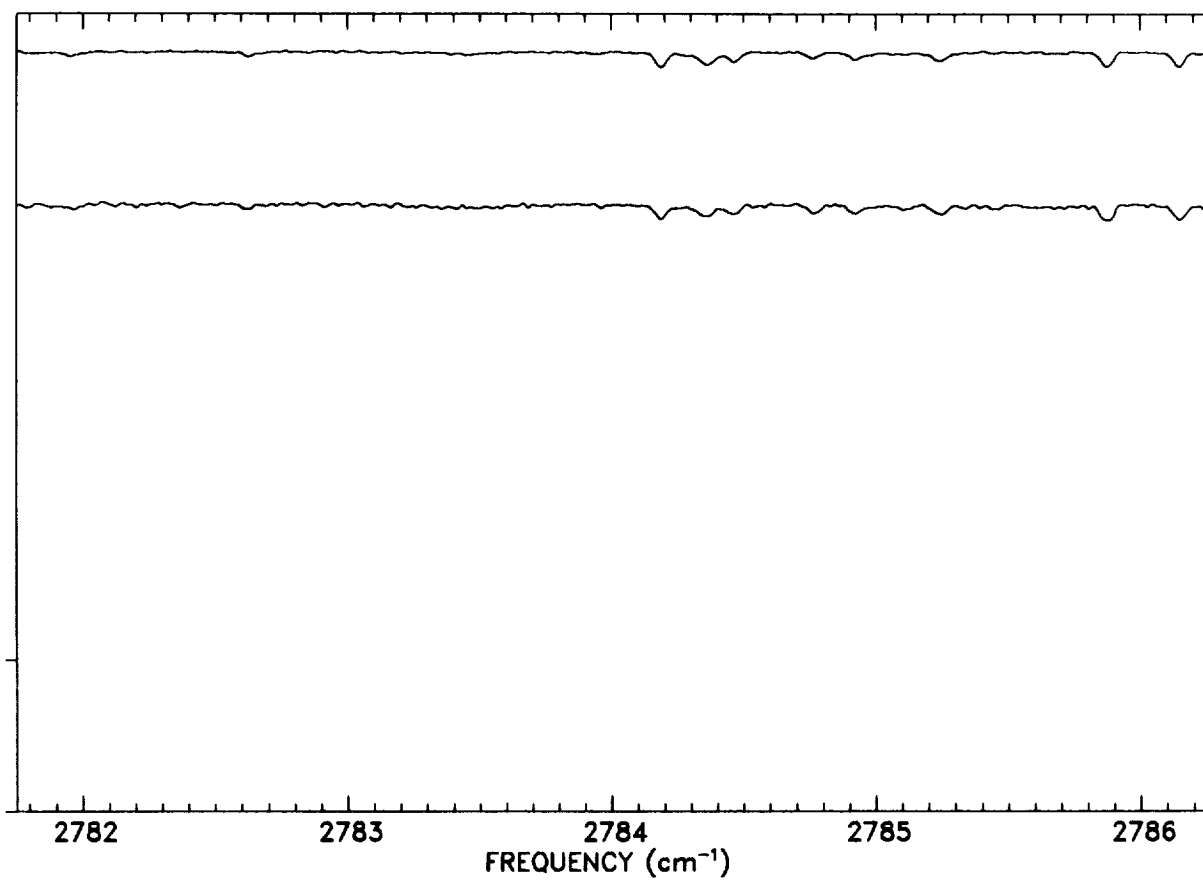


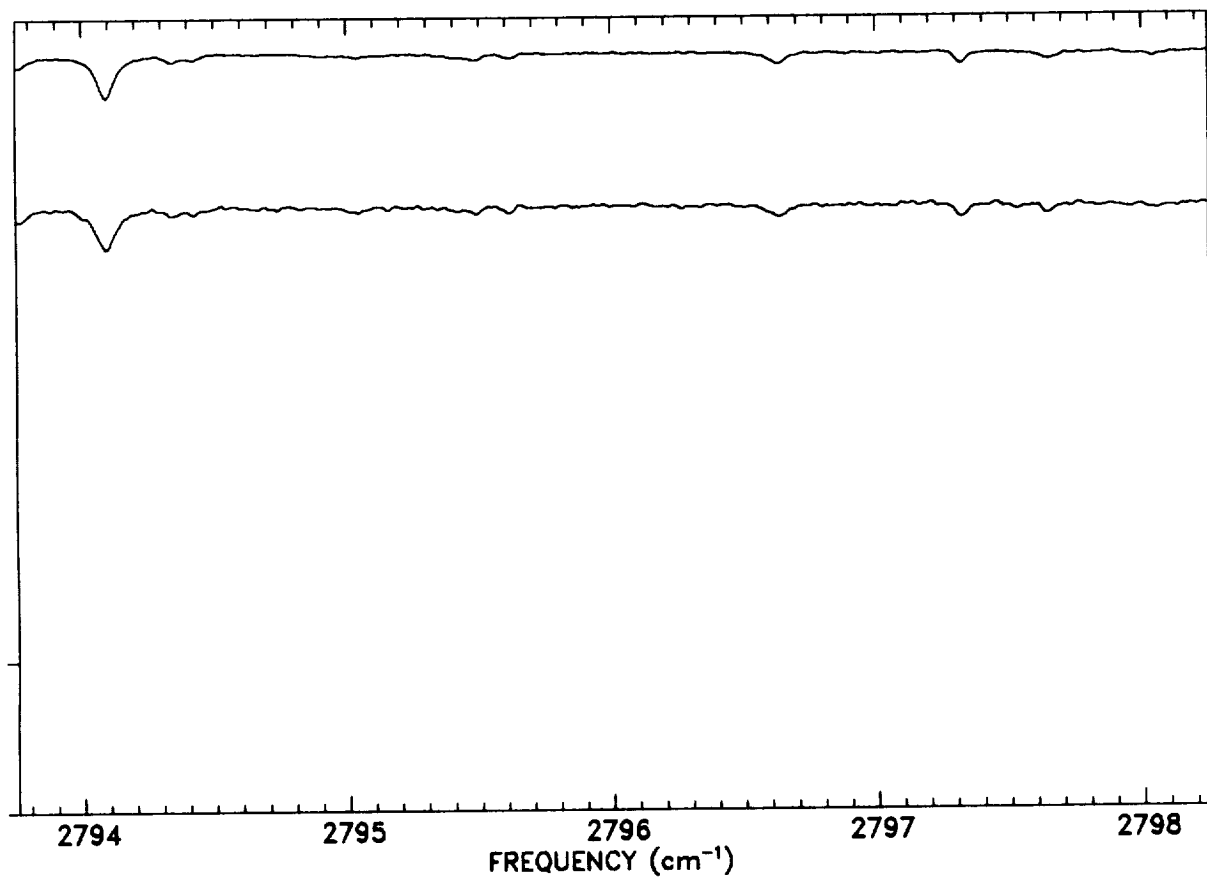
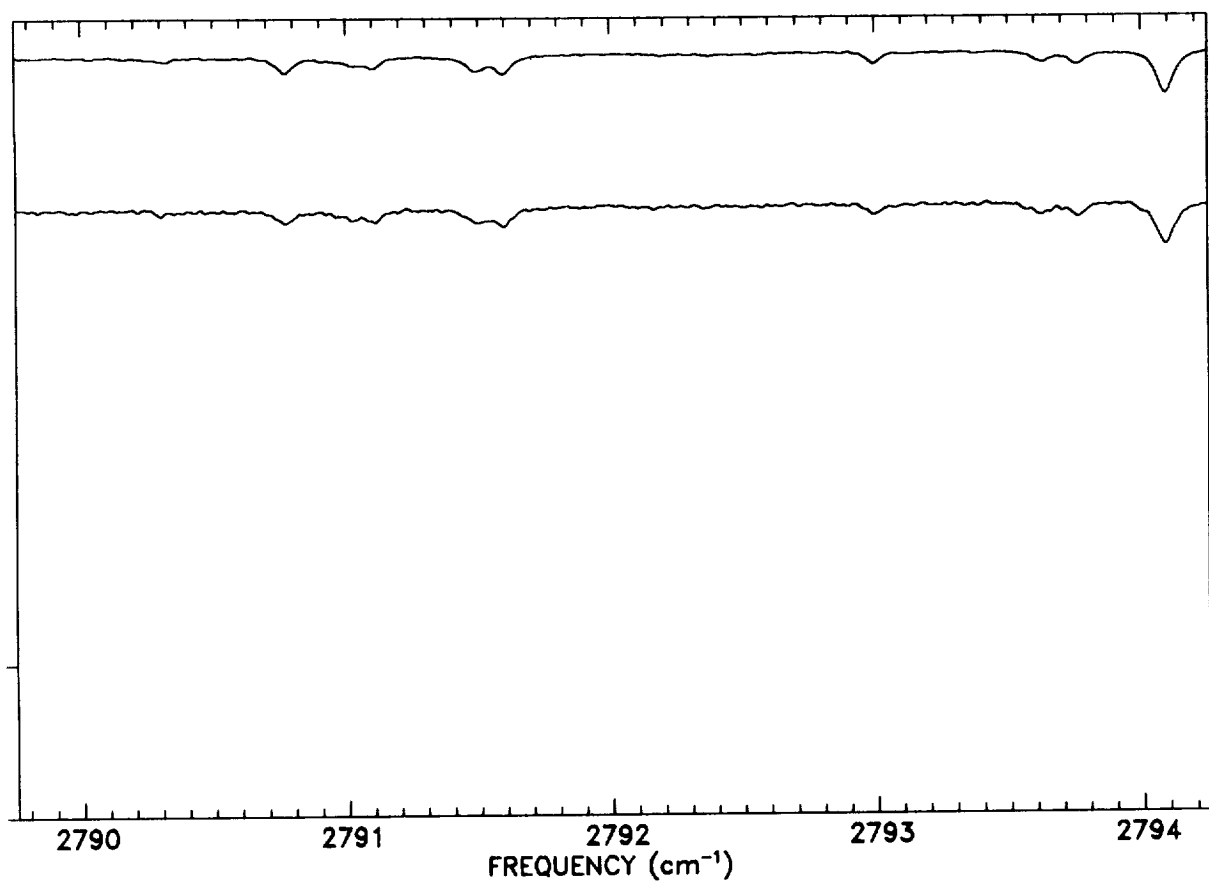


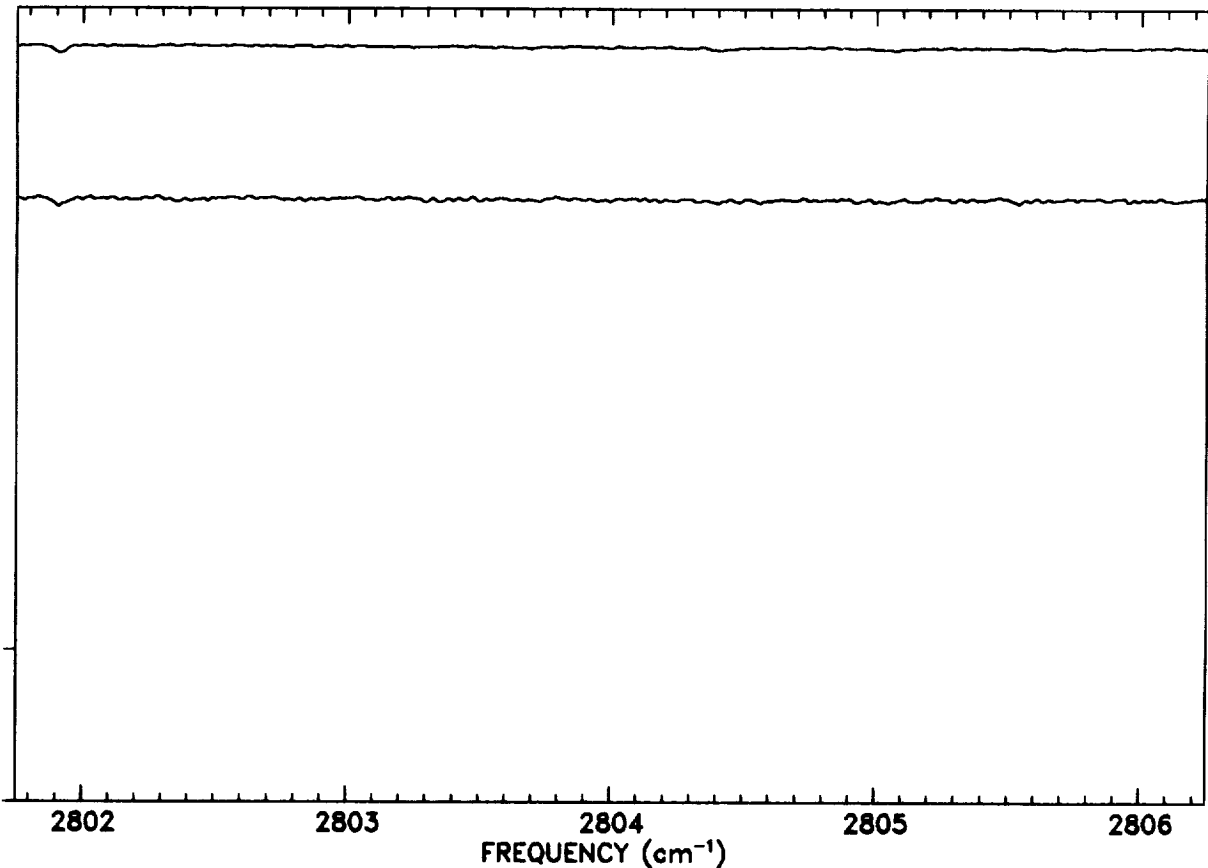
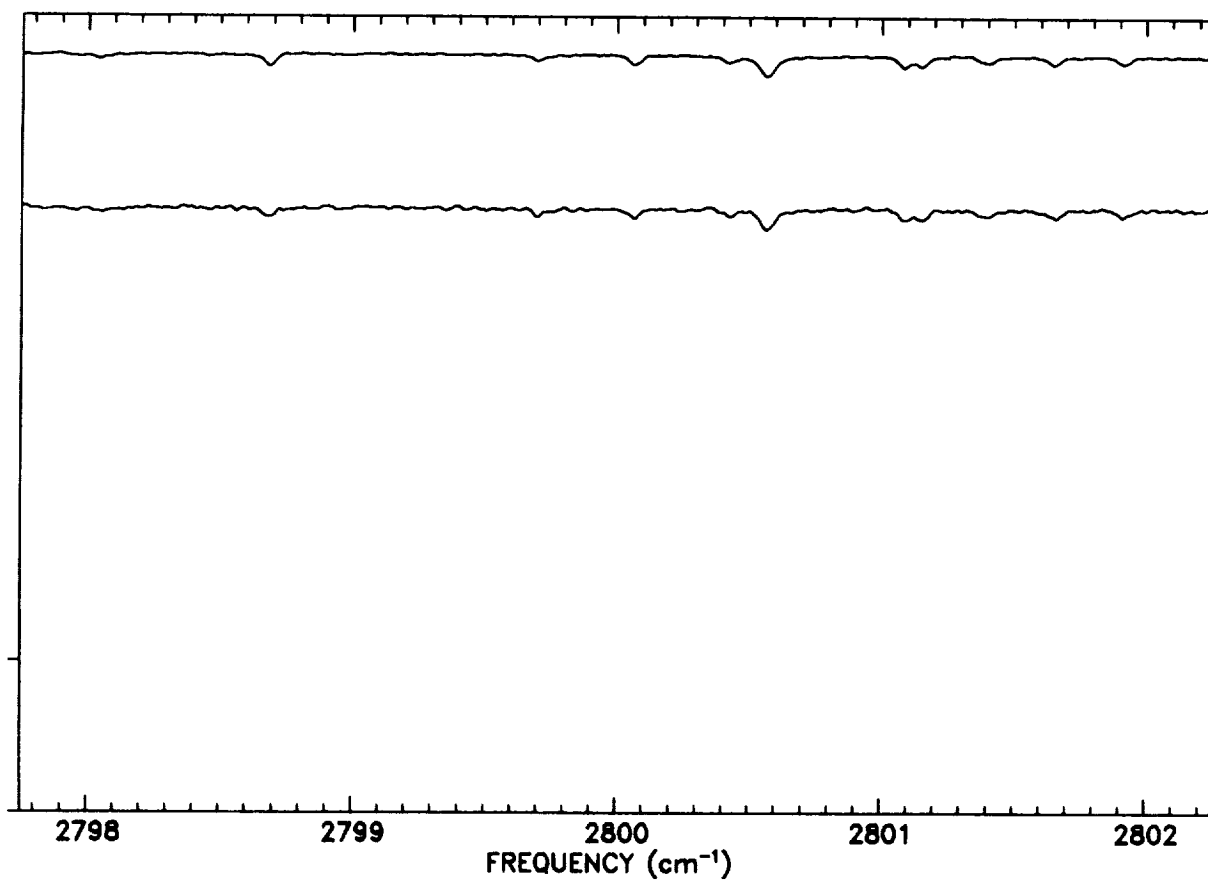


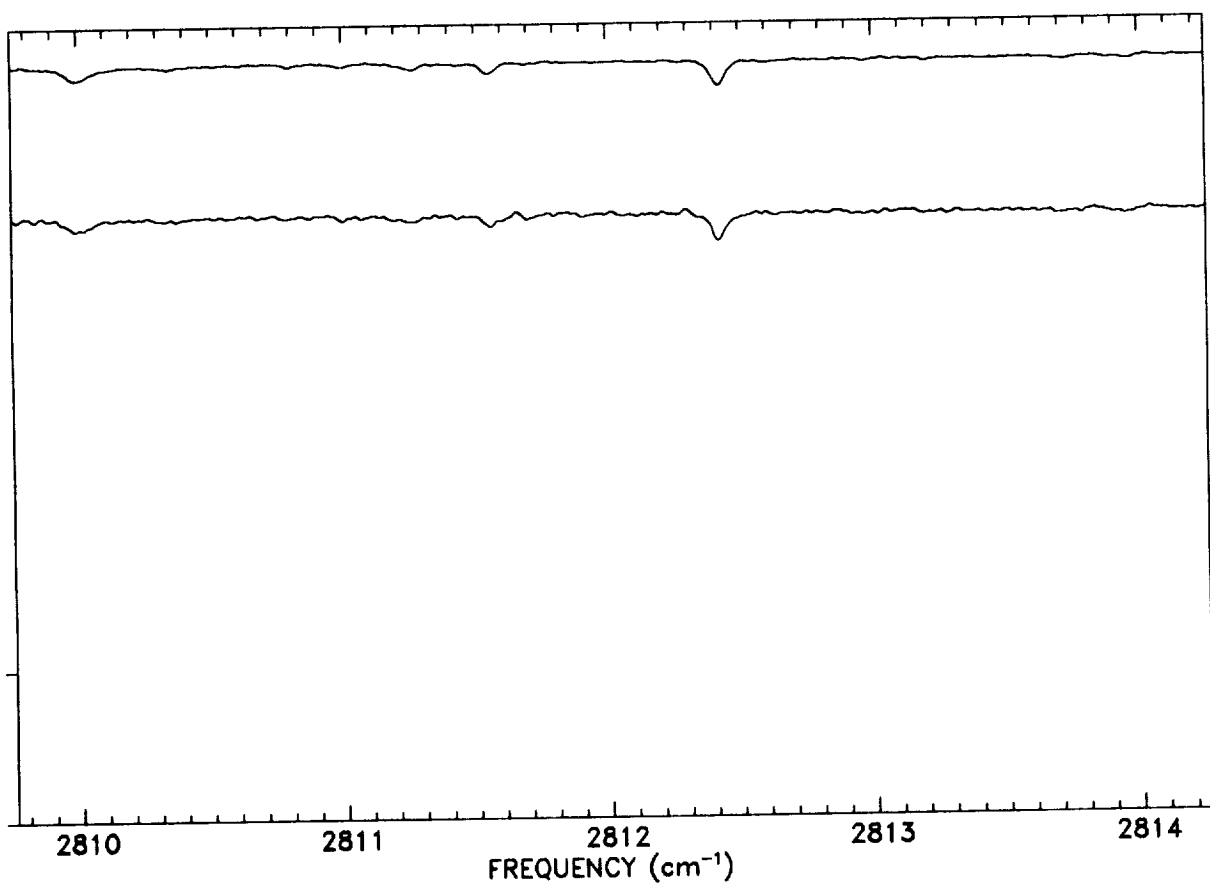
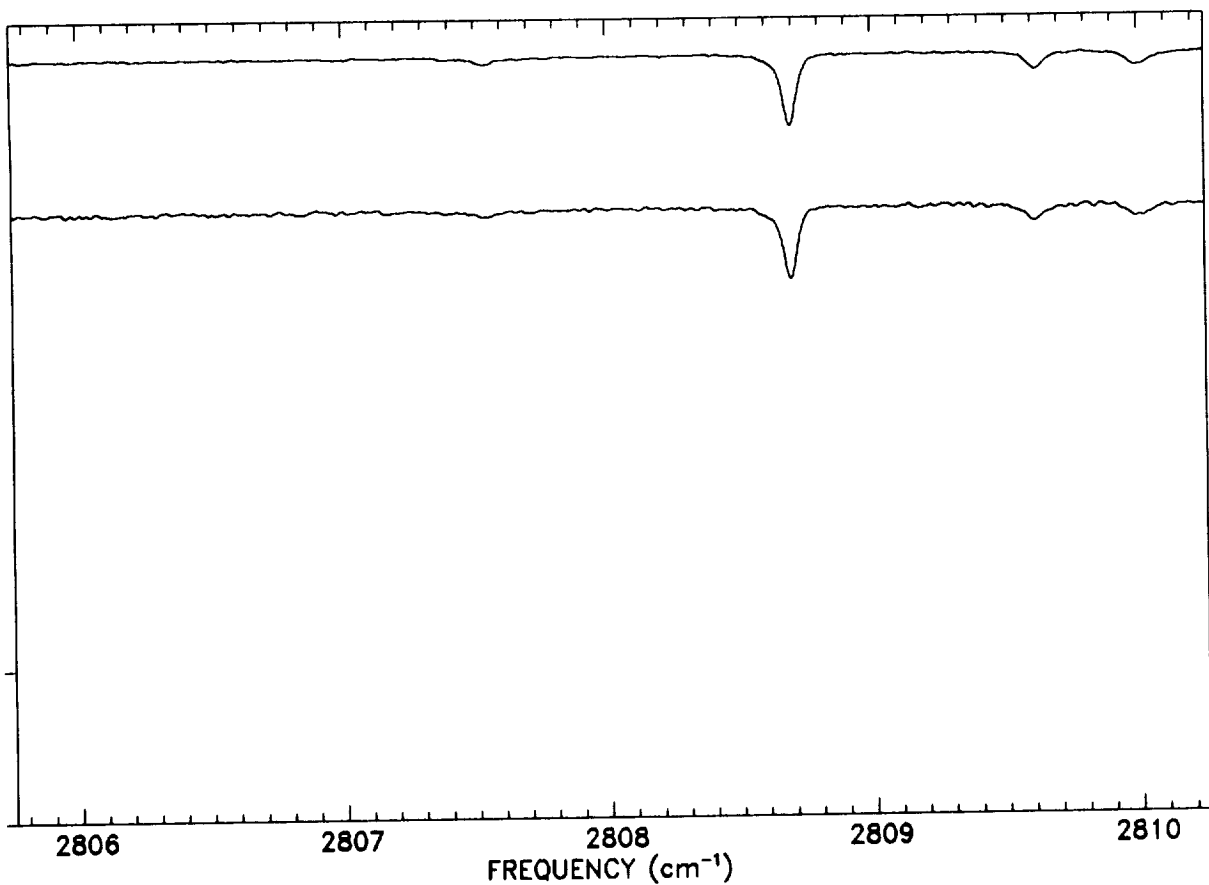


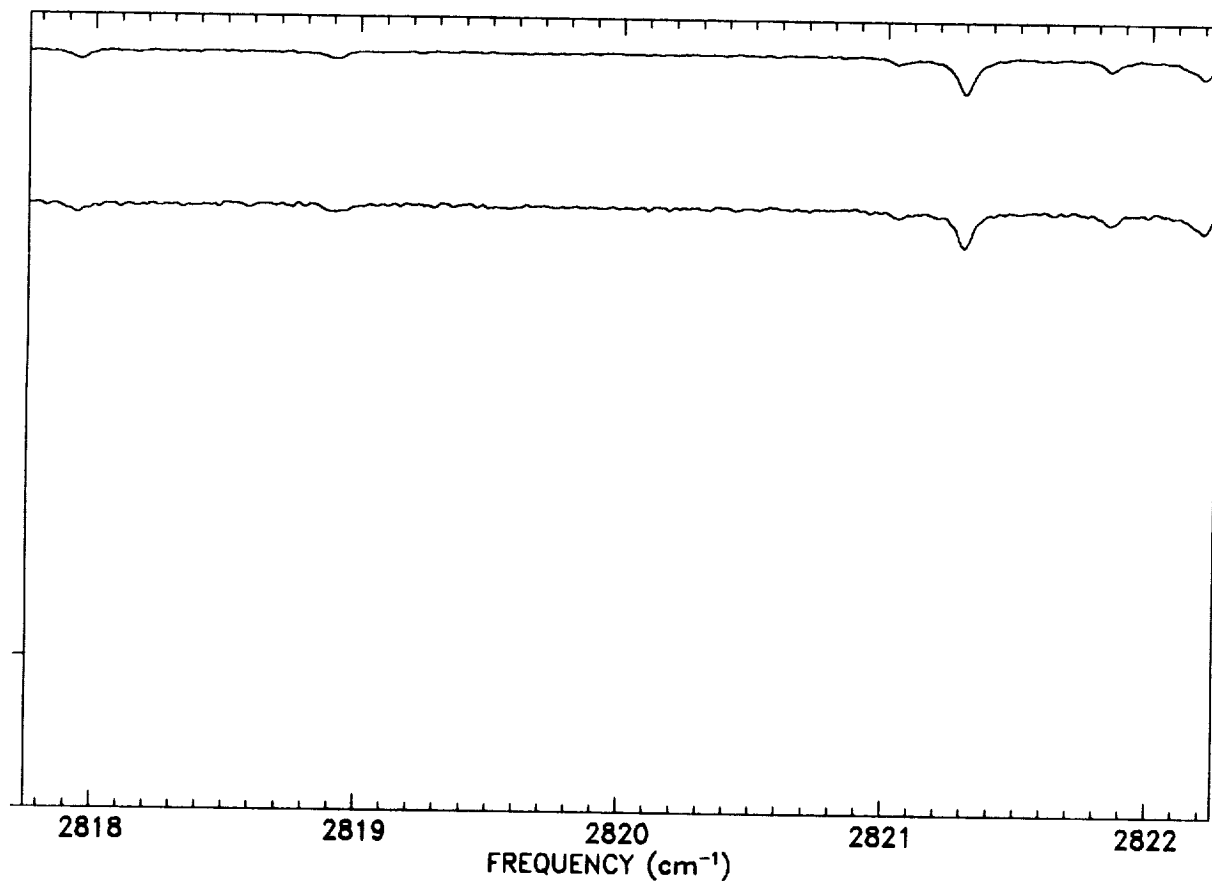
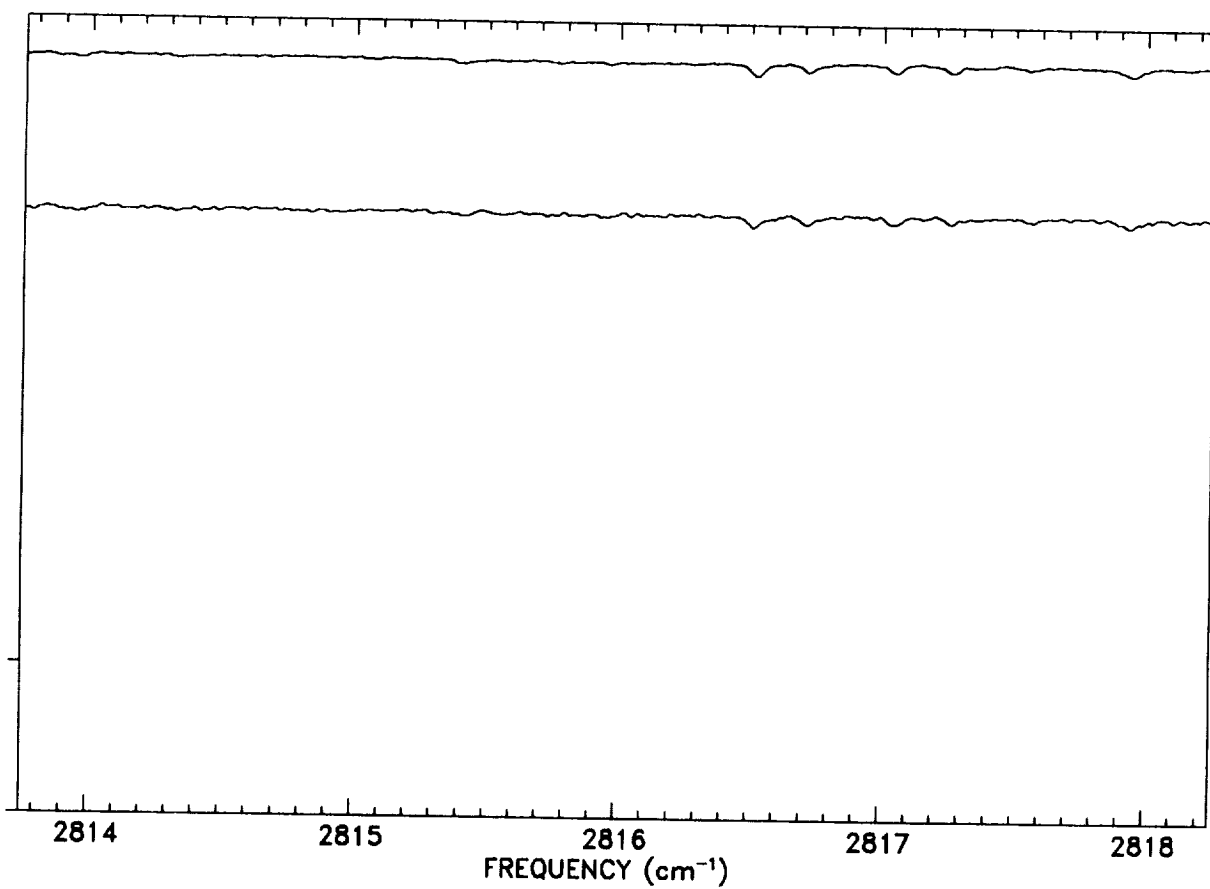


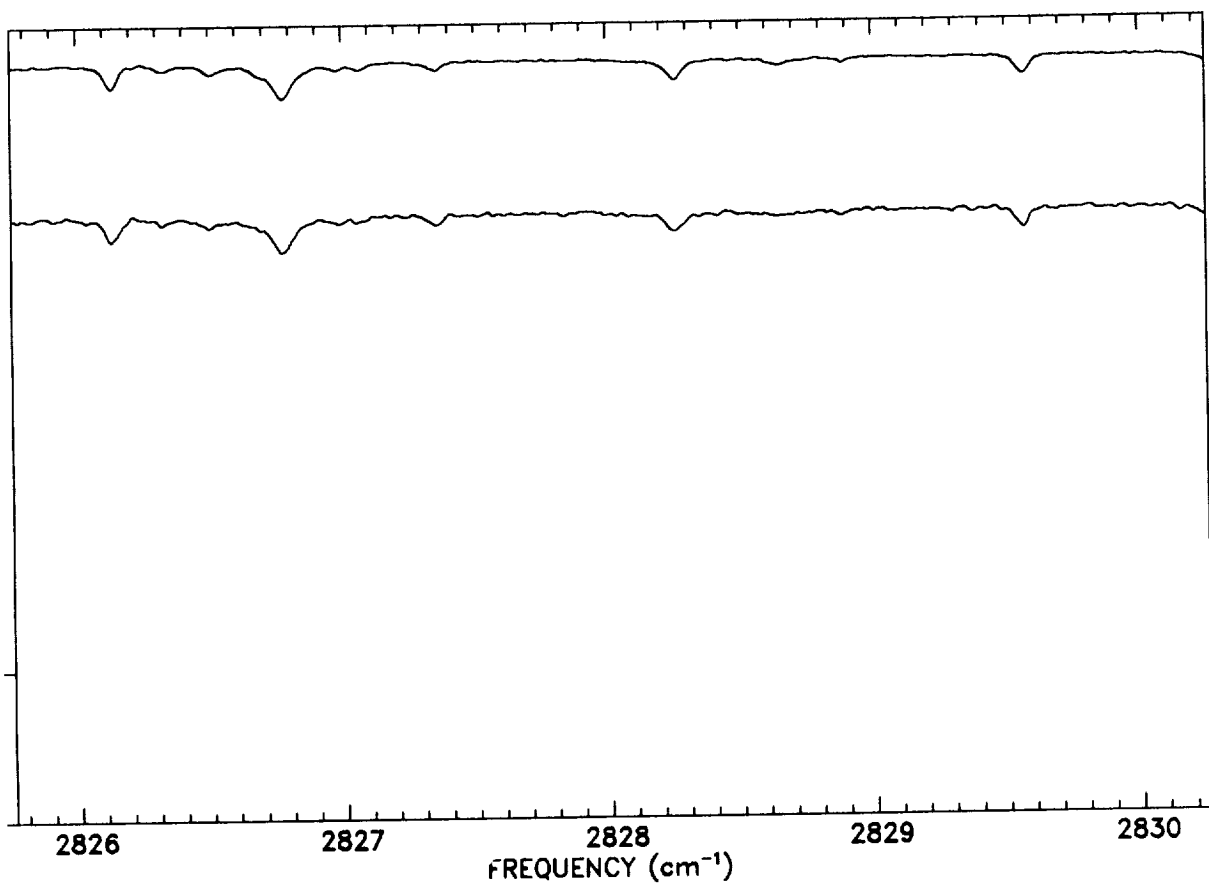
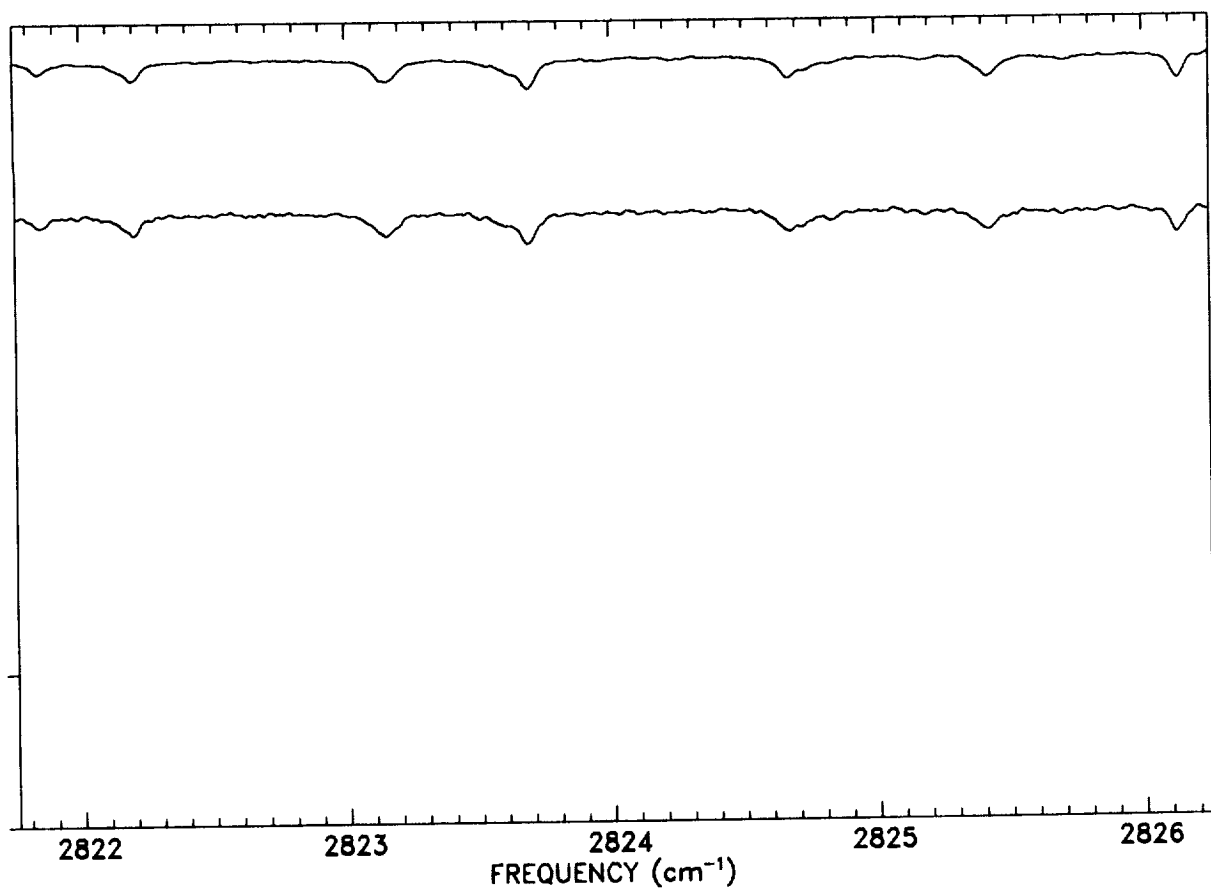


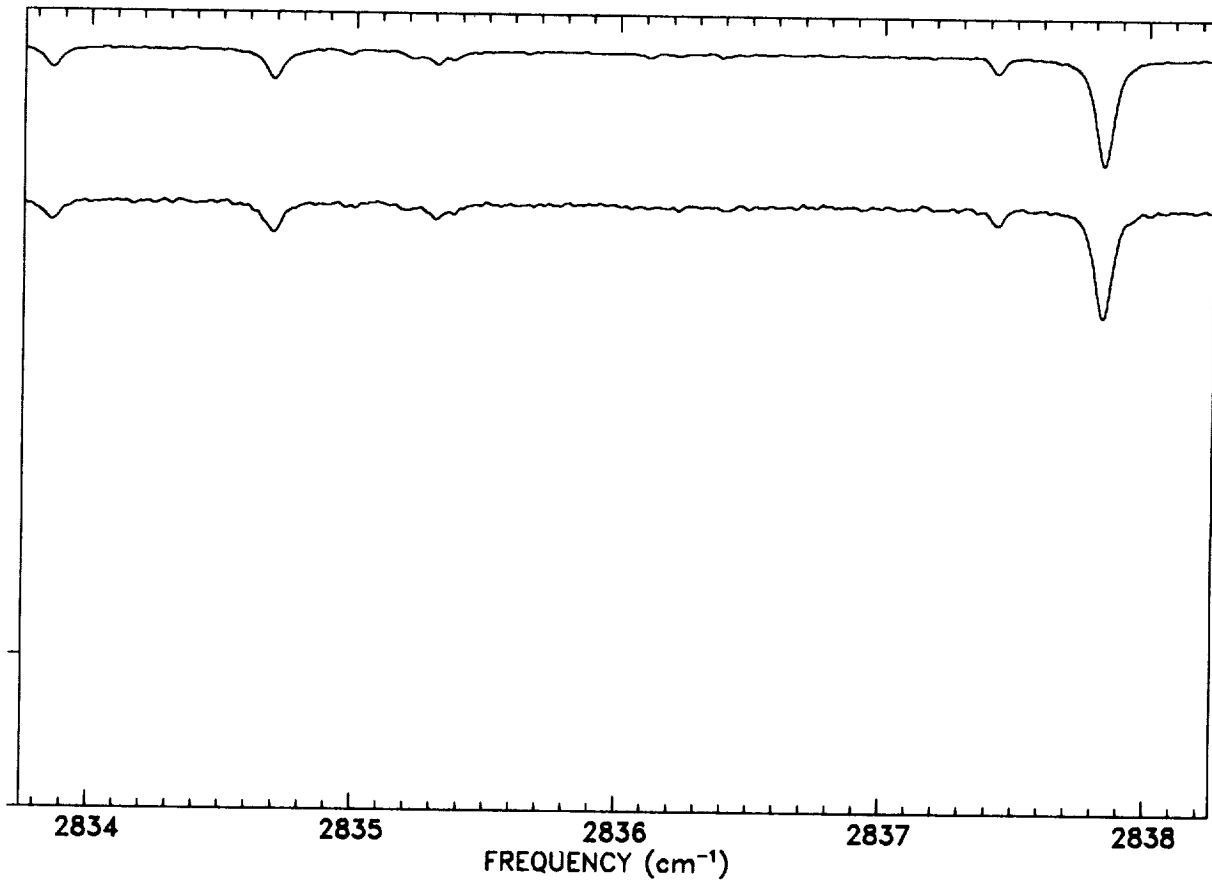
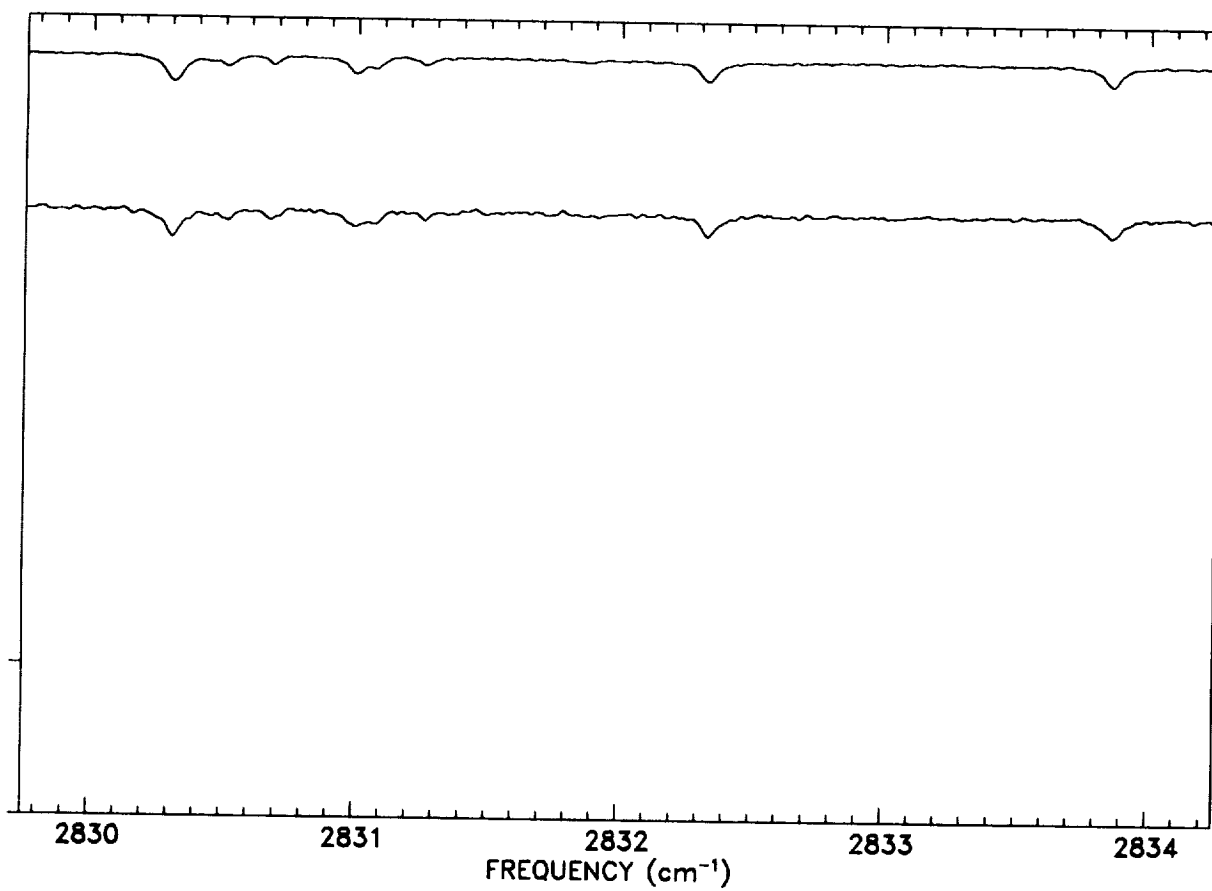


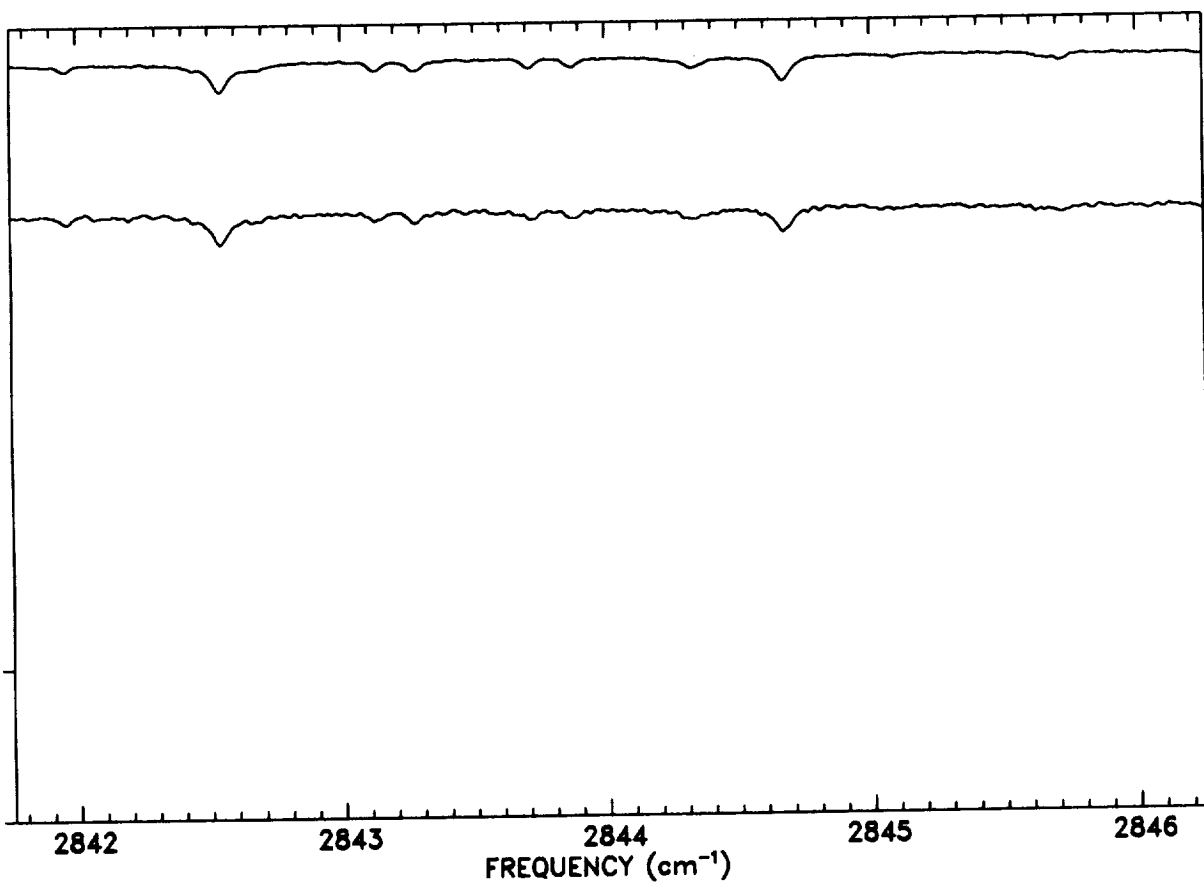
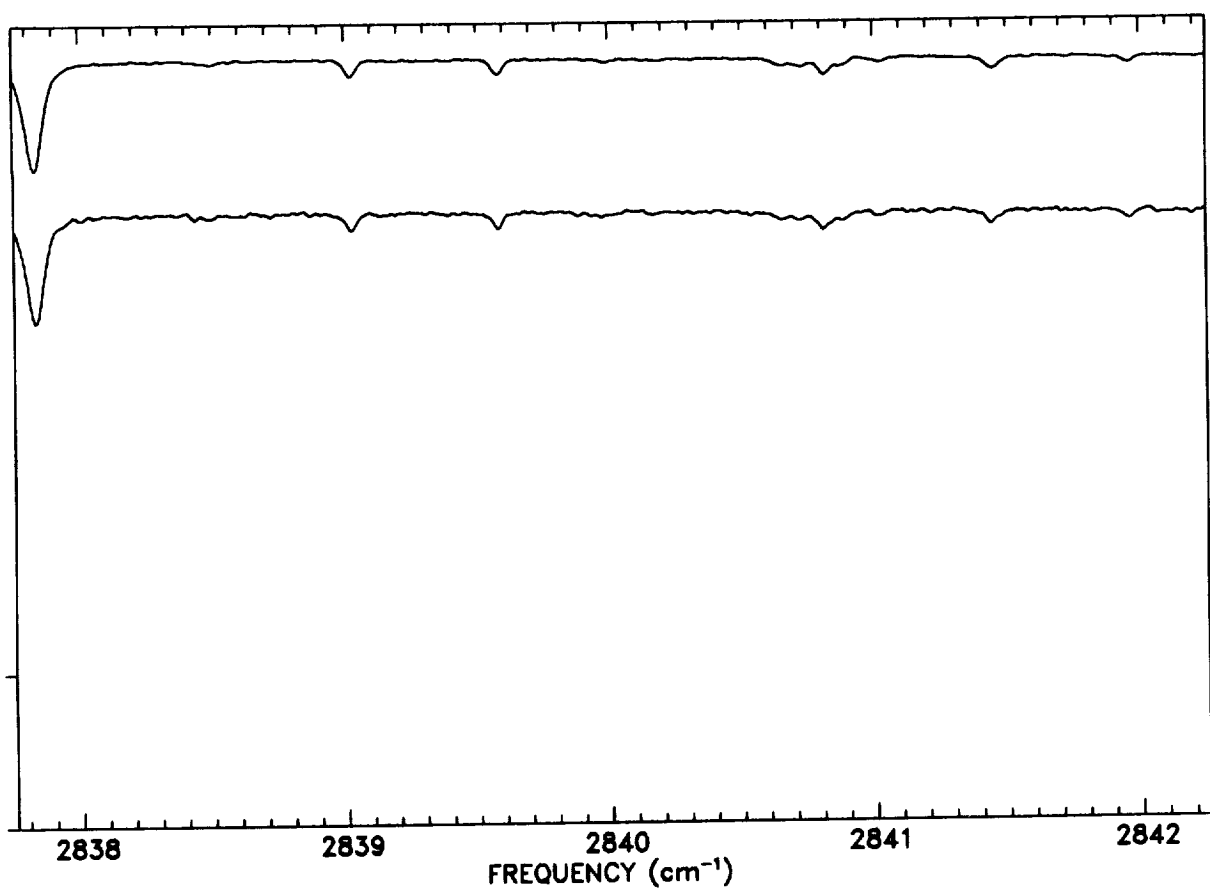


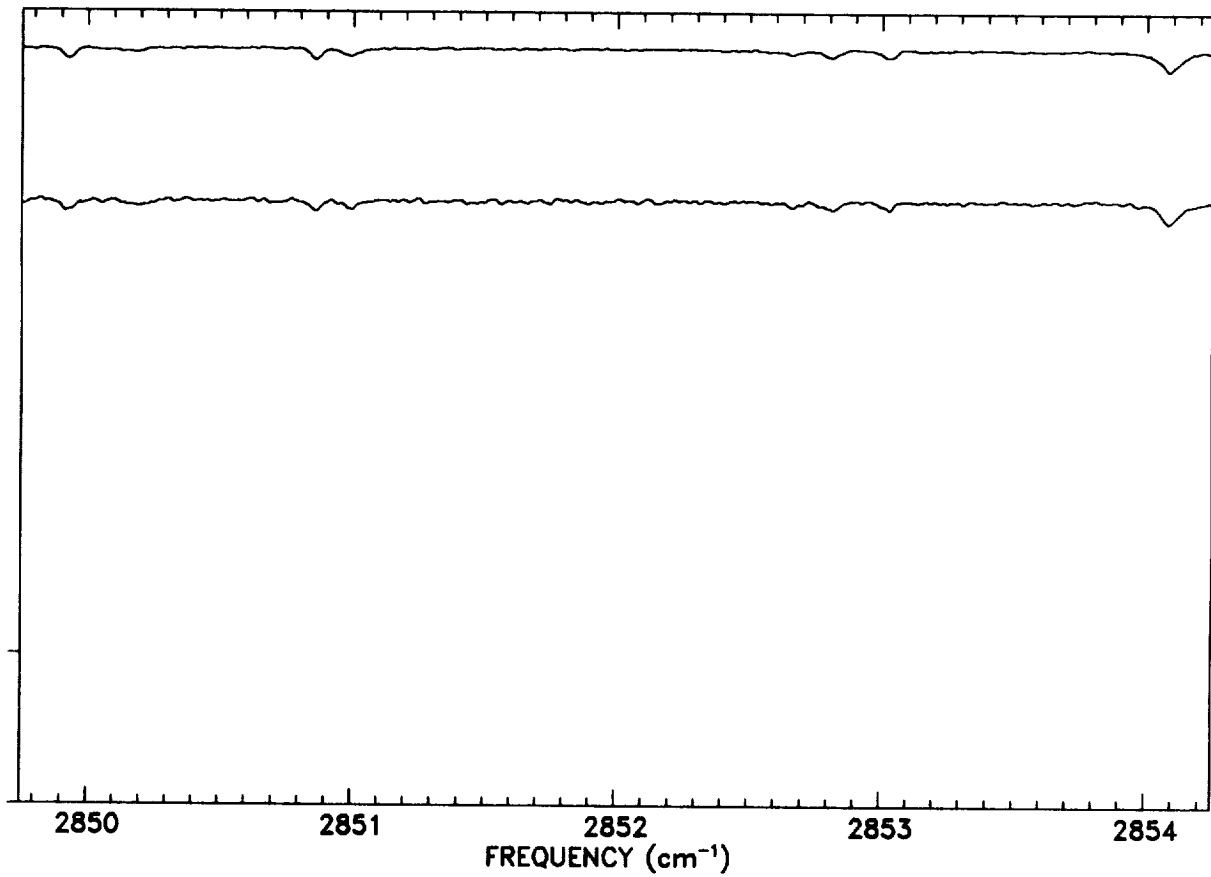
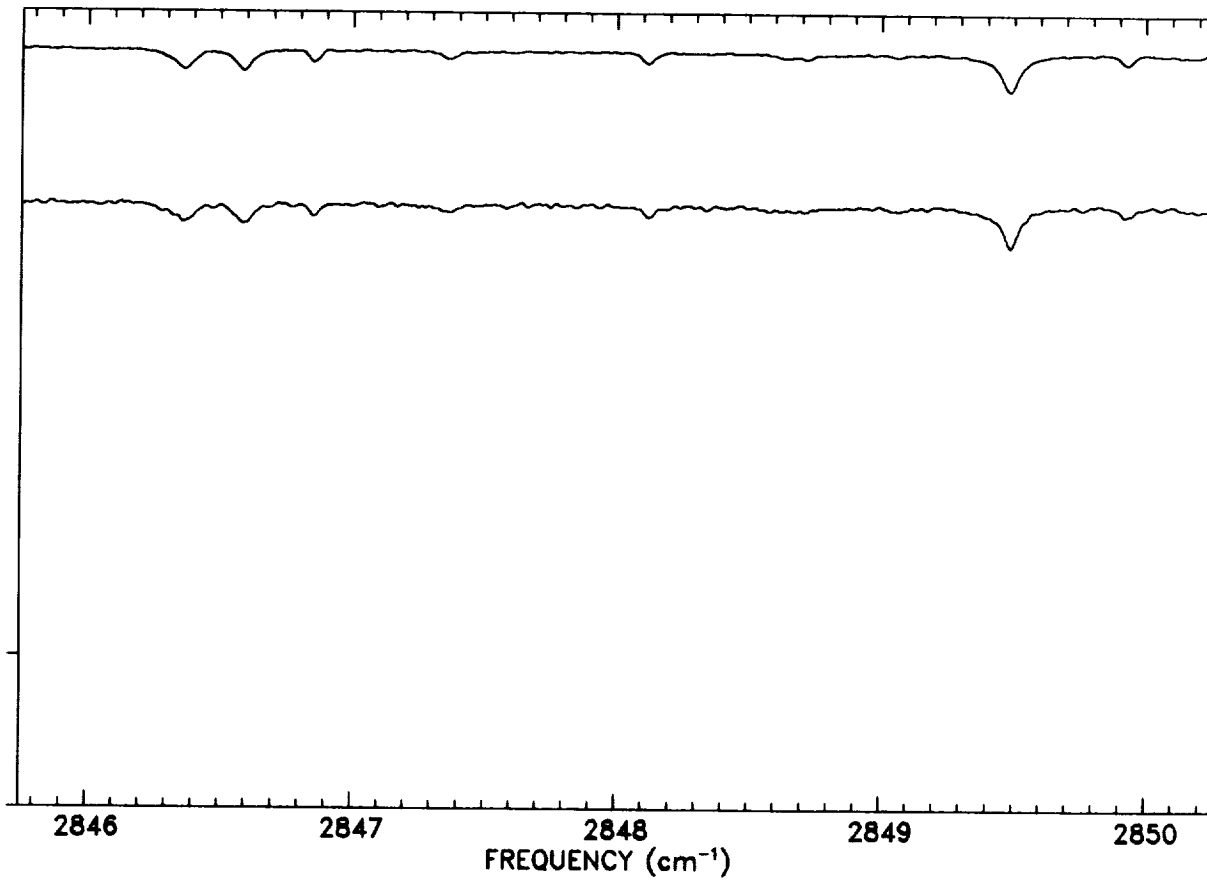


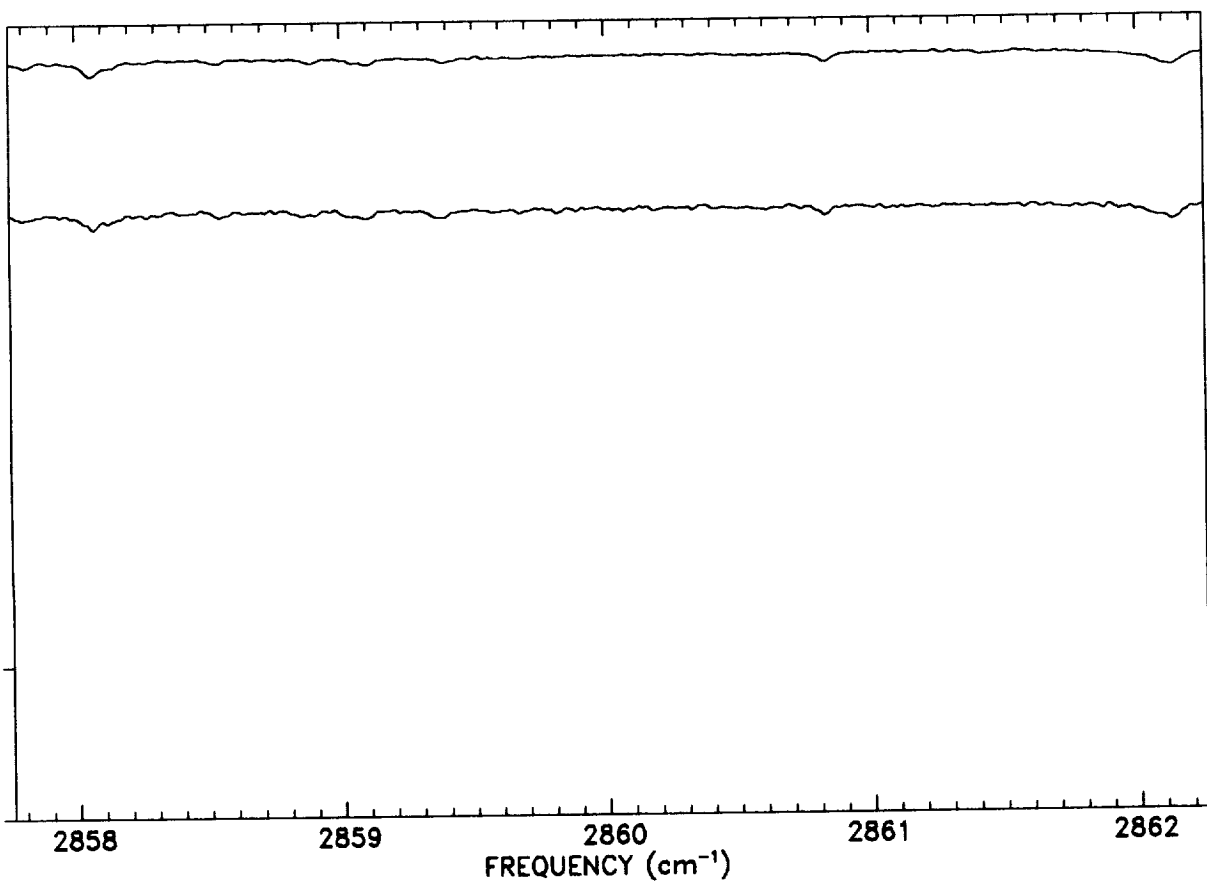
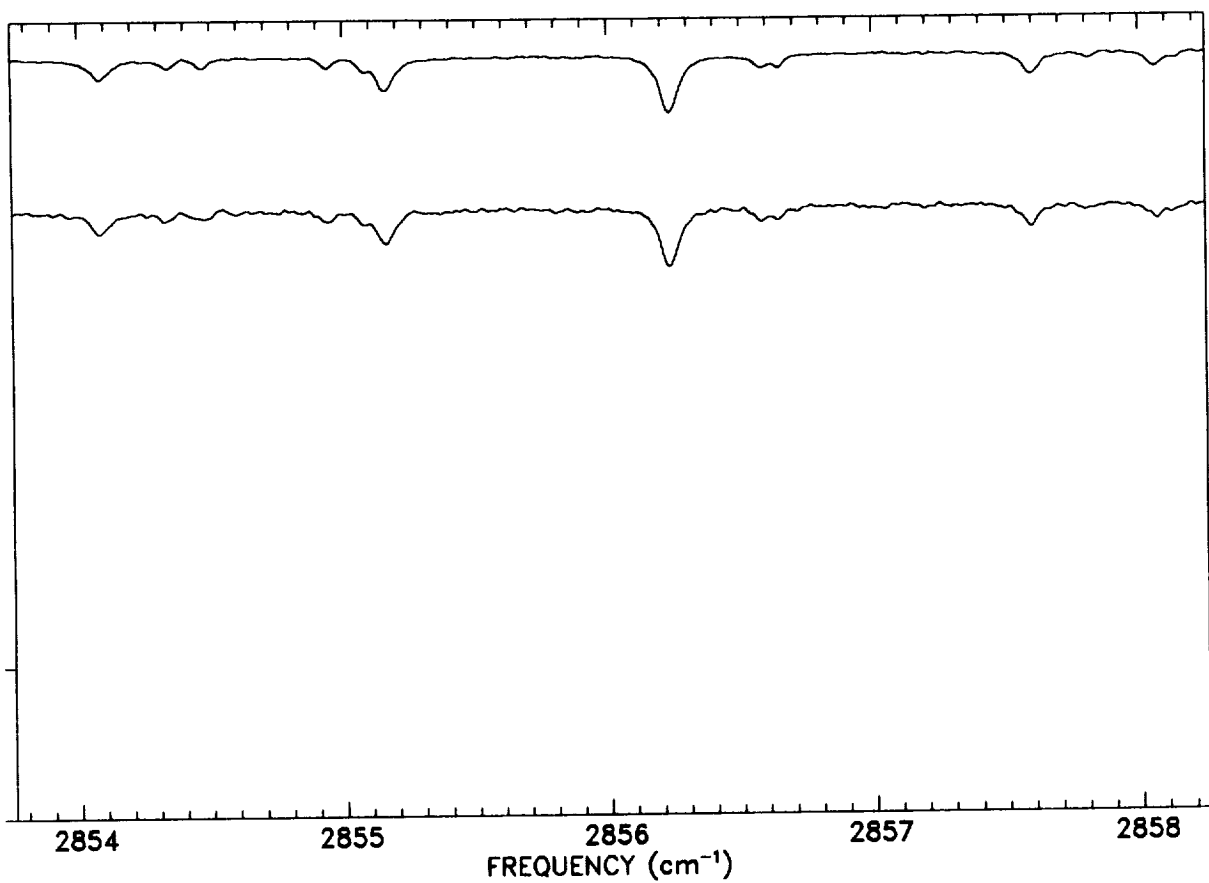


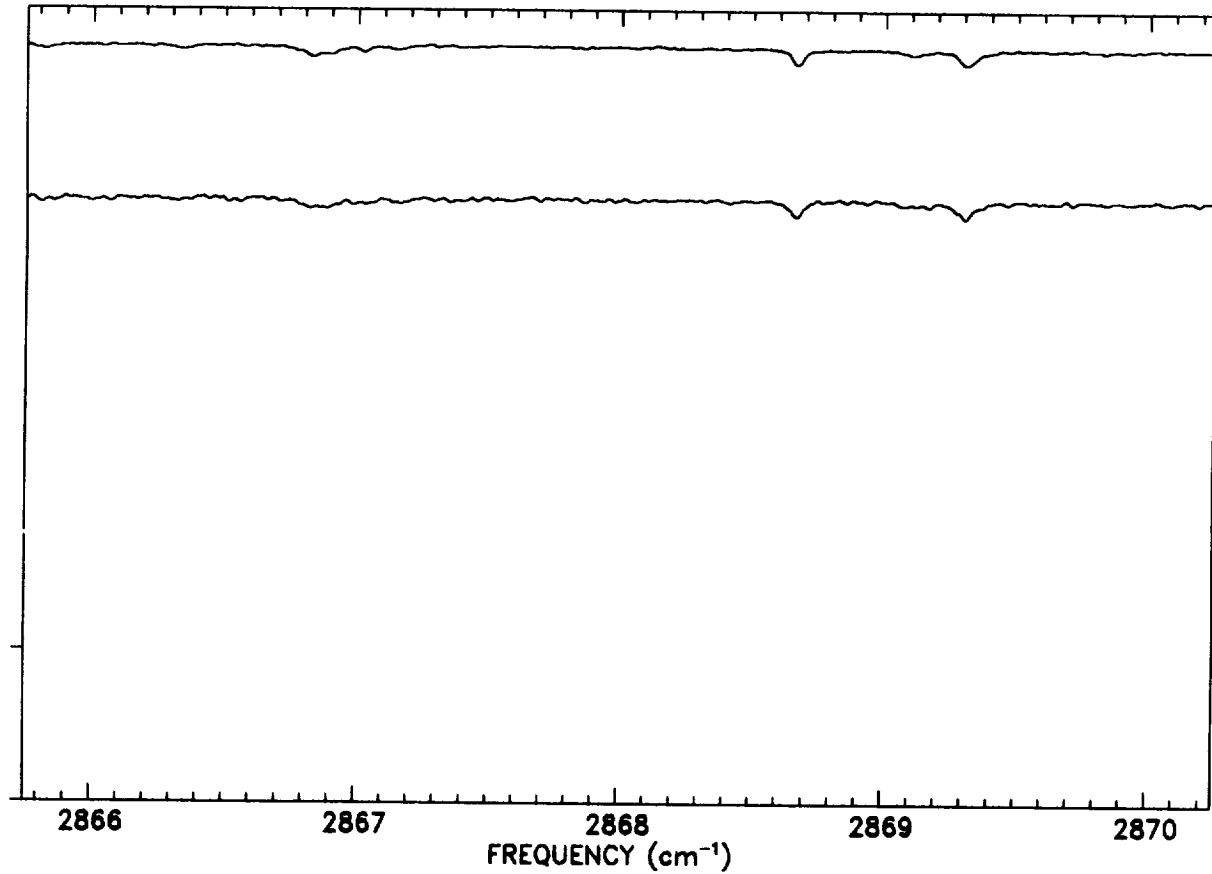
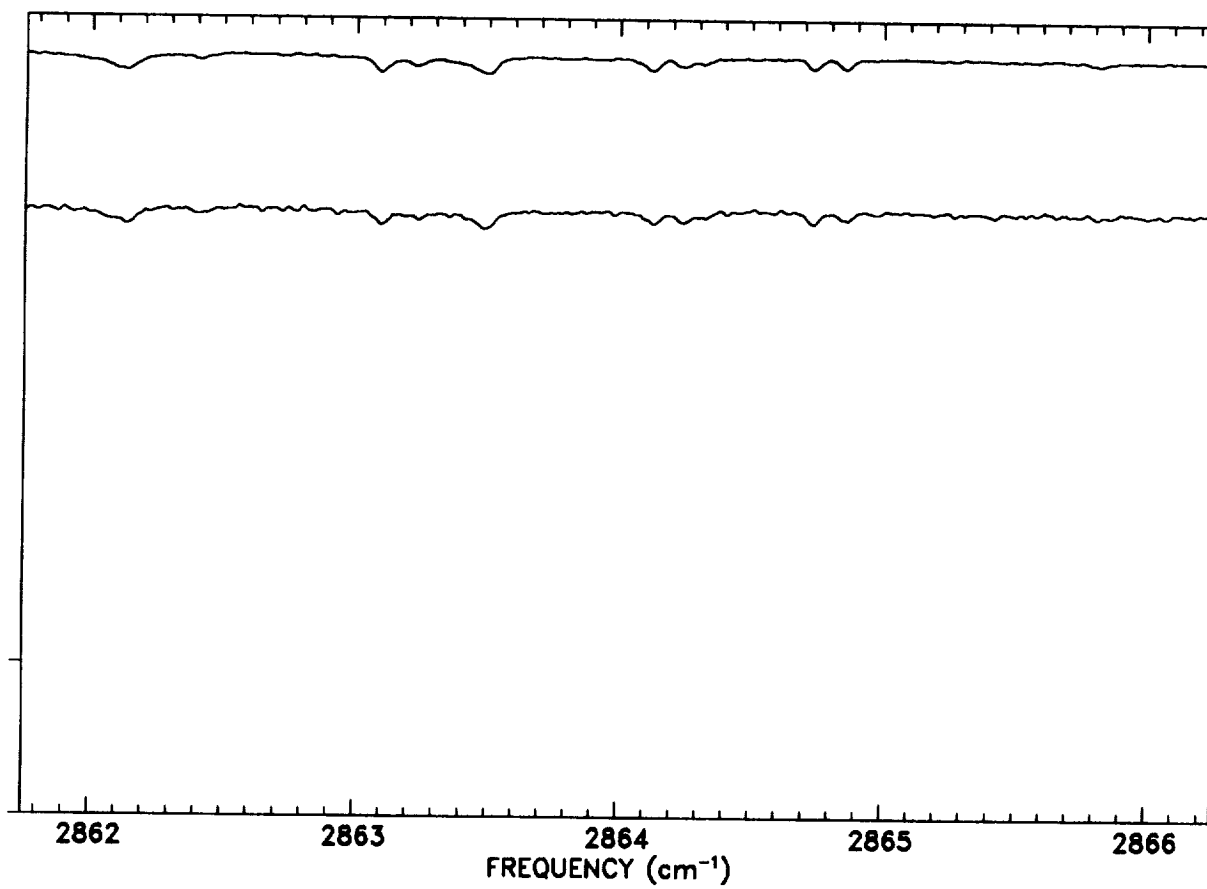


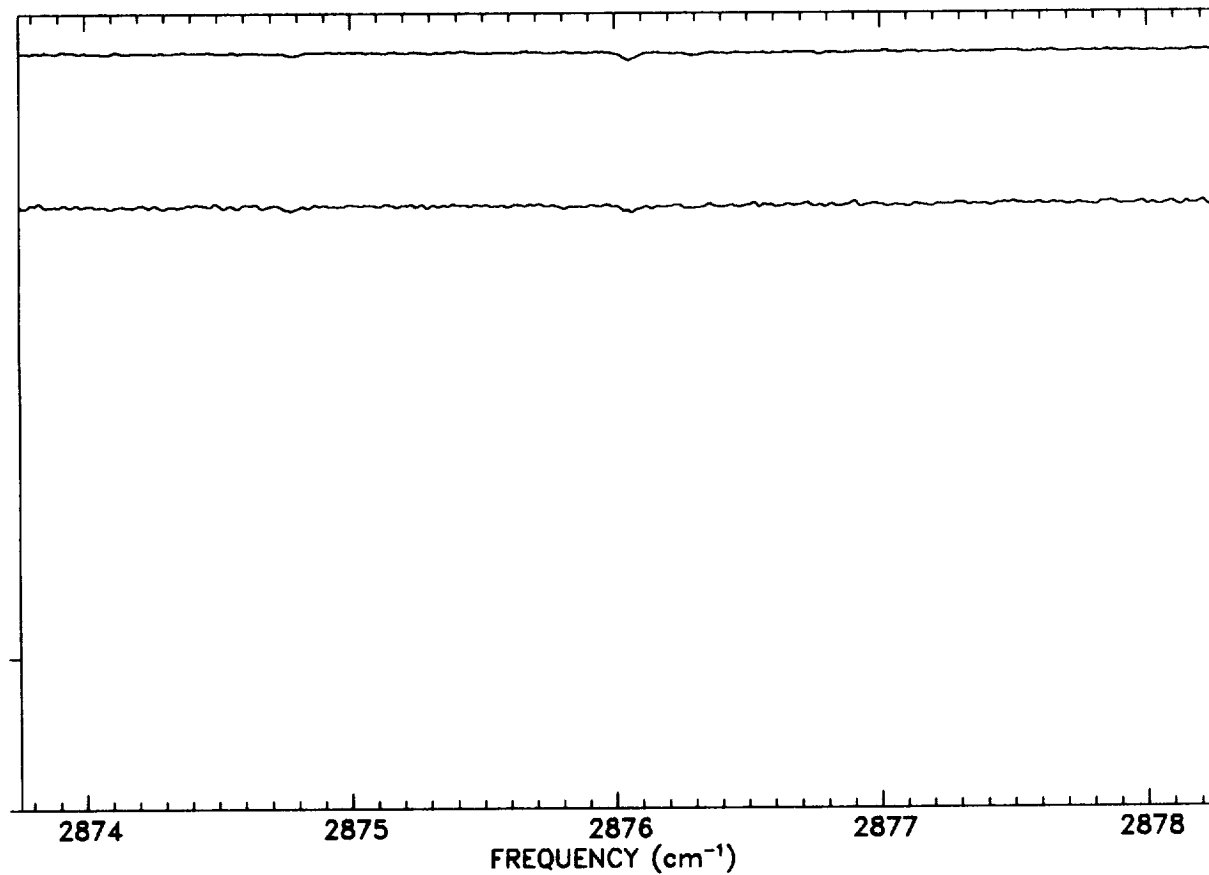
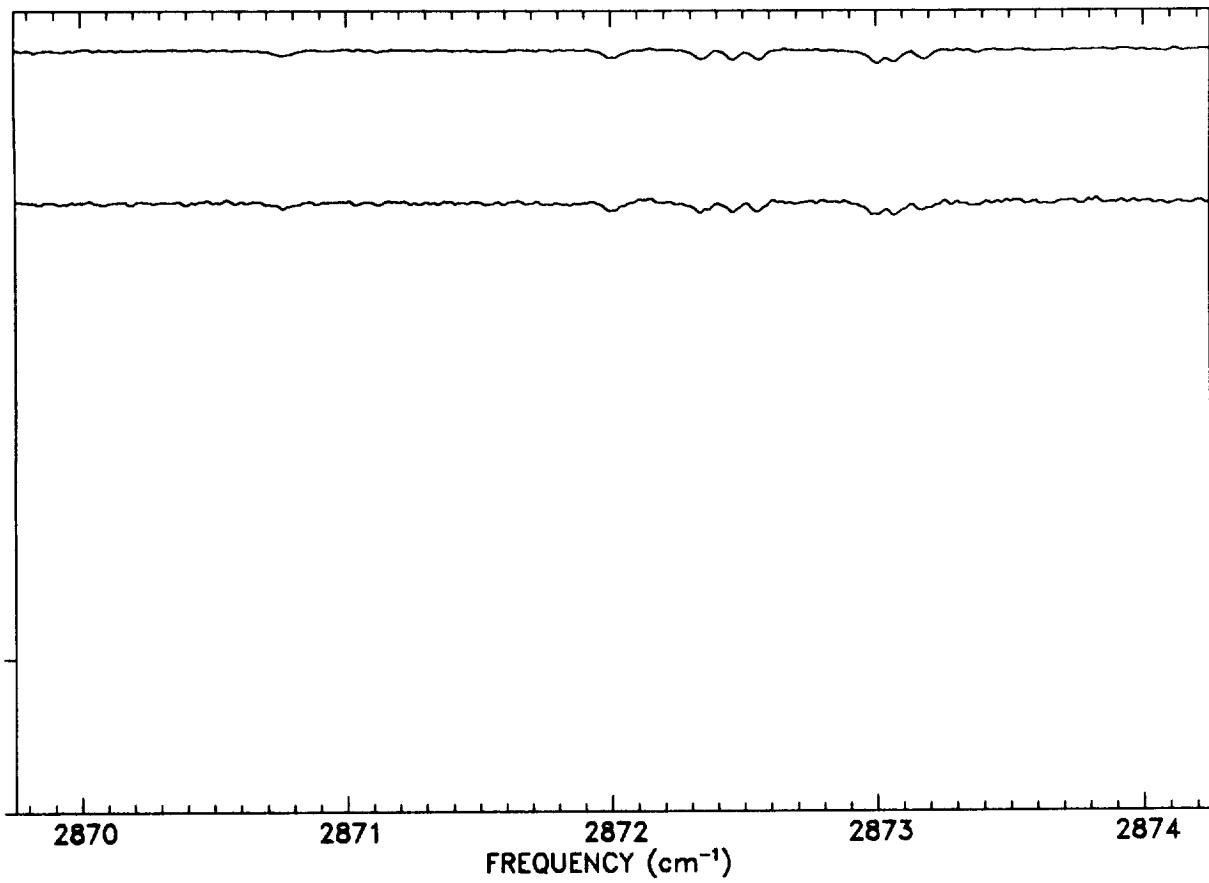


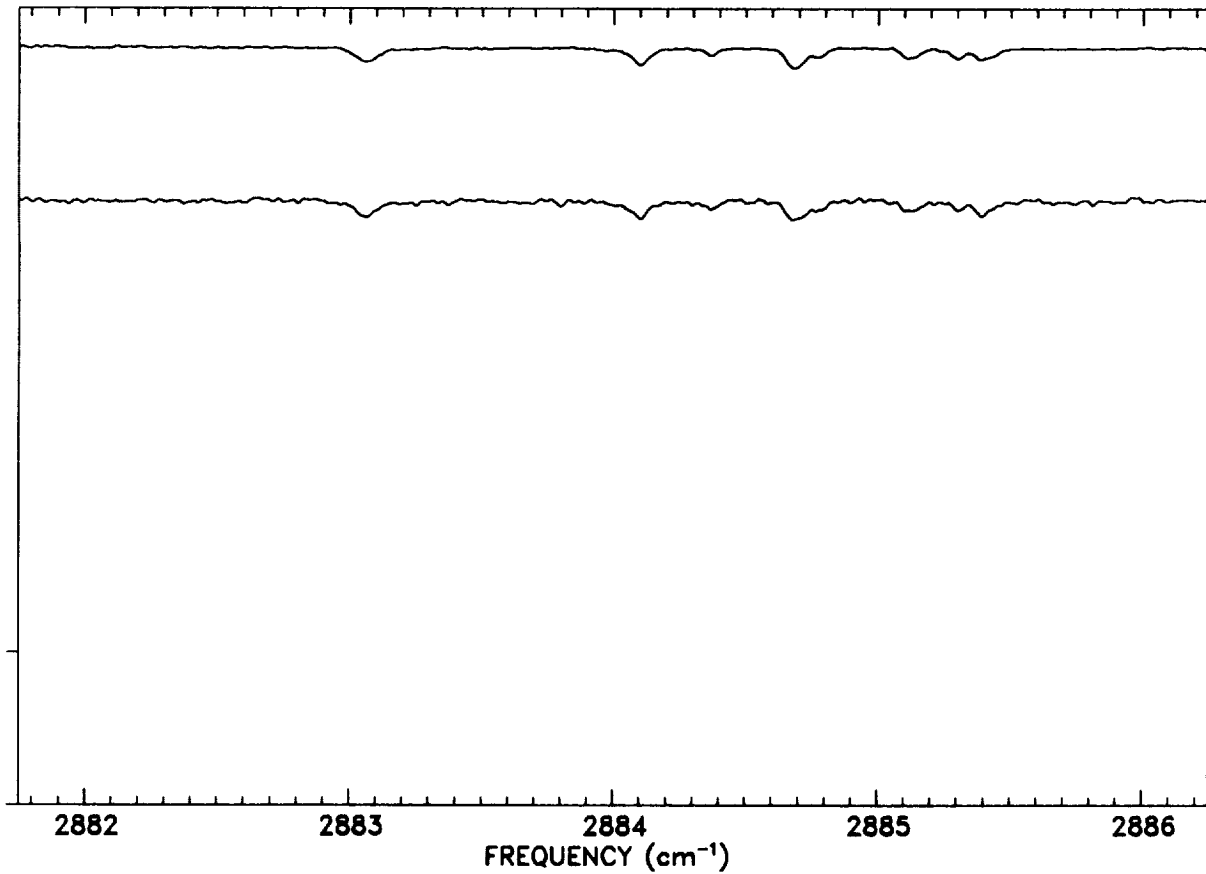
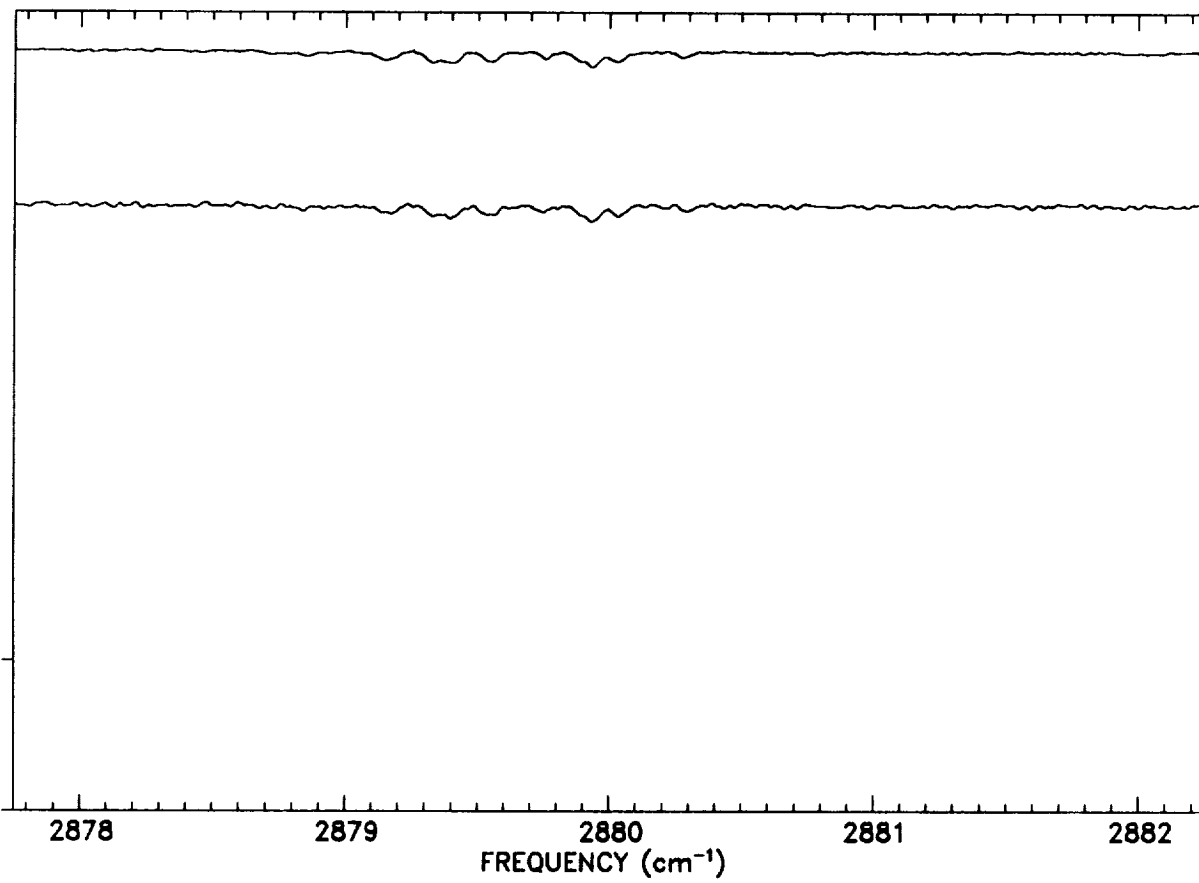


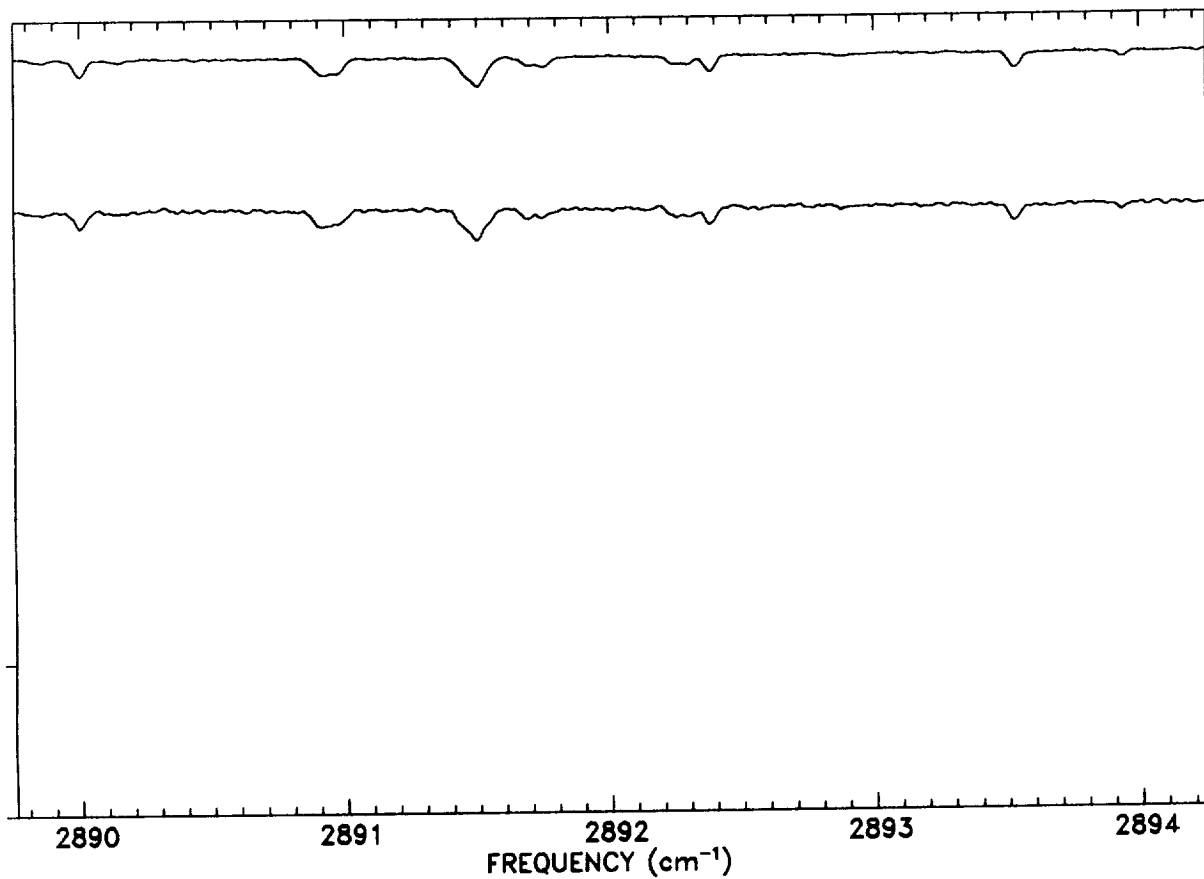
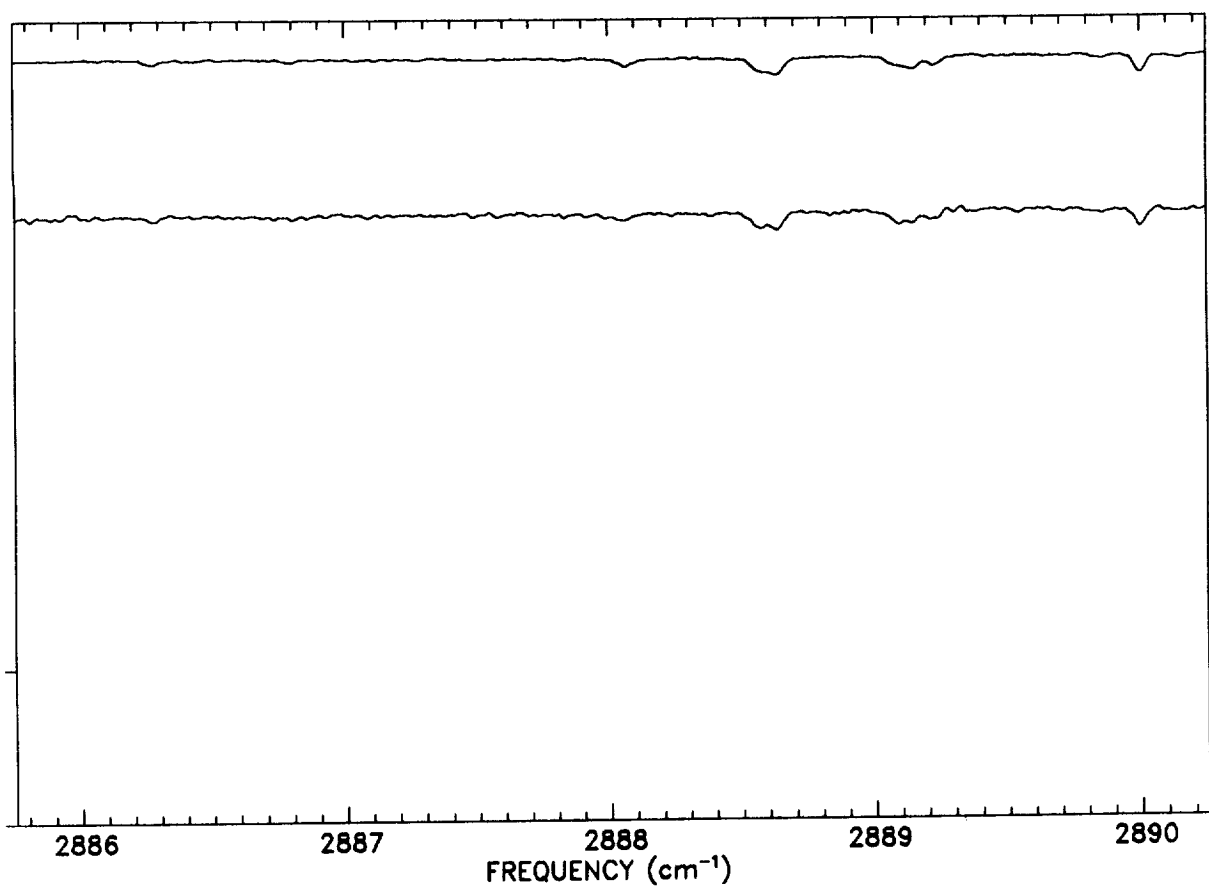


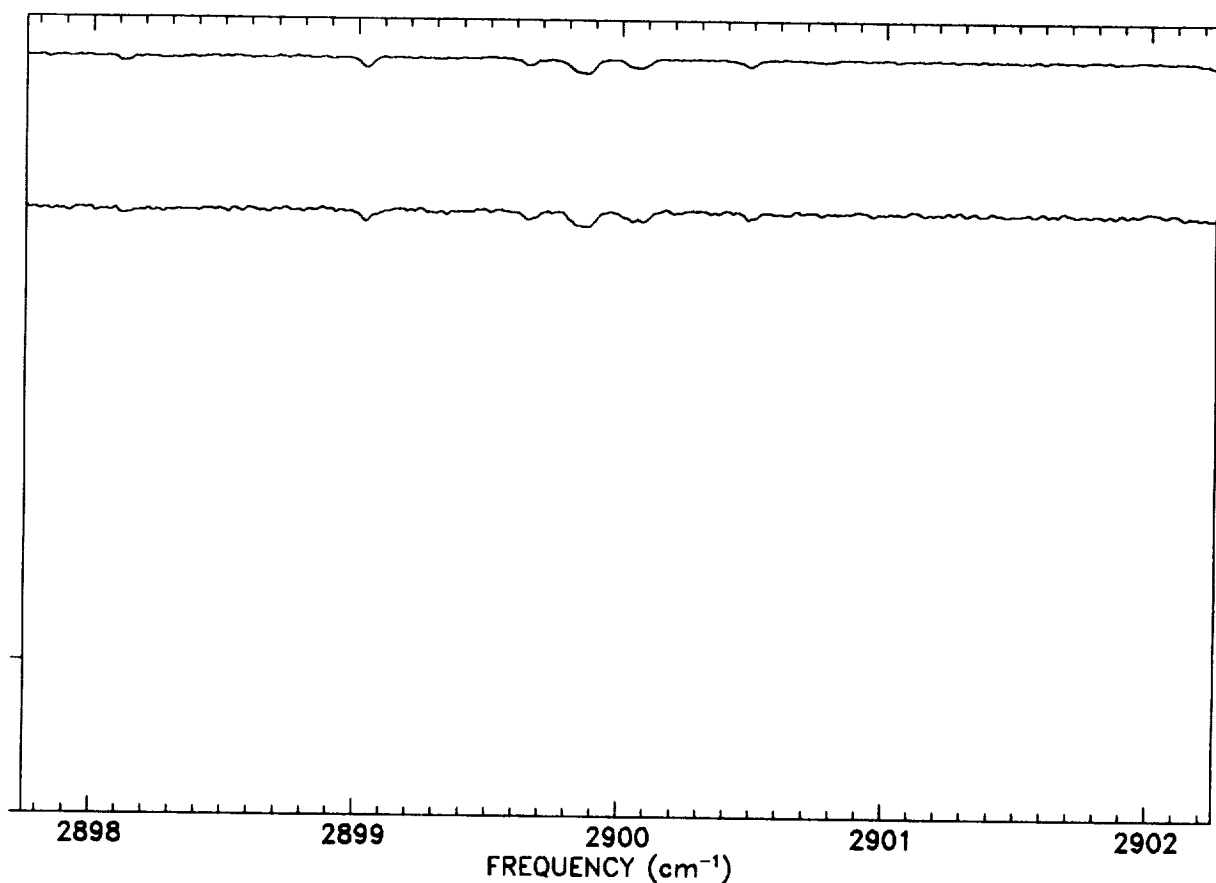
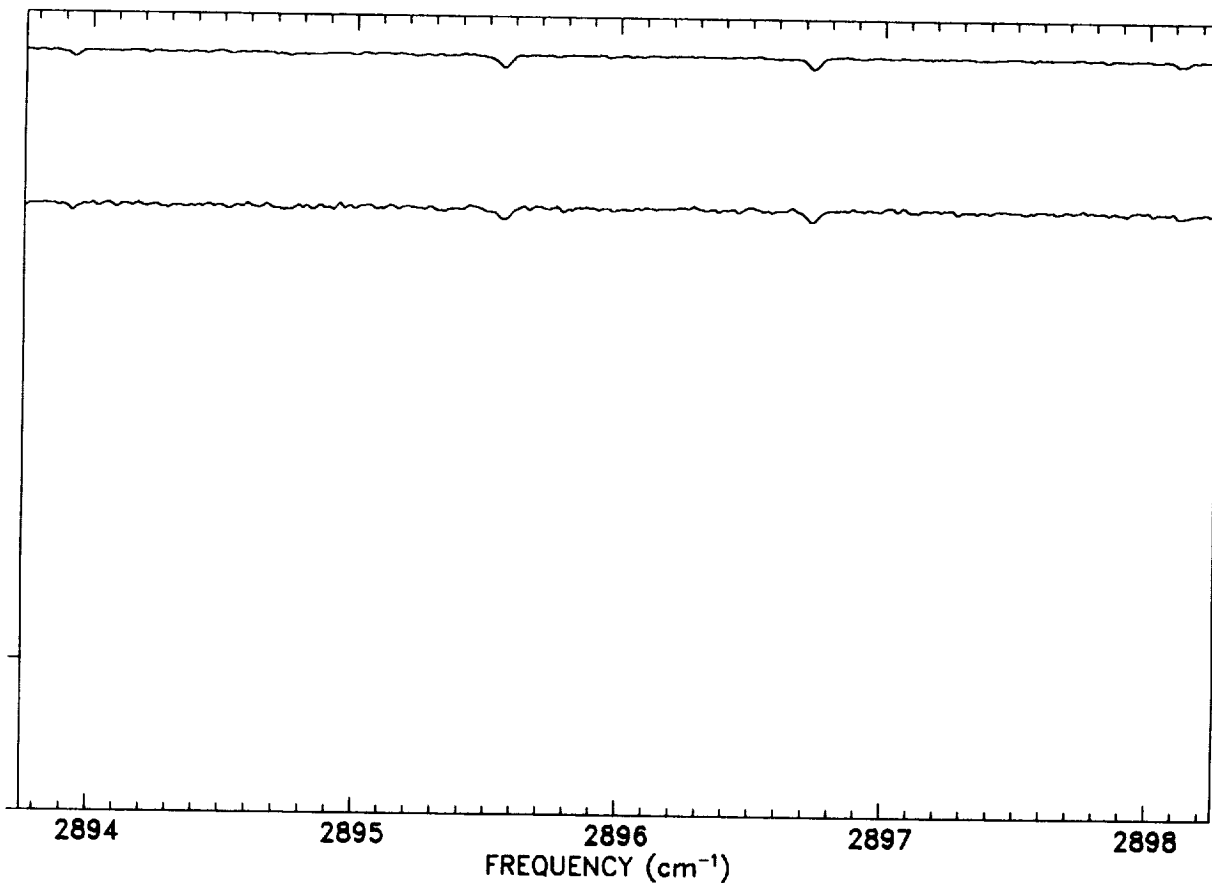


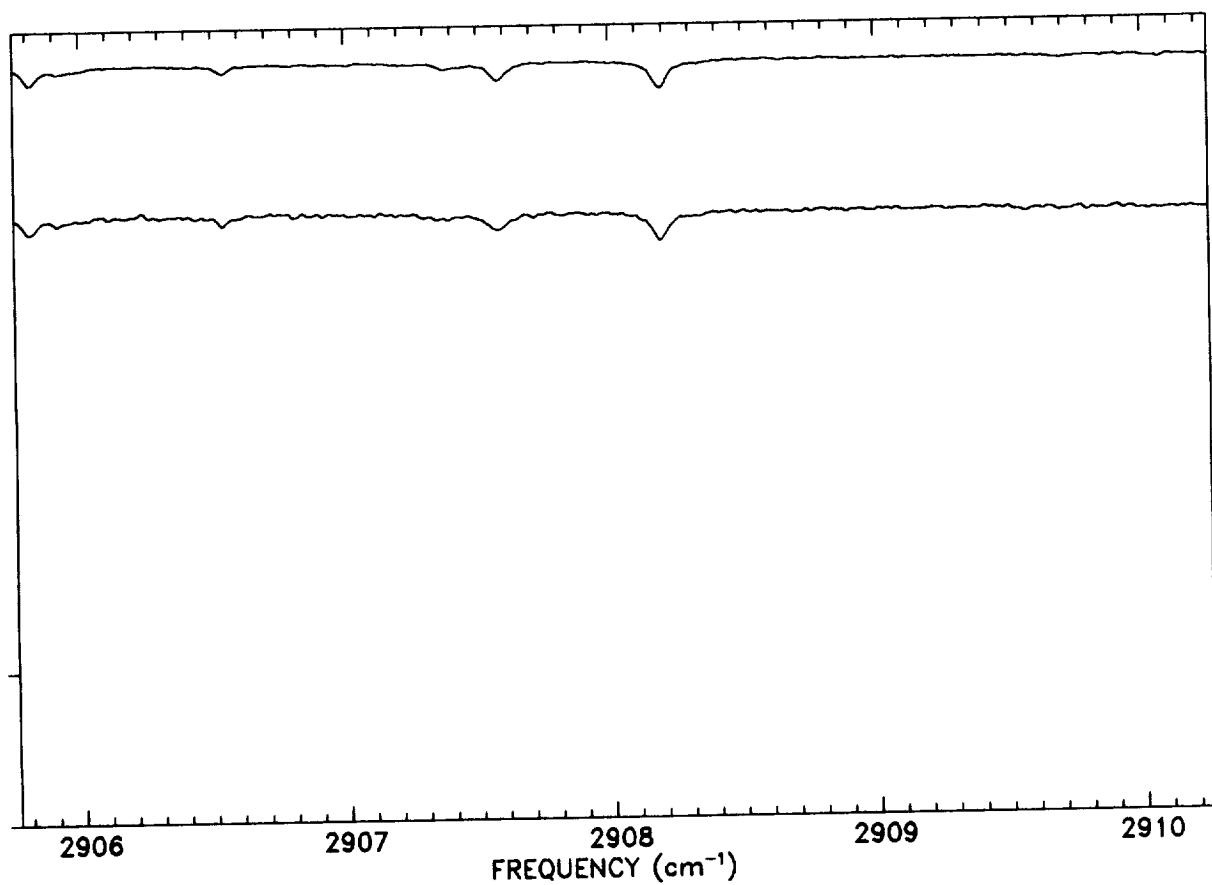
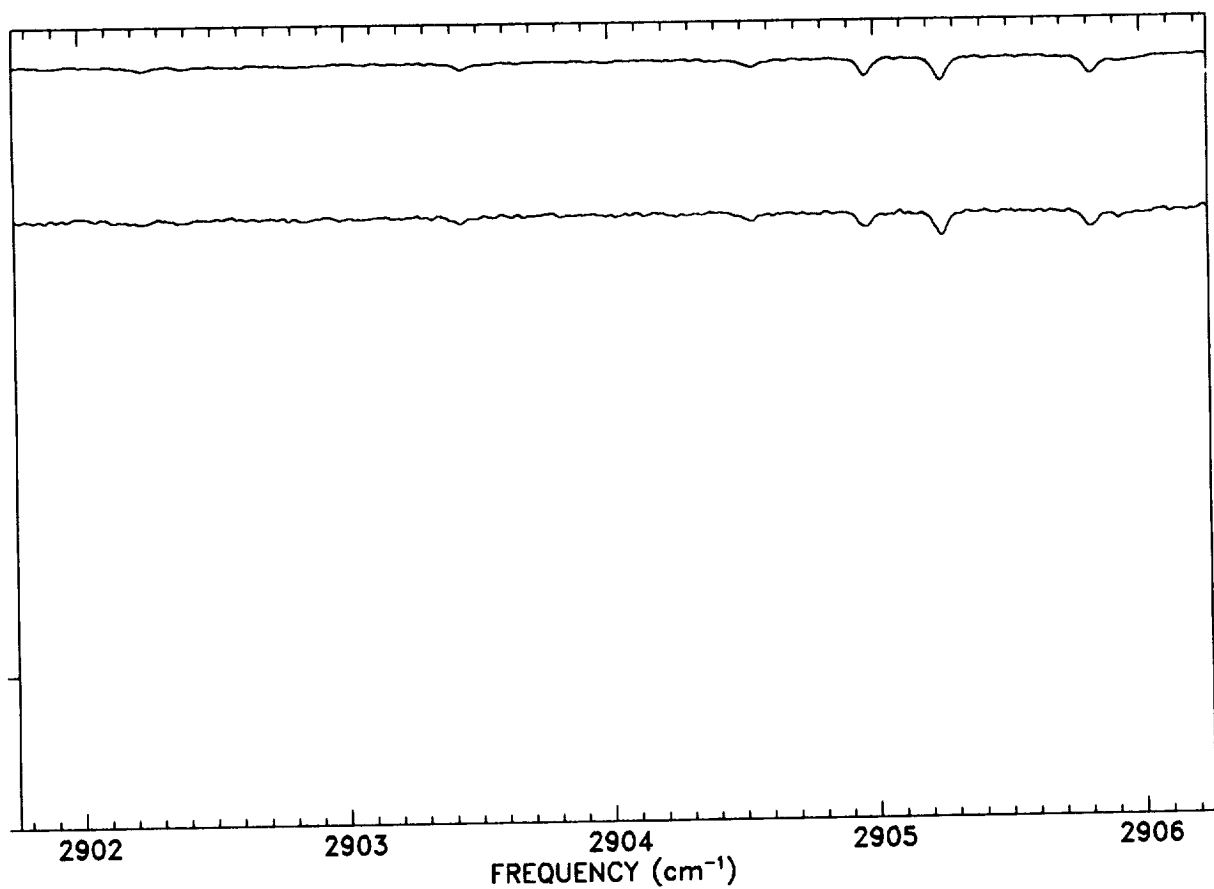


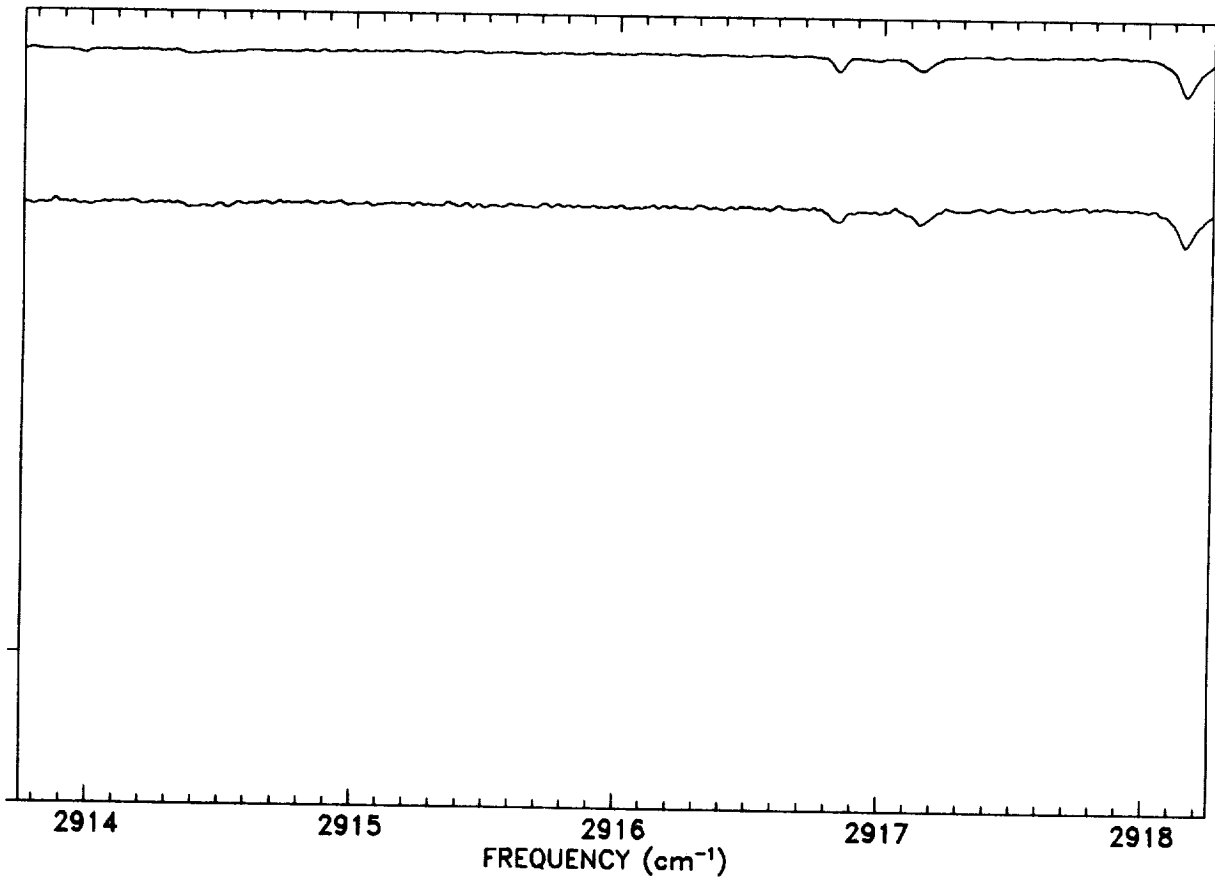
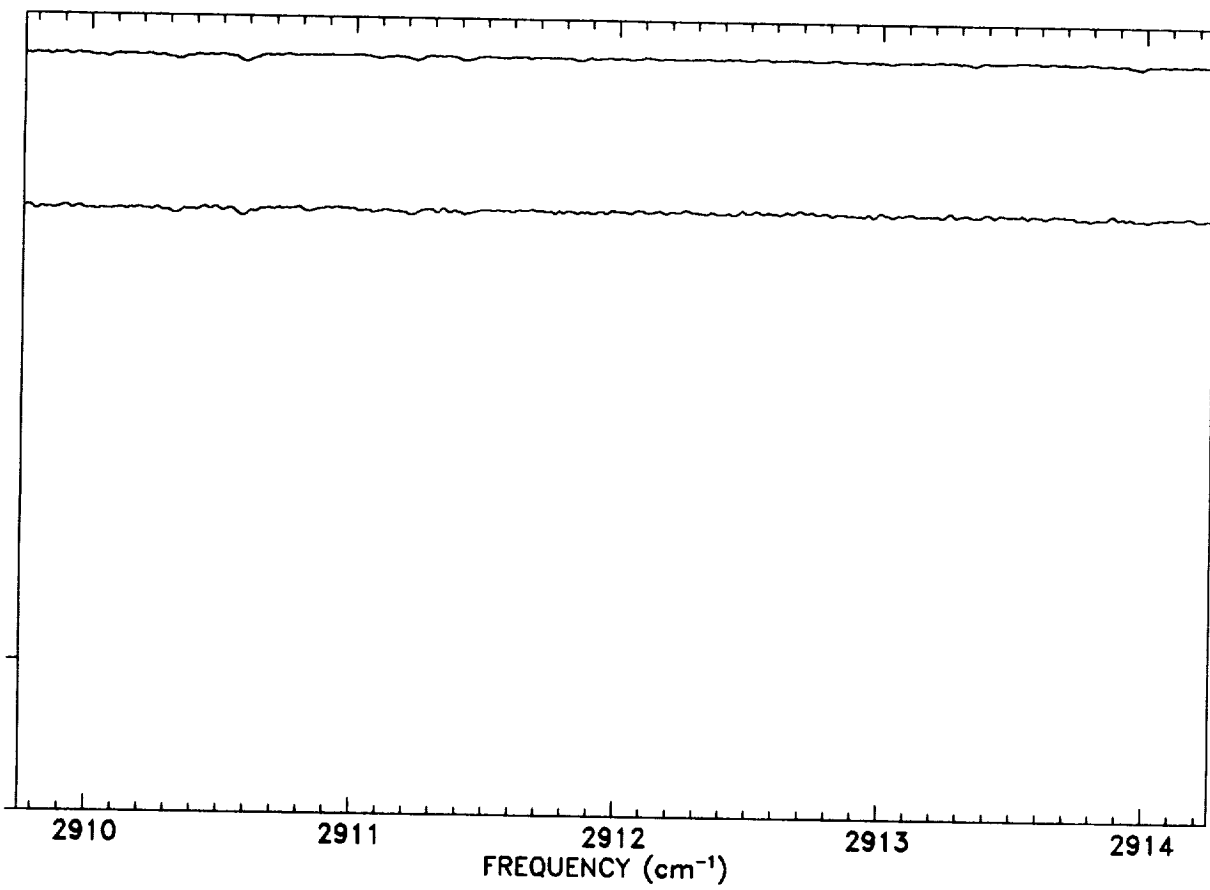


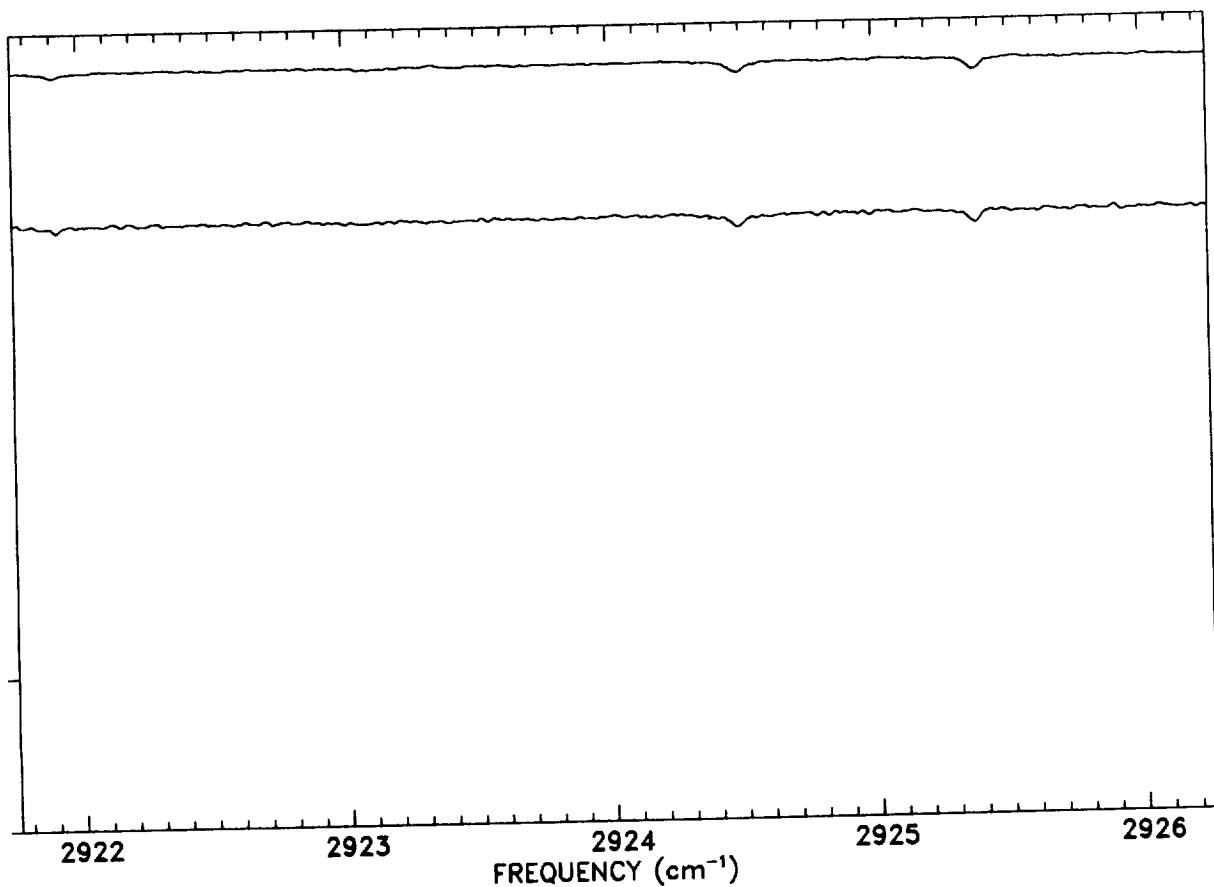
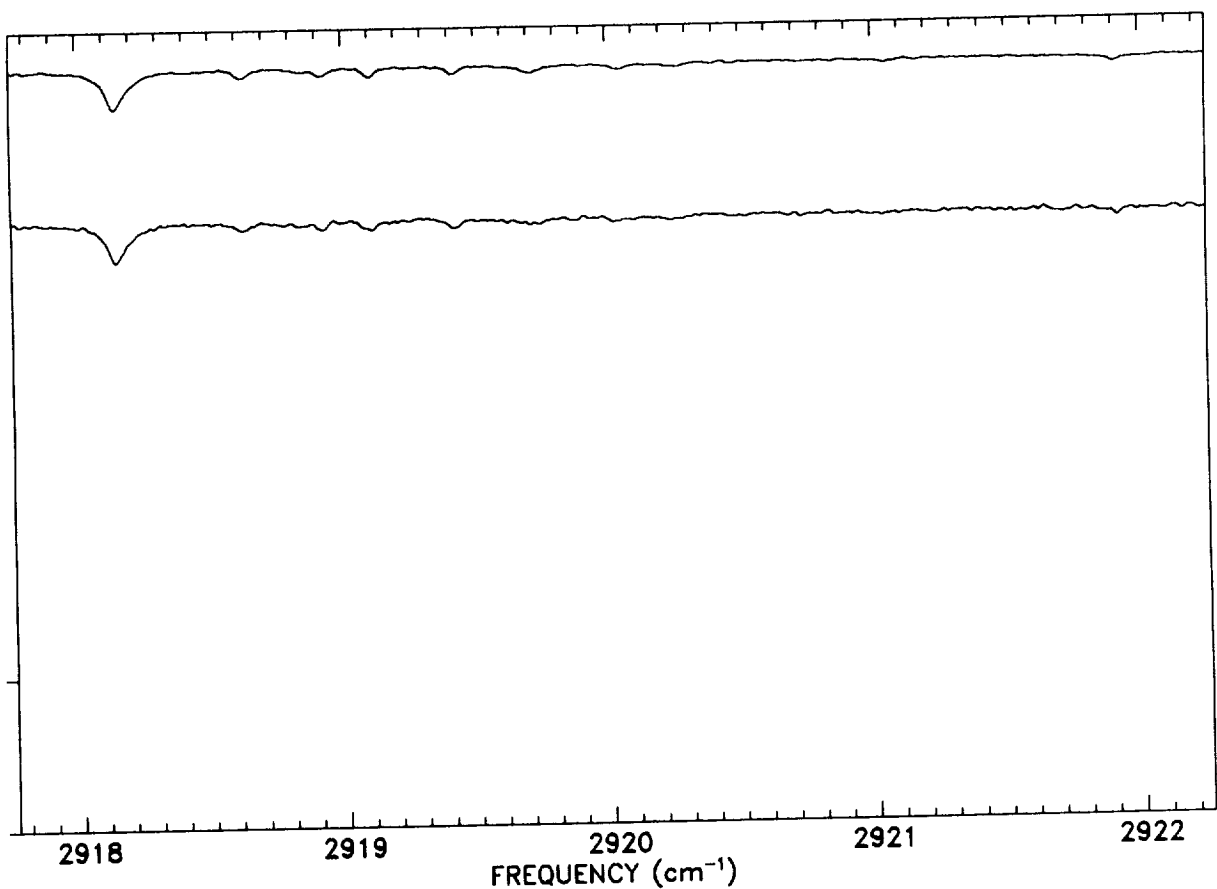


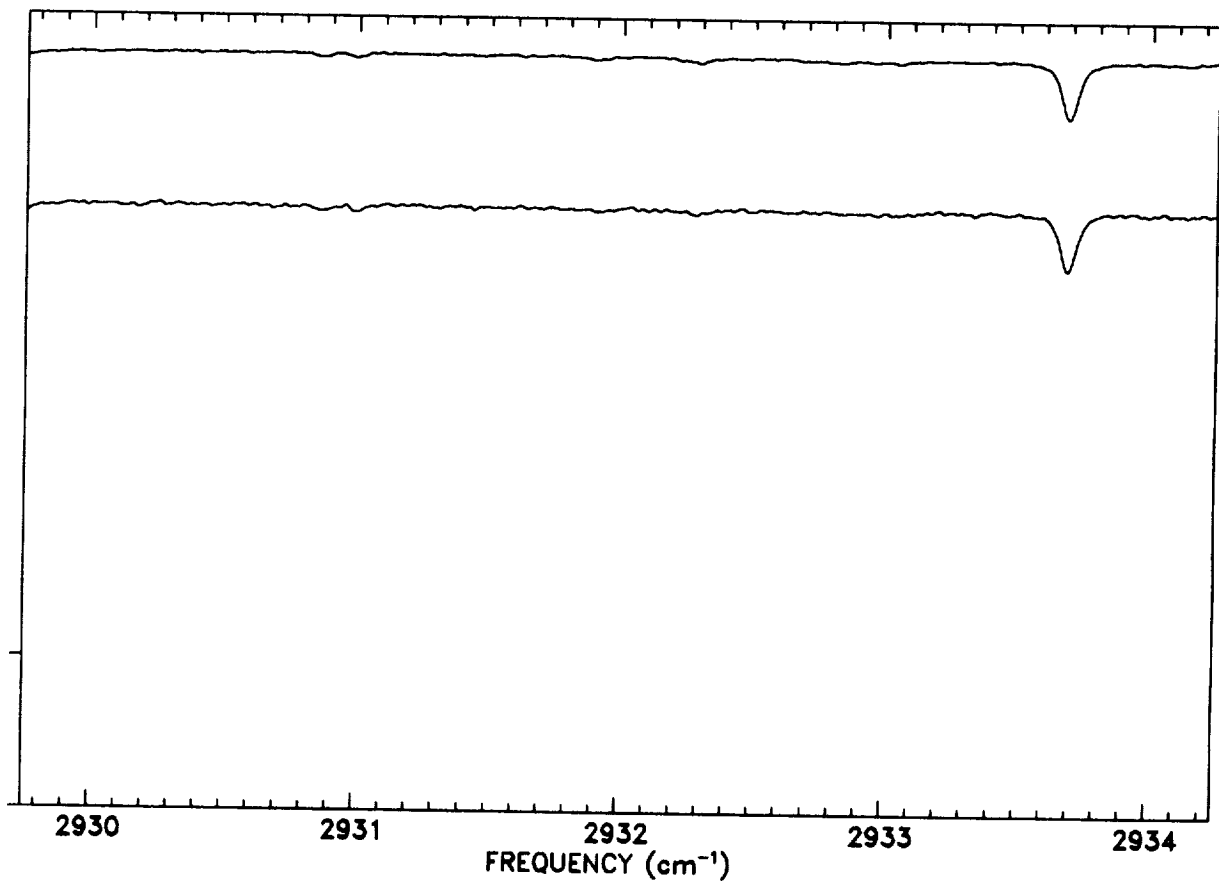
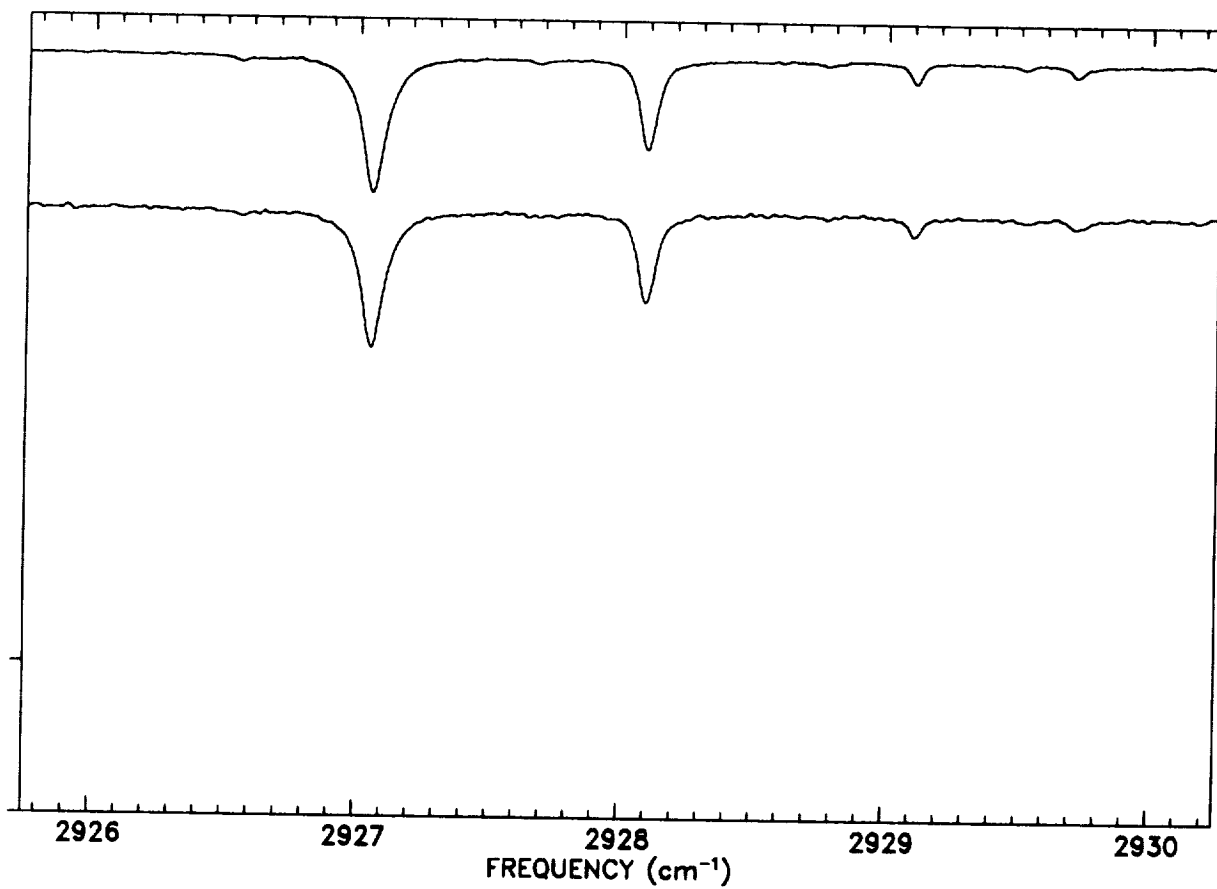


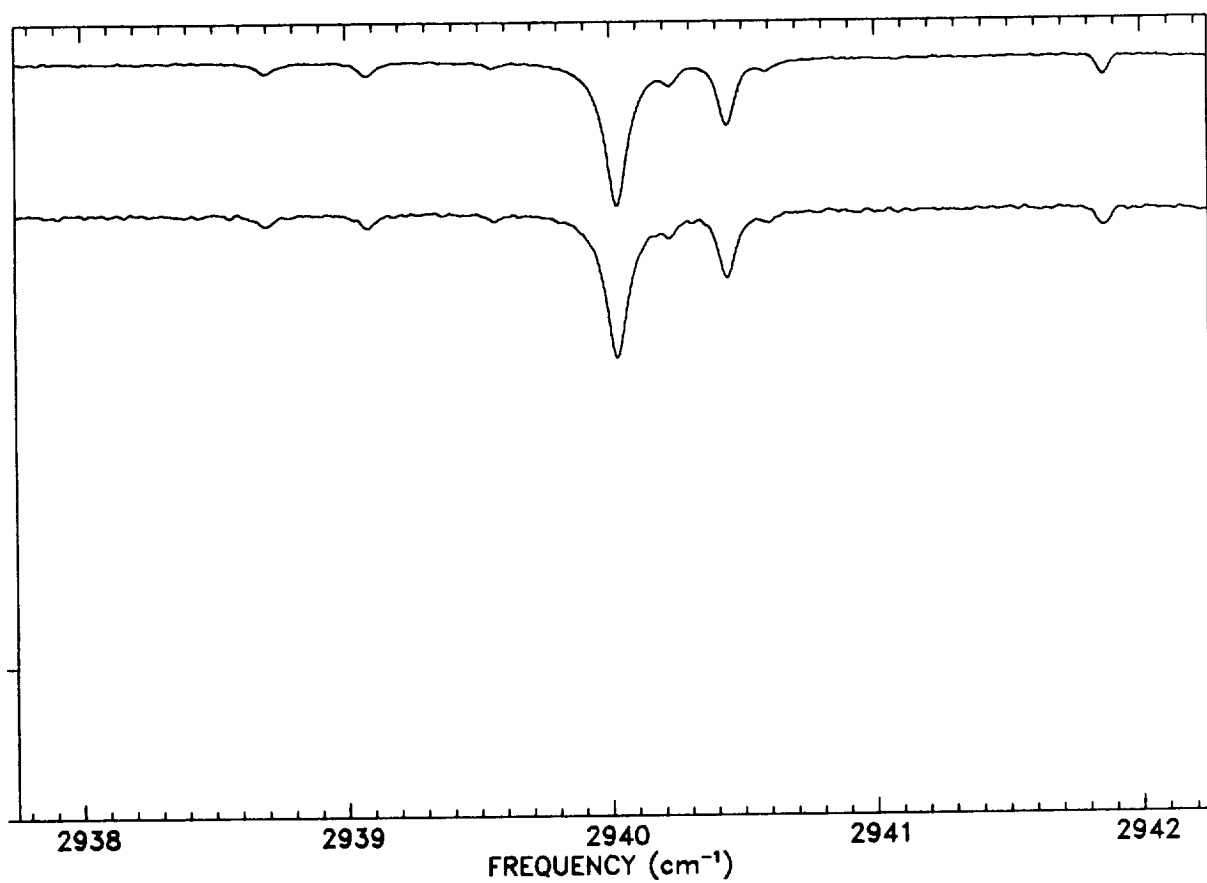
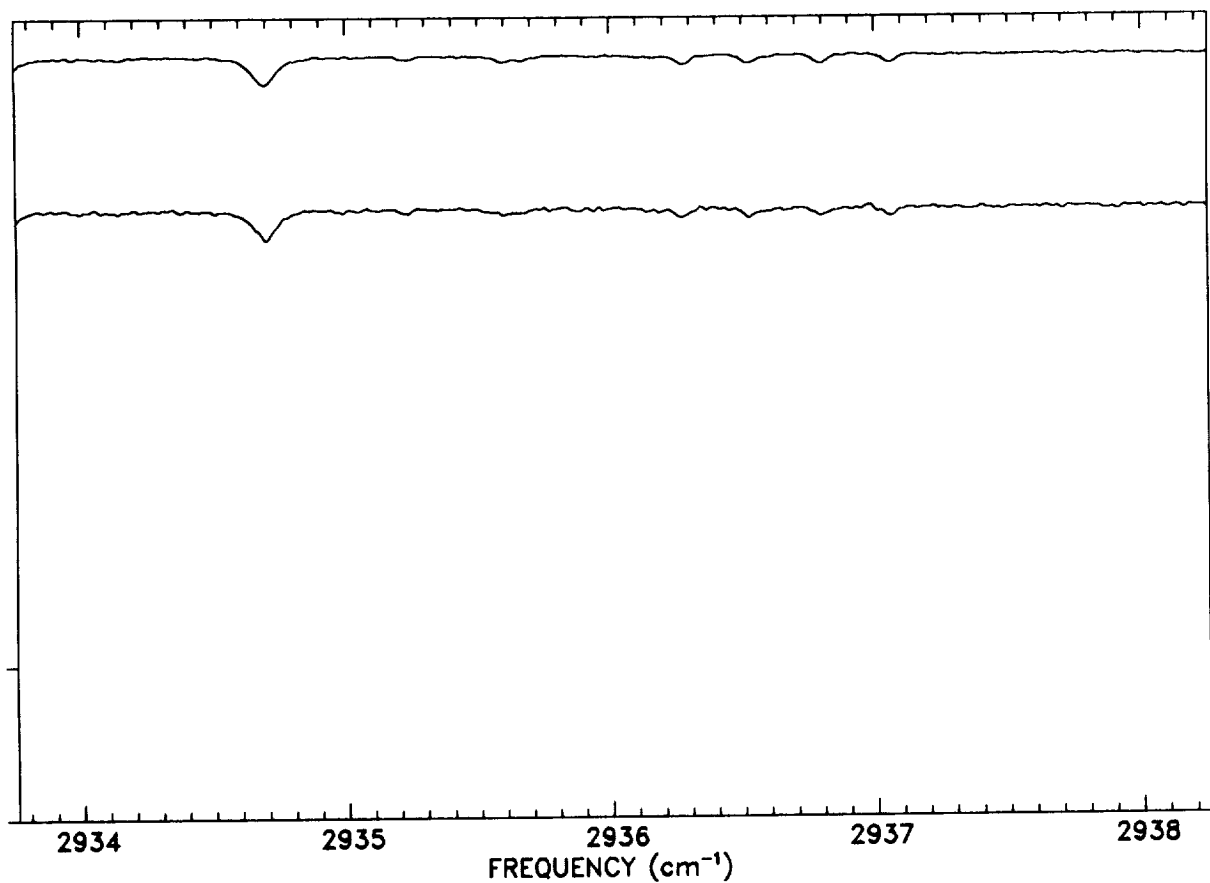


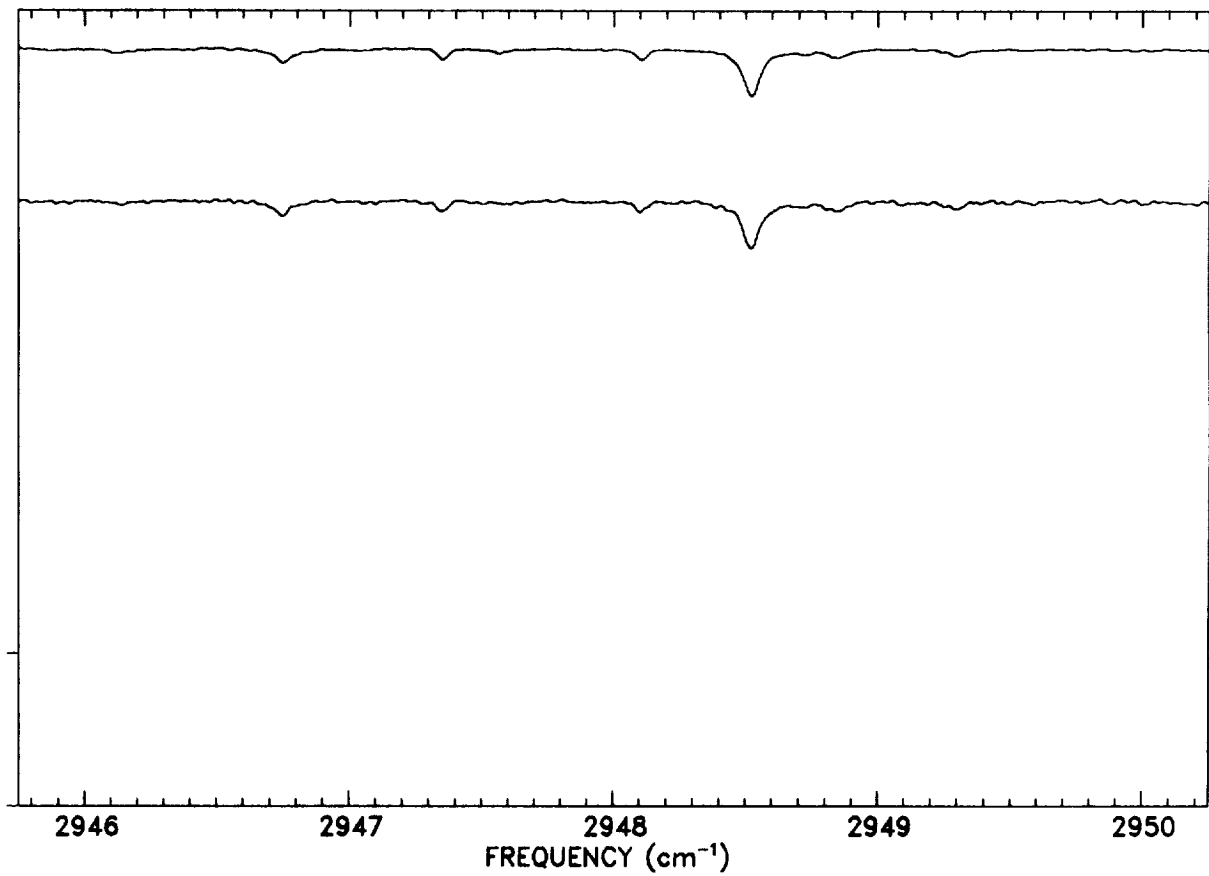
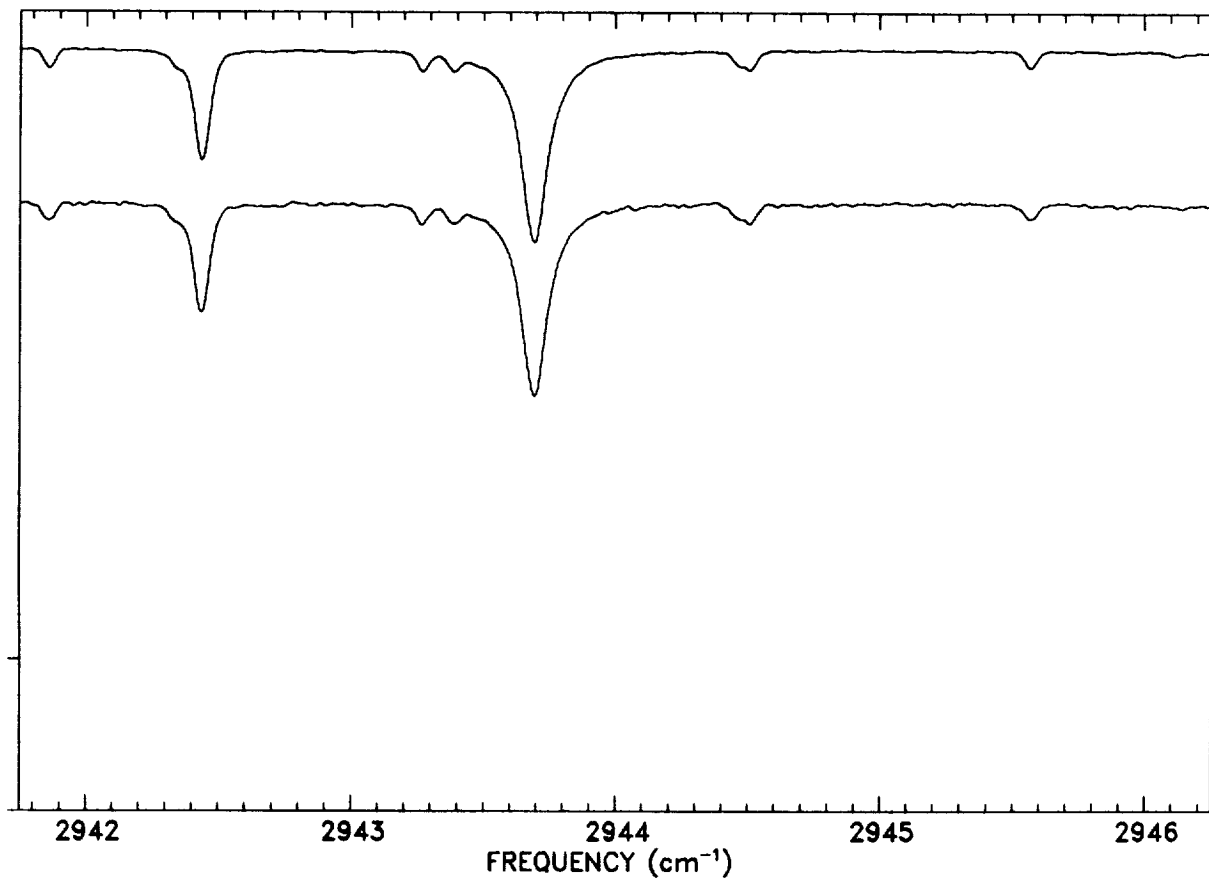


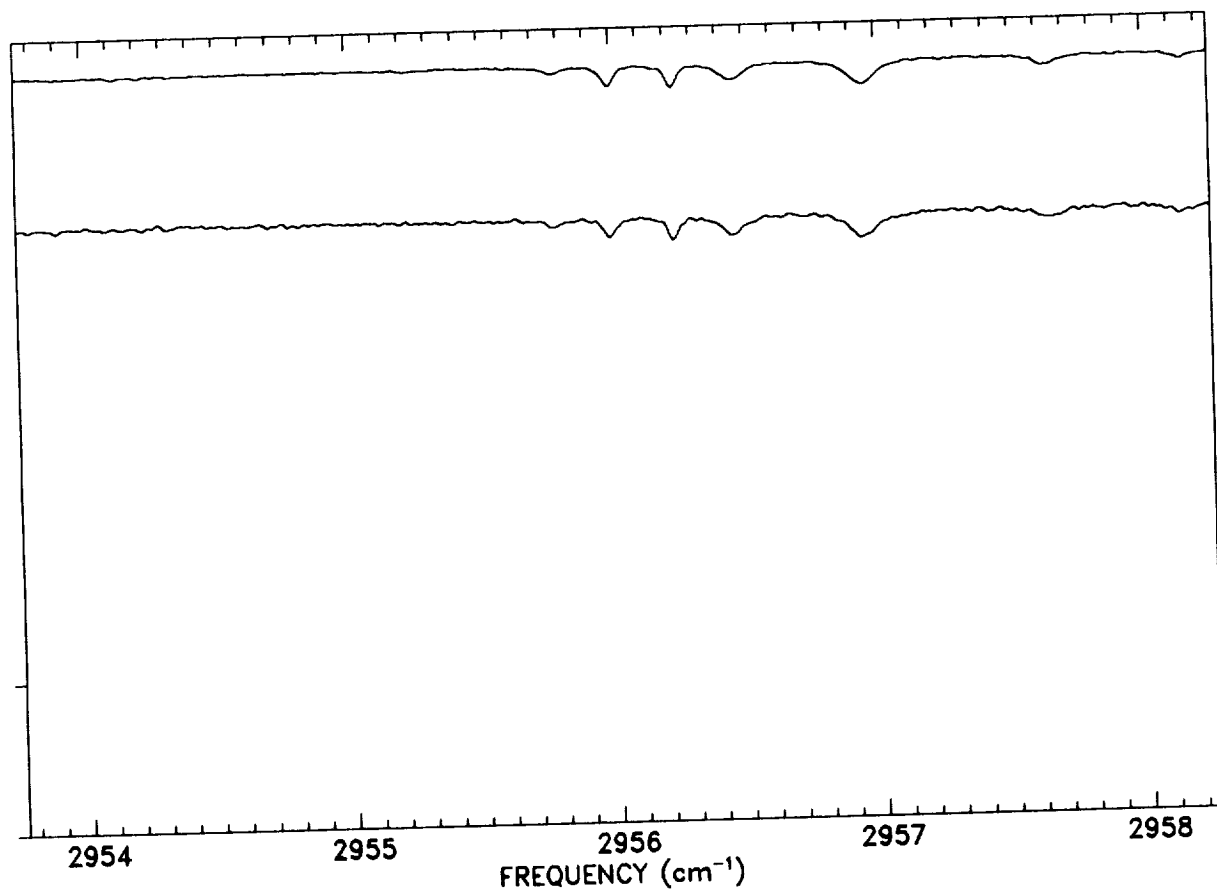
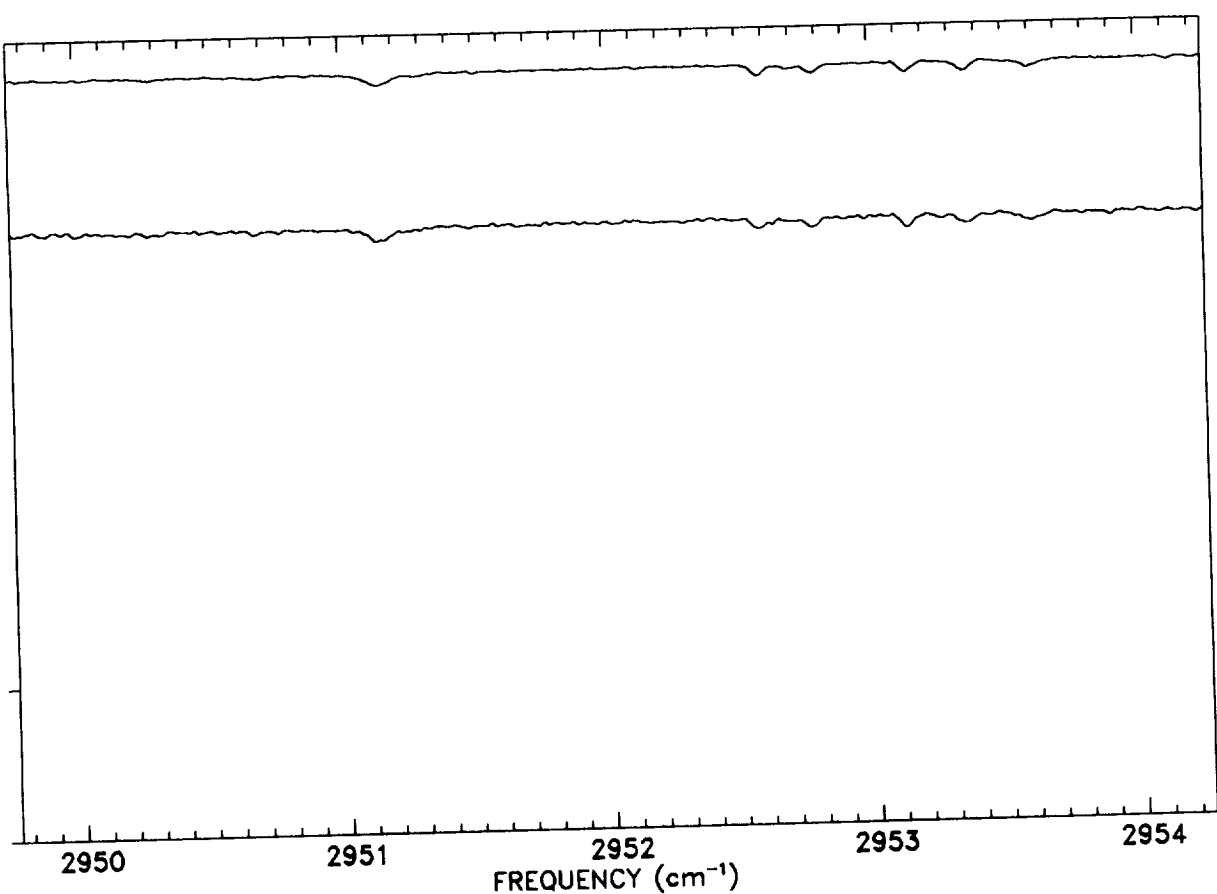


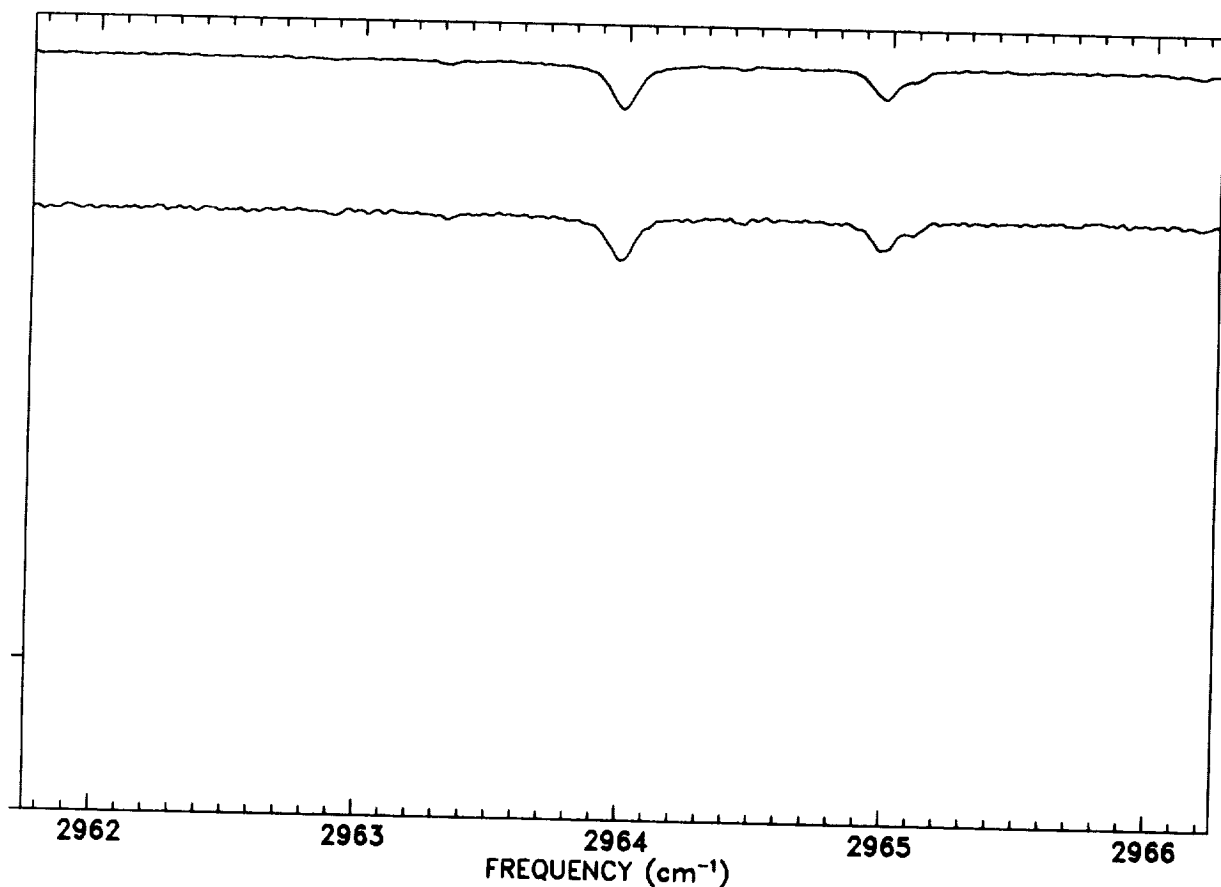
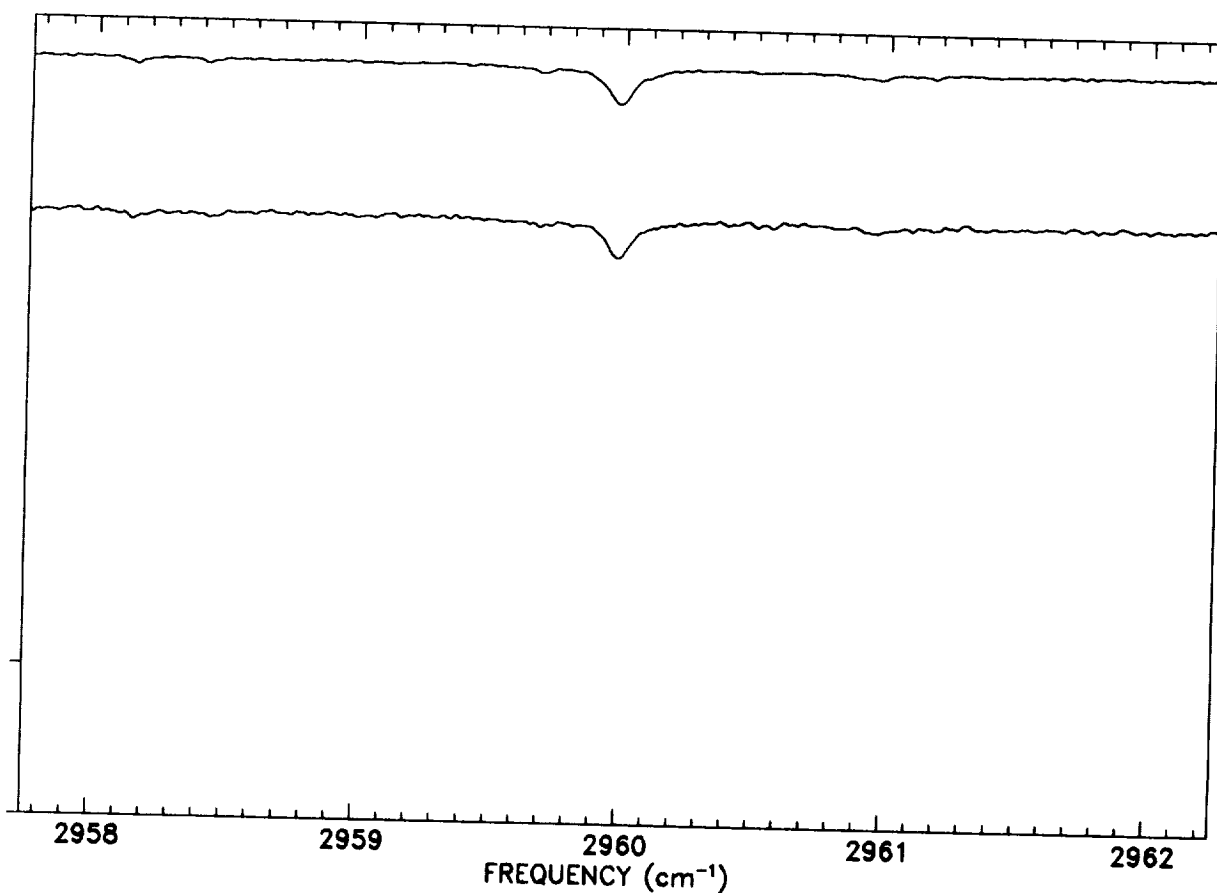


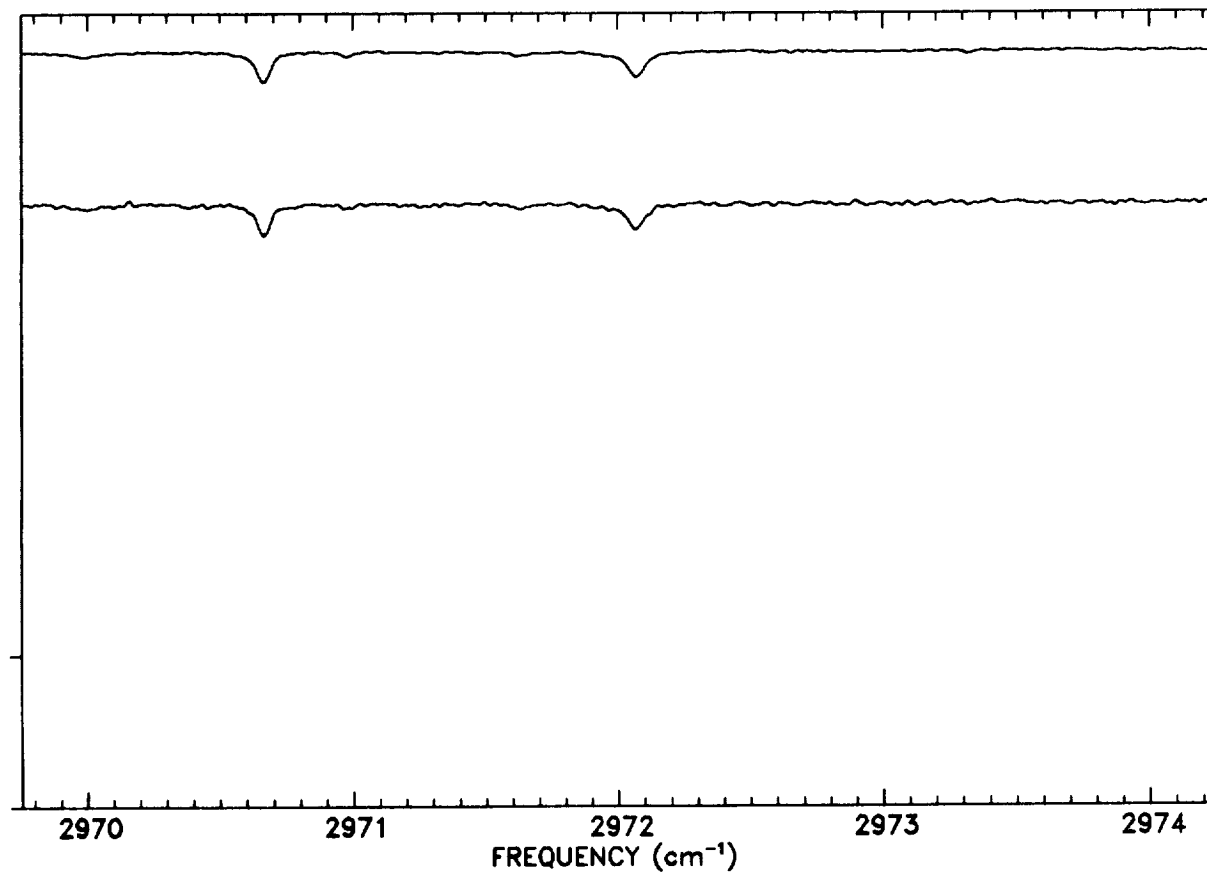
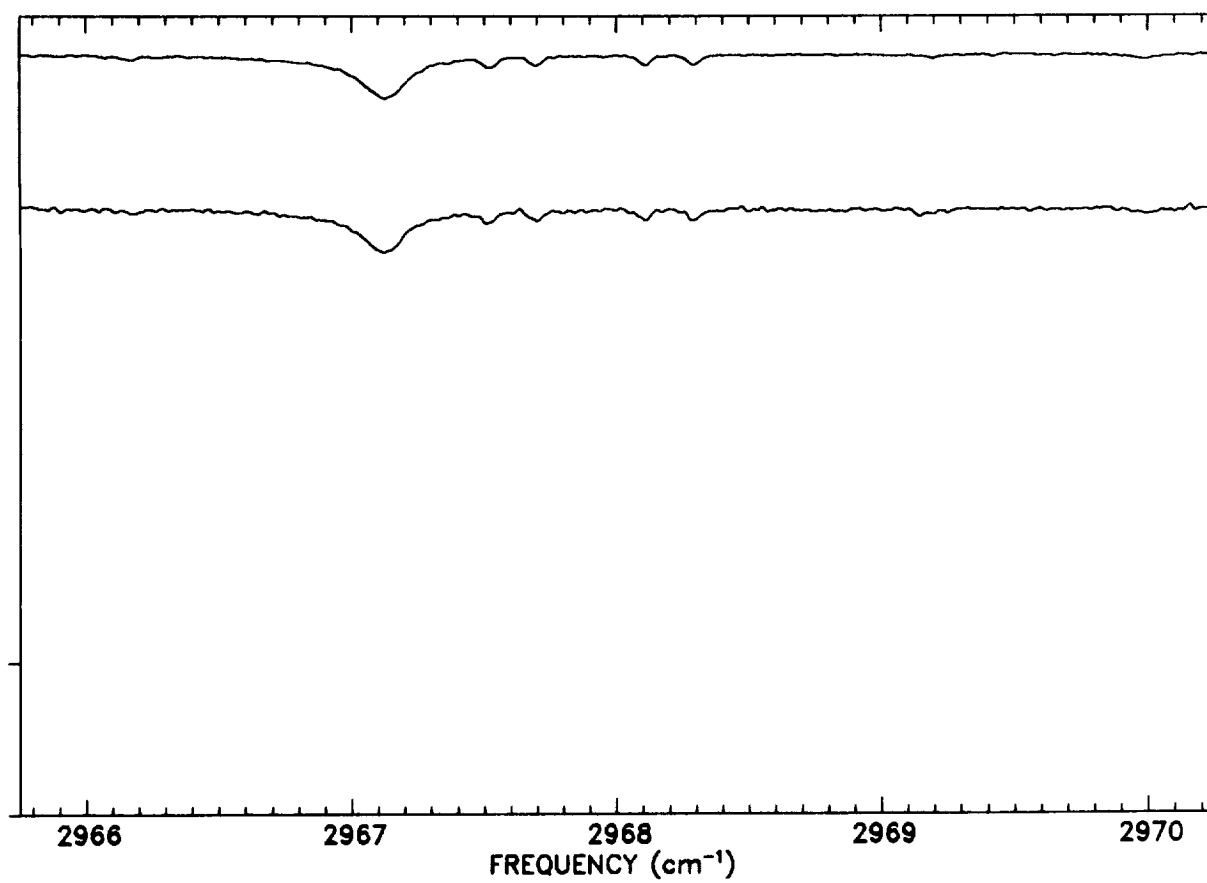


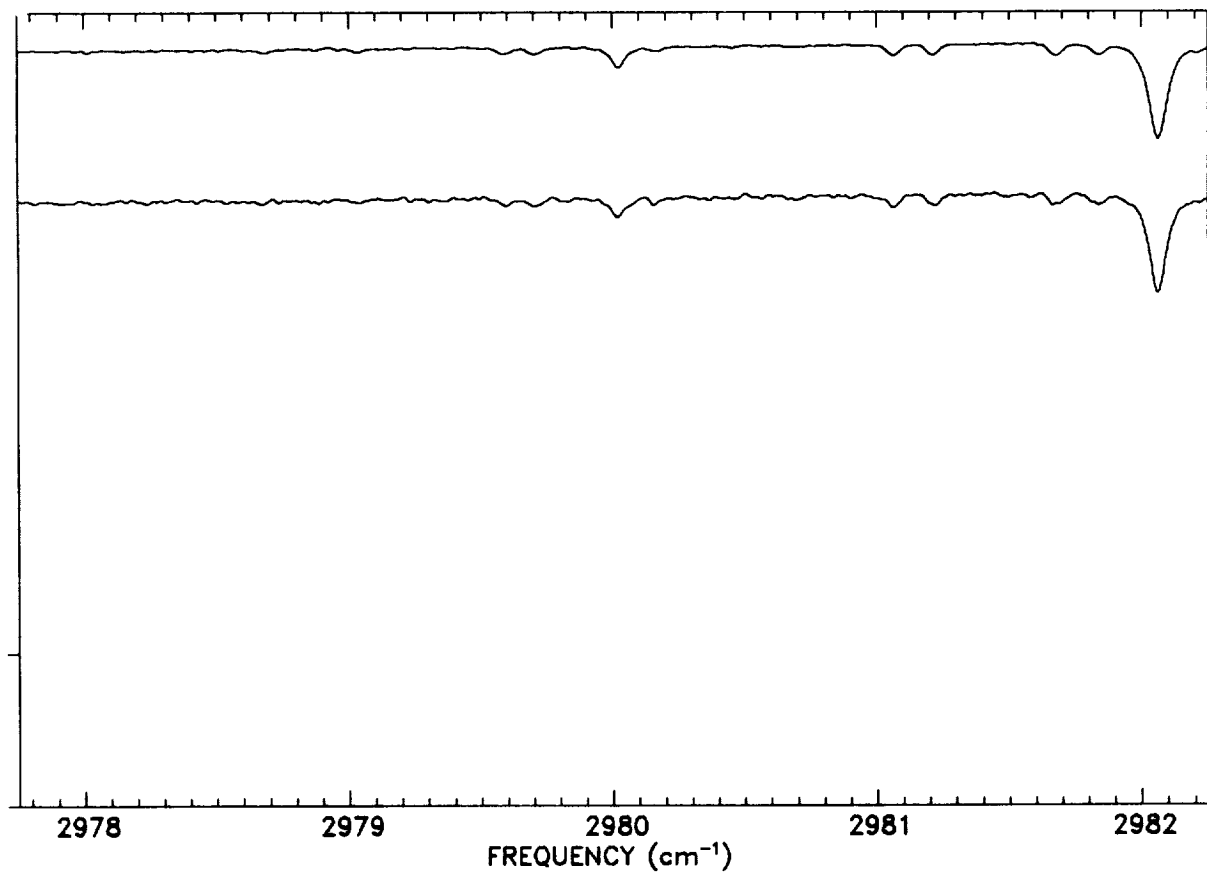
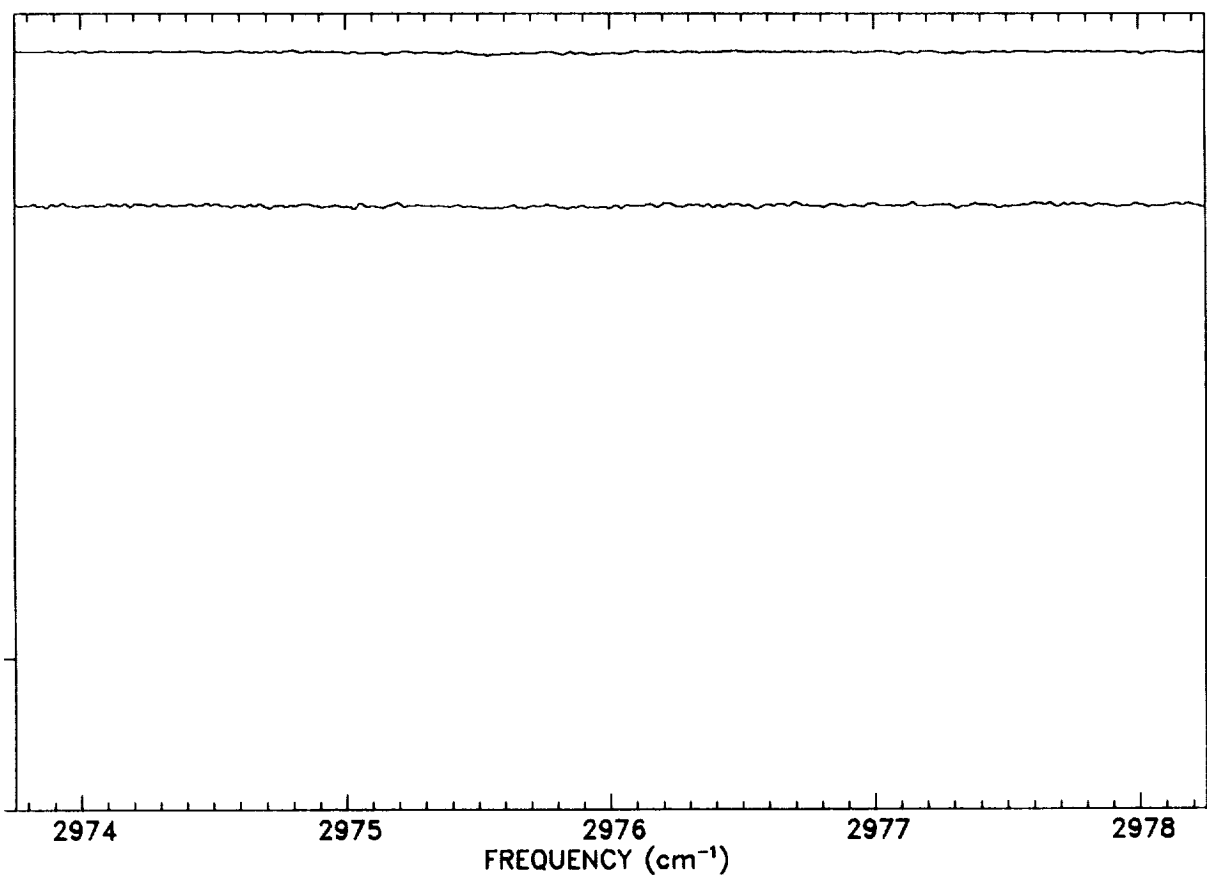


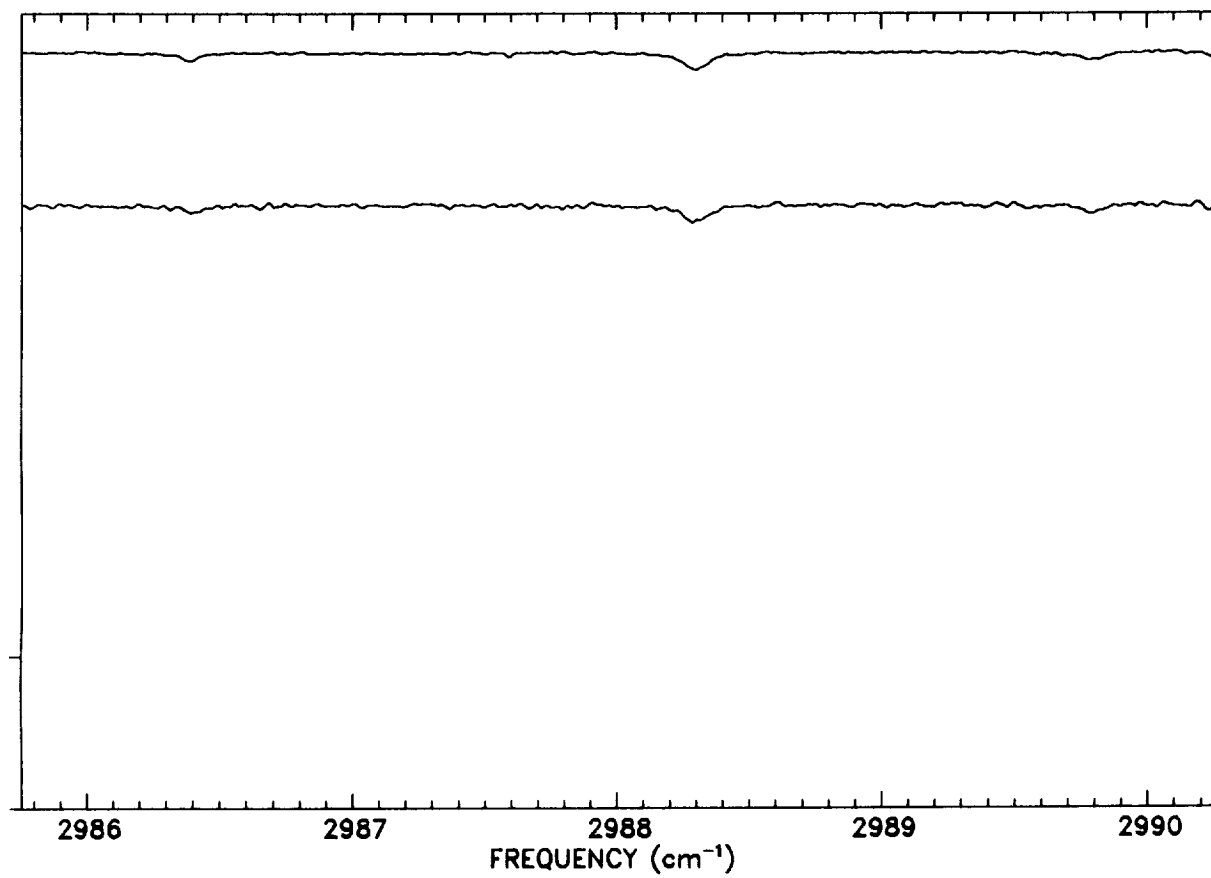
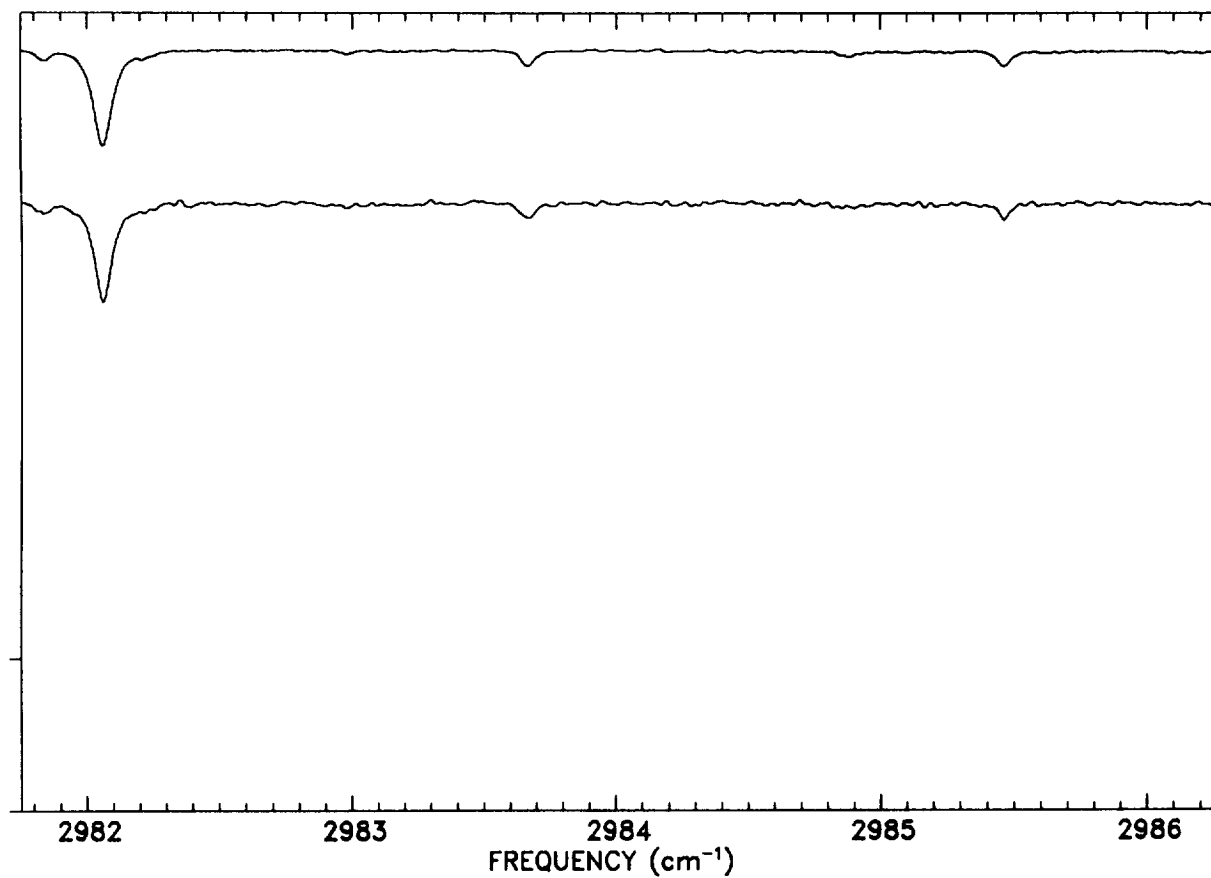


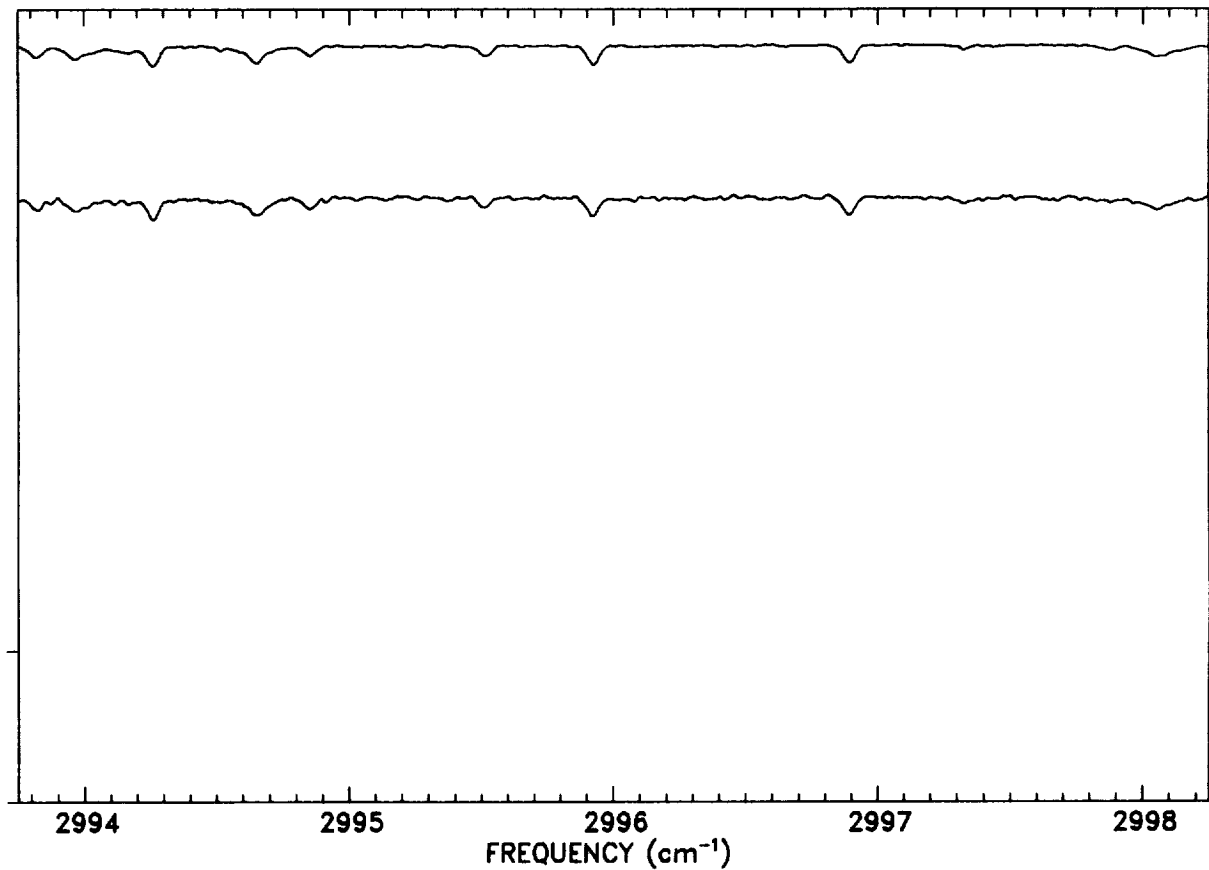
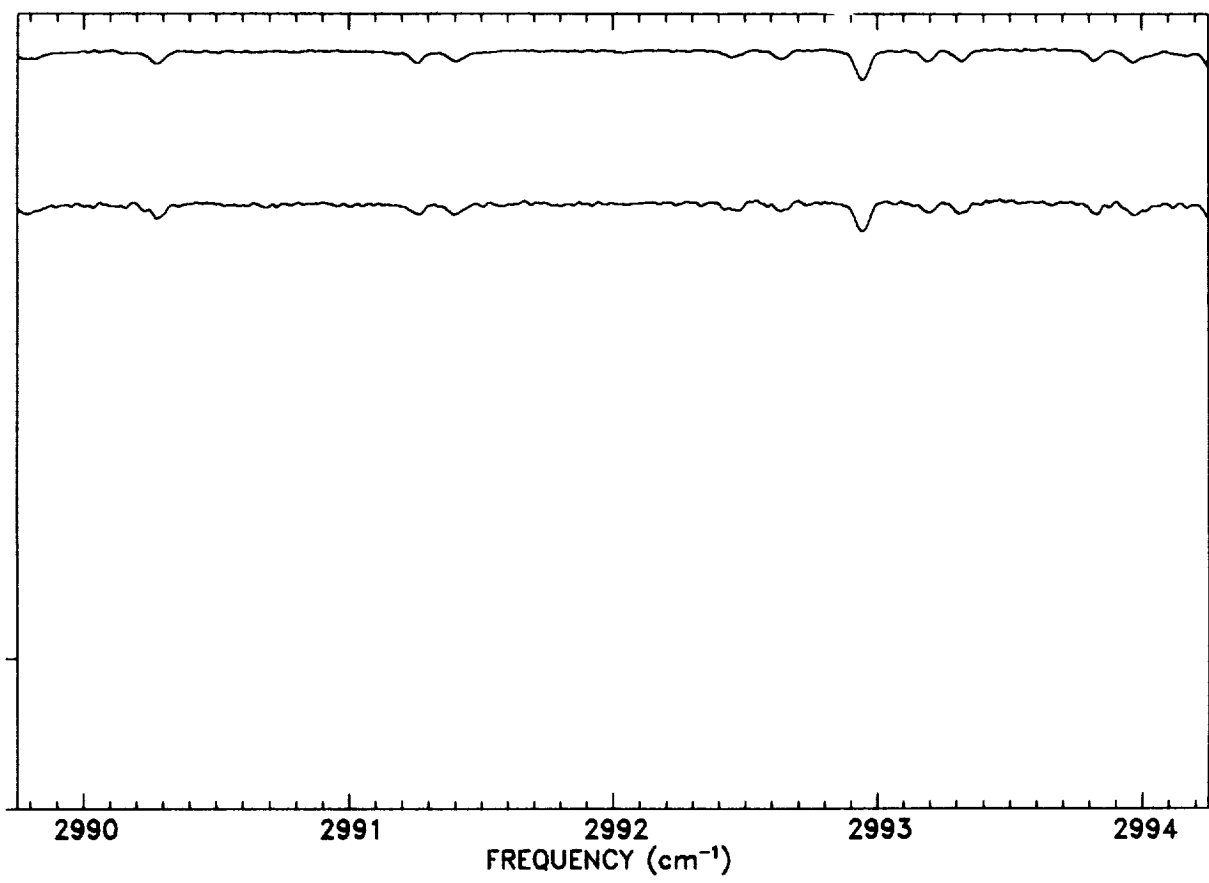


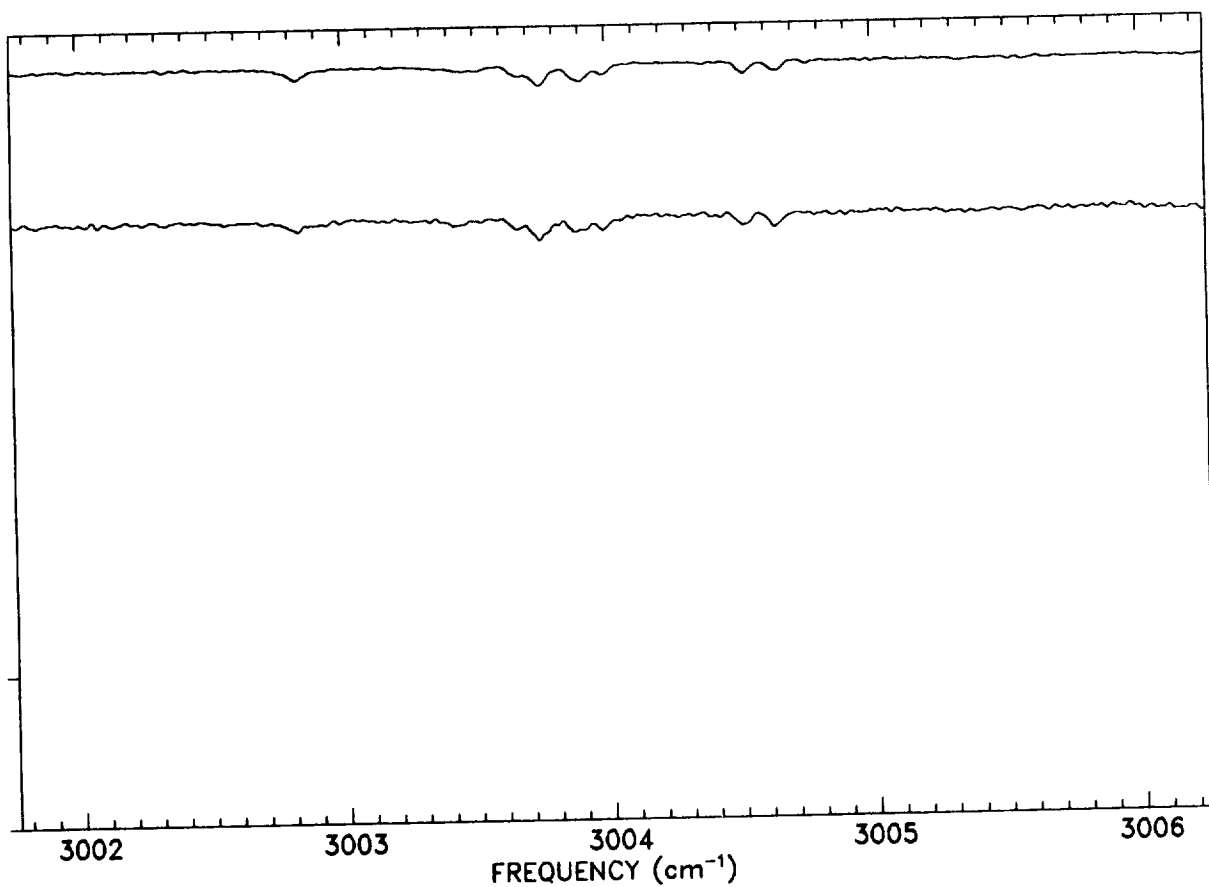
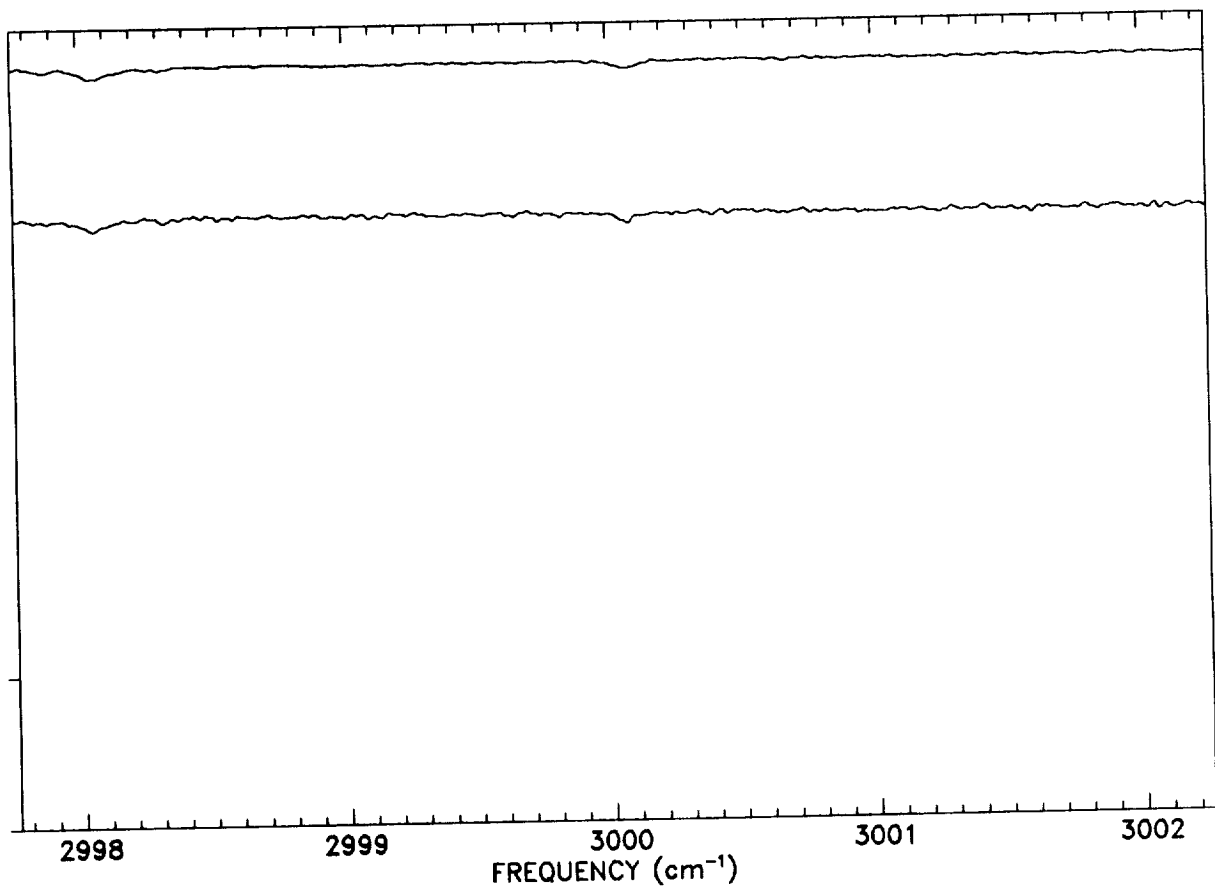


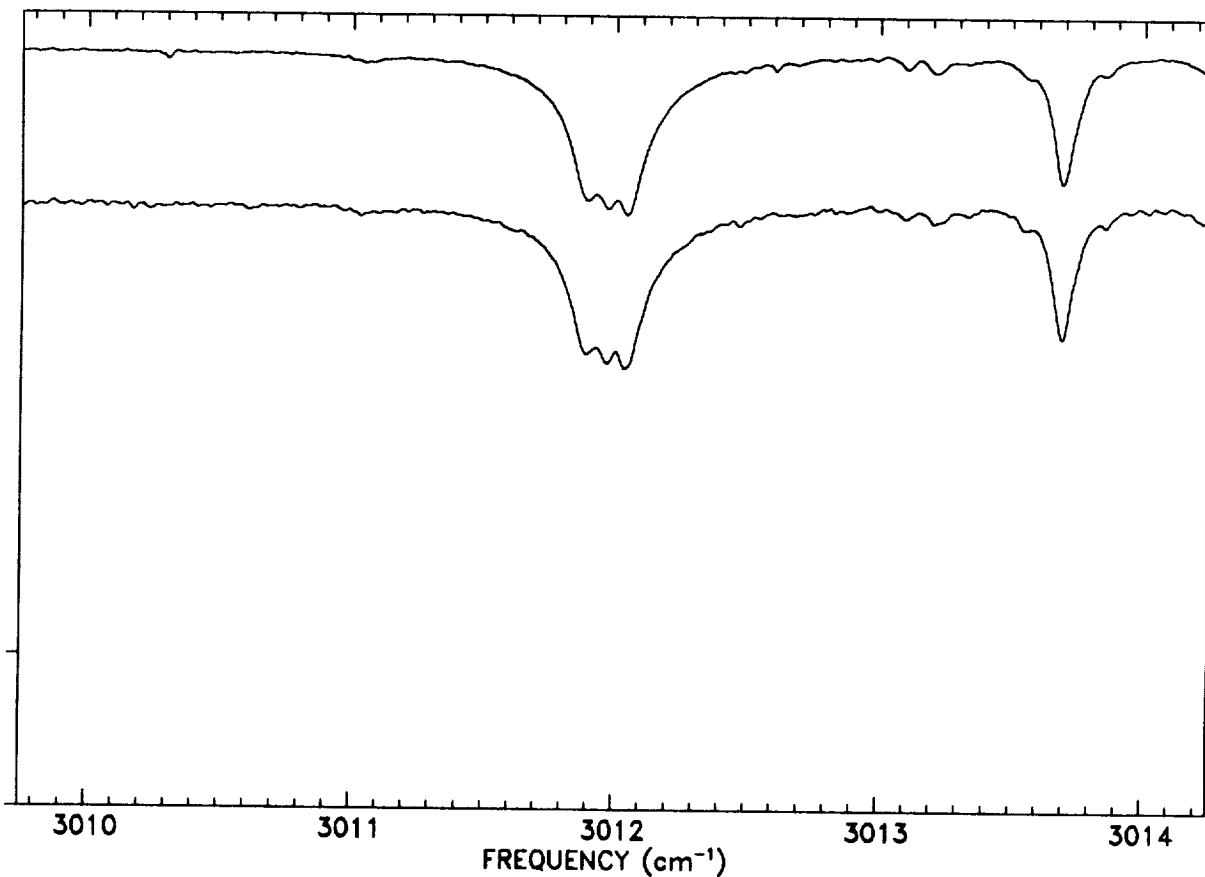
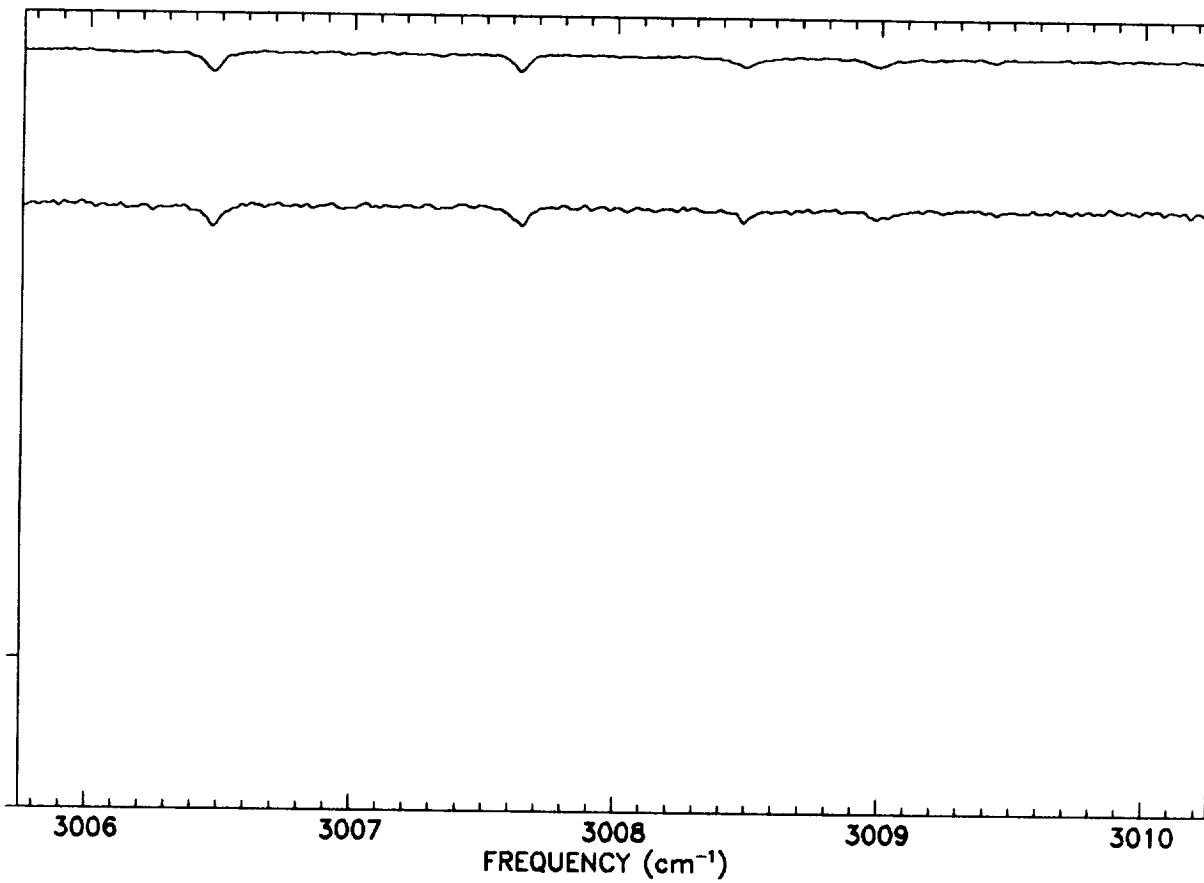


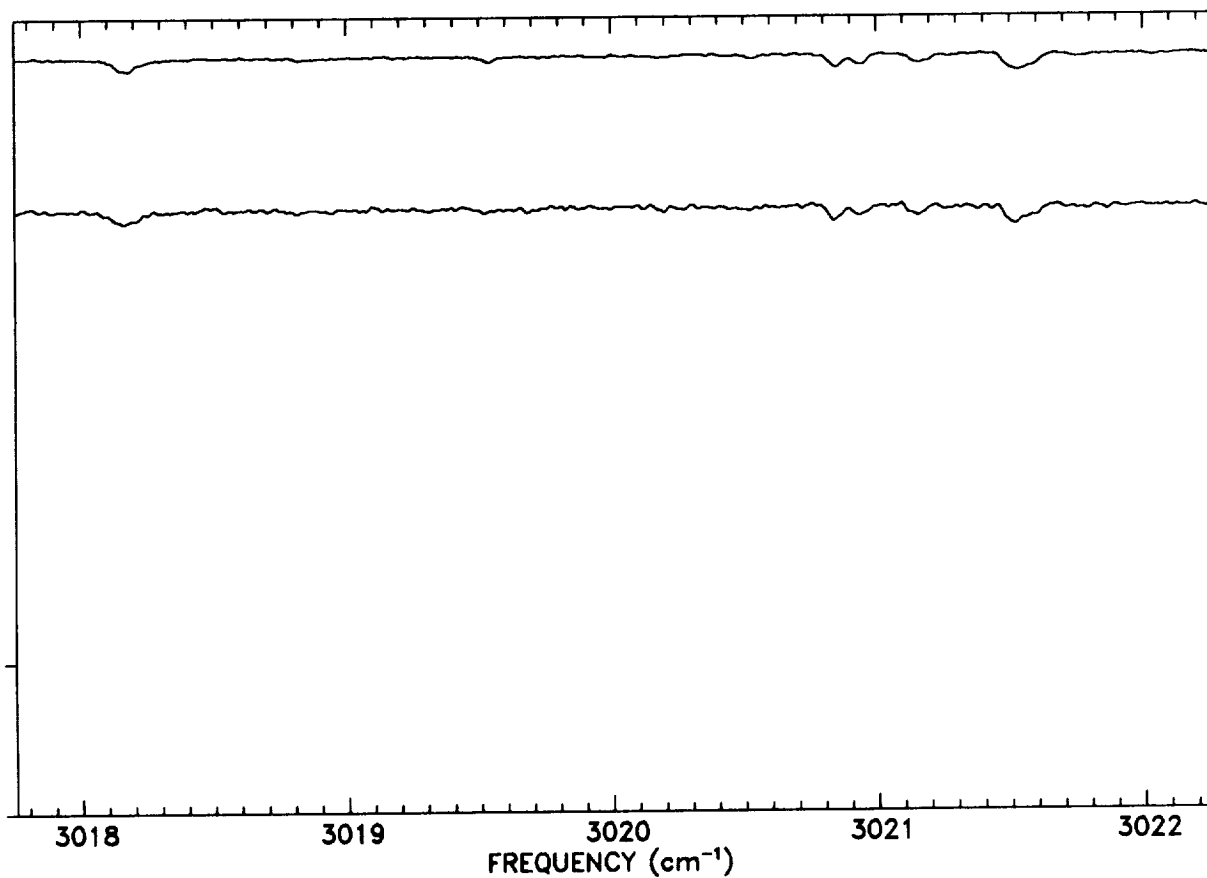
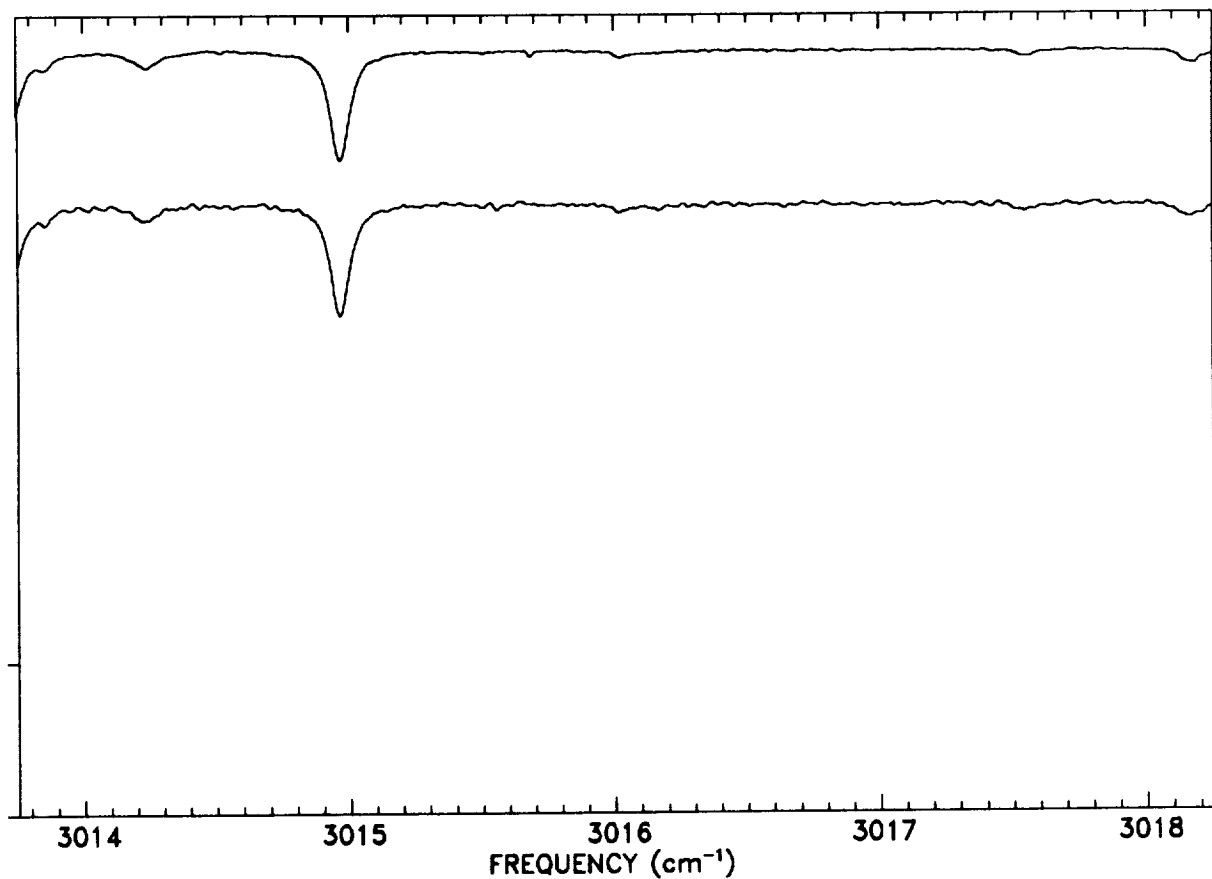


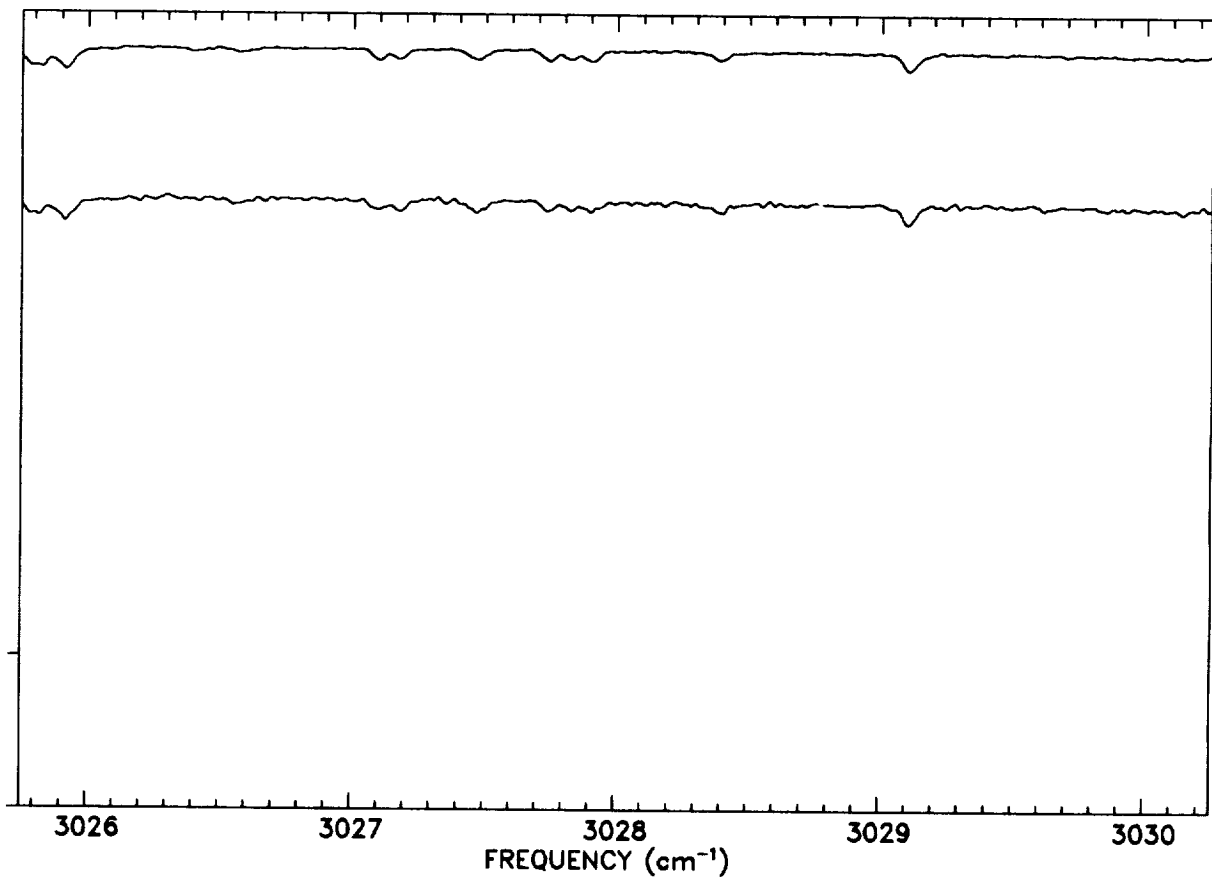
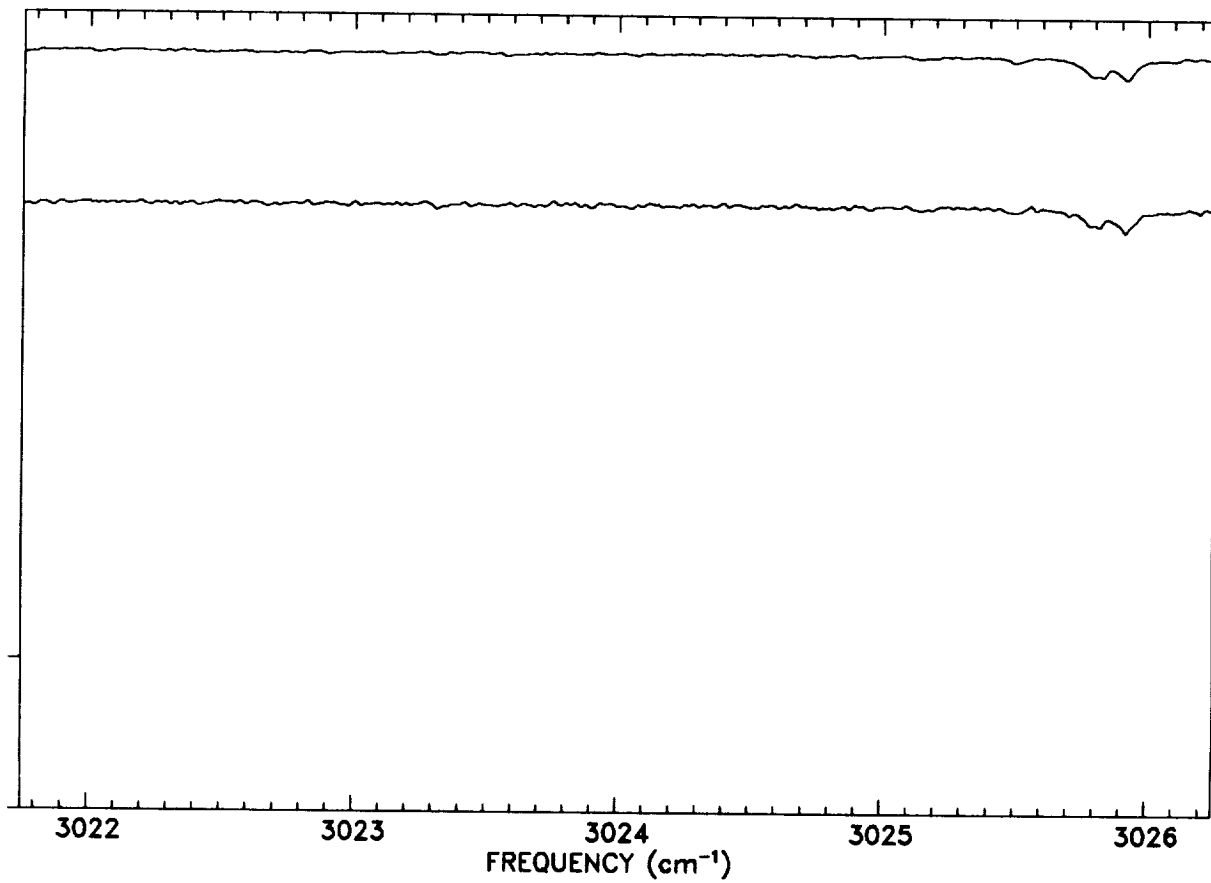


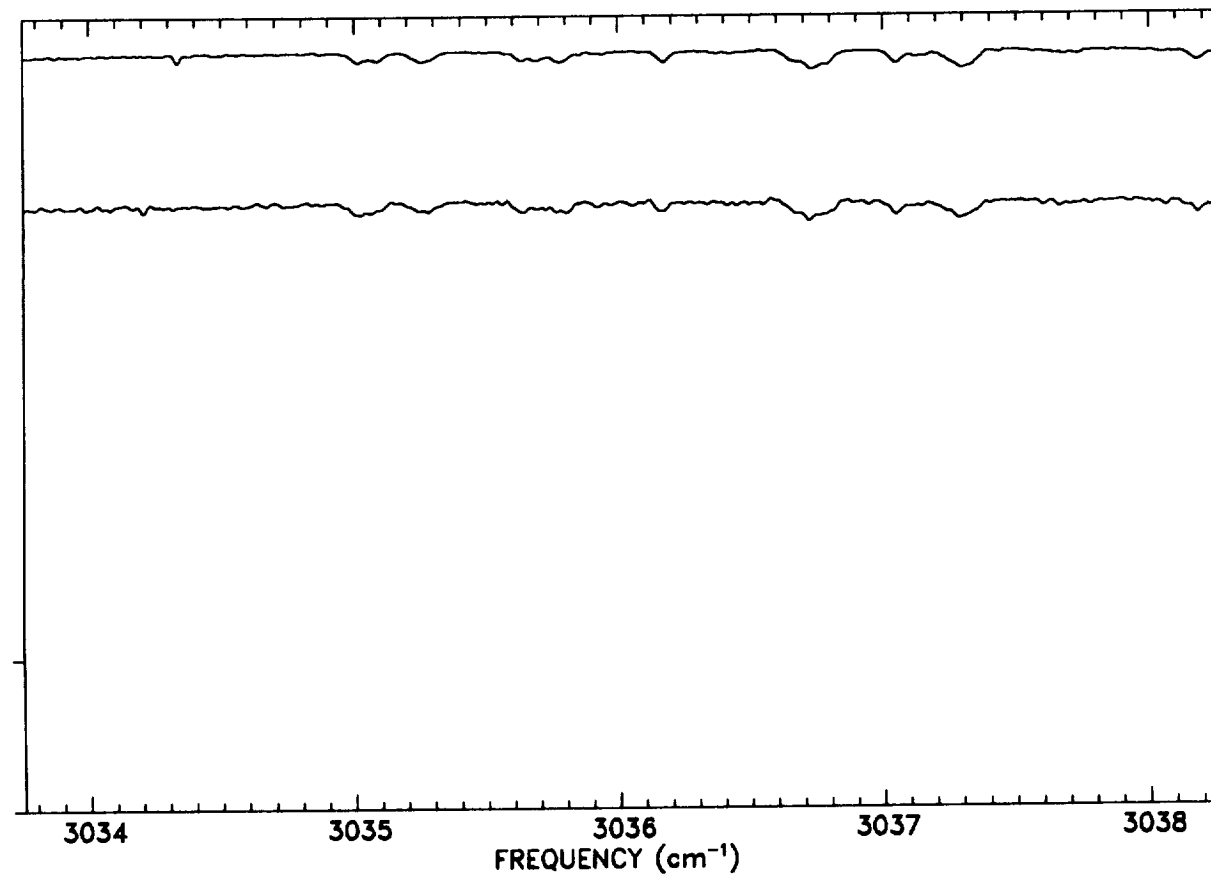
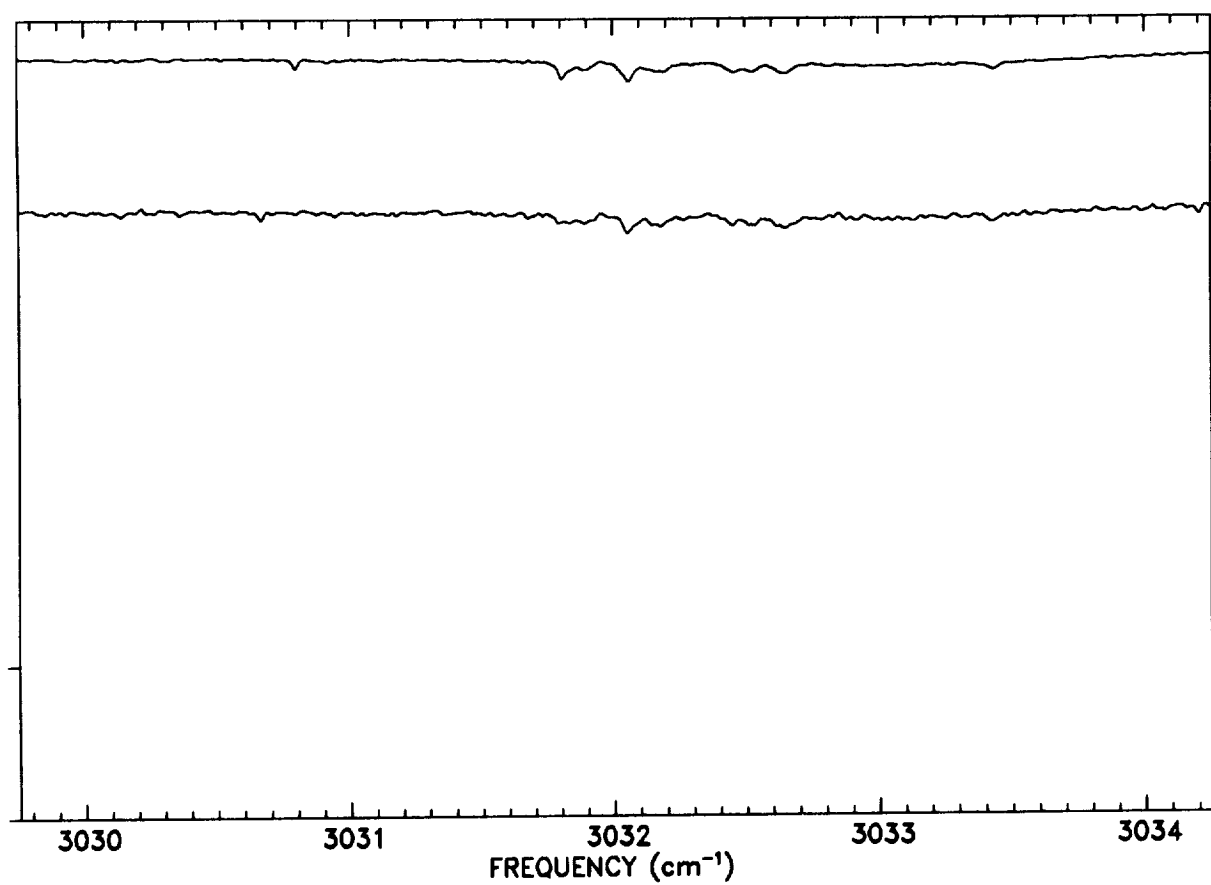


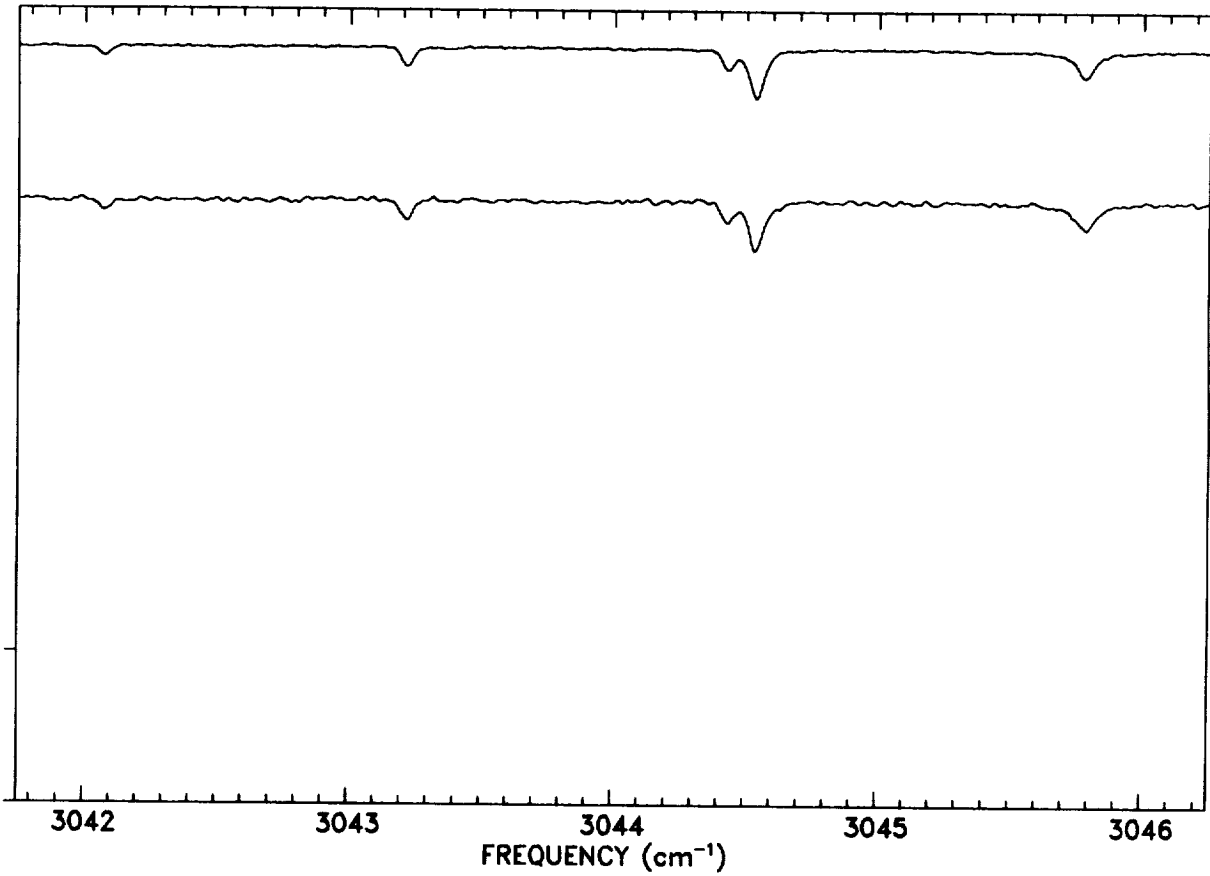
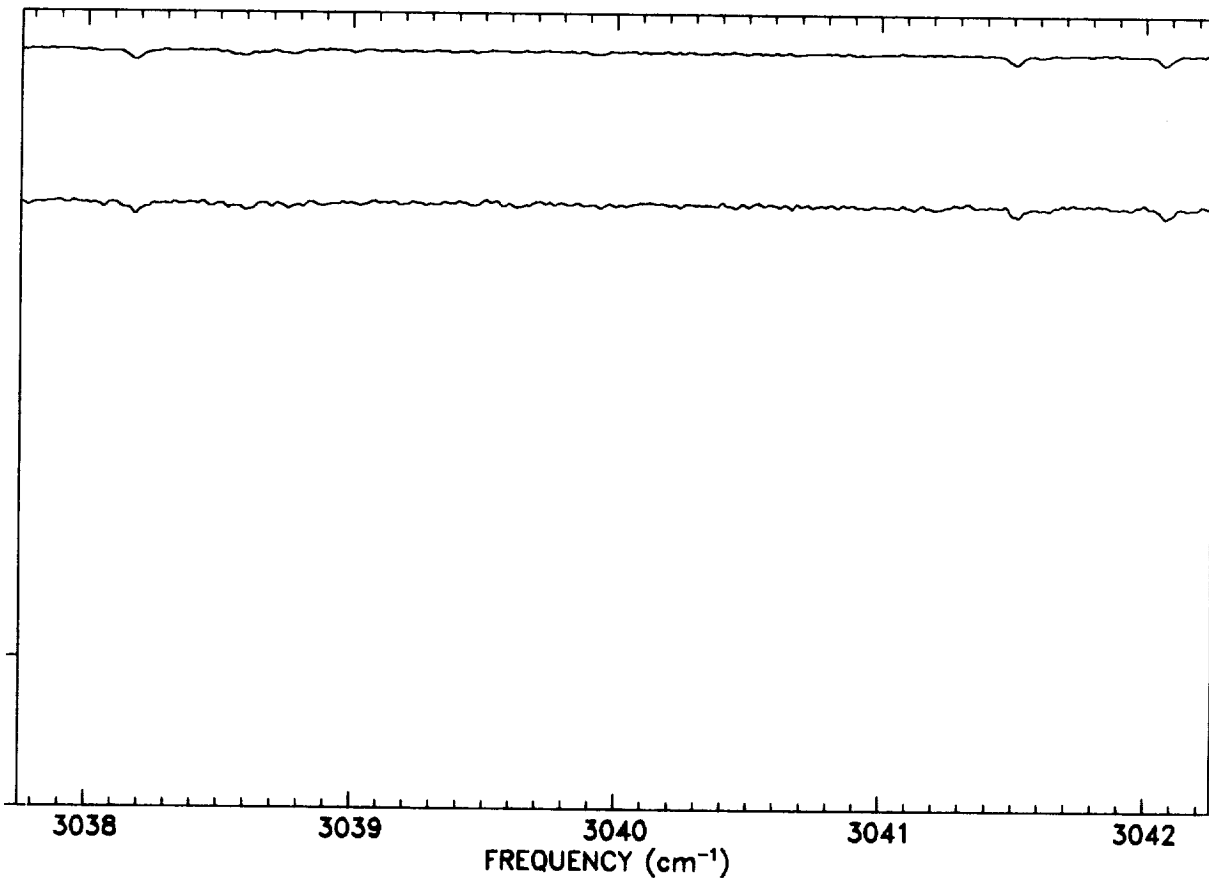


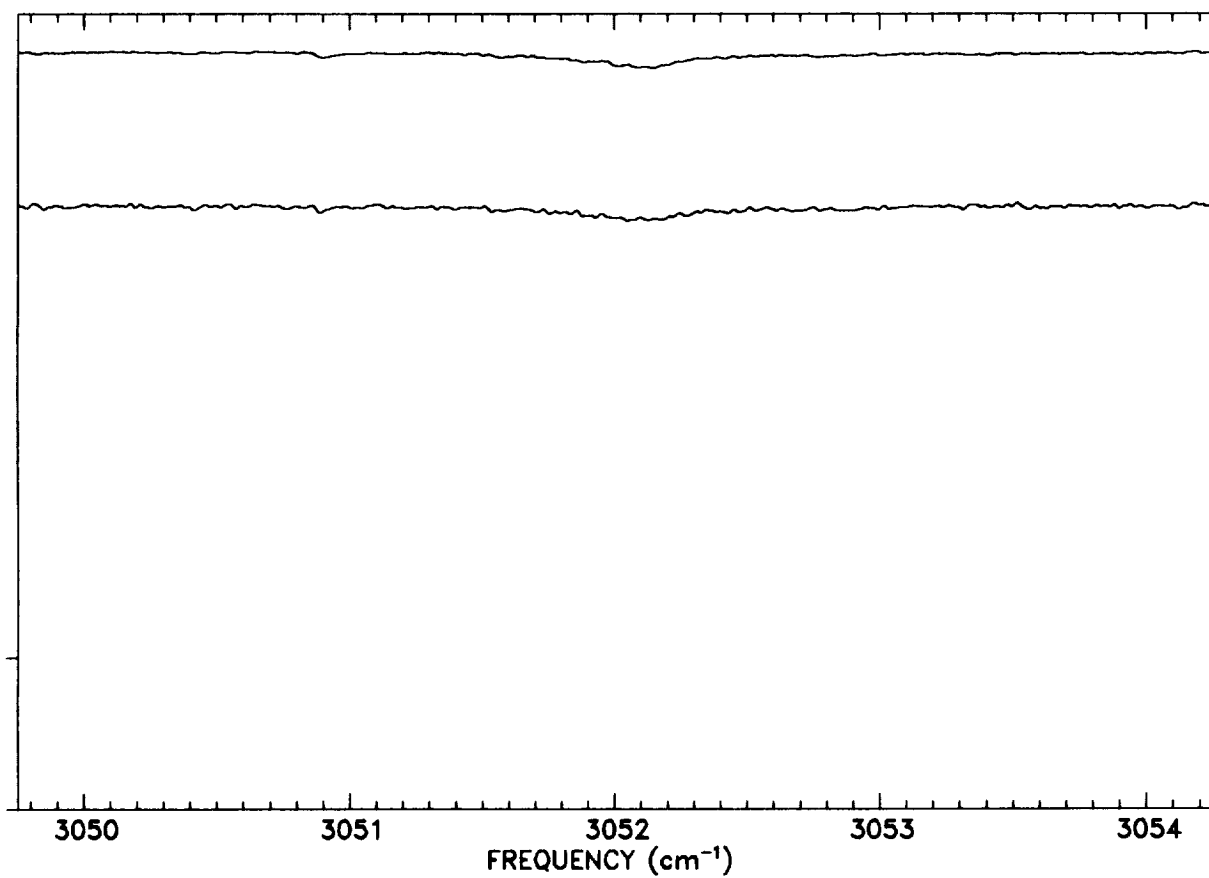
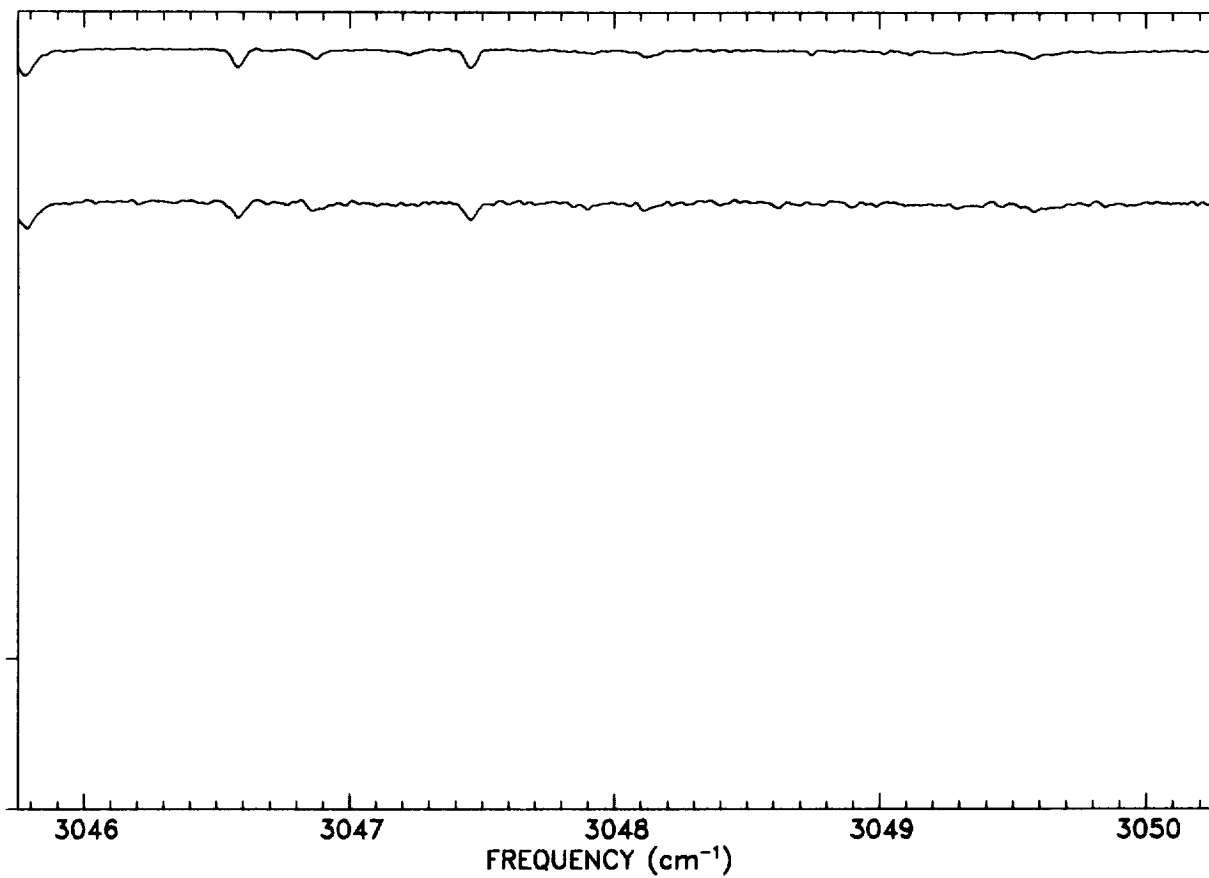


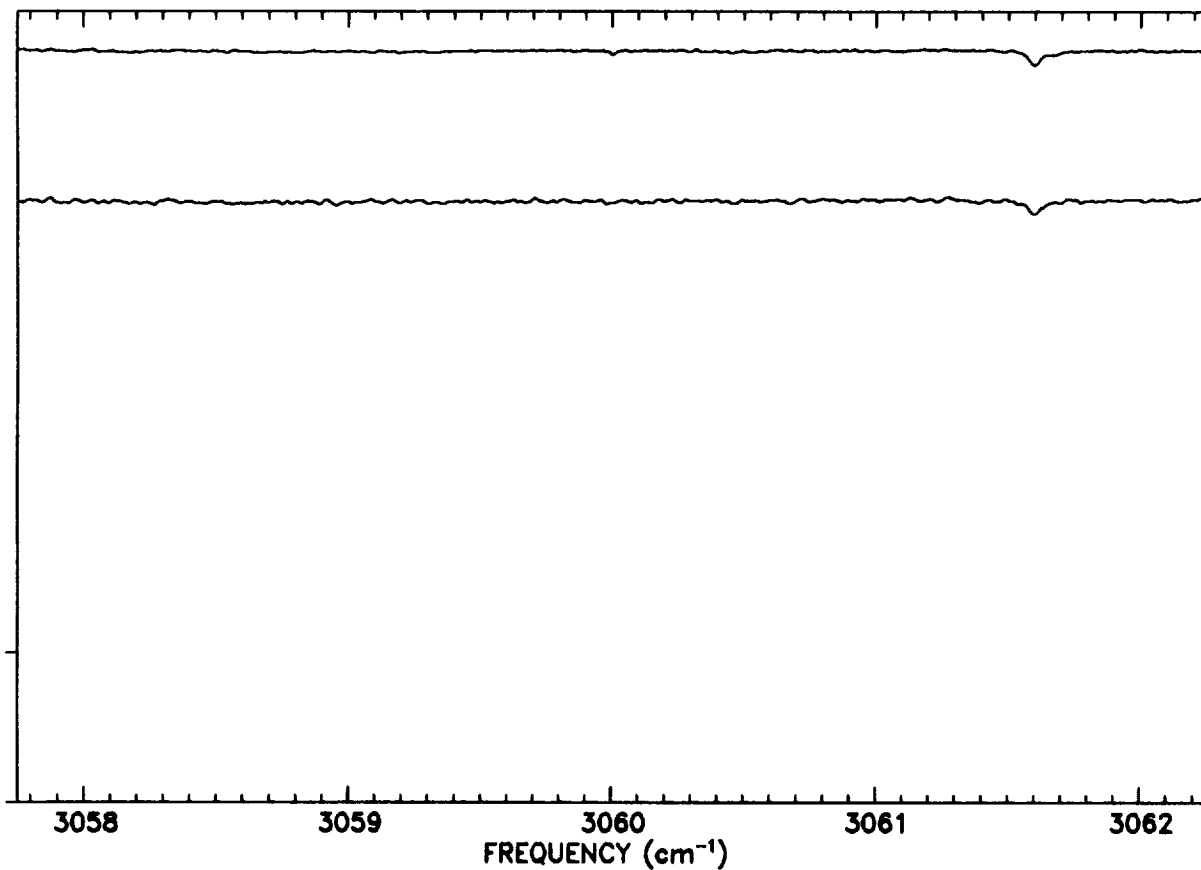
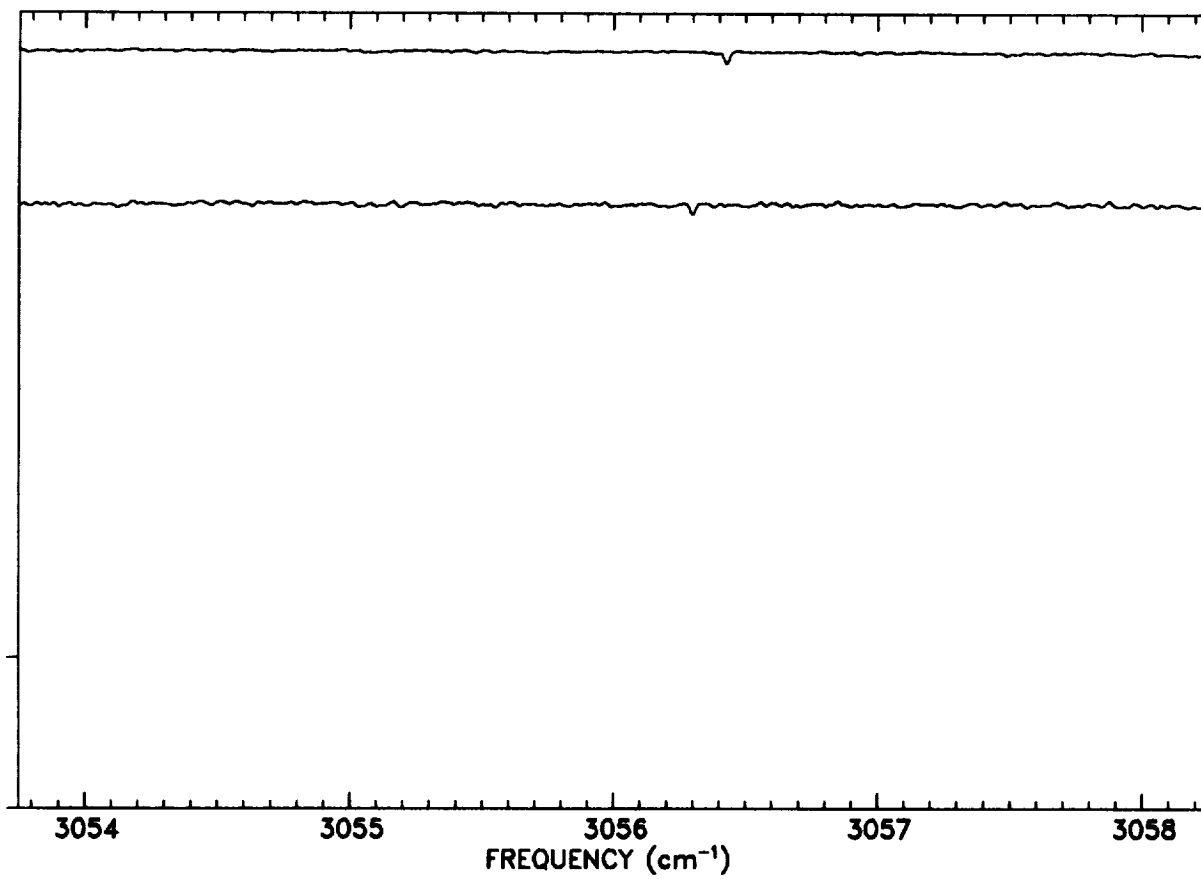


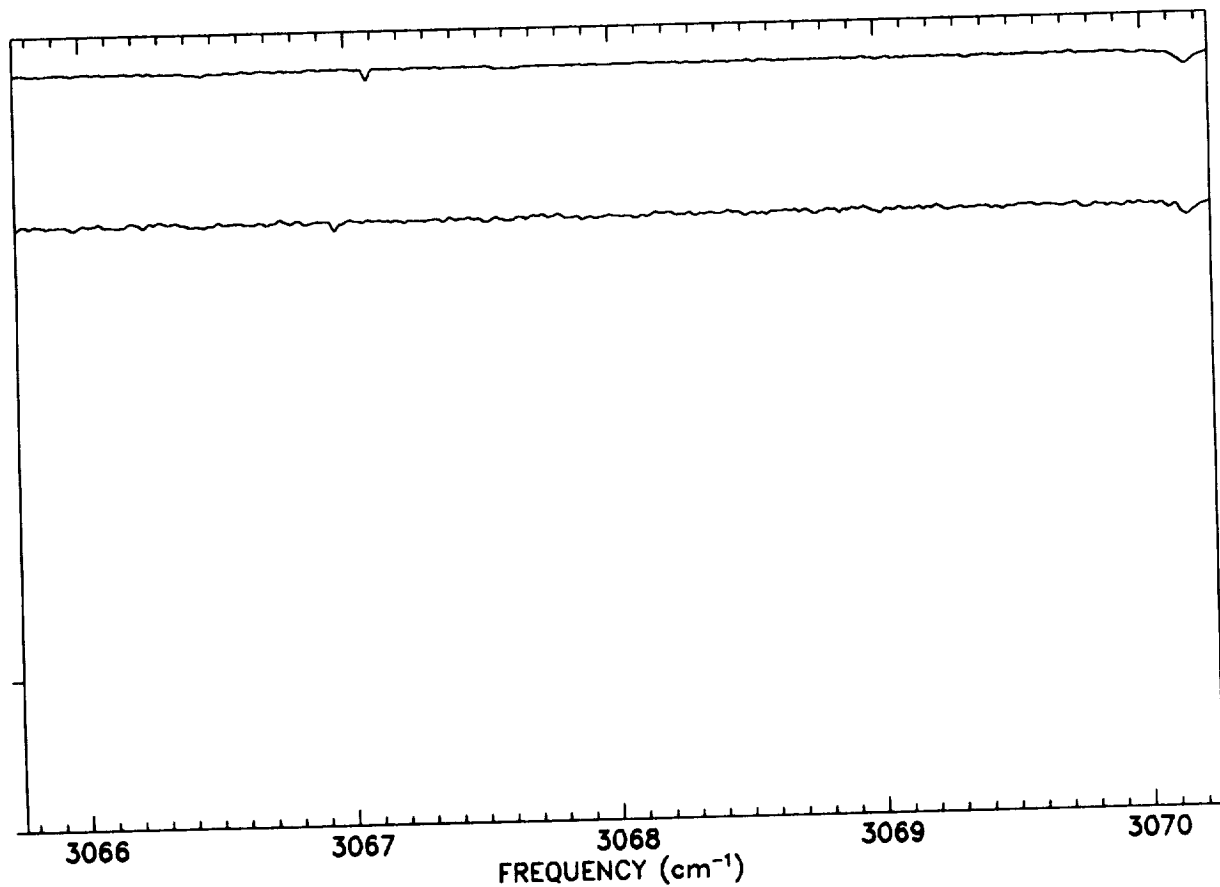
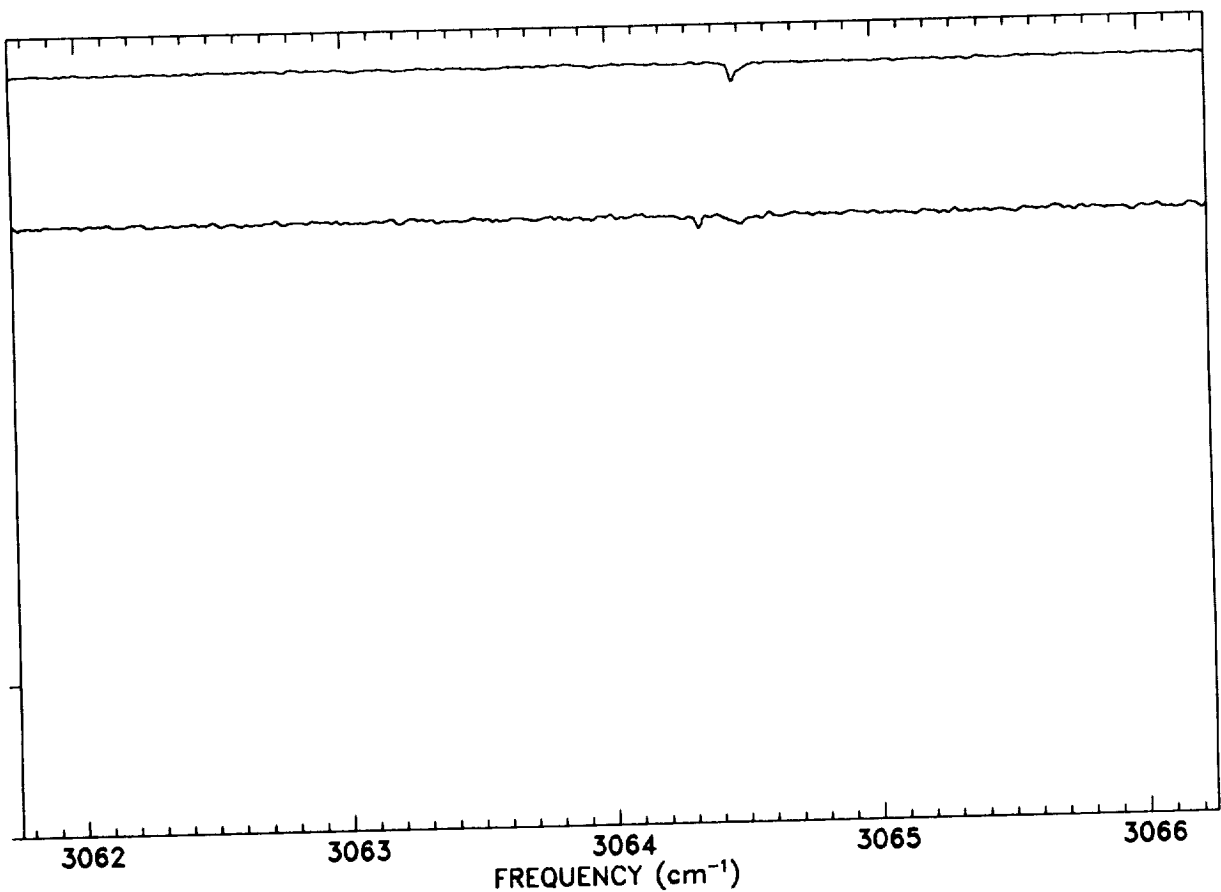


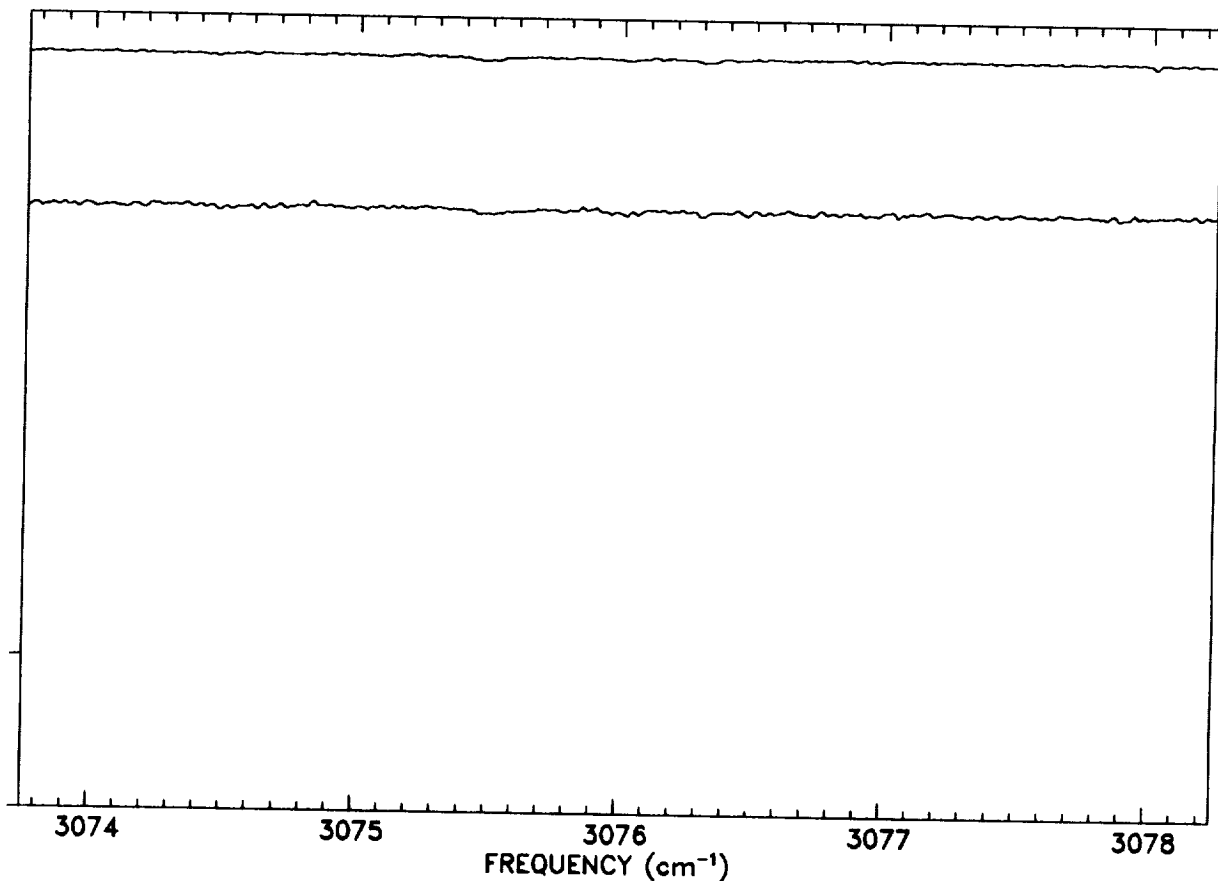
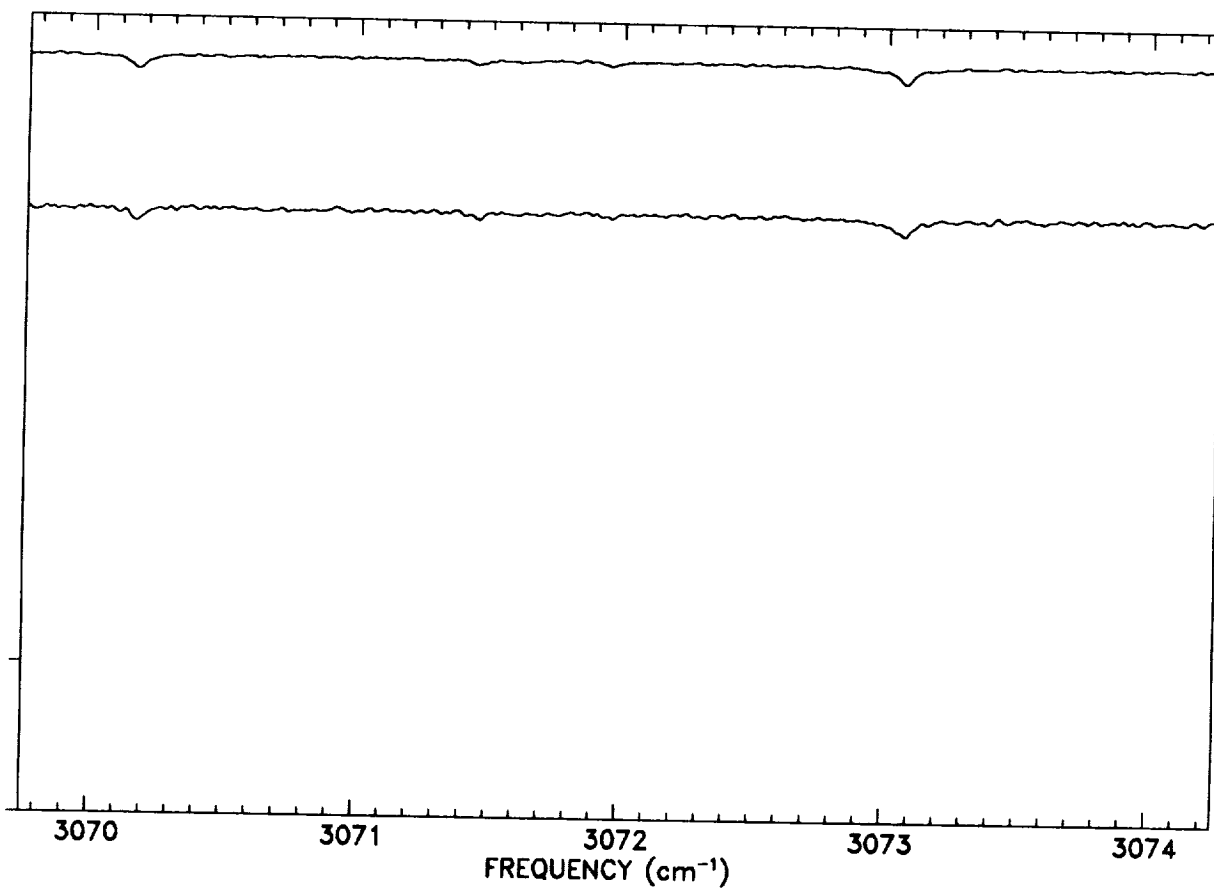


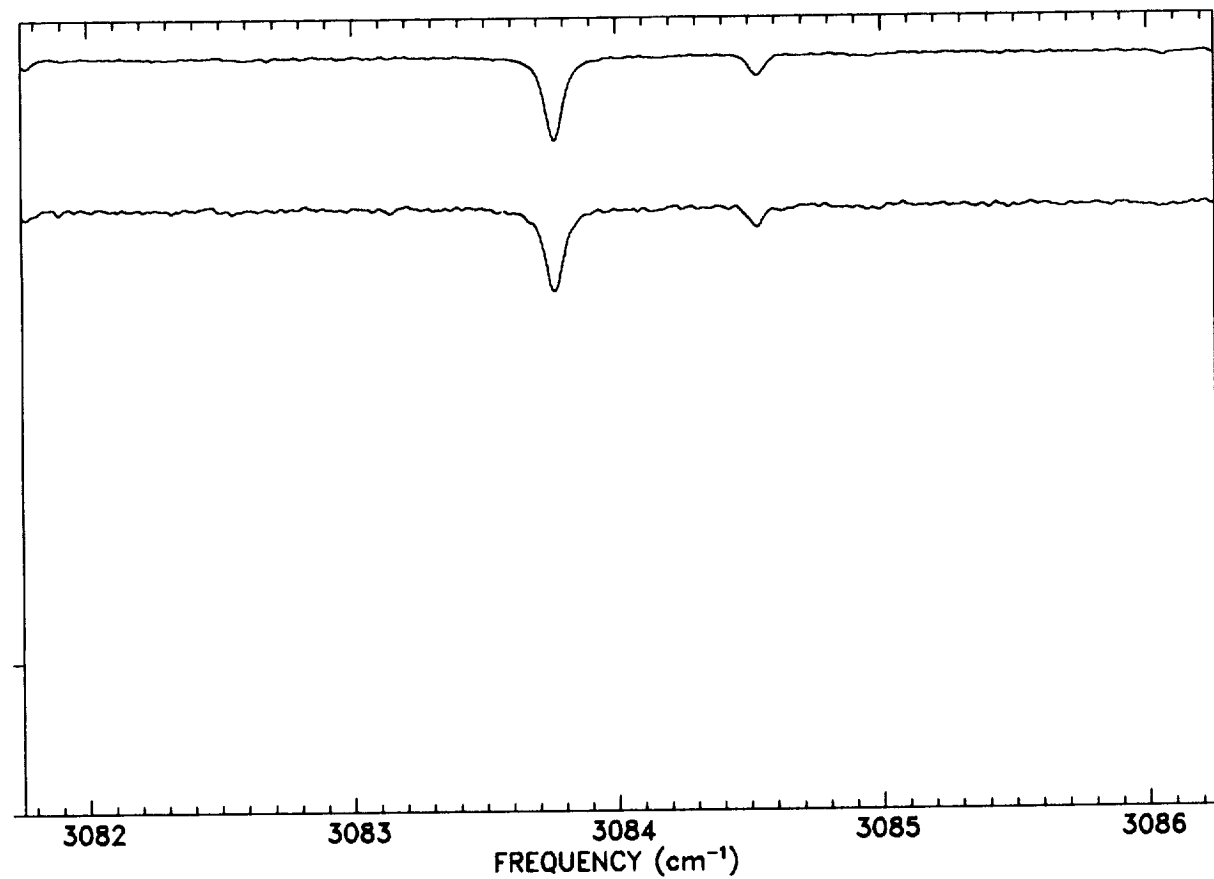
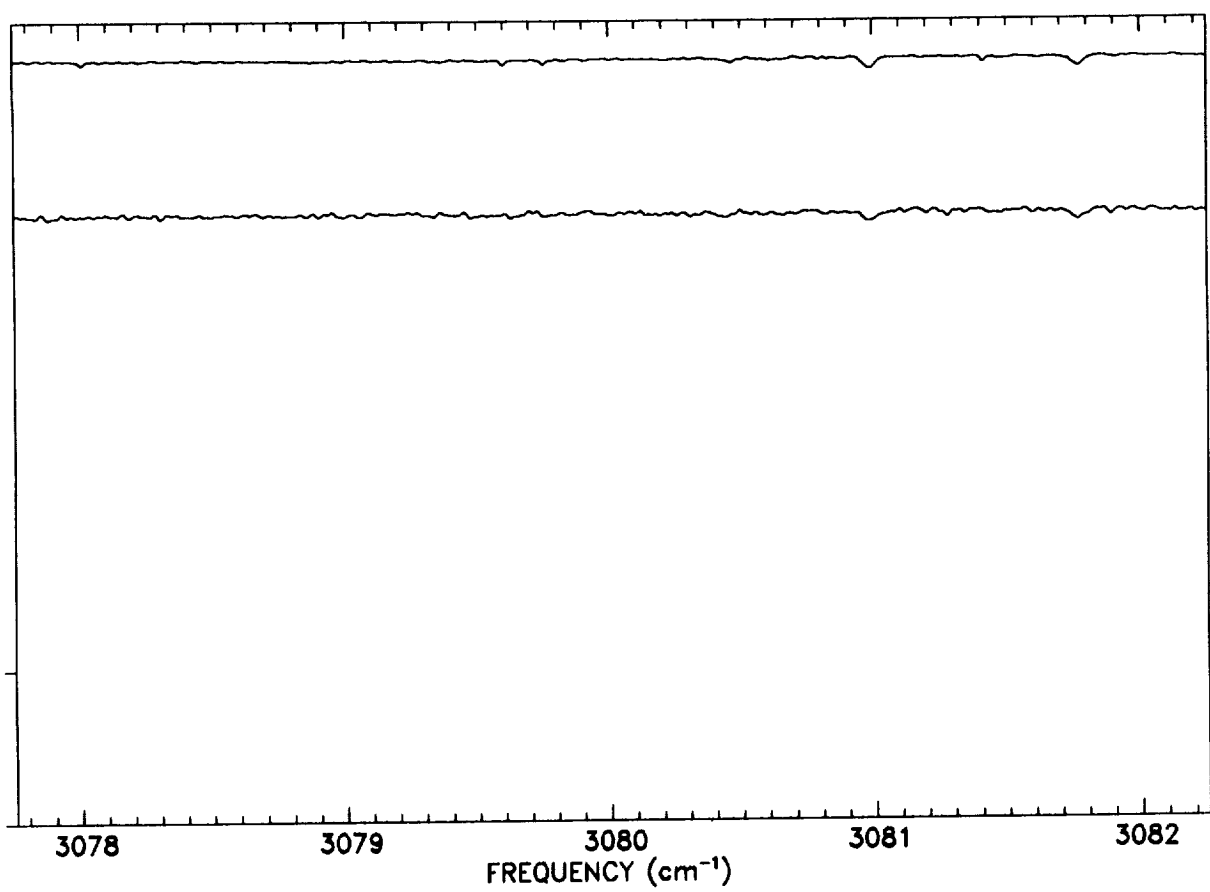


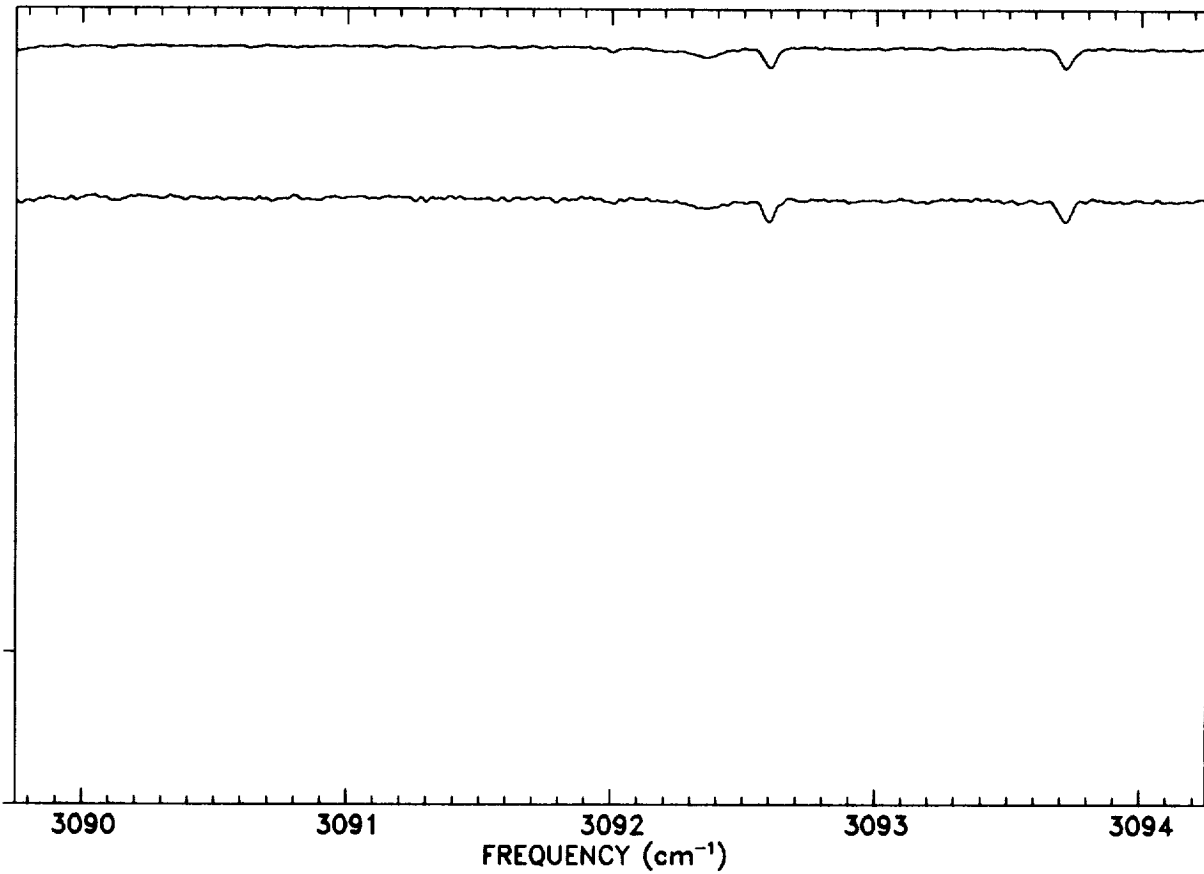
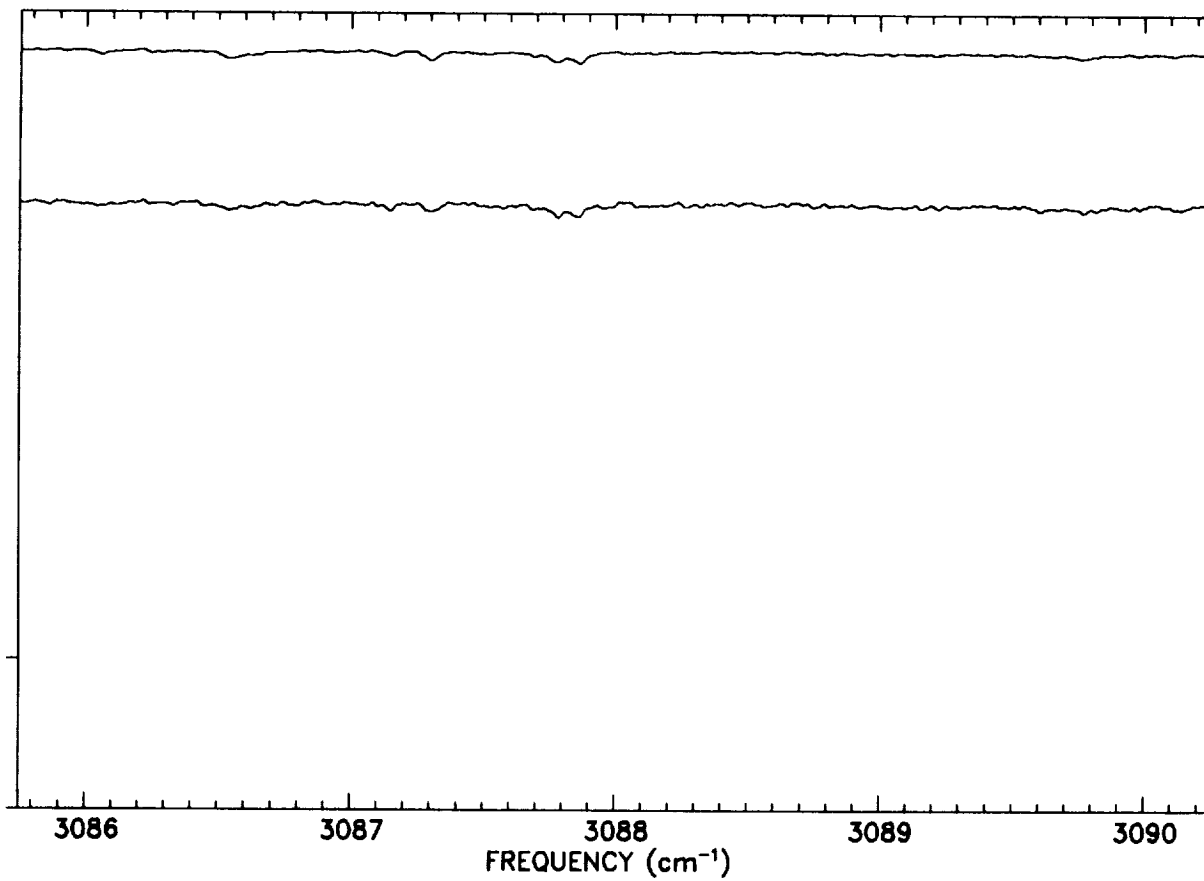


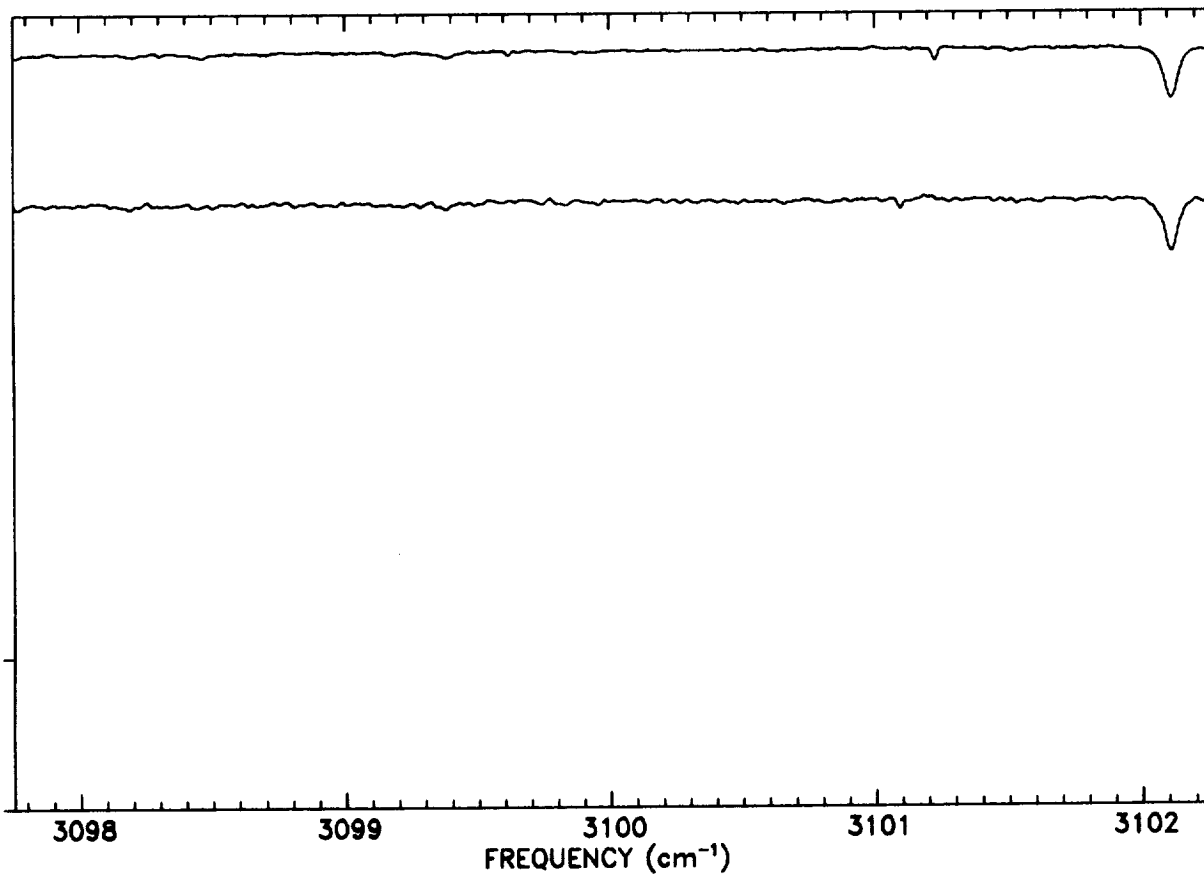
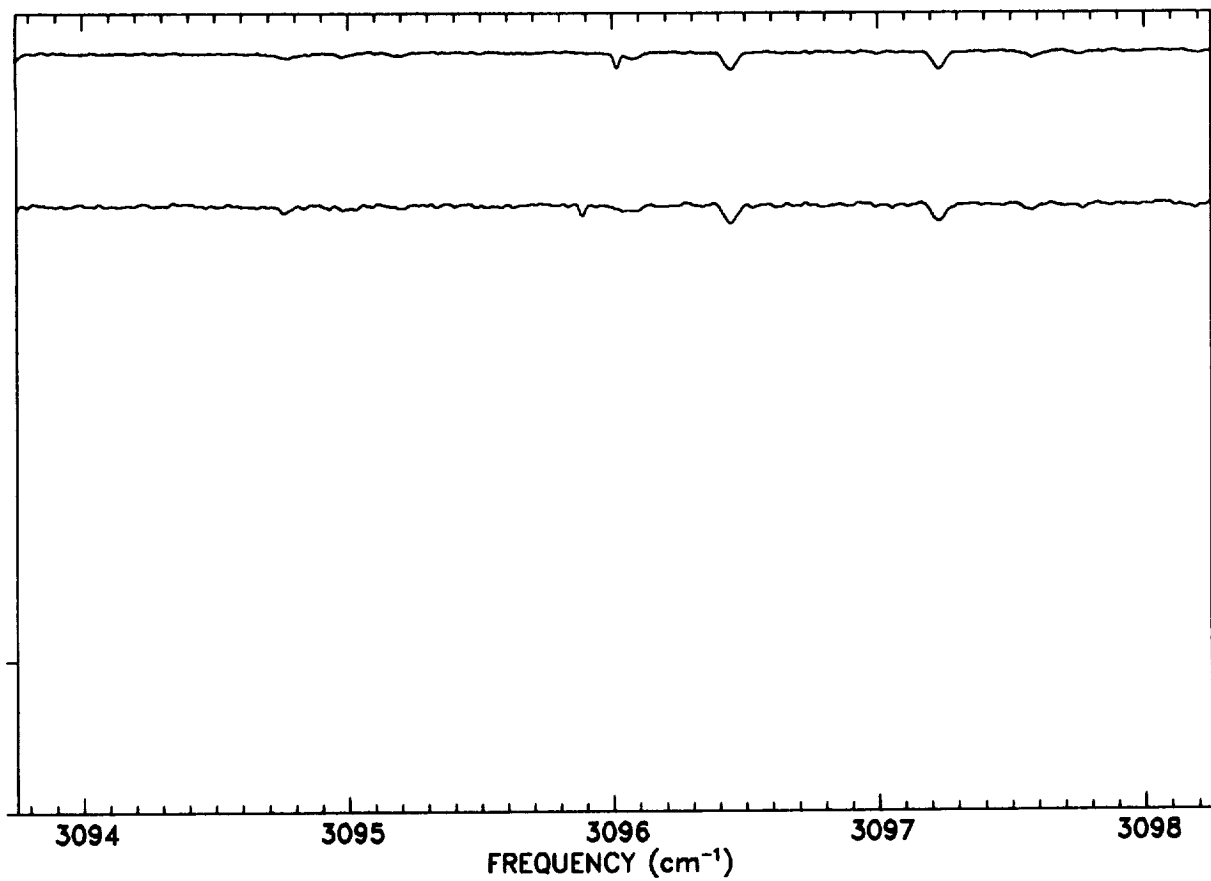


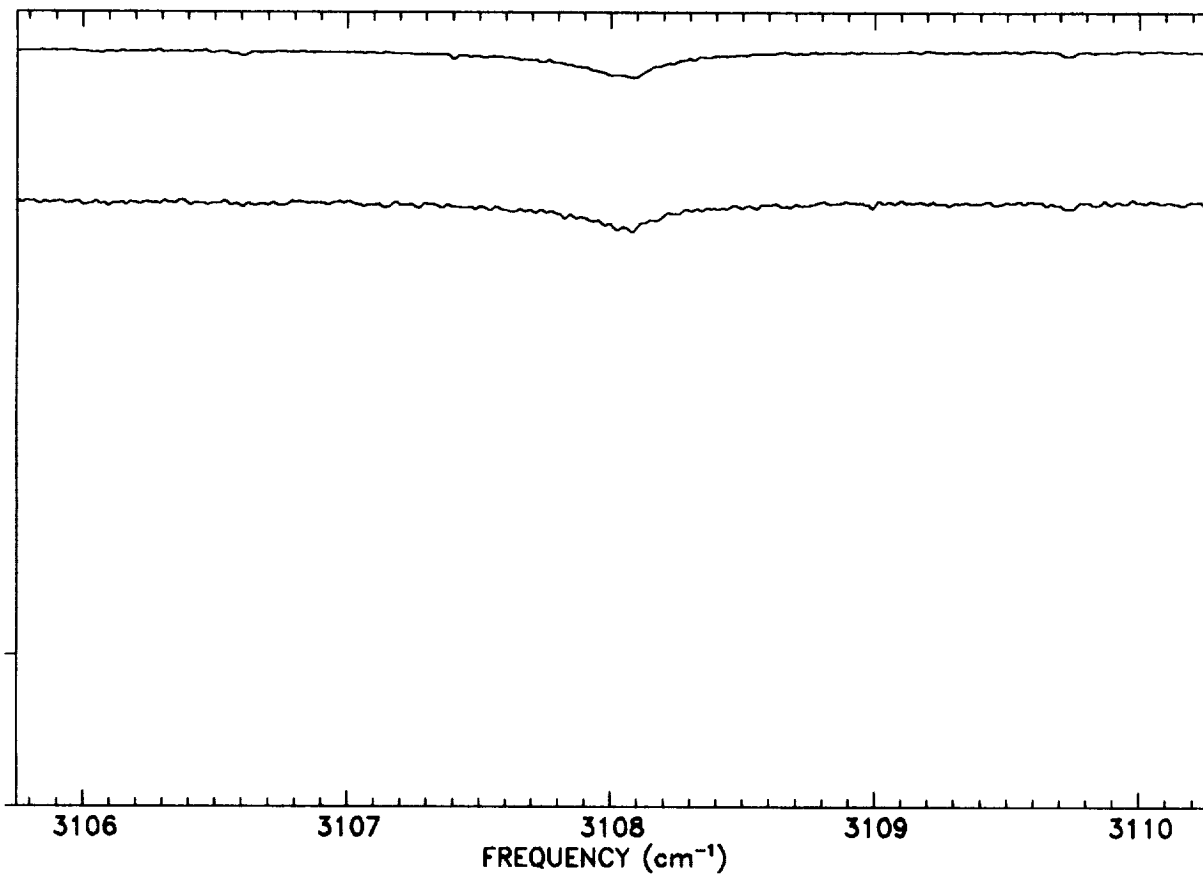
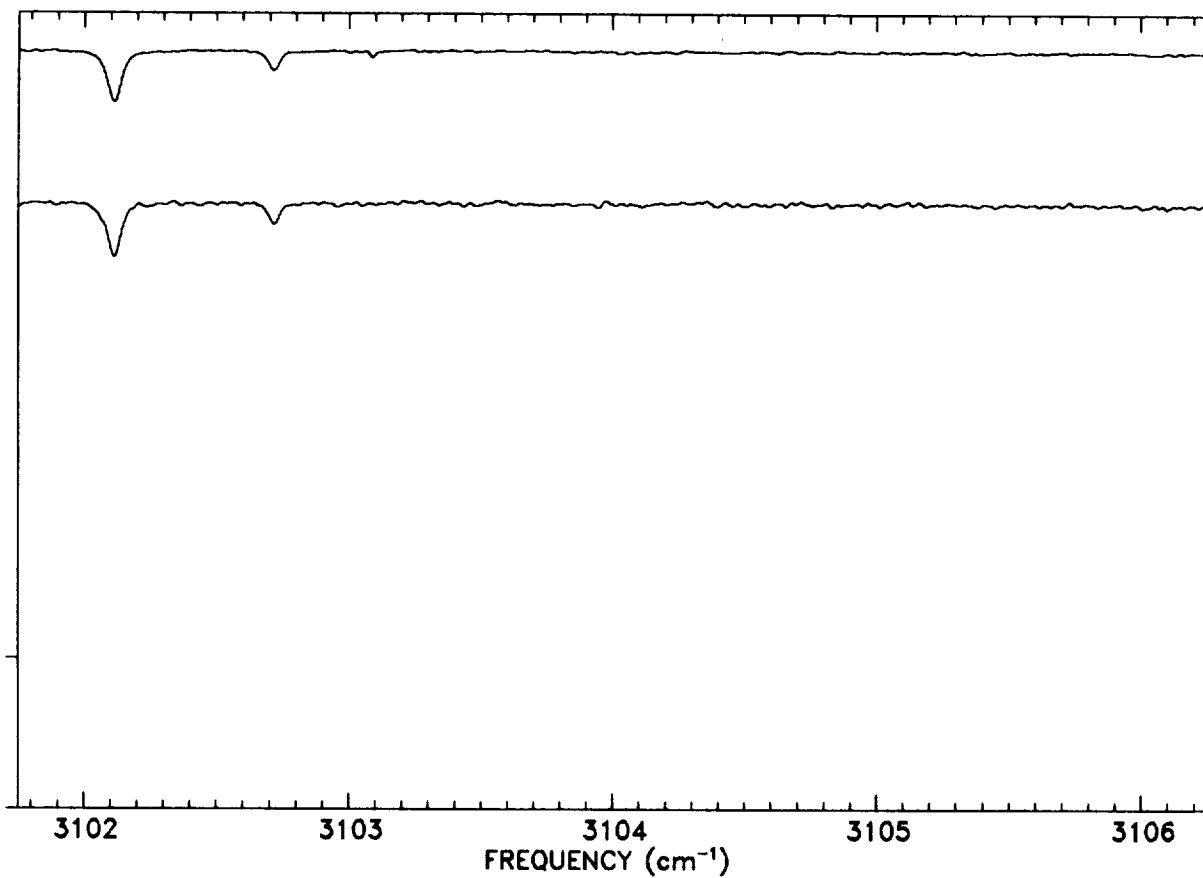


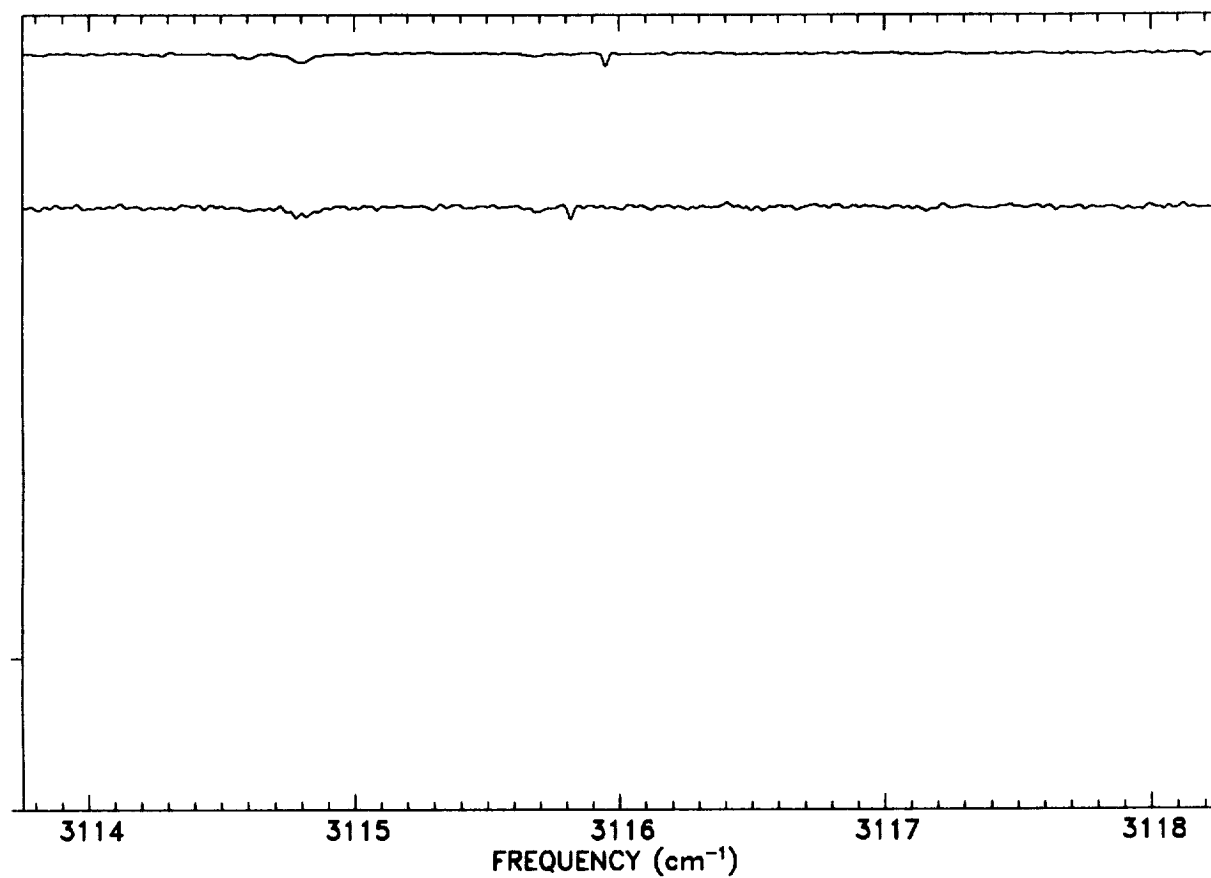
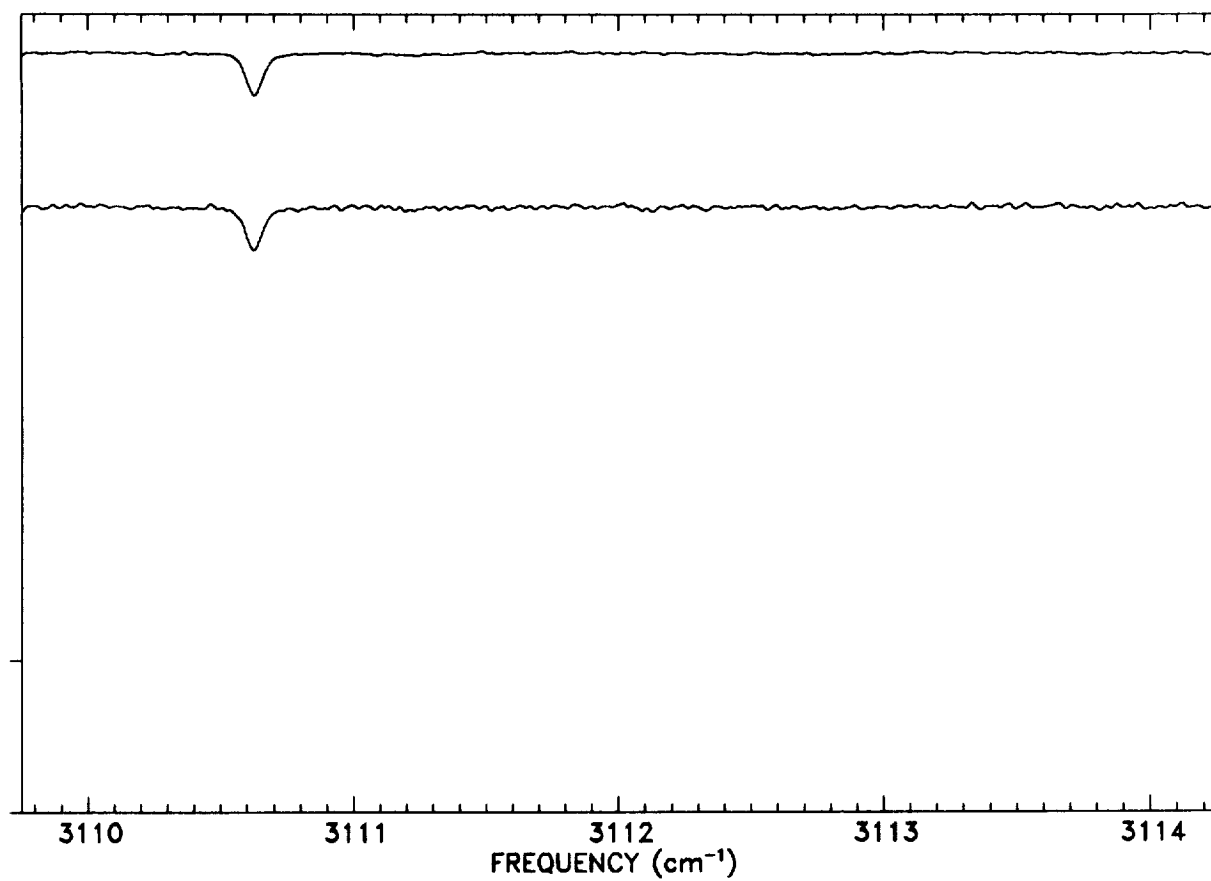


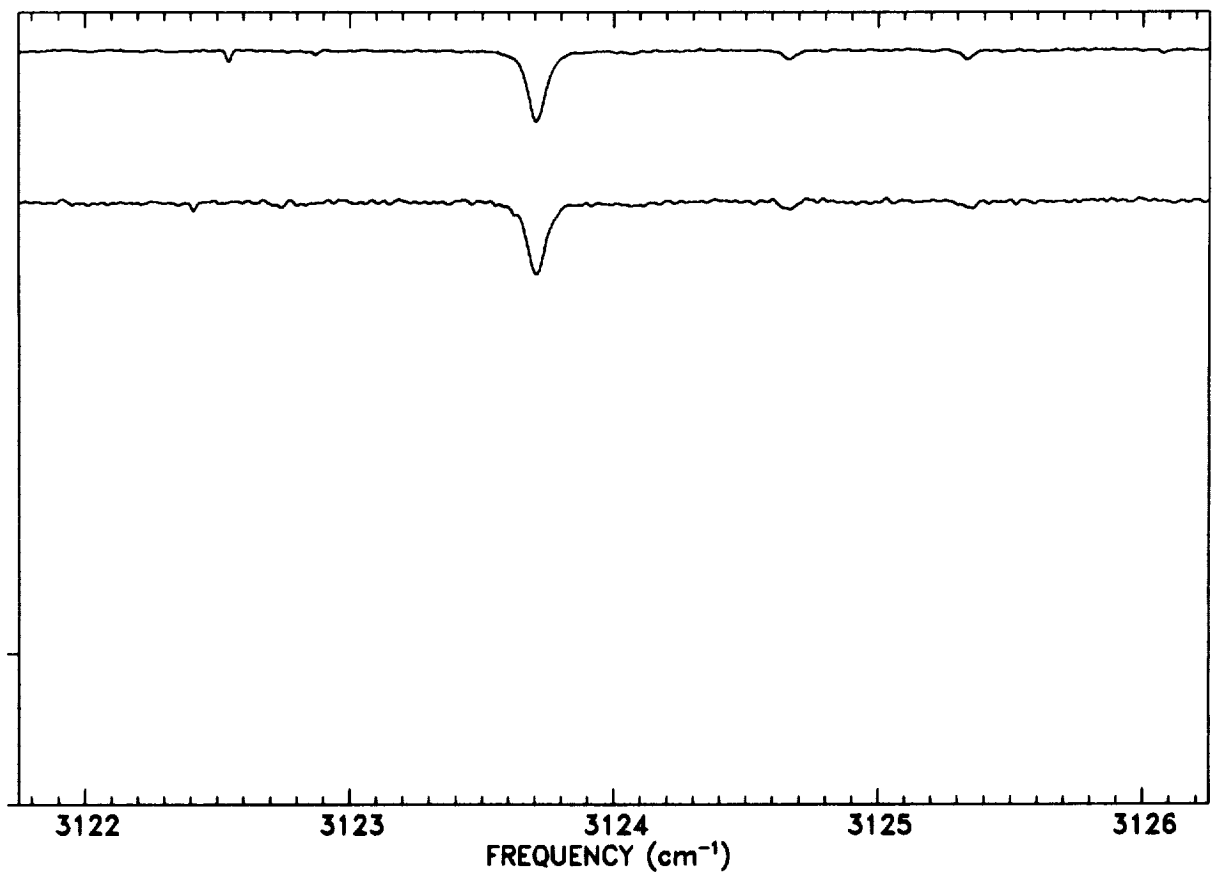
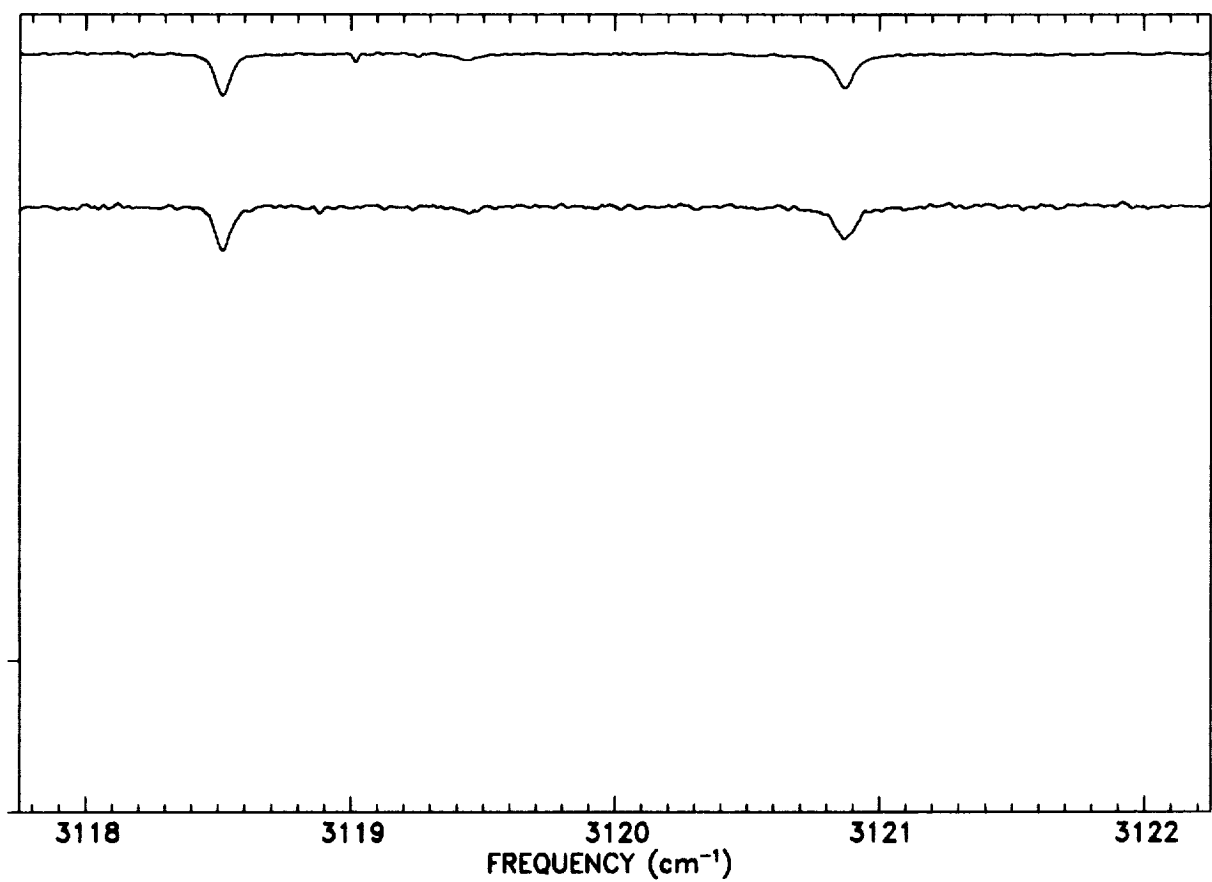


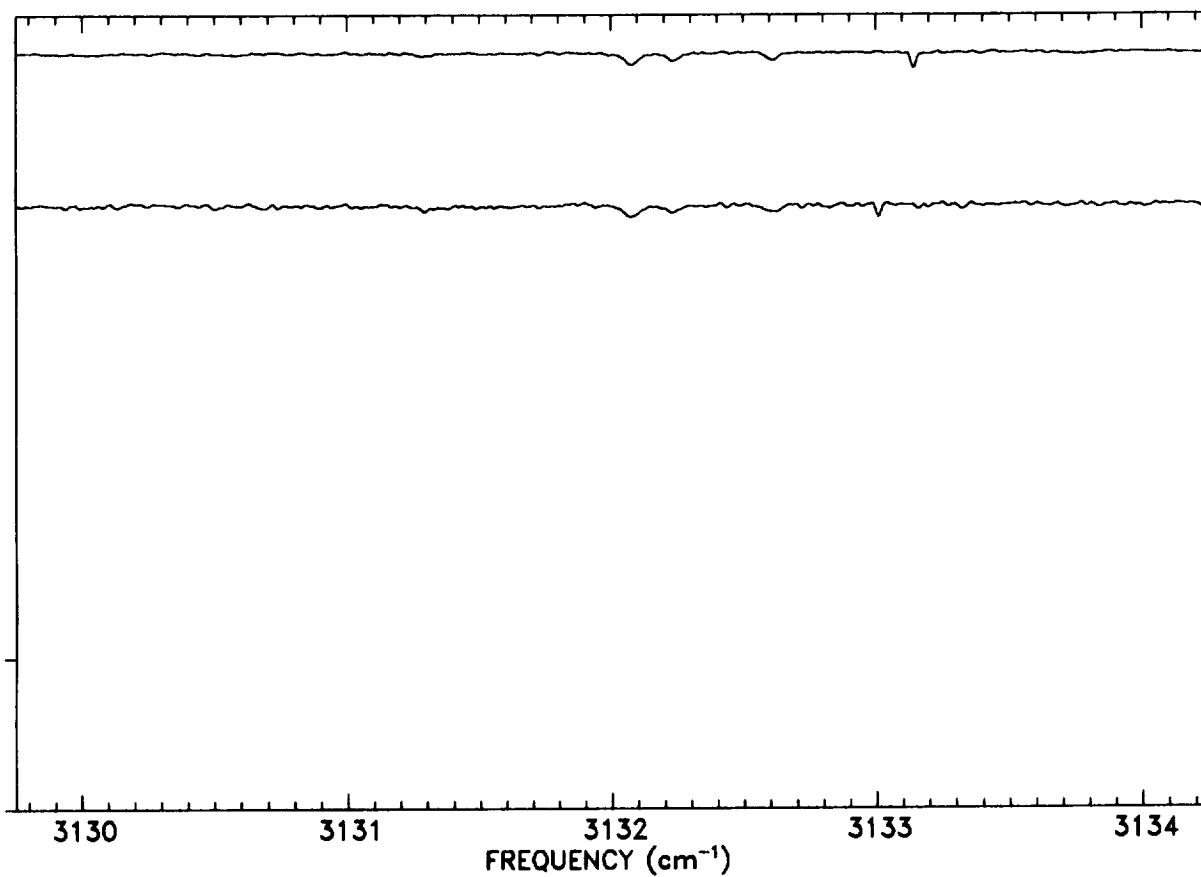
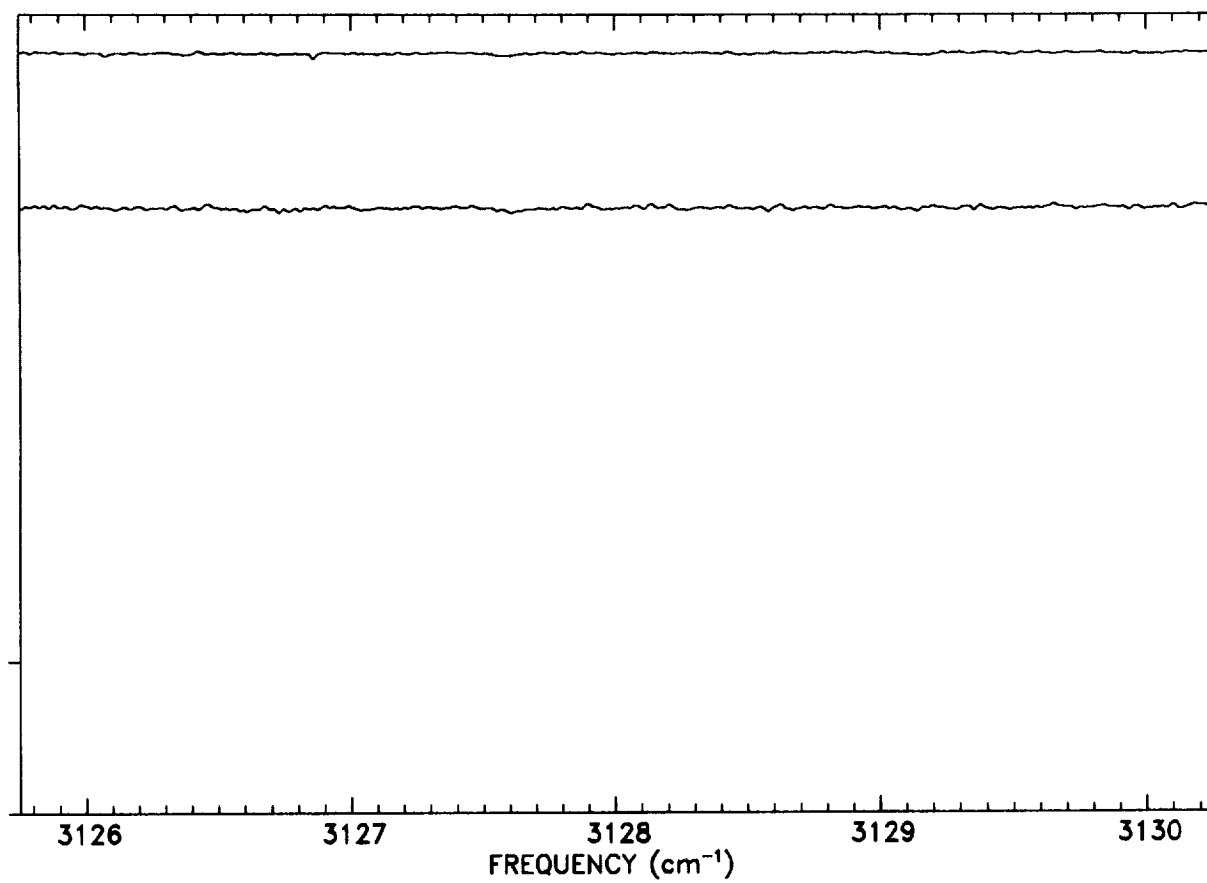


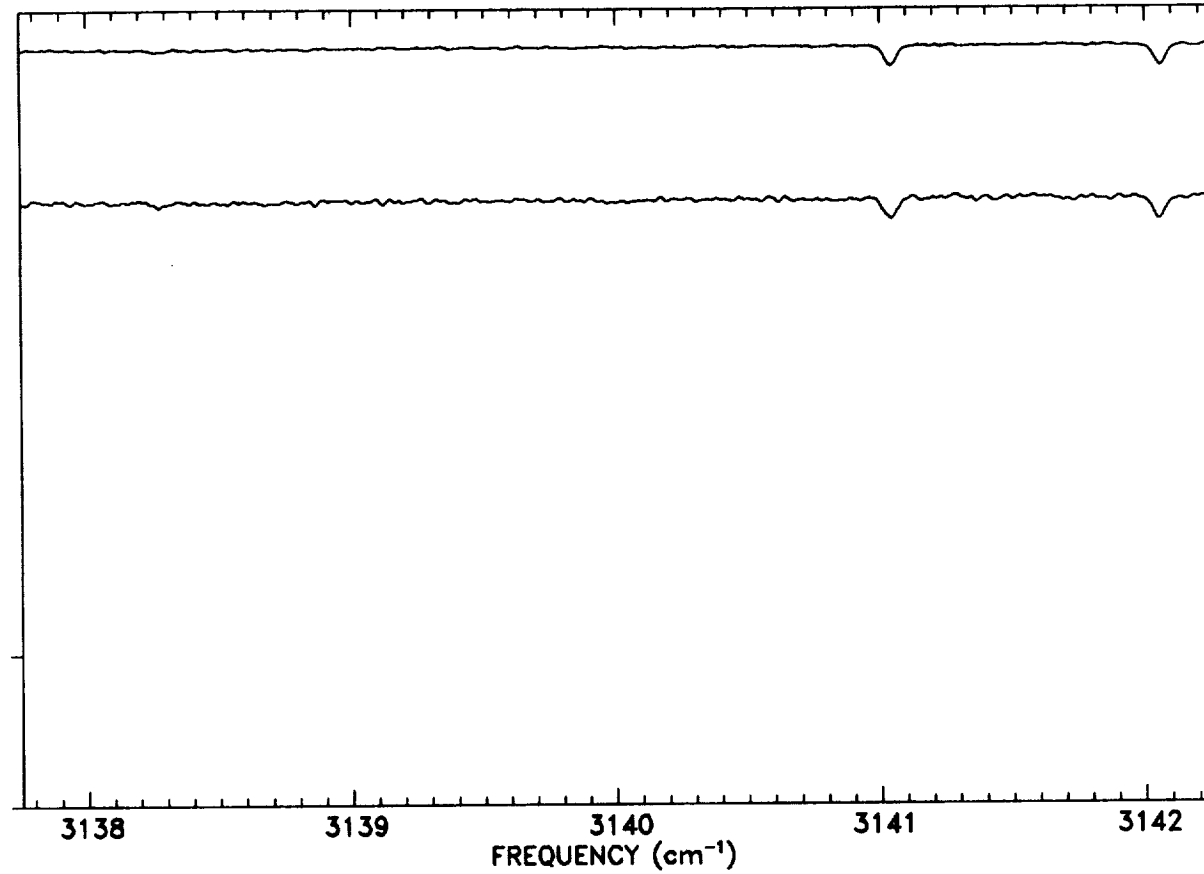
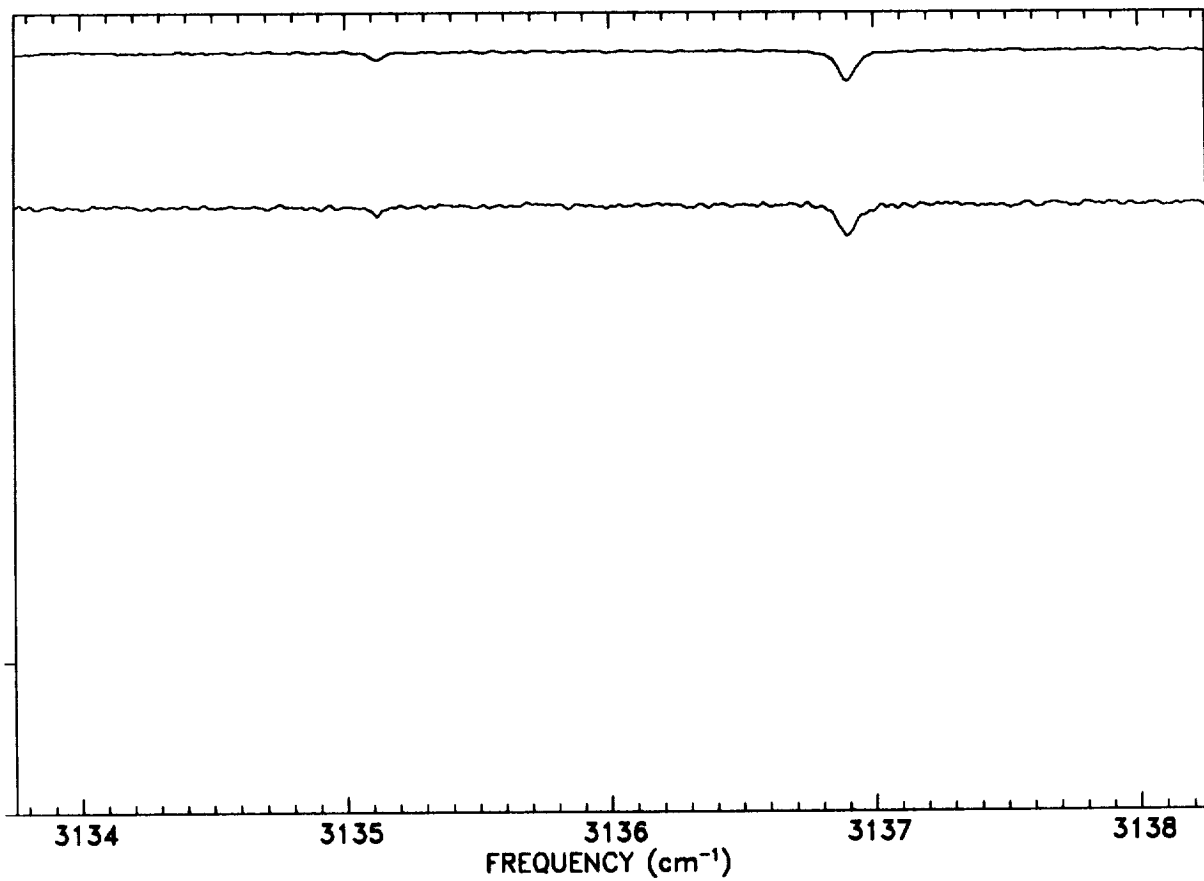


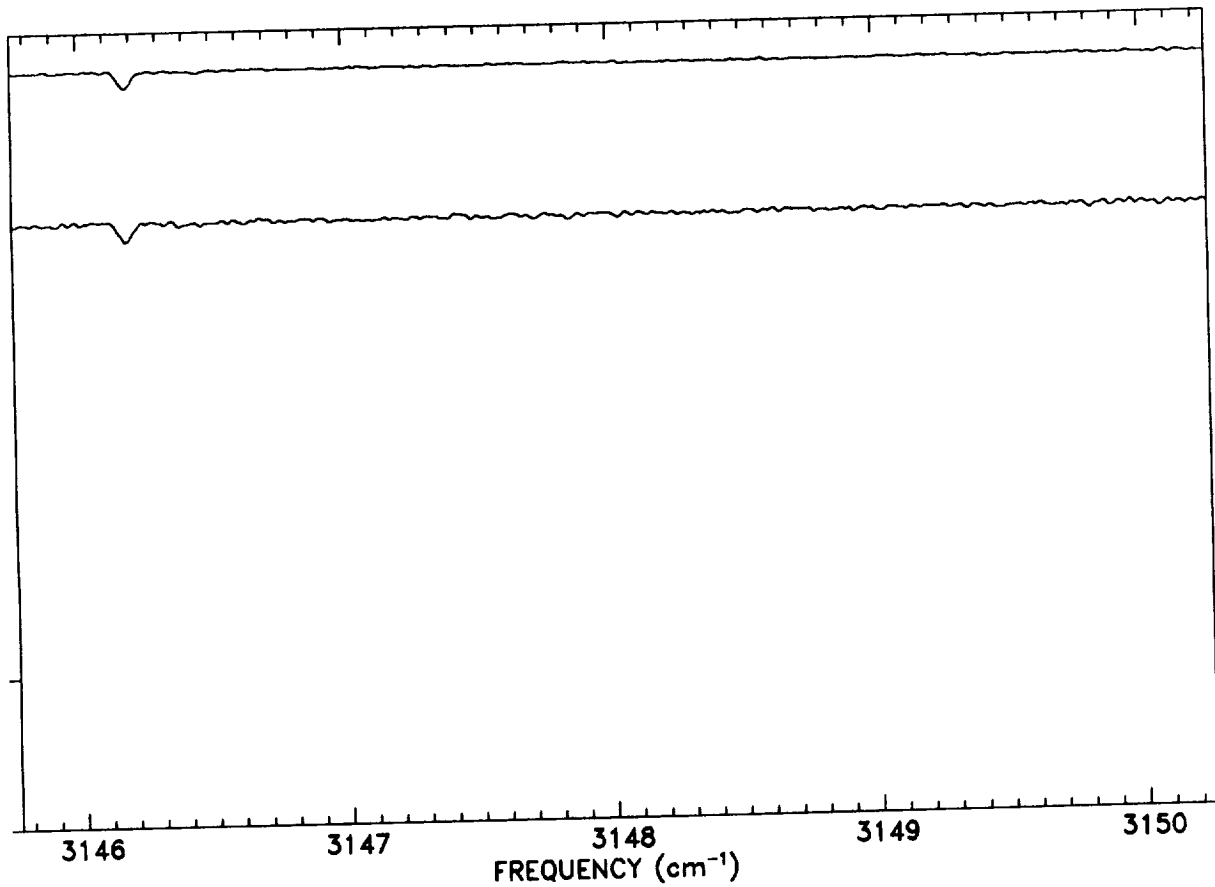
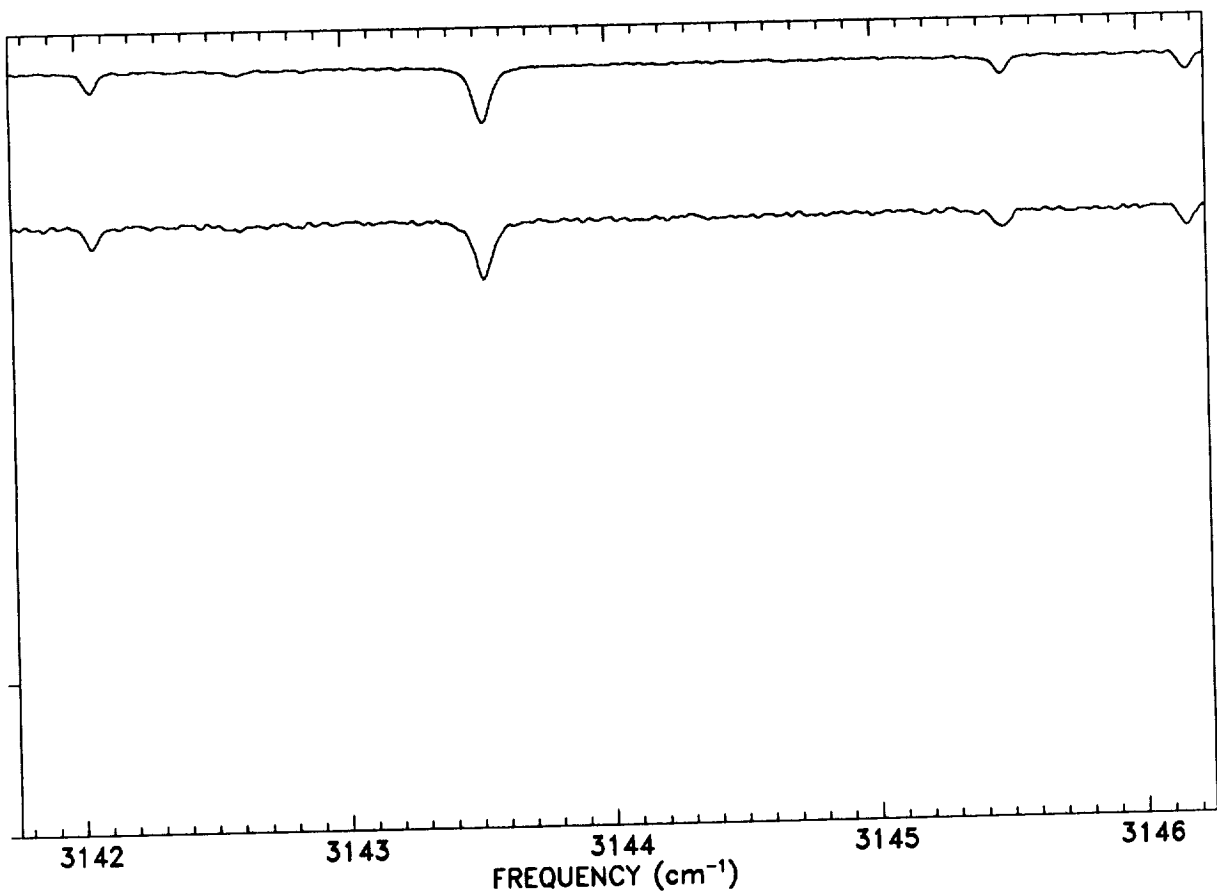


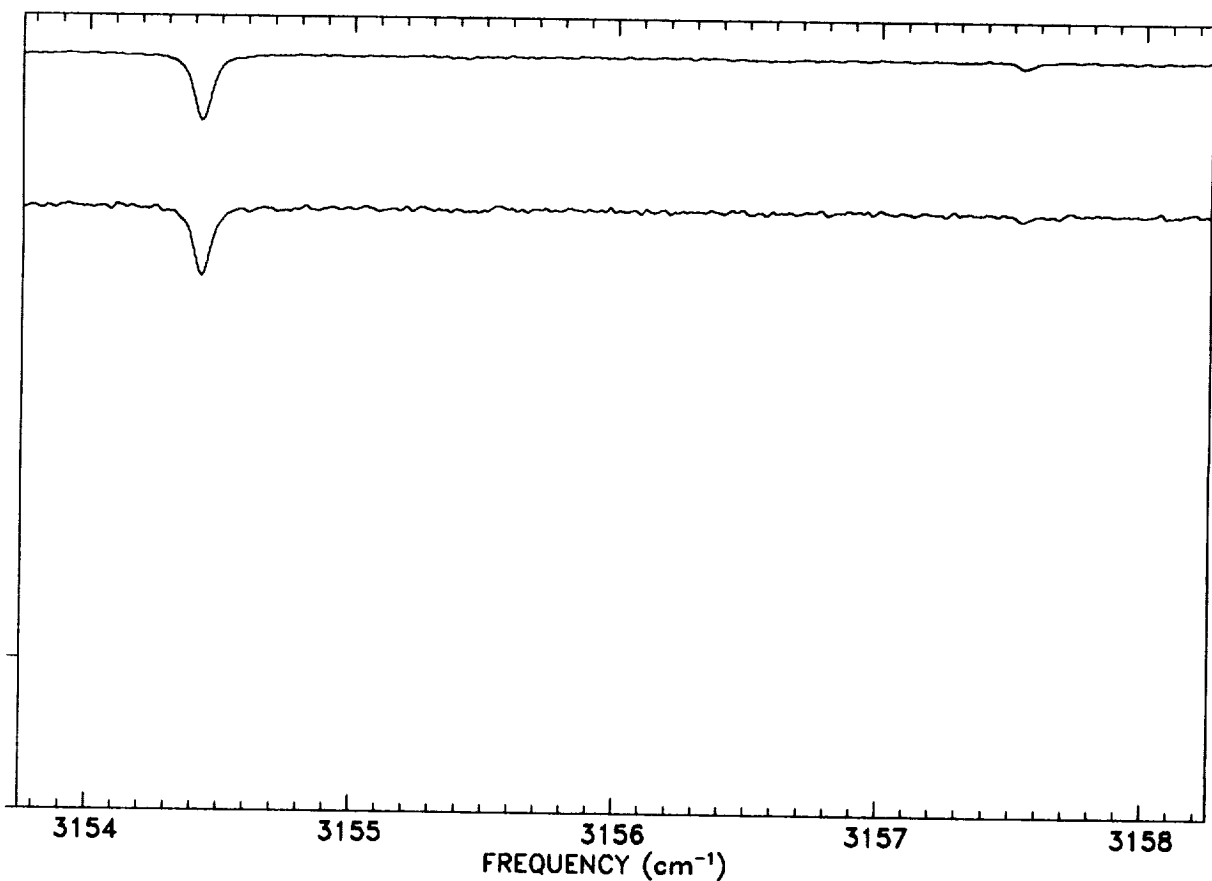
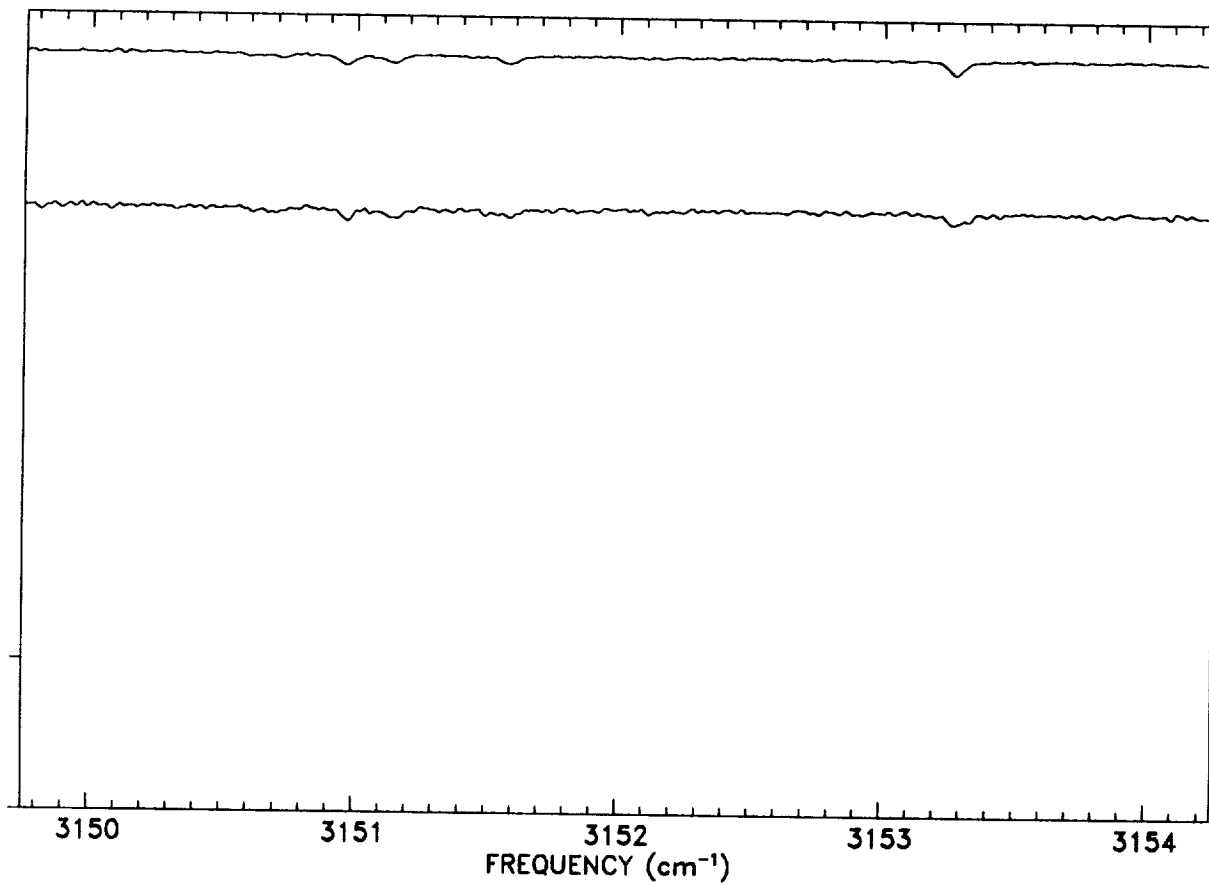


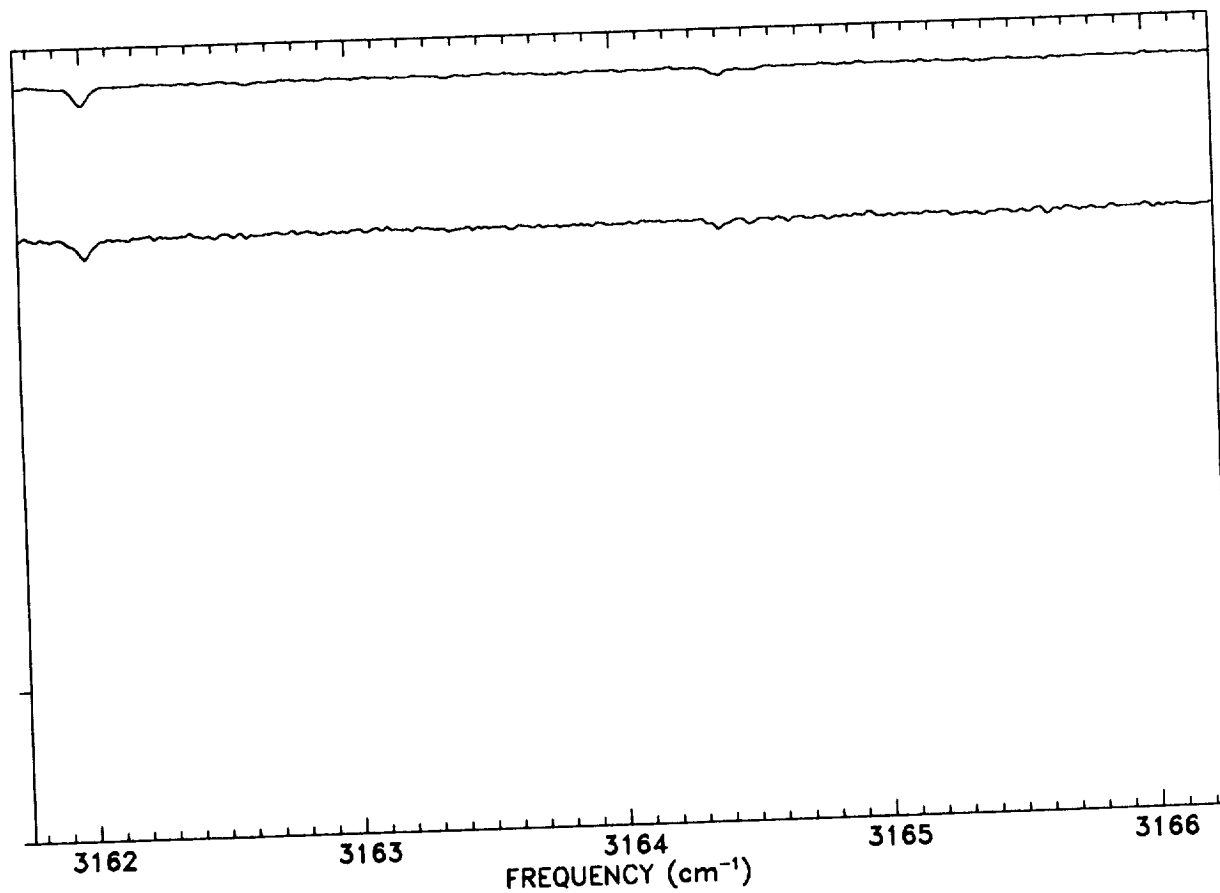
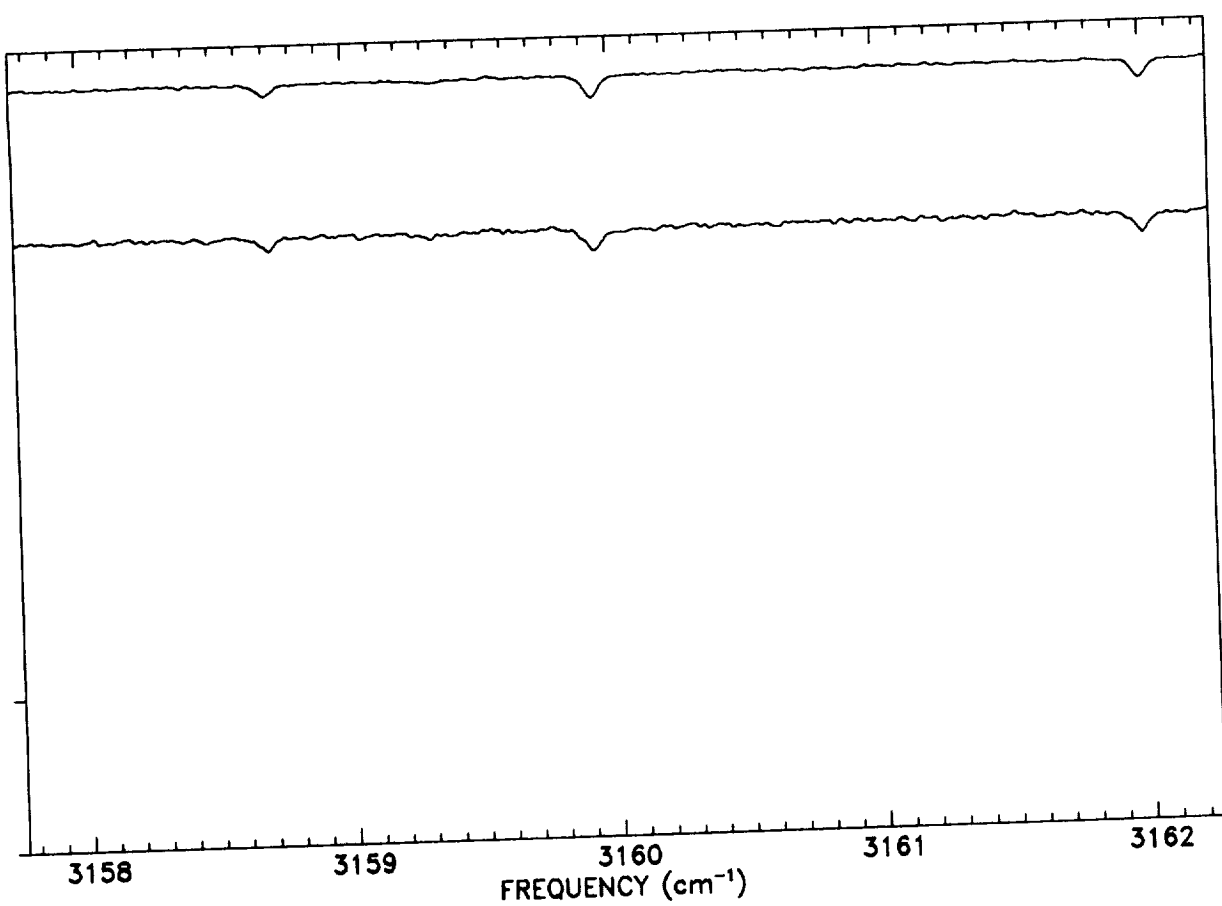


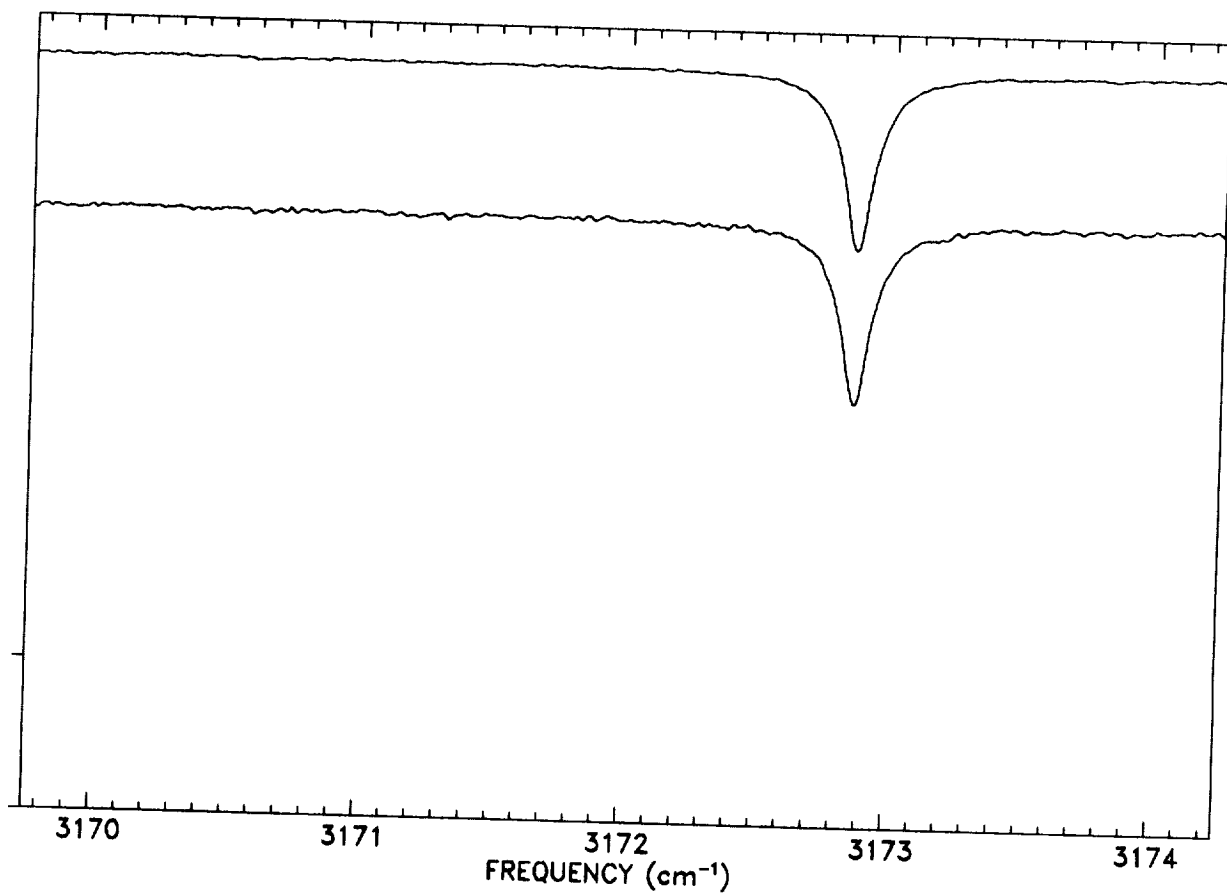
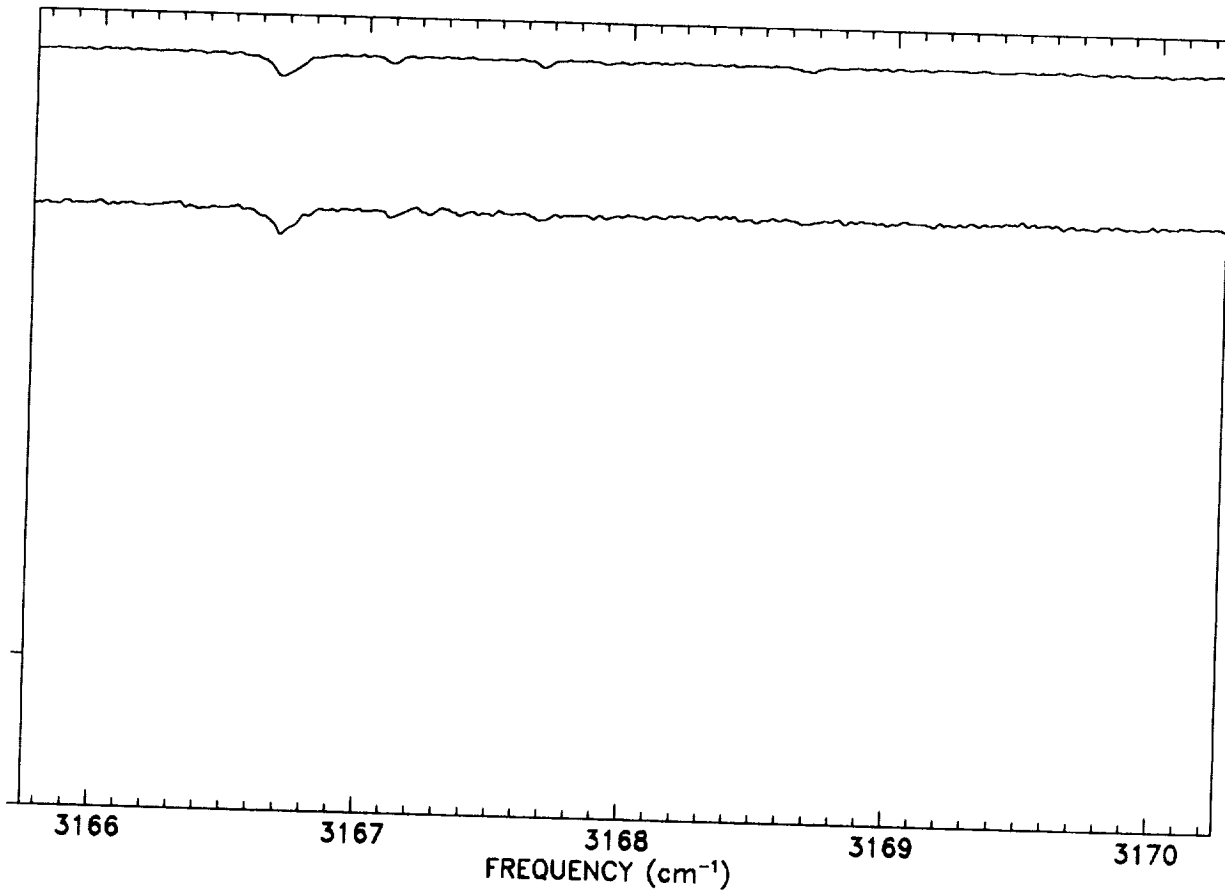


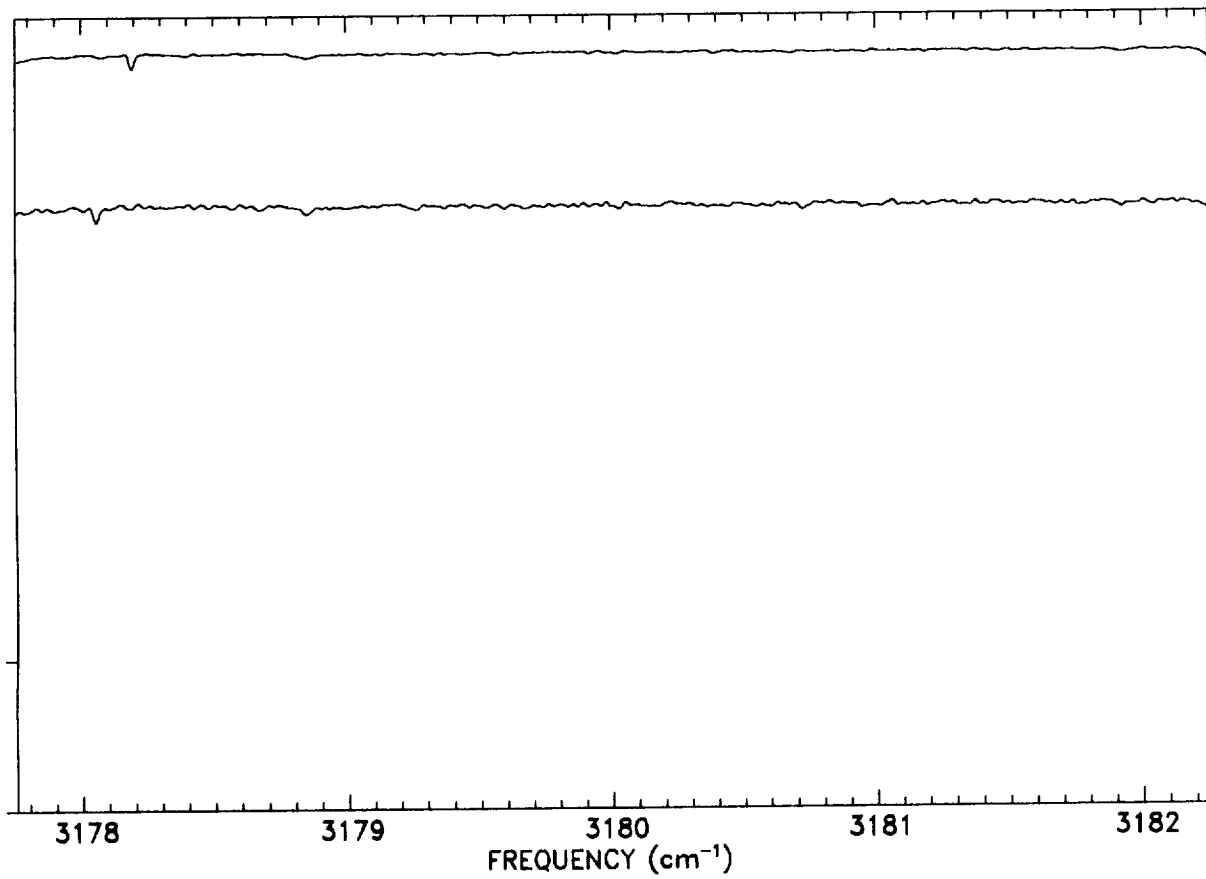
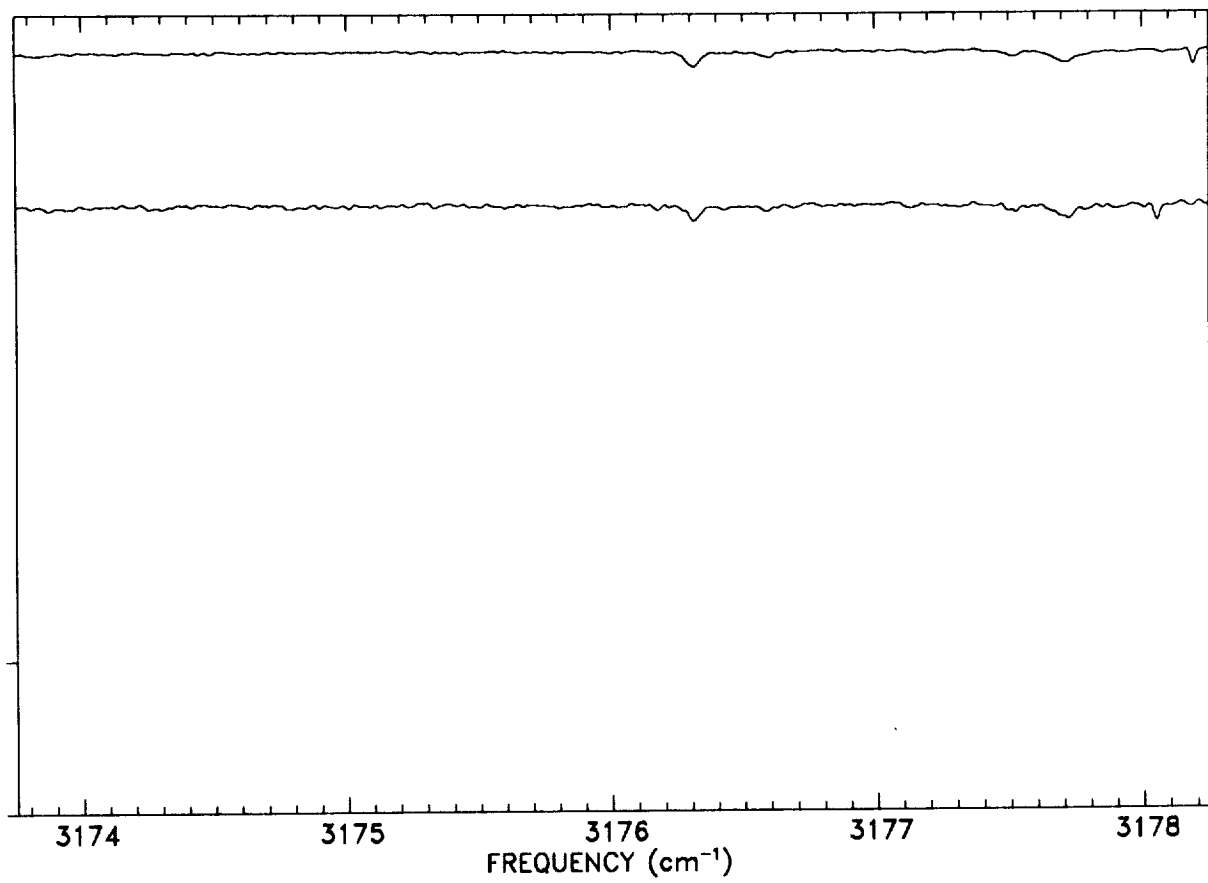


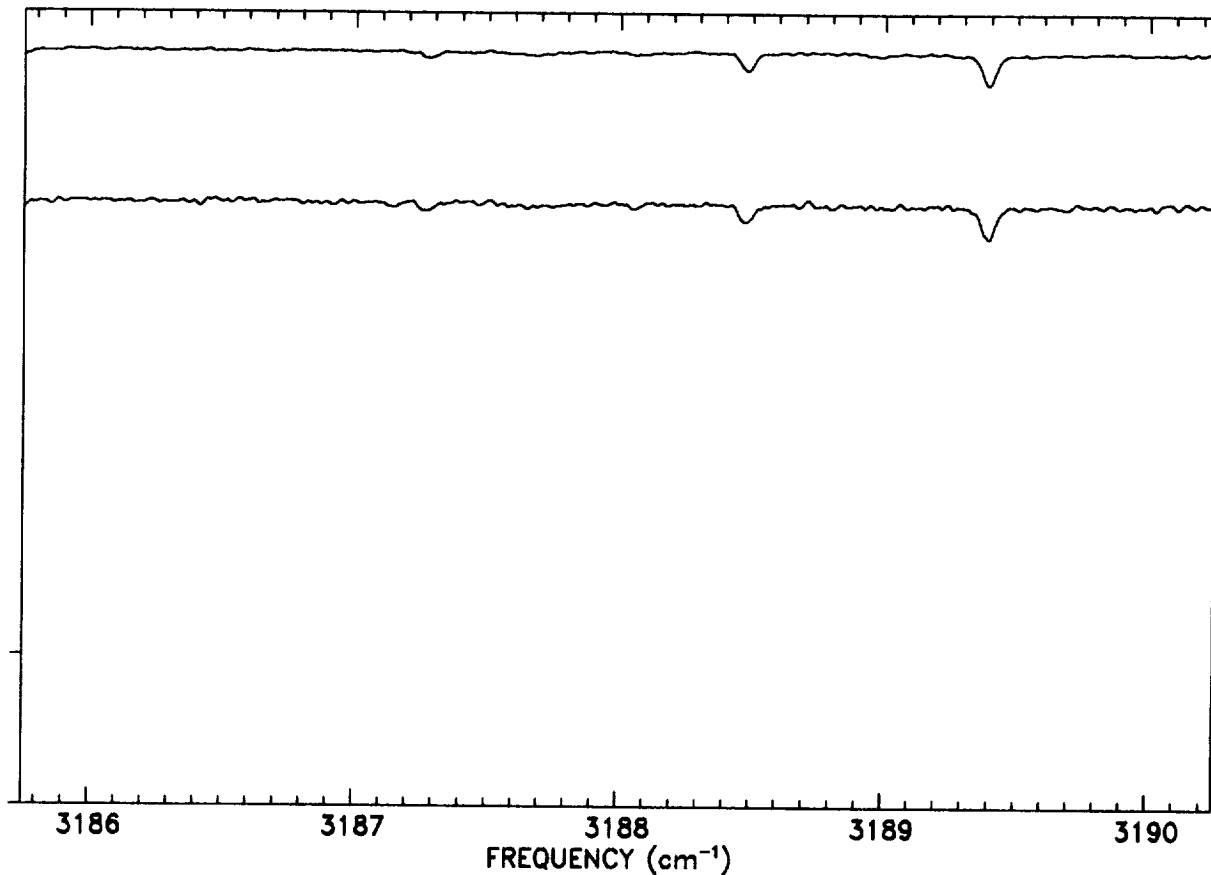
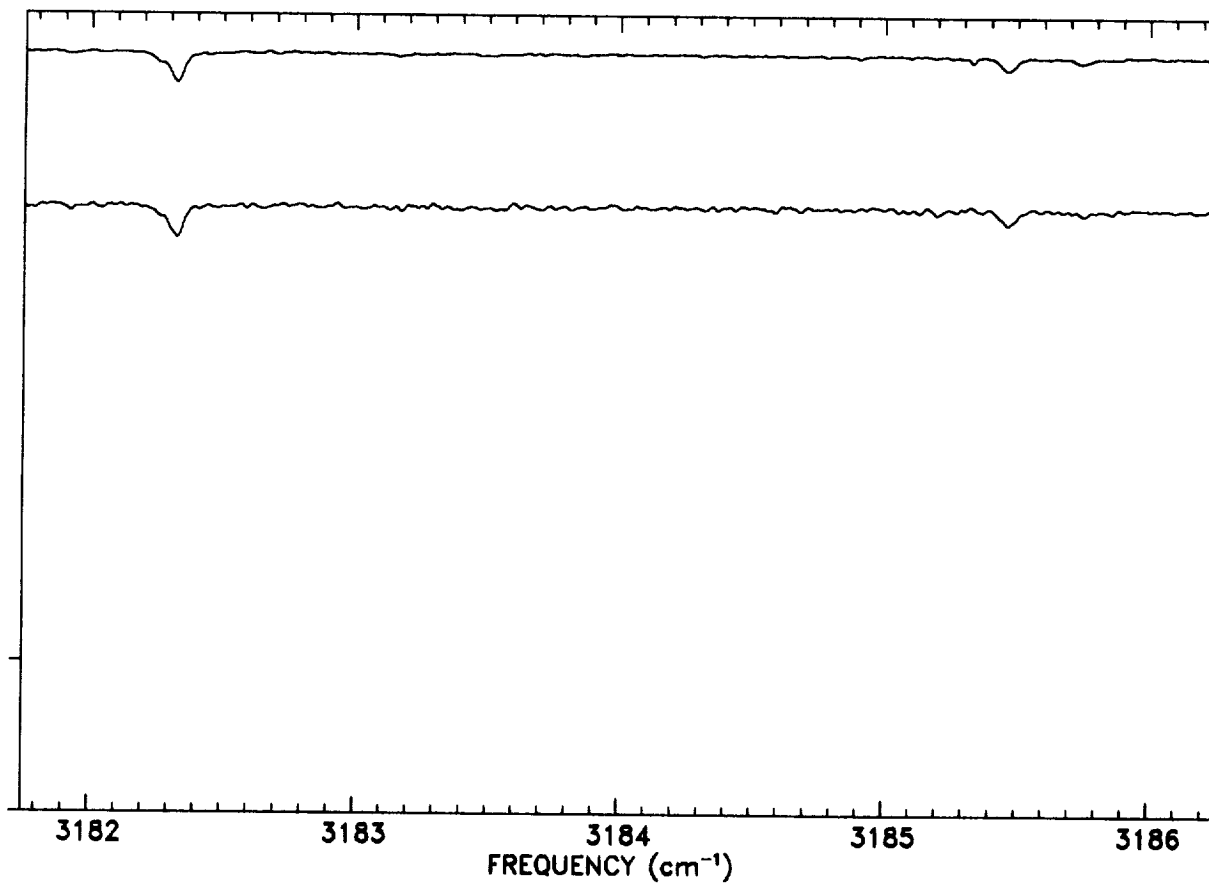


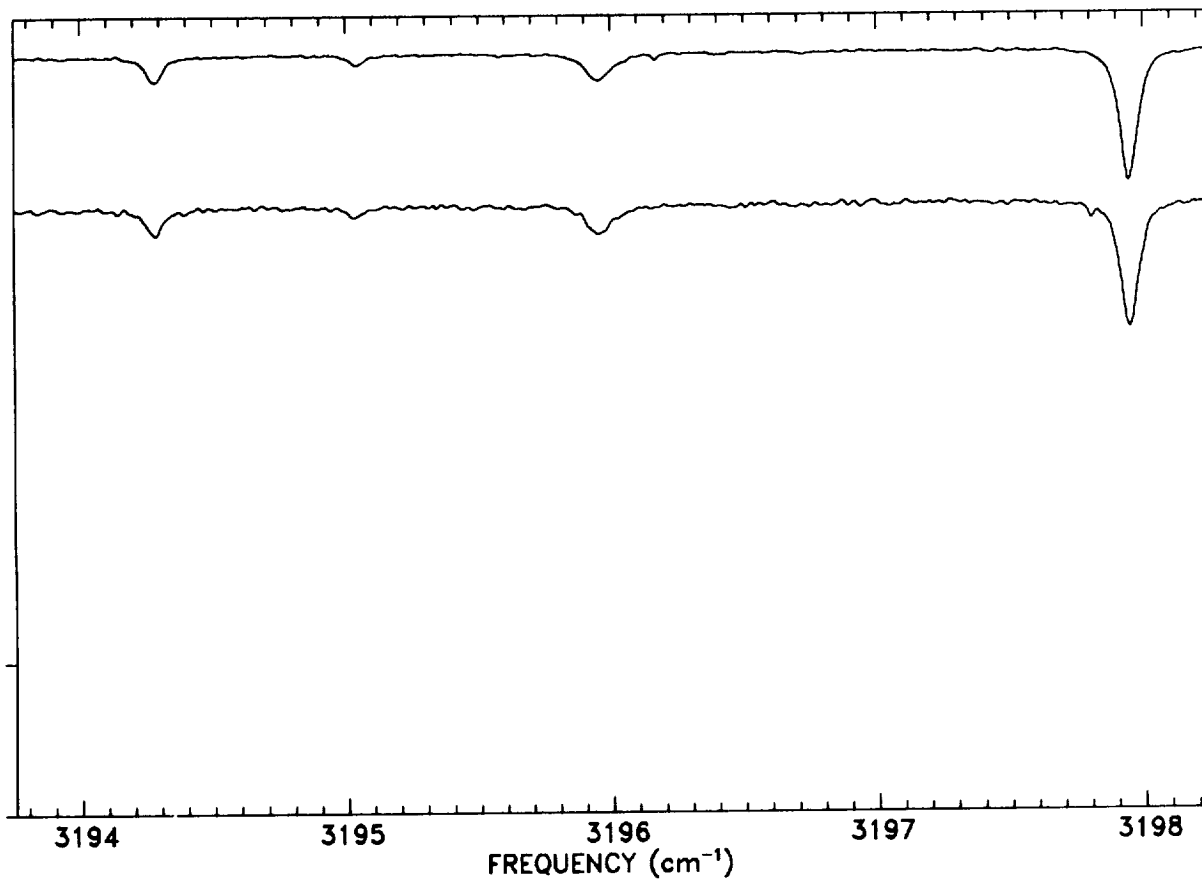
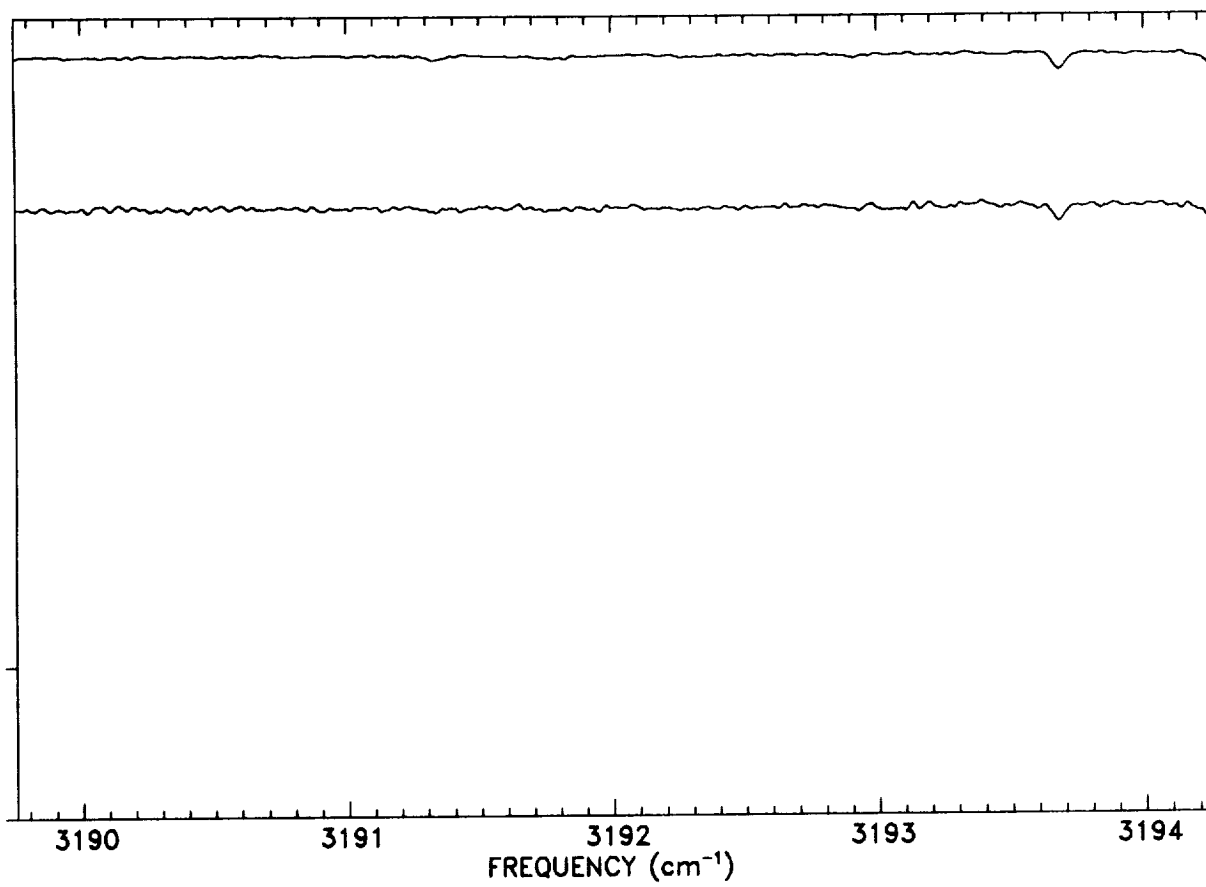


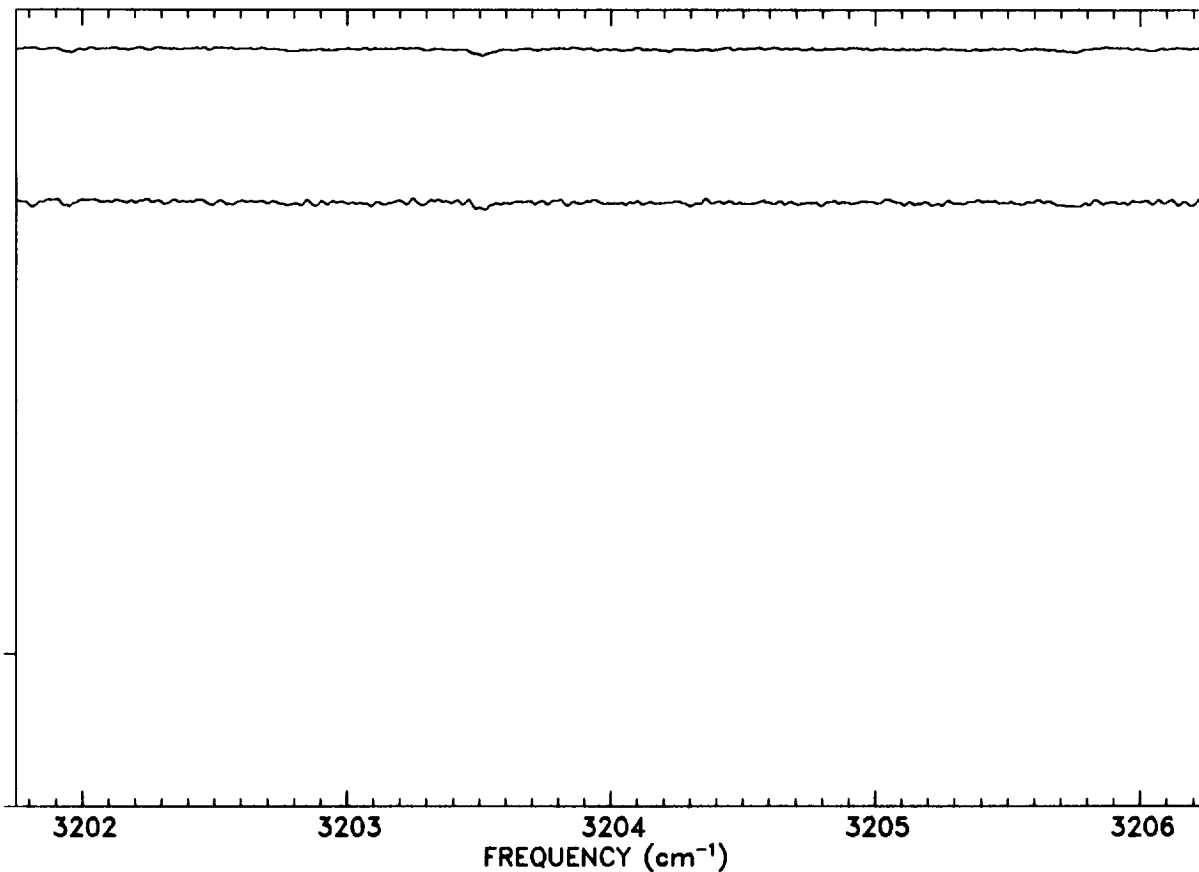
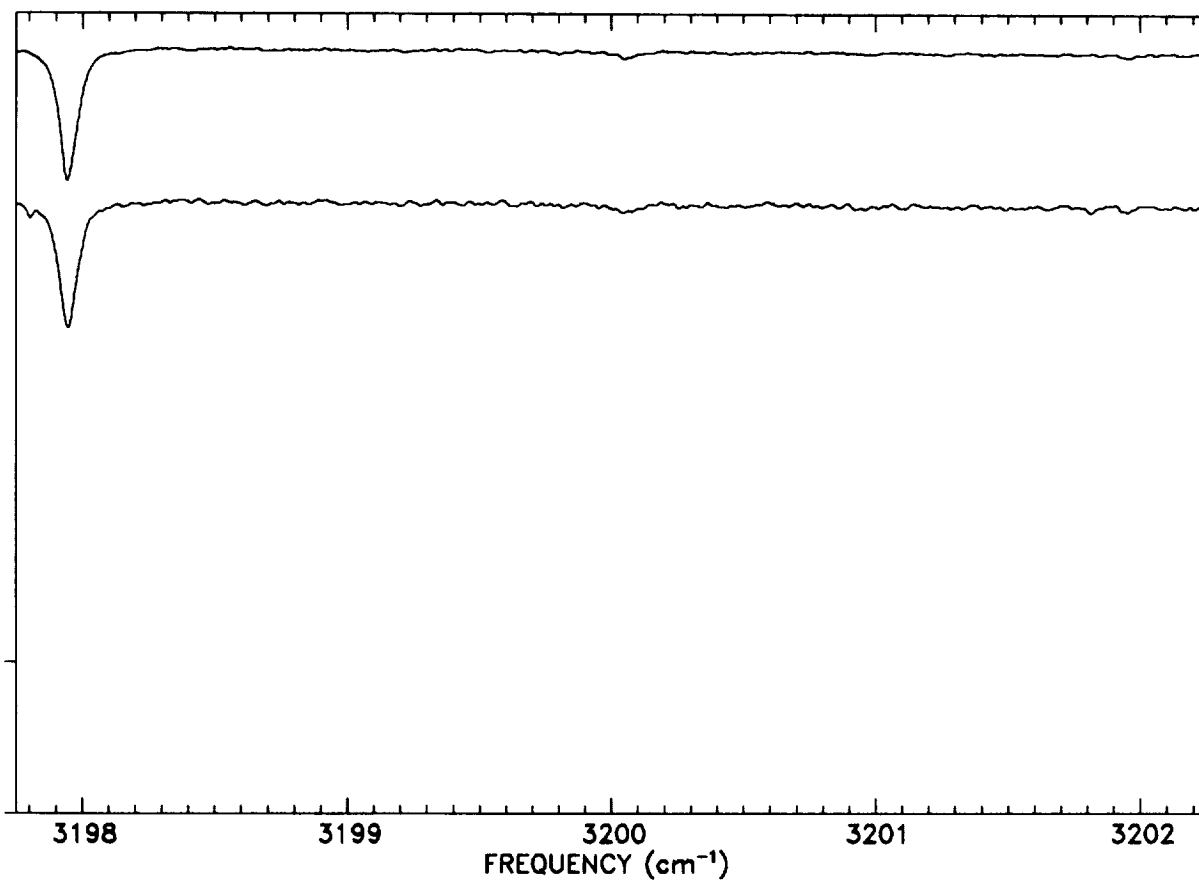


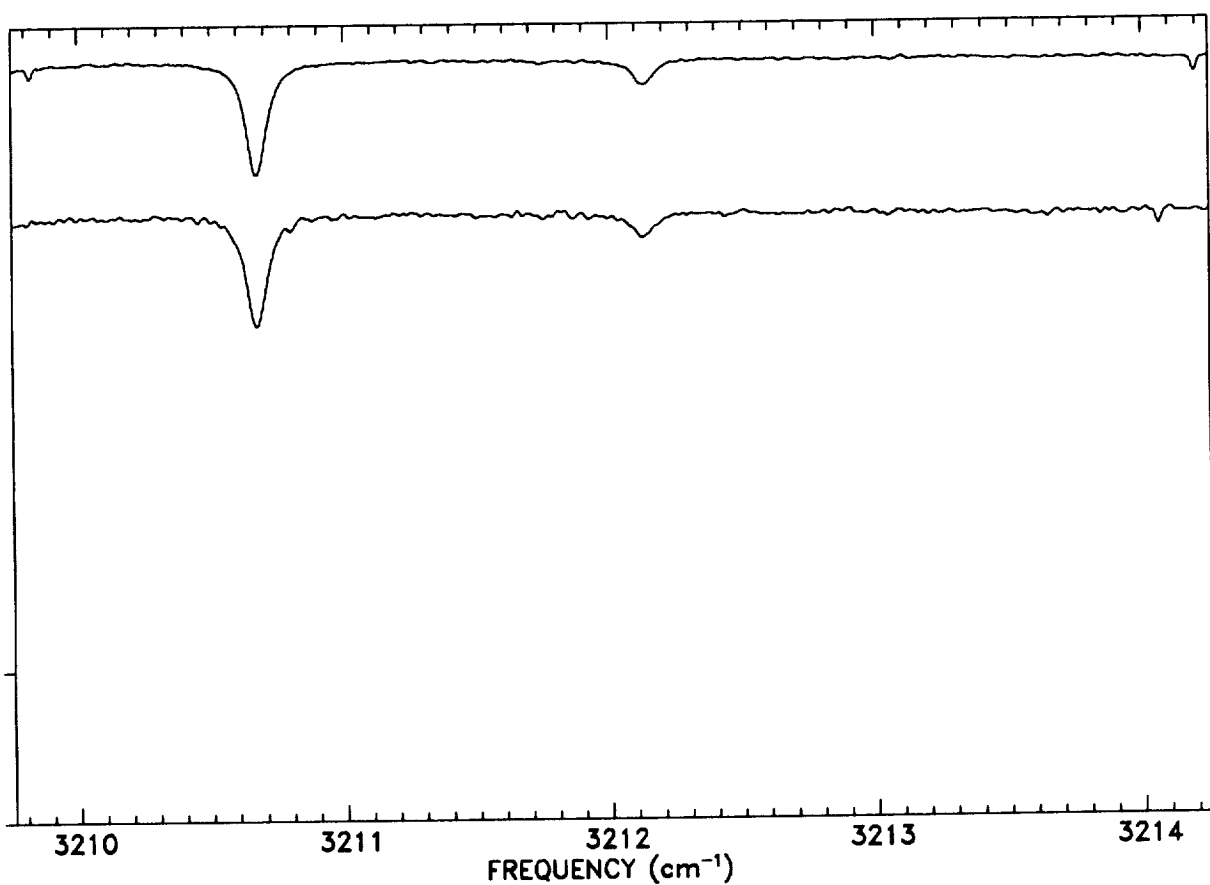
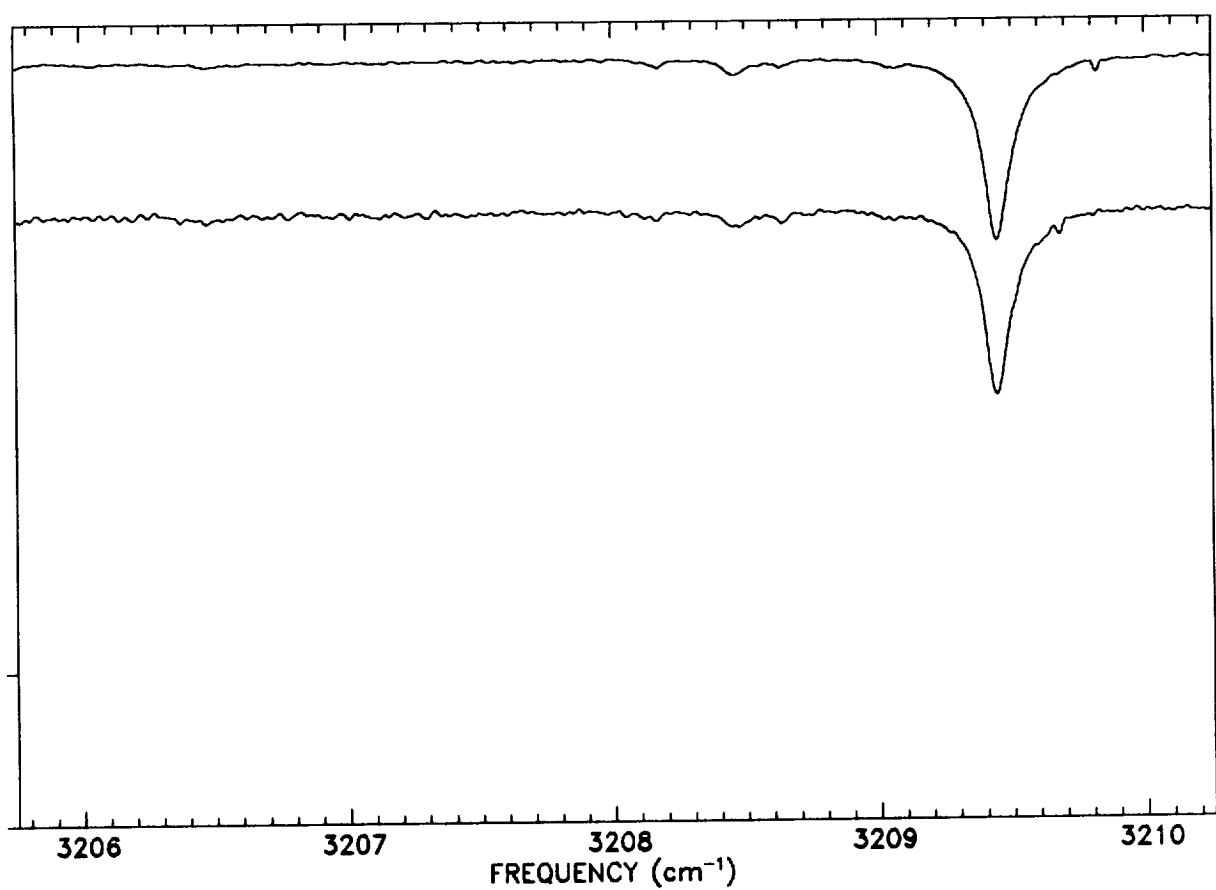


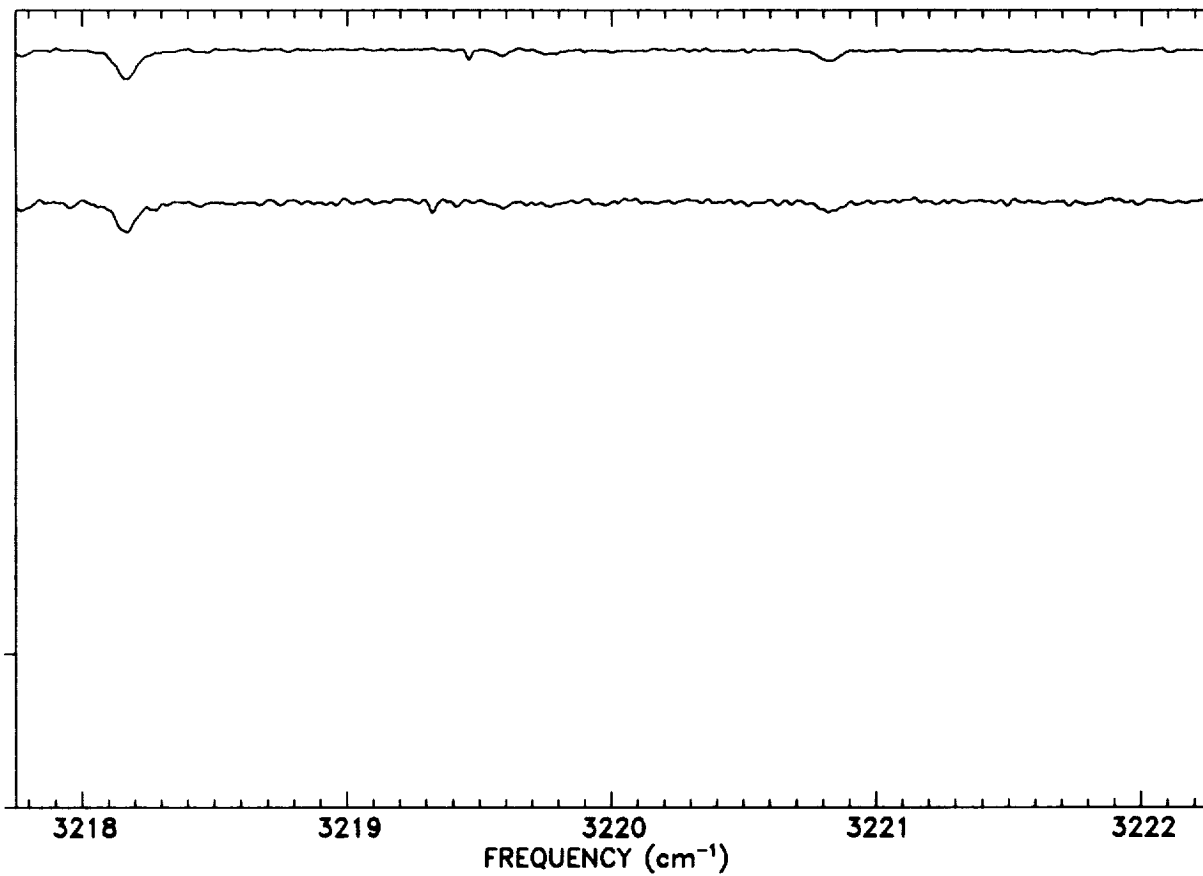
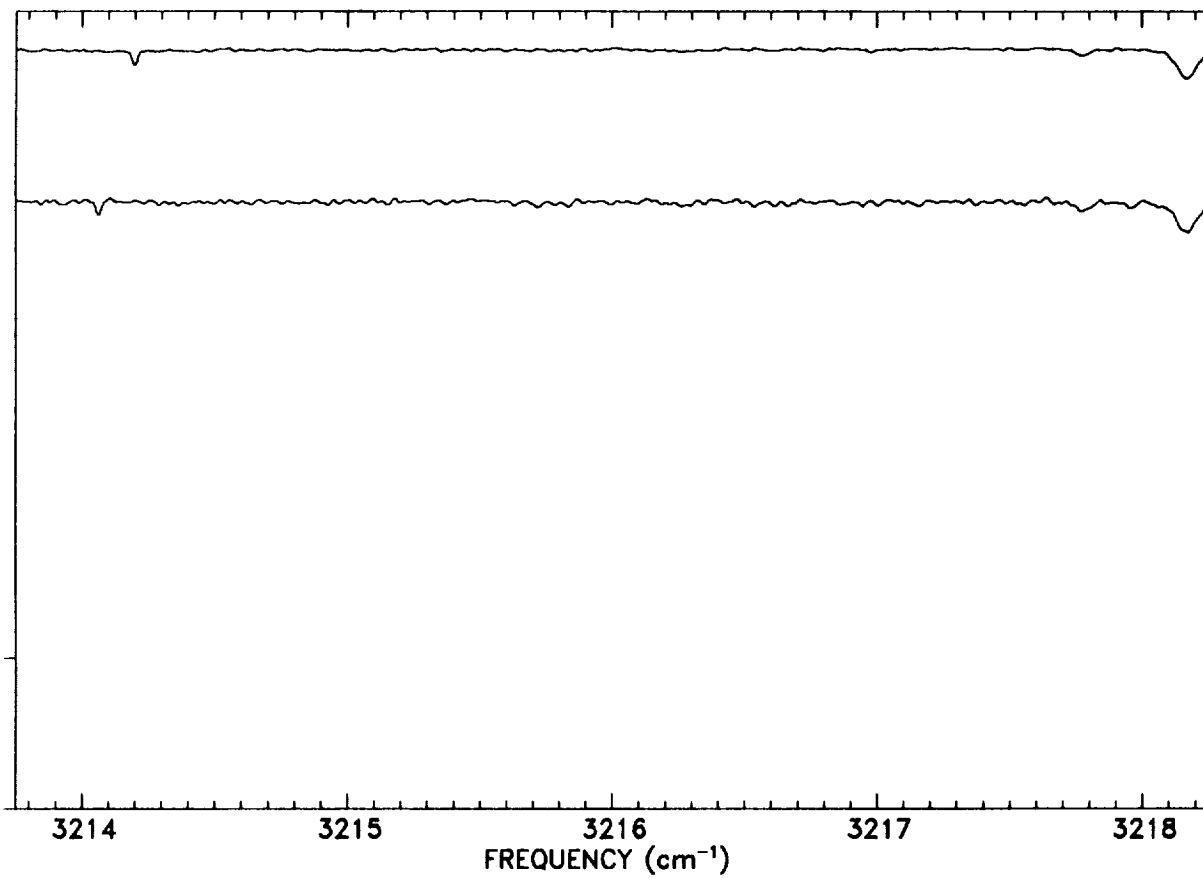


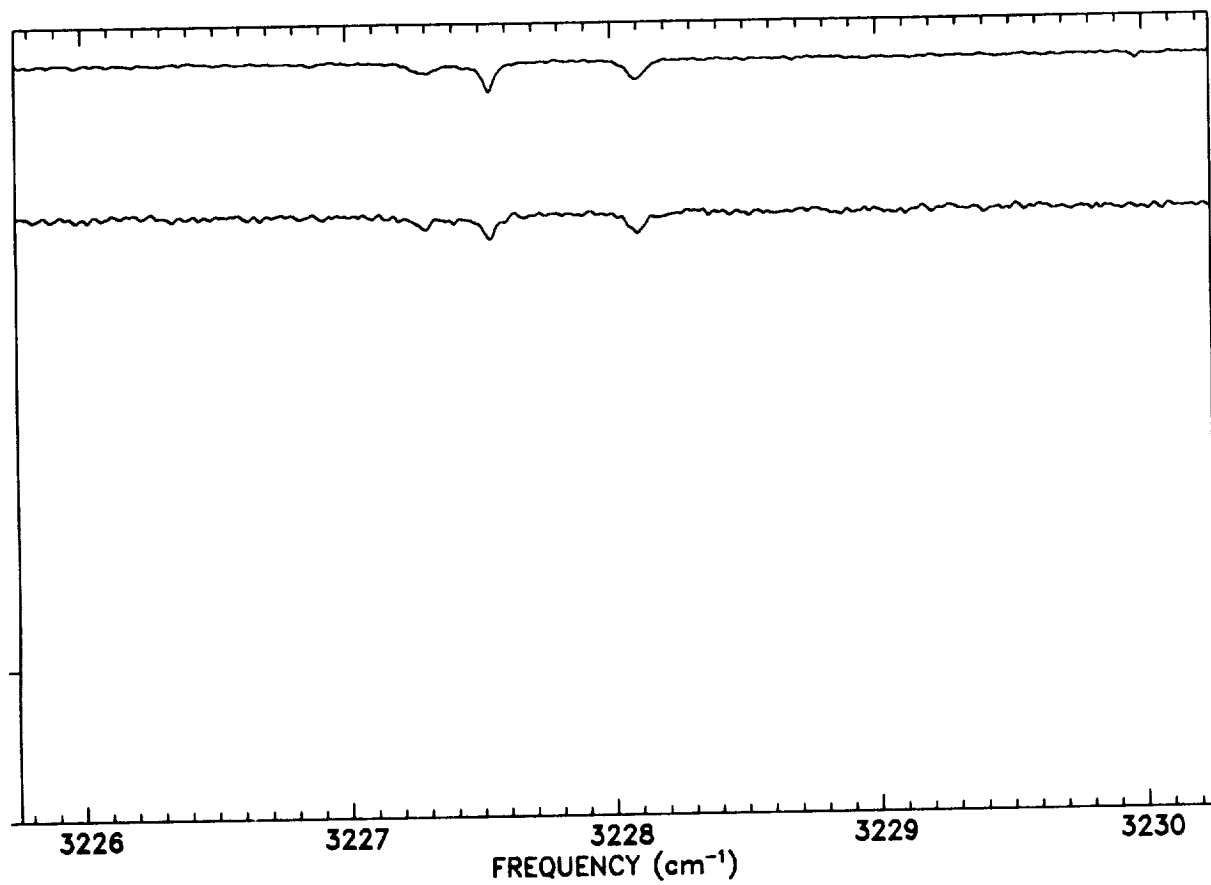
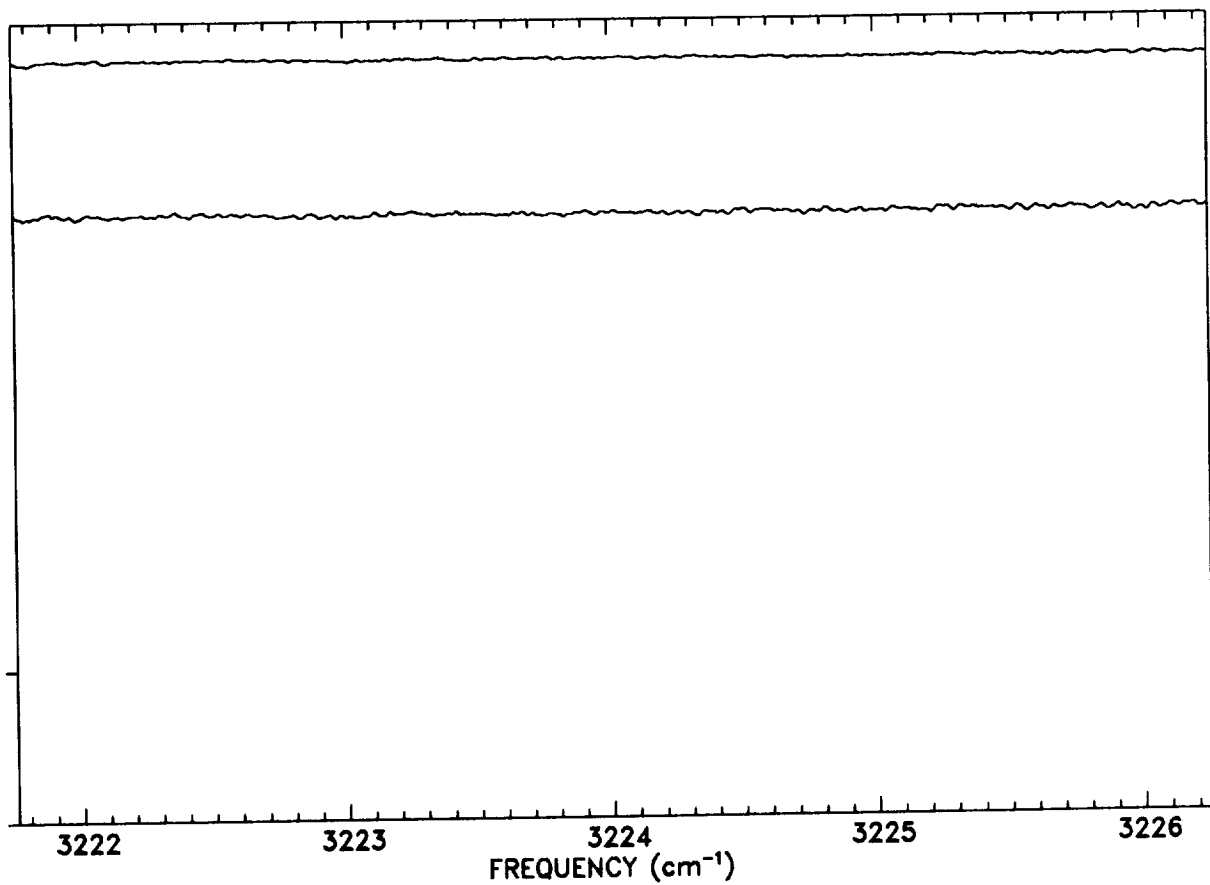


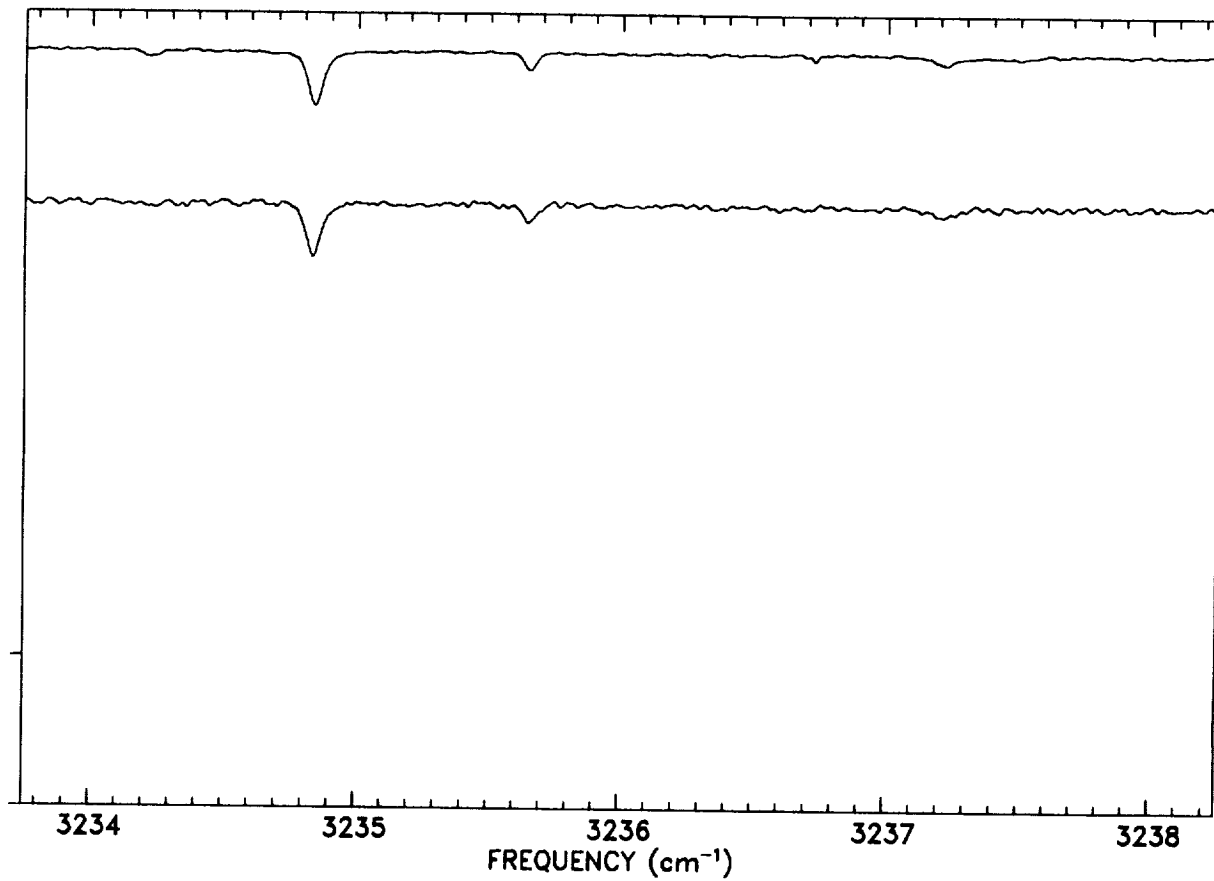
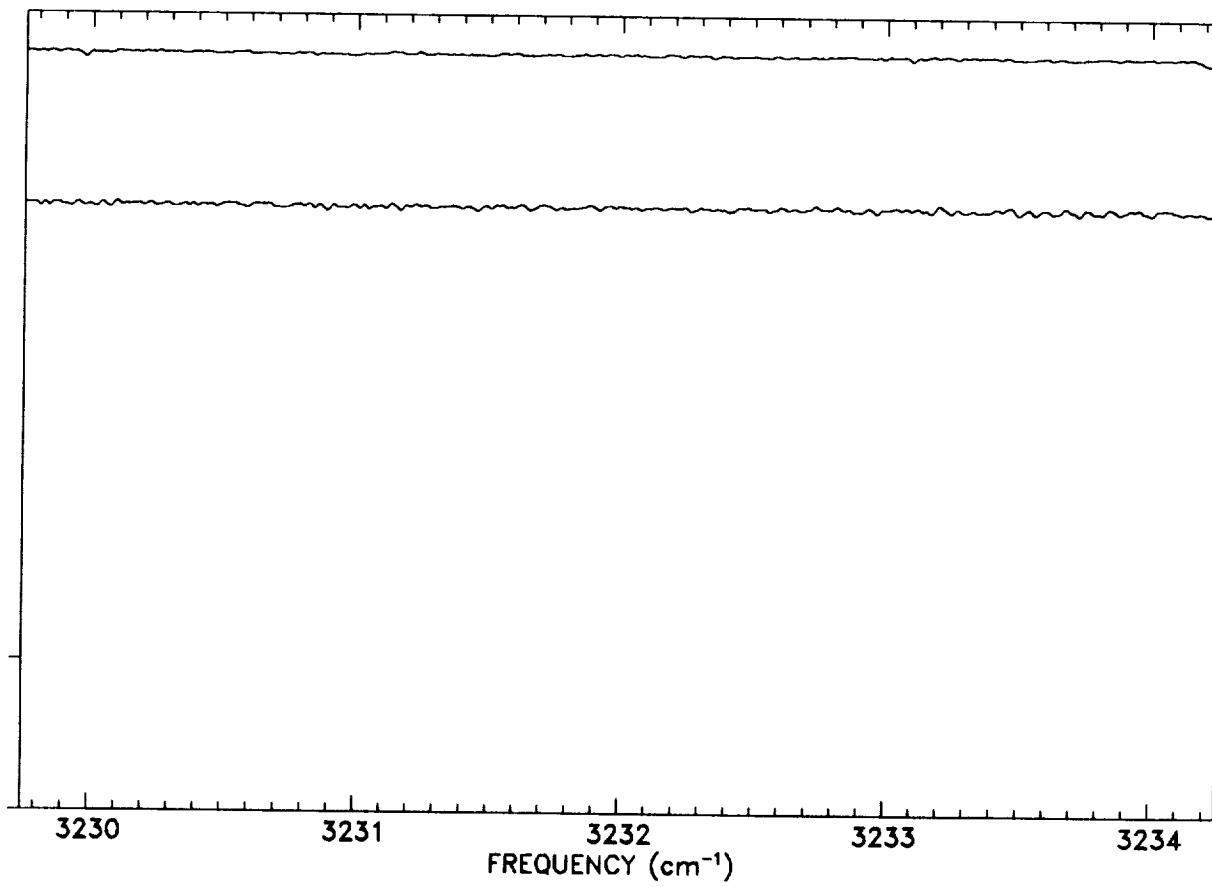


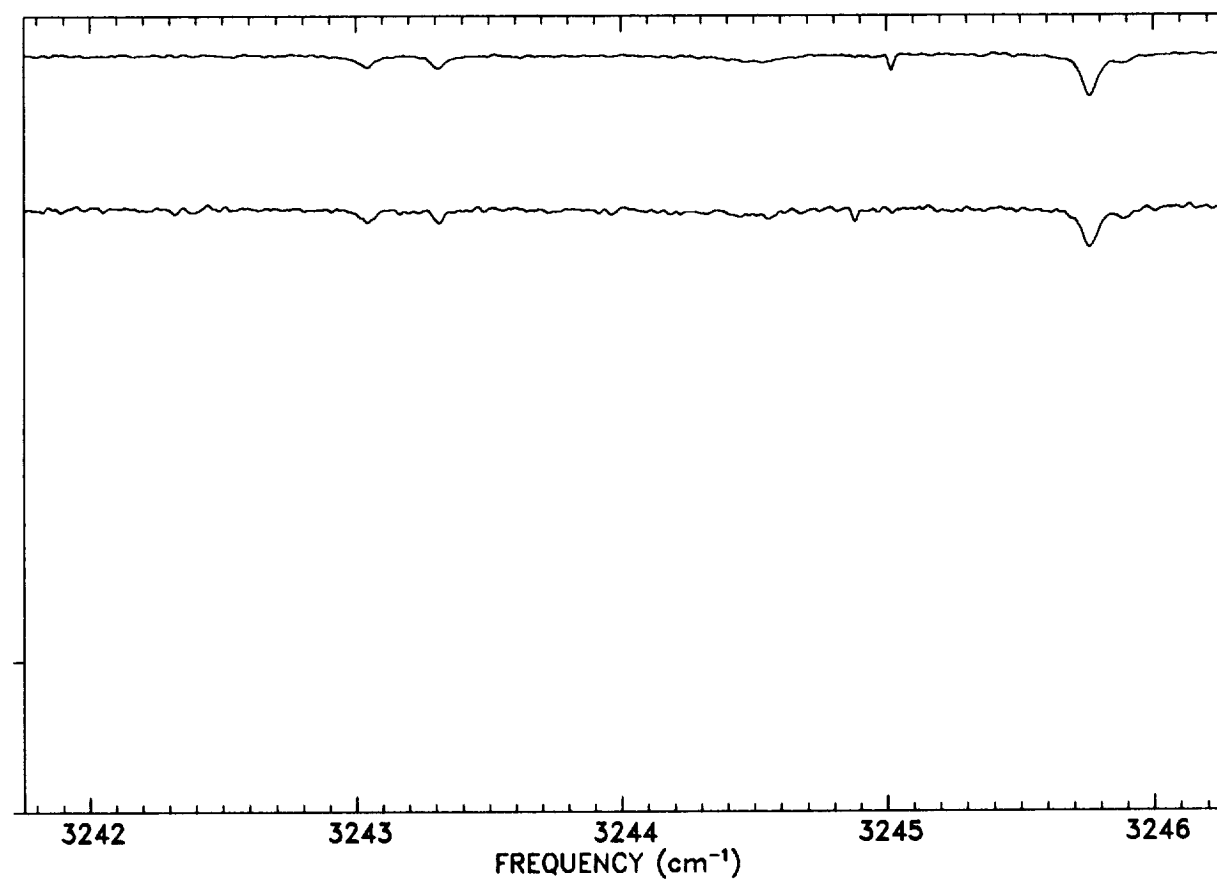
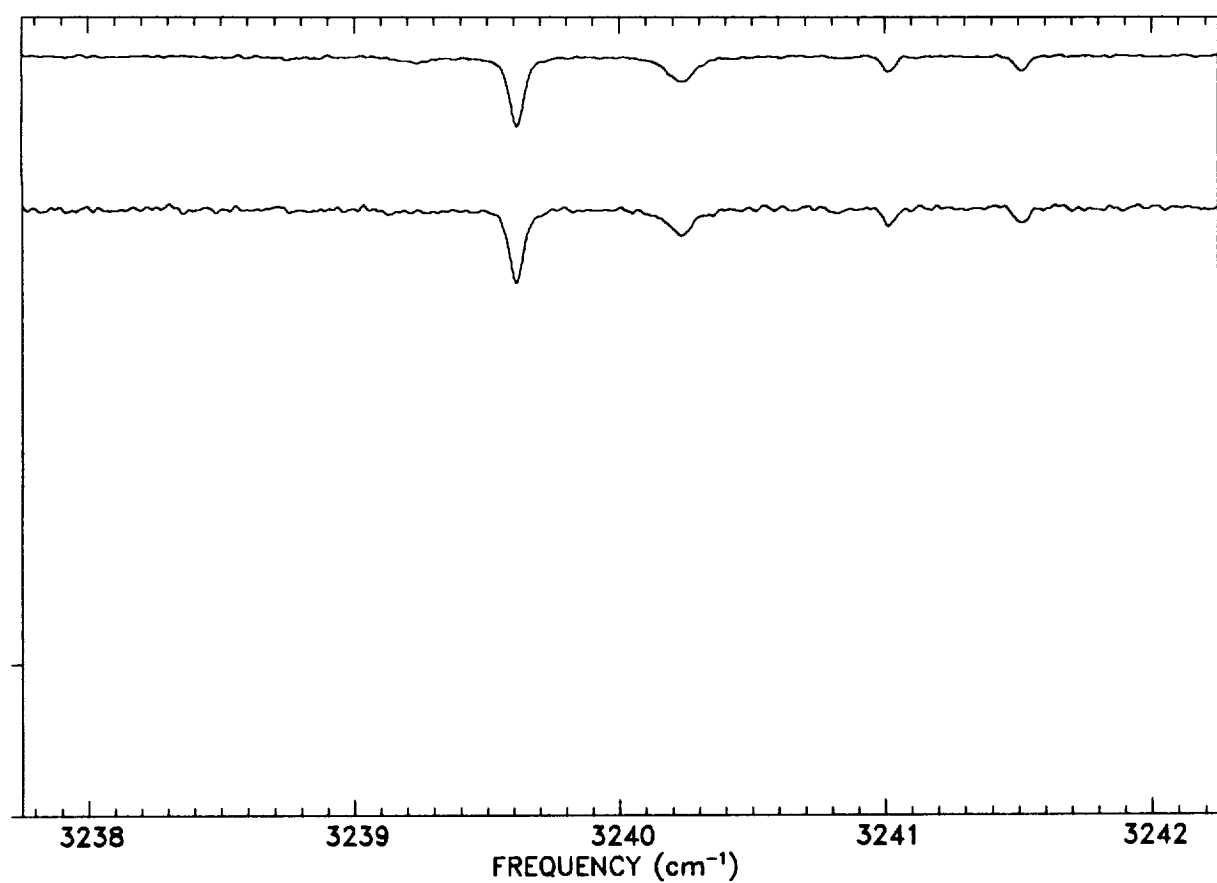


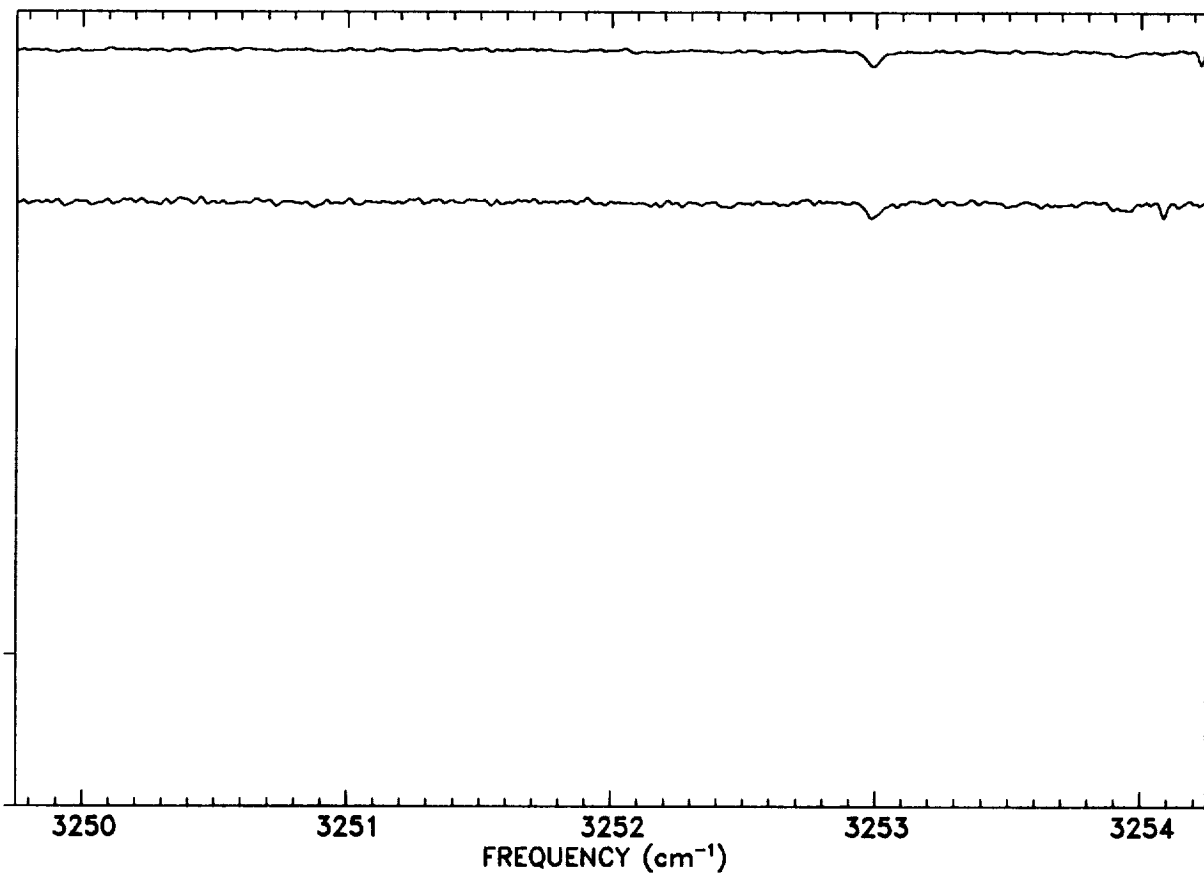
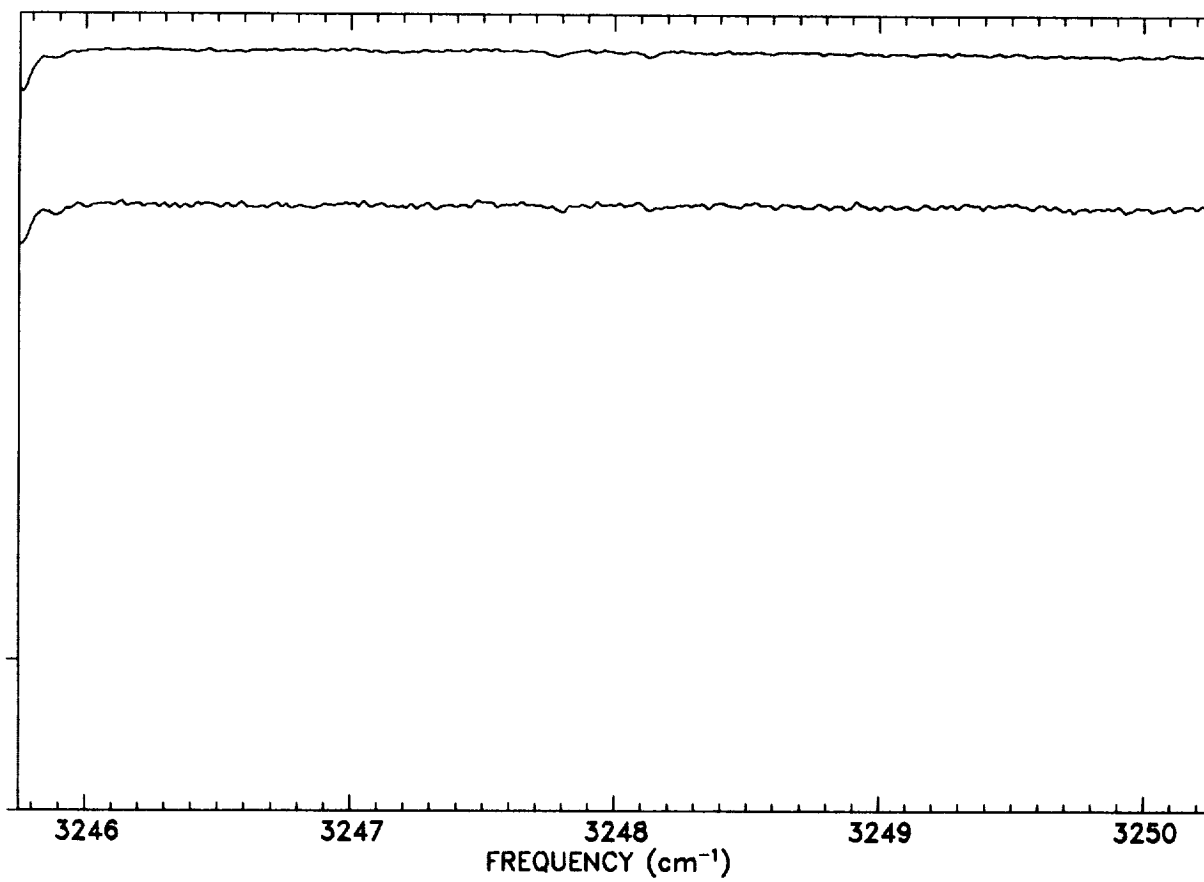


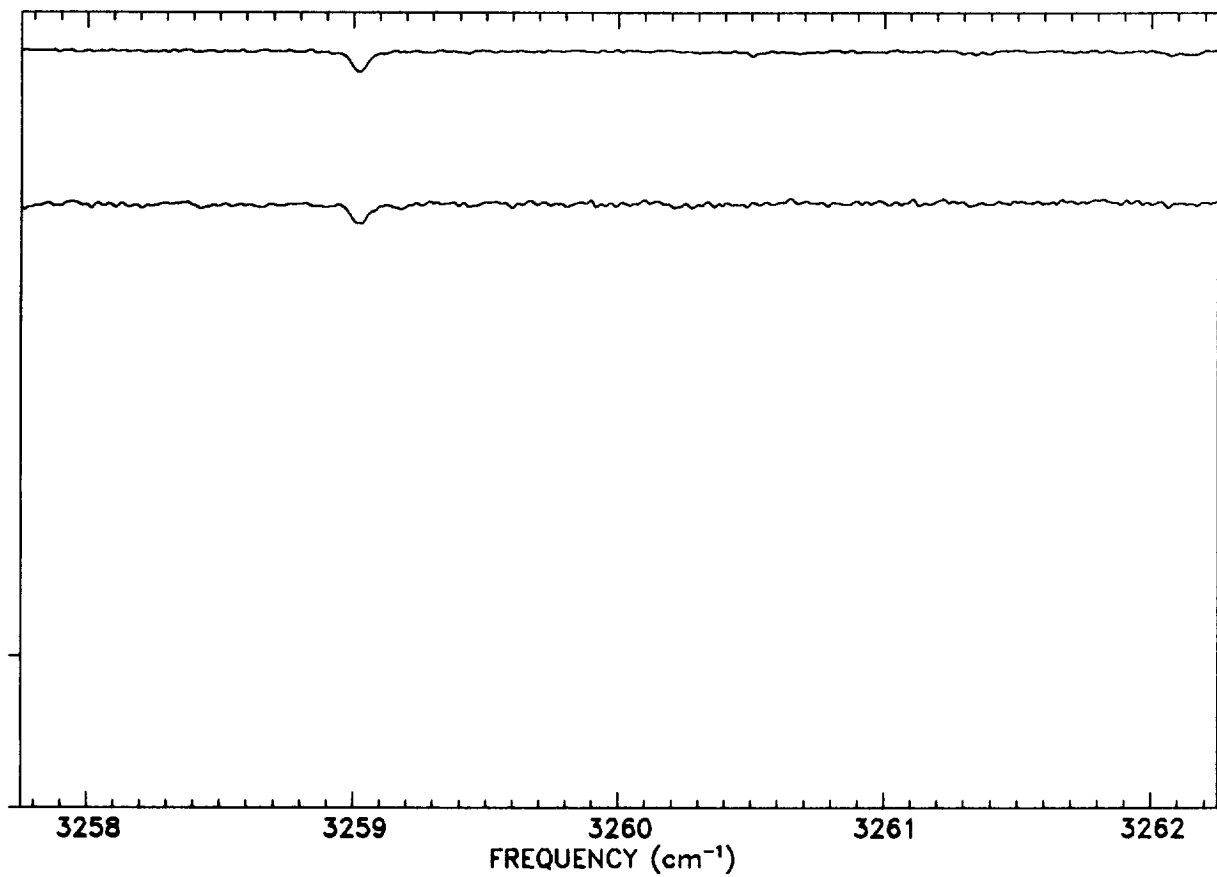
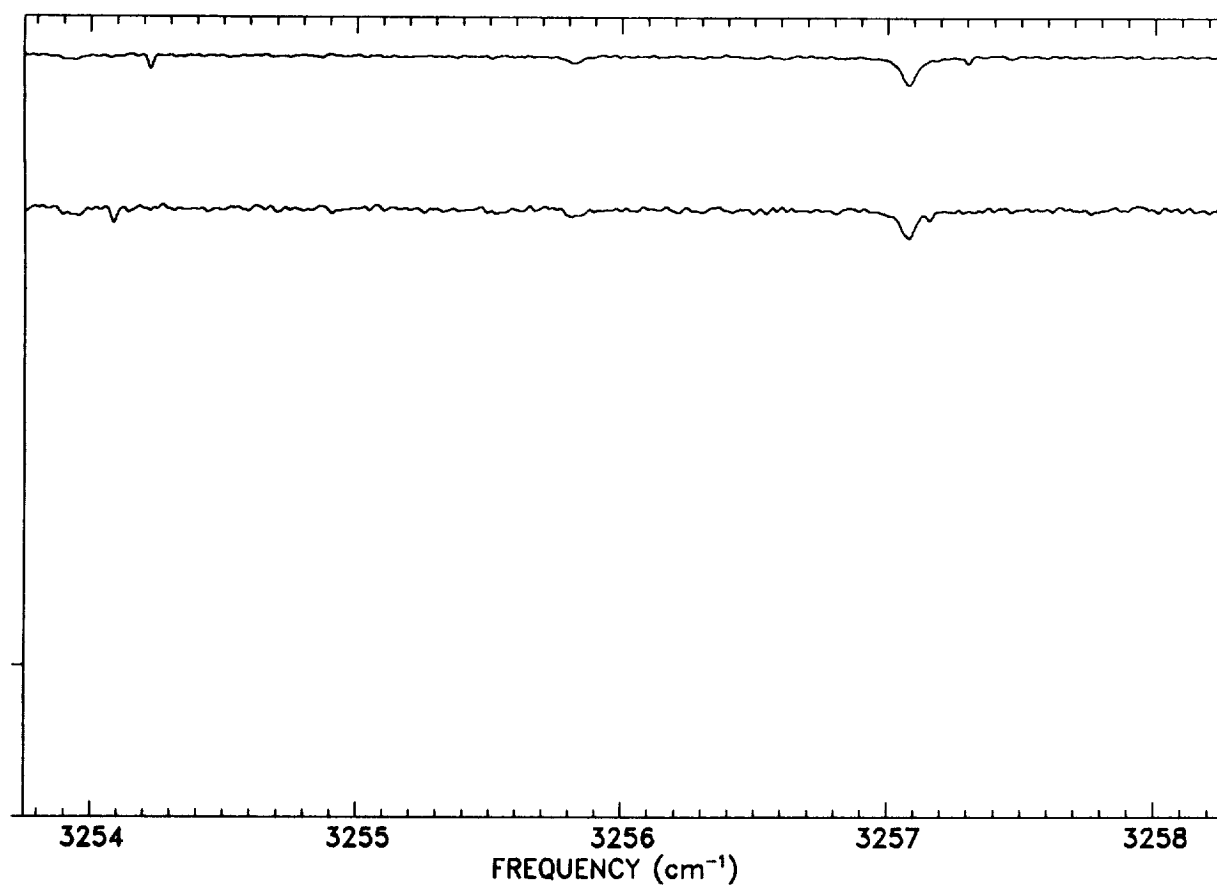


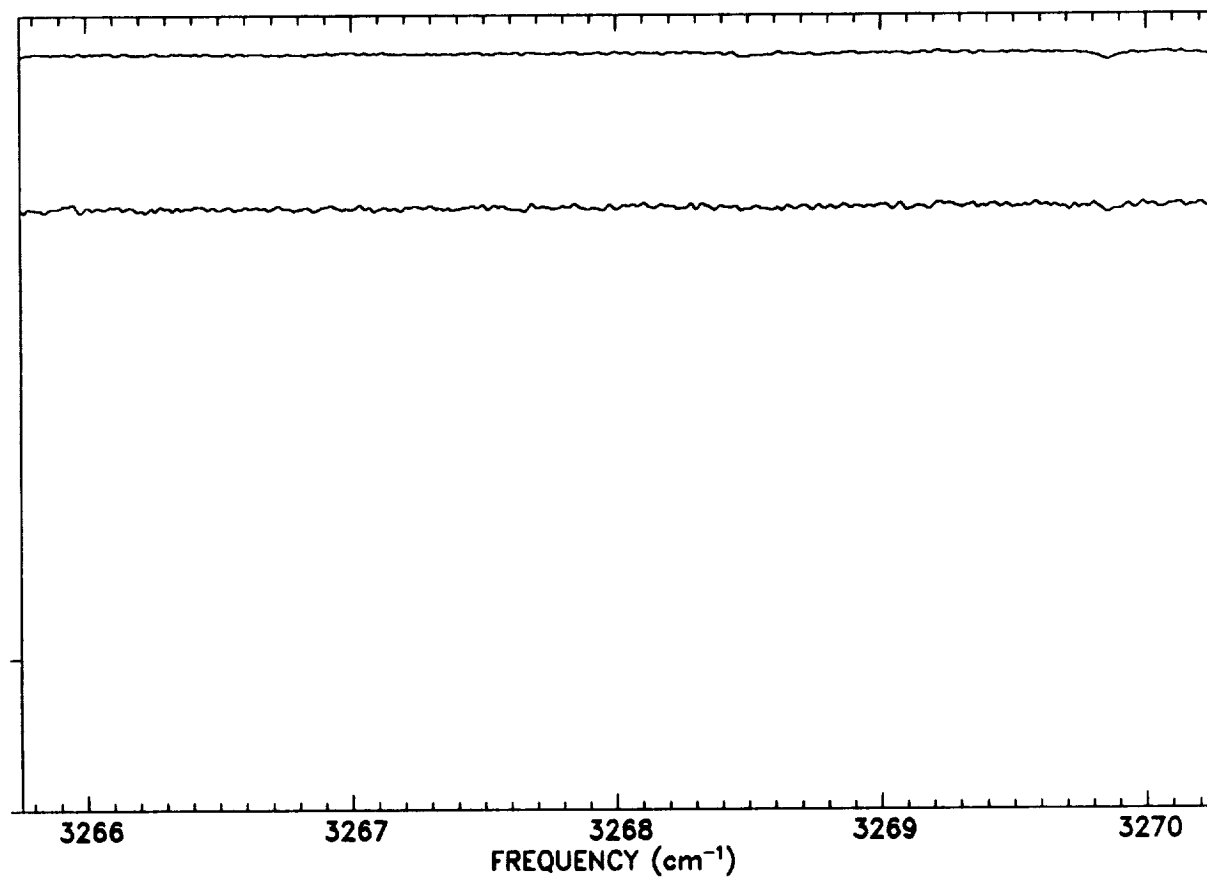
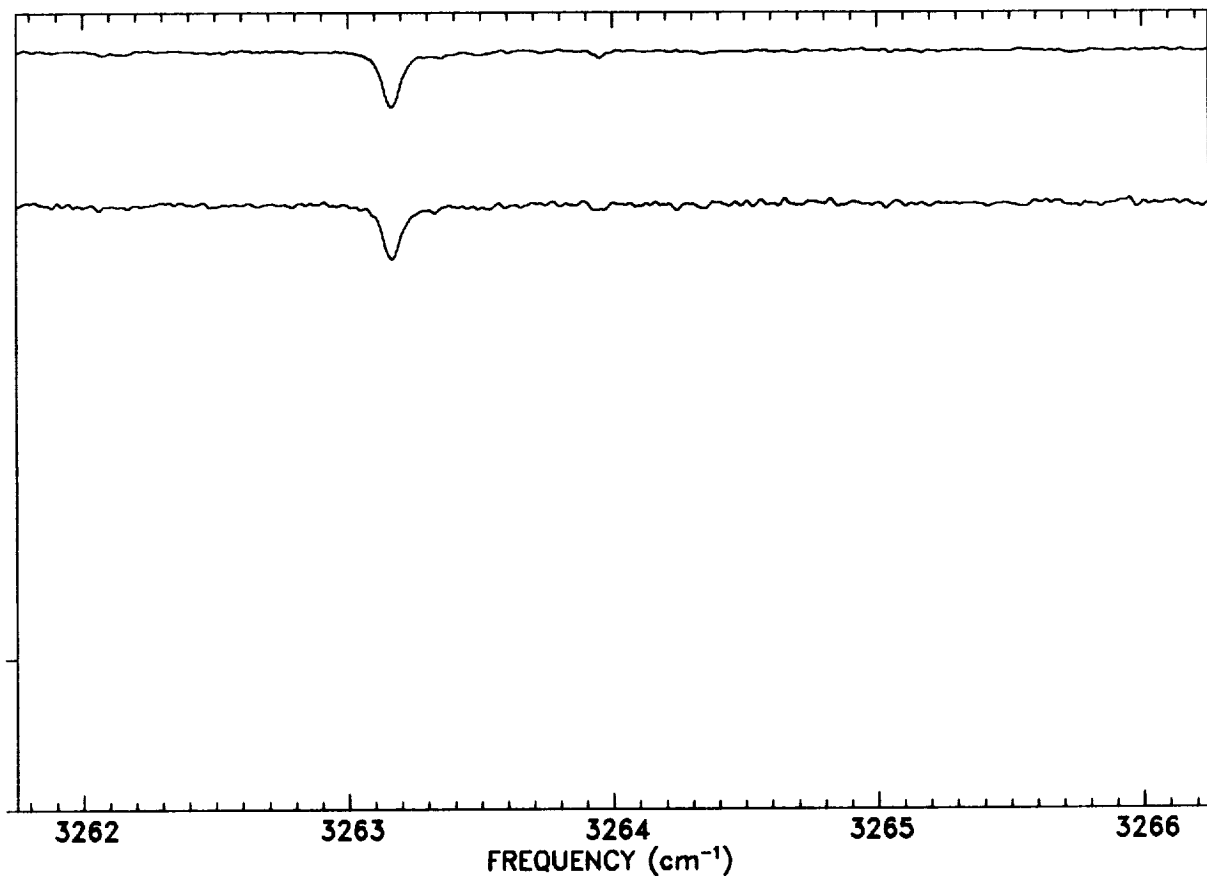


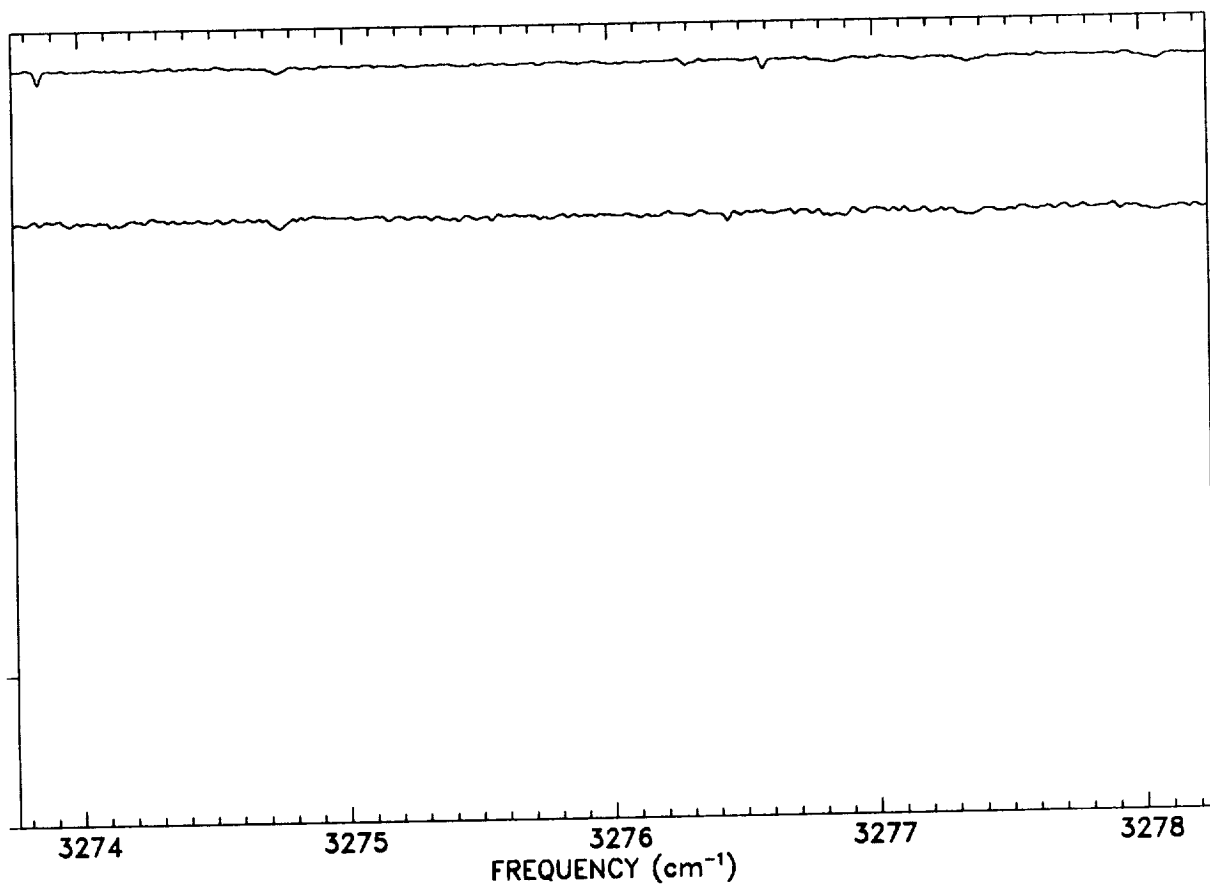
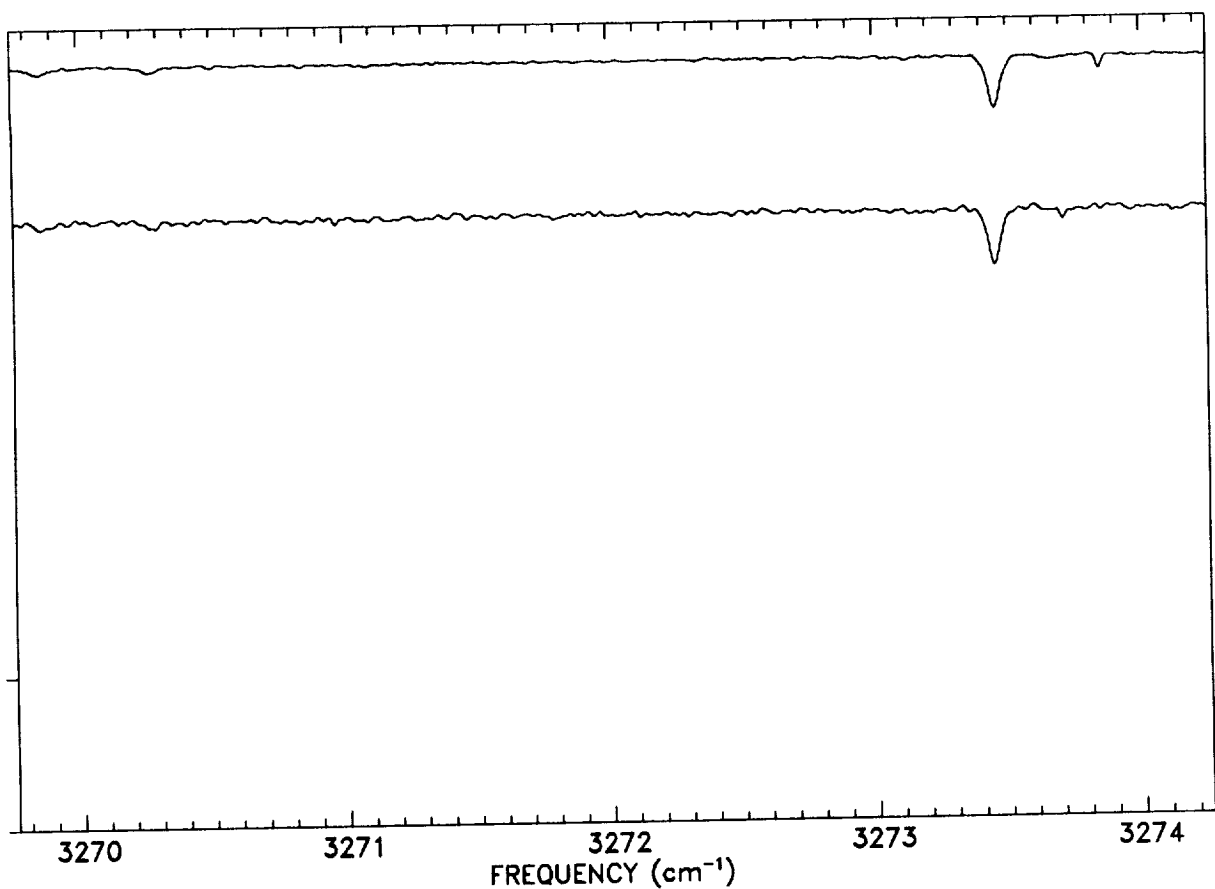


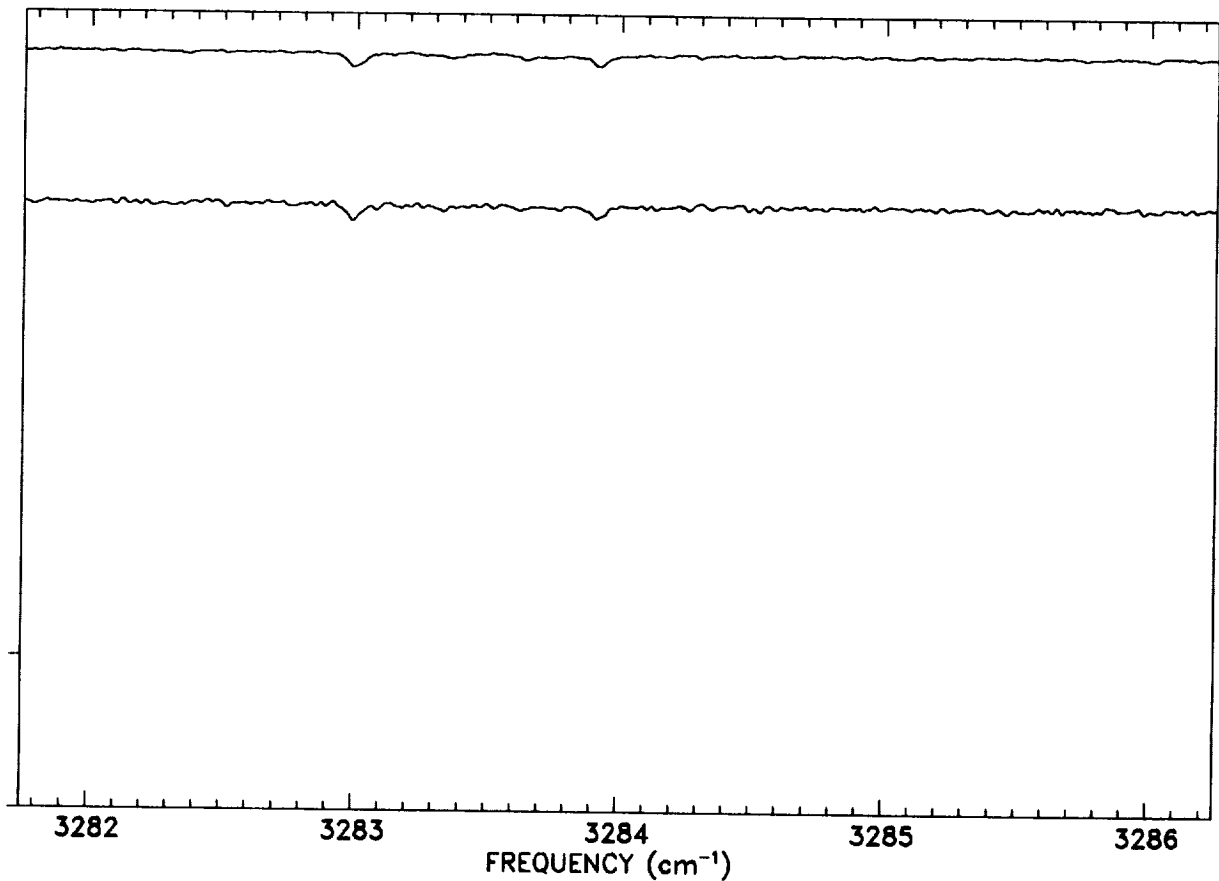
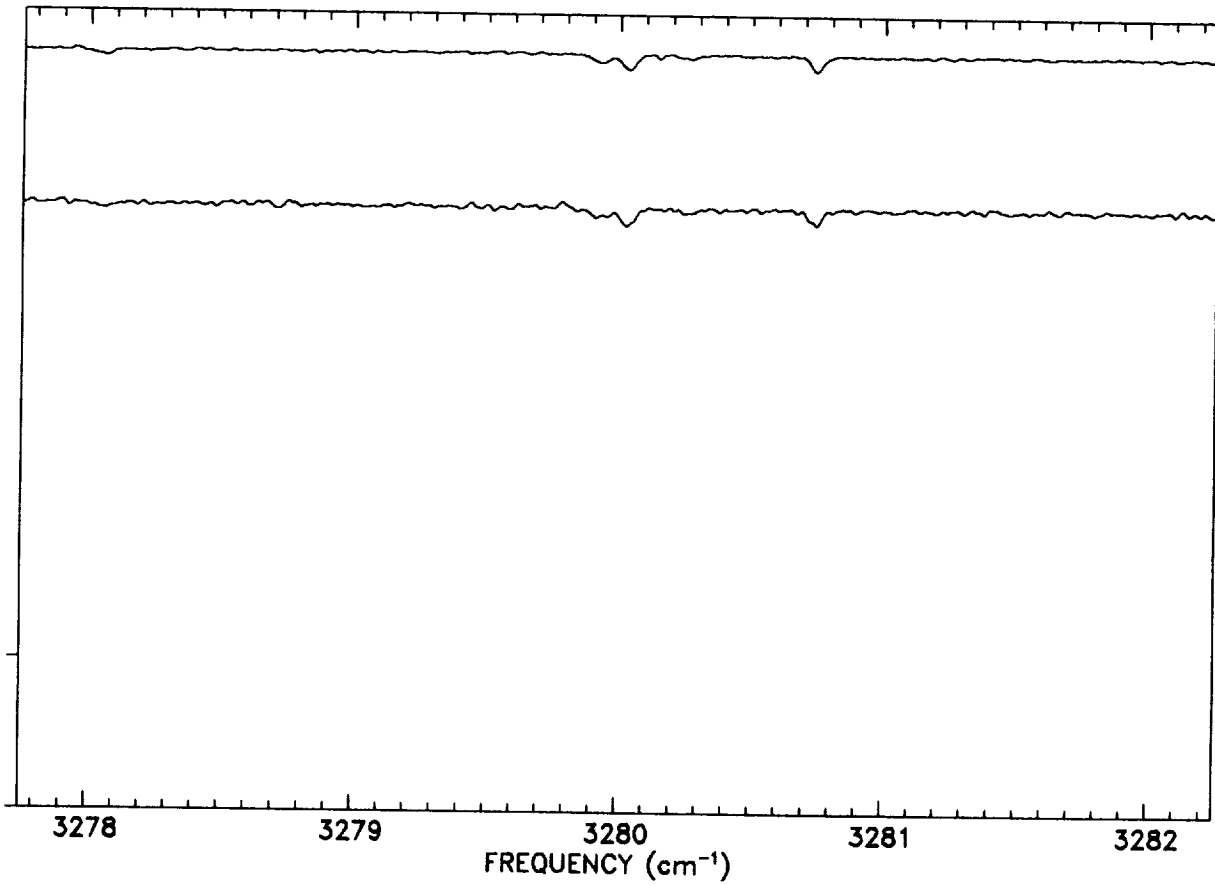


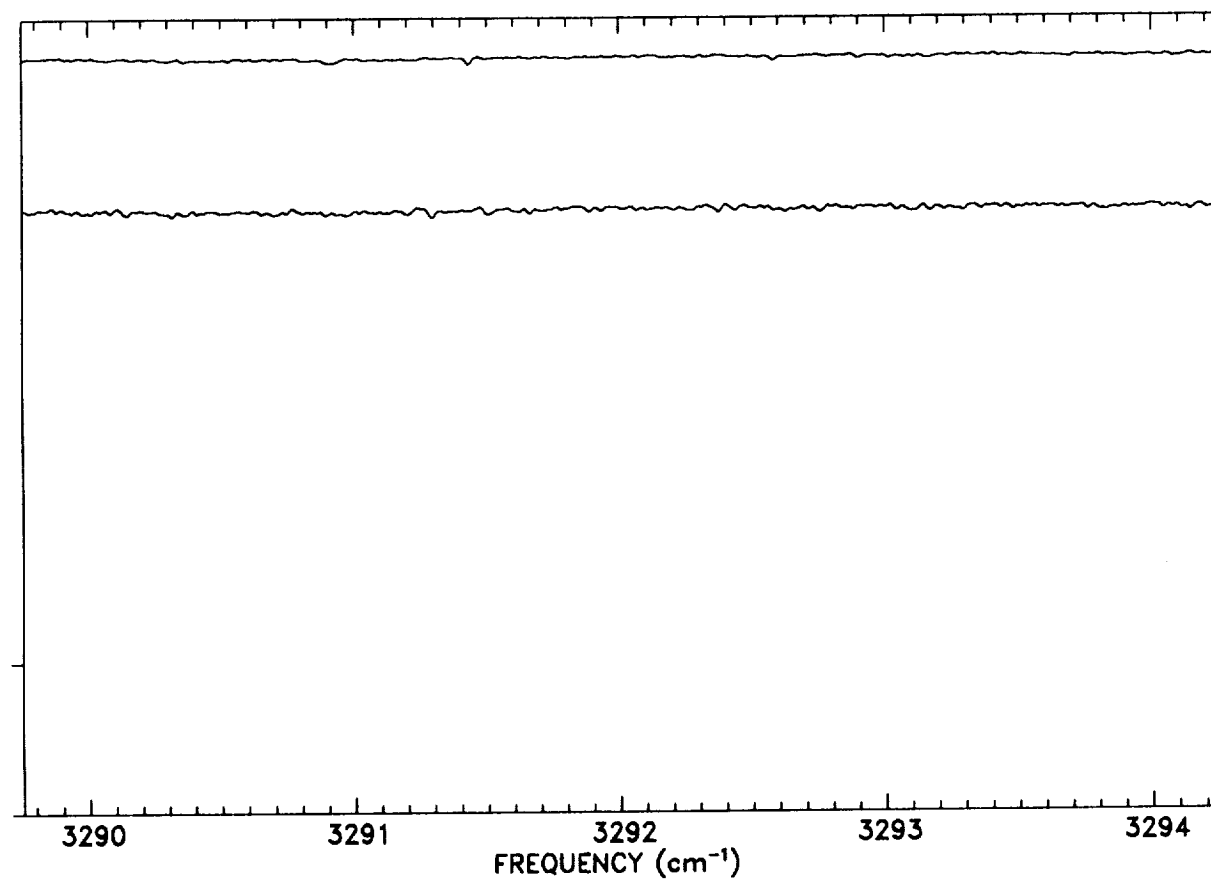
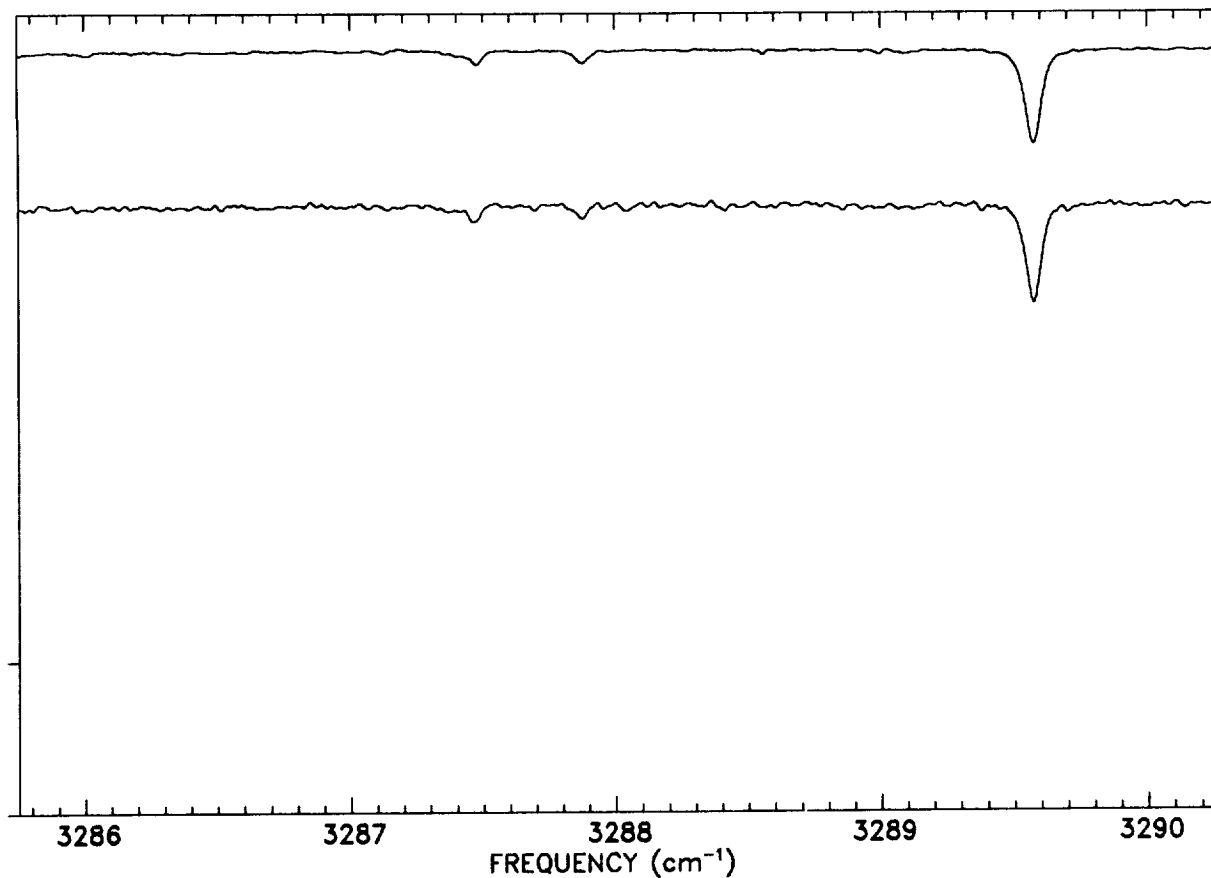


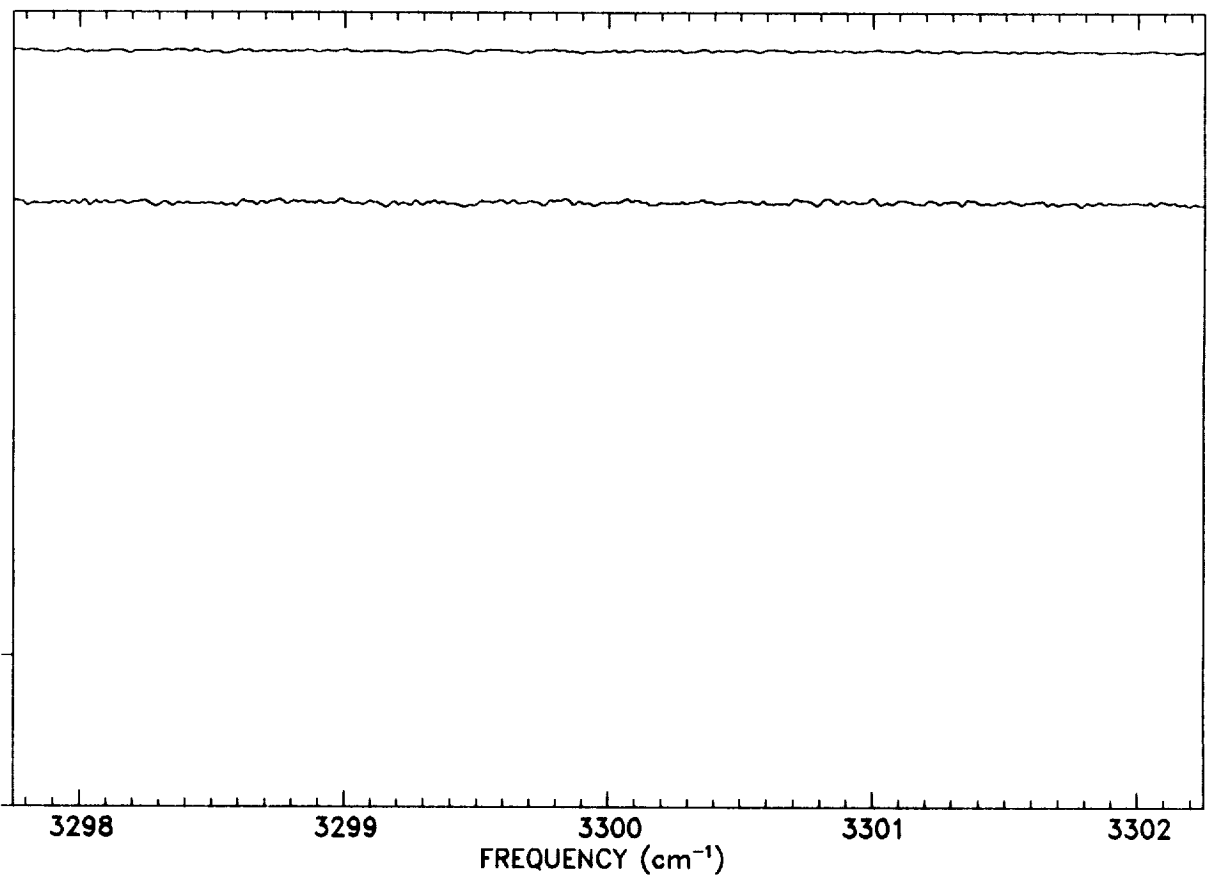
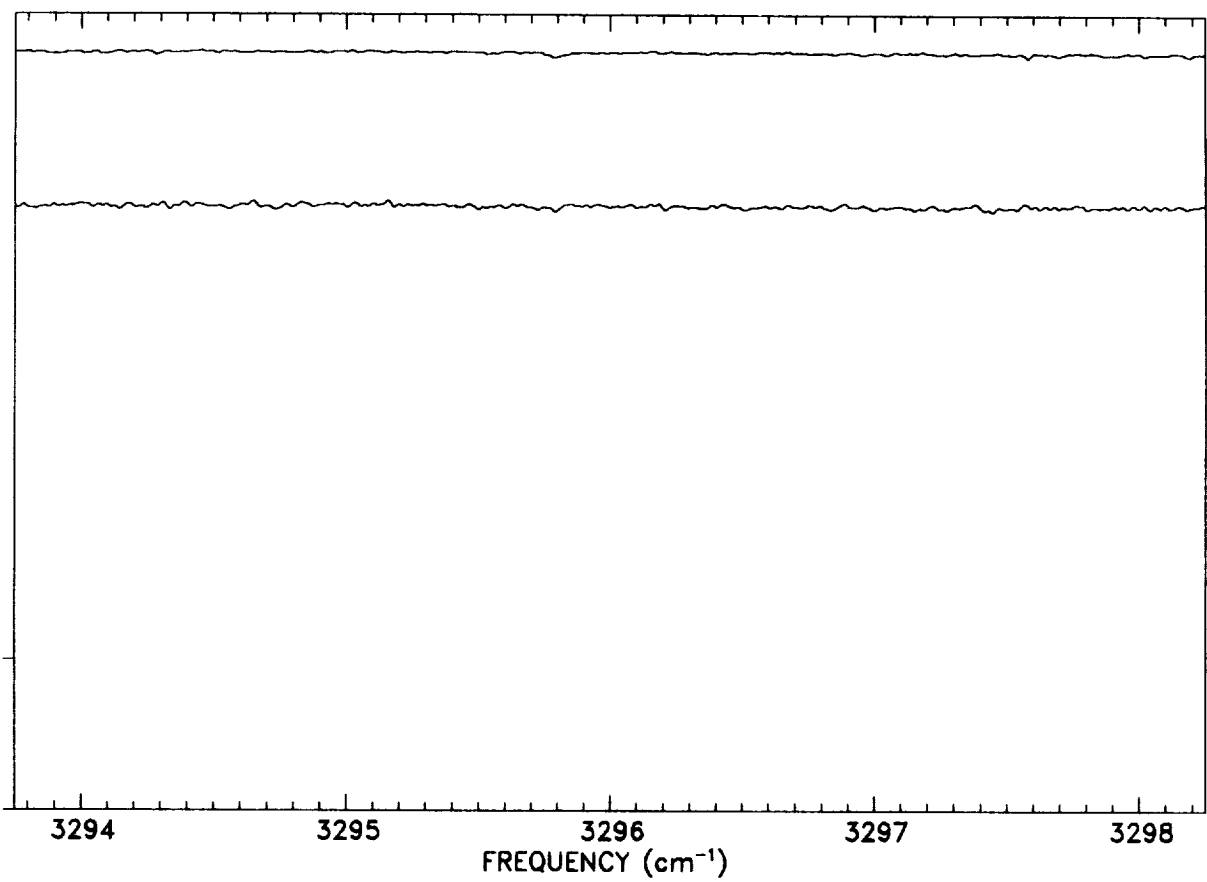


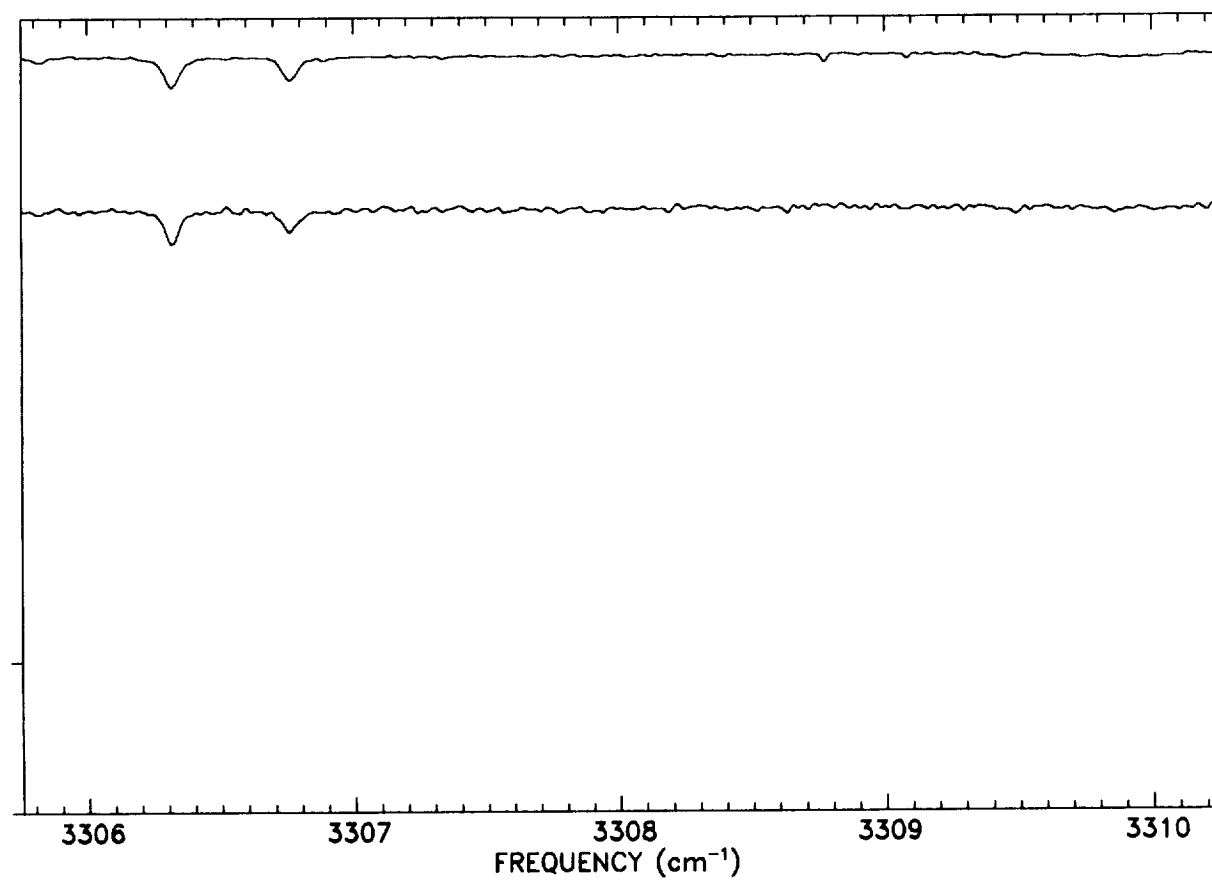
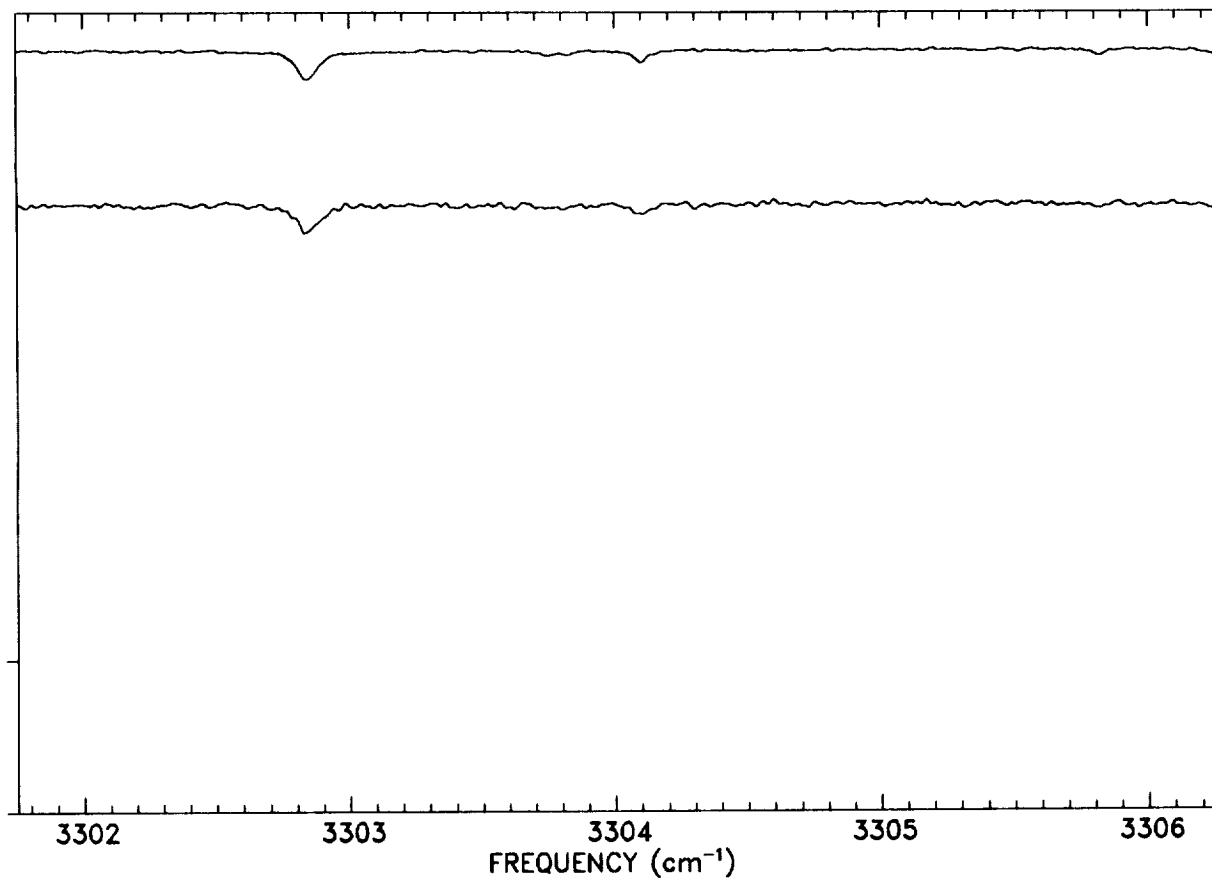


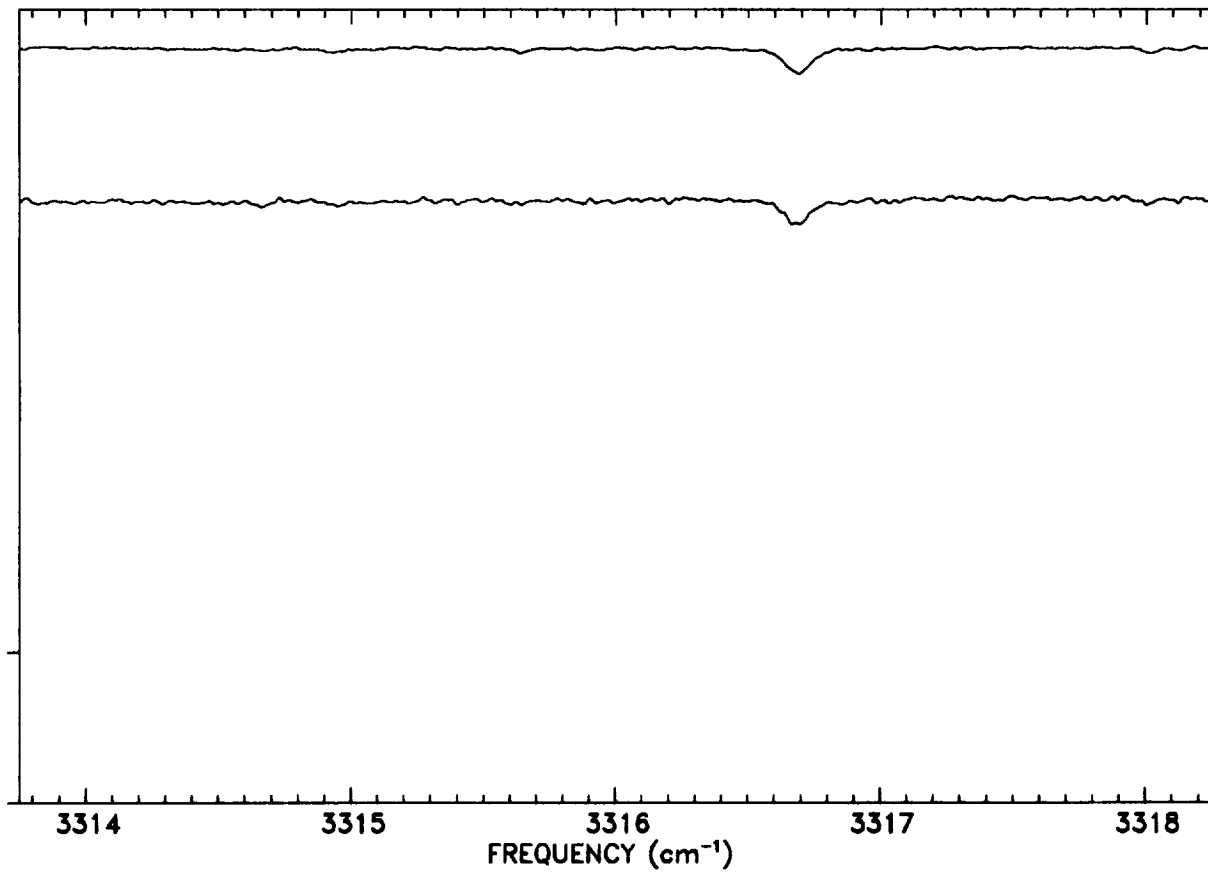
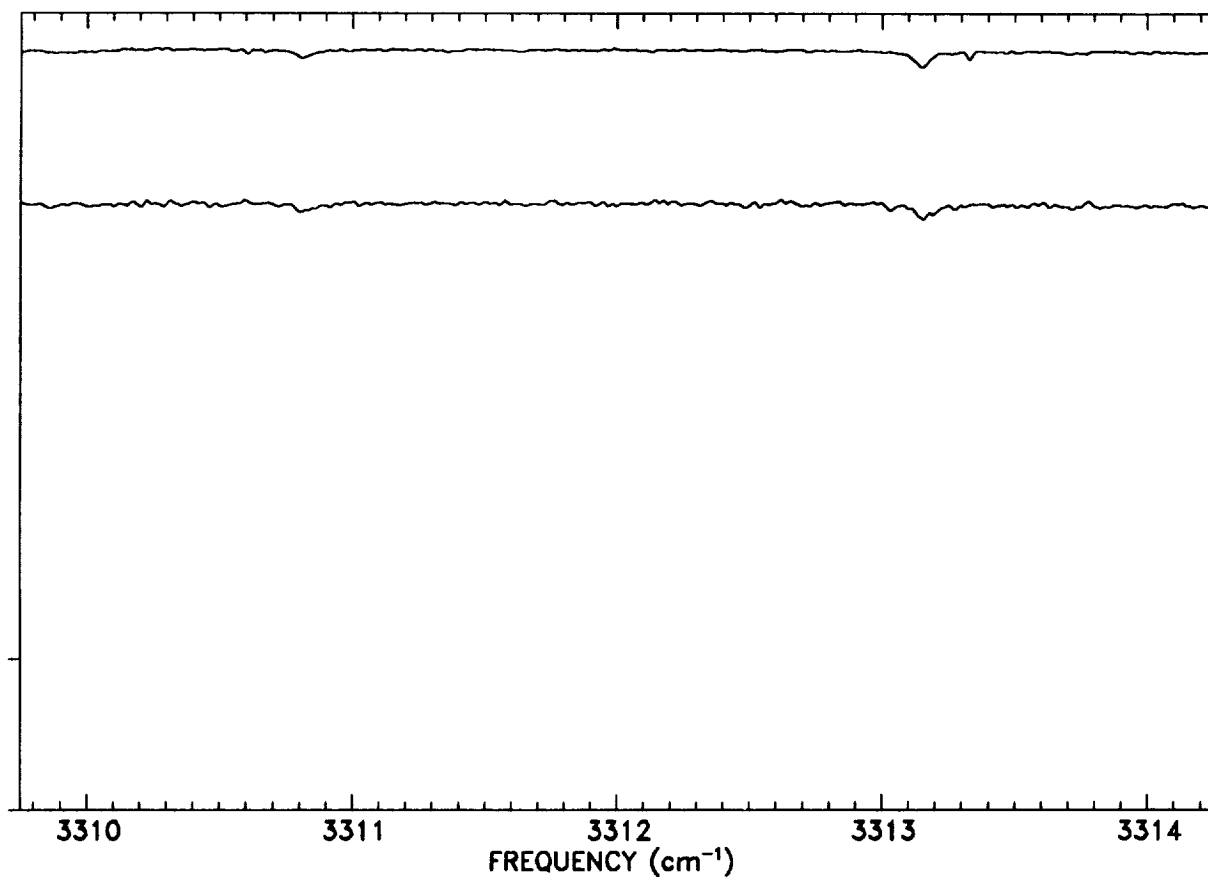


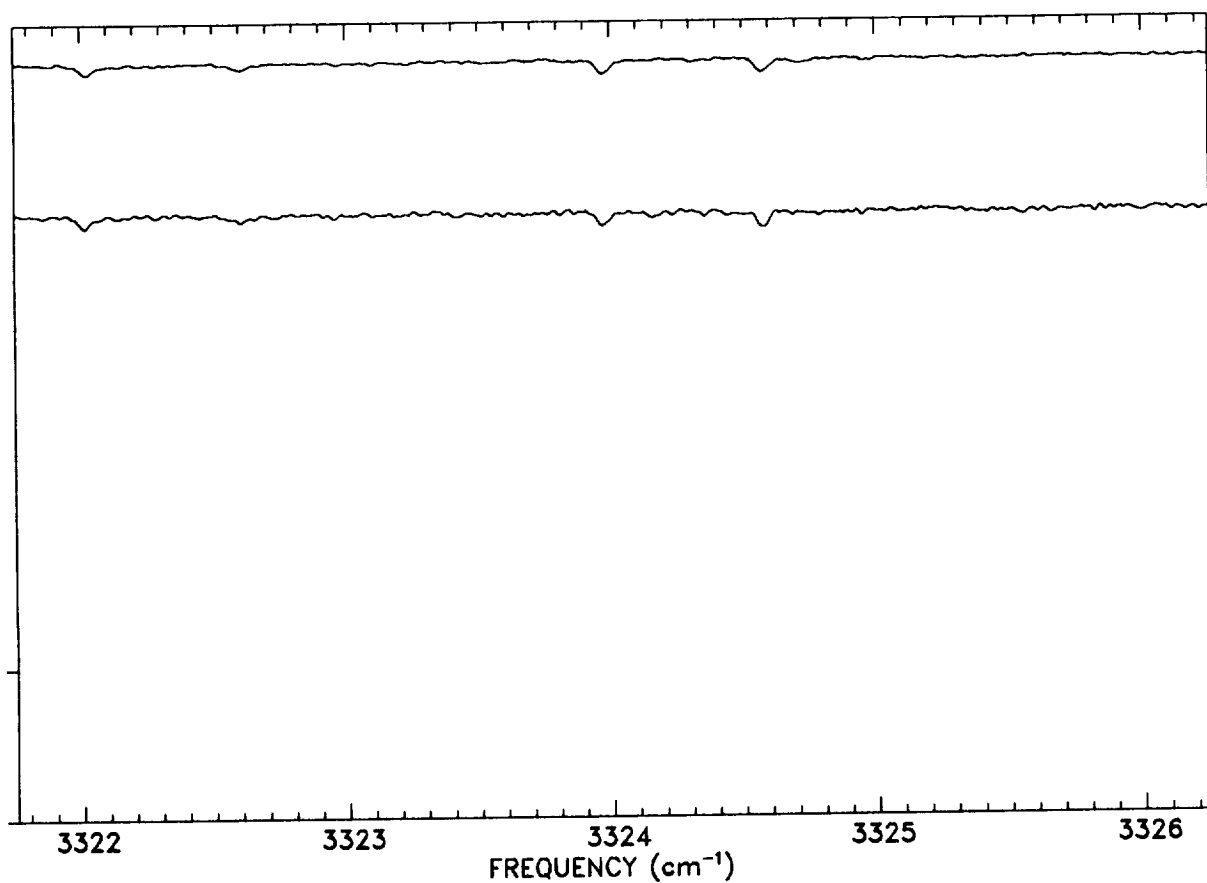
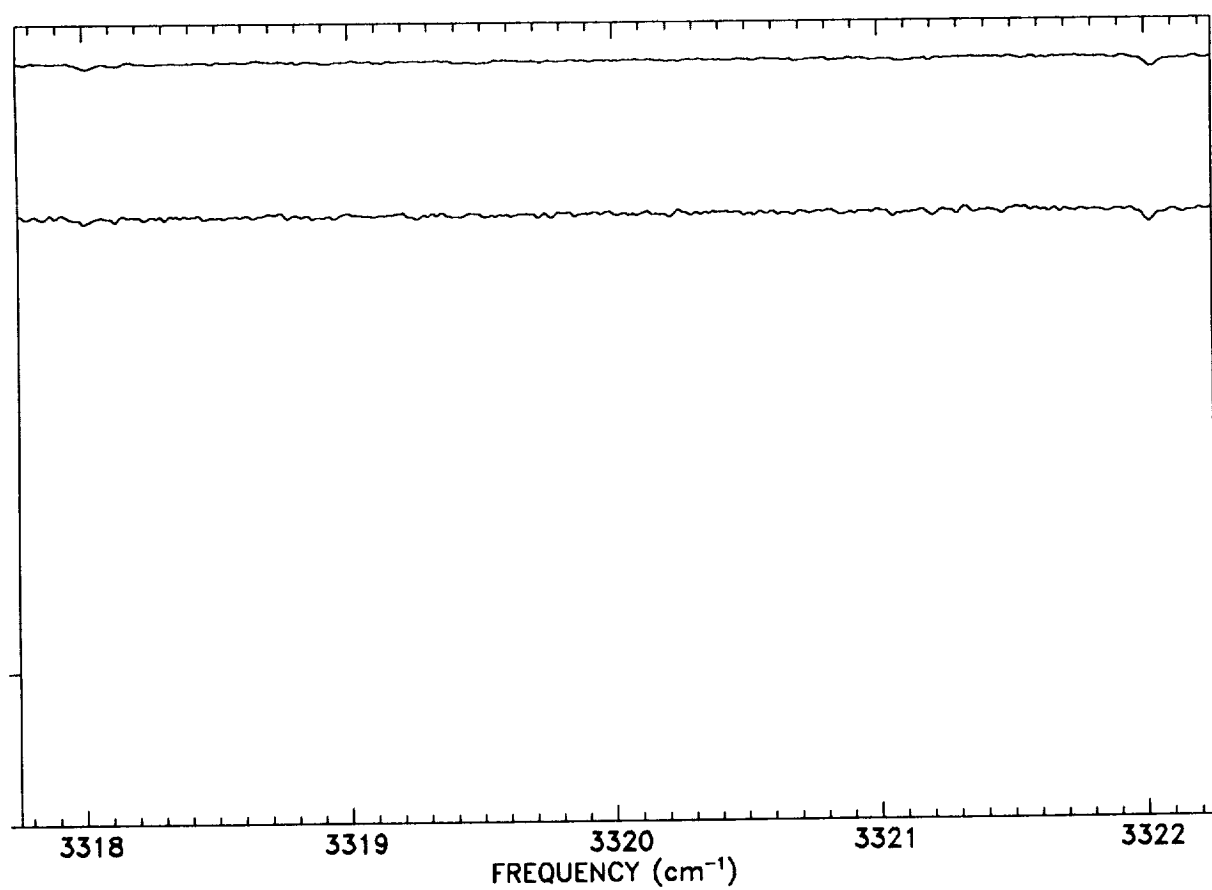


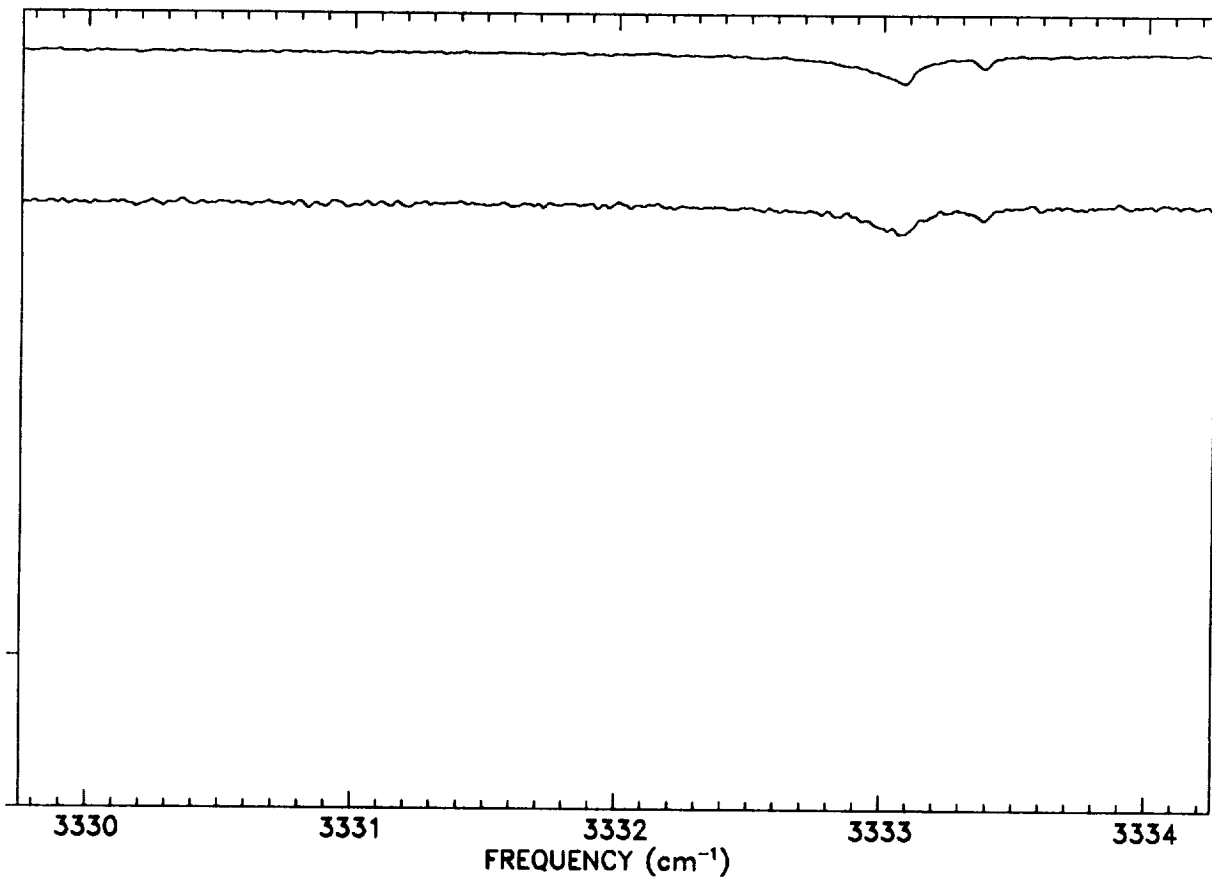
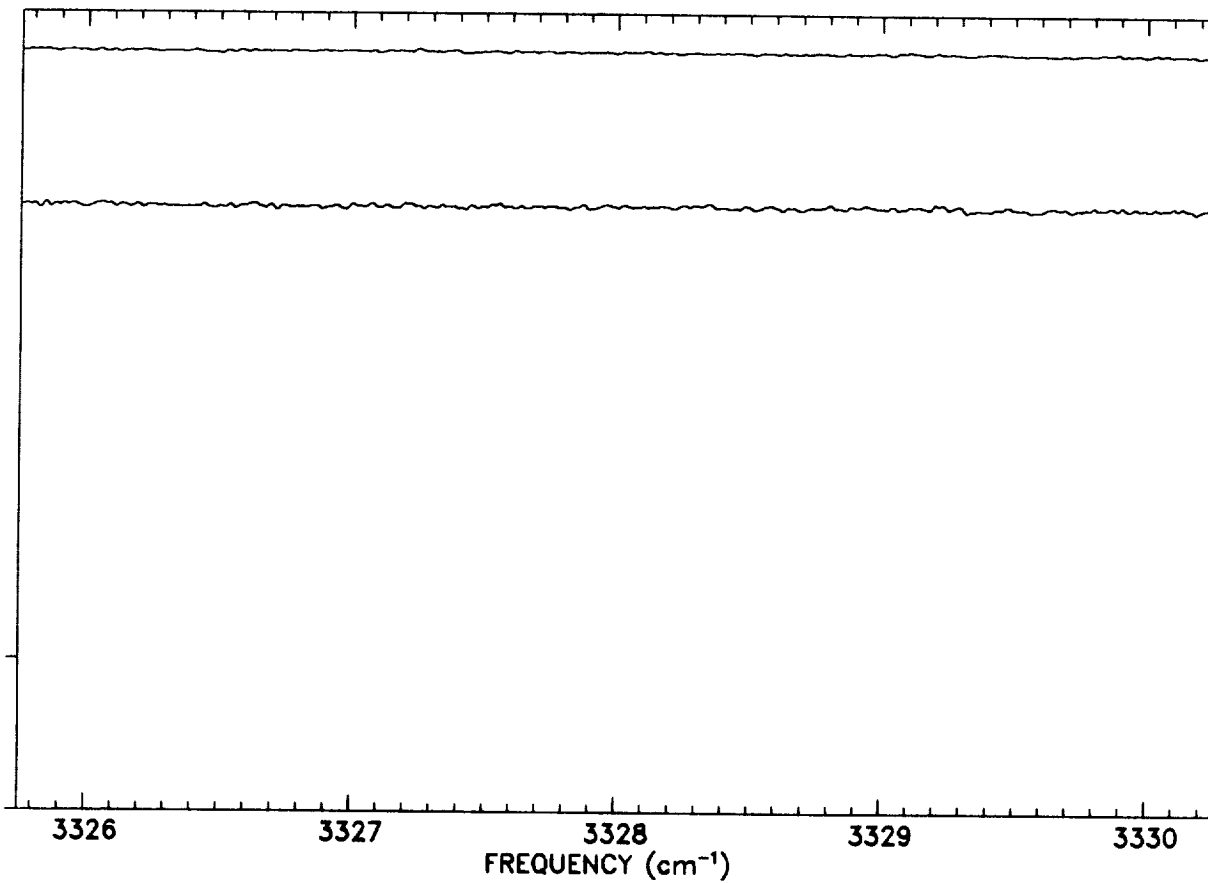


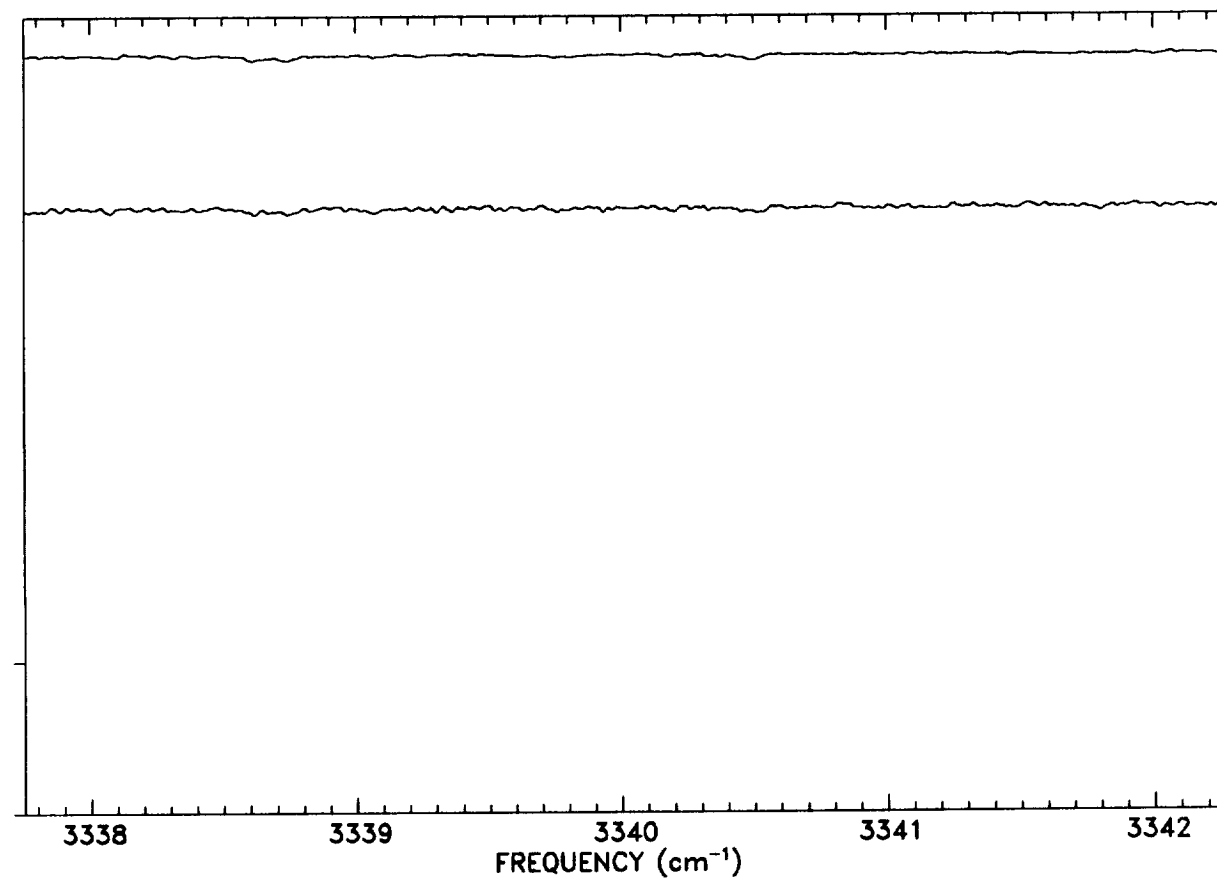
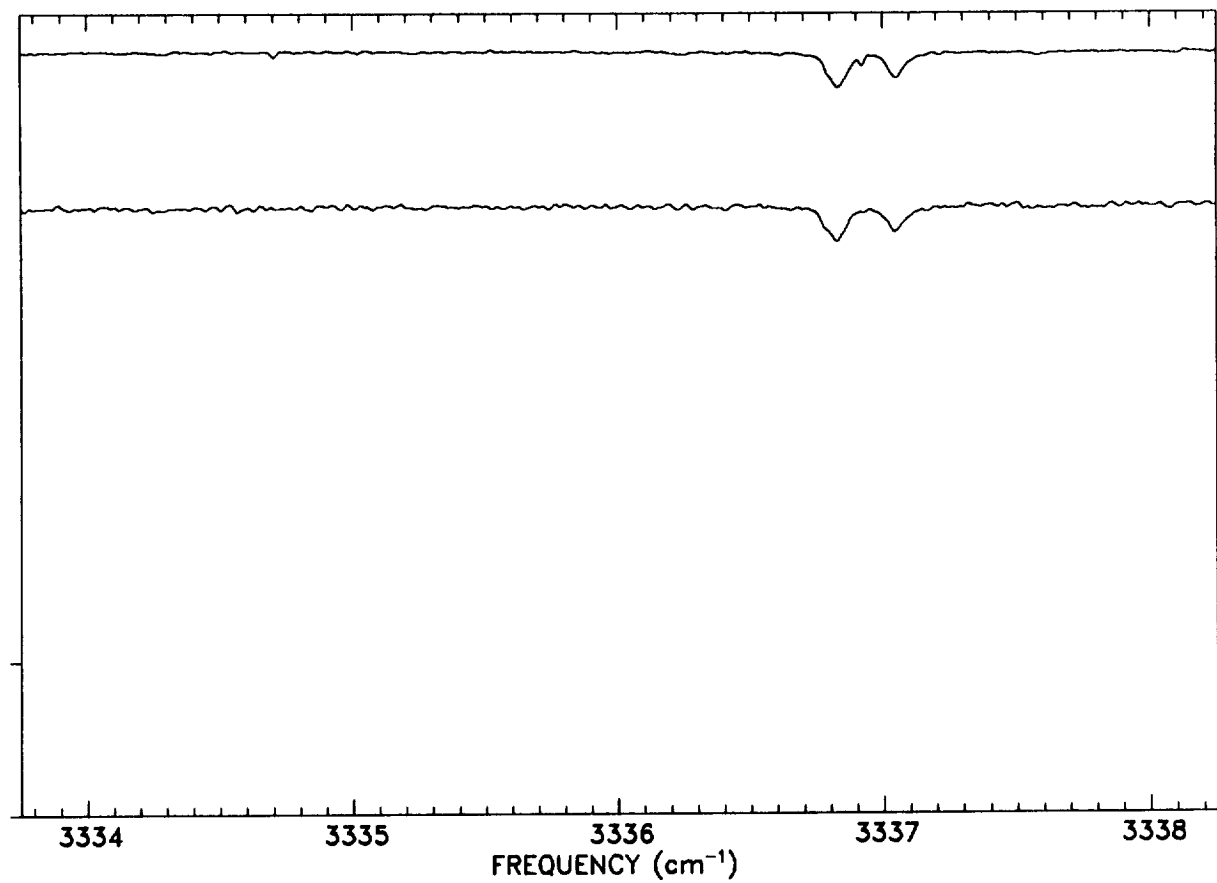


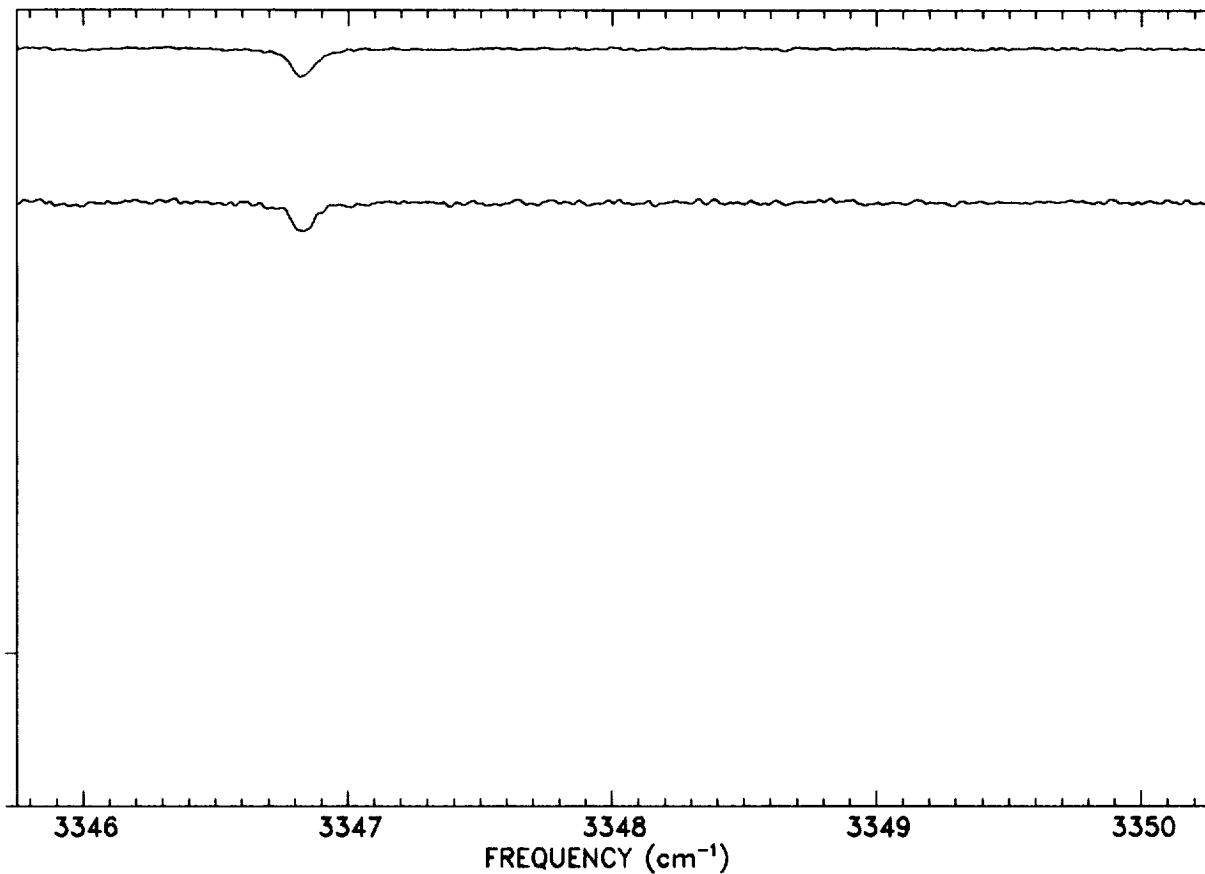
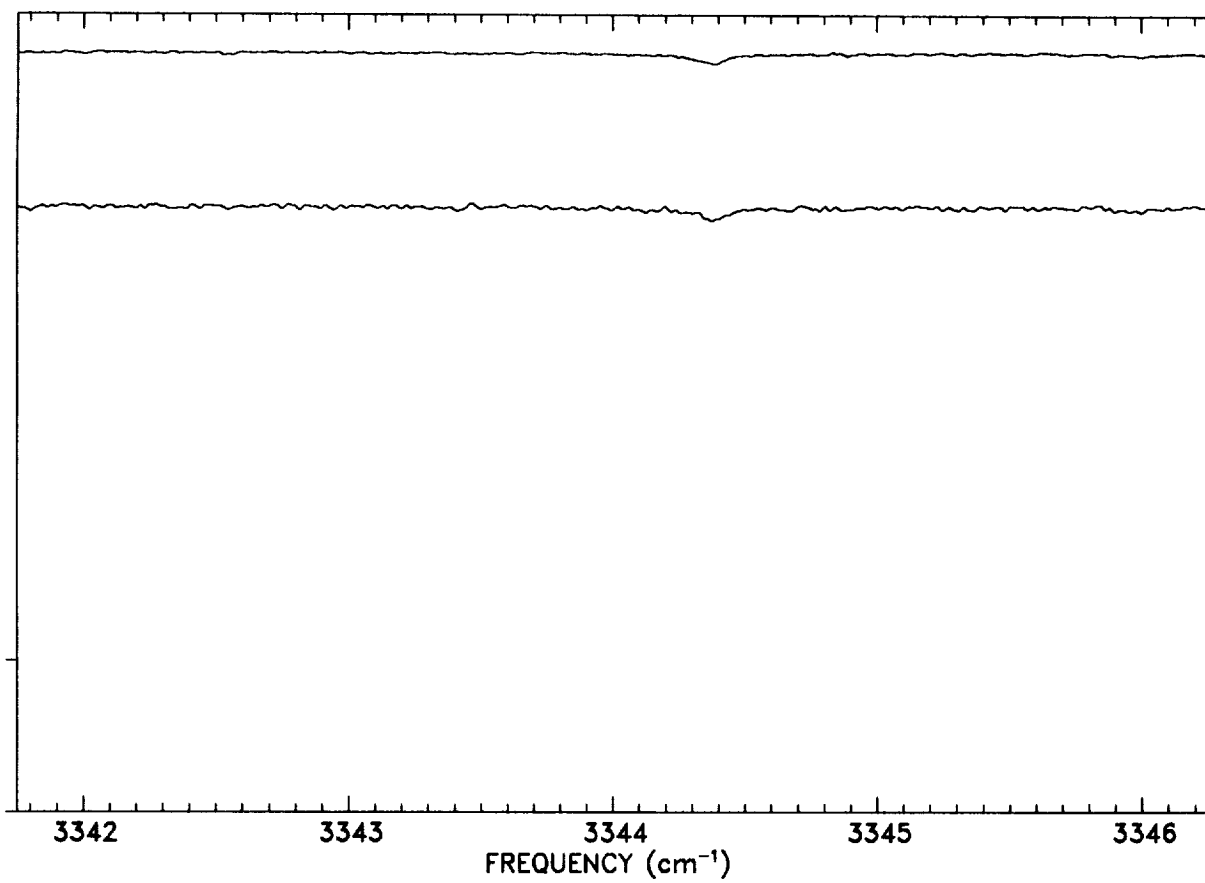


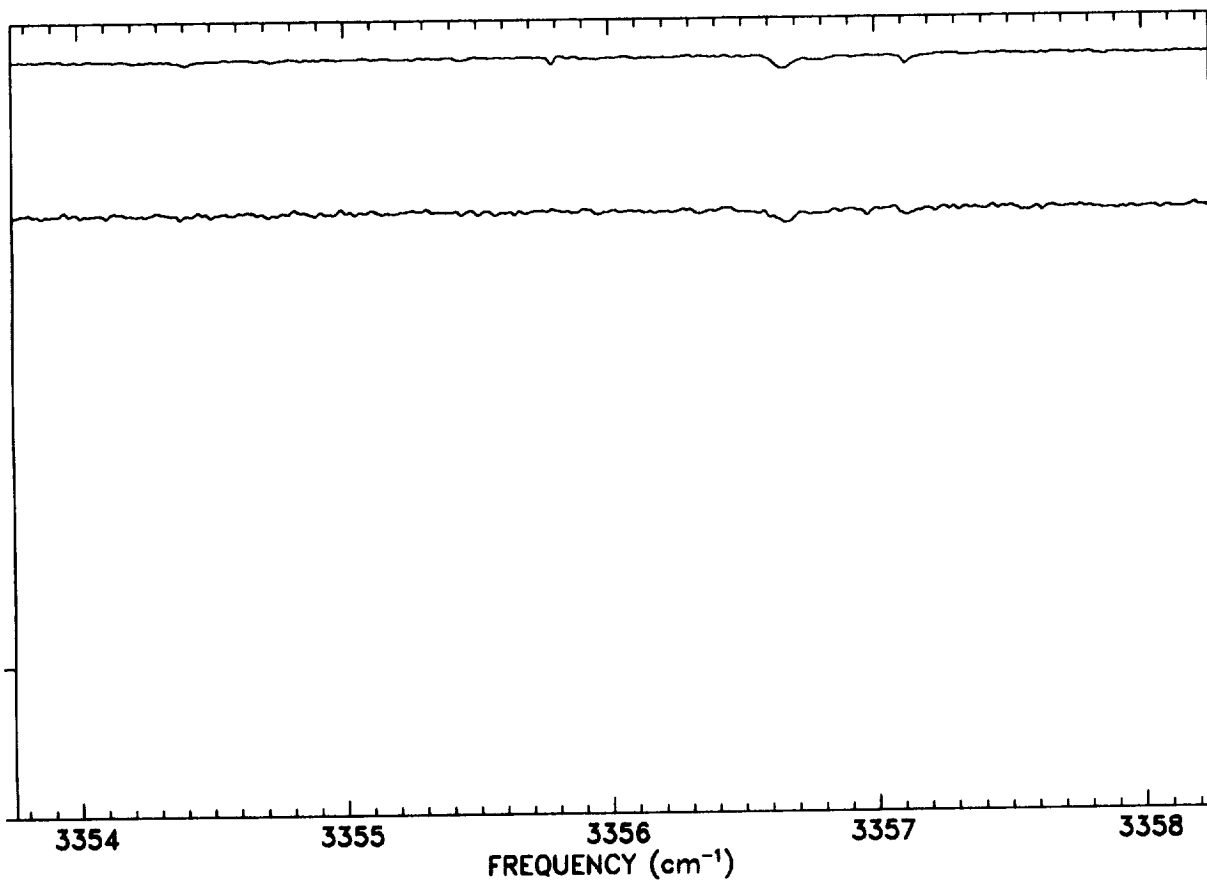
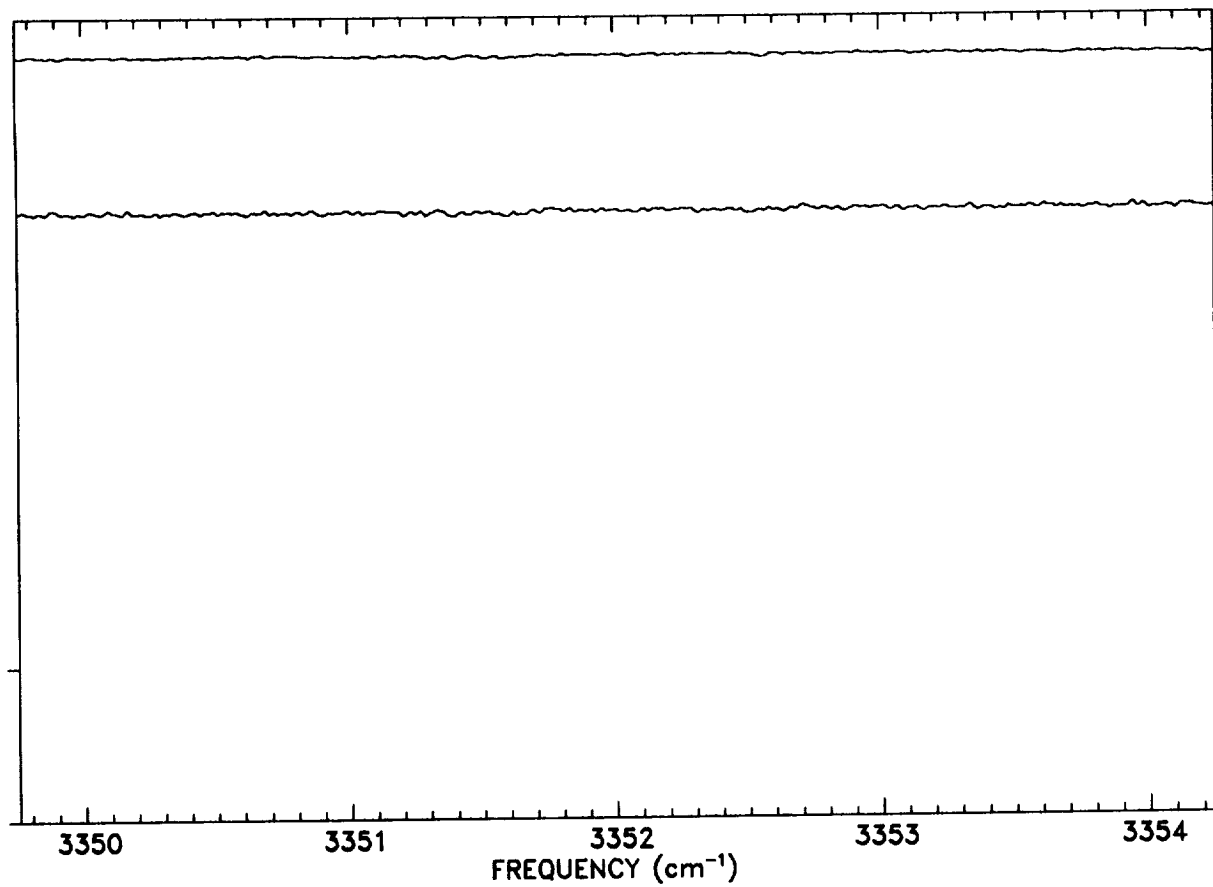


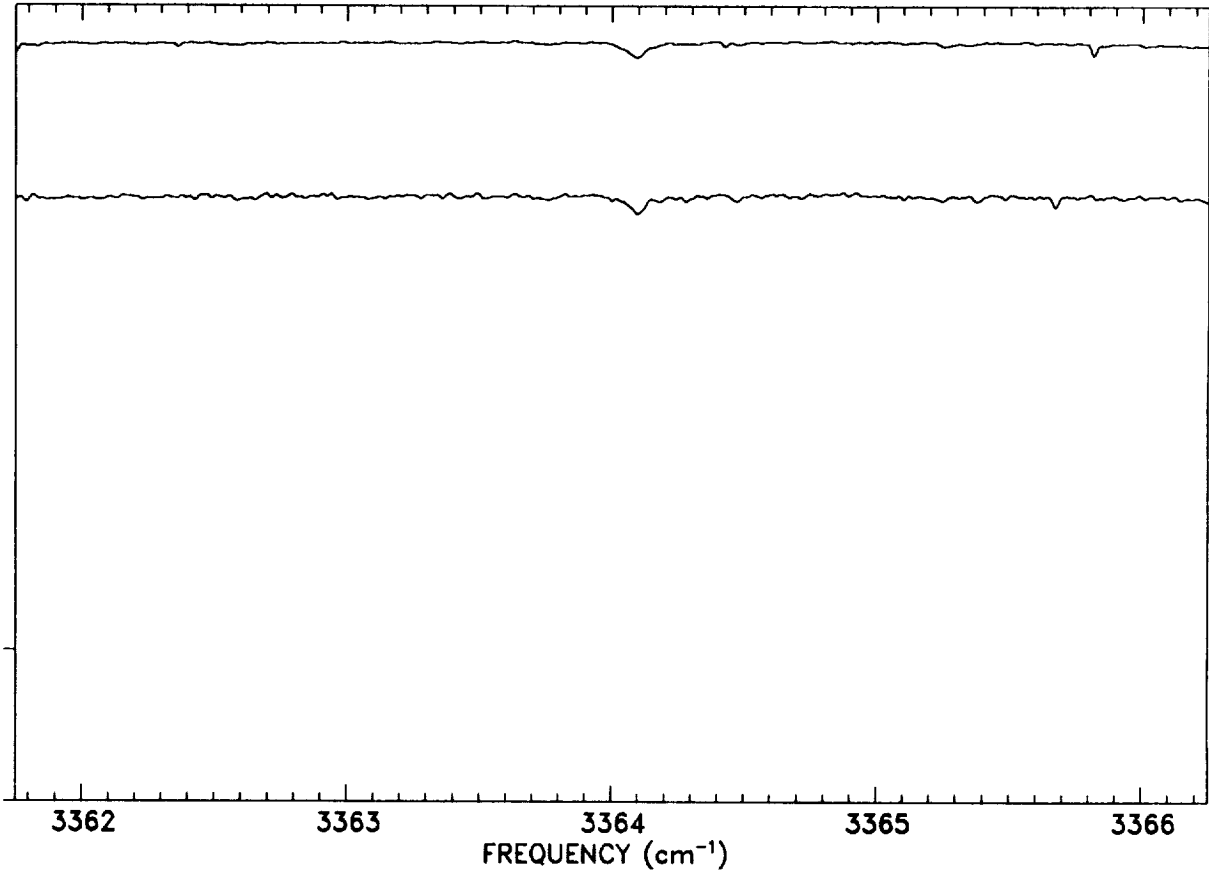
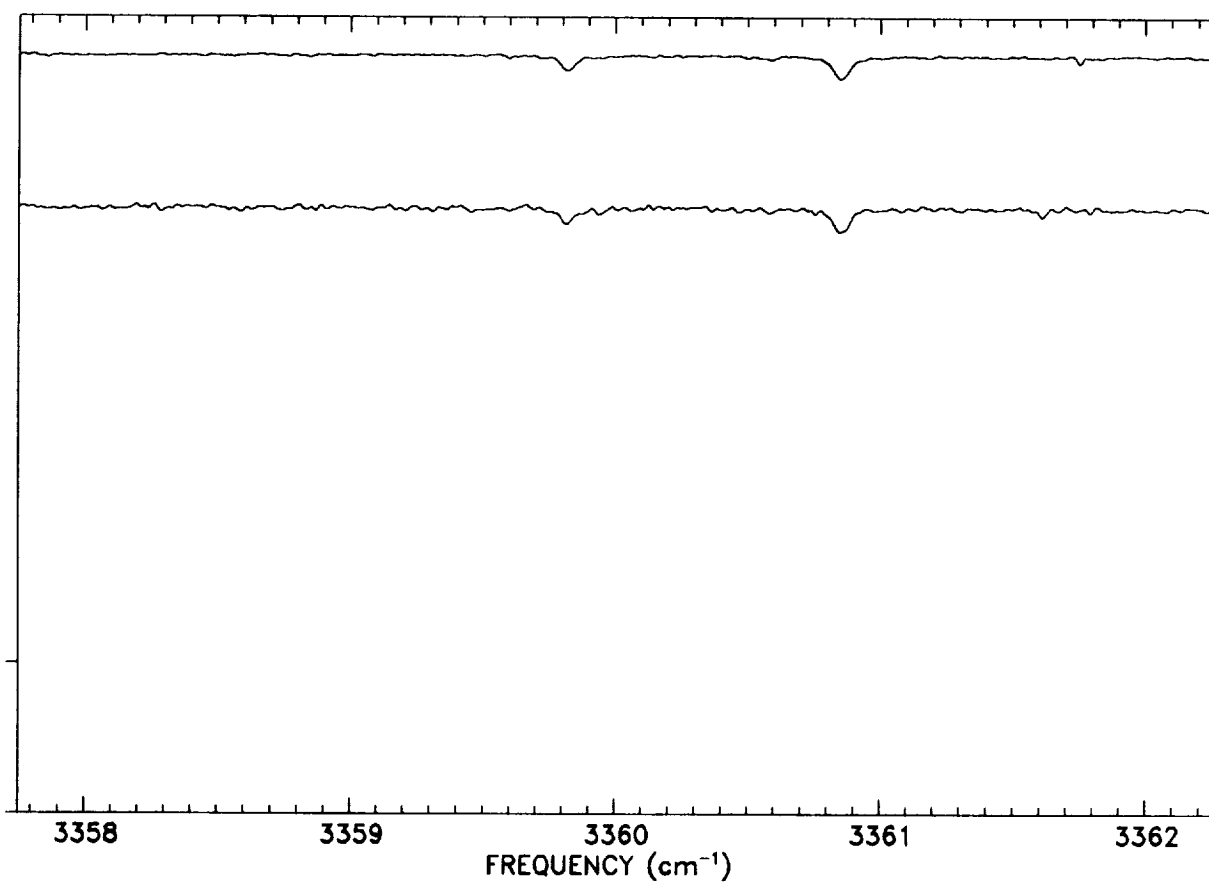


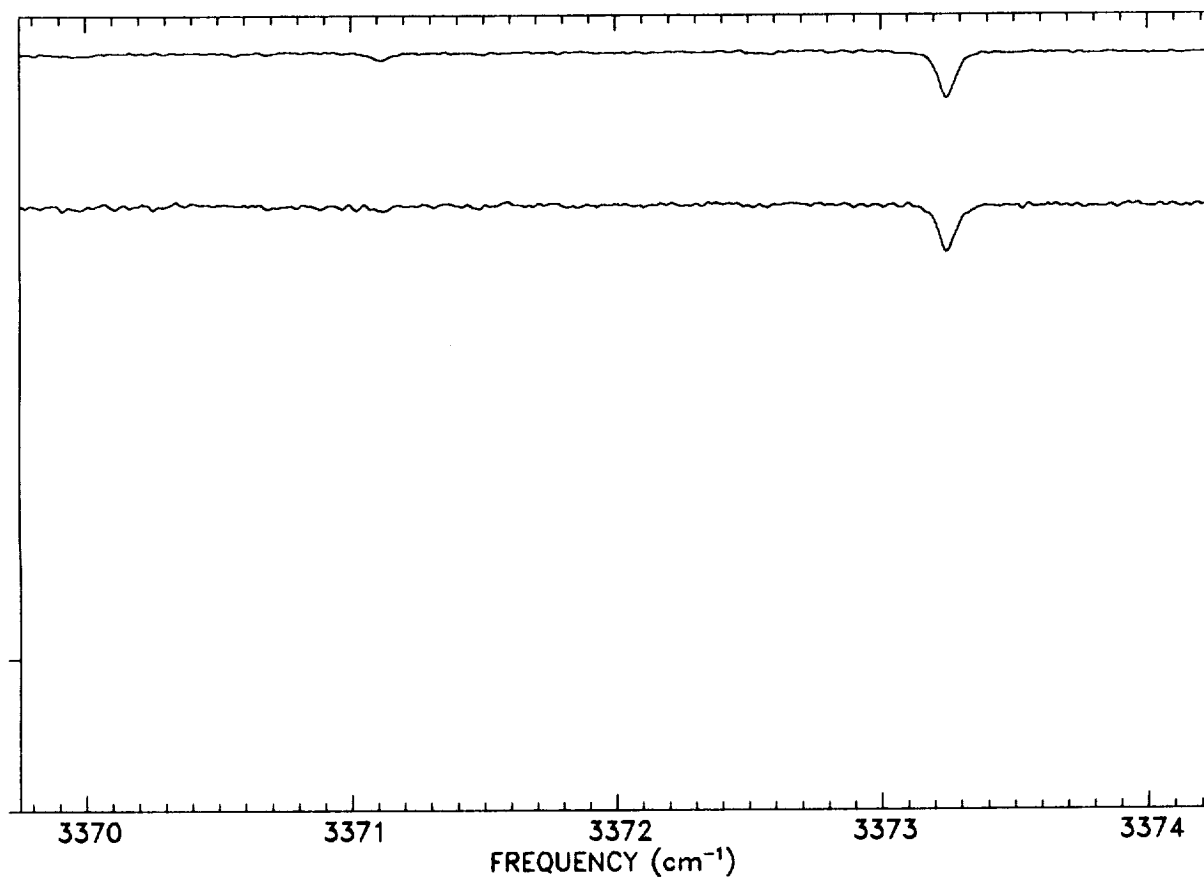
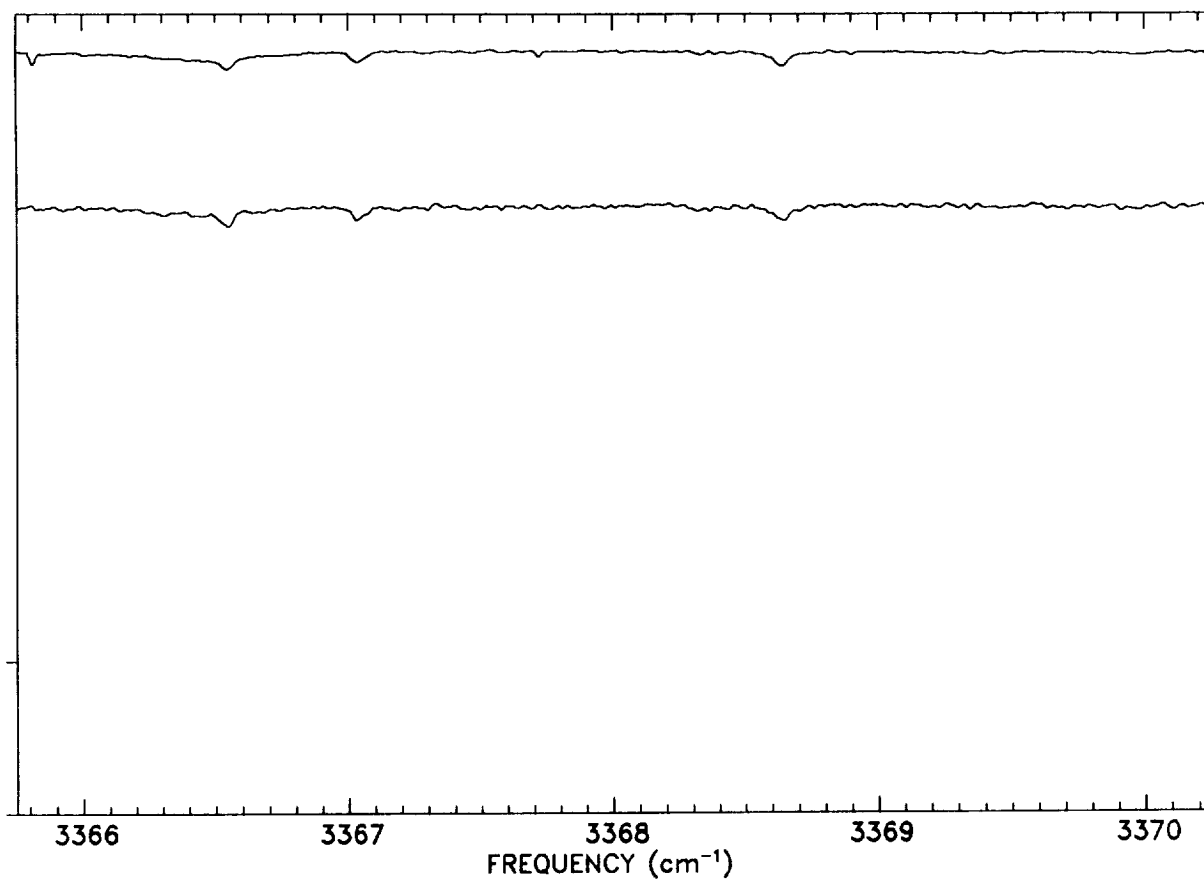


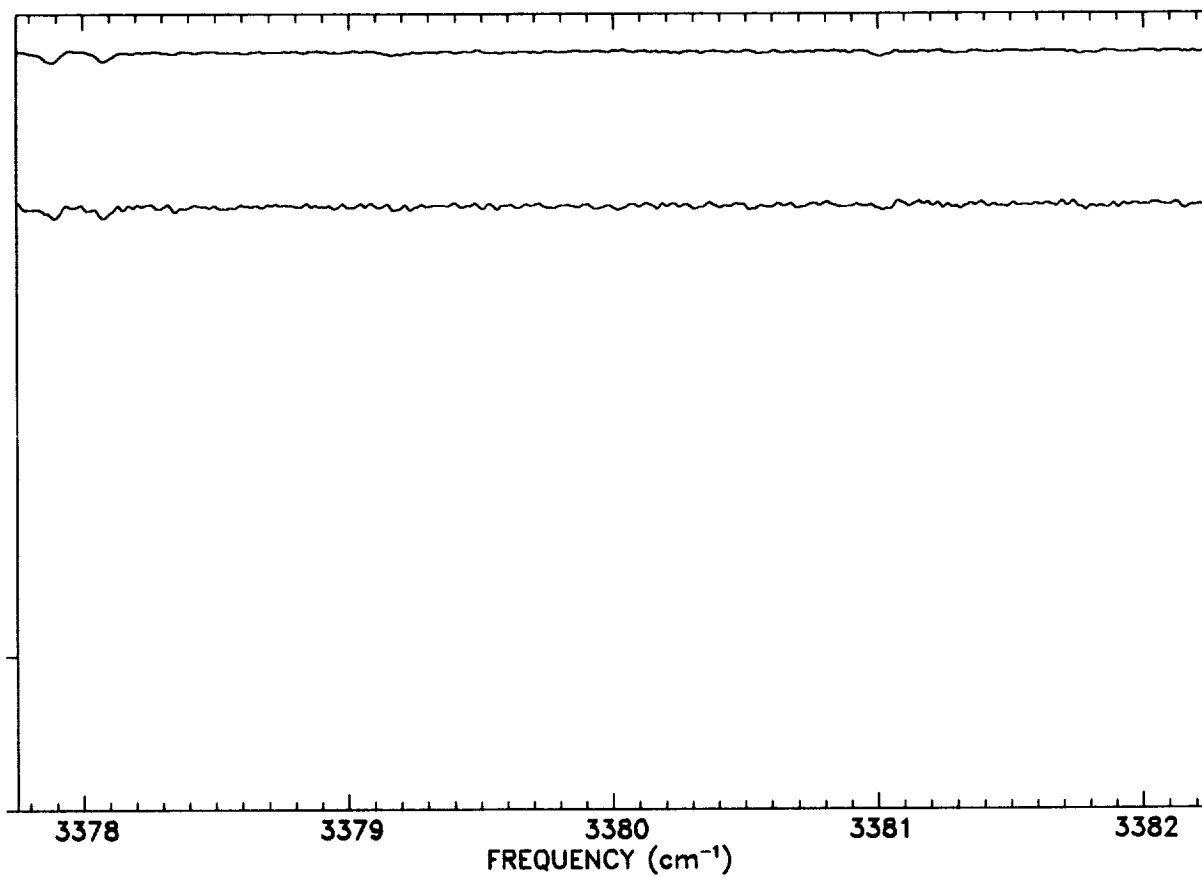
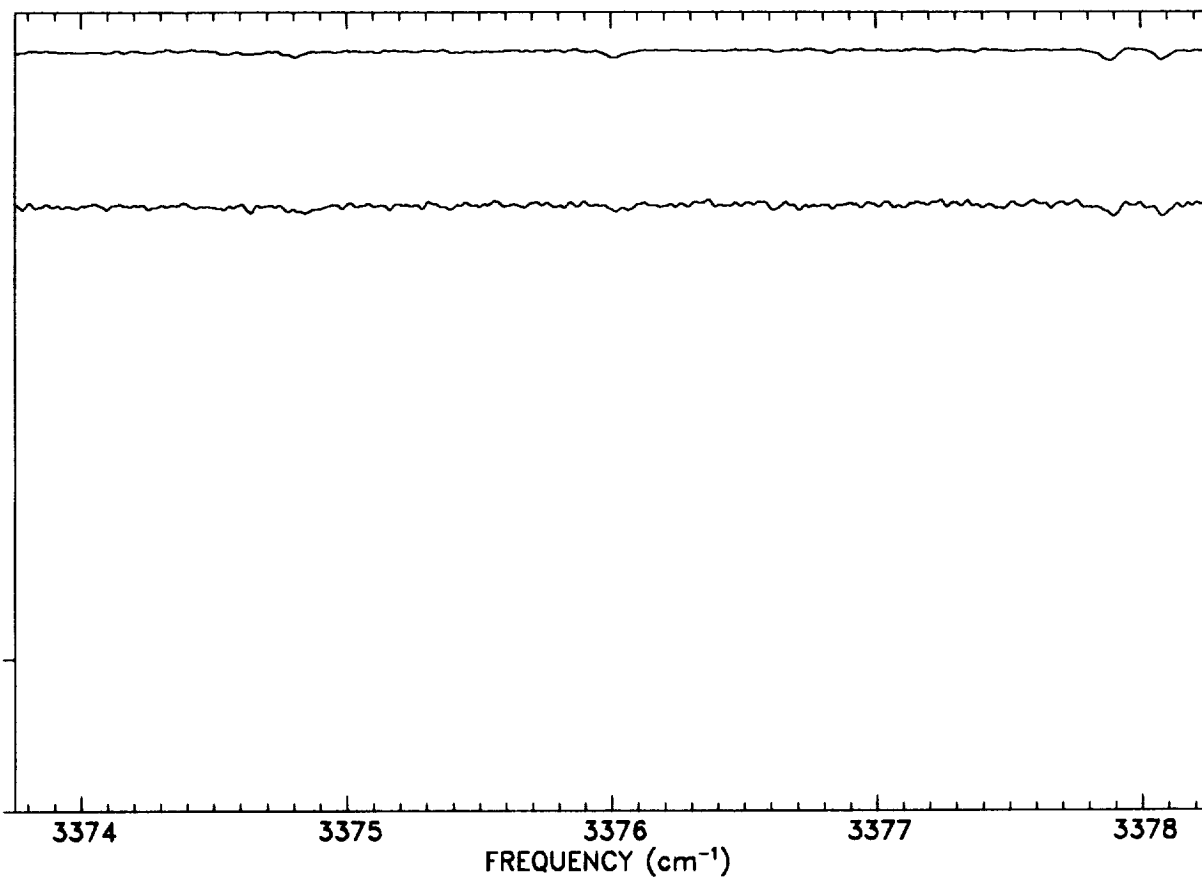


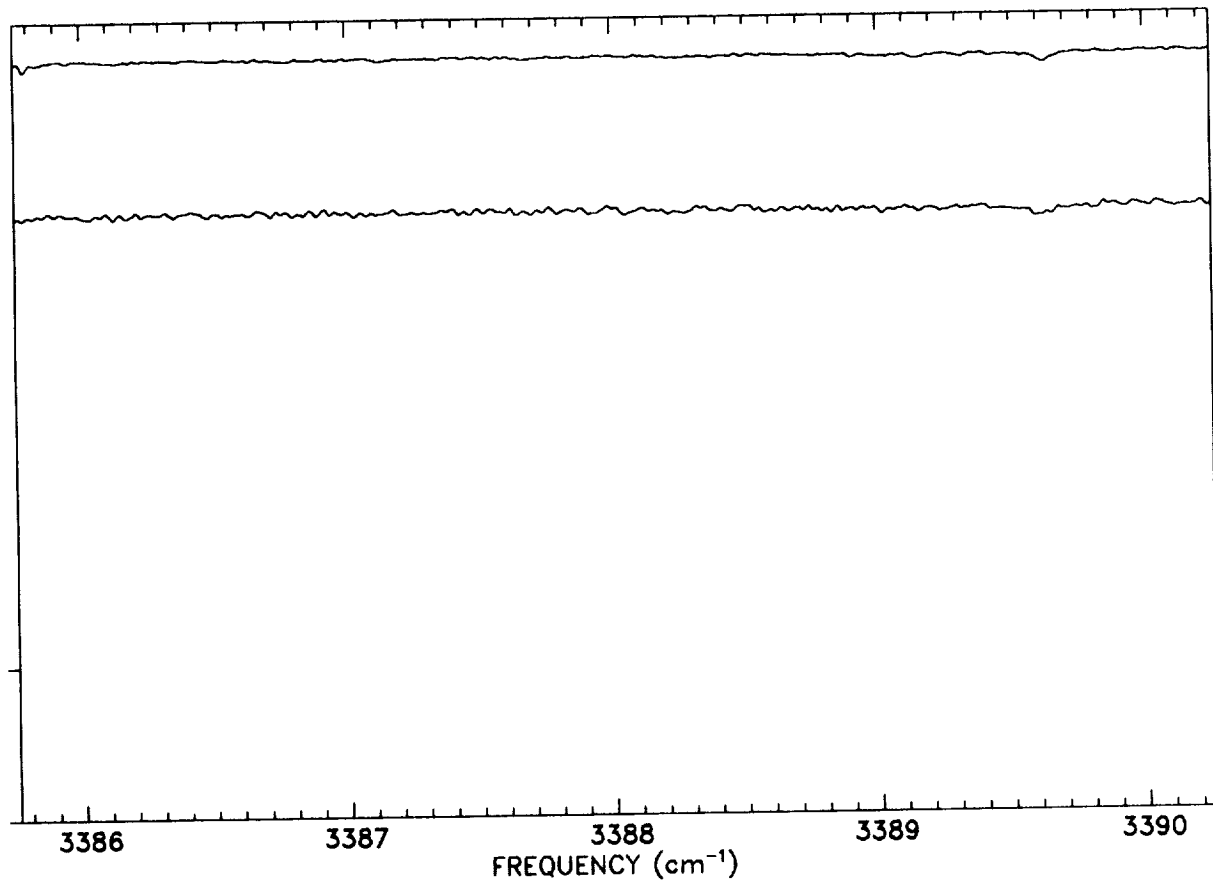
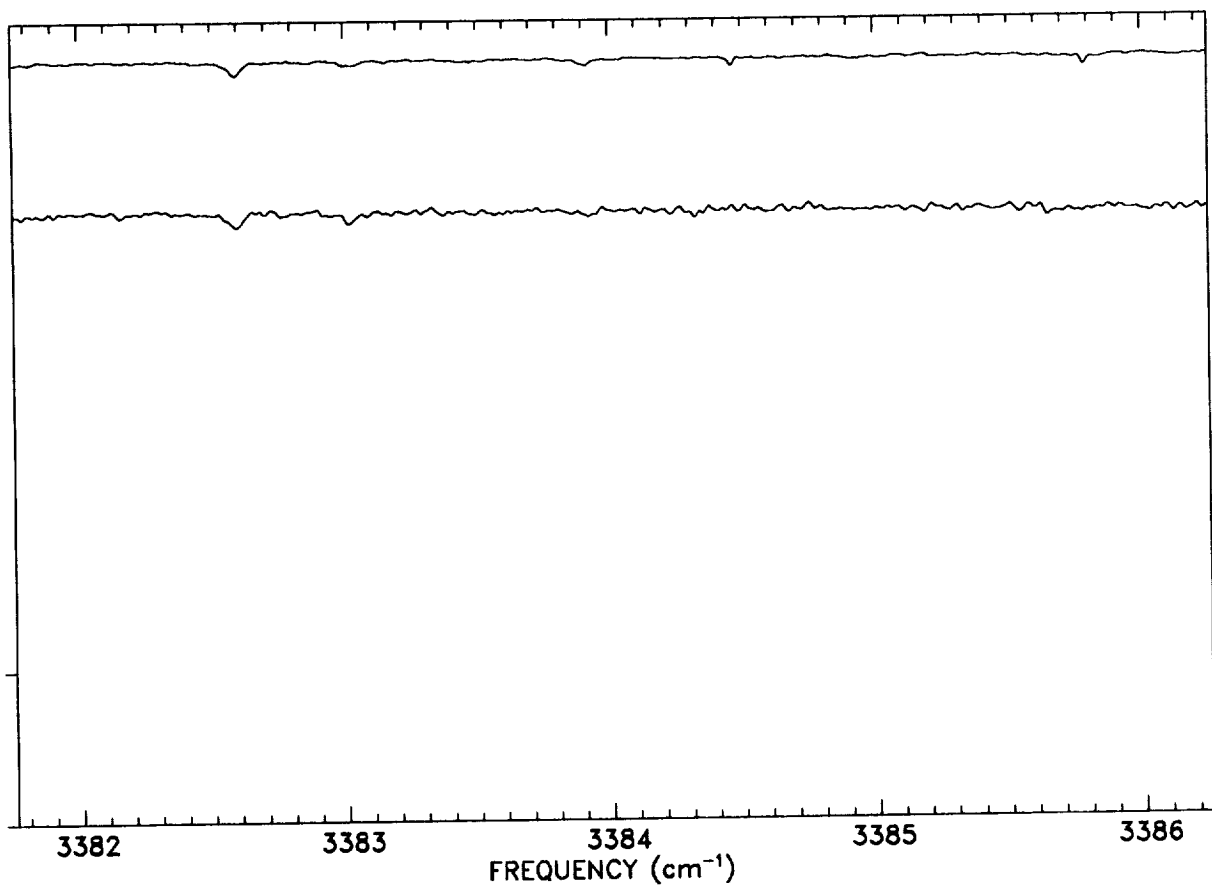


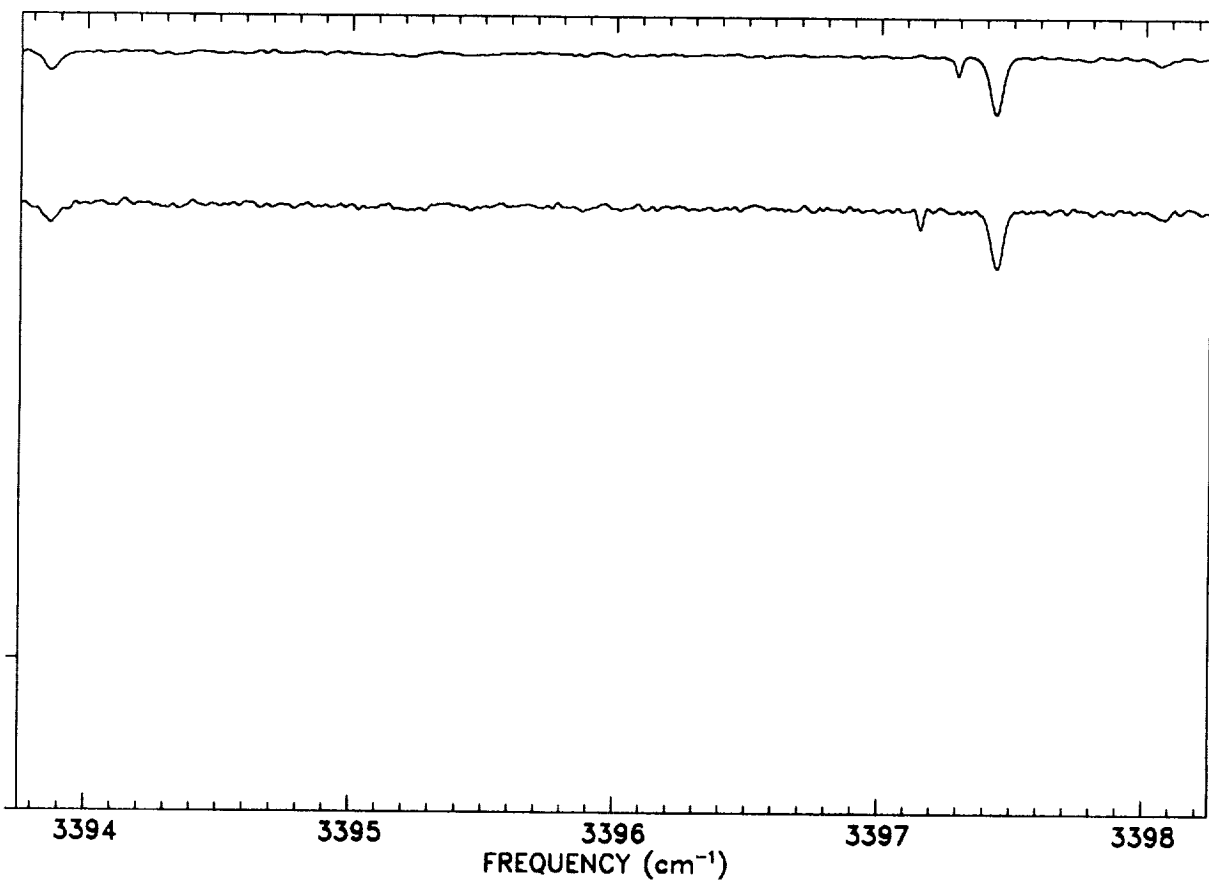
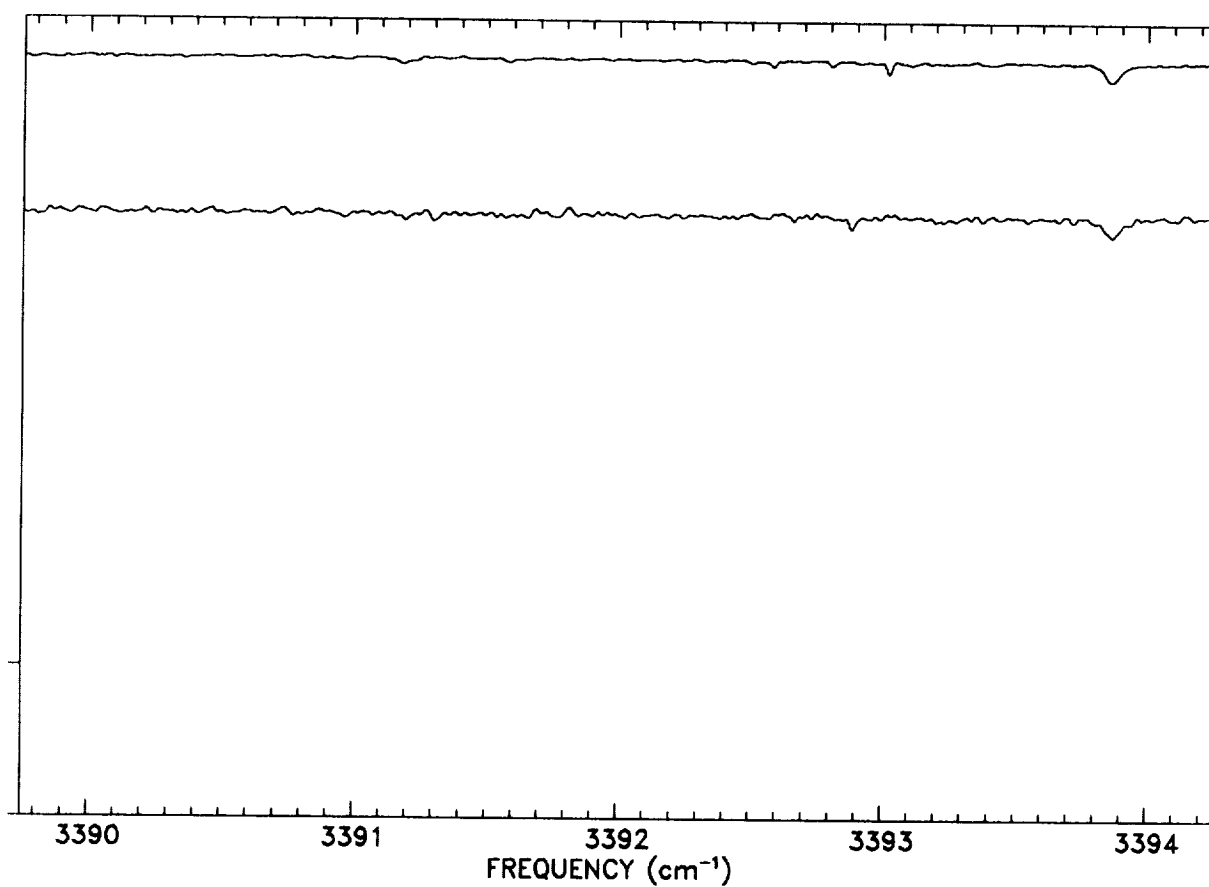


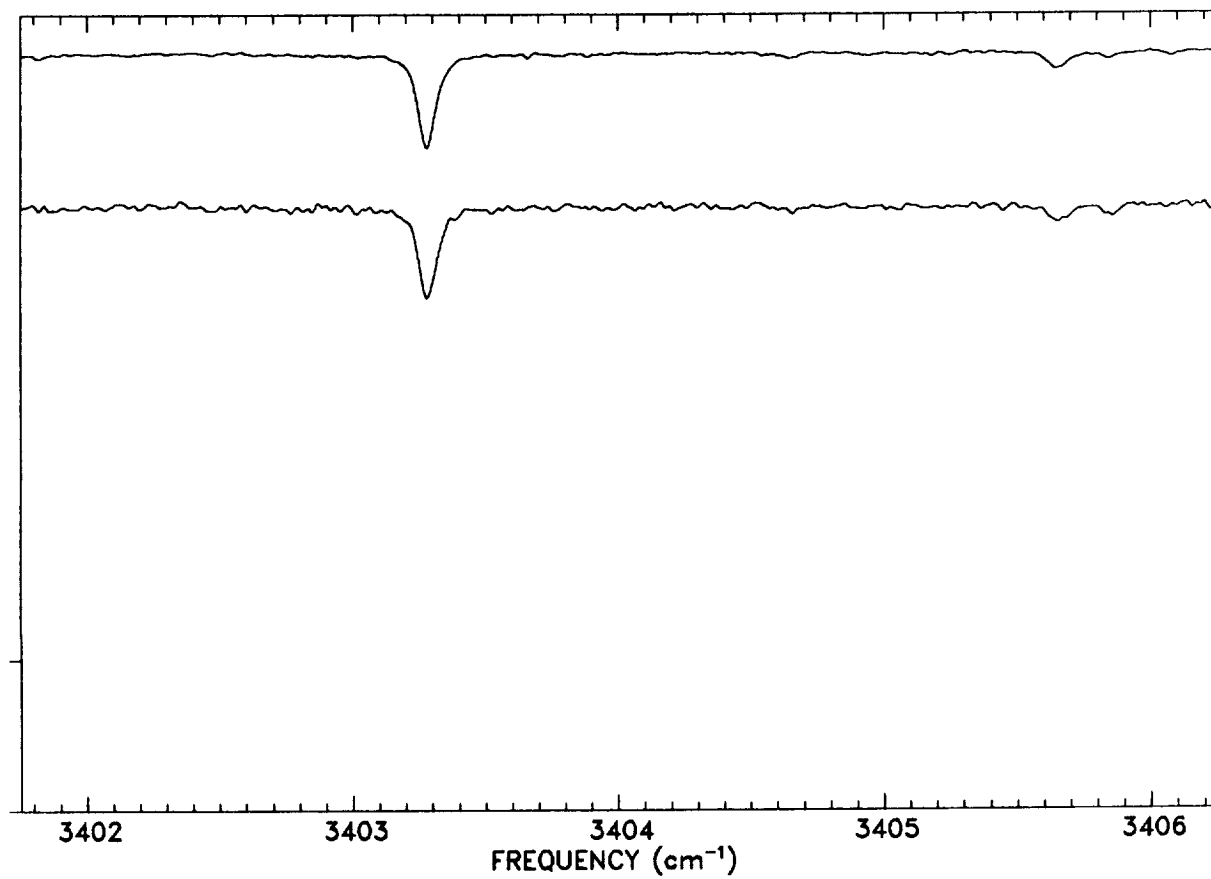
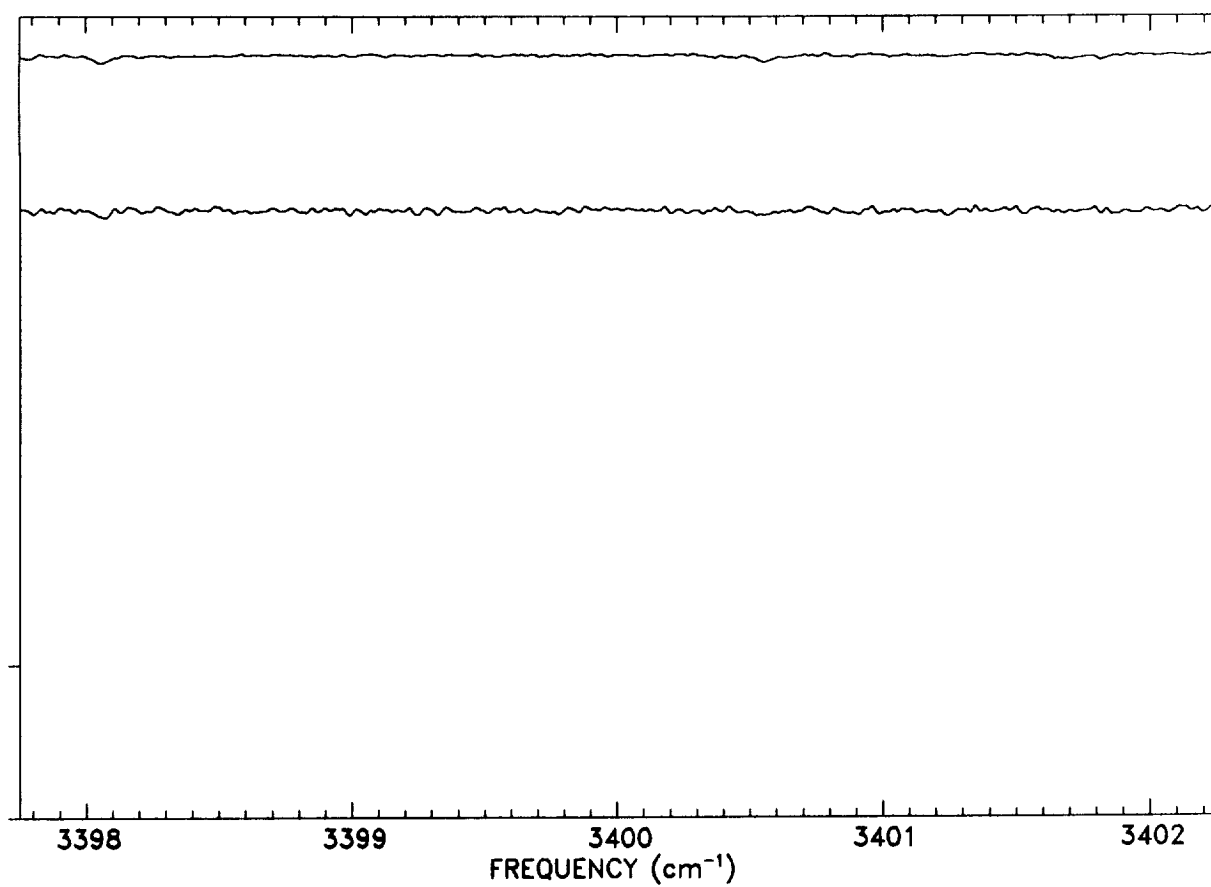


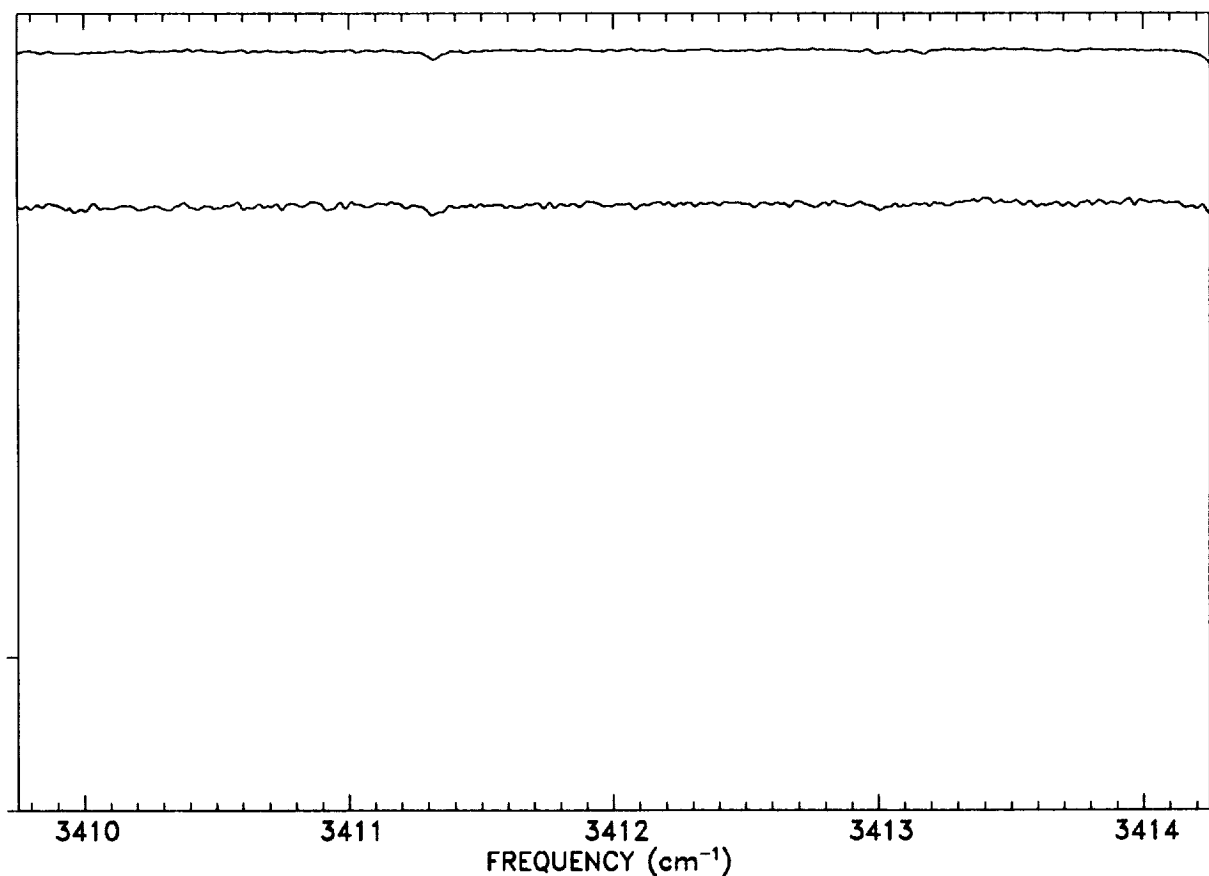
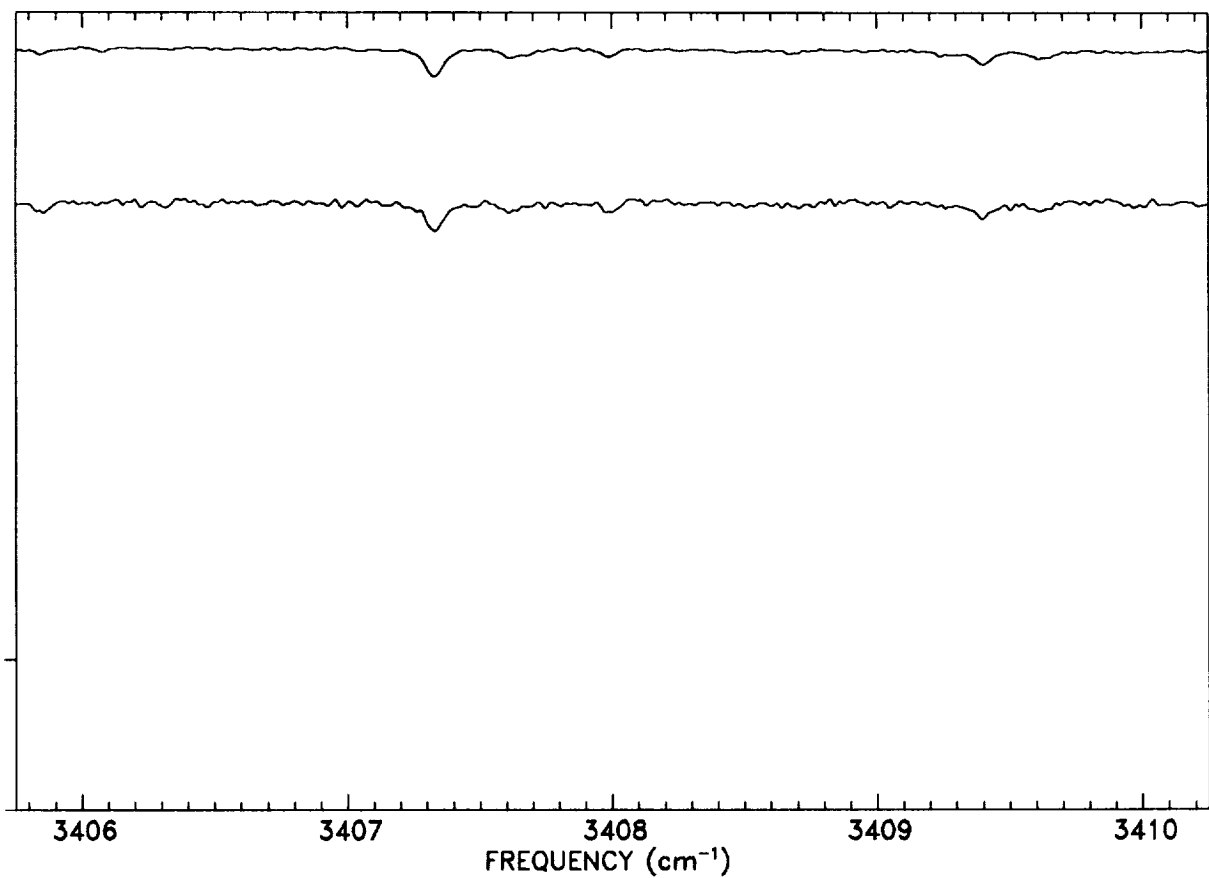


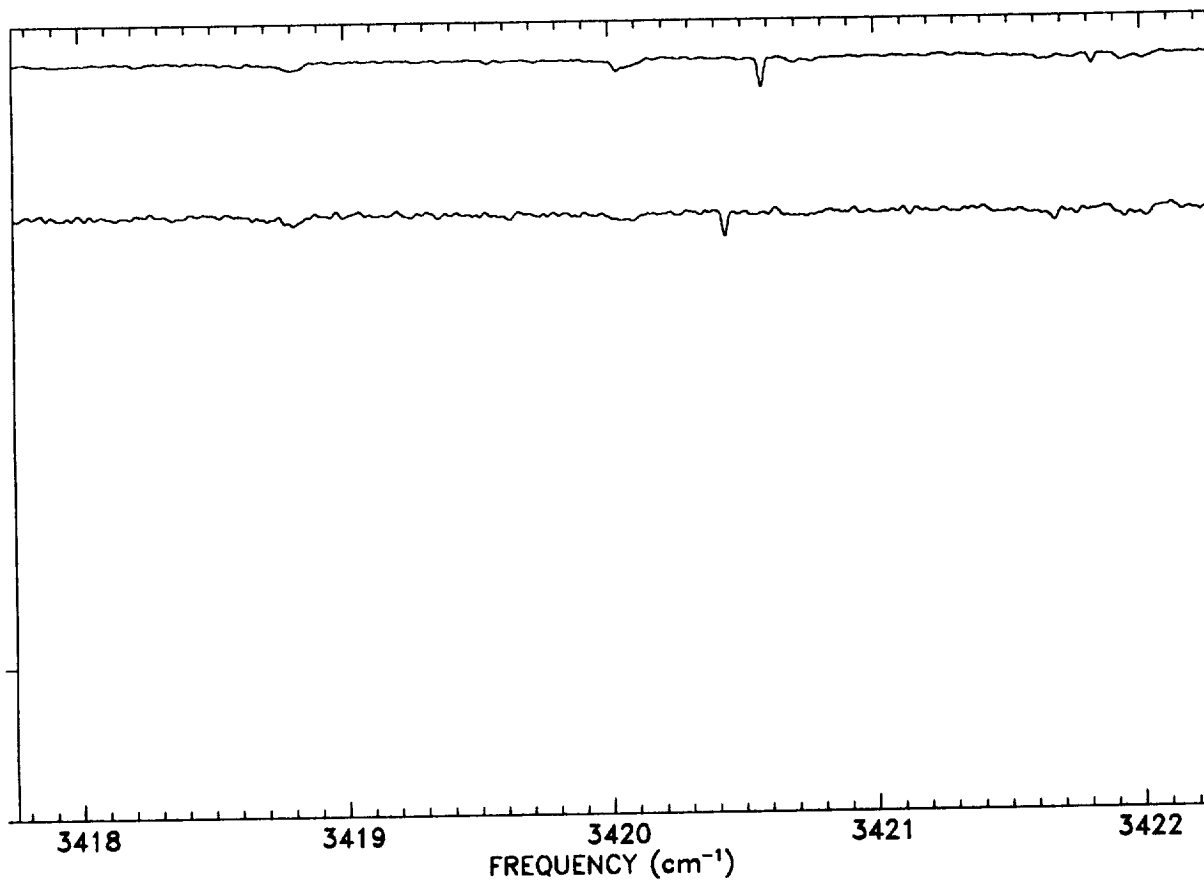
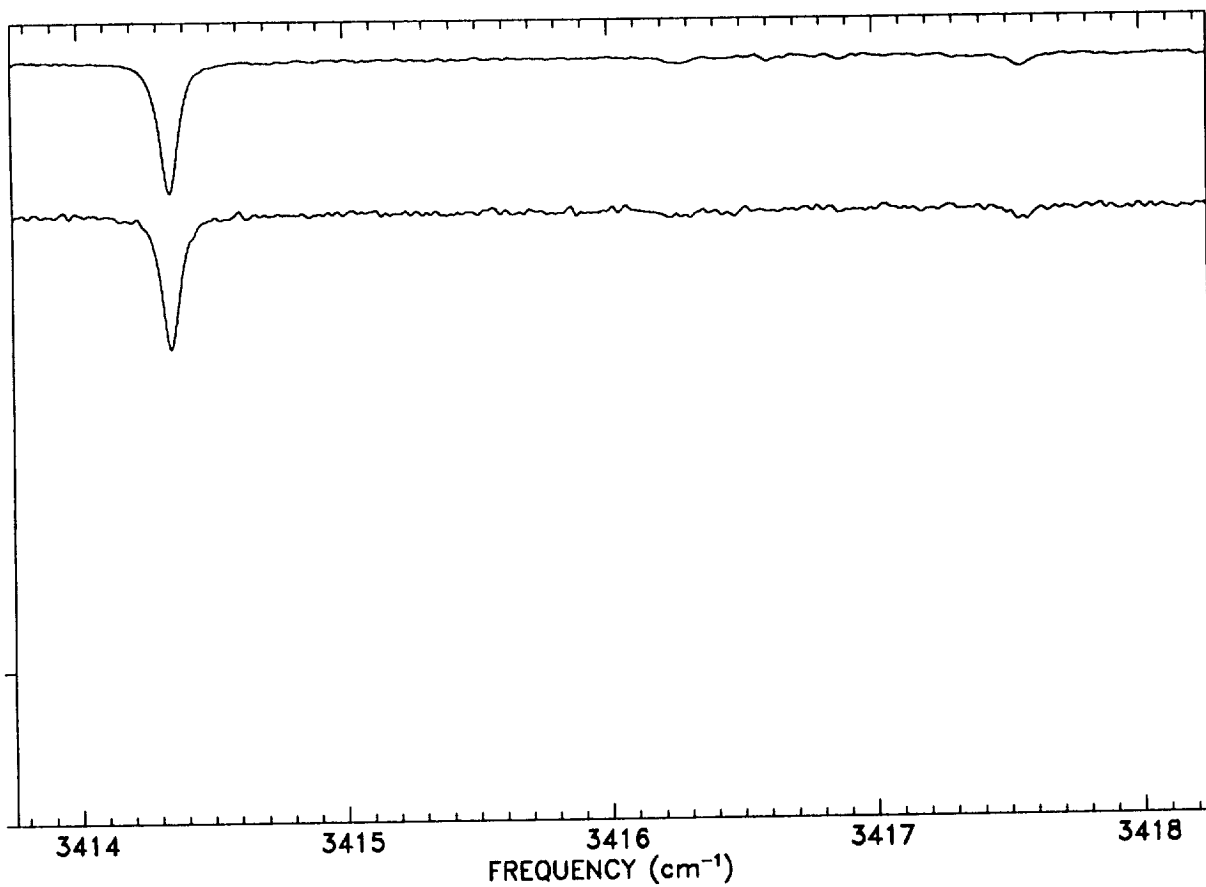


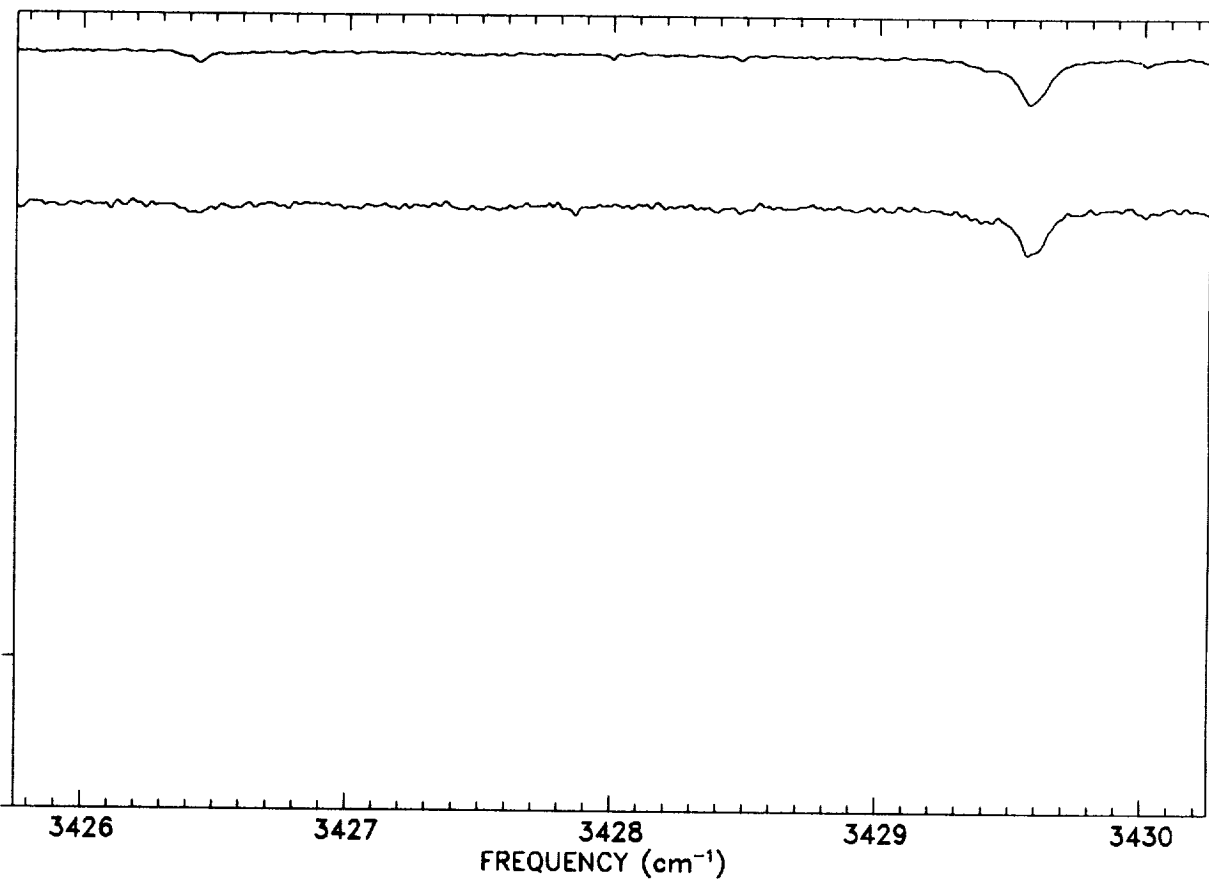
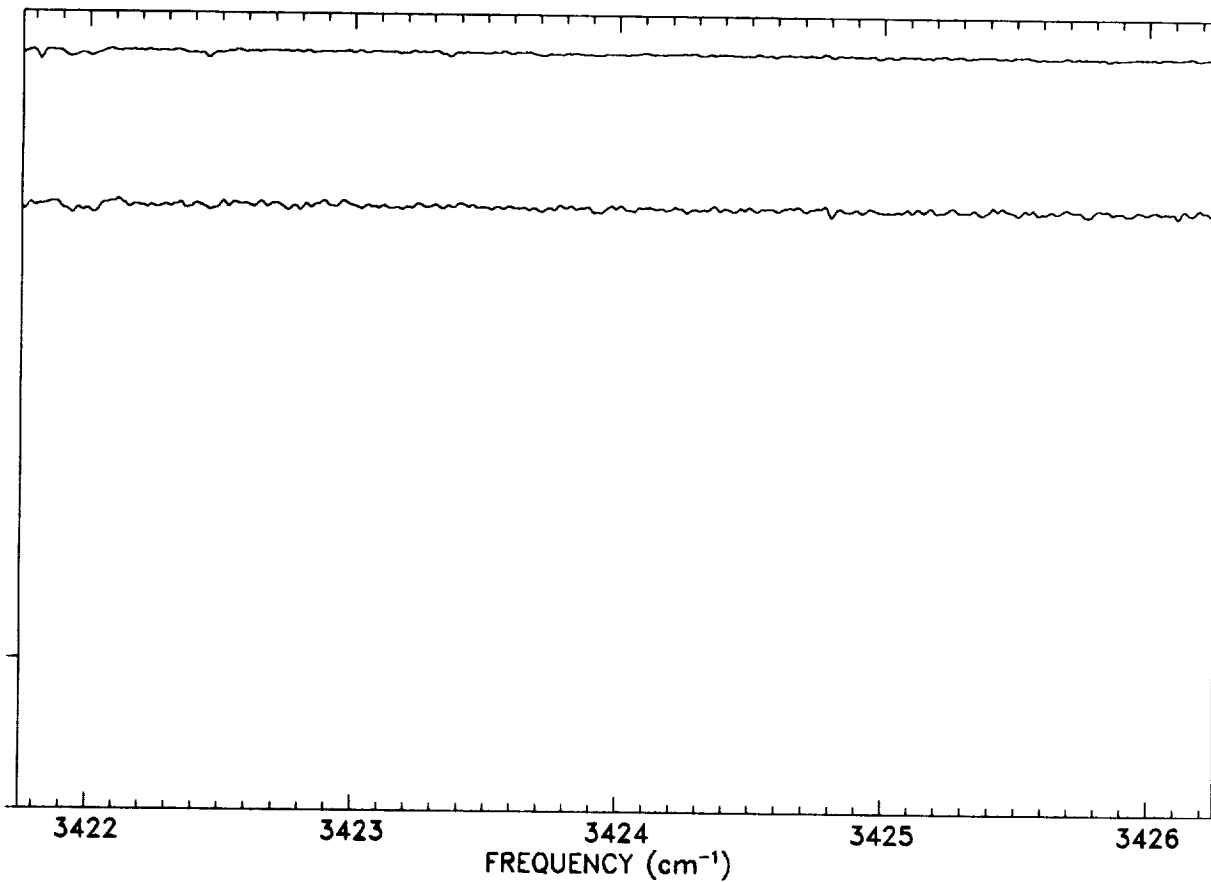


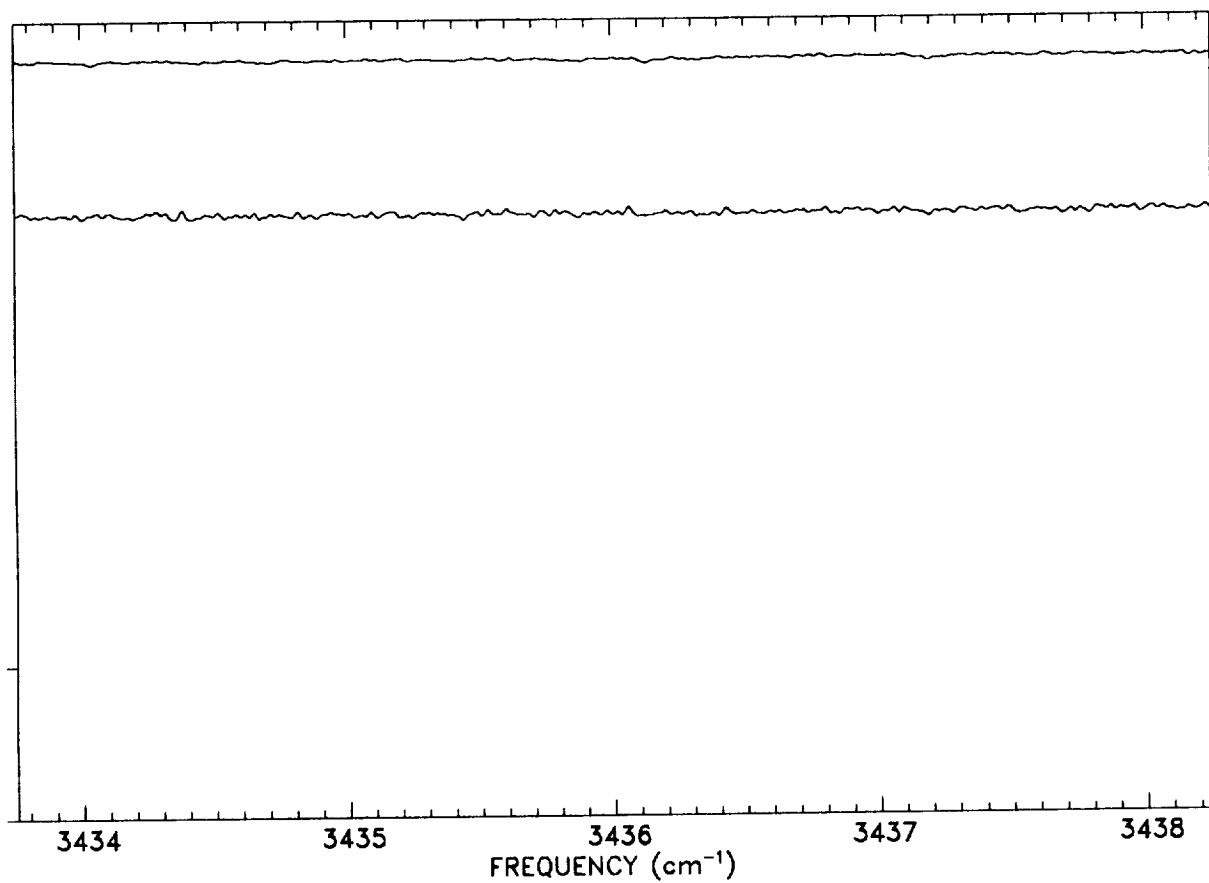
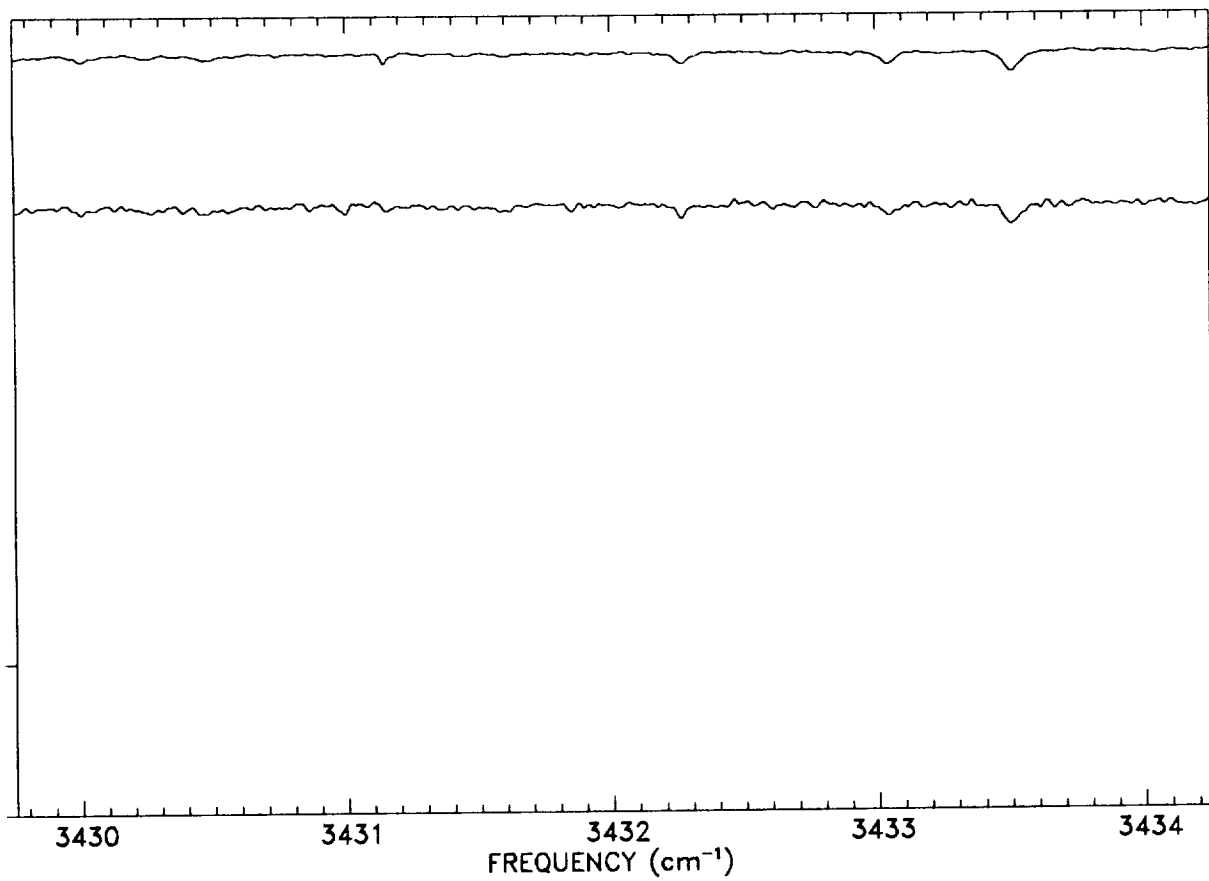


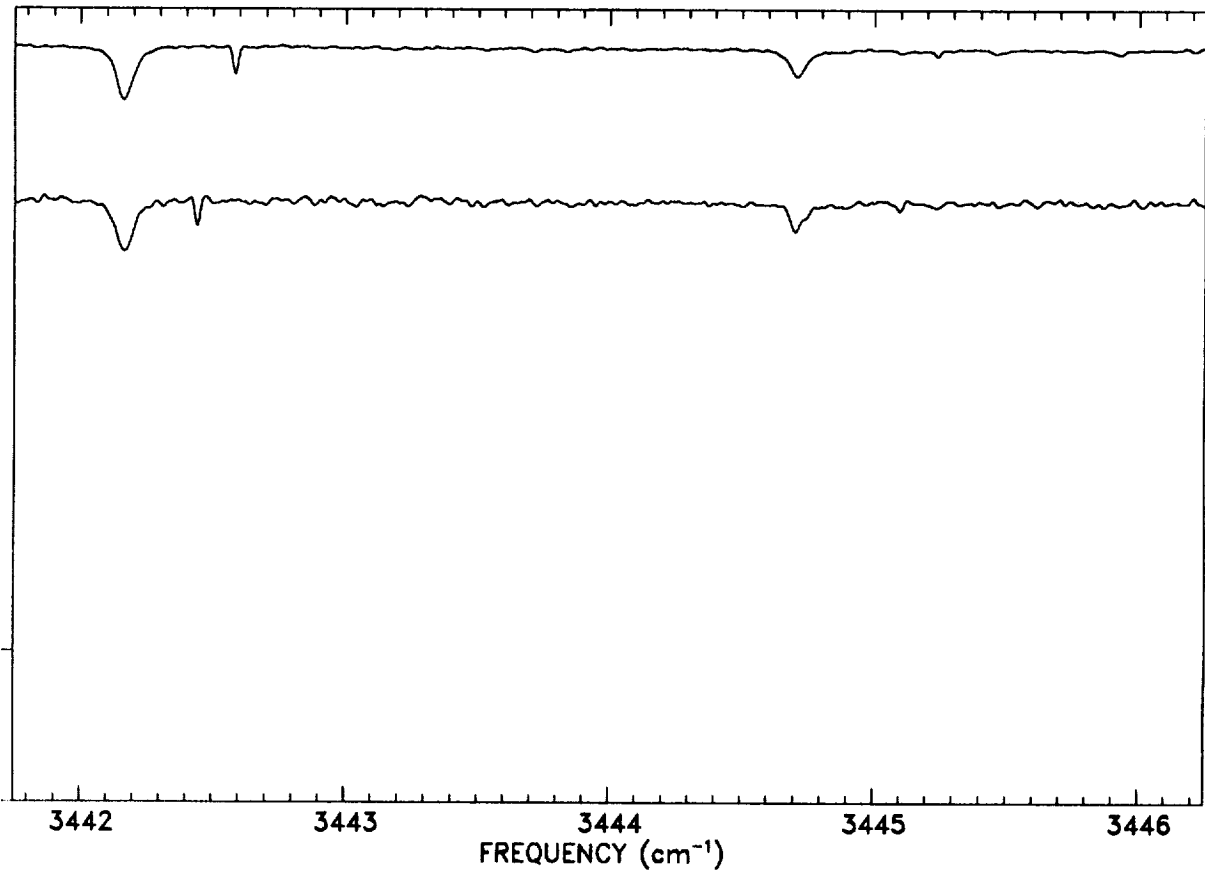
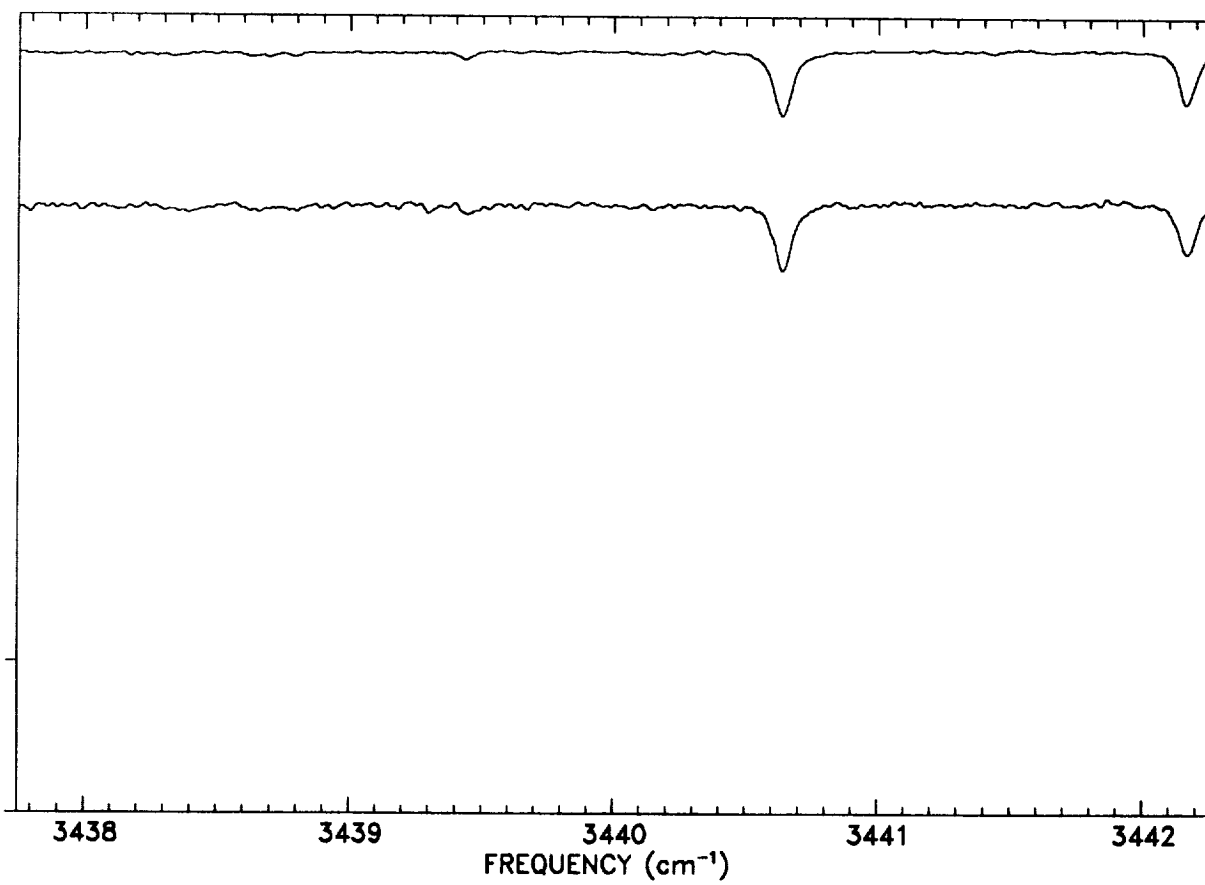


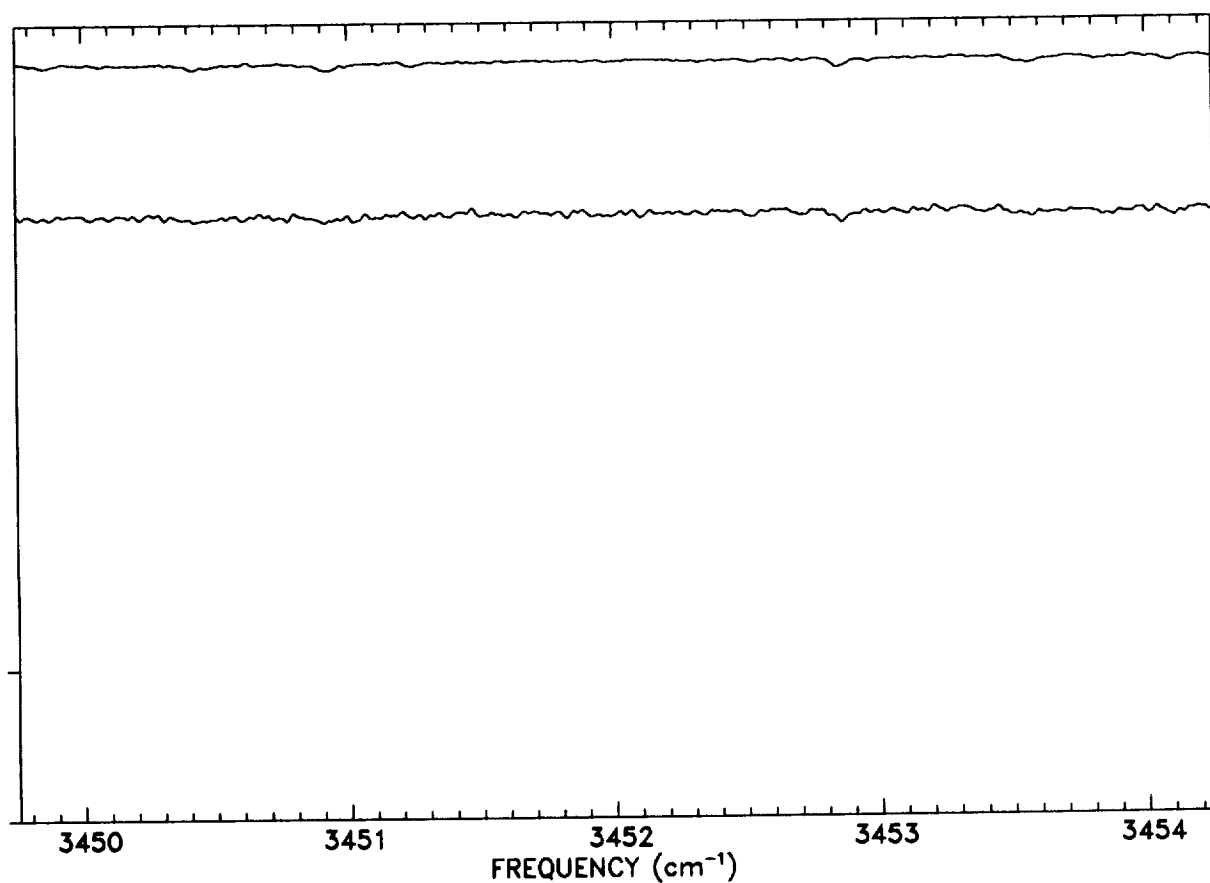
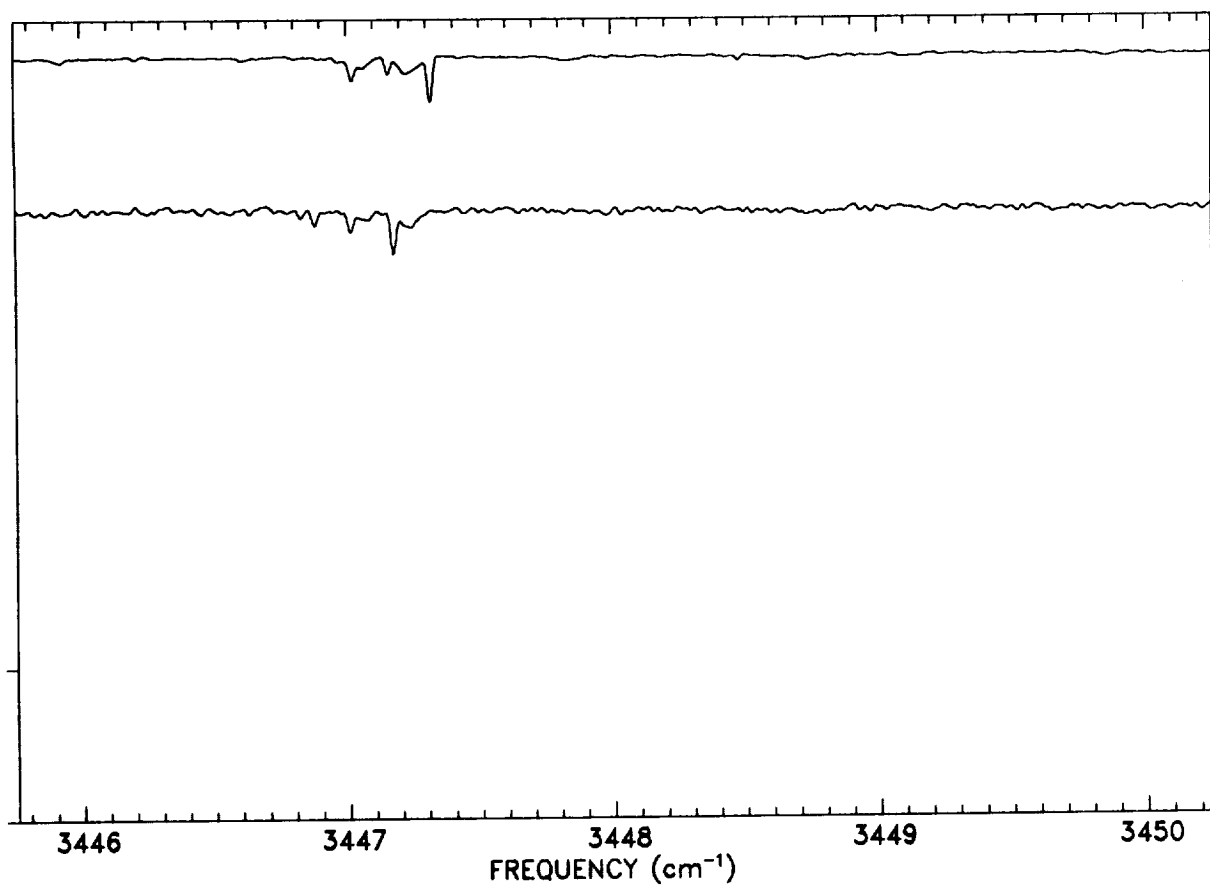


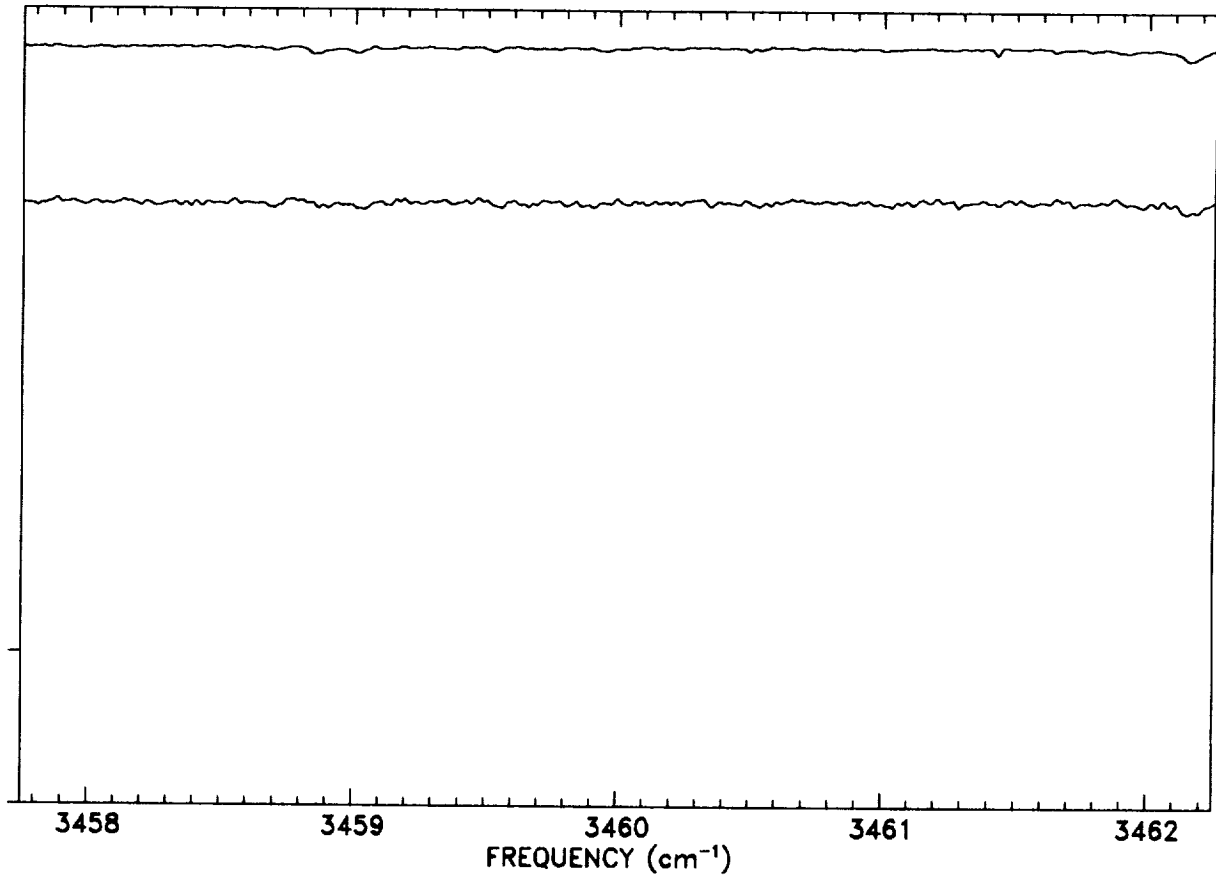
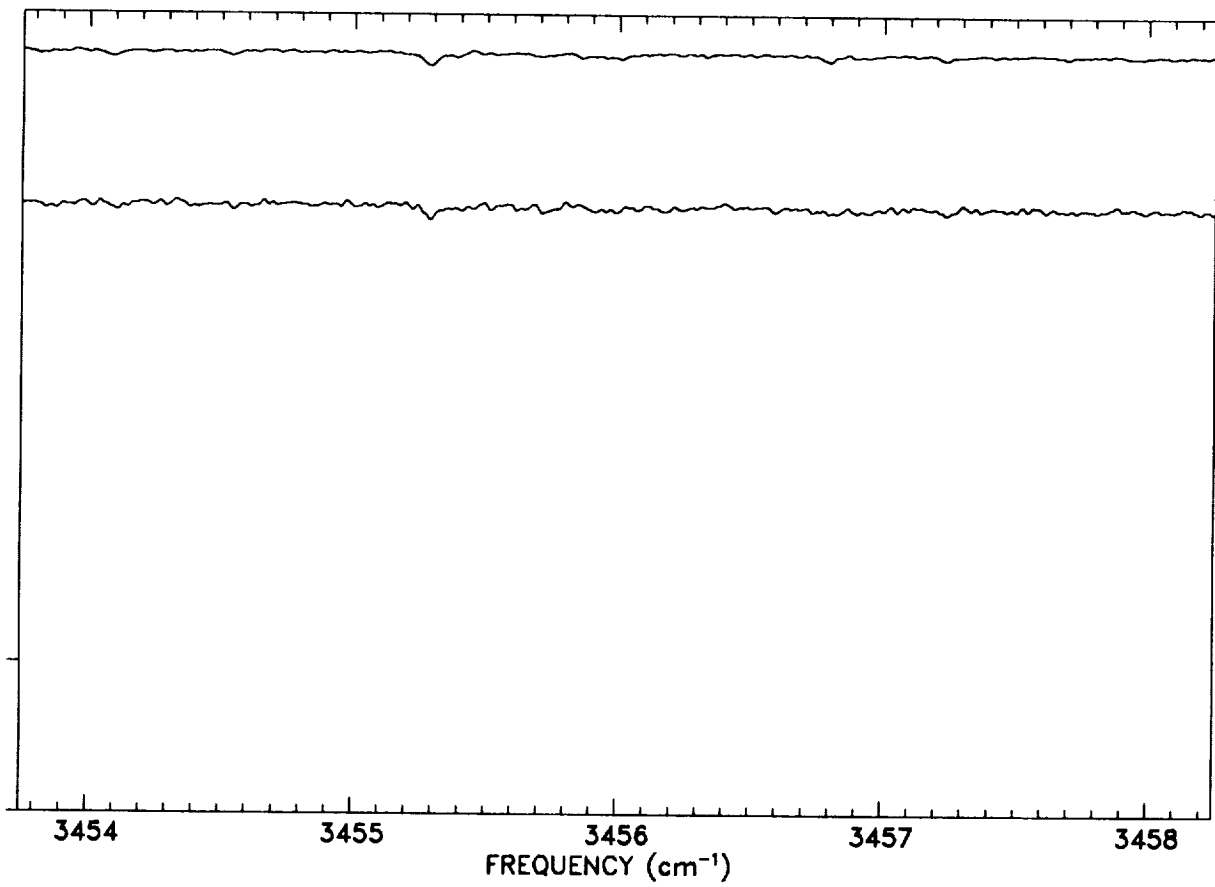


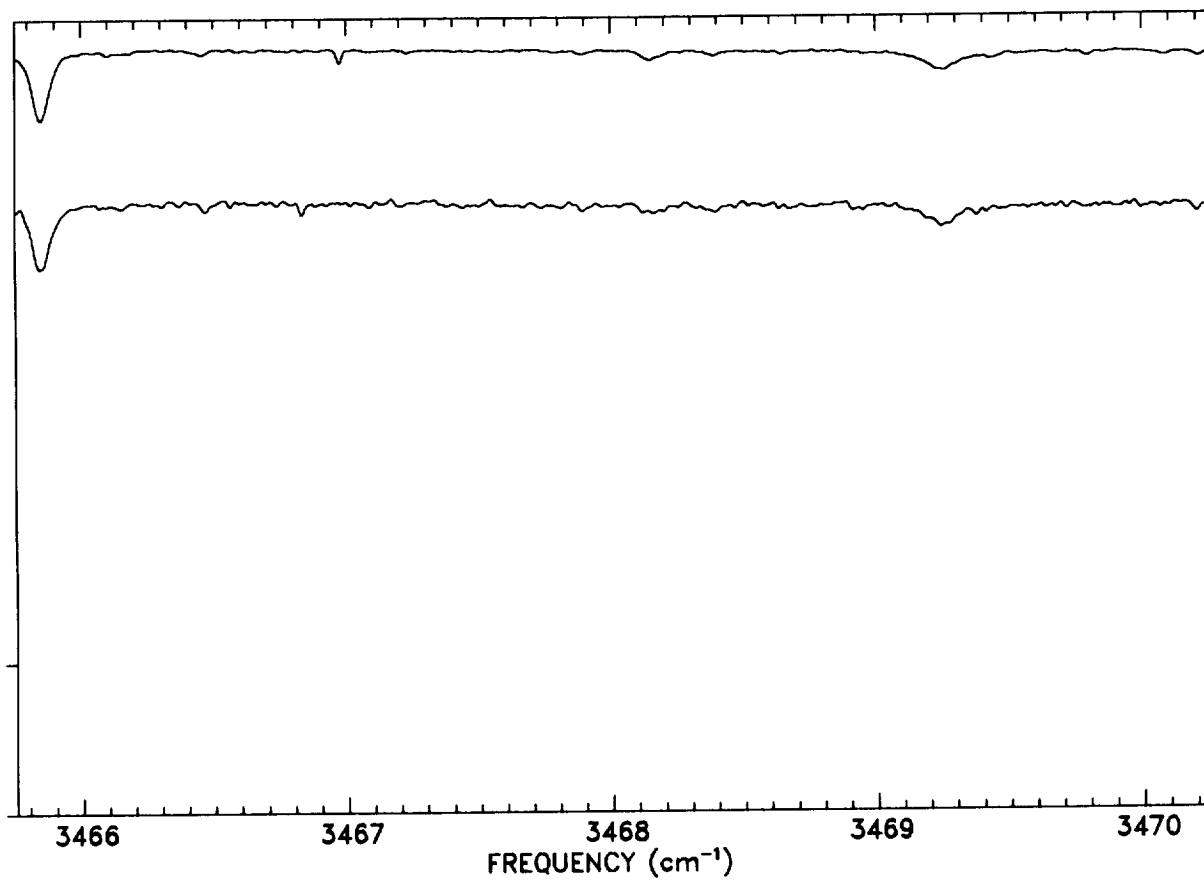
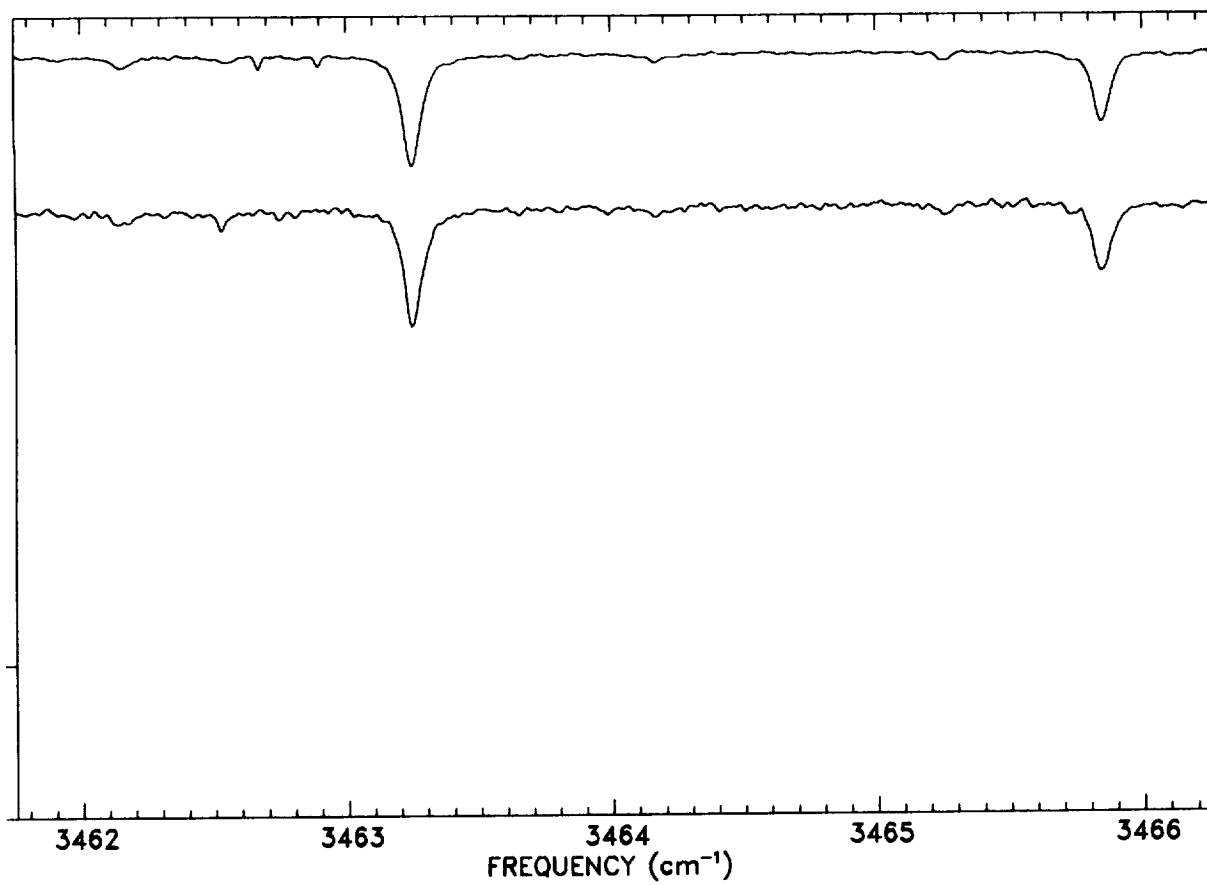


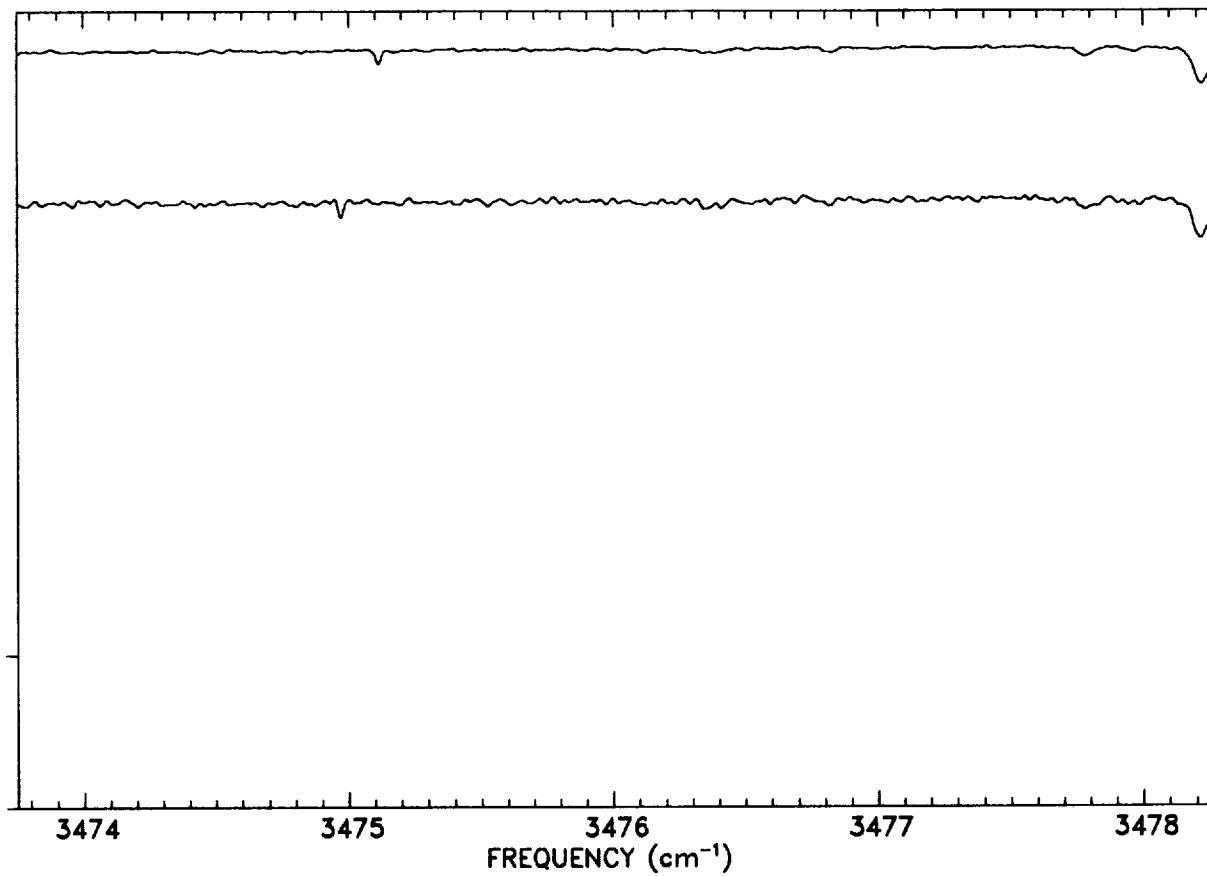
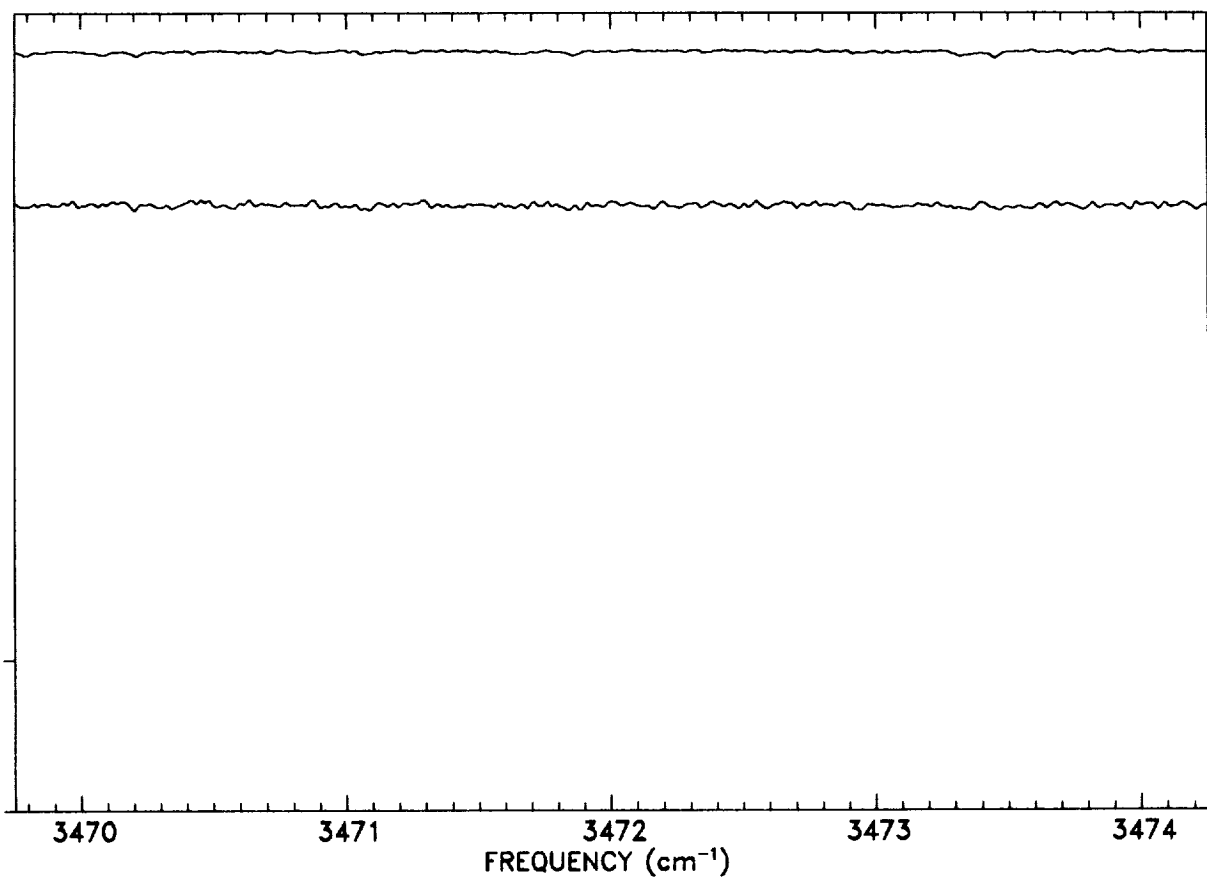


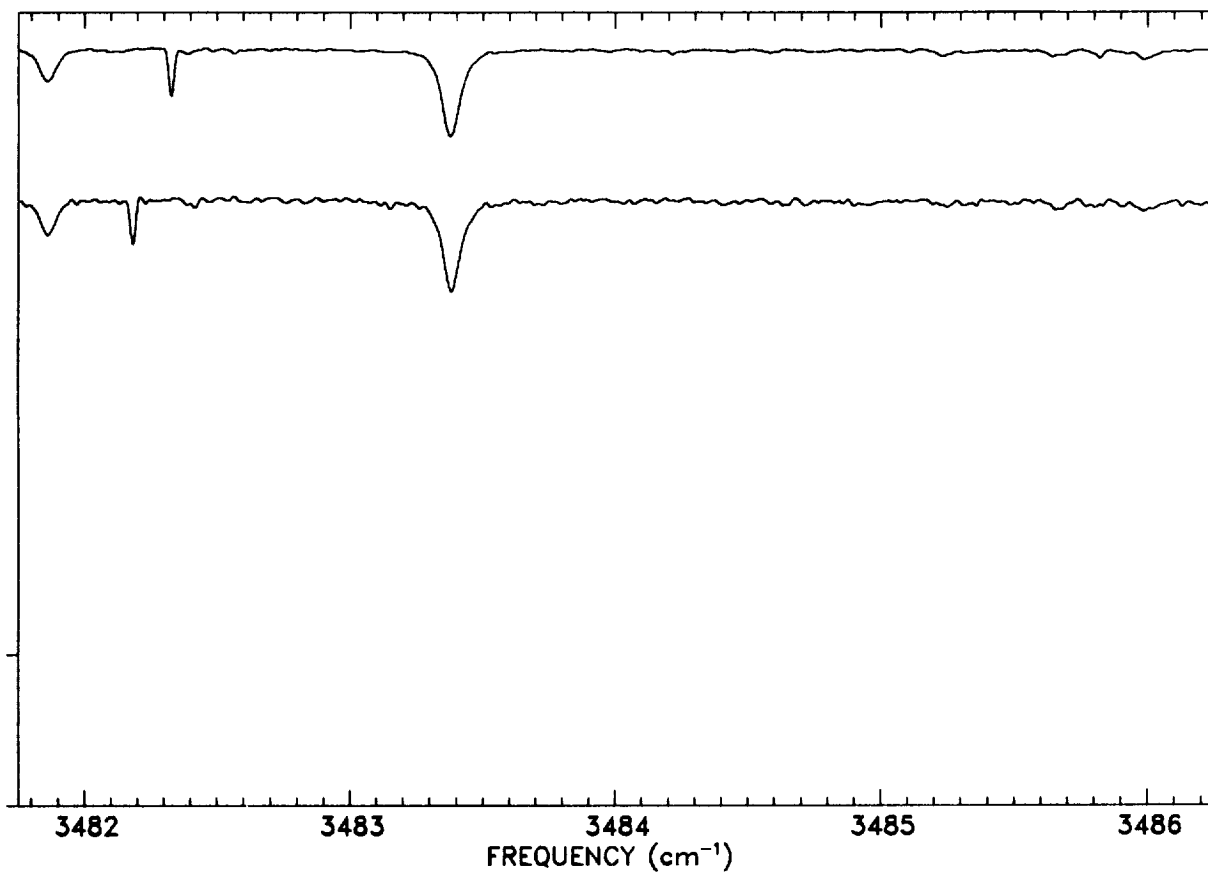
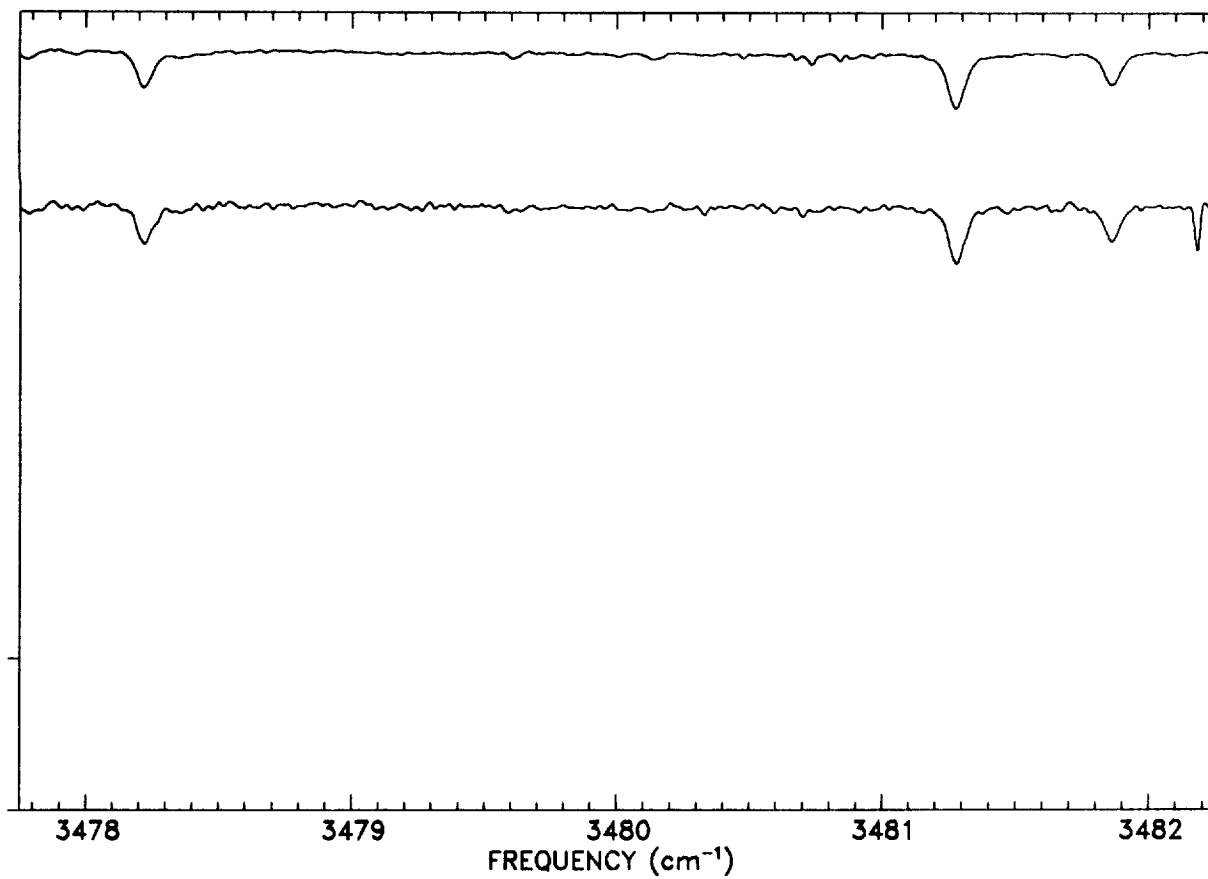


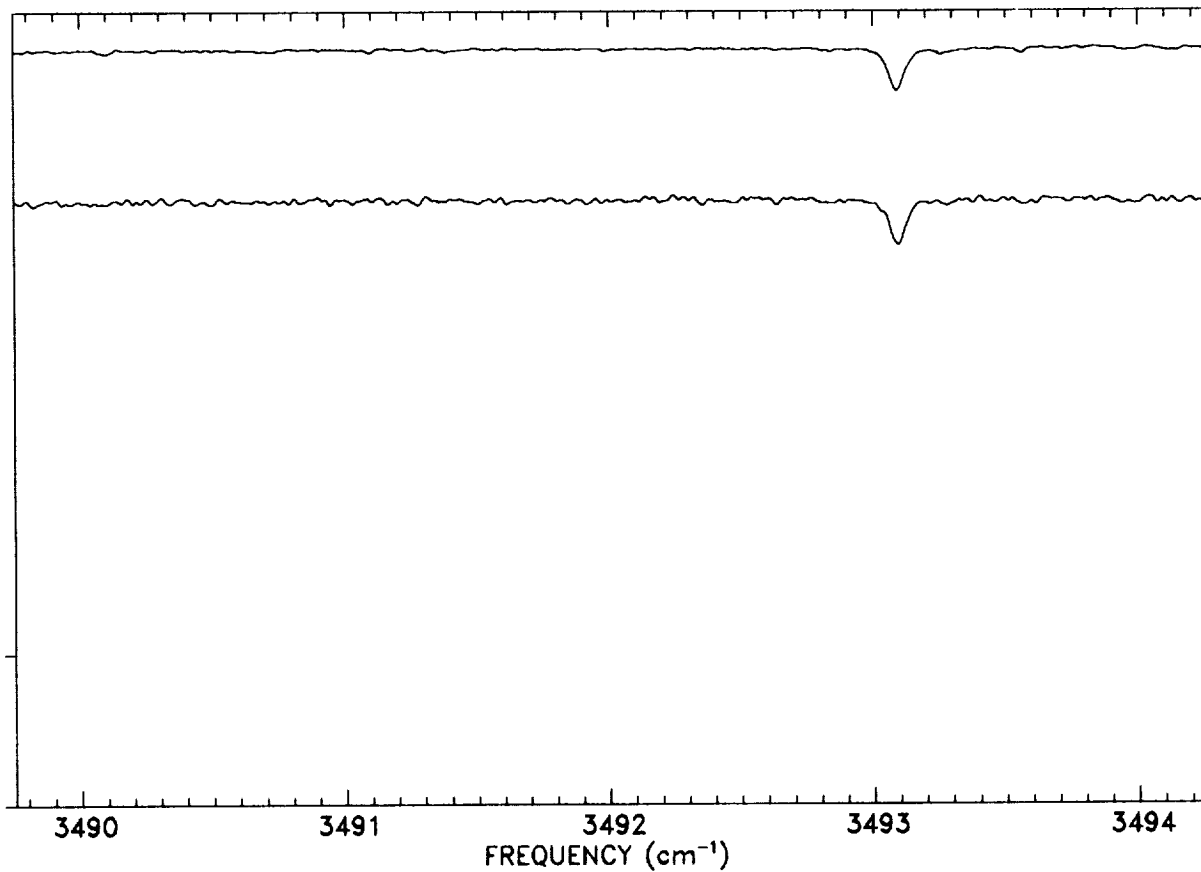
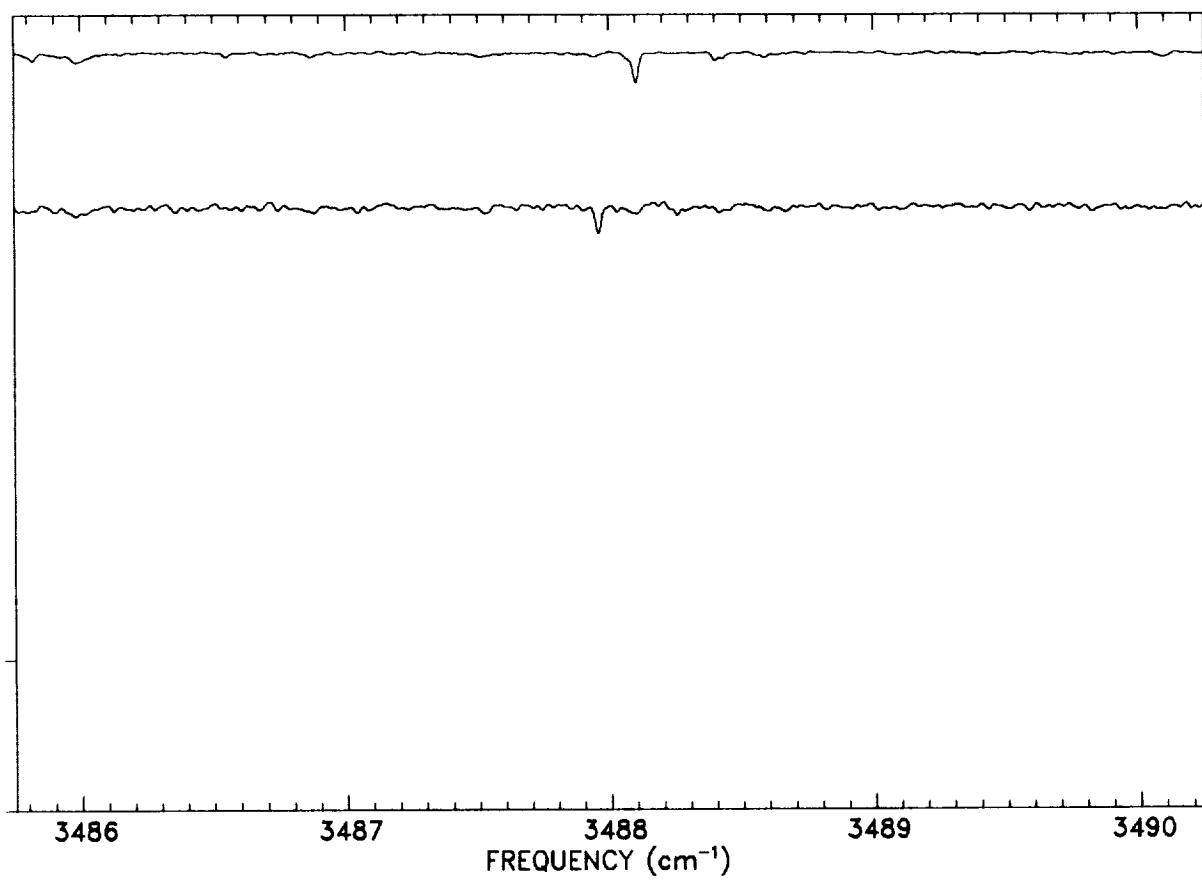


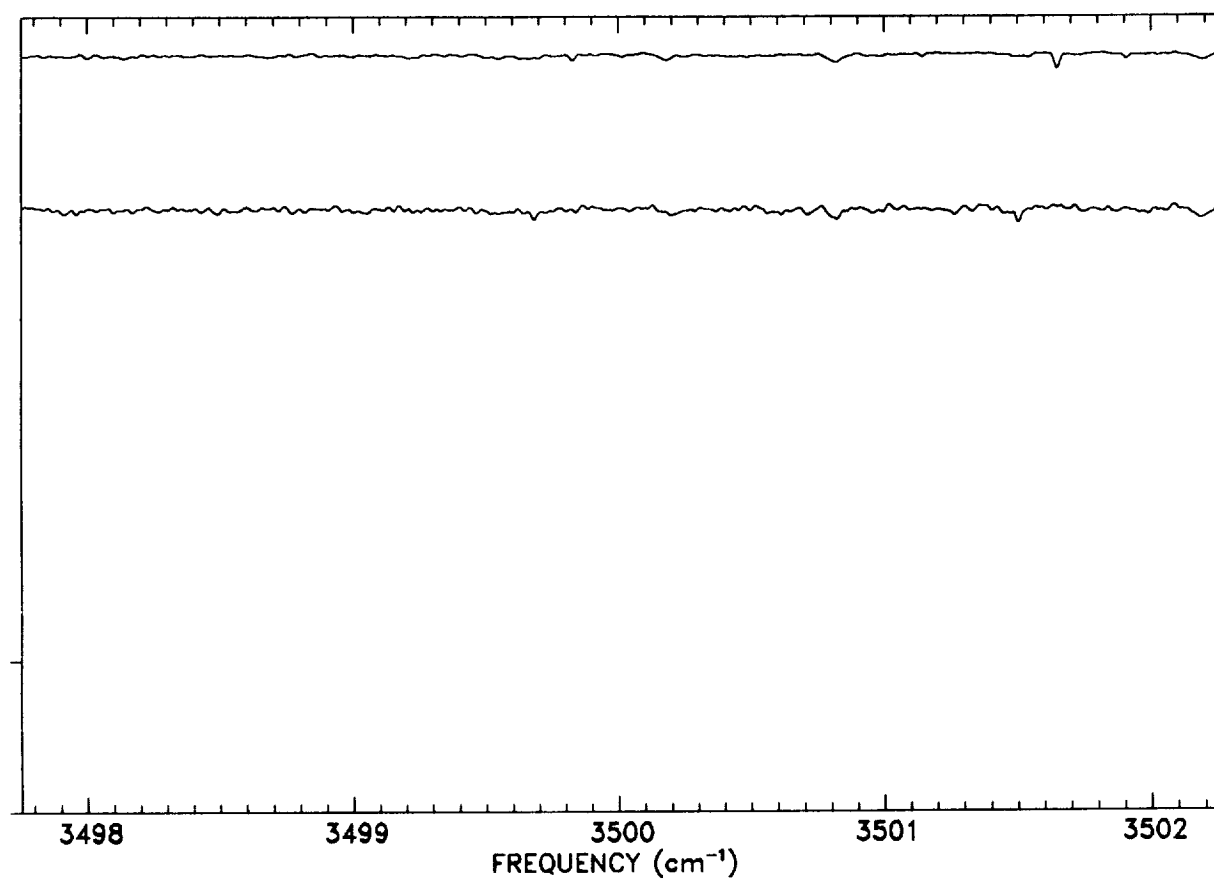
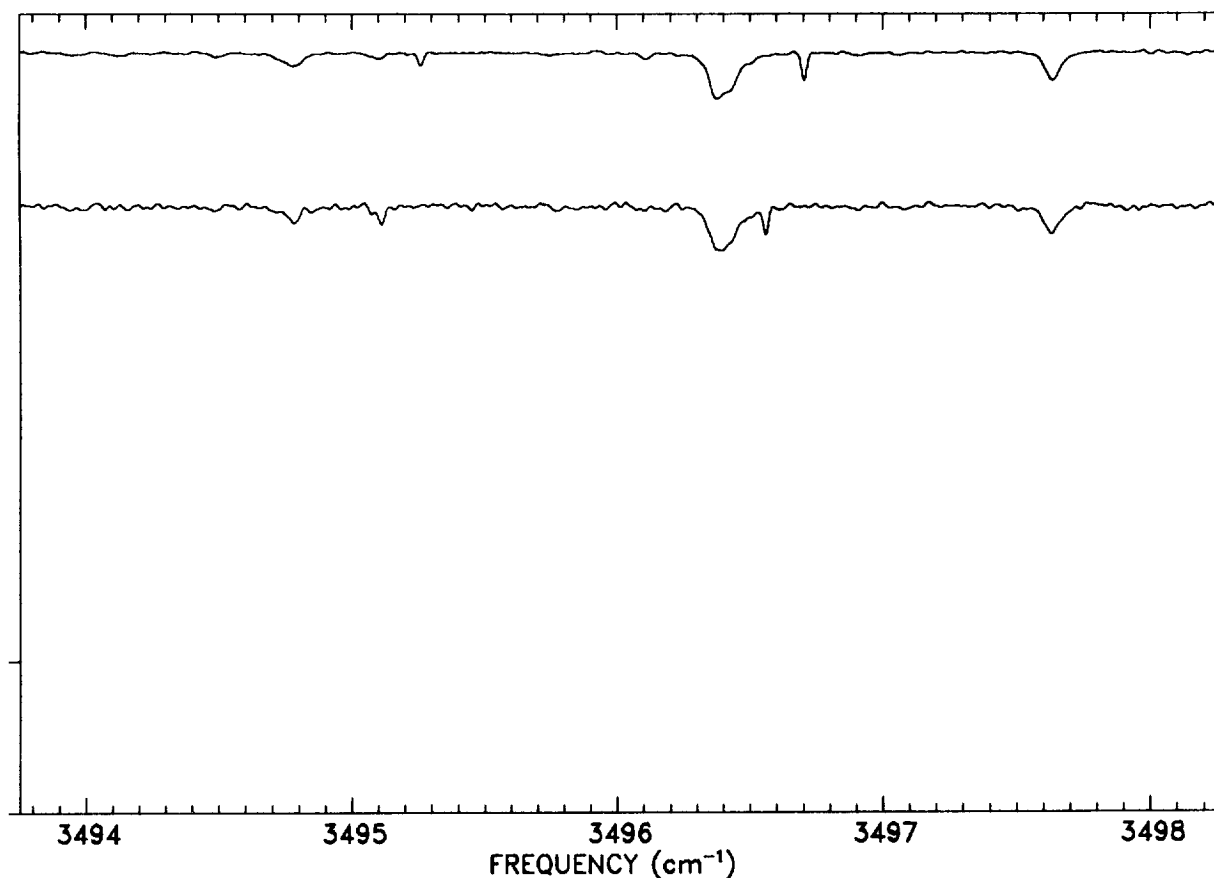


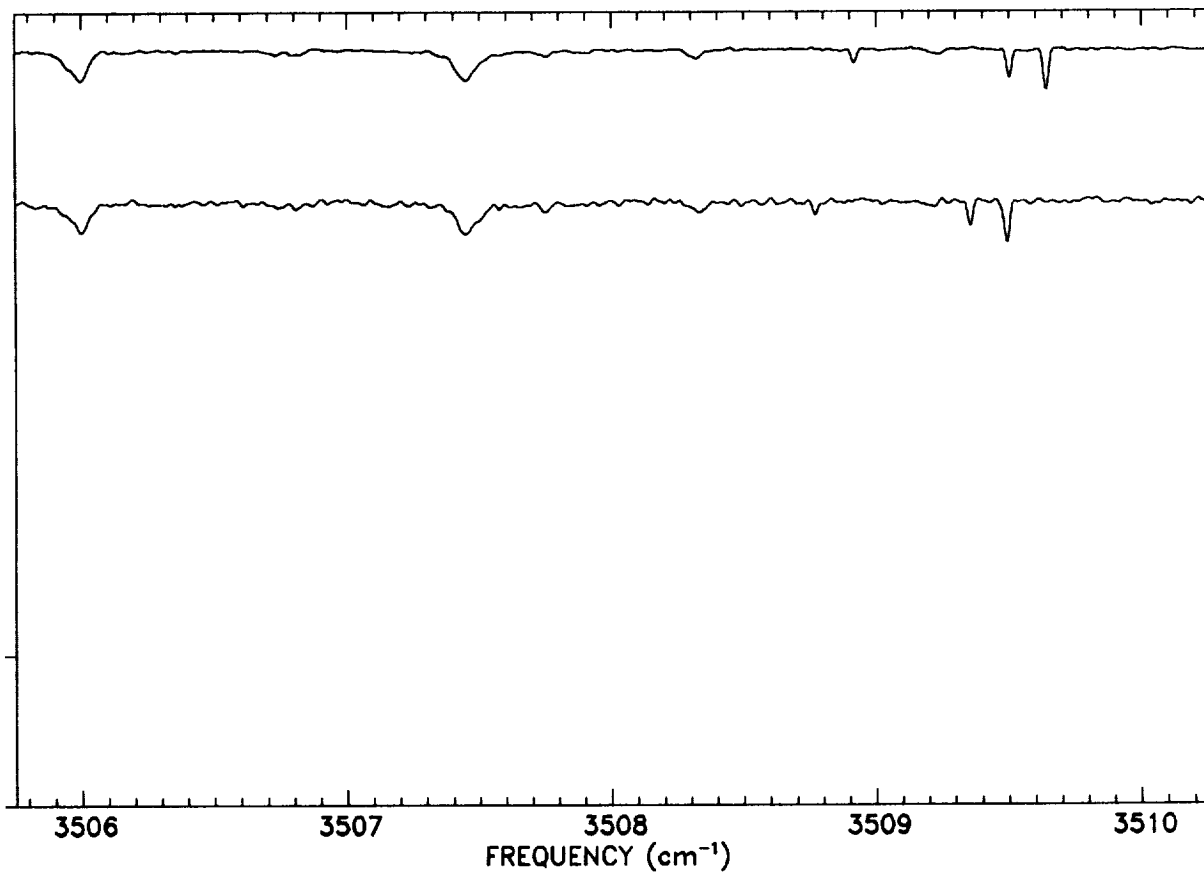
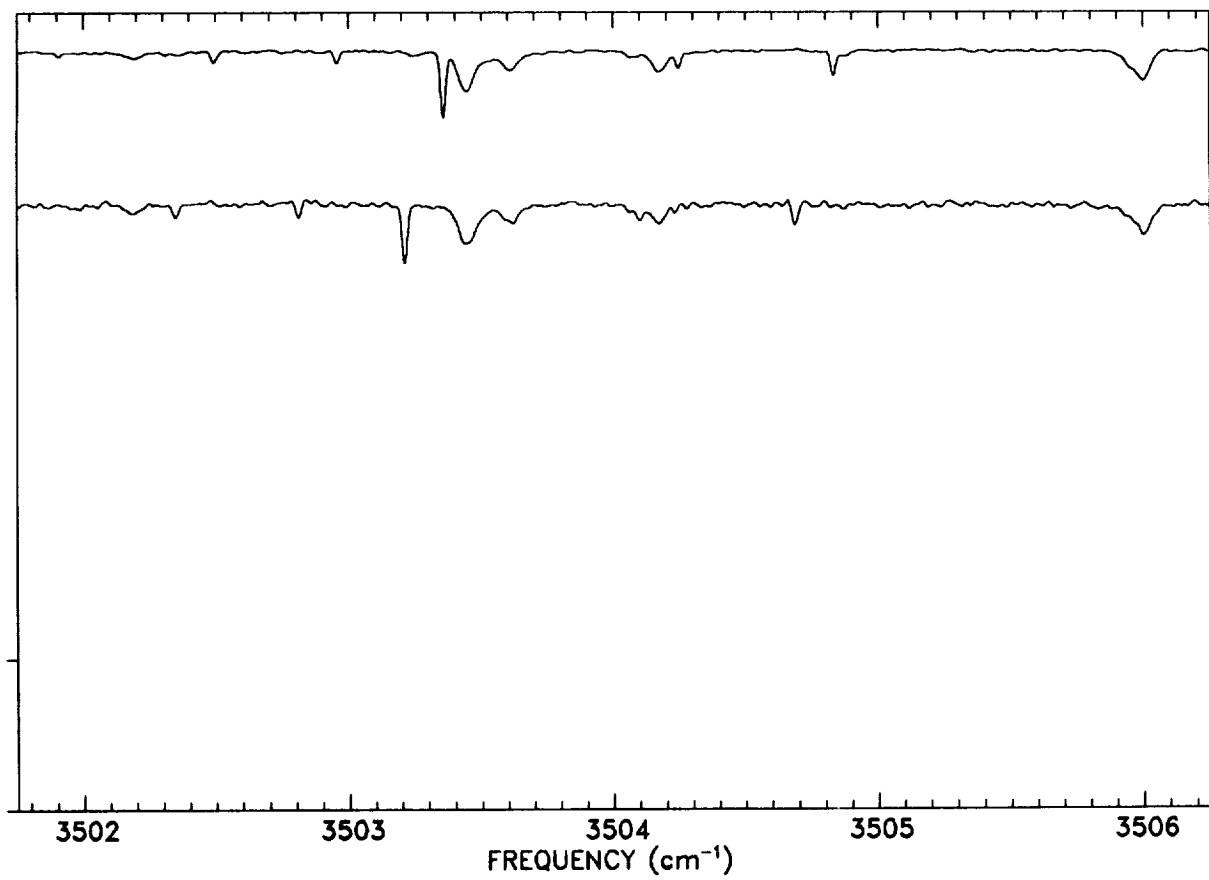


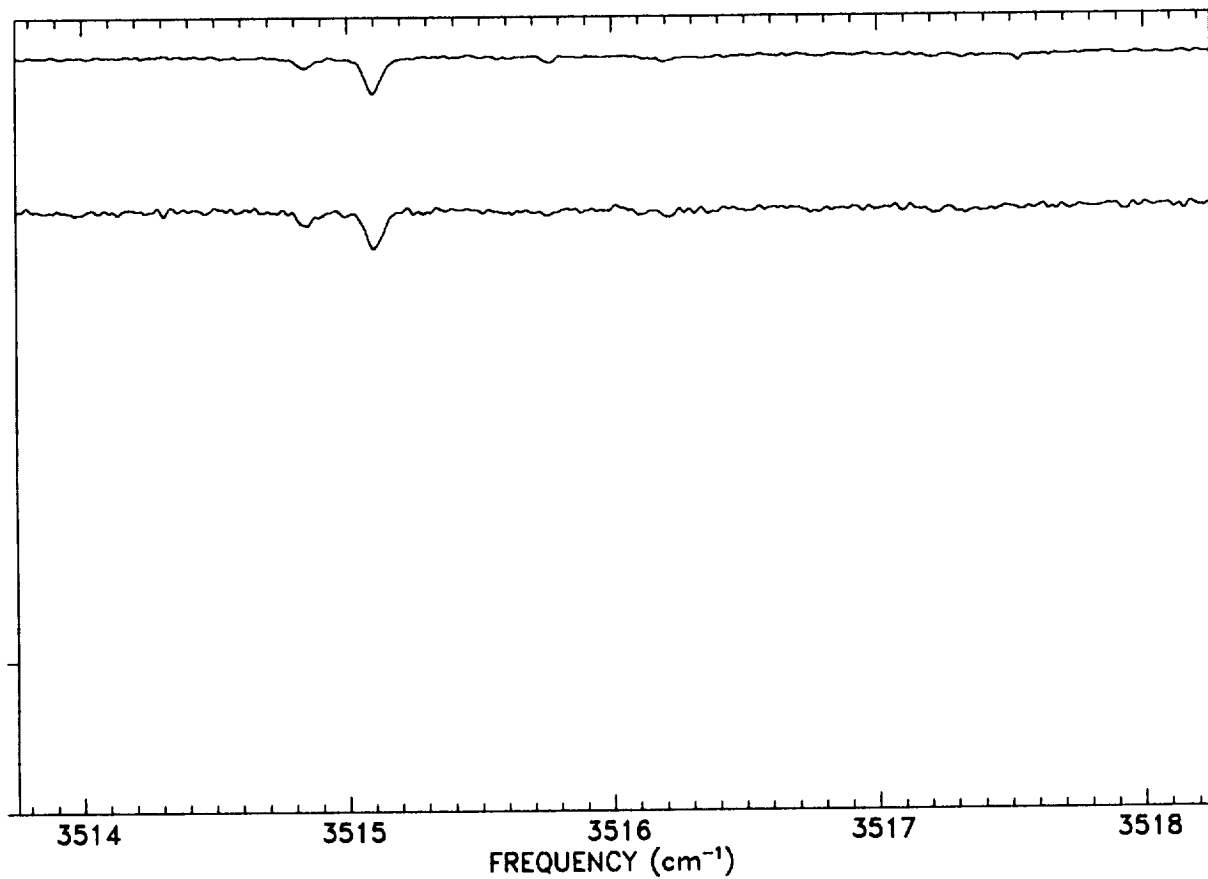
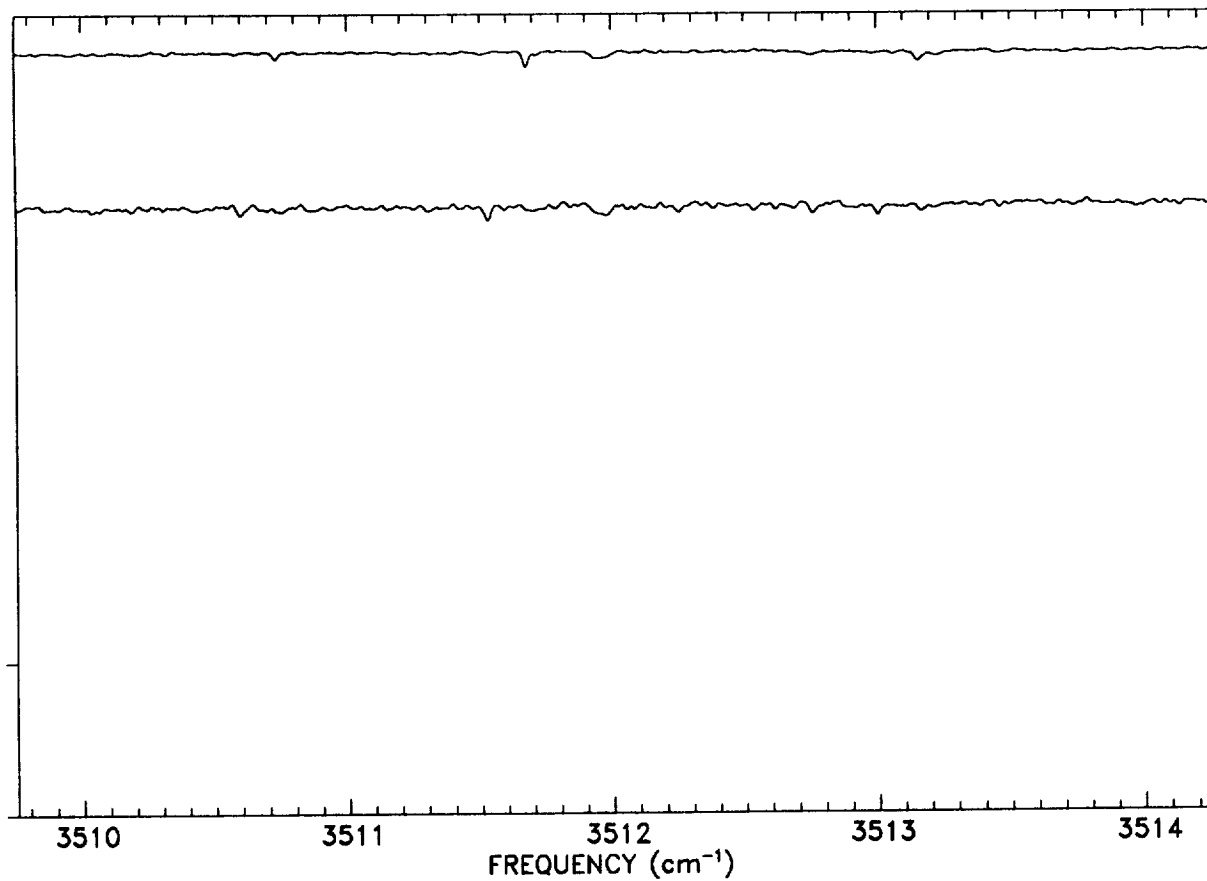


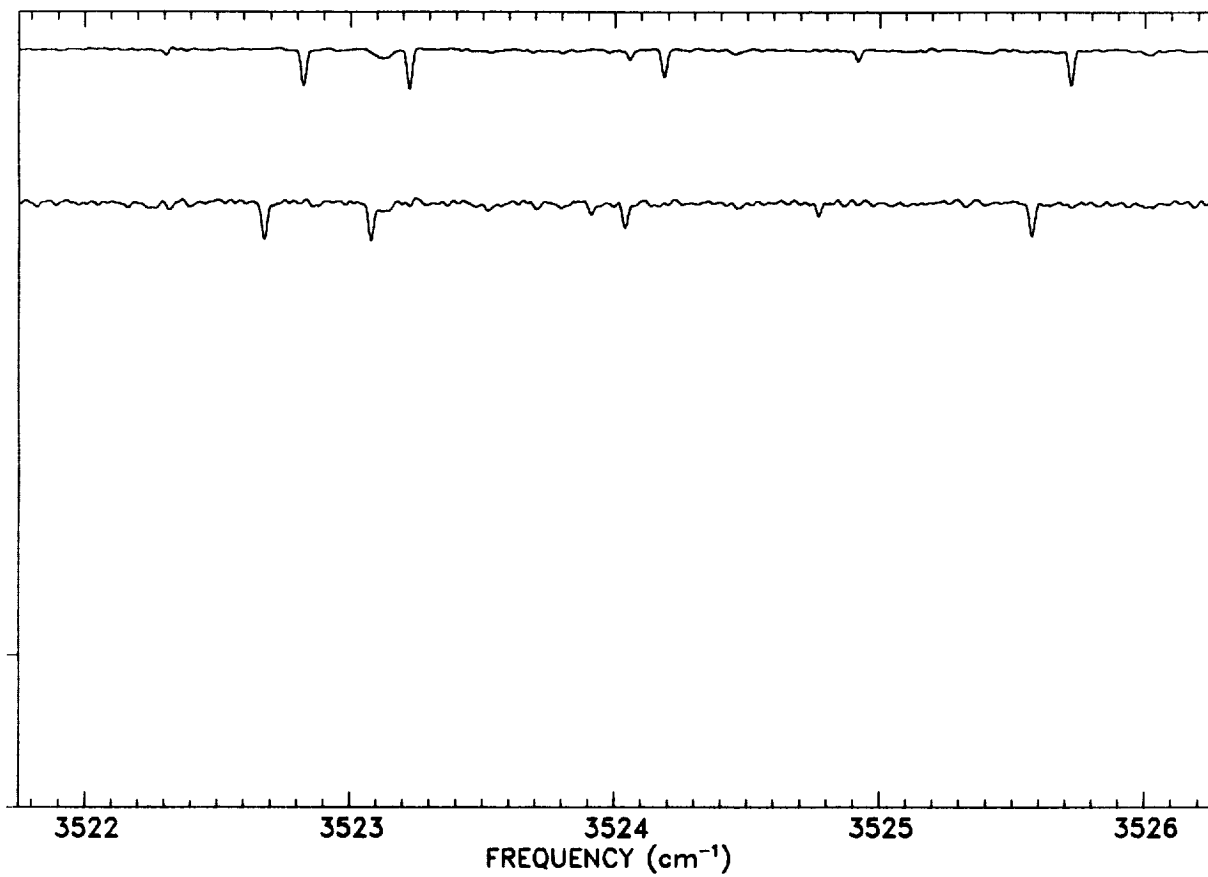
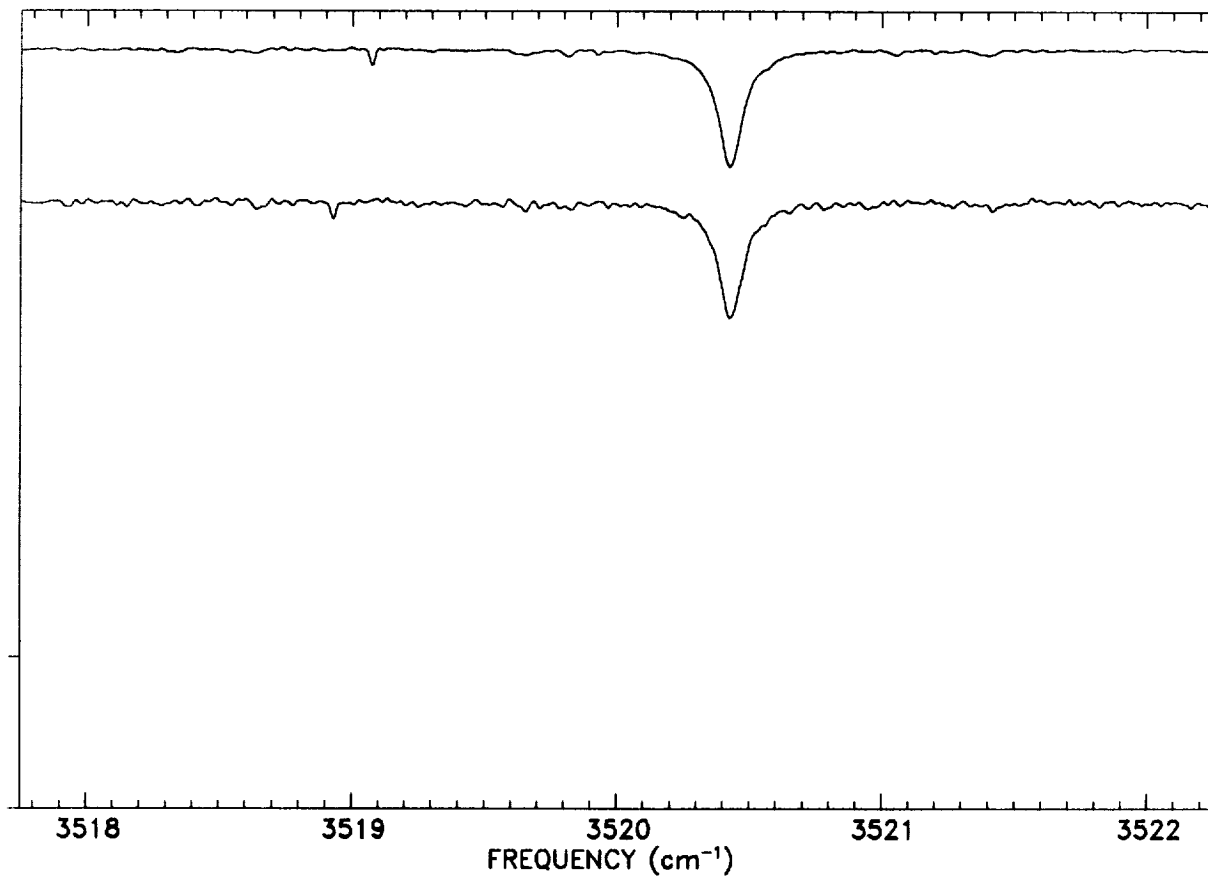


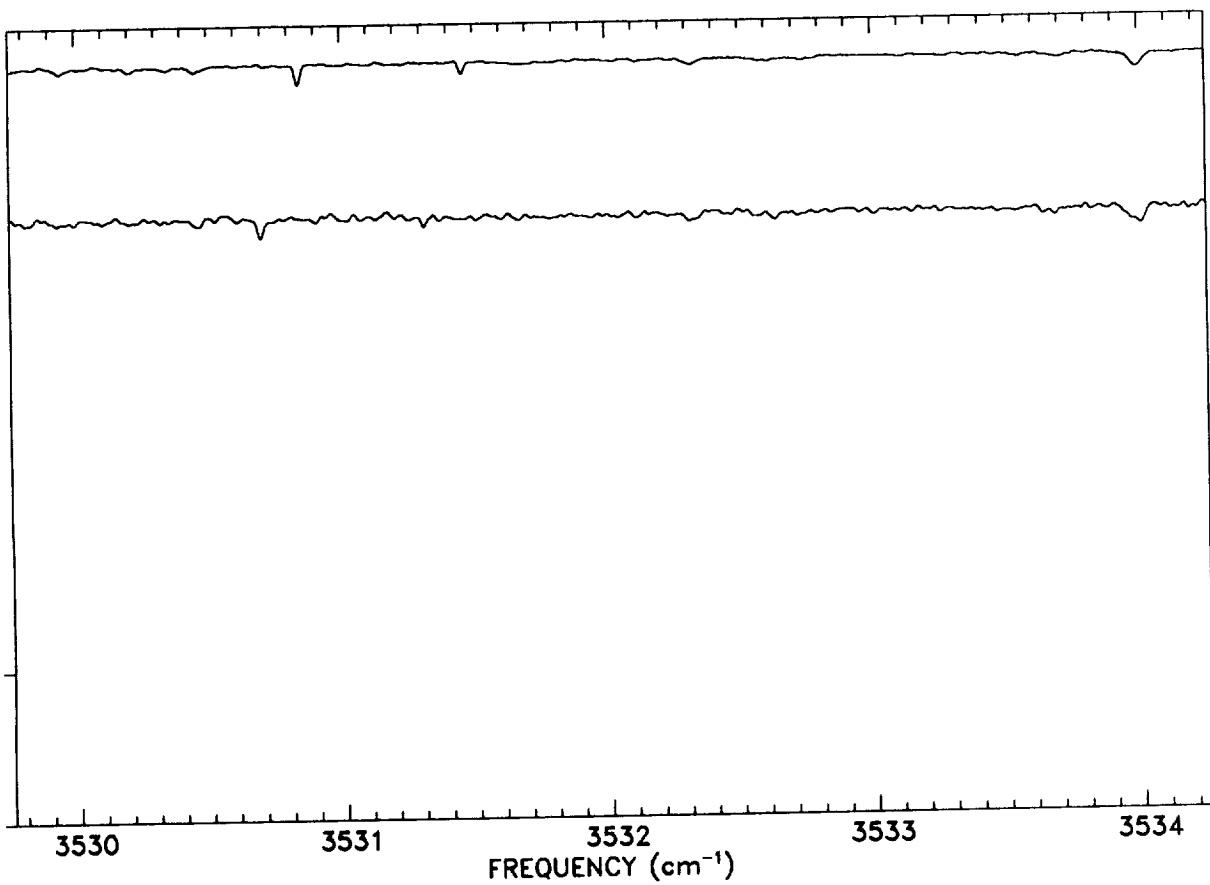
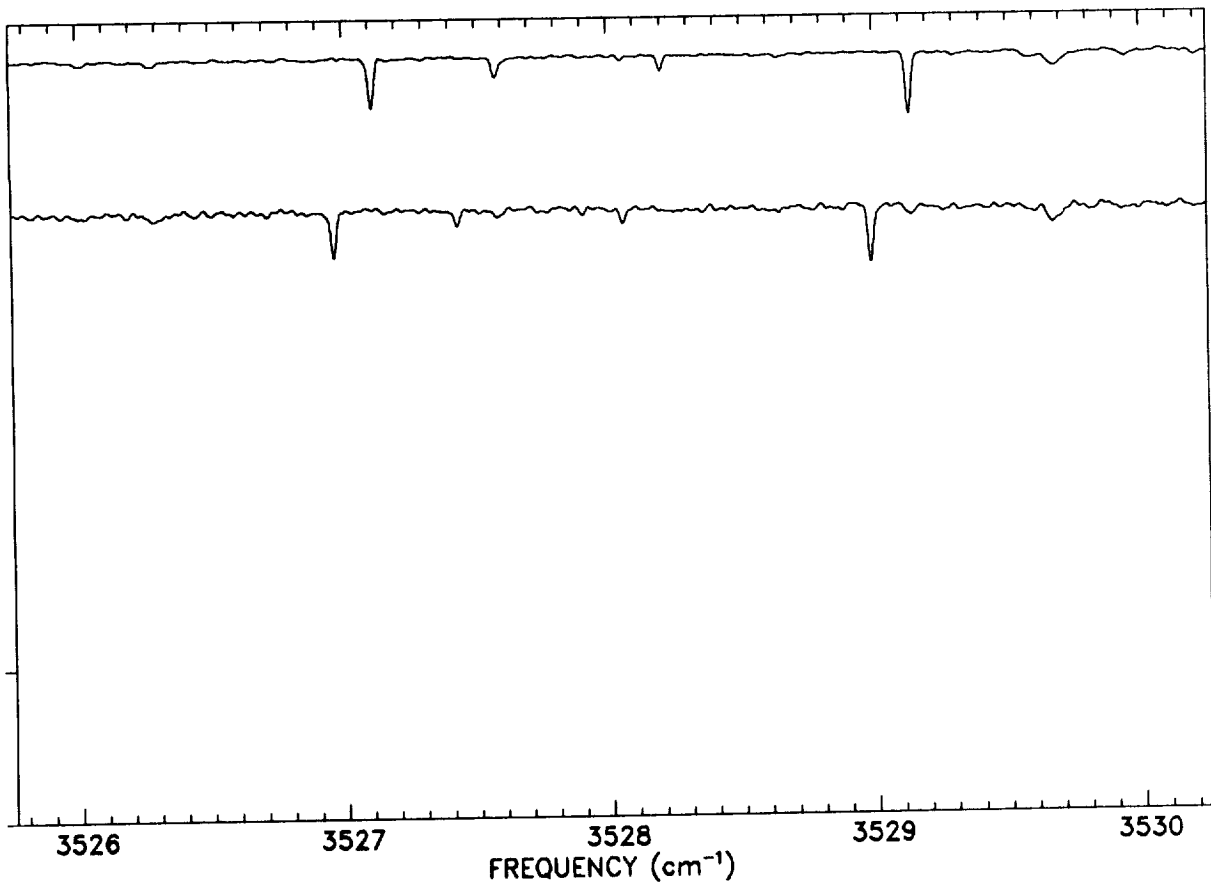


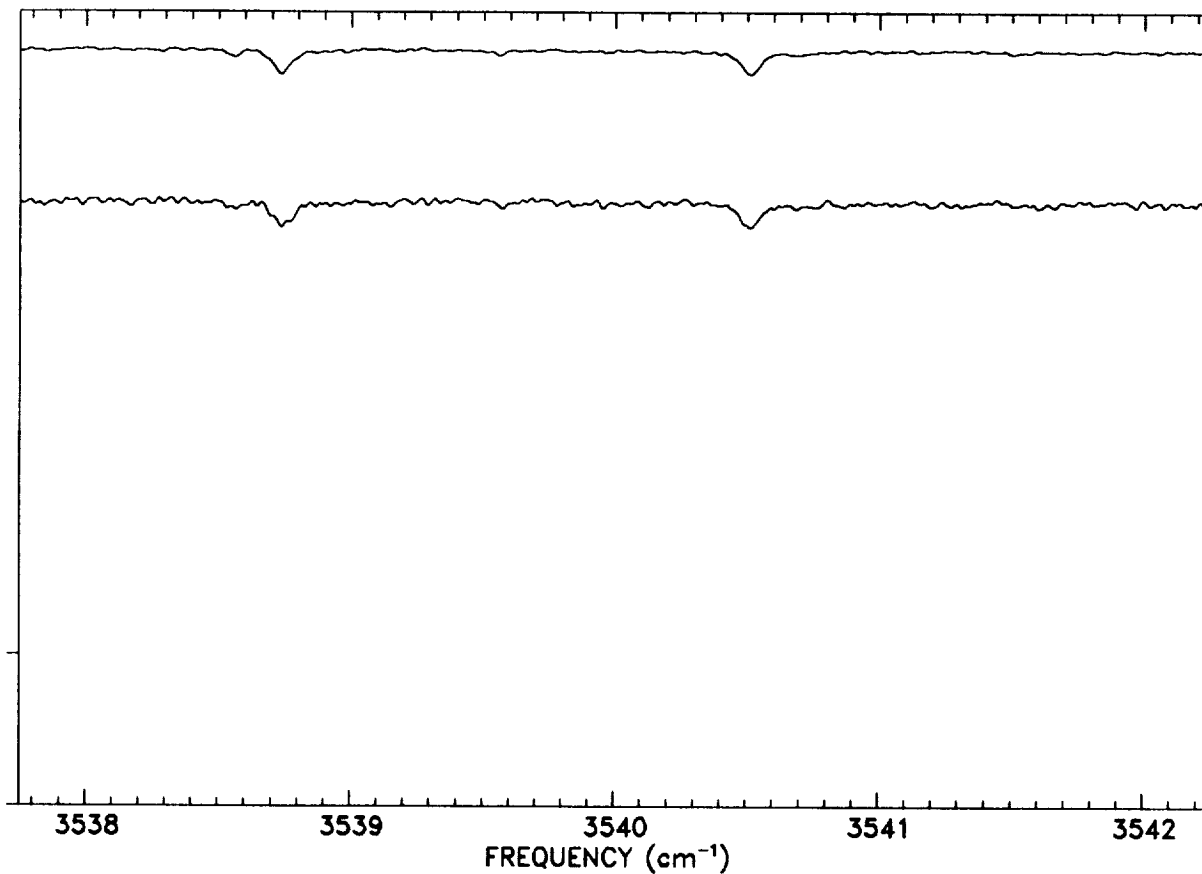
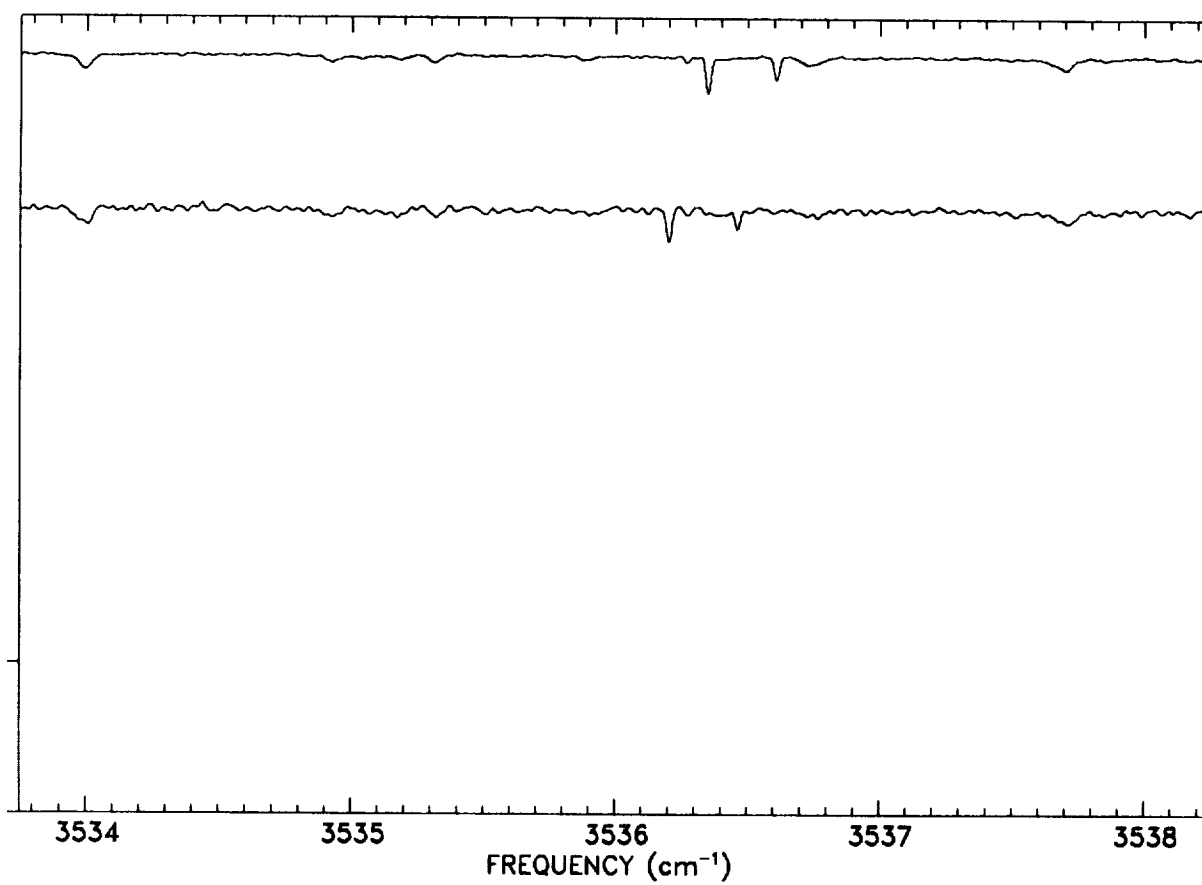


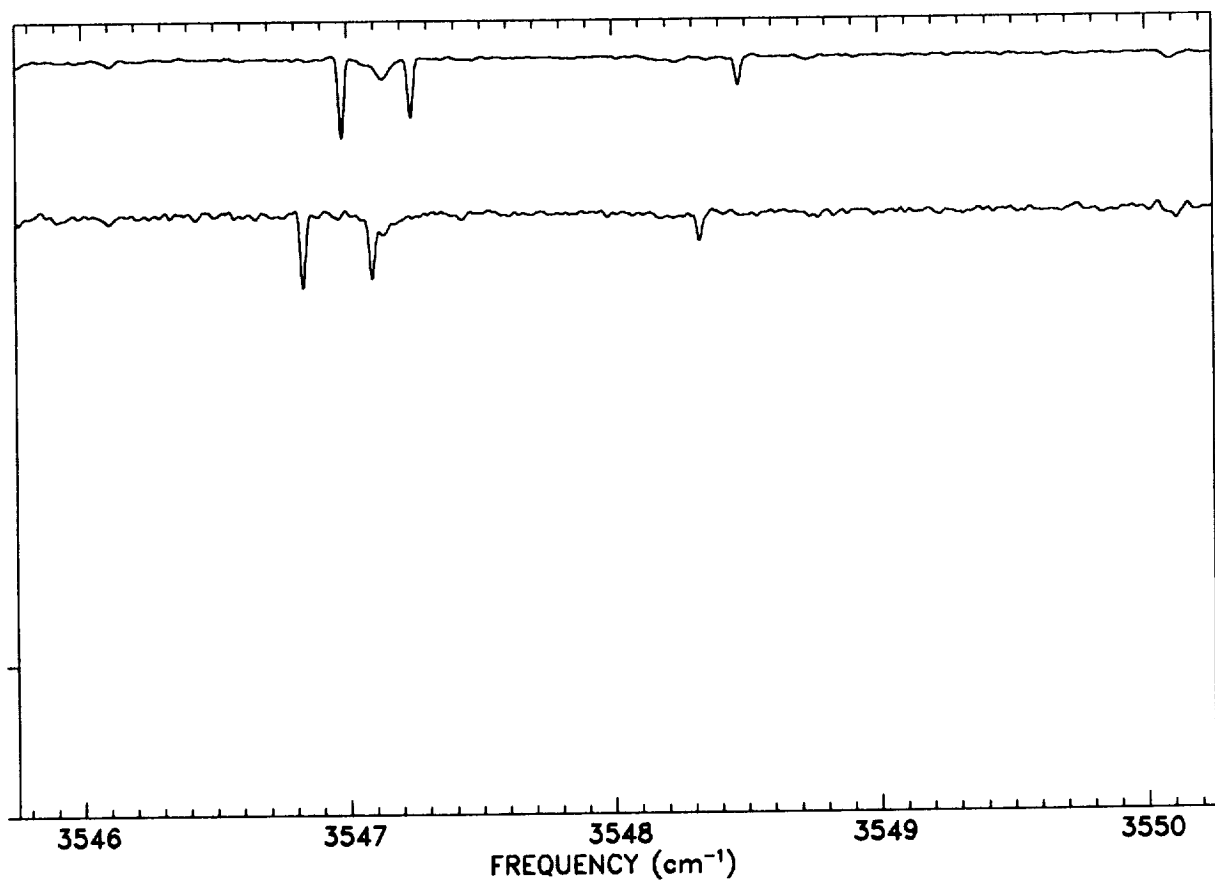
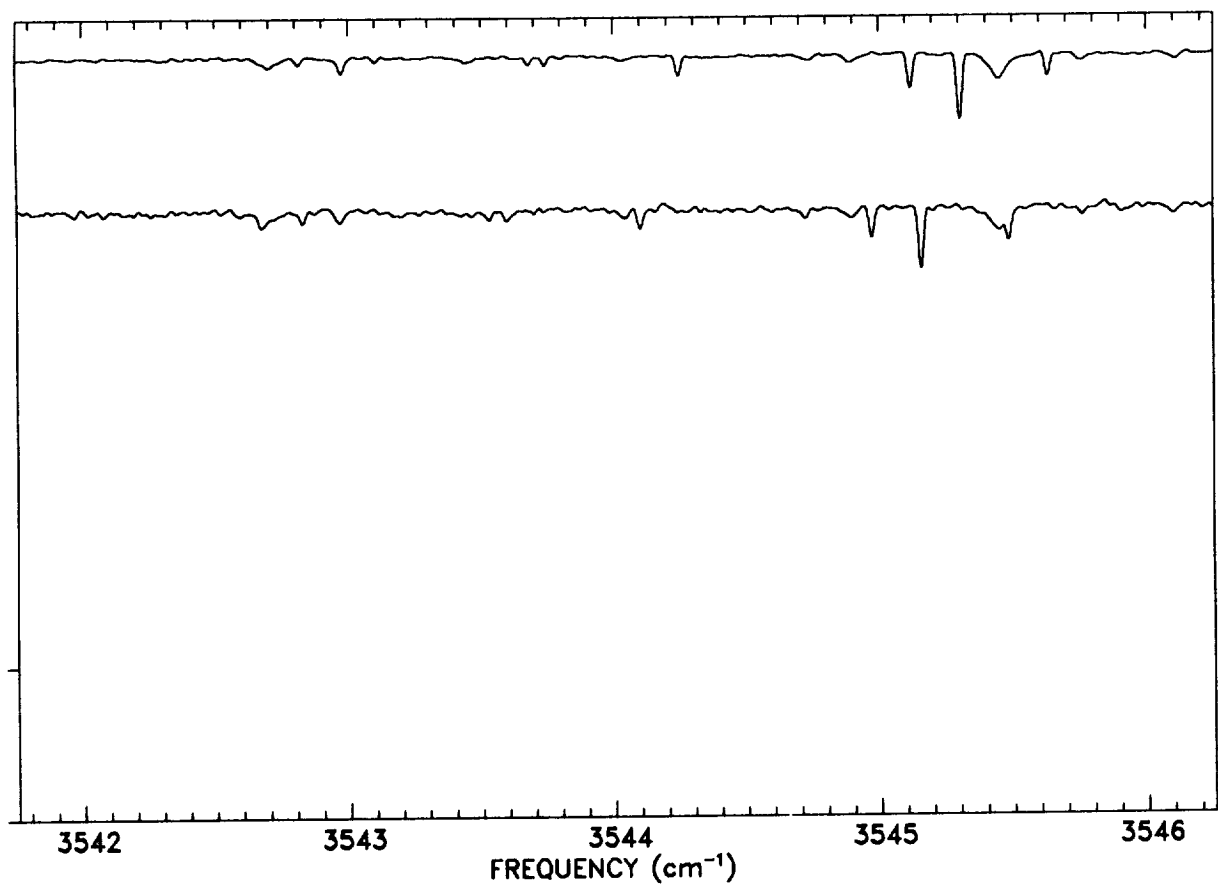


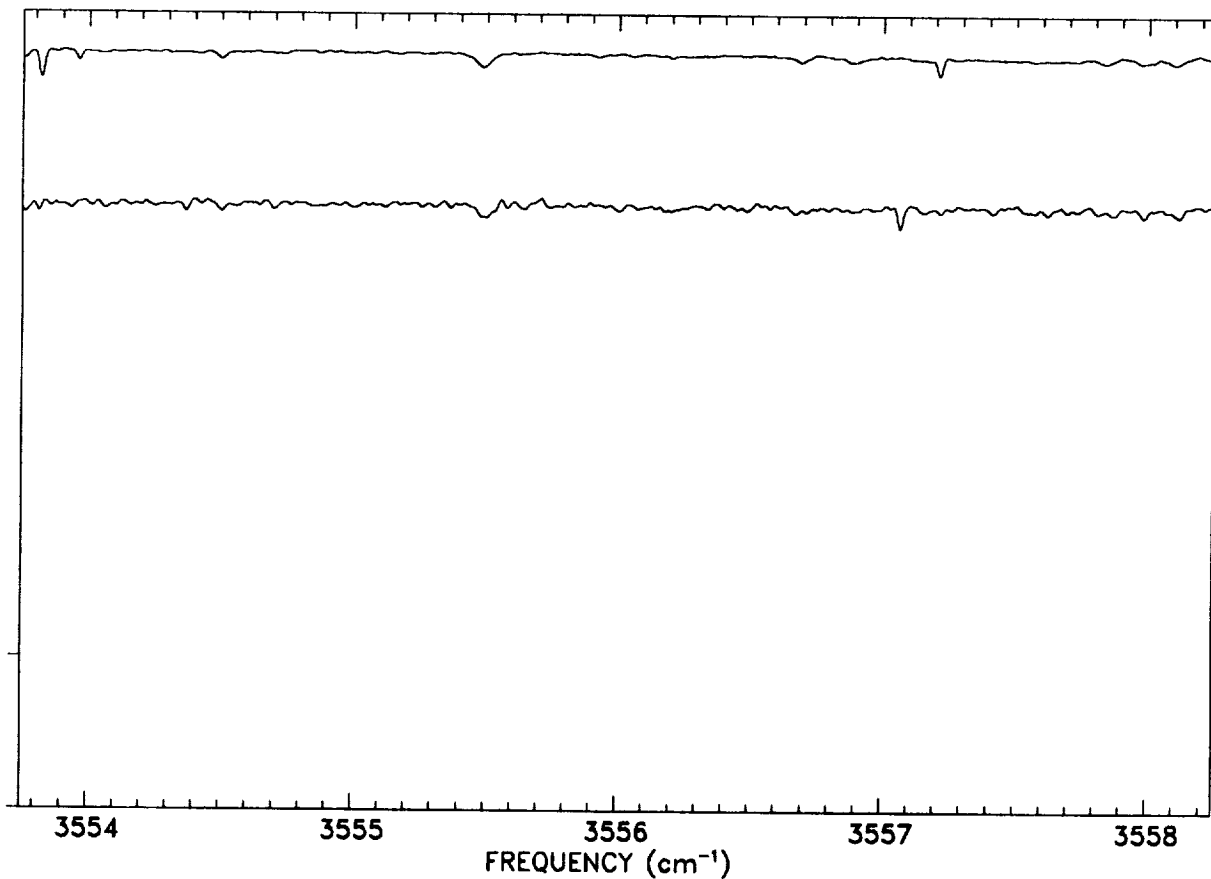
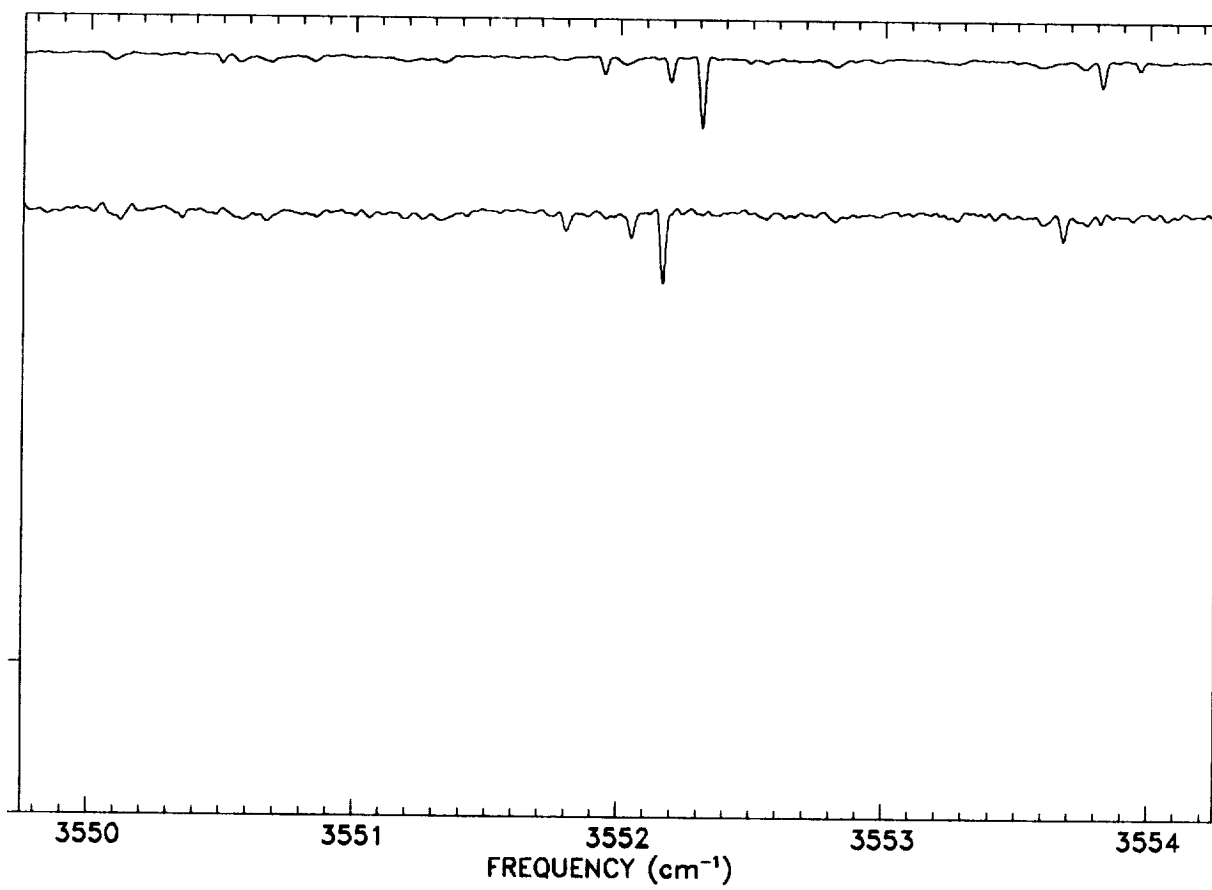


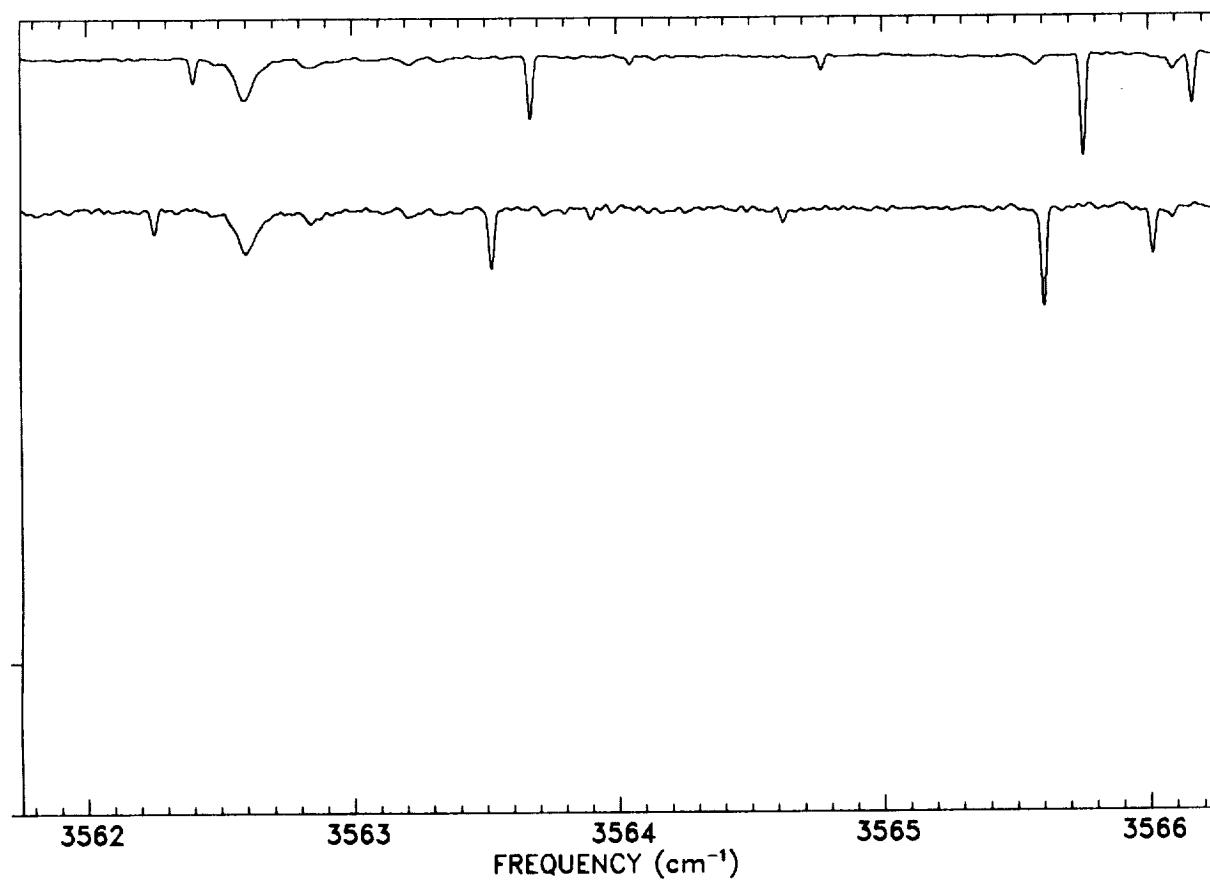
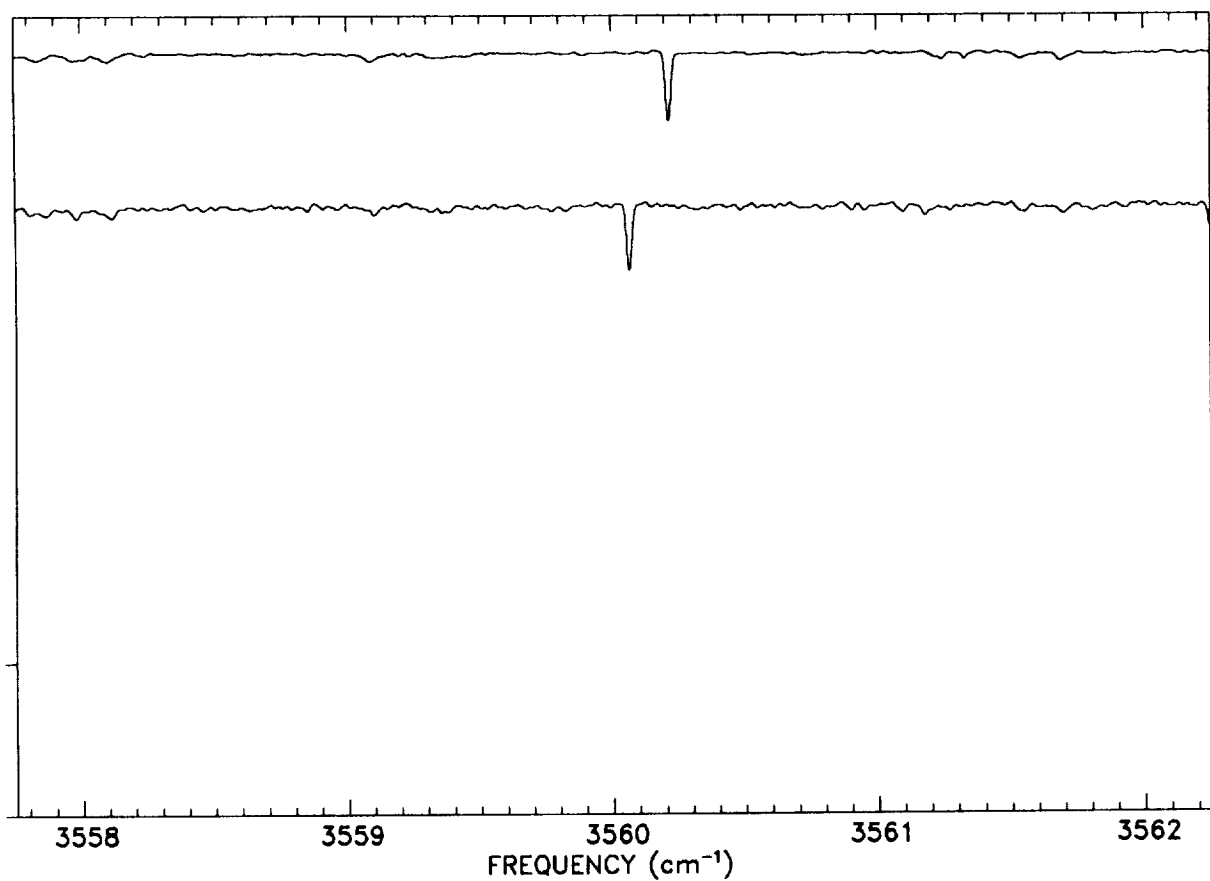


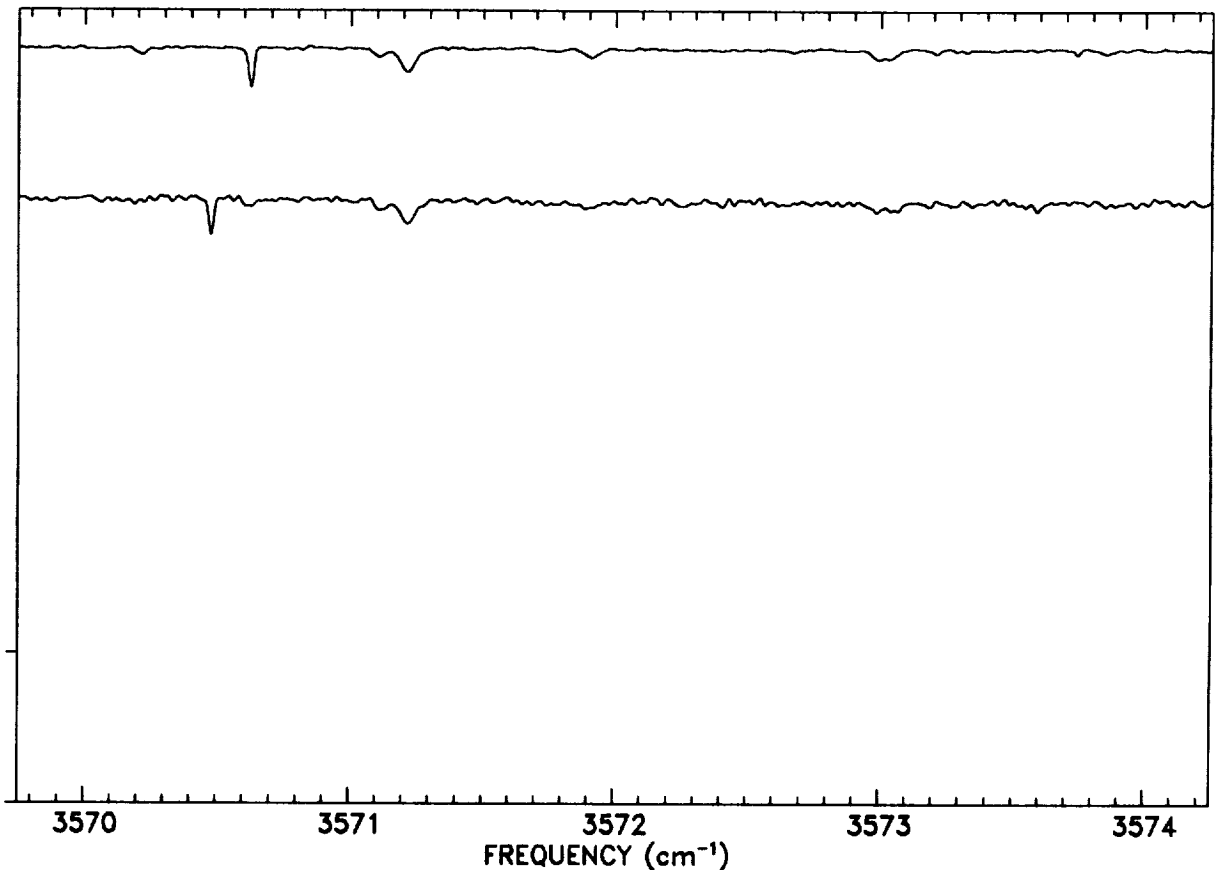
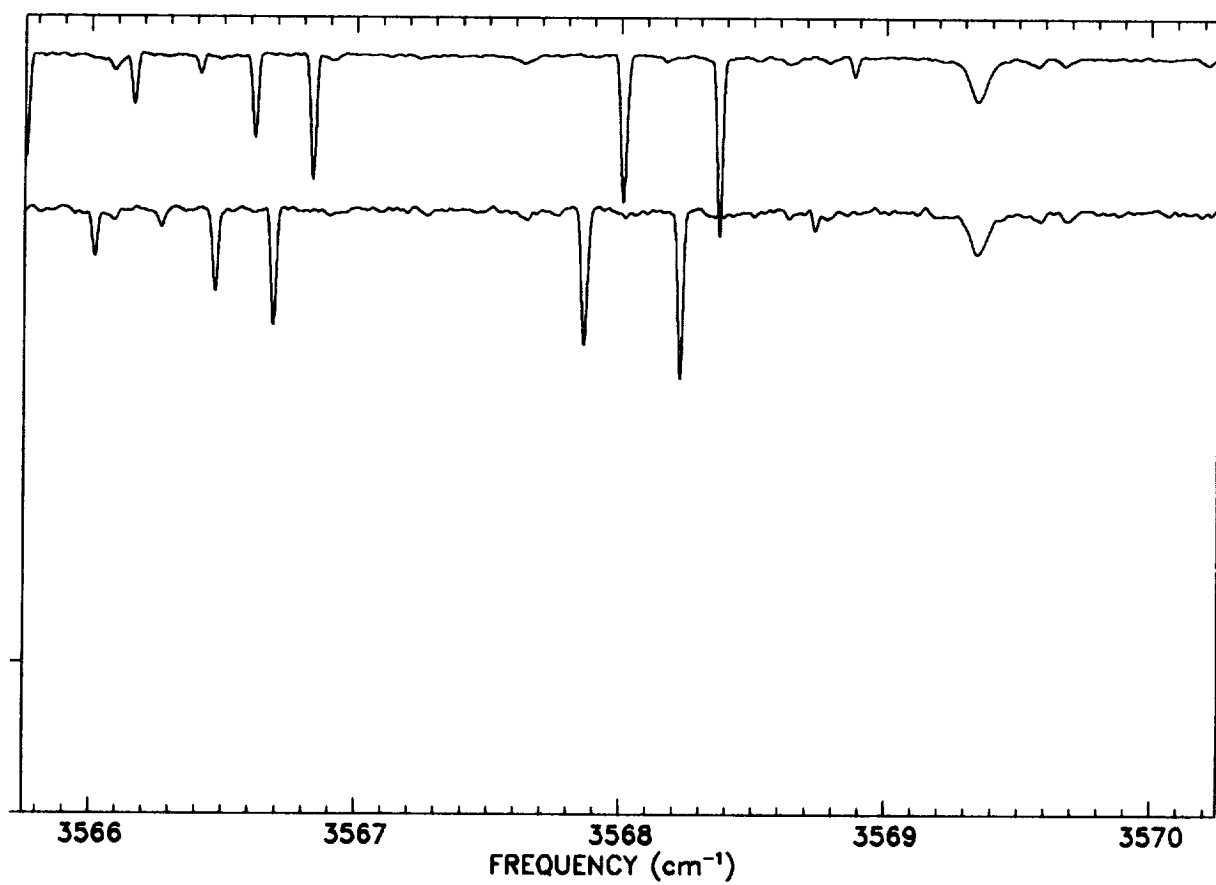


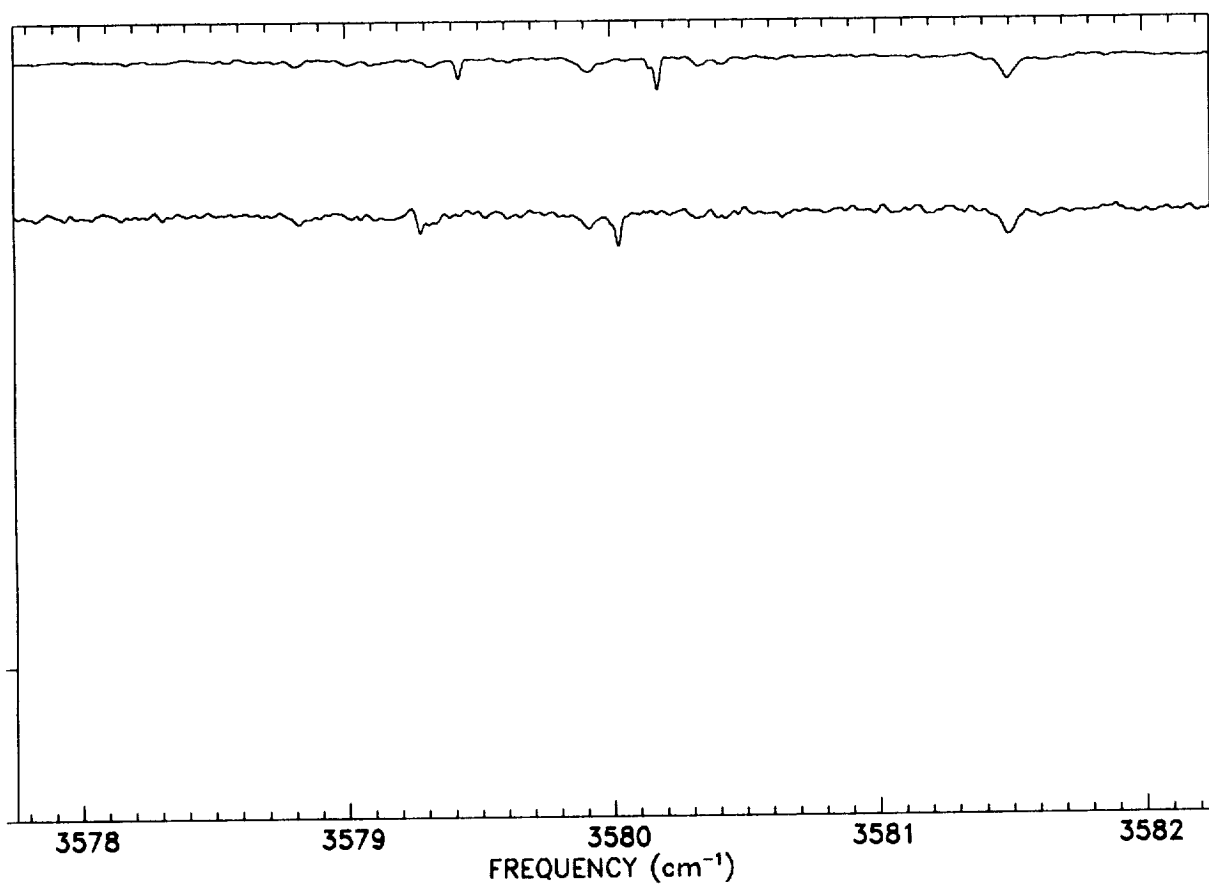
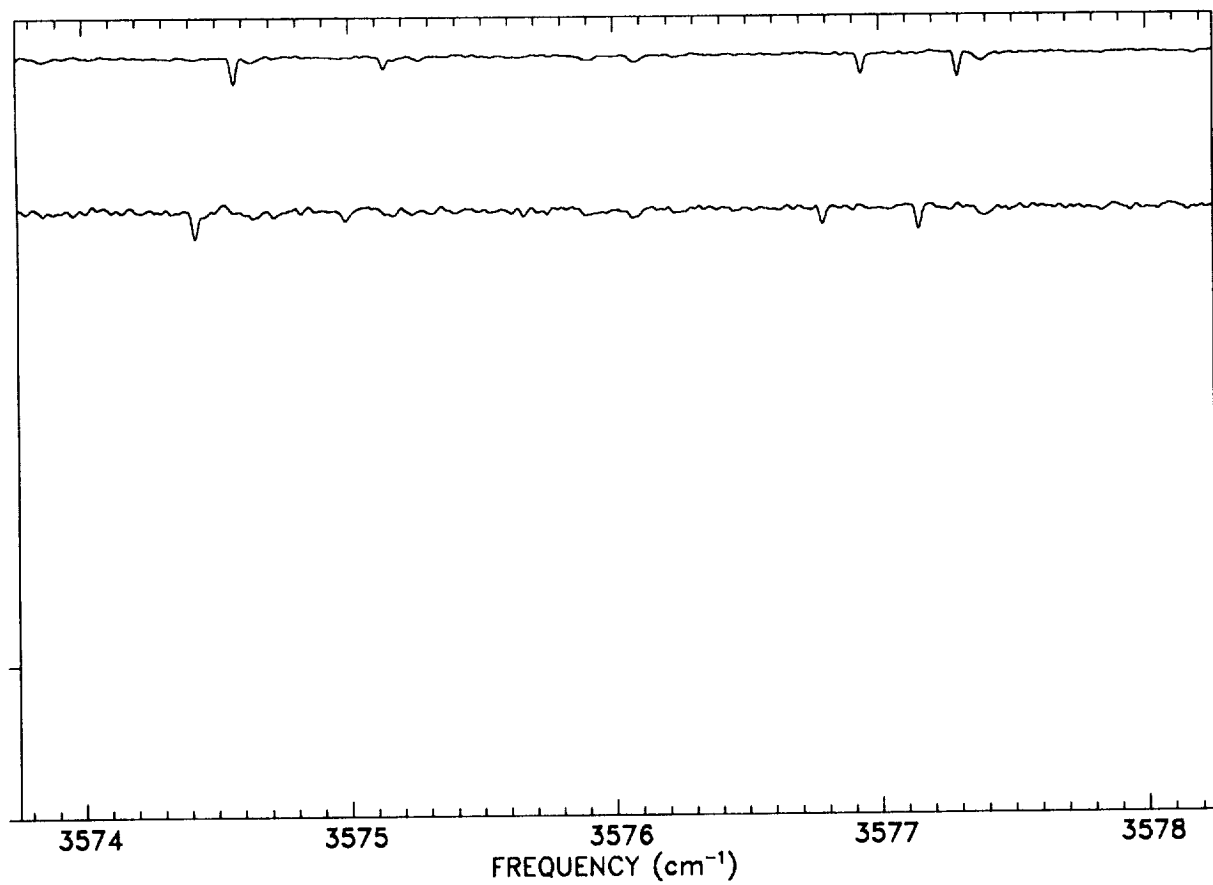


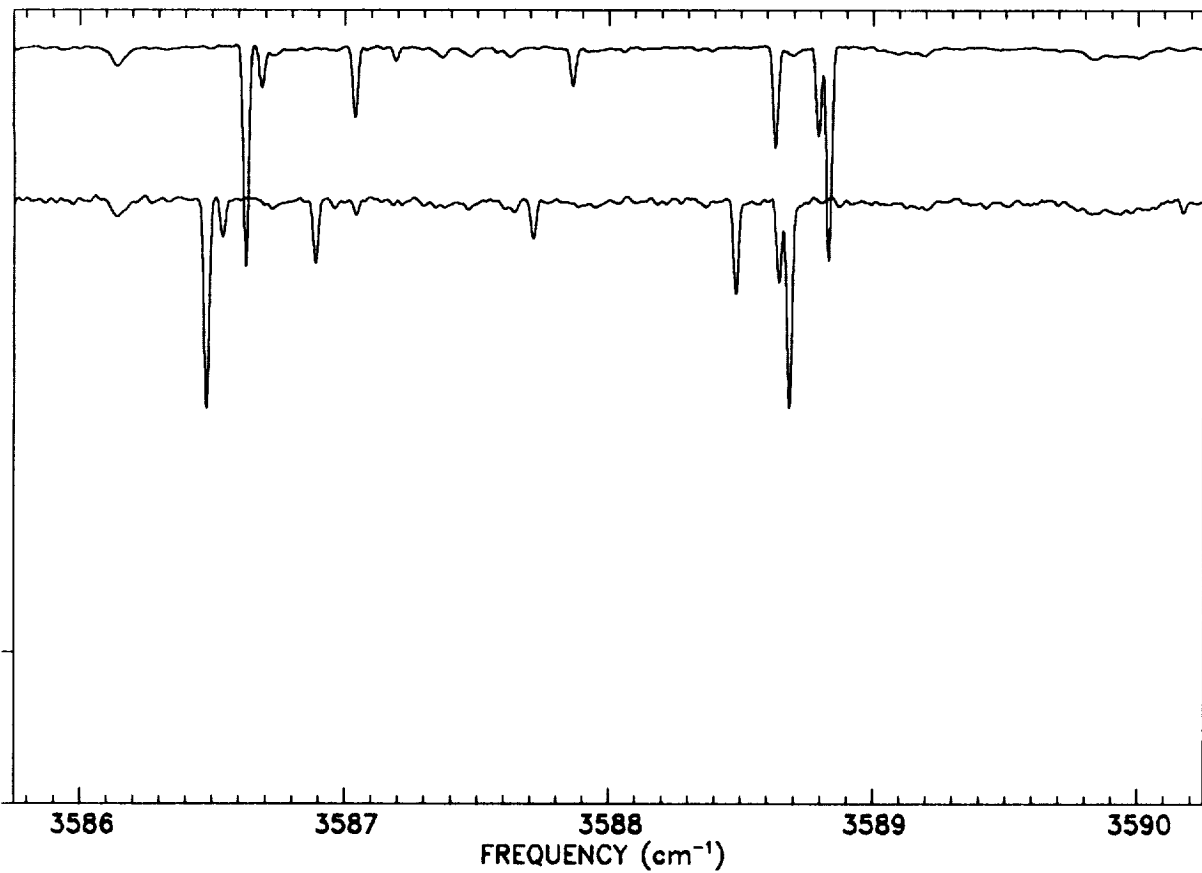
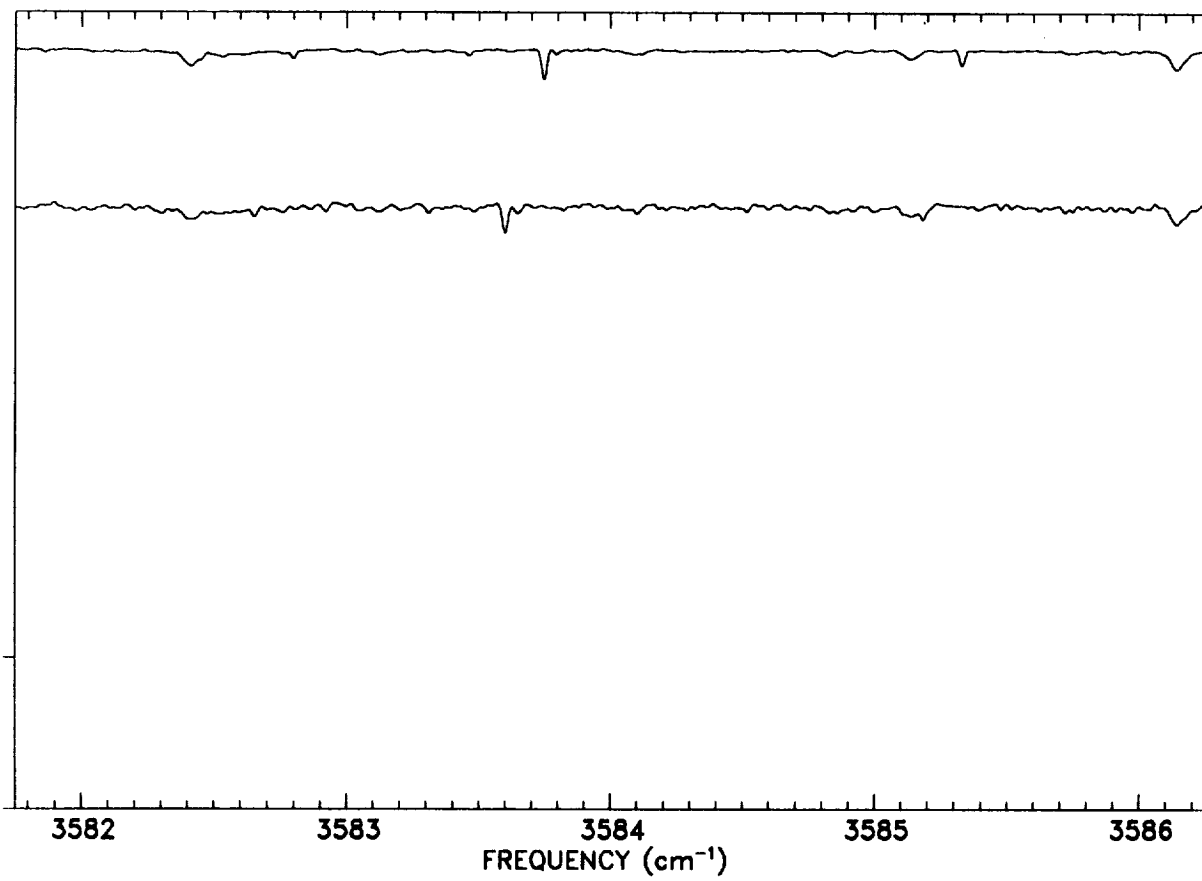


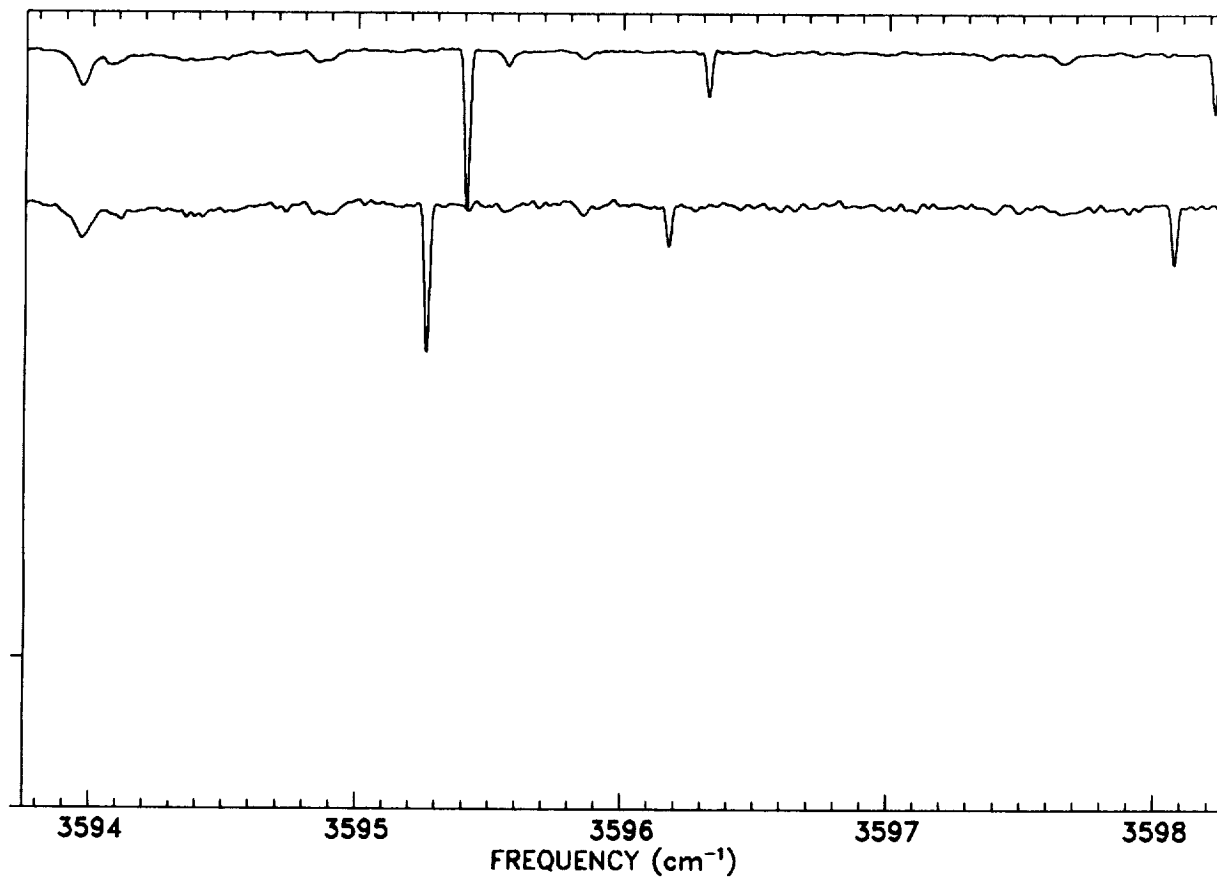
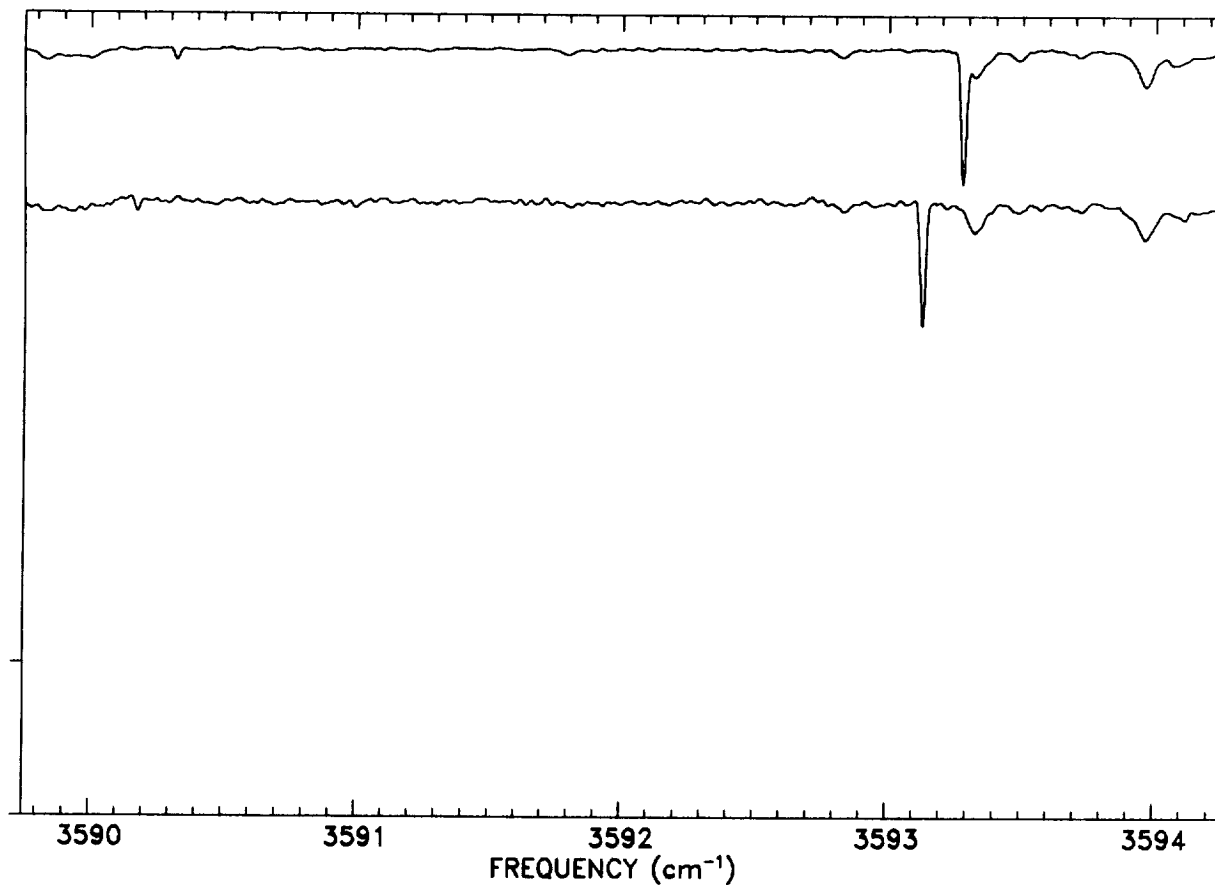


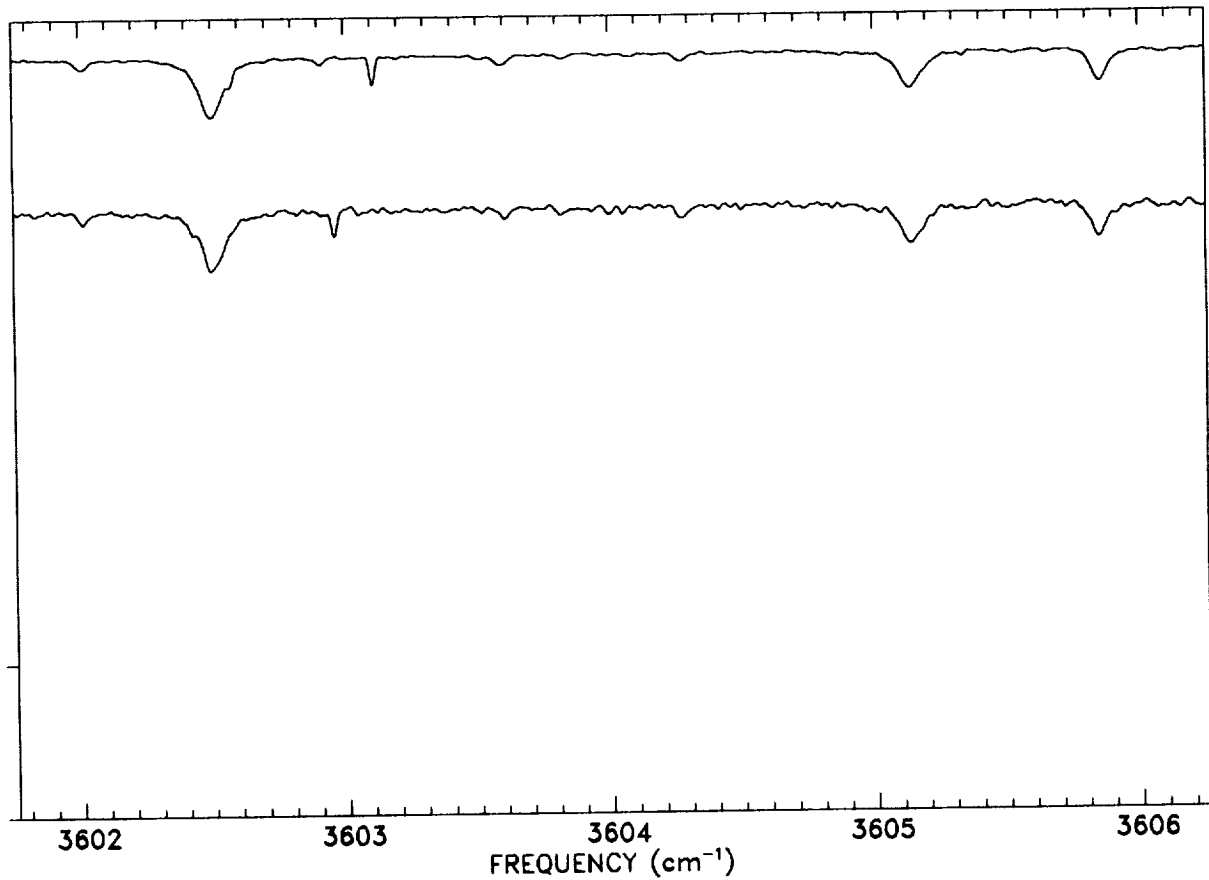
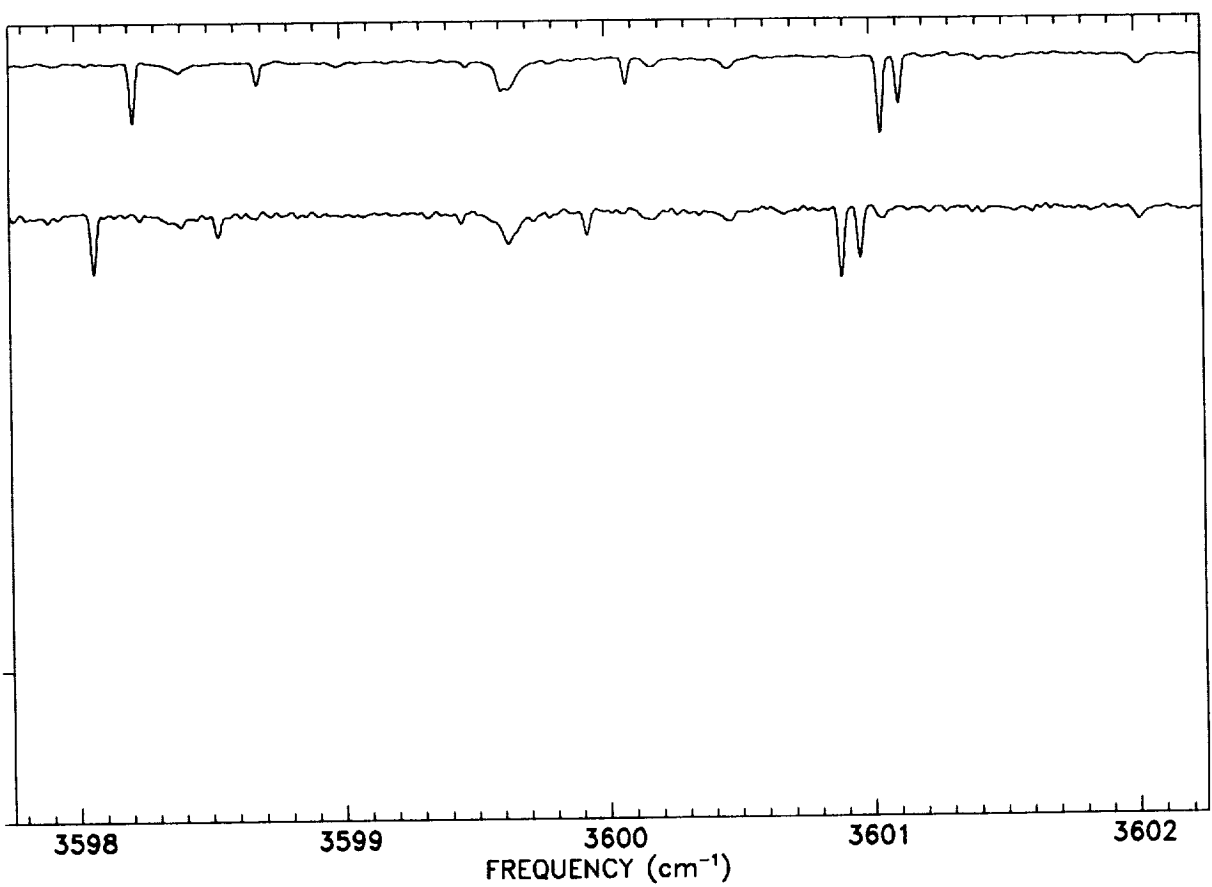


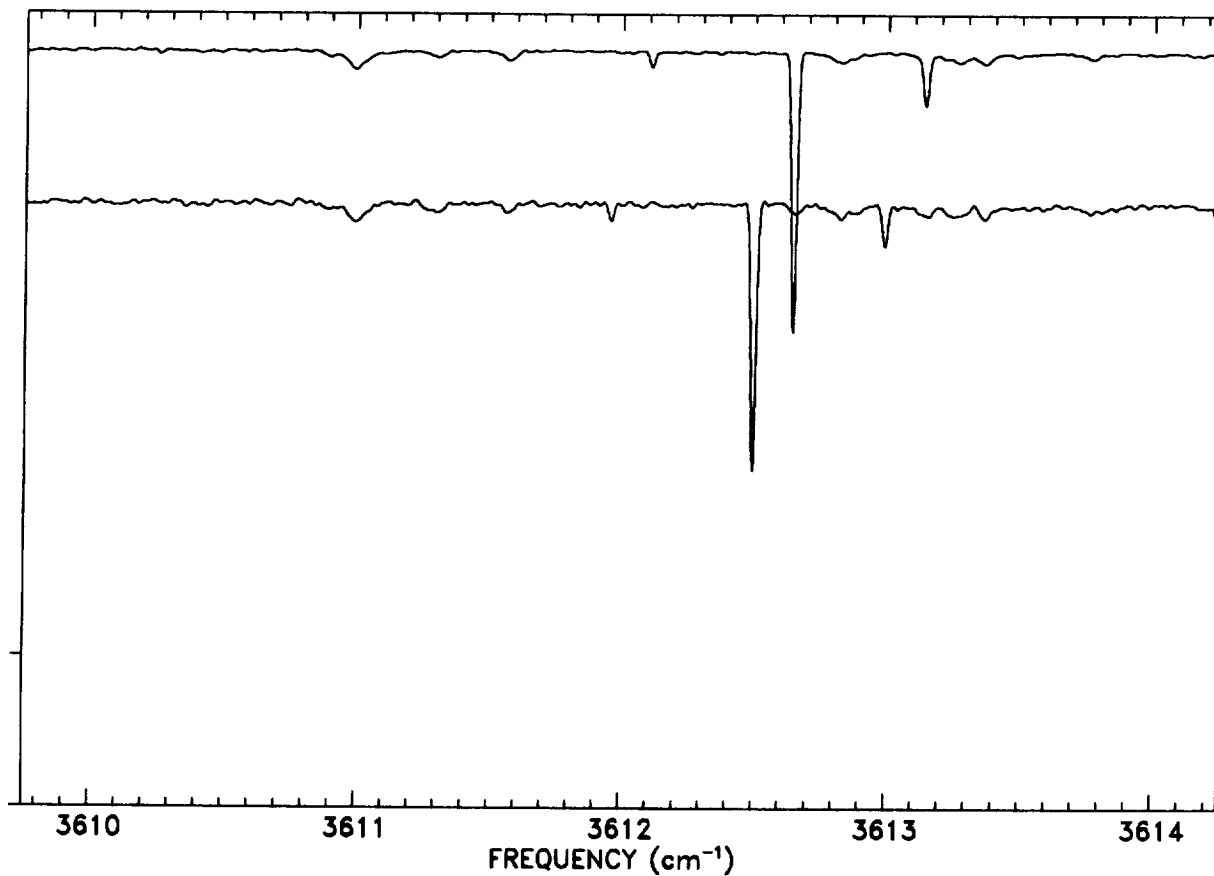
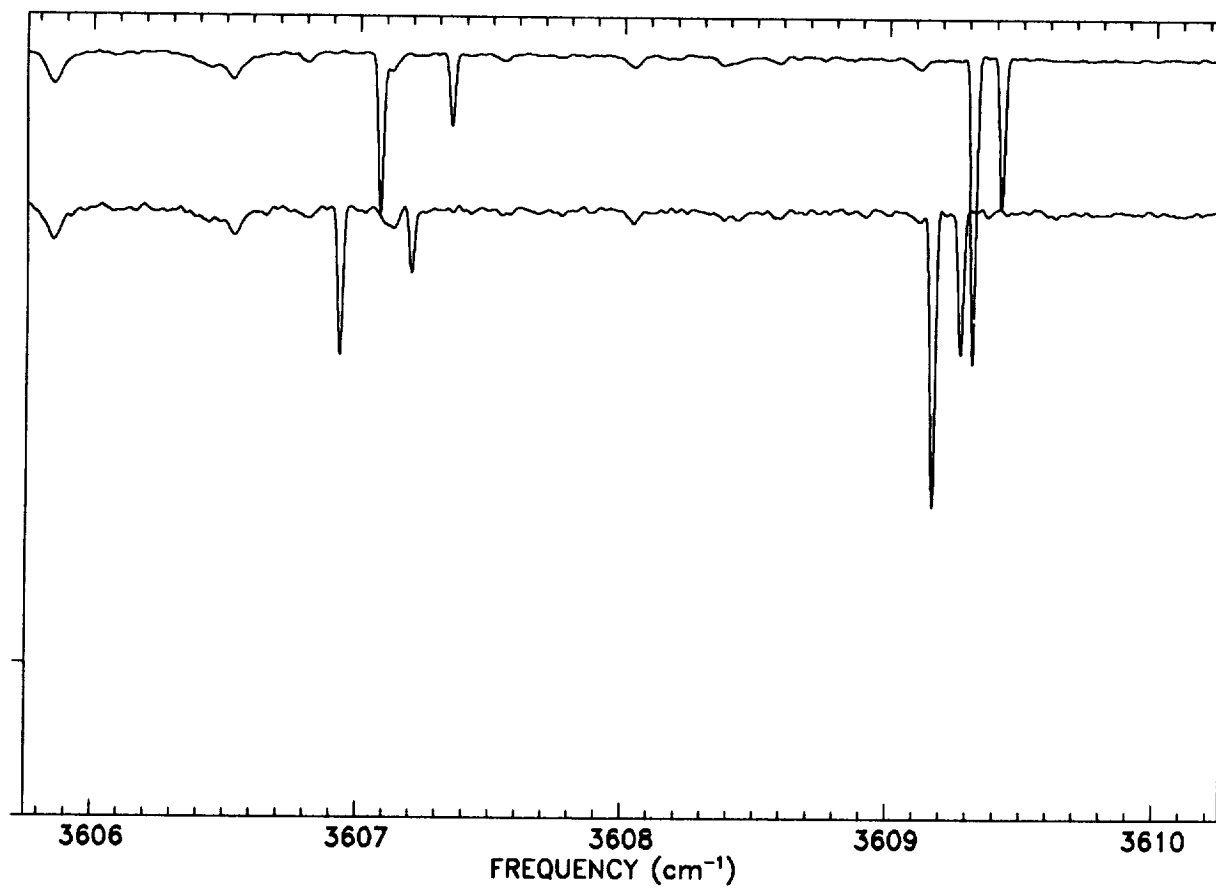


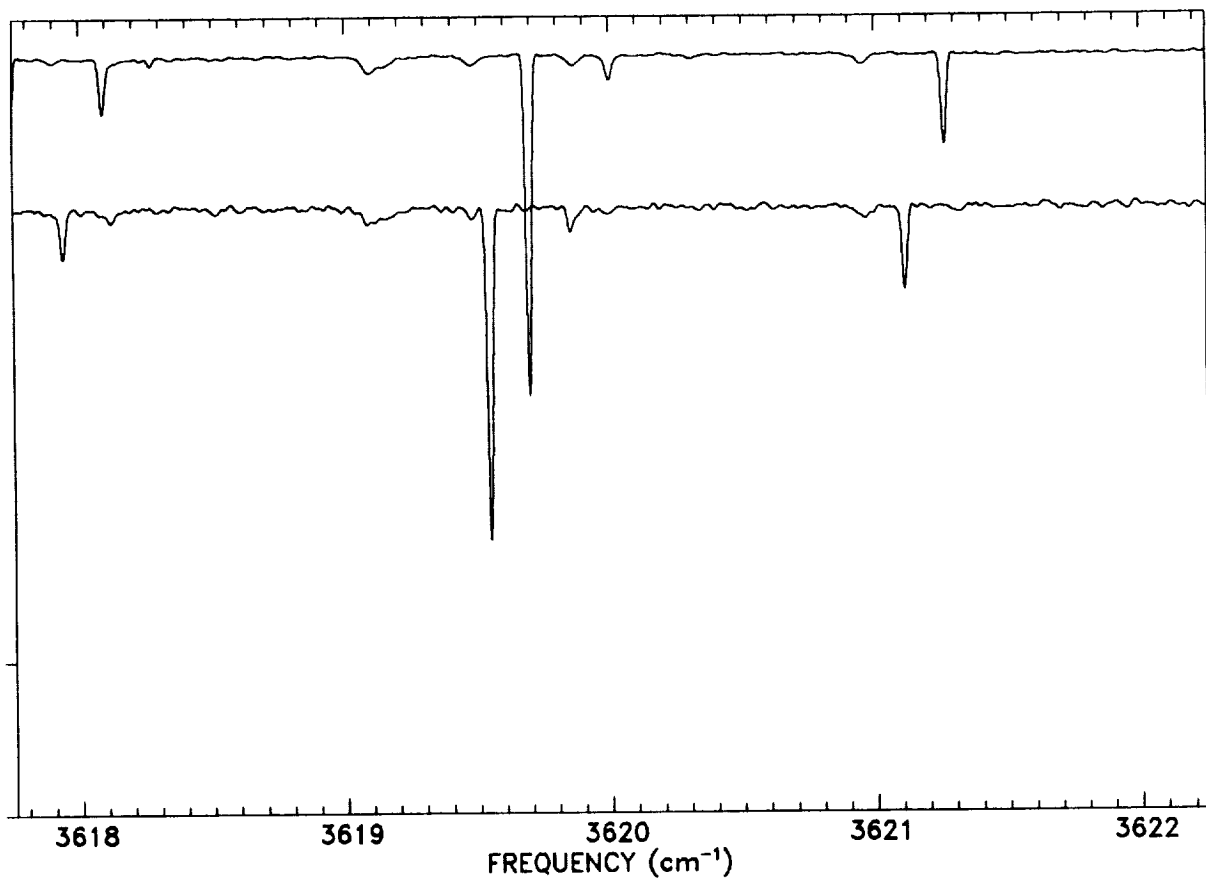
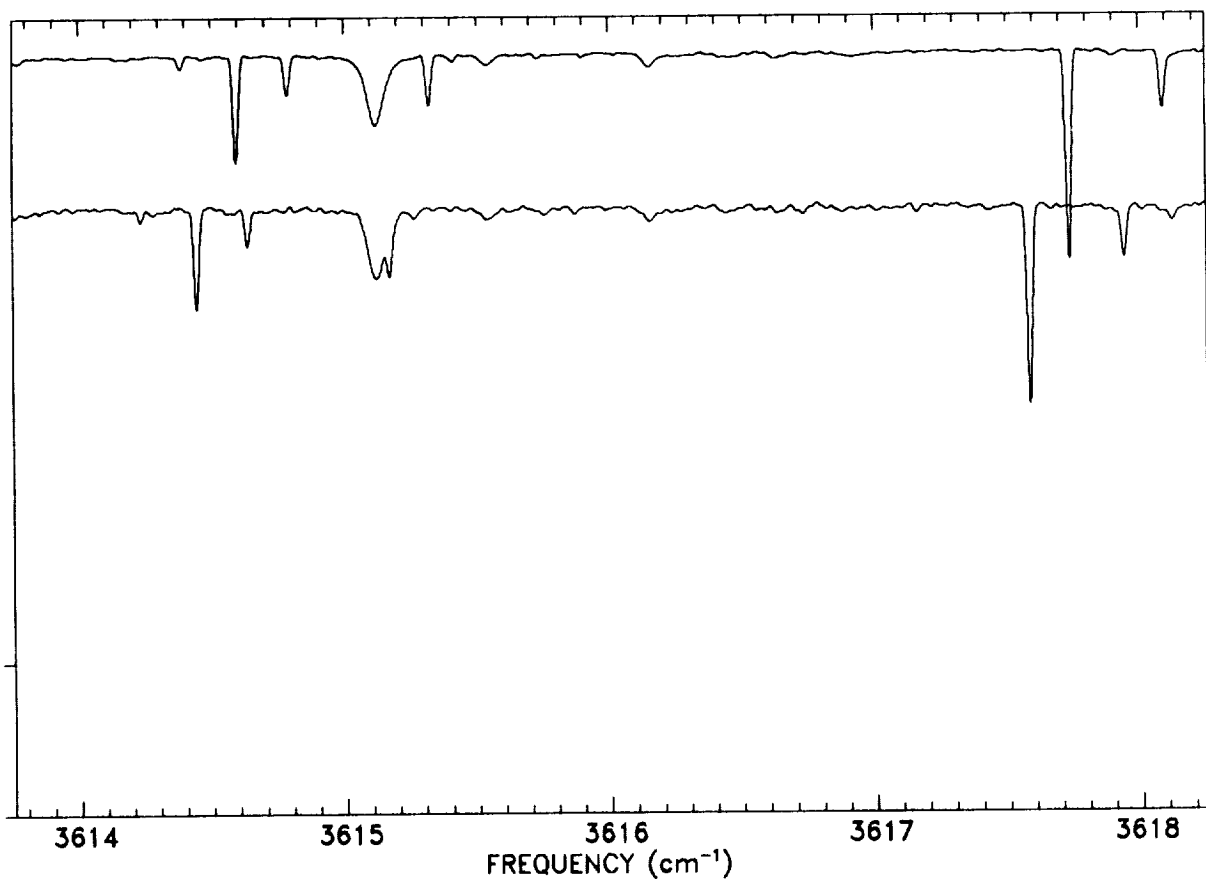


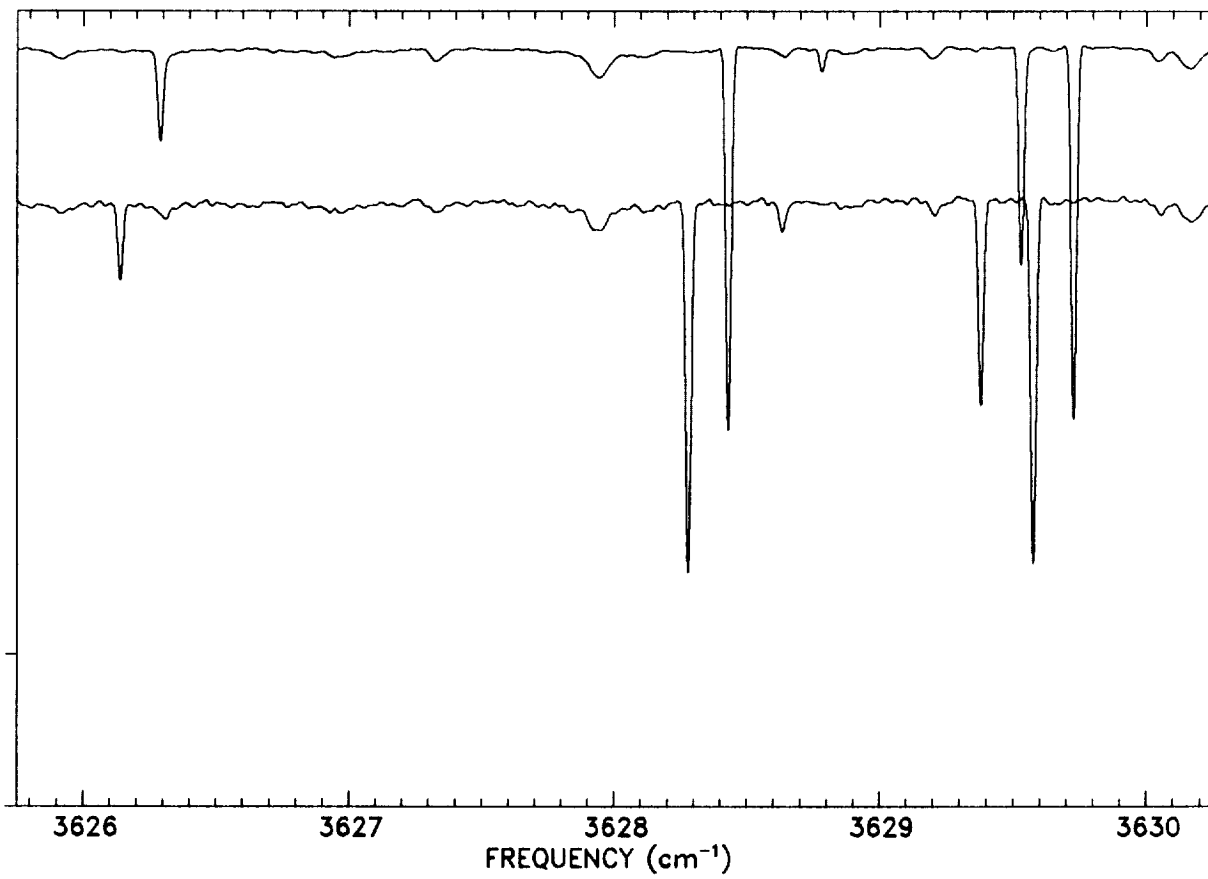
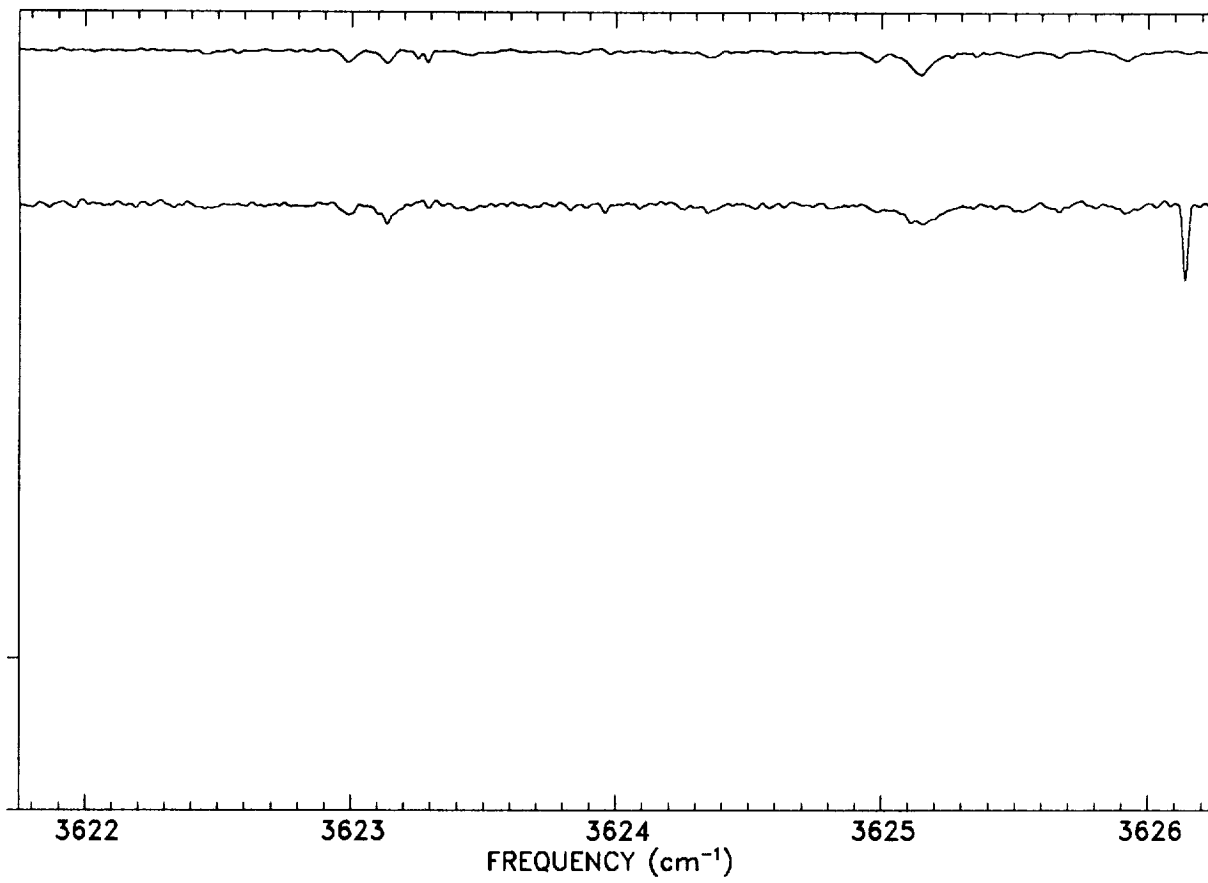


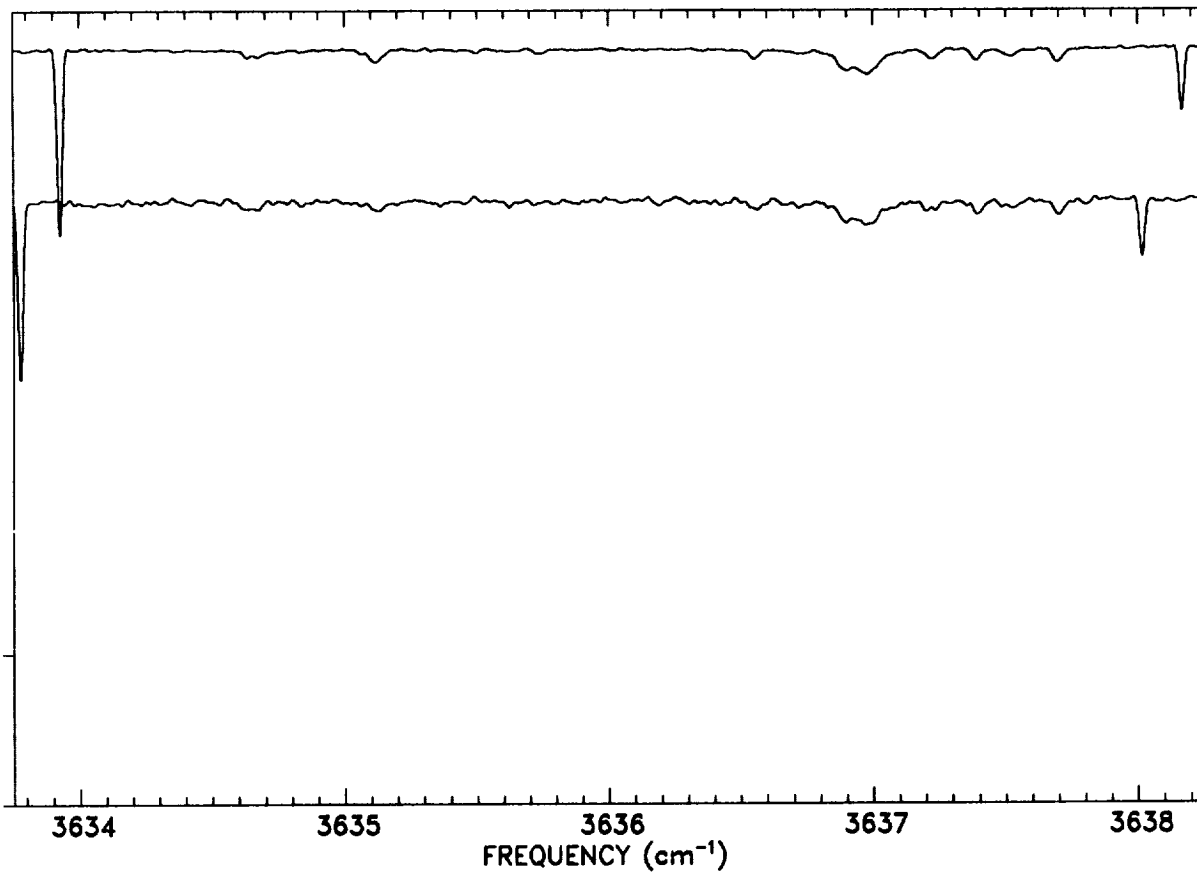
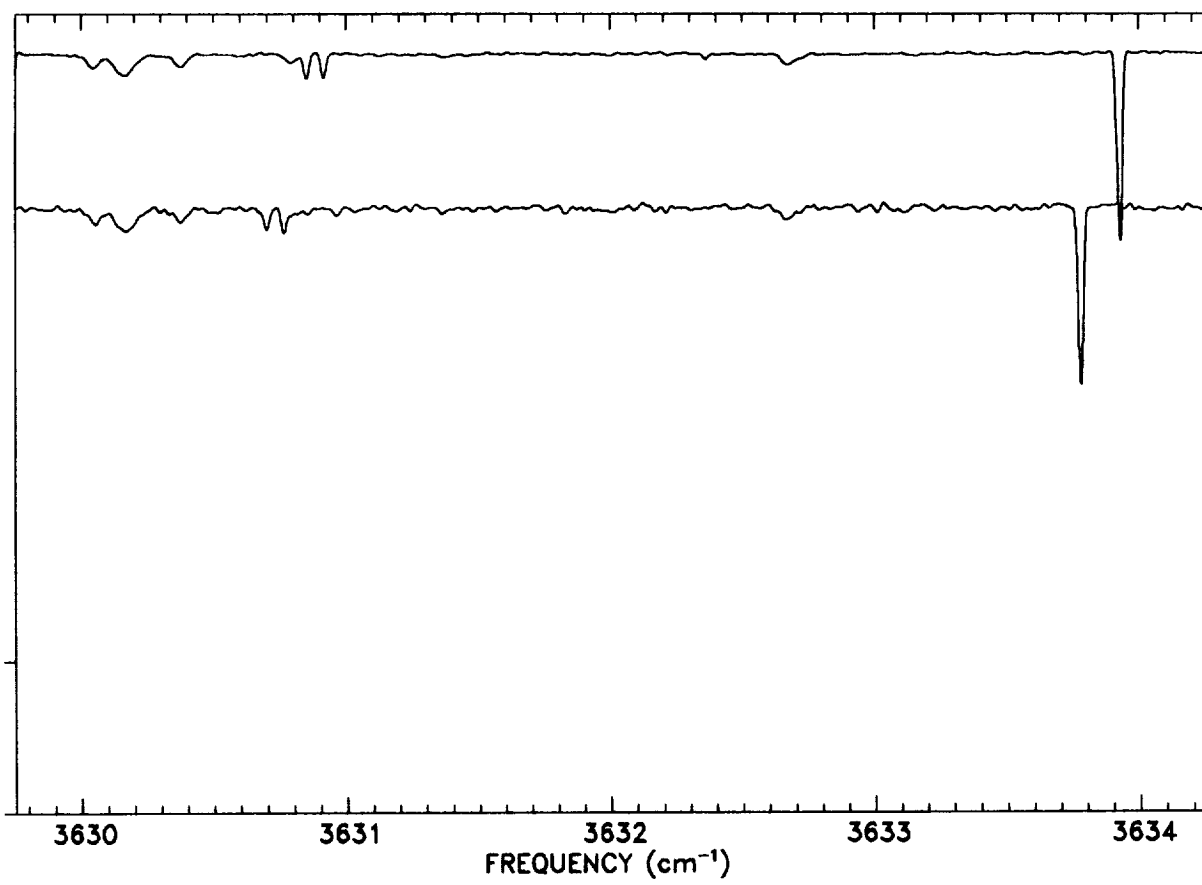


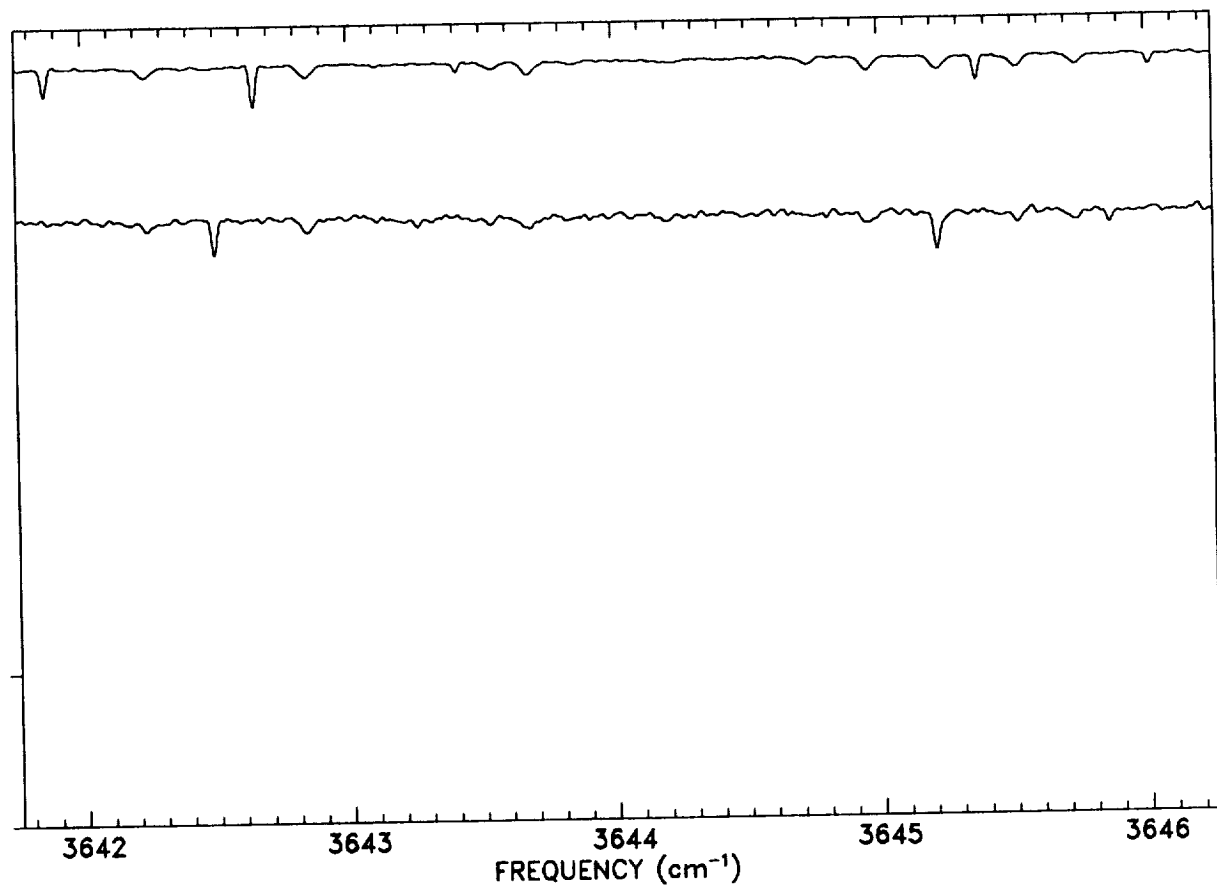
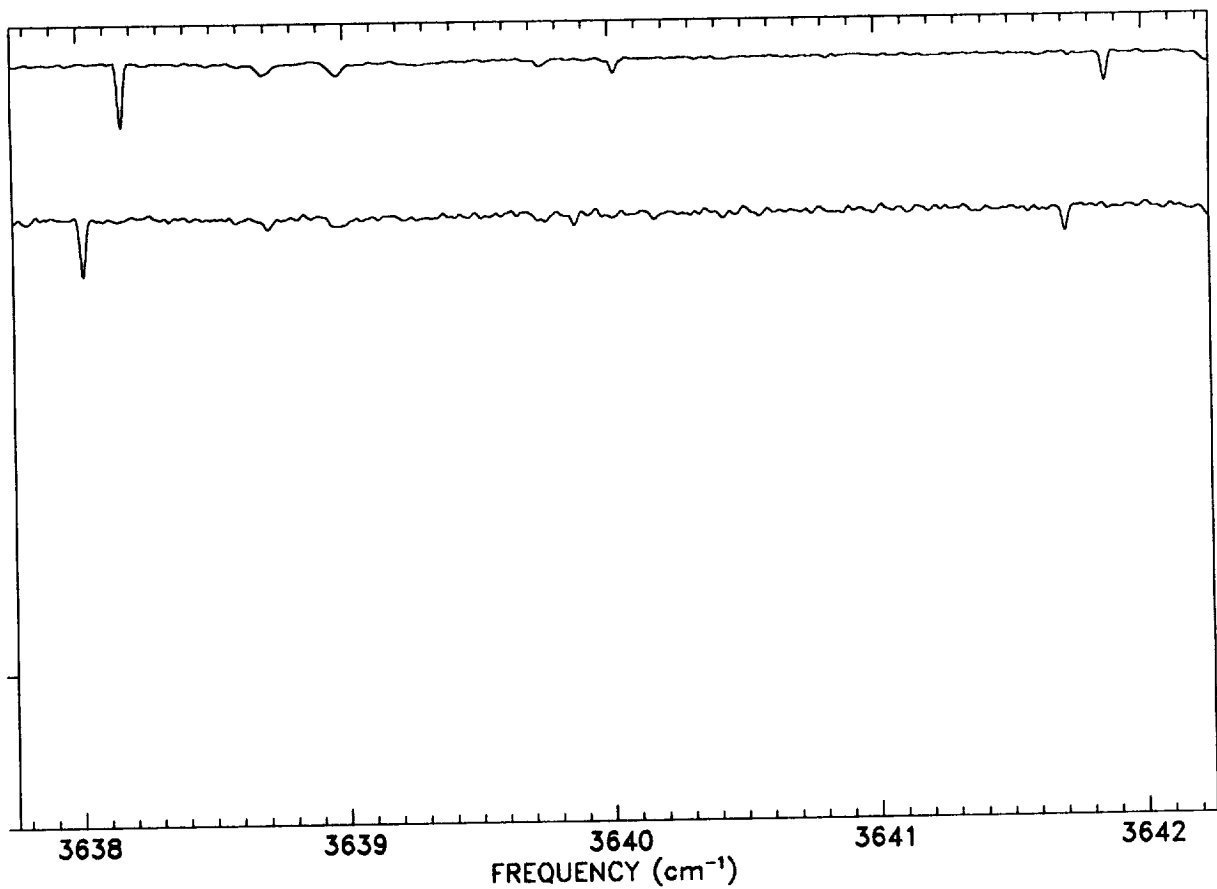




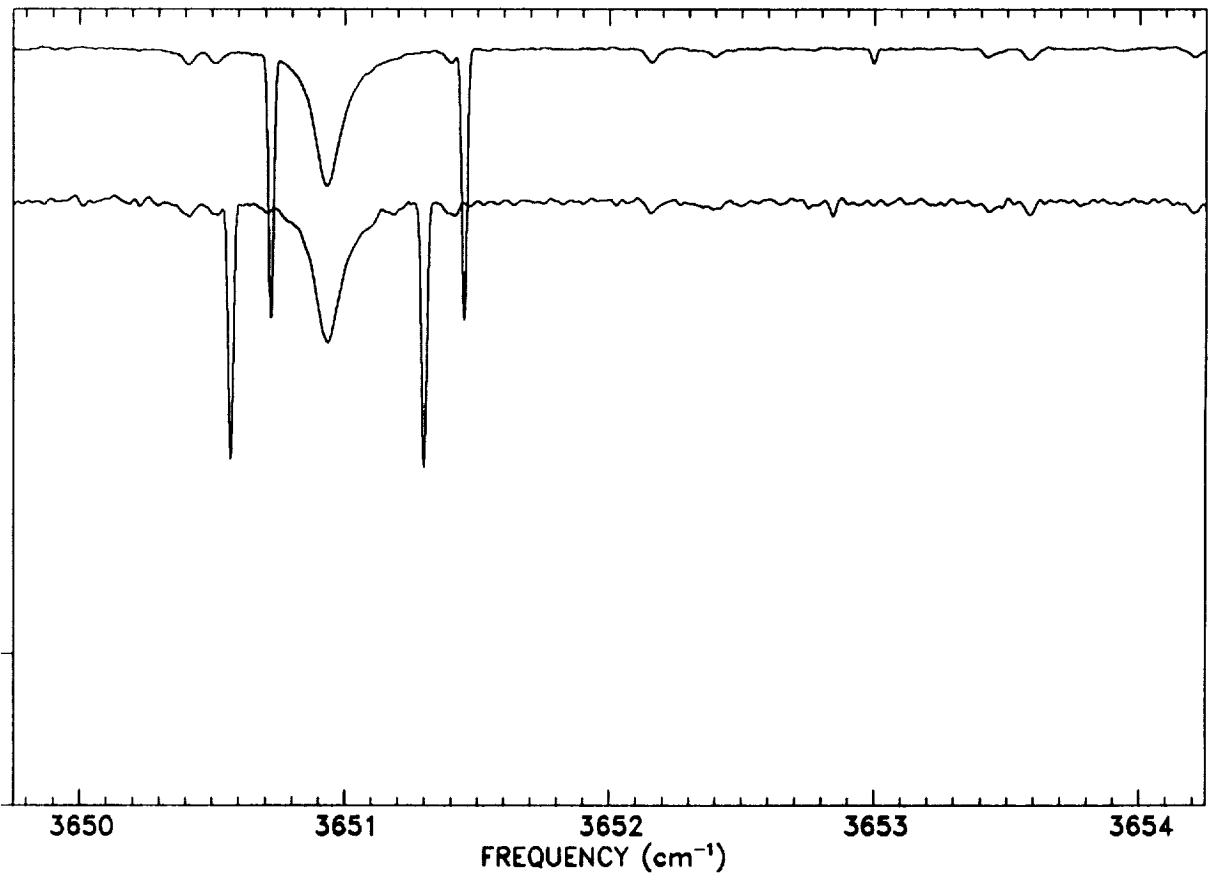
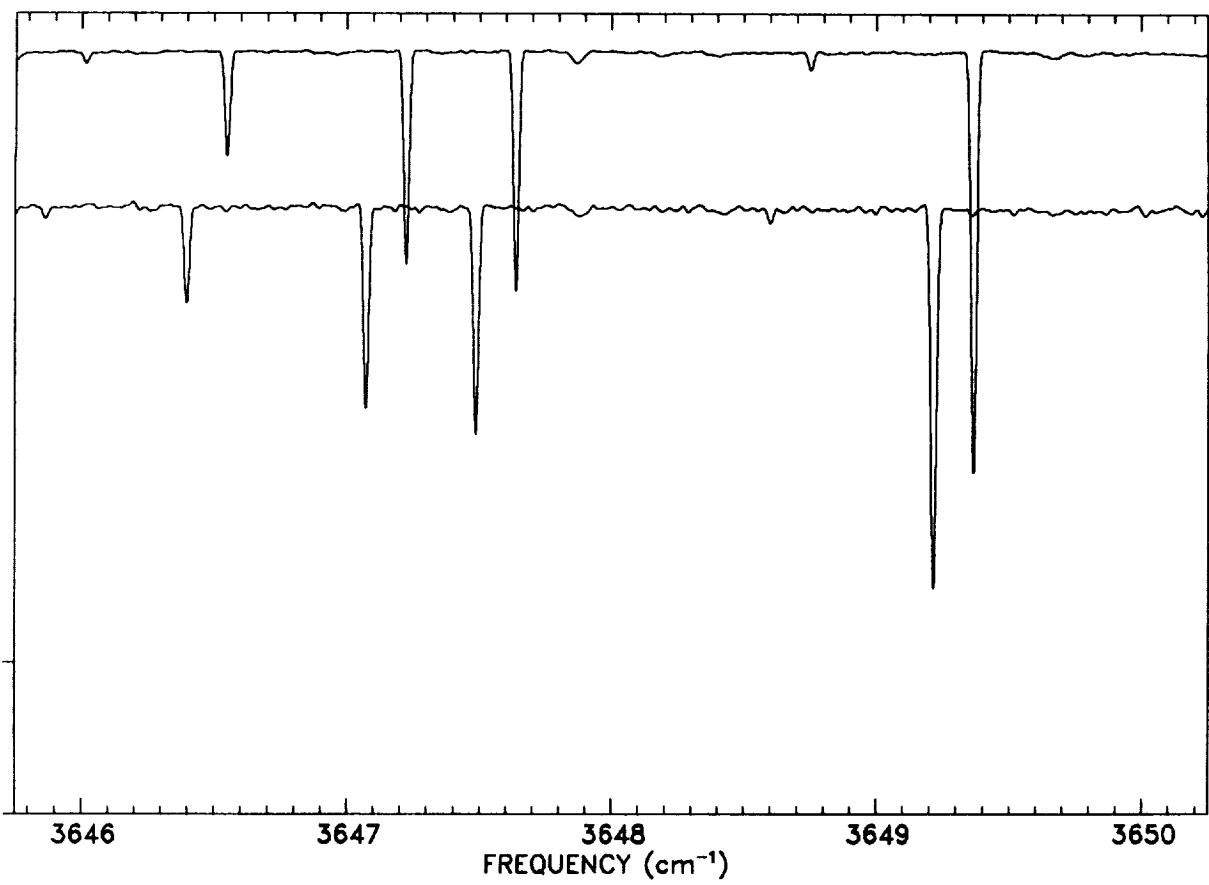


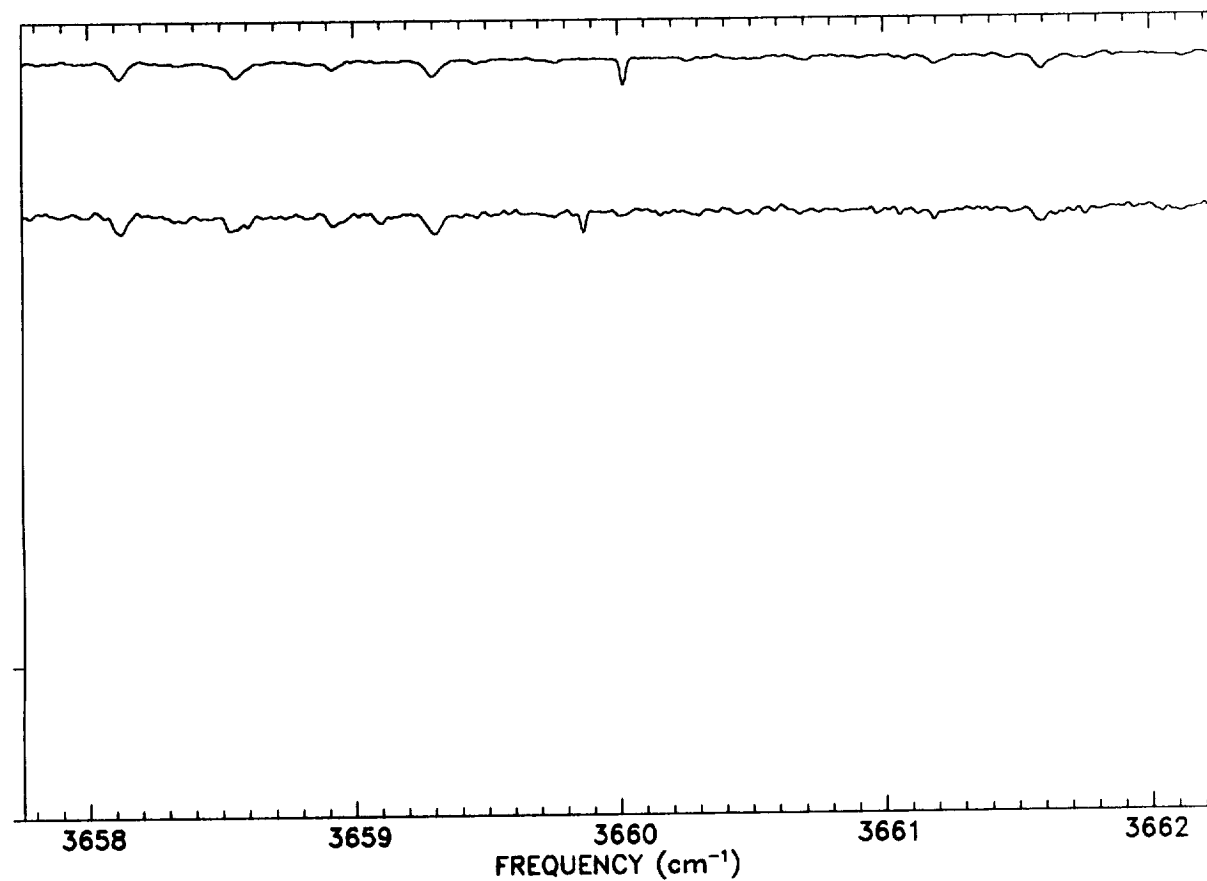
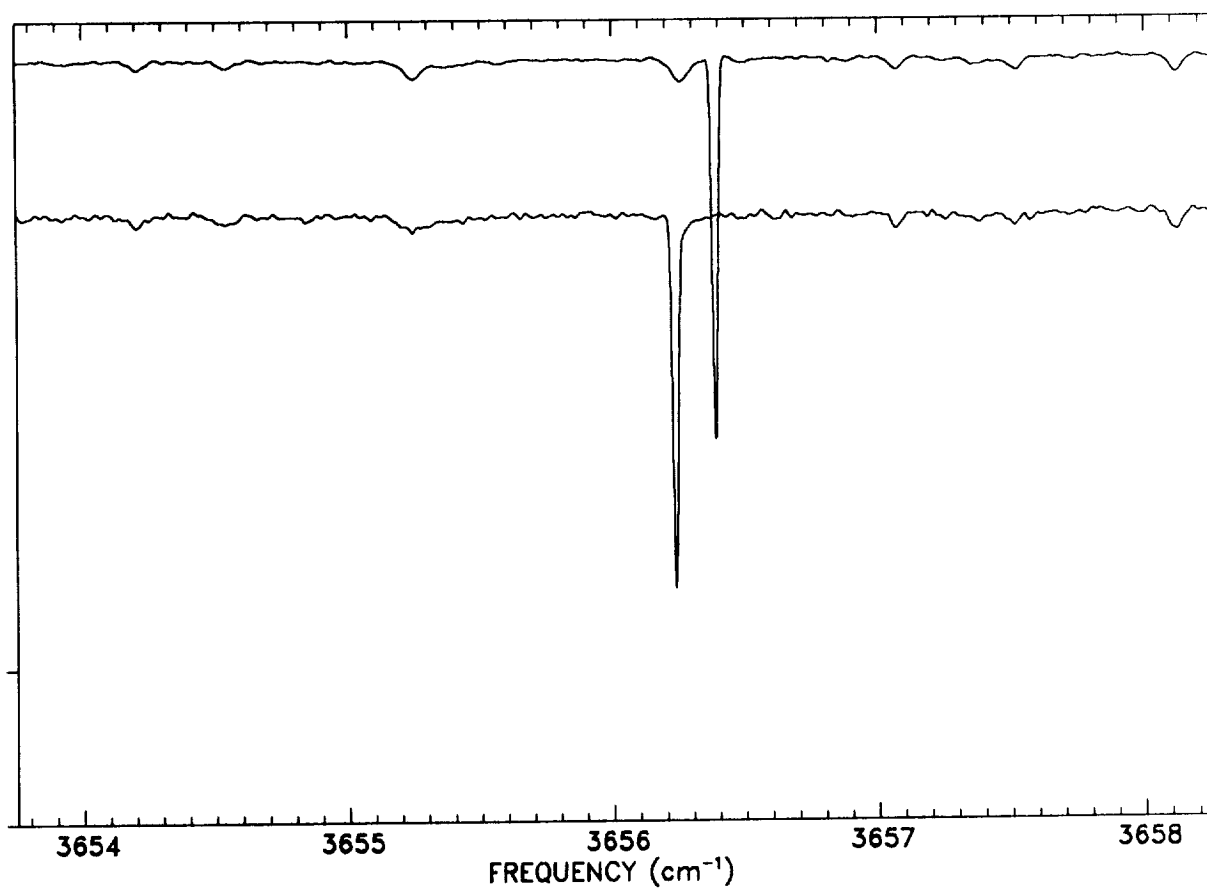


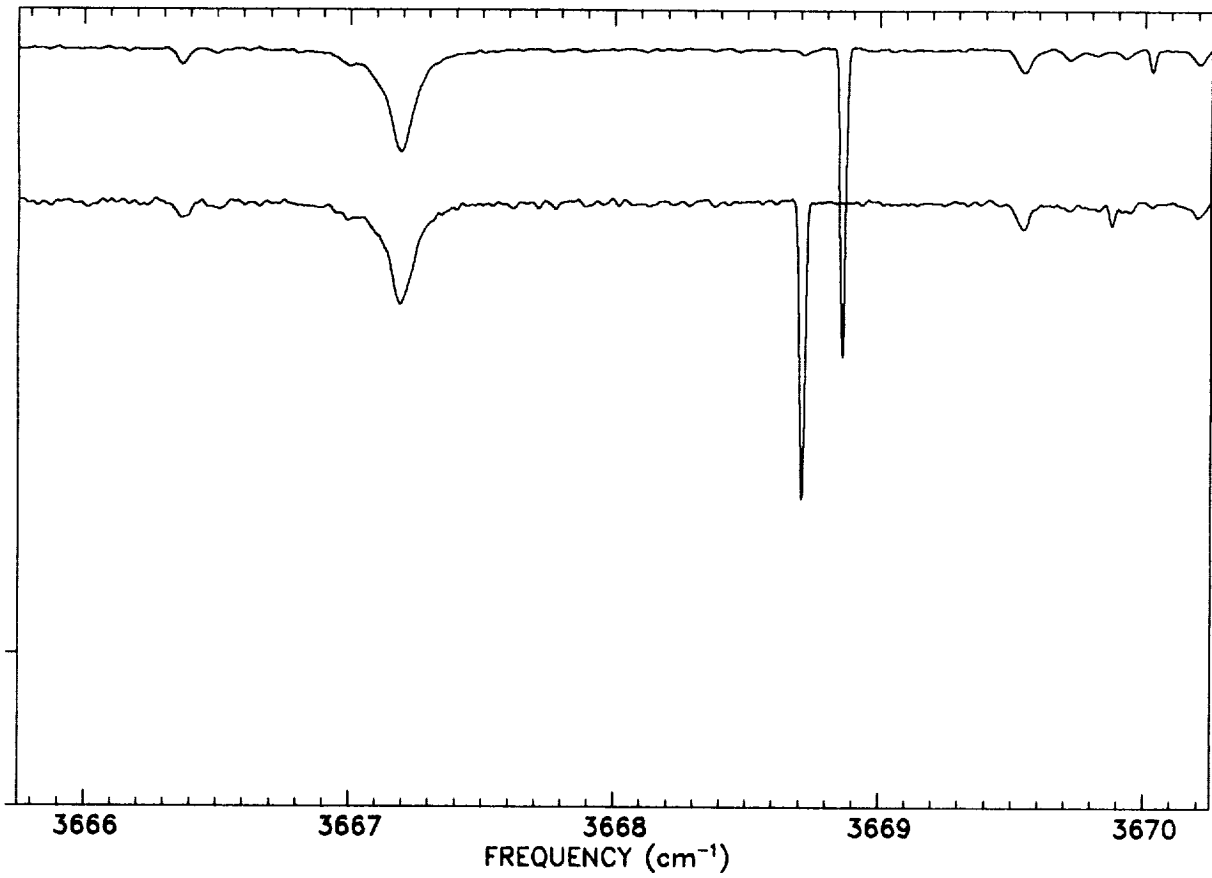
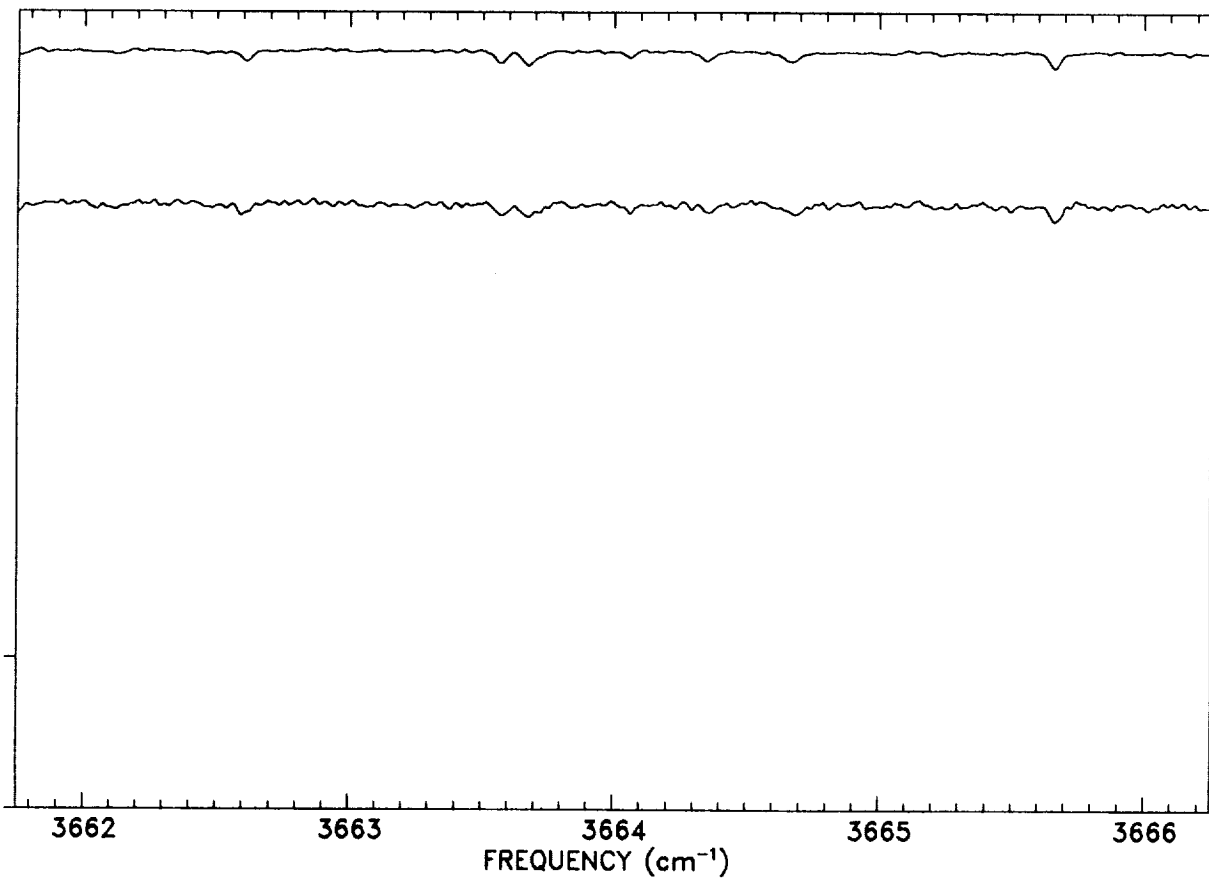


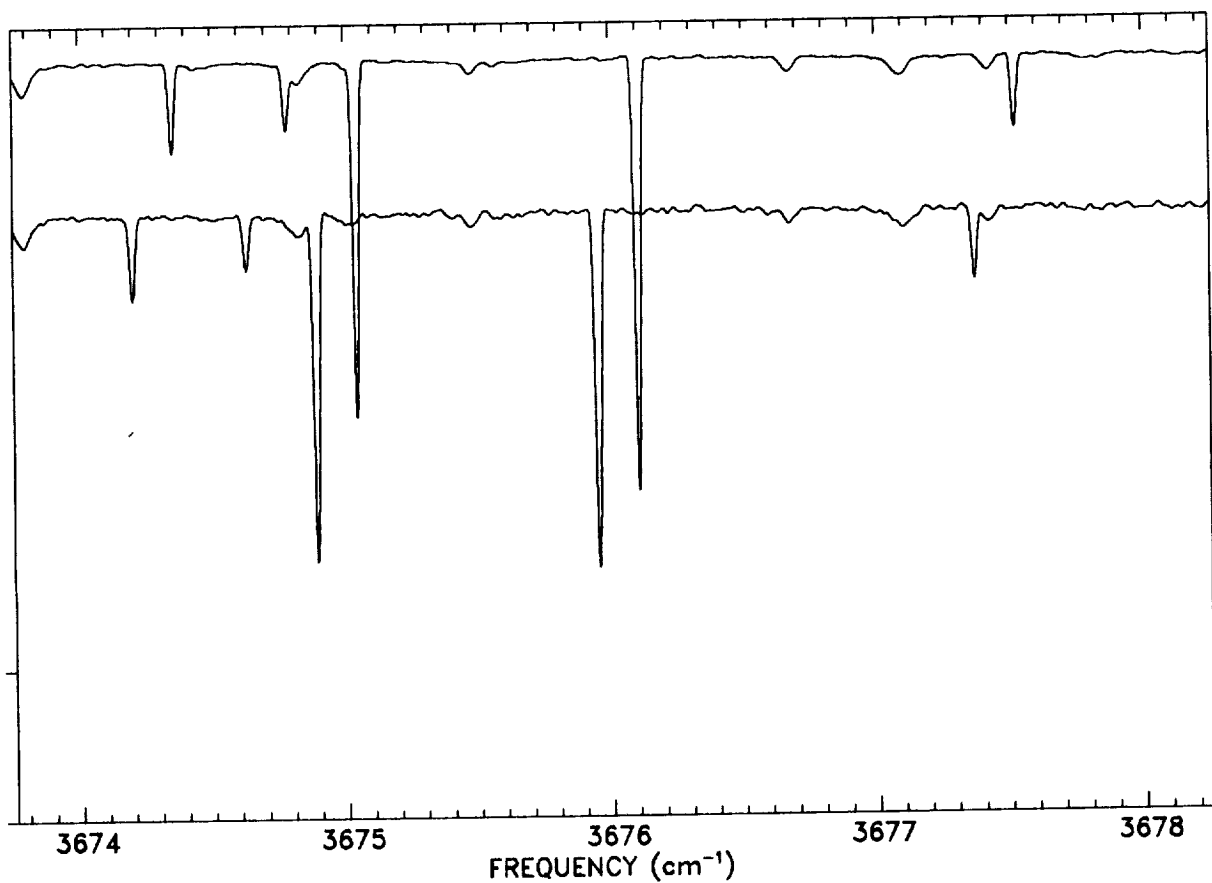
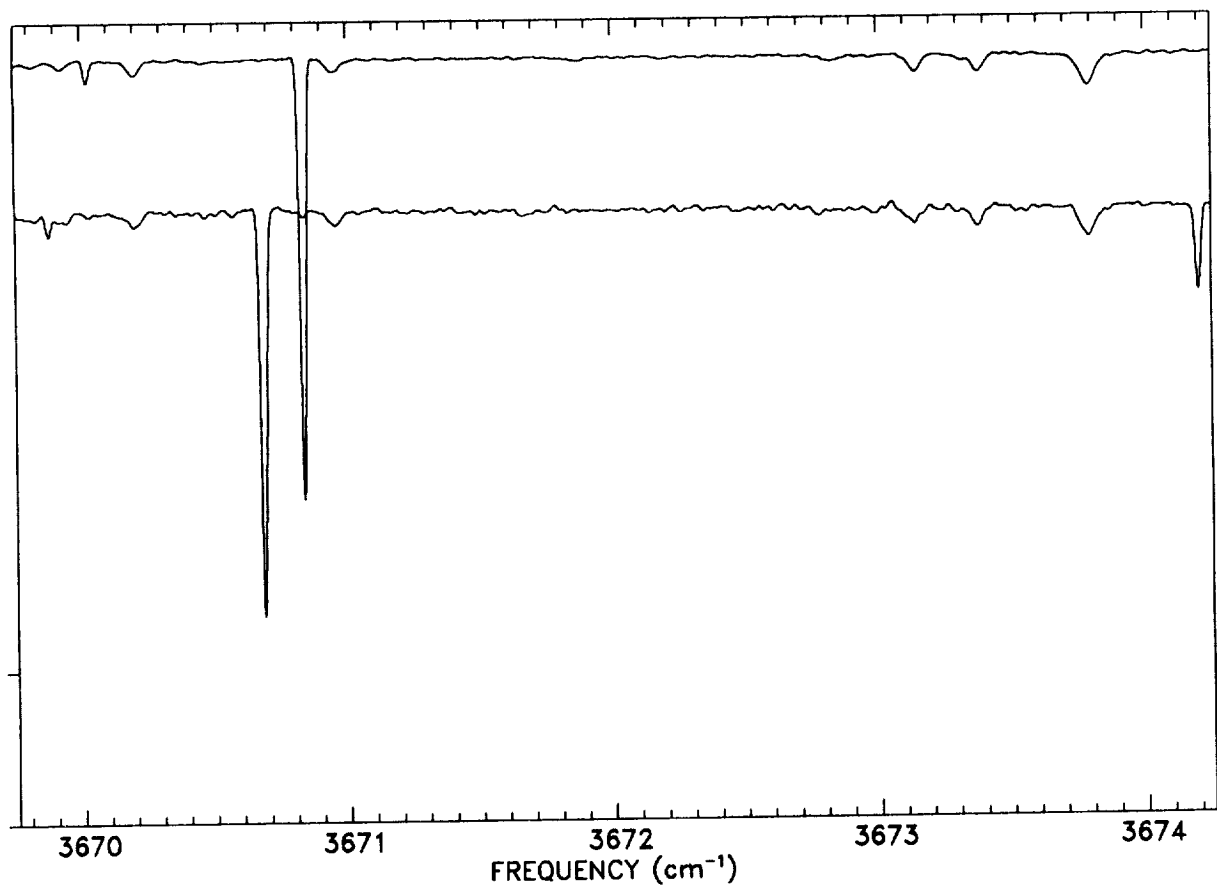


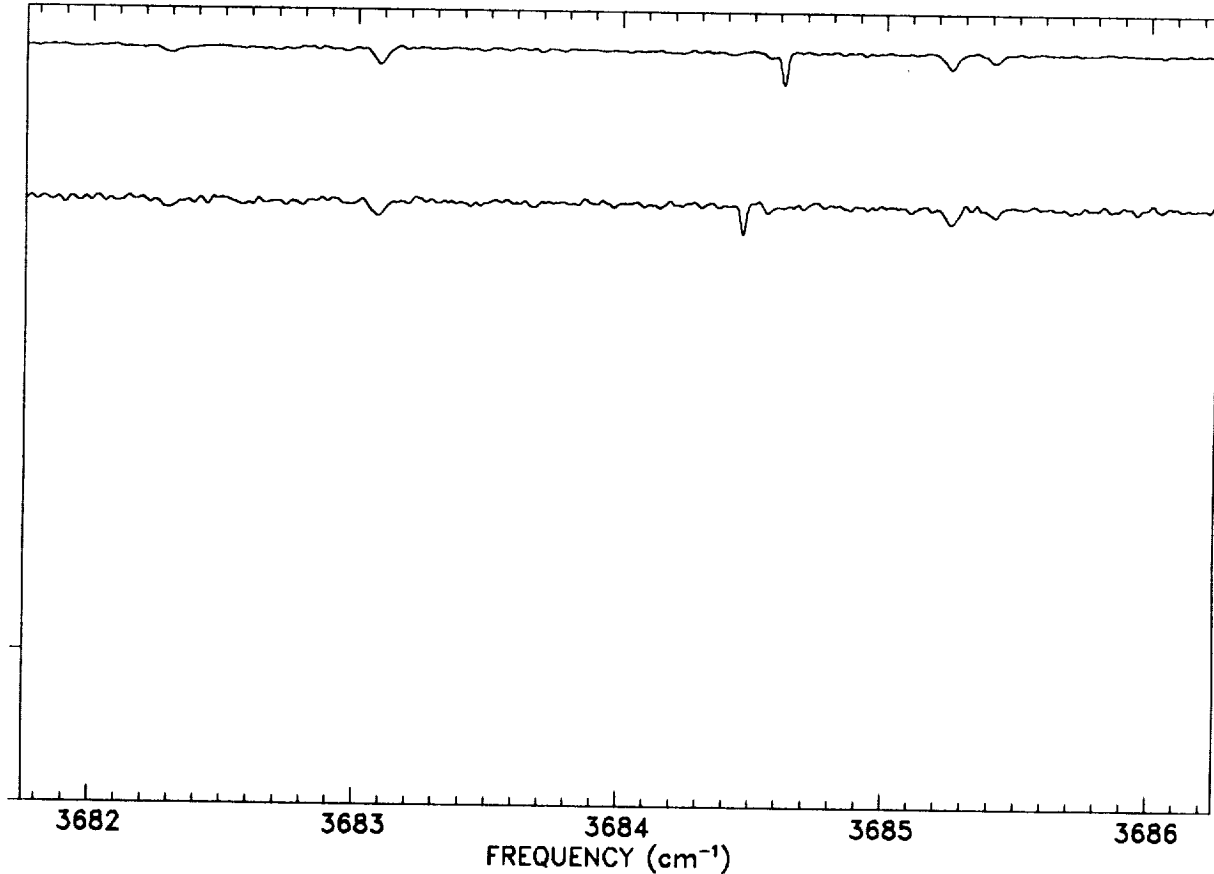
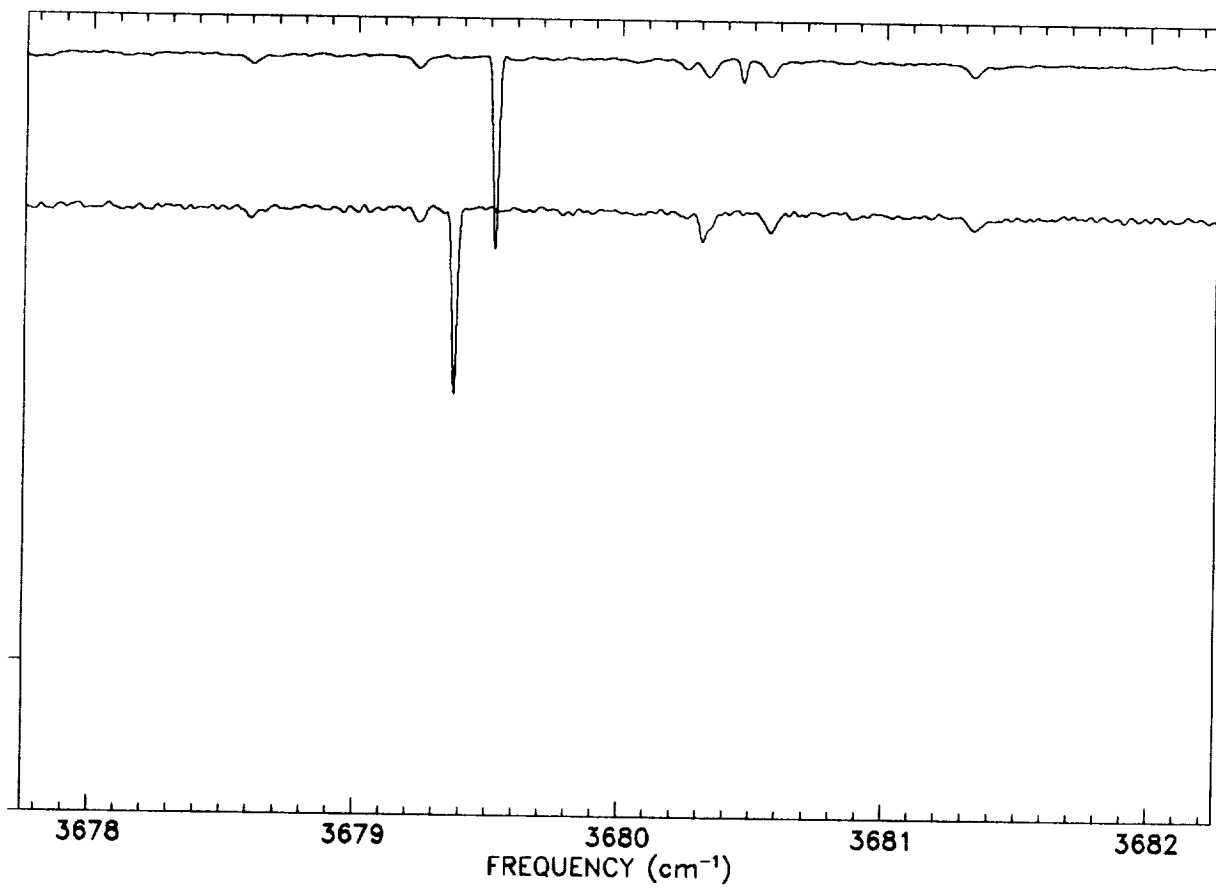
C - S

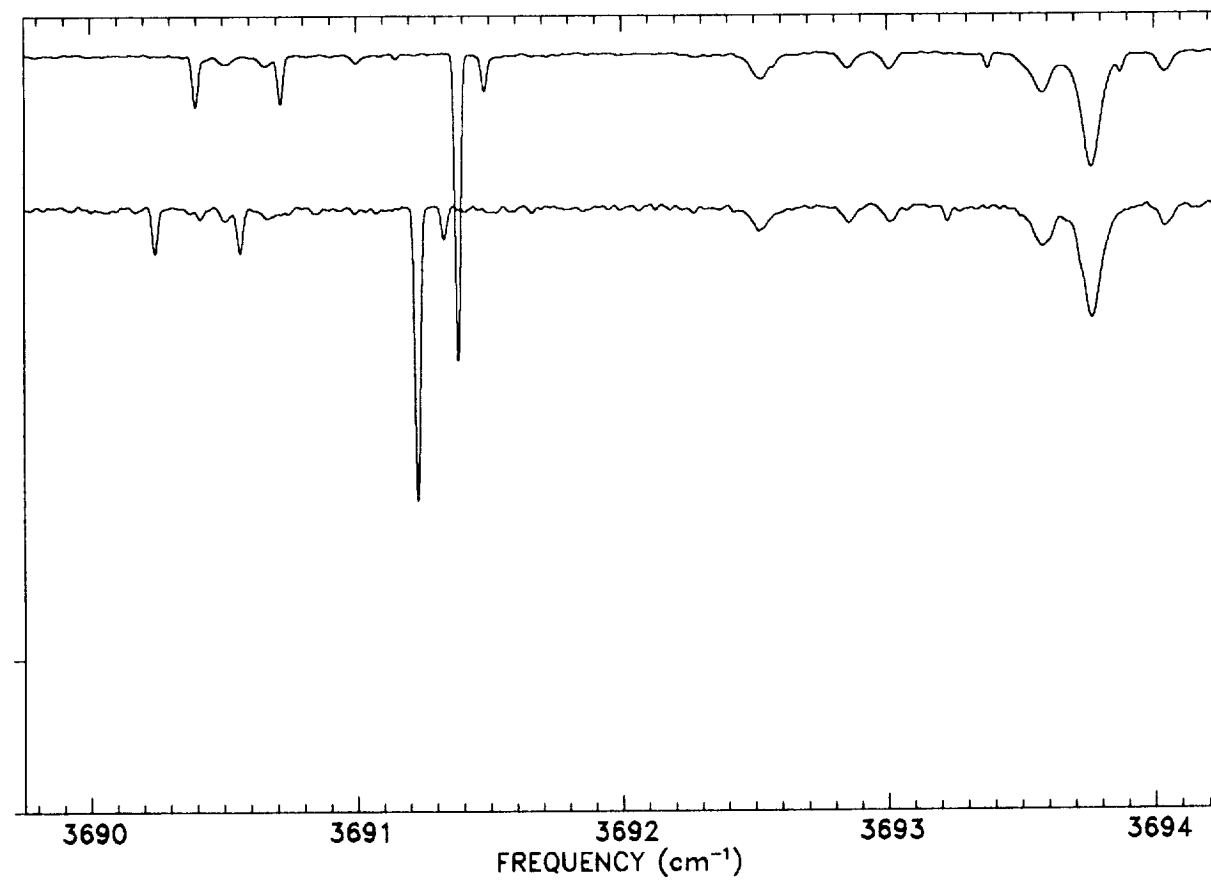
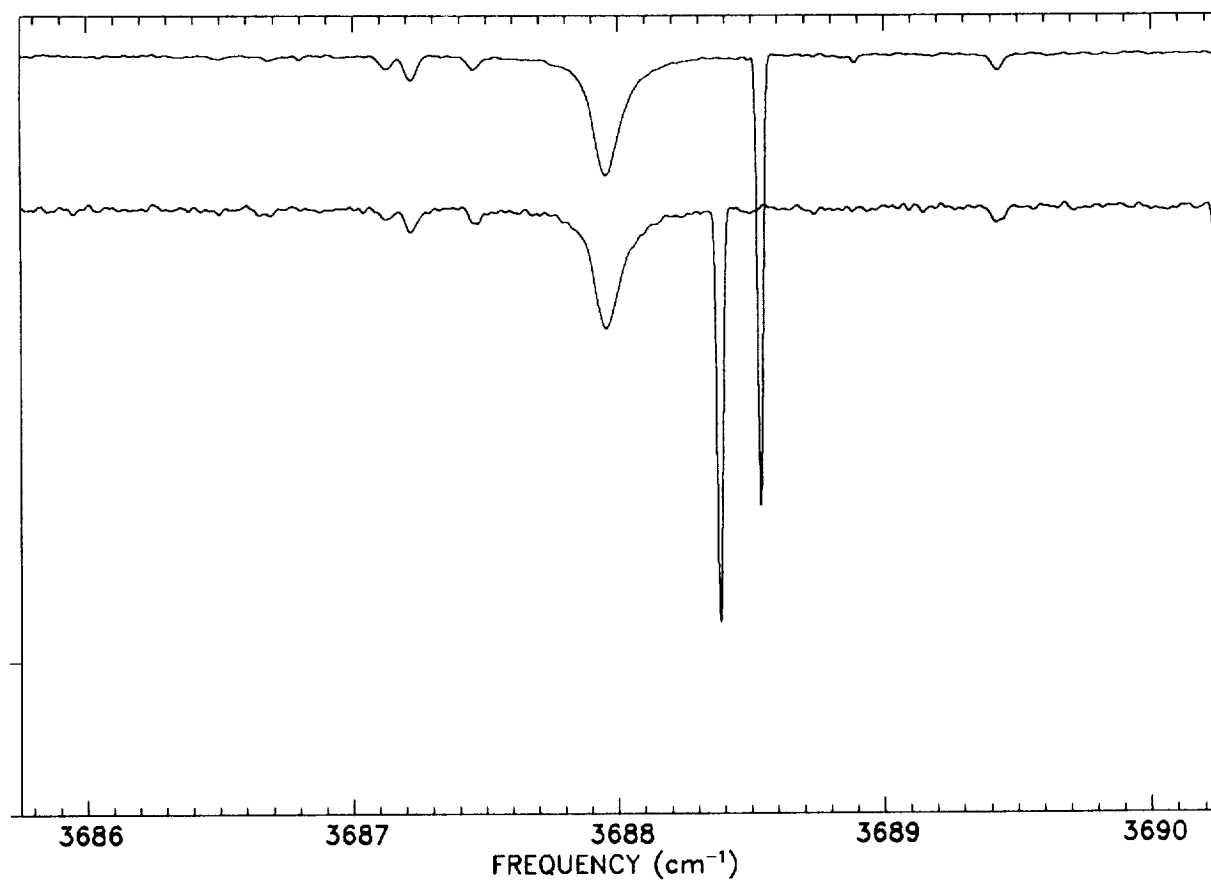


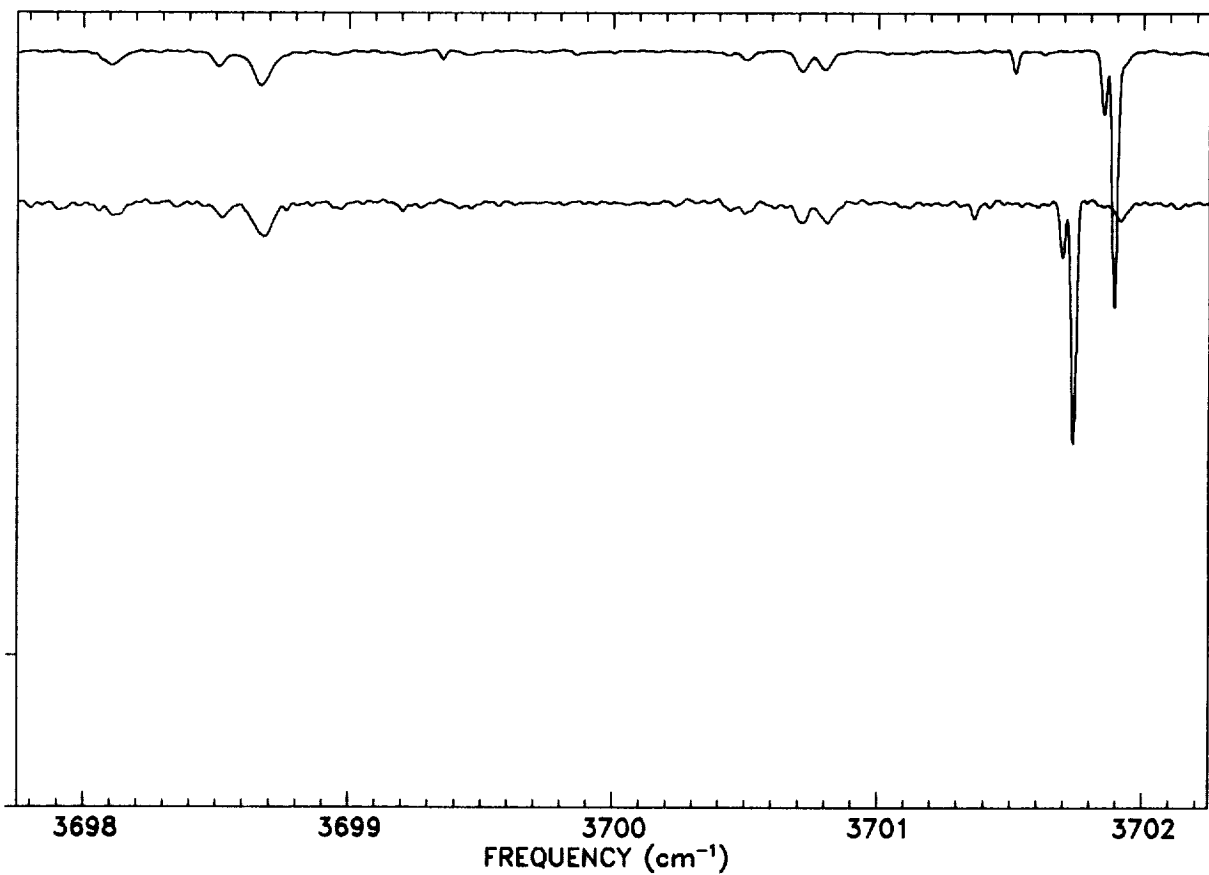
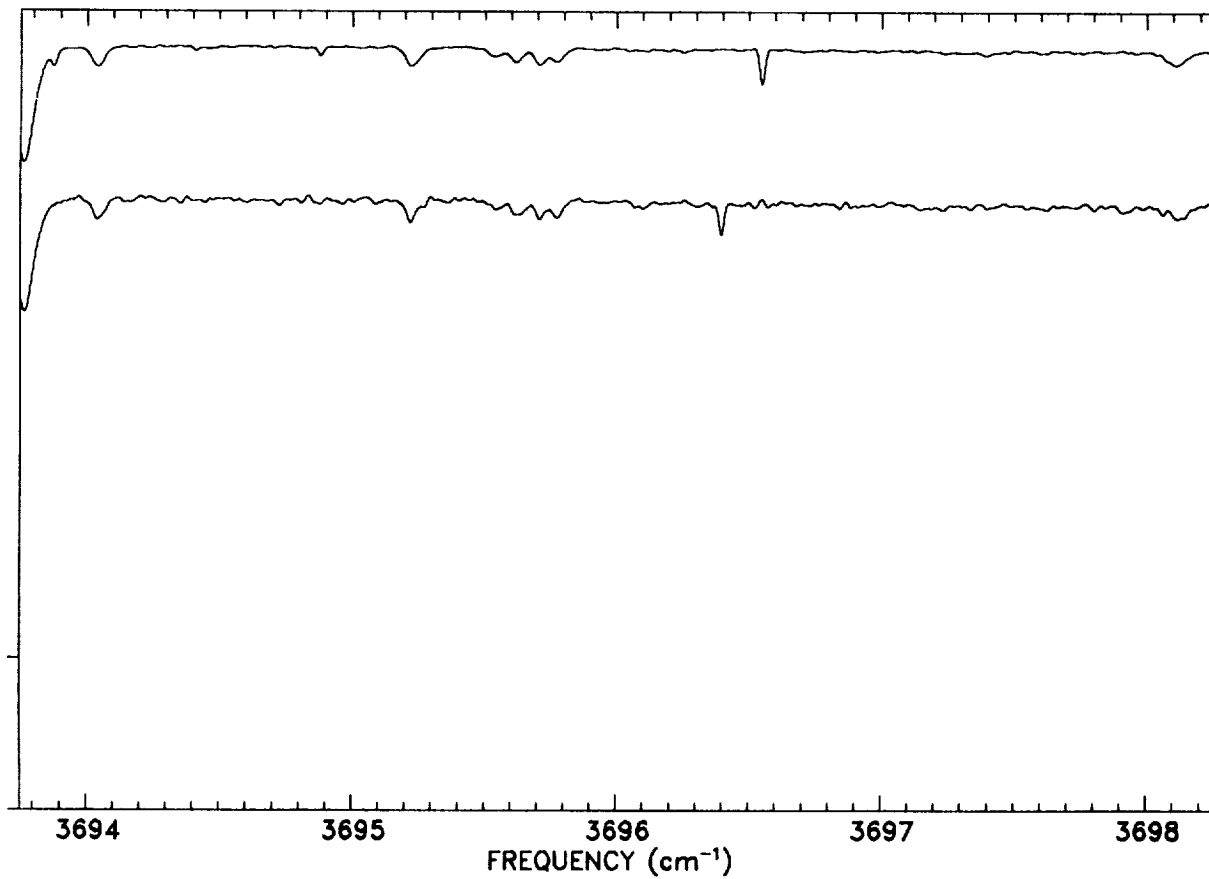


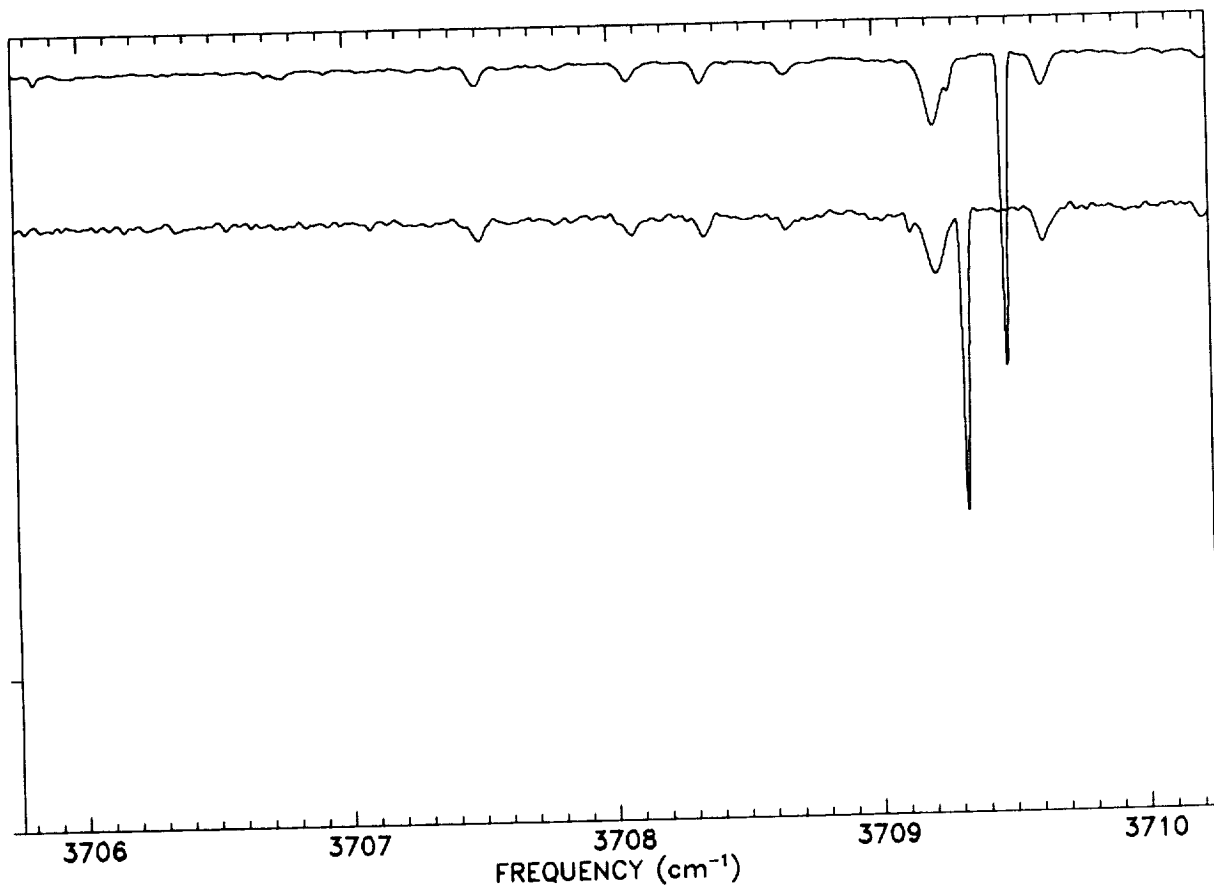
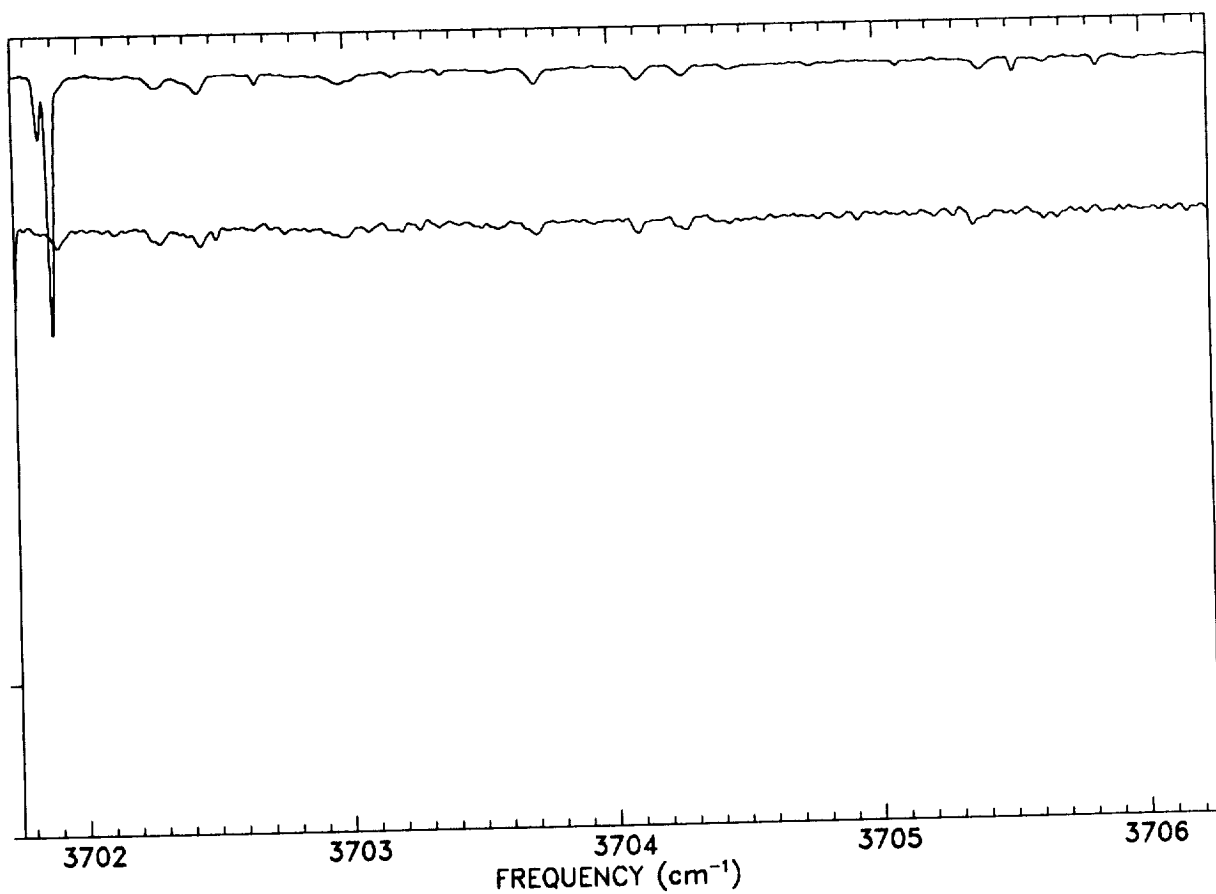


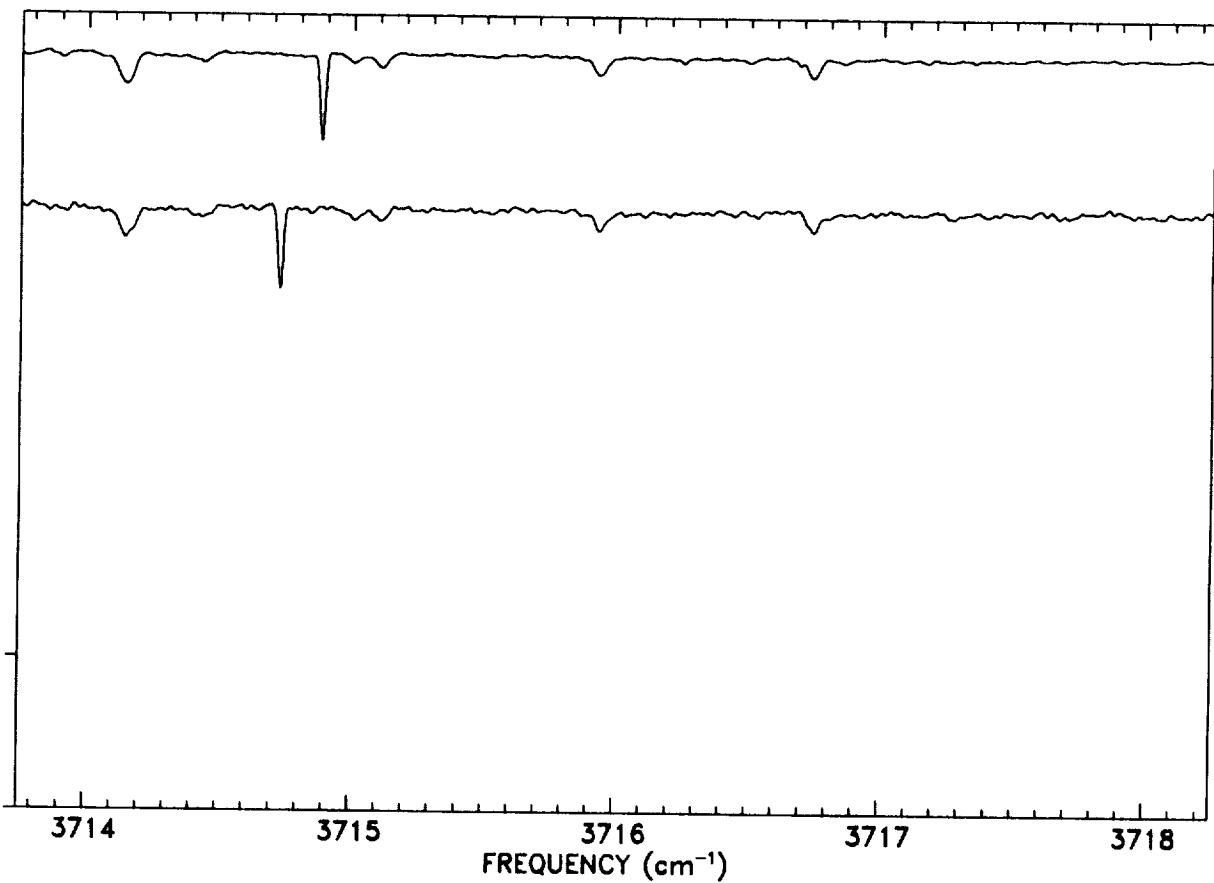
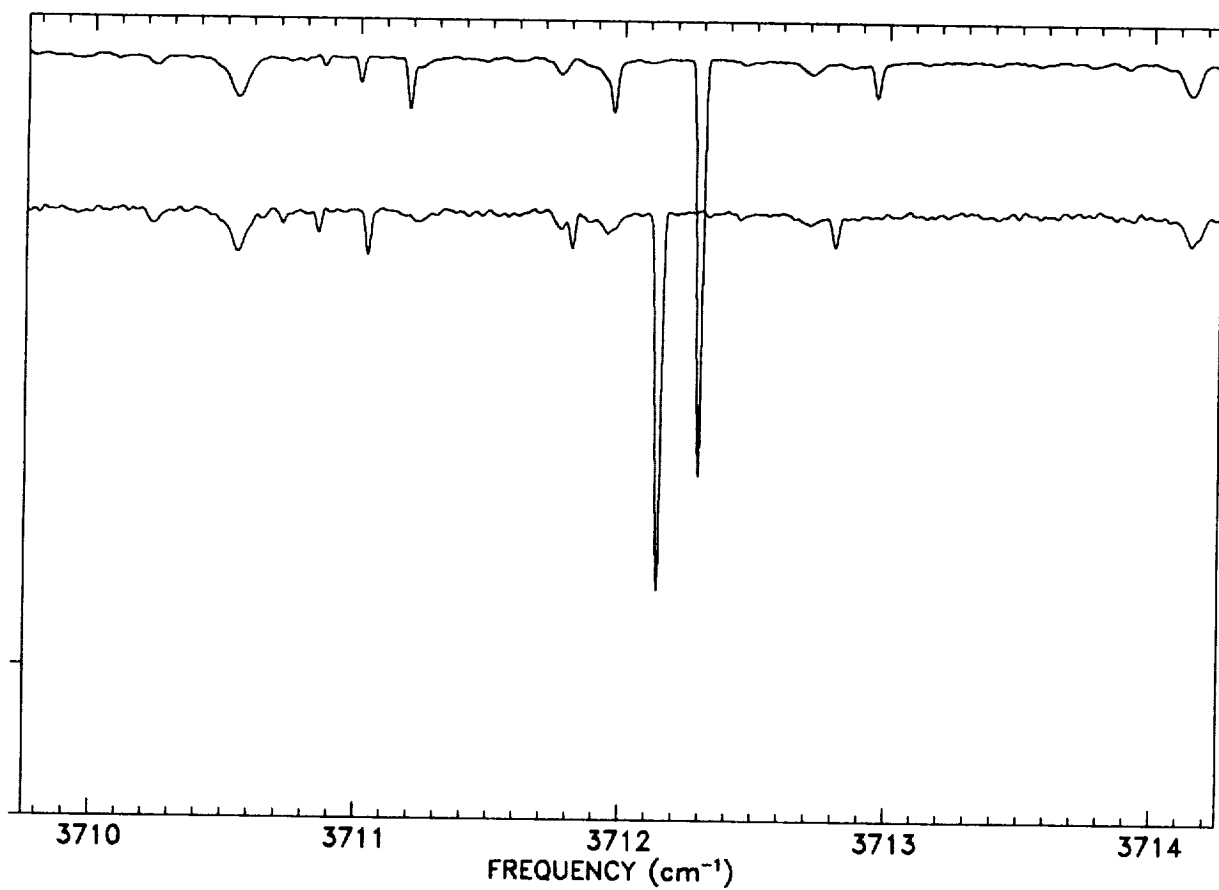


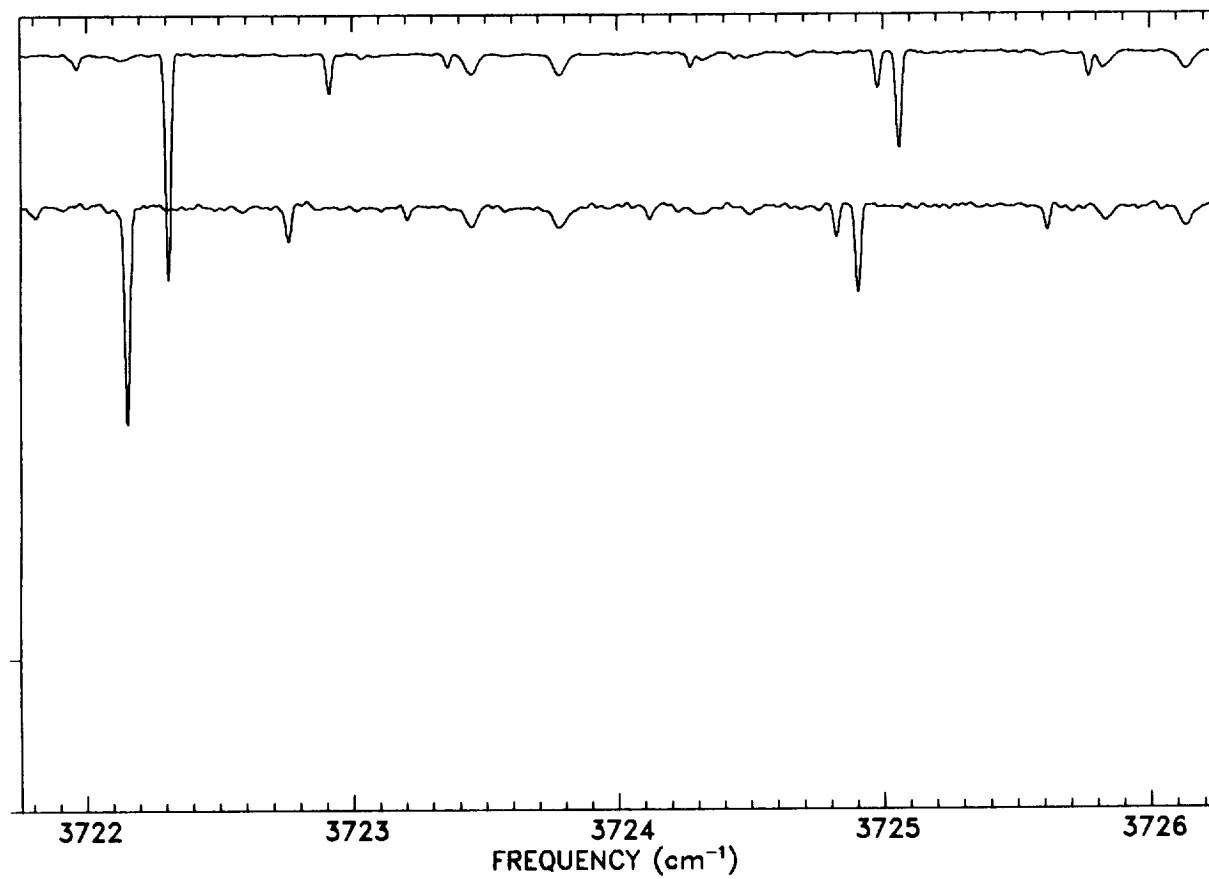
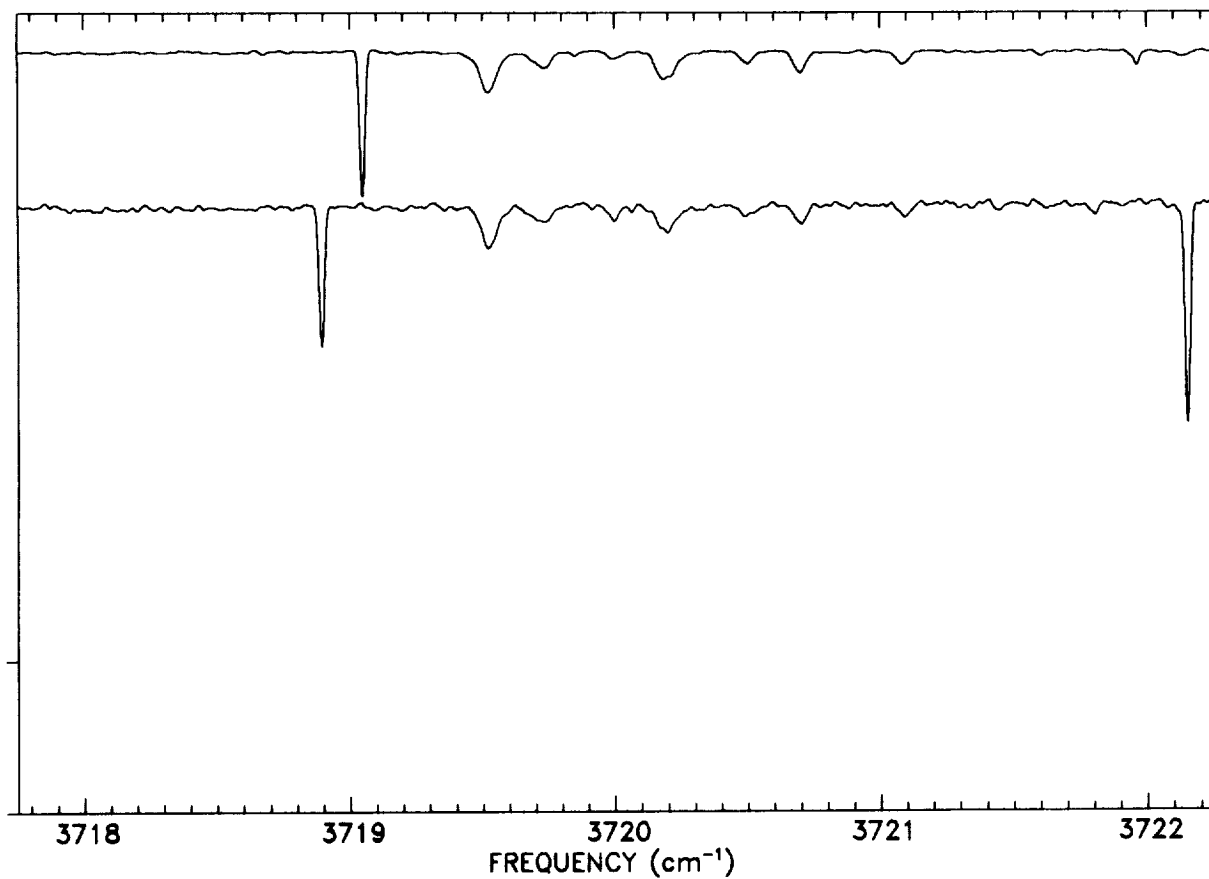


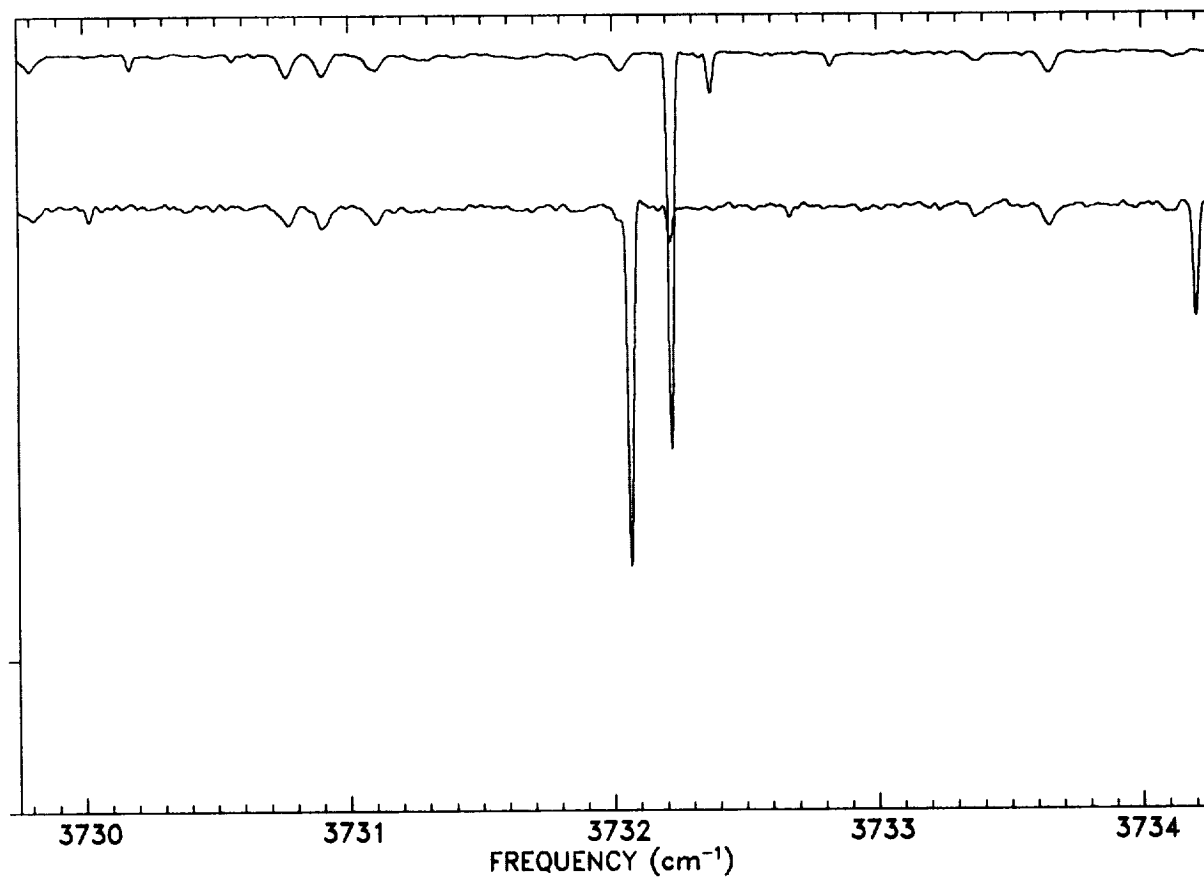
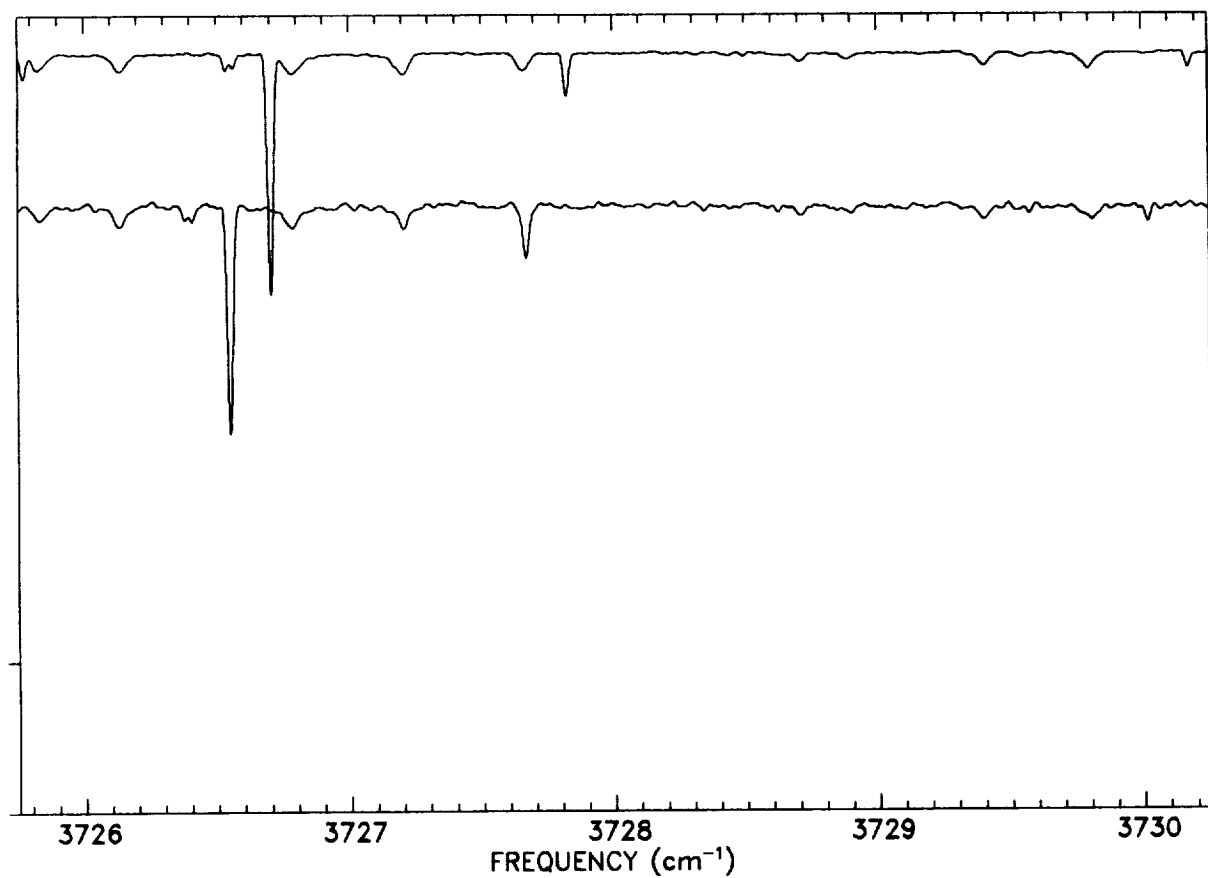


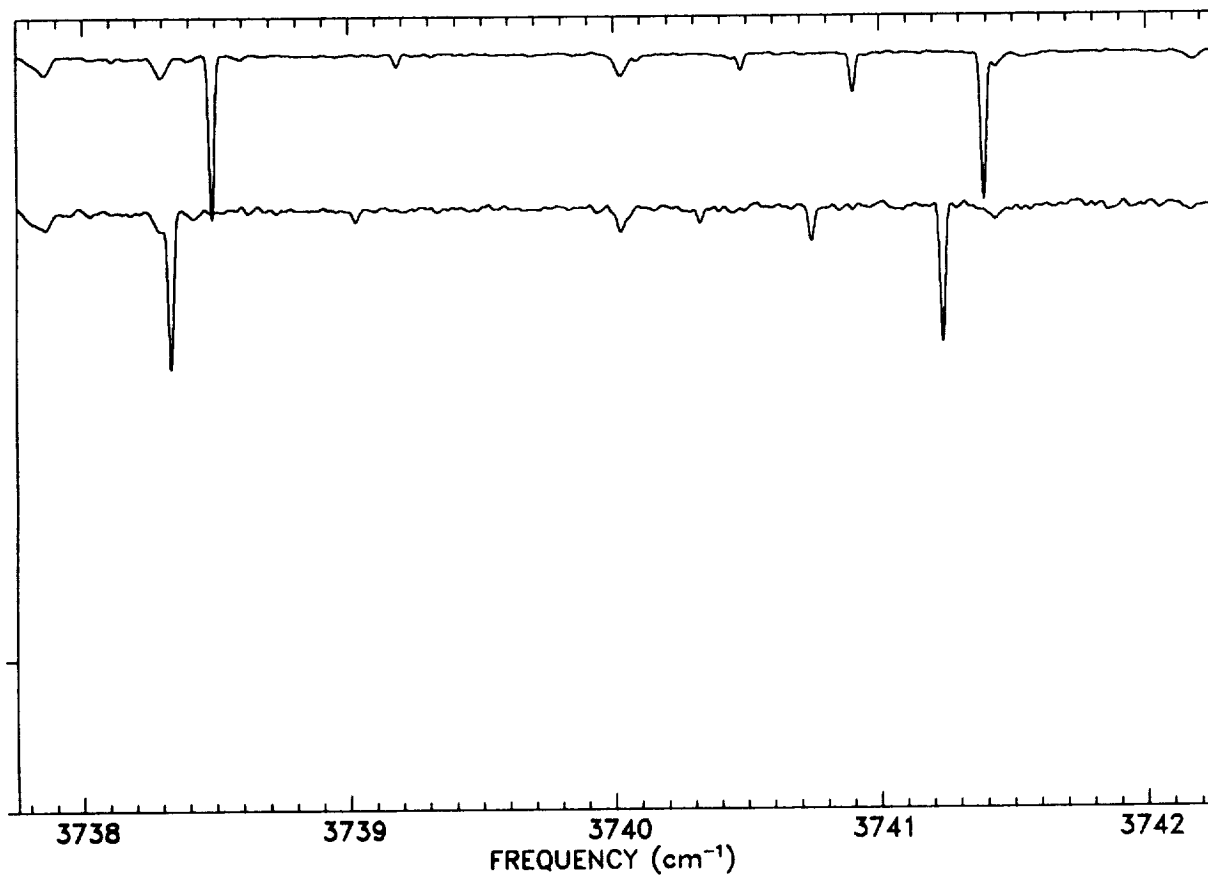
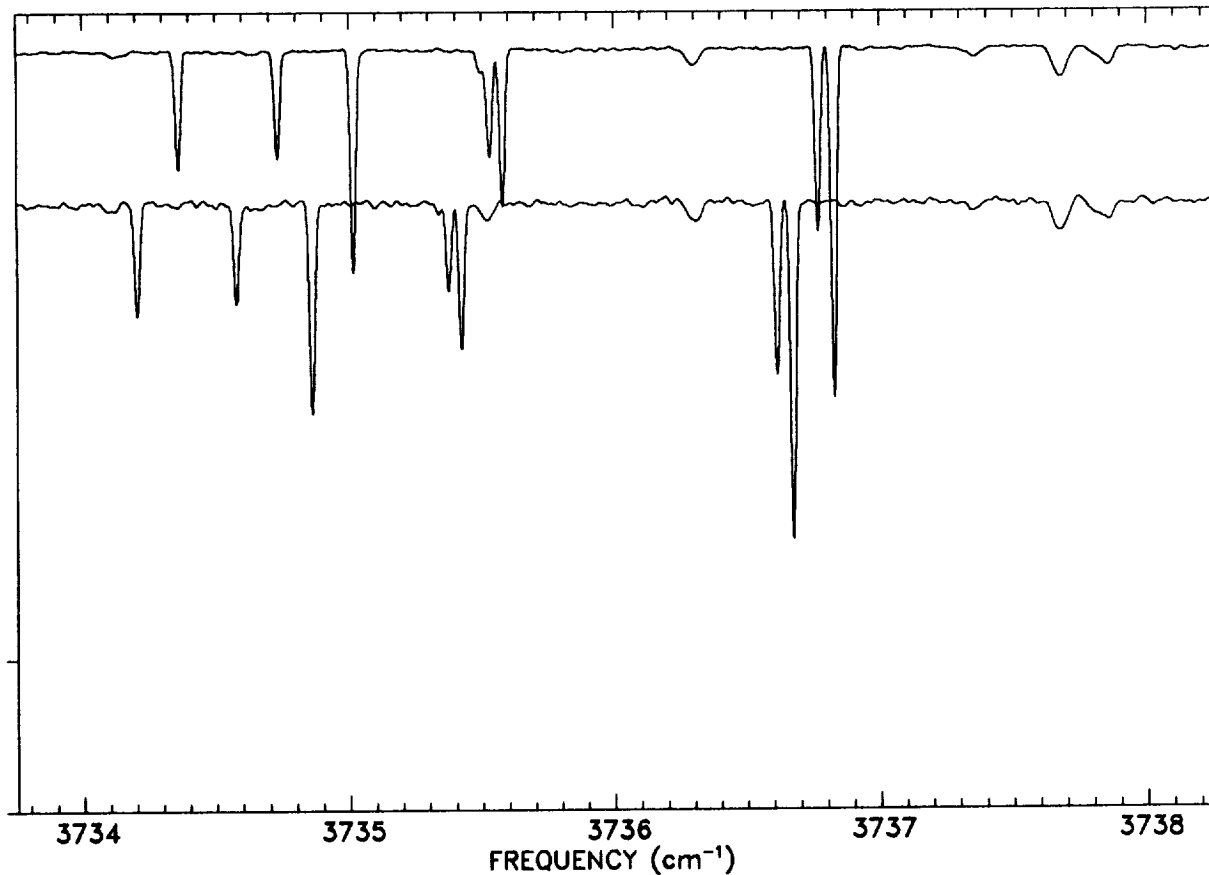


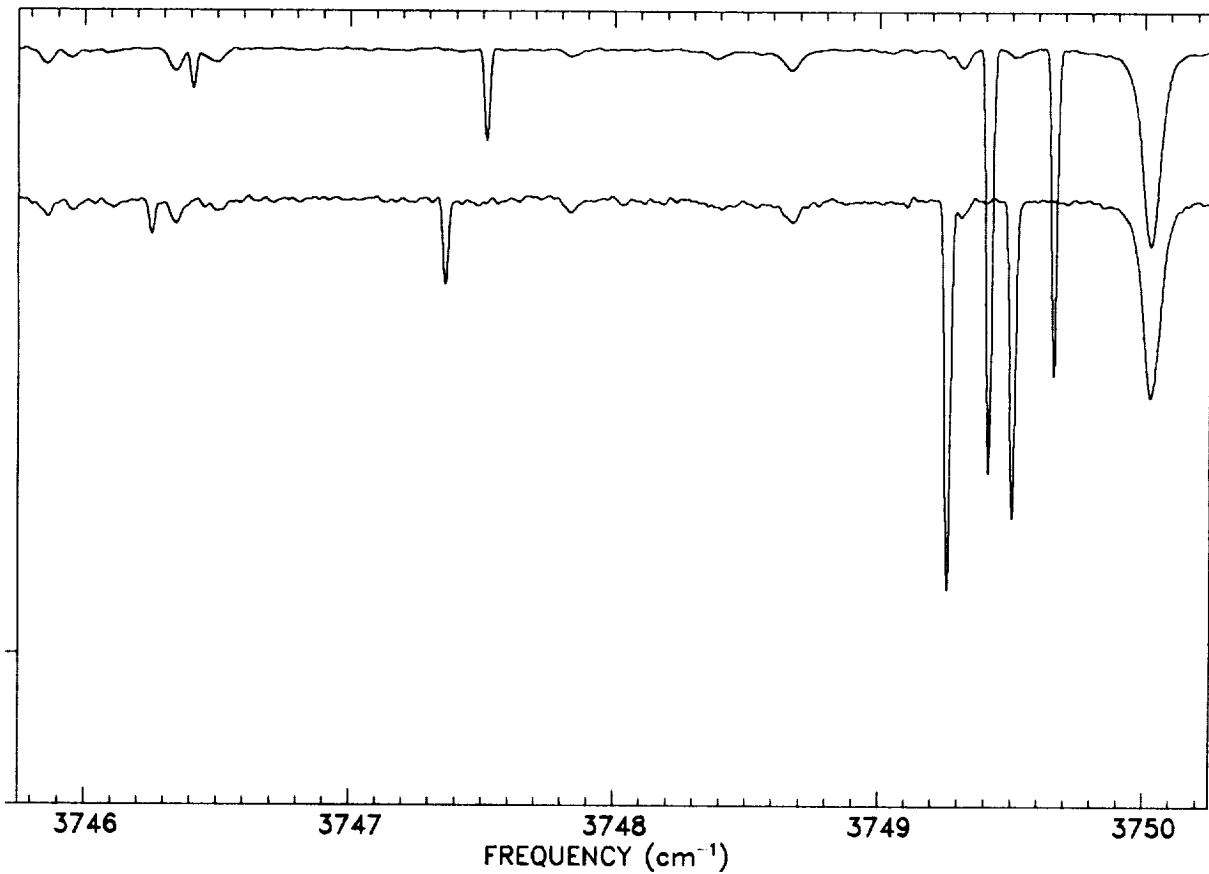
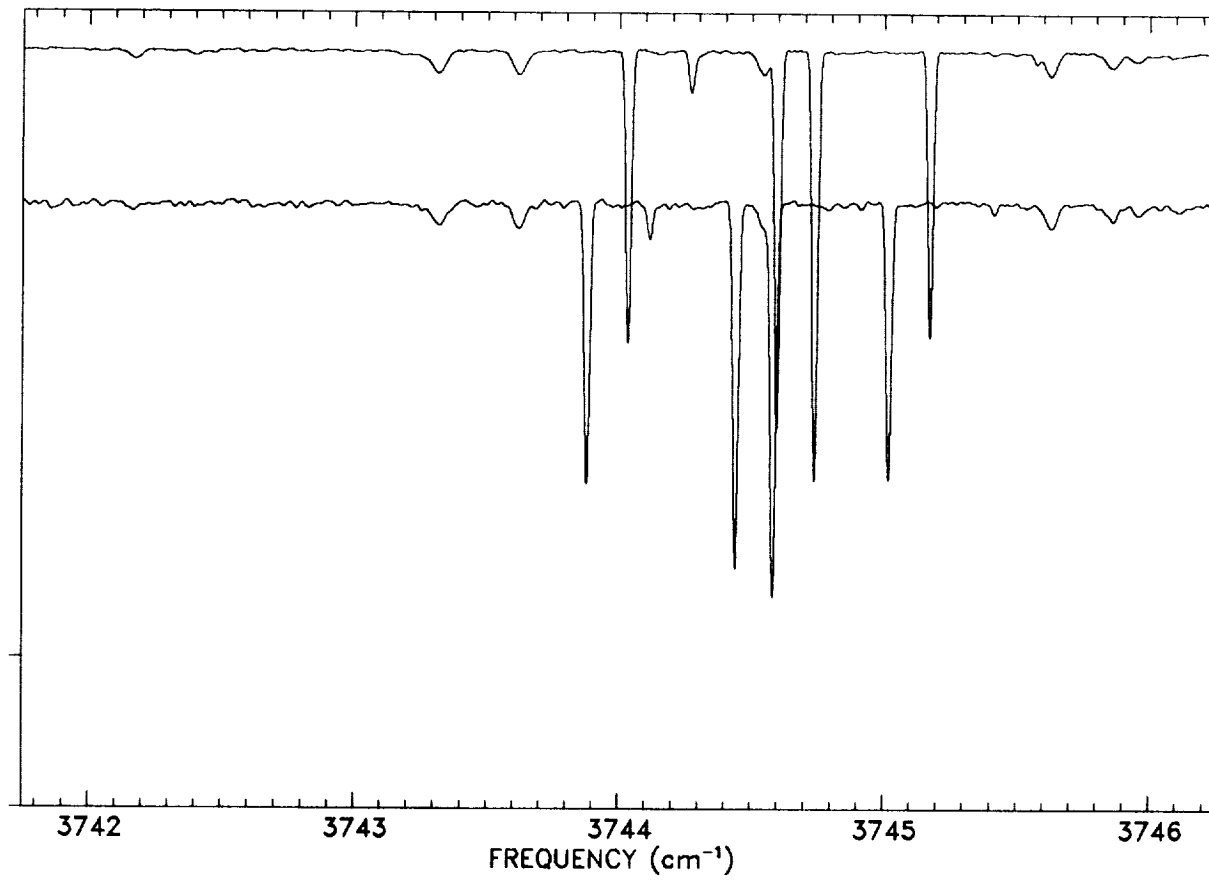


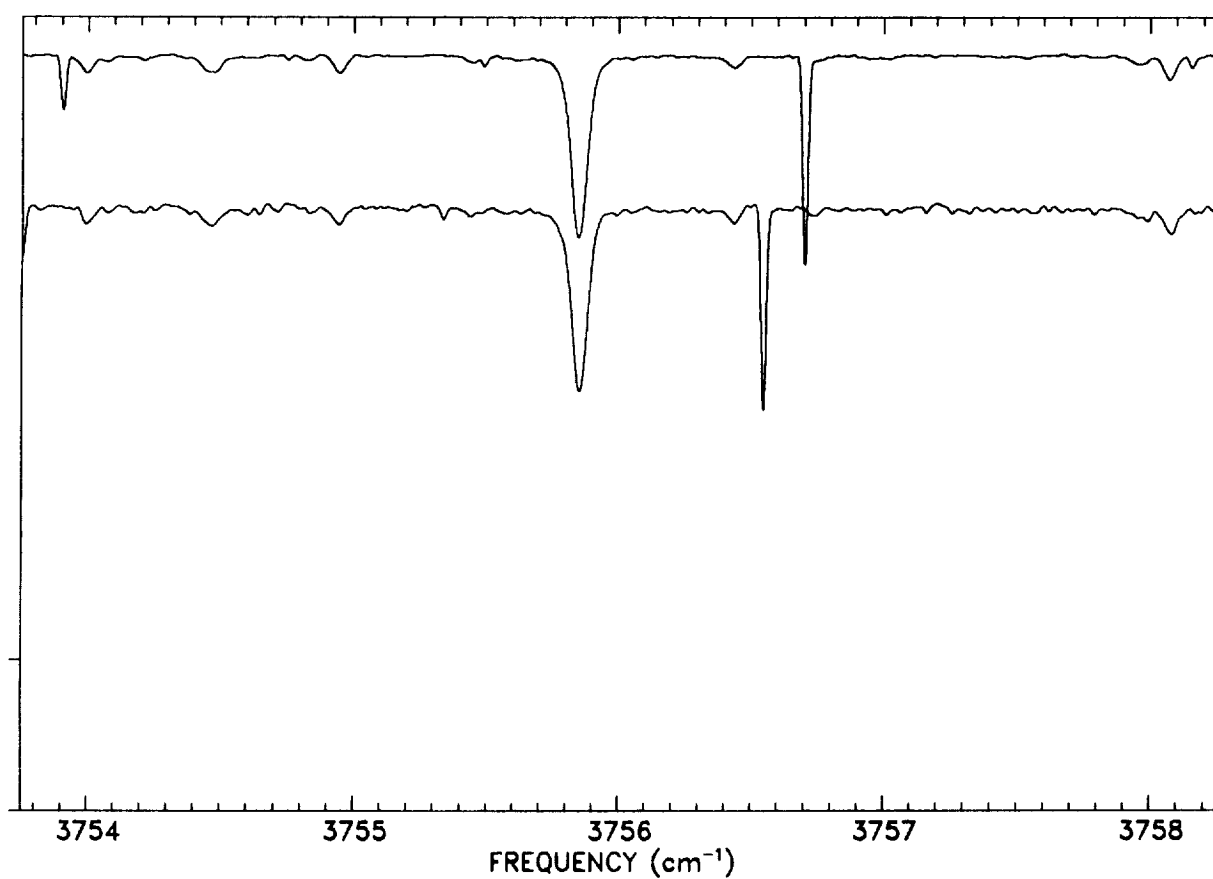
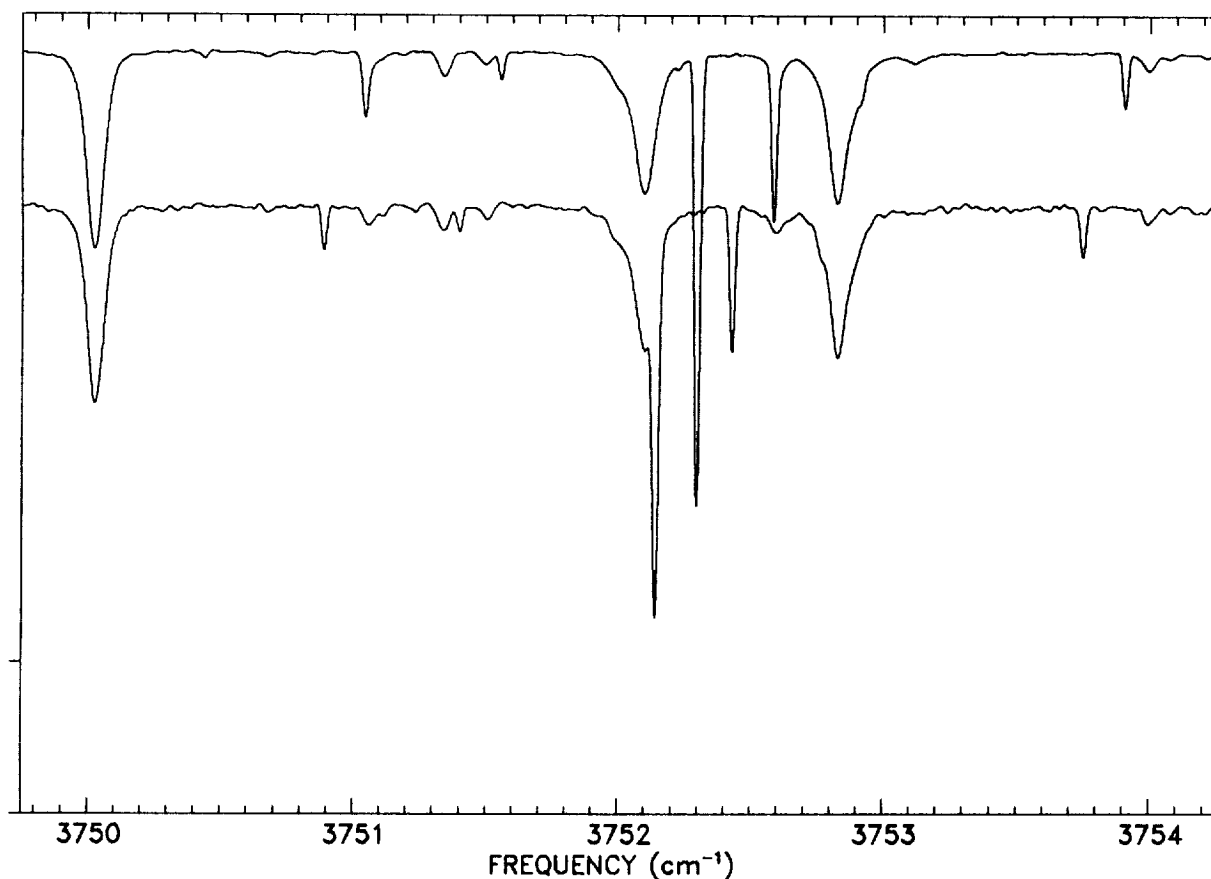


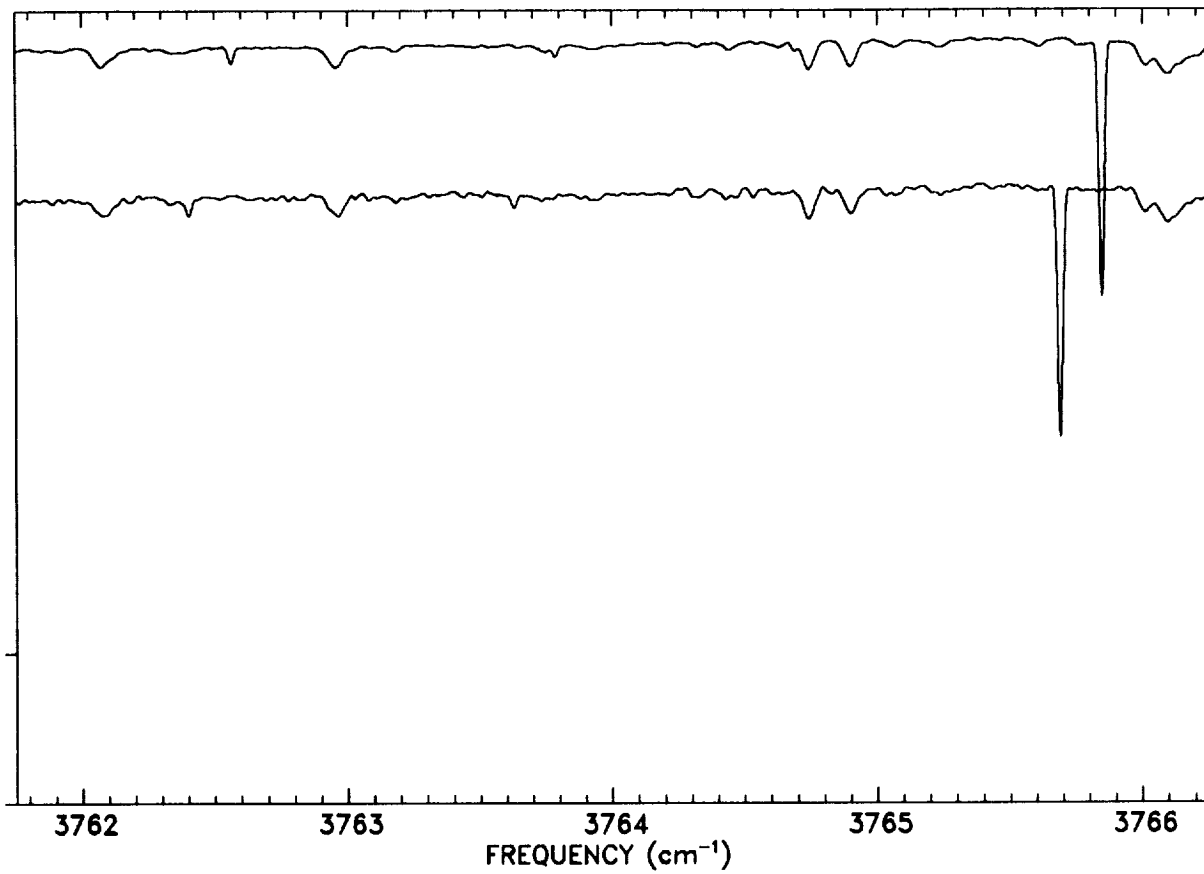
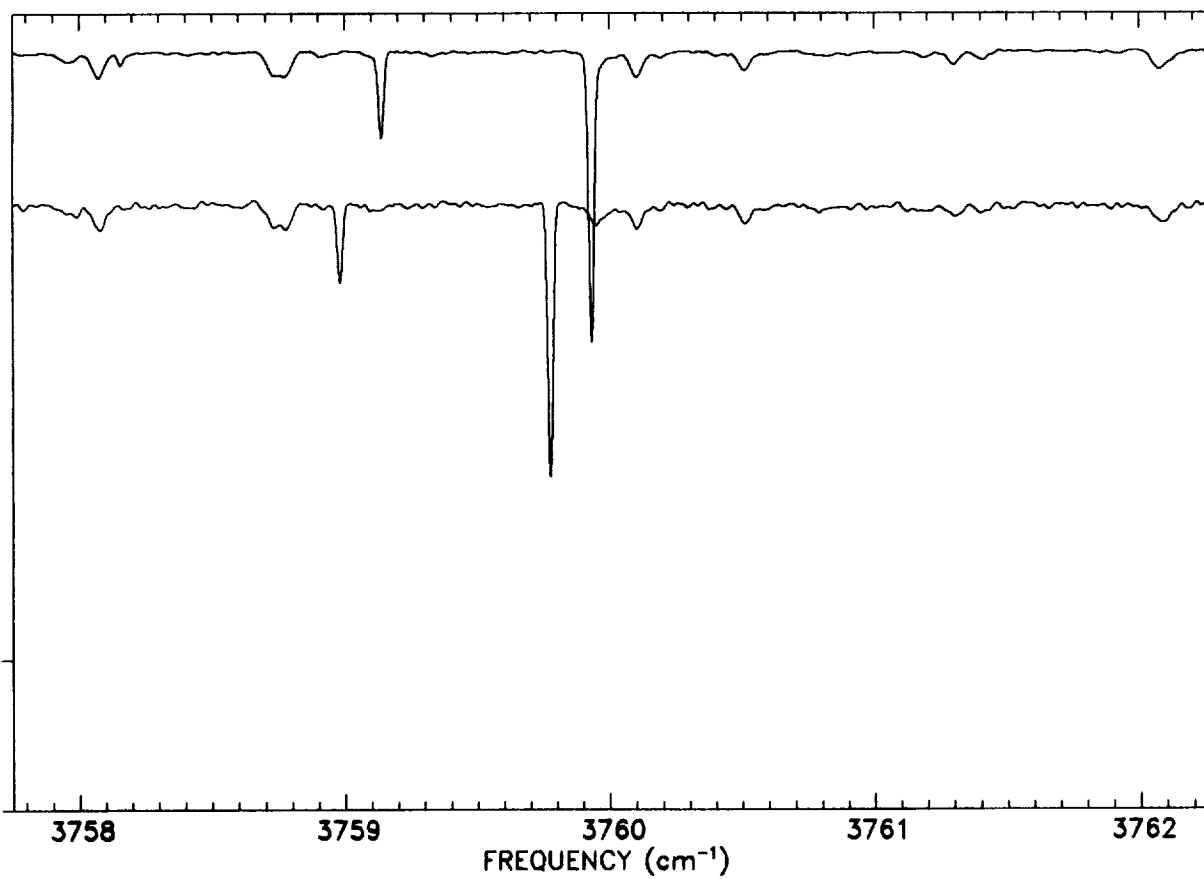


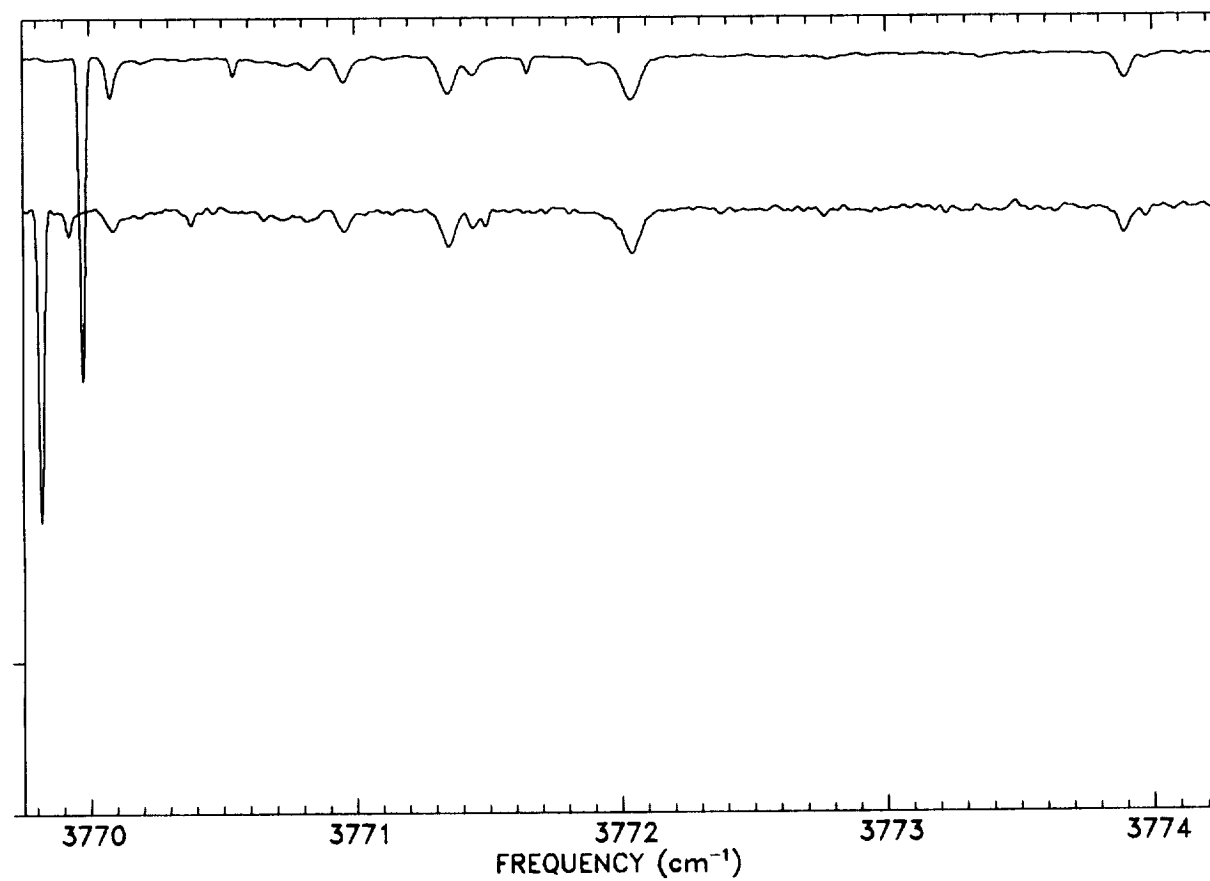
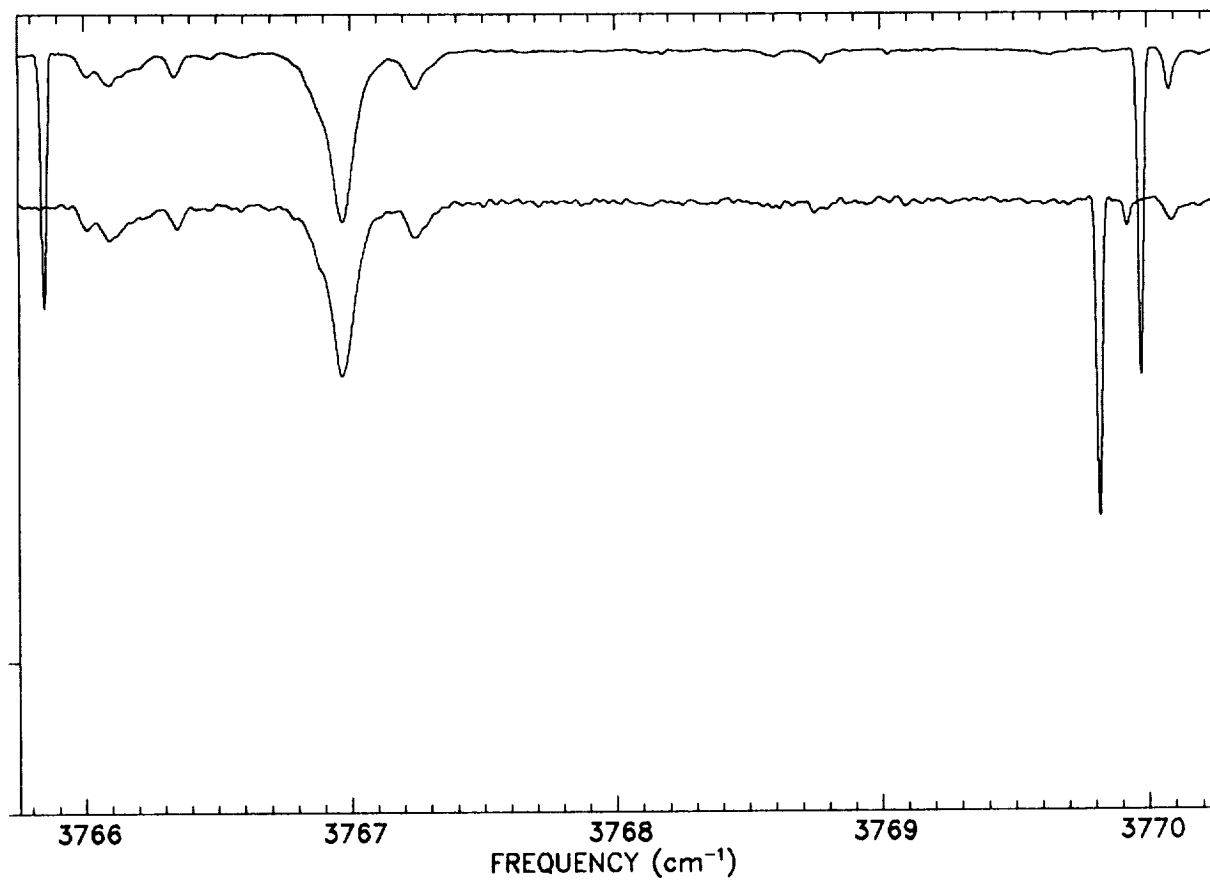


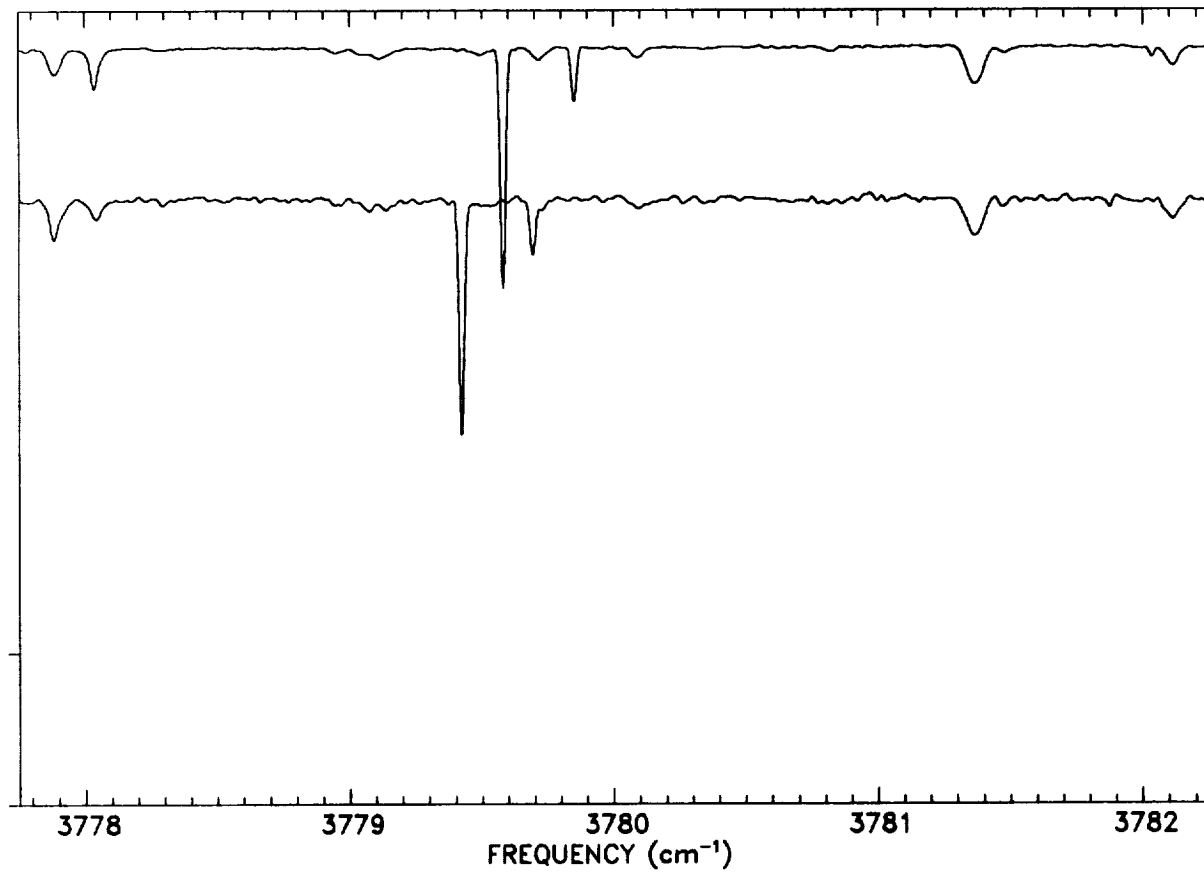
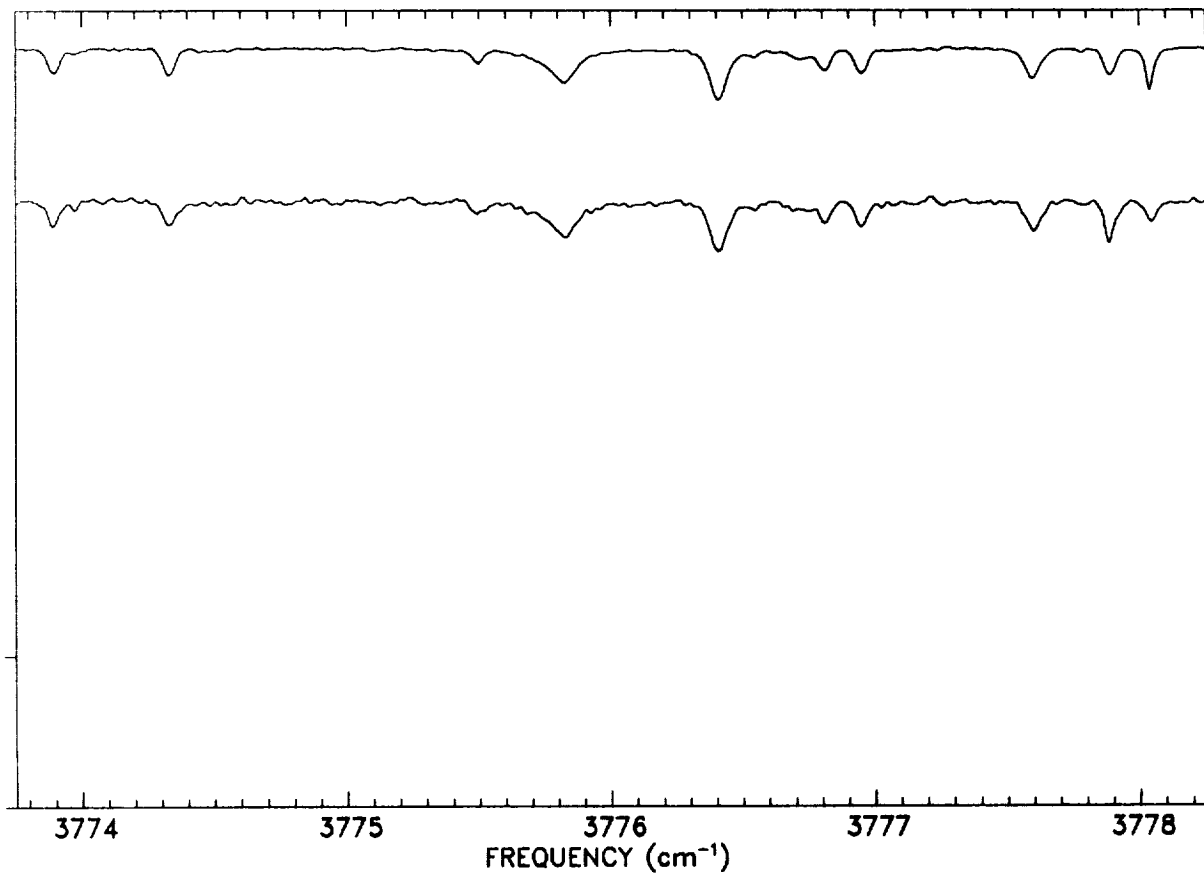


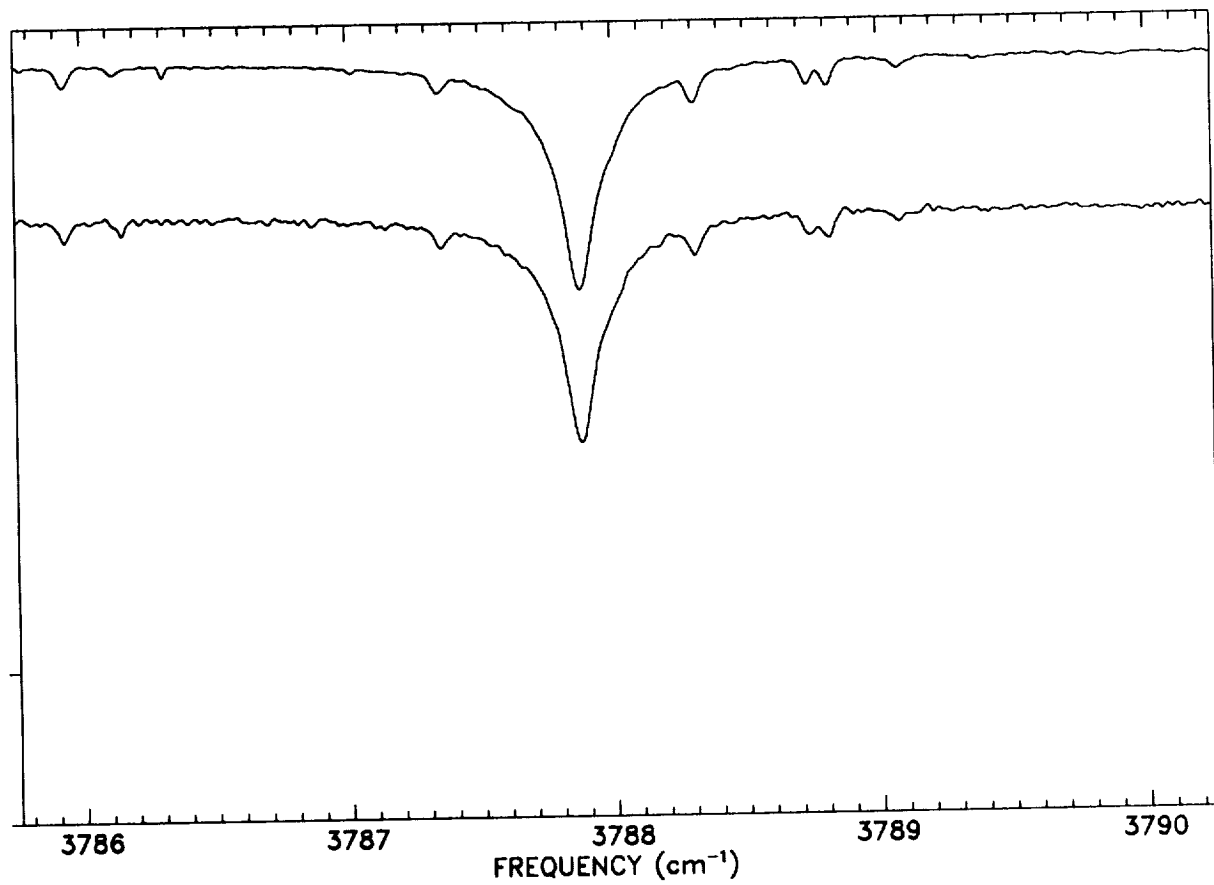
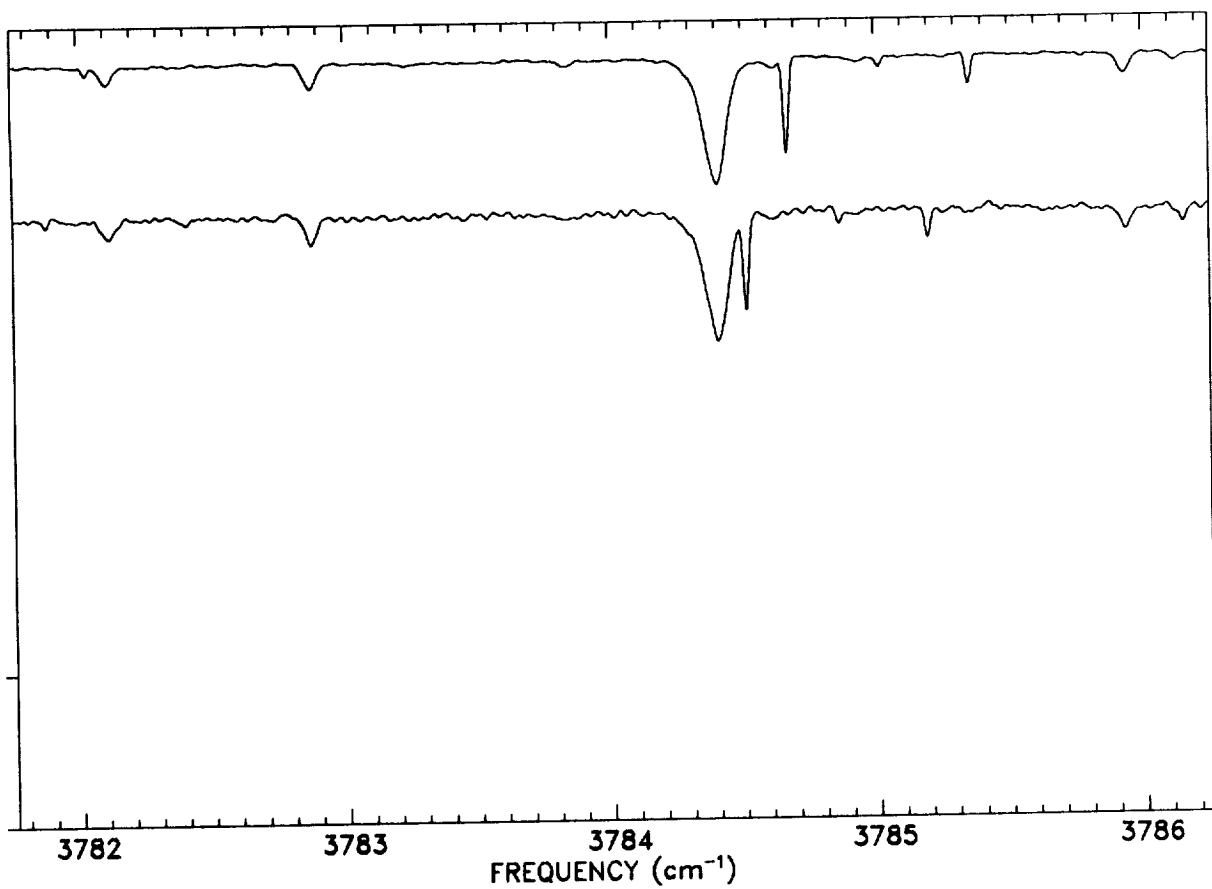


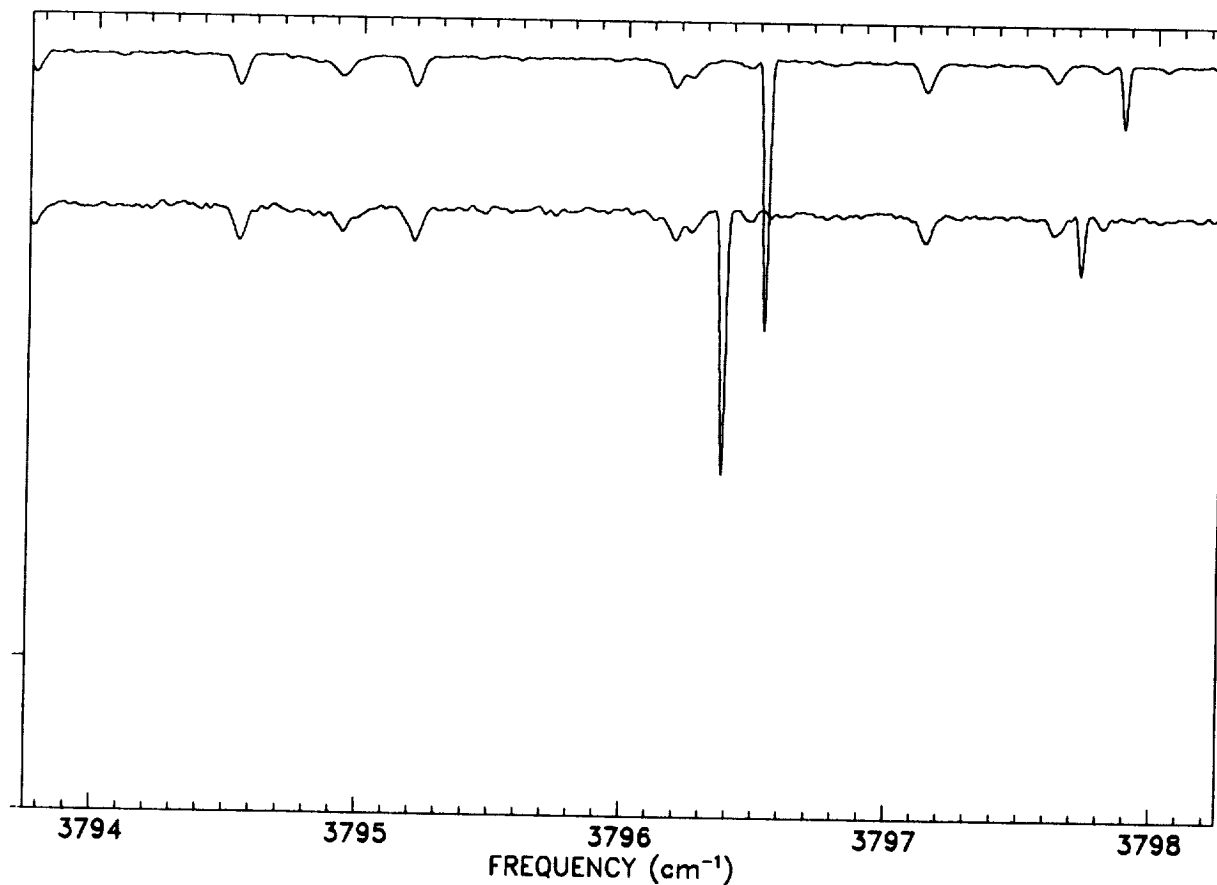
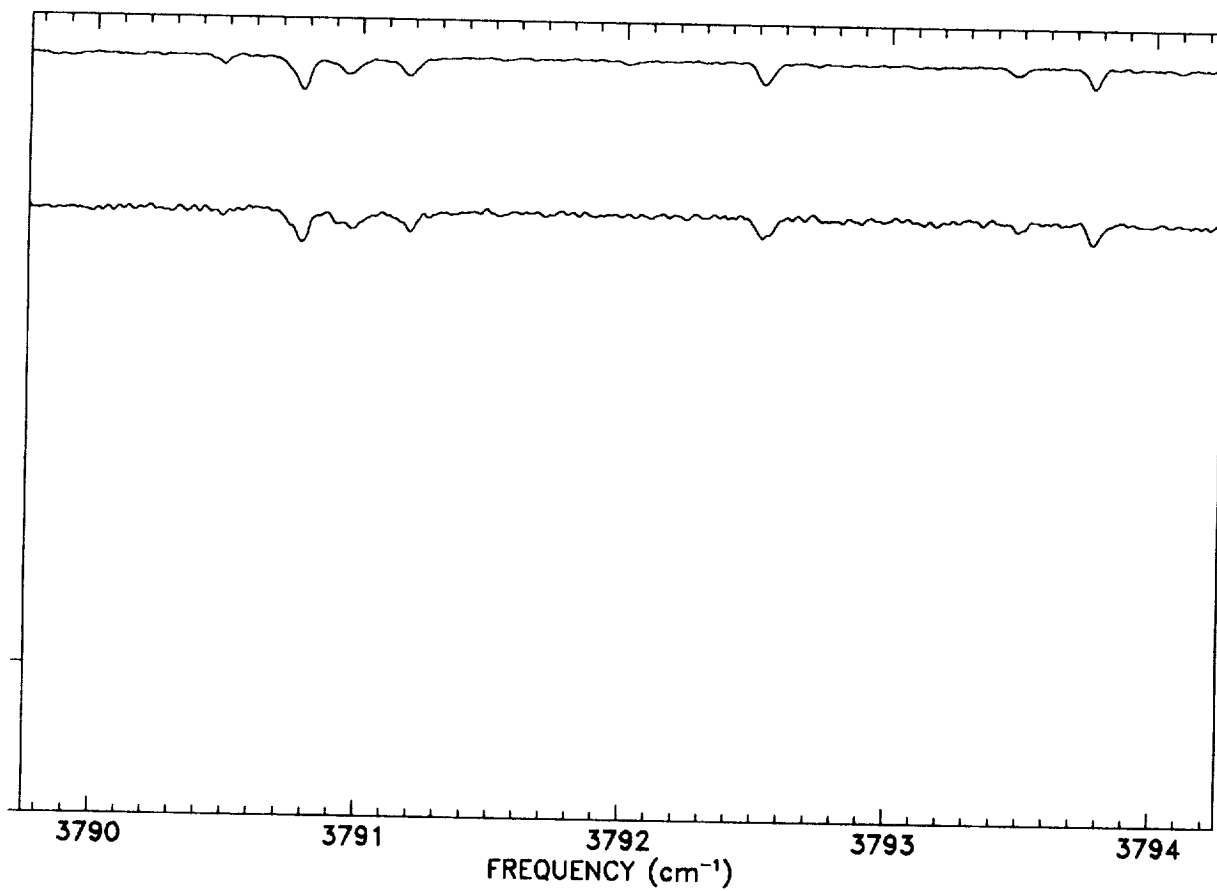


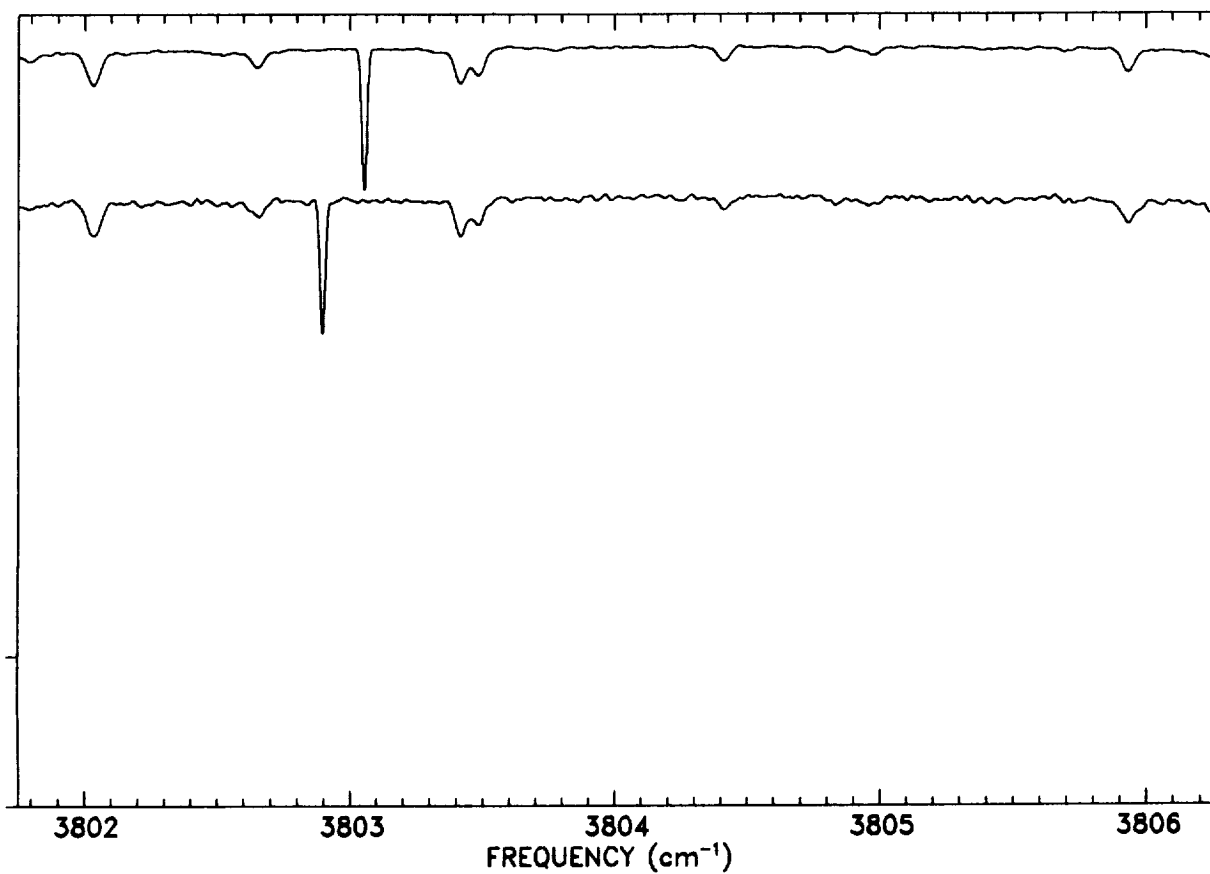
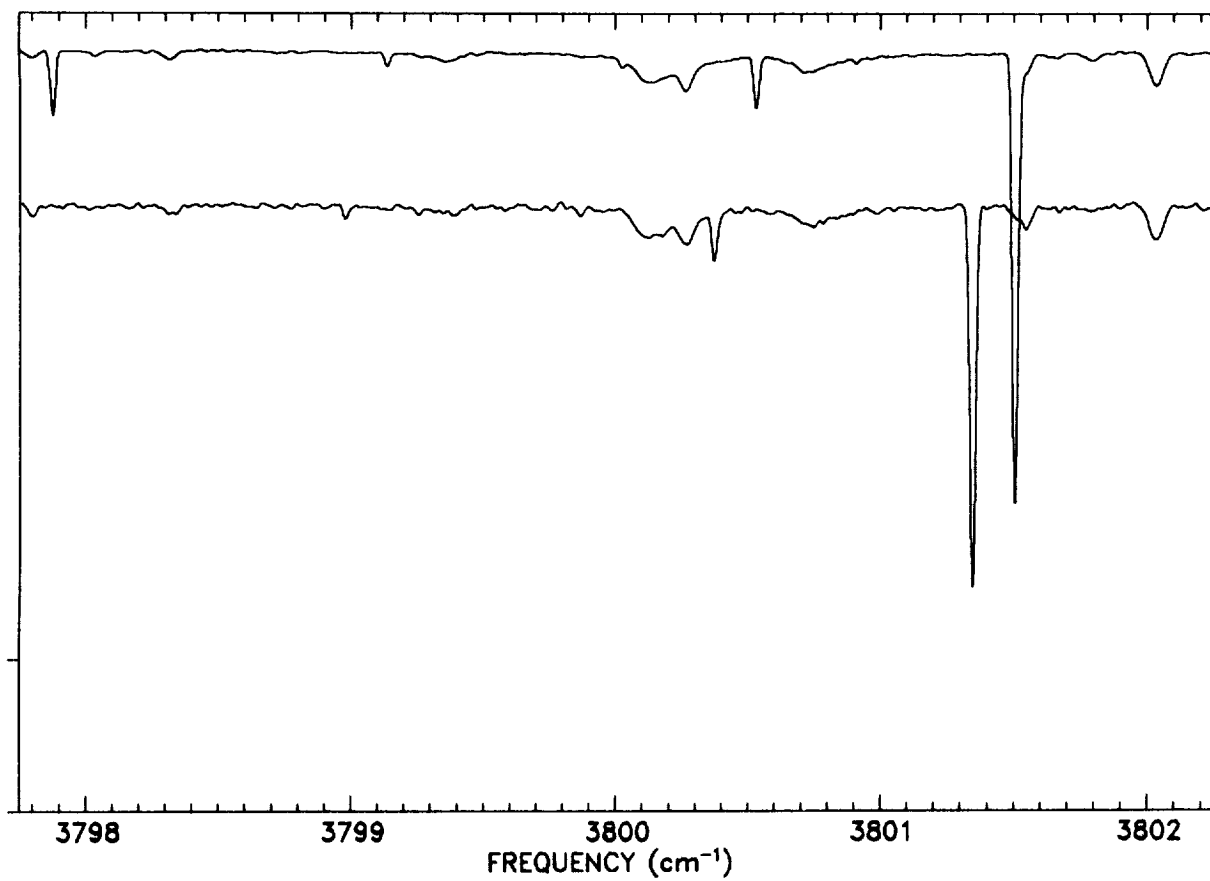


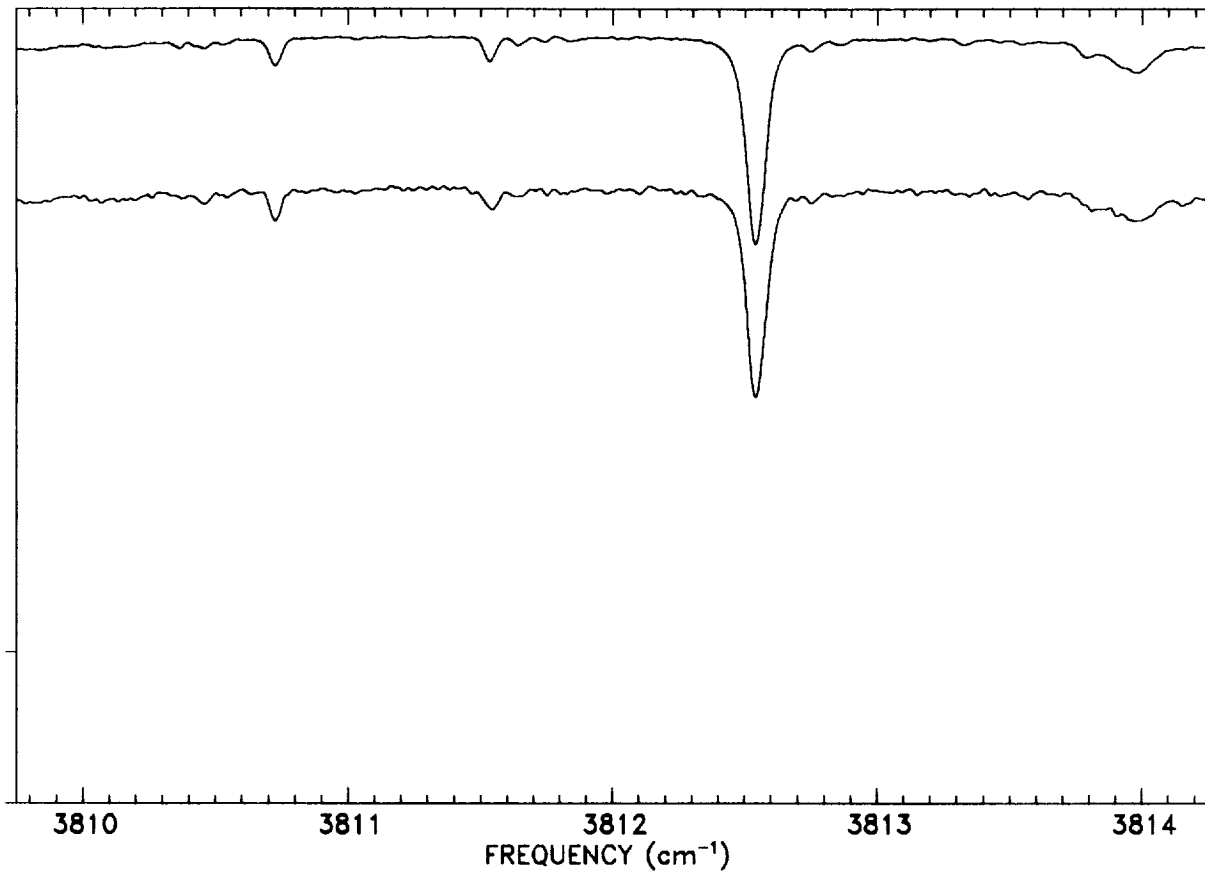
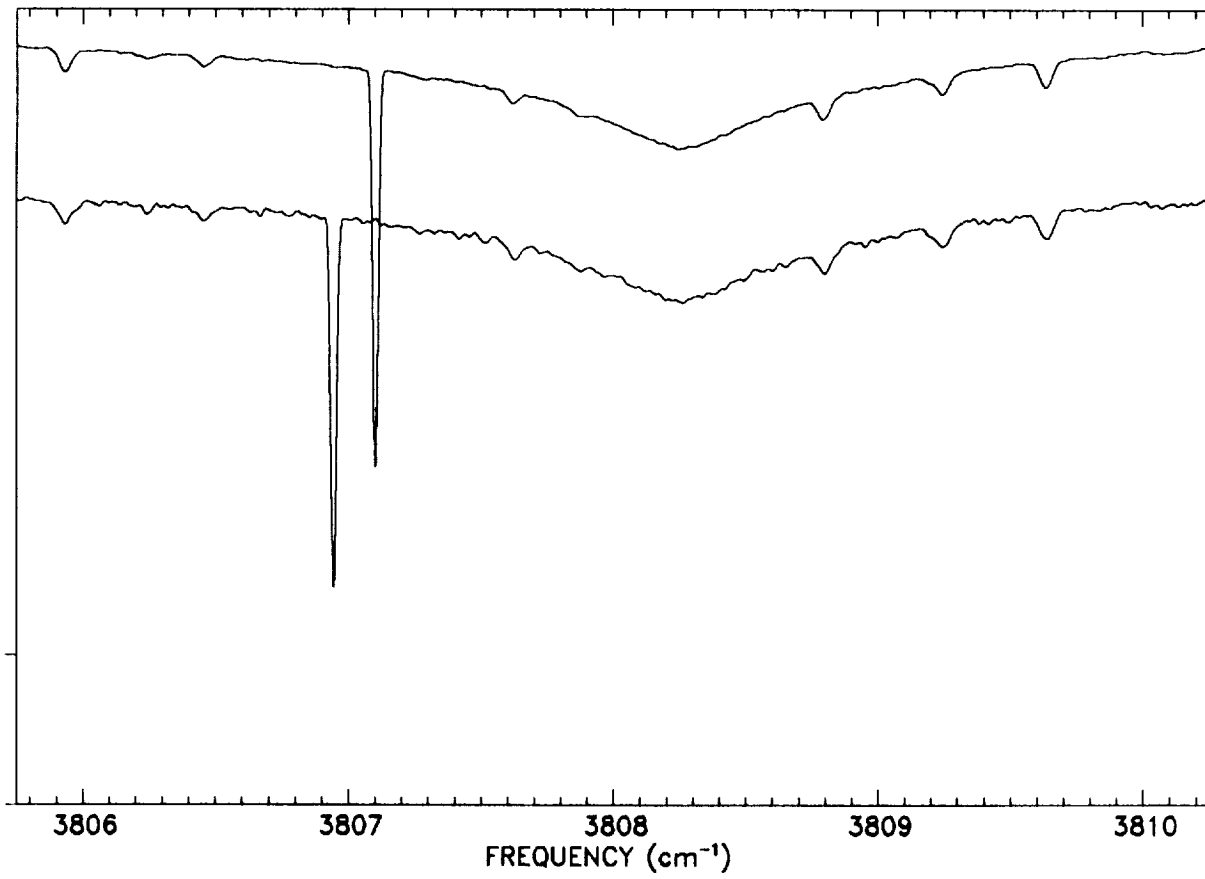


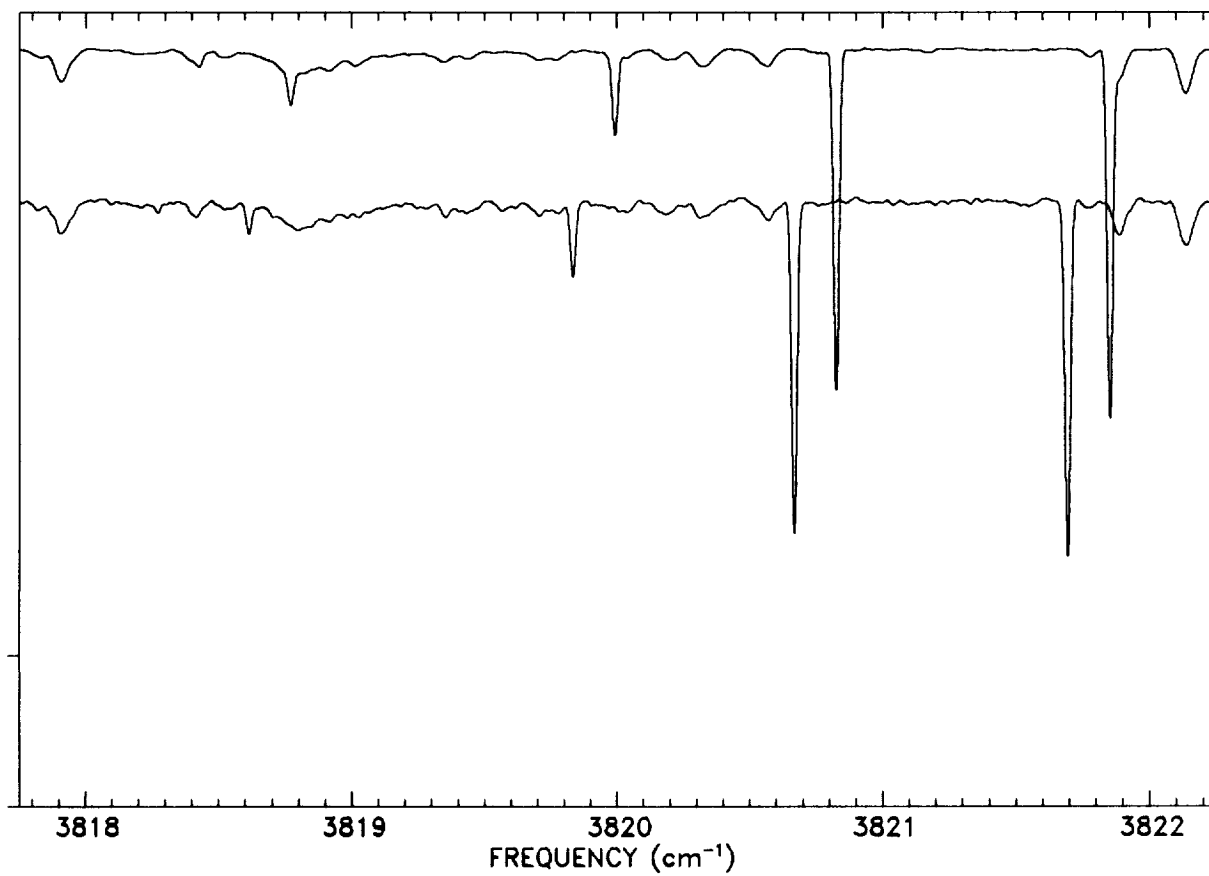
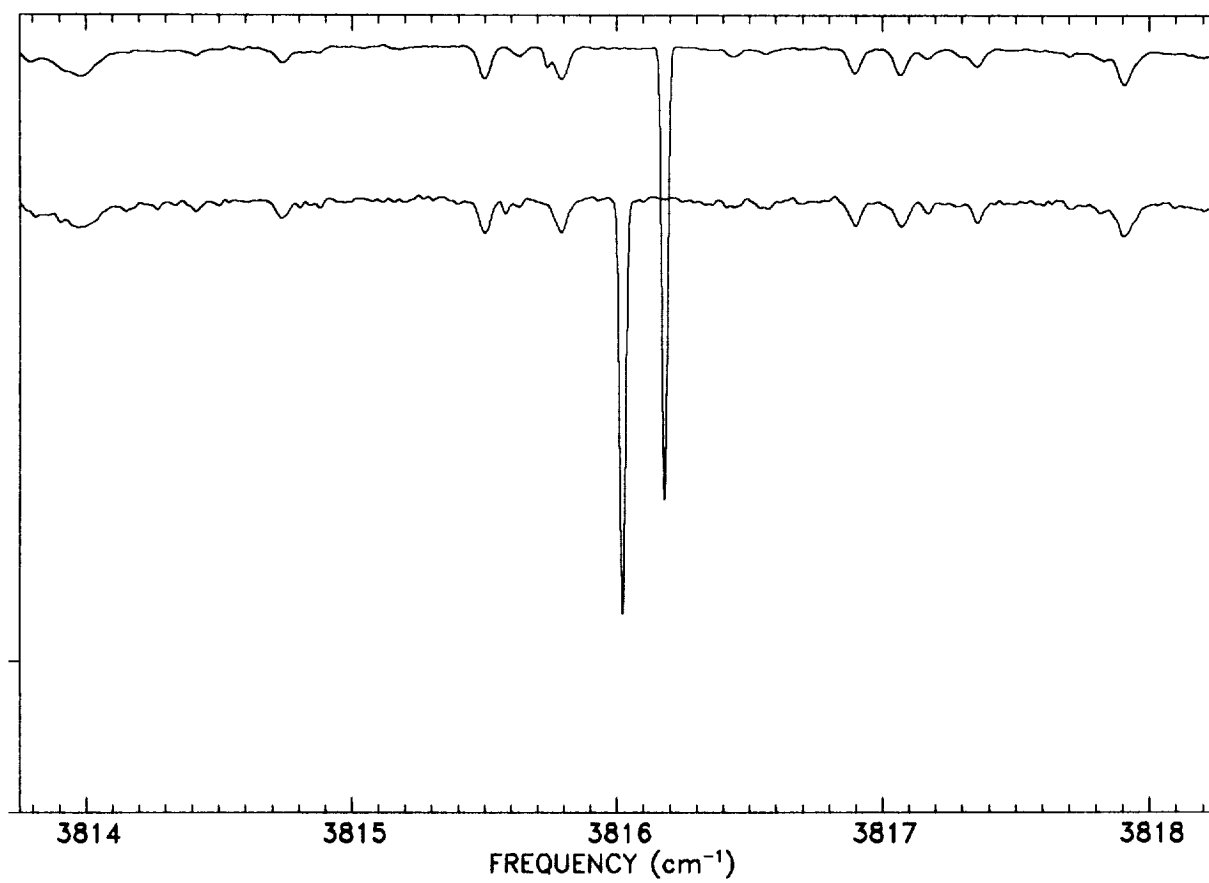


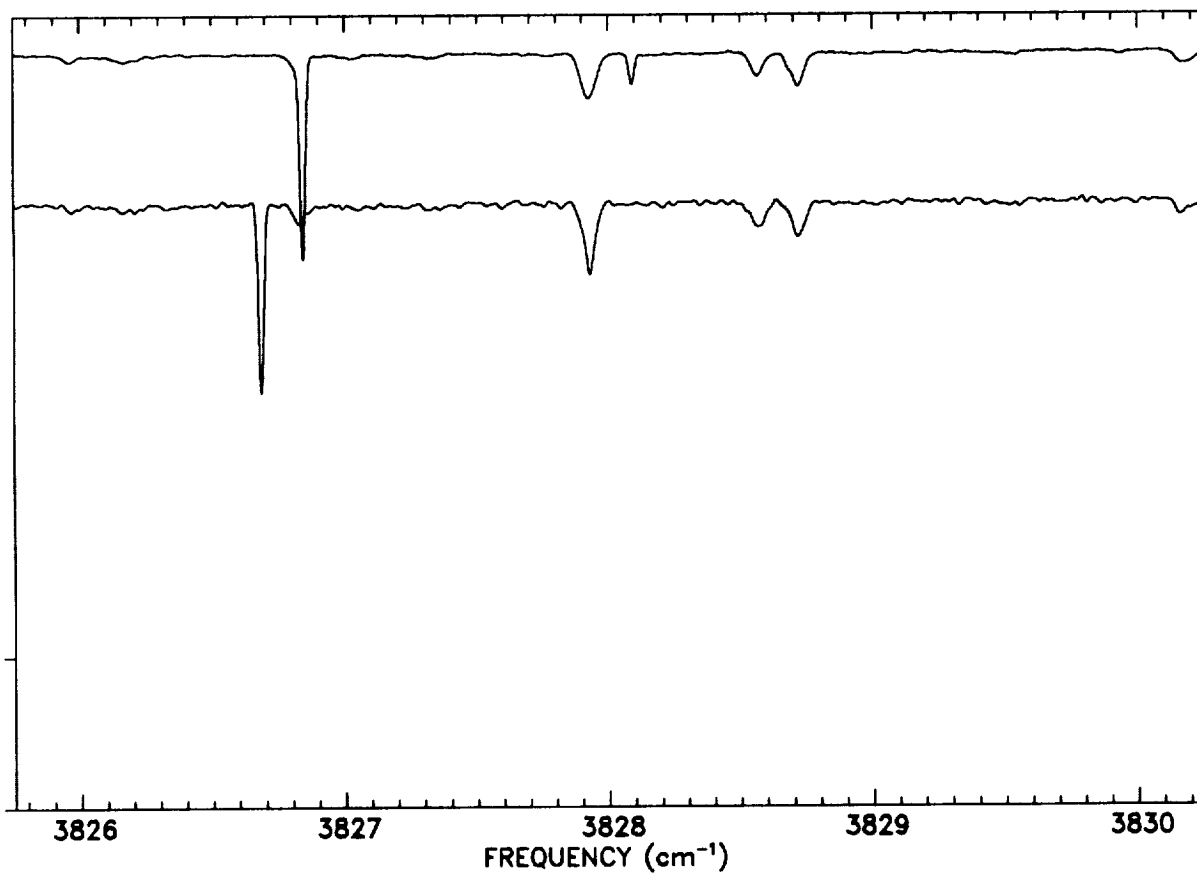
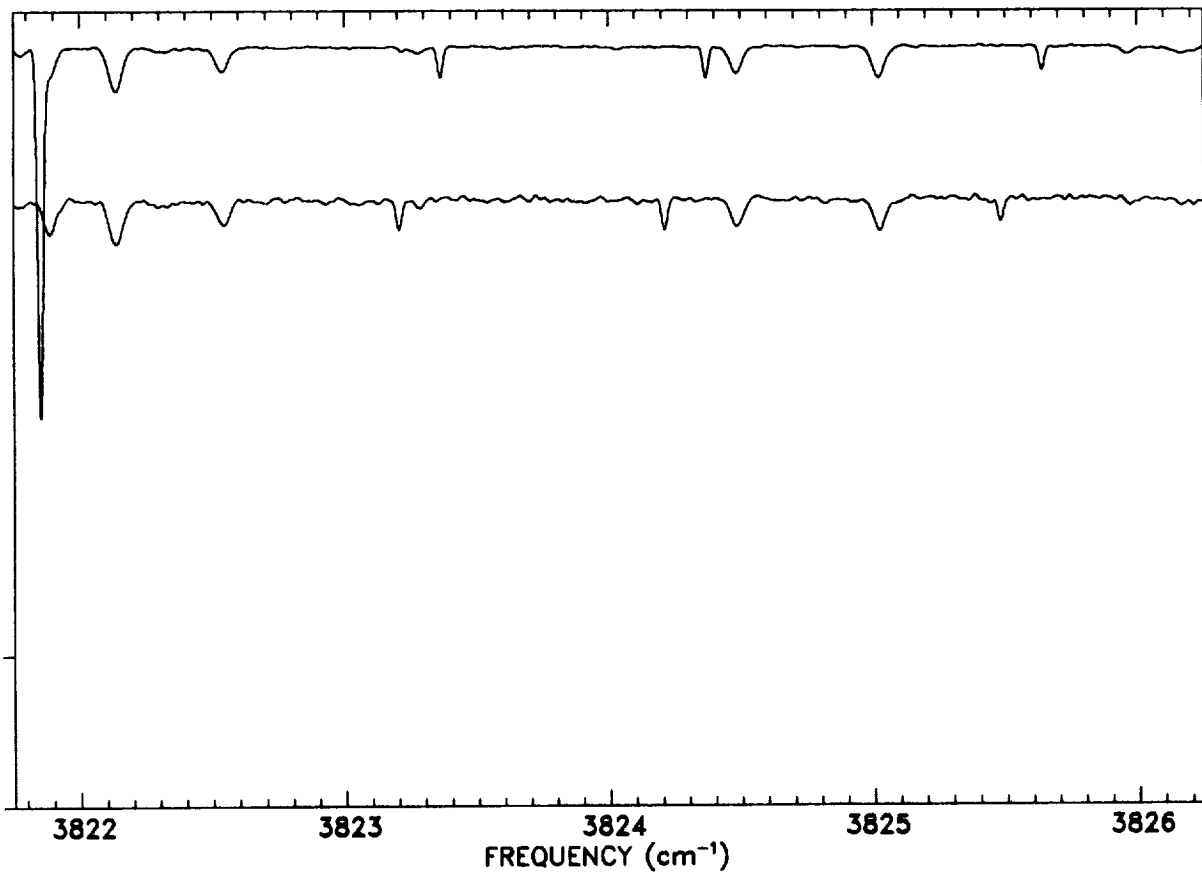


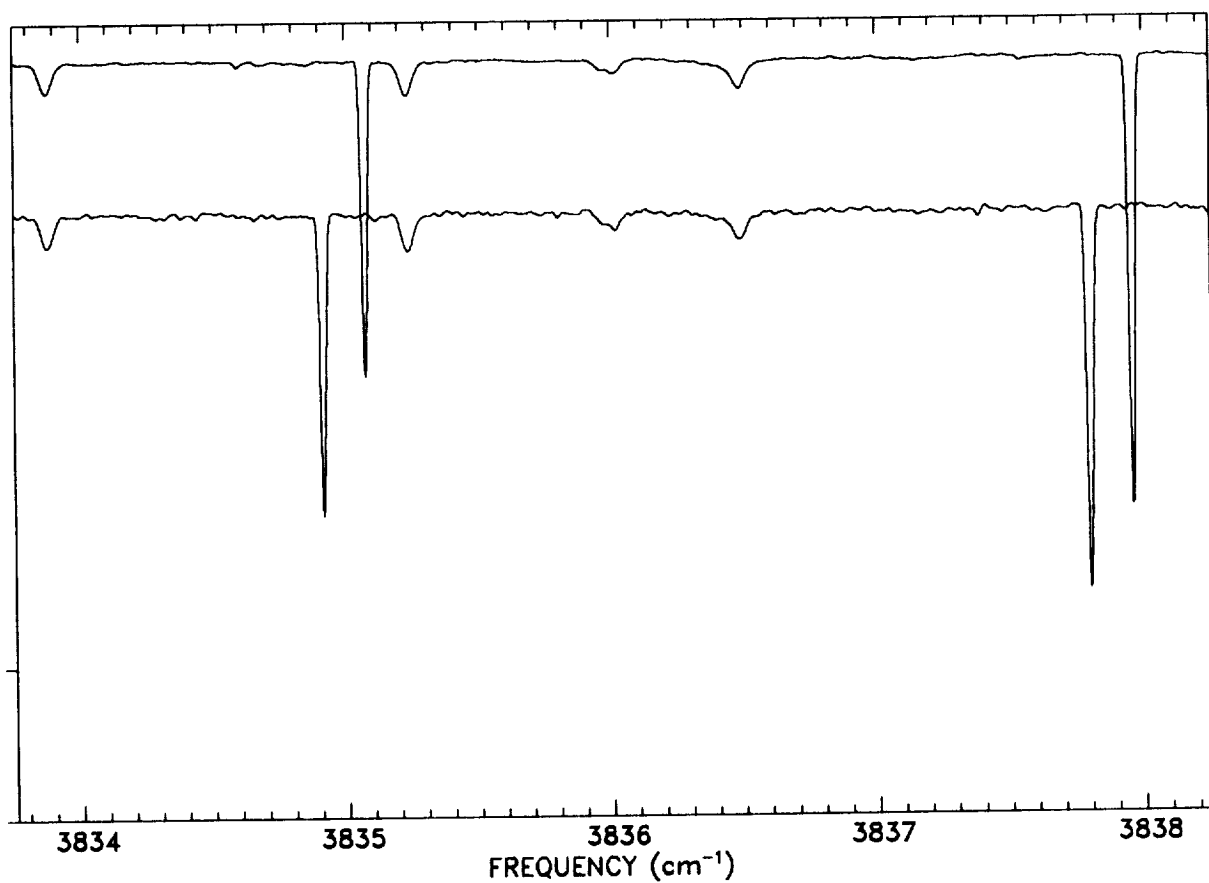
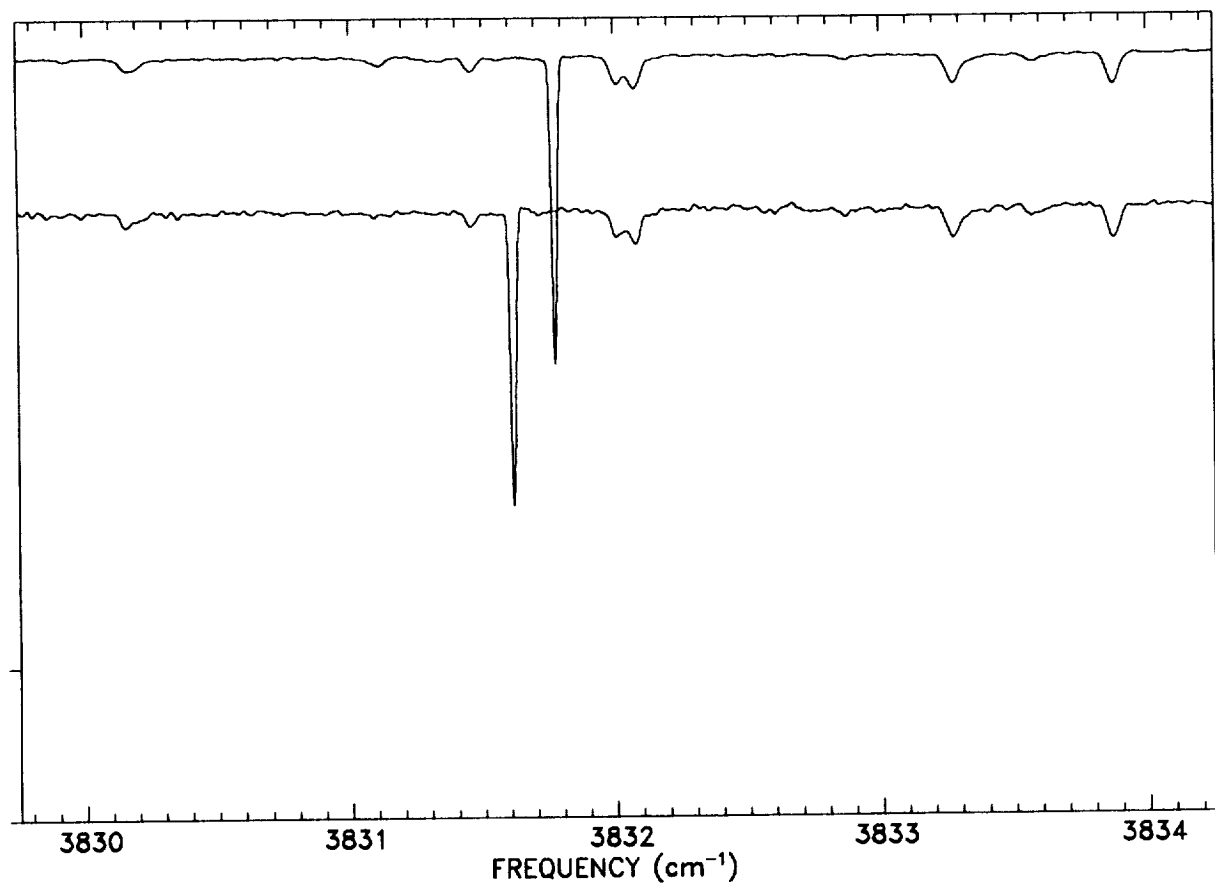


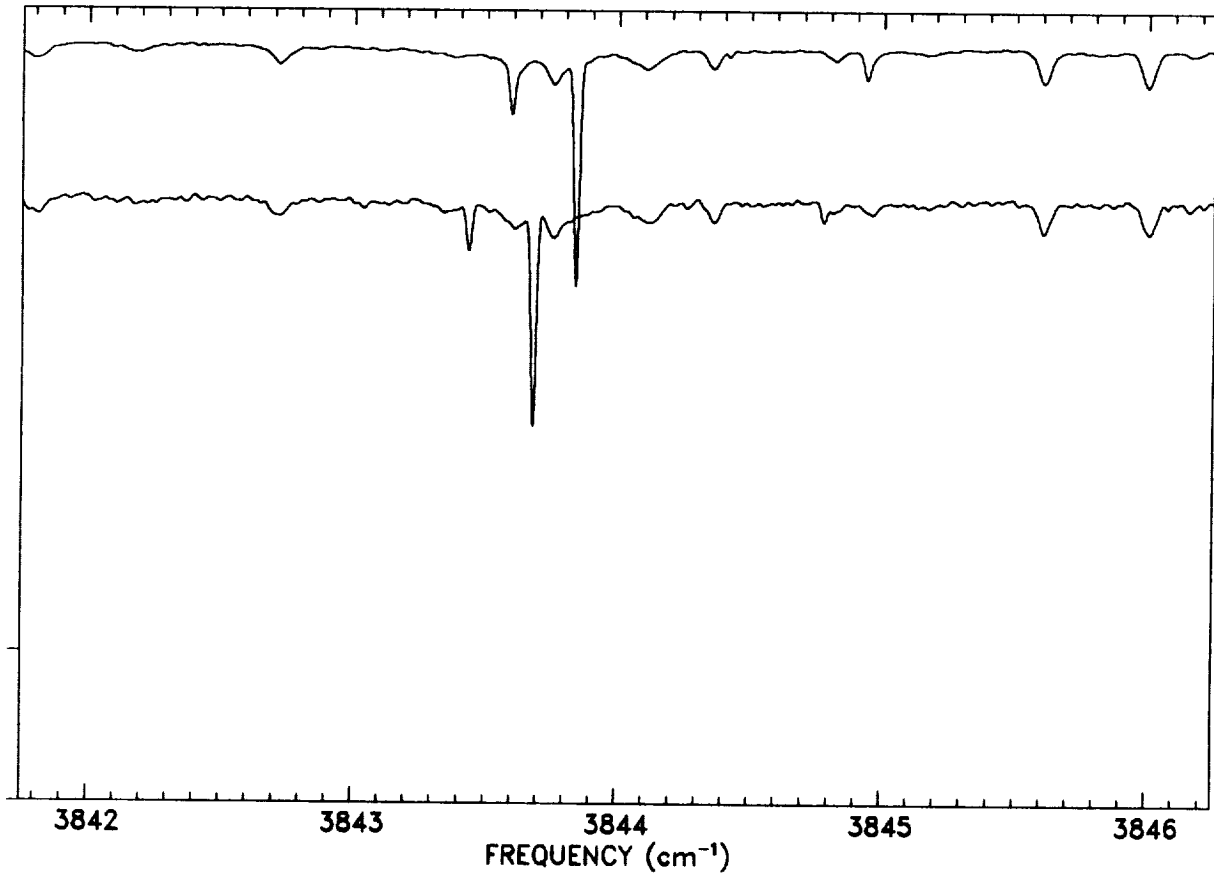
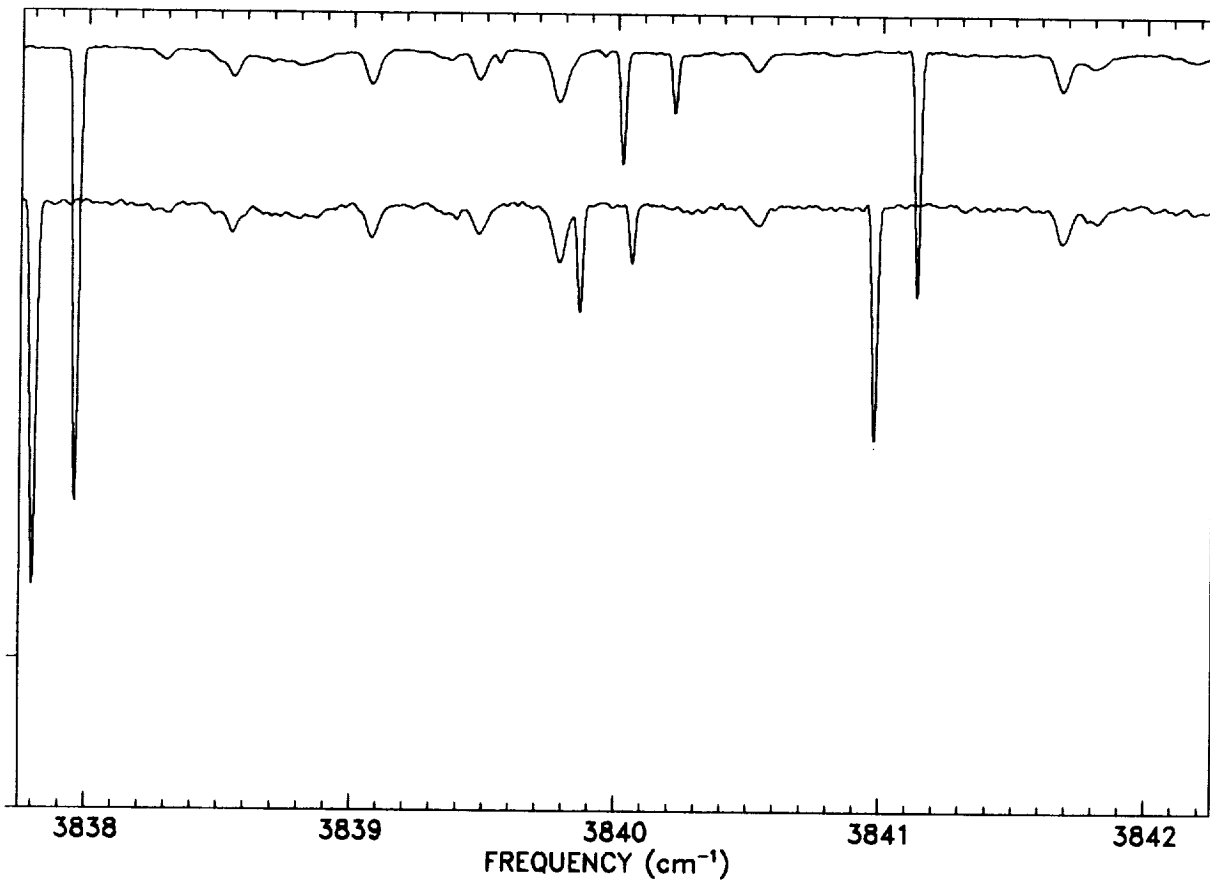


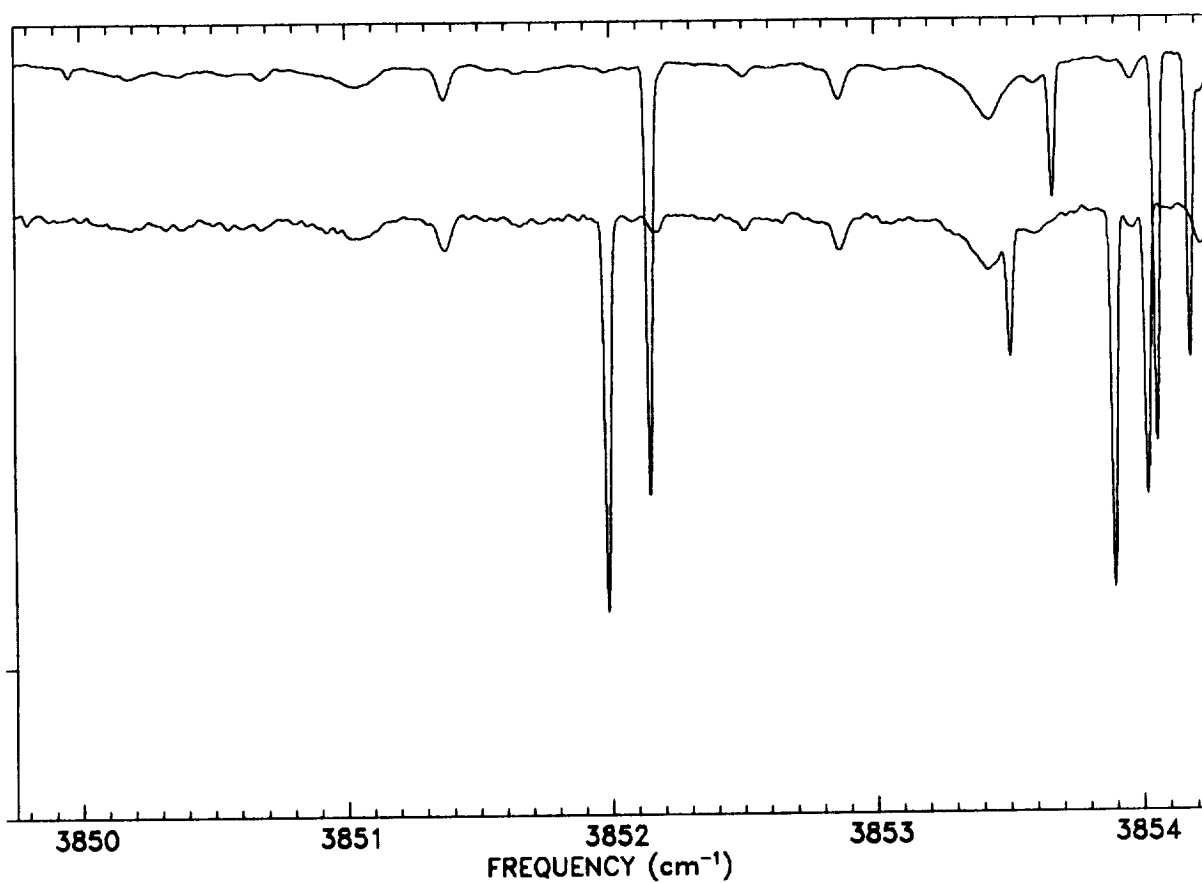
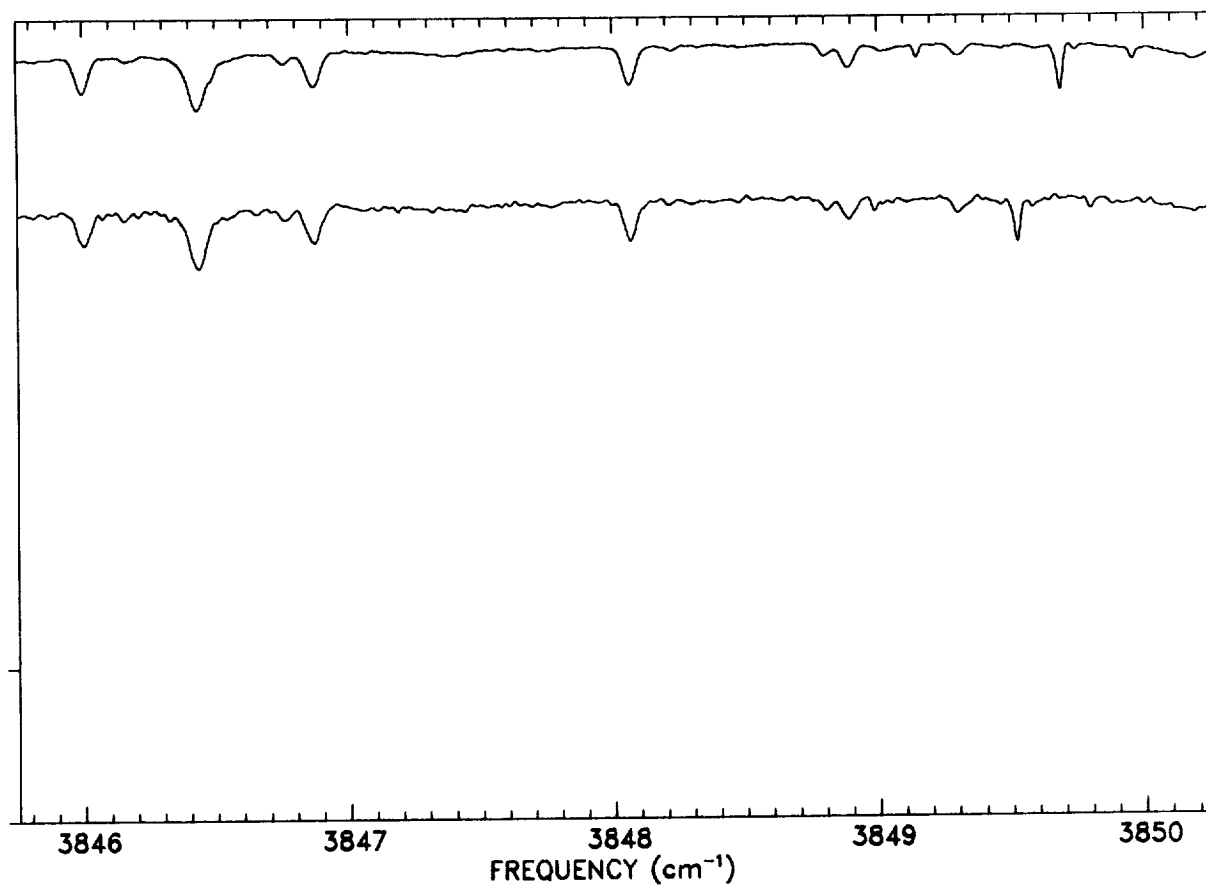


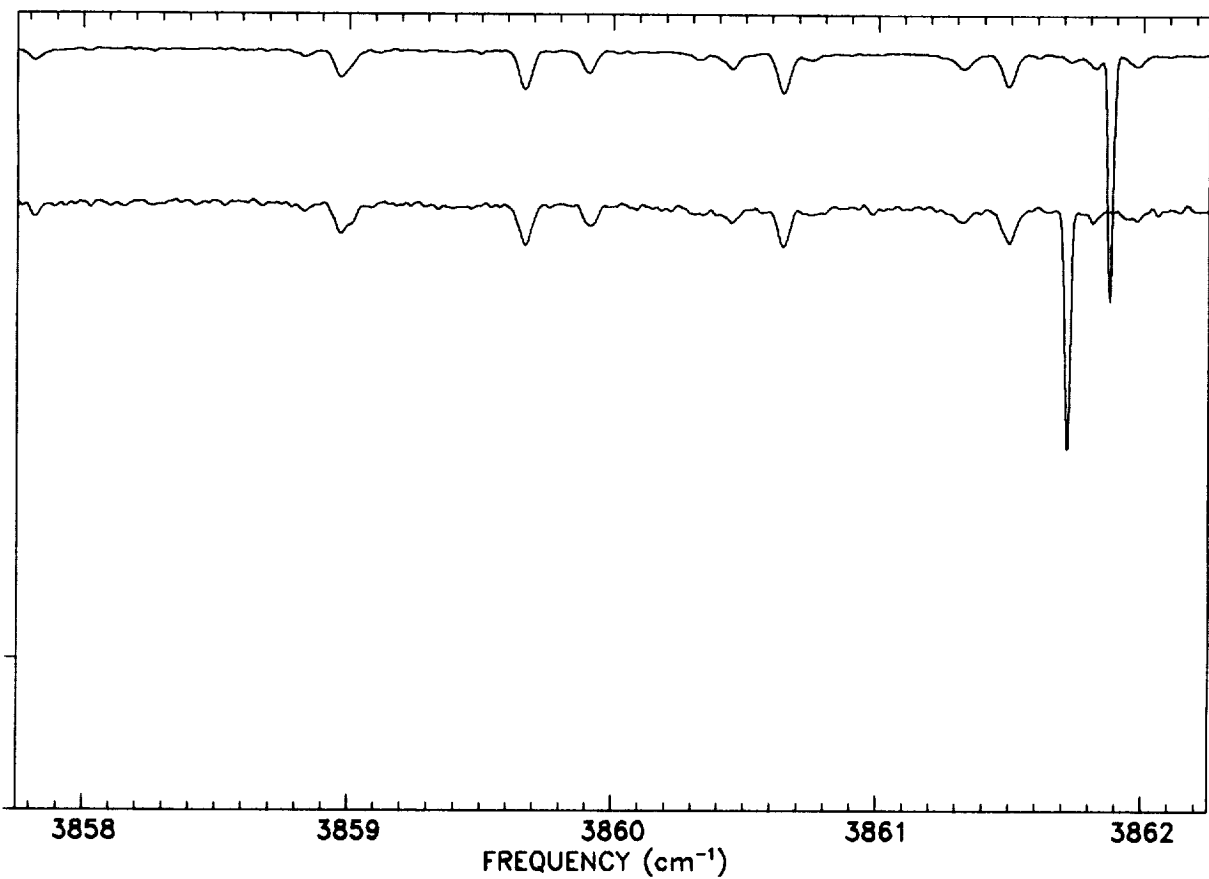
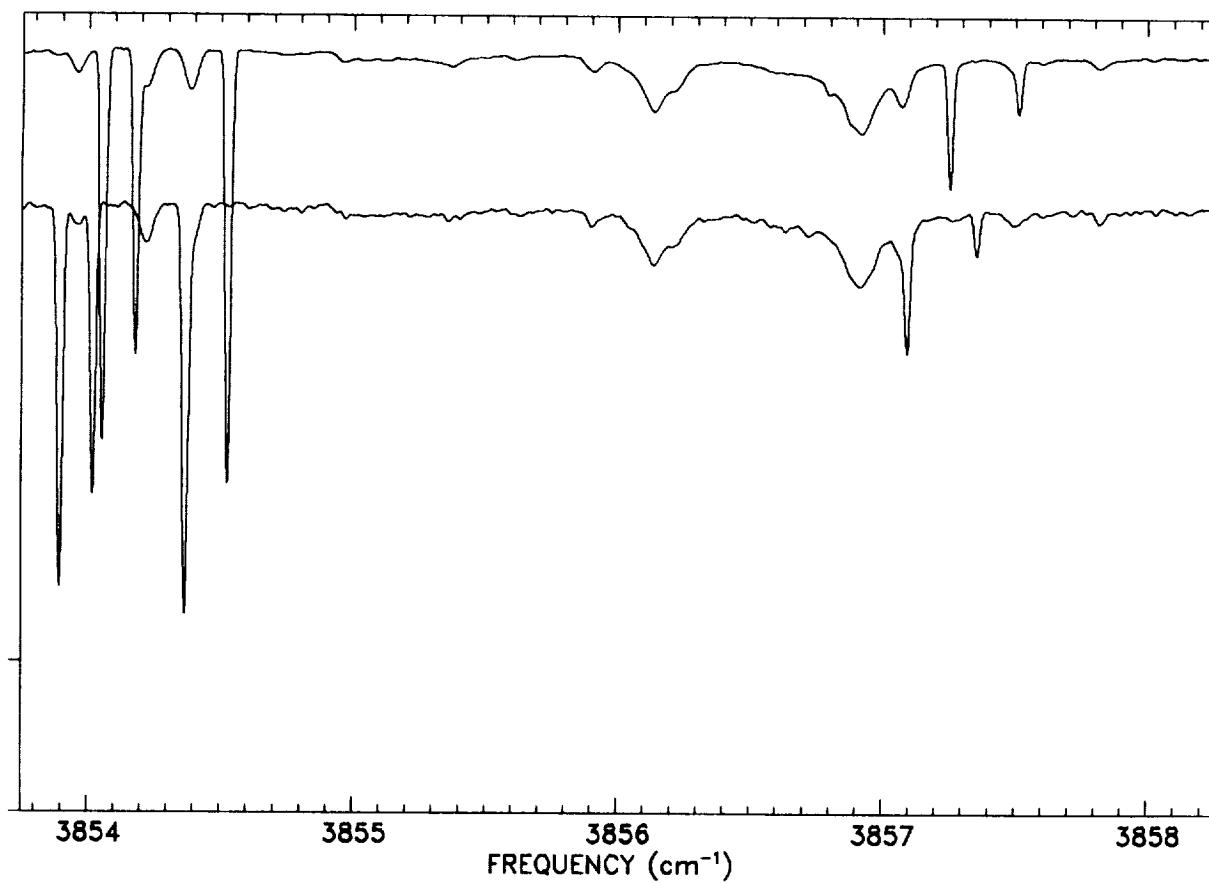


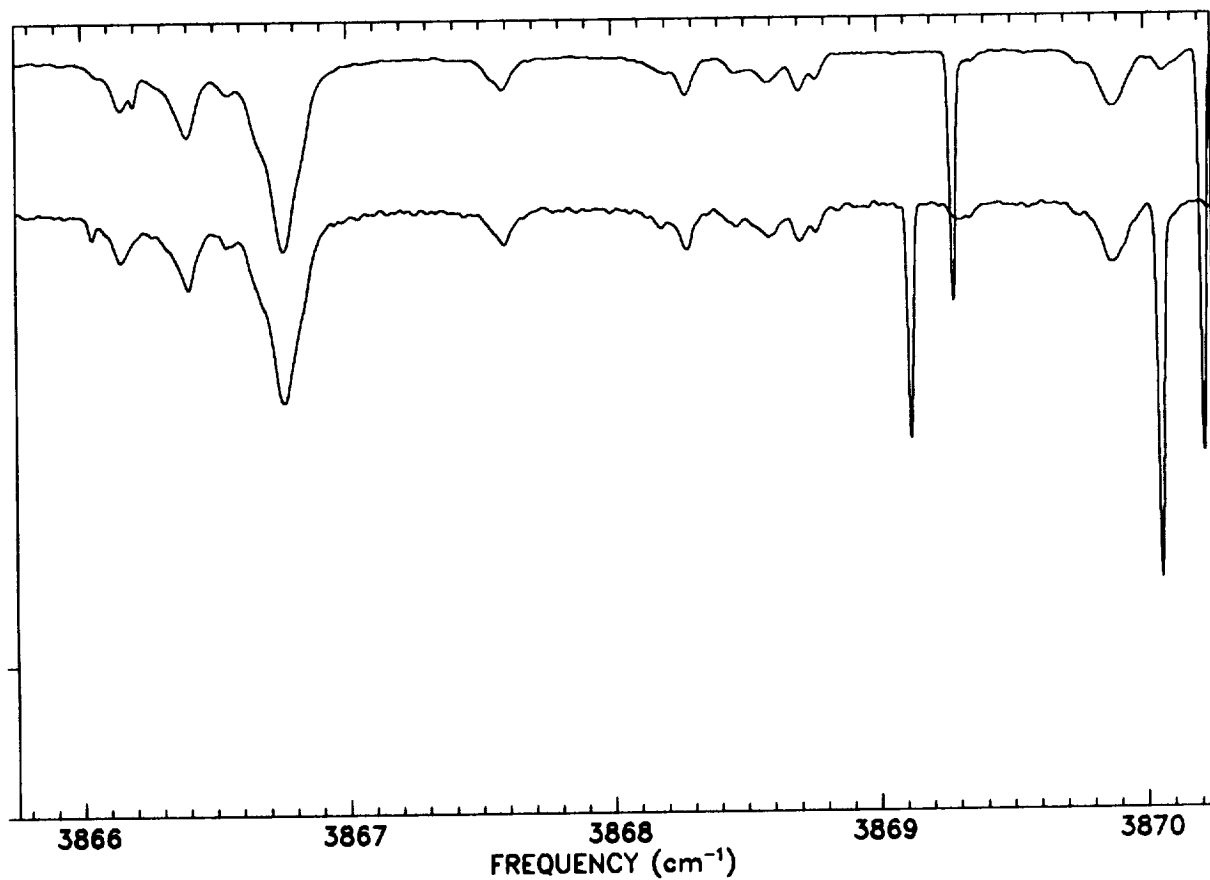
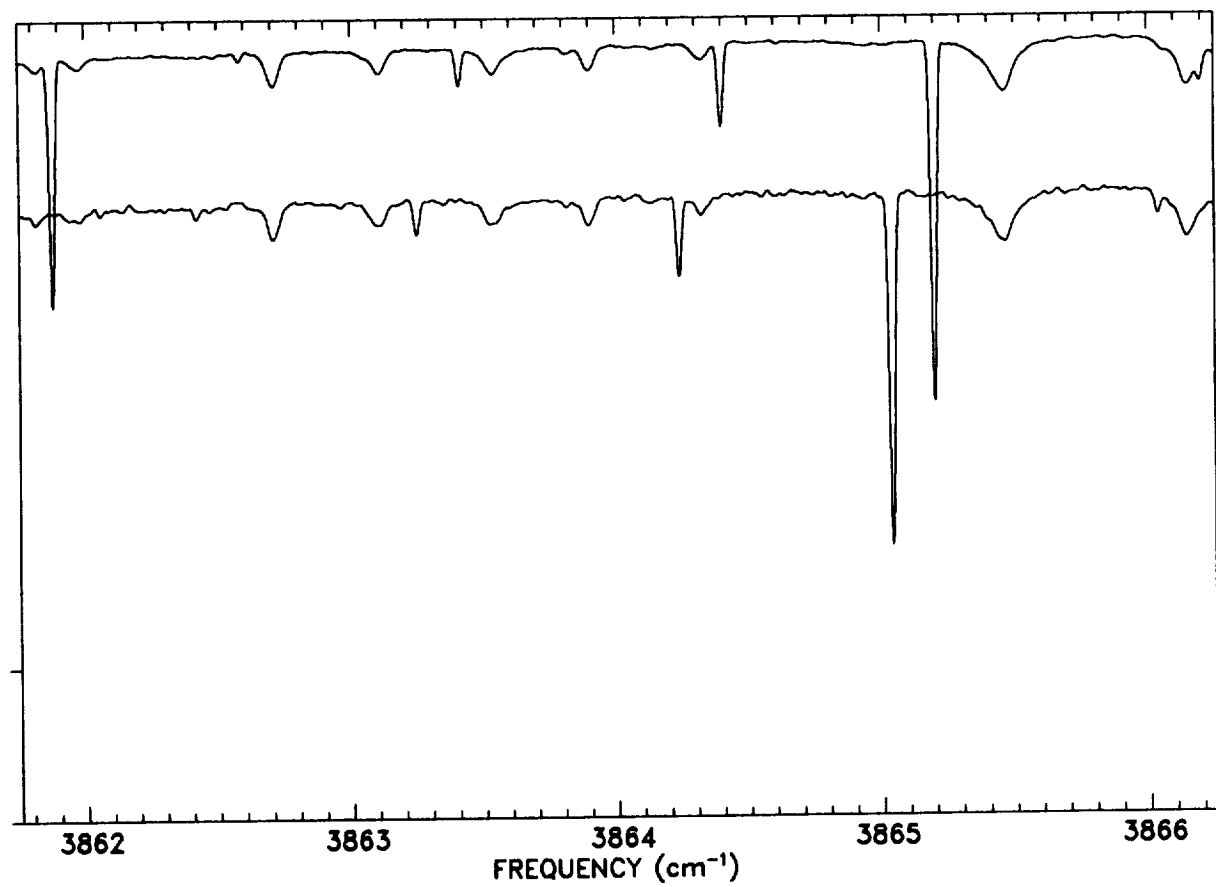


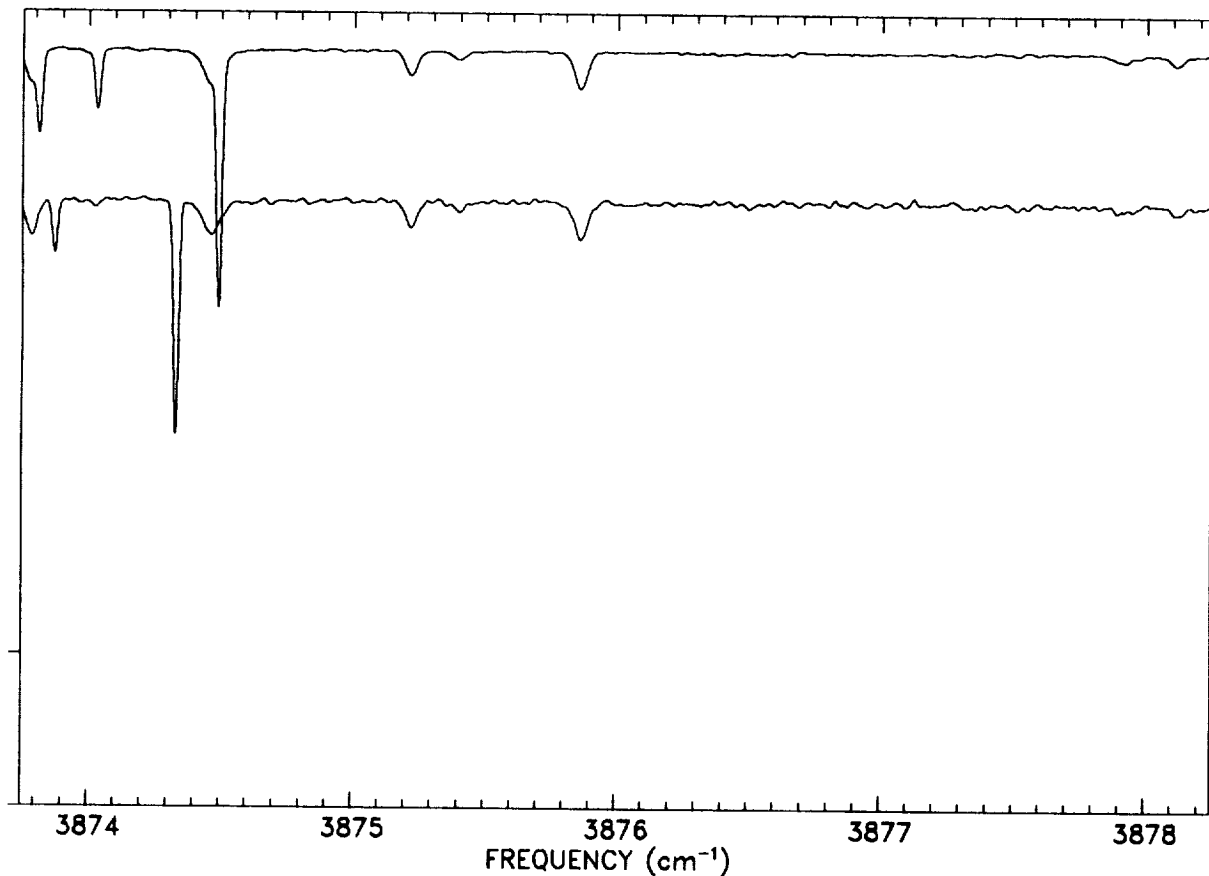
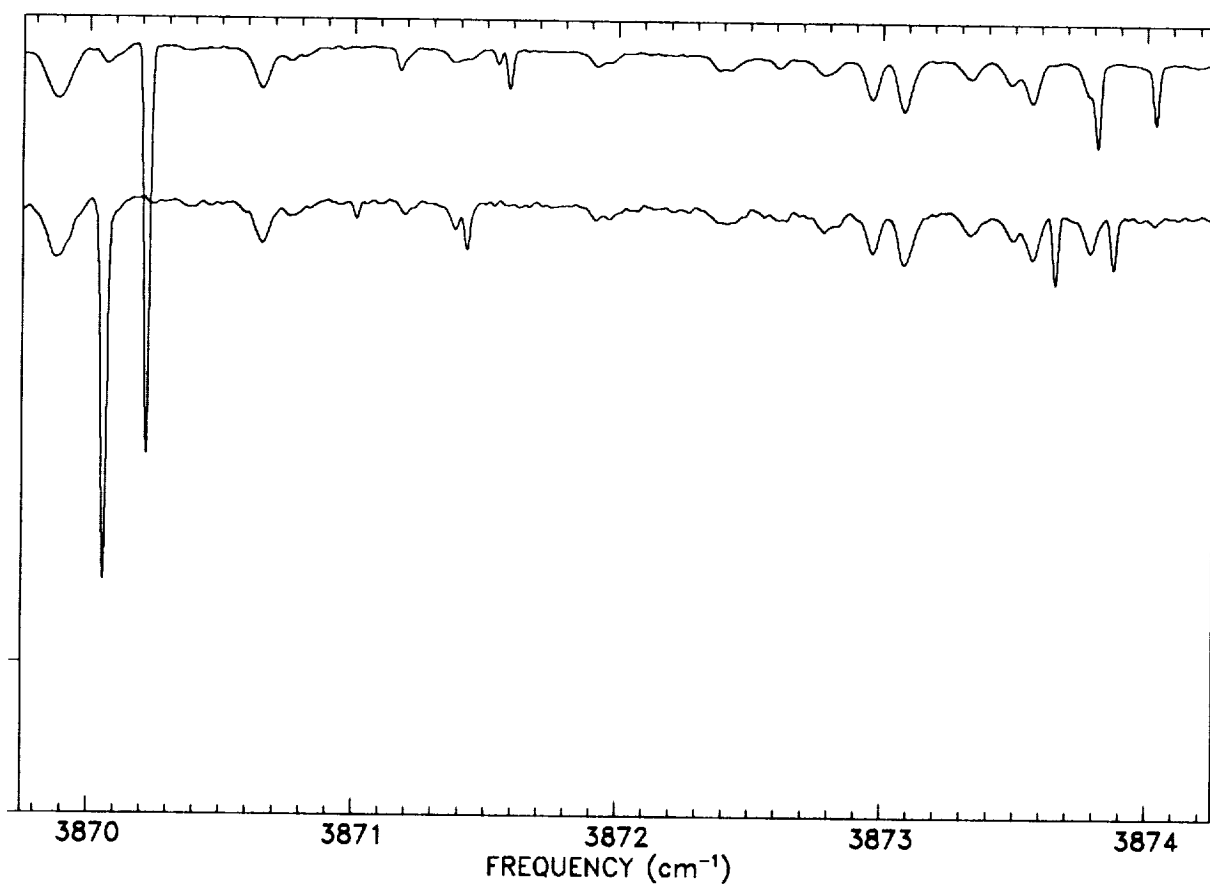


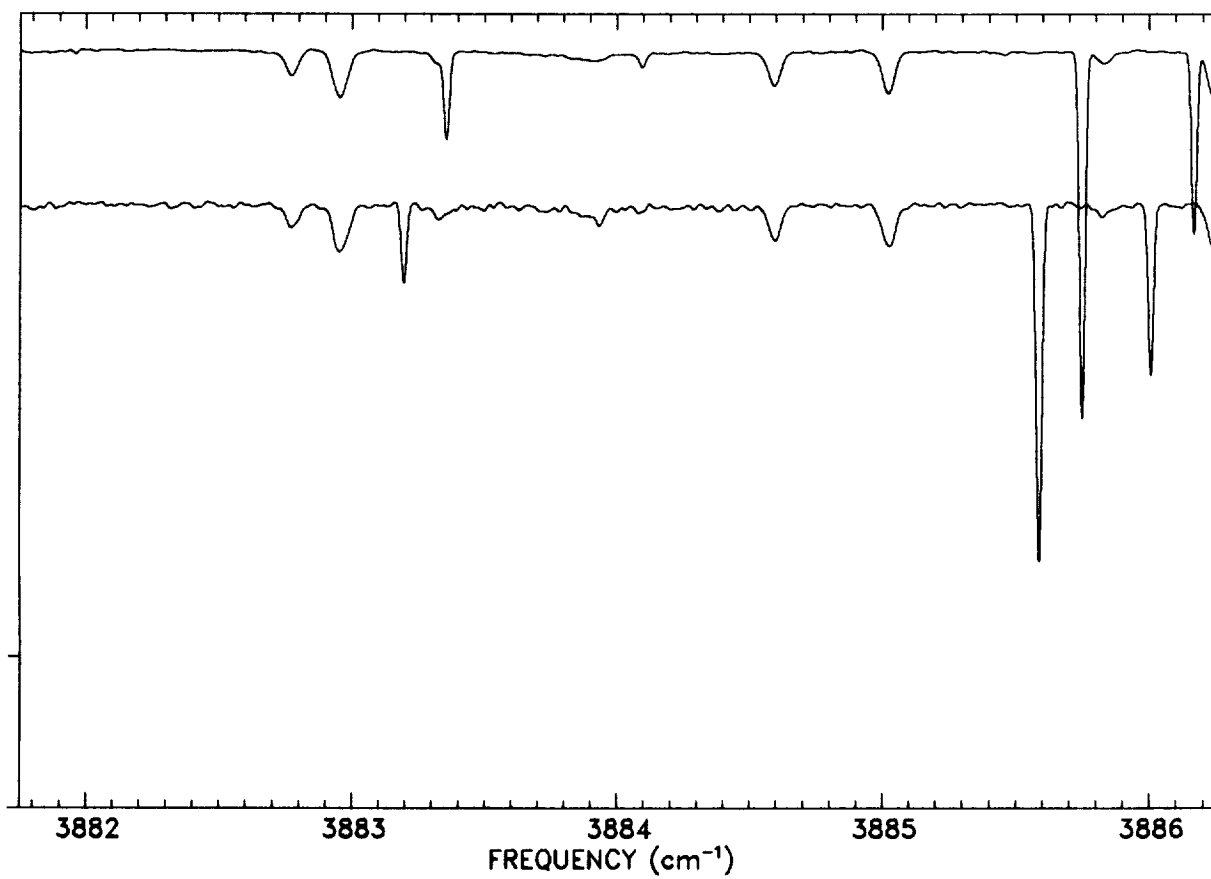
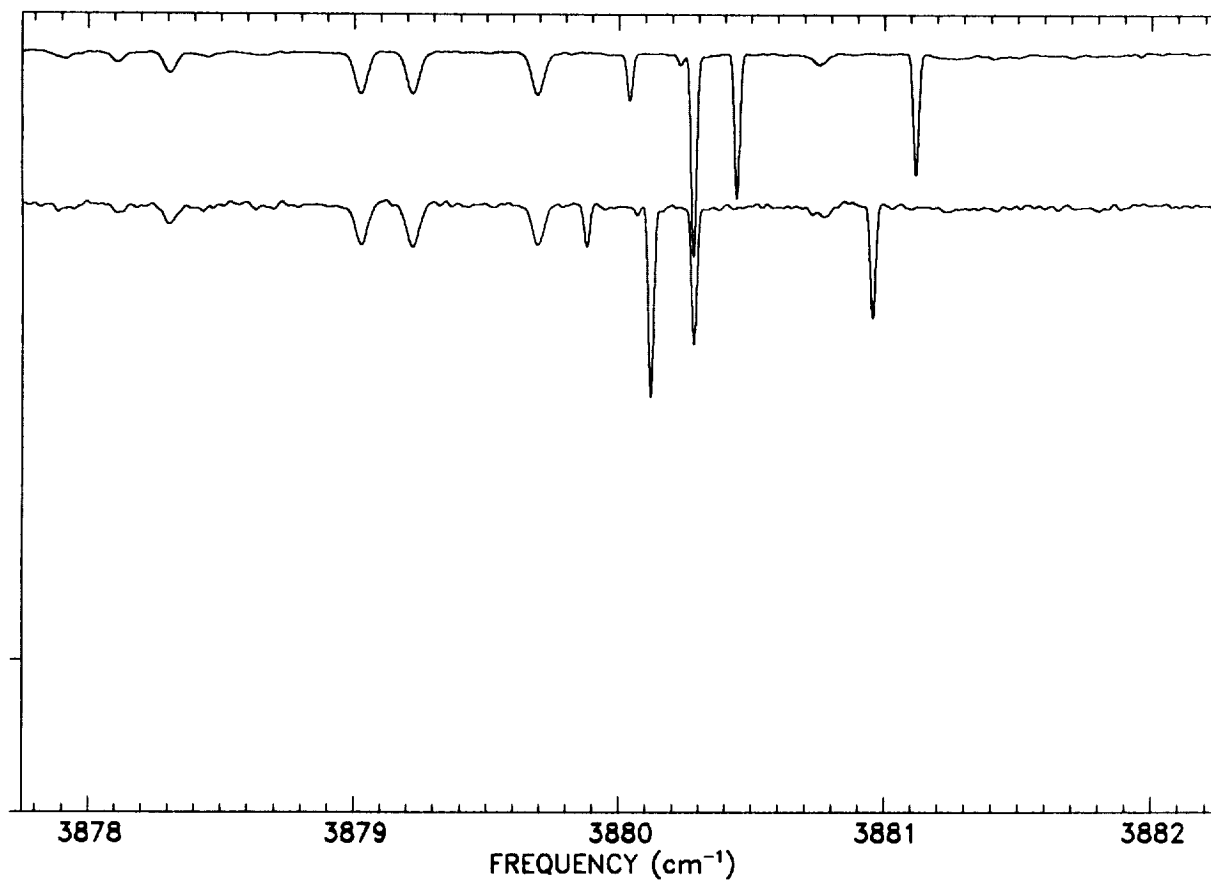


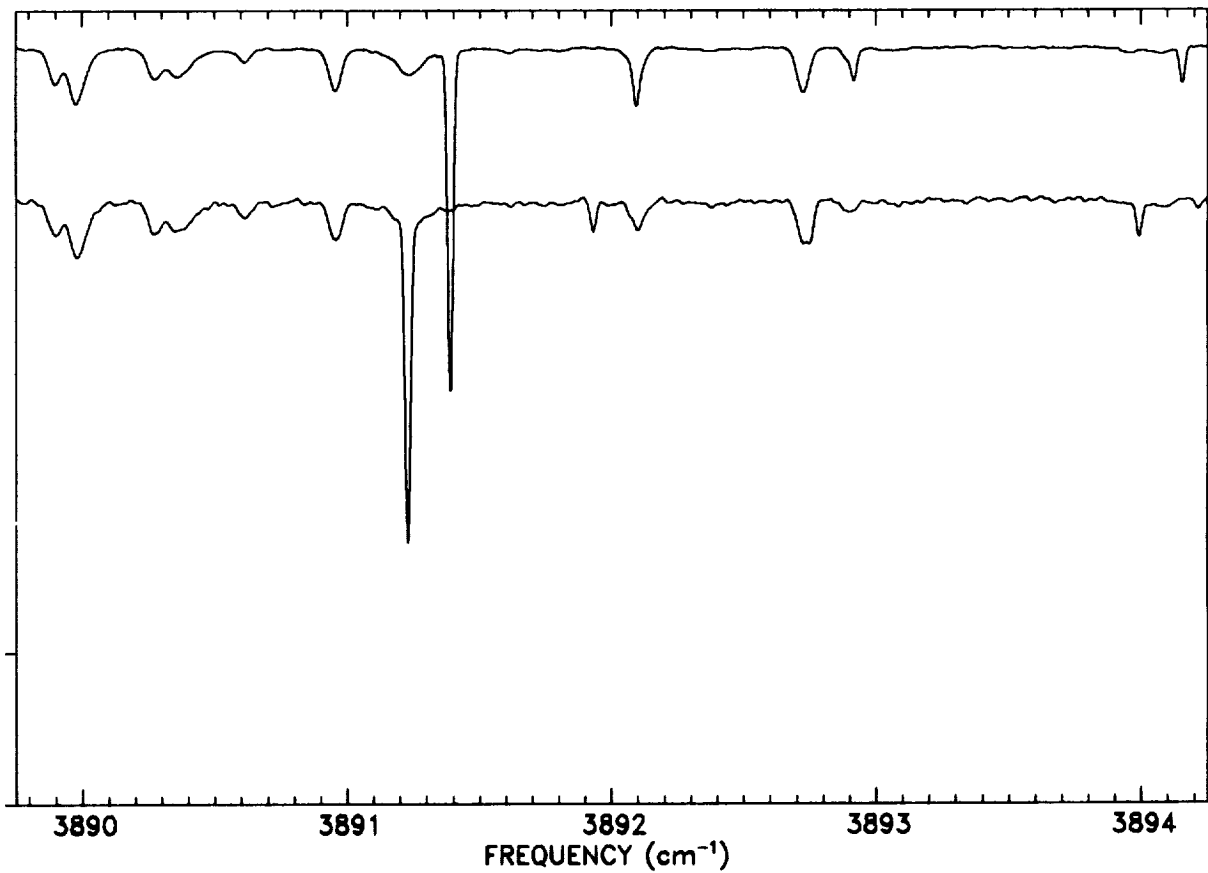
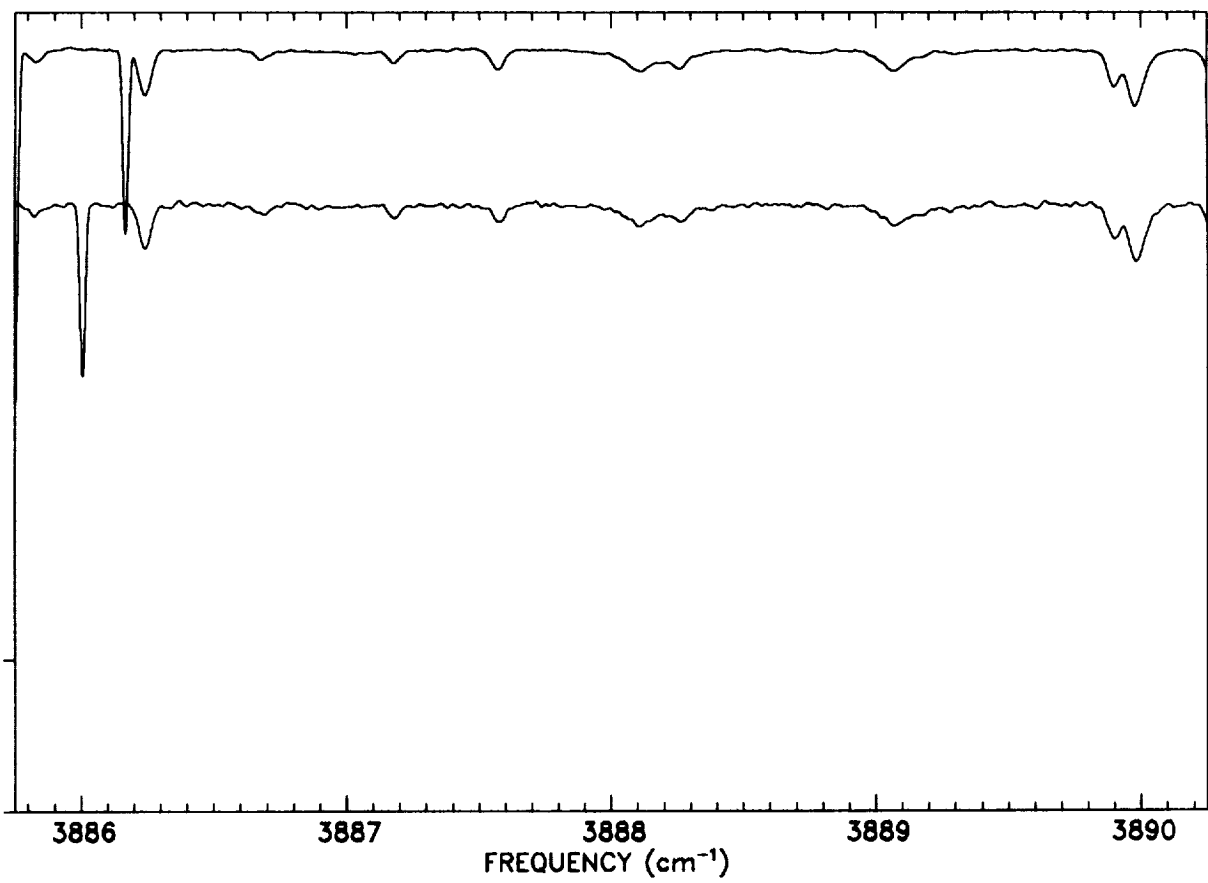


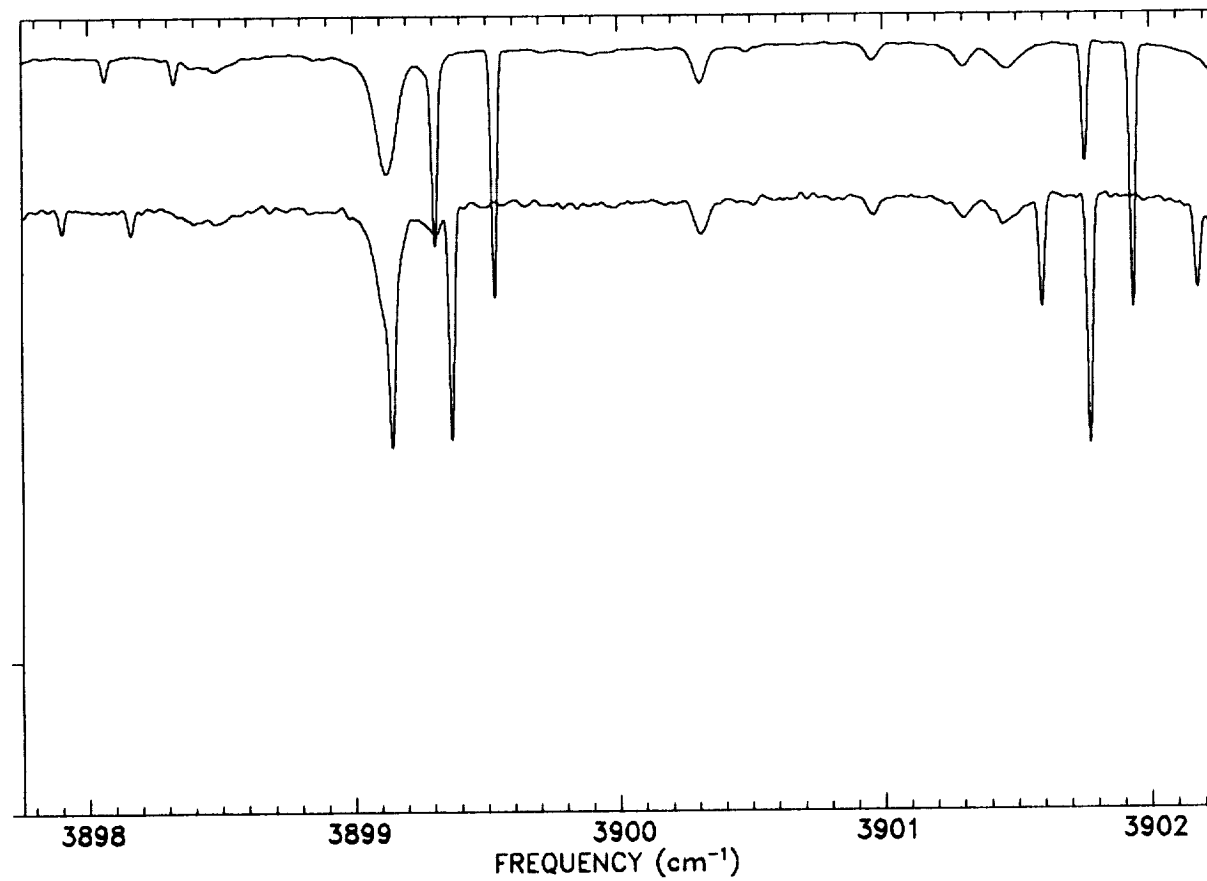
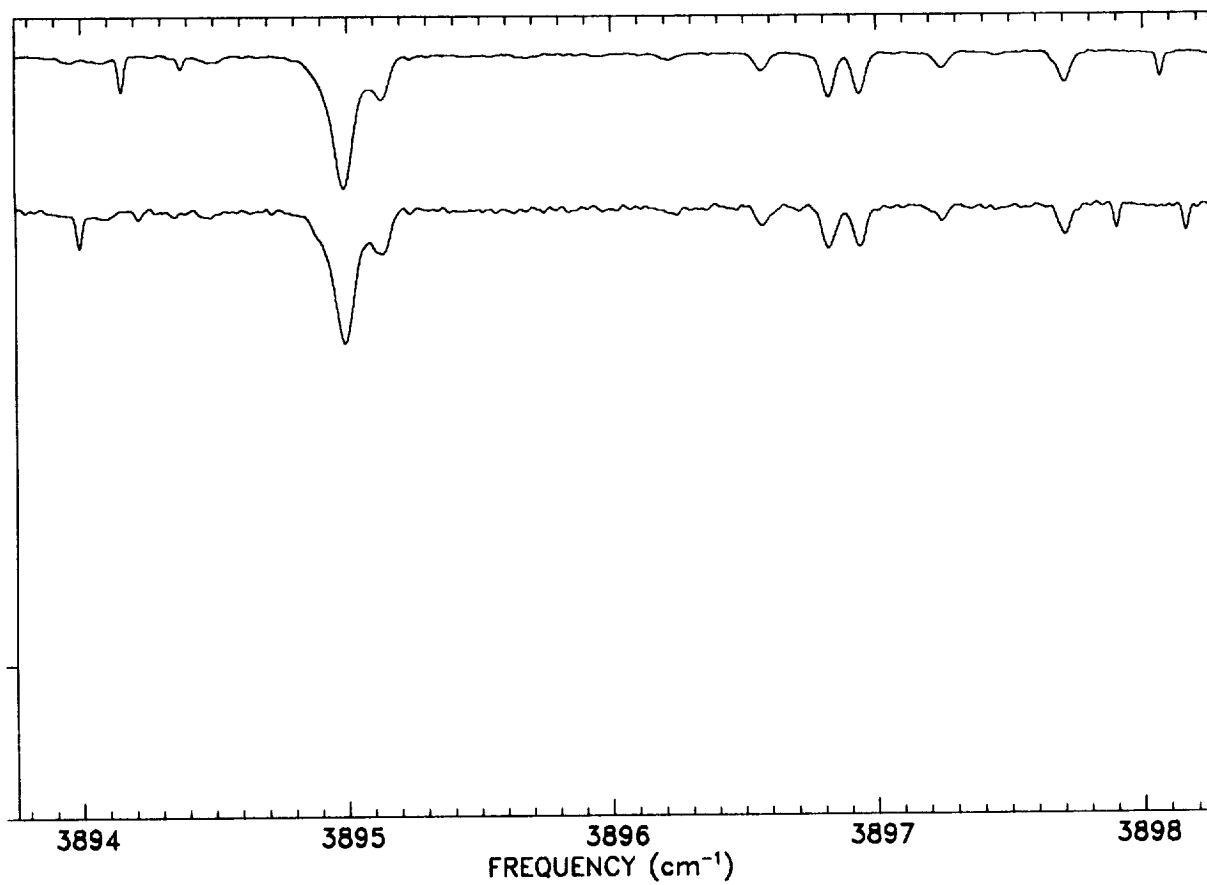


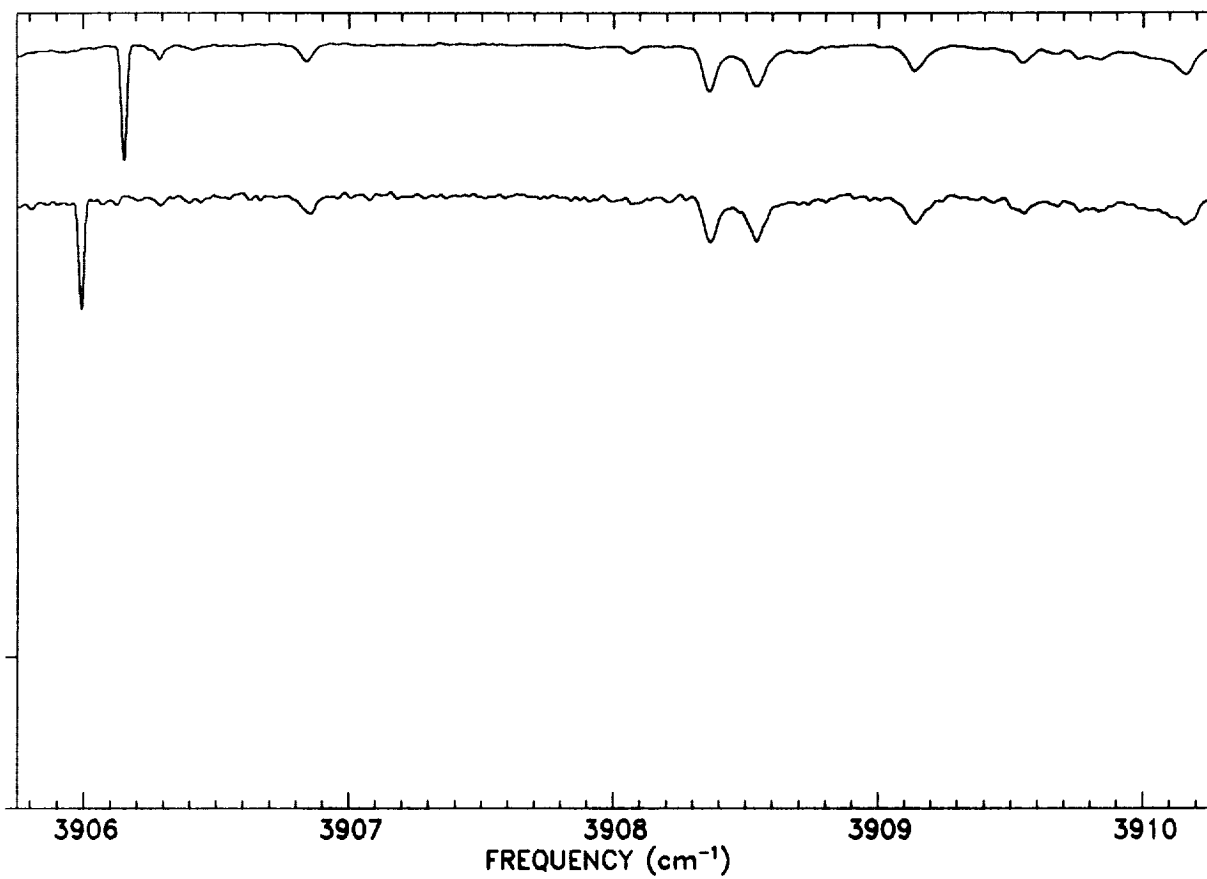
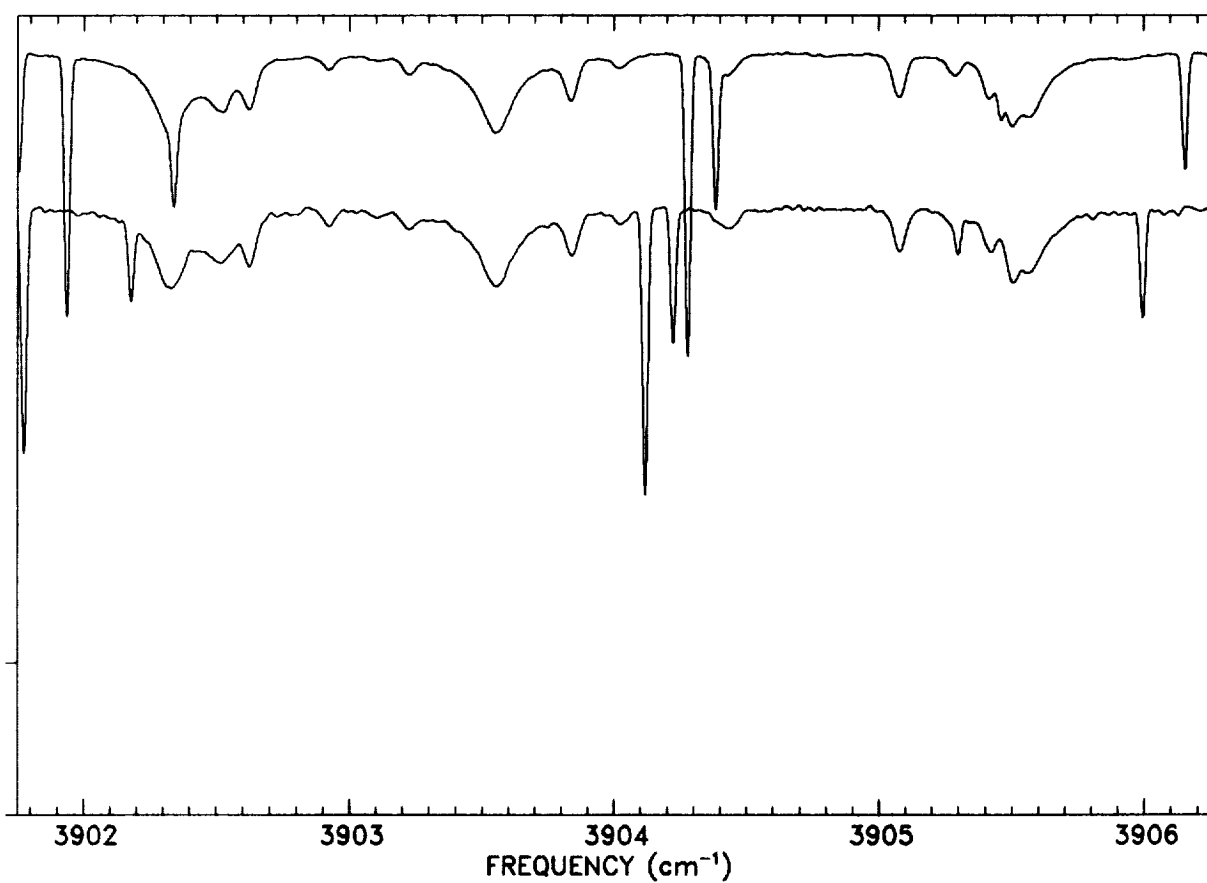


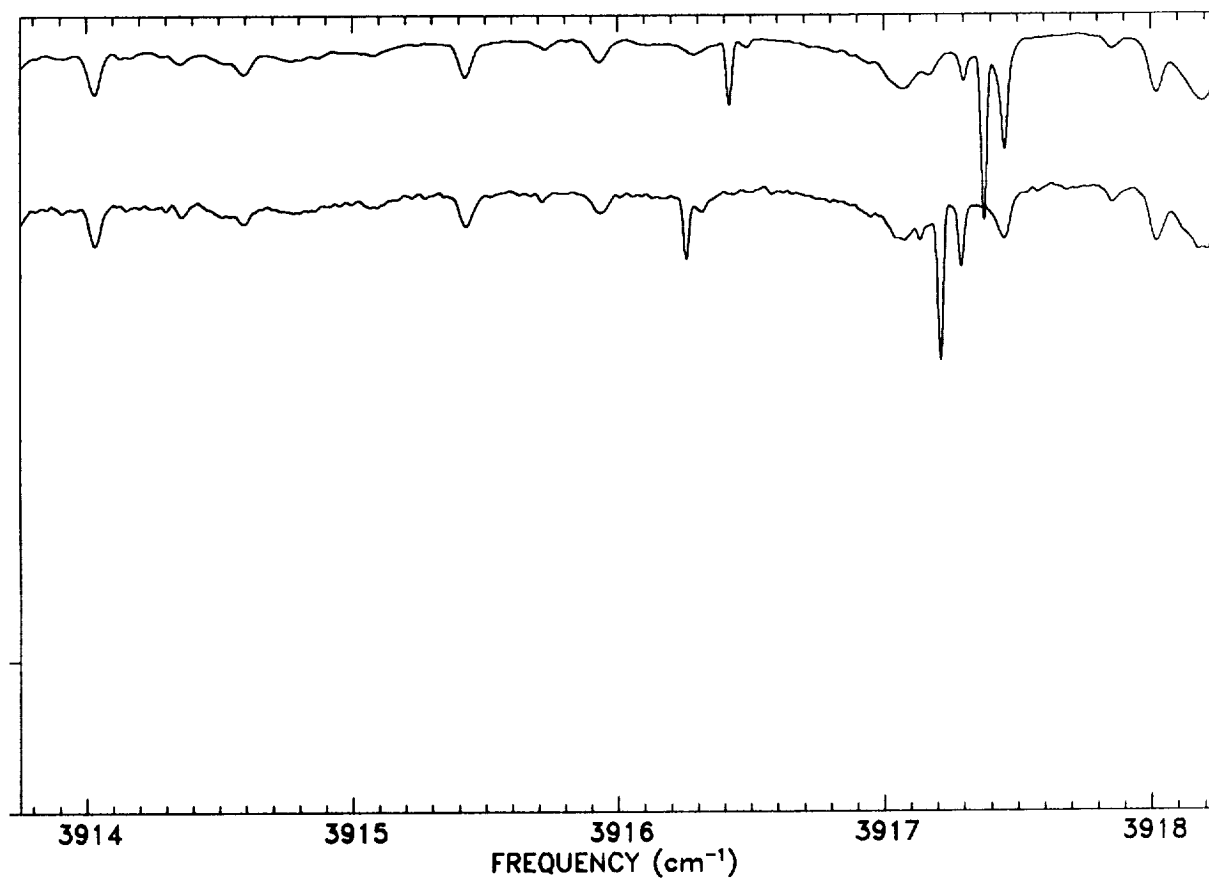
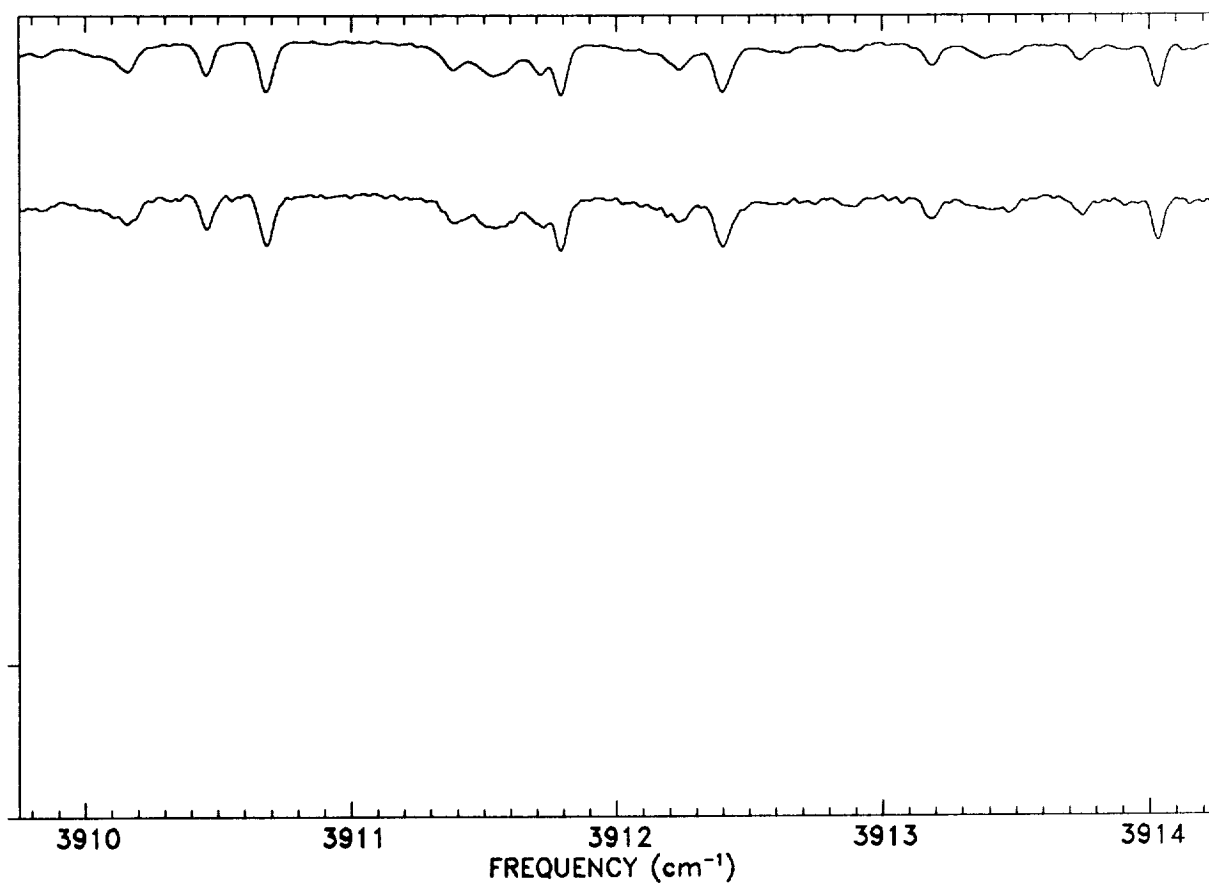


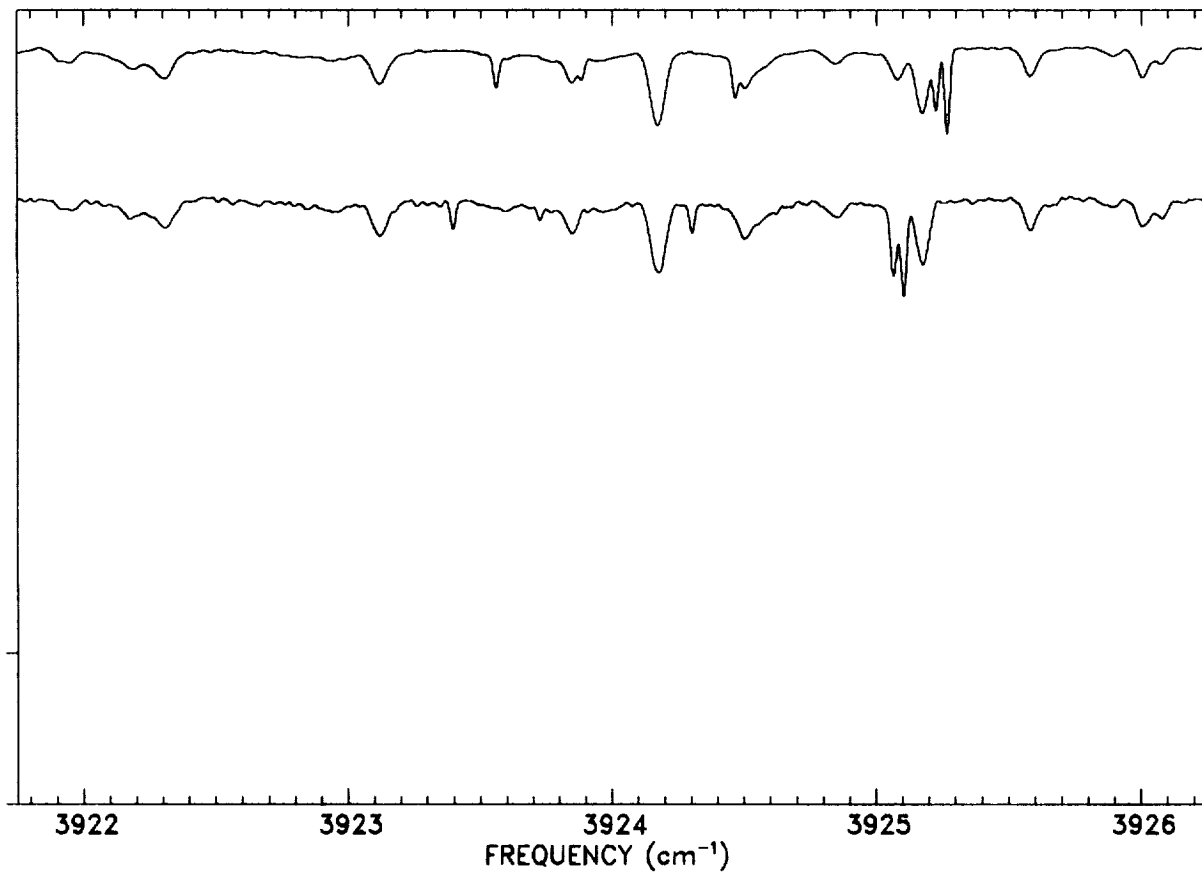
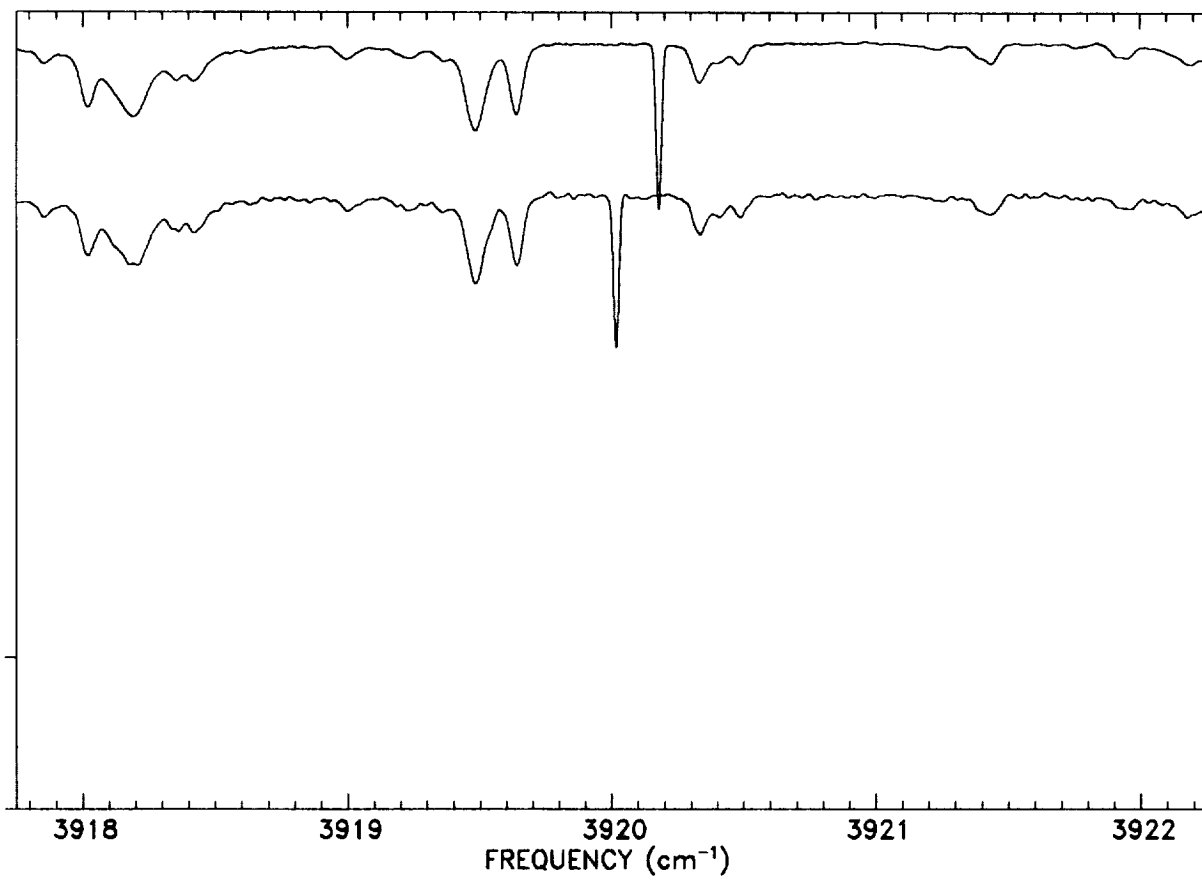


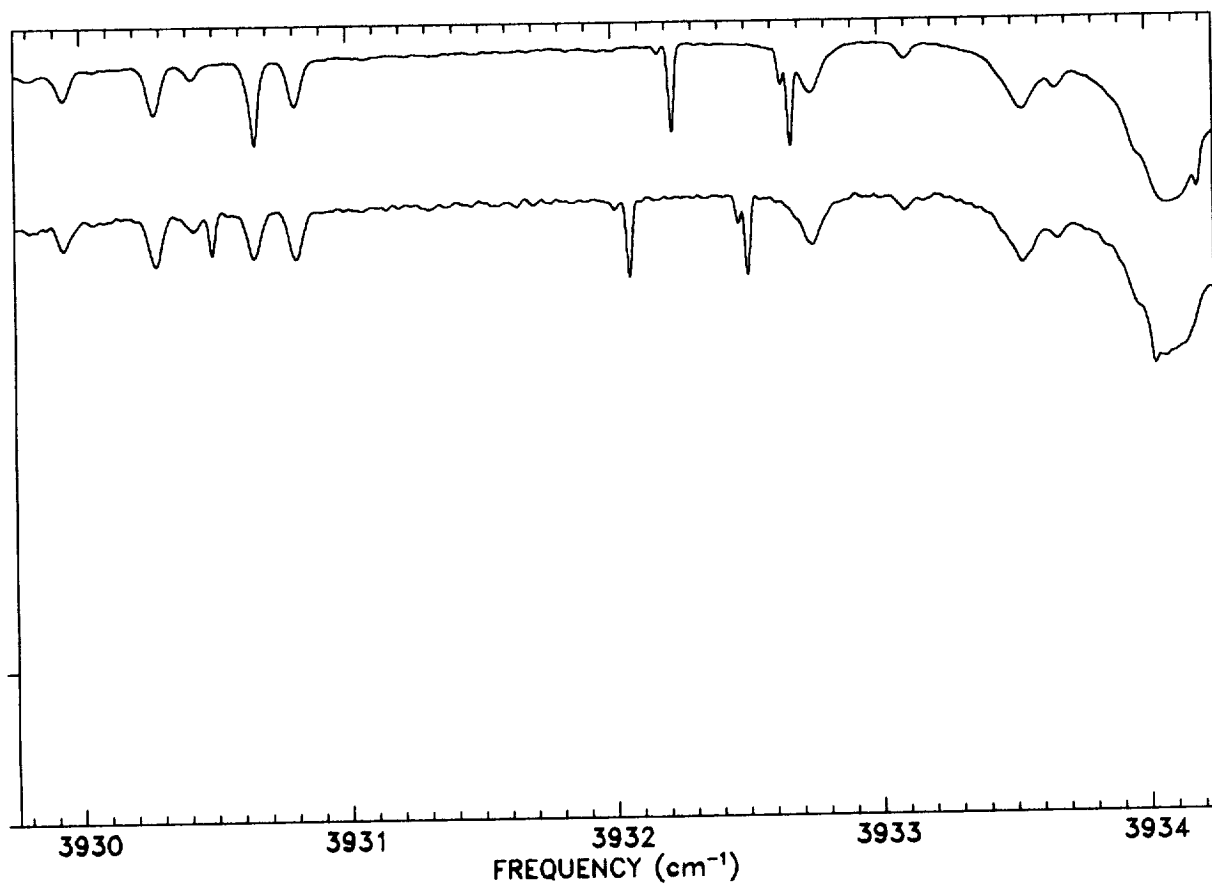
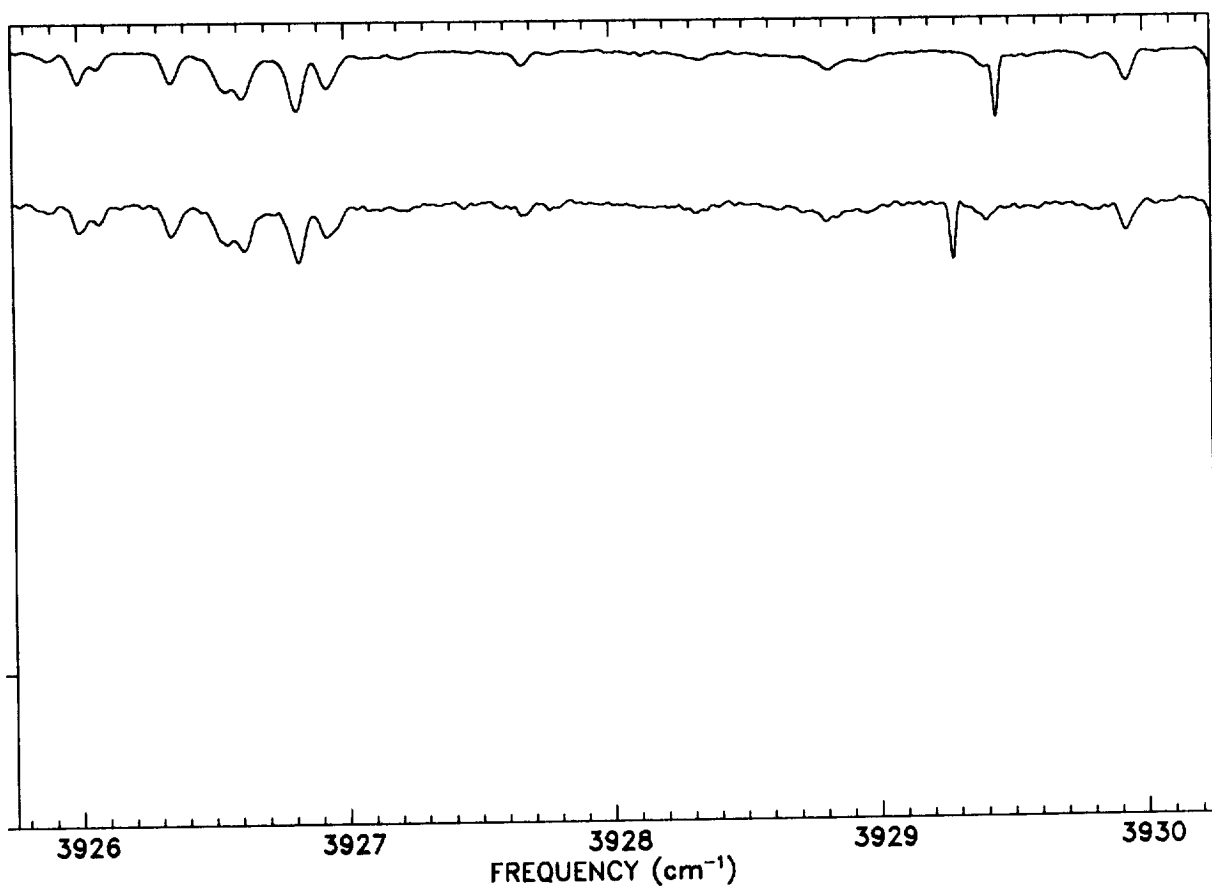


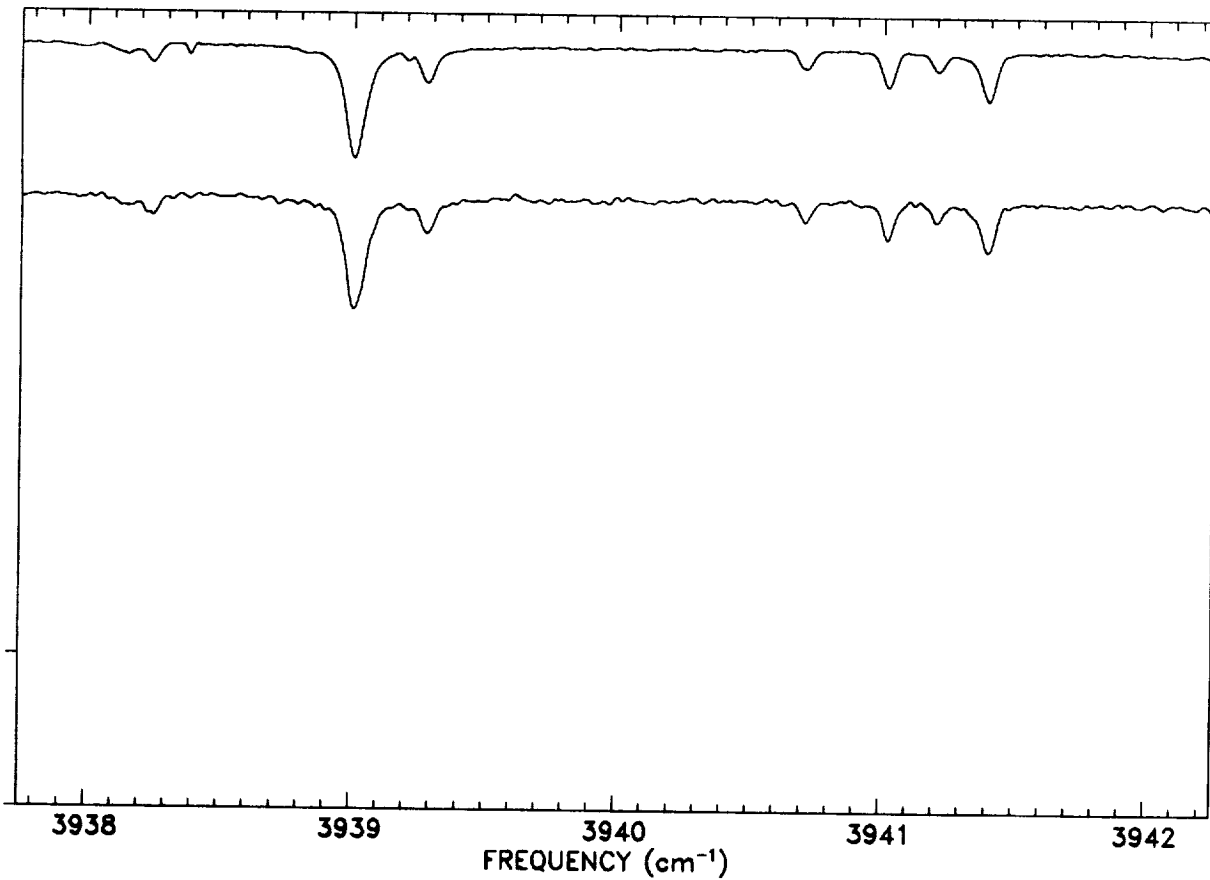
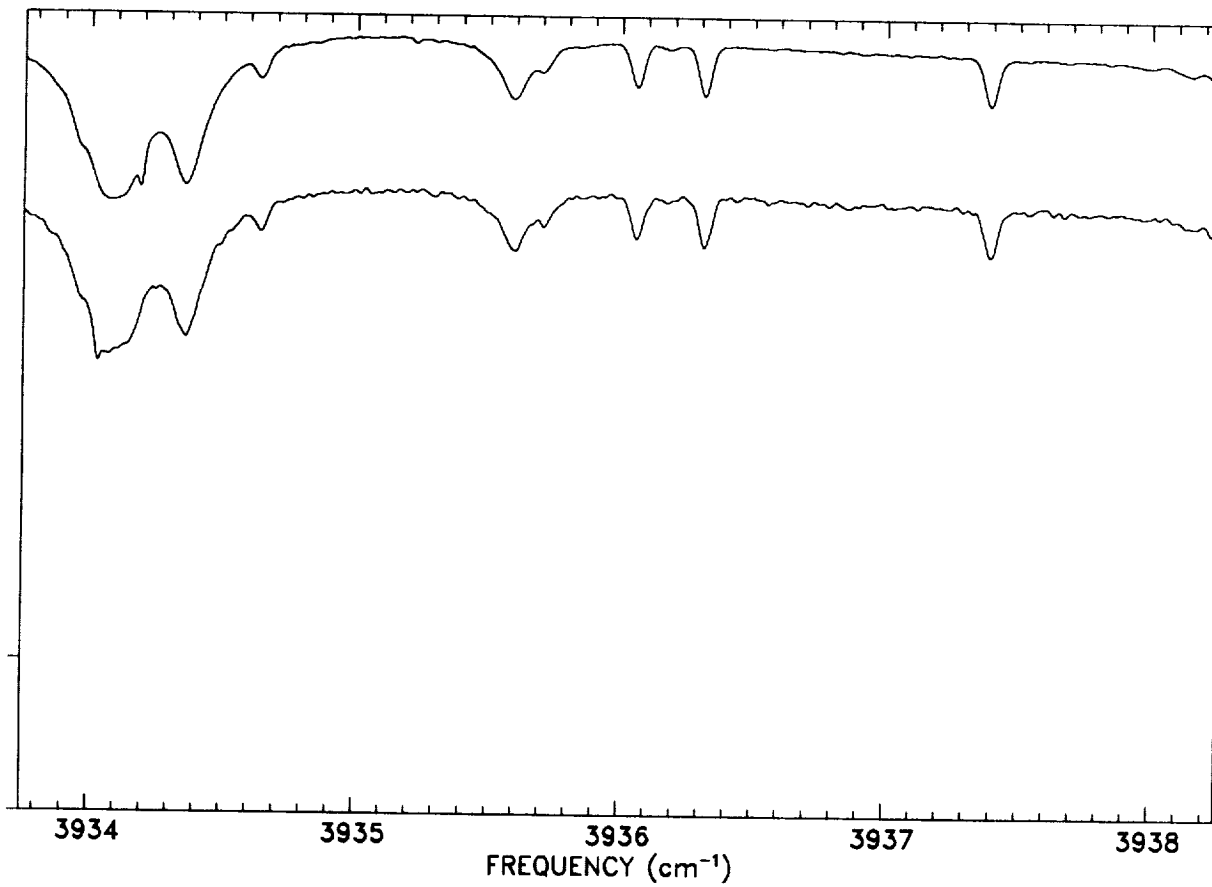


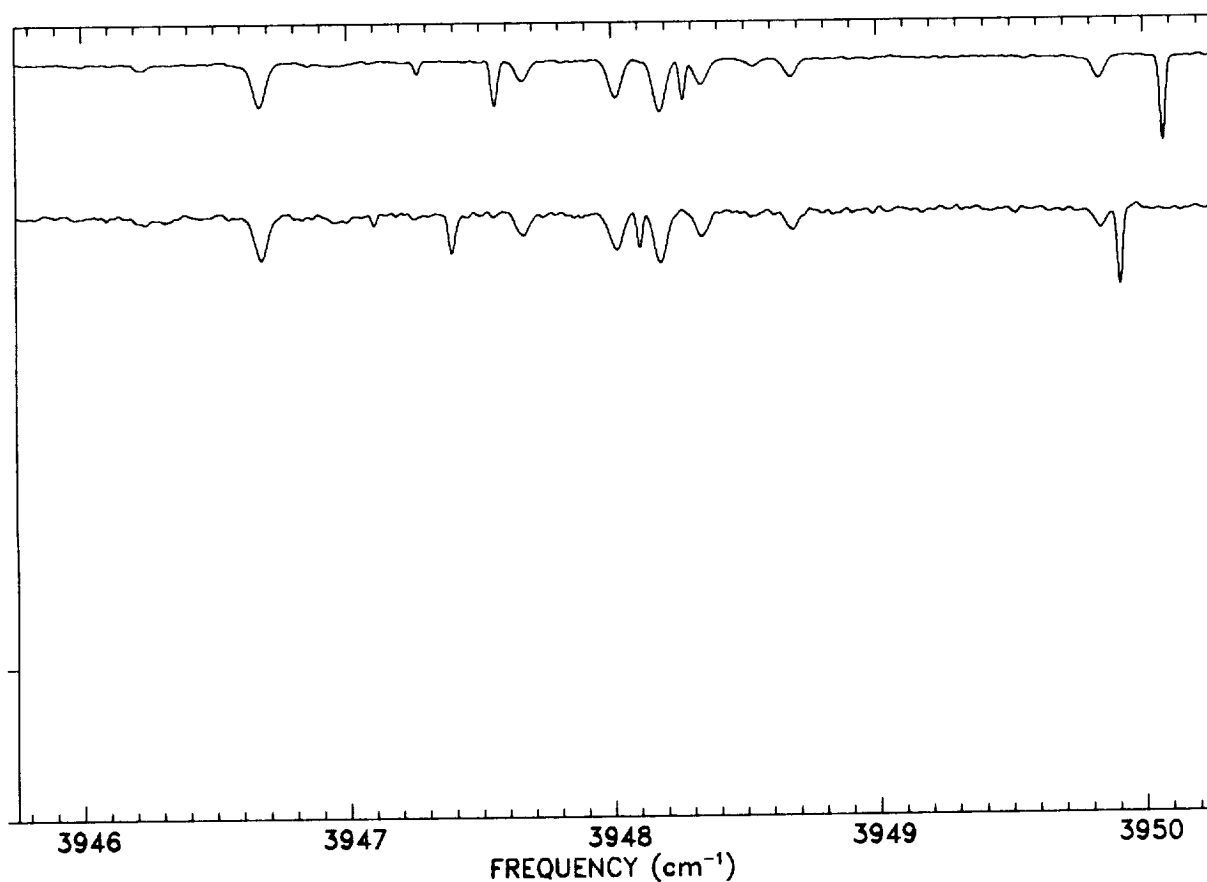
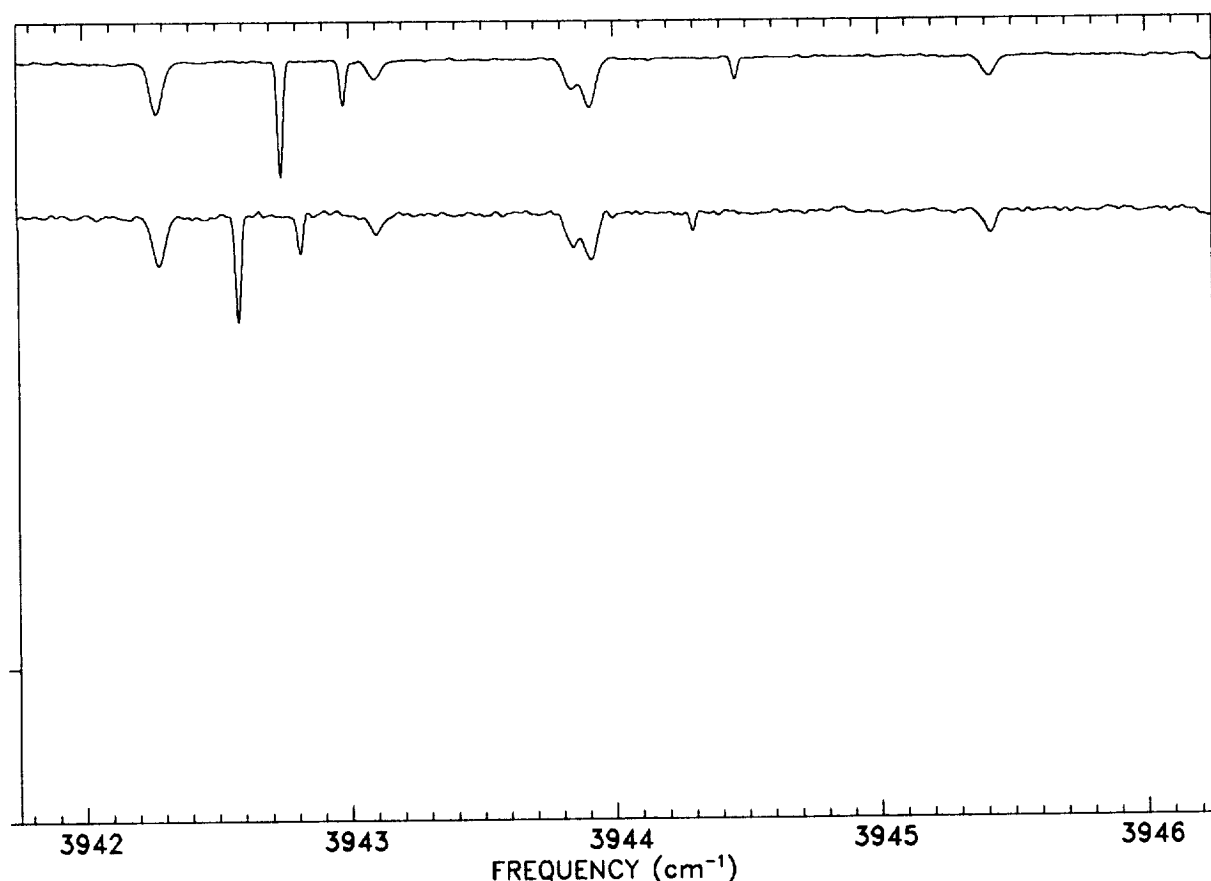


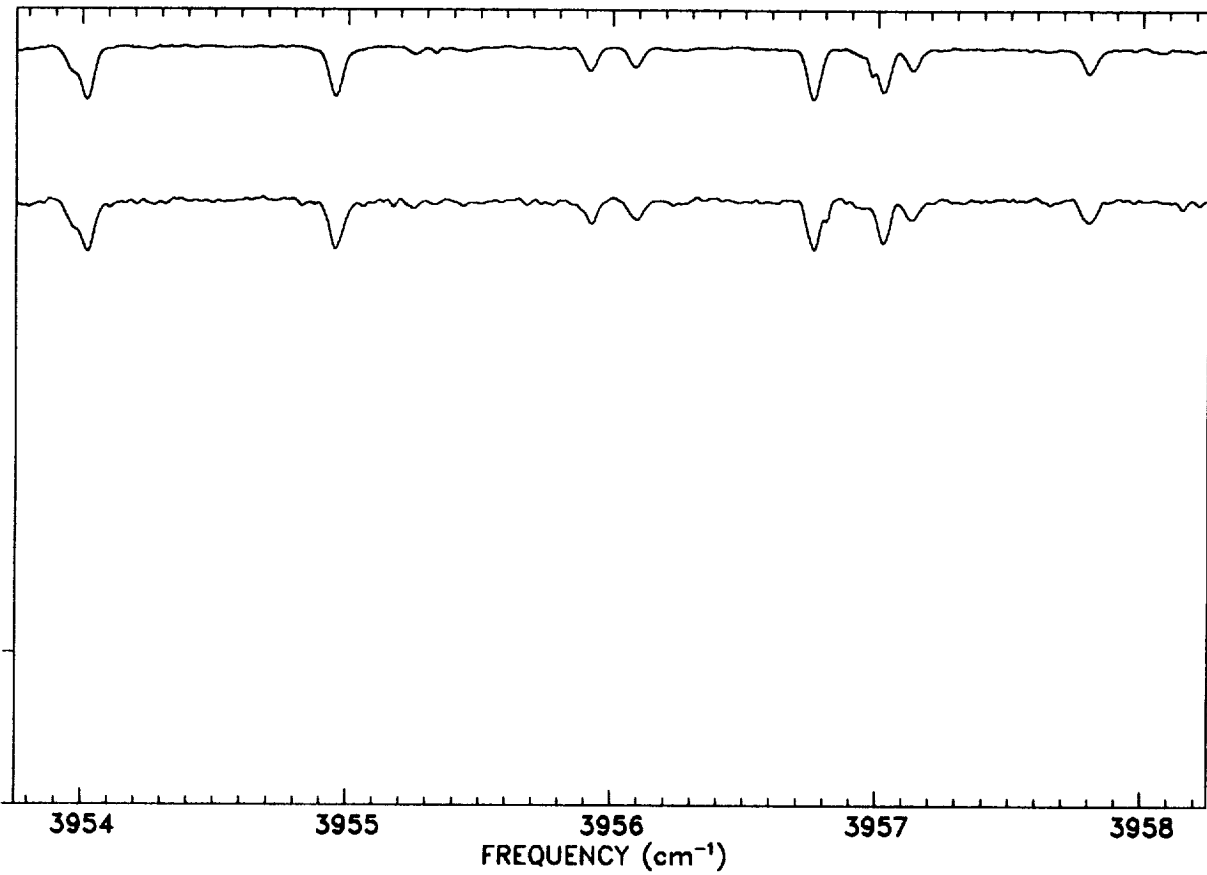
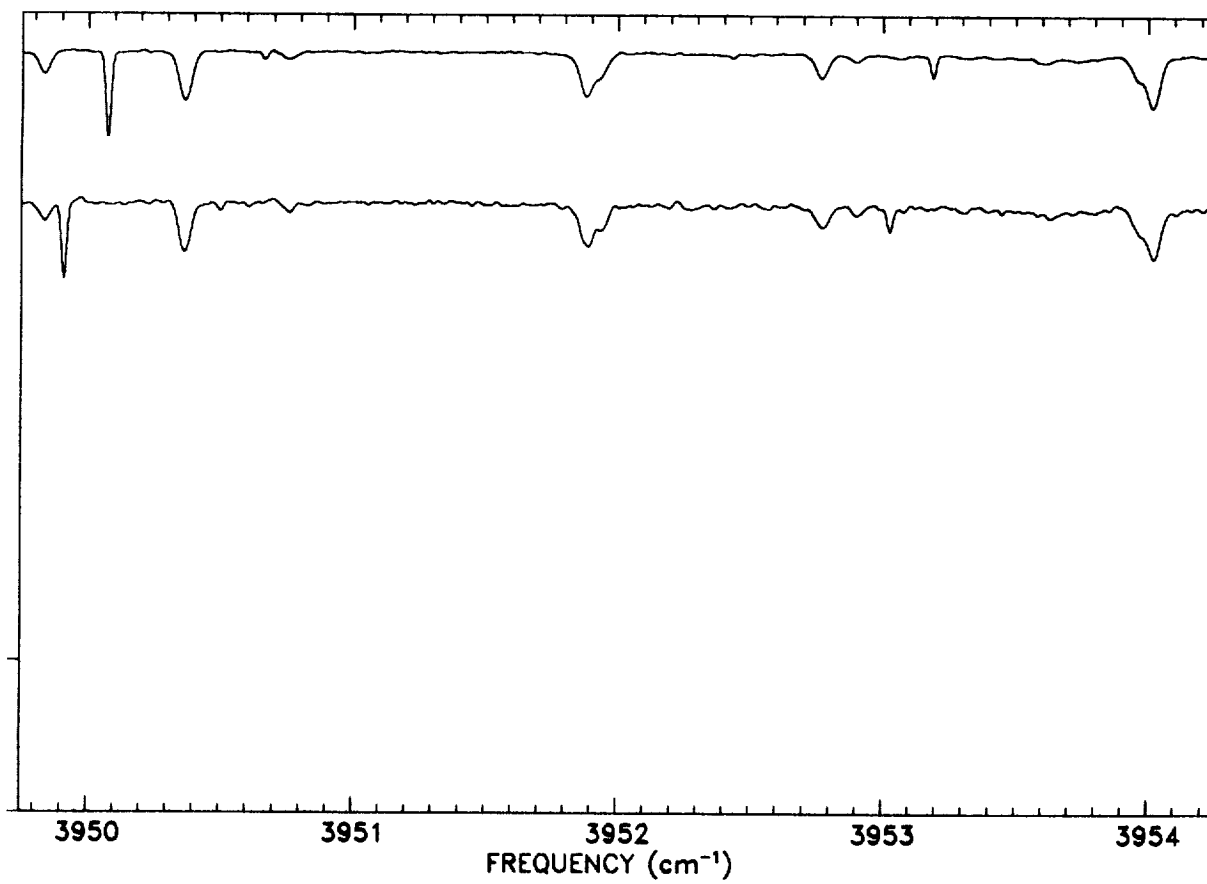


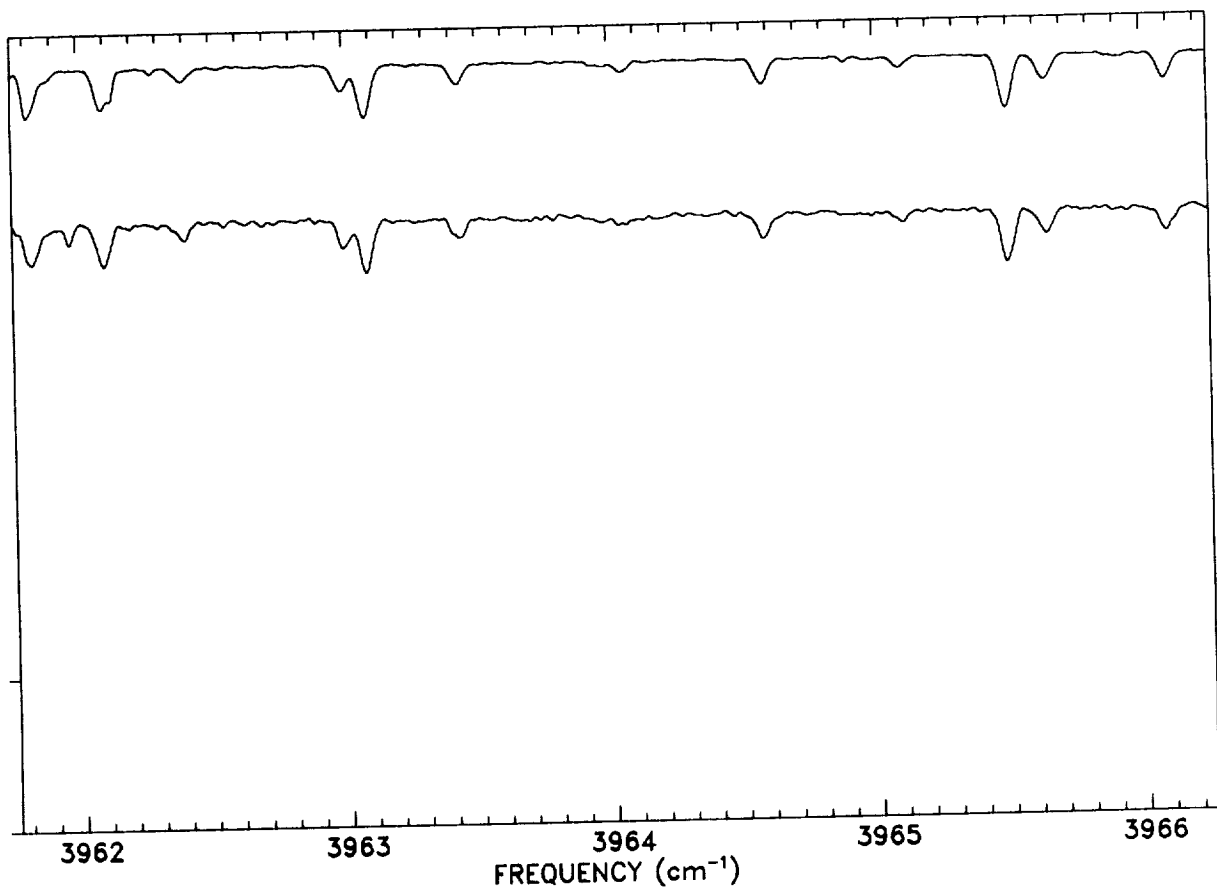
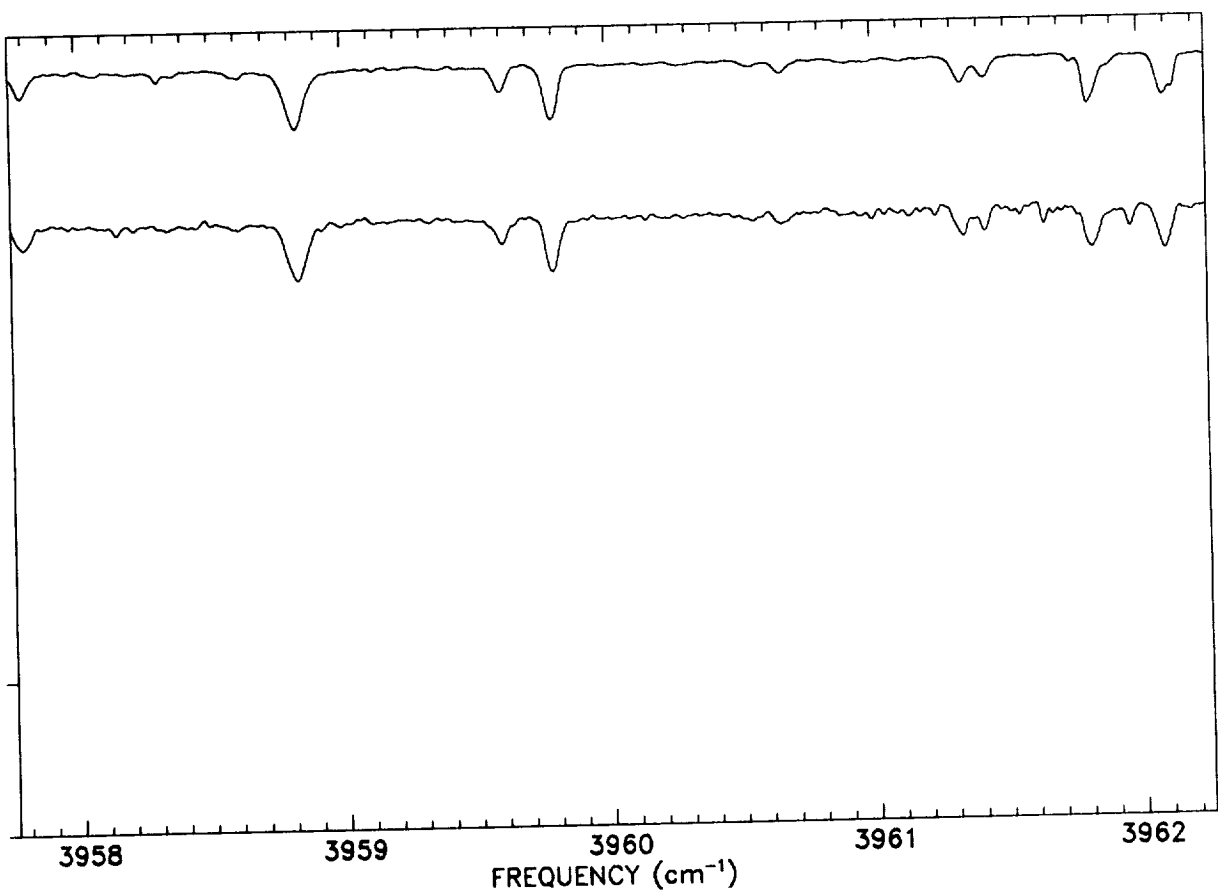


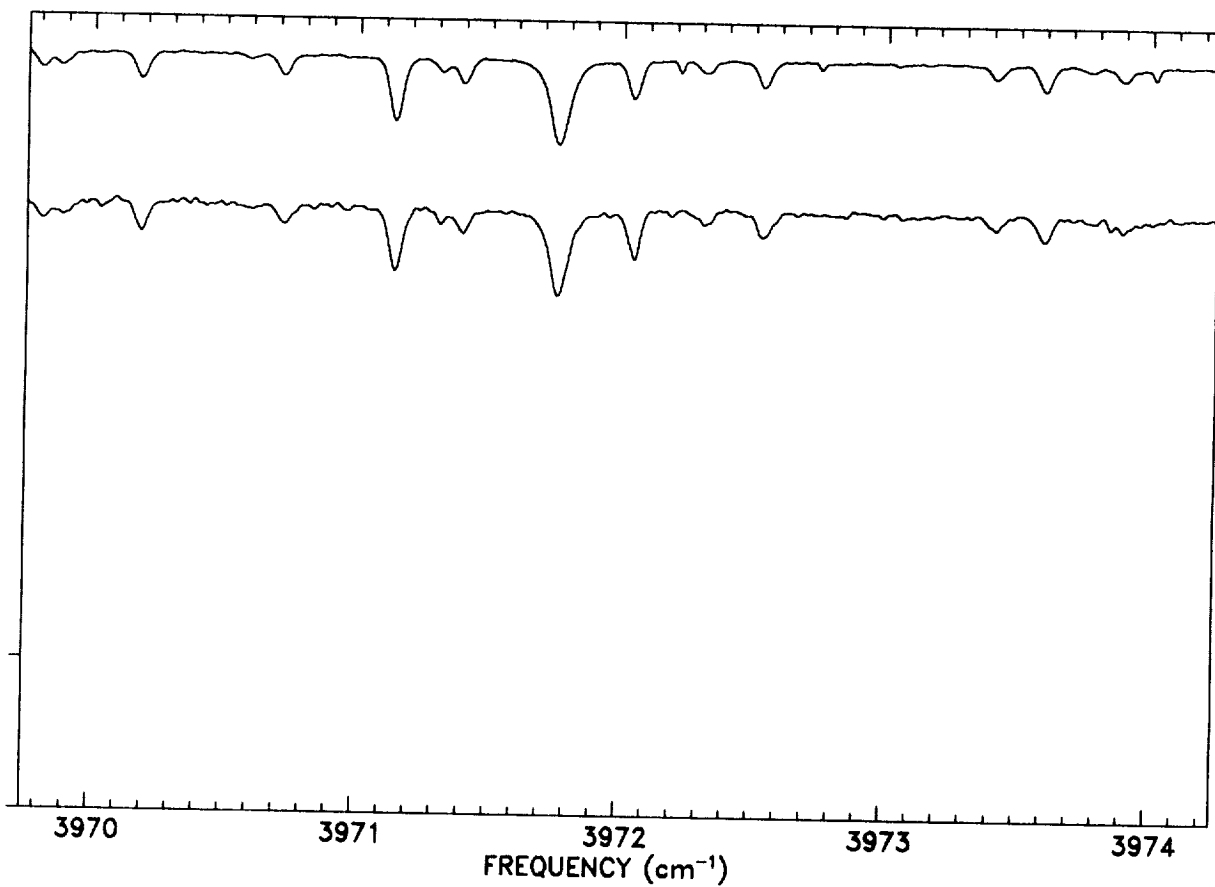
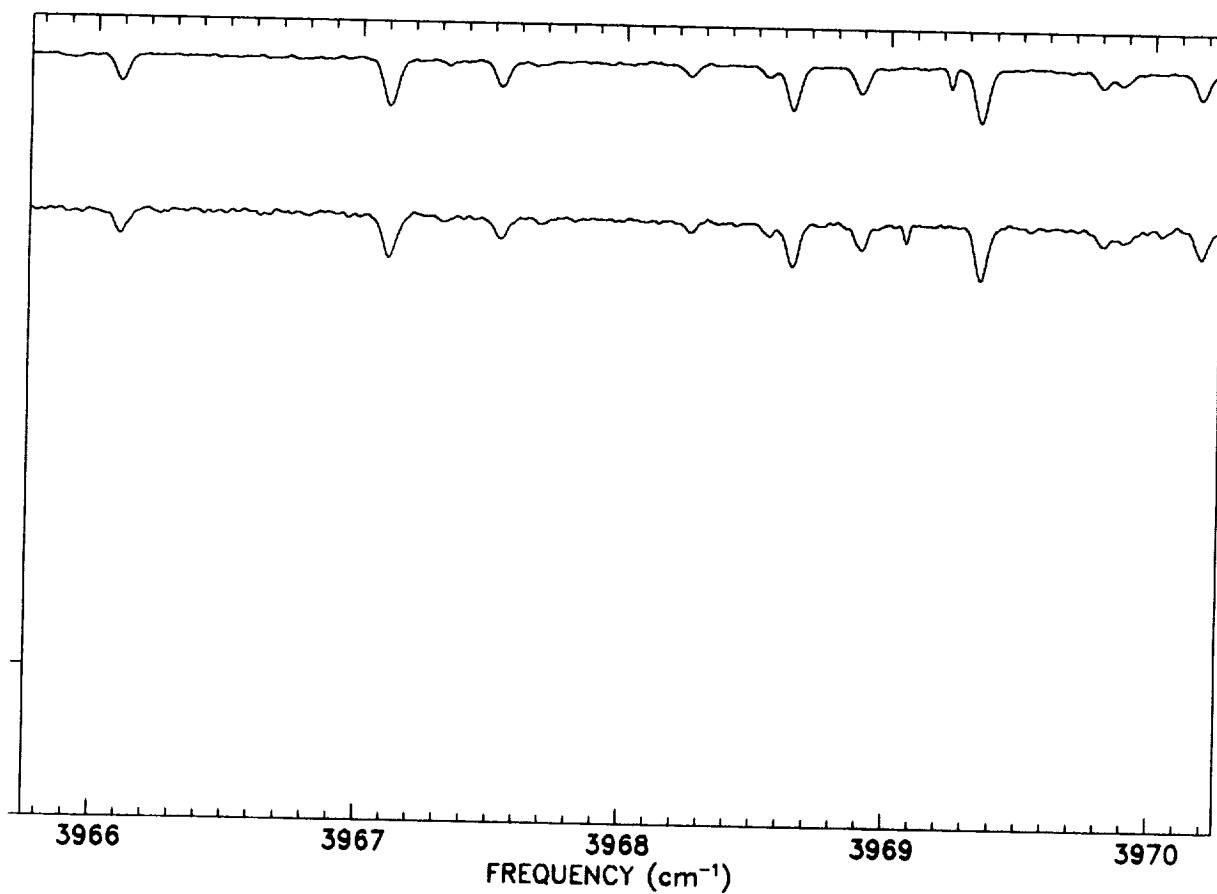


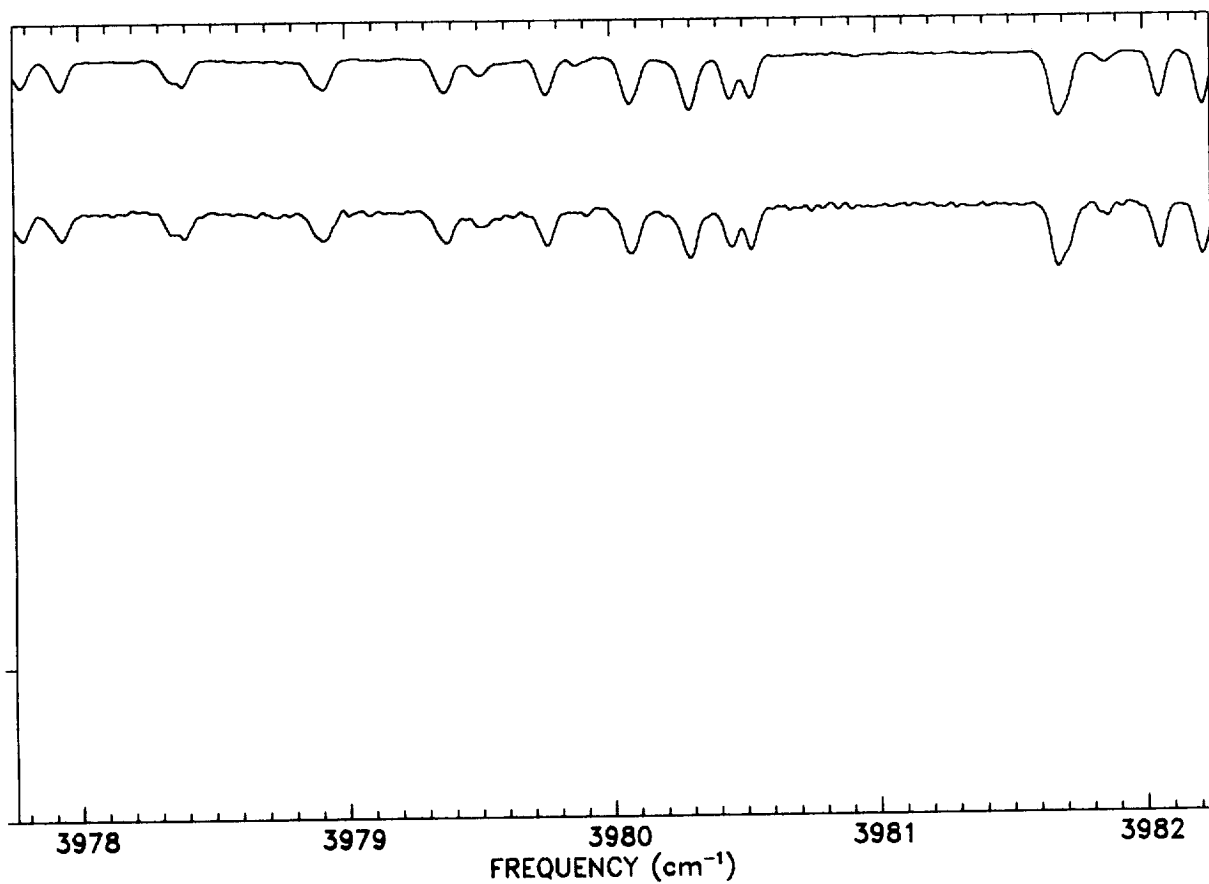
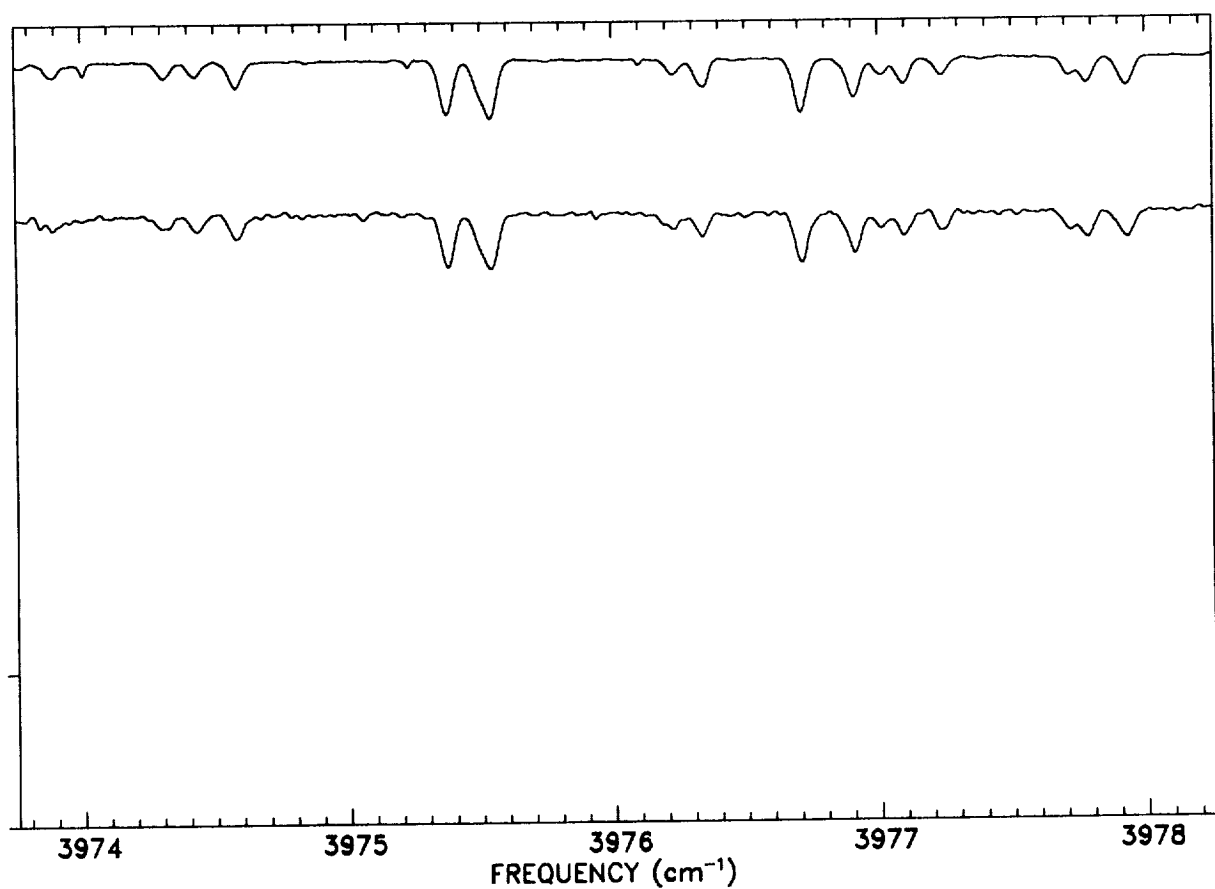


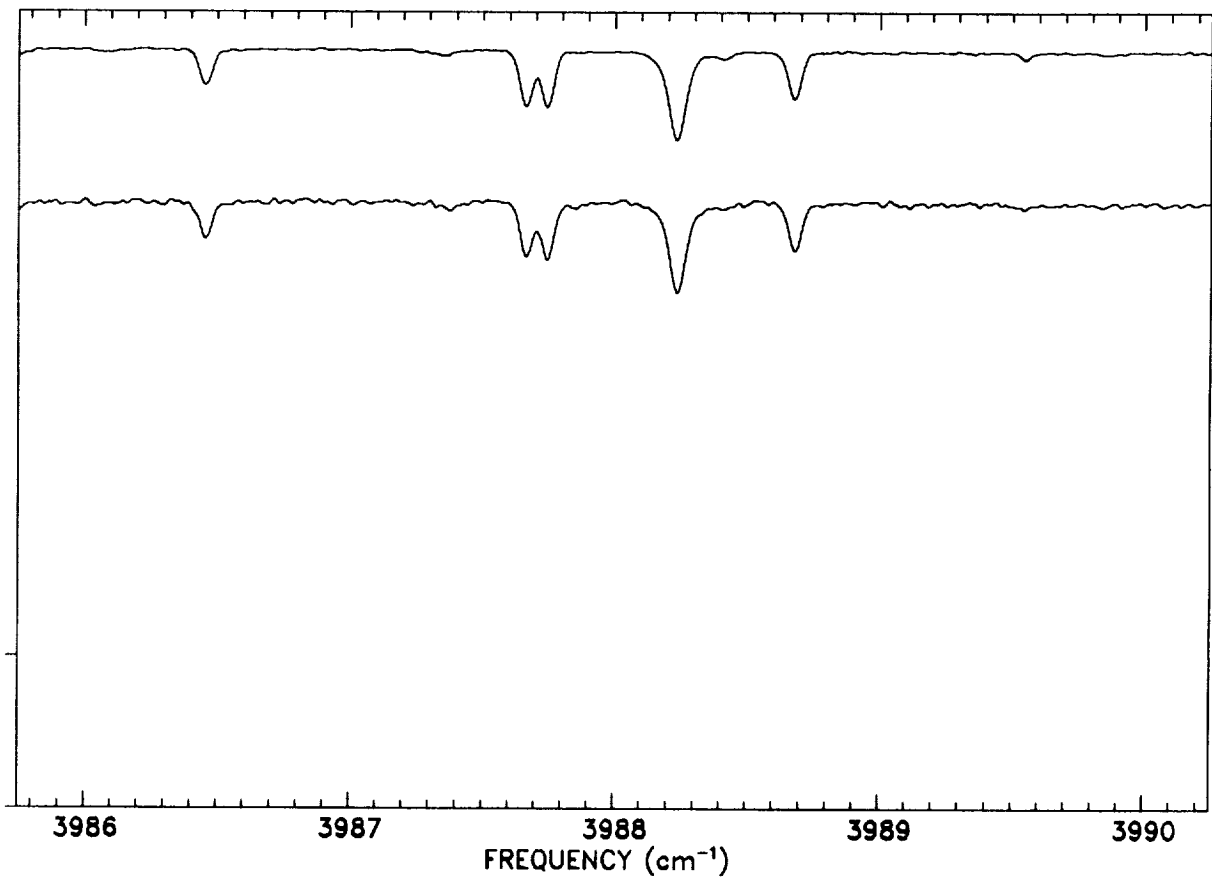
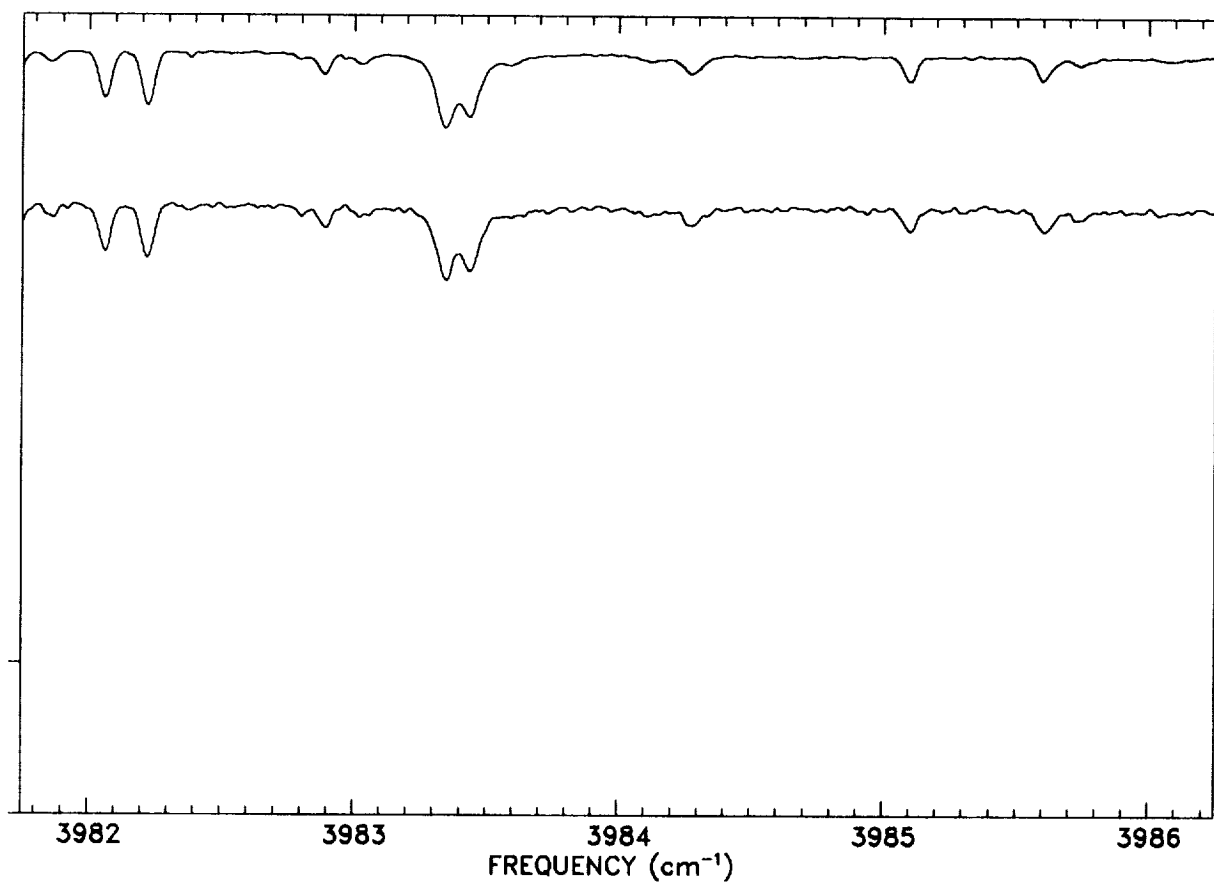


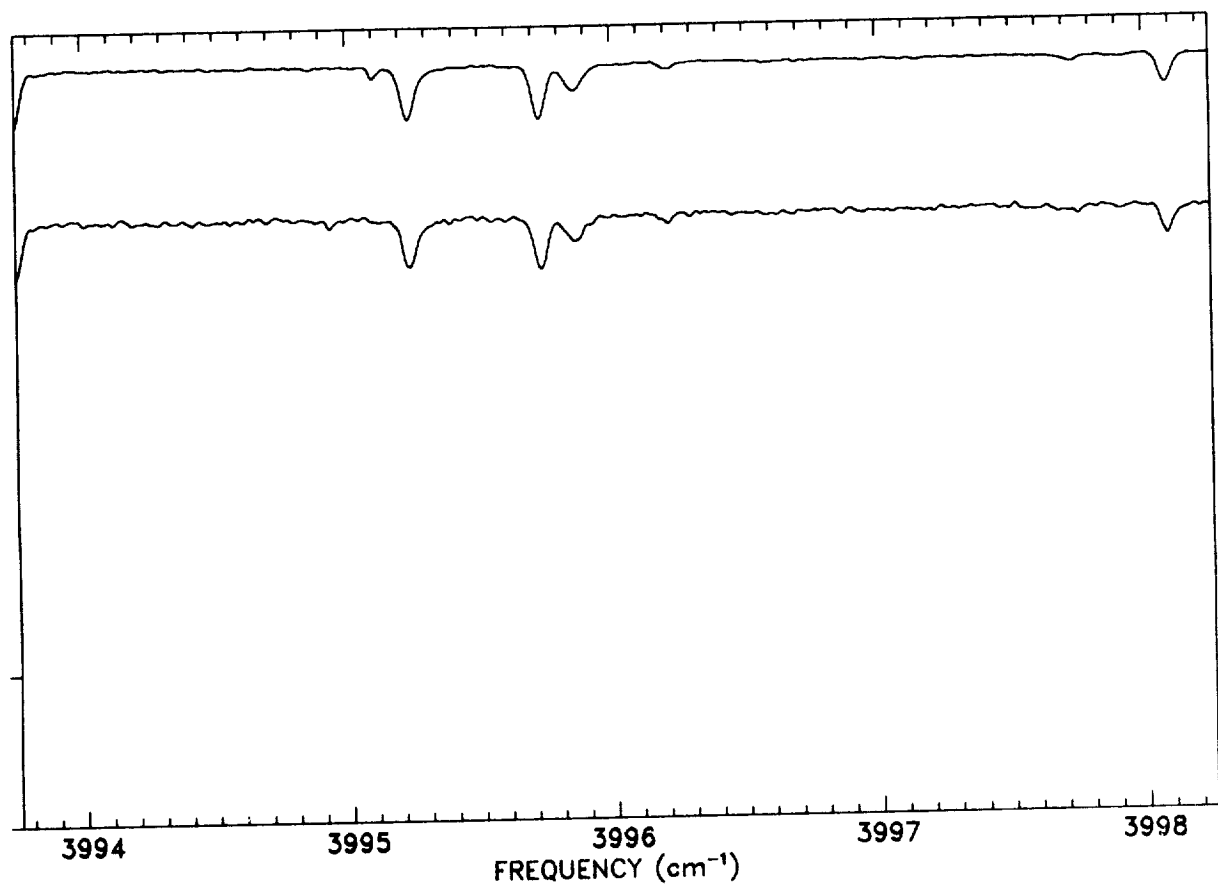
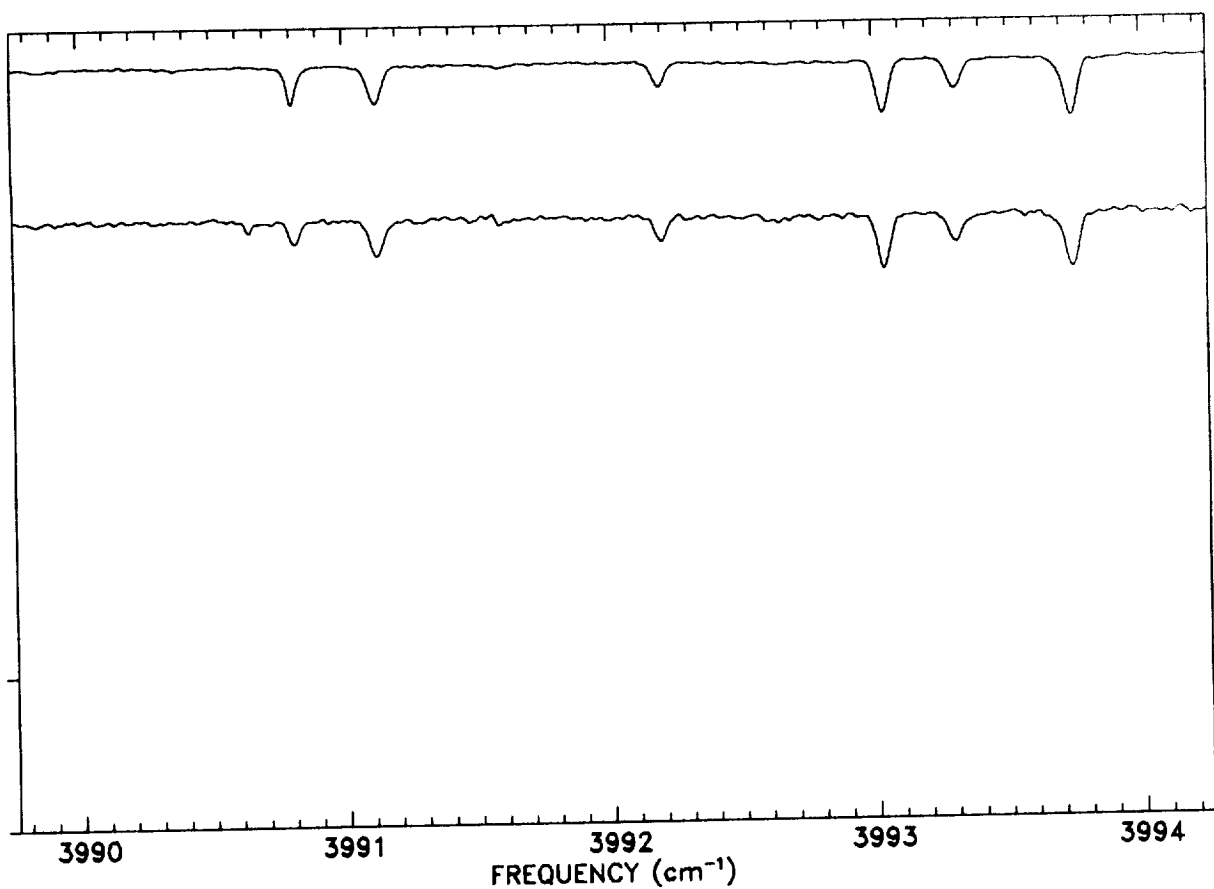


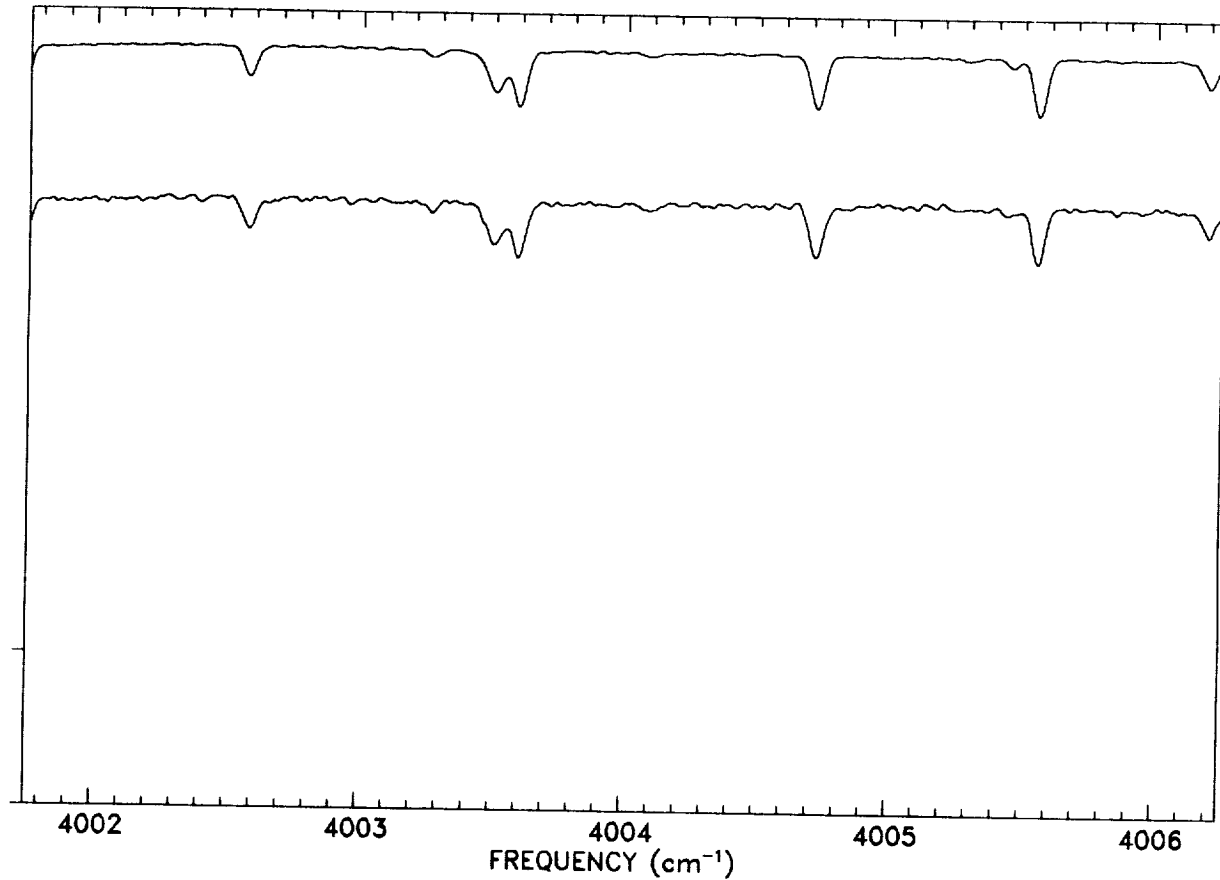
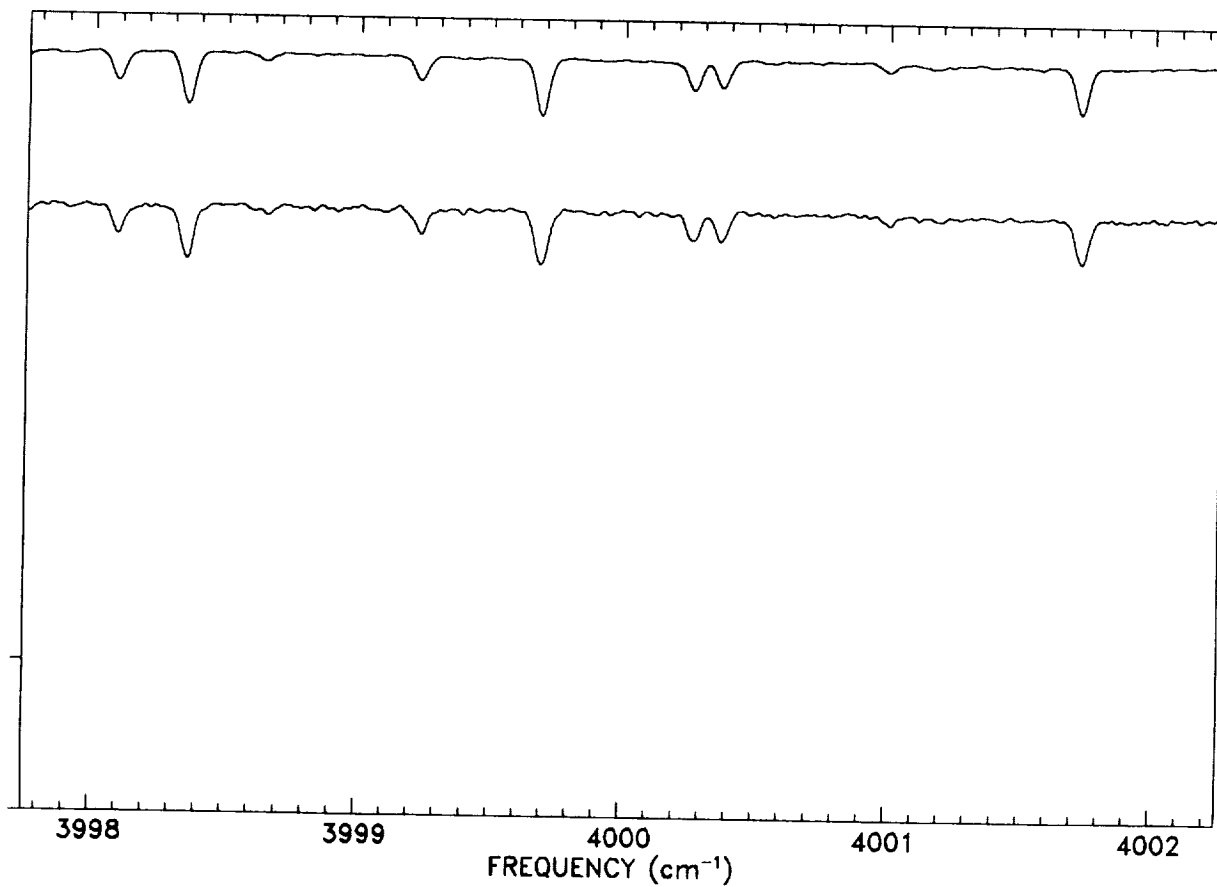


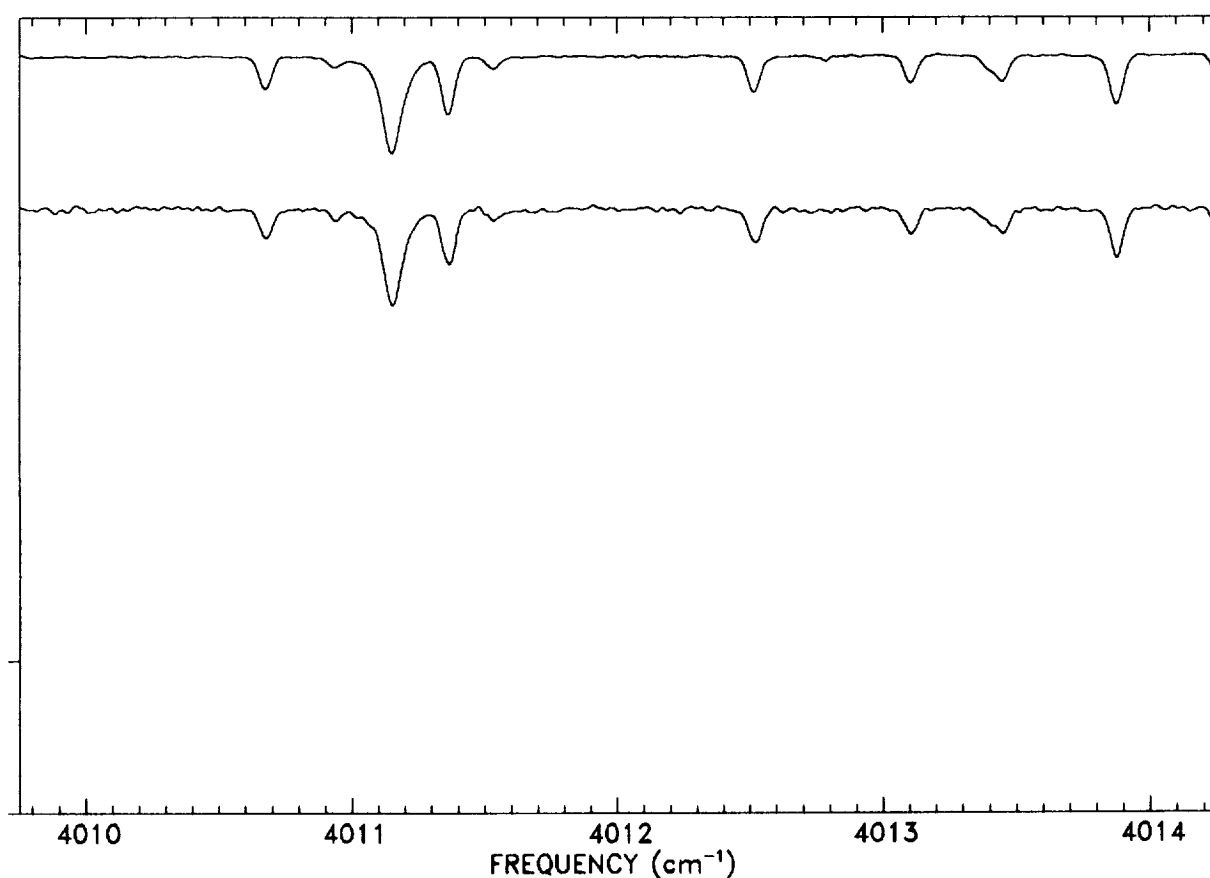
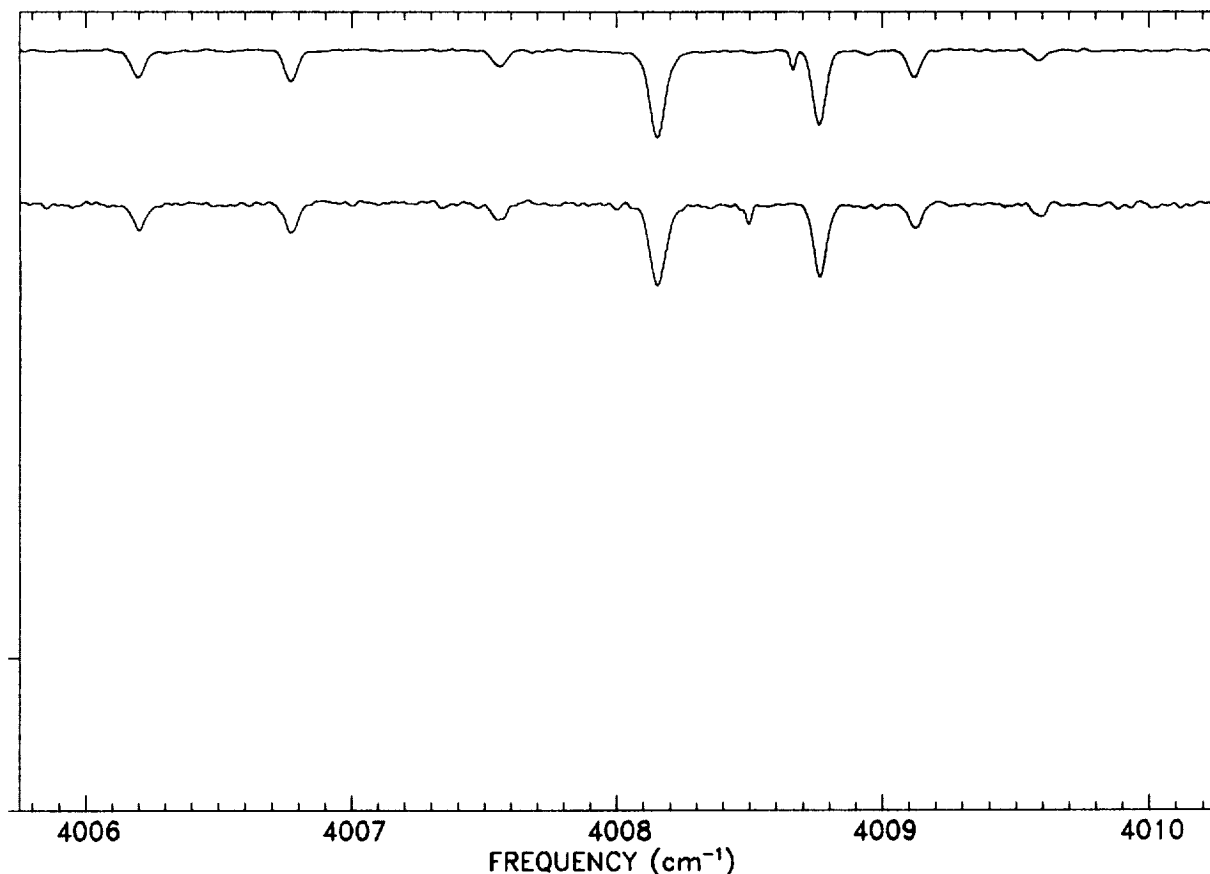


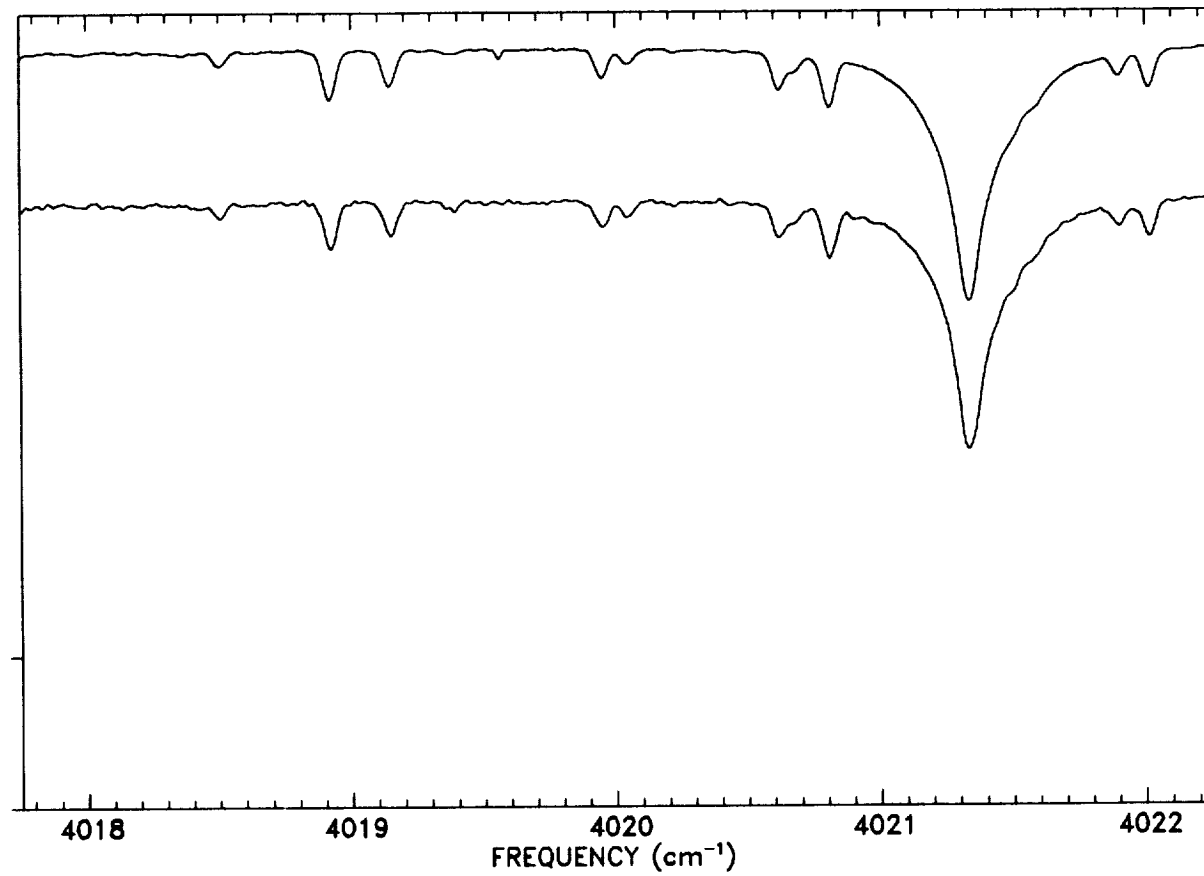
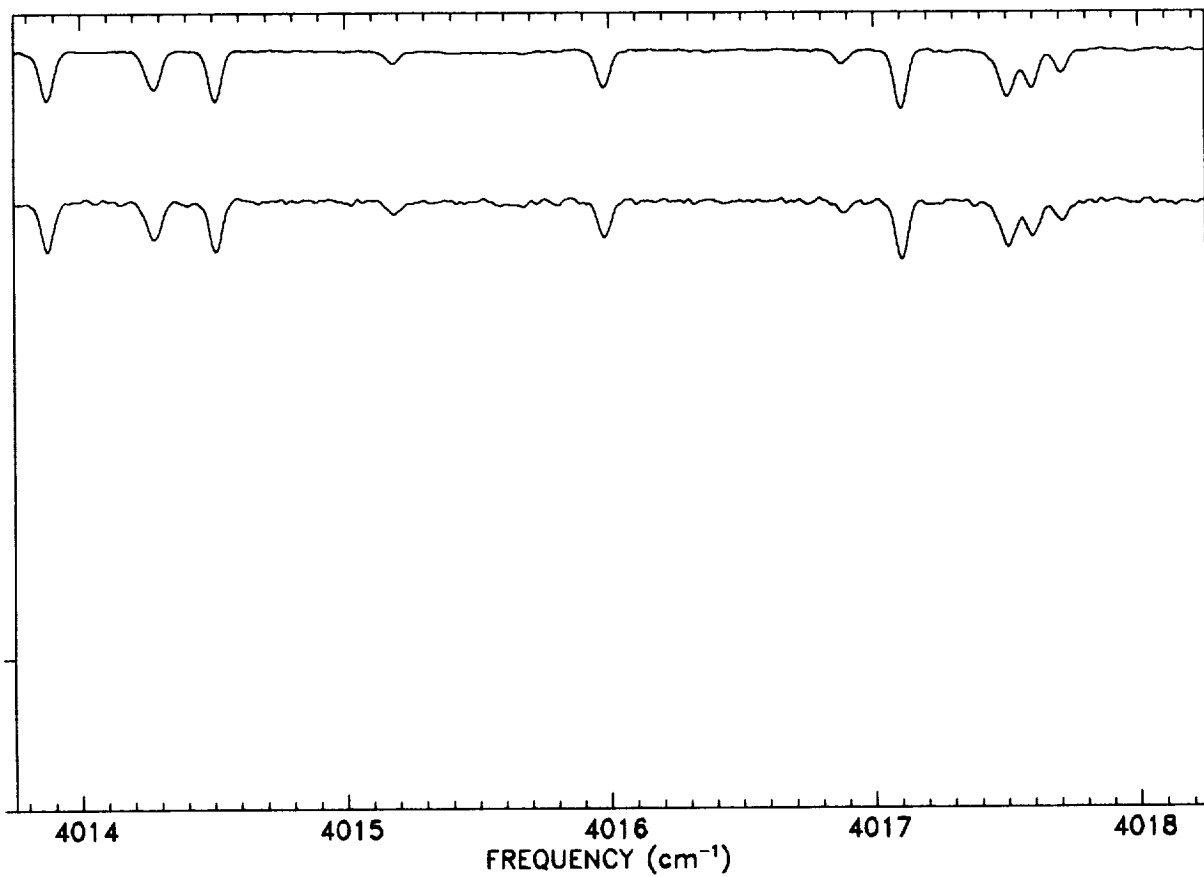


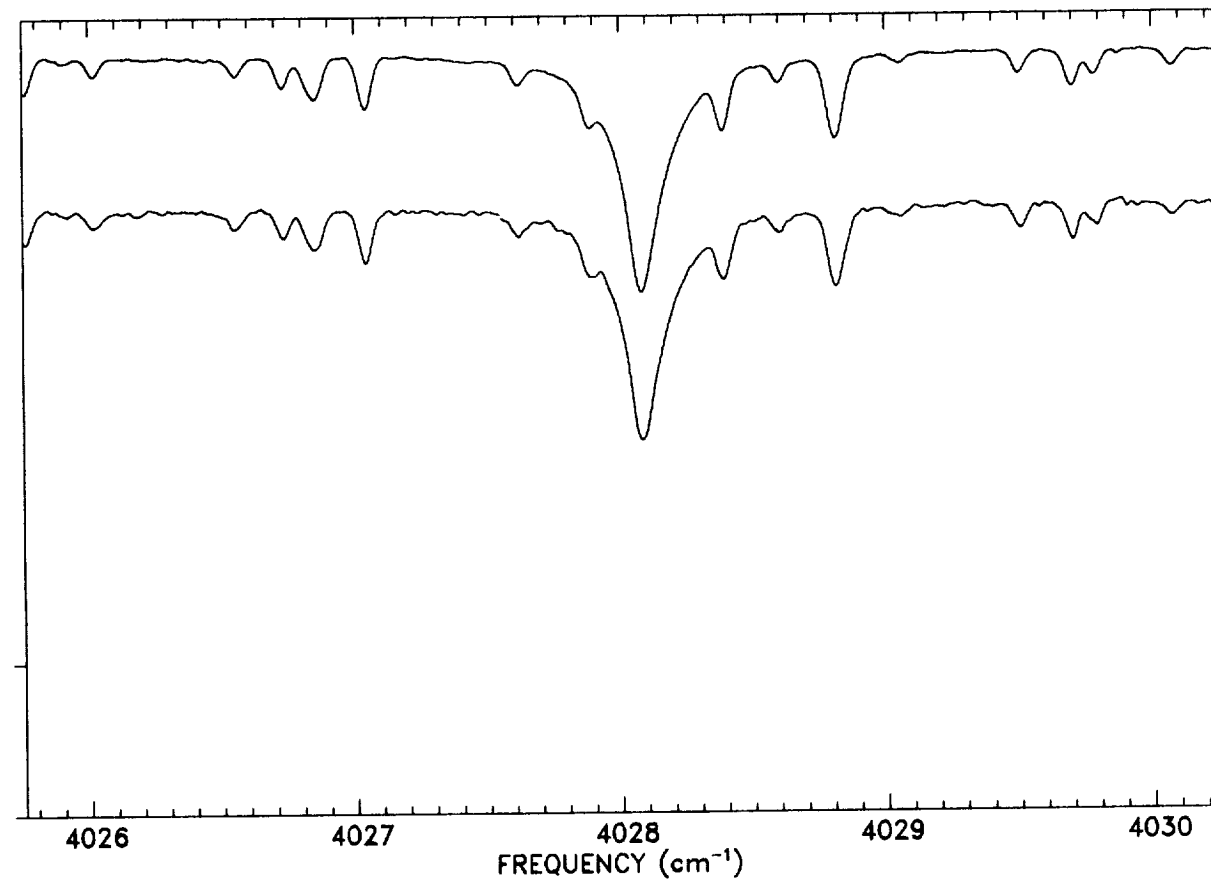
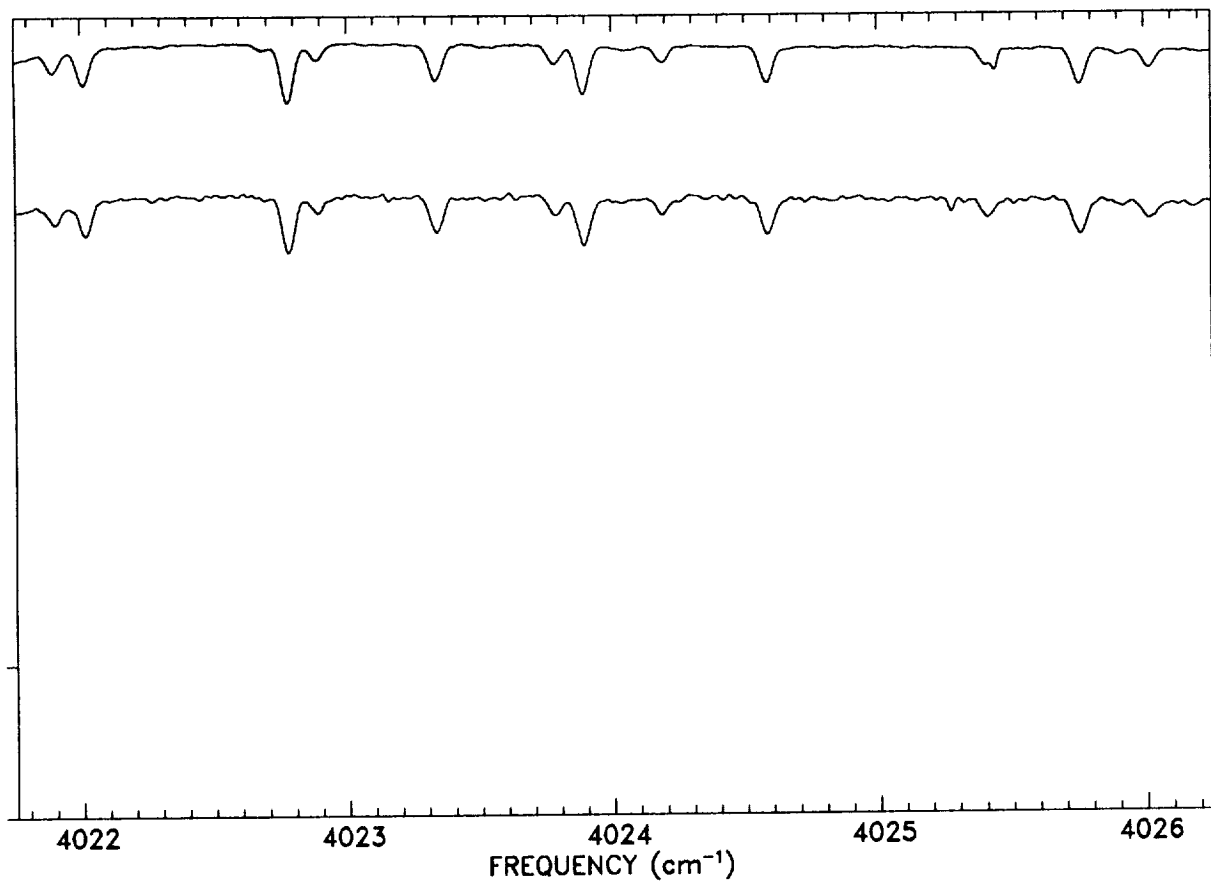


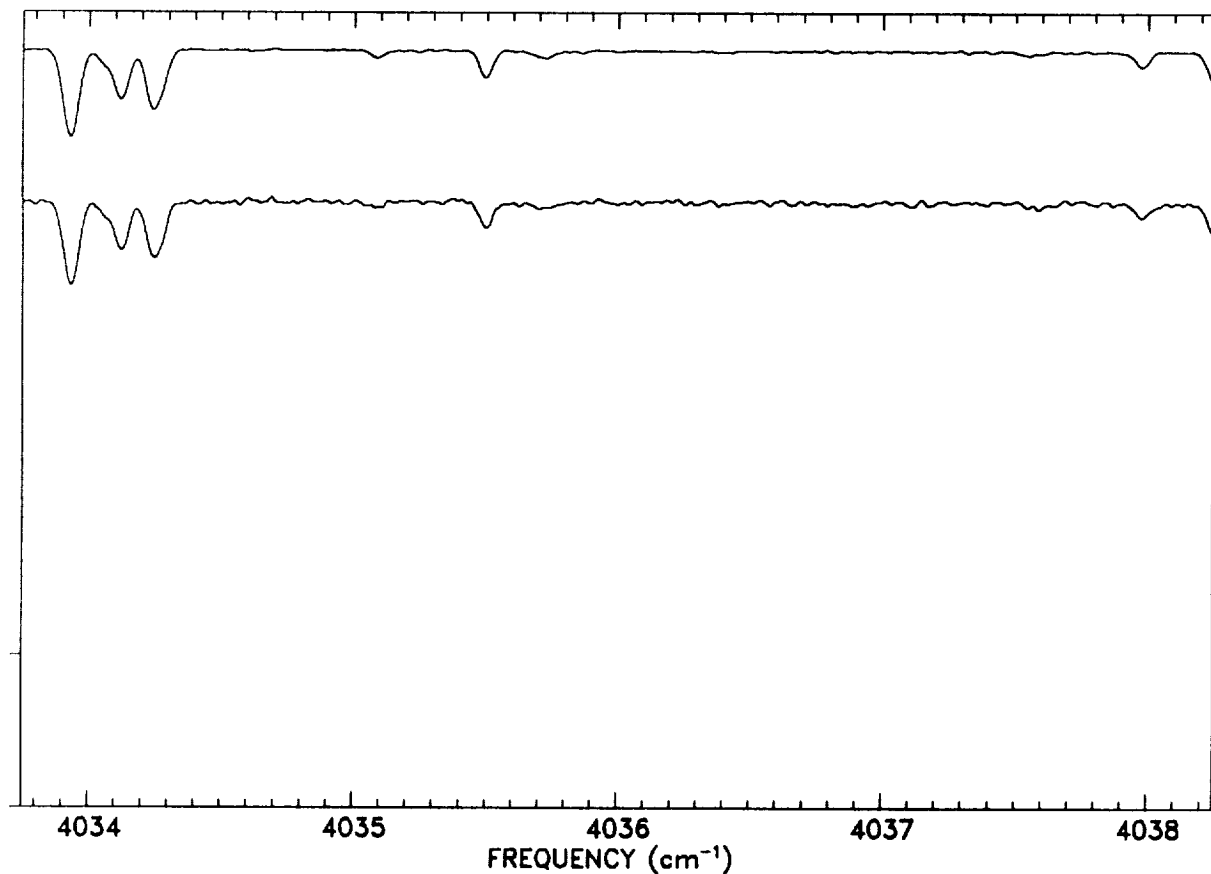
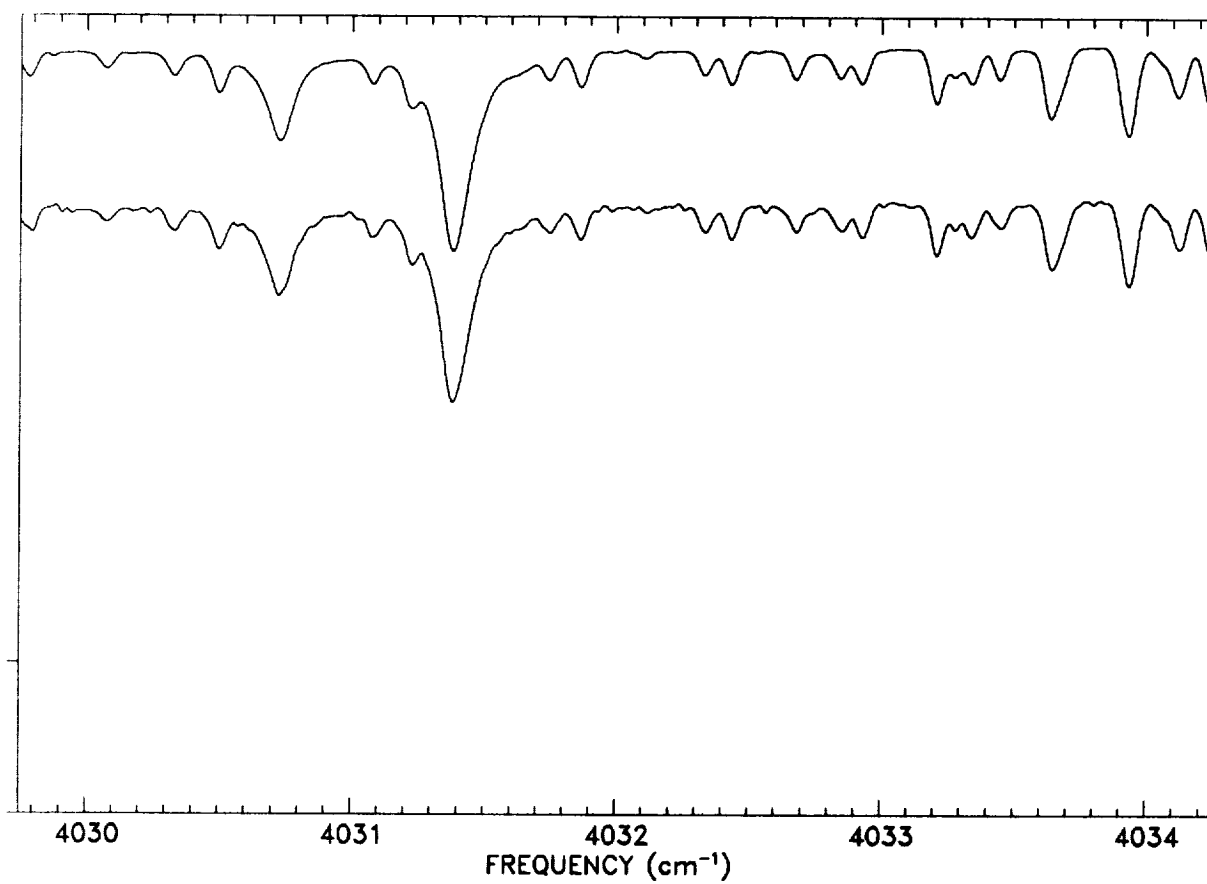


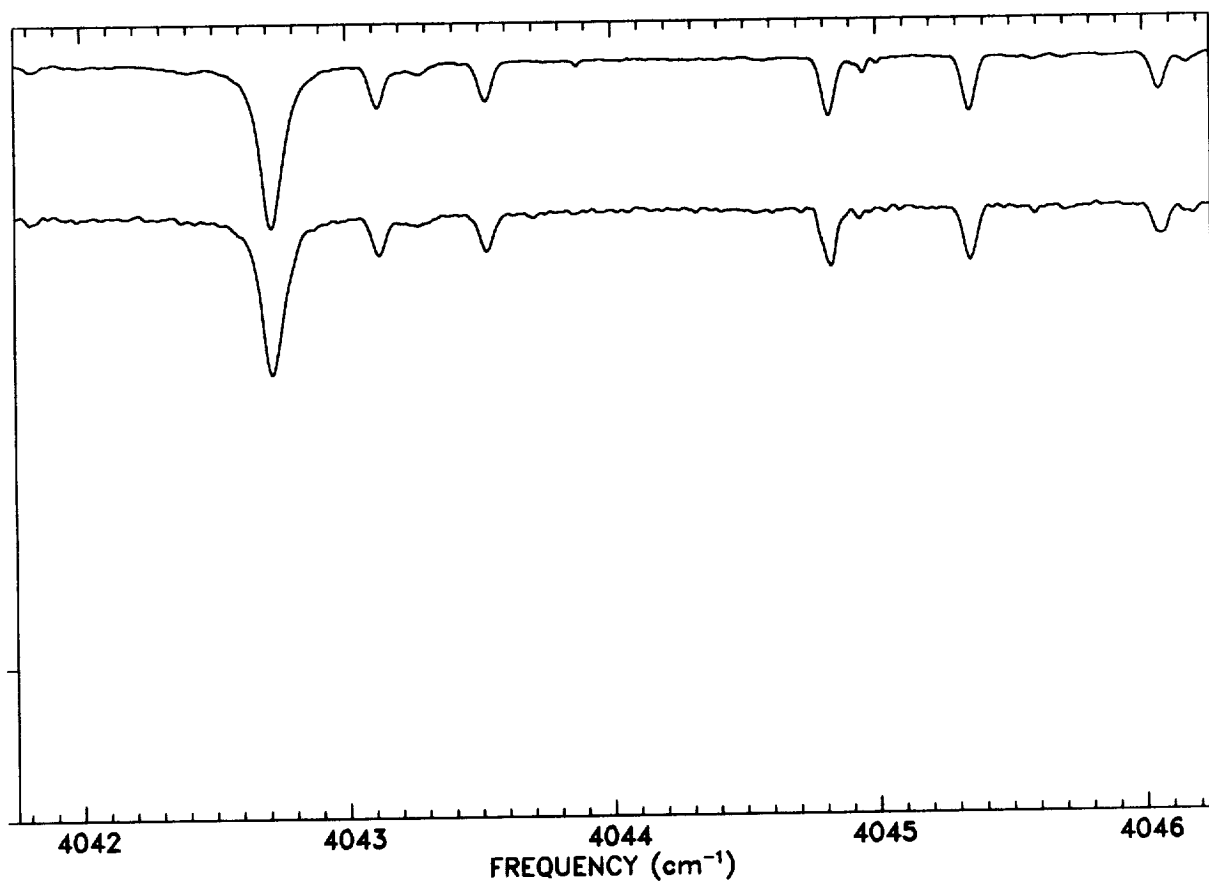
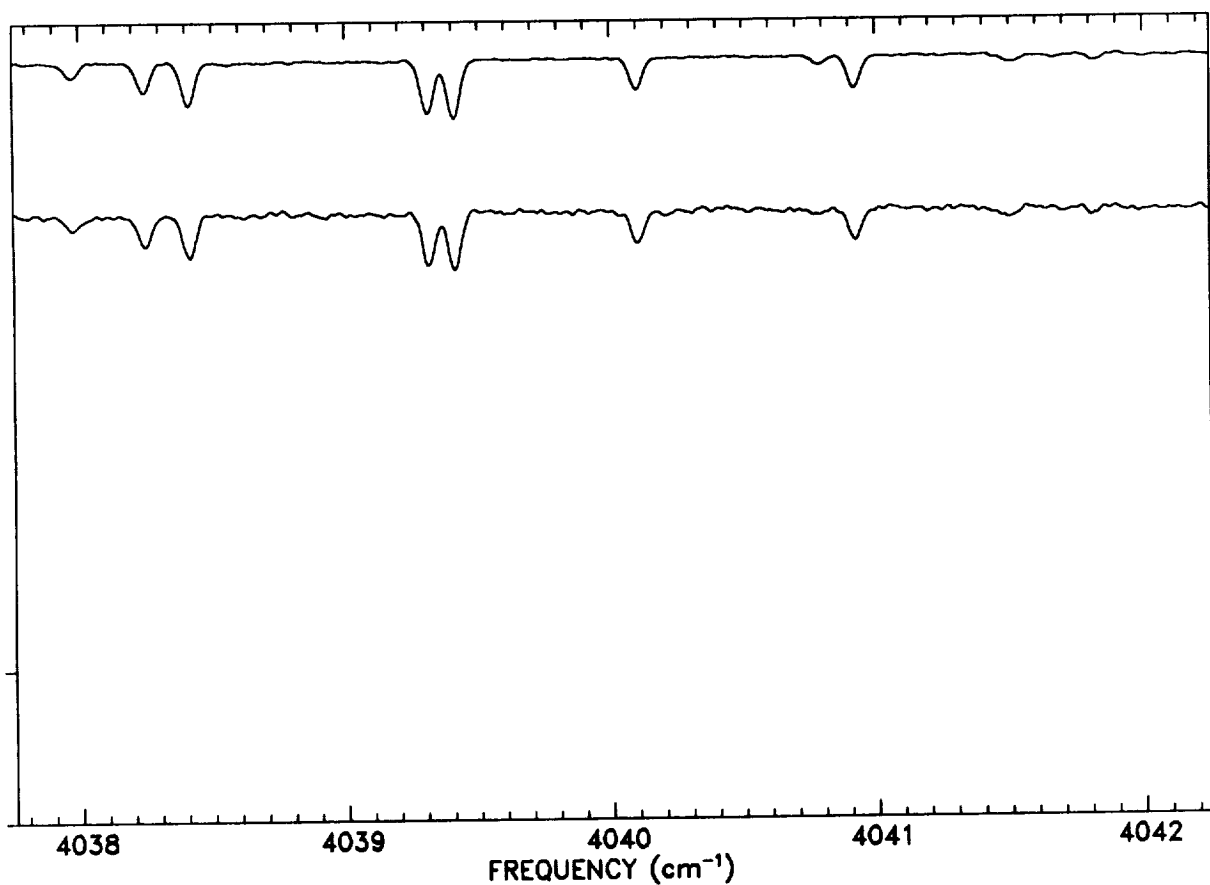


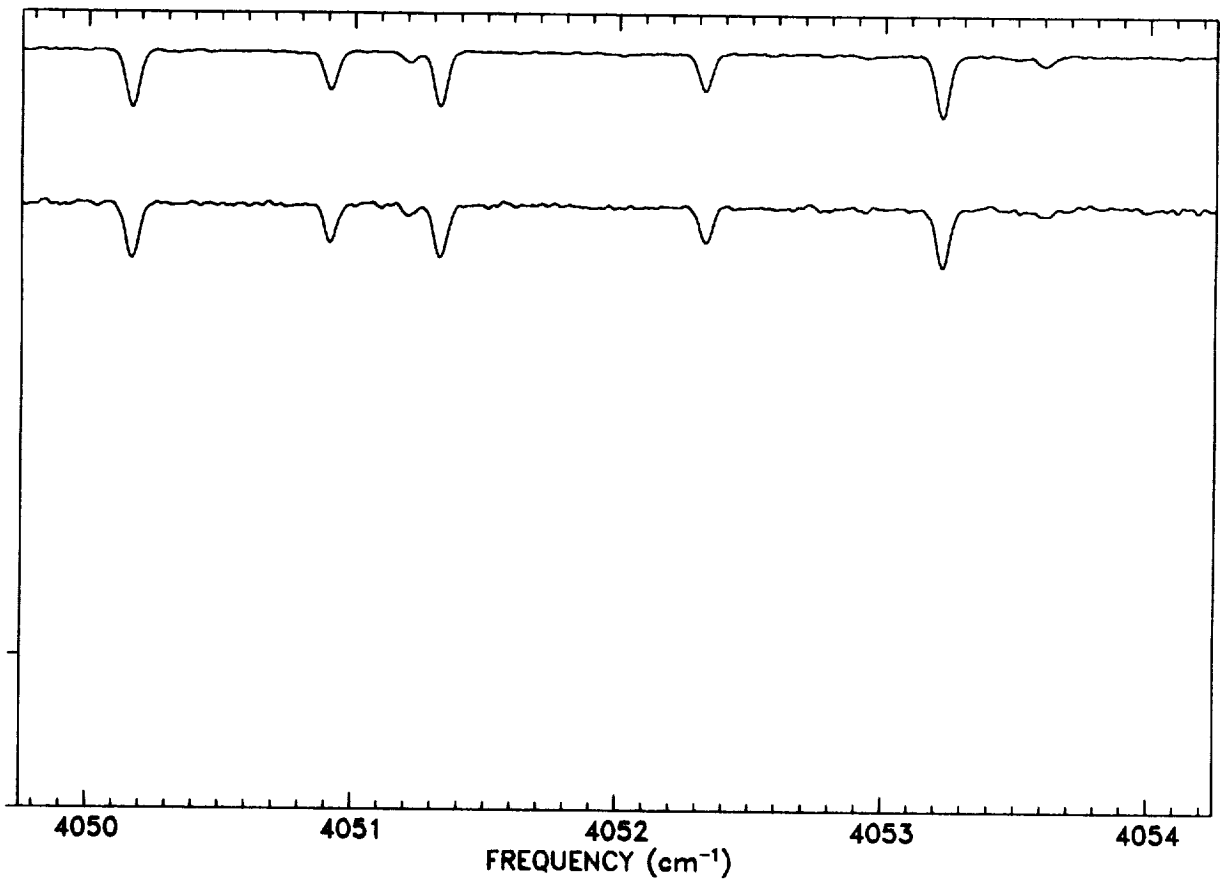
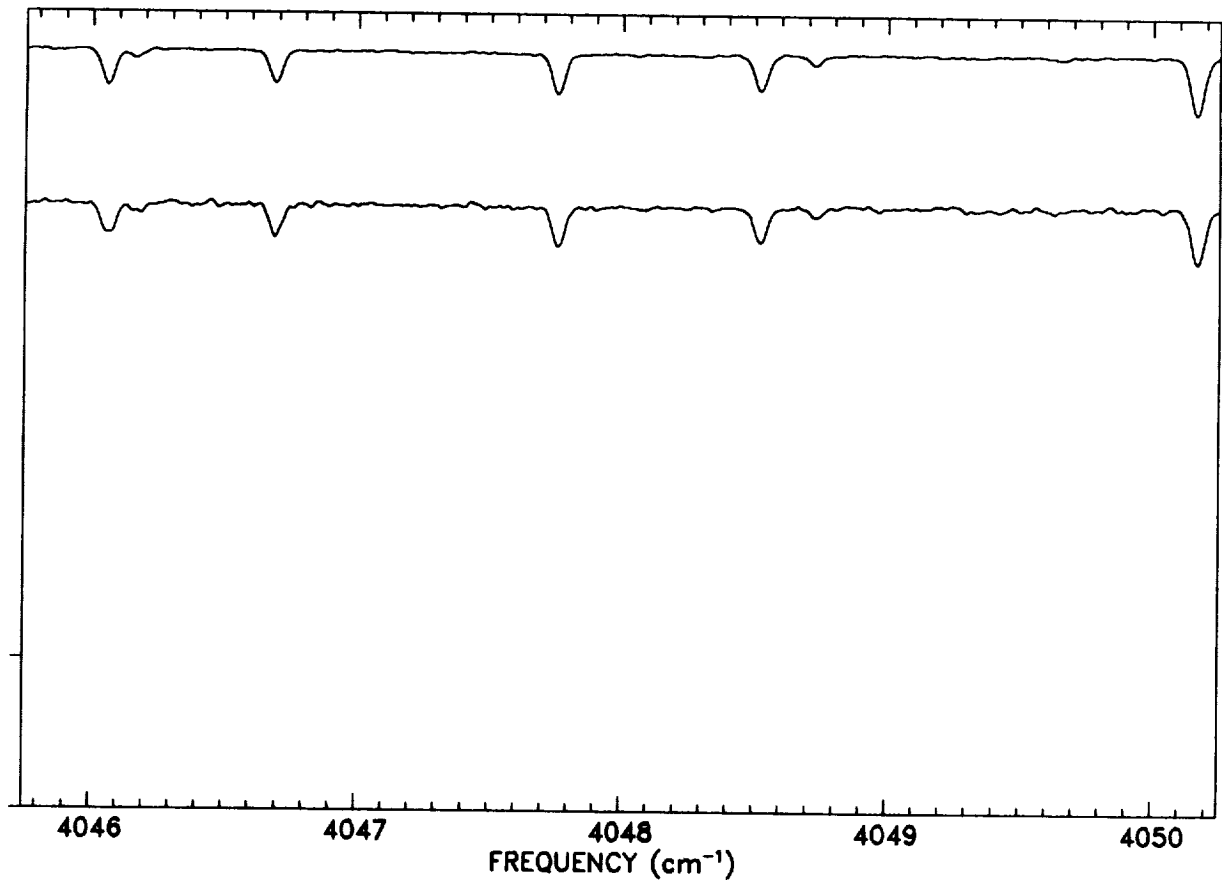


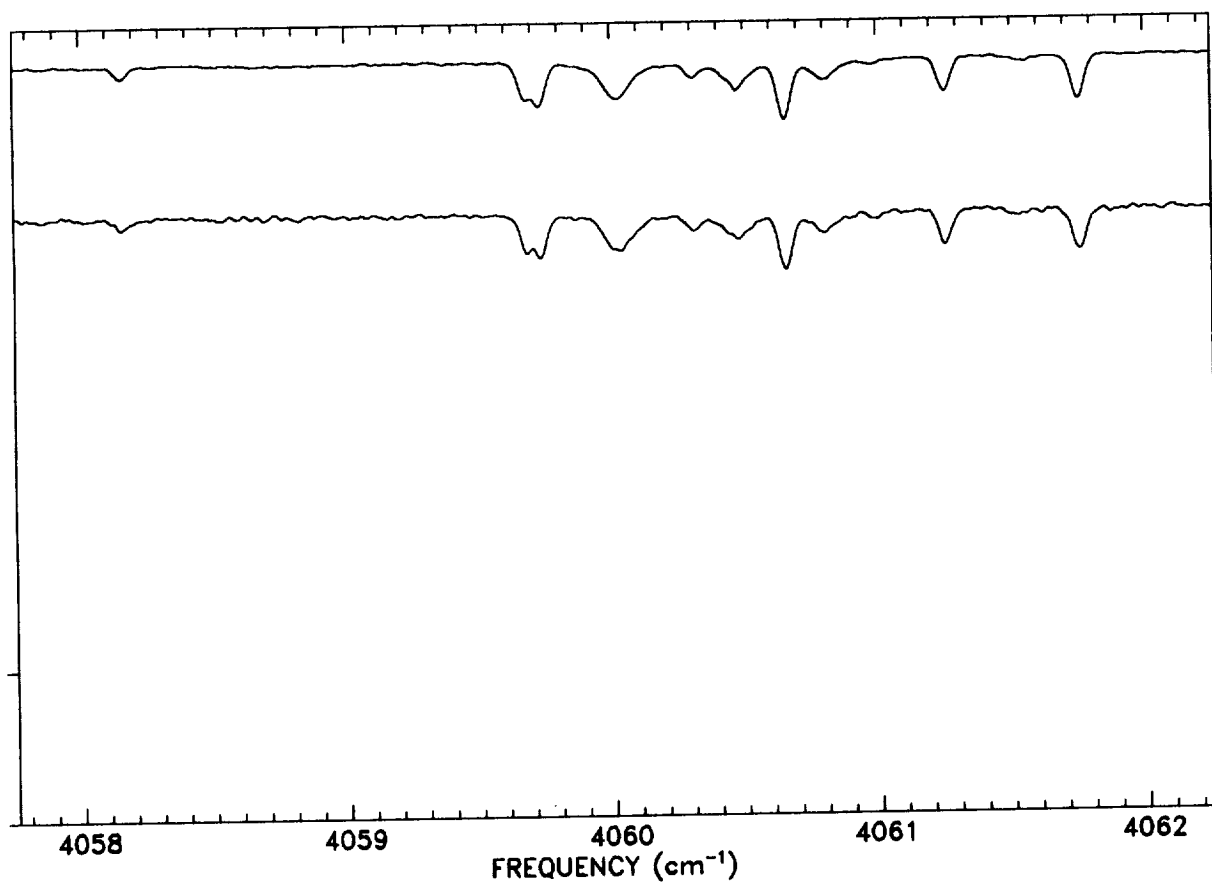
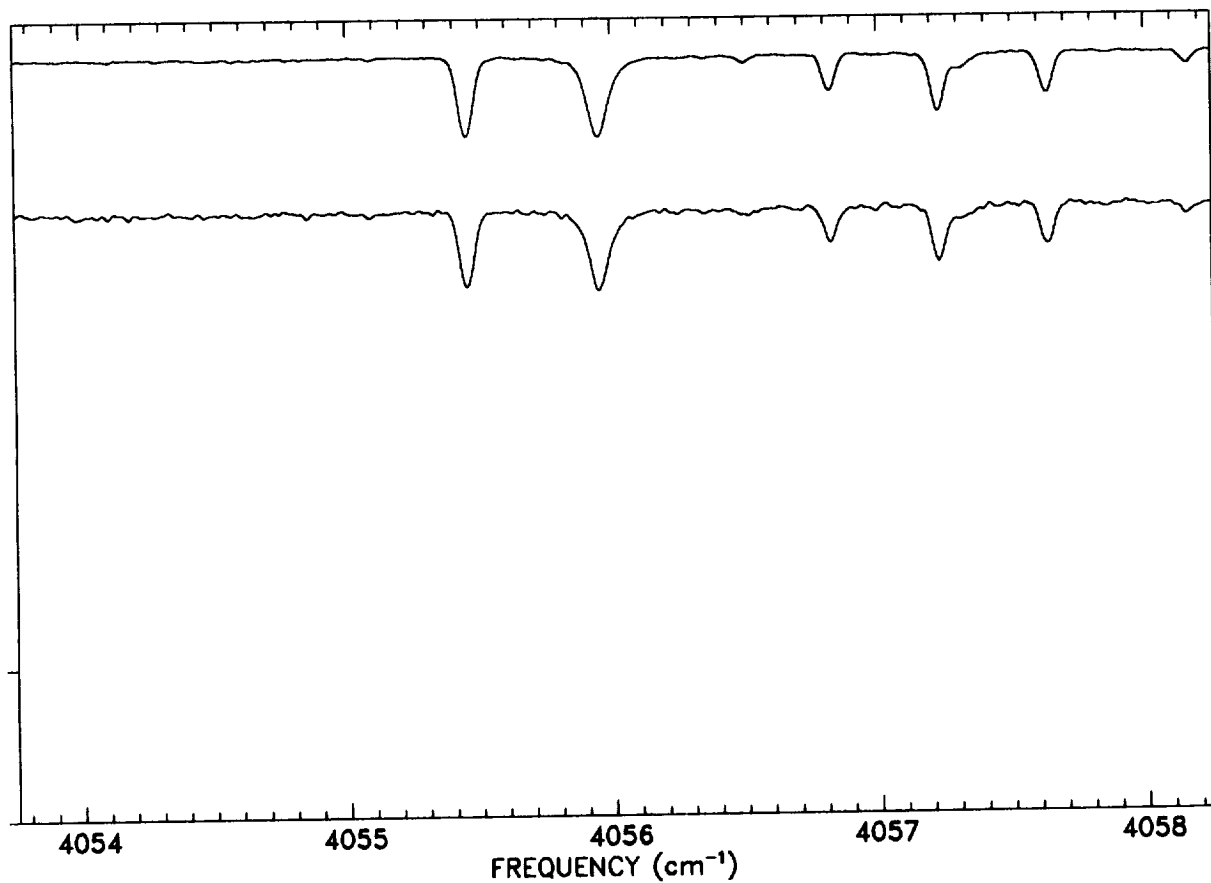


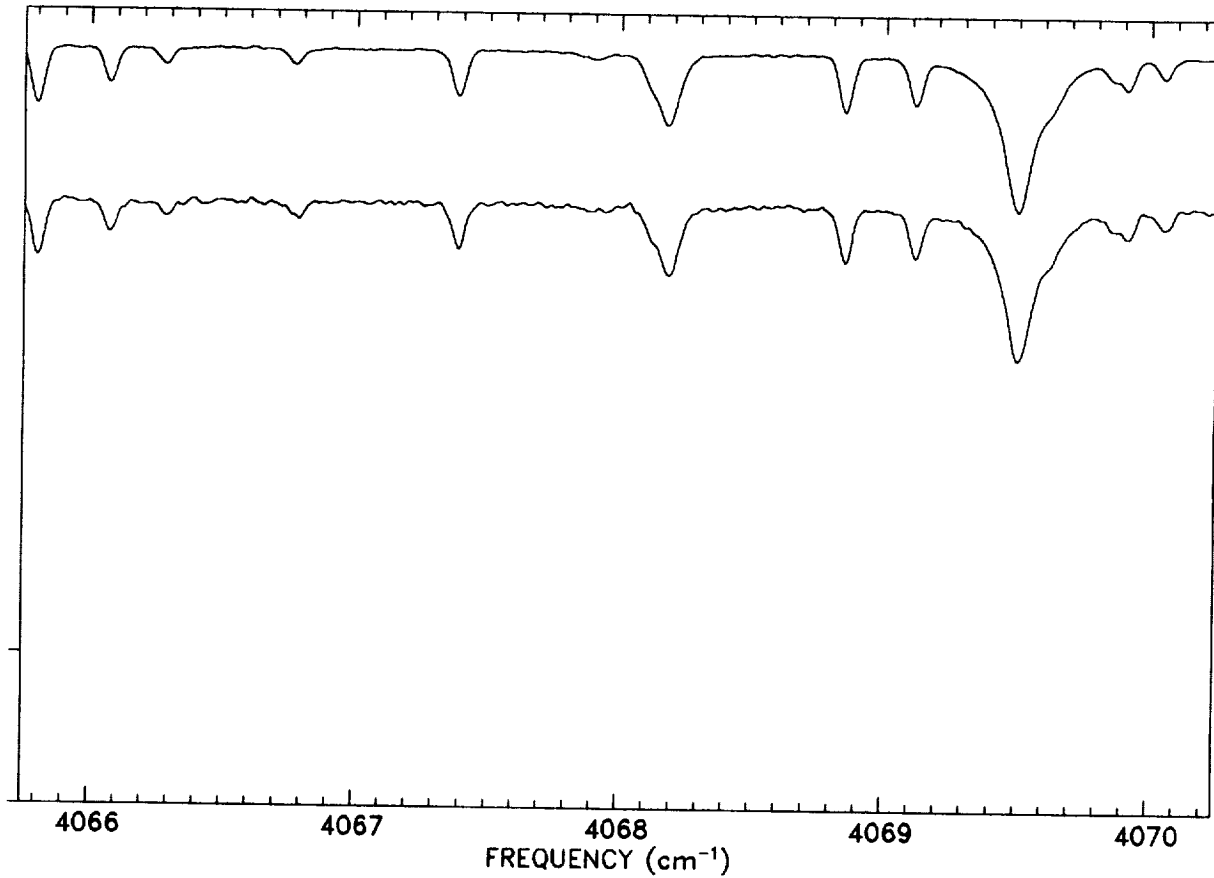
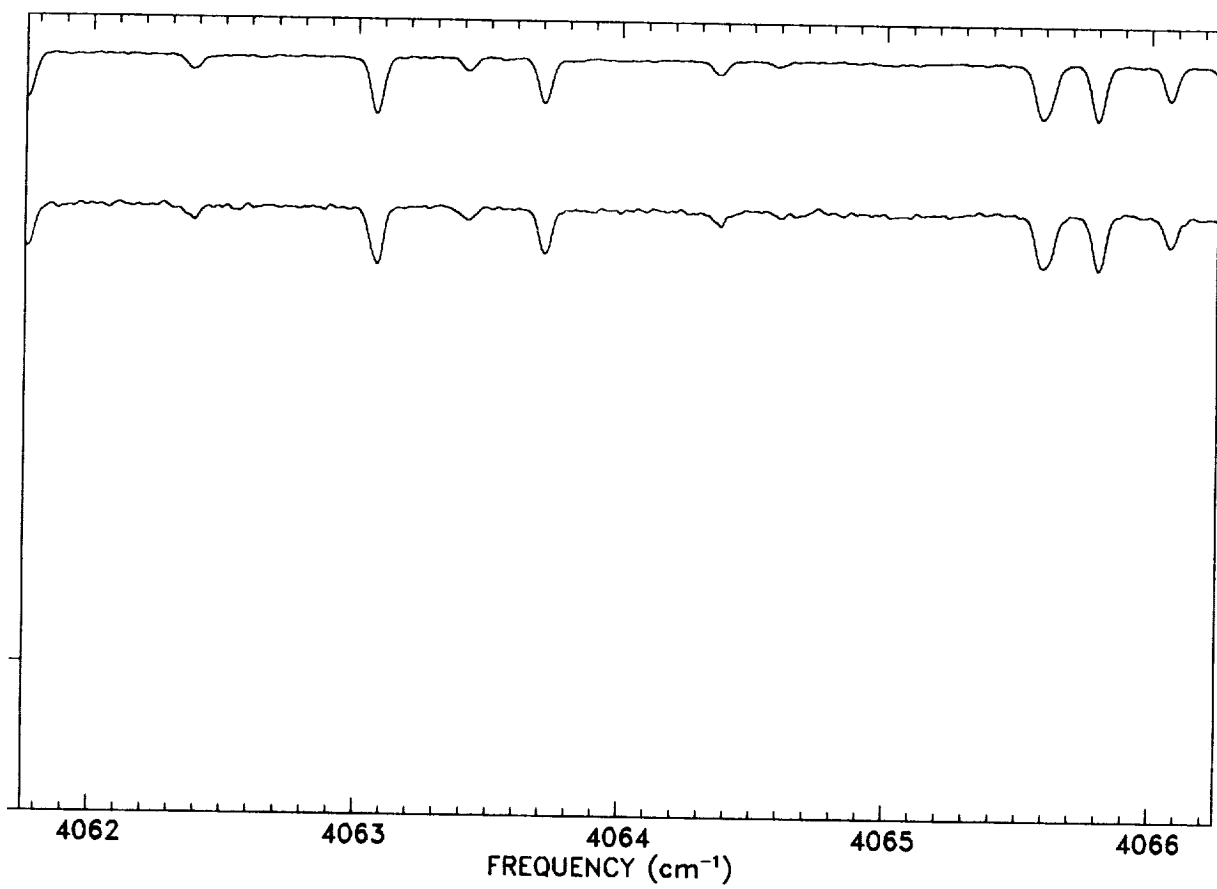


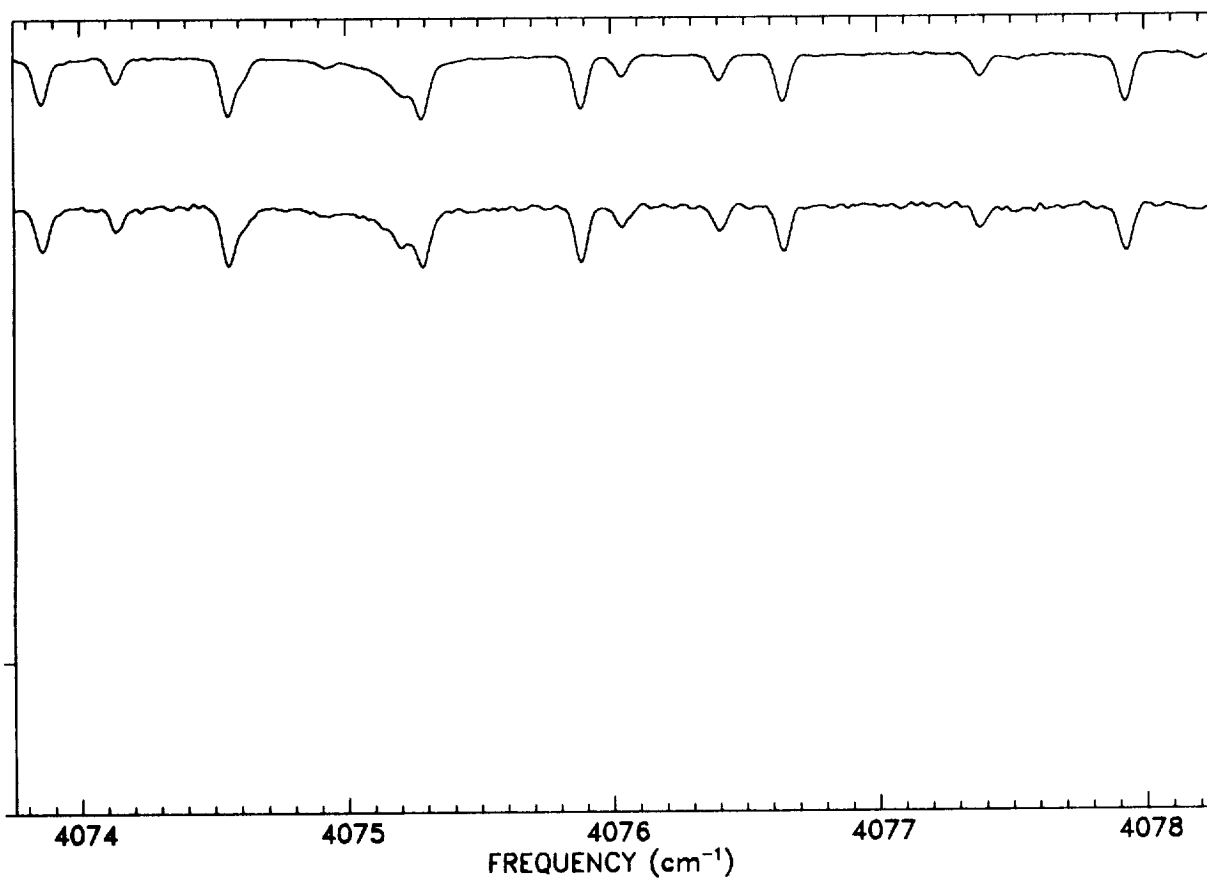
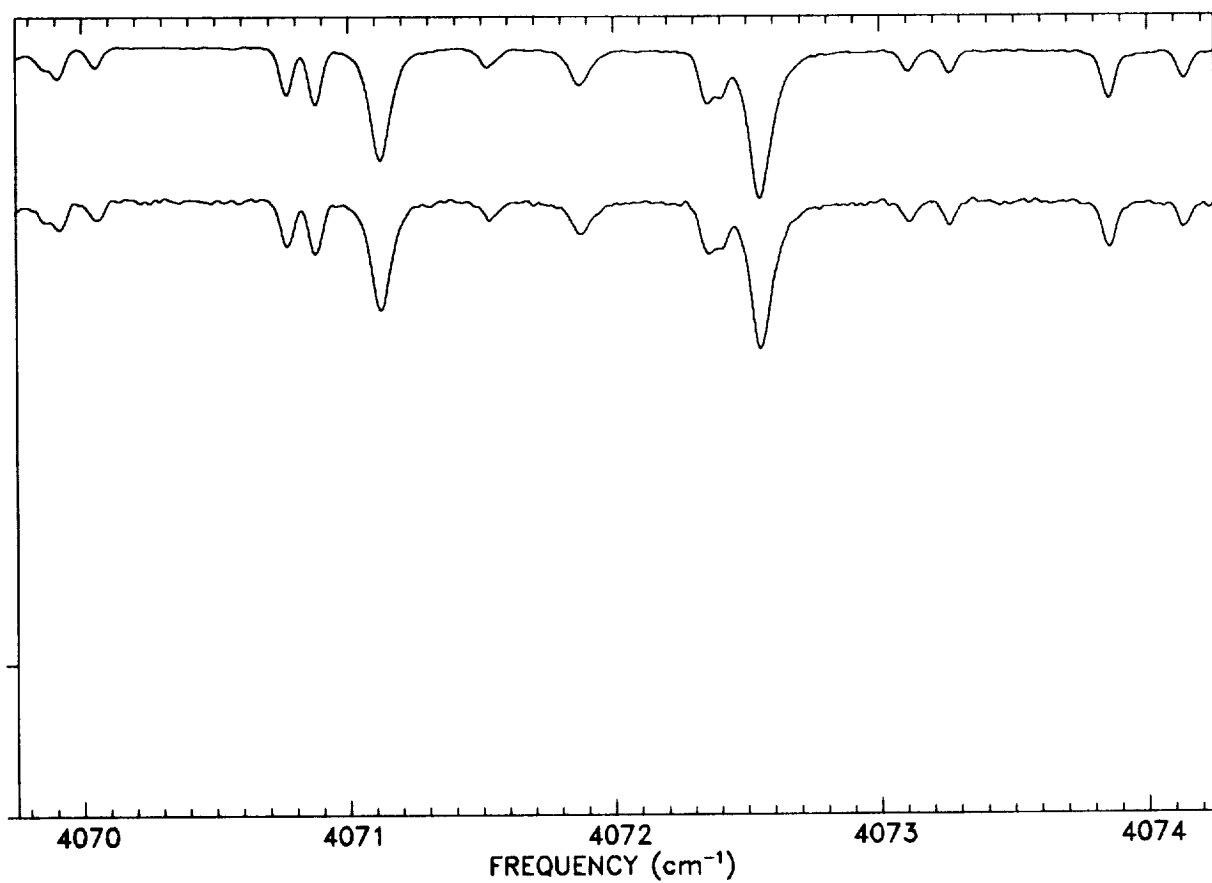


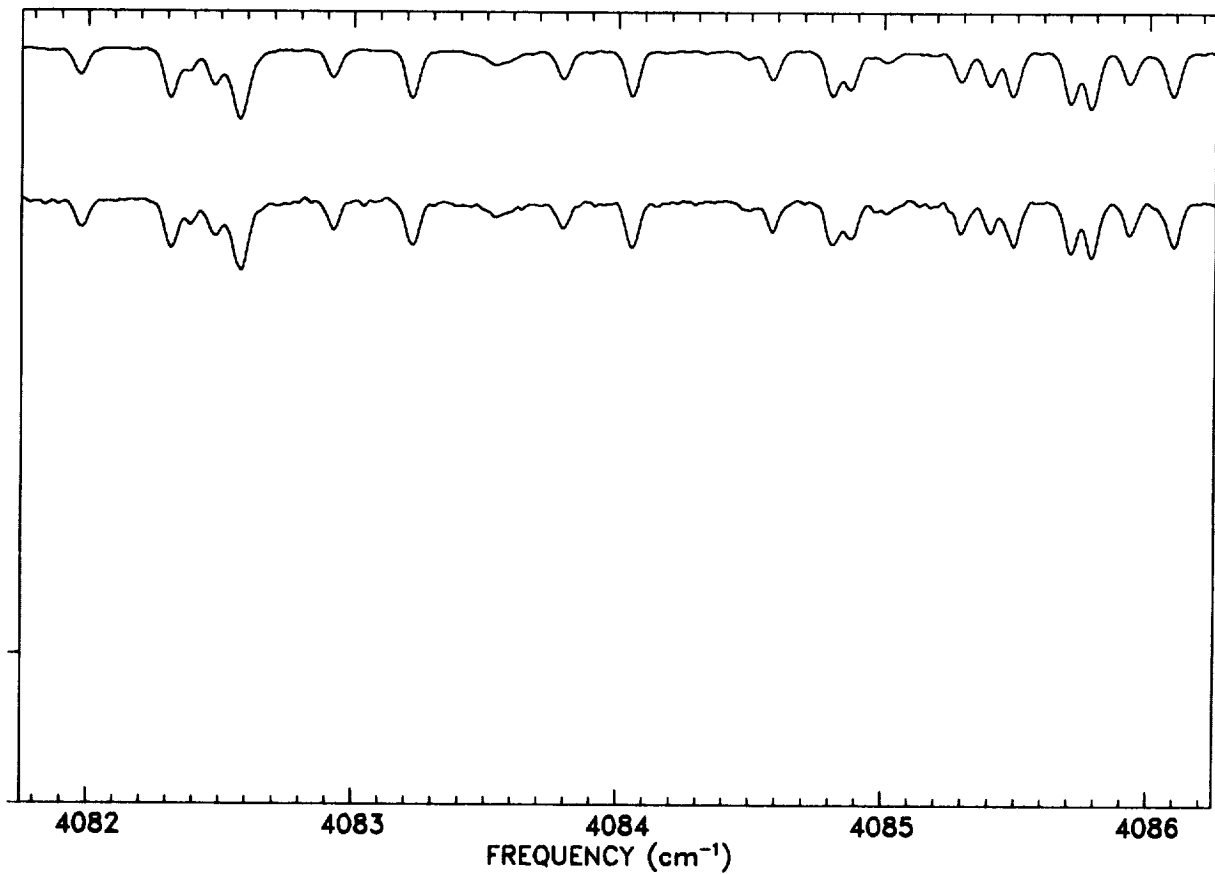
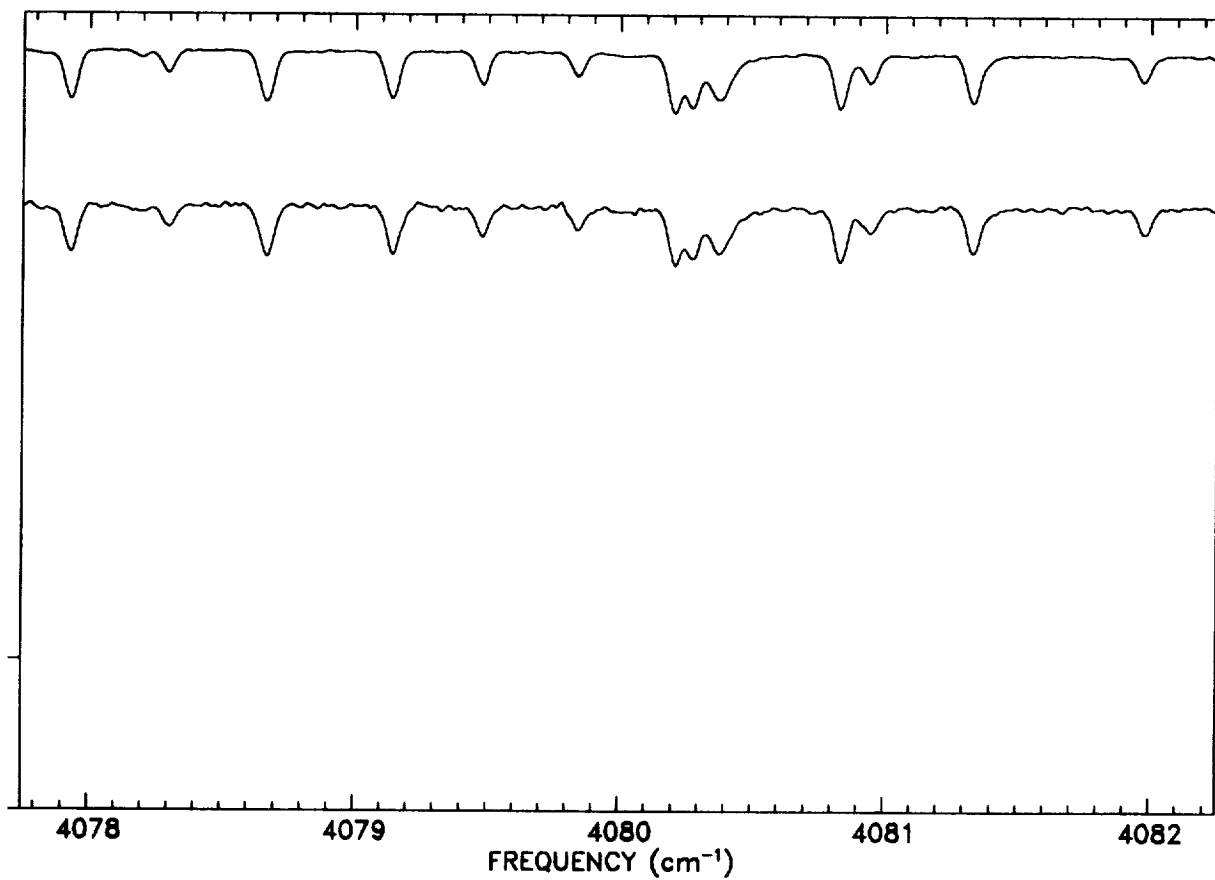


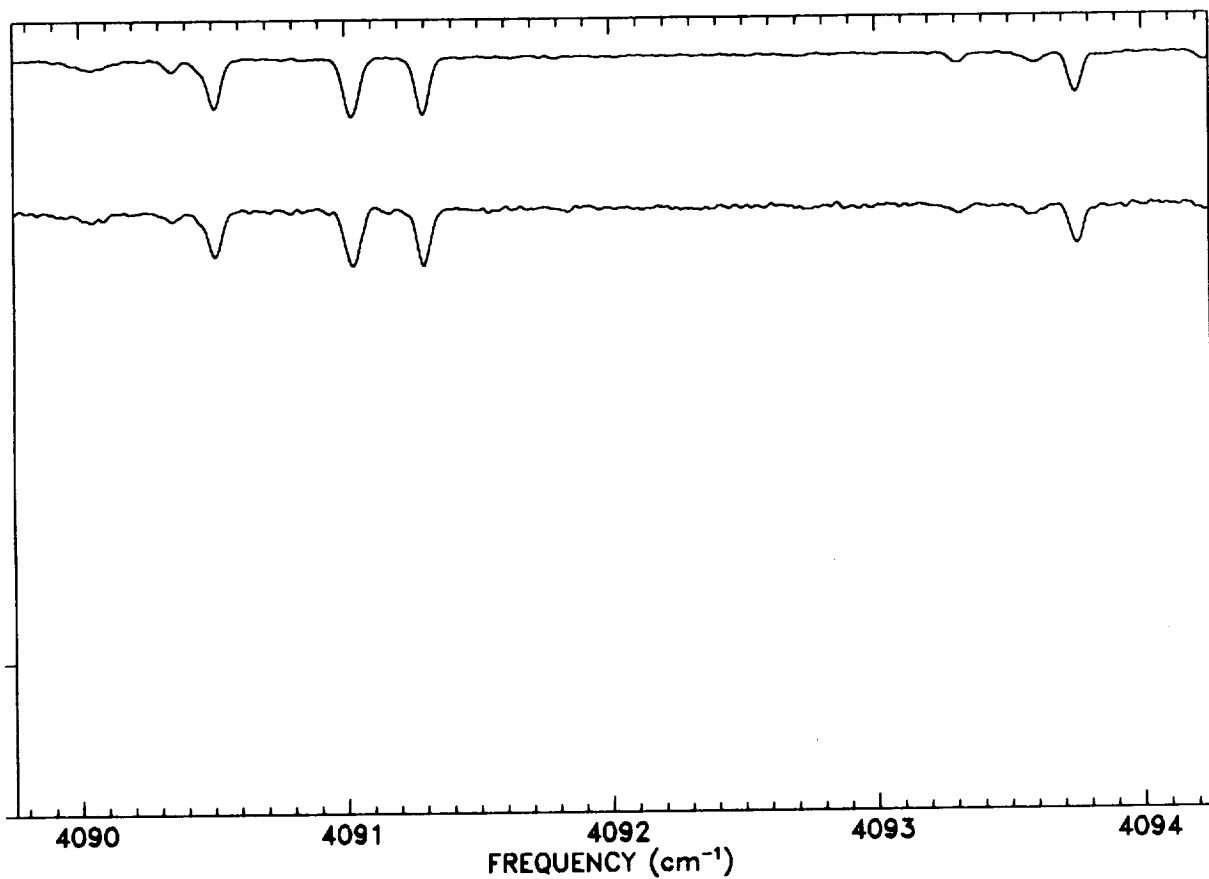
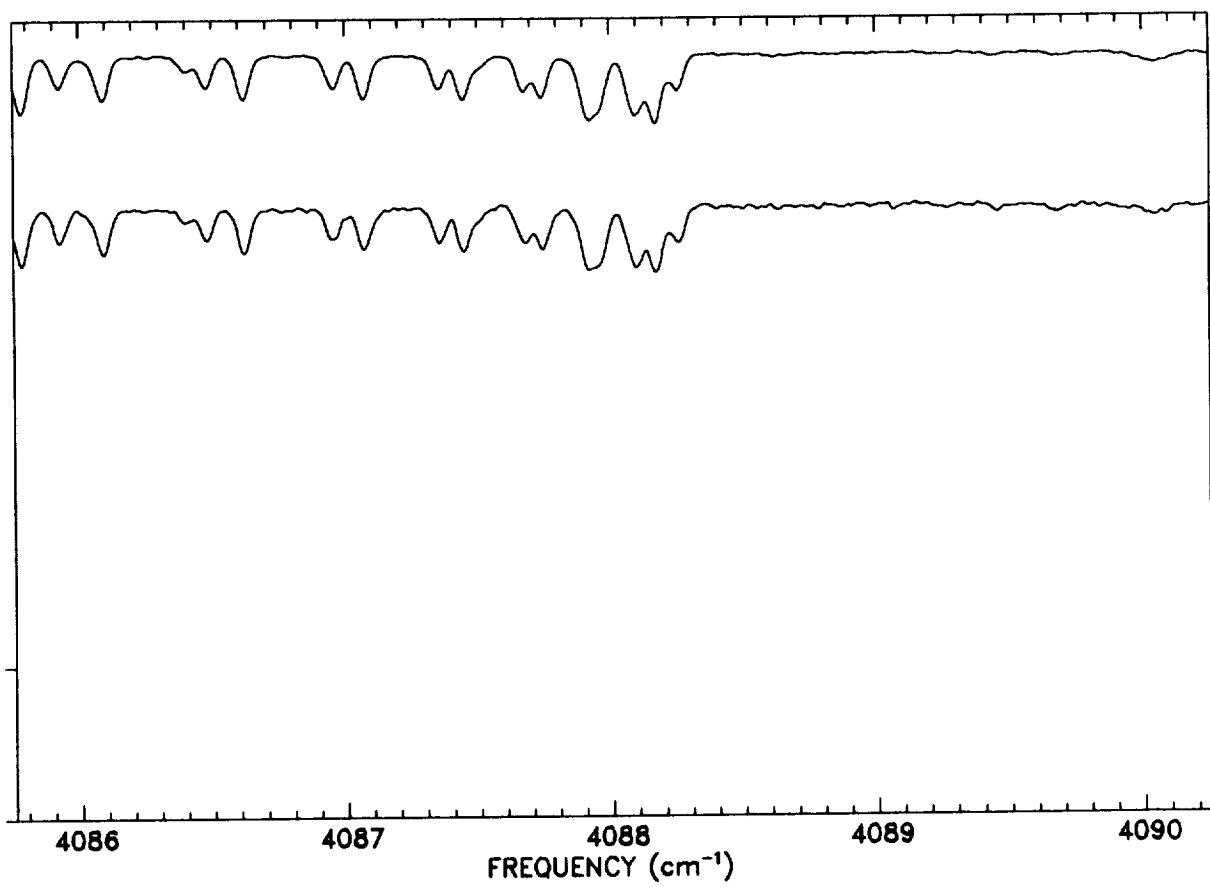


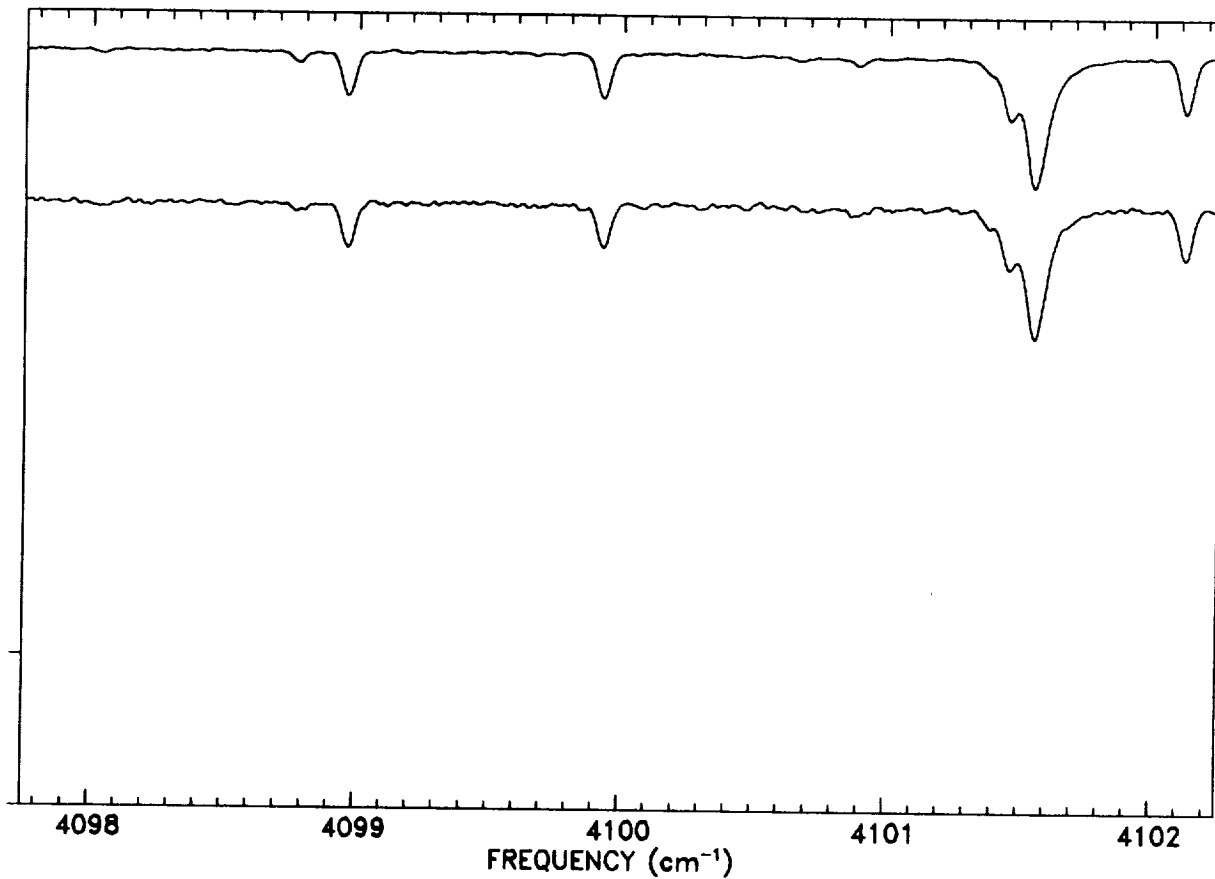
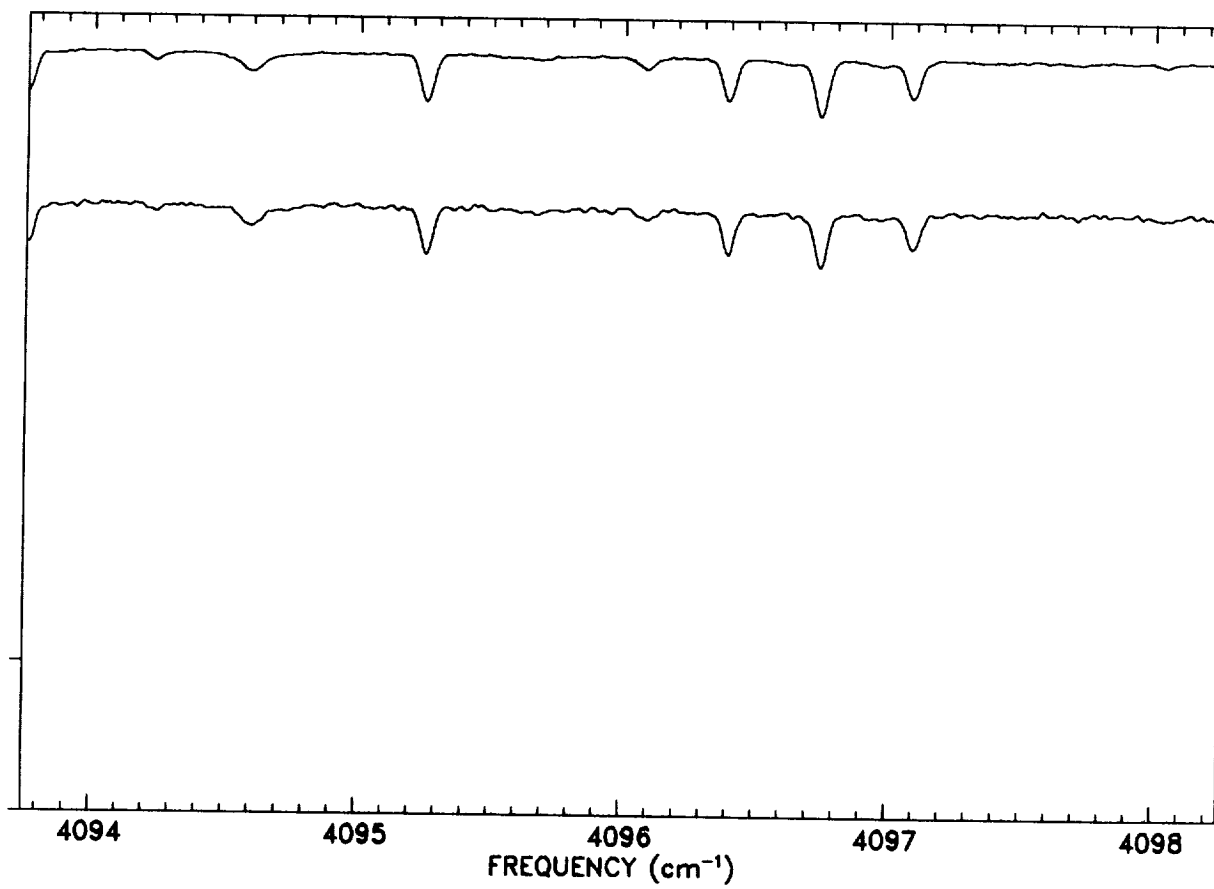


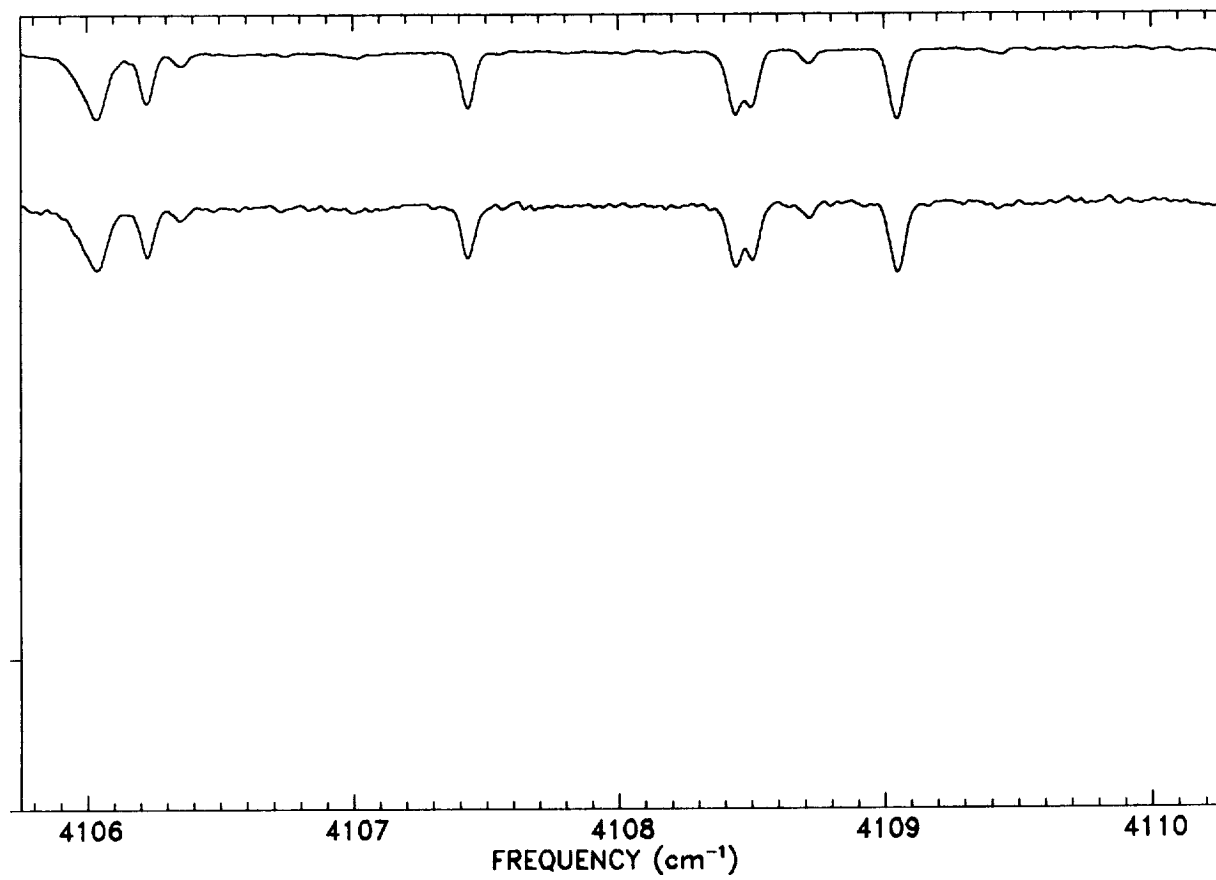
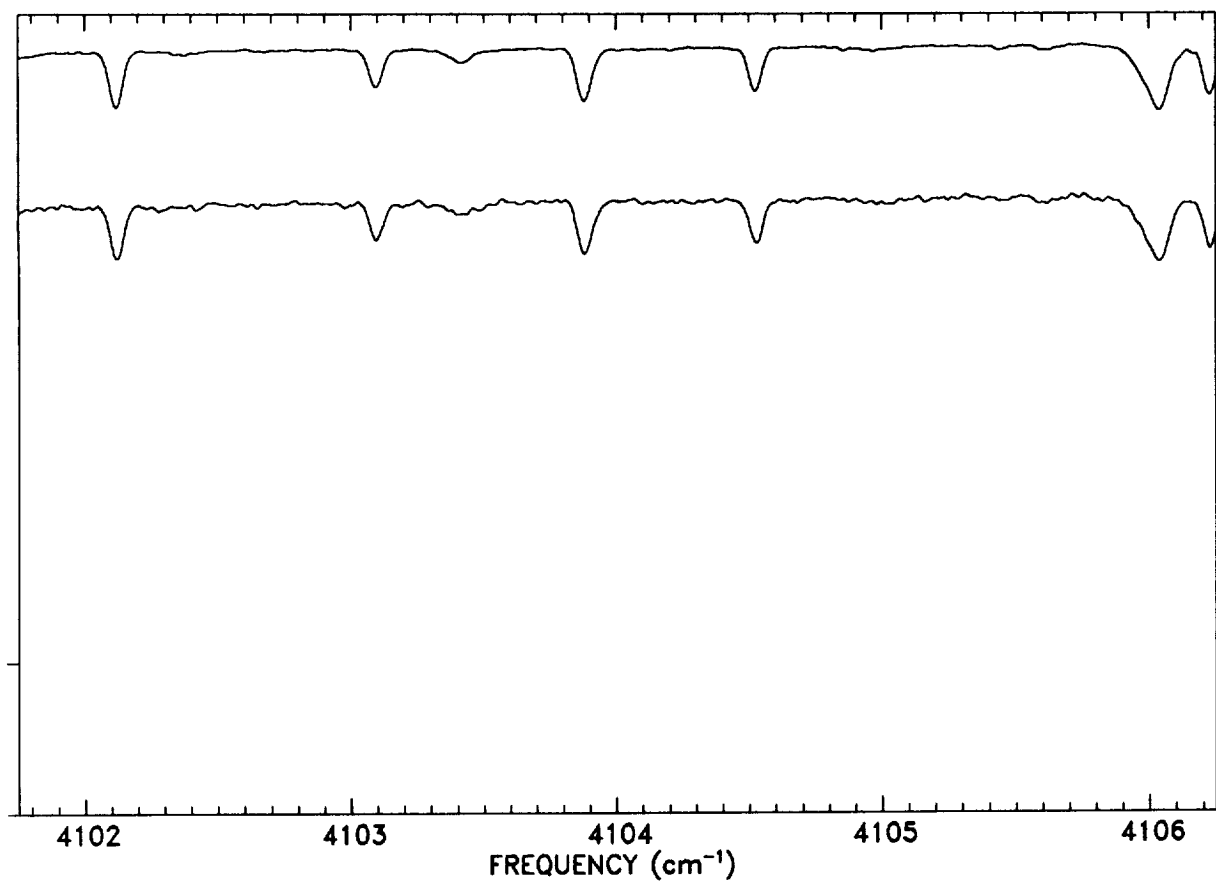


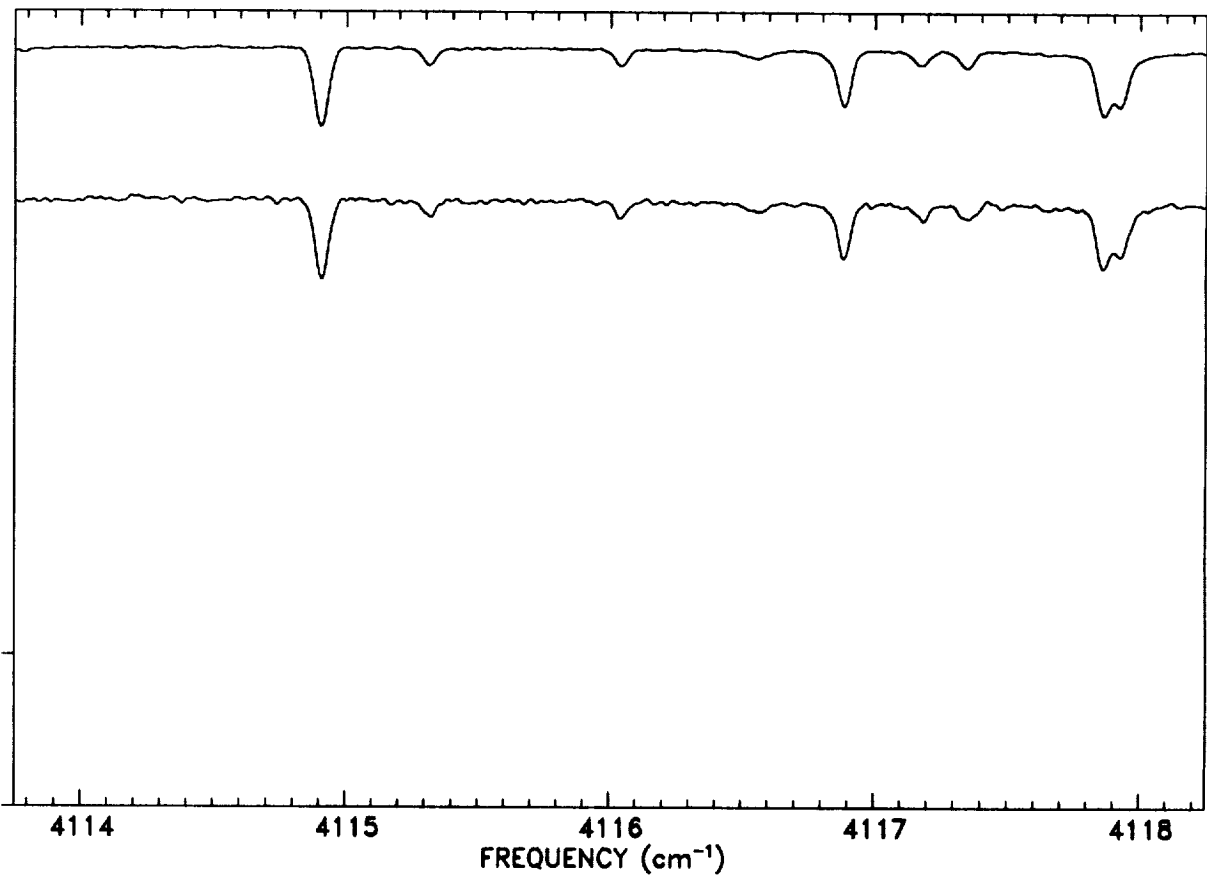
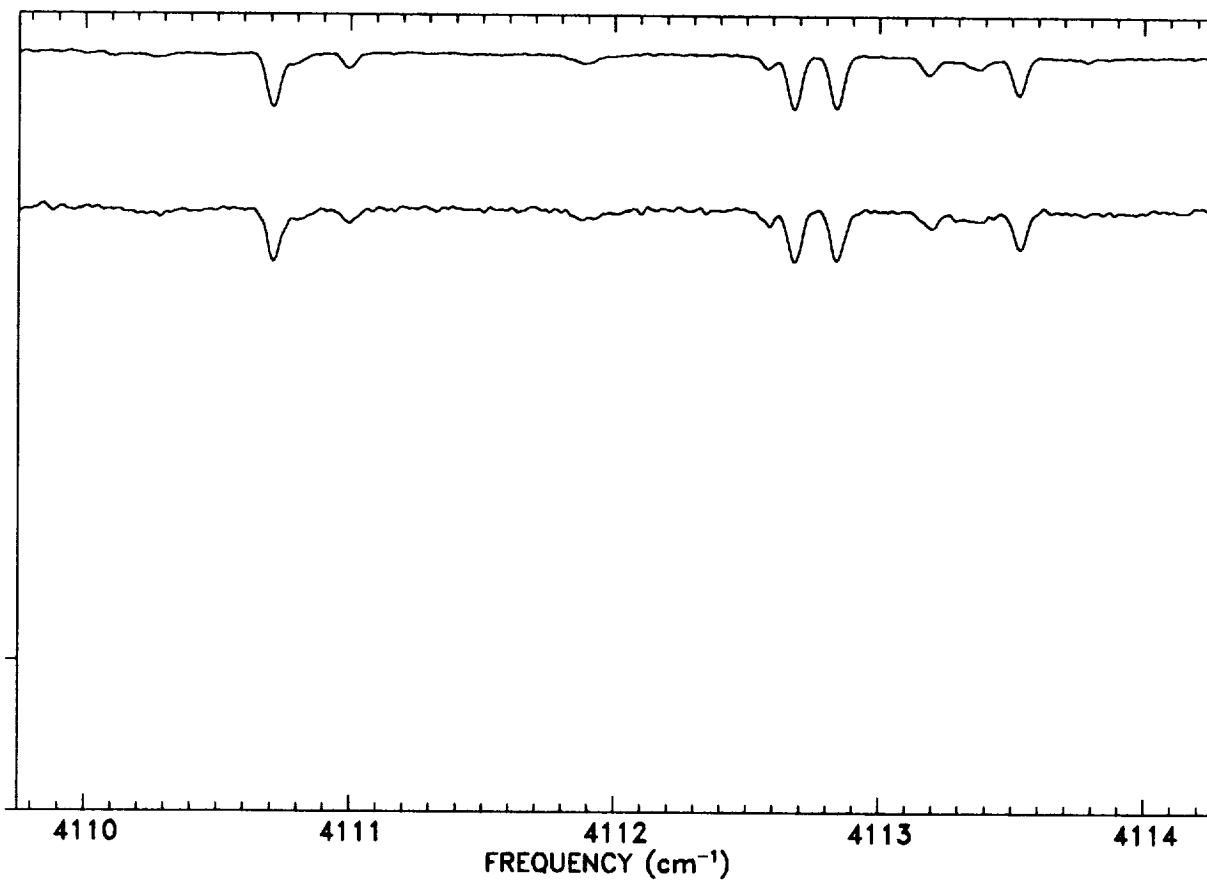


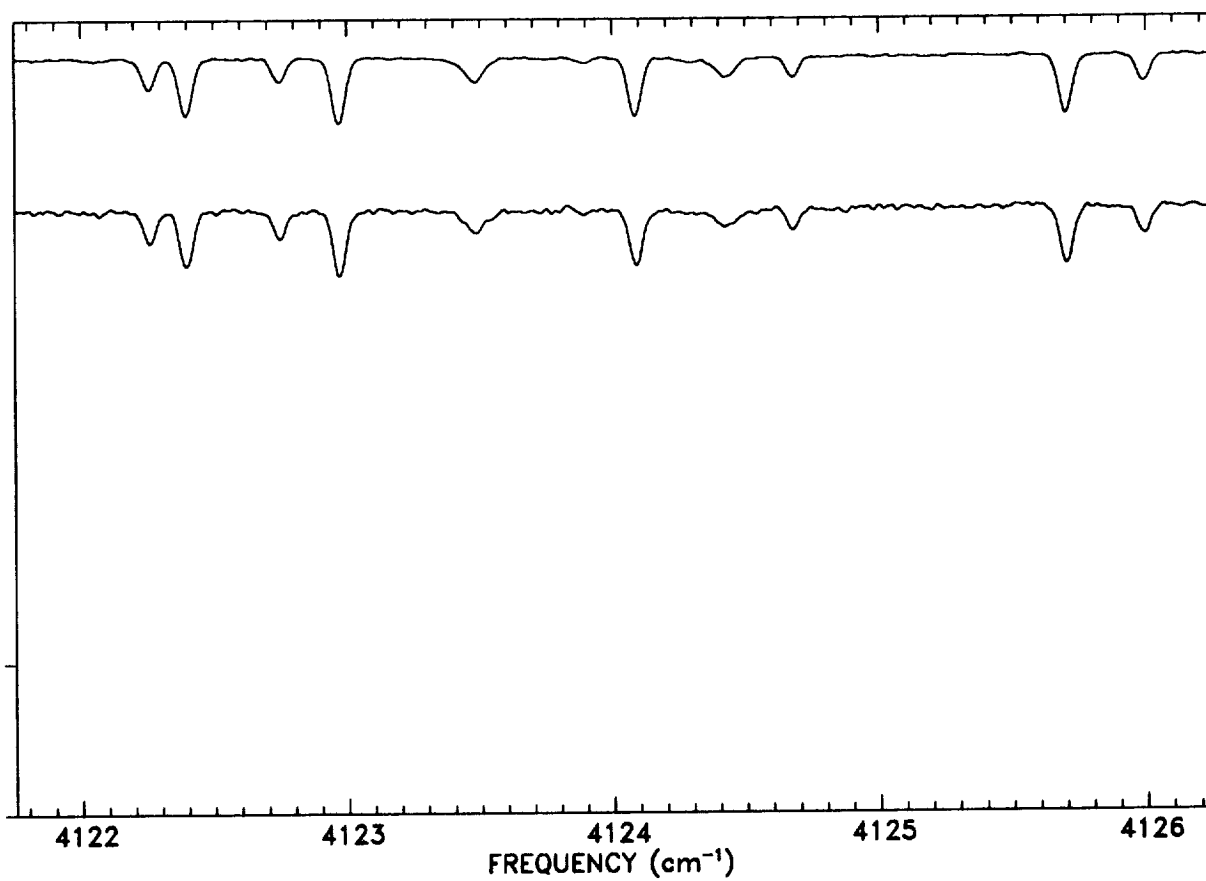
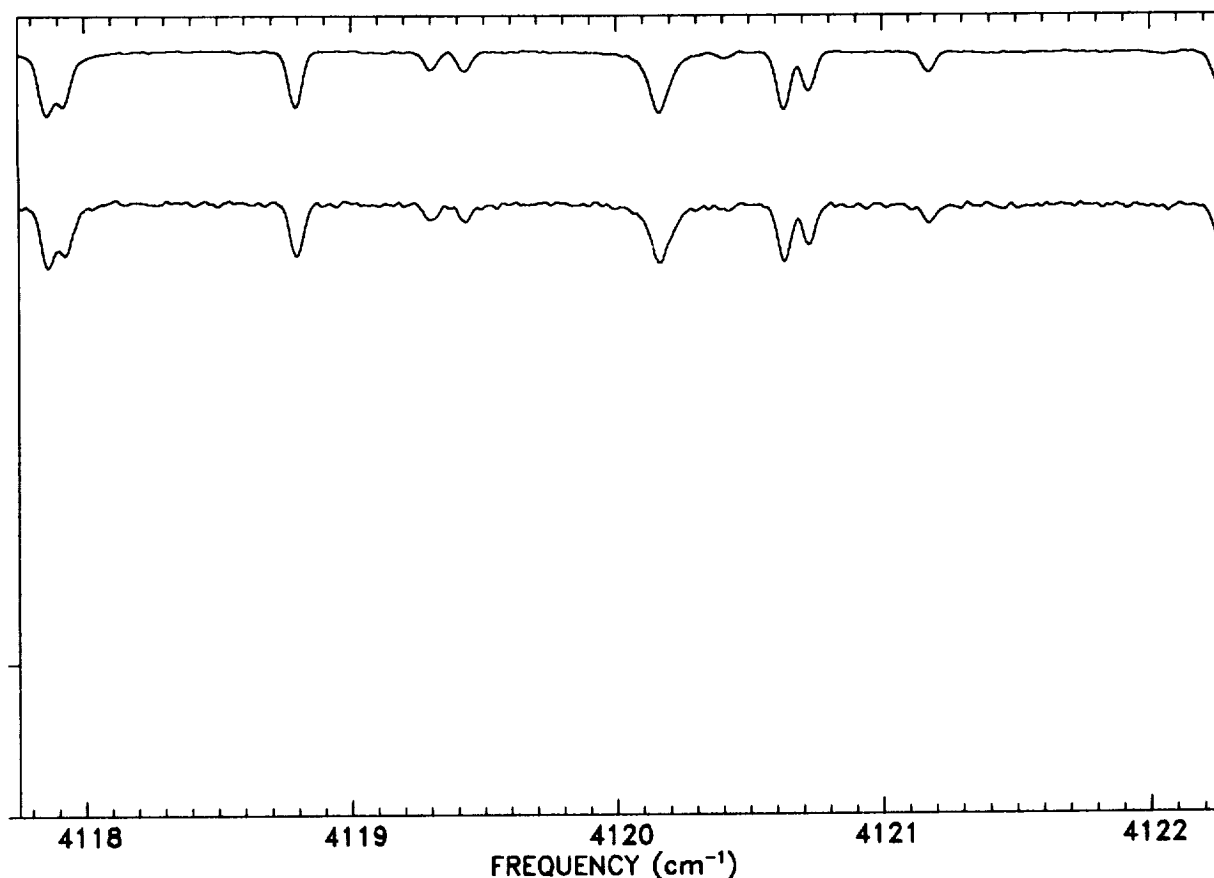


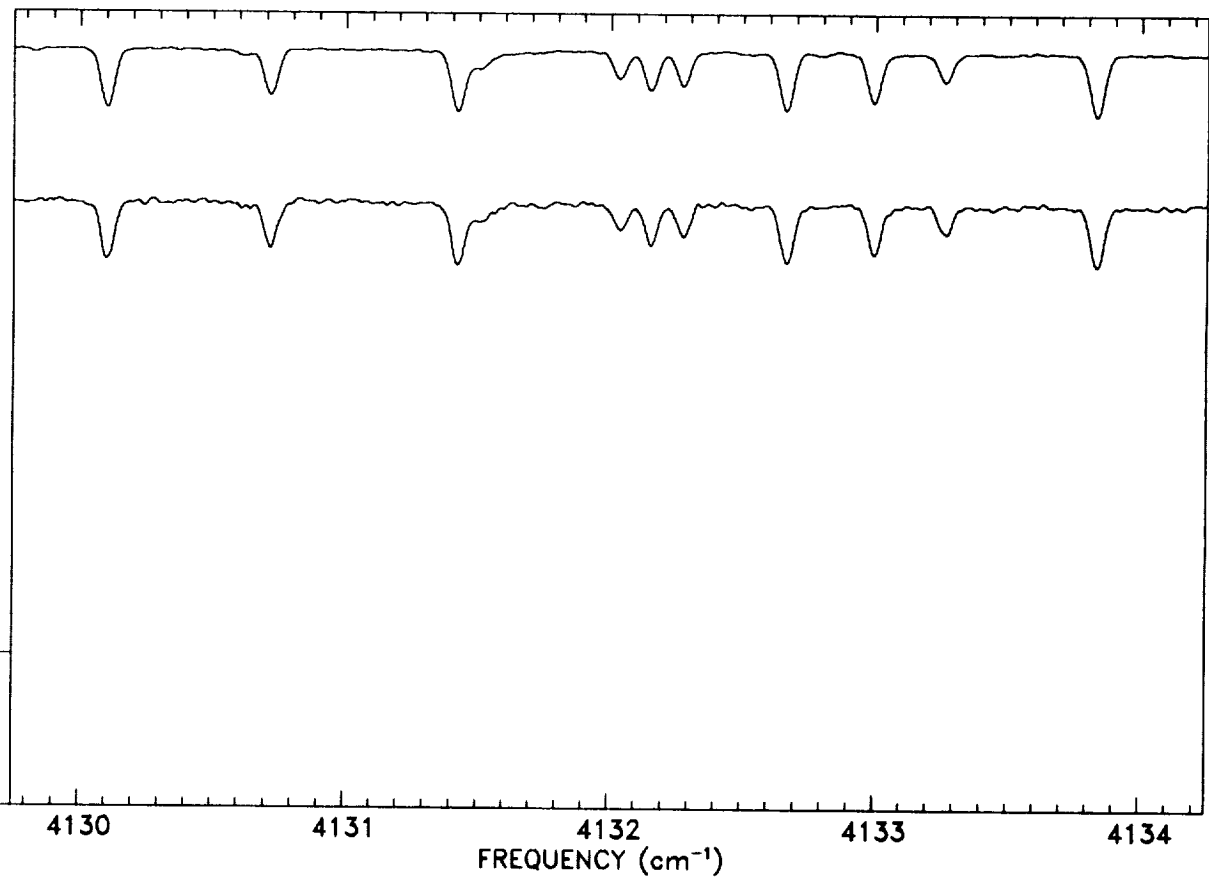
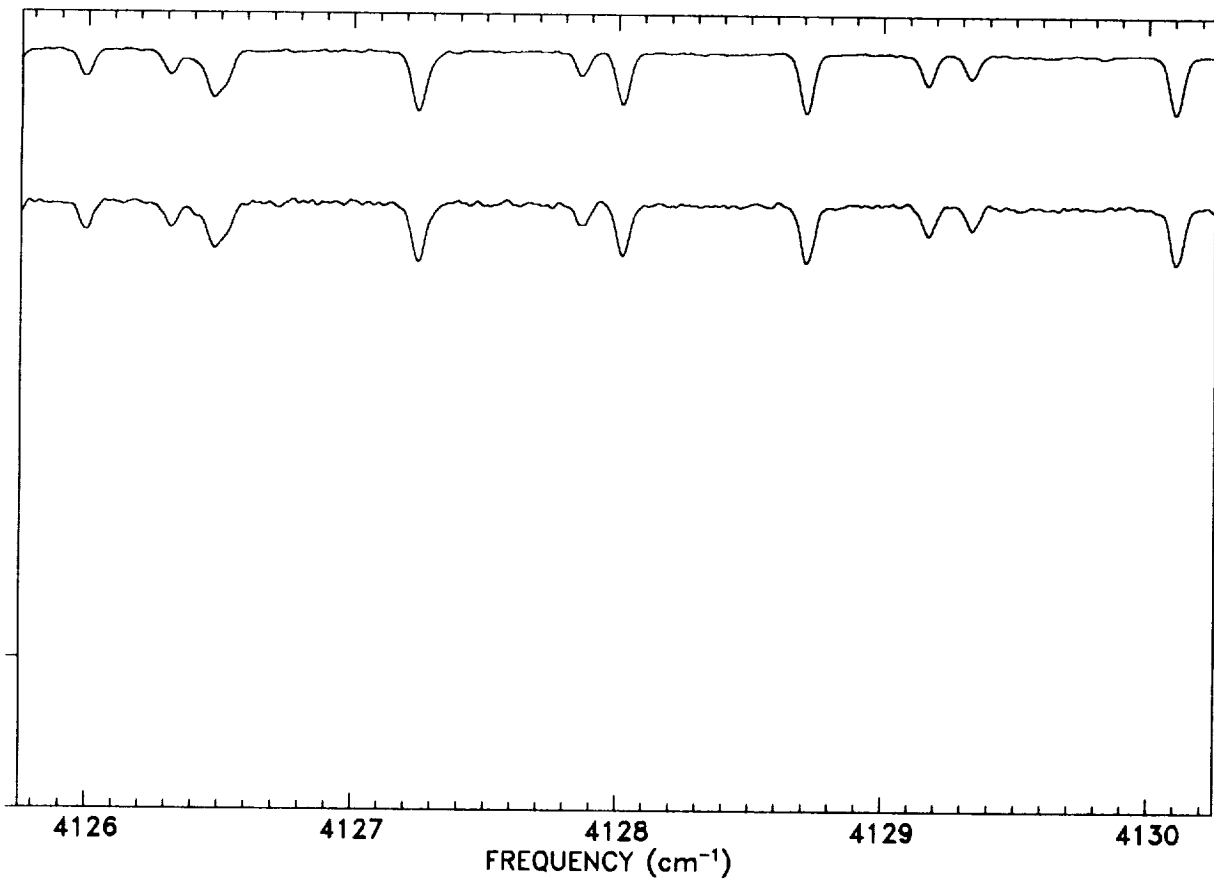


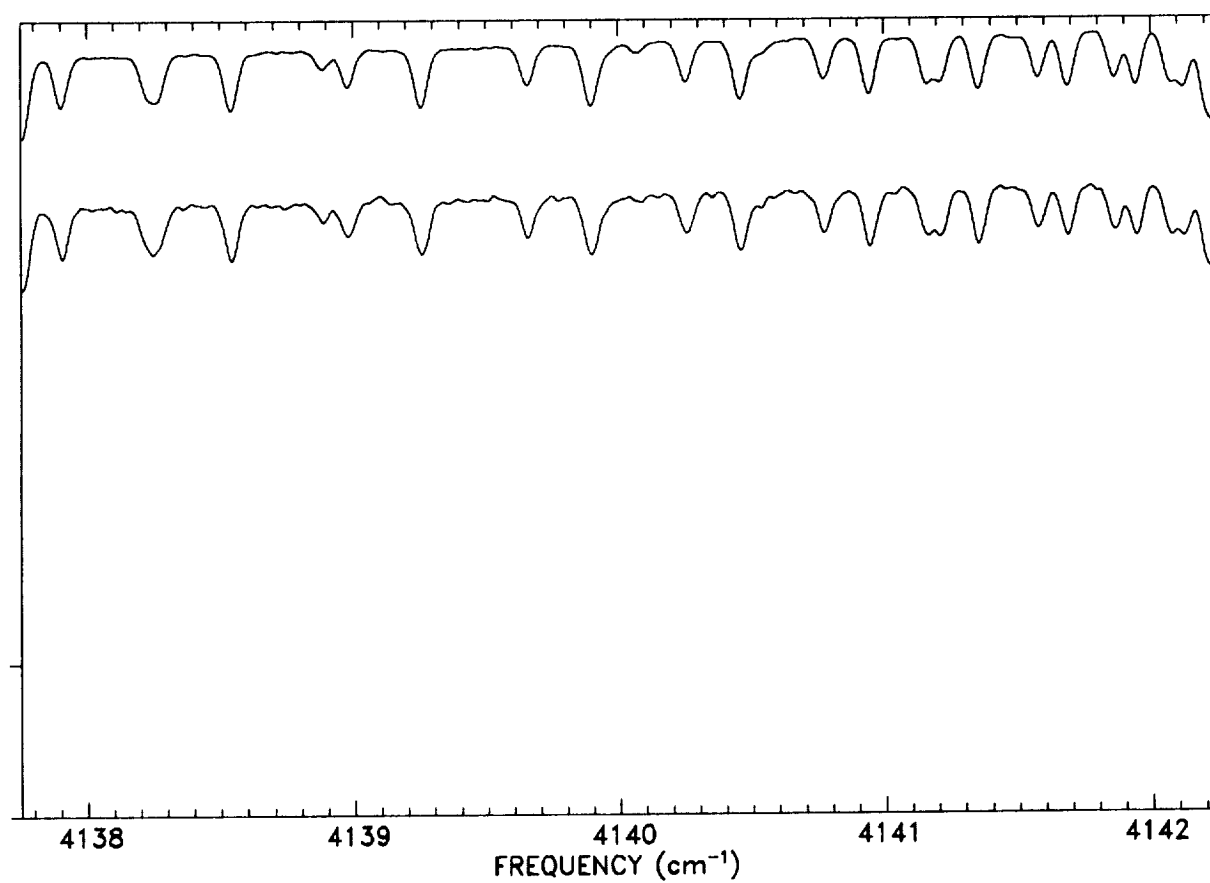
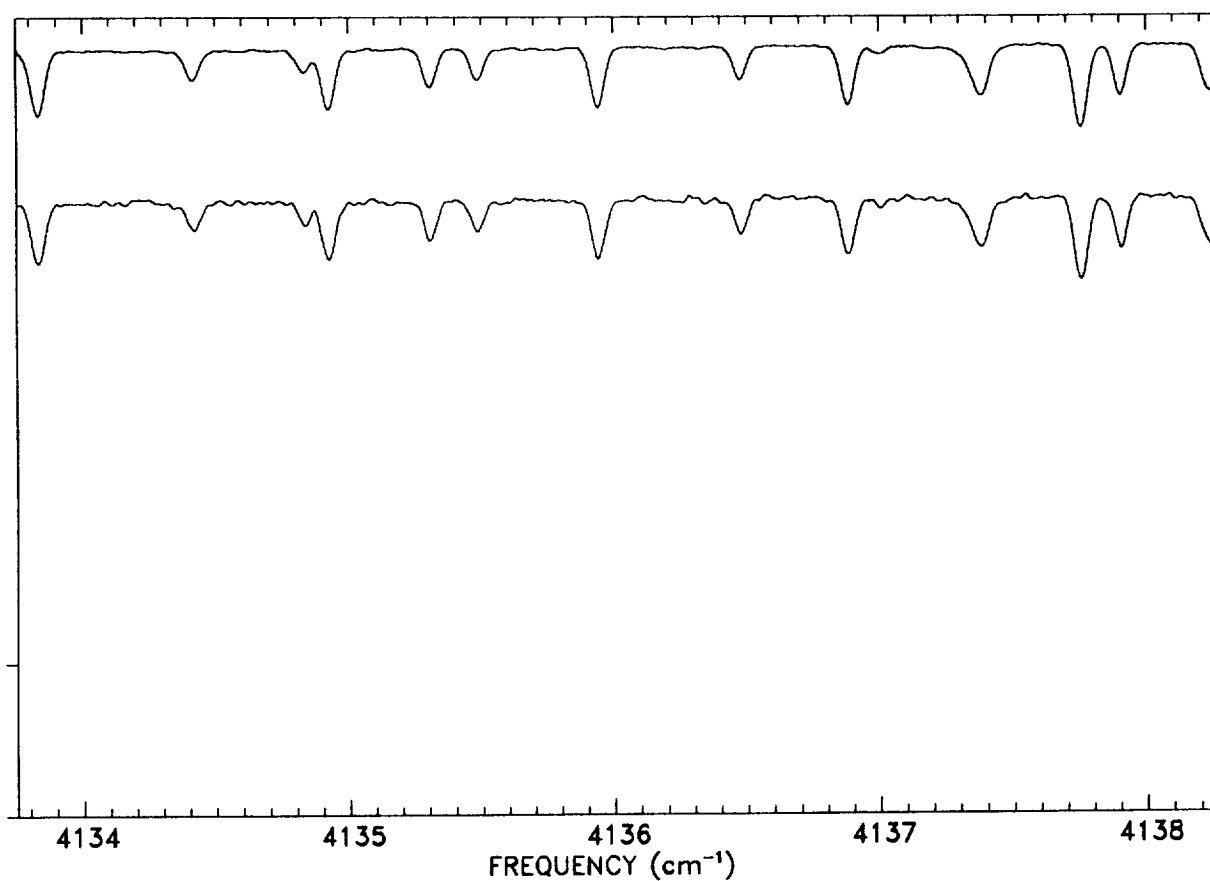


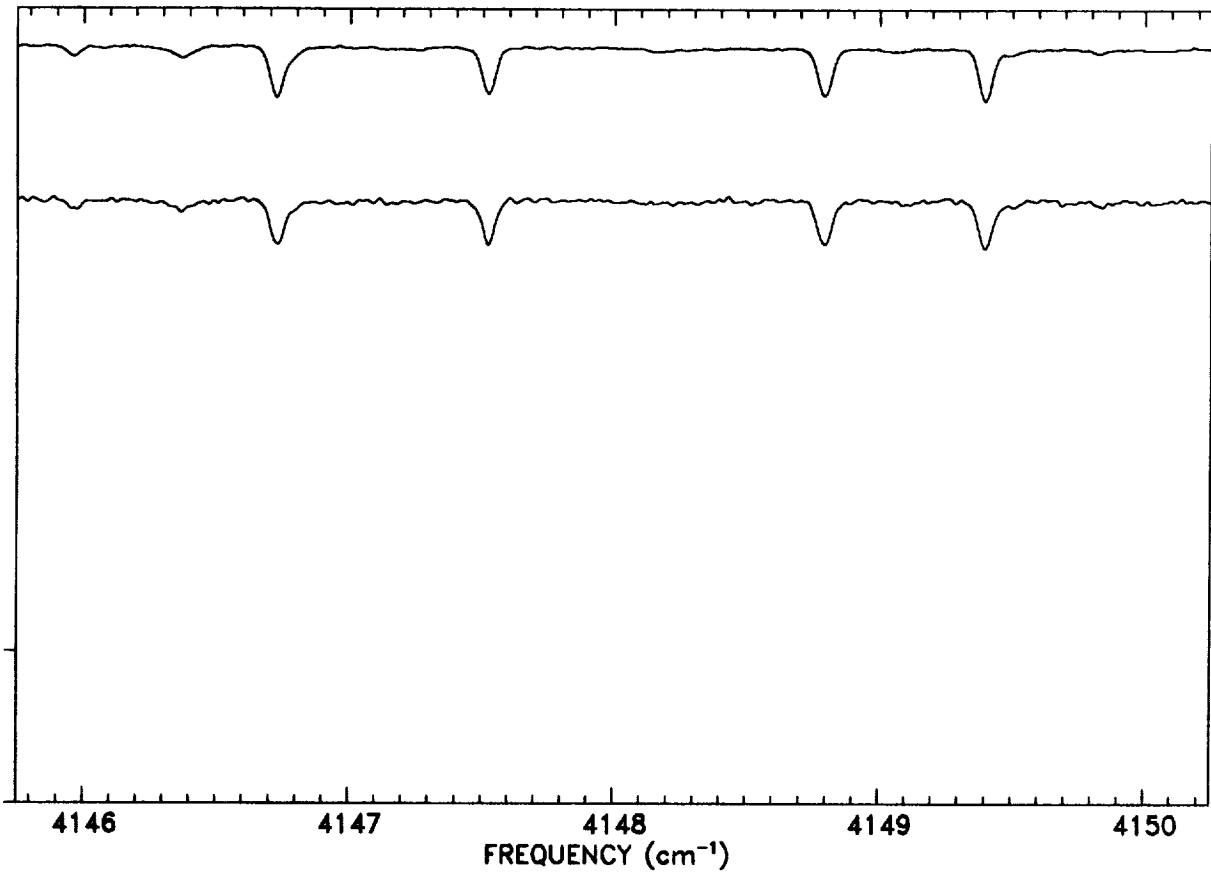
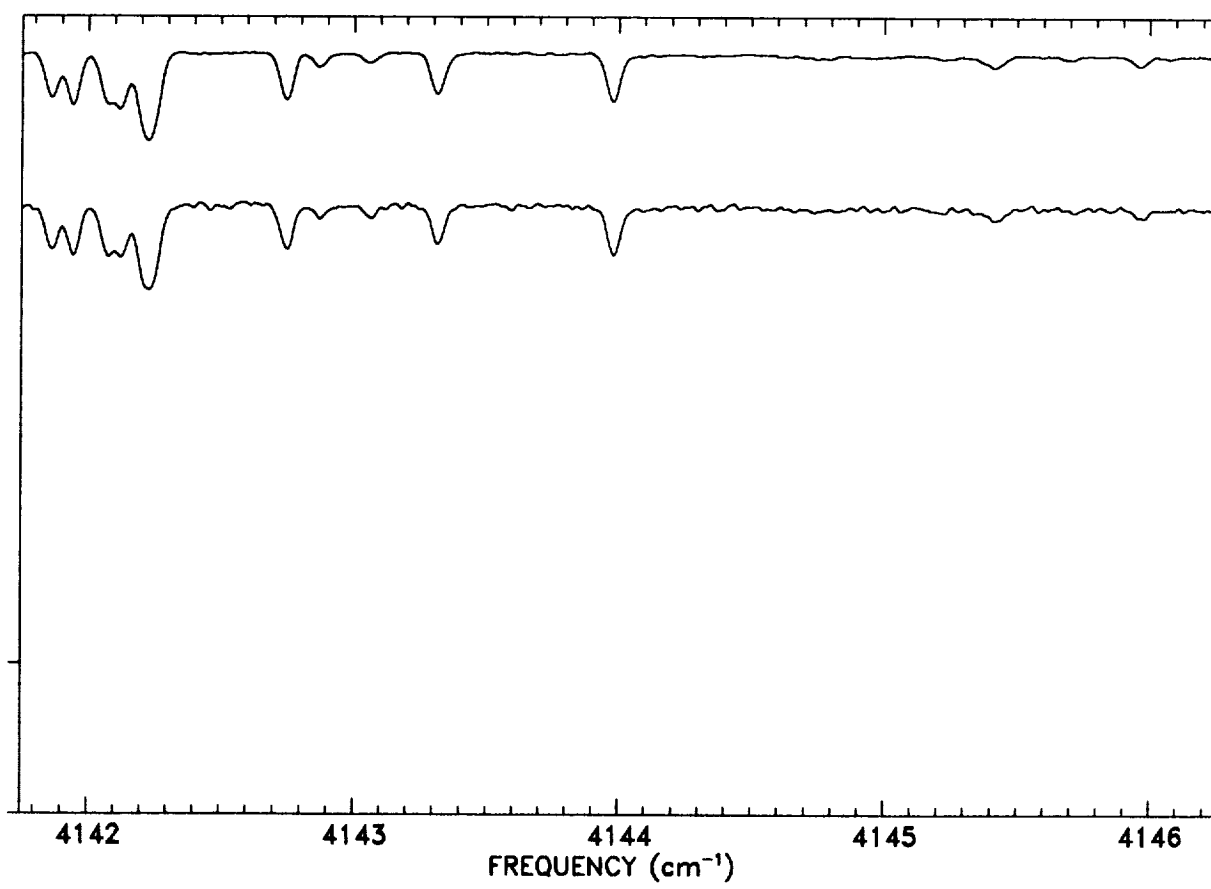


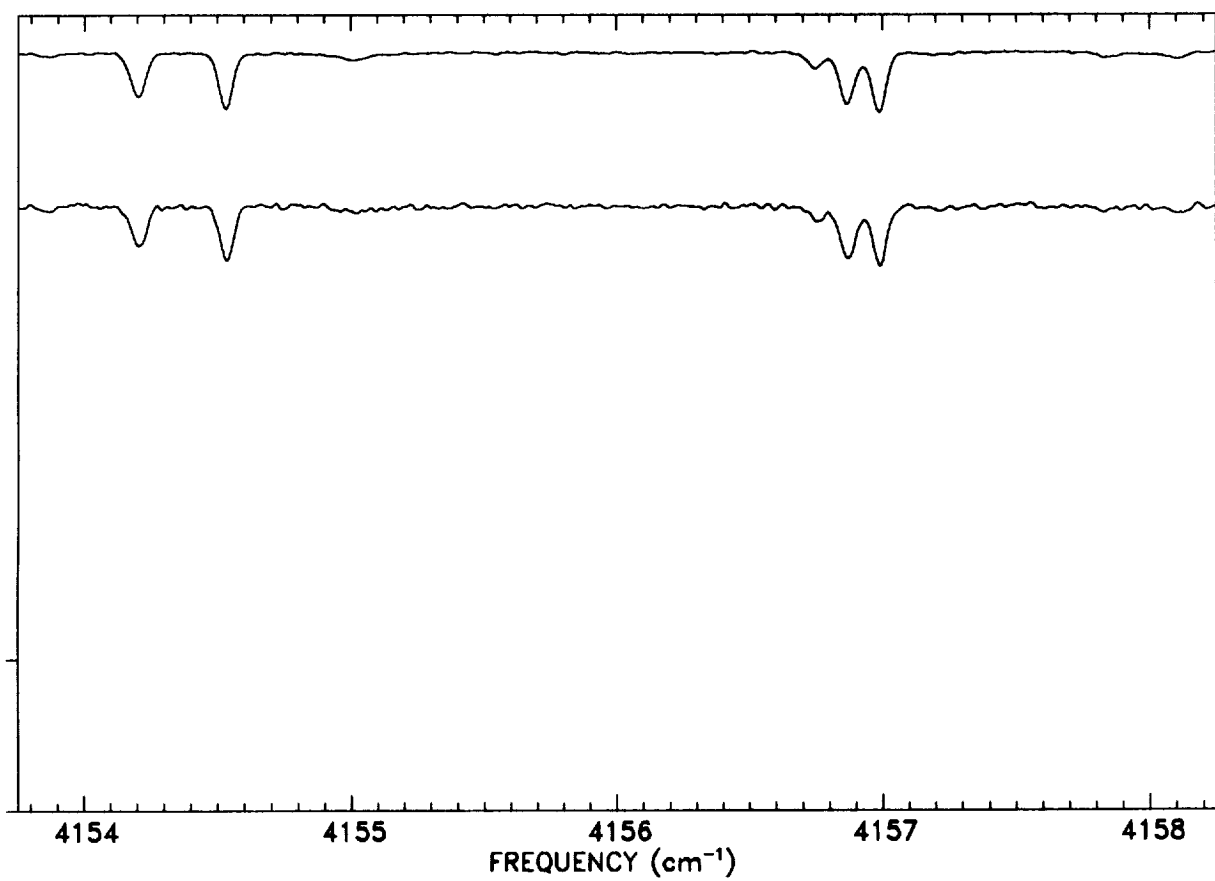
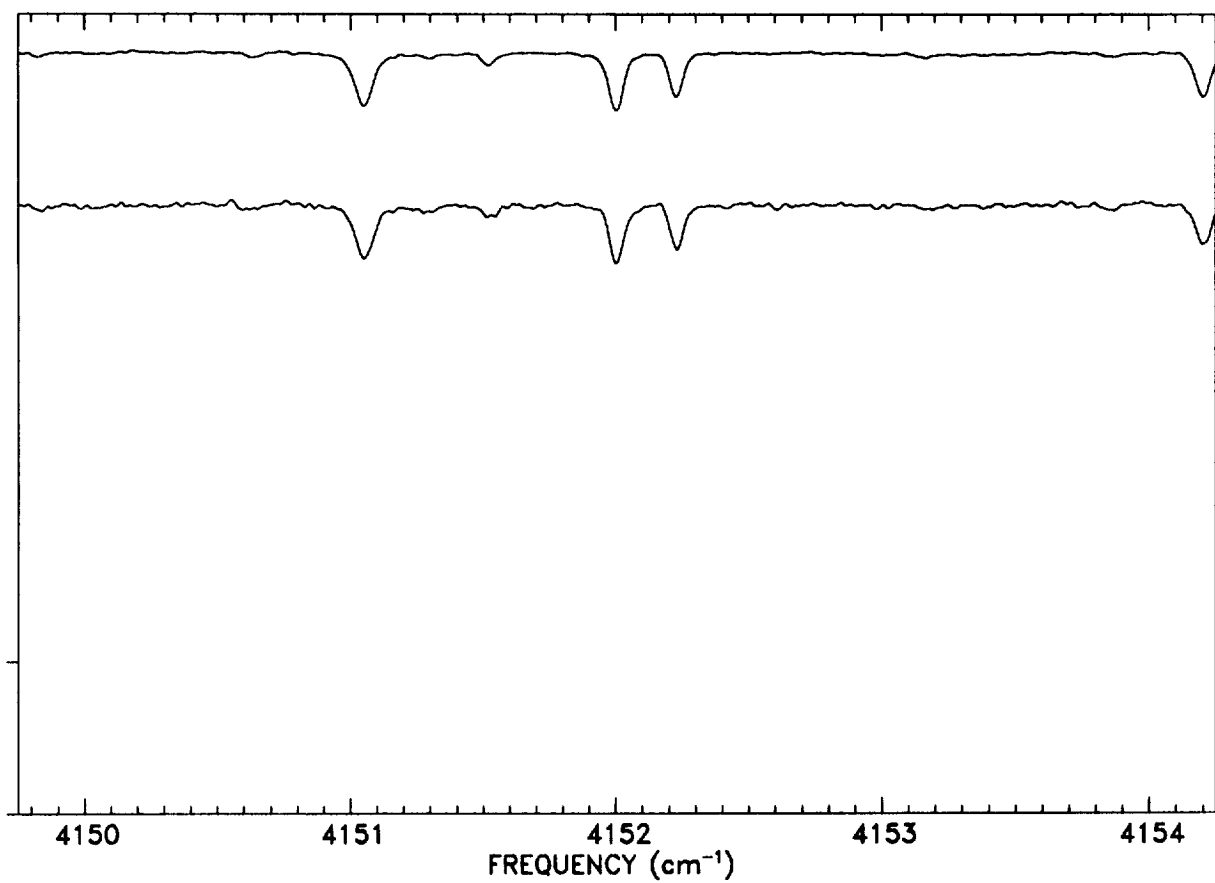


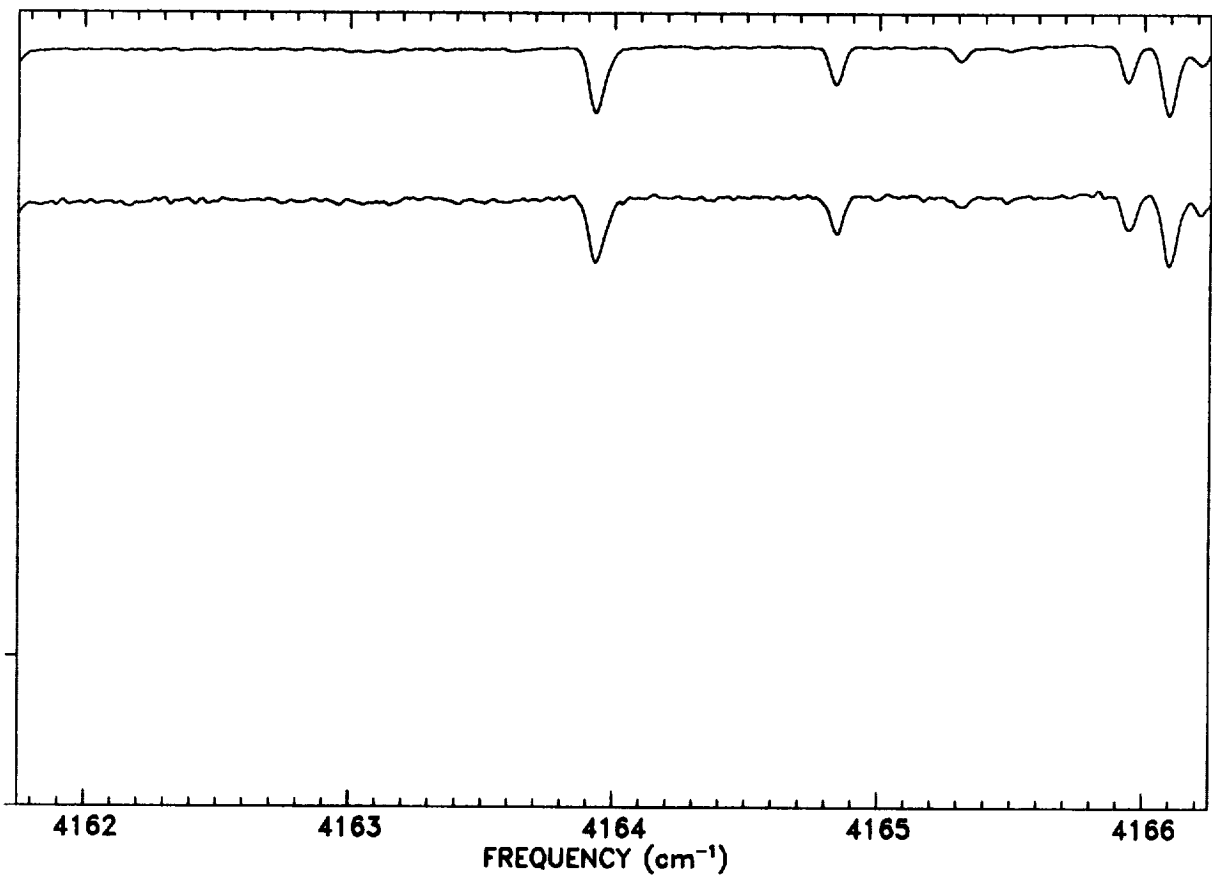
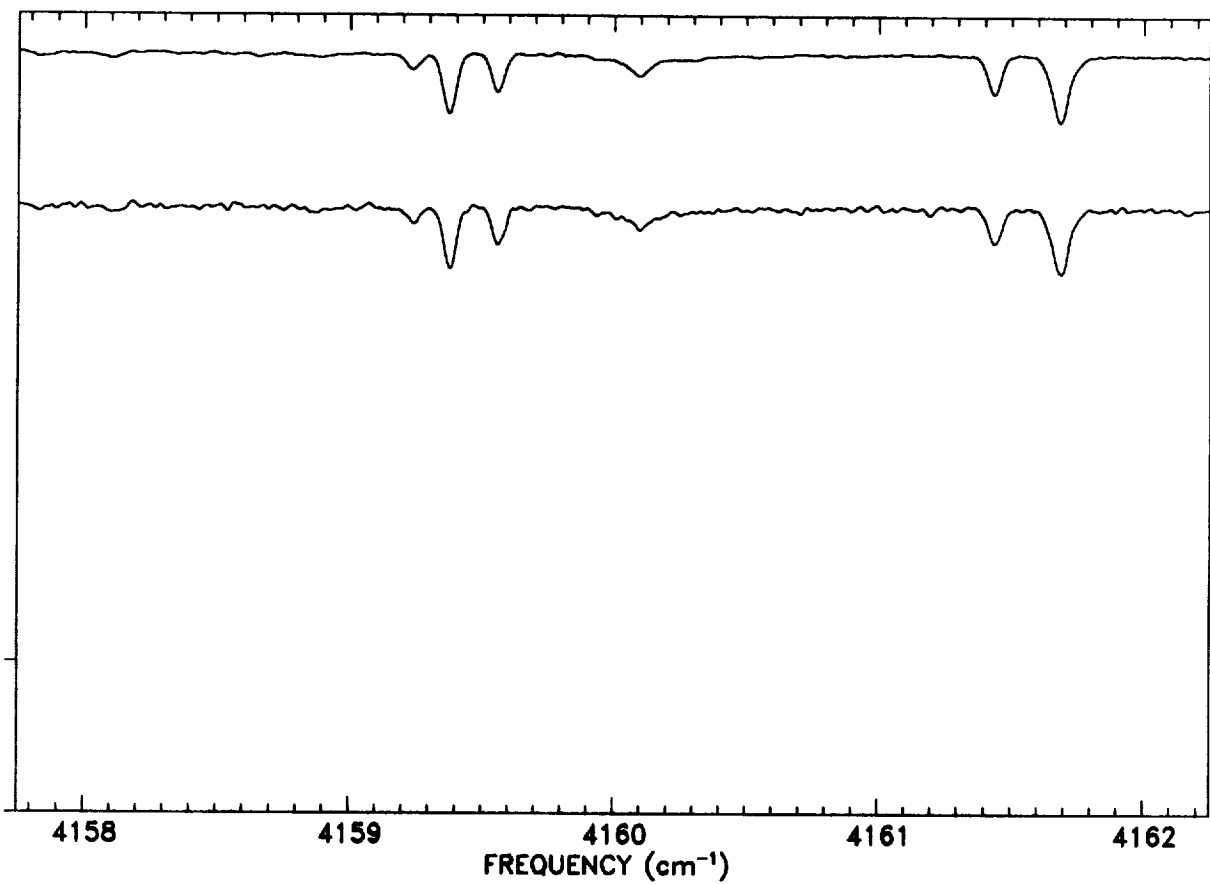


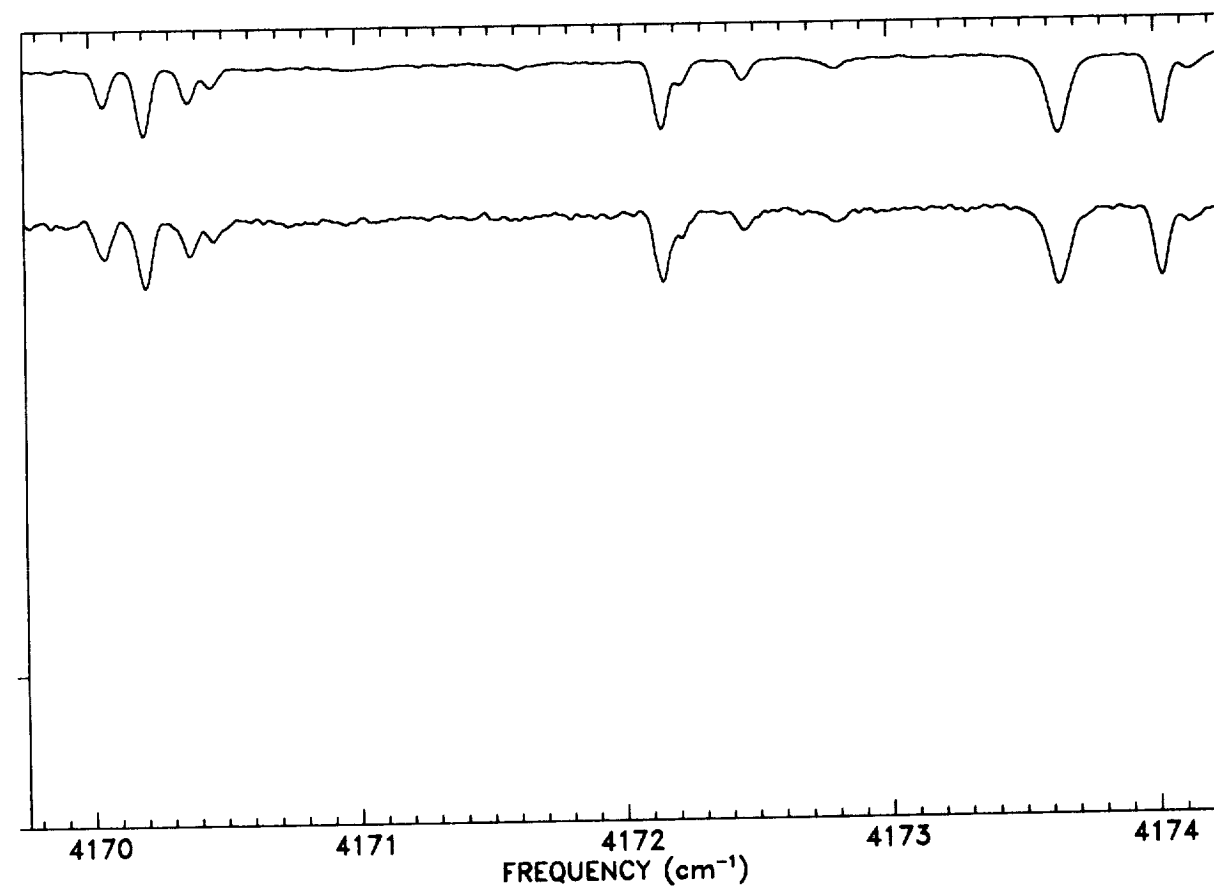
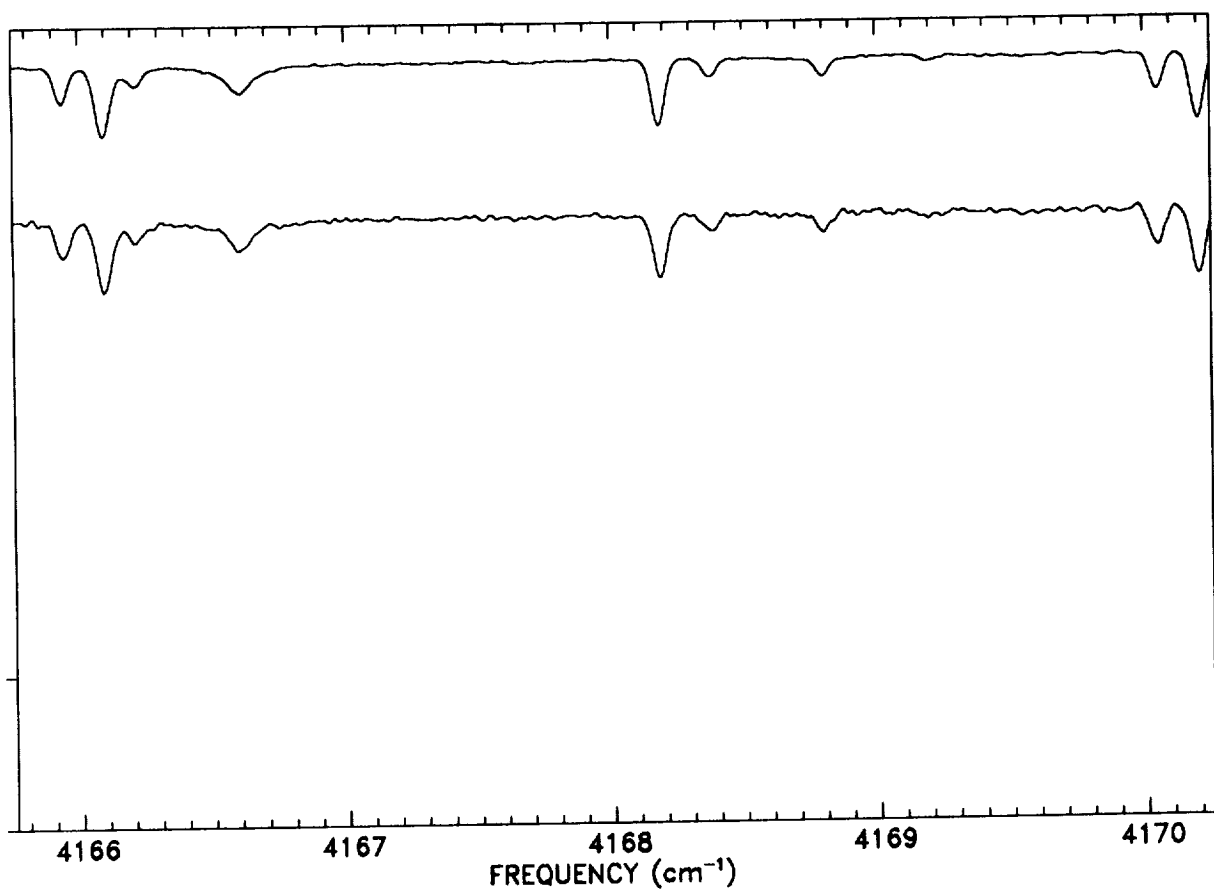


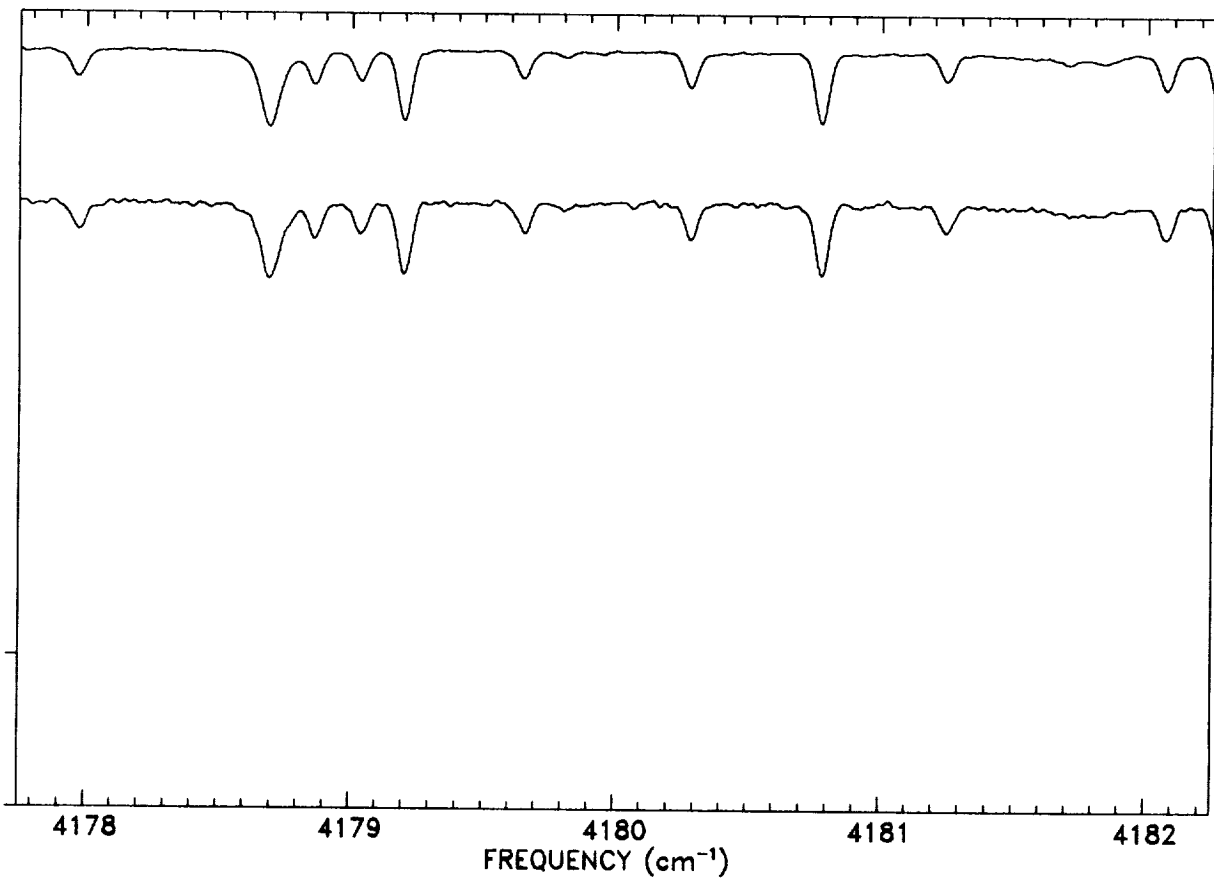
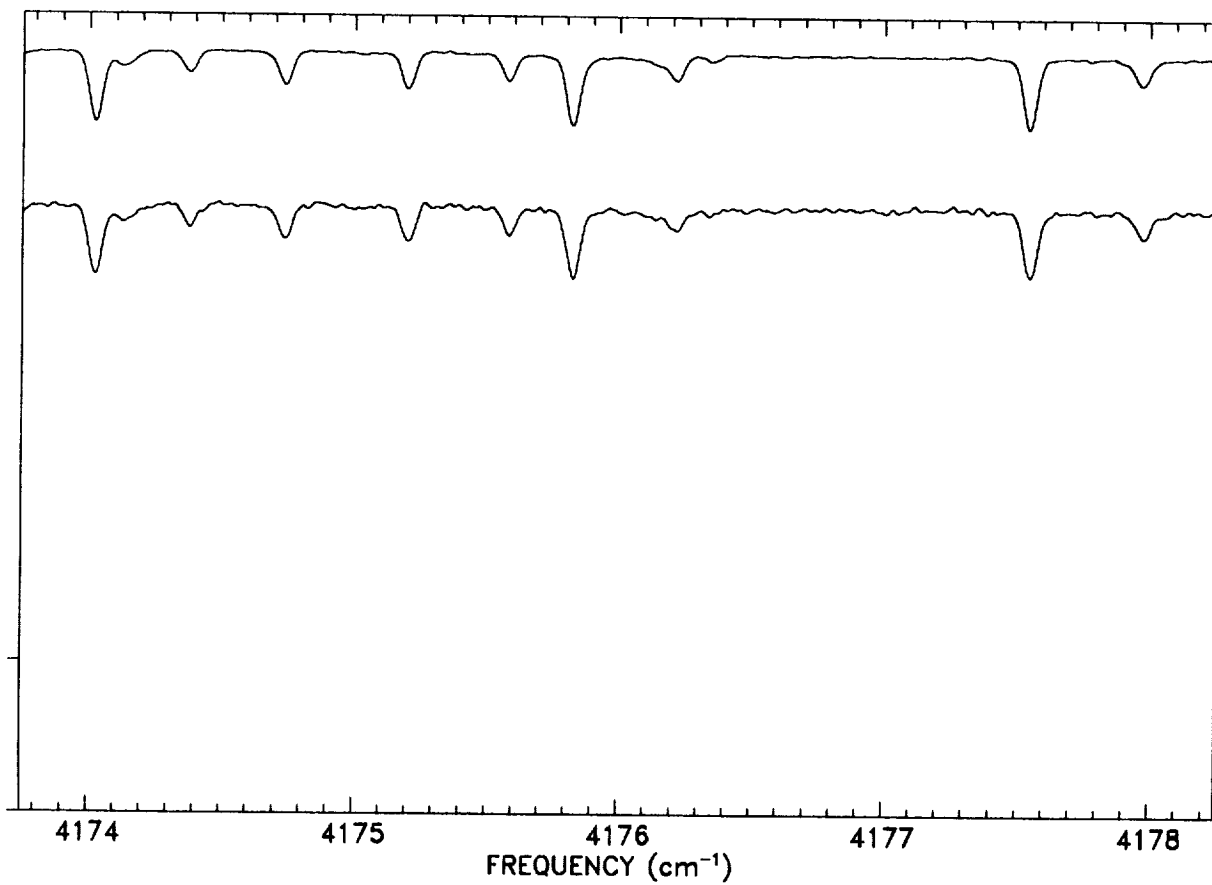


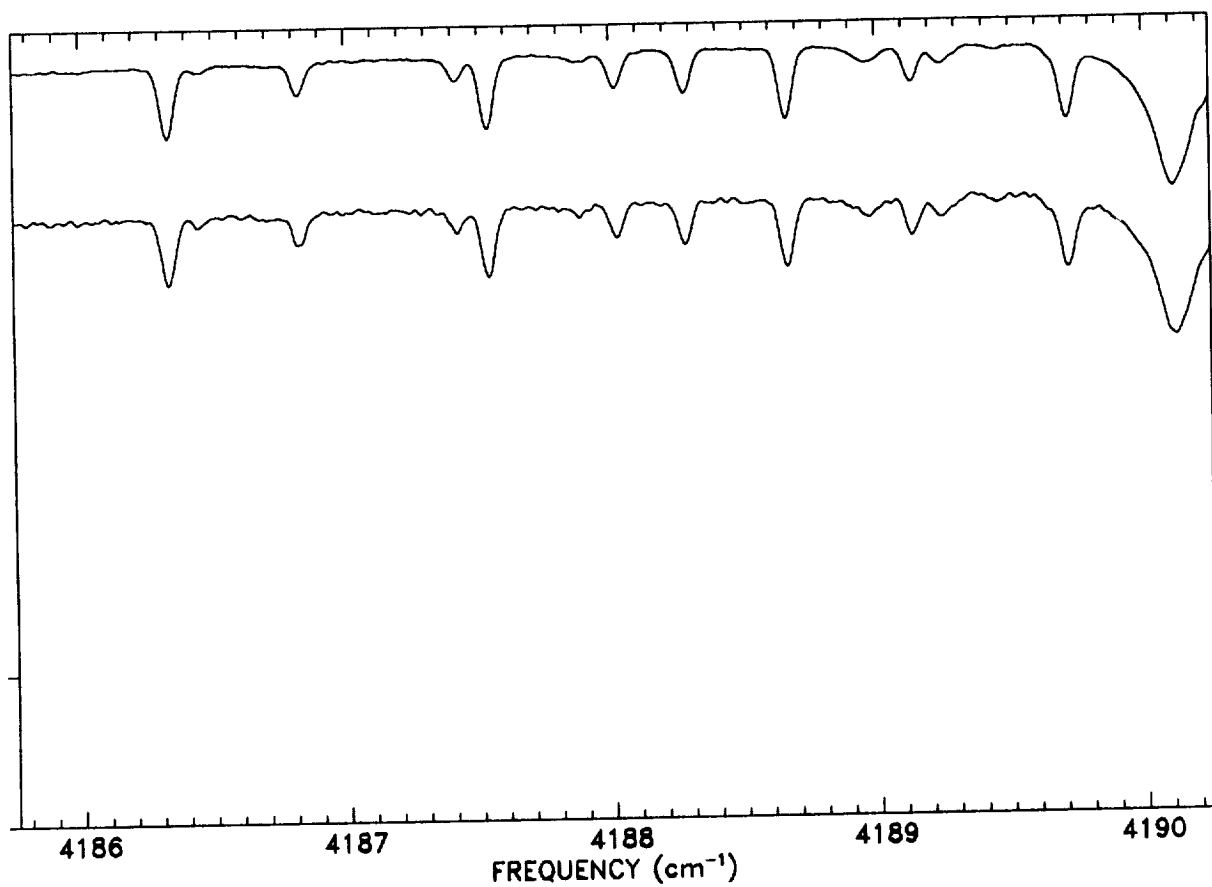
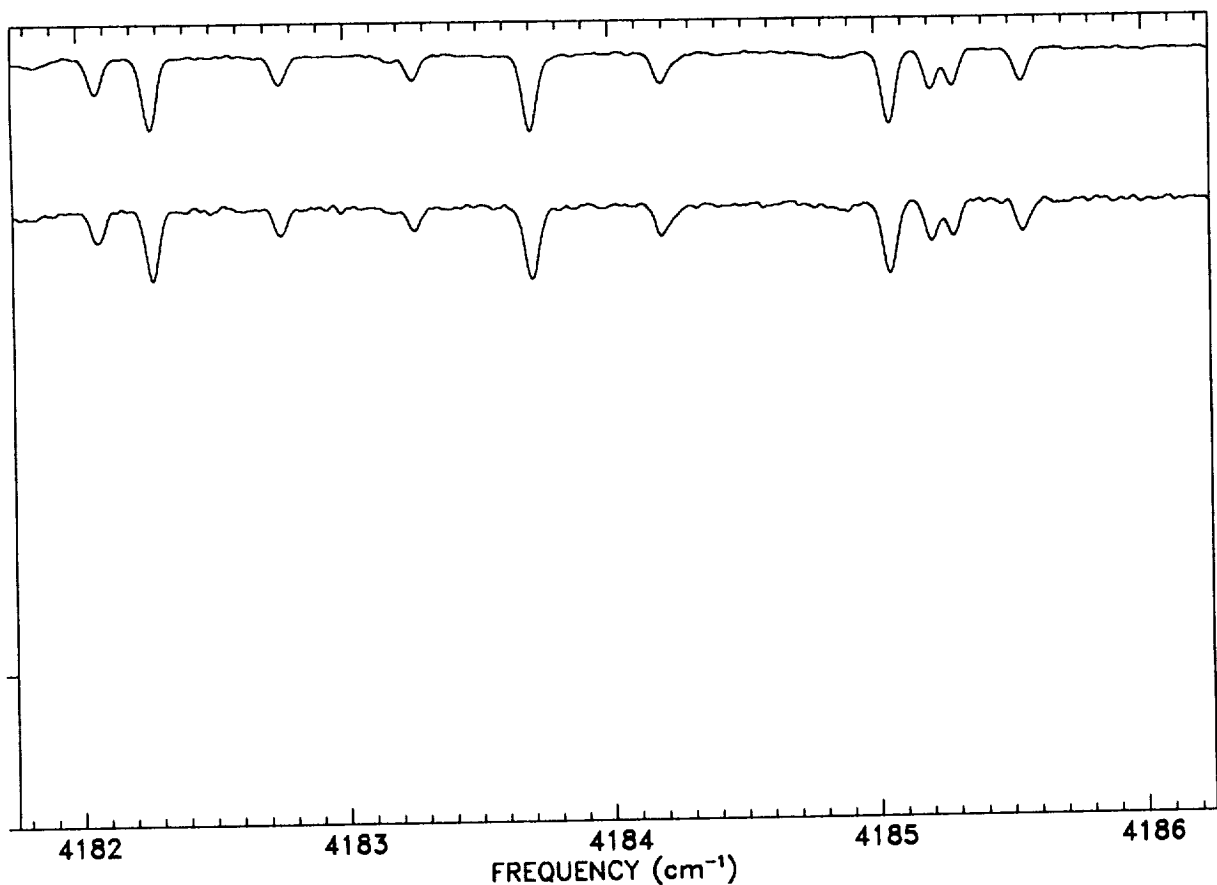


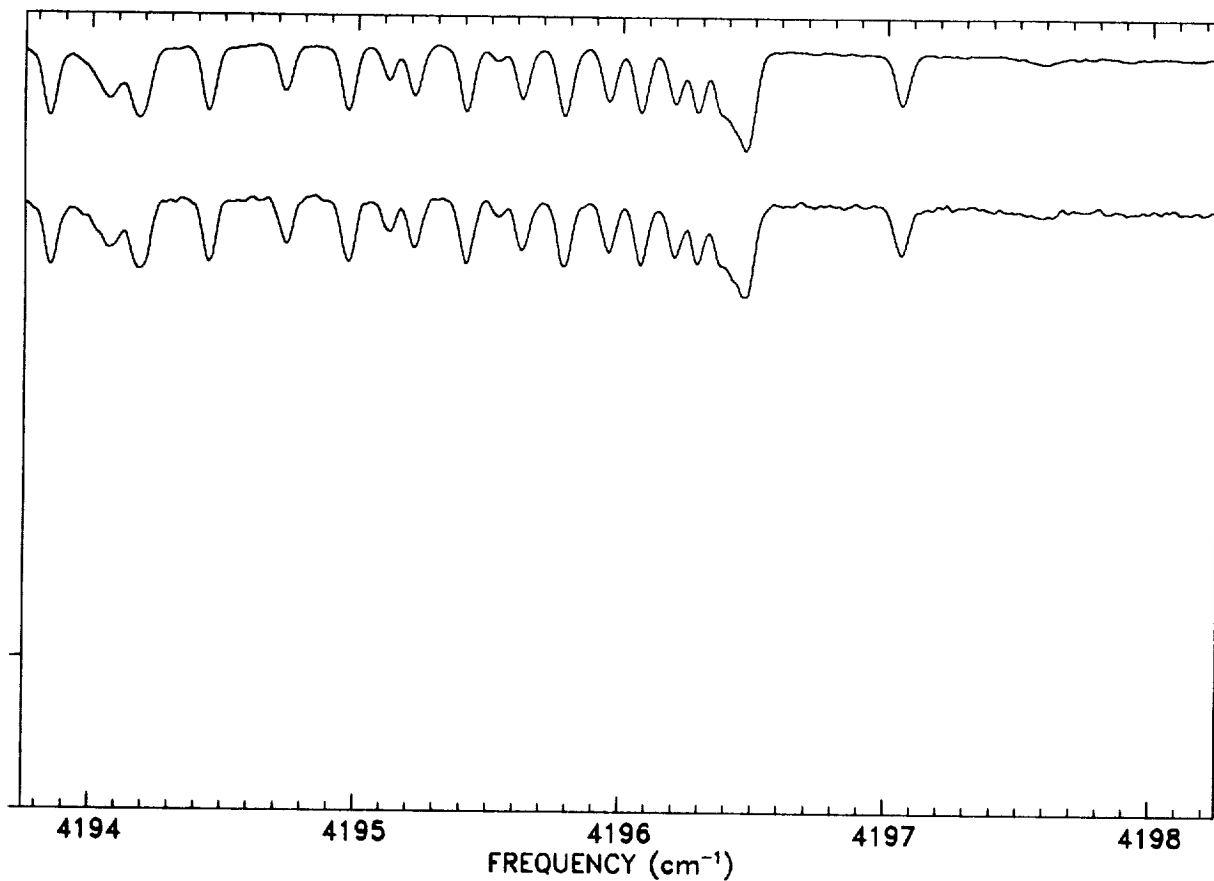
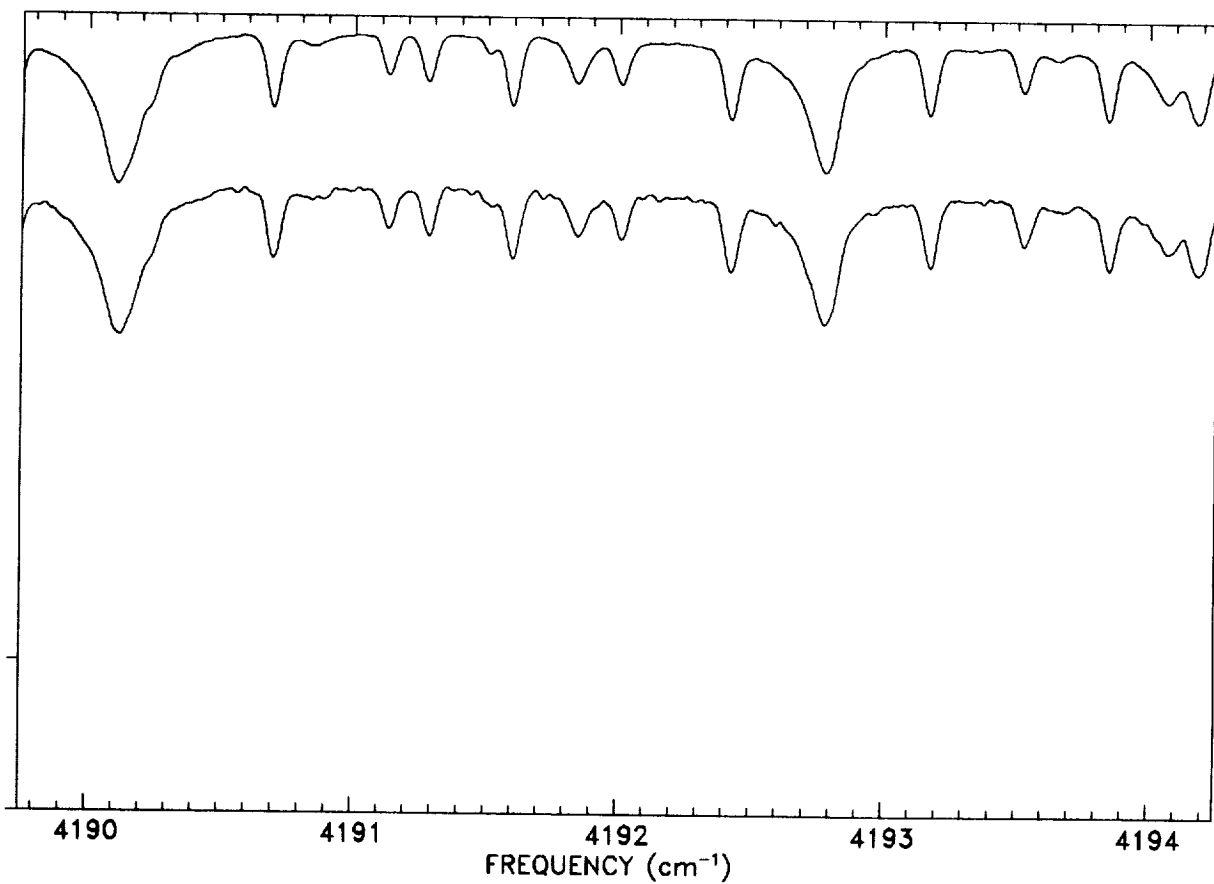


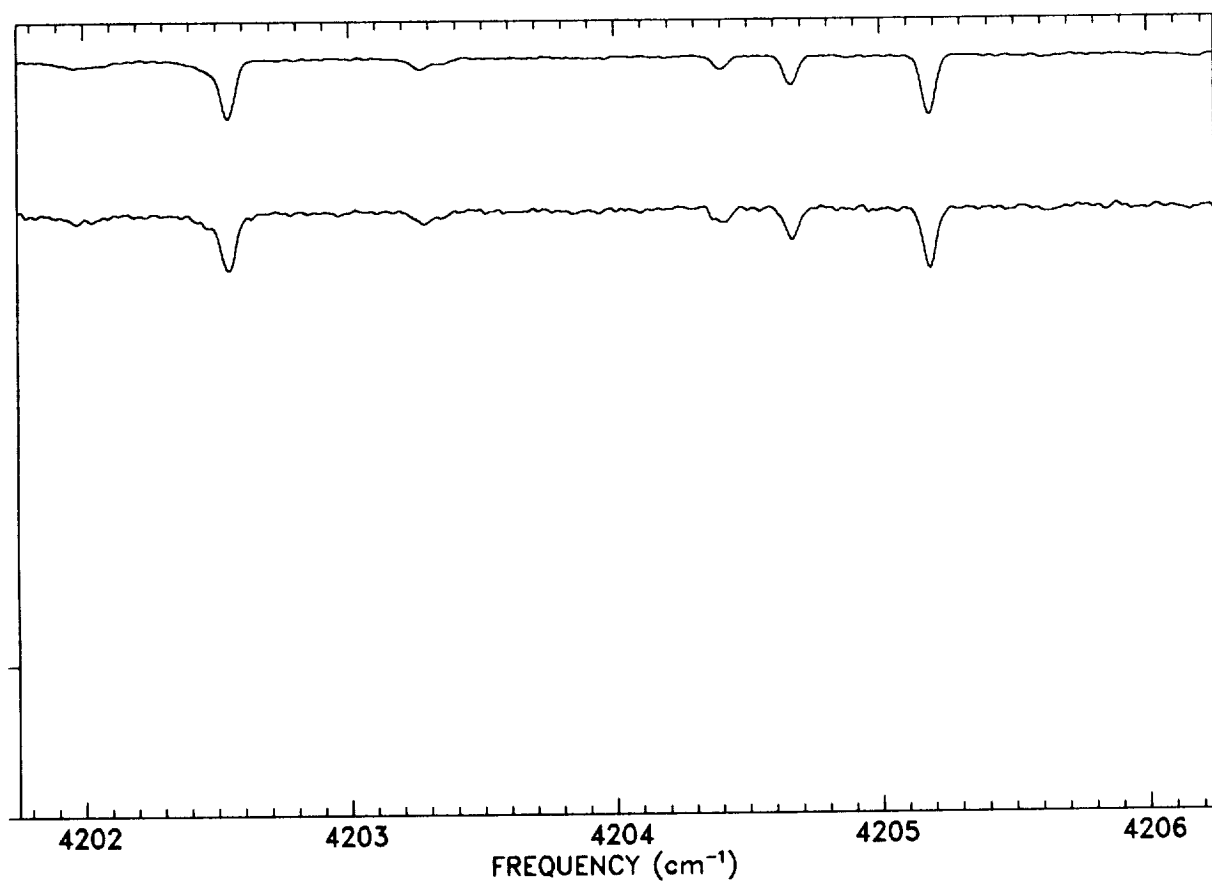
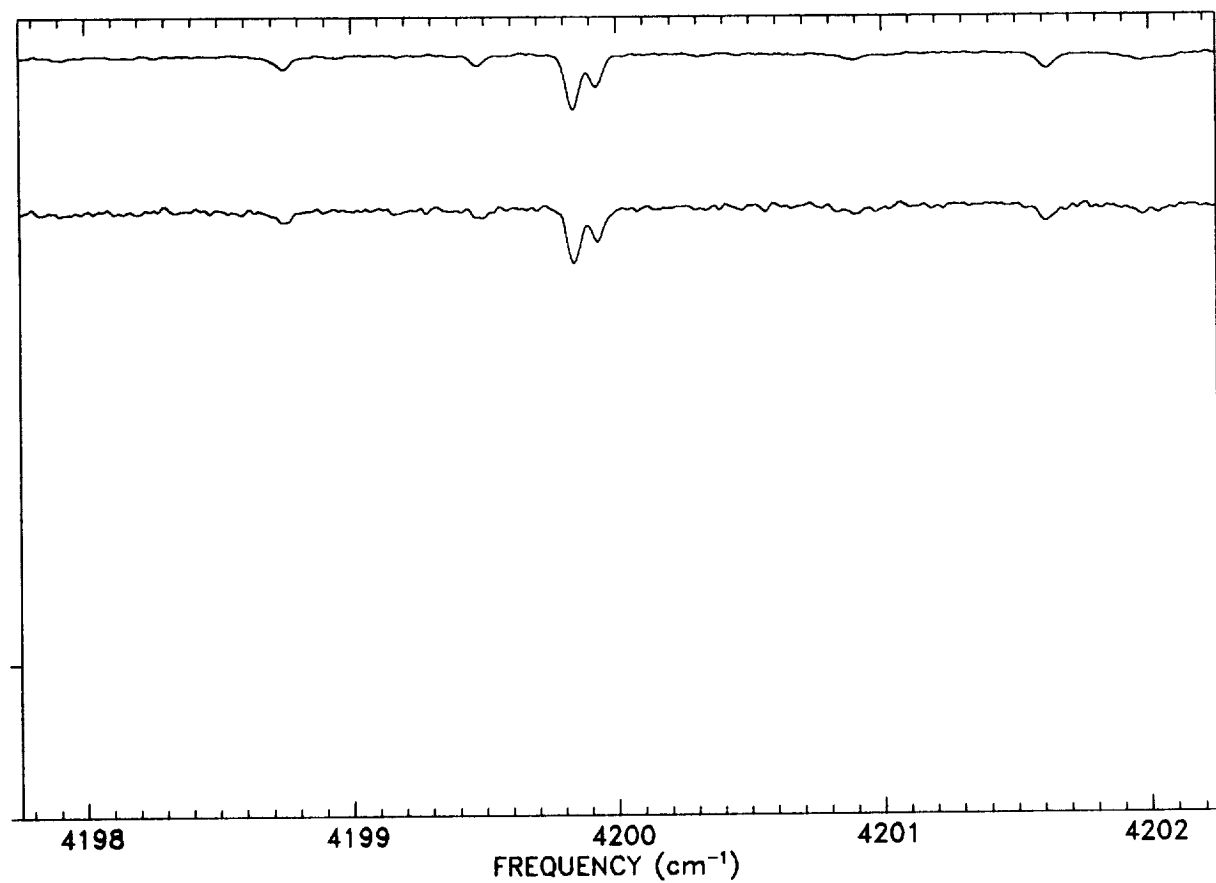


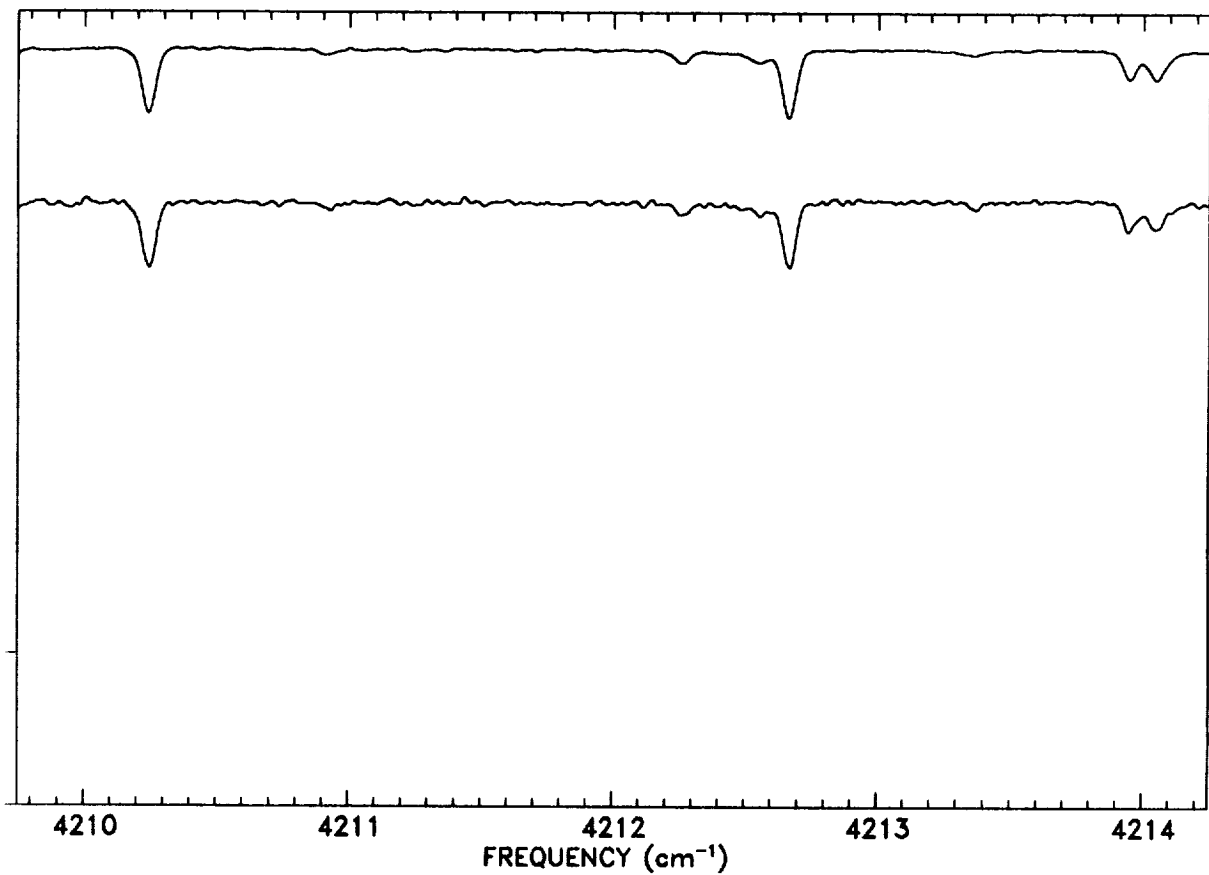
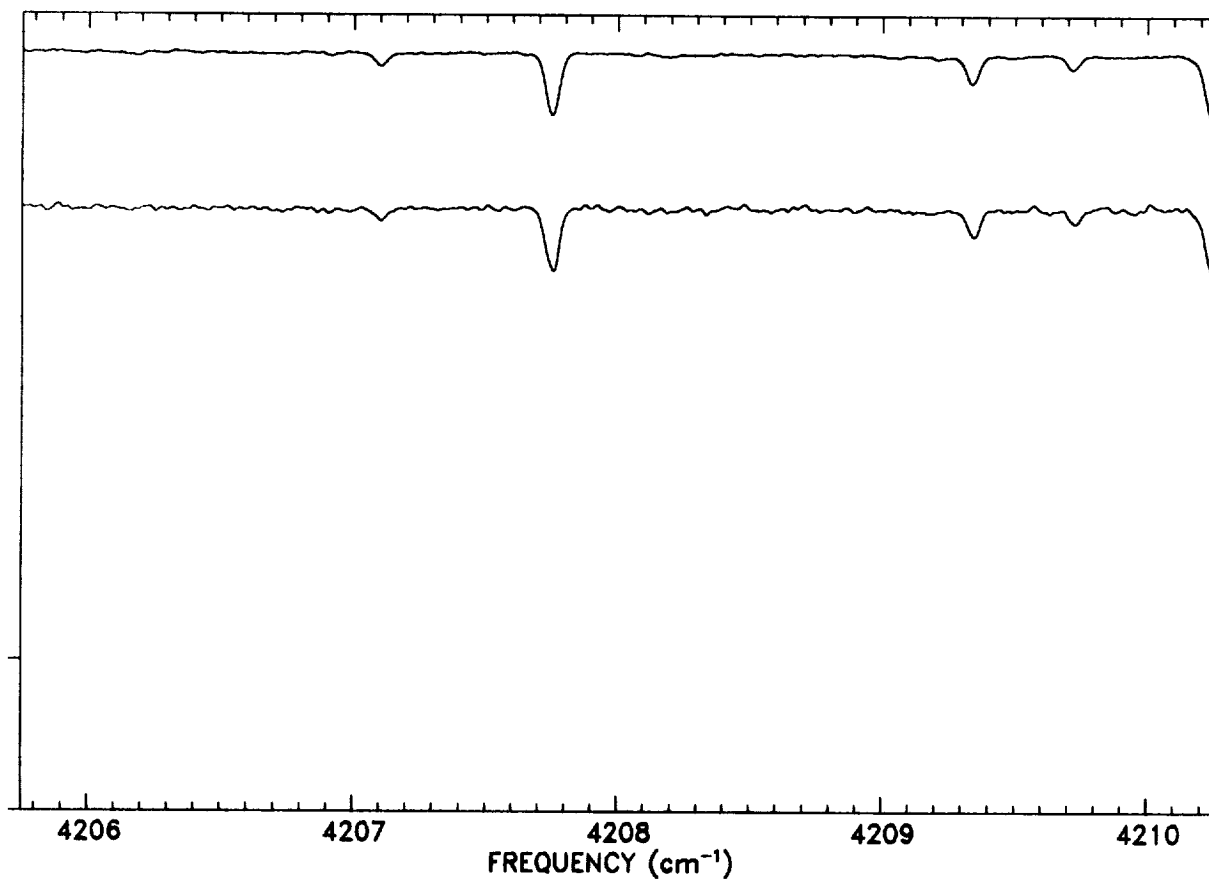


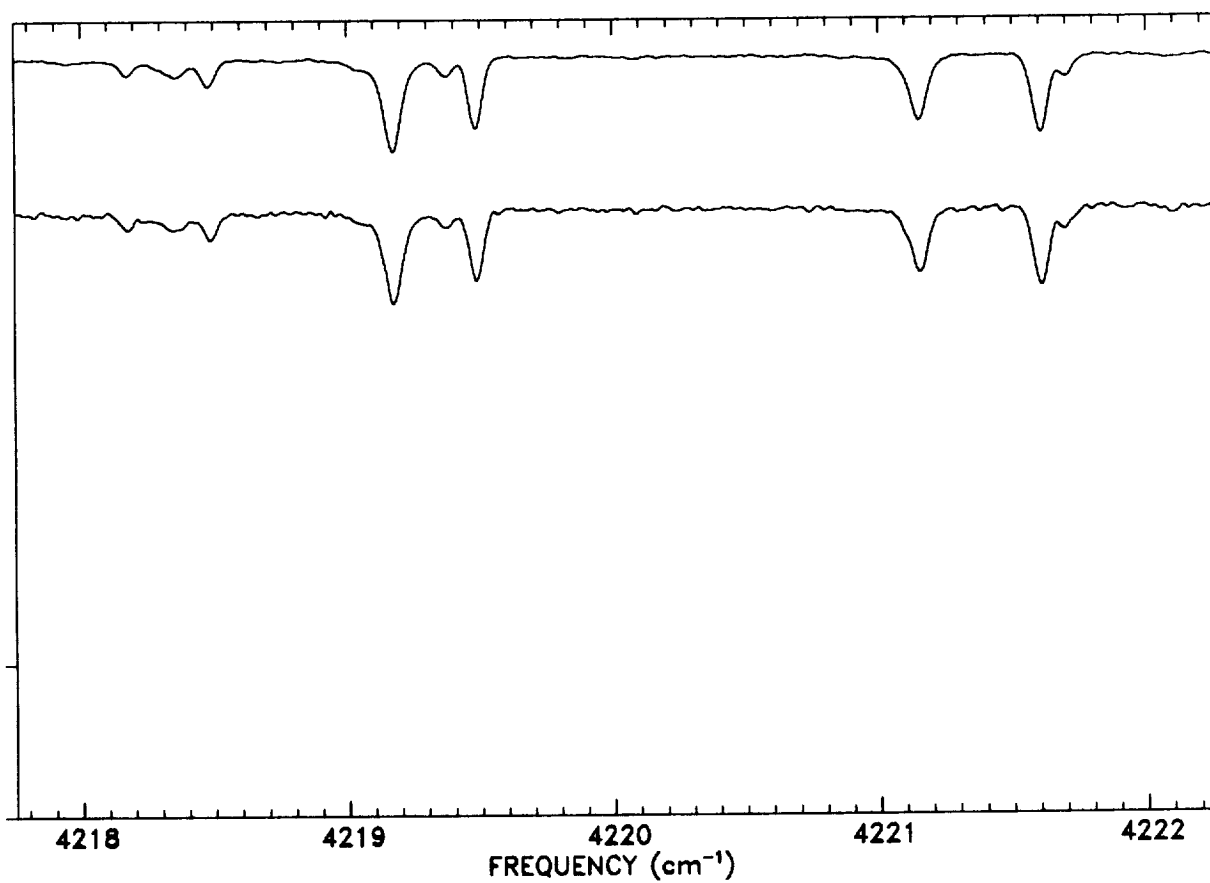
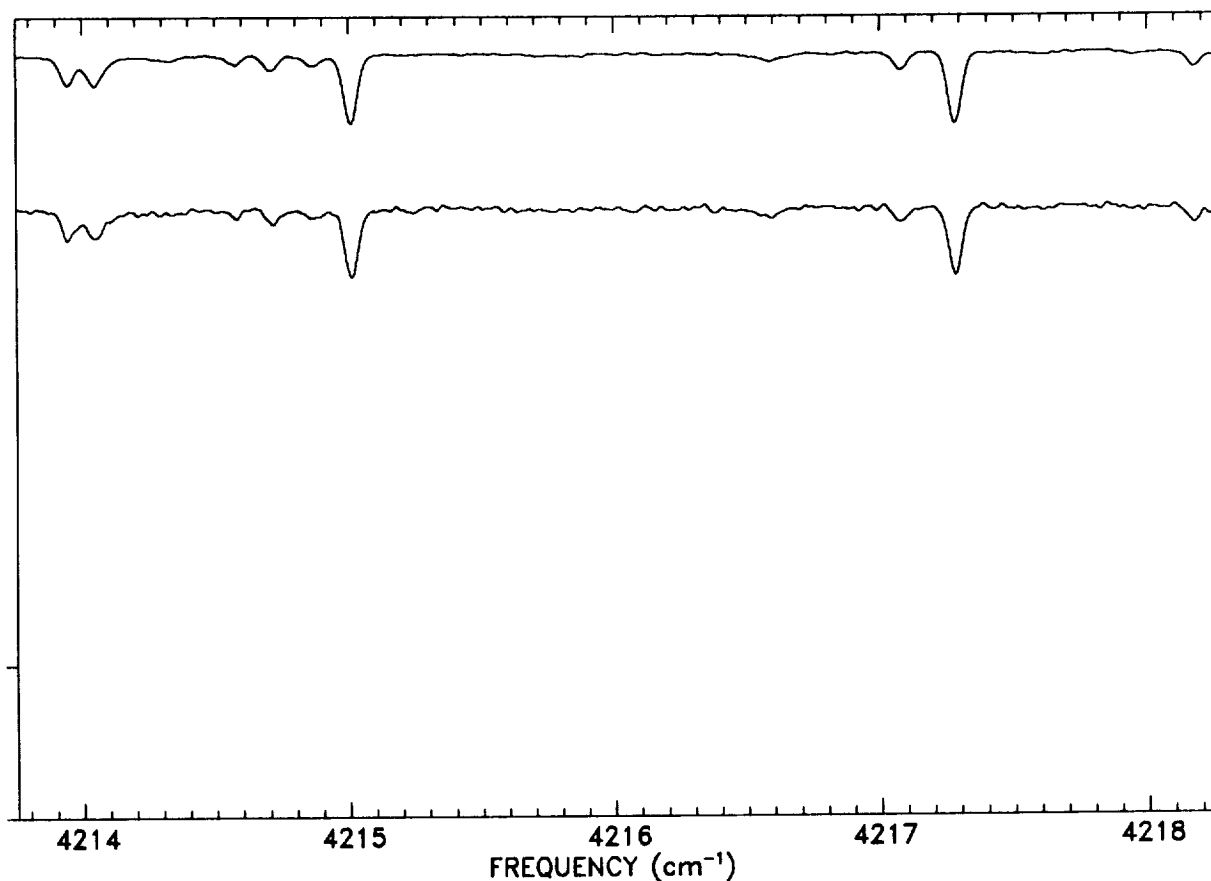


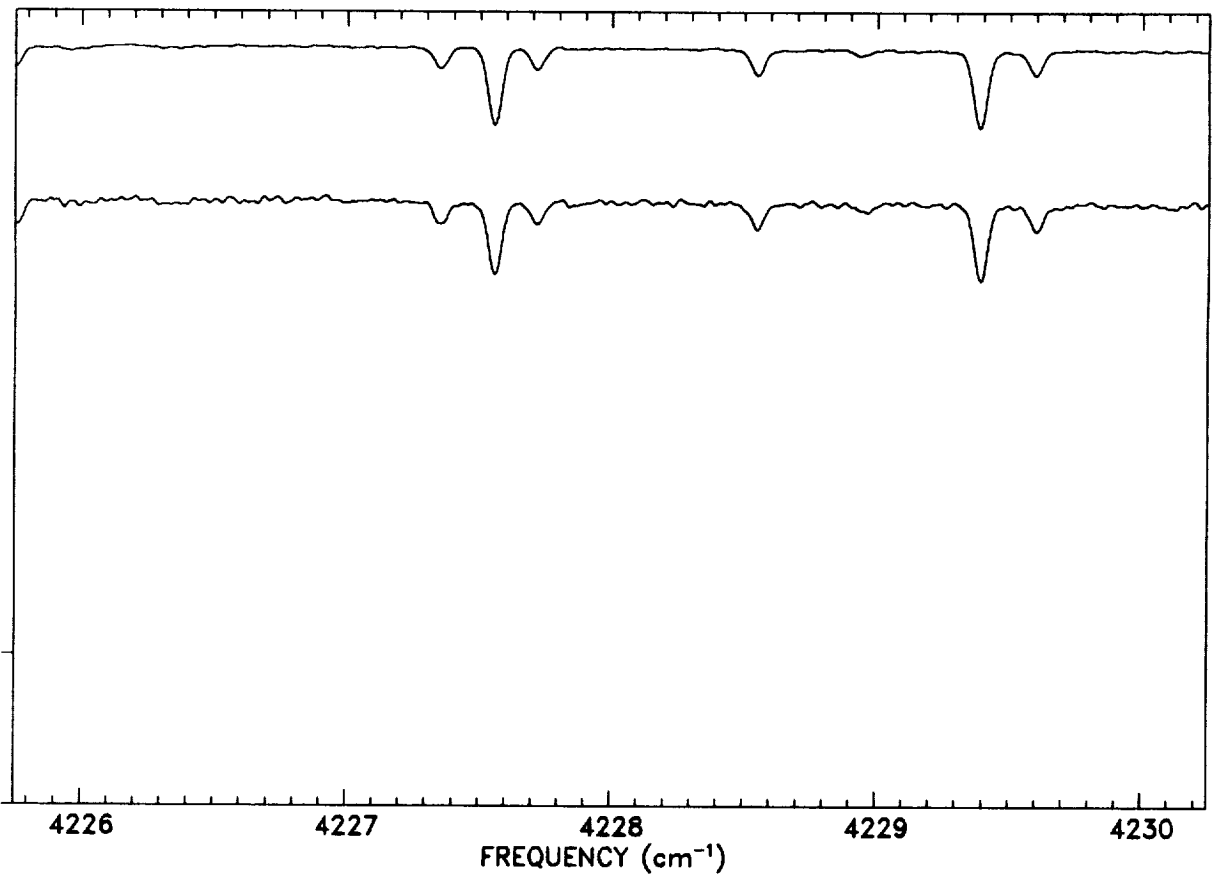
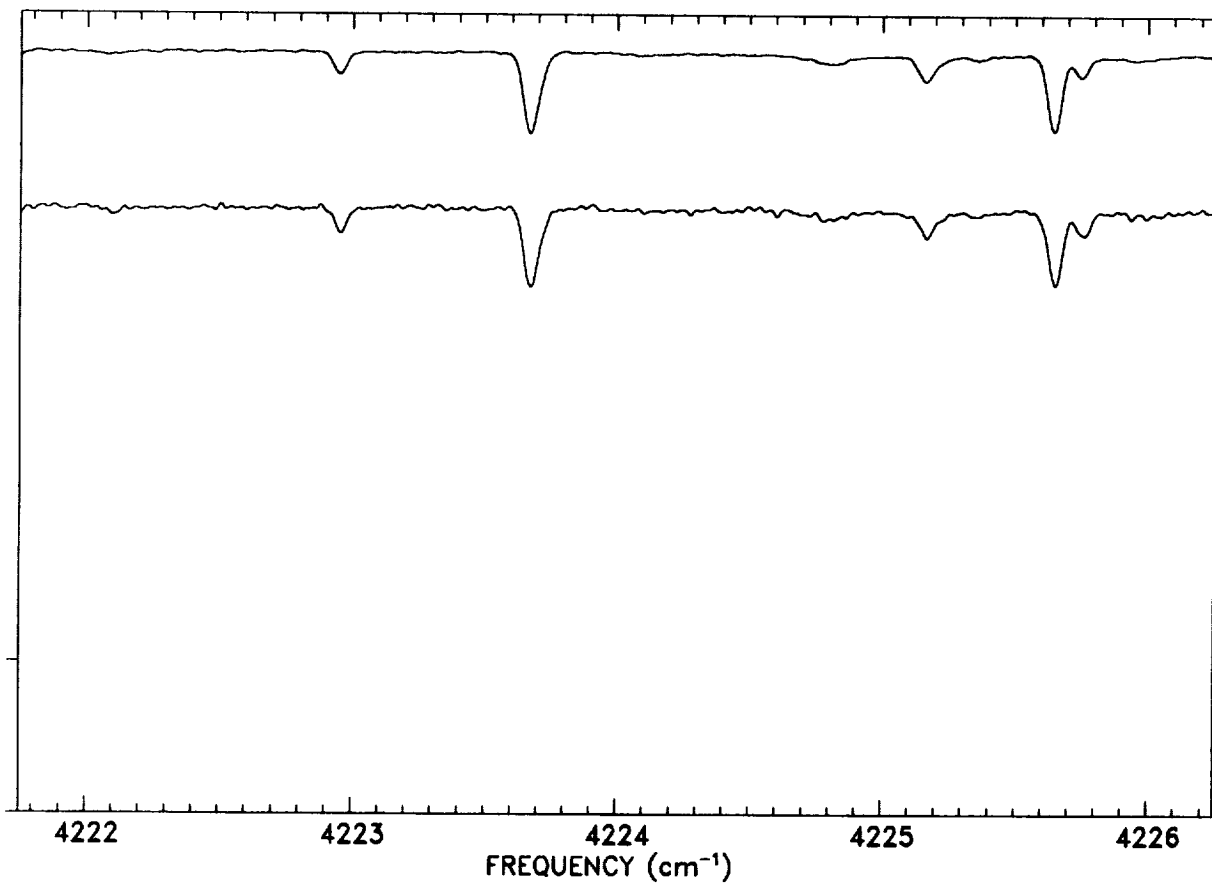


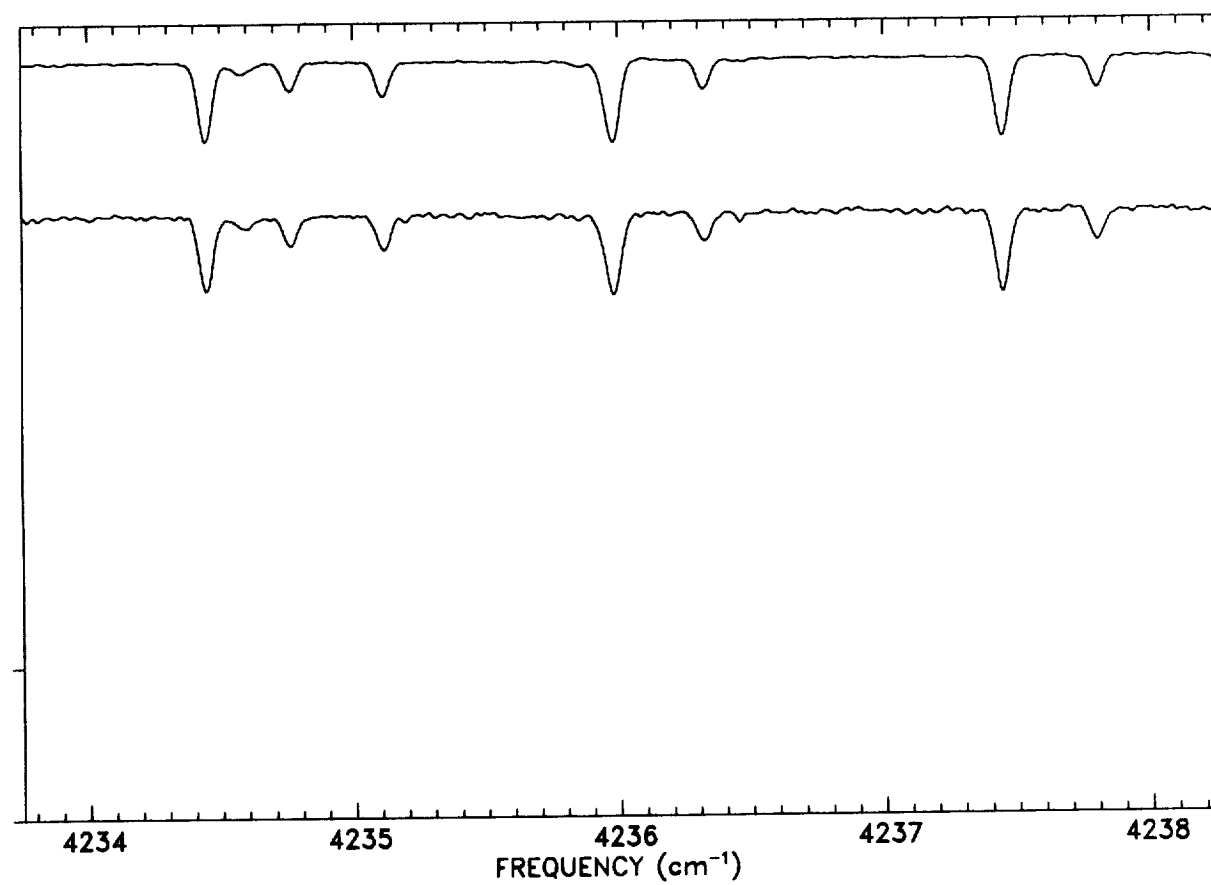
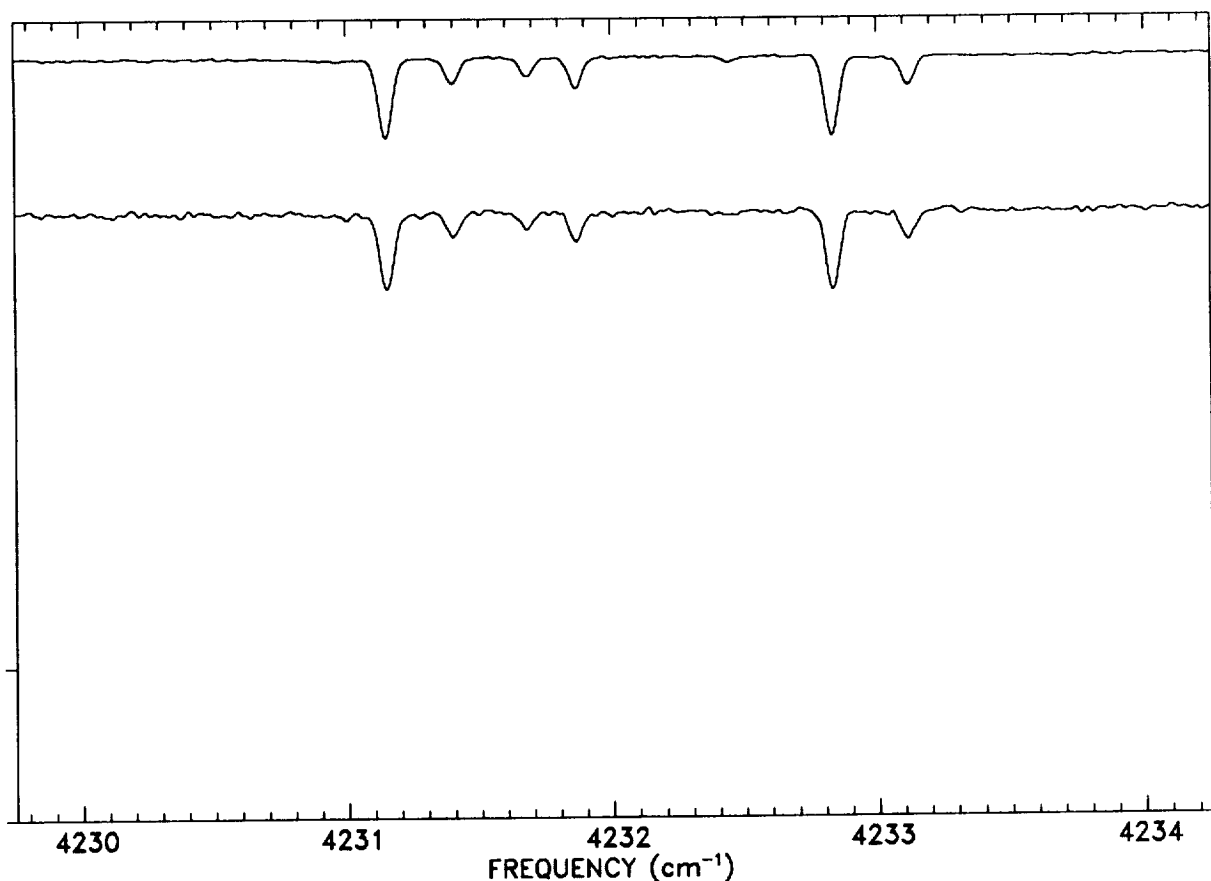


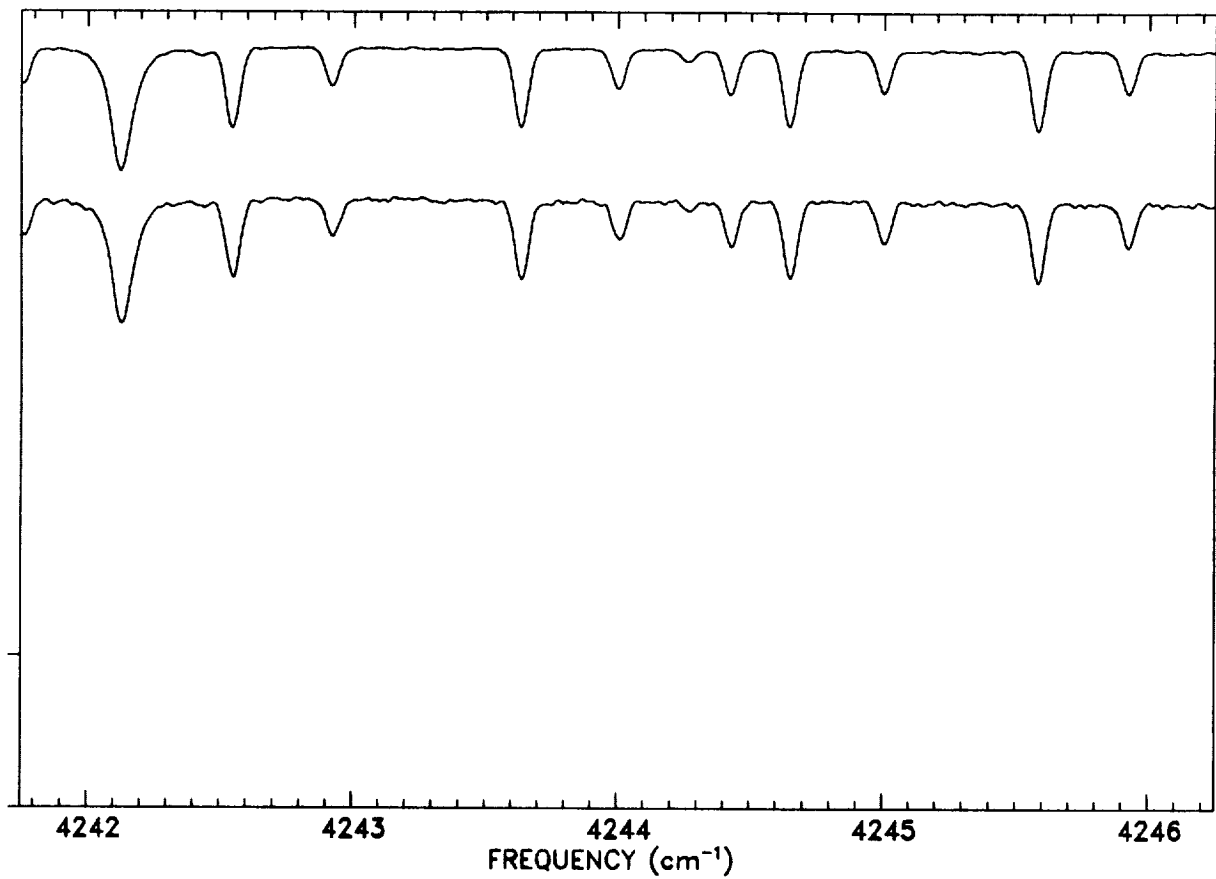
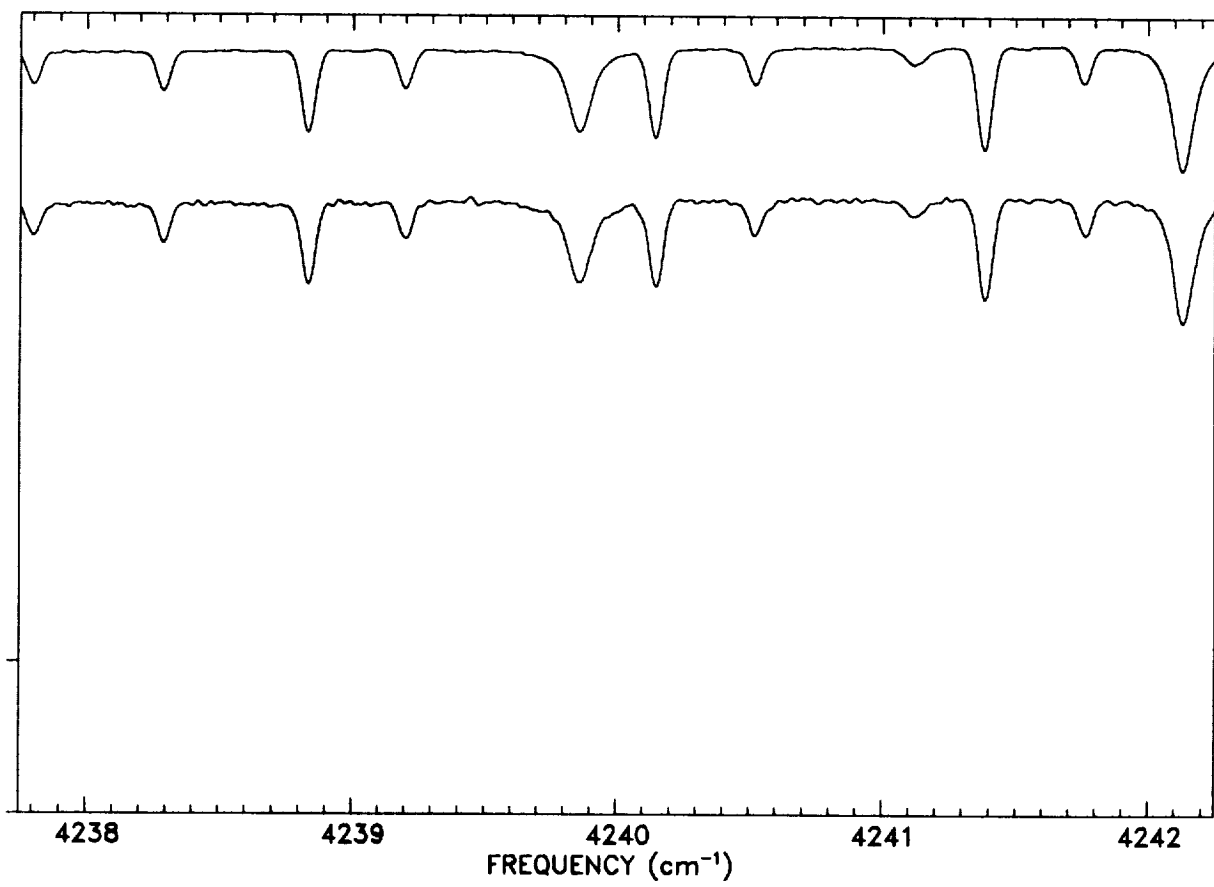


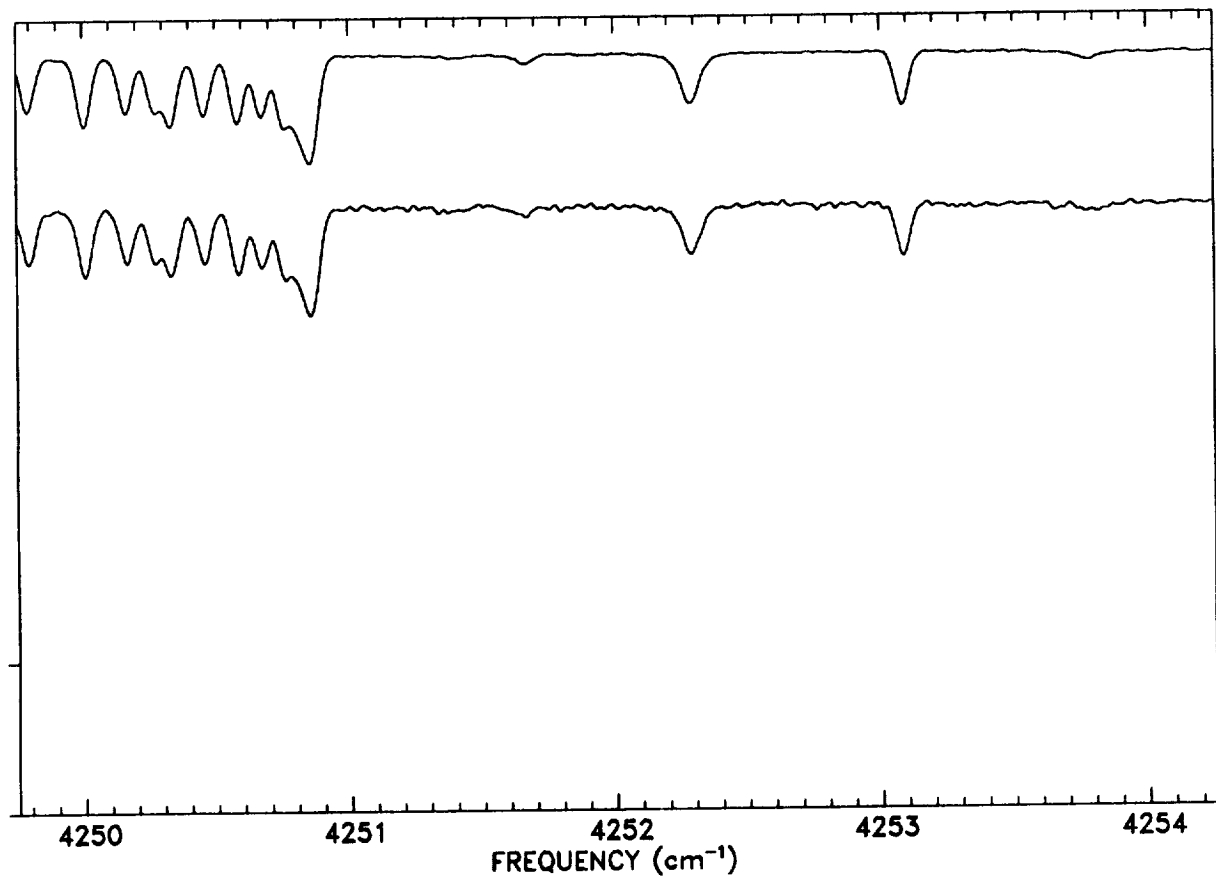
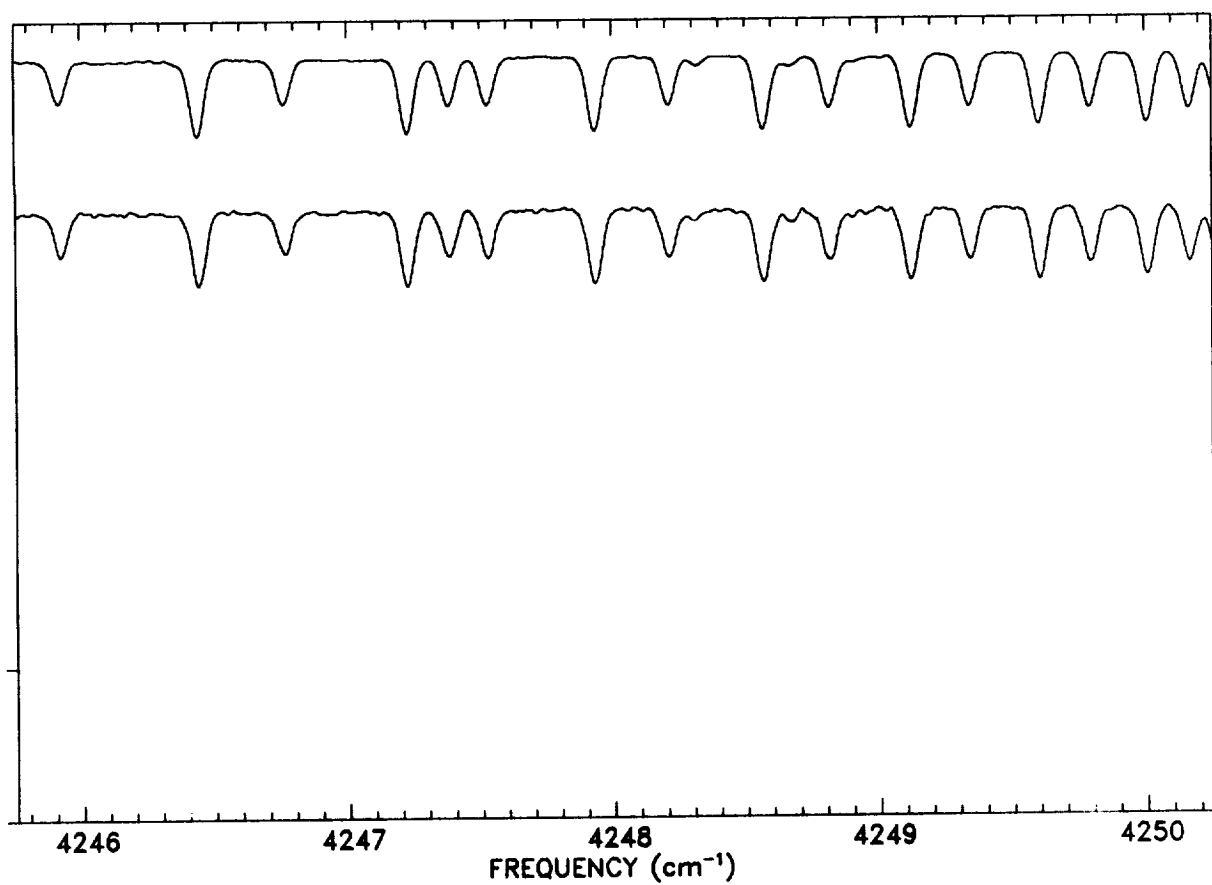


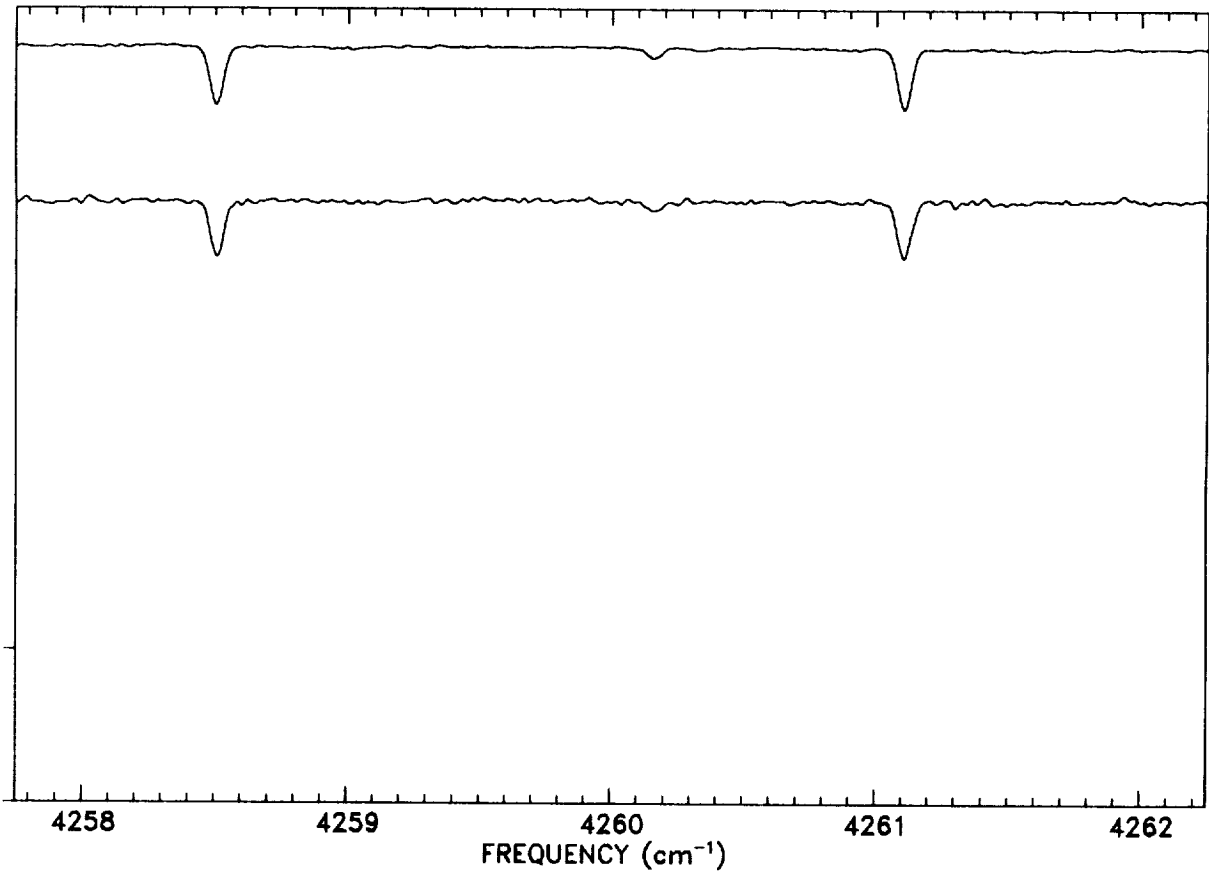
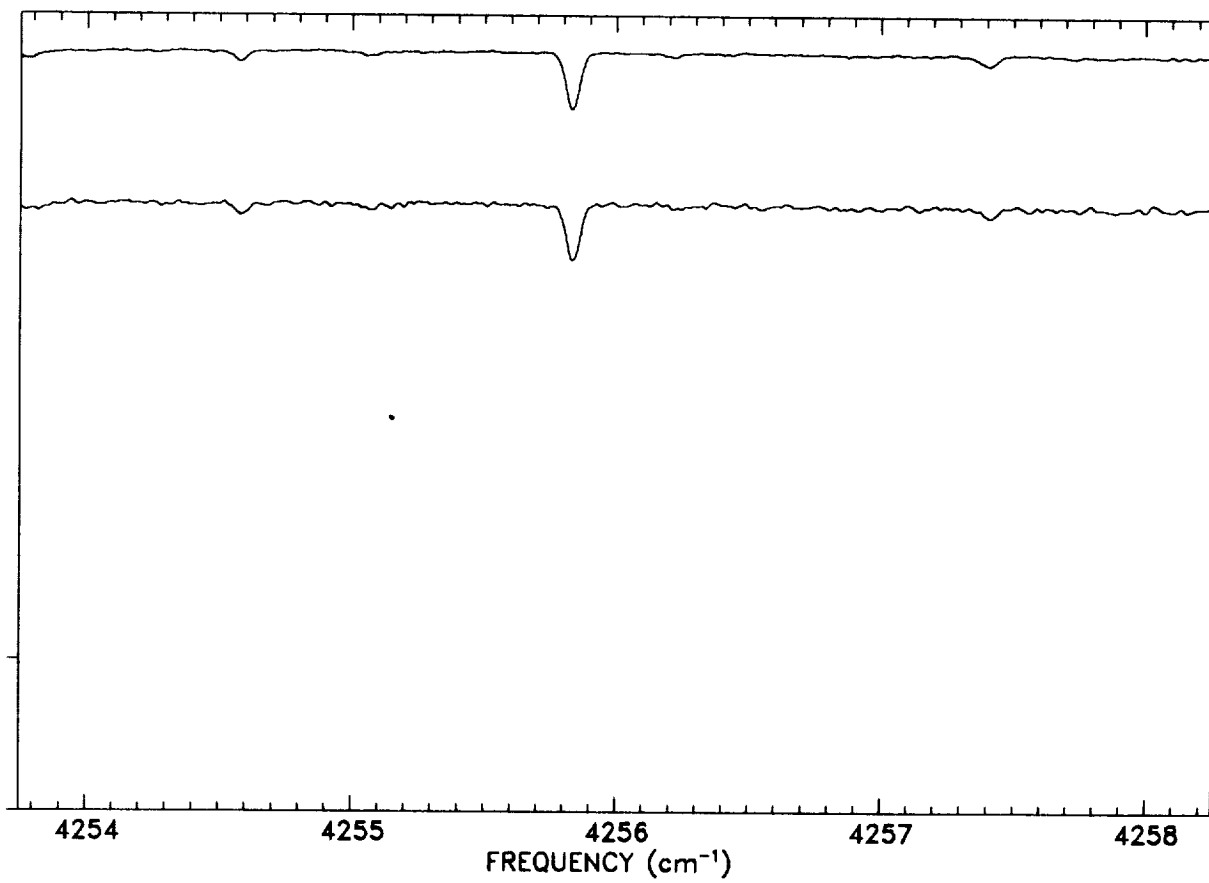


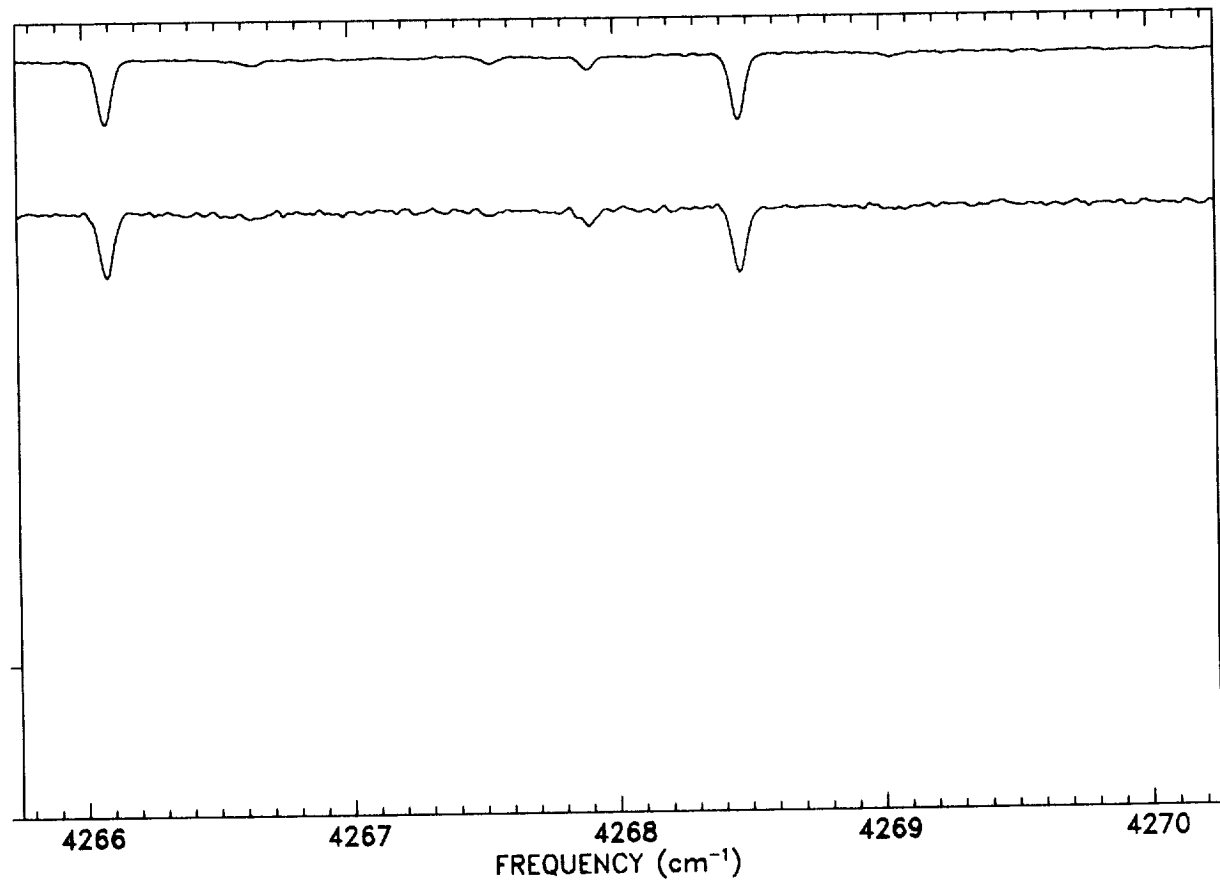
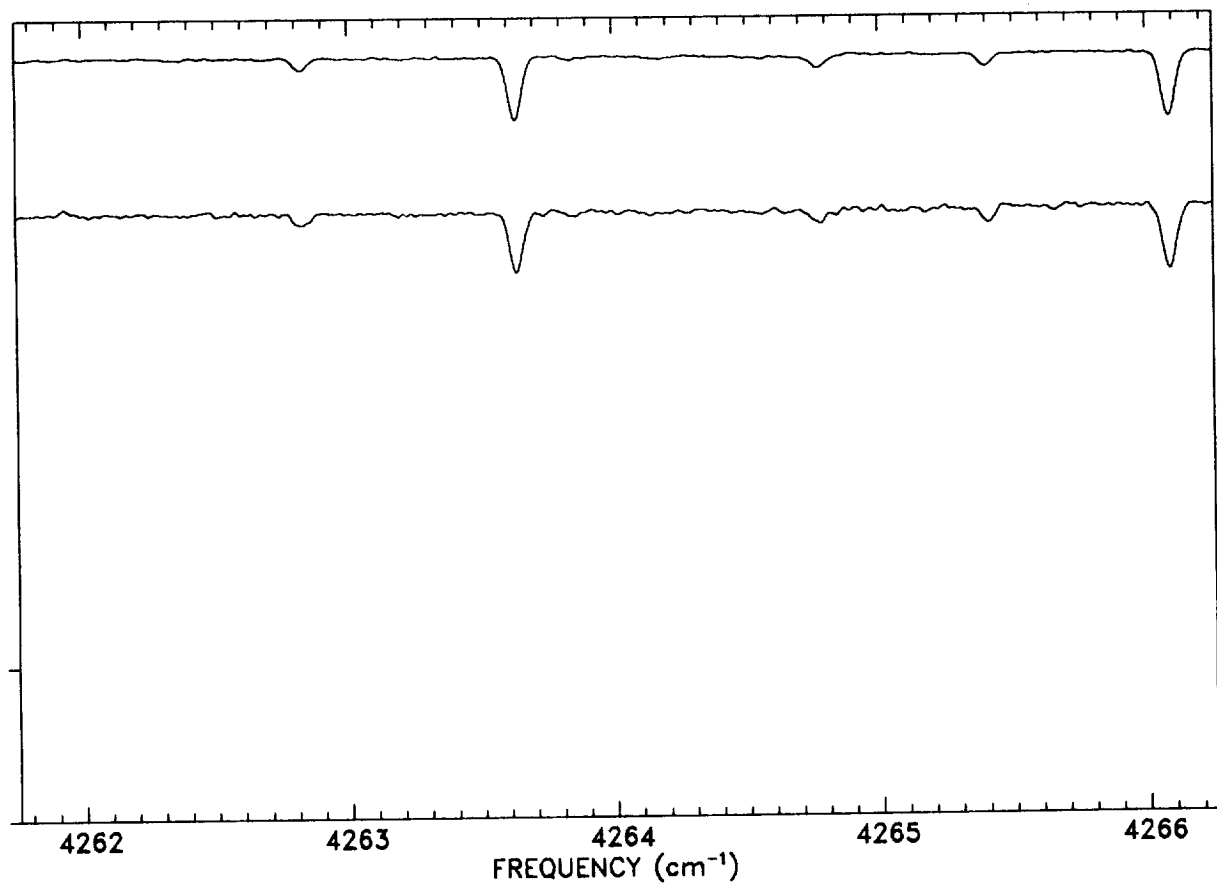


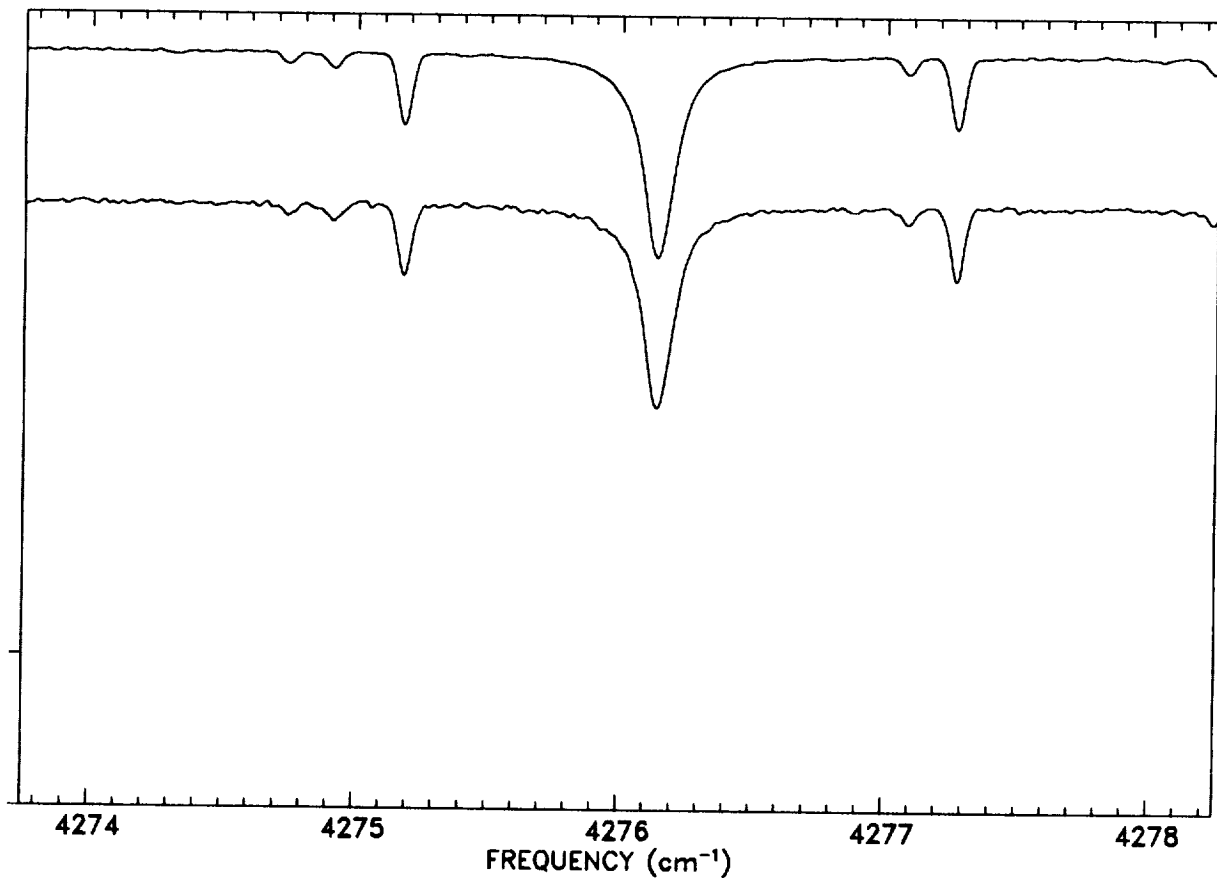
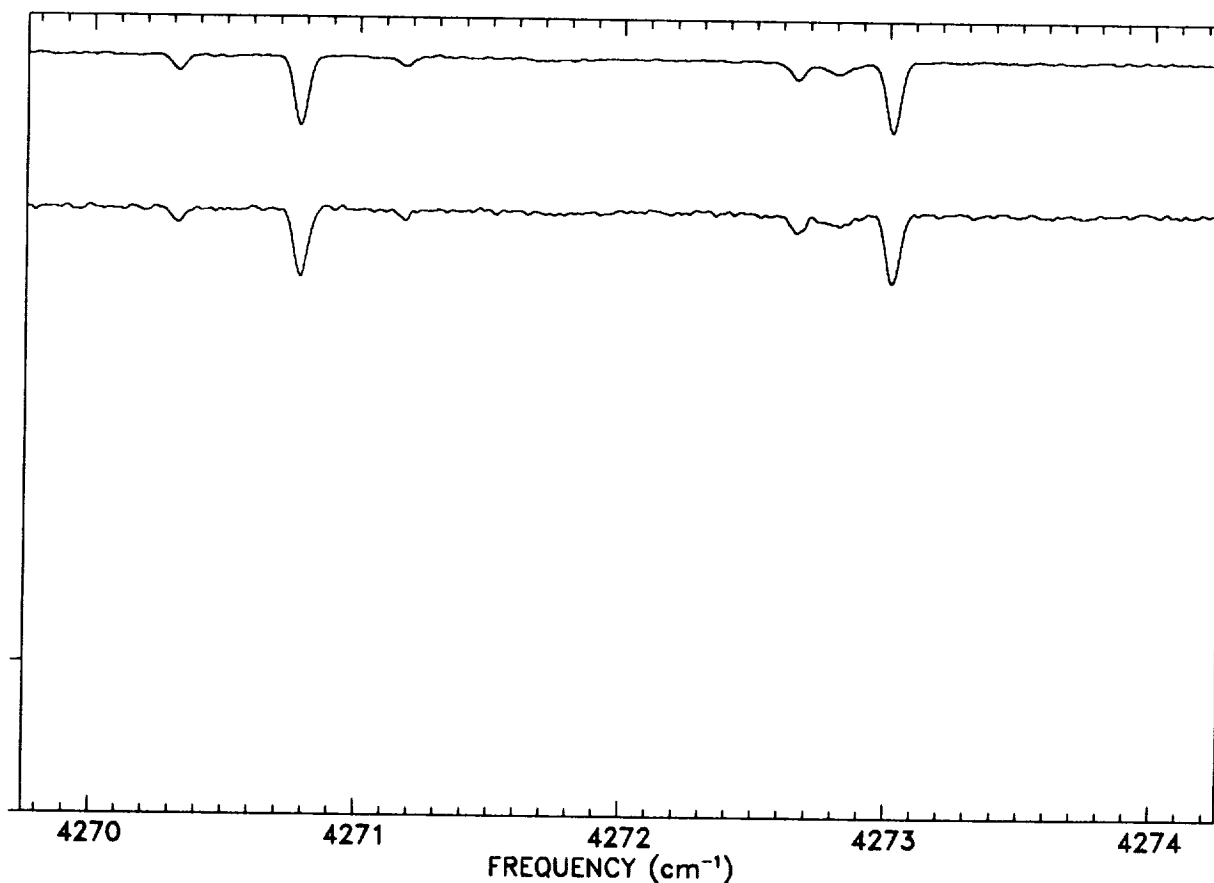


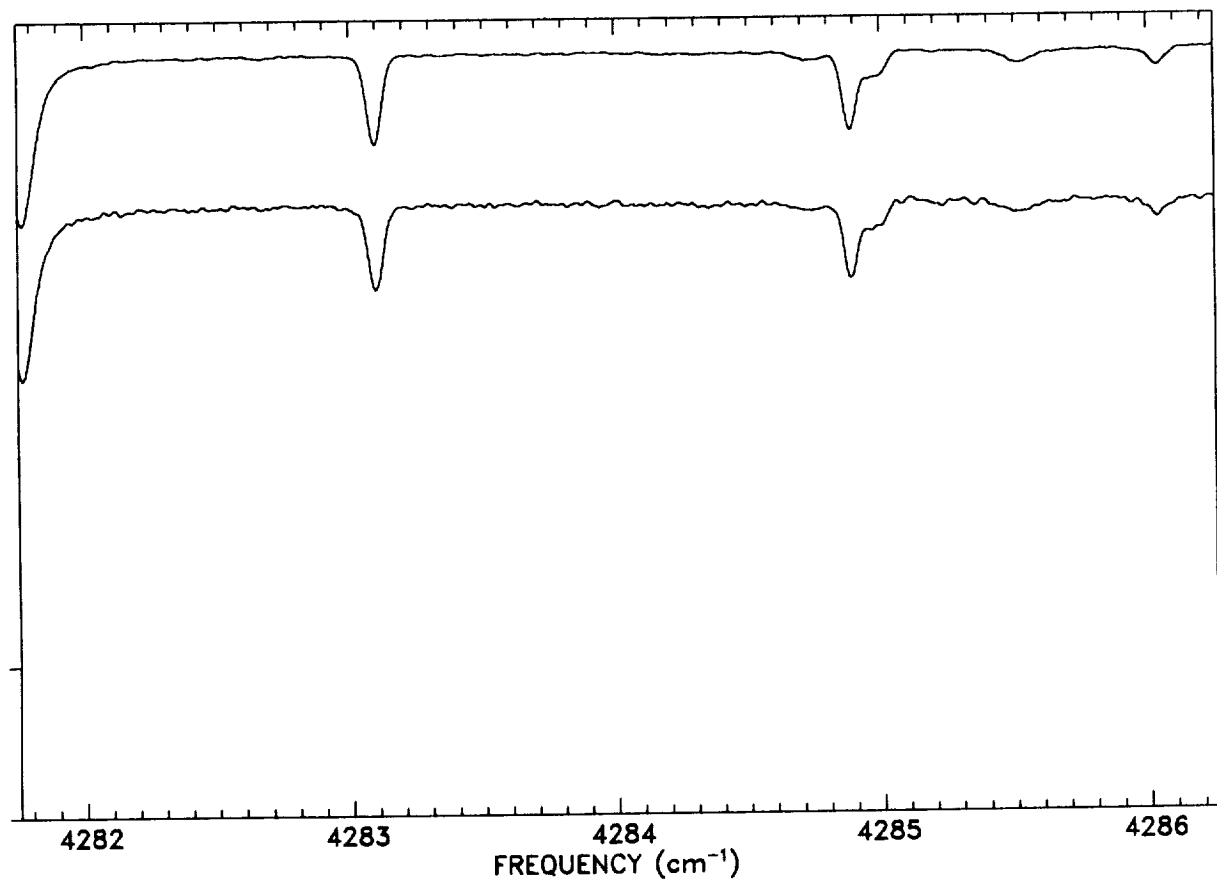
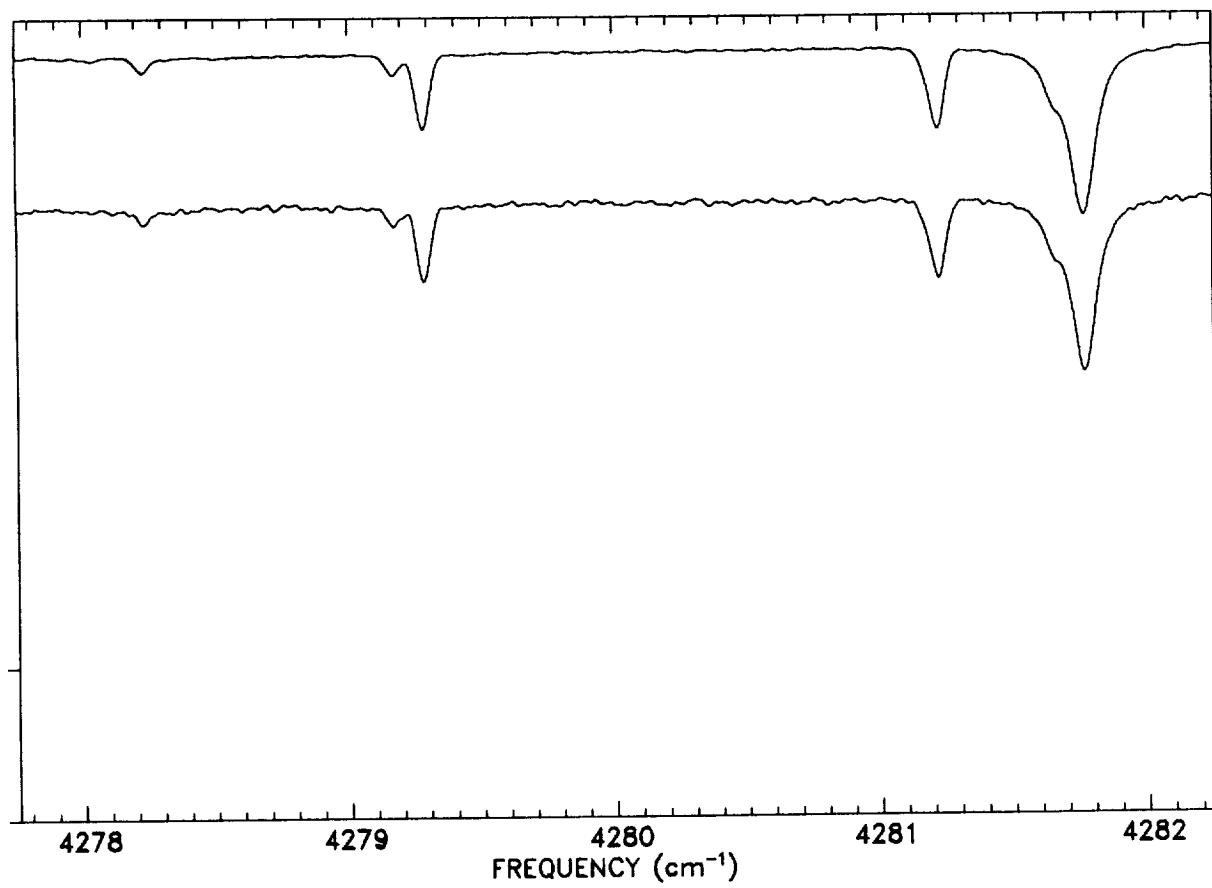


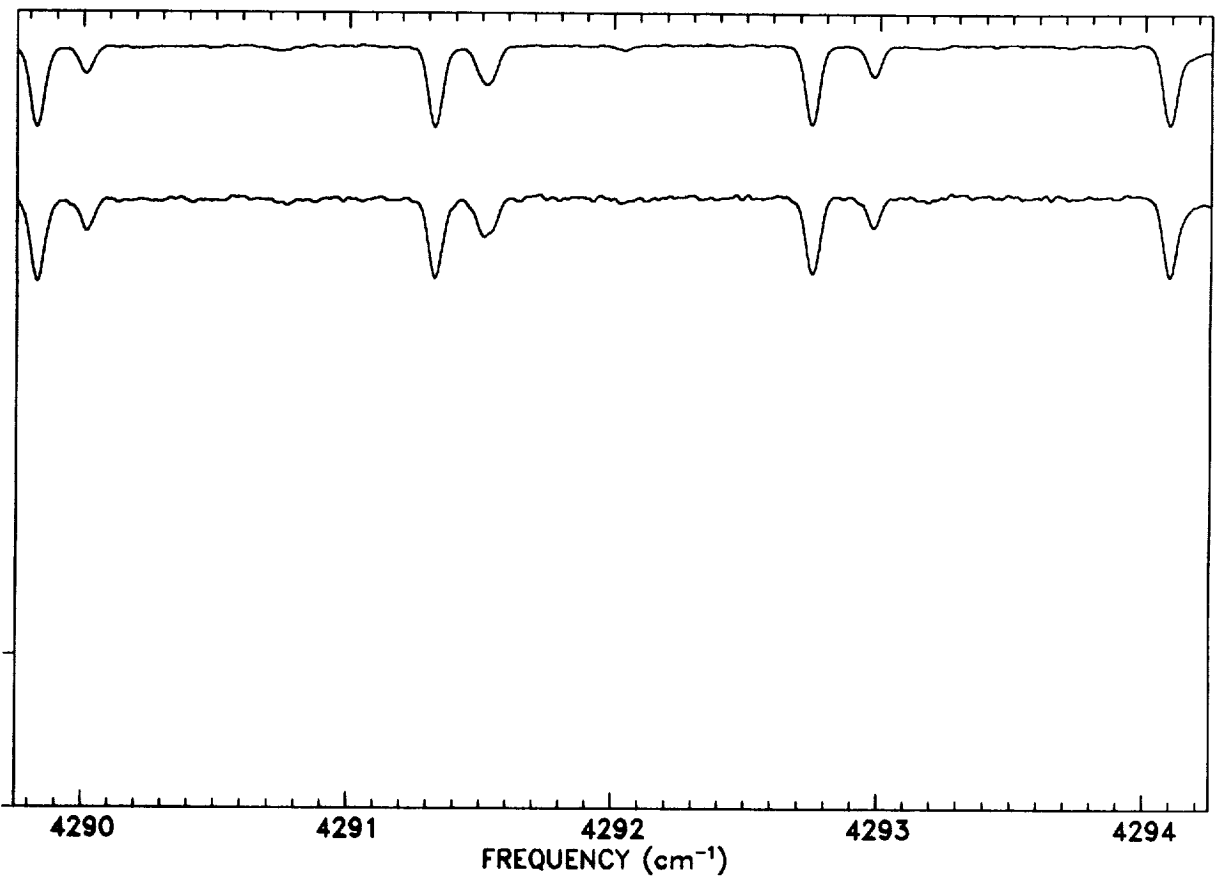
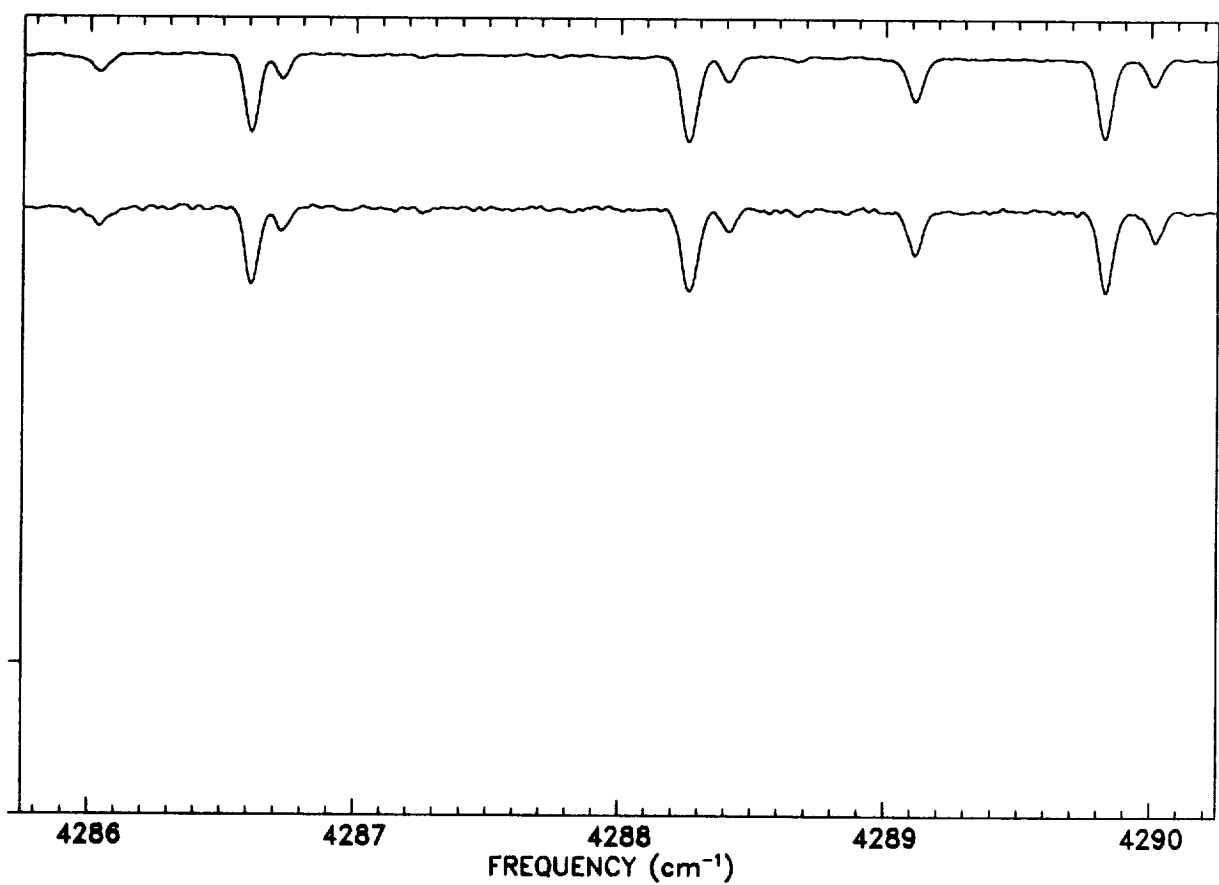


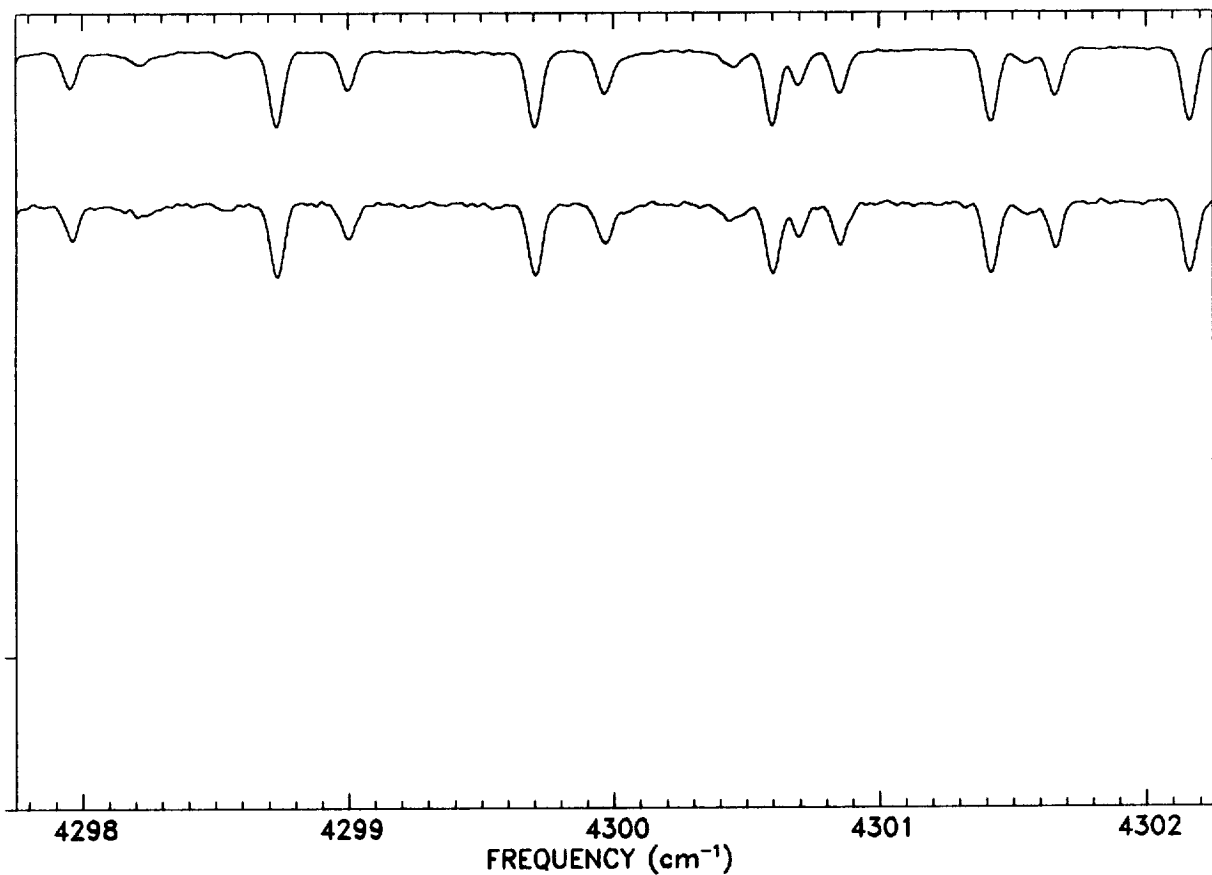
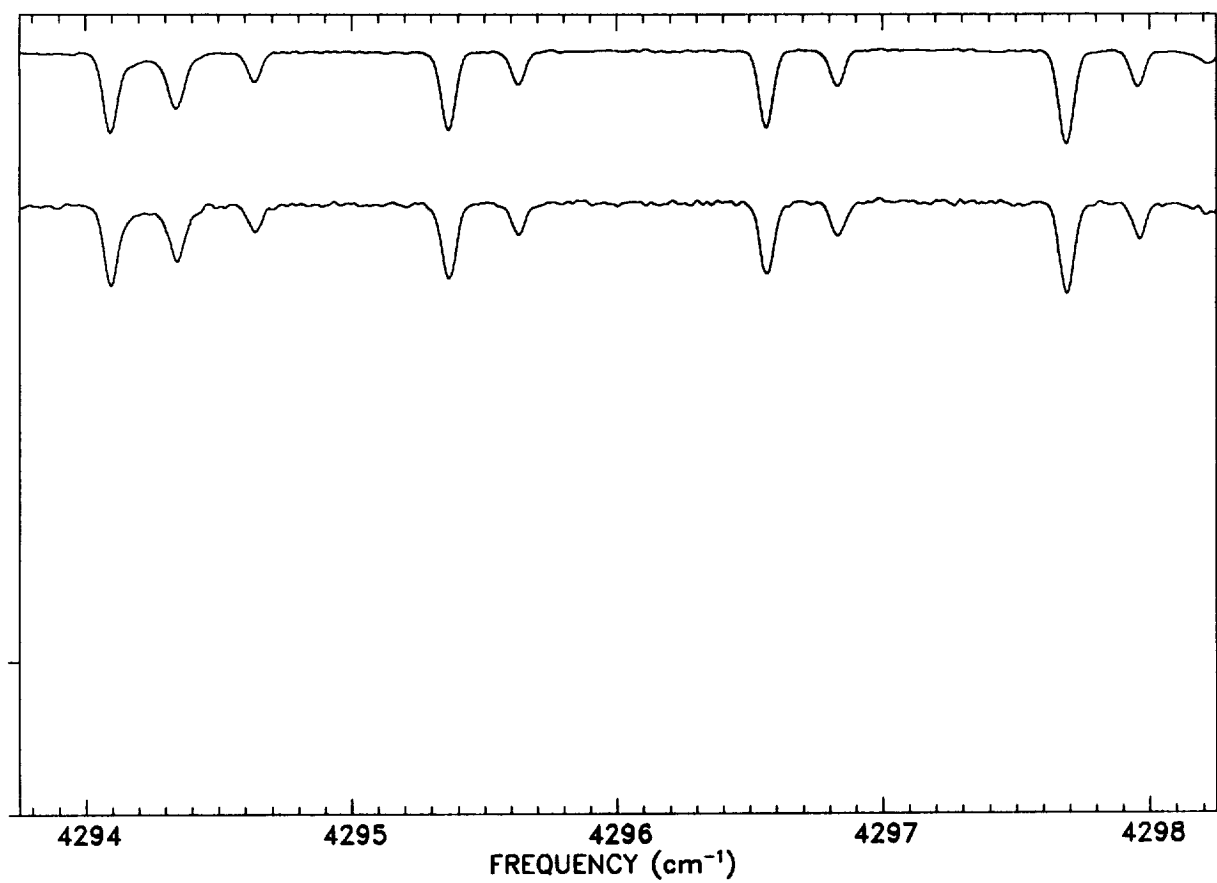


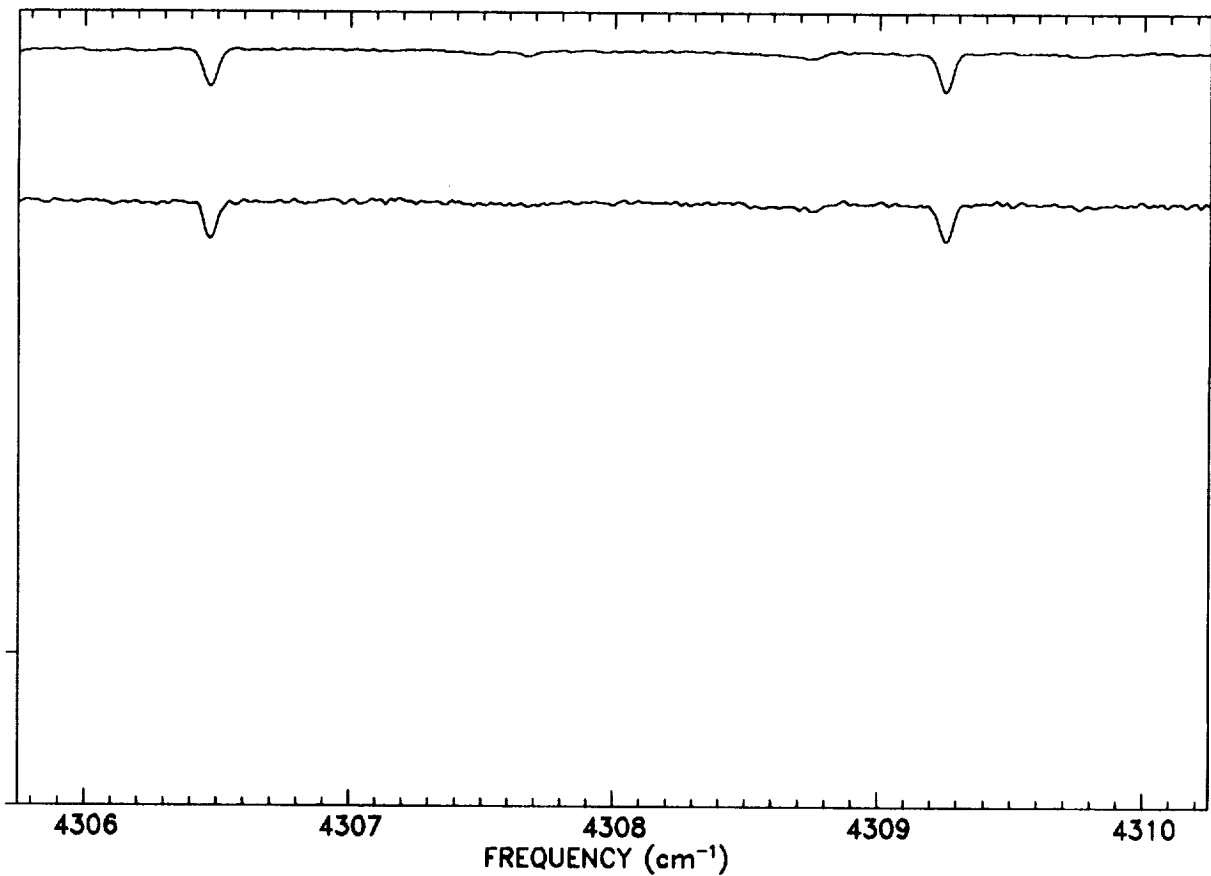
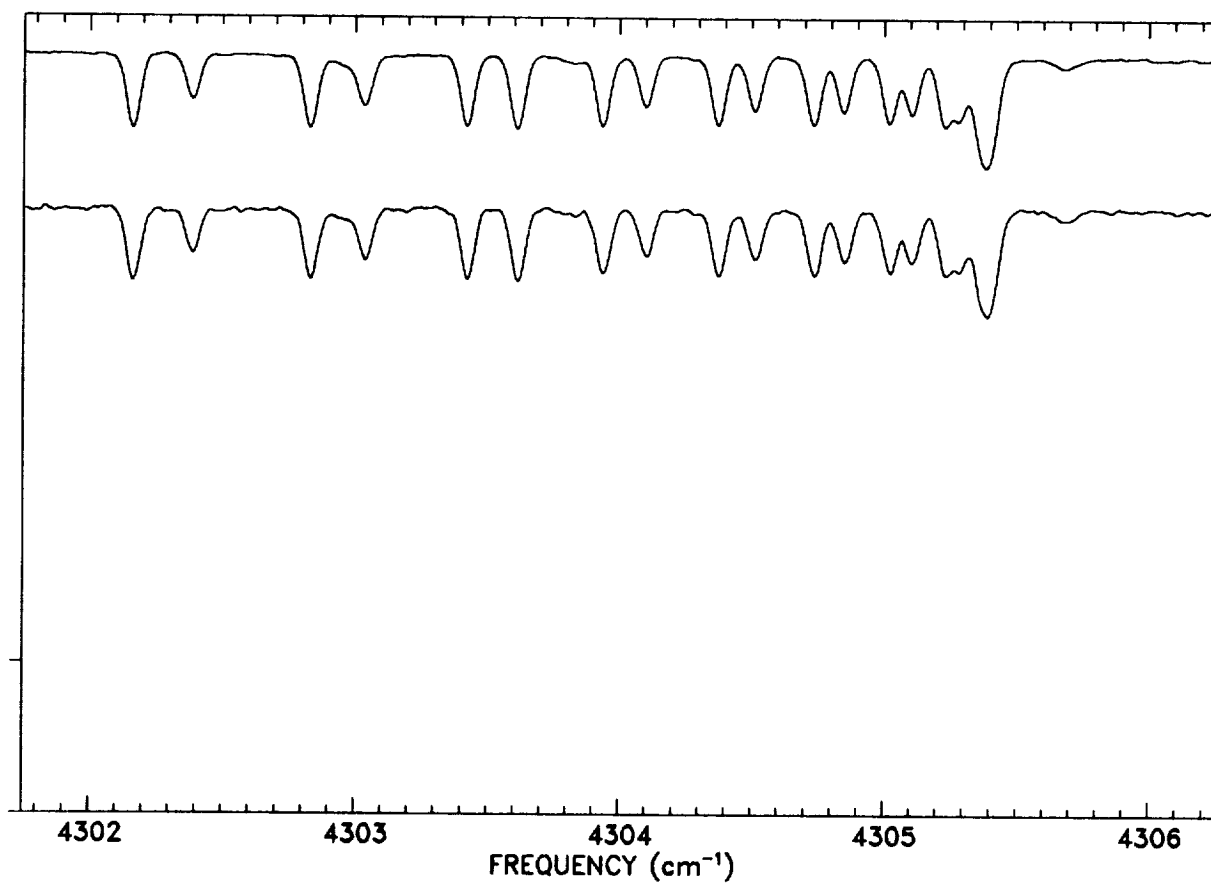


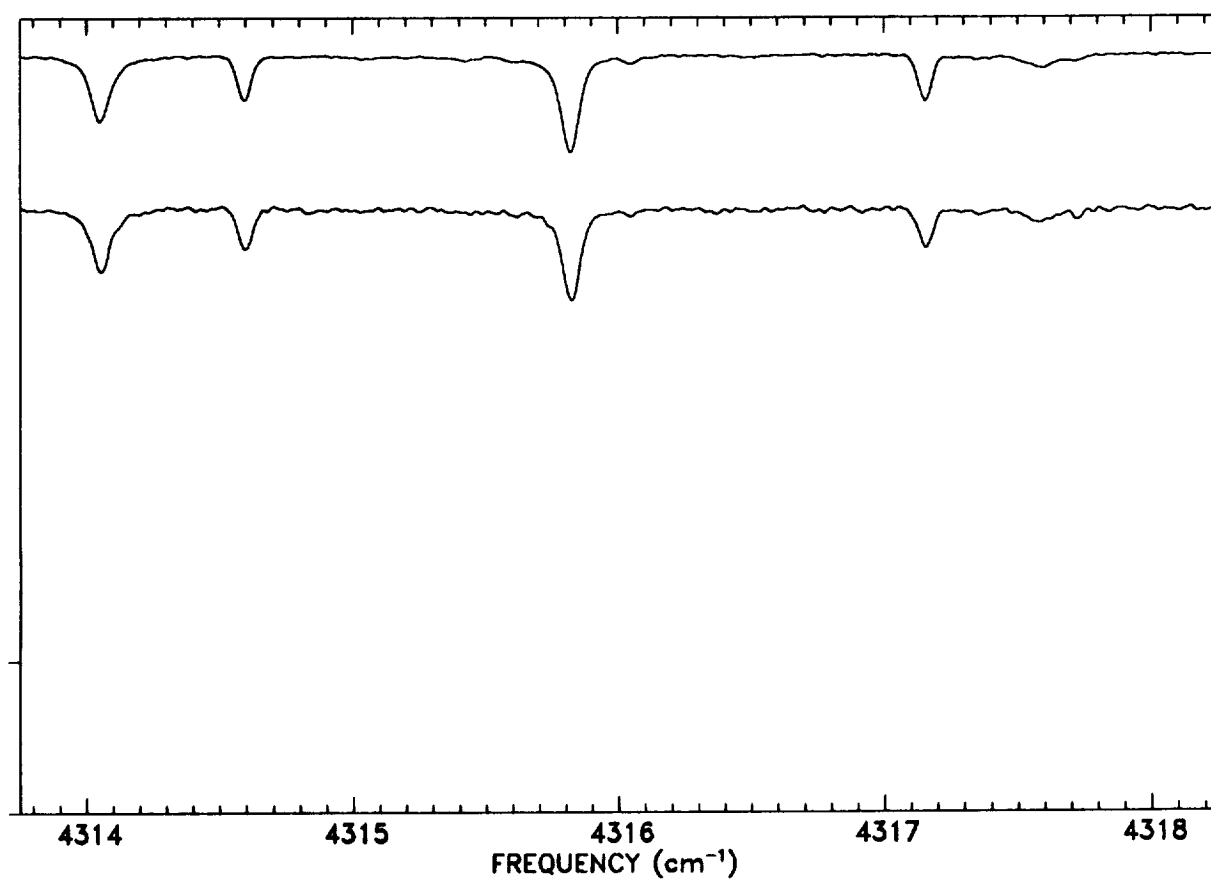
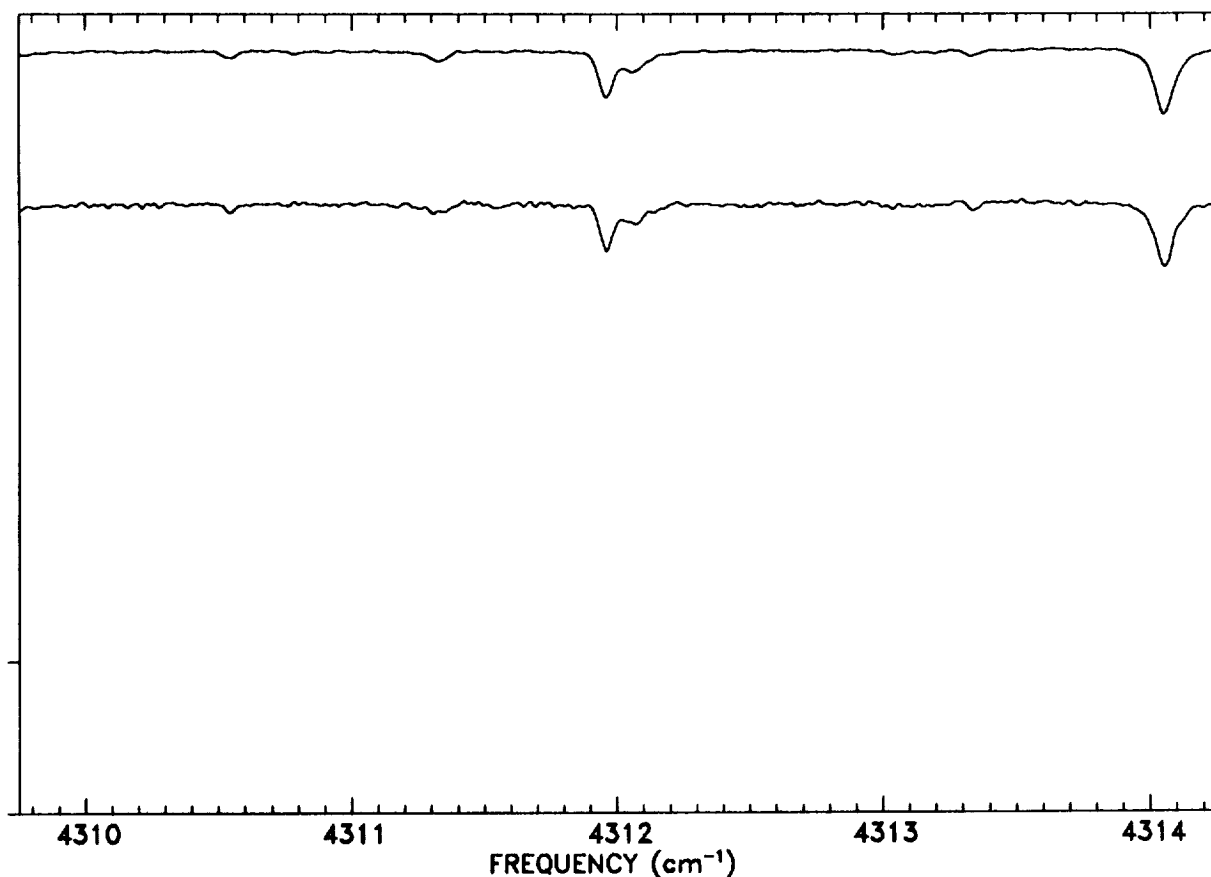


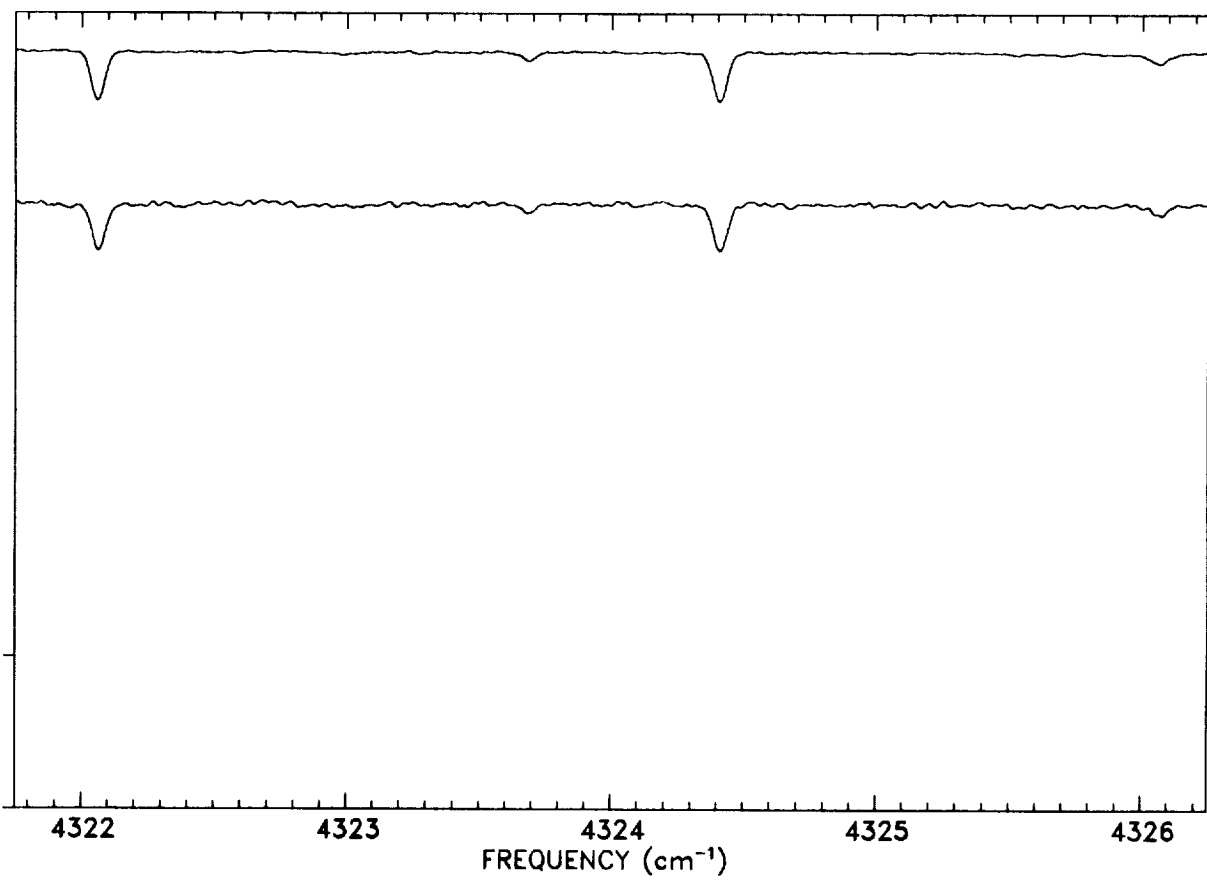
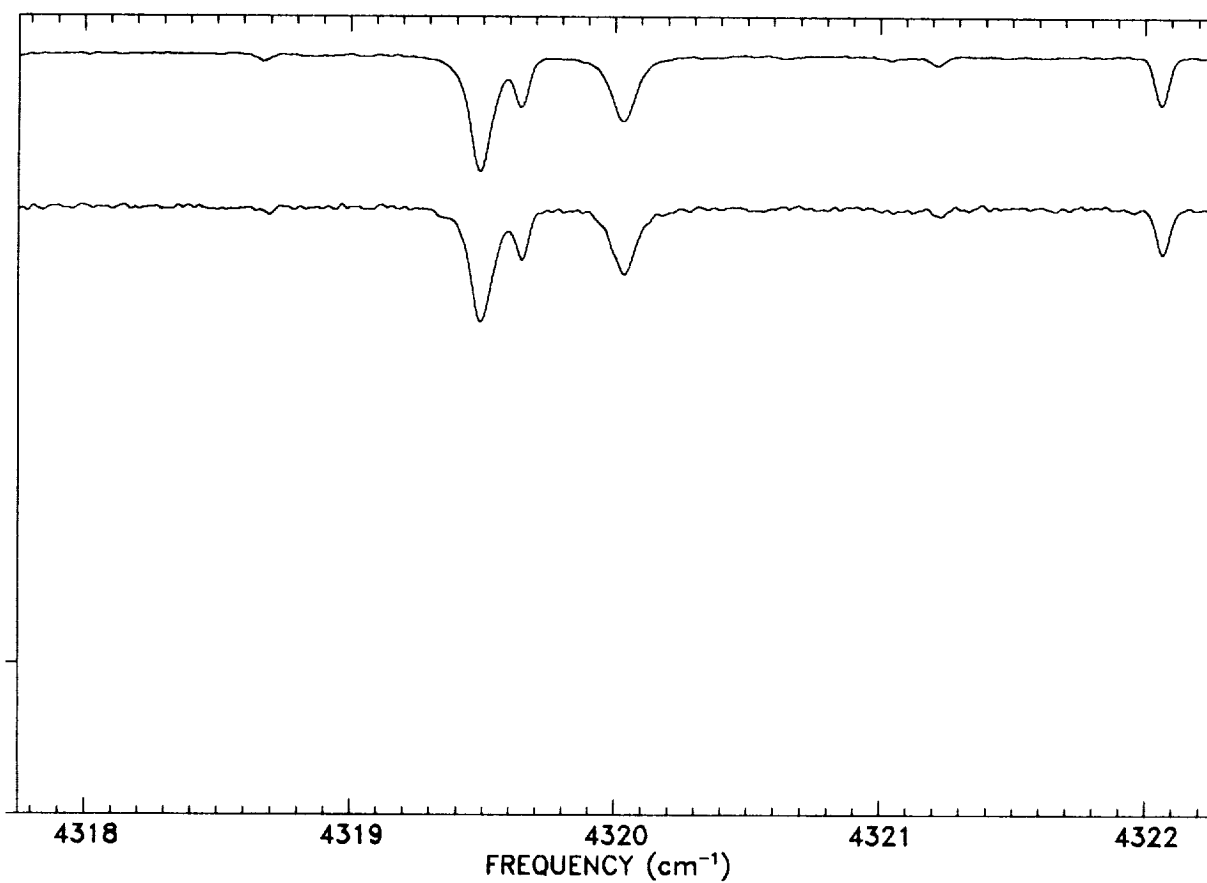


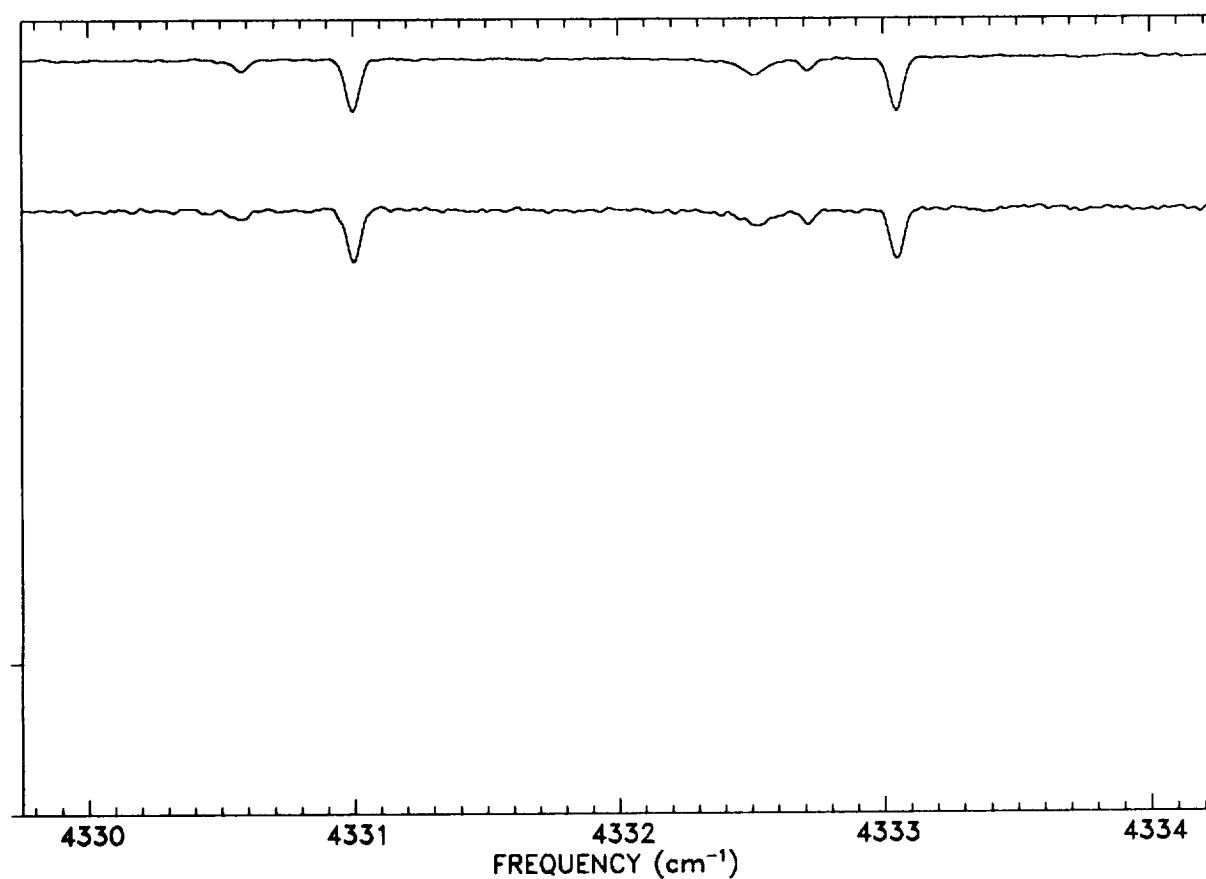
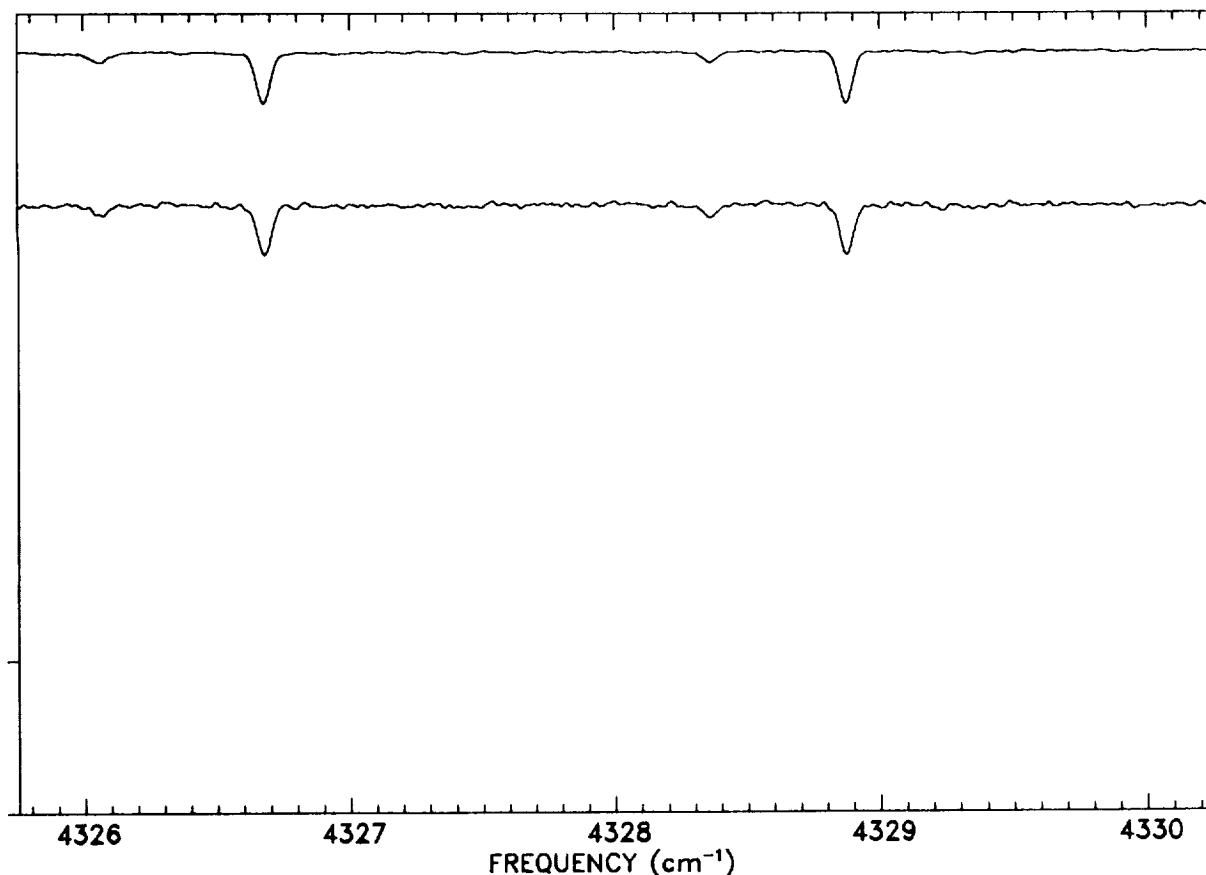


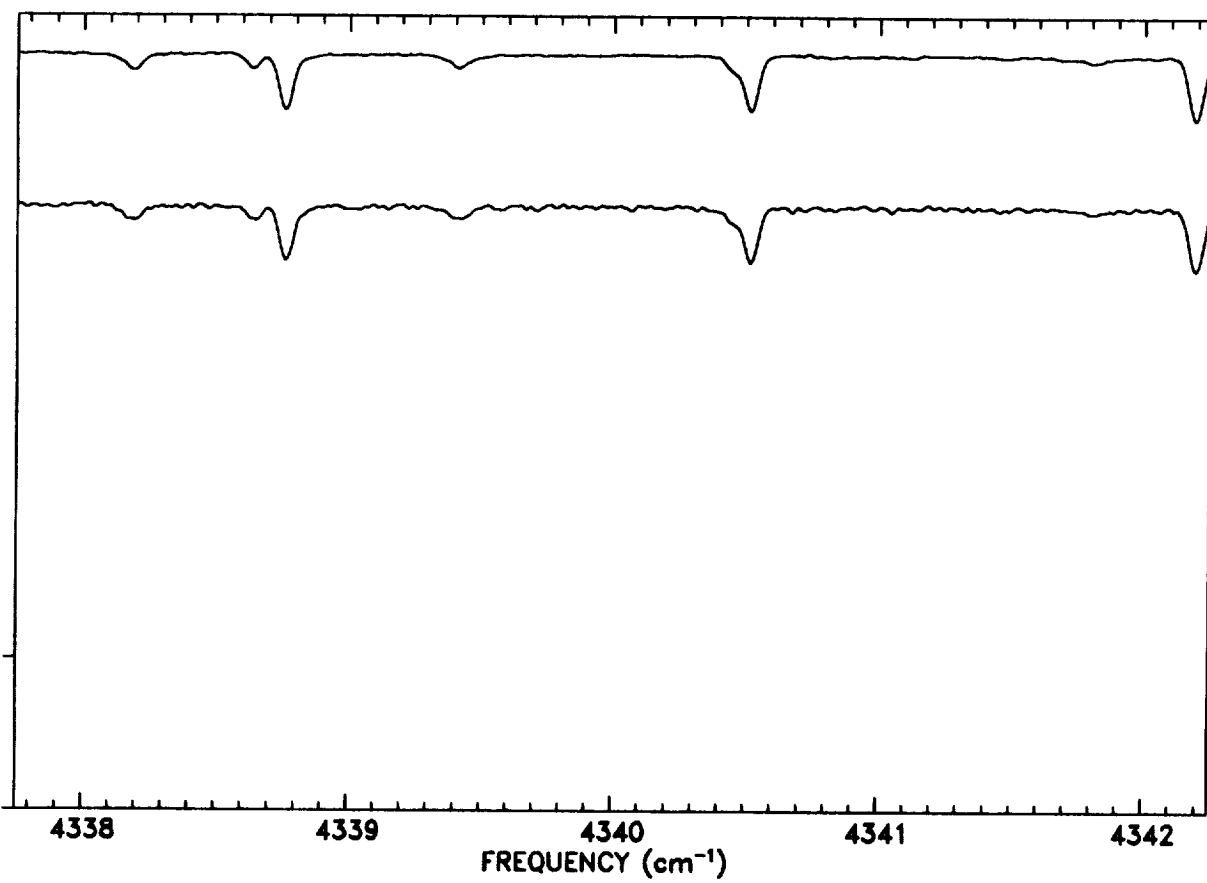
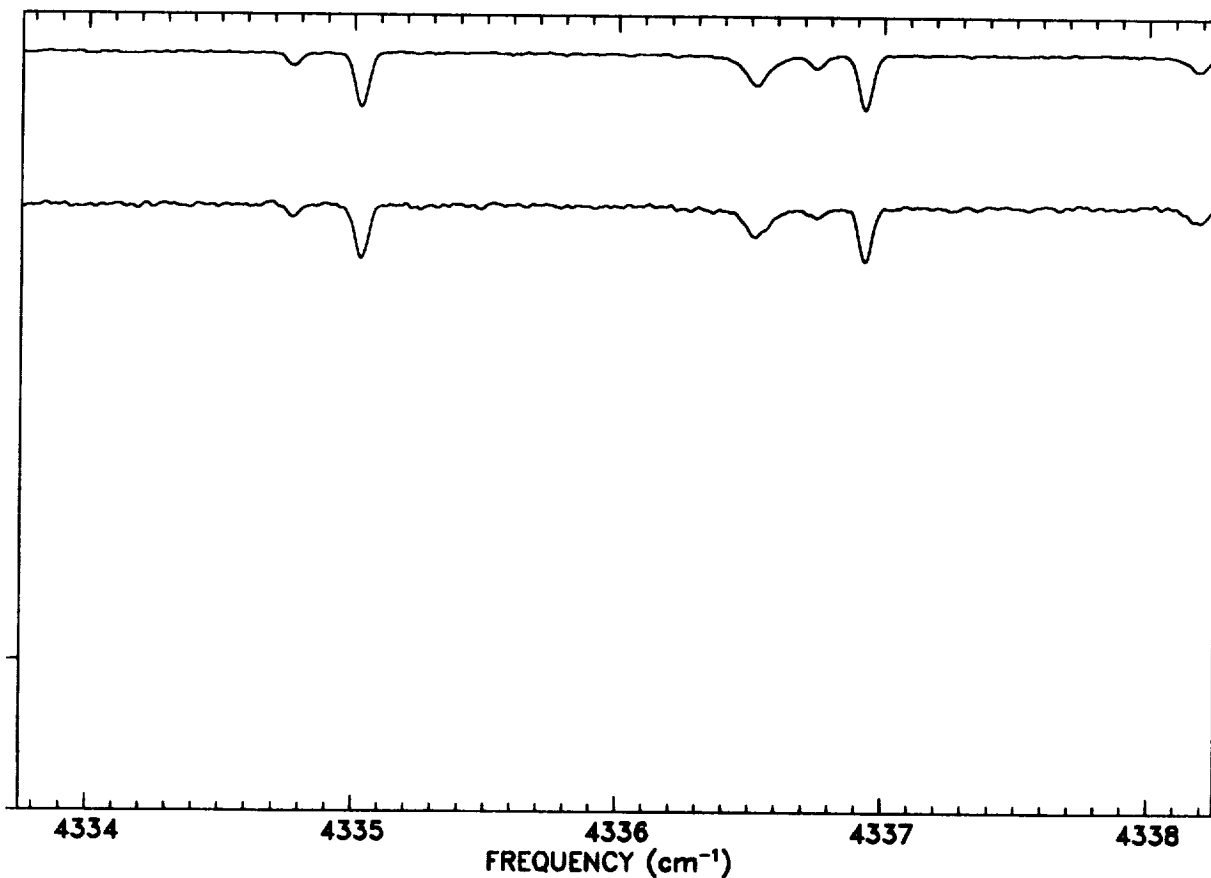


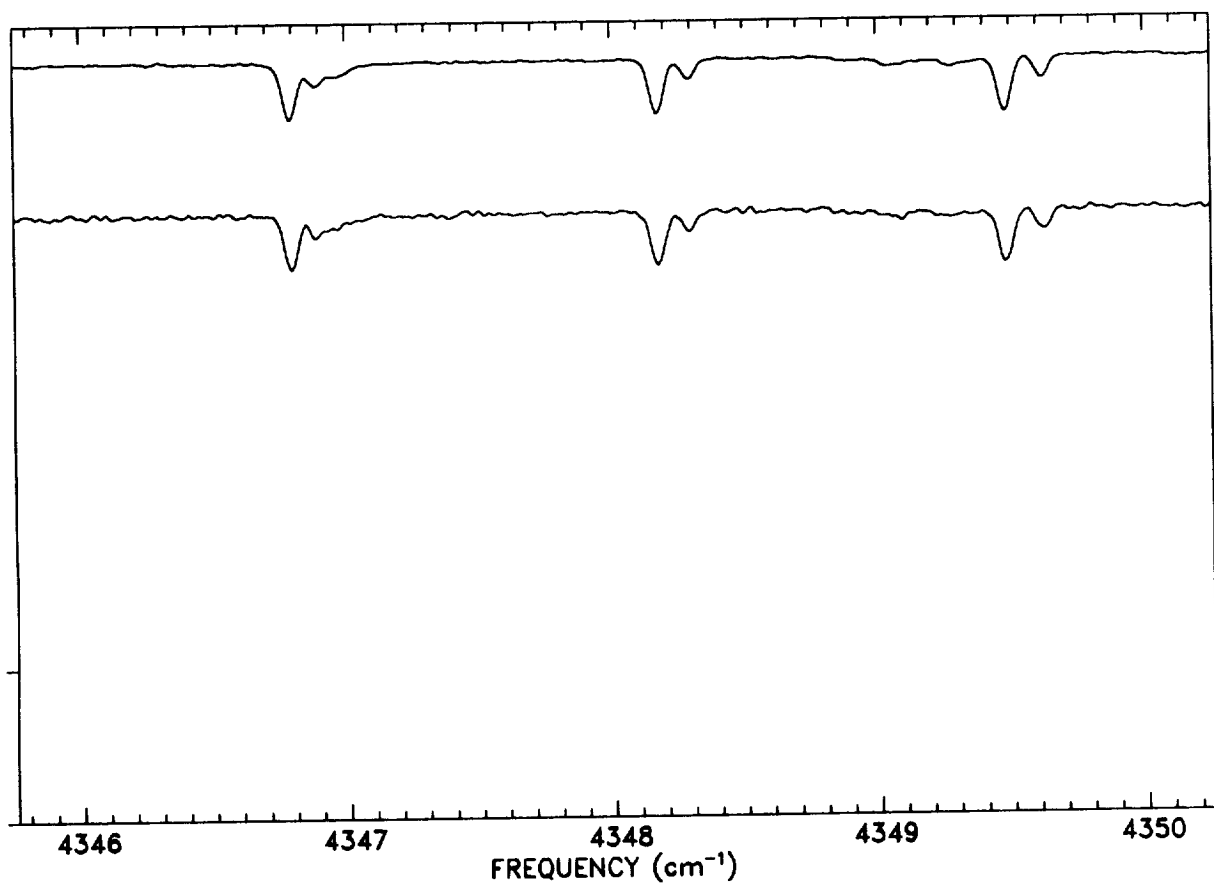
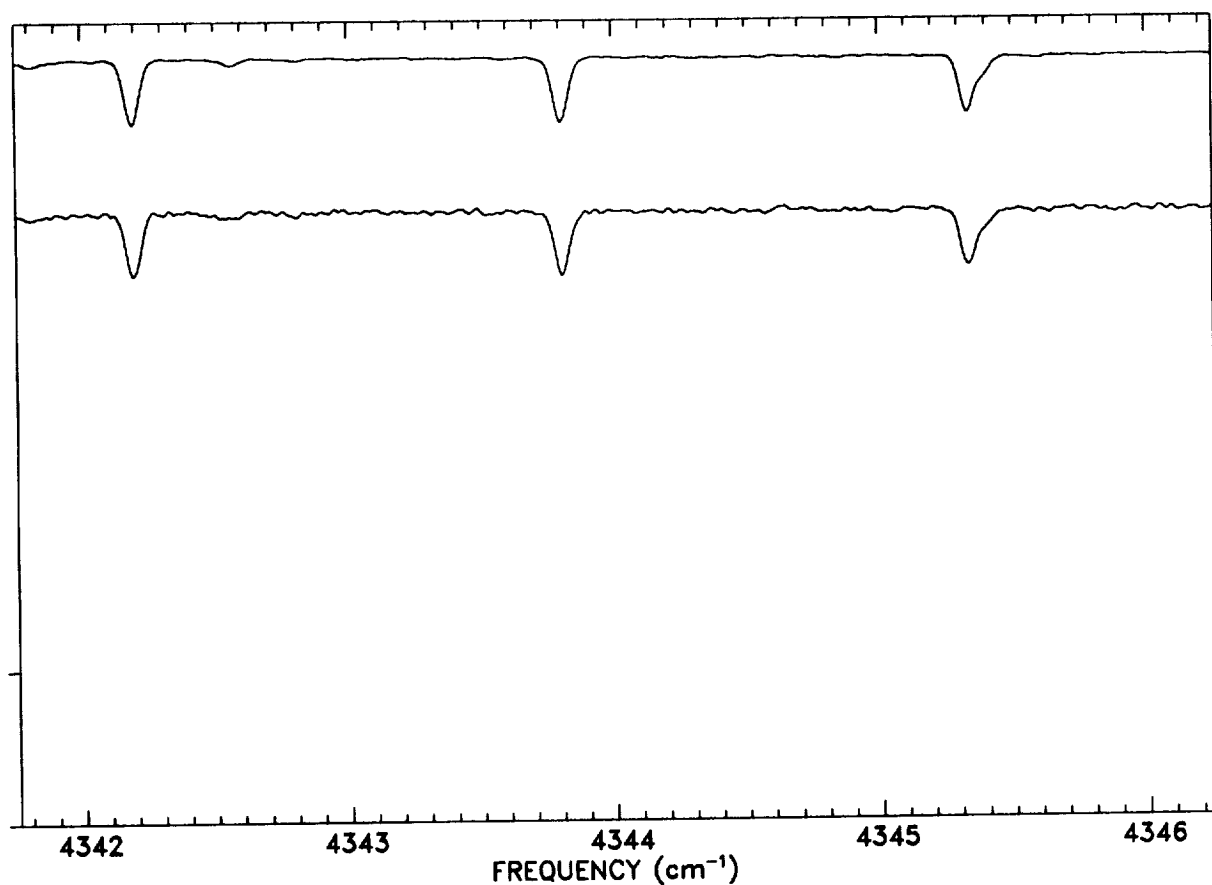


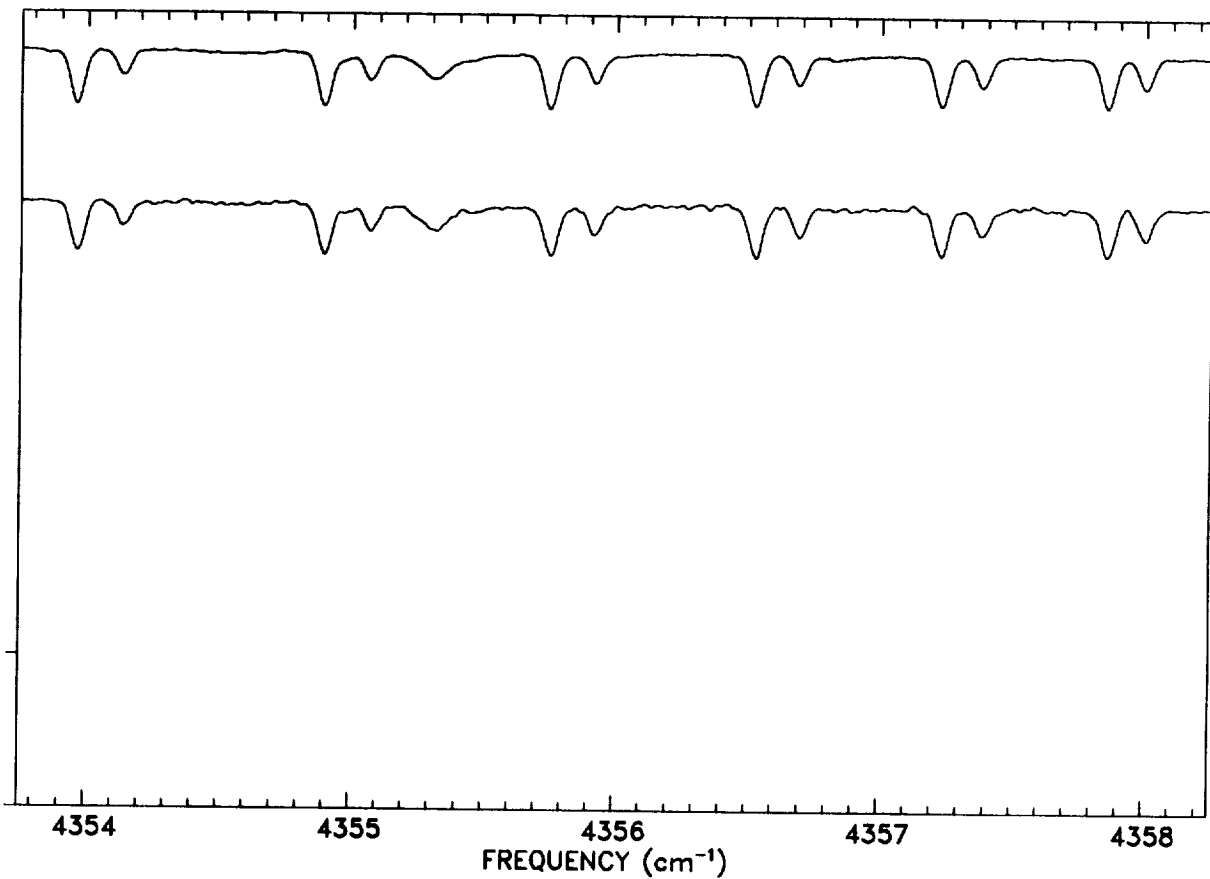
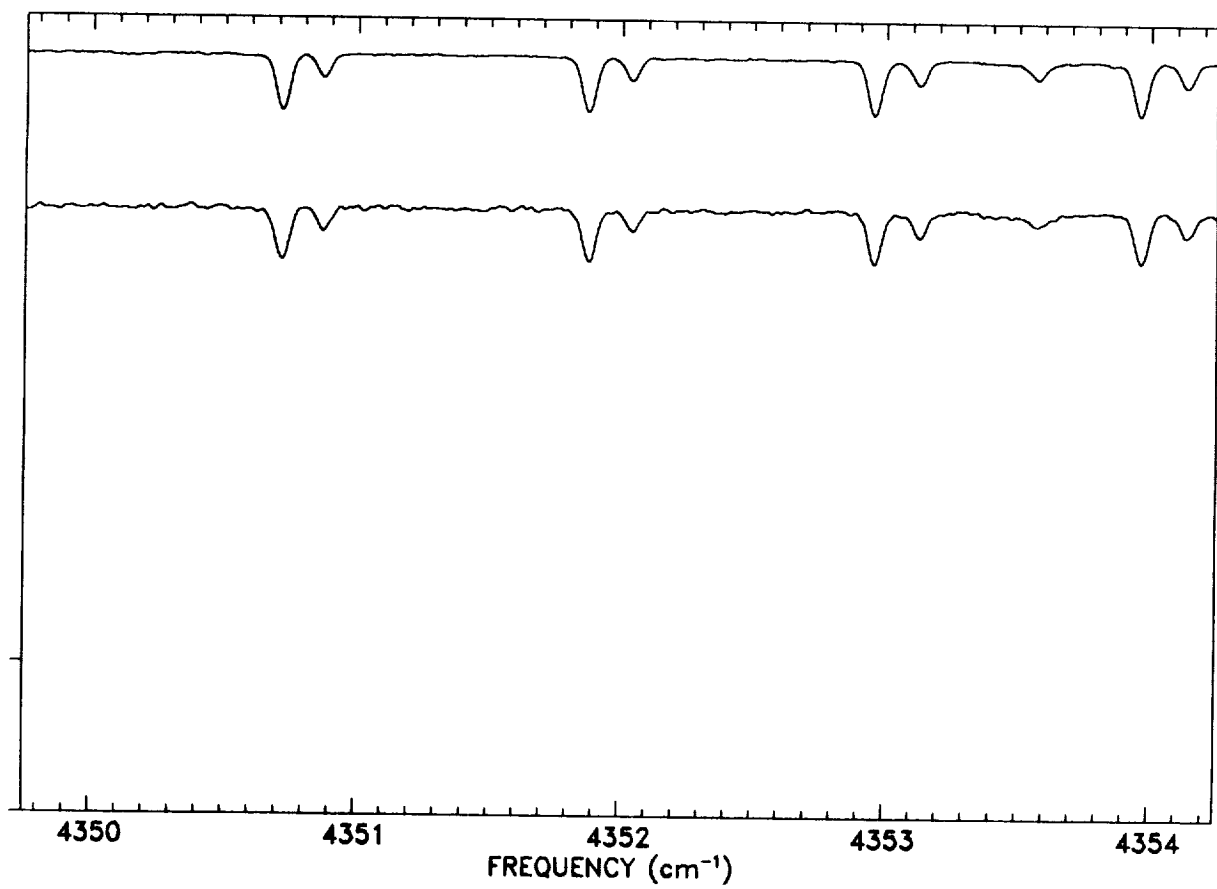


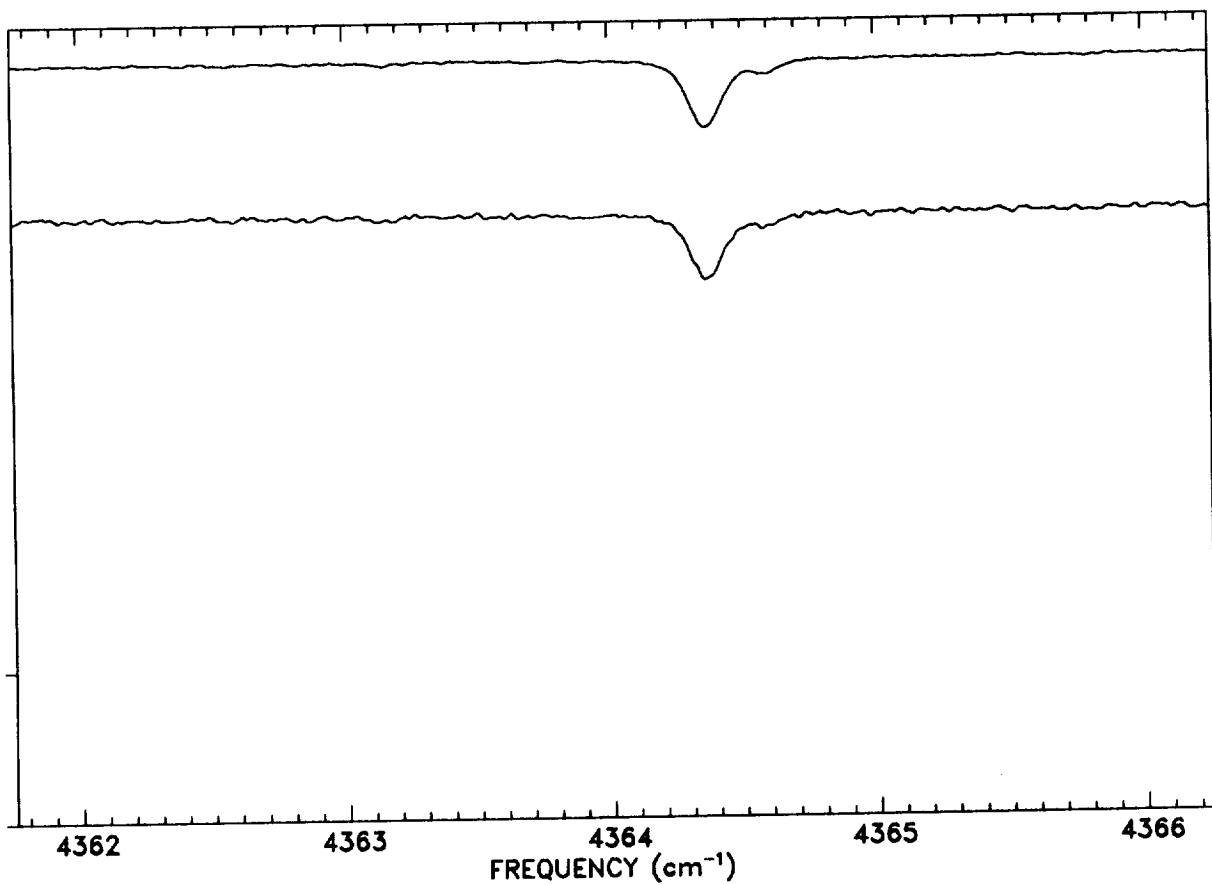
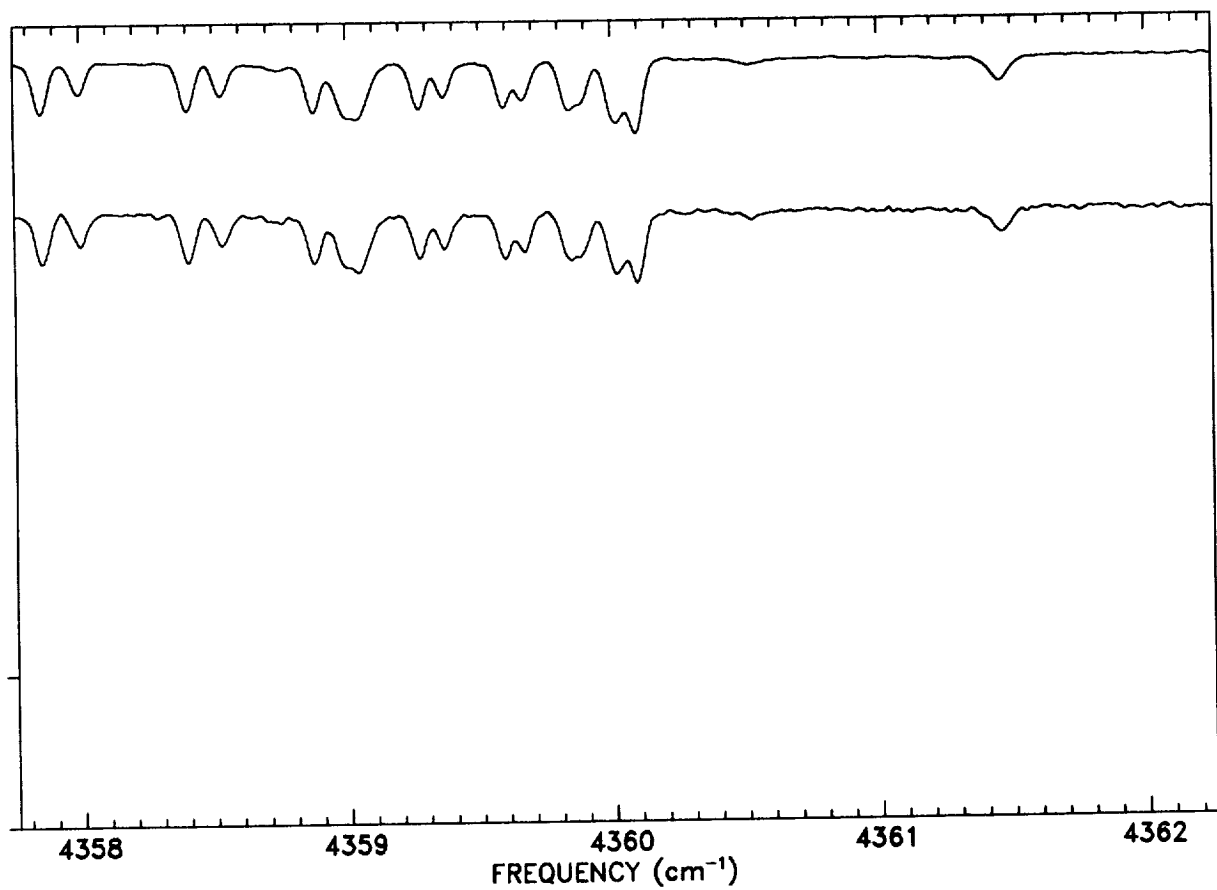


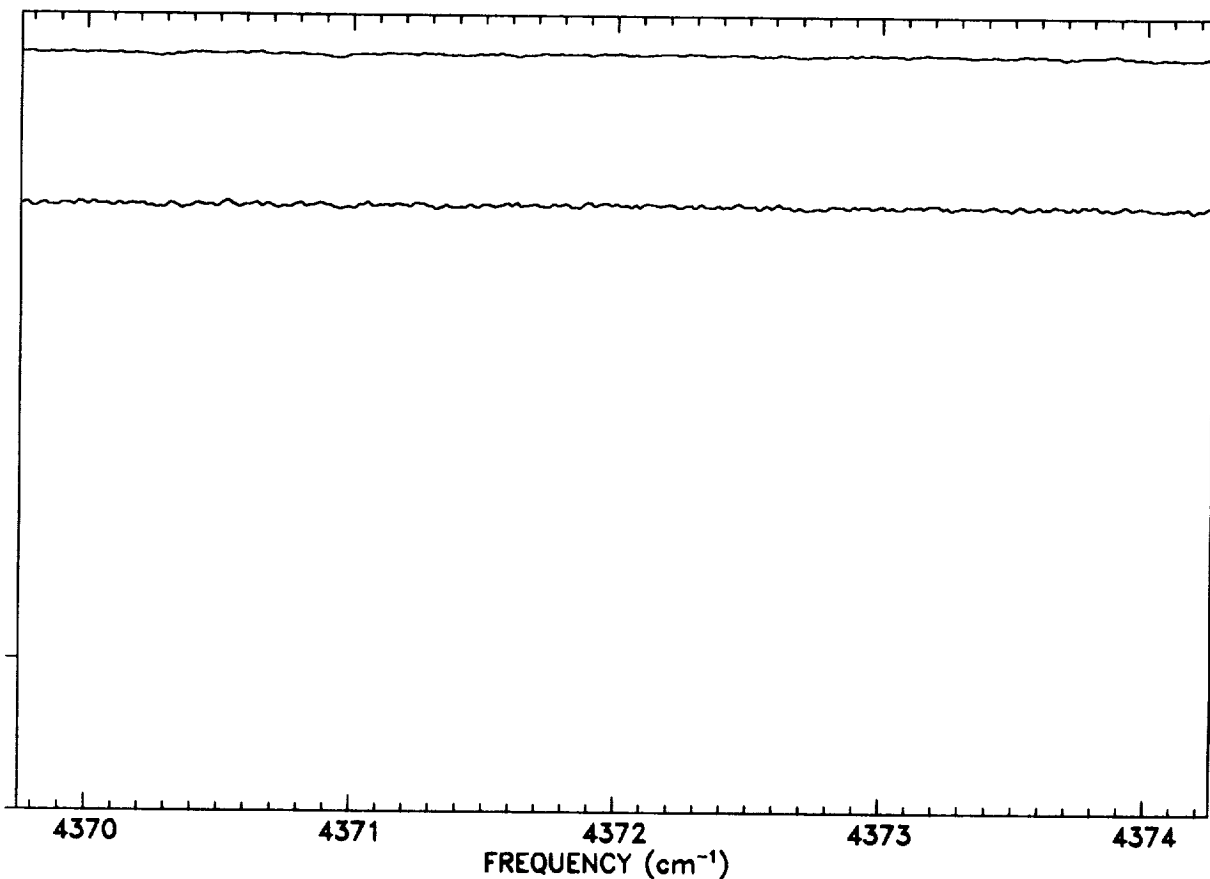
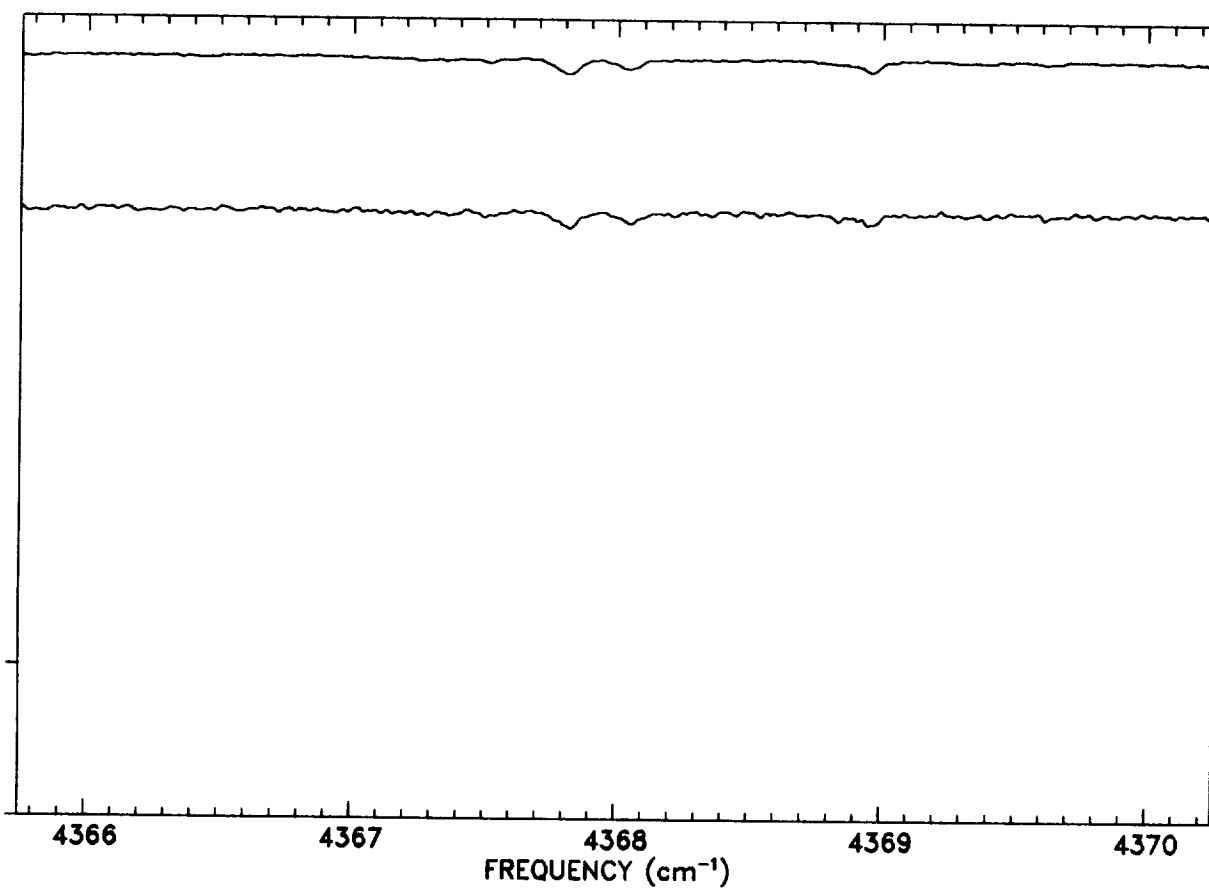


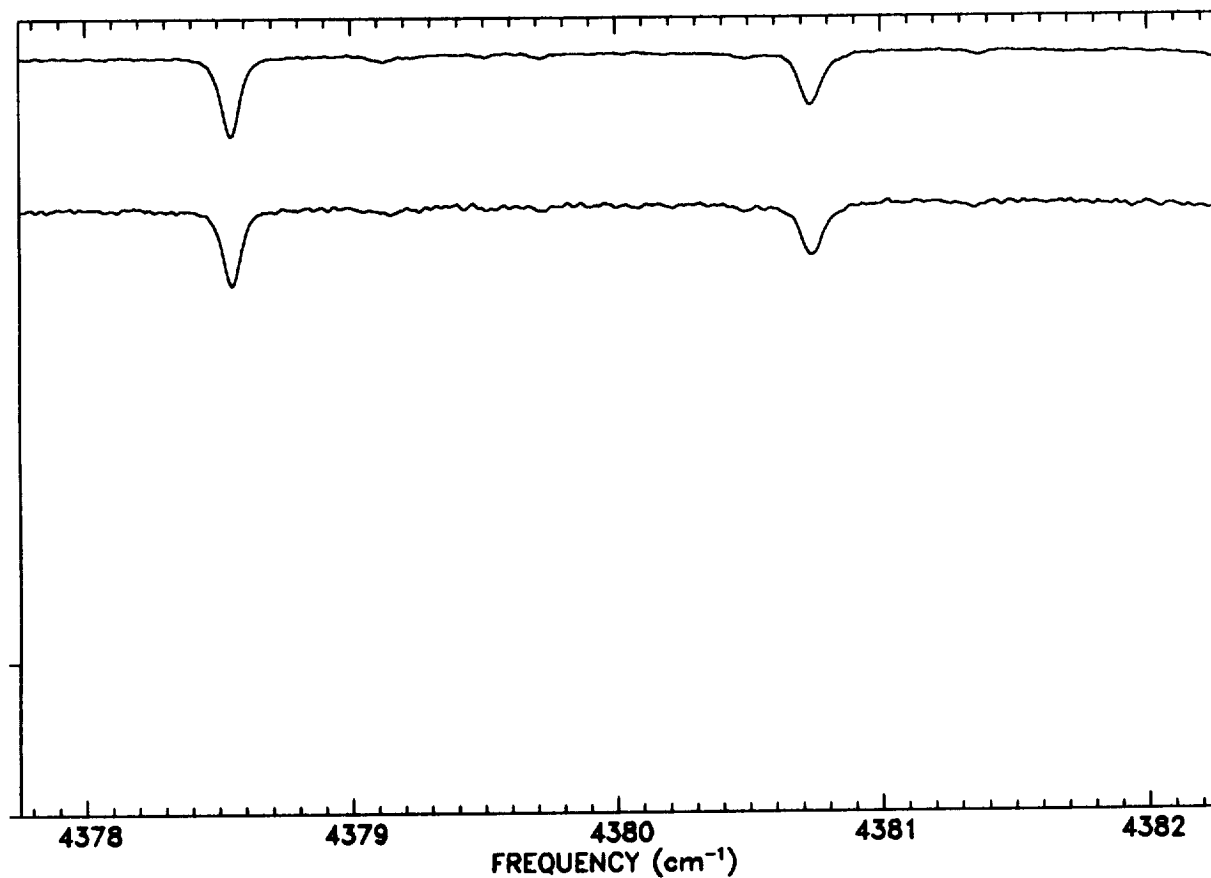
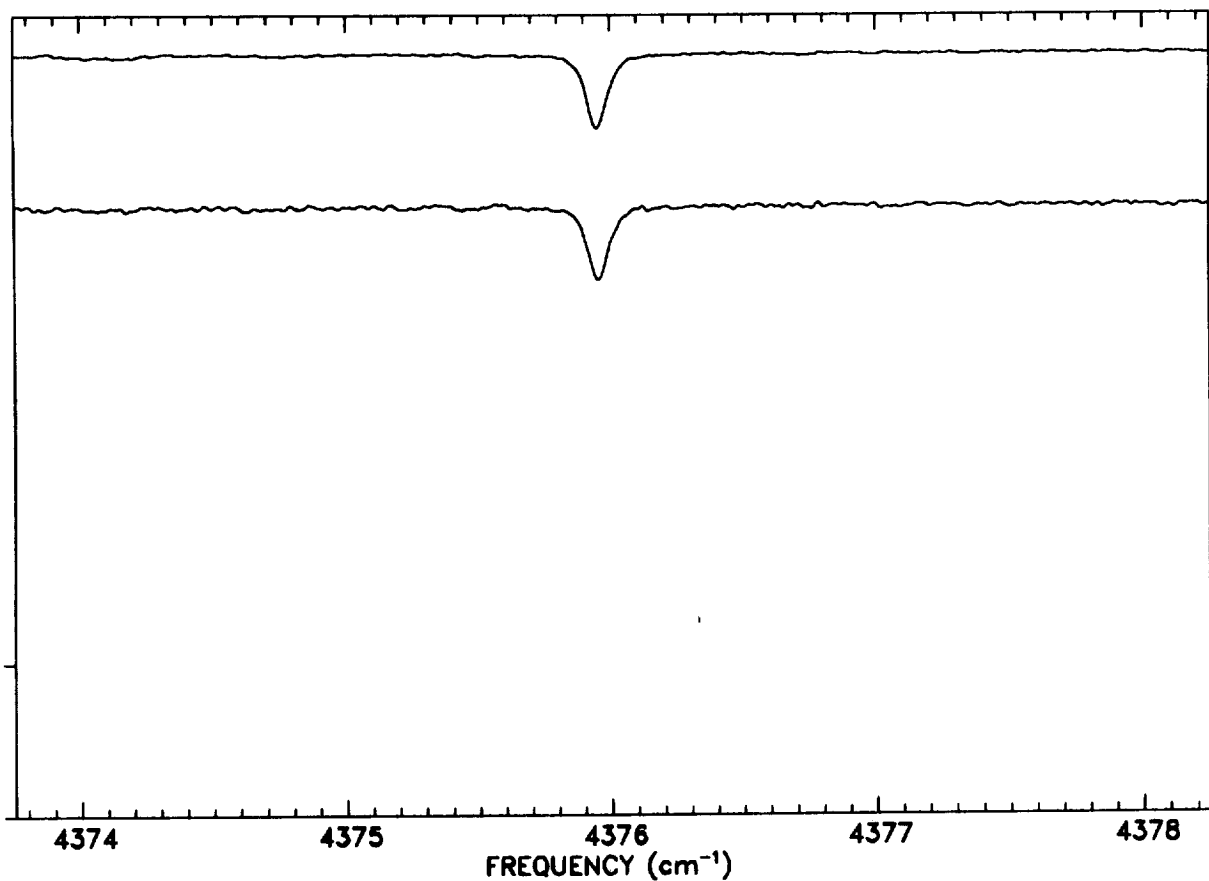


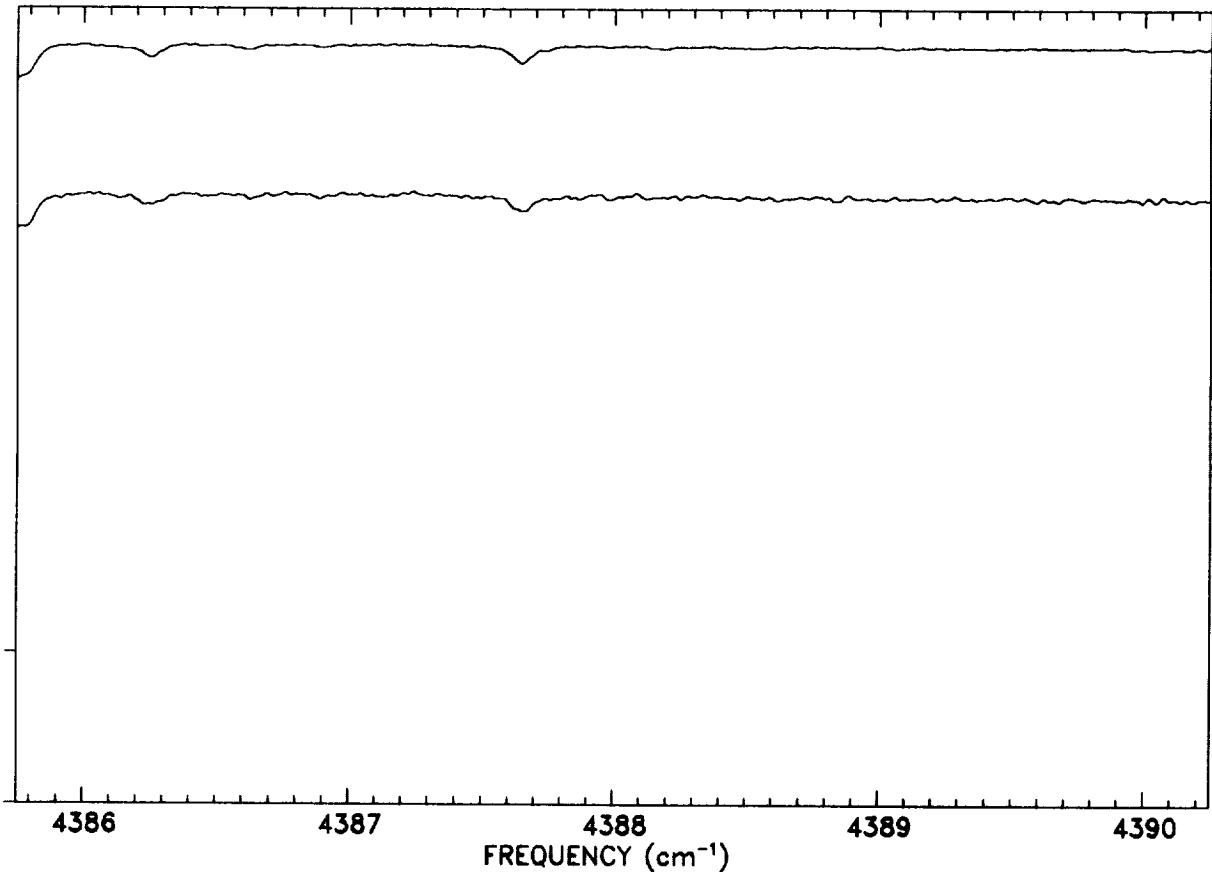
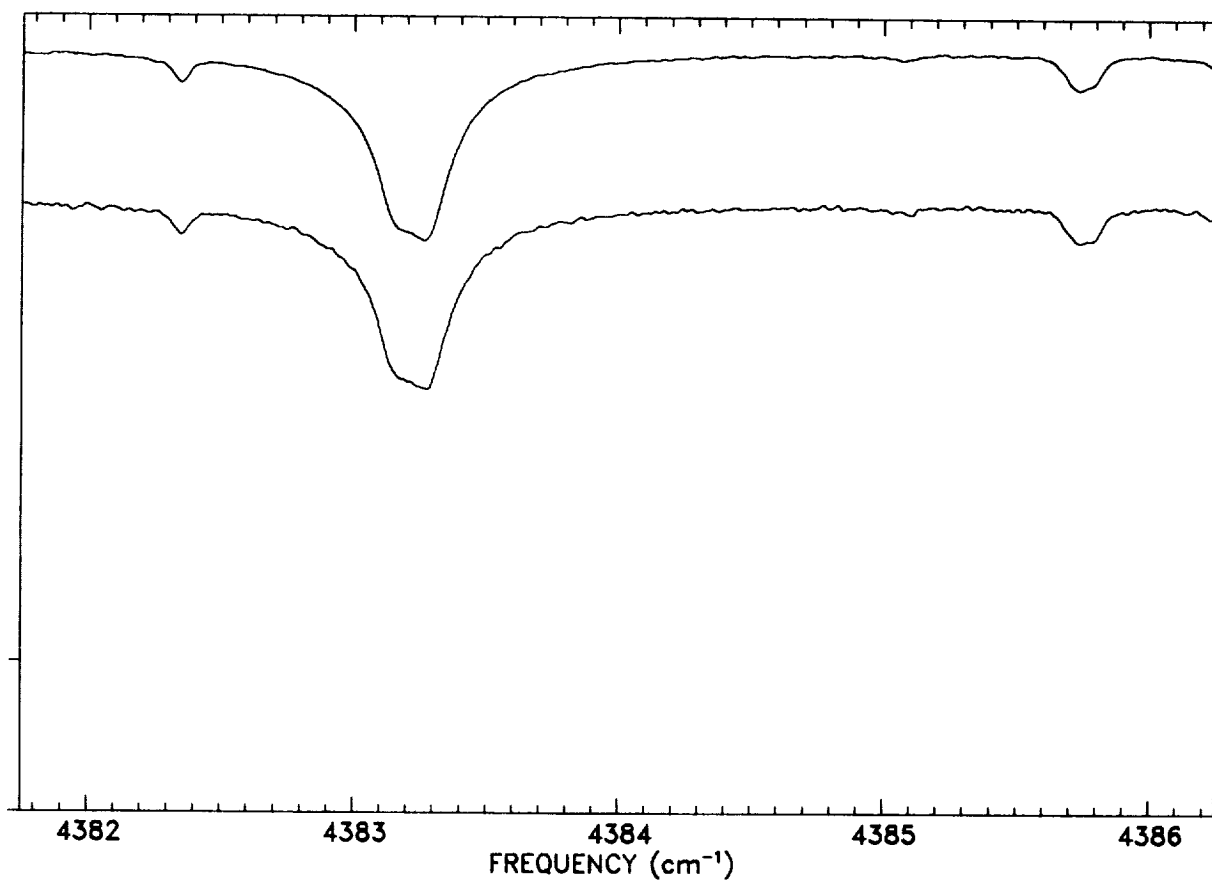


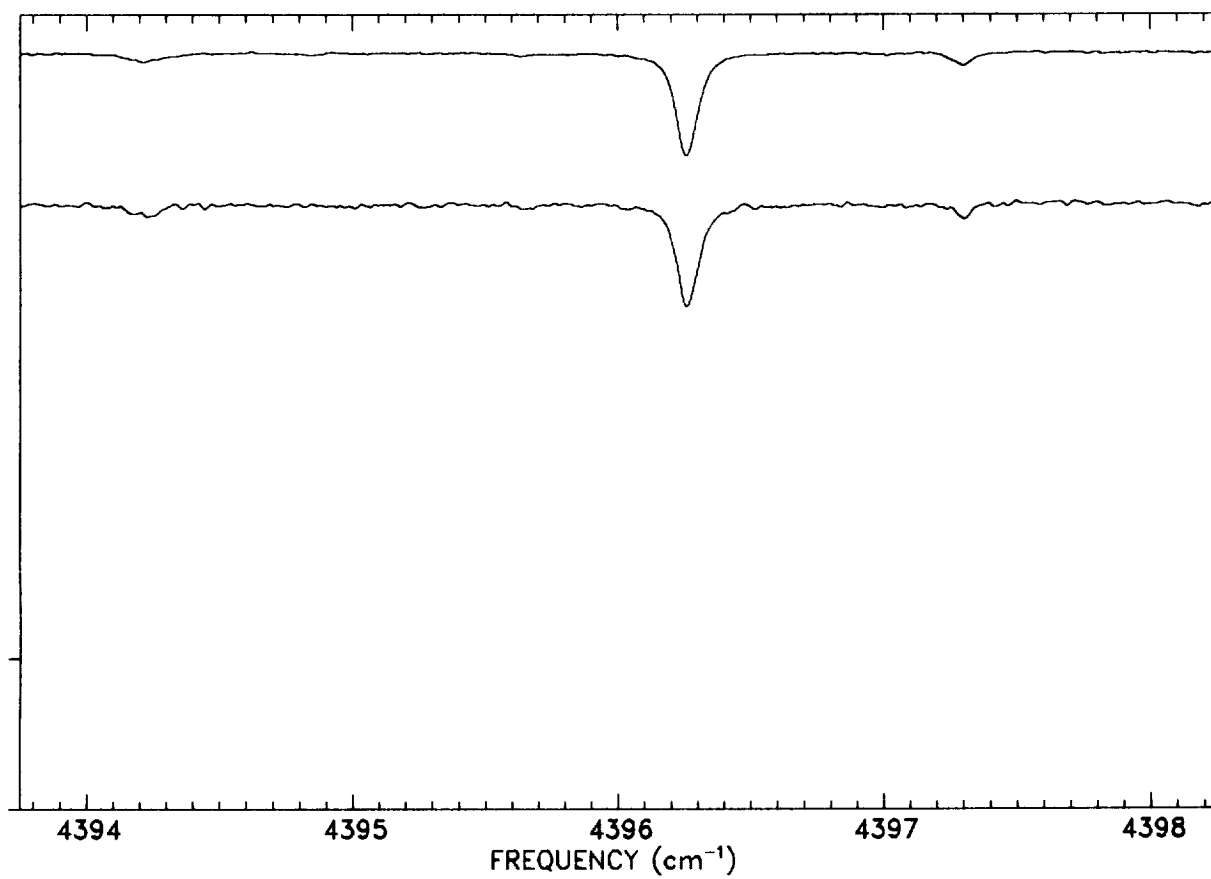
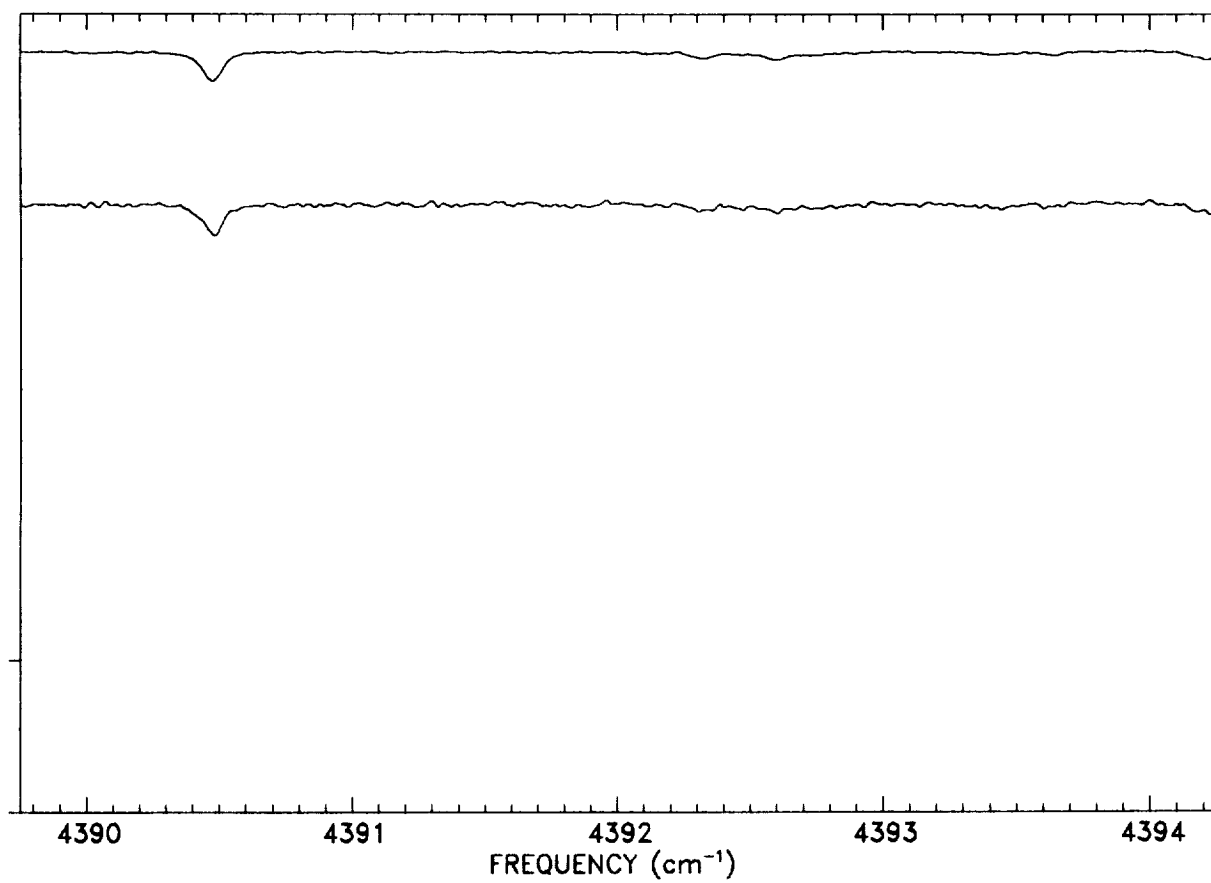


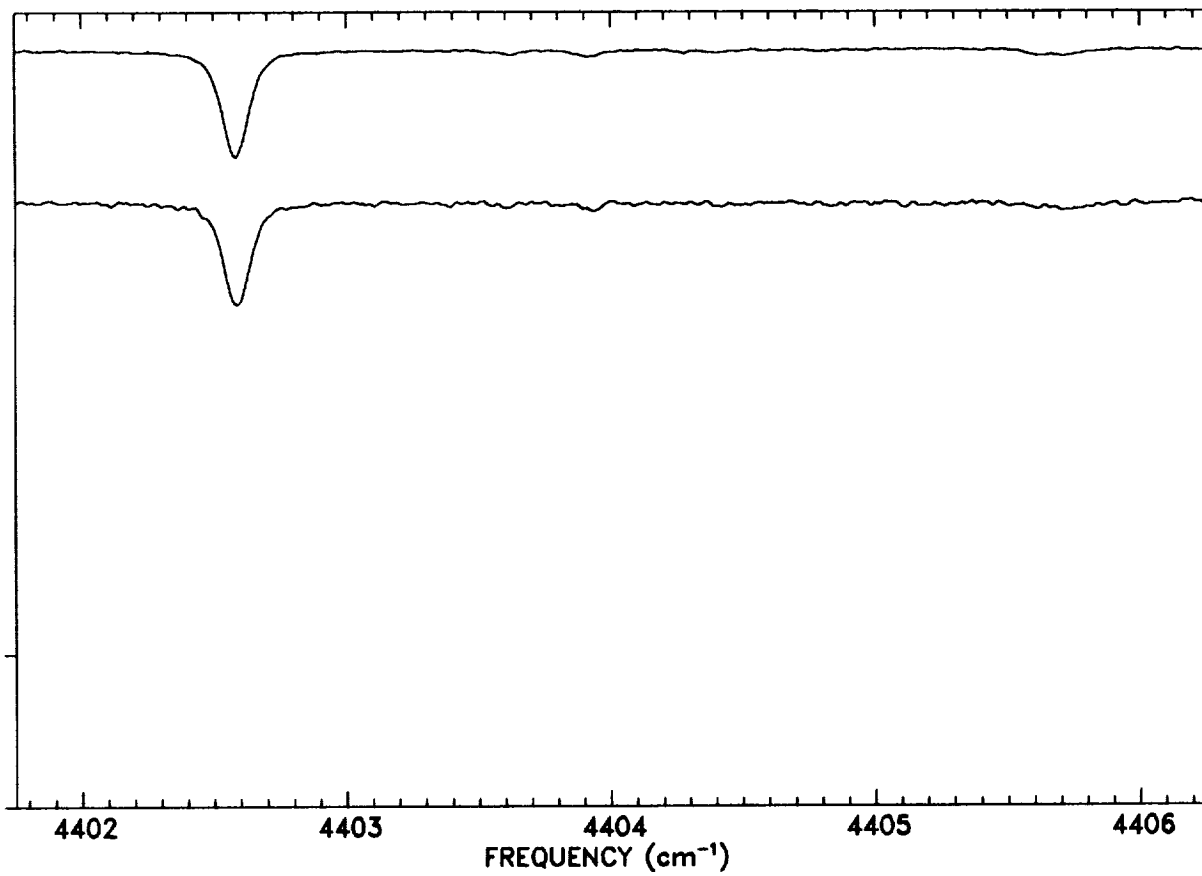
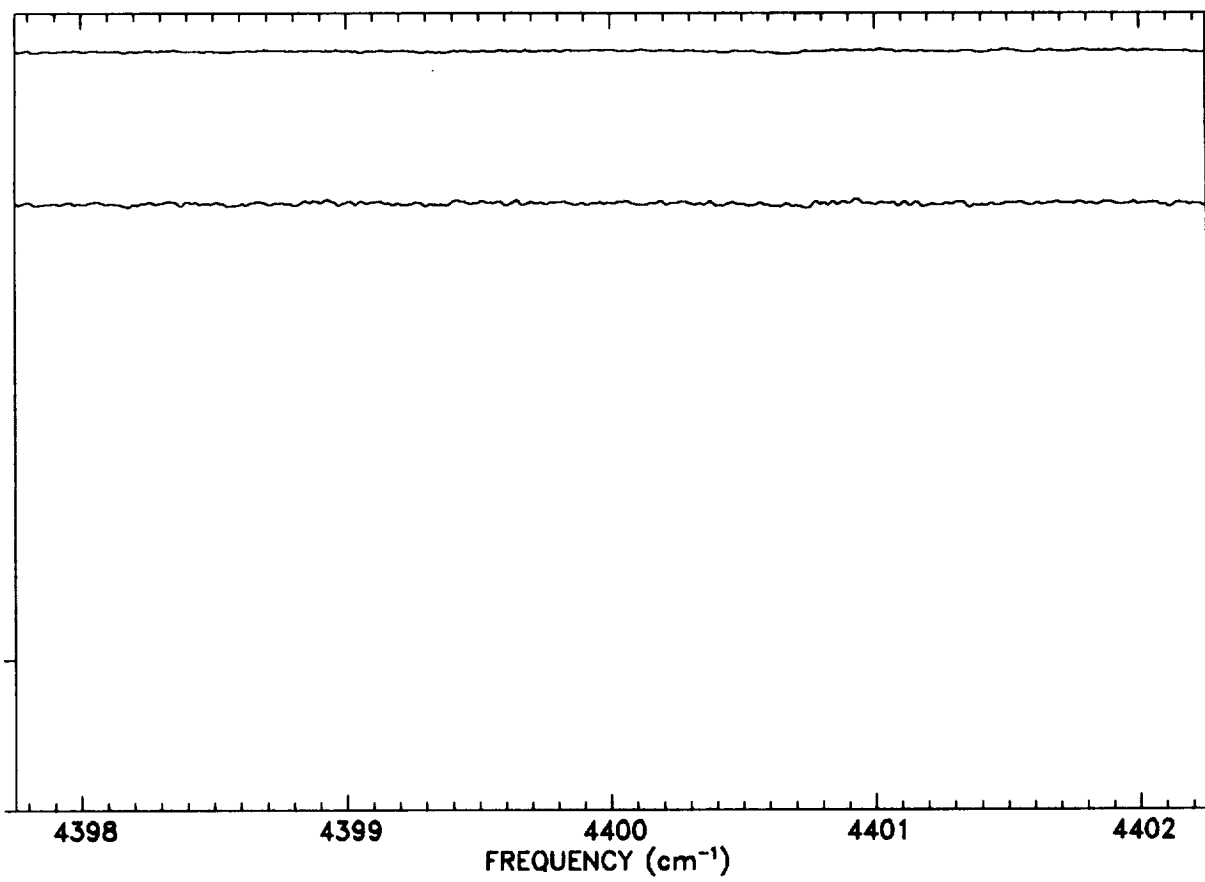


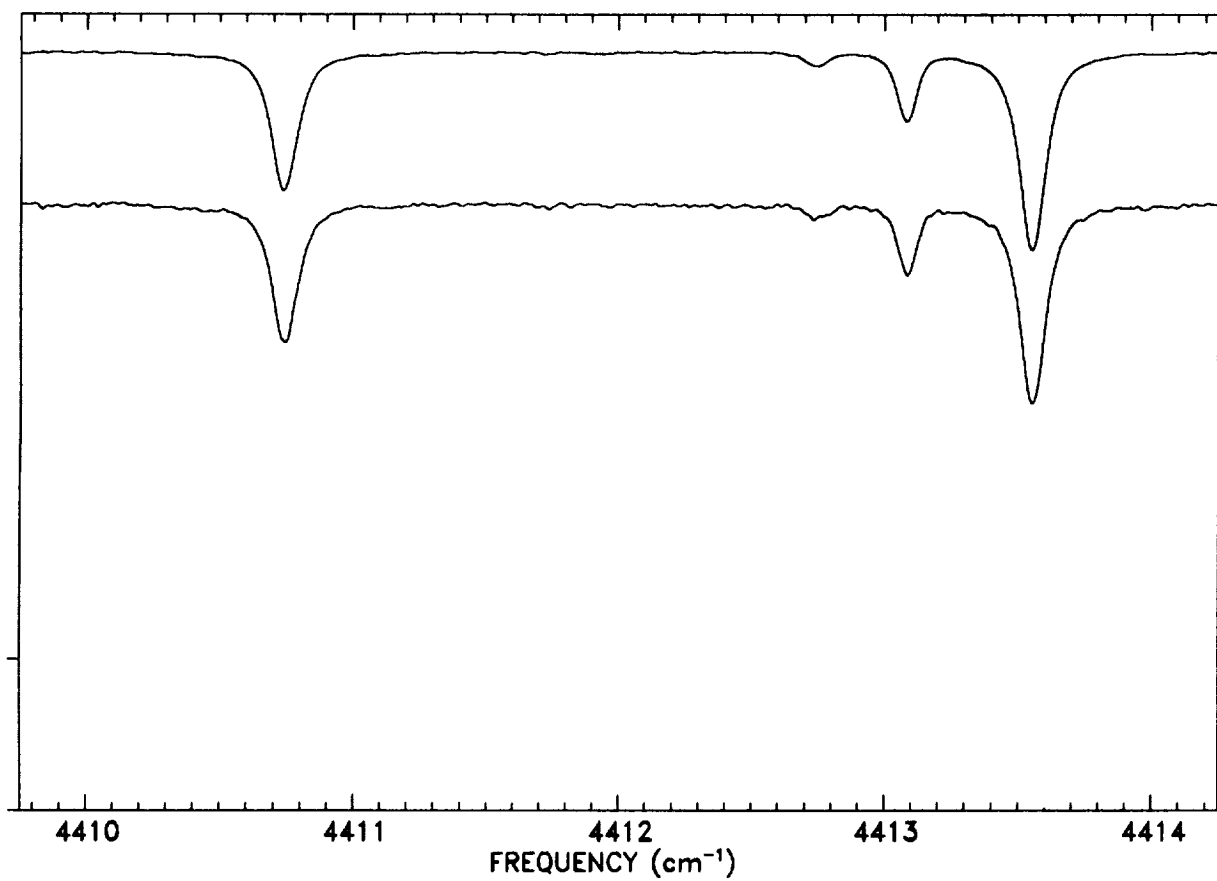
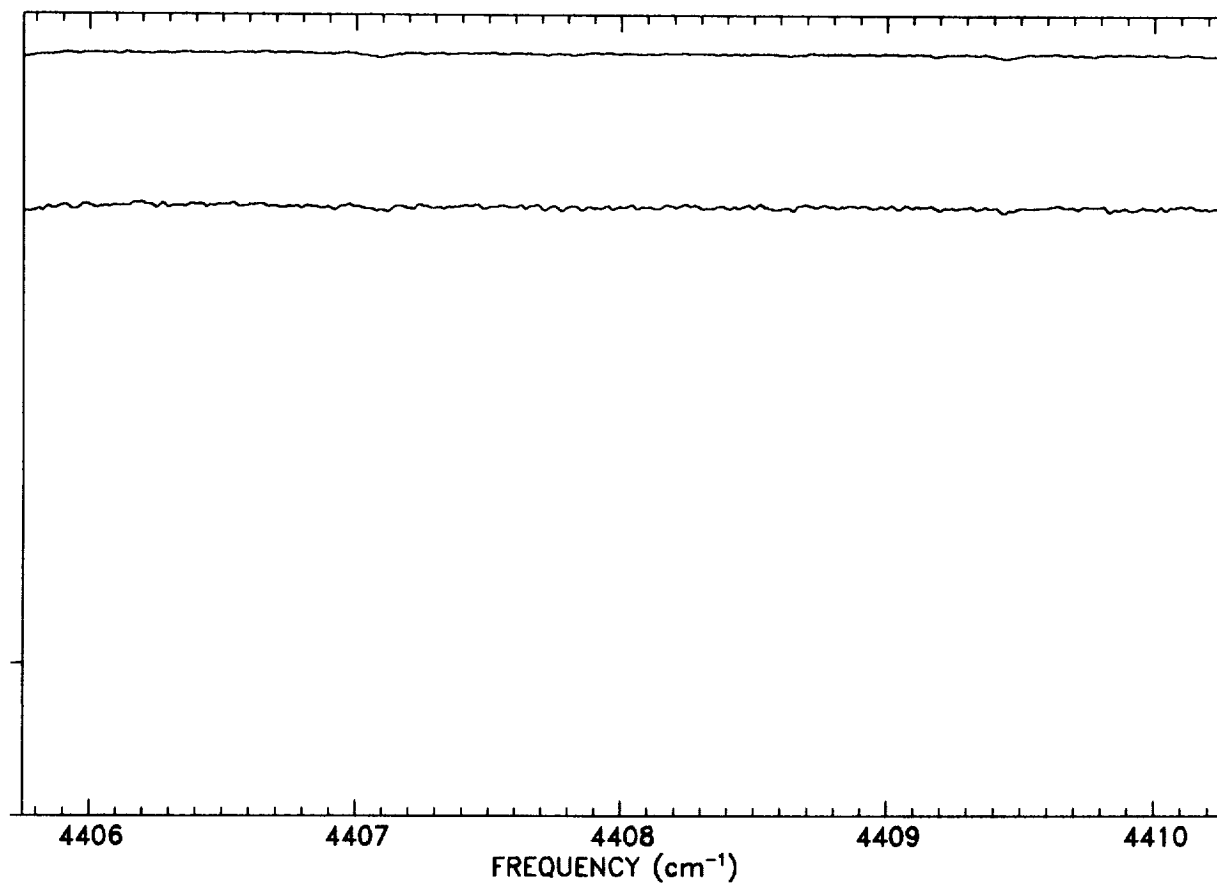


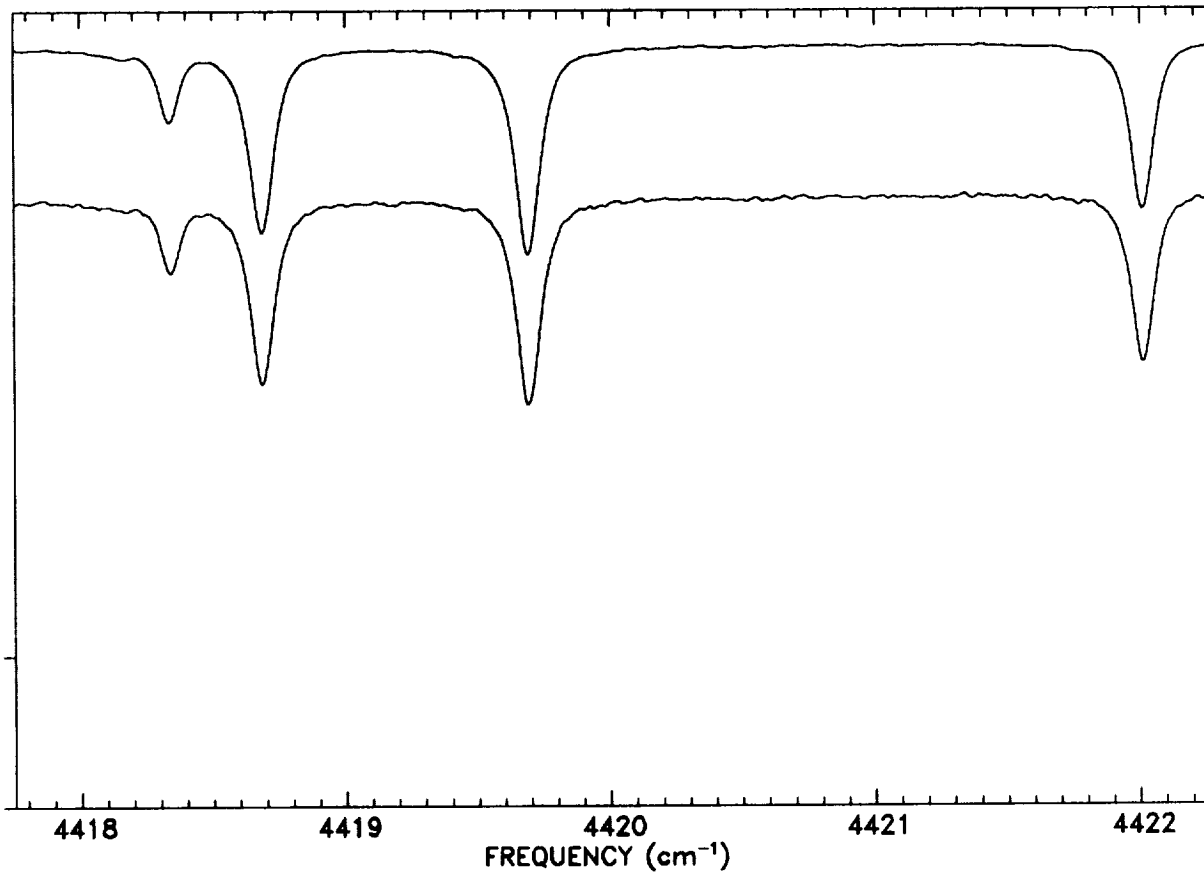
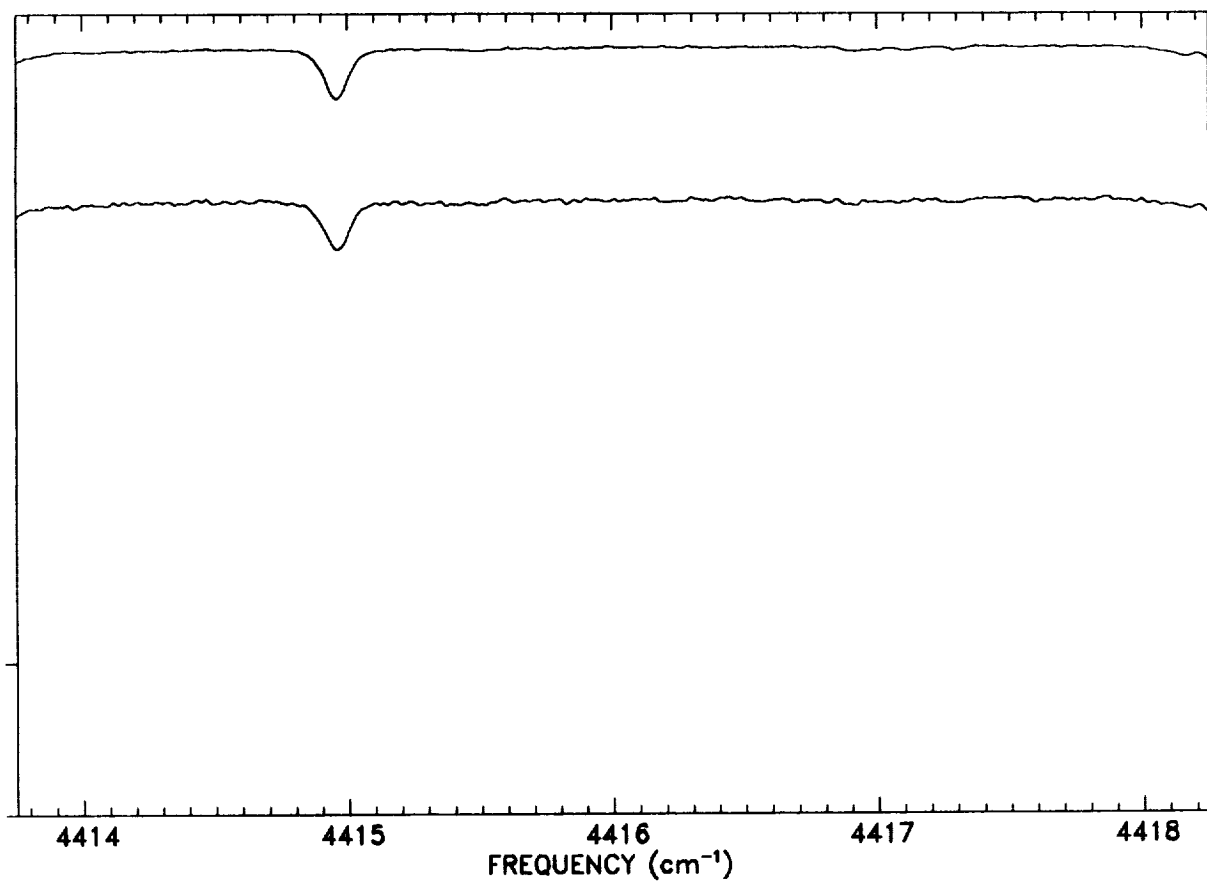


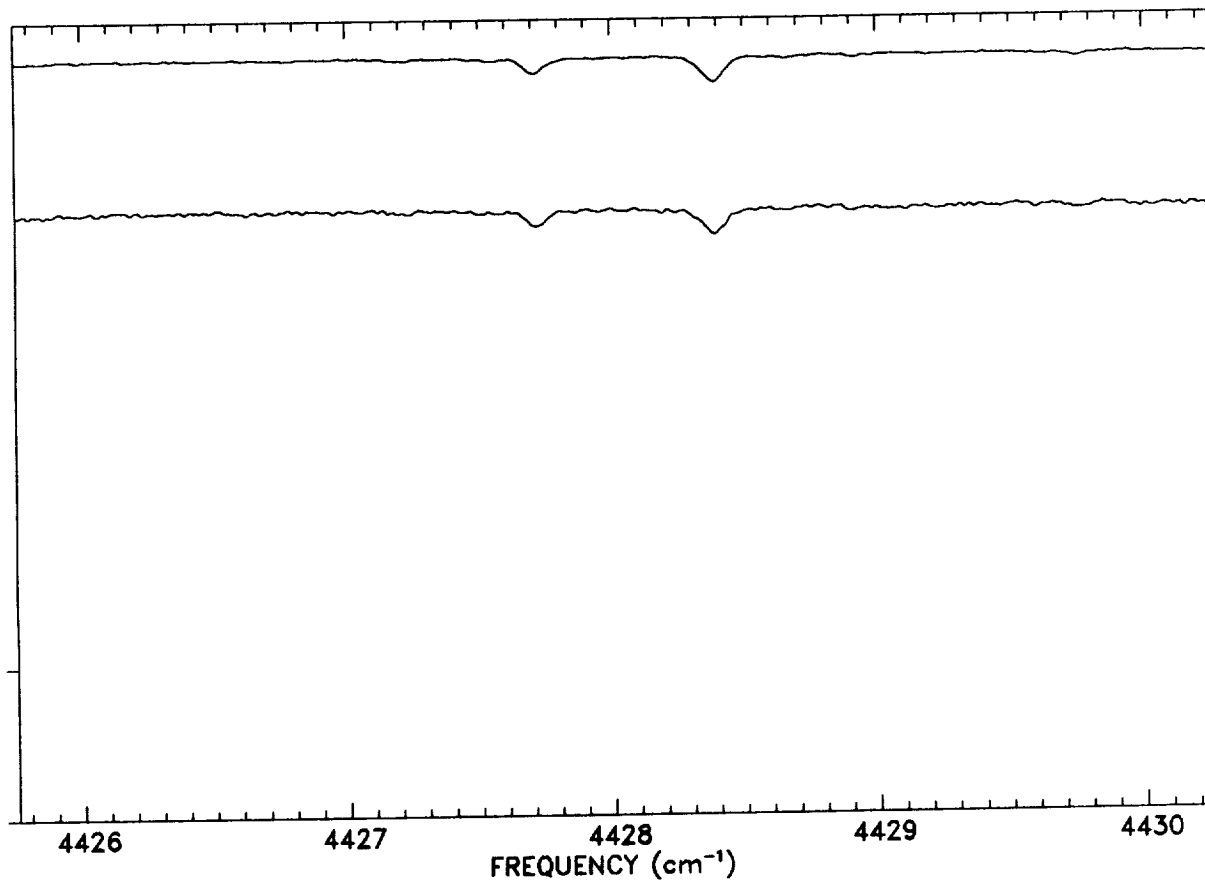
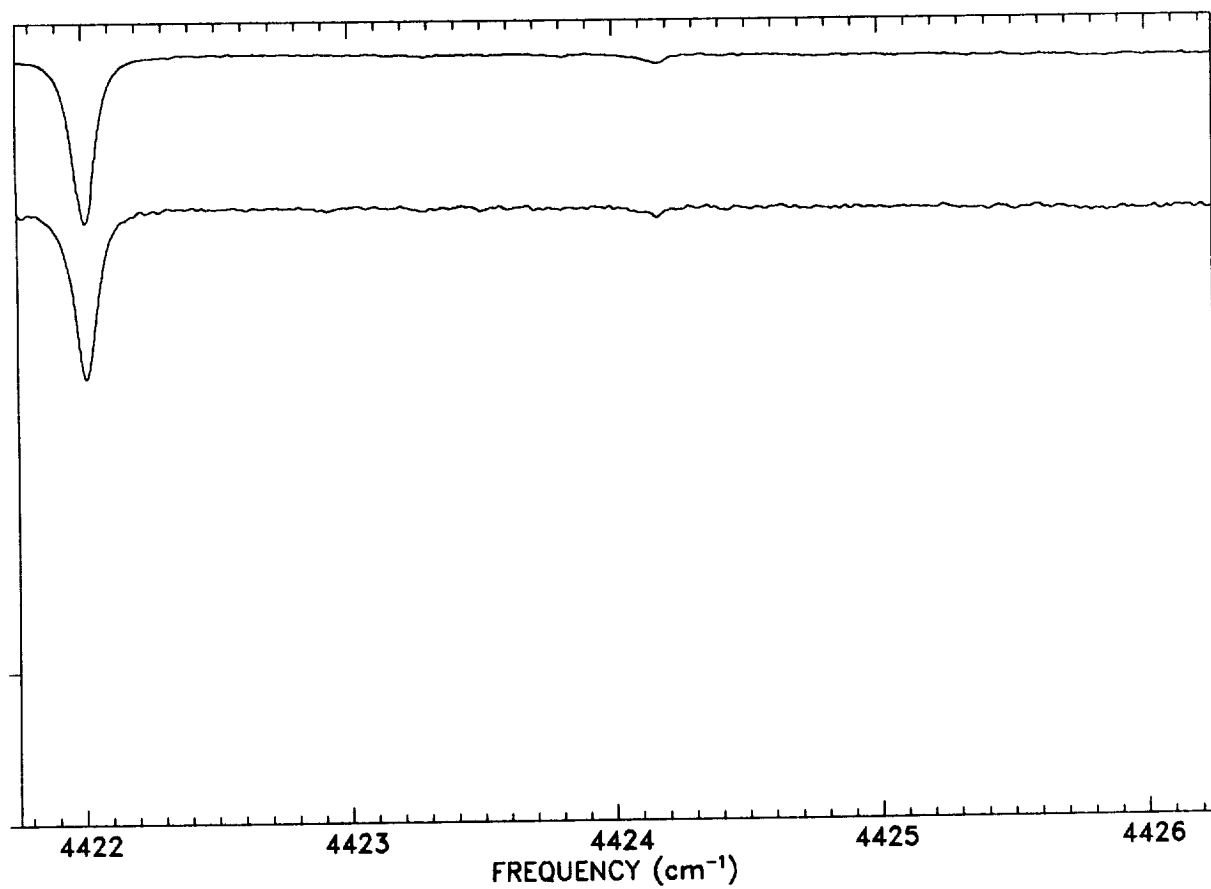


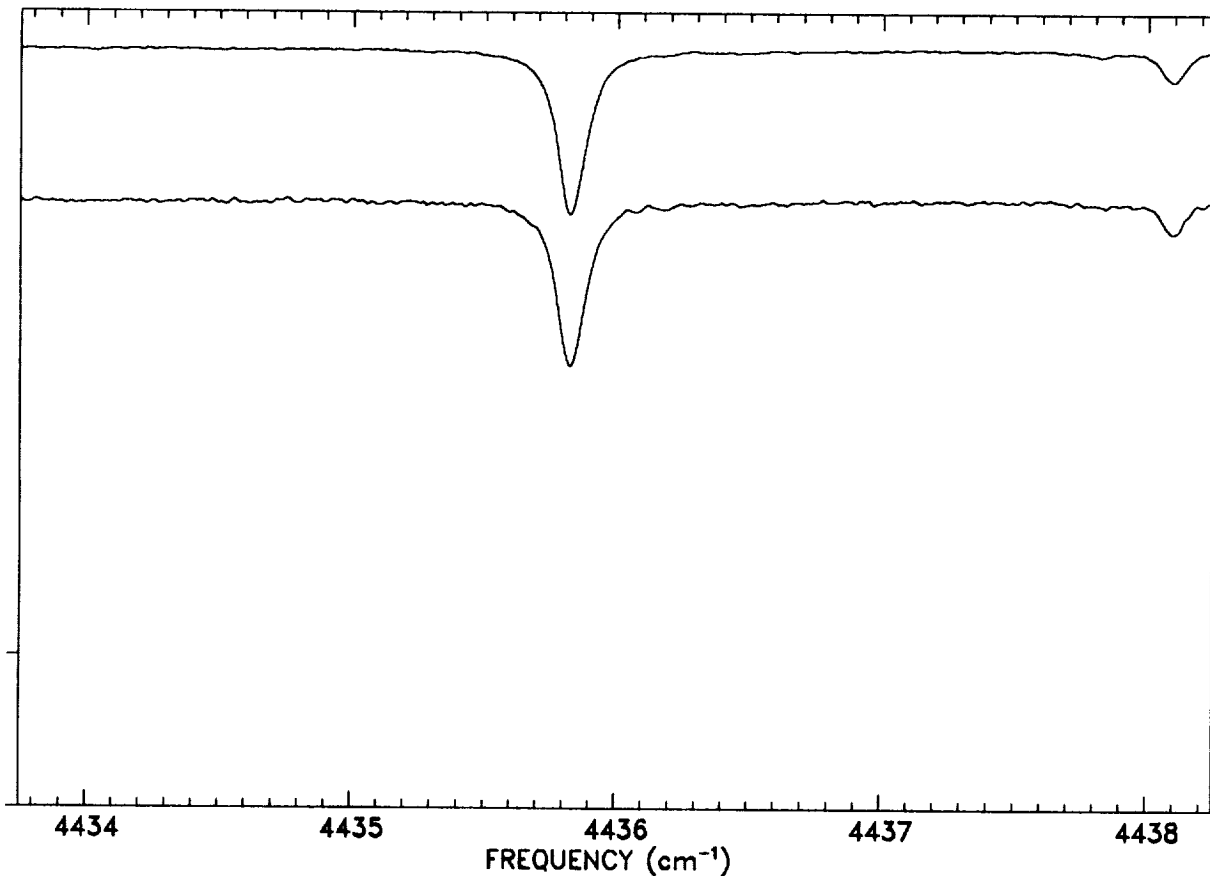
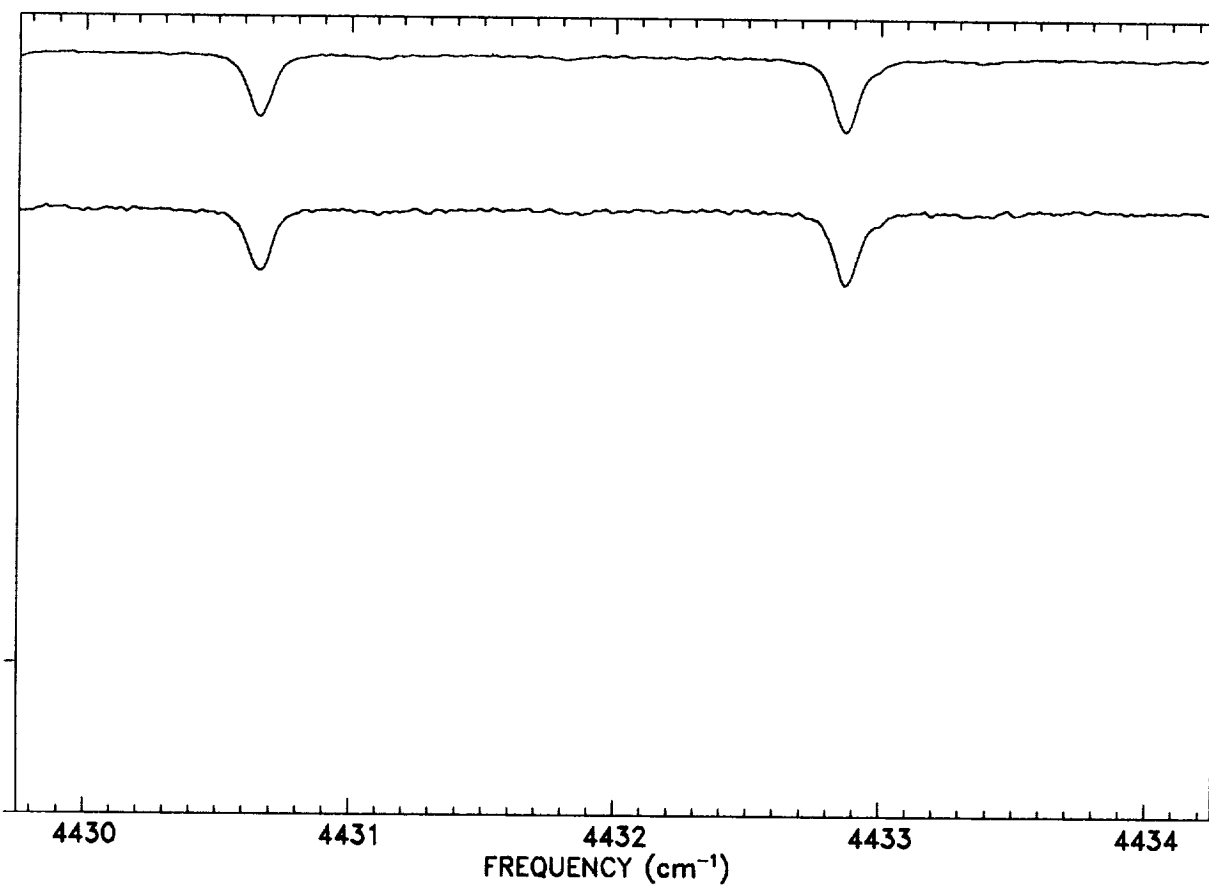


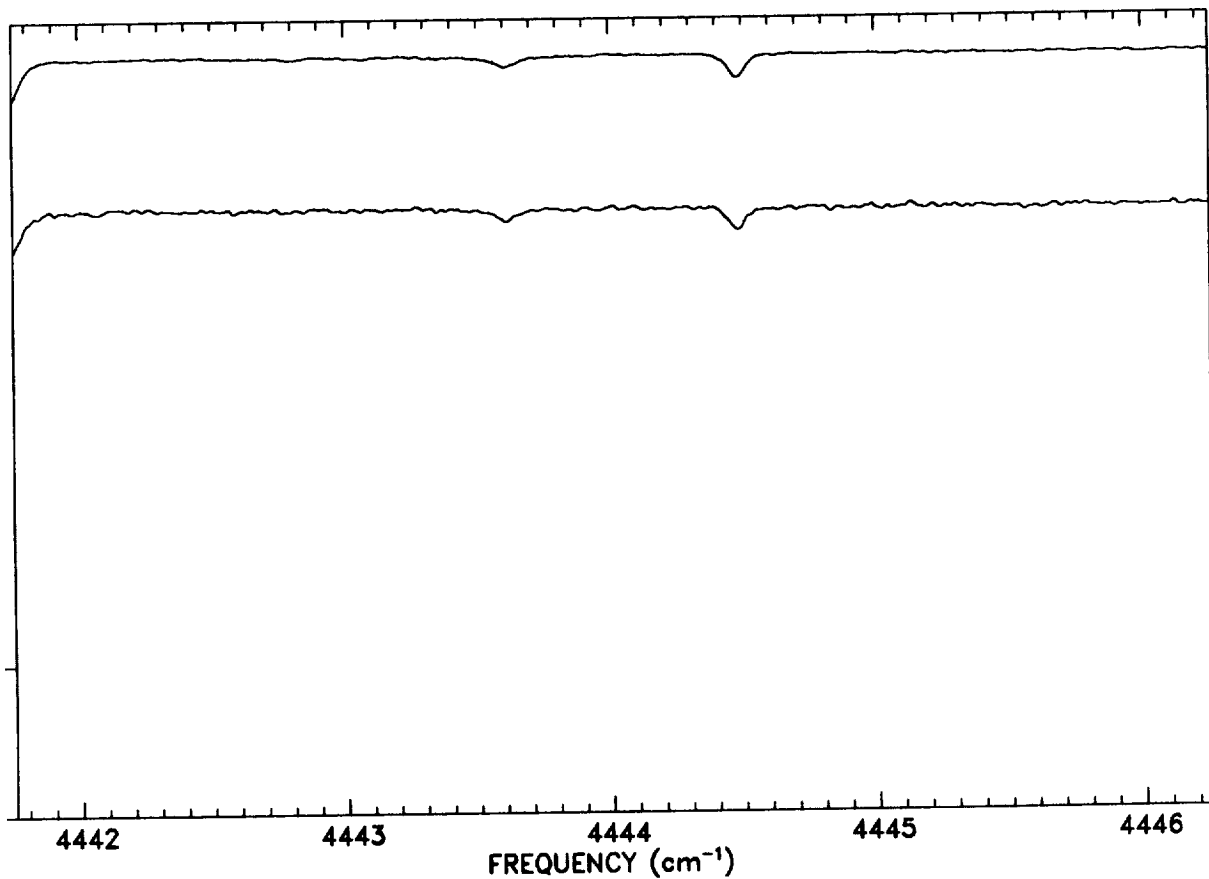
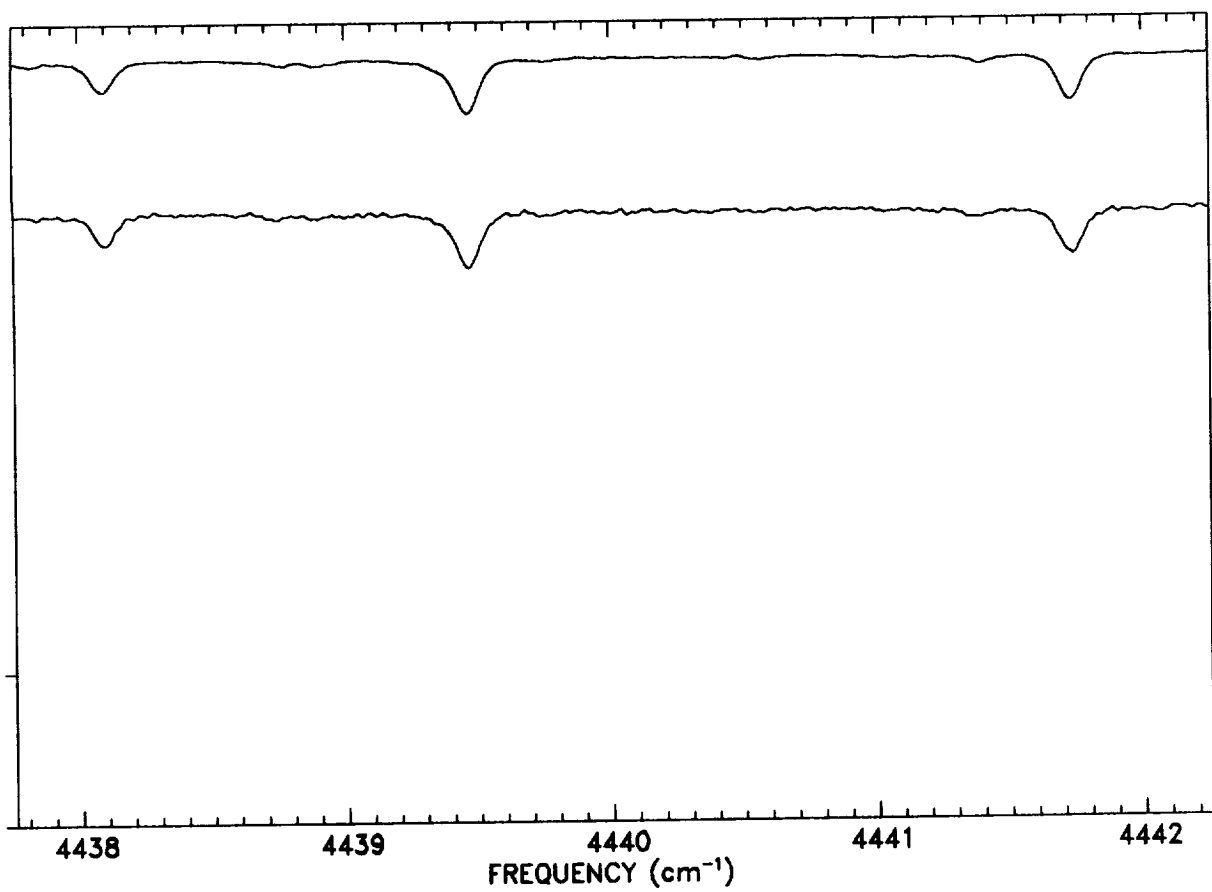


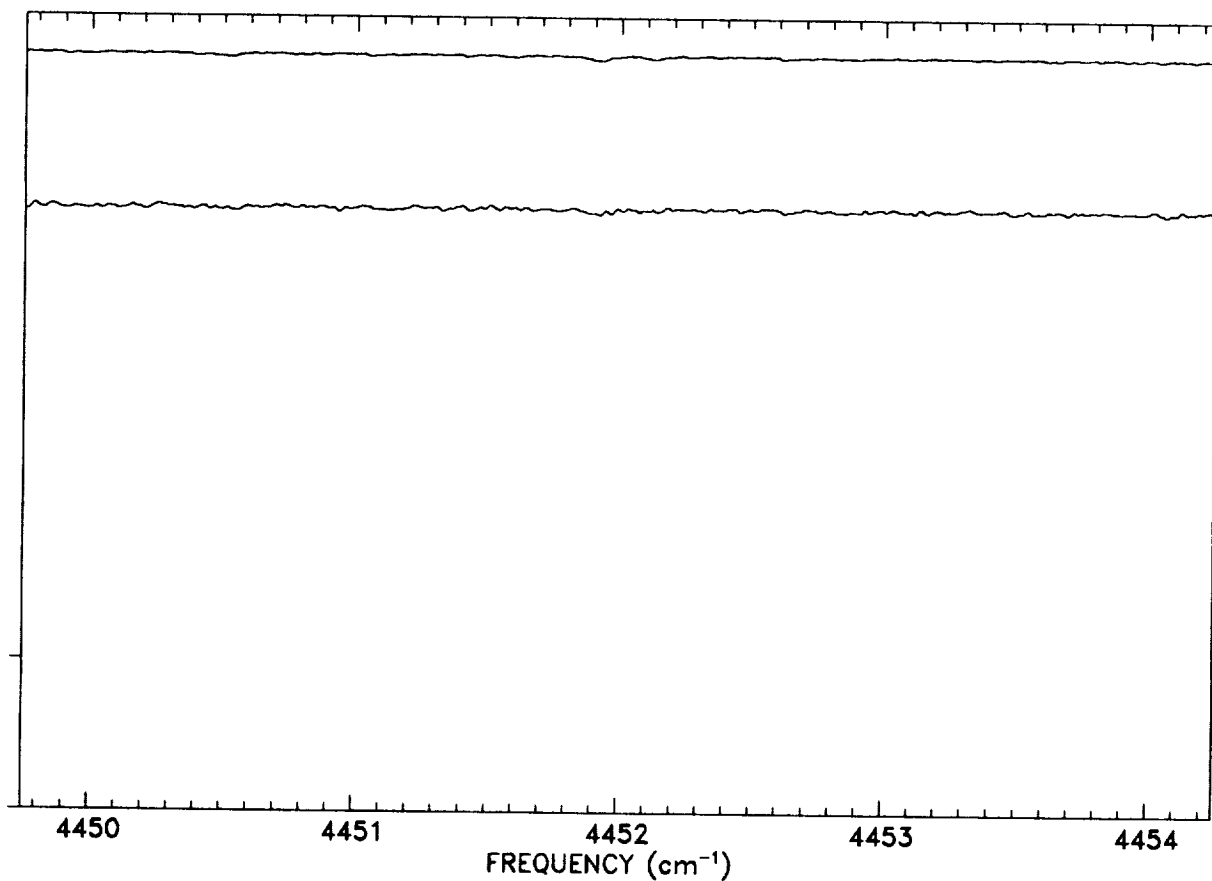
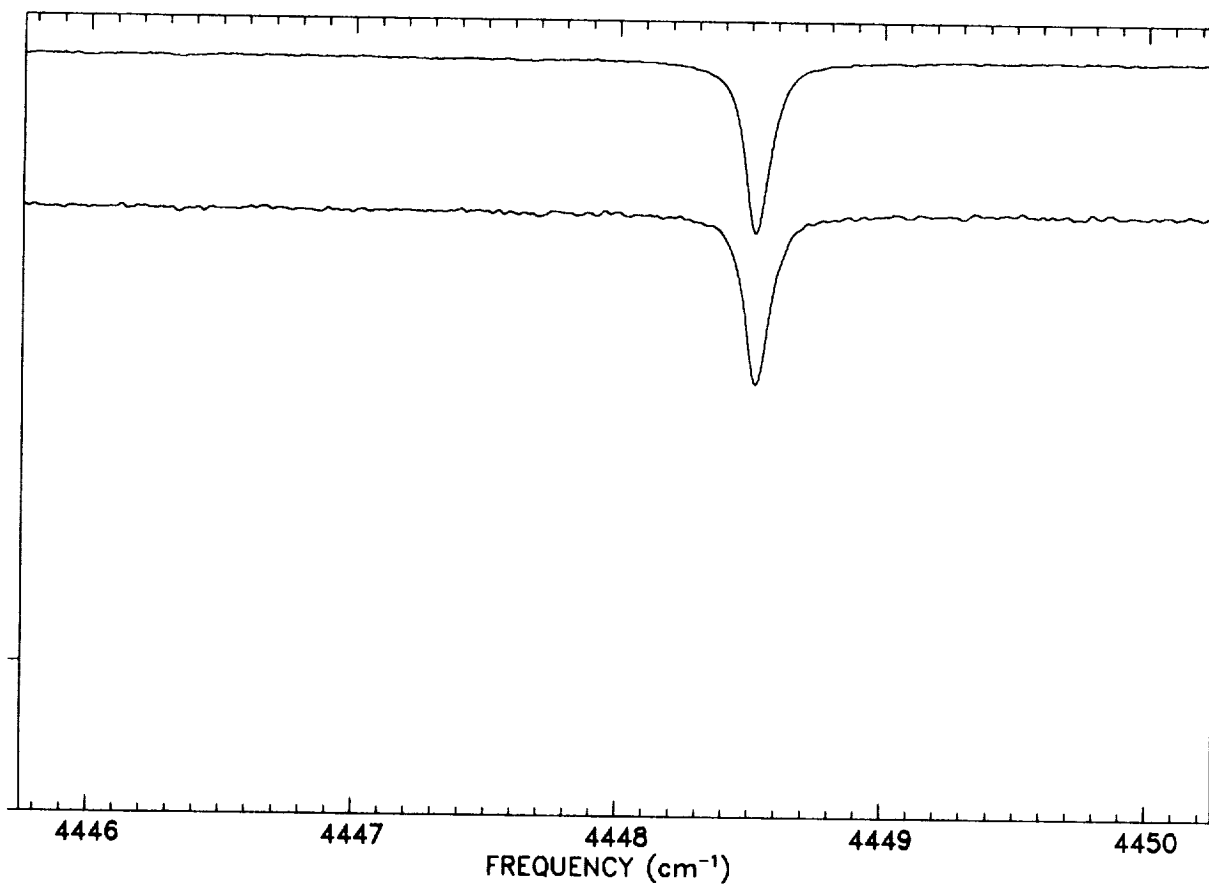


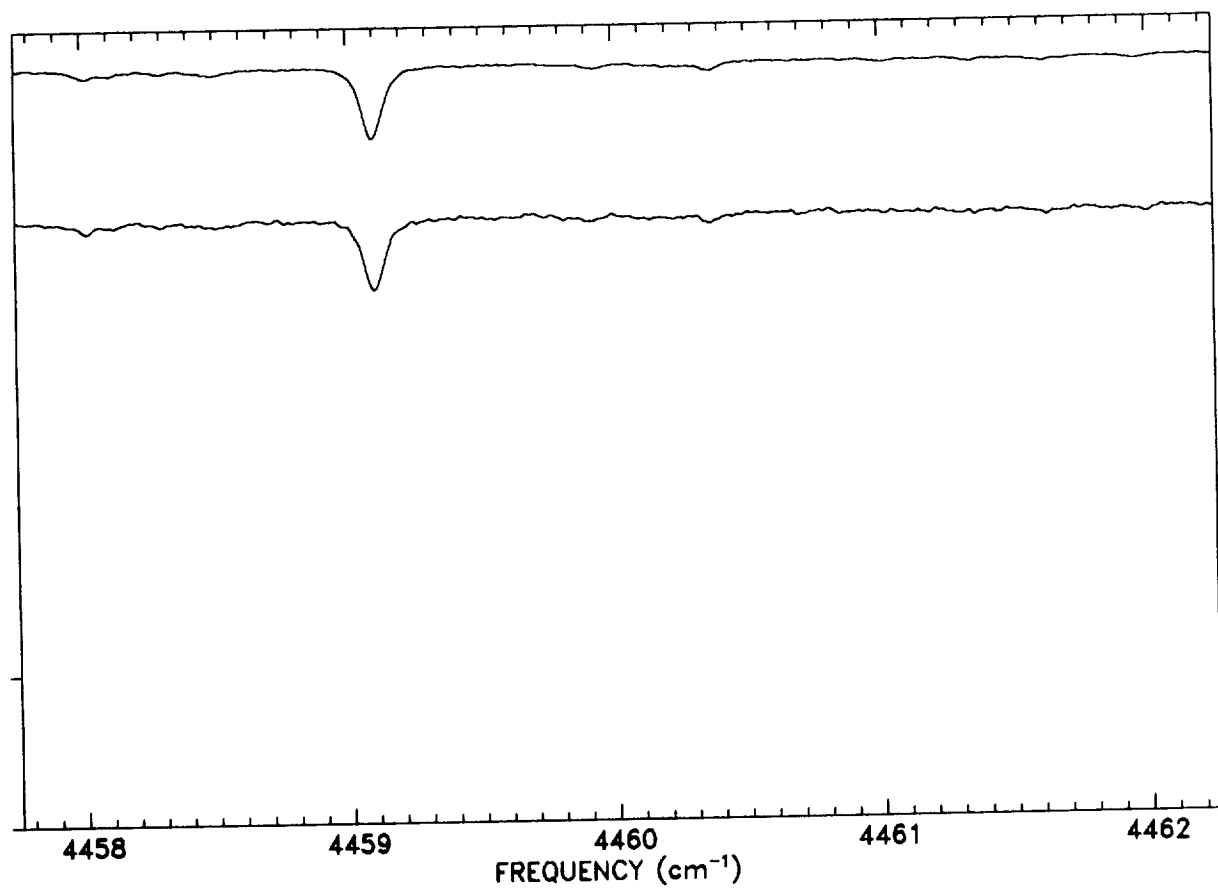
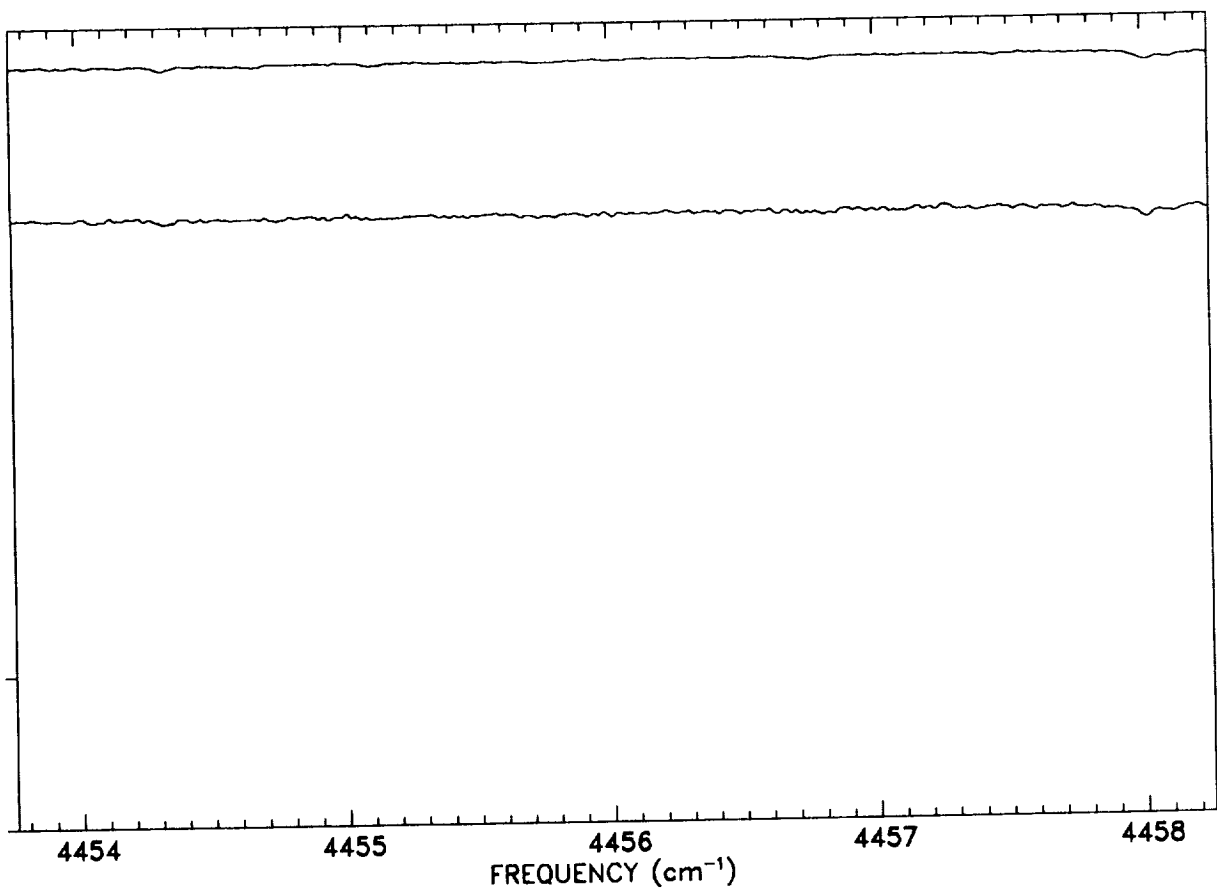


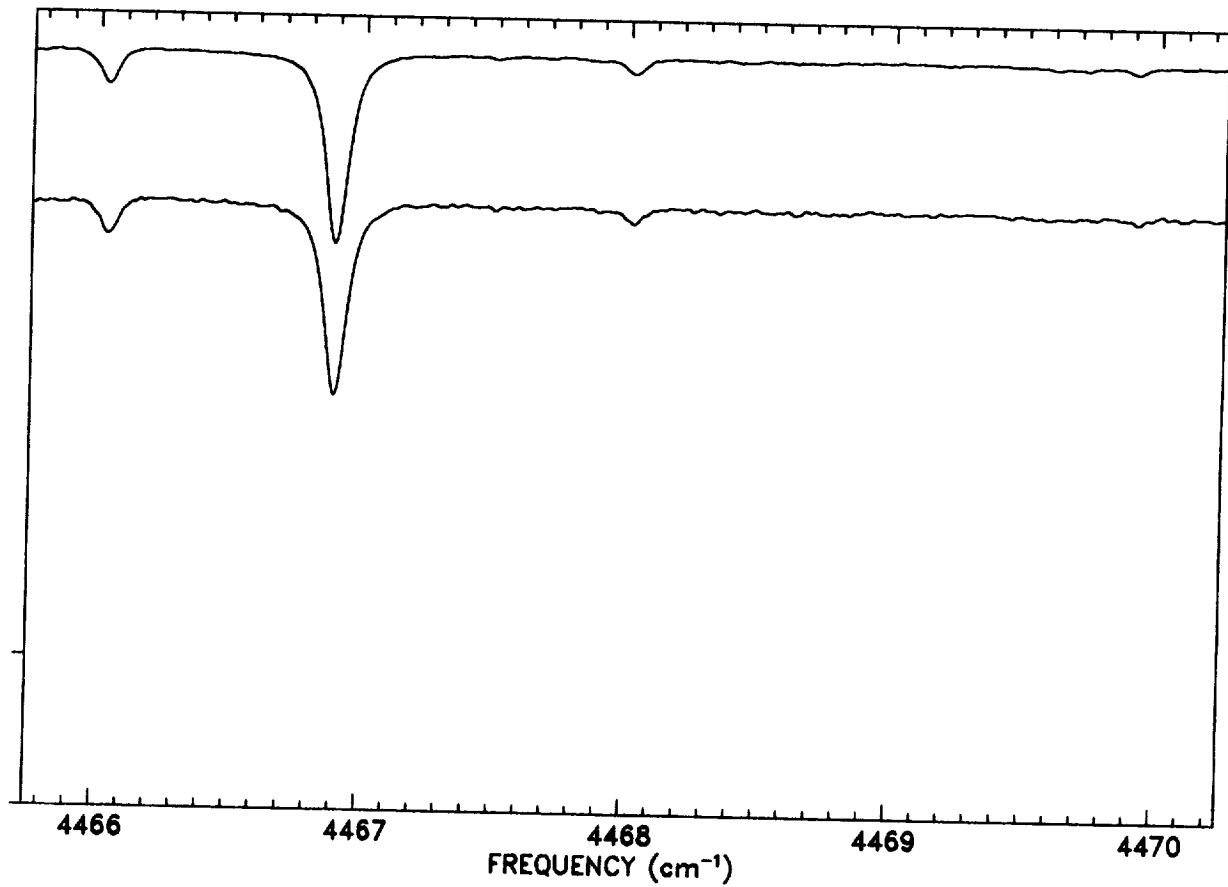
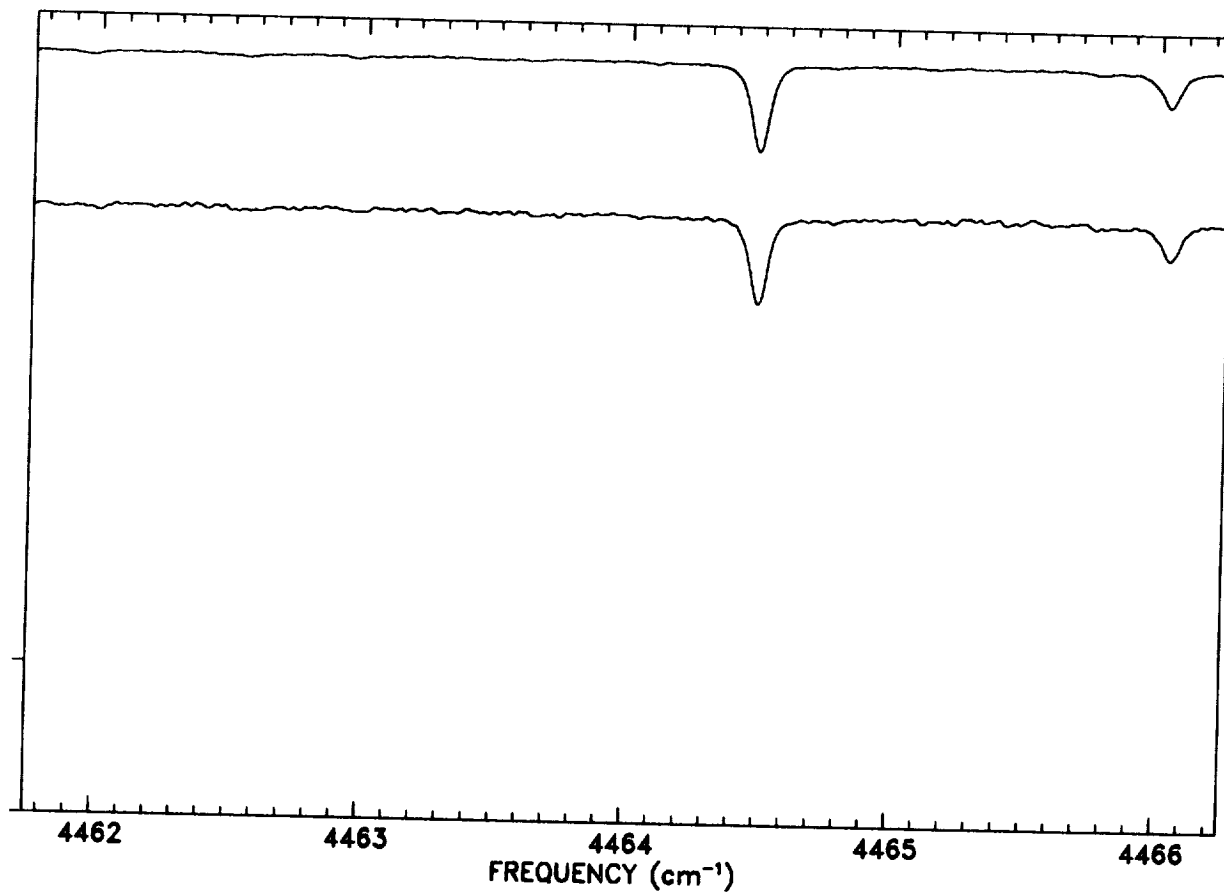


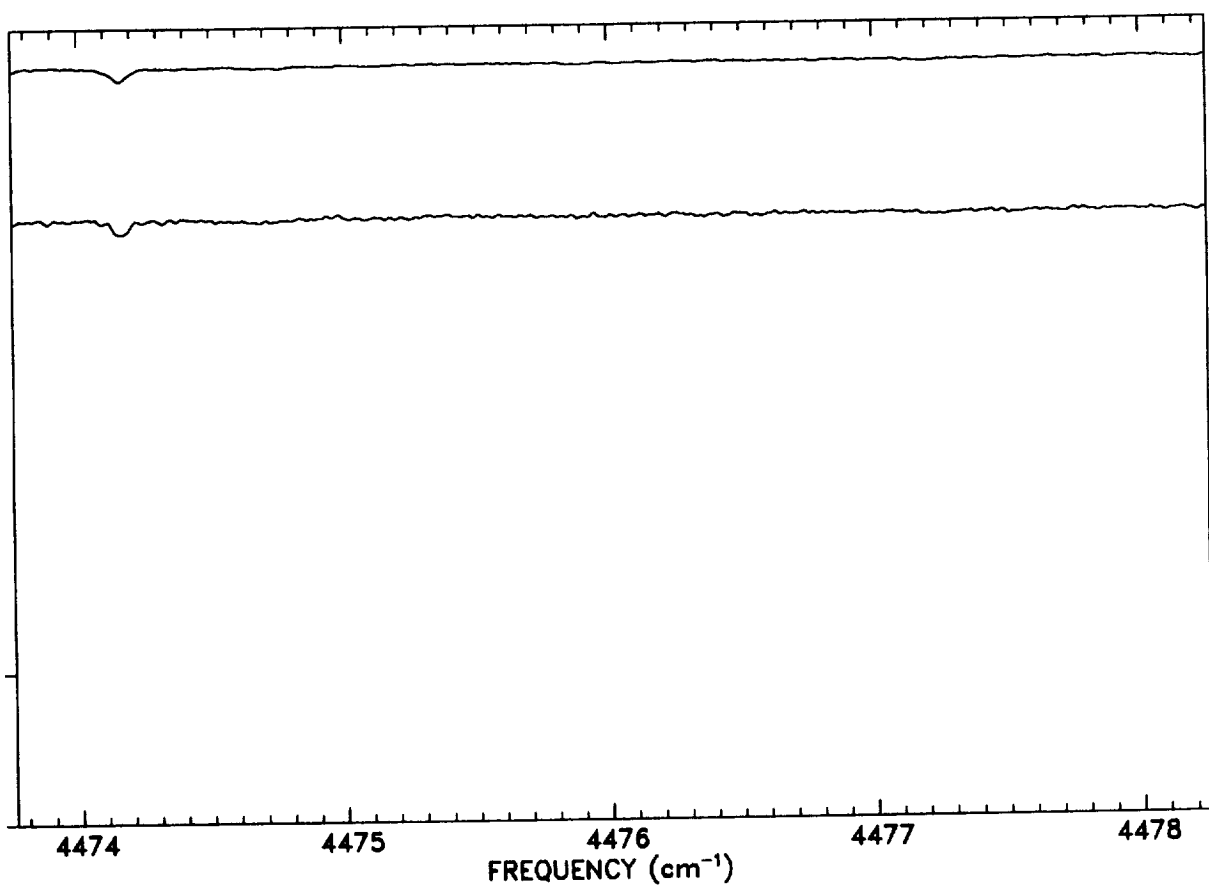
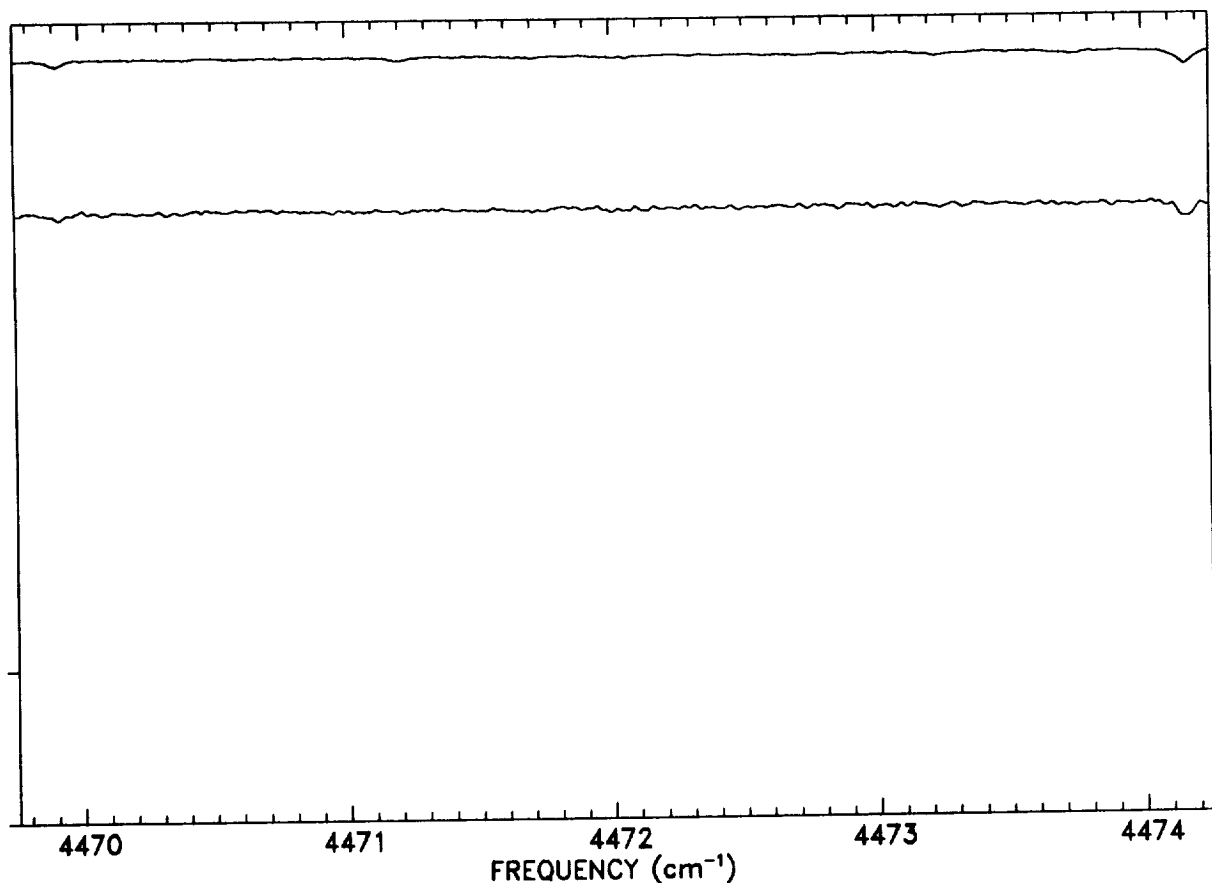


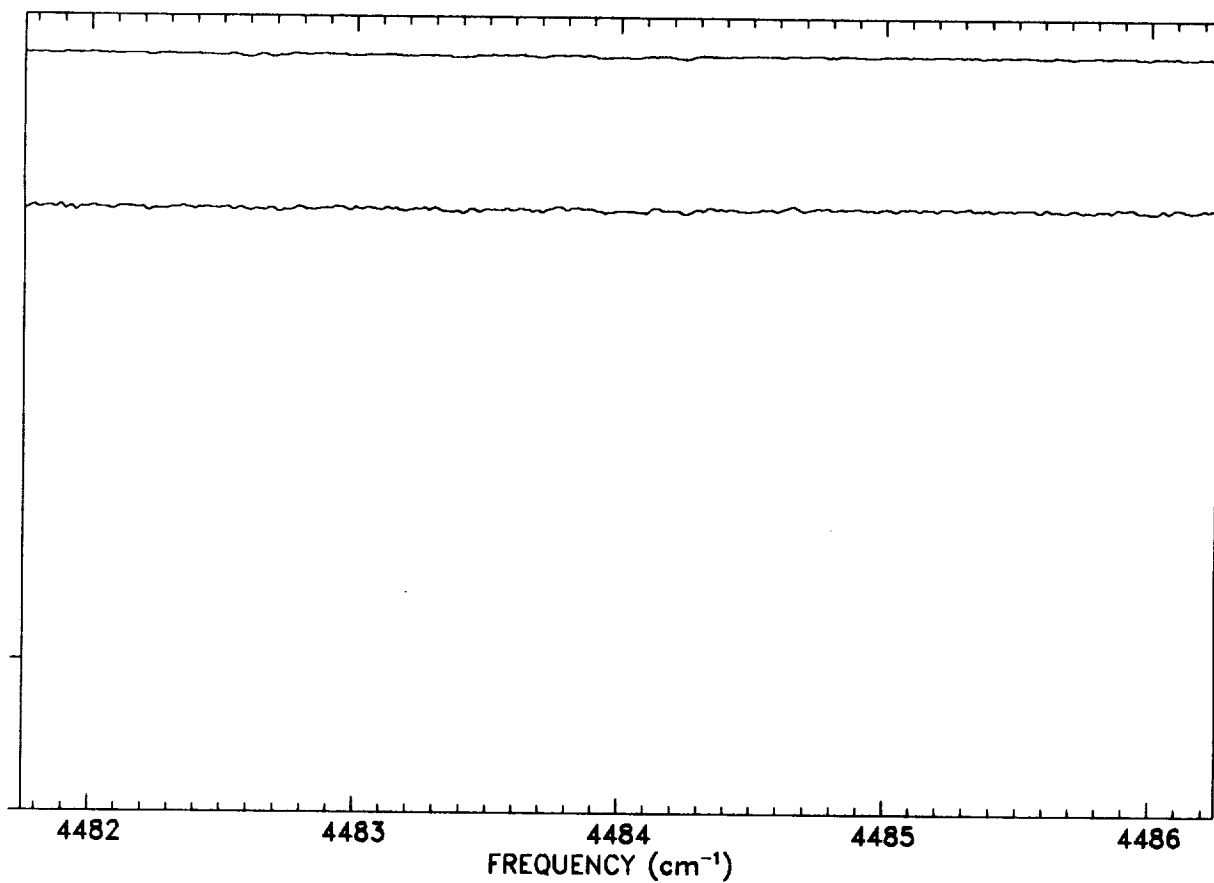
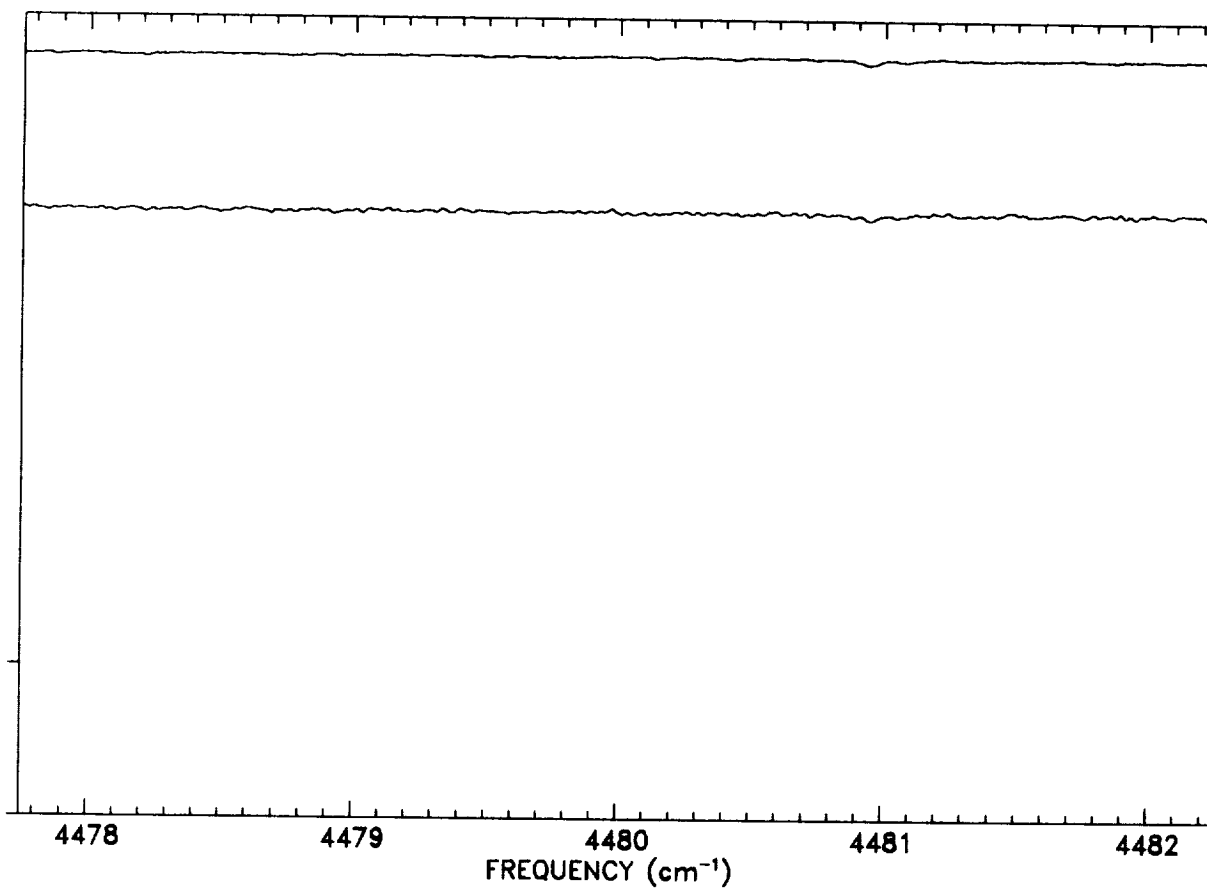


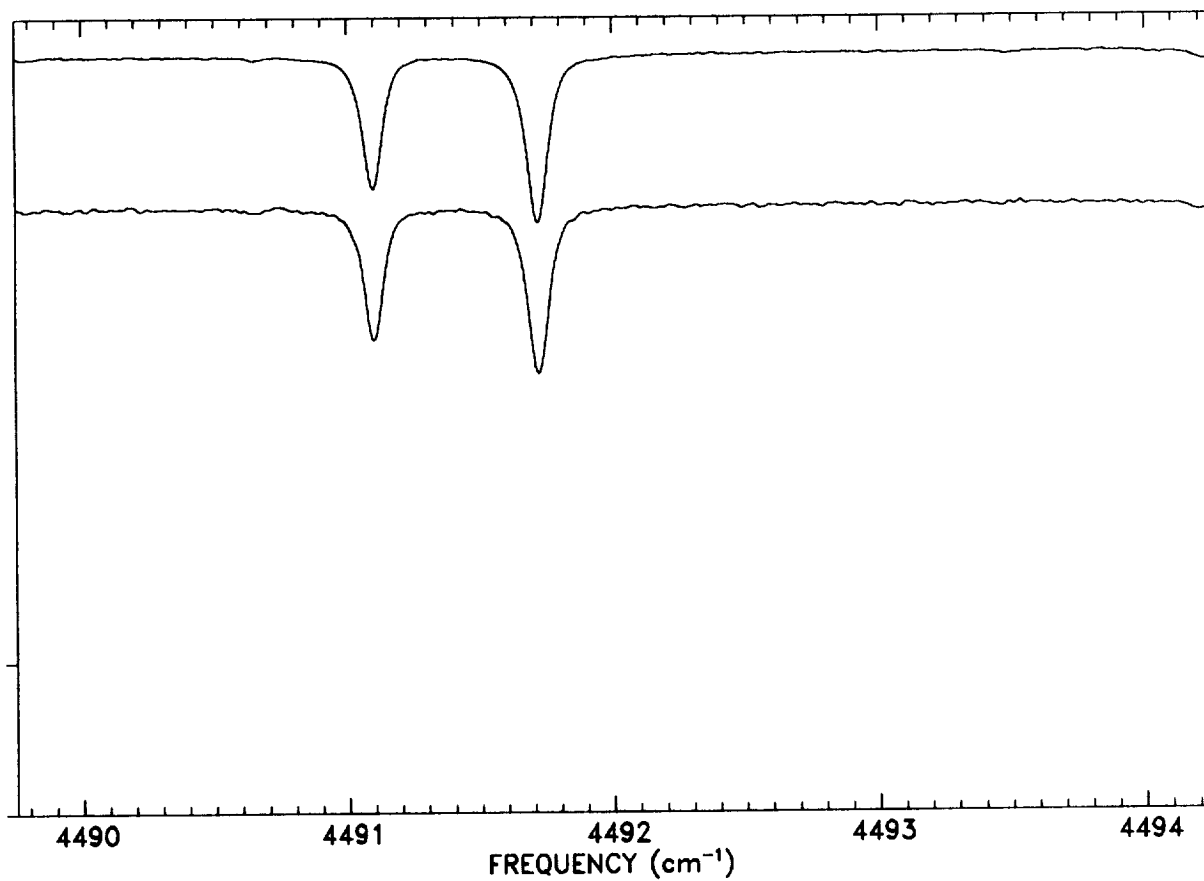
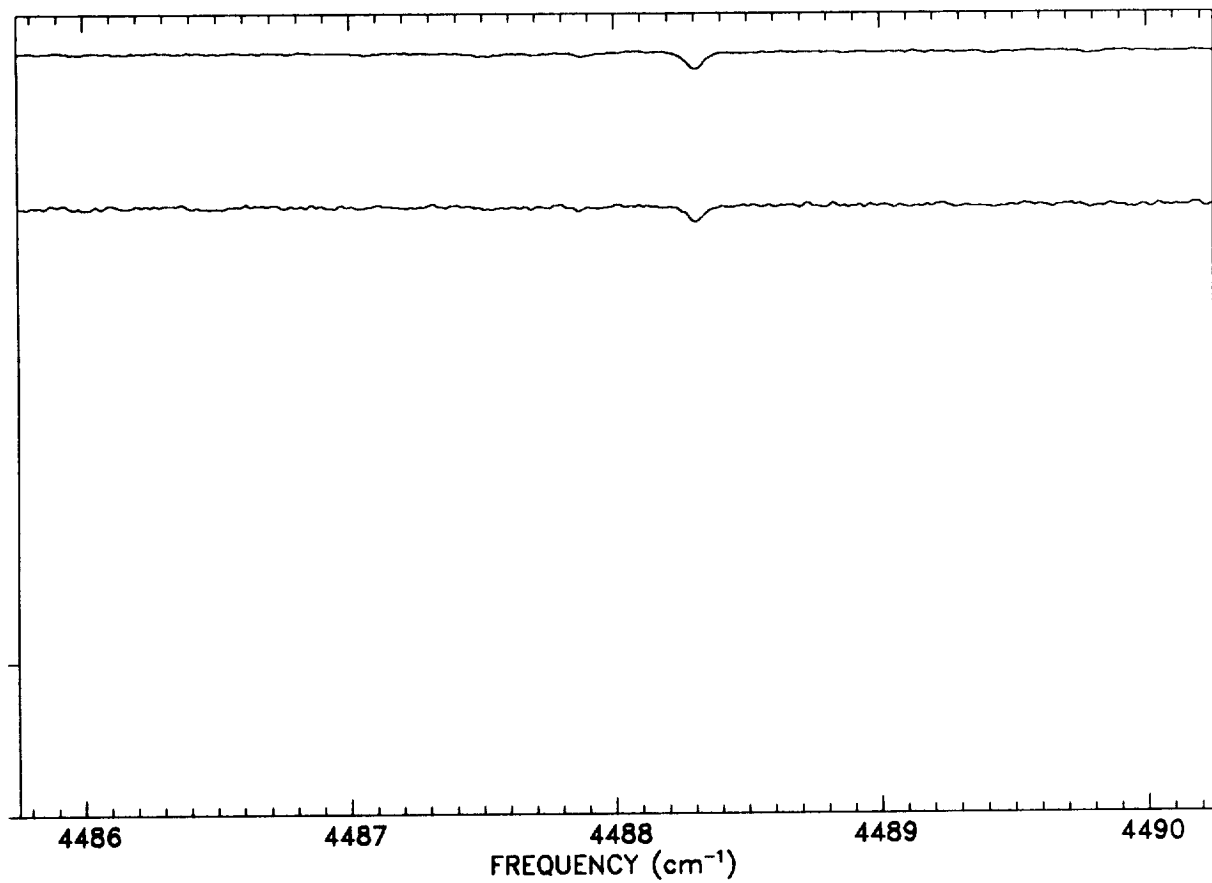


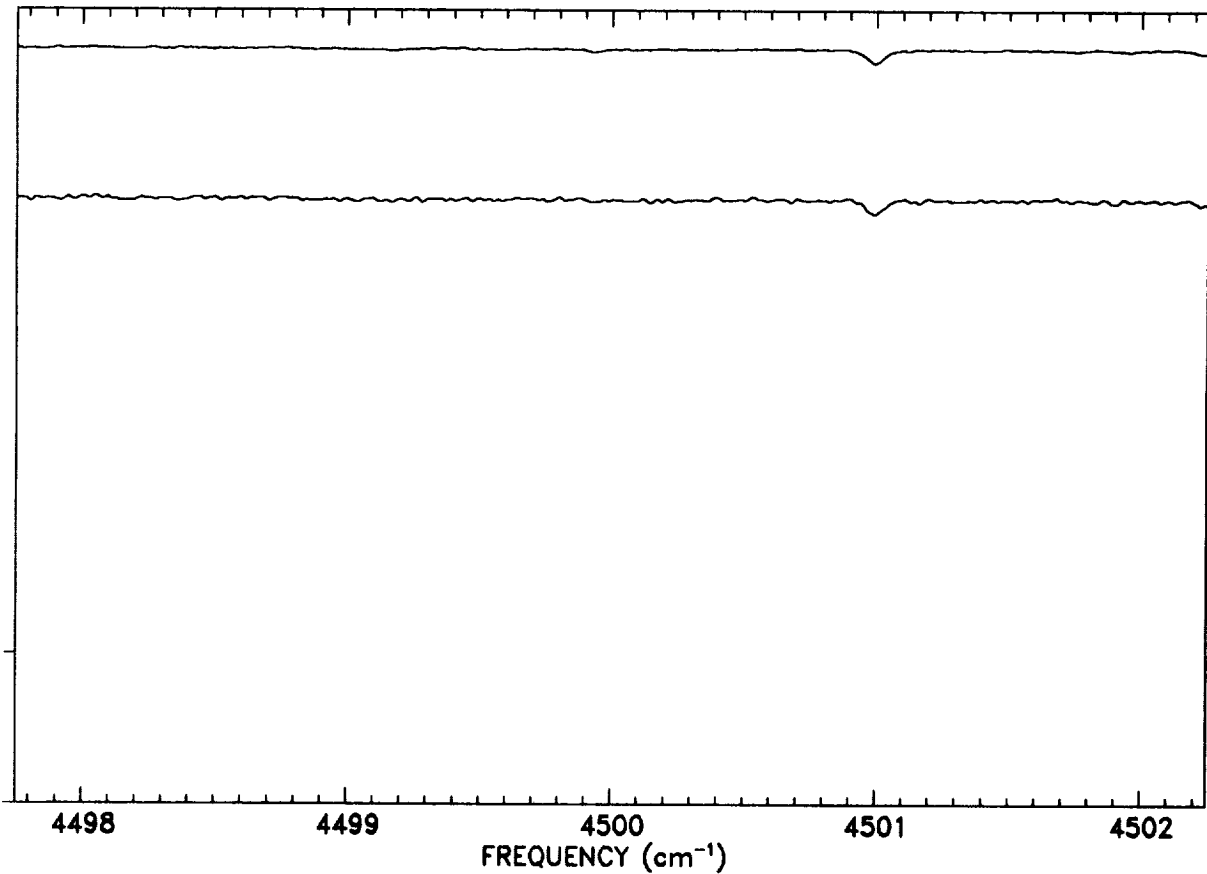
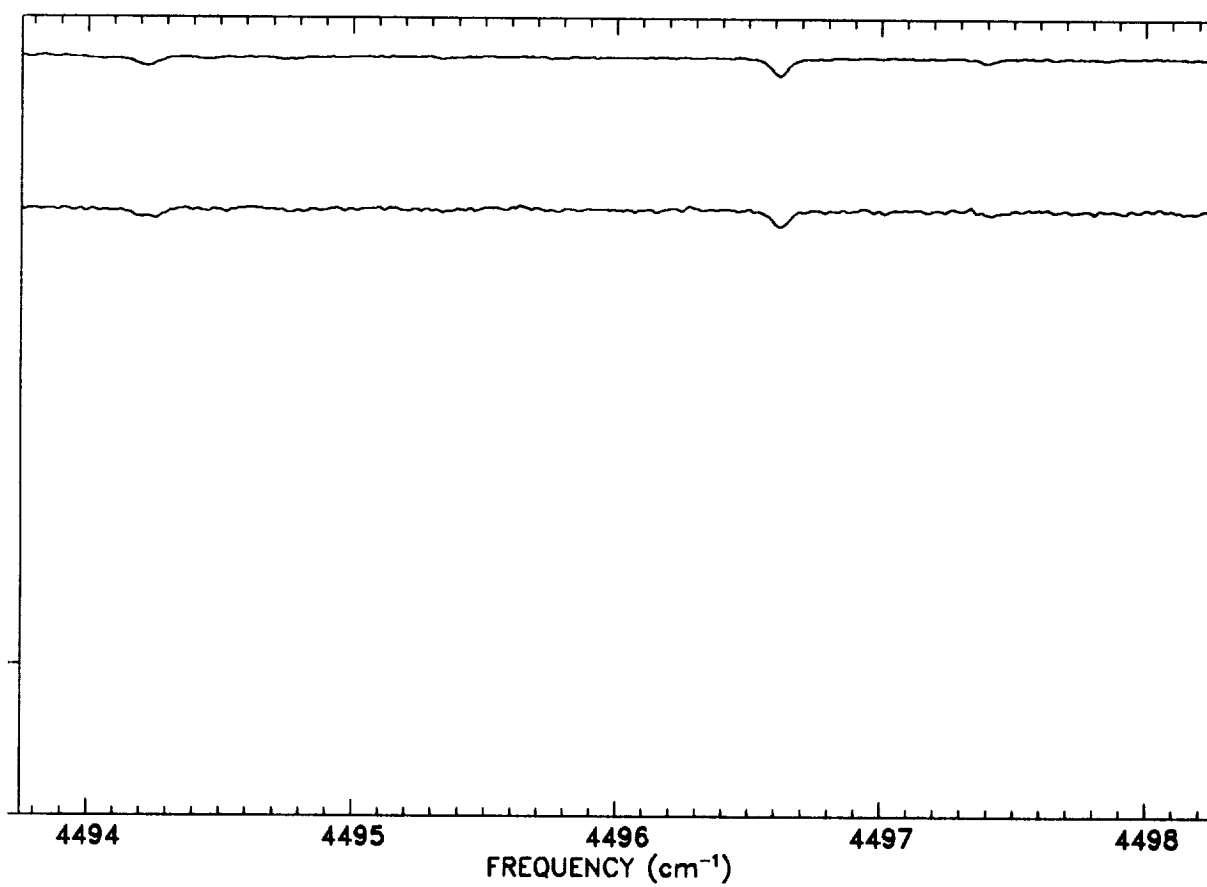


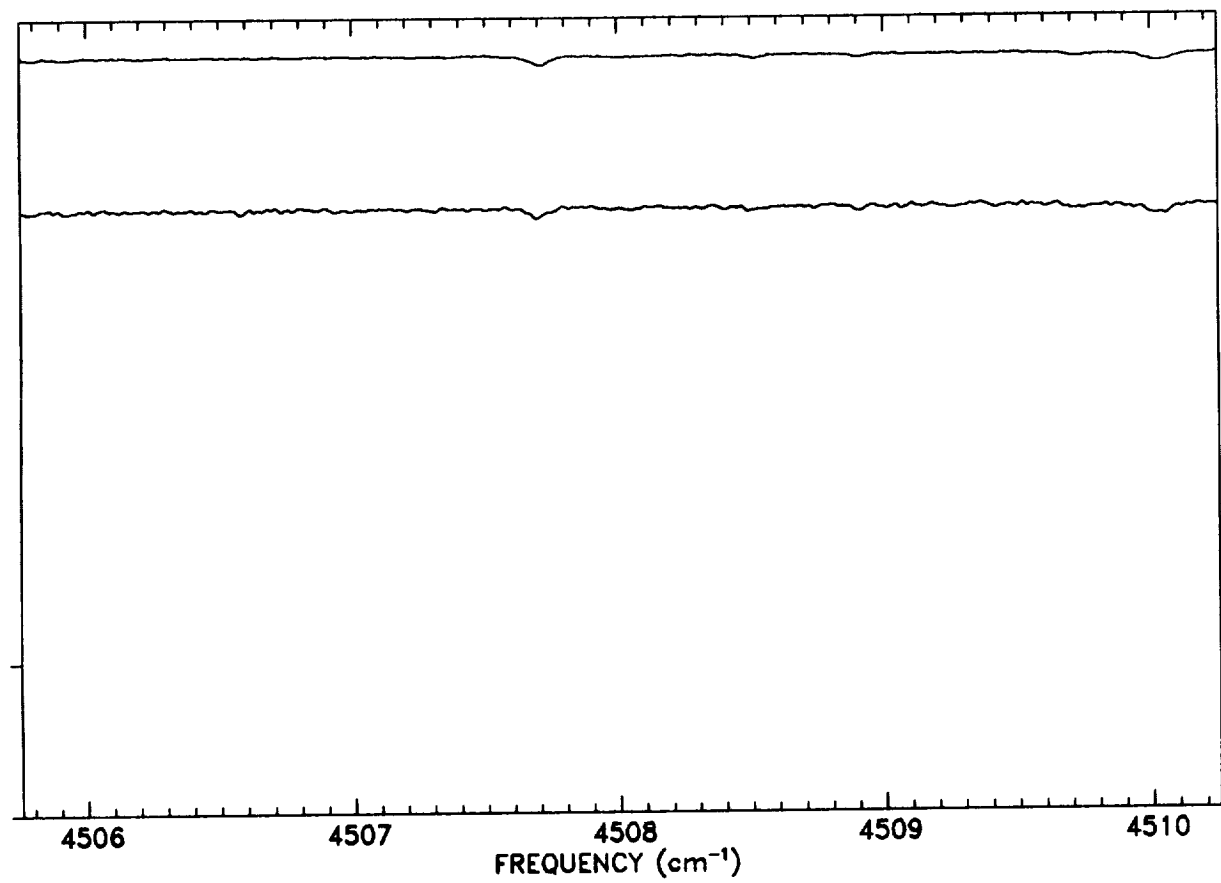
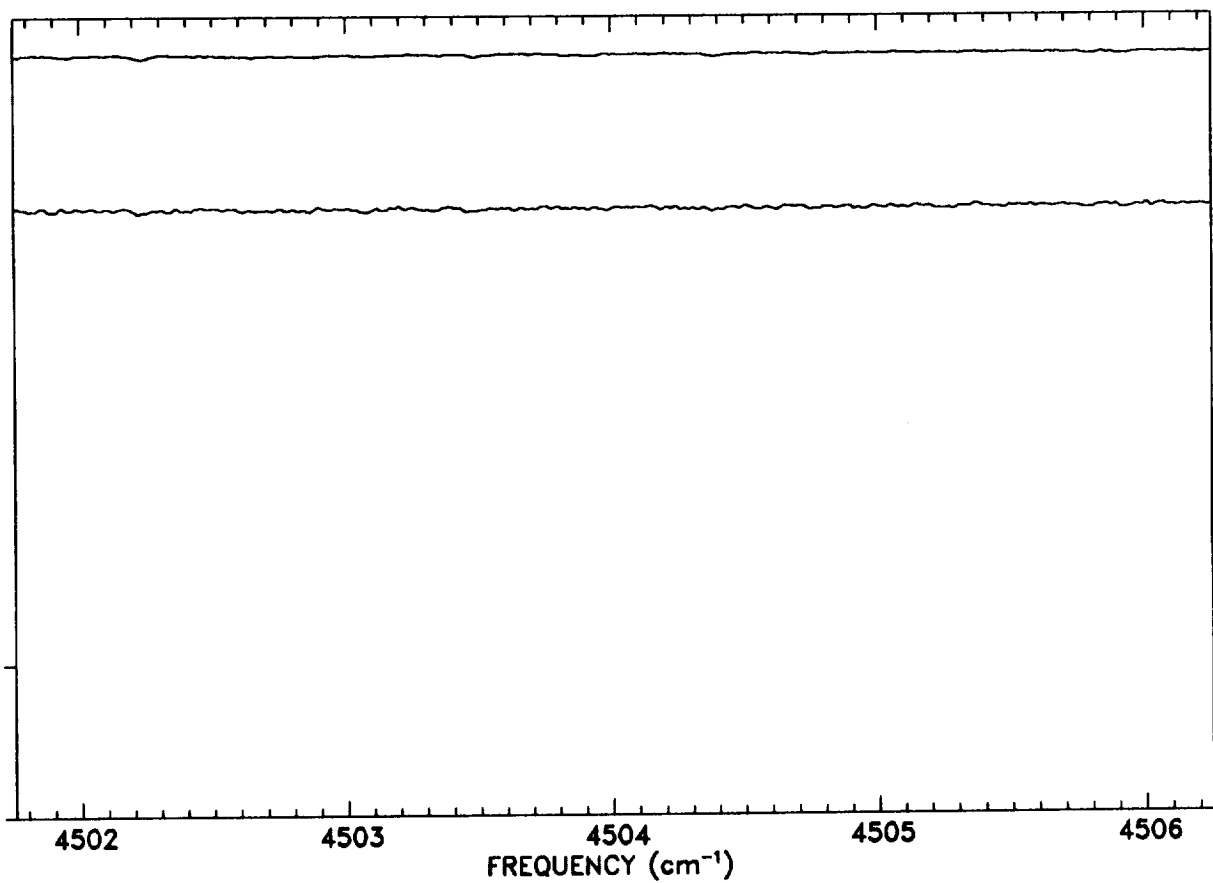


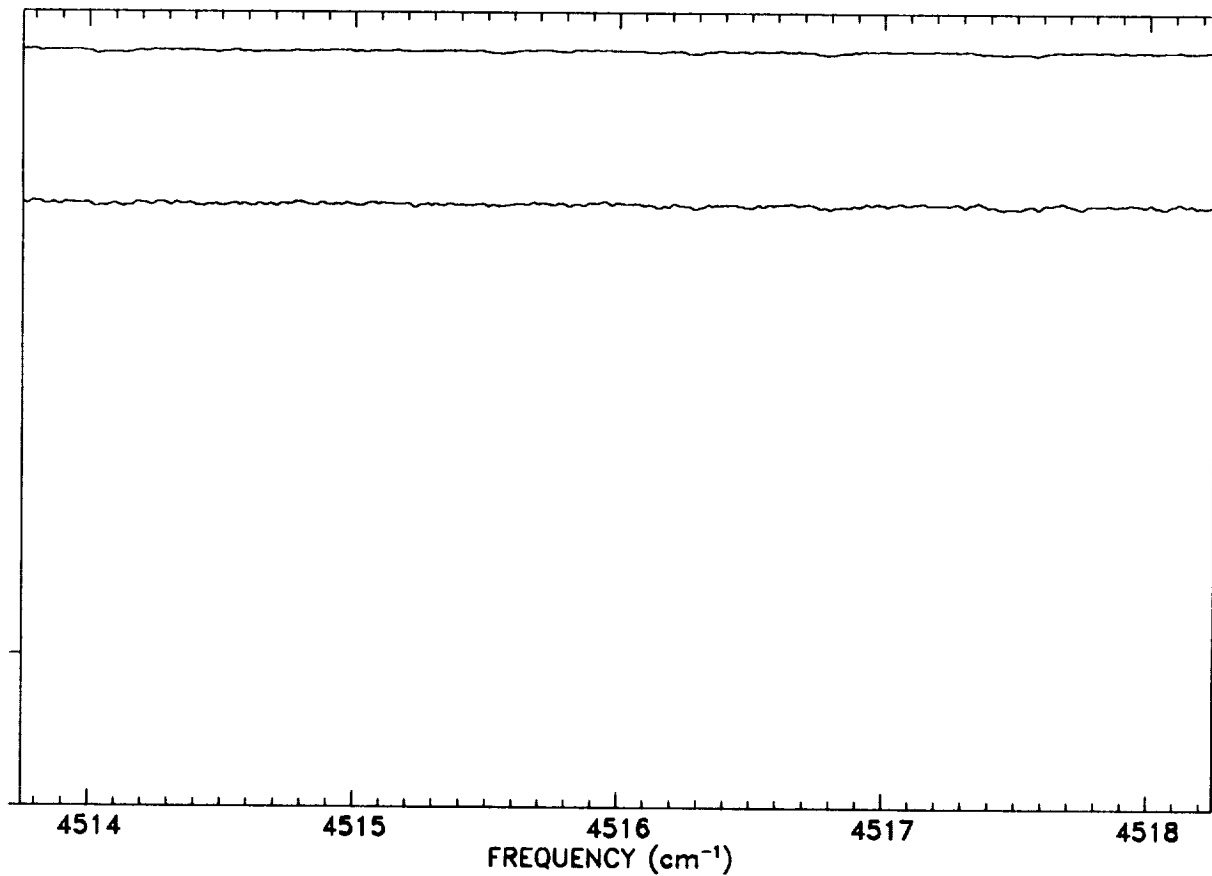
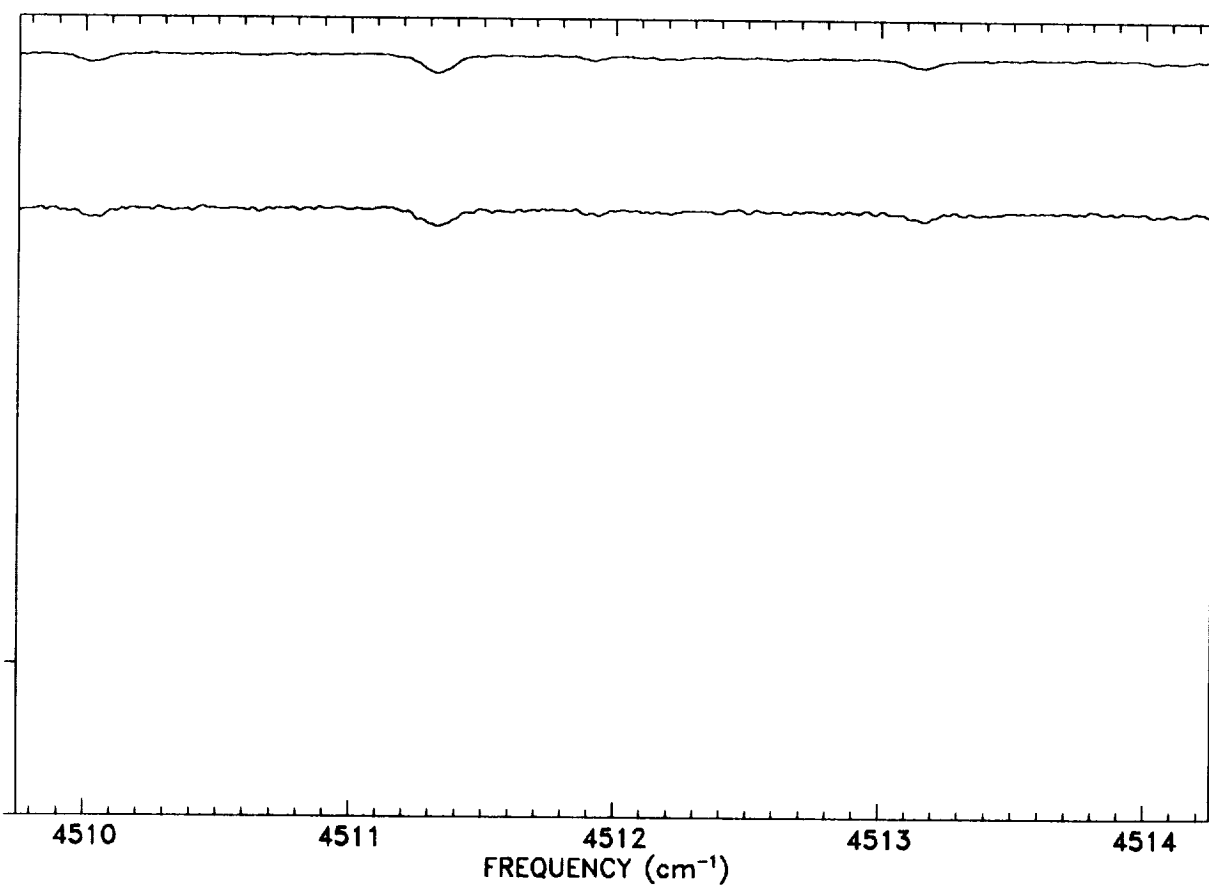


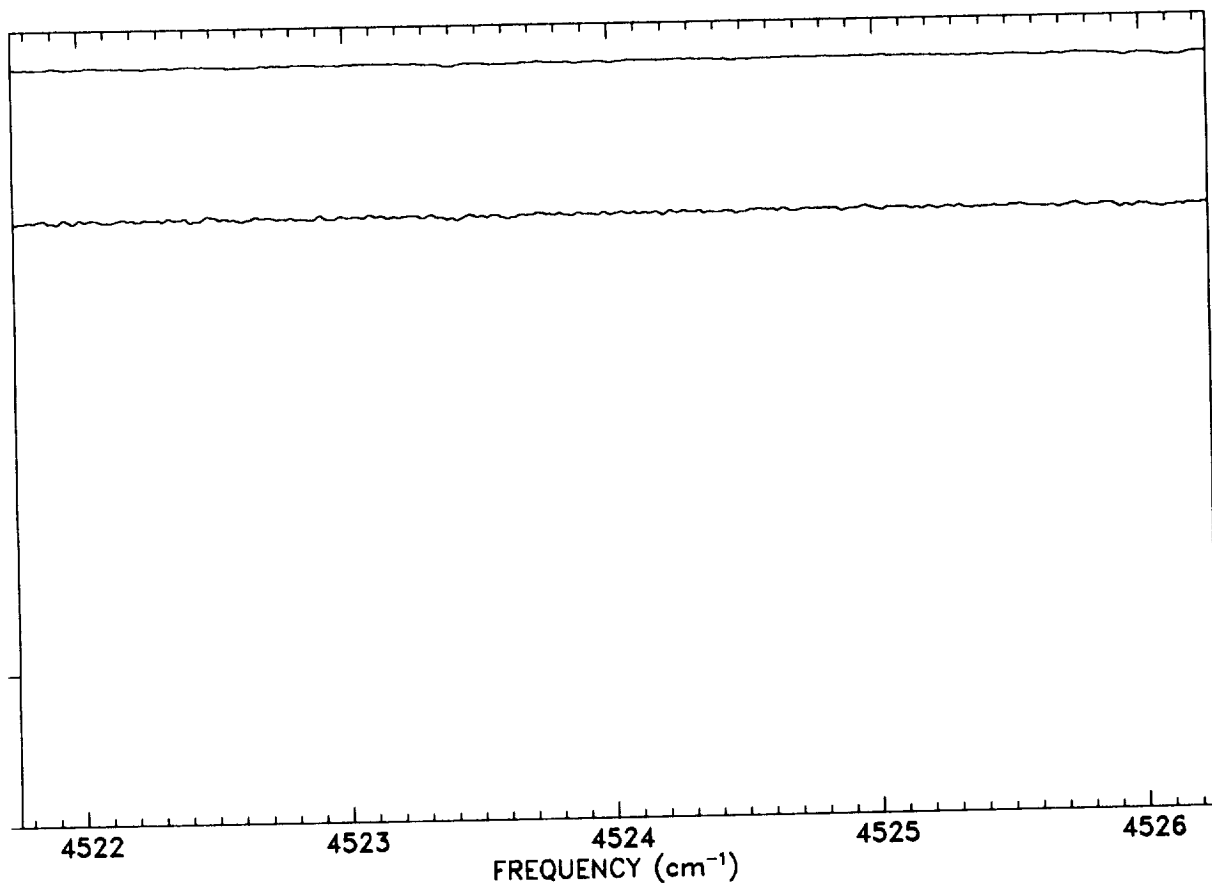
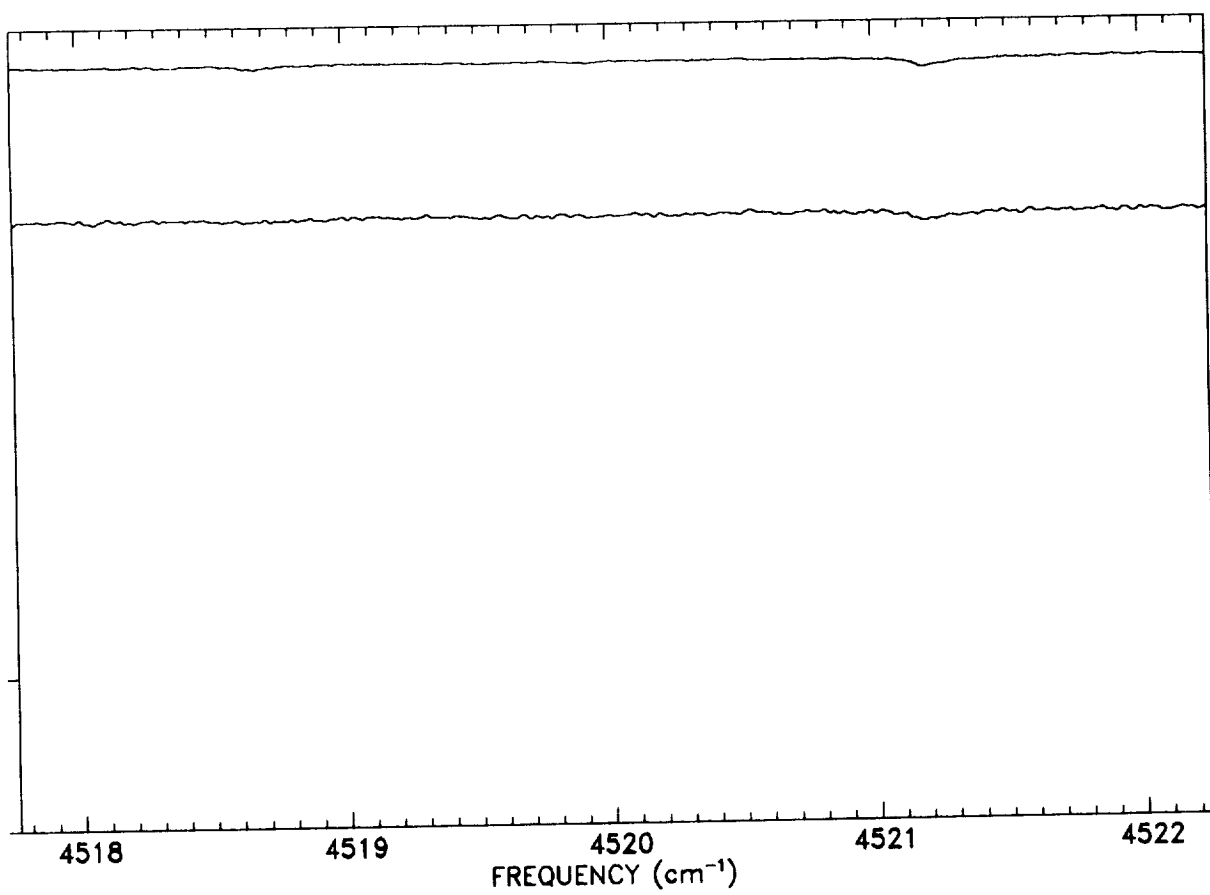


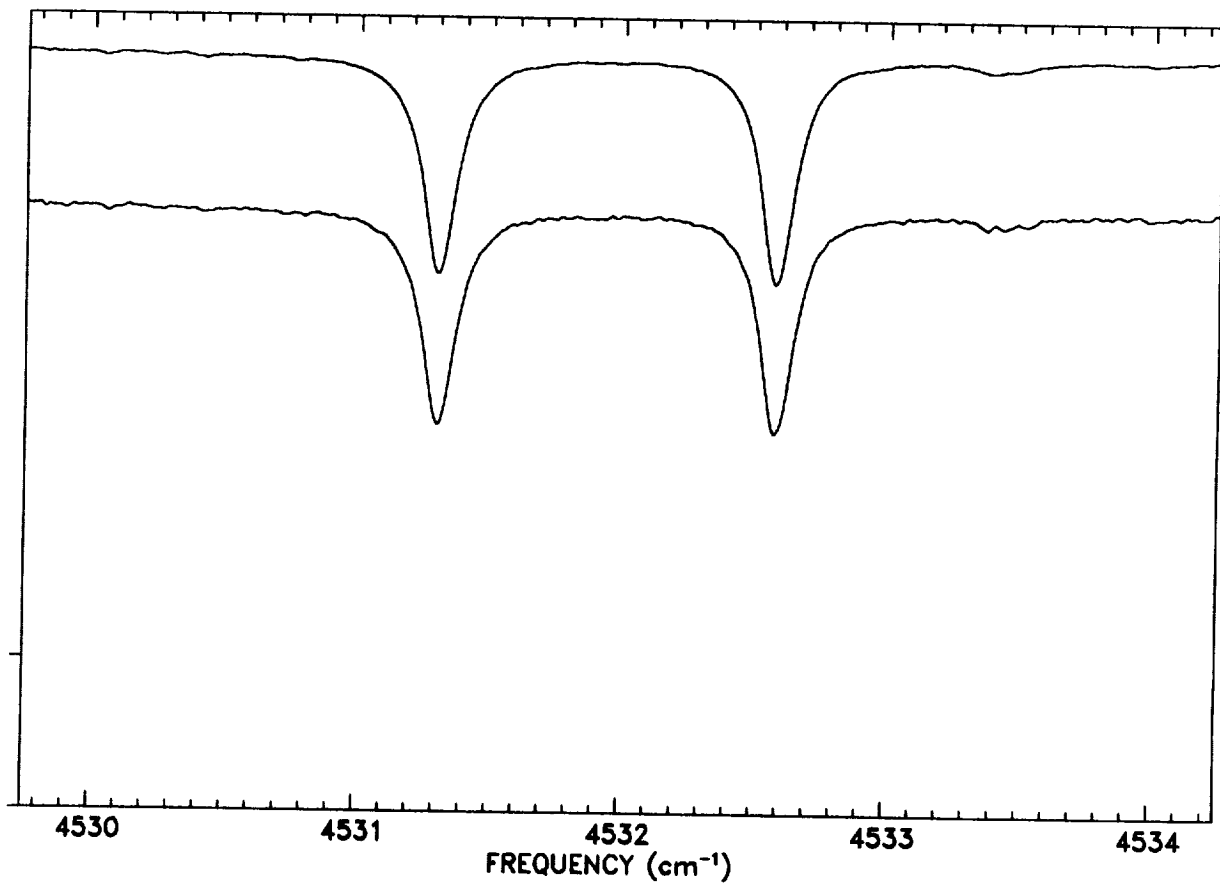
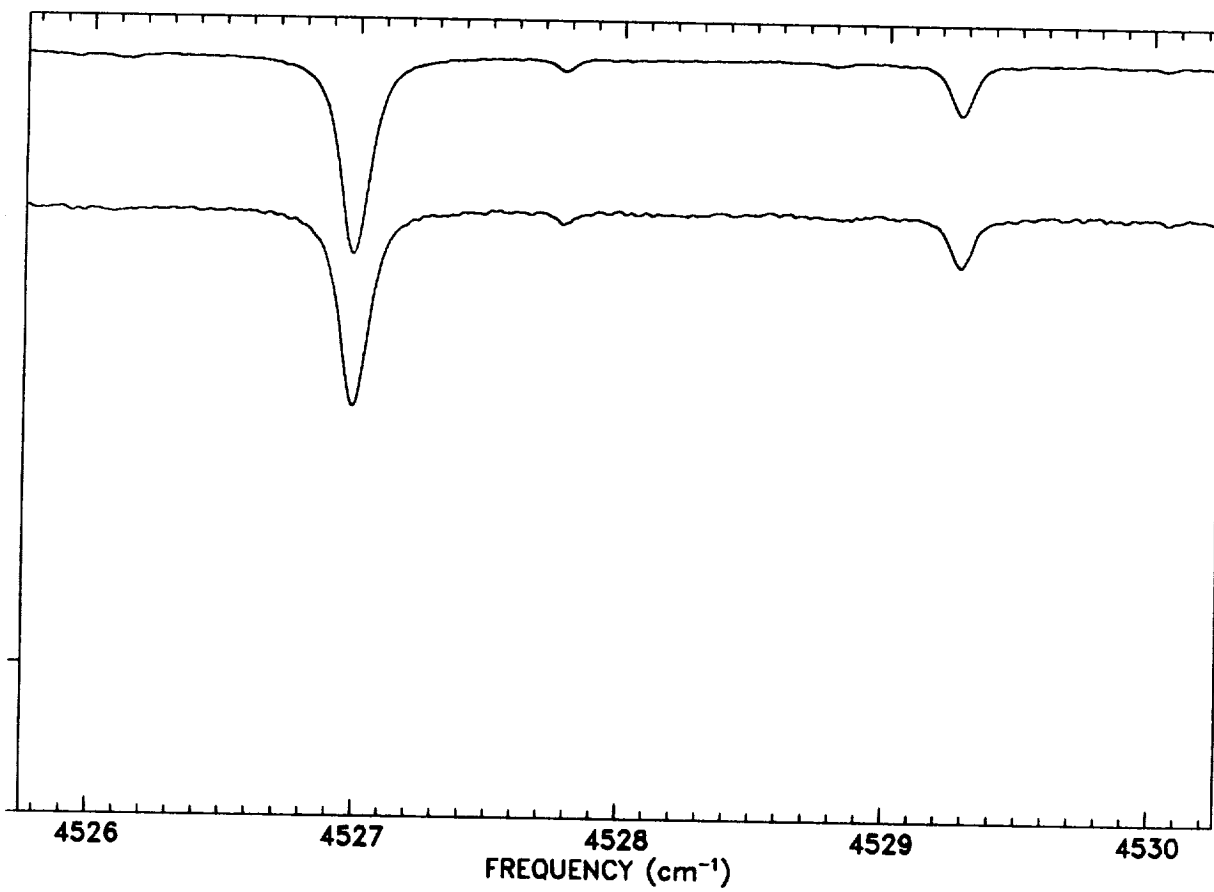


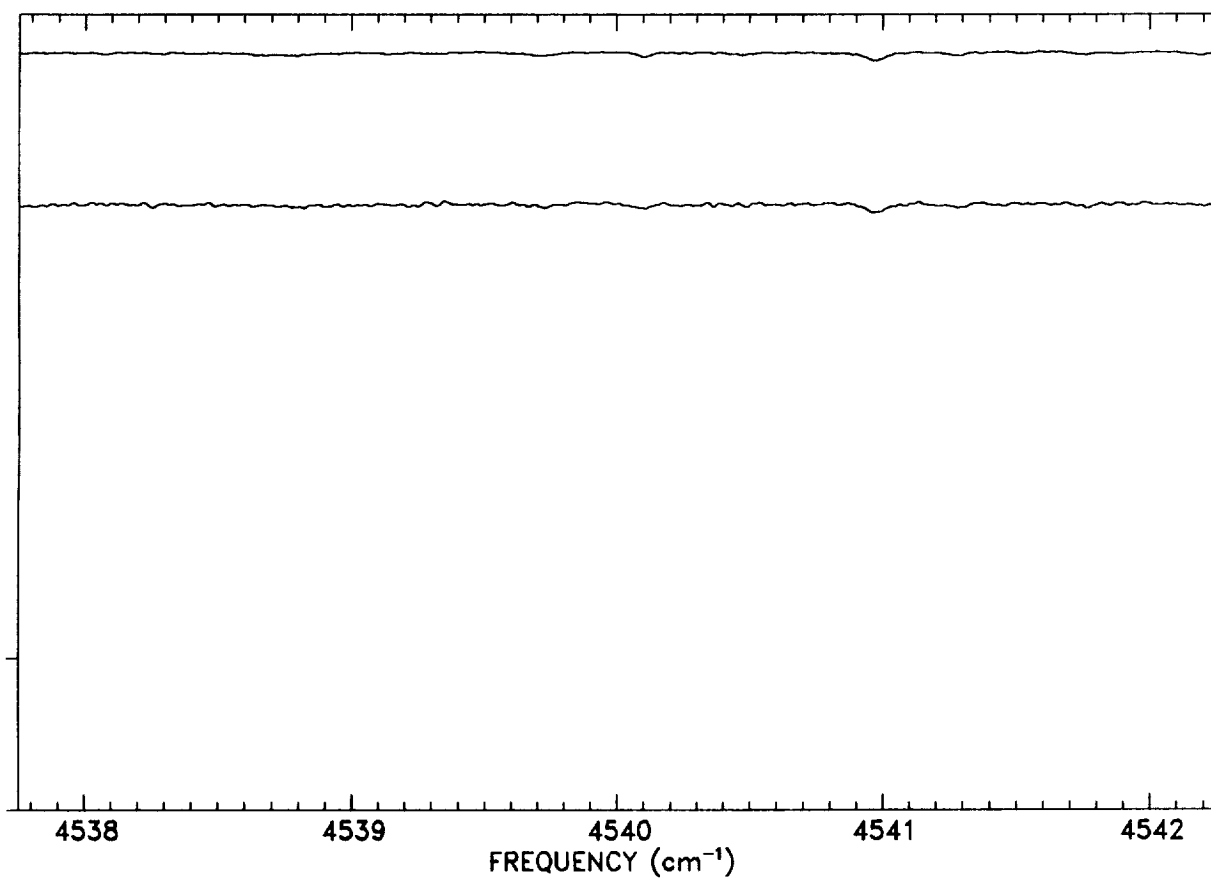
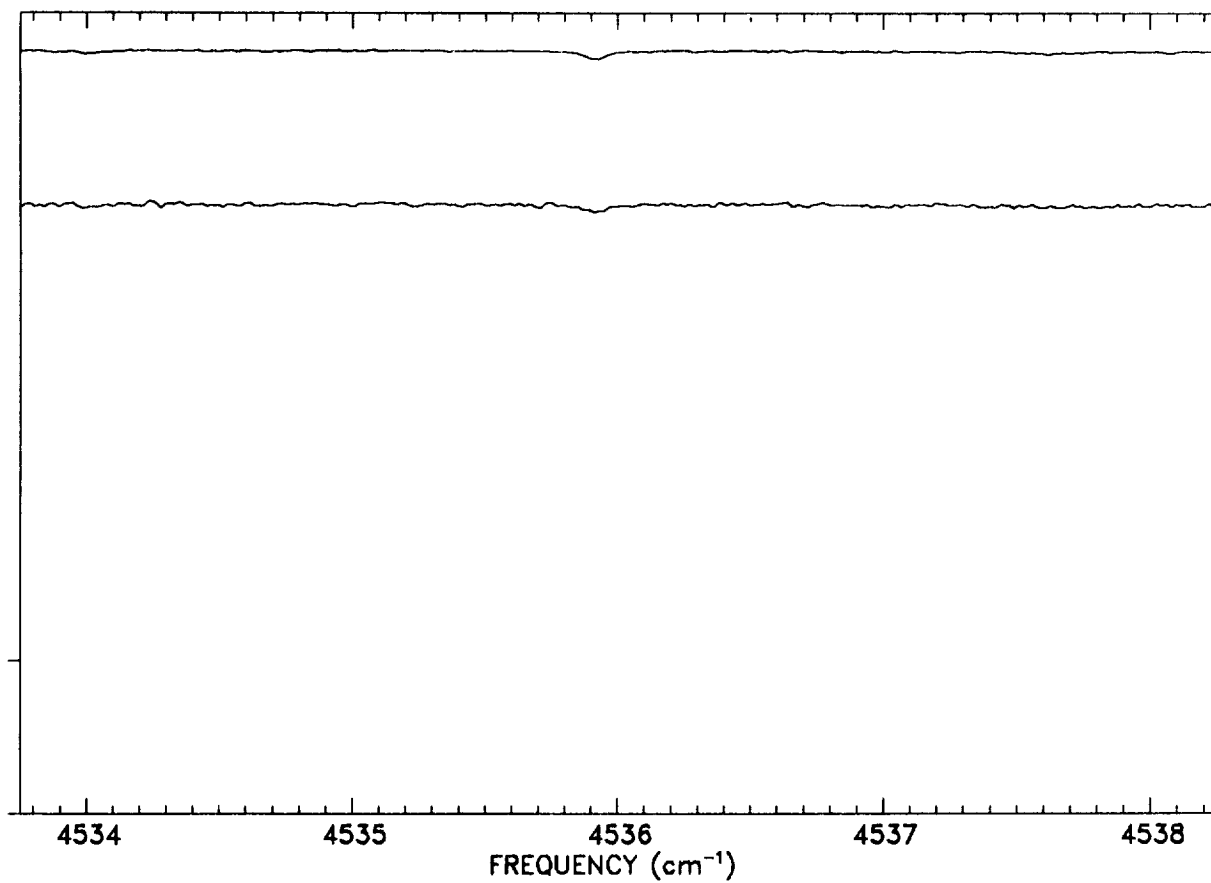


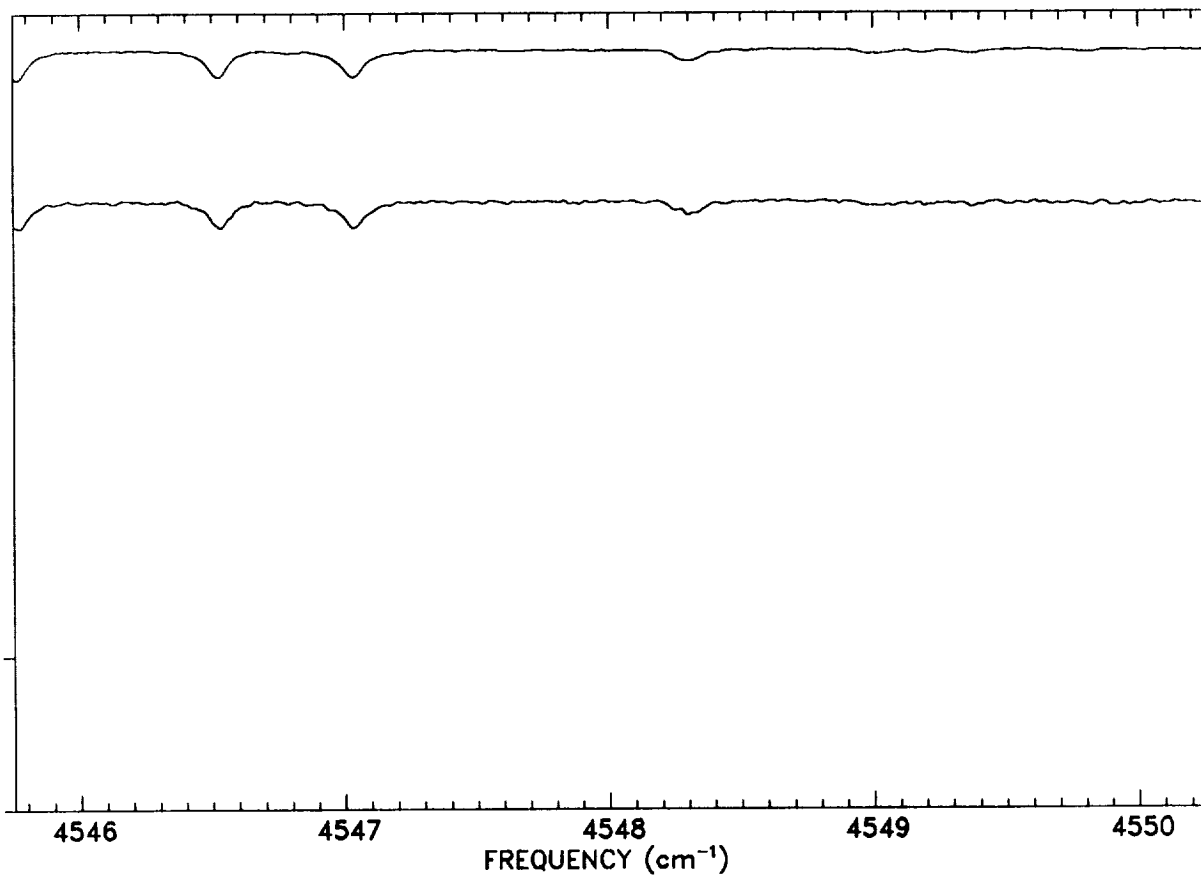
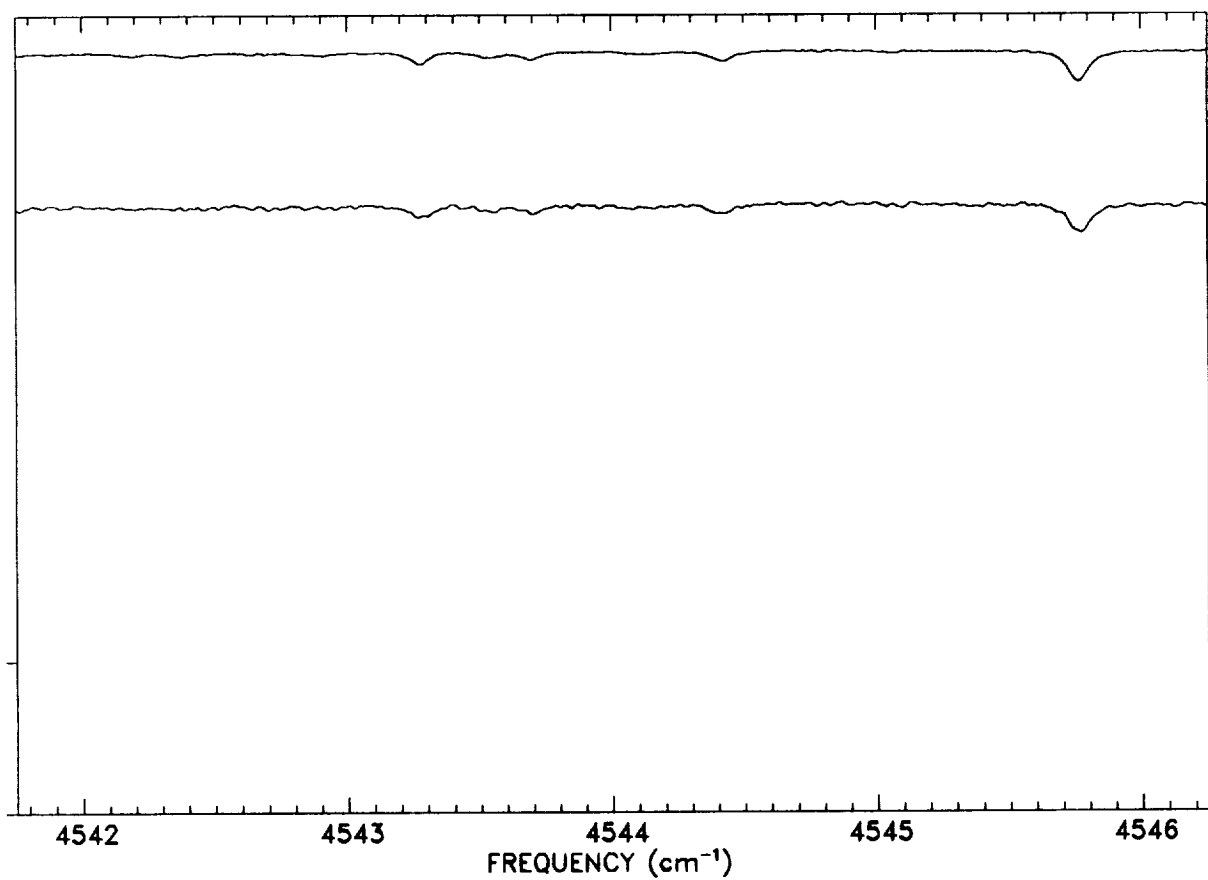


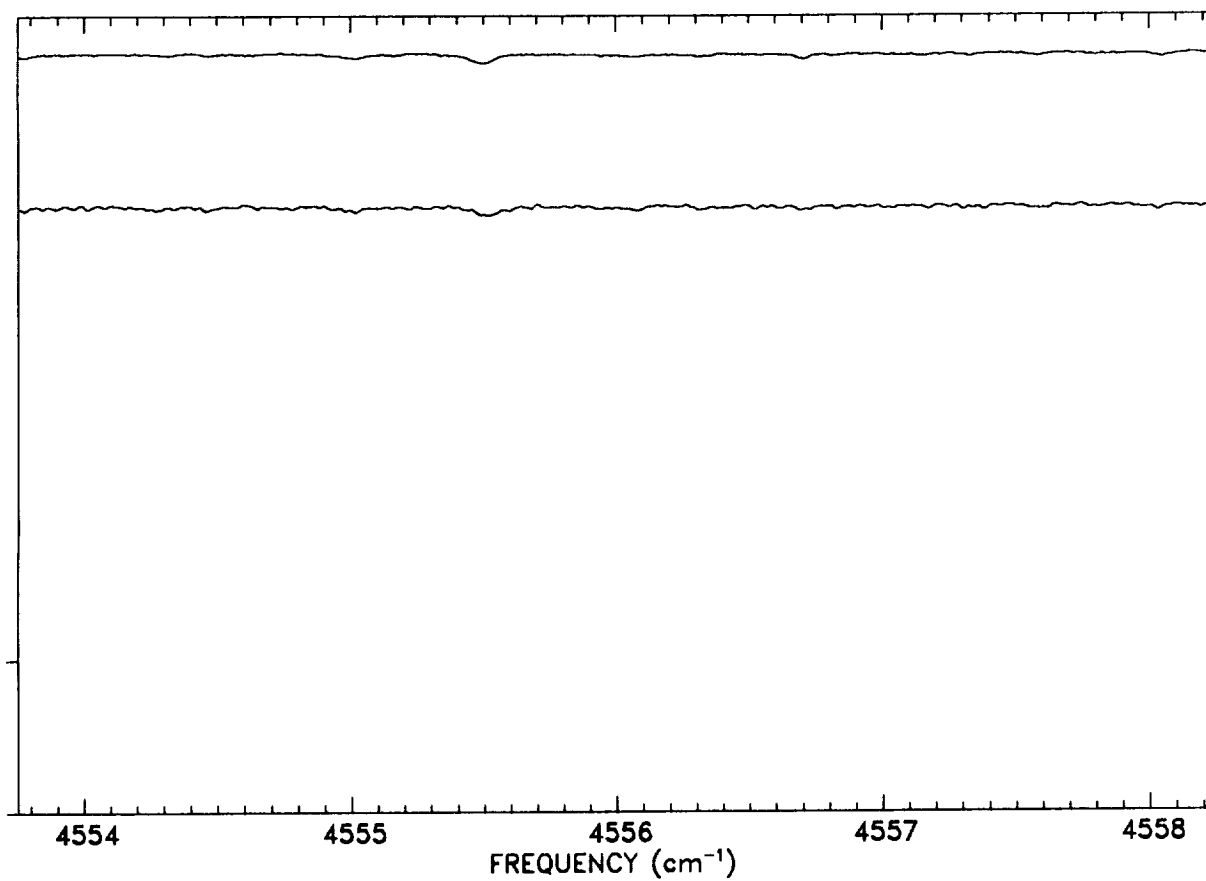
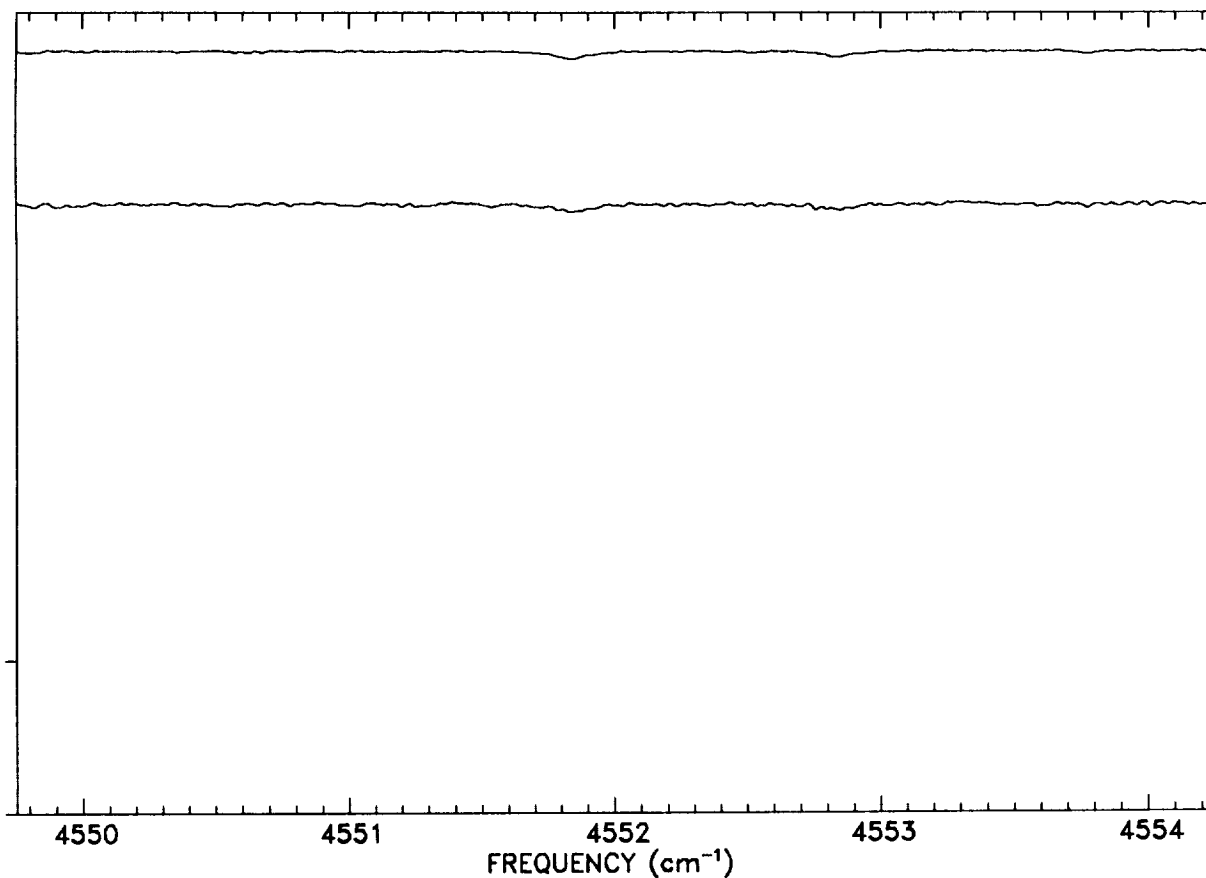


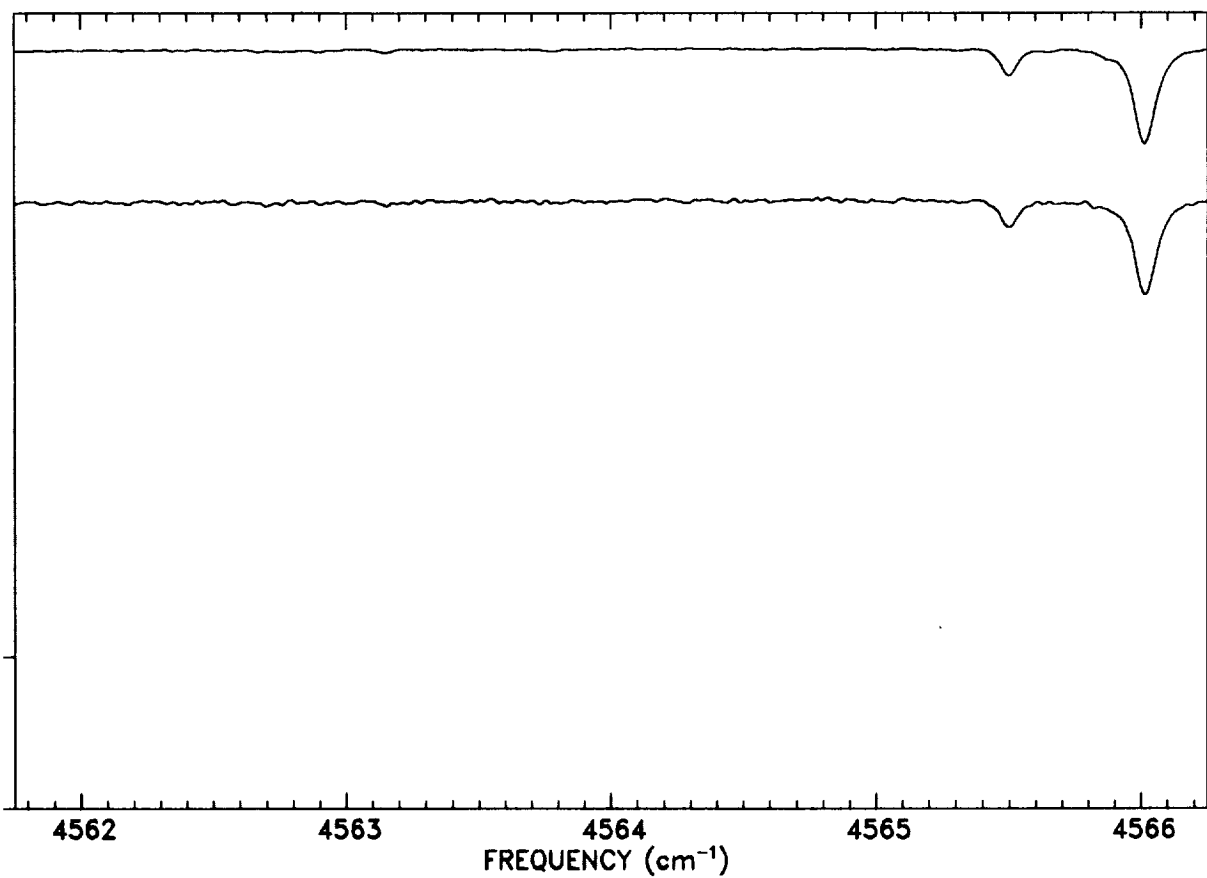
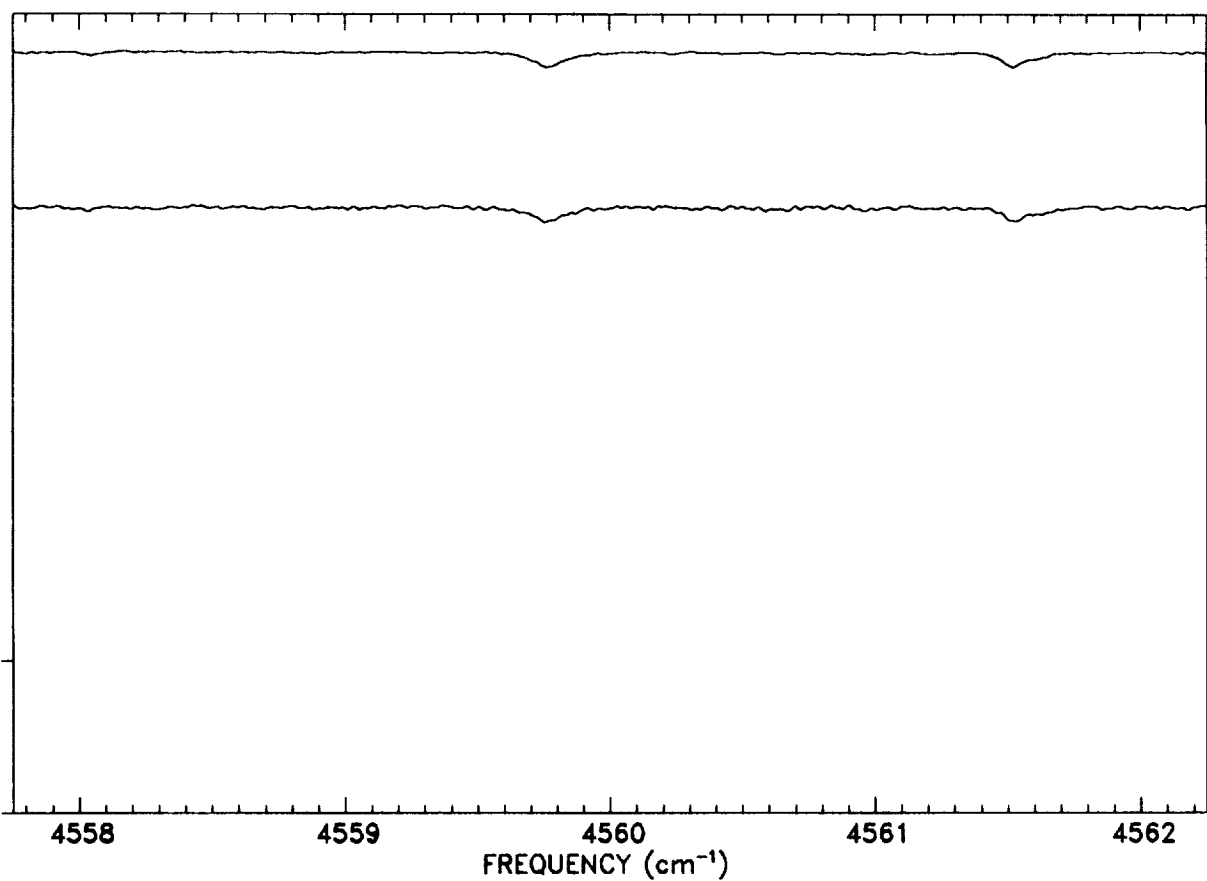


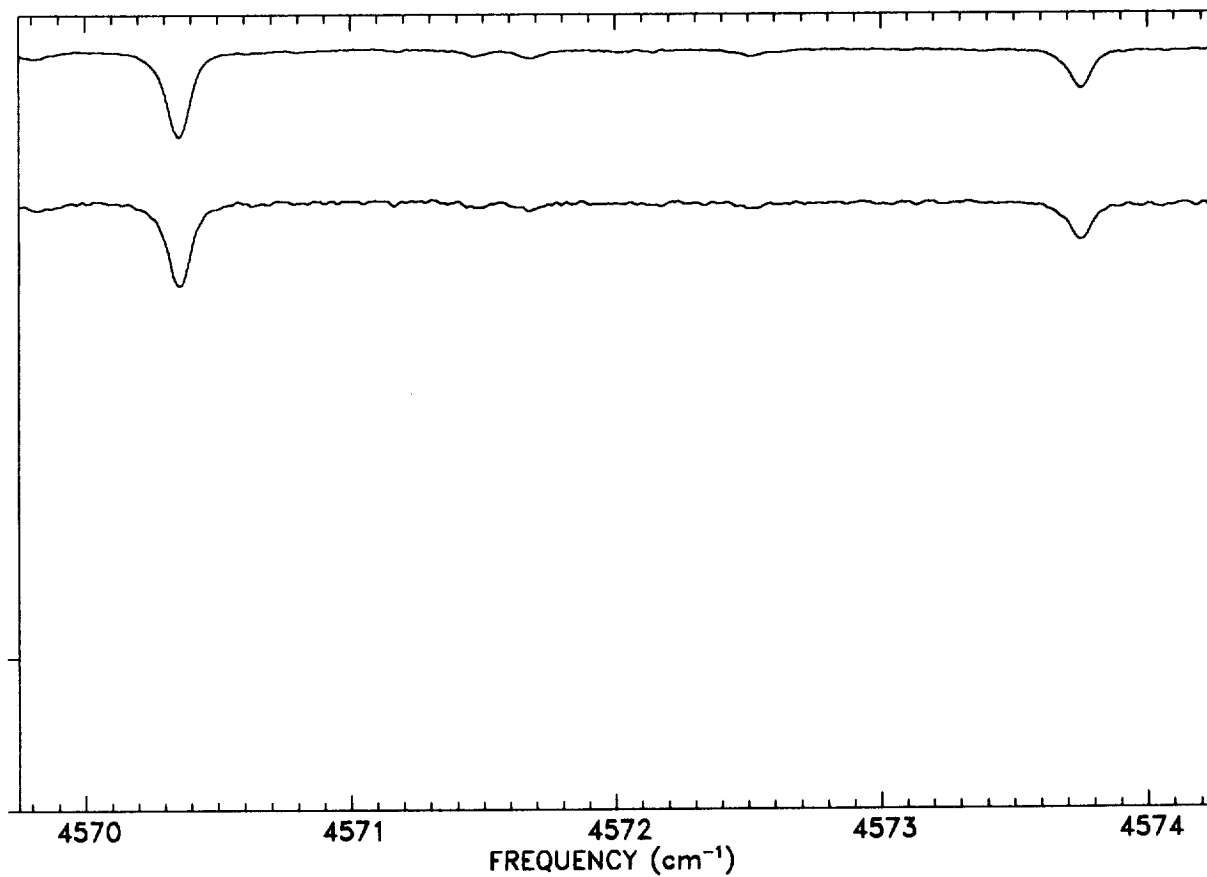
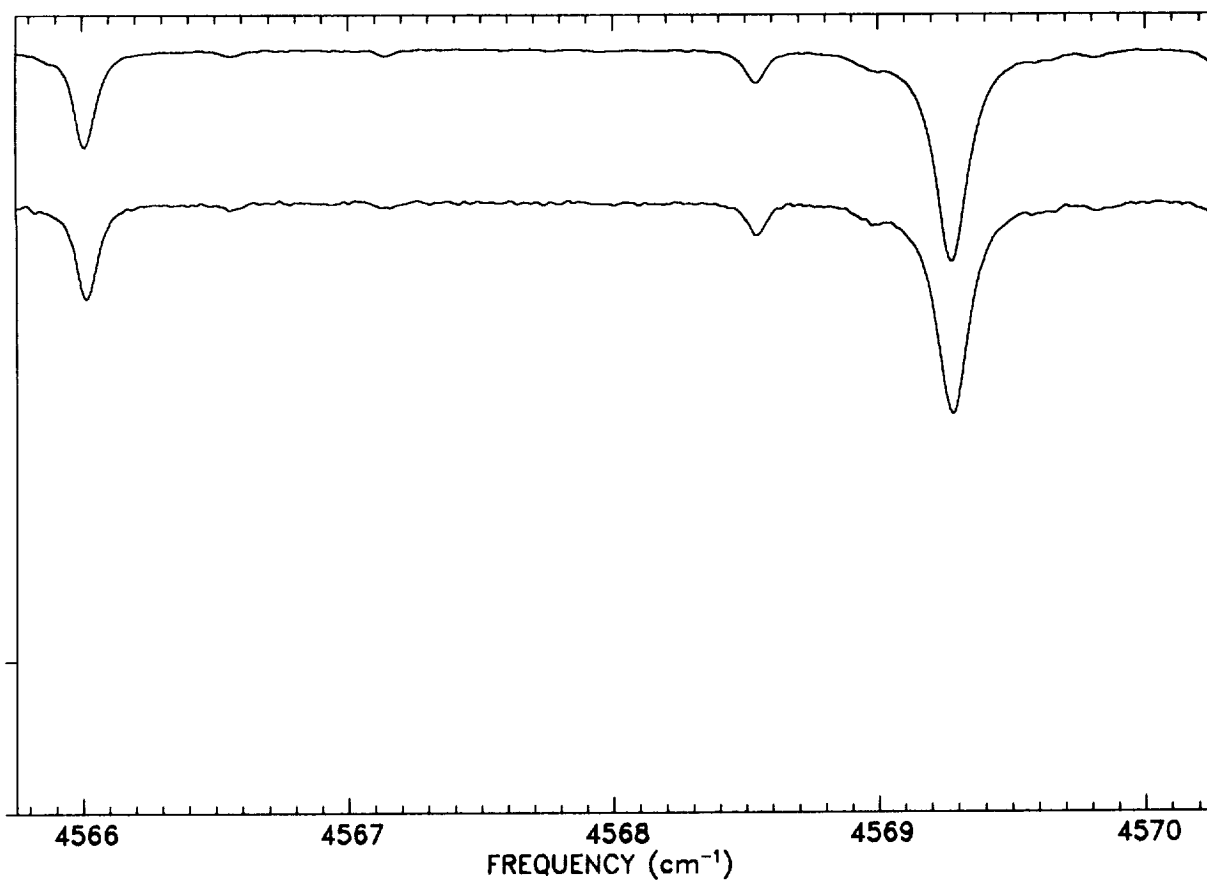


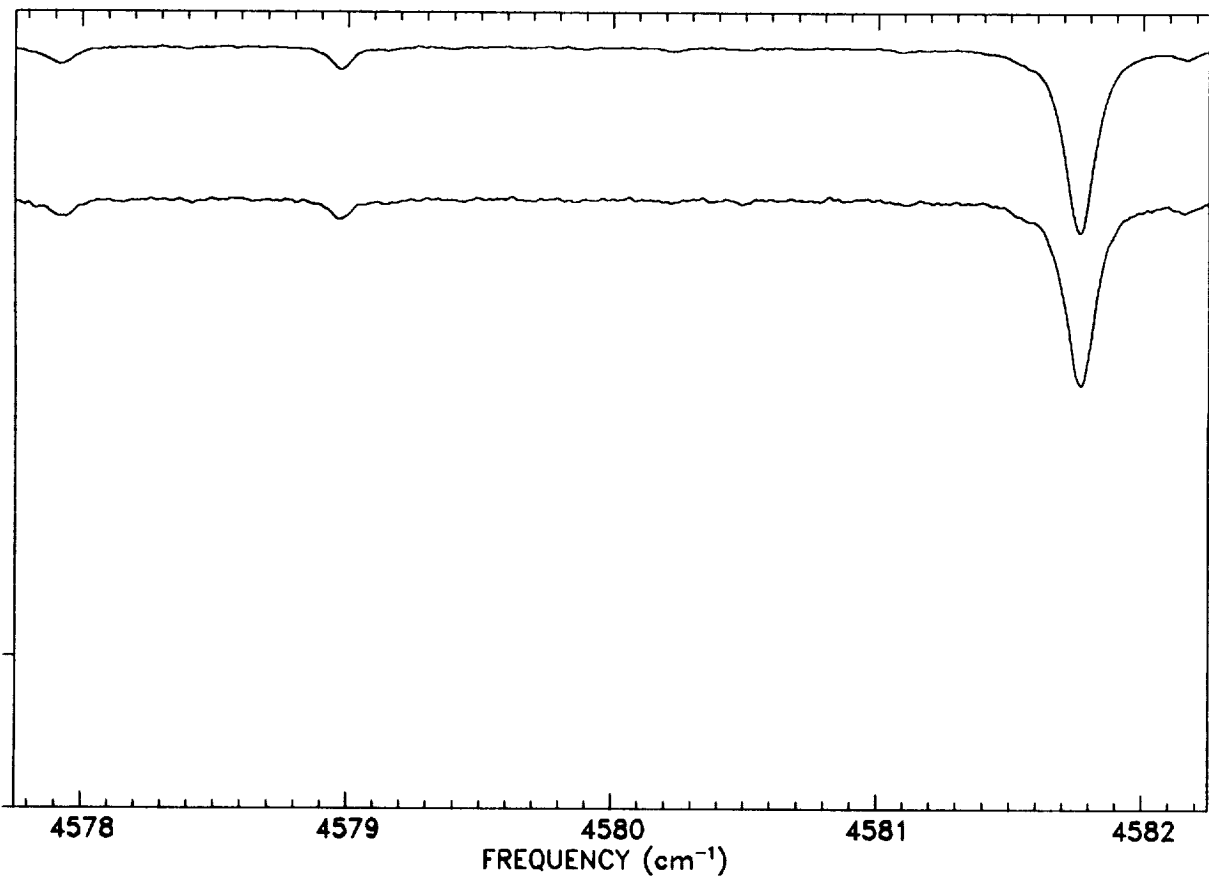
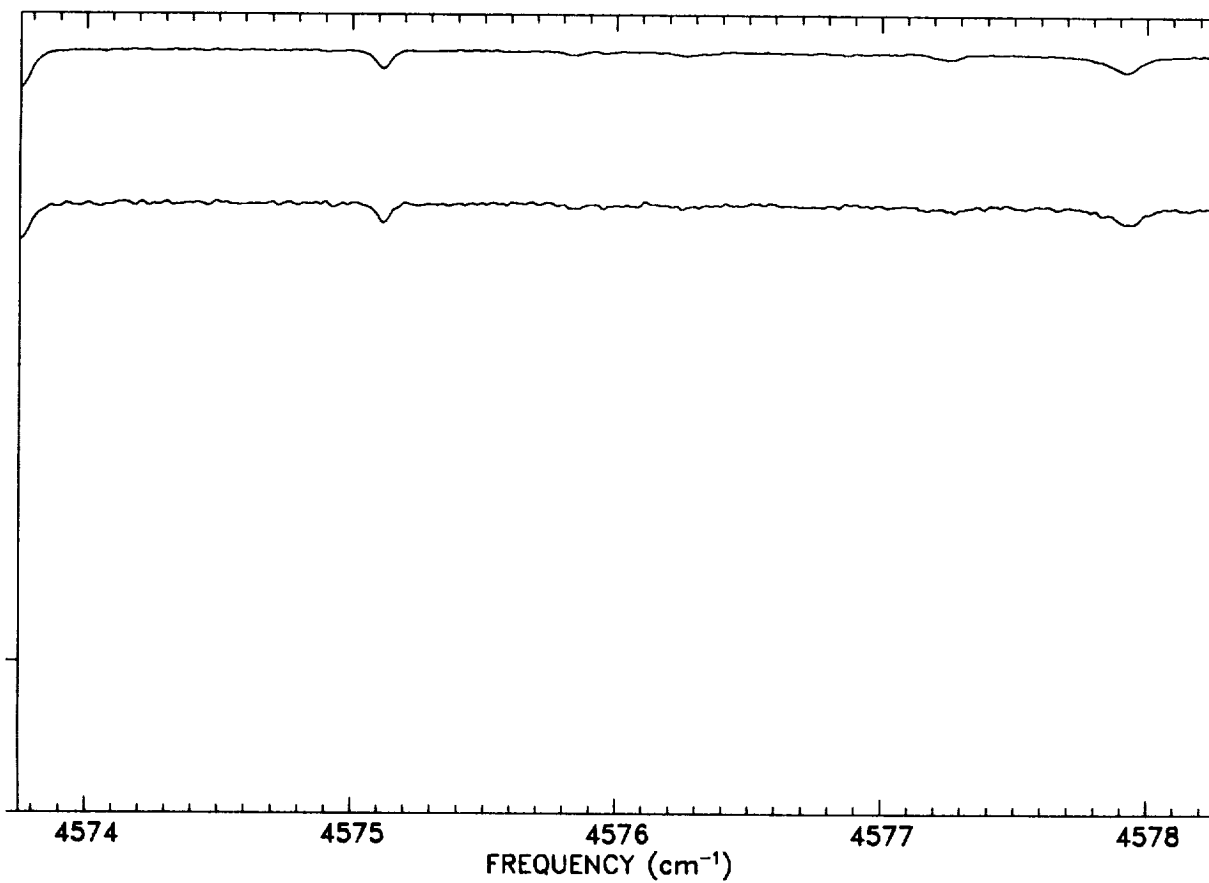


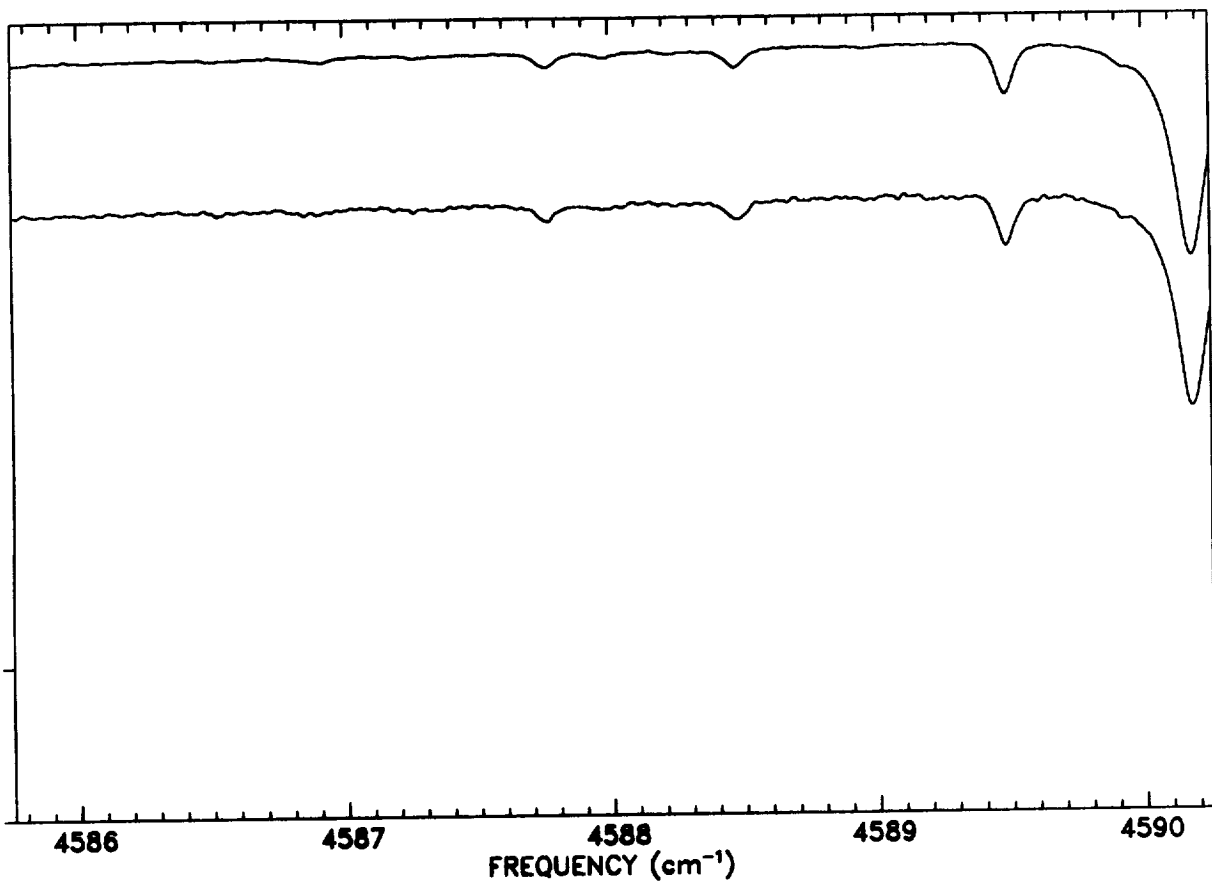
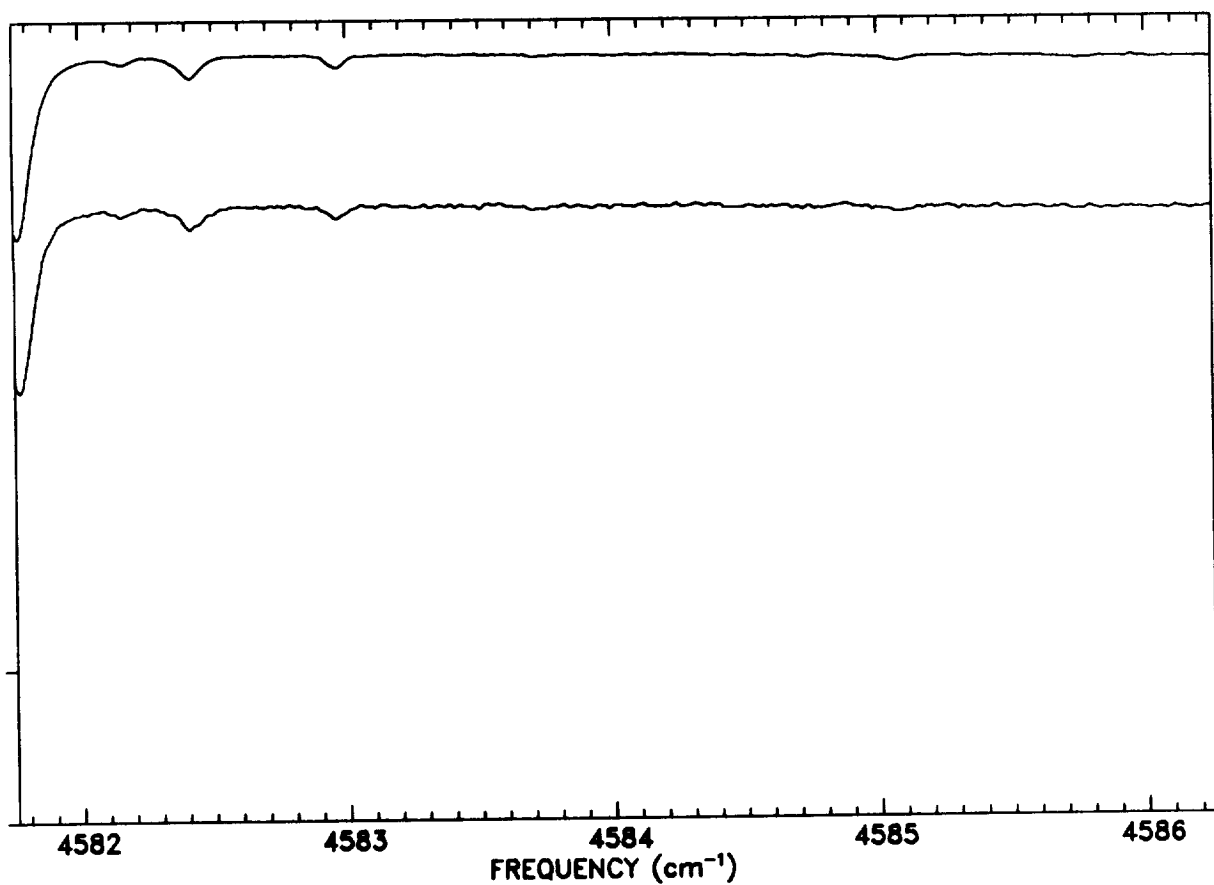


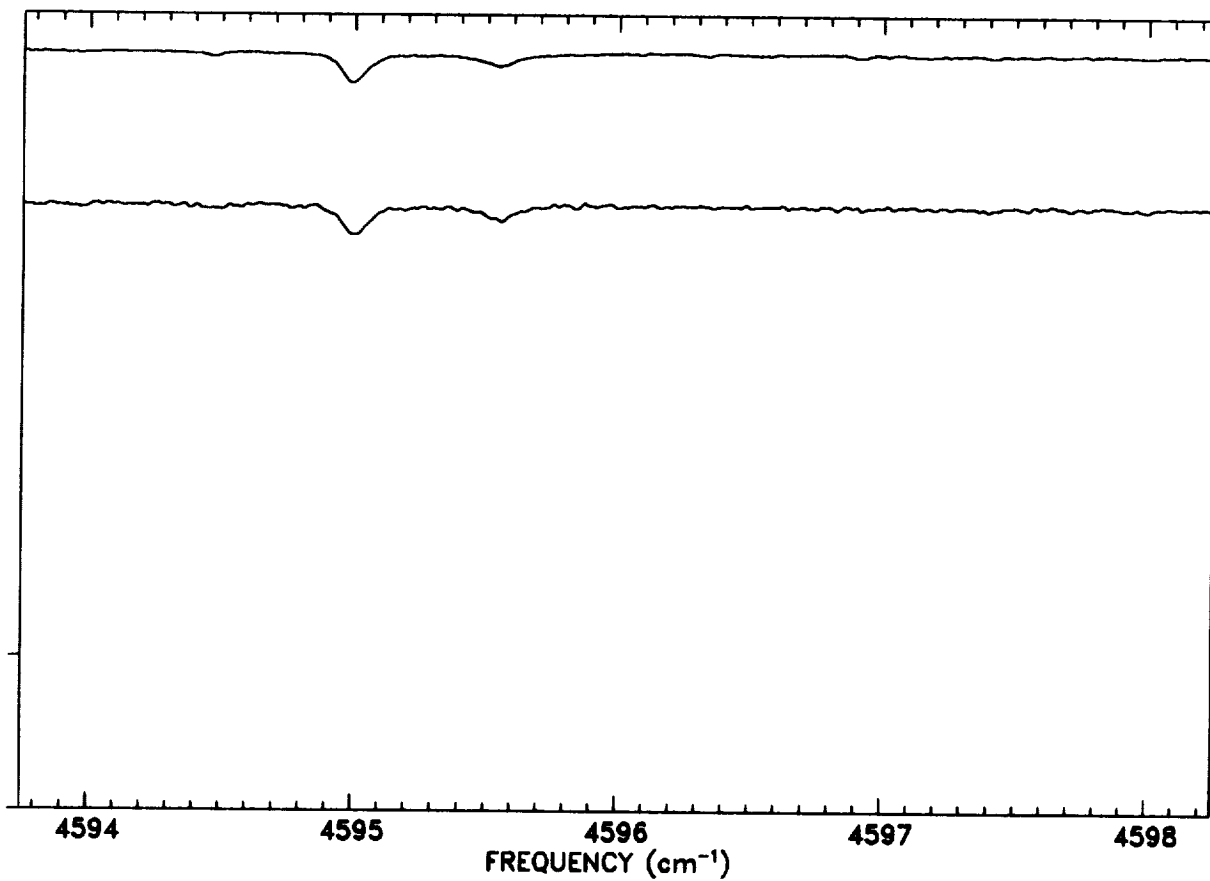
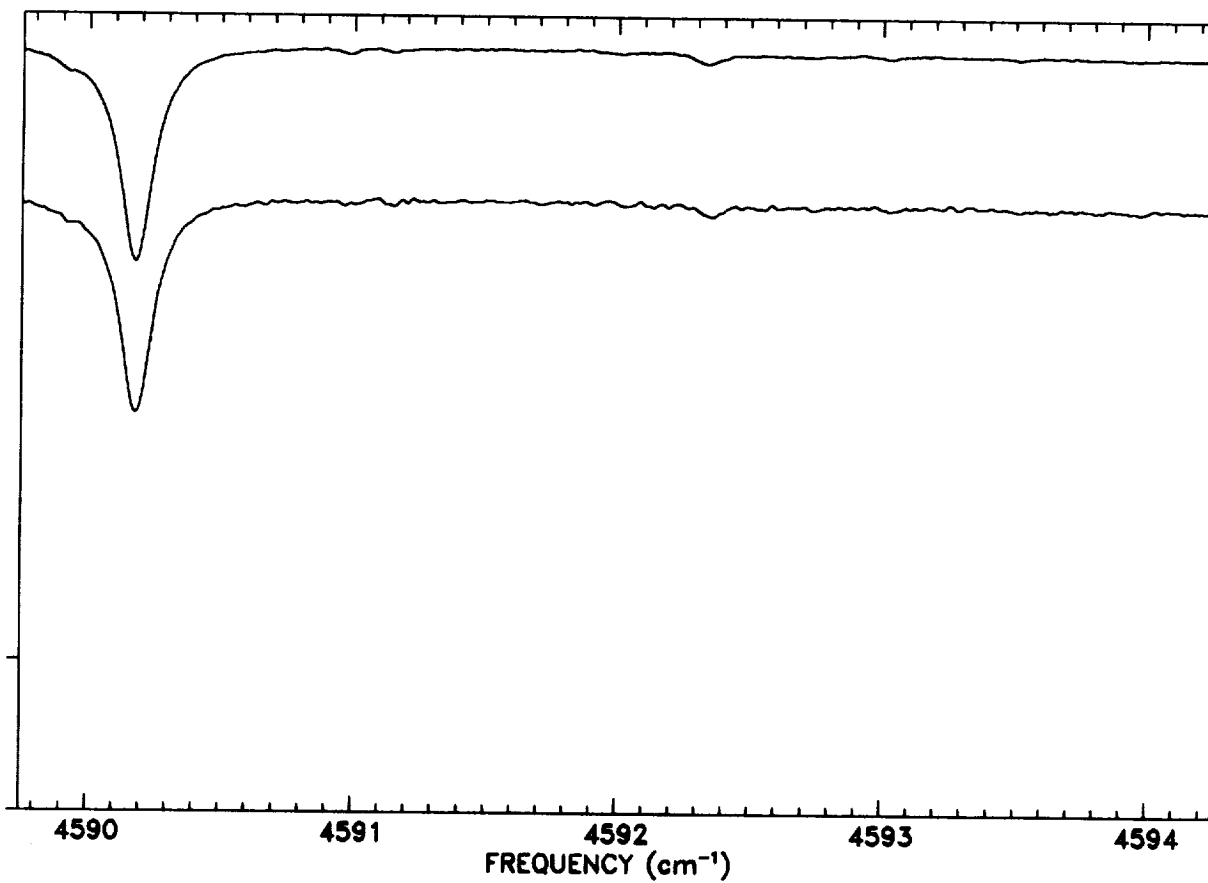


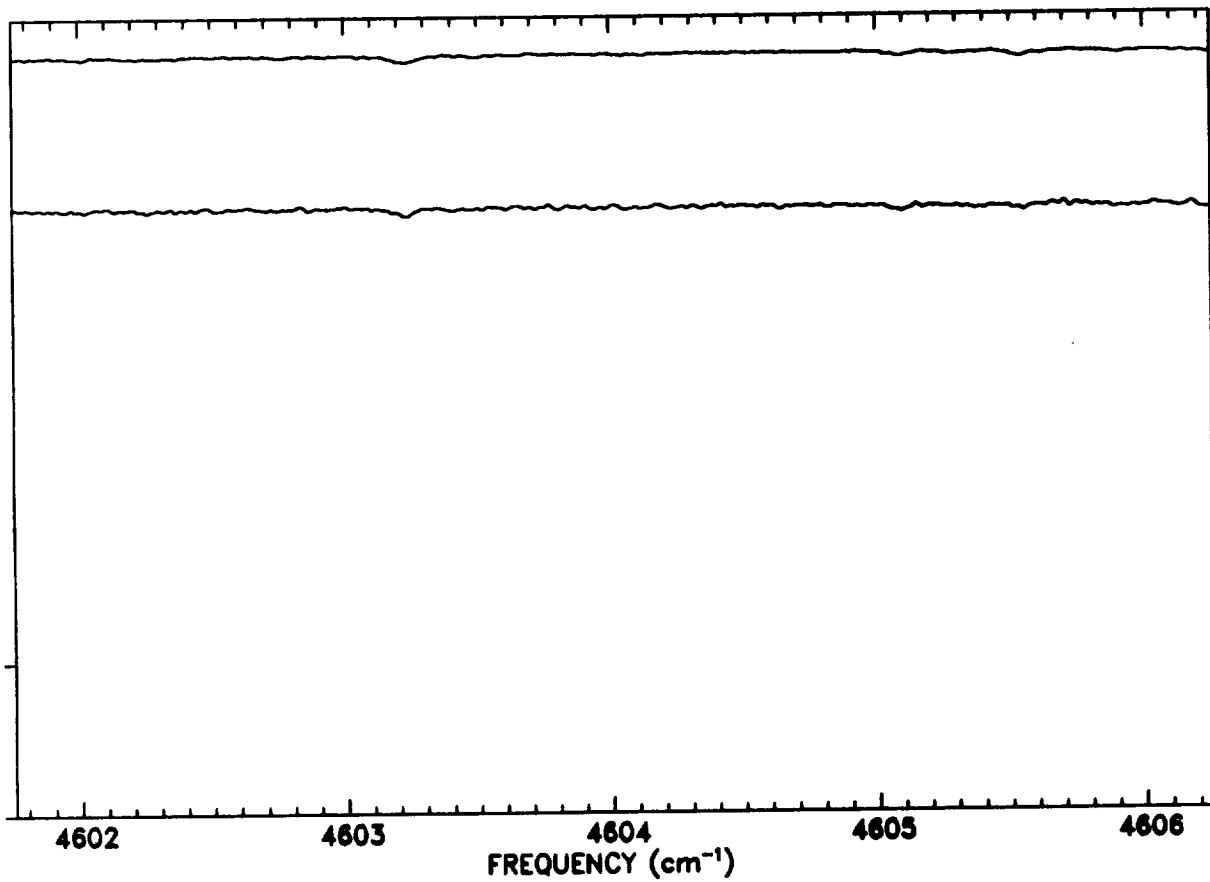
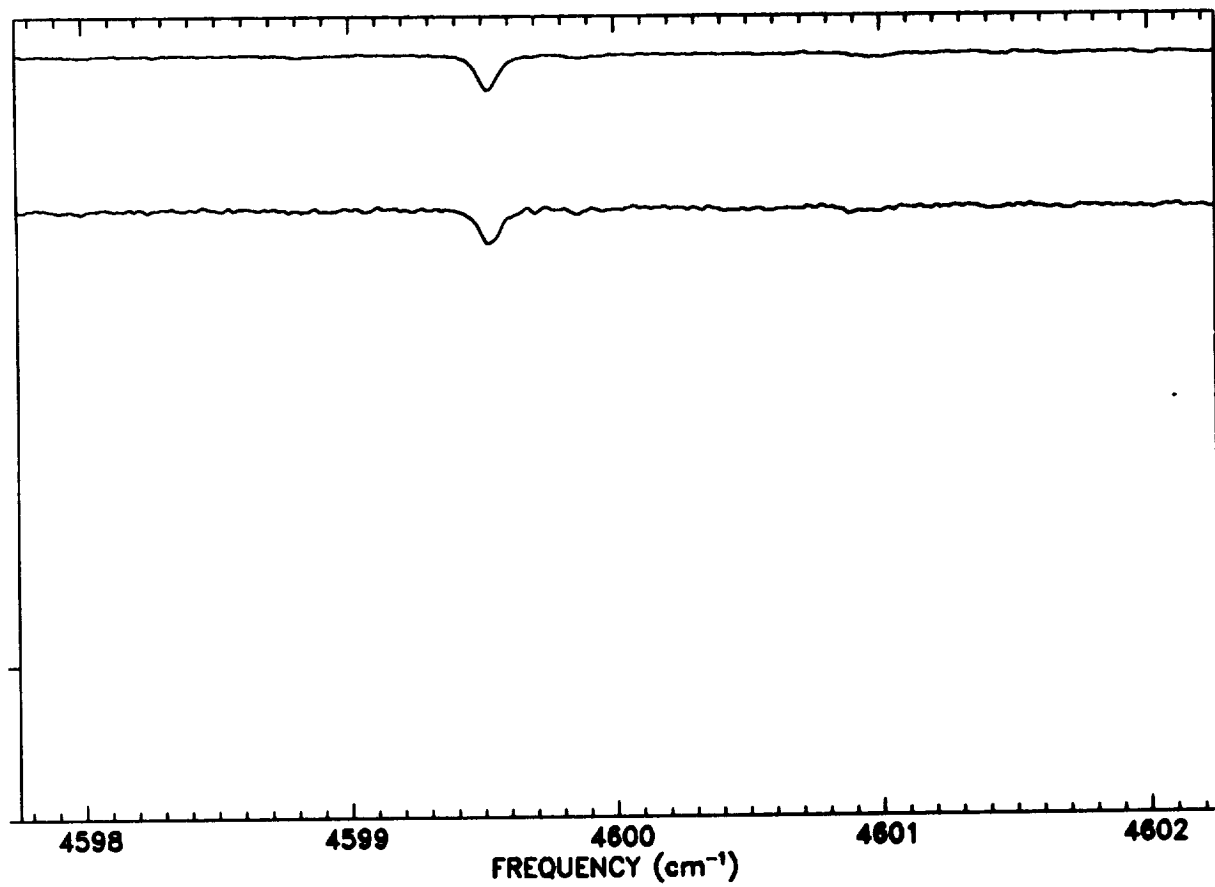


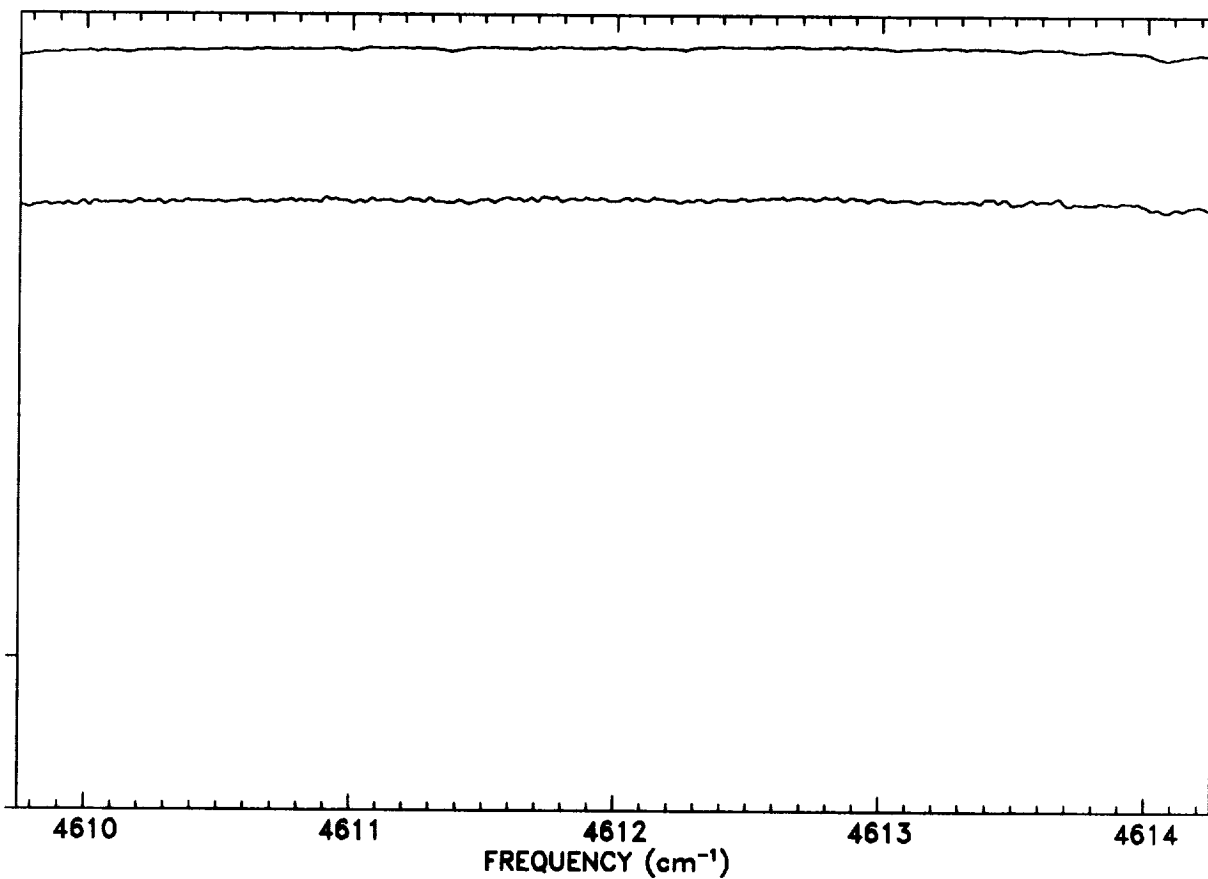
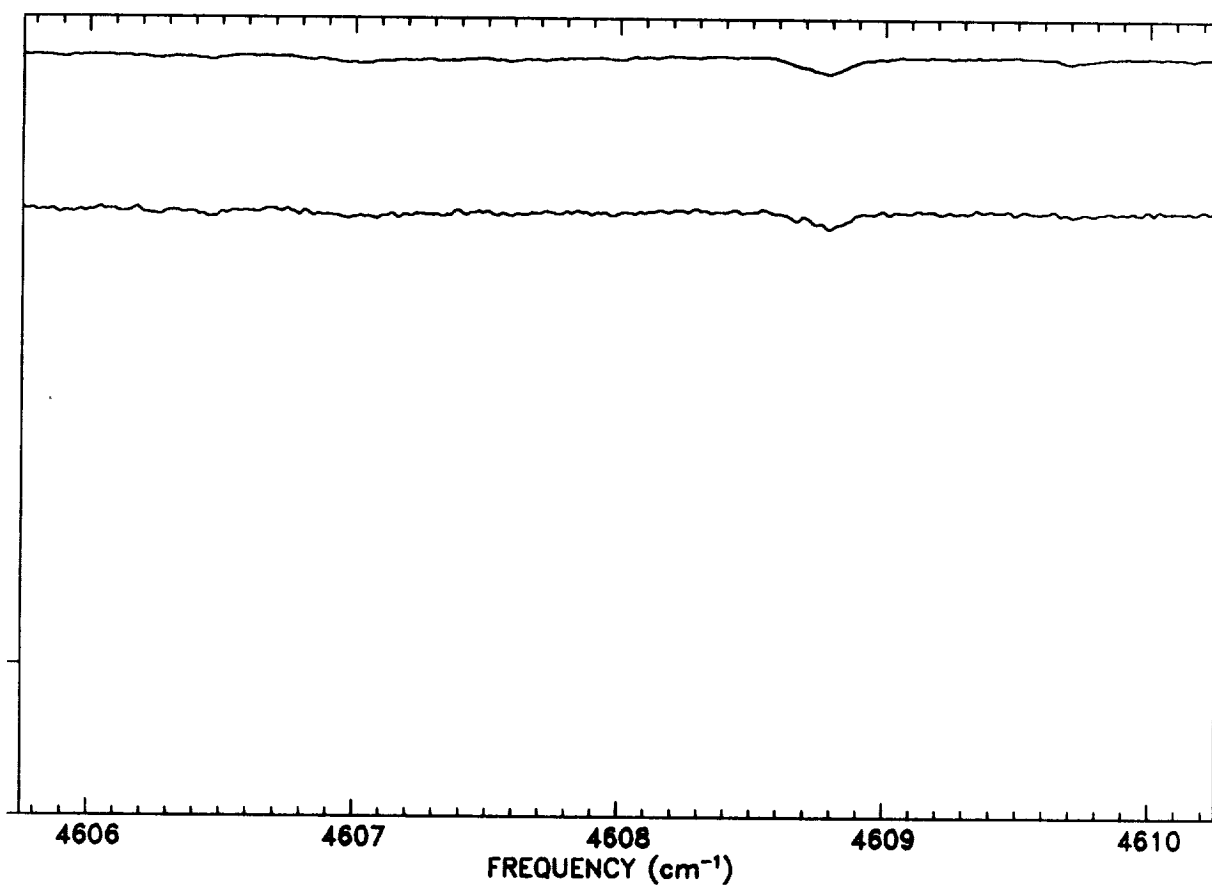


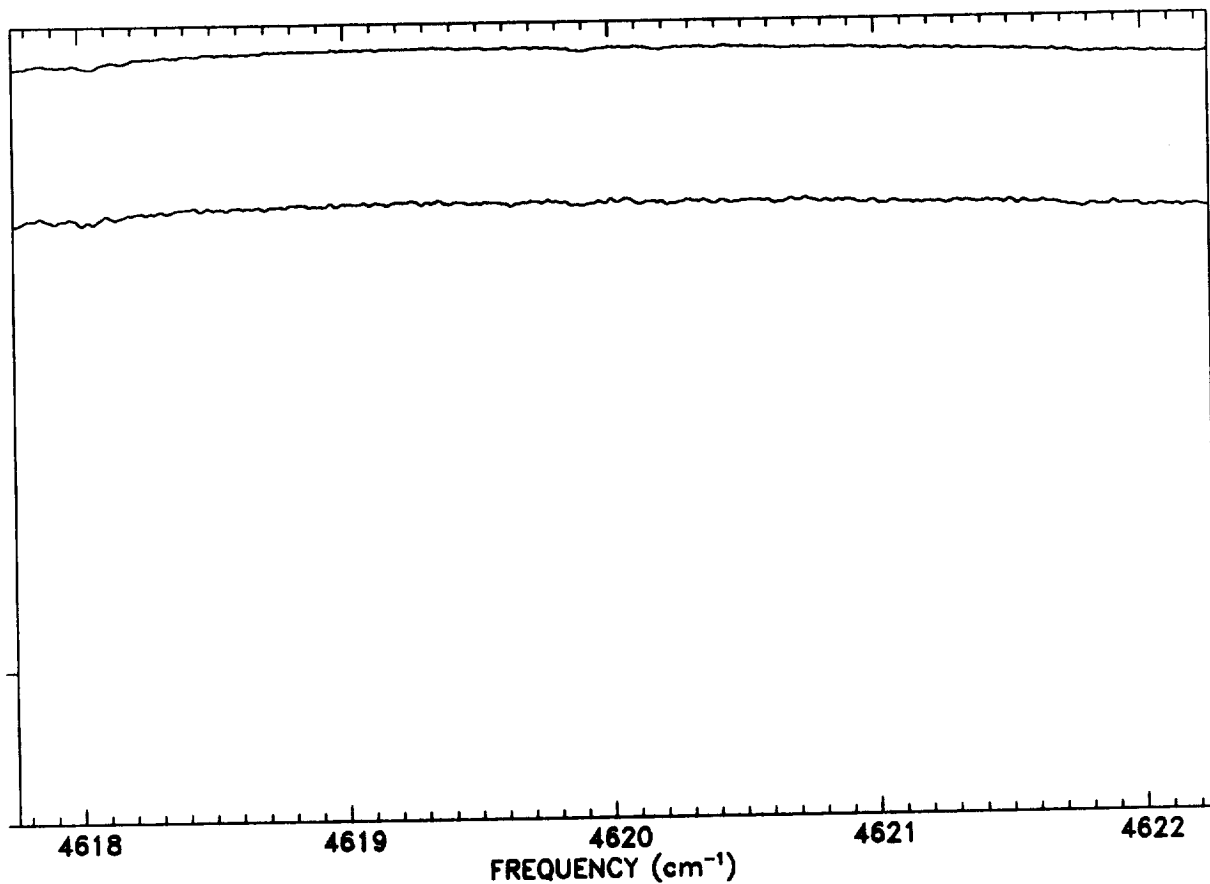
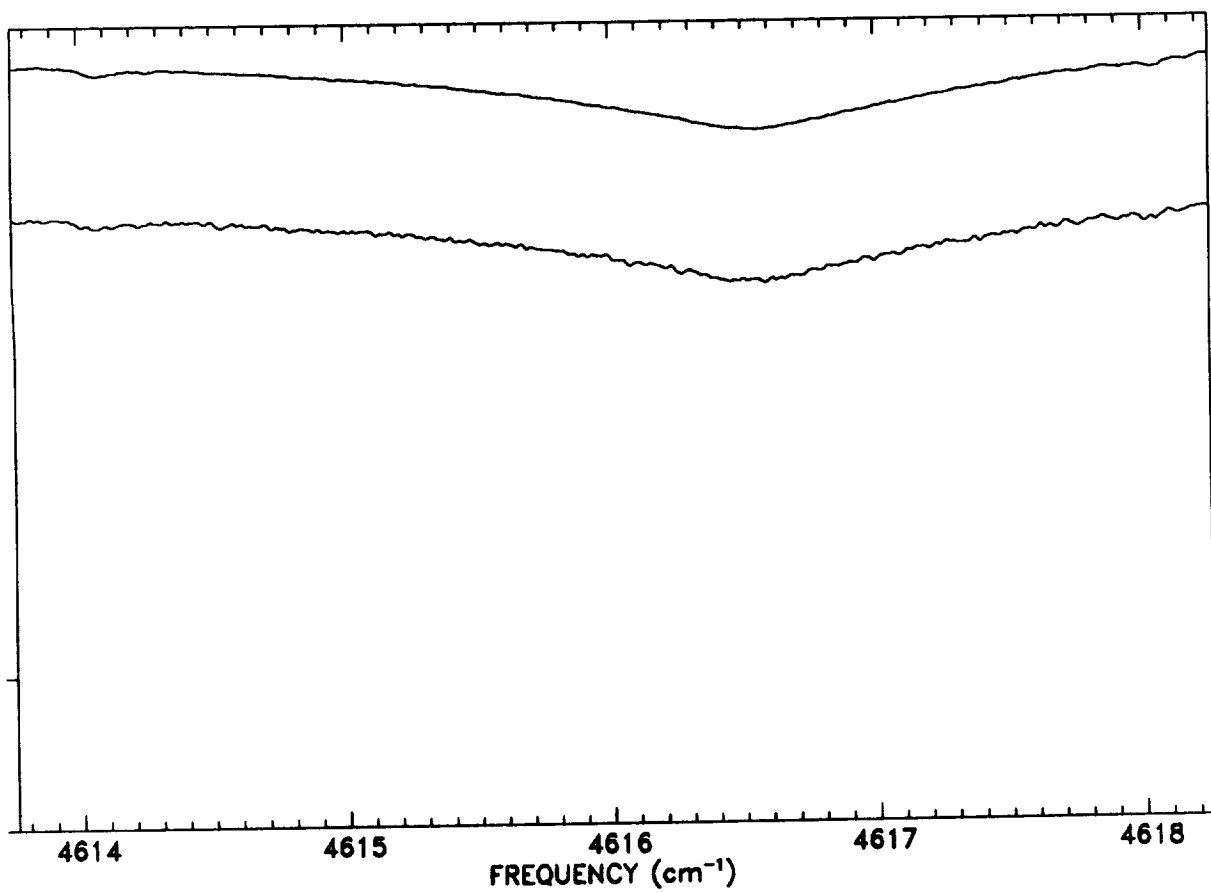


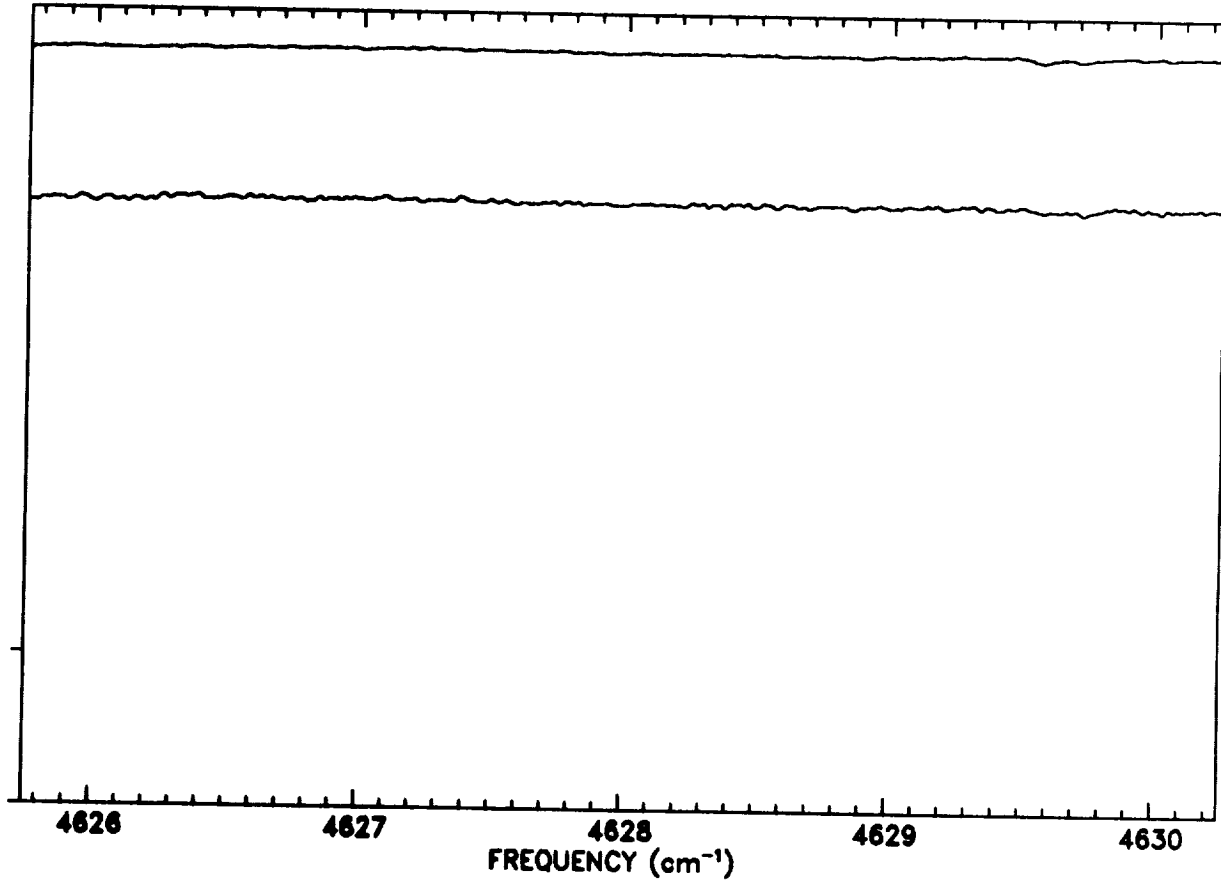
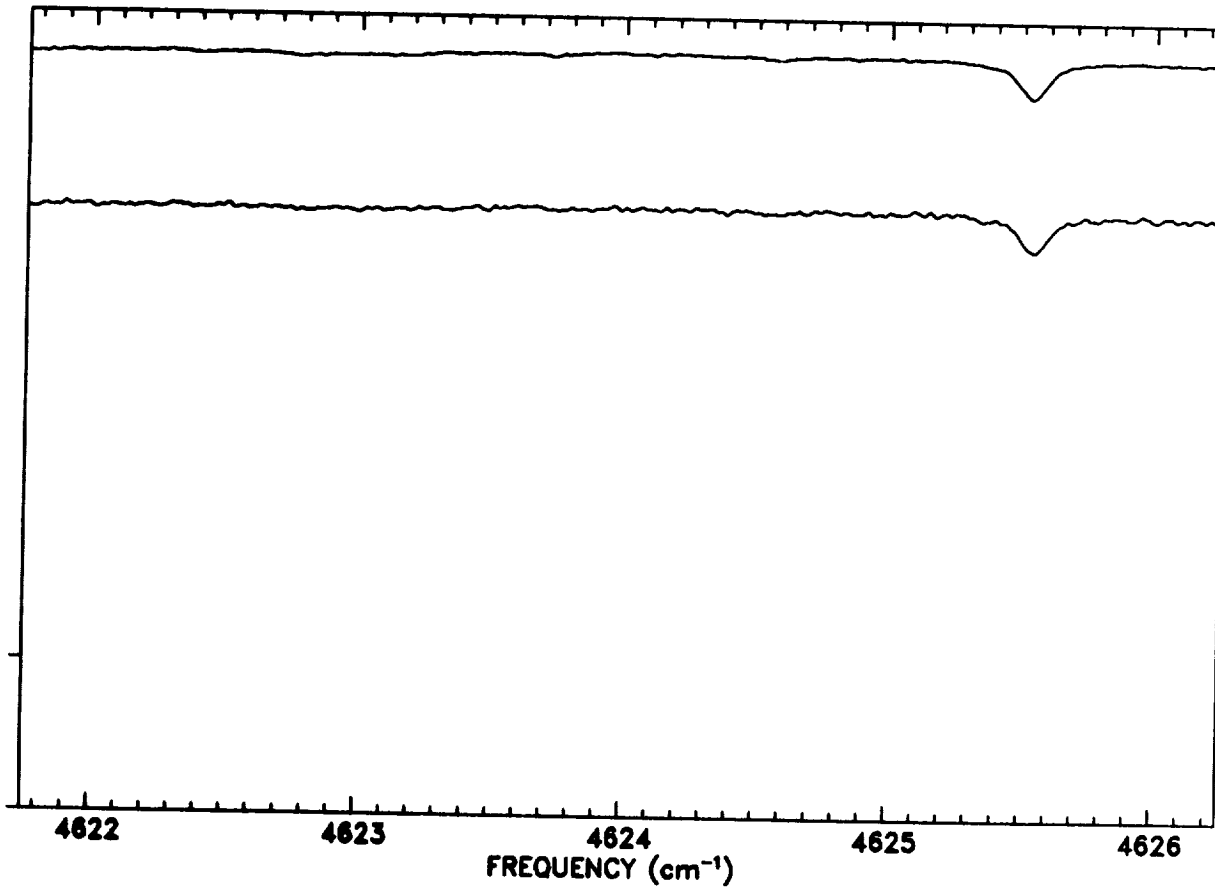


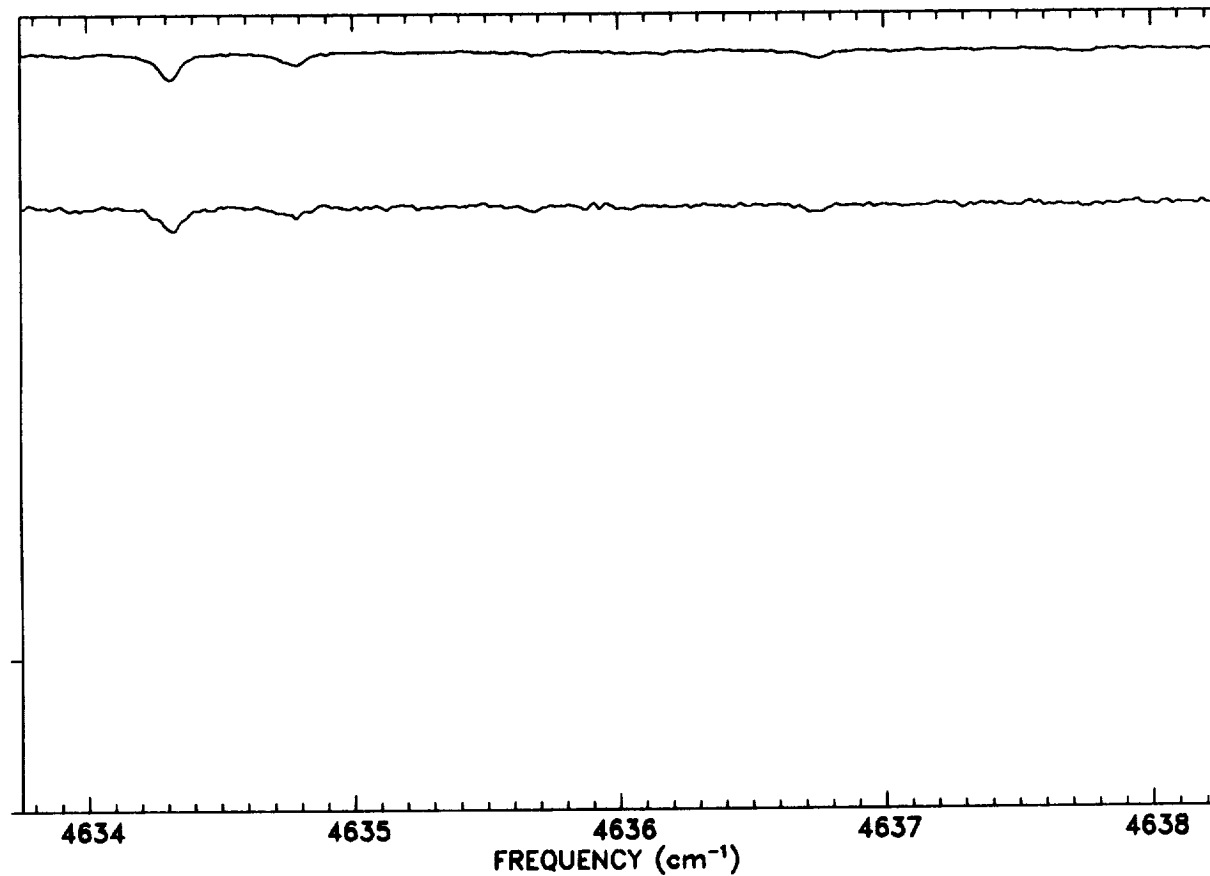
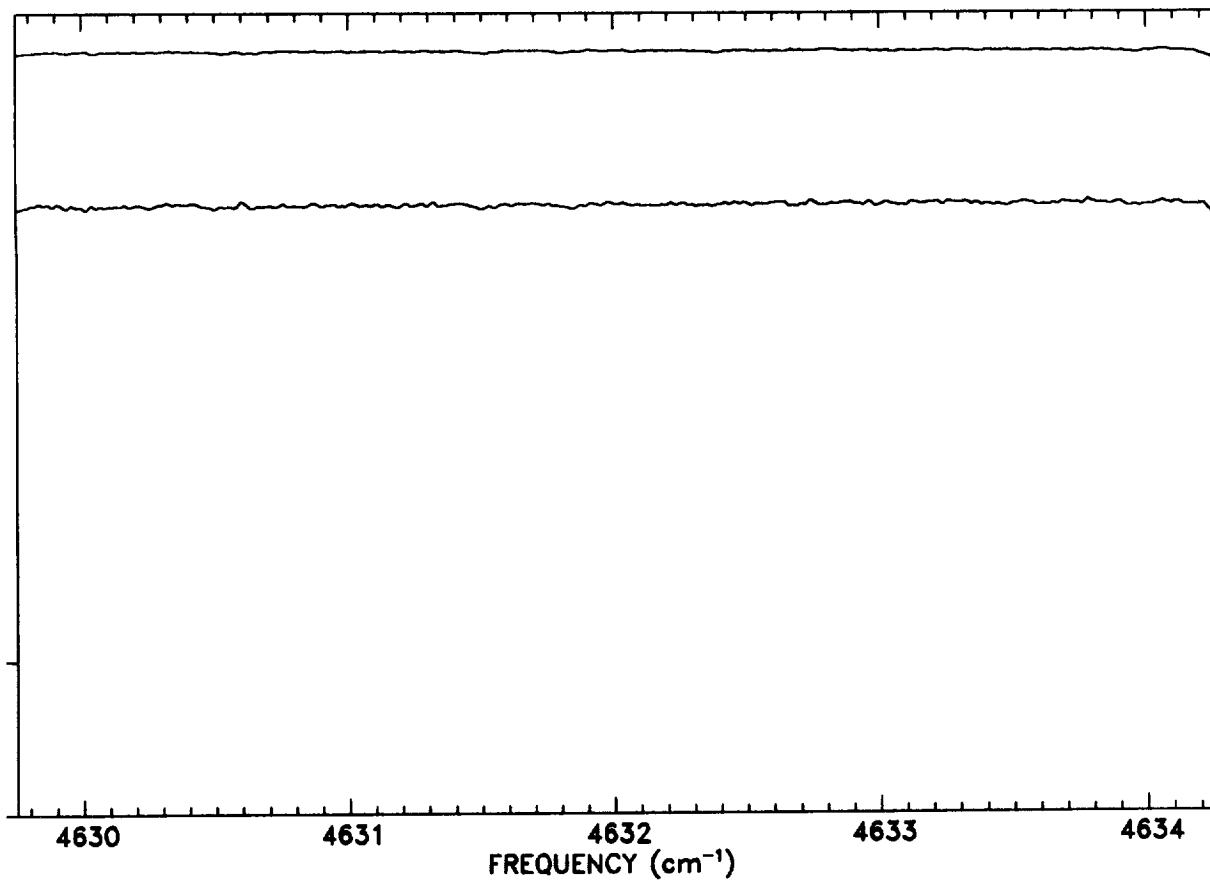


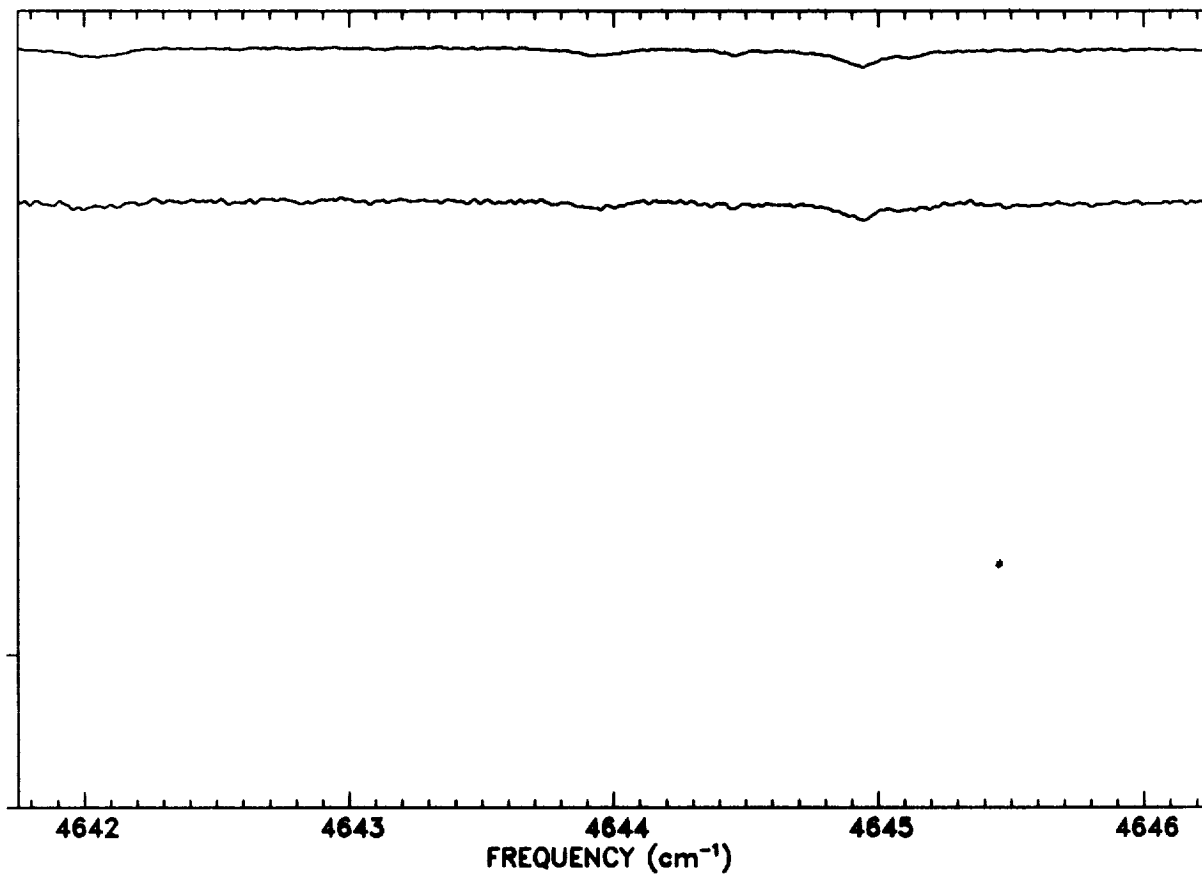
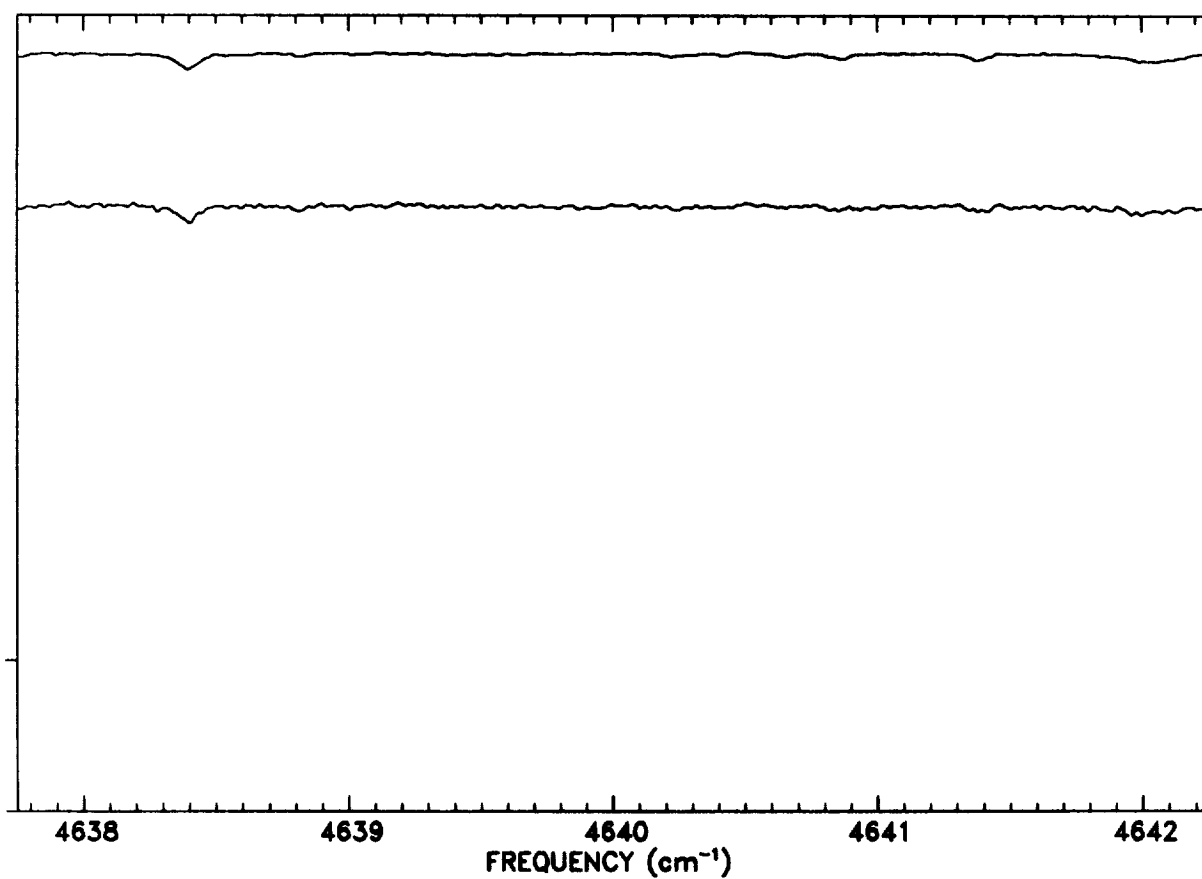


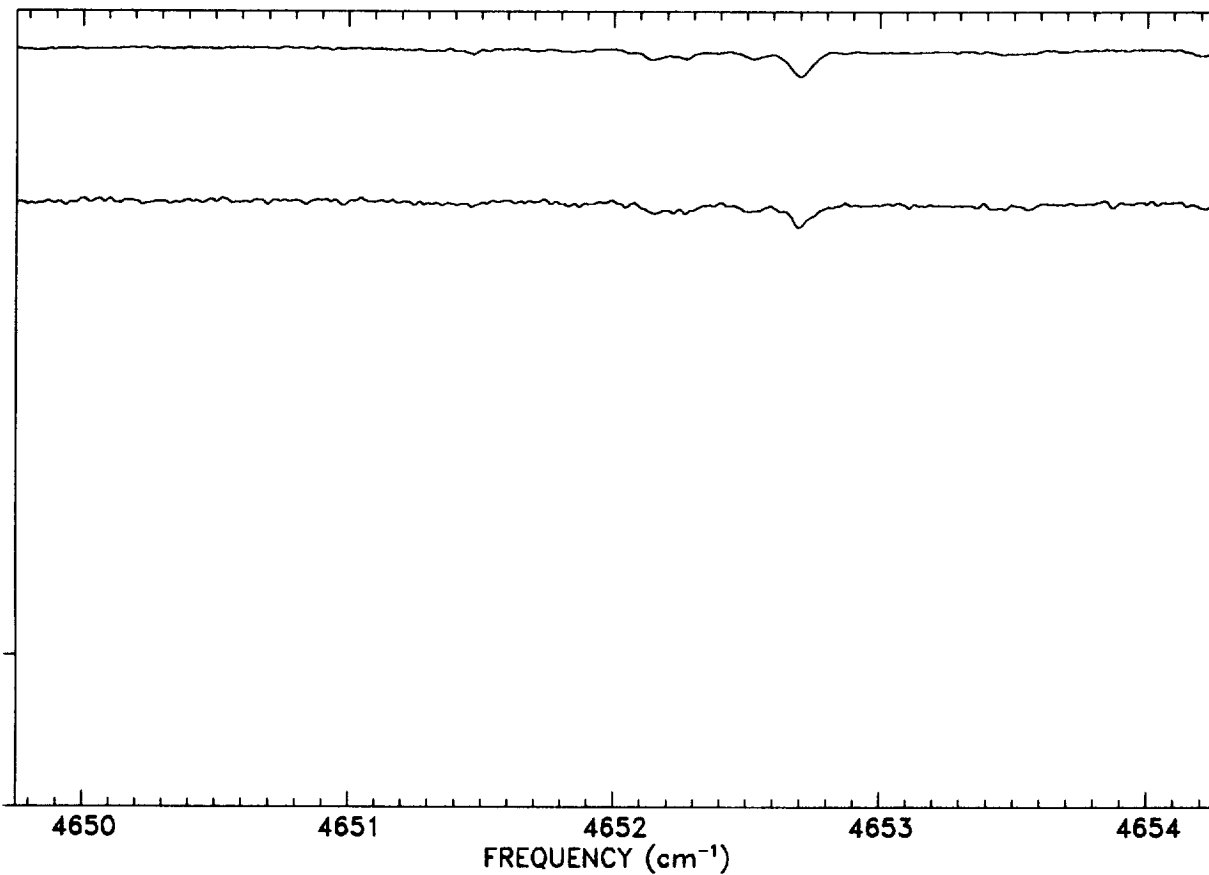
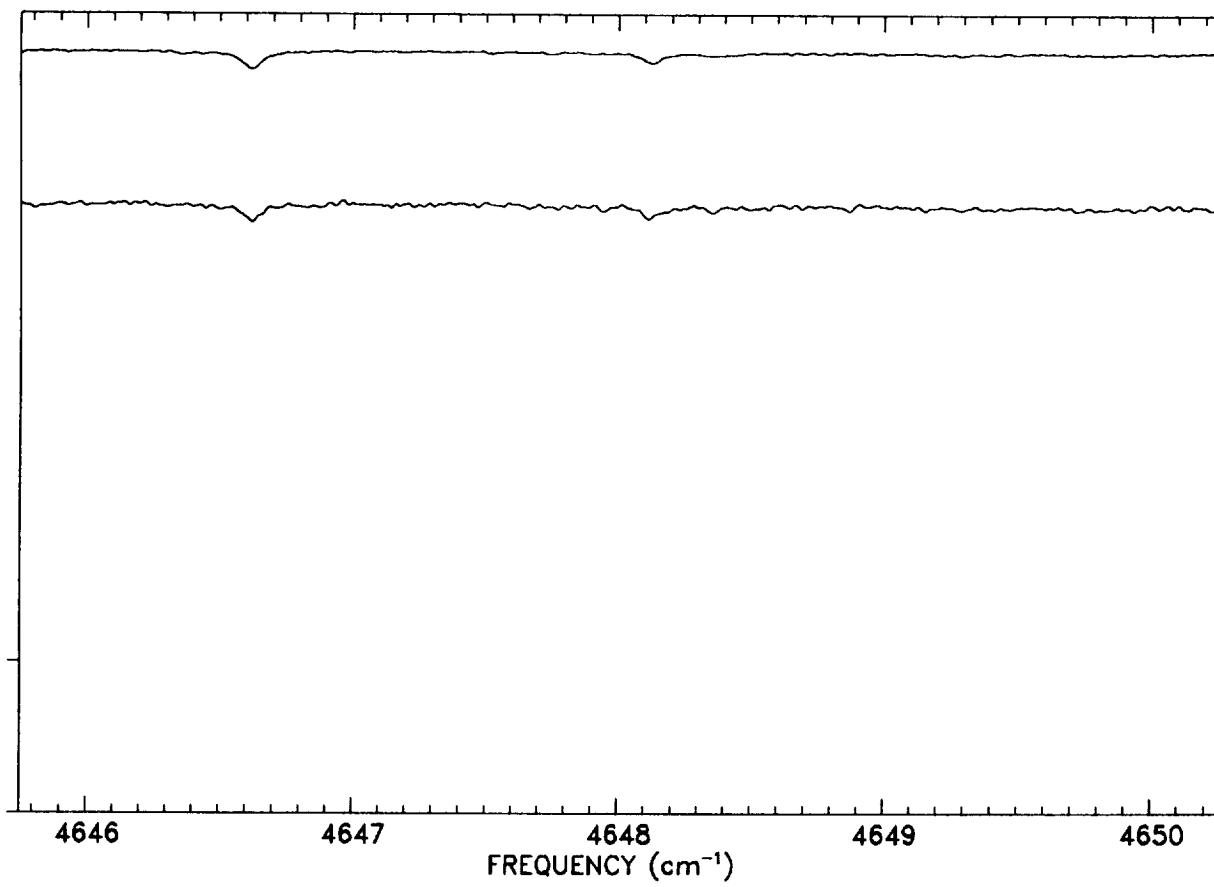


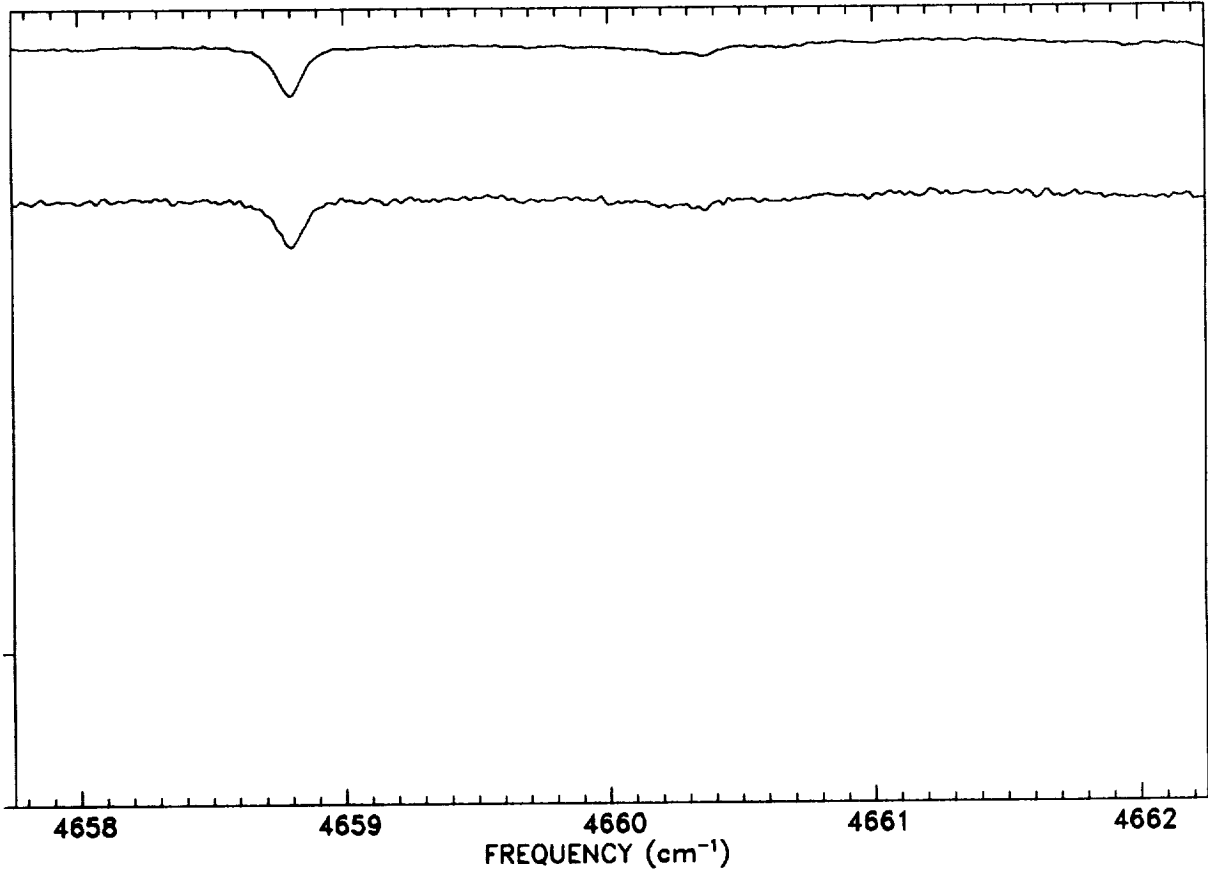
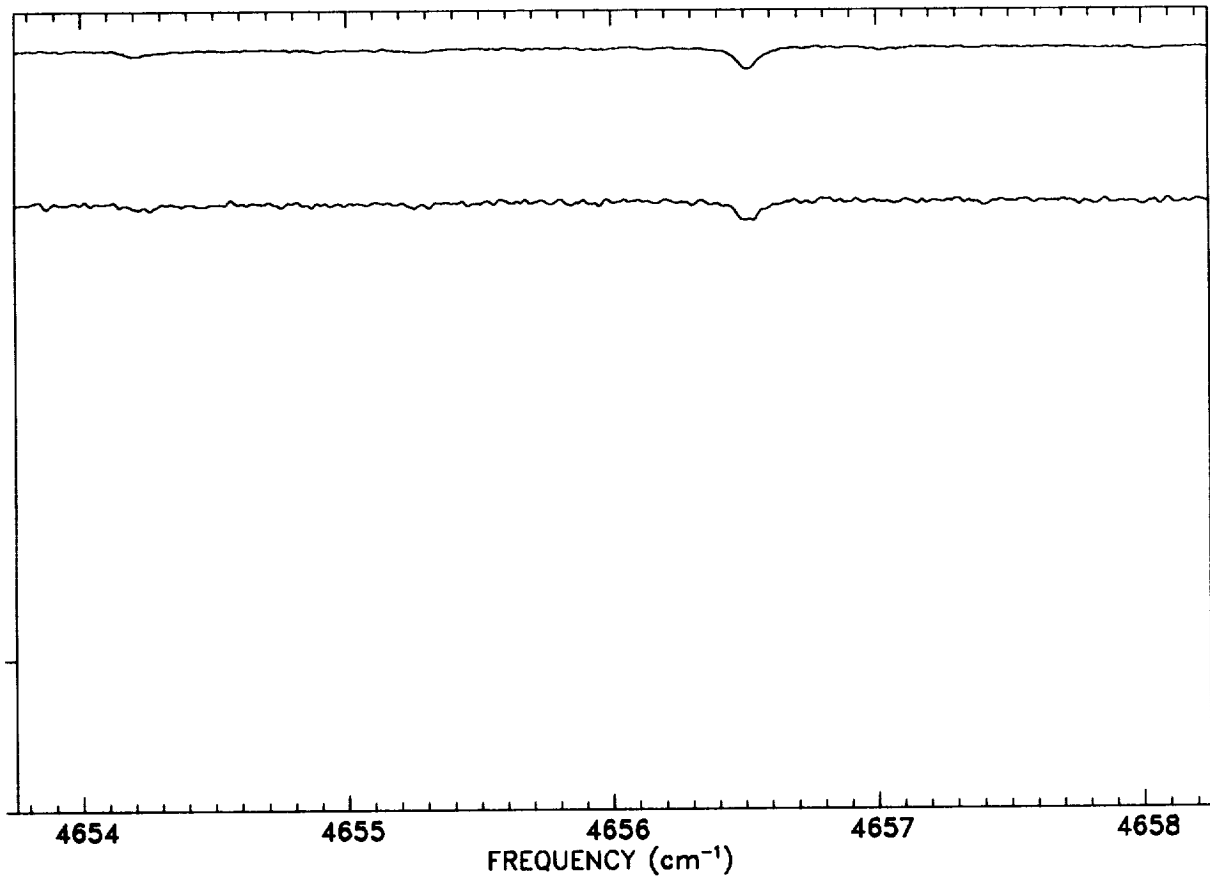


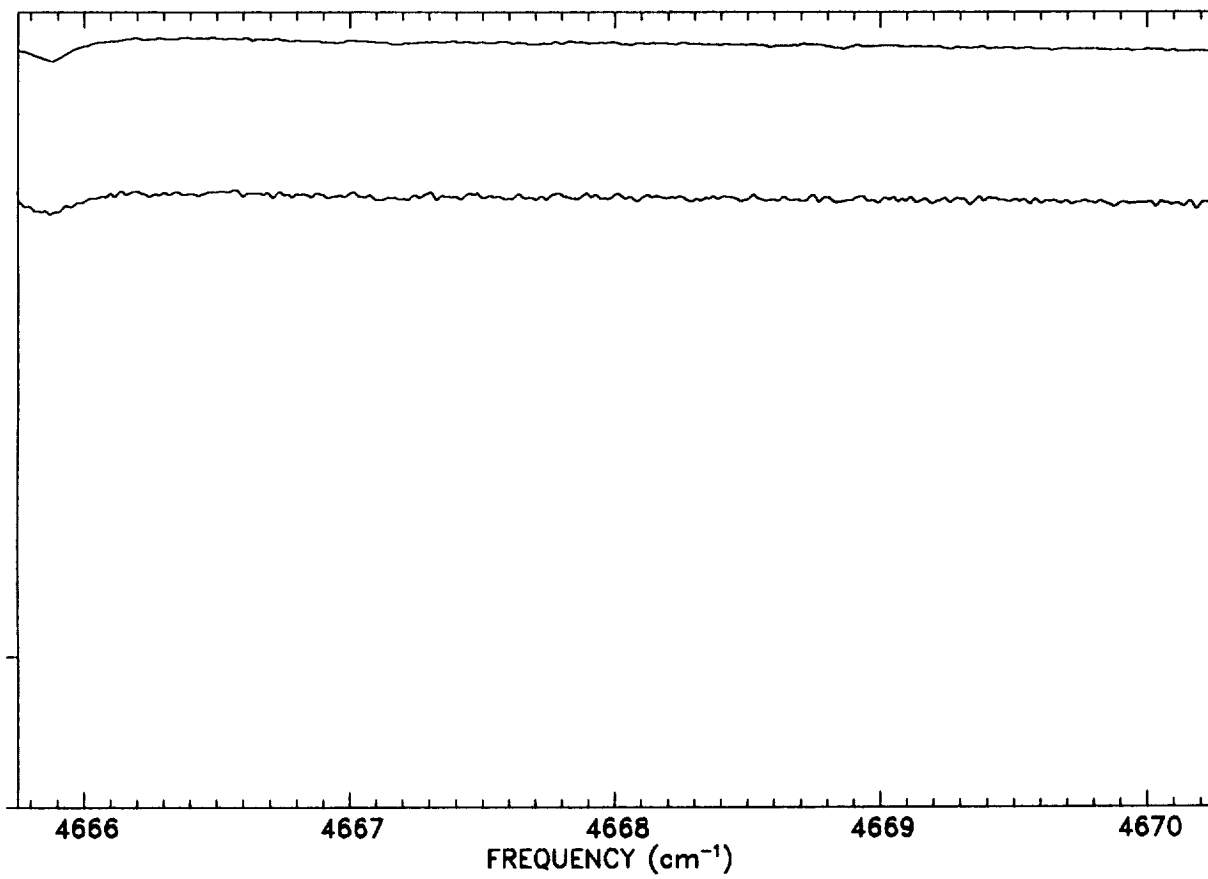
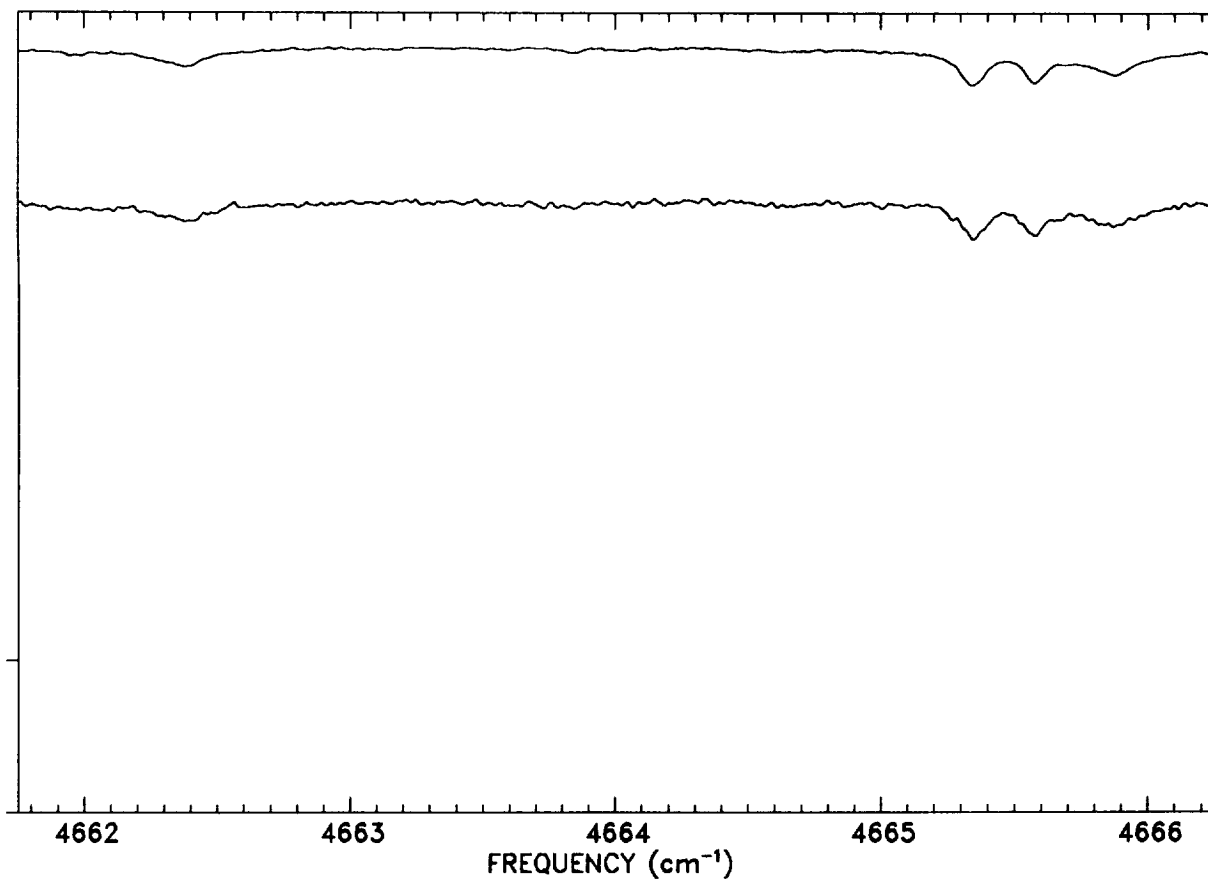


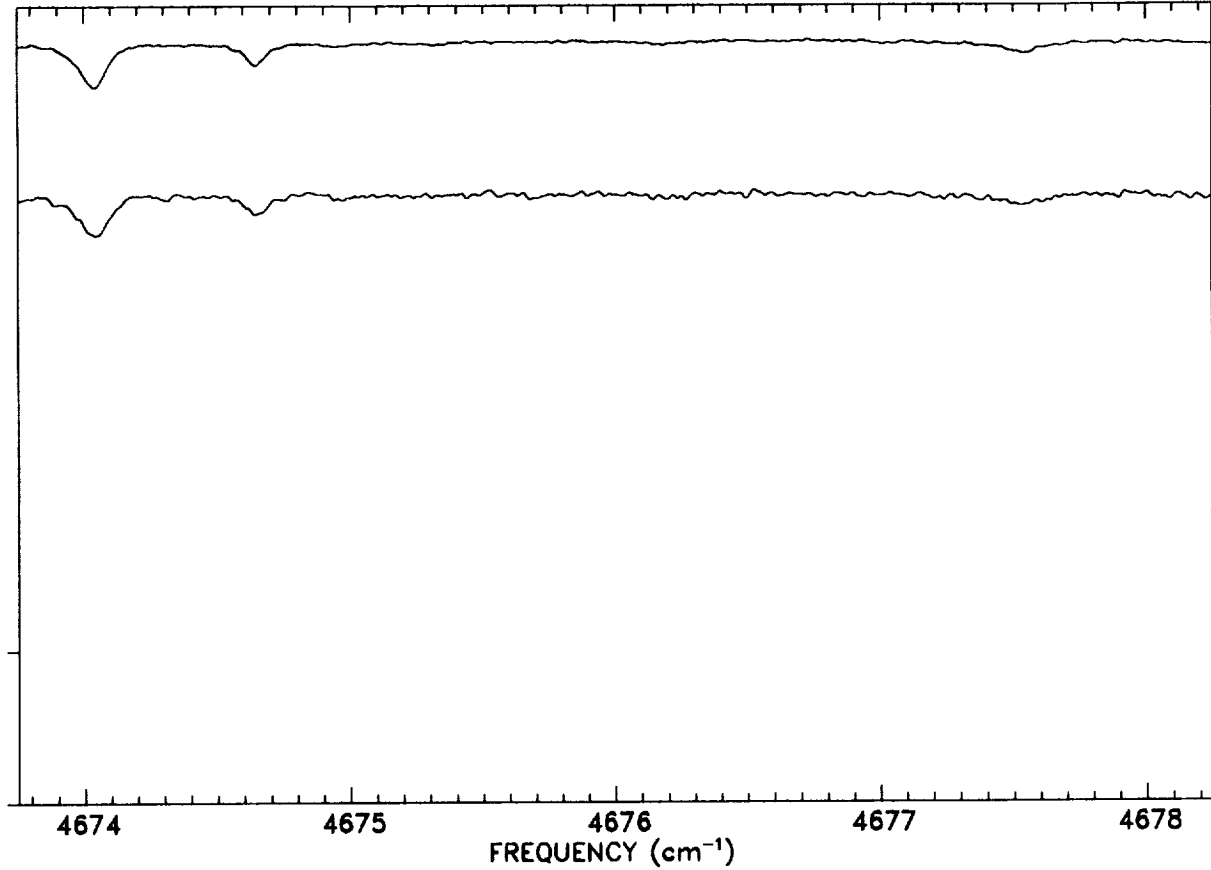
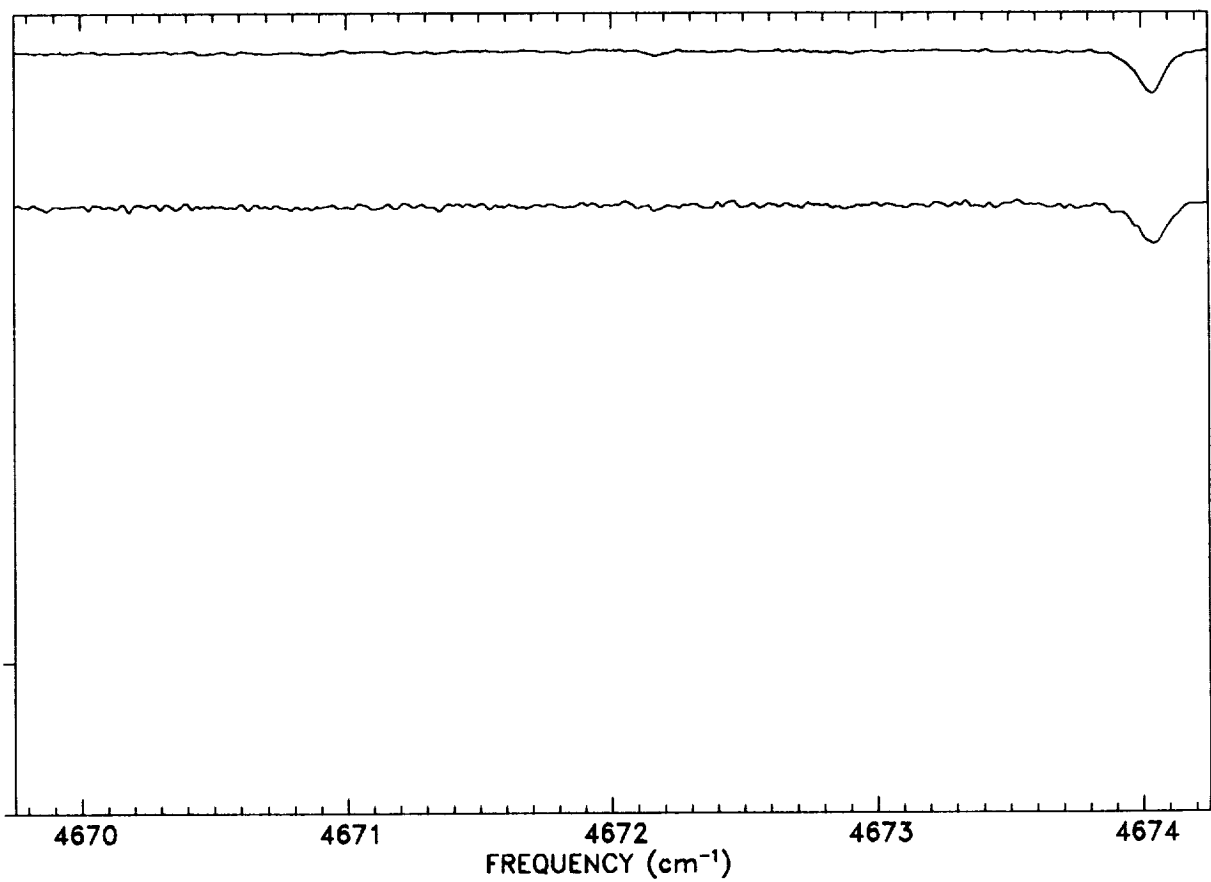


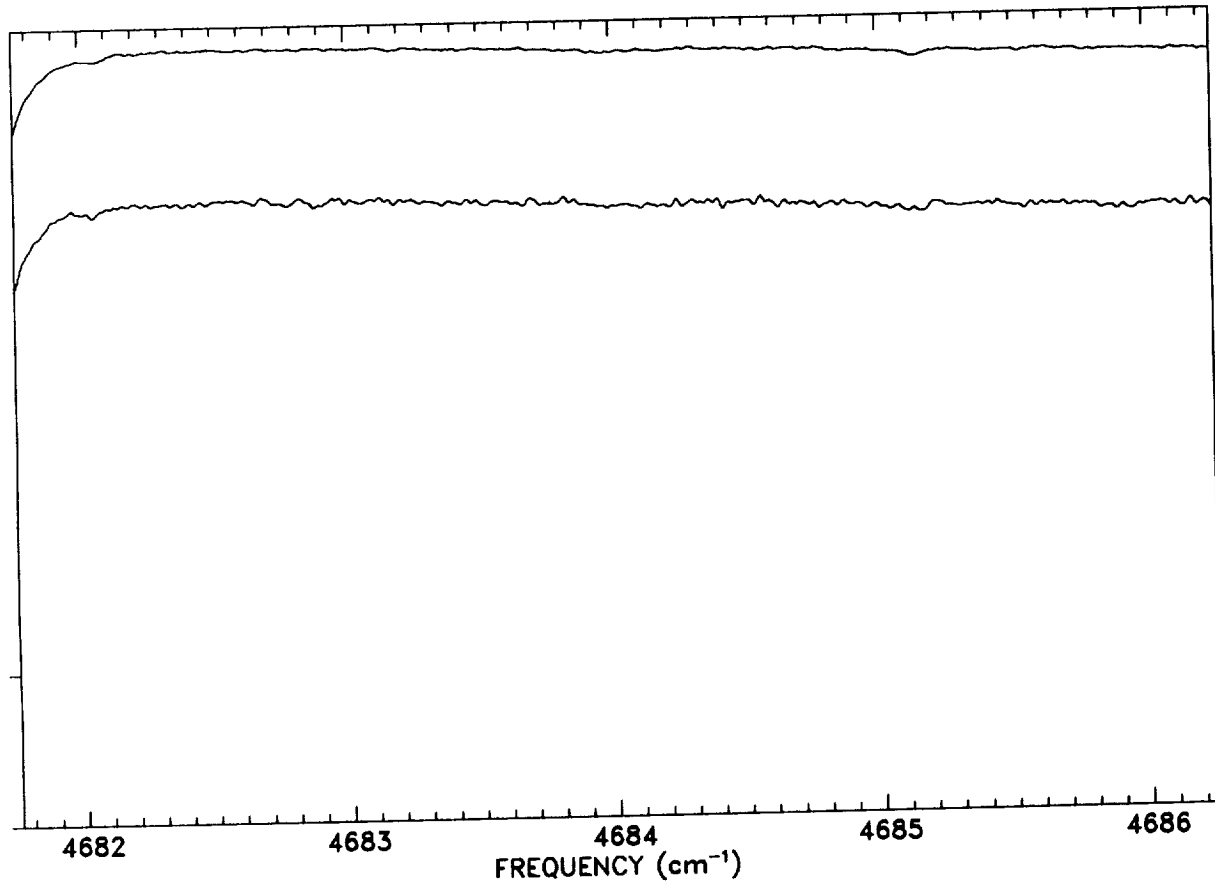
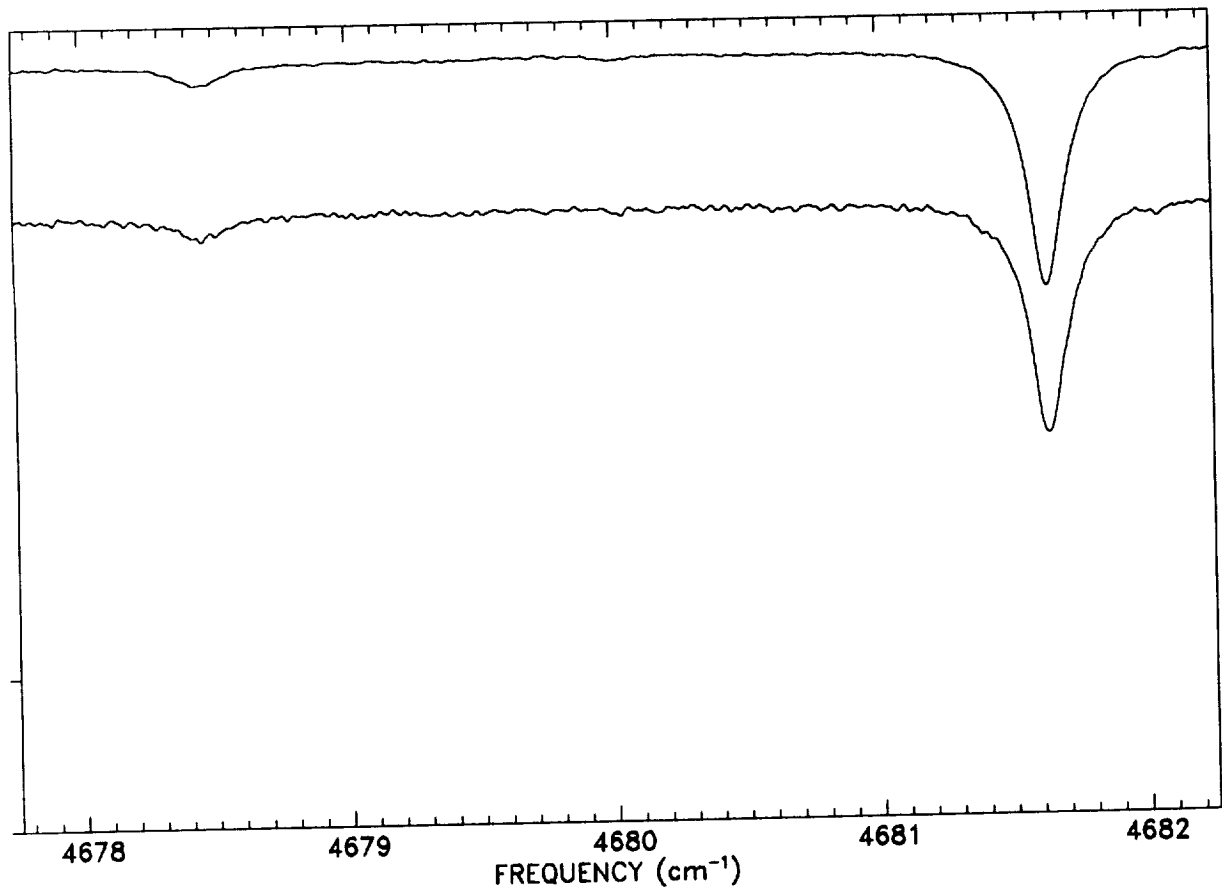


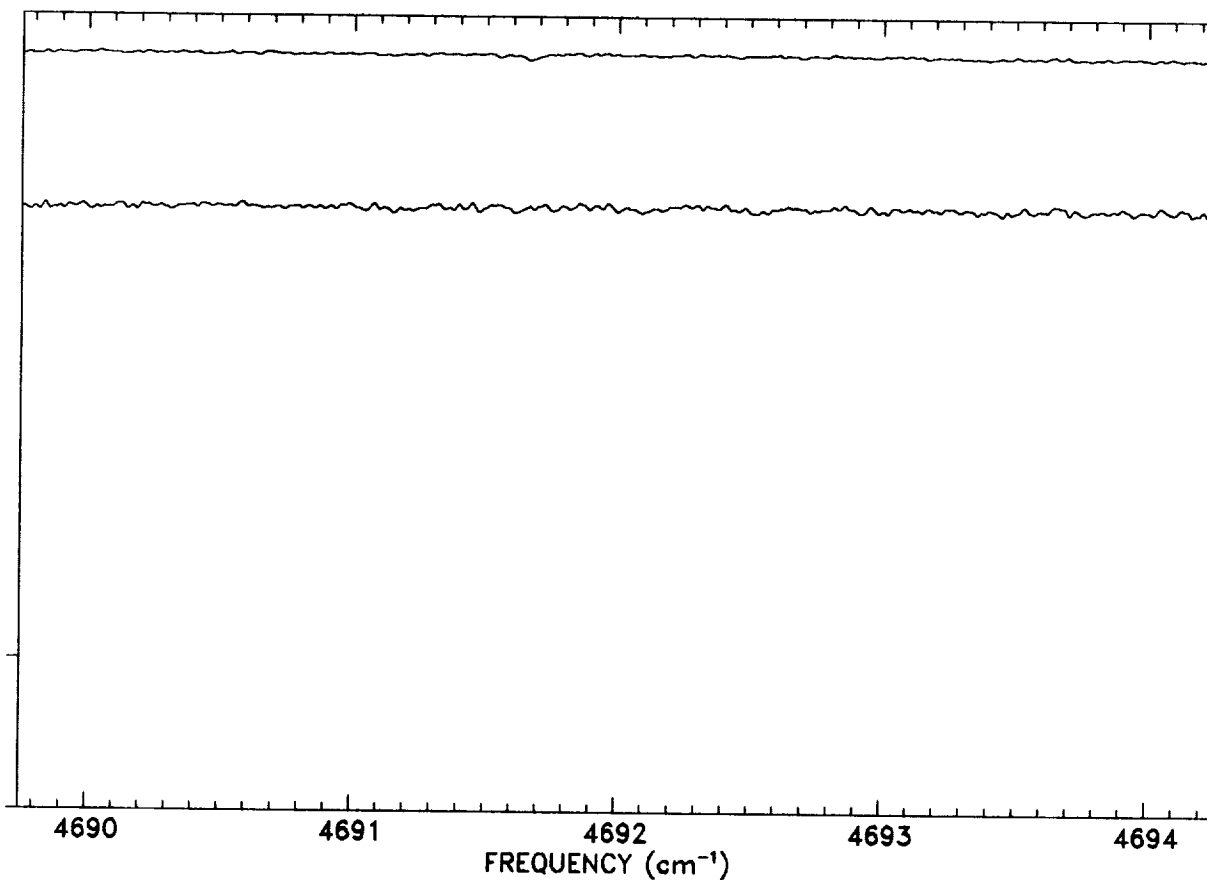
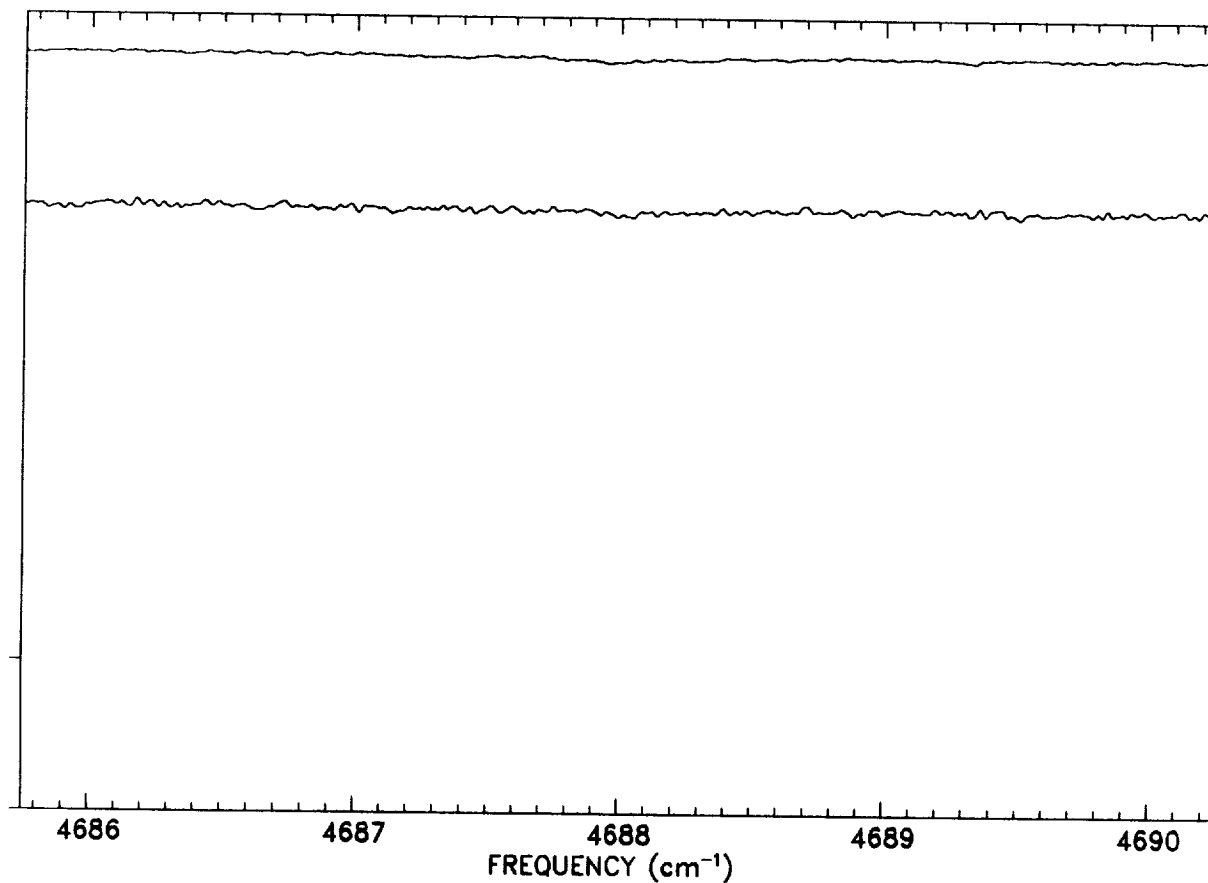


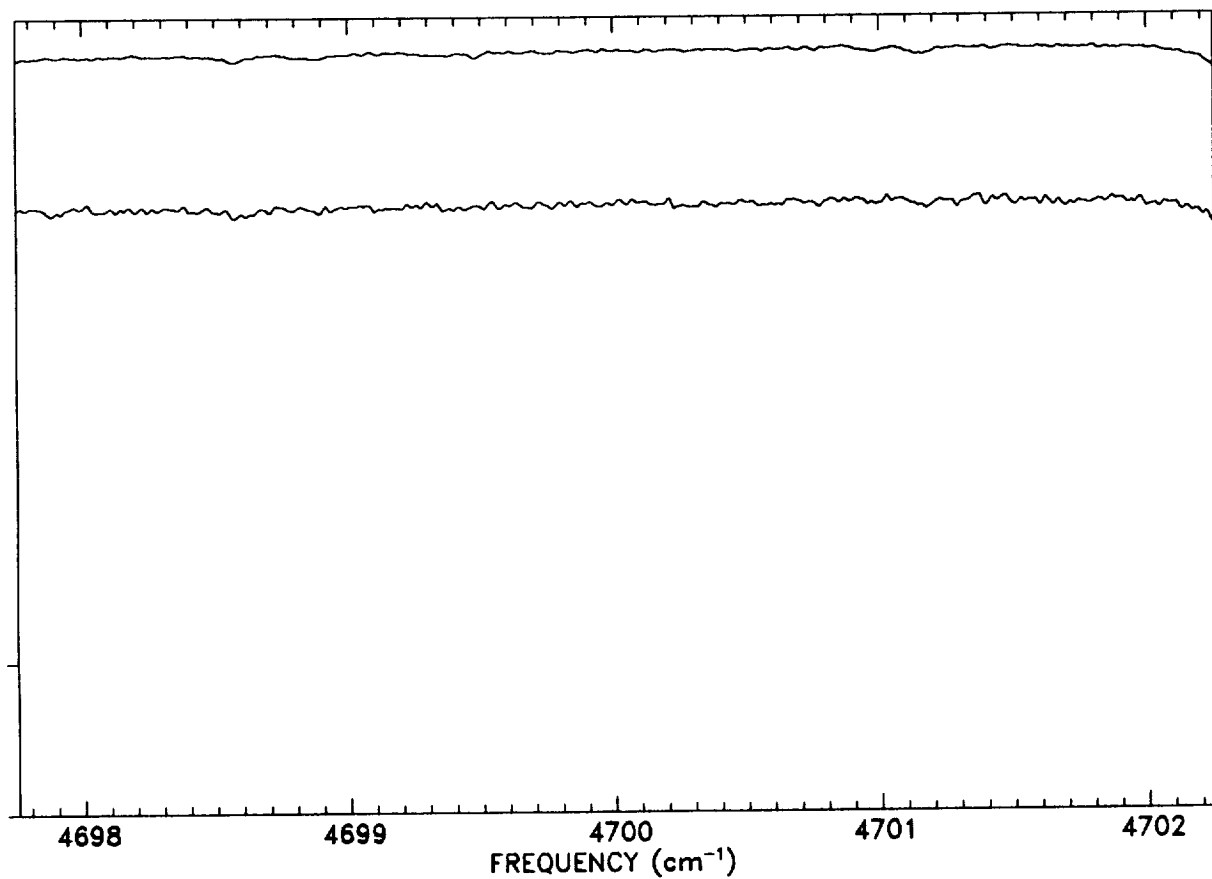
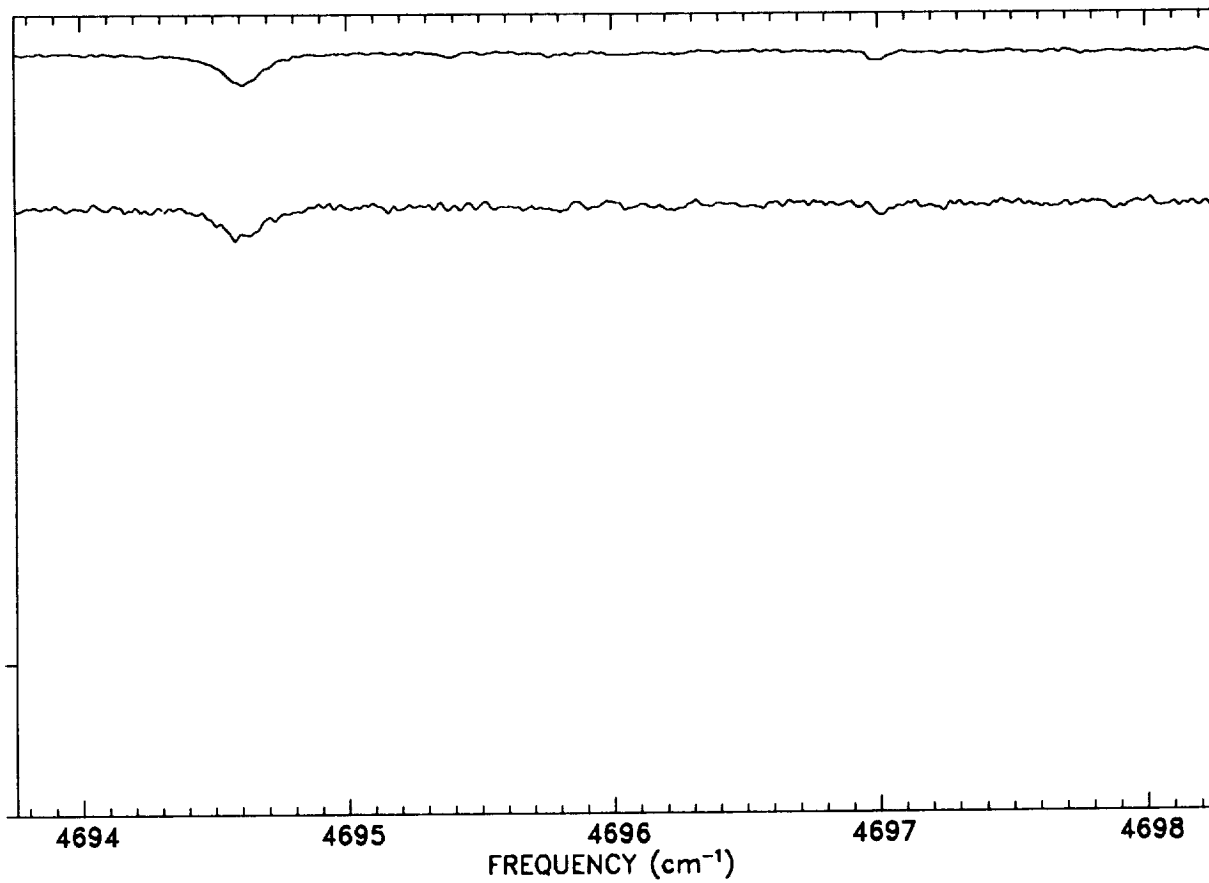


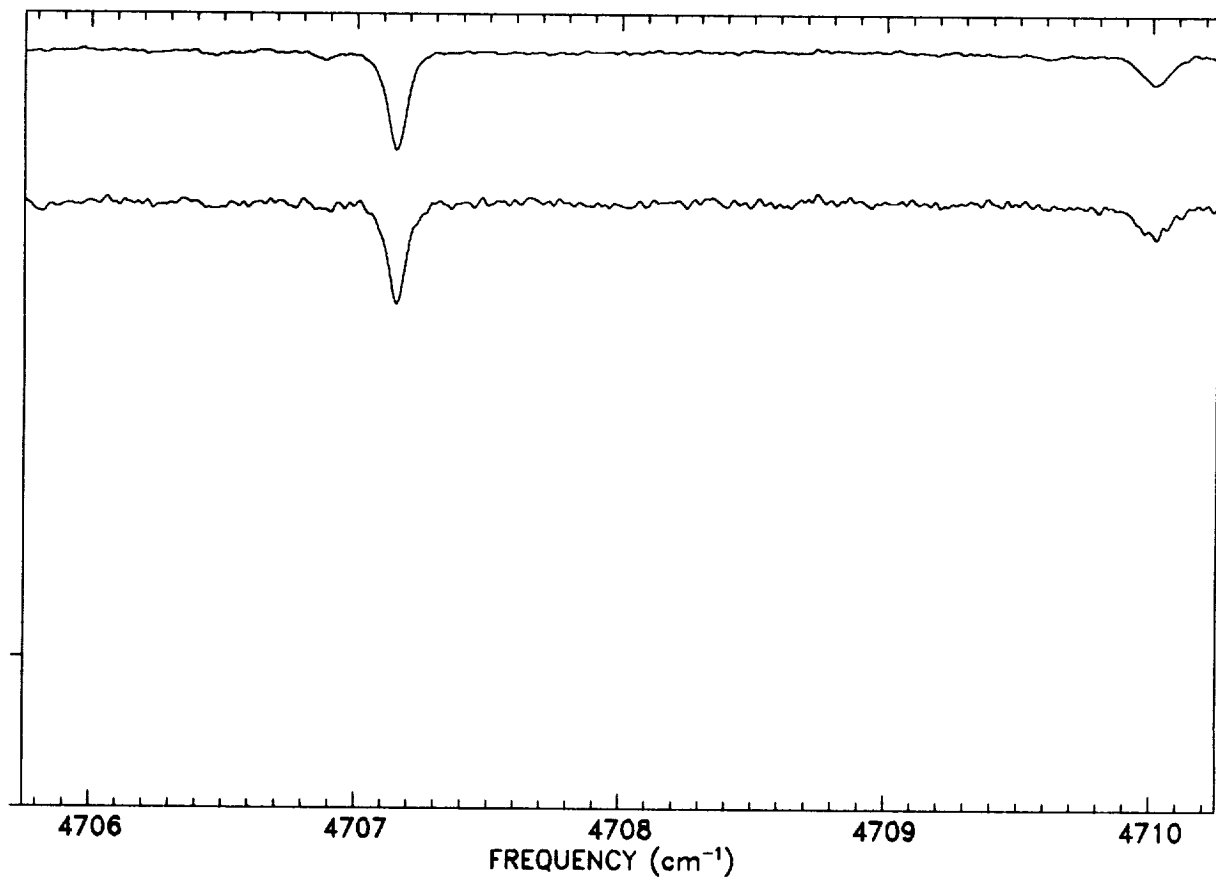
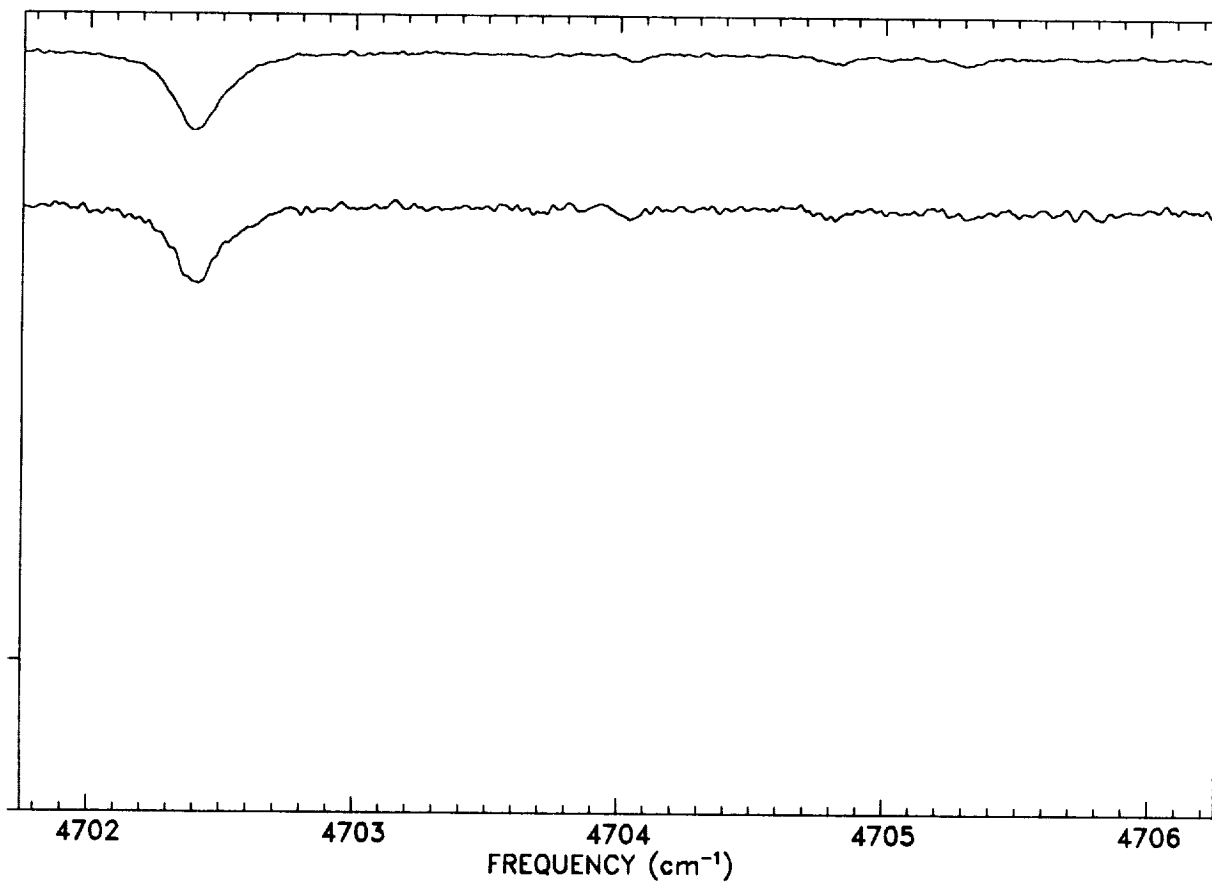


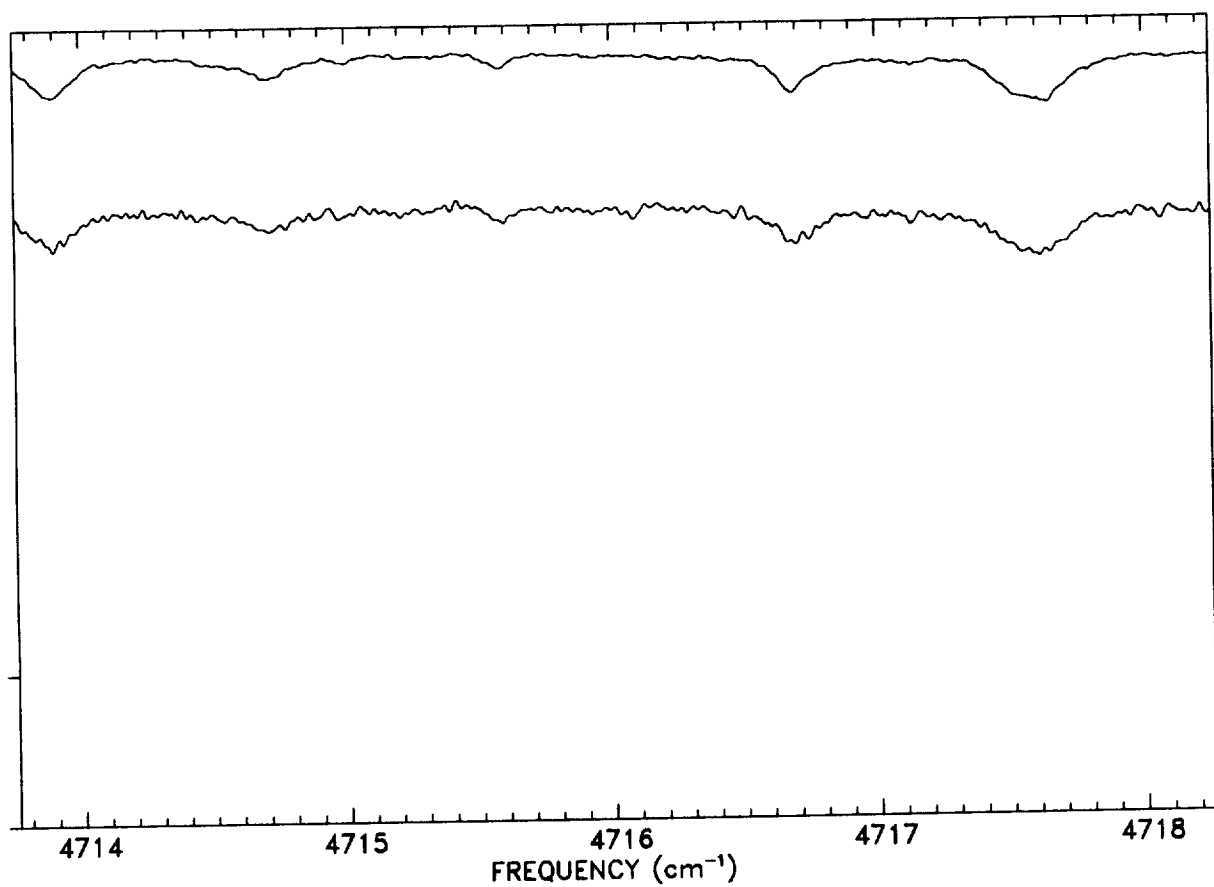
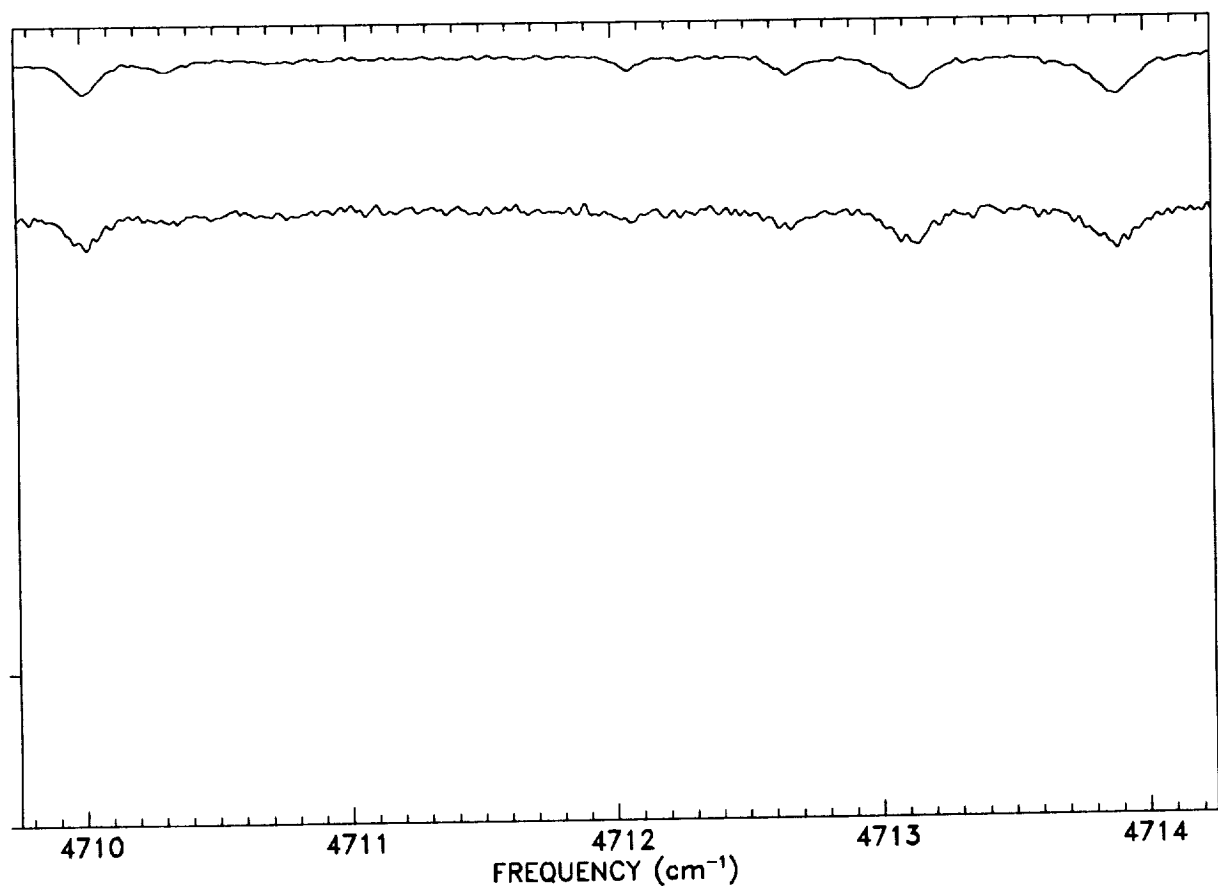


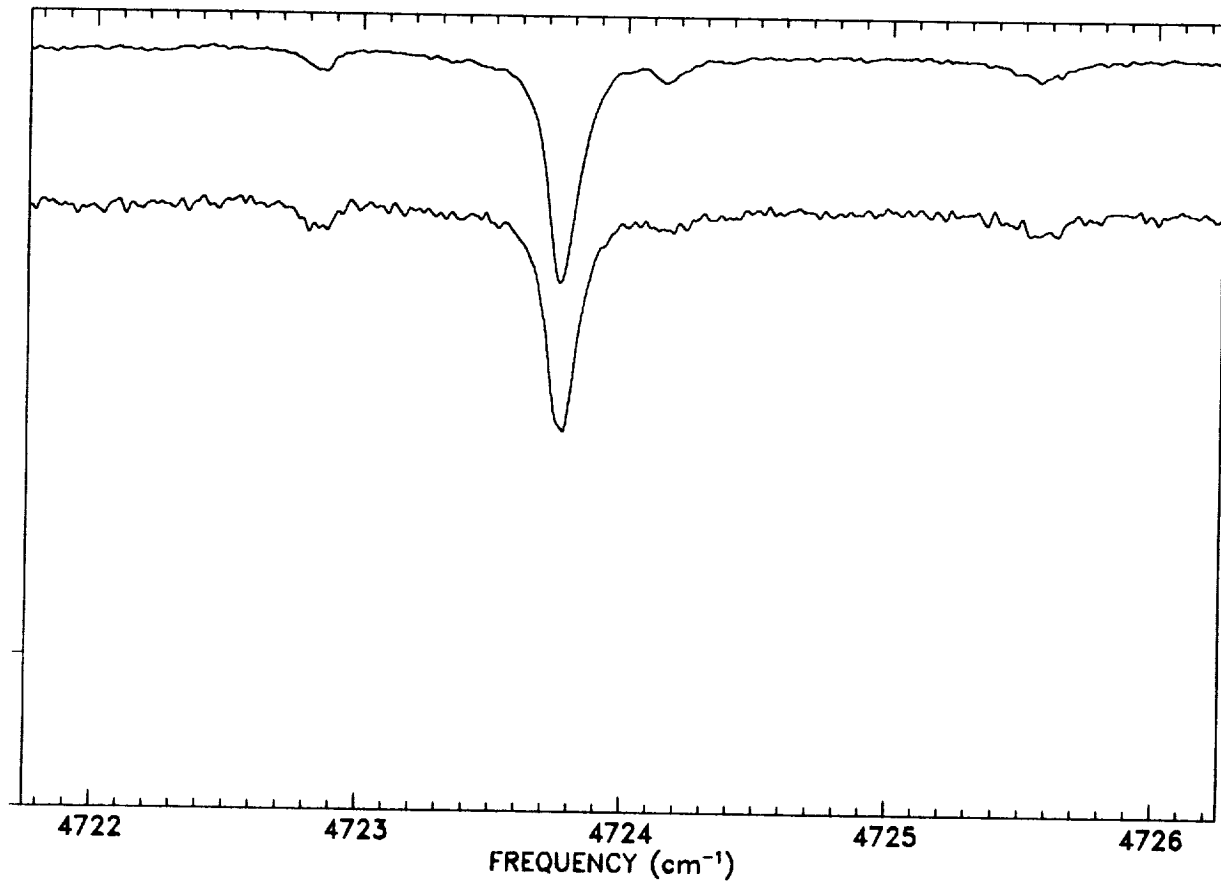
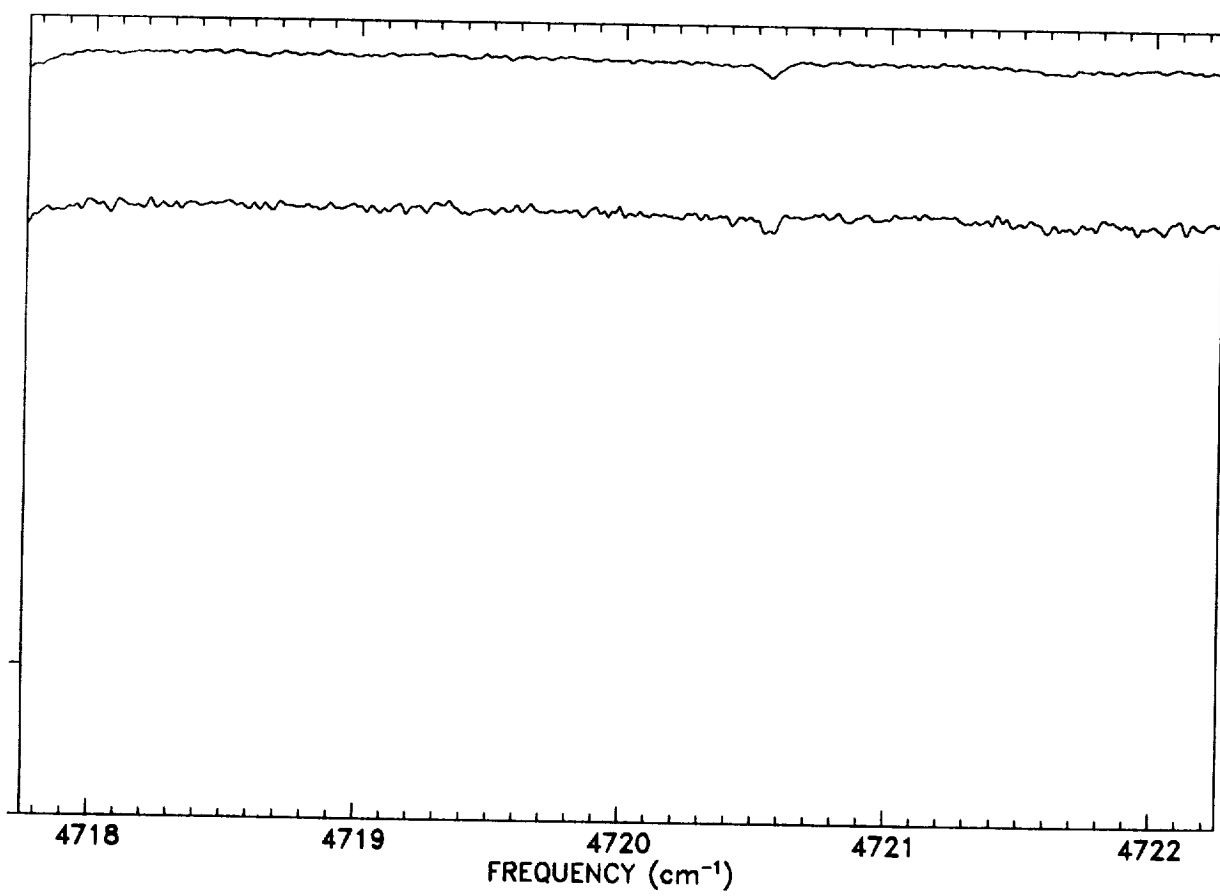


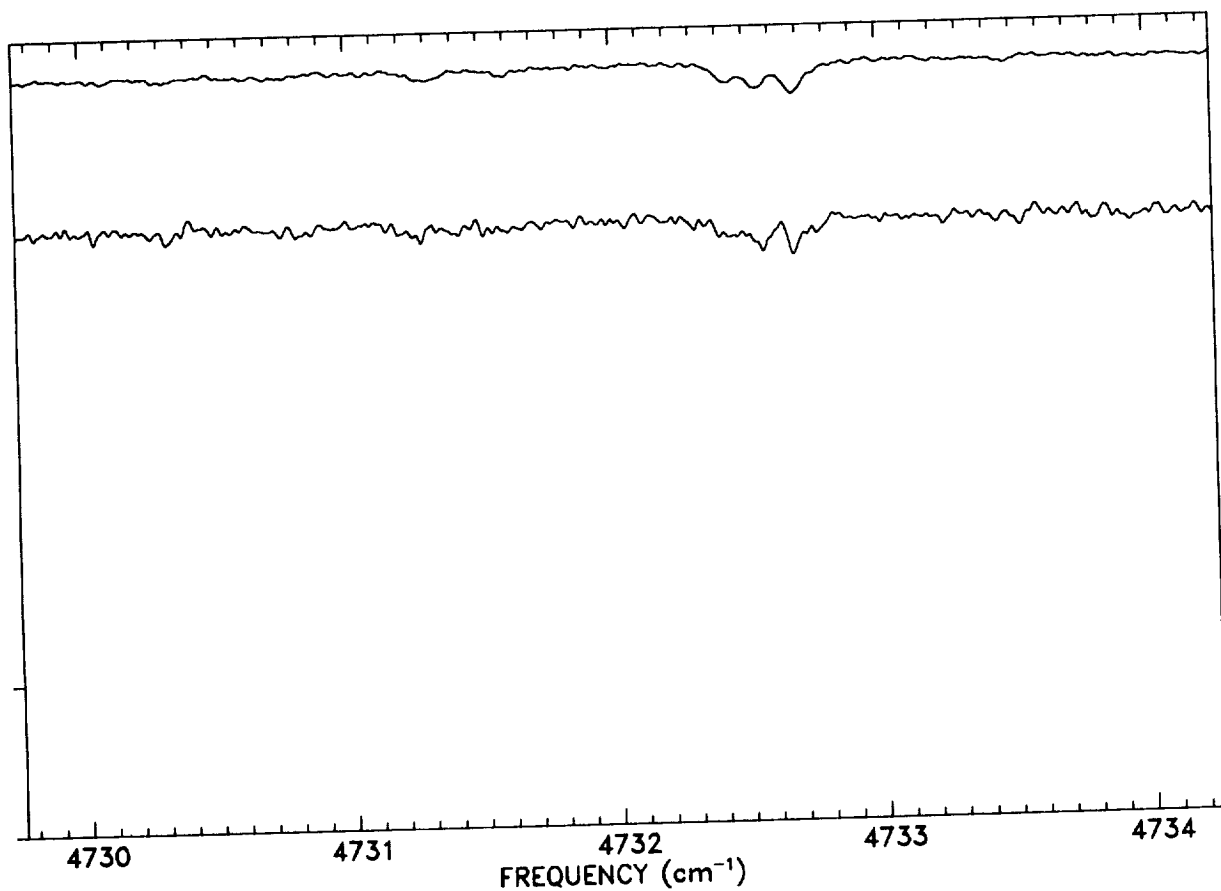
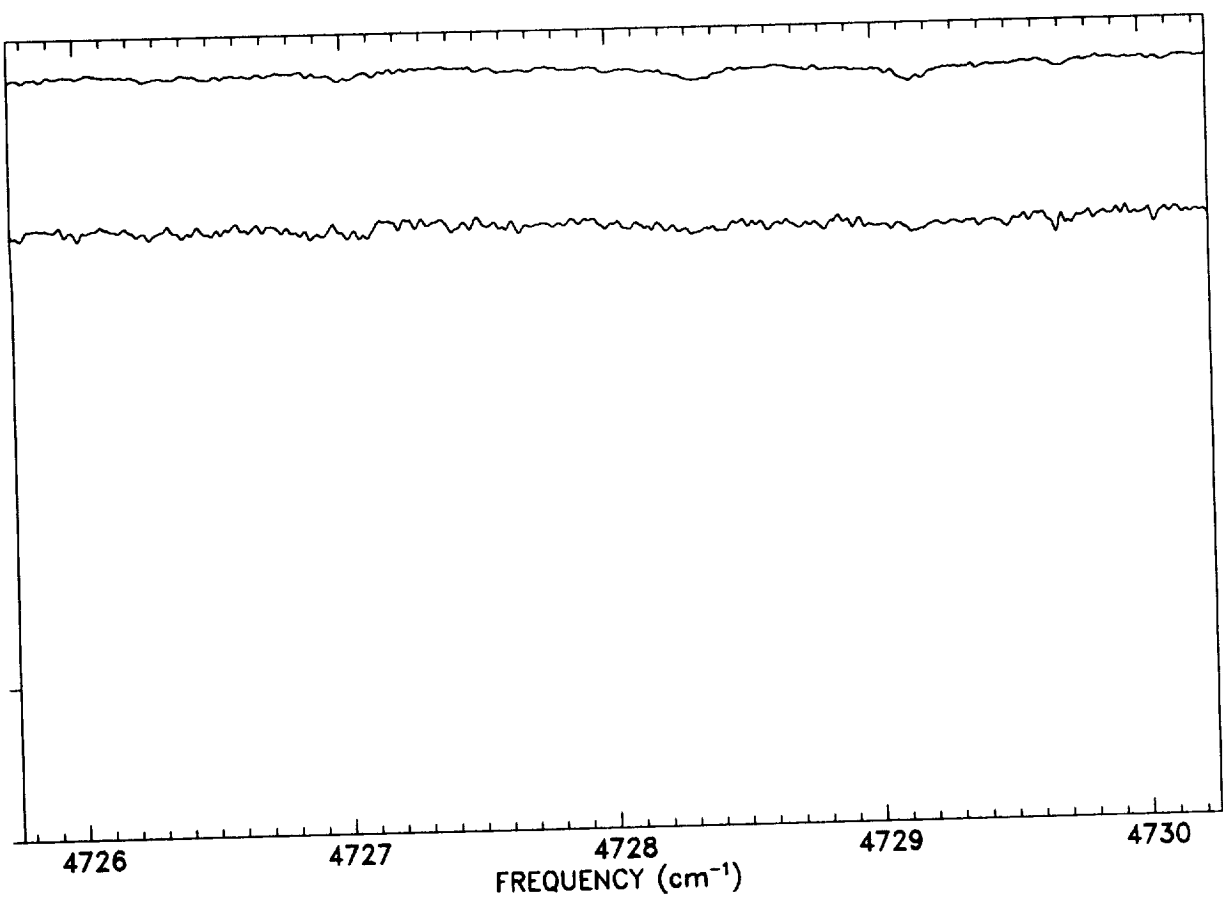


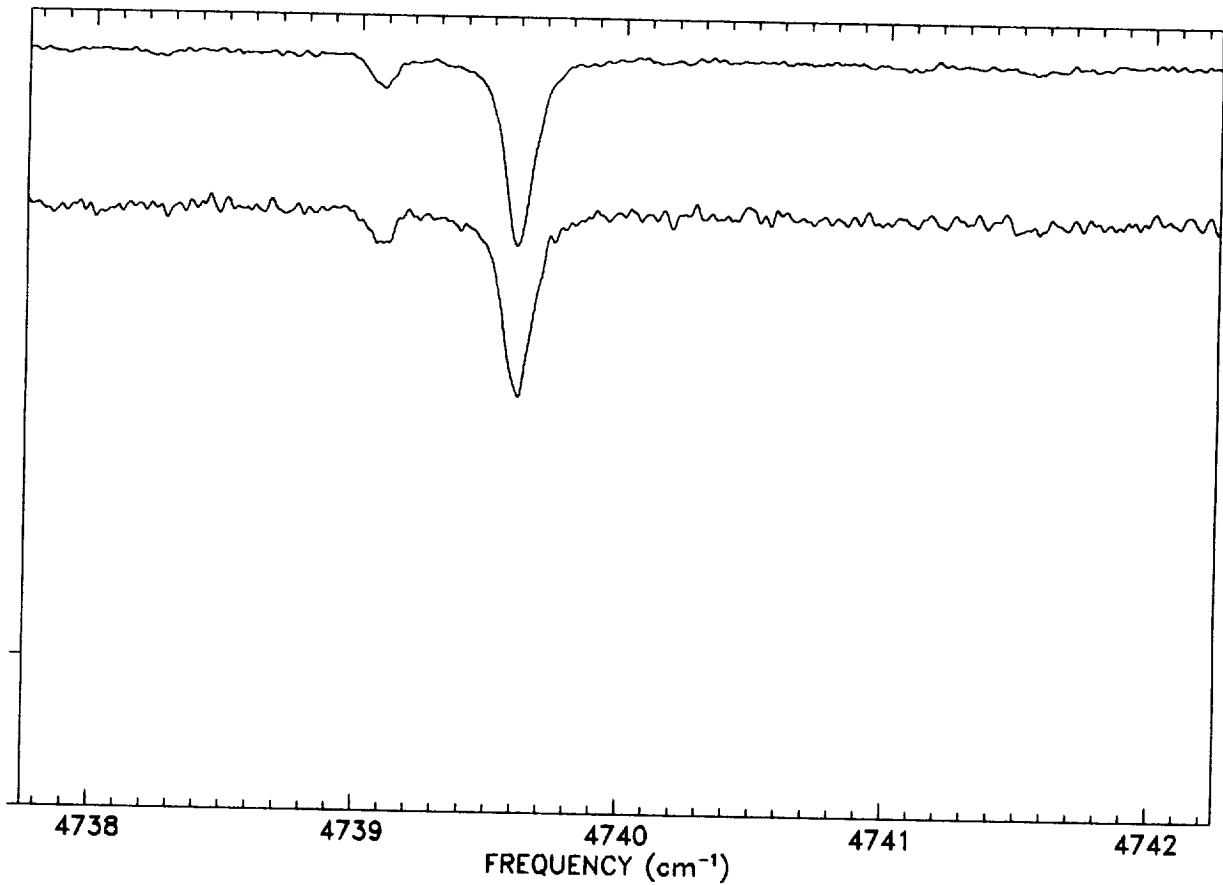
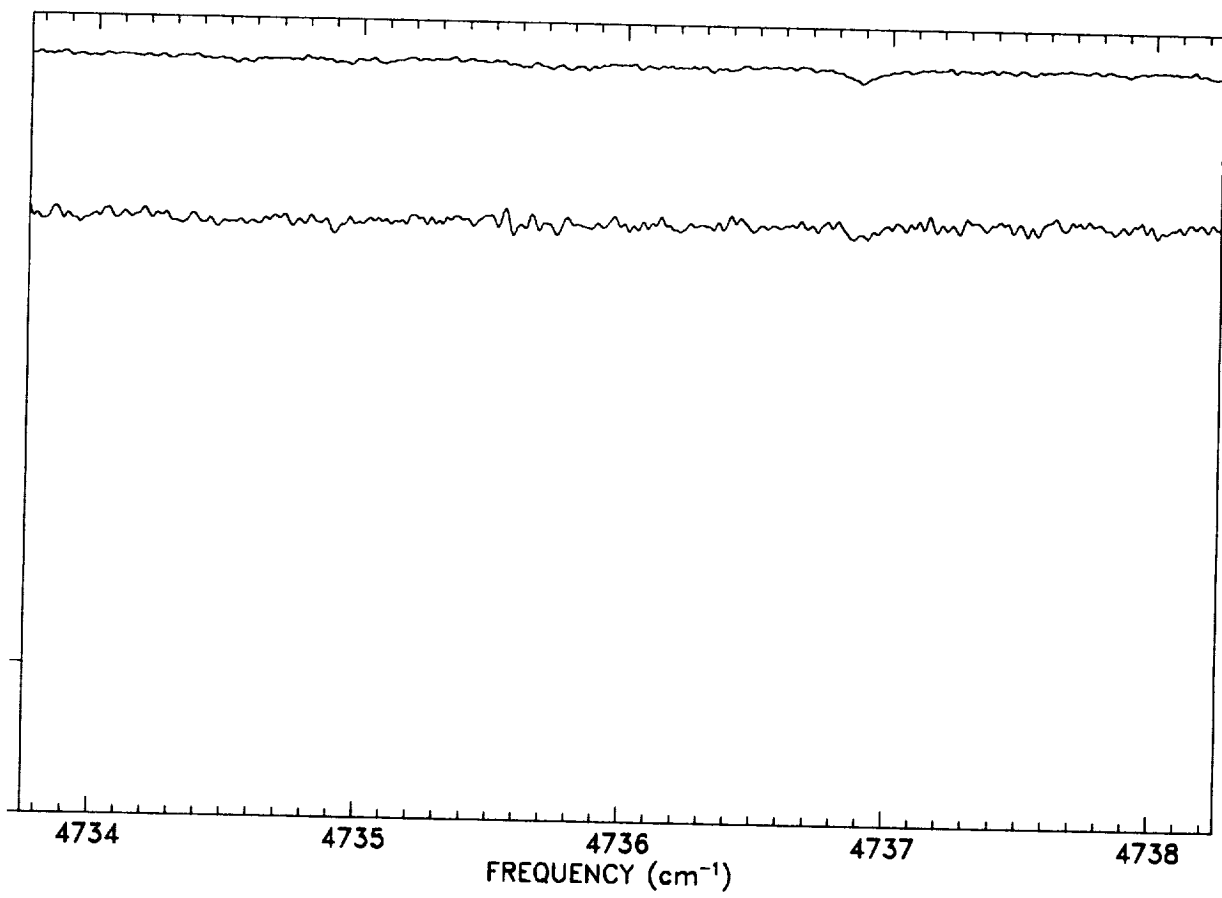


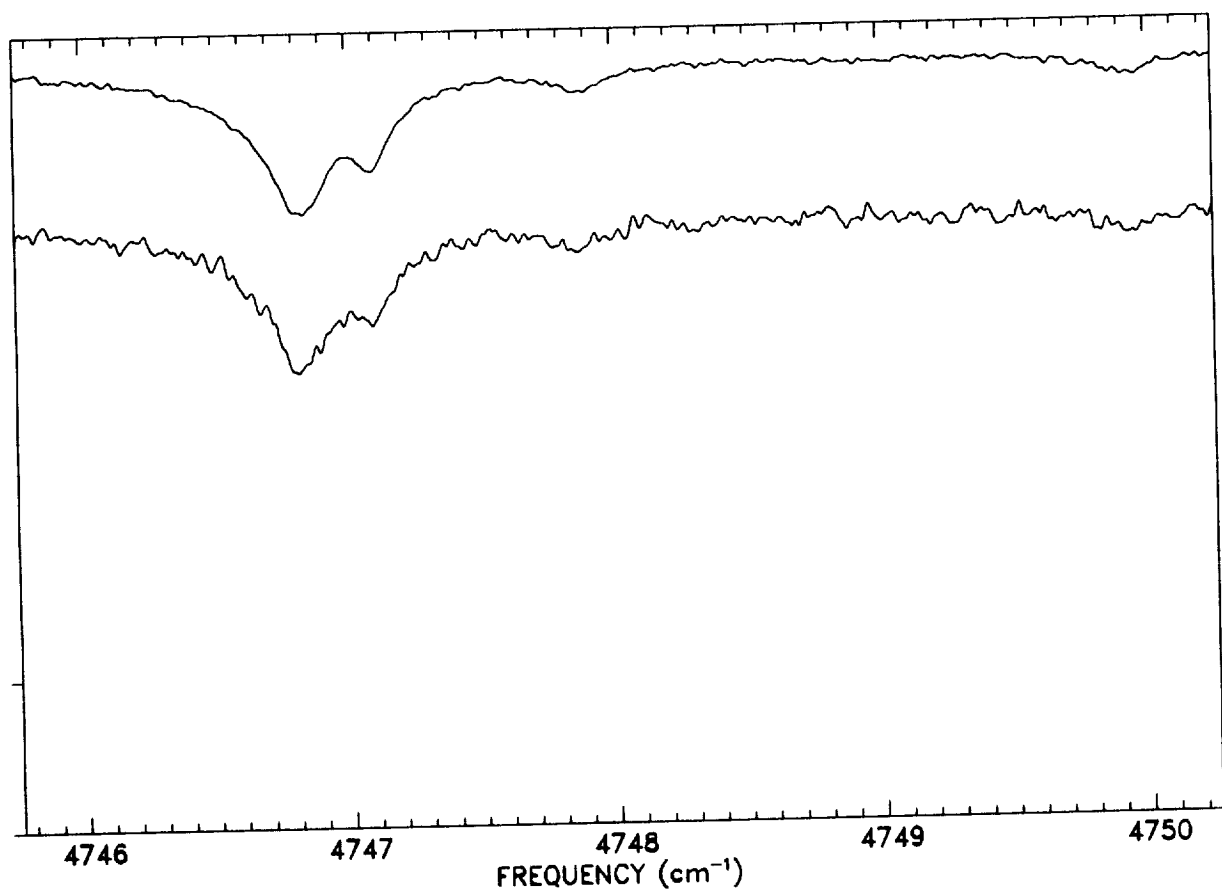
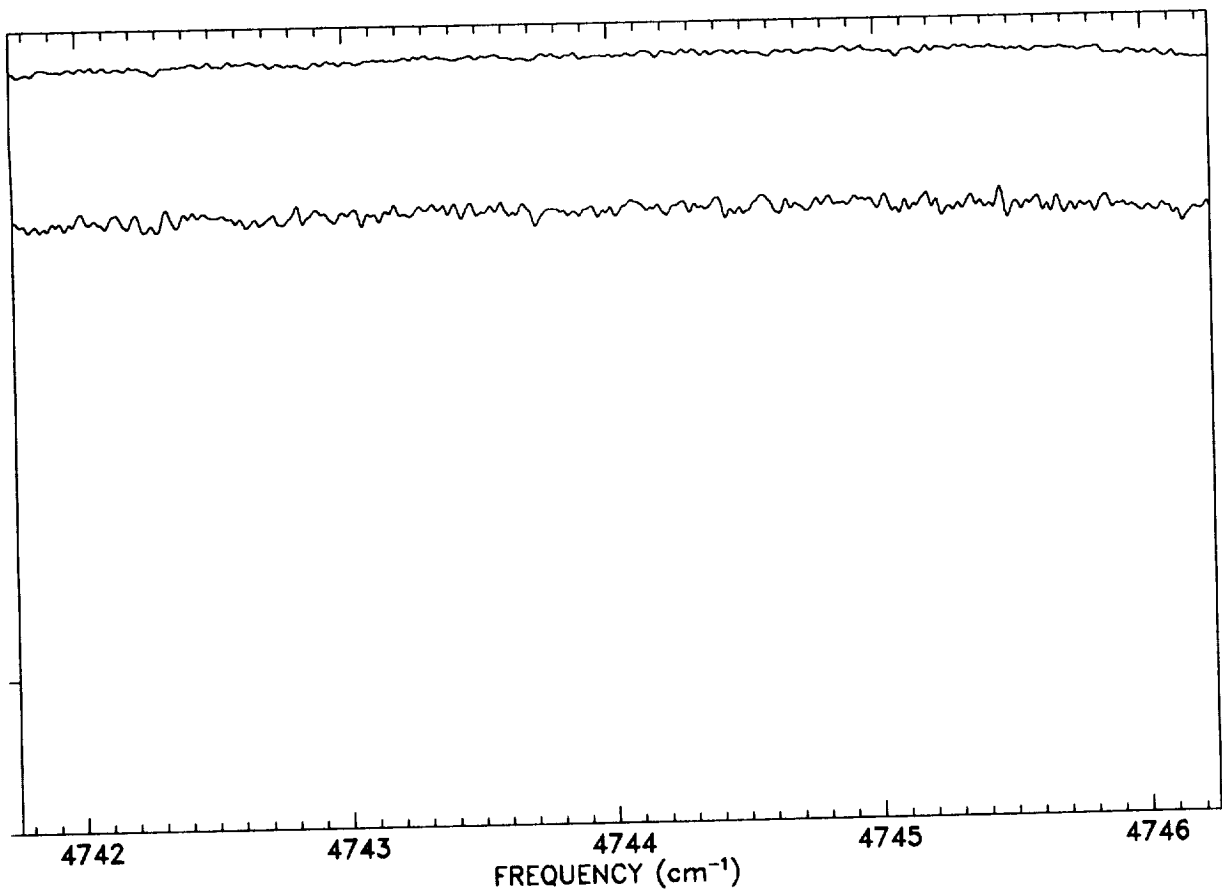


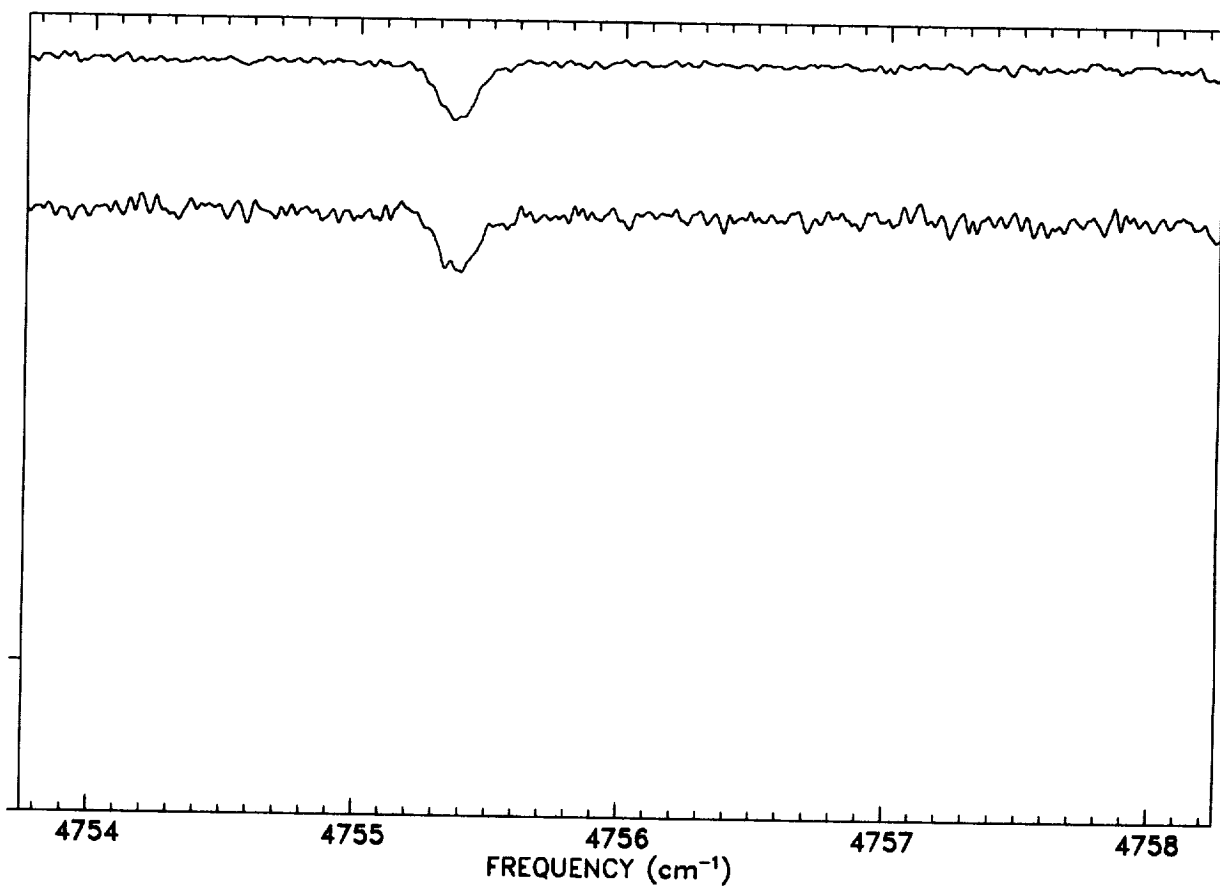
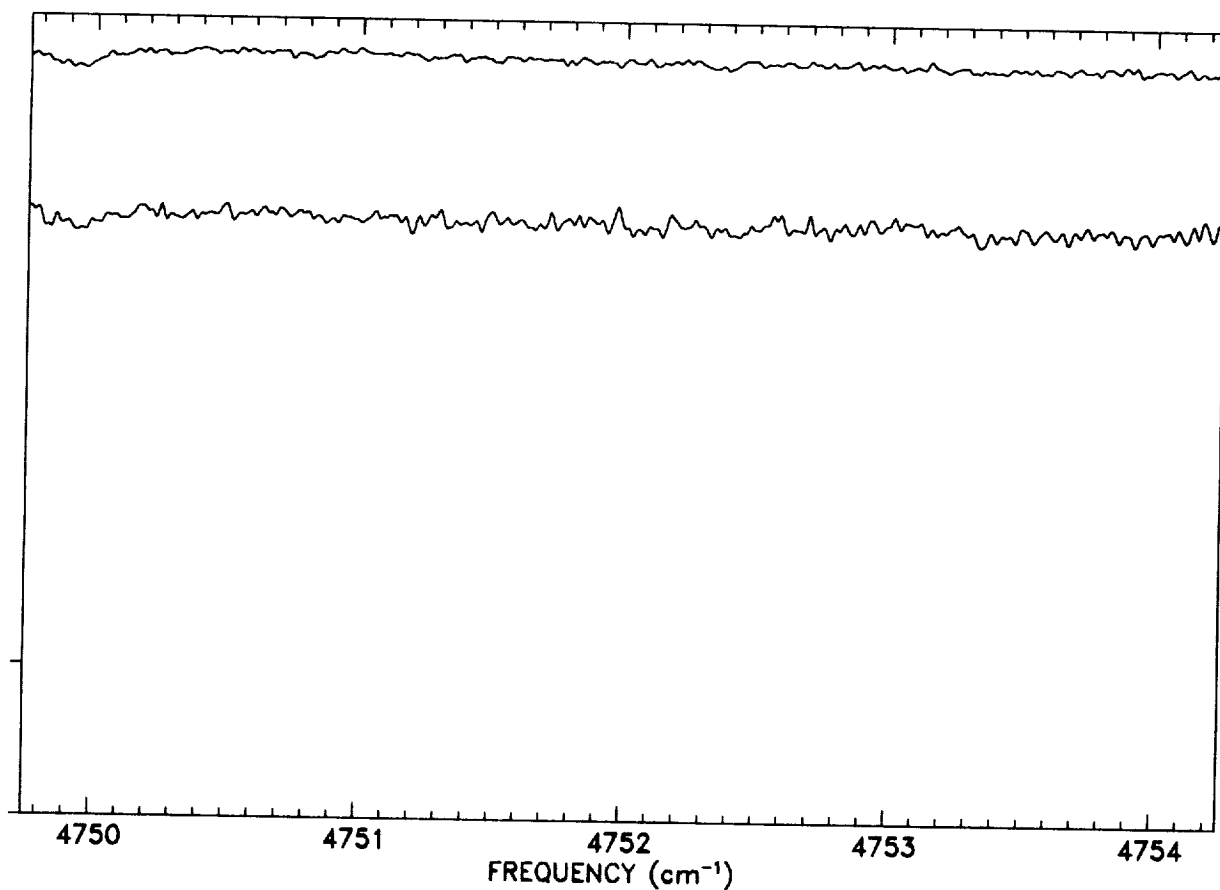


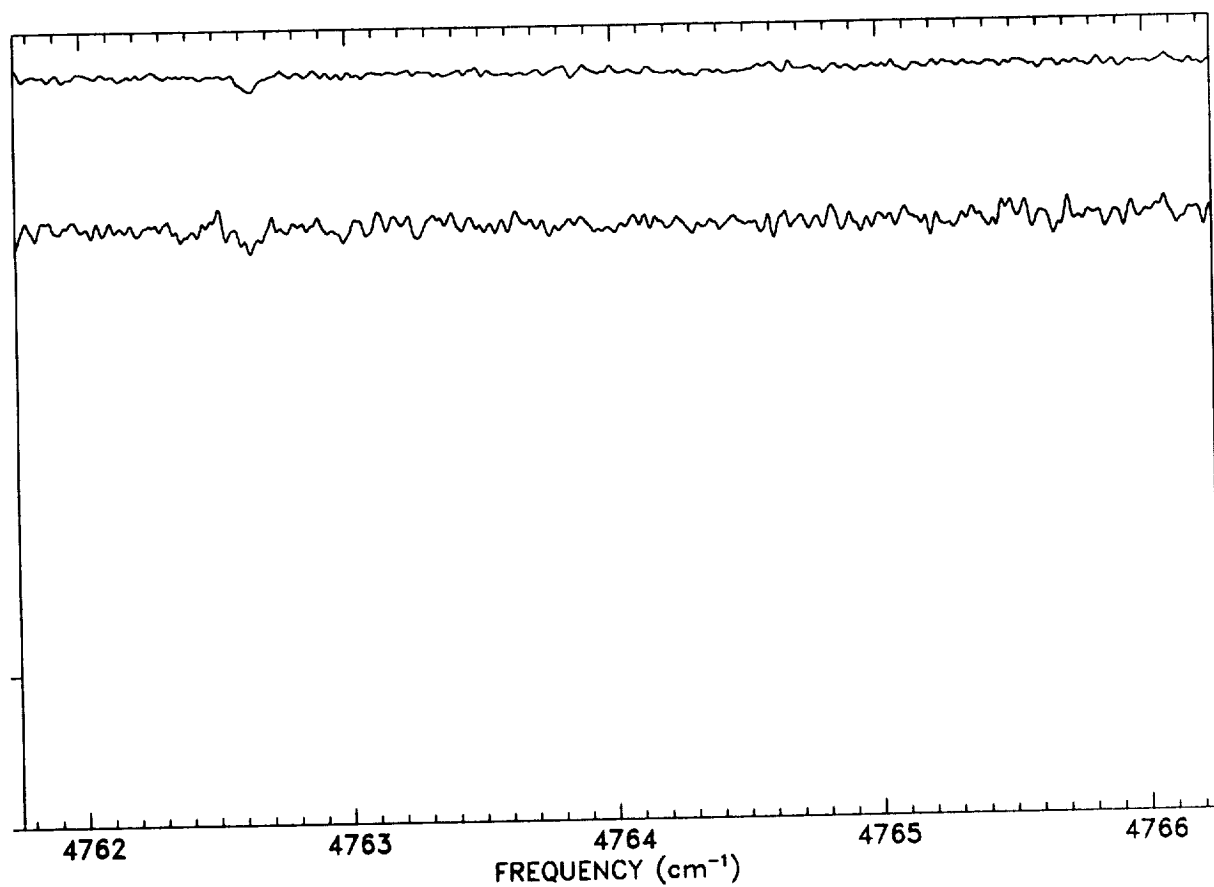
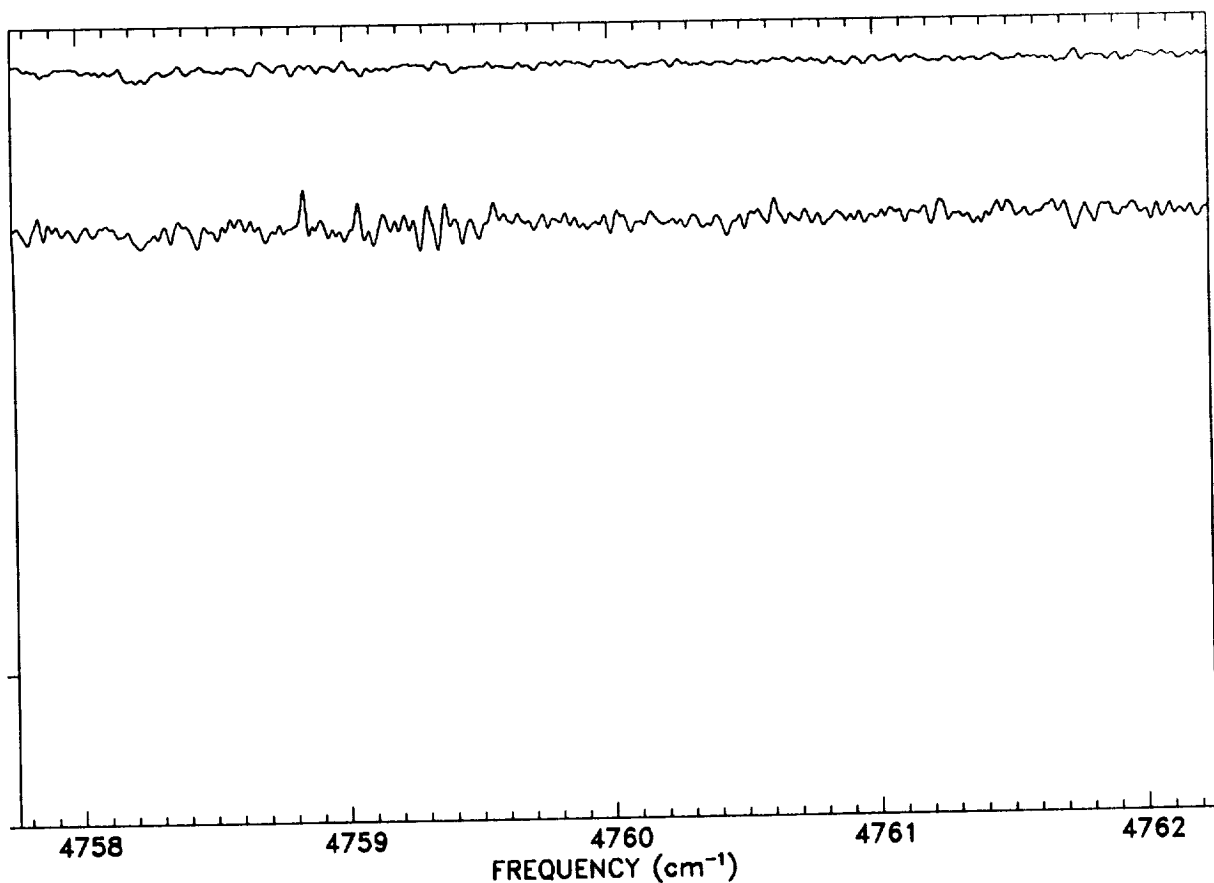


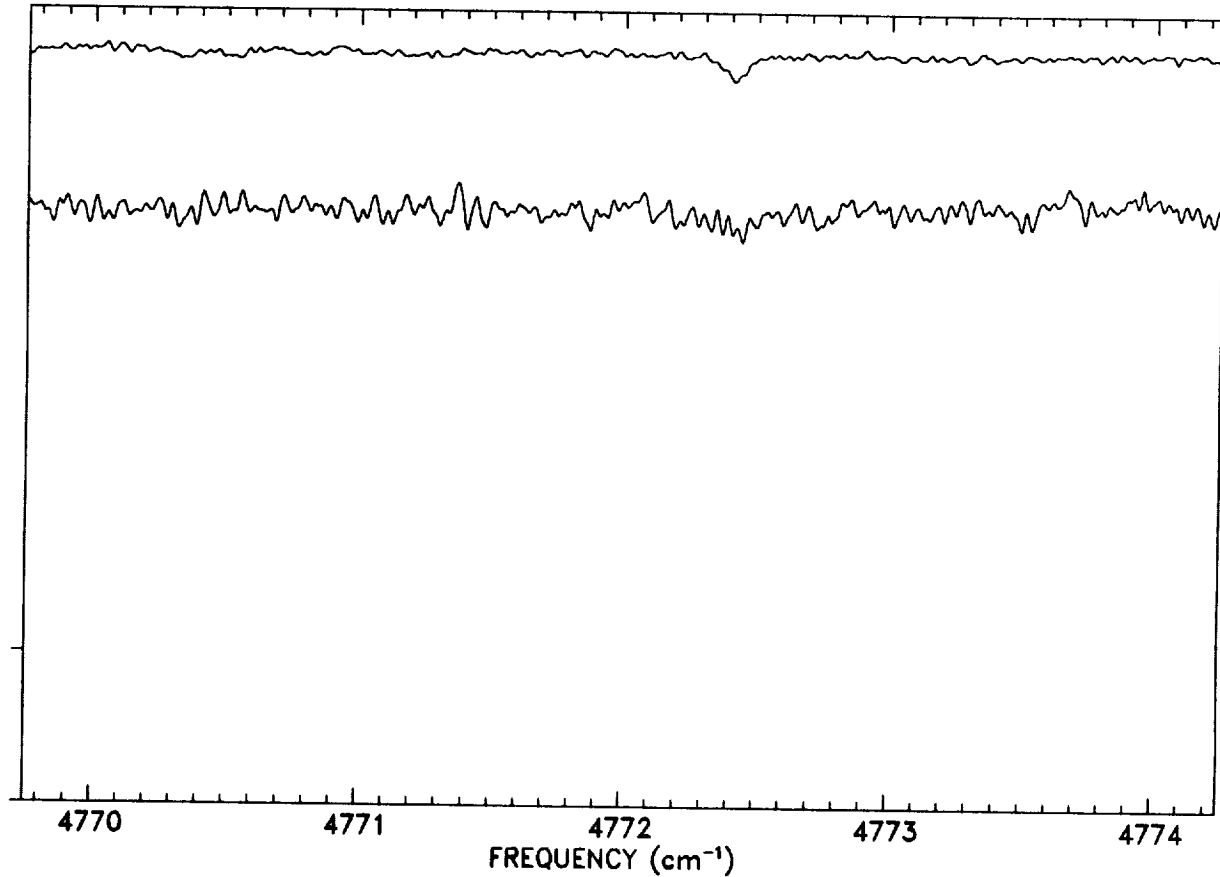
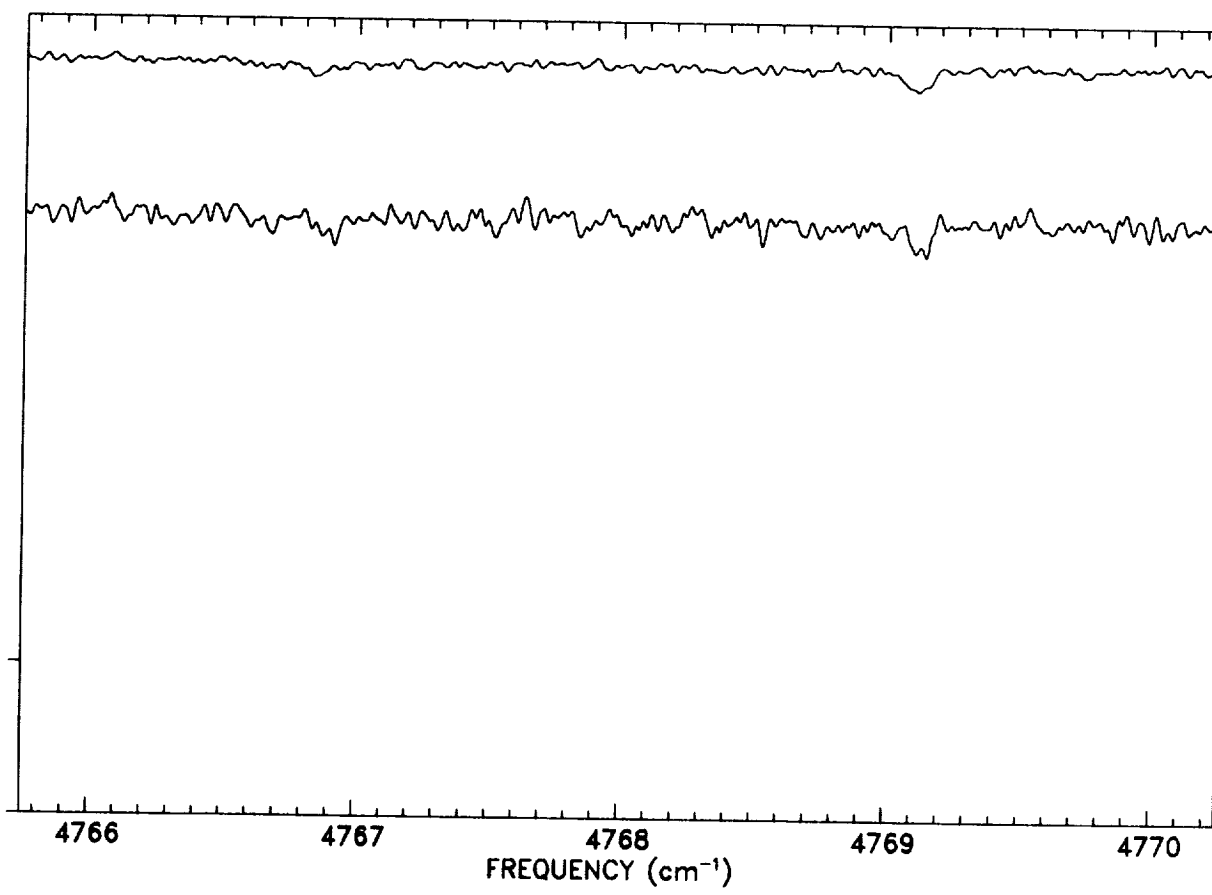


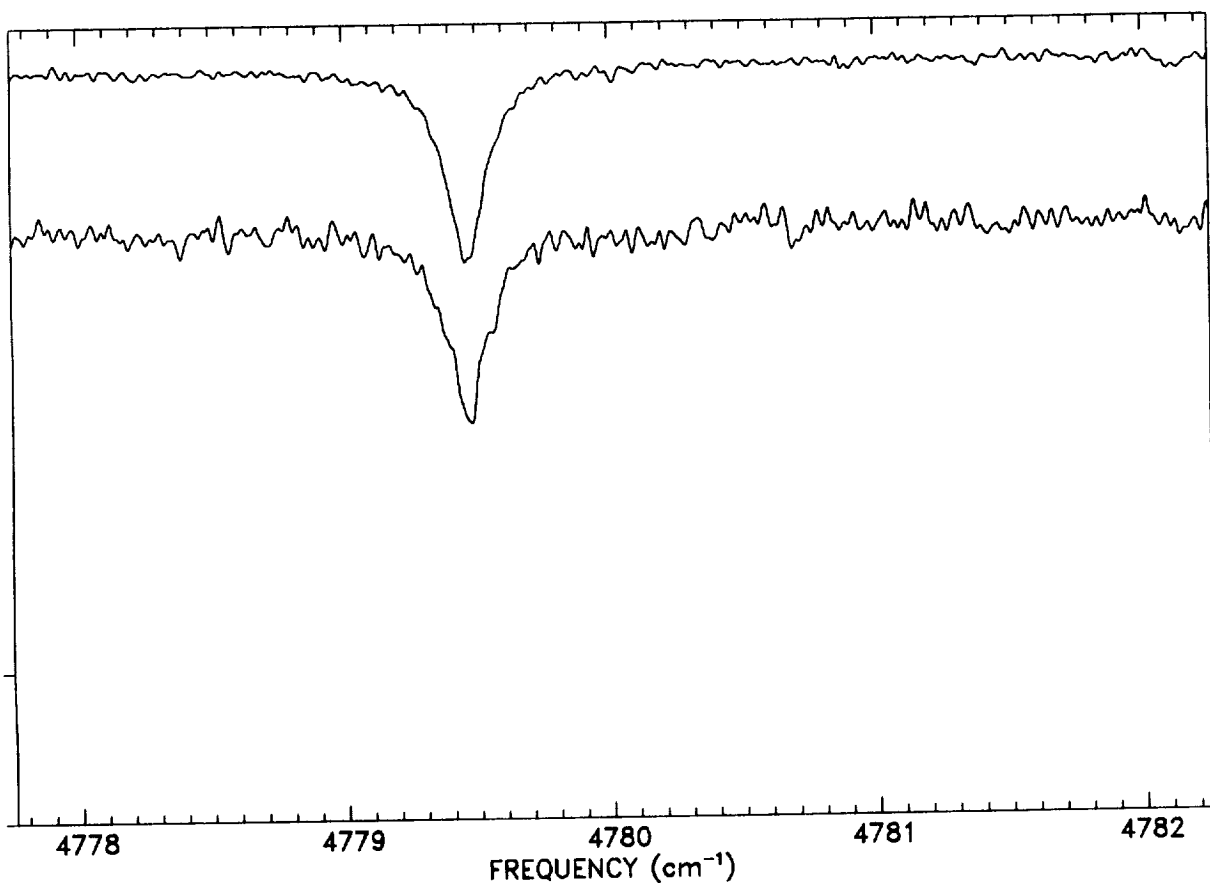
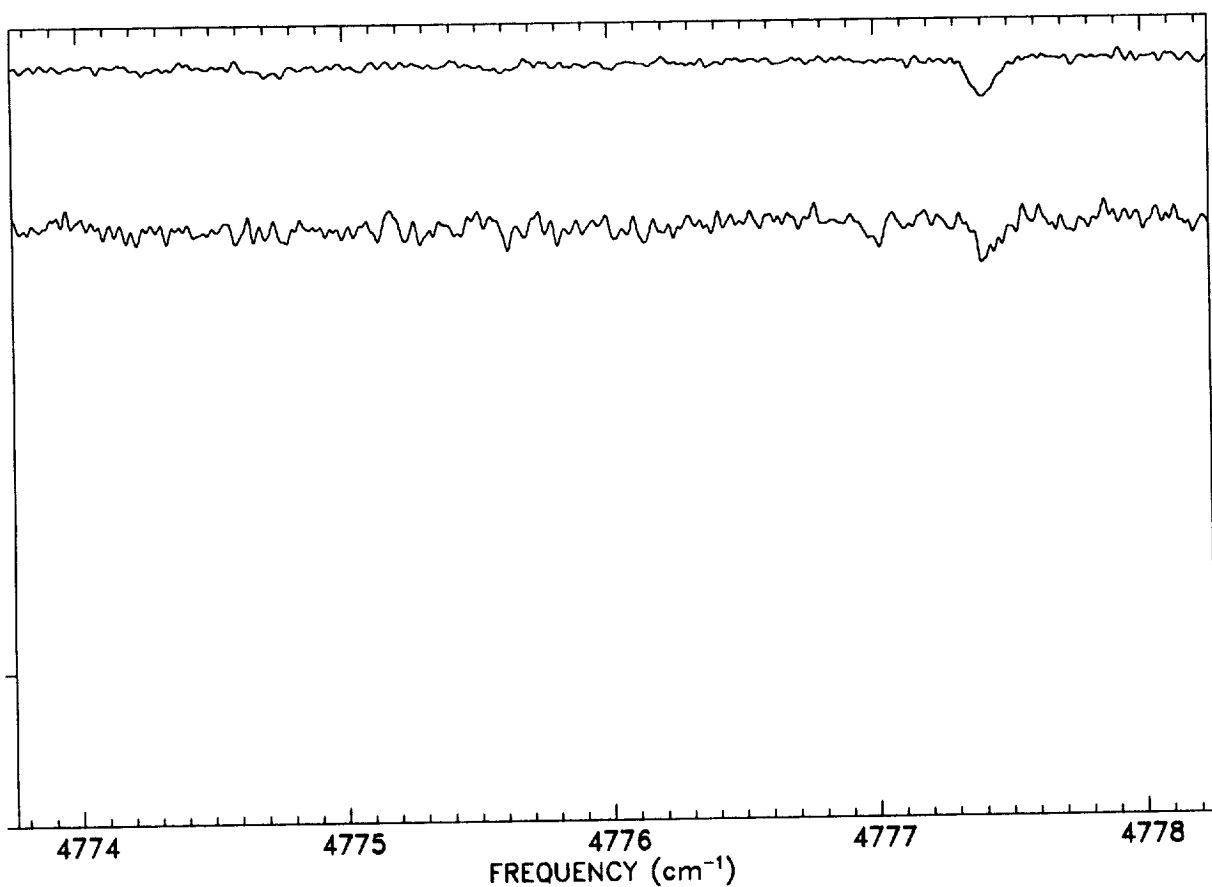


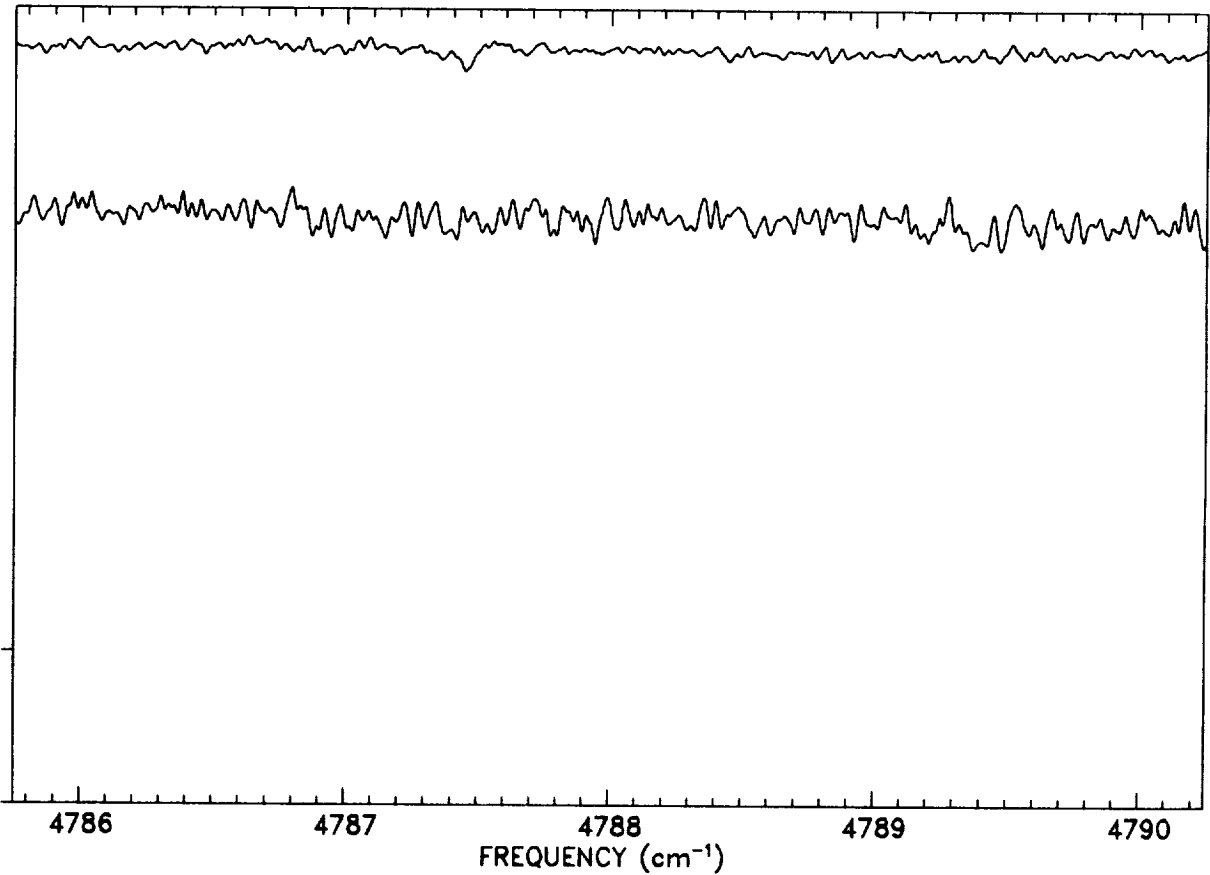
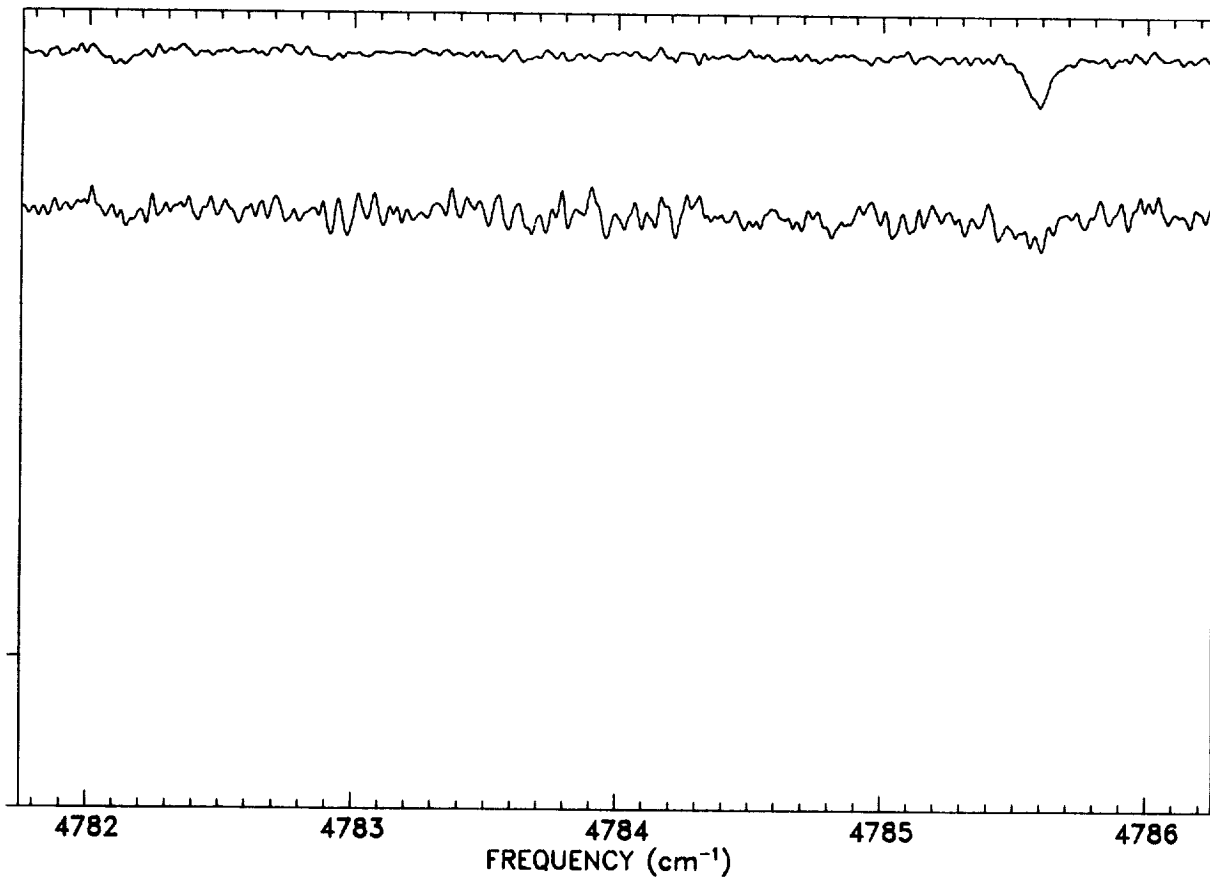


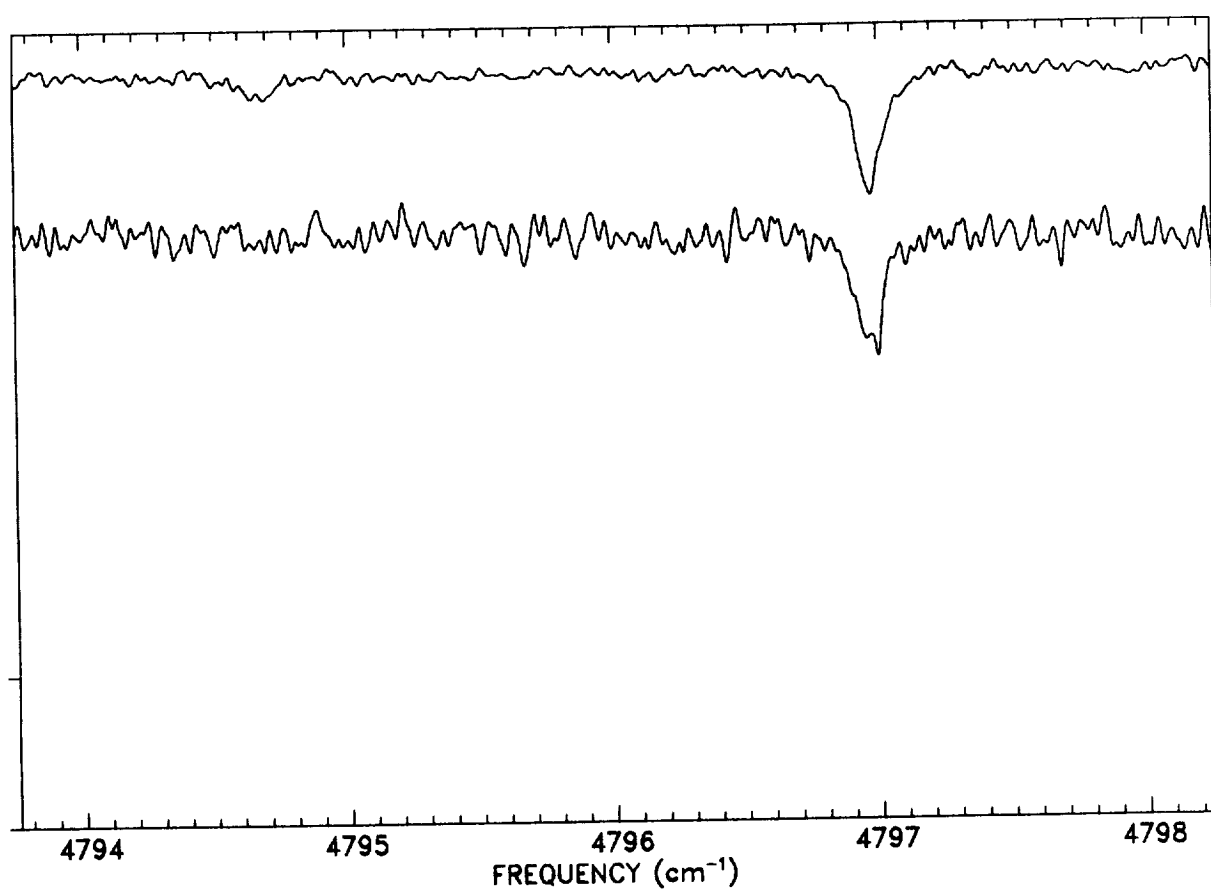
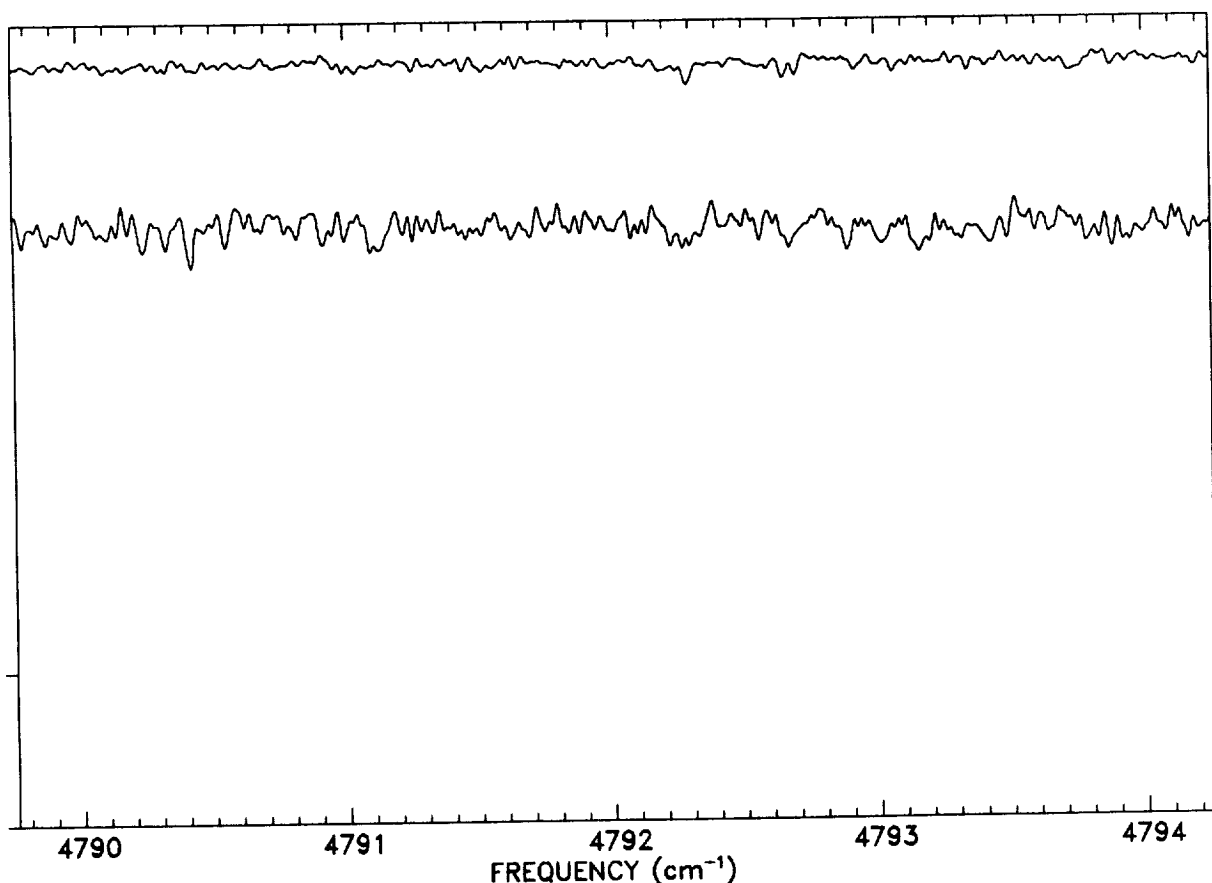














Report Documentation Page

1. Report No. NASA RP-1224, Vol. I	2. Government Accession No.	3. Recipient's Catalog No.	
4. Title and Subtitle A High-Resolution Atlas of the Infrared Spectrum of the Sun and the Earth Atmosphere from Space—A Compilation of ATMOS Spectra of the Region from 650 to 4800 cm⁻¹ (2.3 to 16 μm). Volume I—The Sun		5. Report Date August 1989	
7. Author(s) Crofton B. Farmer and Robert H. Norton		6. Performing Organization Code	
9. Performing Organization Name and Address Jet Propulsion Laboratory California Institute of Technology 4800 Oak Grove Drive Pasadena, California 91109		8. Performing Organization Report No. 400-370	
12. Sponsoring Agency Name and Address National Aeronautics and Space Administration Washington, D.C. 20546-0001		10. Work Unit No.	
15. Supplementary Notes Volume II of RP-1224 entitled "Stratosphere and Mesosphere, 650 to 3350 cm ⁻¹ " is published under separate cover.		11. Contract or Grant No. NAS7-918	
16. Abstract <p>During the period April 29 to May 2, 1985, the Atmospheric Trace Molecule Spectroscopy (ATMOS) experiment was operated for the first time, as part of the Spacelab-3 payload of the shuttle Challenger. The principal purpose of this experiment was to study the distributions of the atmosphere's minor and trace molecular constituents. The instrument, a modified Michelson interferometer covering the frequency range from 600 to 5000 cm⁻¹ at a spectral resolution of 0.01 cm⁻¹, recorded infrared absorption spectra of the Sun and of the Earth's atmosphere at times close to entry into and exit from occultation by the Earth's limb. Spectra were obtained that are free from absorptions due to constituents of the atmosphere (i.e., they are "pure solar" spectra), as well as spectra of the atmosphere itself, covering line-of-sight tangent altitudes that span the range from the lower thermosphere to the bottom of the troposphere. This atlas presents a compilation of these spectra arranged in a hardcopy format suitable for quick-look reference purposes. Volume I gives the solar spectrum from 650 to 4800 cm⁻¹, and Volume II covers the stratosphere and mesosphere (i.e., tangent altitudes from 20 to 80 km) for frequencies from 650 to 3350 cm⁻¹.</p>		13. Type of Report and Period Covered Reference Publication	
17. Key Words (Suggested by Author(s)) Atmospheric radiation; Atmospheric transmission; Infrared; Solar spectrum		18. Distribution Statement Unclassified-Unlimited Subject Category 46	
19. Security Classif. (of this report) Unclassified	20. Security Classif. (of this page) Unclassified	21. No. of pages 532	22. Price A23

